Surprises and Discoveries in Visible-Light Photocatalysis

Dissertation

Zur Erlangung des Doktorgrades der Naturwissenschaften

(Dr. rer. nat.)

an der Fakultät für Chemie und Pharmazie

der **Universität Regensburg**

vorgelegt von

Santosh K. Pagire

aus

Maharashtra, Indien

2017

The experimental part of this work was carried out between October 2013 and September 2017 at the Institute of Organic Chemistry, University of Regensburg, Germany under the supervision of Prof. Dr. Oliver Reiser.

The thesis was submitted on 06.11.2017

Date of the colloquium: 08.12.2017

Board of Examiners:	PD Dr. Sabine Amslinger	(chair)
	Prof. Dr. Oliver Reiser	(1st referee)
	Prof. Dr. Burkhard König	(2nd referee)
	Prof. Dr. Arno Pfitzner	(examiner)

Dedicated to Sonali

“The journey is what brings us happiness, not the destination.”

-Dan Millman

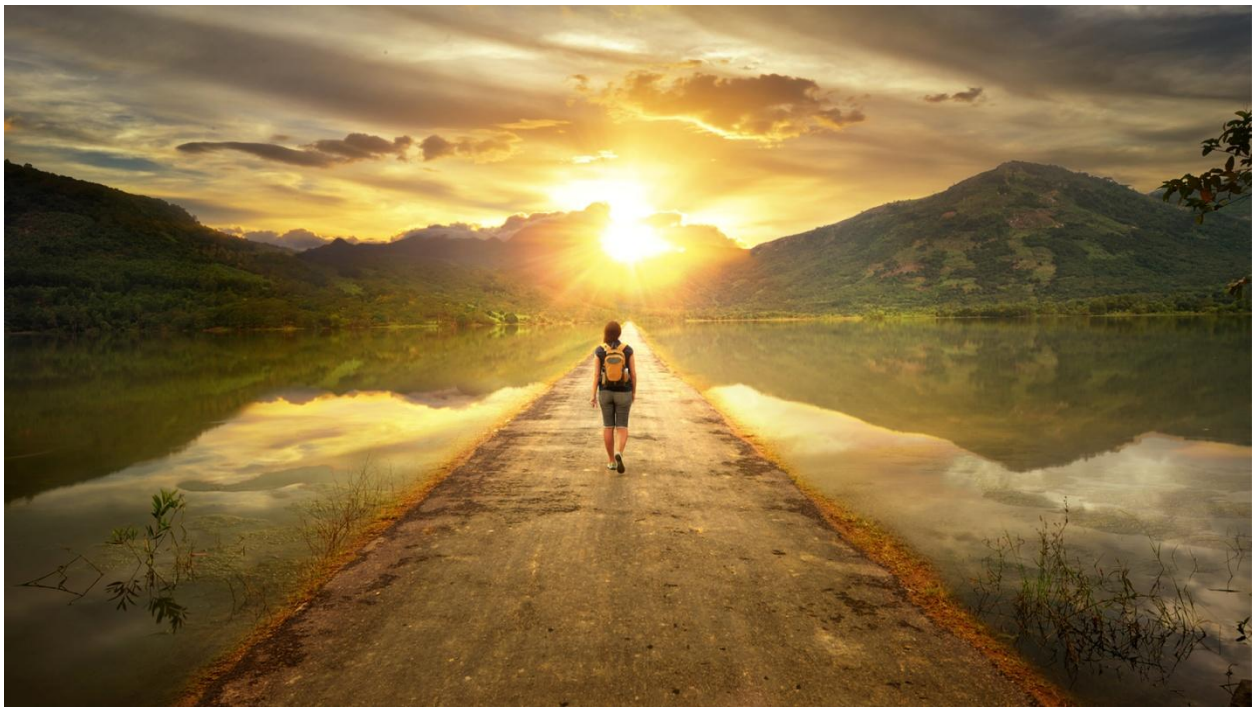

(Image source: Google)

Acknowledgements

The work in this thesis was accomplished through the support, help, and encouragement from numerous people. First and foremost, I wish to express my deep sense gratitude and respect to my research supervisor Prof. Dr. Oliver Reiser, for giving me this unique opportunity to conduct my doctoral studies under his expert supervision and introducing me to the fascinating field of visible-light photocatalysis. I would like to thank him for providing an excellent chemical education, for his never-ending trust in me and in my projects, his continuous support, constructive criticism, open-minded praise, and his special assistance to join the overseas conferences. I particularly appreciated him for providing the unlimited freedom throughout my PhD program at the University of Regensburg. I could have never worked to the best of my capabilities under any kind of mental or physical pressure.

It is my pleasant duty to express my grateful and sincere thanks to Prof. Dr. Burkhard König for being my co-examiner. I am very happy to have him as one of the visible-light photocatalysis experts in my committee. I also thank him for writing recommendation letters in support of my DAAD applications. In addition, I particularly appreciate his offer to collaborate on a review article for *Angewandte Chemie*. I also thank Prof. Dr. Arno Pfitzner for being the doctoral committee members and referring my thesis. He has accepted my request without any hesitation and delay, thank you! I also like to thank PD. Dr. Sabine Amslinger for being Chairman in my PhD defense. I appreciate her quick response; although she will be on maternity leave immediately after the defense. Many congratulations for becoming a Mother, take care!!!

Generous financial supports from DAAD, GDCh, *iP*UR, and DFG-GRK-1626 during my doctoral studies are gratefully acknowledged. In particular, I appreciate the DAAD for providing full-time PhD scholarship, insurance, family support, and the special assistance for learning/understanding the German language and culture. Beyond that, DAAD has also supported me to attend important scientific and cultural events in Germany.

During my PhD journey, I had the chance to collaborate with excellent and hardworking students: Dr. Suva Paria, Asik Hossain, Lukas Traub, Sabine Kerres, Dr. Vidyasagar Adiyala, Julietta Yedoyan, Dr. Leyre Marzo, the part of my thesis would have never been completed

without them, and I am happy to have many of them as co-authors on my publications. Dr. Sabrina Fürst, Dr. Myungmo Lee, Dr. Sharif Najafishirtari, Dr. Vidyasagar Adiyala, and Maryam Homafar were fantastic labmates, we spent a great time together in- and outside the lab. My special thanks go to Dr. Peter Kreitmeier for his valuable assistance, constant help, support in all the technical aspects and computer problems. I was happy to share one of my important publications together with him. I thank Klaus Döring, Helena Konkel, Roxane Harteis, and Brigitte Eichenseher for their technical assistance. I also thank Mrs. Antje Weigert for helping me in official works, especially, her assistance in getting the University funding at the later stage of my PhD. I also thank new secretary, Michaela Schüle for organizing seminar rooms for my defense.

The University of Regensburg has a fabulous infrastructure for research. Many people have contributed to my work from various departments by making my life easier: the friendly staffs from the NMR department, the Mass-Service, and the X-Ray crystallography are gratefully acknowledged. Mrs. Regina Hoheisel is also acknowledged for carrying out cyclic voltammetry experiments. She is one of the coolest and pleasant personalities I have ever seen in my life.

I would like to take this opportunity to thank my Indian seniors: Dr. Dattatraya Bagal, Dr. Suva Paria, Dr. Rizwan Shaikh, Dr. Indrajit Ghosh, Dr. Uttam Chakraborty, Dr. Tamal Ghosh, and Dr. Somnath Das for being my moral supporters and their valuable assistance during my research stay at Regensburg. I will certainly miss the Regensburg, as it was not only a wonderful experience as a PhD student, but I am fortunate to have fantastic friend circle outside the University of Regensburg. Especially, I got amazing friends during the Cricket season. I would definitely miss the quality time we spent together.

Finally, I would like to acknowledge whole Reiser group for their constant help and support, I always felt proud to be a member of this beautiful family. However, most of the times, I felt language was the main barrier to have a great communication. Nevertheless, I tried to communicate with my “broken” German, thanks to the DAAD!!! I thank Martin Hoffman and Dr. Sabrina Fürst for their special assistance in translating a summary of the thesis into a German version.

I have an amazing wife (Sonali) and I feel she is the most deserving person whom I would like to dedicate my PhD thesis. She is one of the inspirations I have in my life; she trusted me in all my decisions and has been continuously supporting me over the last 6 years and never lost her trust in my bad times. The more happiness was added to my life when my princess (Aaradhya) was born on 20th of June 2013. Though, I missed the opportunity to hold her in my hands at the time of her birth. However, later this year, we blessed with a new prince, Aaditya. We are indeed a very happy family now; I had never dreamed such a beautiful life I could get…

Words fall short to thank my "strong" mother and my both the brother's (my two arms) for their help and never-ending love over the years. The biggest part of my success is definitely due to their scarifications and endless care.

Last but not the least; I would like to thank everyone who has supported me on this wonderful ride. There have been too many names and faces that have passed through my life and all of you have helped me to grow just not as an organic chemist but also as a good person.

All in all, I had never imagined that someday I would defend my PhD thesis in Germany. It's an unbelievable journey!!! The dreams do come true if you have faith in yourself….. "*Where there is a will, there is a way*."

Publications, Presentations, and Participations

Publications:

1. **S. K. Pagire**, P. Kreitmeier, O. Reiser

   Visible-Light-Promoted Generation of α-Ketoradicals from Vinyl-Bromides and Molecular Oxygen: Synthesis of Indenones and Dihydroindeno[1,2-c]chromenes**.**

   Angew. Chem. Int. Ed., **2017**, *56*, 10928-10932; **DOI:** 10.1002/anie.201702953 (English edition).

   Bildung von α-Ketoradikalen aus Vinylbromiden und molekularem Sauerstoff mit sichtbarem Licht: Synthese von Indenonen und Dihydroindeno[1,2-c]chromenen.
   Angew. Chem., **2017**, *129*, 11068-11072; **DOI:** 10.1002/ange.201702953 (German edition).

2. L. Marzo, **S. K. Pagire**, O. Reiser, B. König
   Visible-Light Photocatalysis: Does it make a Difference?

   Angew. Chem. Int. Ed. **2017** (manuscript submitted).

3. **S. K. Pagire**, A. Hossain, L. Traub, S. Kerres, O. Reiser
   Photosensitised Regioselective [2+2]-Cycloaddition of Cinnamates and related Alkenes.

   Chem. Commun. **2017**; **DOI**: 10.1039/C7CC06710K. *This paper also featured as a cover of a journal.*

4. **S. K. Pagire**, O. Reiser
   Tandem cyclization of vinyl radicals: A Sustainable Approach to Indolines utilizing Visible-Light Photocatalysis.

   Green Chem. **2017**, *19*, 1721-1725; **DOI:** 10.1039/C7GC00445A.

5. **S. K. Pagire**, A. Hossain, O. Reiser
   Temperature Controlled Selective C-S or C-C Bond Formations: First Photocatalytic Sulfonylation of unactivated Heterocycles utilizing Aryl Sulfonyl Chlorides.

   ACS Catal. **2017** (manuscript under revision).

6. A. Hossain, **S. K. Pagire**, O. Reiser
   Visible-Light-Mediated Synthesis of Pyrazines from Vinyl-Azides utilizing the Photocascade Process.
   Synlett. **2017**, *28*, 1707-1714; **DOI:** 10.1055/s-0036-1590888.
   [Note: This work was published in the *special issue of heterocycles for ISHC Congress, Regensburg 2017. It is also selected for the "best paper of the year award" in top 3 papers by the editorial board of Synlett*].

7. **S. K. Pagire**, S. Paria, O. Reiser
   Synthesis of β-hydroxysulfones from Sulfonyl Chlorides and Alkenes utilizing Visible-Light Photocatalytic Sequences.
   Org. Lett. **2016**, *18*, 2106-2109; **DOI:** 10.1021/acs.orglett.6b00734.
   [Note: this work was also highlighted in *ChemInform* **2016**, *47*, 39; **DOI:** 10.1002/chin.201639089, in *Organic Chemistry Portal*, (ID: J54-Y2016; www.organic-chemistry.org/abstracts/lit5/398.shtm), and in *nature INDEX*, https://www.natureindex.com/article/10.1021/acs.orglett.6b00734]. (*Times cited: 25, Google Scholar).*

Oral and Poster Presentations:

1) *Poster and Oral Presentation*: **S. K. Pagire**, A. Hossain, O. Reiser: Temperature Controlled Selective C-S or C-C Bond Formations: First Photocatalytic Sulfonylation of unactivated Heterocycles utilizing Aryl Sulfonyl Chlorides: In the International Society of Heterocyclic Chemistry (ISHC) at University of Regensburg, Germany (2017).

2) *Poster Presentation:* **S. K. Pagire**, S. Paria, O. Reiser: Synthesis of β-Hydroxysulfones from Sulfonyl Chlorides and Alkenes utilizing Visible-Light Photocatalytic Sequences: (poster presentation): In the international ACS Conference "Chemistry of the people, by the people, for the people" at Philadelphia, USA (2016); Funding(s): *i*PUR and GDCh.

3) *Poster and Oral Presentation:* **S. K. Pagire**, P. Kreitmeier, O. Reiser: Visible-Light Photoredox Catalysis: An Unprecedented Synthesis of Complex Molecules: In the "25th Lecture-conference on photochemistry" at Jena, Germany (2016); Funding: GDCh.

4) *Poster Presentation:* **S. K. Pagire**, S. Paria, O. Reiser: Synthesis of β-Hydroxysulfones from Sulfonyl Chlorides and Alkenes utilizing Visible-Light Photocatalytic Sequences: In the "20th Lecture-conference" at Weimar, Germany (ORCHEM 2016); Funding: GDCh.

5) *Oral Presentation:* **S. K. Pagire**: "Activation of Vinyl-Bromides by Energy and an Electron transfer Process" in the GRK-1626 photocatalysis - 29th Seminar day in Regensburg at the University of Regensburg, Germany (2017).

6) *Oral Presentation:* **S. K. Pagire**: "Molecular Oxygen: Drives life and Organic Synthesis" in the annual Christmas meeting at the University of Regensburg, Germany (2016).

Participations:

1) Participated in the GRK-1626 photocatalysis meeting "24th Seminar day in München with exhibition Fine Art meets Science" at Technical University Munich (TUM), Germany **(**2016).

2) Participated in the "DAAD scholars scientific meeting" at the University of Würzburg, Germany (2014).

3) Participated in the "4th INDIGO Research Conference and intensive course on Organocatalysis" at the University of Regensburg, Germany (2013).

Abbreviations

AIBN	azobisisobutyronitrile	mmol	millimole
atm	atmosphere	mol %	mole percent
ATRA	atom transfer radical addition	Mp	melting point
Ar	aryl	MS	mass spectroscopy
bpy	2,2'-bipyridine	nd	not determined
Bu	butyl	ν	frequency
$CDCl_3$	deuterated chloroform	Na_2SO_4	sodium sulfate
CFL	compact fluorescent lamp	^{n}-Bu	*n*-butyl
CV	cyclic voltammetry	nm	nanometer
δ	chemical shift	NMR	nuclear magnetic resonance
DCM	dichloromethane	nr	no reaction
dap	2,9-bis(para-anisyl)-1,10-phenanthroline	Nu	nucleophile
d.r.	diastereomeric ratio	^{n}-Pr	*n*-propyl
$dF(CF)_3ppy$	2-(2,4-difluorophenyl)-5-(trifluoromethyl) pyridine	*o*-	*ortho*-
dtbbpy	4,4'-di-tert-butyl-2,2'-bipyridine	OAc	acetate
DIPEA	*N*,*N*-diisopropylethylamine	*p*-	*para*
DMF	dimethyl formamide	PC	photocatalyst
ε	Molar extinction coefficient	PE	petroleum ether
e.g.	exempli gratia (*Latin*: for example)	phen	phenanthroline
E/Z	entgegen/zusammen	ppm	parts per million
$E_{1/2}$	standard reduction	Ph	phenyl
ed.	Edition	Pr	propyl
Ed.	Editor	ppy	2-phenylpyridine
EtOAc	ethylacetate	Q	quencher
EI	electron impact (MS)	Φ	quantum yield
equiv	equivalents	quant.	quantitative
ESI	electronspray ionization (MS)	redox	reduction-oxidation
Et	ethyl	R_f	retardation factor
eV	electronvolt	rt	room temperature
et al.	et alia (*Latin*: and others)	SCE	saturated calomel electrode
FC	ferrocene	SET	single electron transfer
FTIR	Fourier transform infrared spectroscopy	t	time
g	gram	τ	lifetime
GC	gas chromatography	TEMPO	(2,2,6,6-Tetramethylpiperidin-

			1-yl)oxyl
h	hour	Tf	triflyl (= trifluoromethane sulfonyl)
HRMS	high resolution mass spectrometry	Ts	tosyl (= 4-toluenesulfonyl)
Hz	Hertz	^{t}-Bu	*tert-butyl*
i.e.	it est (*Latin*: that is)	THF	tetrahydrofuran
^{i}-Pr	*iso*-propyl	TLC	thin layer chromatography
IR	infrared spectroscopyl	TMS	trimethylsilyl
ISC	inter system crossing	Ts	tosyl
J	coupling constant	UV	ultraviolet
L	ligand; liter	V	Volt
λ_{max}	wavelength of maximum	vis	visible
LED	light emitting diode	vs	versus (*Latin*: against)
LRMS	low resolution mass spectroscopy	W	watt
M	metal; molar (mol L^{-1})	wt%	weight percent
m	milli (10^{-3}); multiplet	X	arbitrary halogen
m-	meta		
m/z	mass to charge ratio		
Me	methyl		
MeCN	acetonitrile		
MHz	mega hertz		
min	minute		
mL	milliliter		
MLCT	metal-to-ligand charge transfer		

Table of Contents

1 Surprises and discoveries in visible-light photocatalysis

1.1 Introduction to the visible-light photocatalysis:

The development of safer and sustainable methods for organic synthesis is one of the important goals of modern chemical research era. In fact, a number of classical, as well as some current synthetic methodologies, use toxic and explosive reagents at enforced reaction conditions. On the other hand, more than hundred years ago, an Italian photochemist, Giacomo Ciamician[1] (a nine-time Nobel Prize nominee) recognized that sunlight could be used as a renewable, unlimited, safer, and cleaner energy source for the organic syntheses (Figure 1.1).

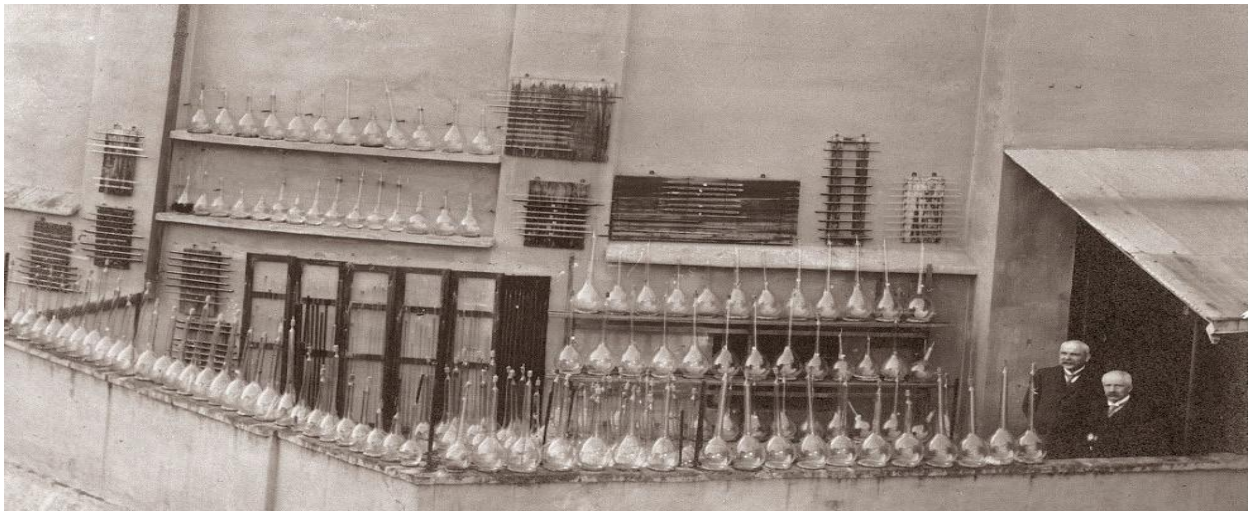

Figure 1.1: *Visible-light mediated organic synthesis is an old idea*: This photograph is from the balcony of Giacomo Ciamician's laboratory (1913).

He predicted for the first time the bright future of photochemistry owing to the vast natural abundance of solar energy. He wrote: *"On the arid lands there will spring up industrial colonies without smoke and without smokestacks; forests of glass tubes will extend over the plains and glass buildings will rise everywhere; inside of these will take place the photochemical processes that hitherto have been the guarded secret of the plants, but that will have been mastered by human industry which will know how to make them bear even more abundant fruit than nature, for nature is not in a hurry and mankind is. And if in a distant future the supply of coal becomes completely exhausted, civilization will not be checked by that, for life and civilization will continue as long as the sun shines"*[1]

To that end, intensive research works have been committed to originate photoredox catalysts that are able to absorb visible-light and to promote the desired chemical transformations between small organic molecules. Indeed, visible-light photocatalysis technology has recently received remarkable recognition from synthetic chemists because of its prevalent applications in organic synthesis and its significance for sustainable developments in chemistry.[2,3,4]

In our day-to-day life, a number of important processes involve photochemistry. The primary example is photosynthesis, in which most plants use the sunlight to convert CO_2 and H_2O into glucose and releases molecular oxygen as a by-product. Not only plants but human being also relies on photochemistry for the generation of Vitamin D with sunlight. The Grotthuss-Draper law states that "*only the light that is absorbed by a system or molecule can bring about a photochemical change or photochemical reaction*." The Stark-Einstein law says that "*every photon that is absorbed will cause a chemical or physical reaction*."

Upon absorbing photons directly from the light source, the reactant molecule is excited to the new energy maxima, which is typically called as an excited state. If the reactant molecule is unable to absorb the required photon or if the required light source of a particular wavelength is not available then a "photosensitizer" is employed, which absorbs the photon and transfer the energy to the reactant. This process is known as "photosensitization". The reverse process is called "quenching" – when a photoexcited state is deactivated by a chemical compound.

In principle, inorganic metal complexes and organic dyes are employed as photosensitizers (or photocatalysts).[3] The most commonly employed photocatalysts are poly-pyridyl or phenanthroline based complexes of [Ru], [Ir], or [Cu]: such as, $[Ru(bpy)_3Cl_2]$, *fac*-$[Ir(ppy)_3]$, $[Ir(ppy)_2(dtb\text{-}bpy)PF_6]$, $[Ir\{dF(CF_3)ppy\}_2(dtb\text{-}bpy)PF_6]$, $[Cu(dap)_2Cl]$ etc. (Figure 1.2).

Besides inorganic compounds, organic compounds[4,5] are also used as a visible-light photocatalyst, a few of these are eosin Y, flavin, fluorescein, 9,10-dicyanoanthracene, rose Bengal, Rhodamine 6G etc. These complexes absorb visible-light of the electromagnetic spectrum to give stable, long-lived photoexcited states. Typically, the lifetime of the excited species is sufficiently longer [Table 1.1; e.g. 2300 ns for $Ir[dF(CF_3)ppy]_2(dtbbpy)PF_6$] that it may engage in bimolecular electron-transfer reactions in competition with deactivation pathways.

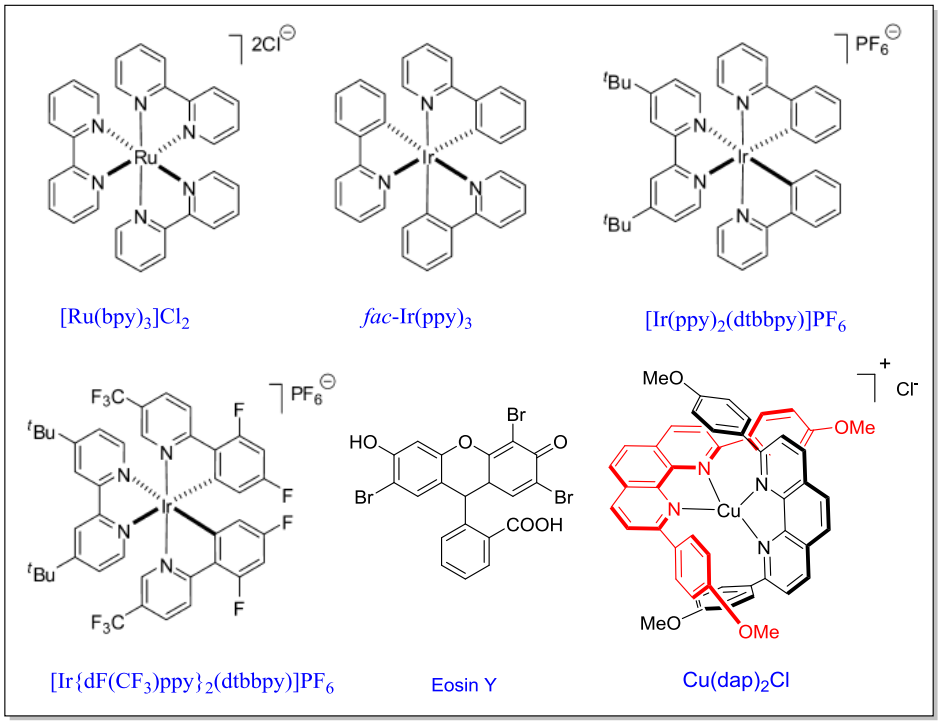

Figure 1.2: Some typical photoredox catalysts.

Entry	Photocatalyst	$E_{1/2}$ (M^*/M^+) (V)	$E_{1/2}$ (M^+/M) (V)	Excitation λ_{max} (nm)	Excited state lifetime, τ (ns)
1	$Ru(bpy)_3^{2+}$	-0.81	+1.29	437	1100
2	$Ru(phen)_3^{2+}$	−0.87	+1.26	422	500
3	$Ir[dF(CF_3)ppy]_2(dtbbpy)^+$	−0.89	+1.69	380	2300
4	*fac*-$Ir(ppy)_3$	−1.73	+0.77	375	1900
5	$Ir(ppy)_2(dtbbpy)^+$	−0.96	+1.21	-	557
6	$Cu(dap)_2^+$	−1.43	+0.62	437	270

Table 1.1 Redox potentials and selected photophysical properties of commonly used visible-light photocatalysts. All potentials are given in volts versus the SCE.[3]

Although most of these species are poor single-electron oxidants and reductants in their ground states; however, upon excitation they become very potent single-electron-transfer reagents. More importantly, the conversion of these bench stable, benign catalysts to redox-active species upon irradiation with simple household light-bulbs or LED's represents a remarkably chemoselective trigger to induce unique and valuable catalytic processes.

In many instances, the photocatalytic reactions occur at milder reaction conditions, typically at room temperature. However, a key challenge for these photochemical reactions is the regeneration of the metal complexes or the catalytic cycle. For this, external stoichiometric reagents are often applied, and in some cases, they may be replaced by simple oxidants or reductants, such as air (oxygen) or amines. In this fashion, besides providing alternate ways for established transformations that allow a broadening of the substrate scope and improvement of reaction conditions, also innovative transformations become possible. Undoubtedly, using visible-light as the ultimate renewable energy resource in combination with catalytic amounts of metal complexes or organic dyes is attractive for developing sustainable chemical transformations.

1.2 Principal modes of activation in visible-light photocatalysis:

1.2.1 An electron transfer: Oxidative or reductive quenching cycles:

In principle, the visible-light photocatalysis operates through two different activation modes: an electron transfer and energy transfer. The principal mode of action in visible-light photocatalysis is to induce an electron transfer to or from a substrate, thus generating radical anions or cations of the substrates, which are often occurred through the extrusion of a leaving group to overall form a neutral radical as the reactive species that typically initiates a chemical transformation. Further manipulation of these reactive intermediates can result in a number of synthetically useful bond forming reactions in a controllable manner.

The commonly established mechanism of a metal-based photocatalyzed (electron transfer) reaction is presented in a Latimer-diagram (Figure 1.3). As mentioned, the exceptional property of the typical photocatalyst (PC) is to absorb the (visible) light to generate a high energy excited singlet state (PC*) through a metal-to-ligand charge transfer (MLCT). Then this singlet excited state undergoes rapid intersystem crossing (ISC) to give the lowest energy triplet MLCT state, which usually has a longer lifetime (Table 1.1) and is capable to perform a single electron transfer (SET) or photoinduced electron transfer (PET) process more efficiently as compared to their ground states.

The redox transformations of PC* occurs either by oxidative or by reductive quenching cycles. In the oxidative quenching cycle, PC* functions as a reductant, reducing some electron acceptor by a SET process. The products of this SET event are the radical anion and the oxidized form of the employed photocatalyst. In general, this oxidized species is a strong oxidant and may accept an electron from some donor (typically from a substrate itself) to give the radical cation and regenerate the photocatalytic cycle. A compound that gains an electron from PC* is said to be an oxidative quencher of the photocatalyst; common oxidative quenchers are viologens, polyhalomethanes, dinitro- and dicyanobenzenes, or aryldiazonium salts etc.

On the other hand, in the reductive quenching cycle, PC* functions as an oxidant, accepting an electron from sacrificial electron donors to give the reduced form of PC. This intermediate is a good reductant and may donate an electron to afford the ground-state species of PC. The most

common reductive quenchers are tertiary amines (e.g. NEt_3, DIPEA etc). To determine whether a reductive or oxidative quenching cycle is operative in a particular reaction, fluorescence quenching (or Stern−Volmer) studies are commonly employed. This technique examines the competition between two deactivation pathways of the photoexcited state: i.e. excited state quenching via electron transfer or by emission process.

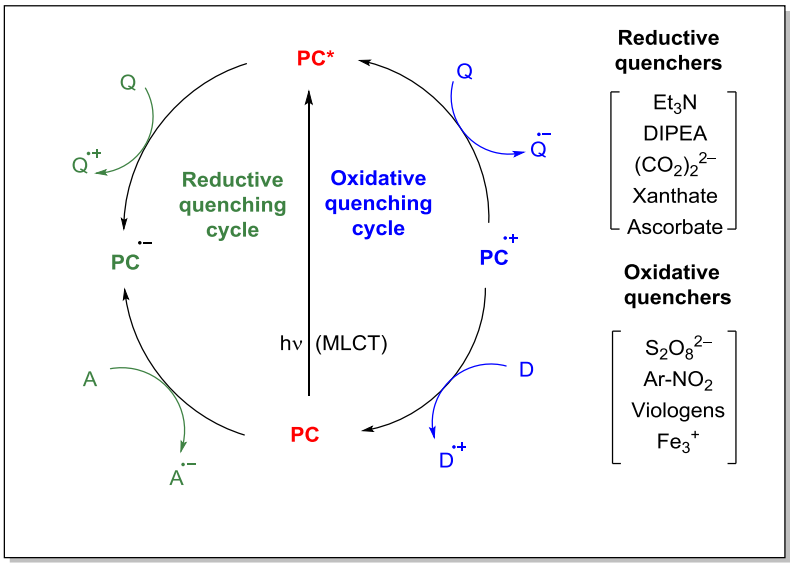

Figure 1.3: General presentation of electron transfer process (PC = photocatalyst; Q = quencher; A = acceptor; D = donor, blue: oxidative quenching cycle; green: reductive quenching cycle).

1.2.2 Energy transfer: A sensitization

The second mode of action is that a photosensitizer transfers energy to a substrate if electron transfer process is thermodynamically unfavorable or redox potential differences between reacting substrates and photocatalysts are considerably high (Figure 1.4).[6]

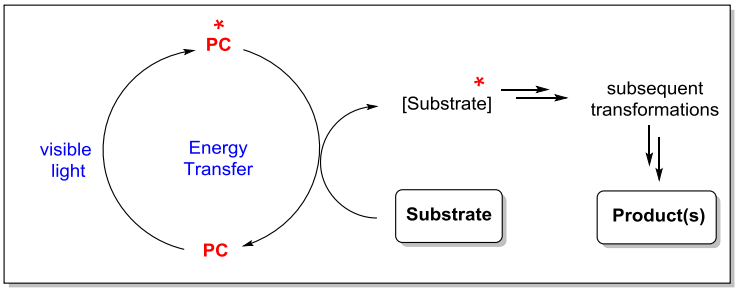

Figure 1.4 General presentation of energy transfer process.

Certainly, this mode of sensitization has a long tradition for synthetic photochemistry. However, most of the traditional processes suffer from major drawbacks: such as the use of high energy UV-light, the use of stoichiometric amounts of sensitizers, longer reaction times, etc. In recent times, the combination of high power visible-light emitting LED's and the discovery of new photocatalysts, which can carry out energy transfer processes much more efficiently, hence hold the promise for new transformations to be discovered.

1.2.3 Energy transfer followed by an electron transfer: A Photocascade Process

Another mode of action in visible-light photocatalysis is that a photosensitizer transfers energy to a substrate if electron transfer process for the first step is thermodynamically unfavorable or in other words, the redox potential differences between reacting substrates and photocatalysts are very high. After the first step of sensitization, the substrate could undergo subsequent transformation to form either a stable intermediate or a first step product. At this stage, this intermediate or product is typically within the reach of redox potentials of the employed photocatalyst, which could subsequently undergo the SET process with the same photocatalyst to form a final product (Figure 1.5). This process is also called as a *photocascade* process.[7] Although, this mode has not been widely applied thus far, however, it certainly holds promise for the future advancements and also needs further mechanistic investigations.

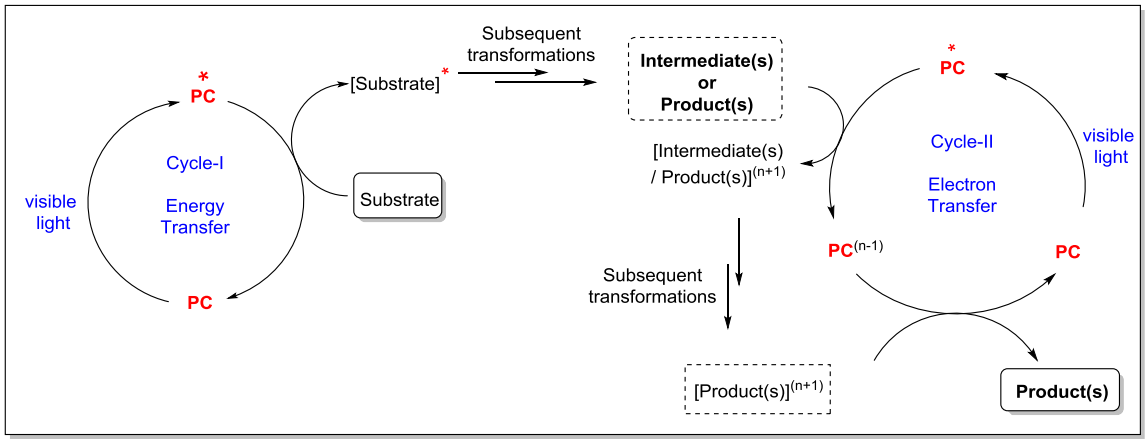

Figure 1.5: General presentation of dual energy- and electron transfer photocascade process.

1.3 Aim of the work and outcomes:

In this regard, I was mainly involved on to develop visible-light photocatalyzed methods in organic synthesis. On that way, along with the introduction of new and mild transformations, I have also recognized practical alternatives to the established classical procedures, which were traditionally operated either by UV-light or by using hazardous/toxic reagents such as *n*-Bu_3SnH/AIBN in stoichiometric amounts at elevated temperature conditions.

In addition, I have also noticed several unique and unprecedented activation modes due to the involvement of highly reactive radical intermediates. Most of the times, the surprising reactions are fascinating and it often leads to the meaningful discoveries in science. However, some reactions also led to the complex reaction mixtures. Despite its apparent randomness, the beauty of identified transformations is well-defined and organized. This has been proved by carrying out several experimental and spectroscopic investigations.

In photochemical reactions, several reactive radical intermediates are involved, thus predicting the plausible reaction mechanisms for new reactions is a challenging task. Nevertheless, I have tried my best to penetrate light into all the possible dark corners of the reaction, to understand the mode of action of a photocatalyst in the preliminary as well as in the later stages, and to identify or characterize the key intermediates involved. Finally, to find suitable applications of these new reactions and to introduce an efficient method for organic synthesis were the key parameters in my doctoral work. Arguably, the disclosed reactions are certainly difficult (impossible in most of the cases!) to accomplish by applying other non-photochemical methods.

Overall, the major part of my doctoral work is a result of unexpected findings; therefore, I summarized my thesis with the title: "*Surprises and discoveries in Visible-Light Photocatalysis*."

1.4 References:

[1] G. Ciamician, *Science* **1912**, *36*, 385.

[2] a) F. Teplý, *Collect. Czech. Chem. Commun.* **2011**, *76*, 859; b) J. M. R. Narayanam, C. R. J. Stephenson, *Chem. Soc. Rev.* **2011**, *40*, 102; c) D. Ravelli, S. Protti, M. Fagnoni, *Chem. Rev.* **2016**, *116*, 9850; d) K. L. Skubi, T. R. Blum, T. P. Yoon, *Chem. Rev.* **2016**, *116*, 10035; e) I. Ghosh, L. Marzo, A. Das, R. Shaikh, B. König, *Acc. Chem. Res.* **2016**, *49*, 1566; f) J. I. Day, K. Teegardin, J. Weaver, J. Chan, *Org. Process Res. Dev.* **2016**, *20*, 1156; g) J.-P. Goddard, C. Ollivier, L. Fensterbank, *Acc. Chem. Res.* **2016**, *49*, 1924; h) A. C. Hernandez-Perez, S. K. Collins, *Acc. Chem. Res.* **2016**, *49*, 1557; i) D. C. Fabry, M. Rueping, *Acc. Chem. Res.* **2016**, *49*, 1969; j) J. C. Tellis, C. B. Kelly, D. N. Primer, M. Jouffroy, N. R. Patel, G. A. Molander, *Acc. Chem. Res.* **2016**, *49*, 1429; k) E. C. Gentry, R. R. Knowles, *Acc. Chem. Res.* **2016**, *49*, 1546; l) S. A. Morris, J. Wang, N. Zheng, *Acc. Chem. Res.* **2016**, *49*, 1957; m) S. P. Pitre, C. D. McTiernan, J. C. Scaiano, *Acc. Chem. Res.* **2016**, *49*, 1320; n) M. H. Shaw, J. Twilton, D. W. C. MacMillan, *J. Org. Chem.* **2016**, *81*, 6898.

[3] C. K. Prier, D. A. Rankic, D. W. C. MacMillan, *Chem. Rev.* **2013**, *113*, 5322.

[4] M. Majek, A. Jacobi von Wangelin, *Acc. Chem. Res.* **2016**.

[5] a) D. P. Hari, B. Konig, *Chem. Comm.* **2014**, *50*, 6688; b) E. Brachet, T. Ghosh, I. Ghosh, B. König, *Chem. Sci.* **2015**, *6*, 987; c) I. Ghosh, B. König, *Angew. Chem. Int. Ed.* **2016**, *55*, 7676; d) I. Ghosh, T. Ghosh, J. I. Bardagi, B. König, *Science* **2014**, *346*, 725.

[6] a) S. K. Pagire, A. Hossain, L. Traub, S. Kerres, O. Reiser, *Chem. Commun.* **2017**, 10.1039/C7CC06710K; b) Z. Lu, T. P. Yoon, *Angew. Chem. Int. Ed.* **2012**, *51*, 10329.

[7] a) A. Hossain, S. K. Pagire, O. Reiser, *Synlett* **2017**, *28*, 1707; b) S. K. Pagire, P. Kreitmeier, O. Reiser, *Angew. Chem., Int. Ed.* **2017**, *56*, 10928; c) J. Xuan, X.-D. Xia, T.-T. Zeng, Z.-J. Feng, J.-R. Chen, L.-Q. Lu, W.-J. Xiao, *Angew. Chem., Int. Ed.* **2014**, *53*, 5653; d) J.-R. Chen, D.-M. Yan, Q. Wei, W.-J. Xiao, *ChemPhotoChem* **2017**, *1*, 148.

2 Shining visible-light on C-X bonds

2.1 Introduction:

The development of catalytic systems for the activation of C-X bonds has been a long-standing goal in organic synthesis.[1] In particular, the cross coupling reactions, such as the Stille,[2] the Kumada,[3] the Suzuki-Miyaura,[4] the Negishi[5] coupling or cross-coupling of organolithium reagents,[6] are vastly developed and extensively applied in organic chemistry. Among them, the Ar-X (aryl halides) or Alk-X (alkyl halides) activation is one of the popular classes of activation in organic synthesis by both, classical[1] as well as by visible-light photocatalysis.[7] However, on the other hand, the activation of vinyl-X (vinyl halides) is also a close topic of interest, though it is less studied and yet underdeveloped area.[8] Nevertheless, in few cases, the synthetic utility of vinyl halides is established in radical[9] as well as in classical[10] reactions.

2.2 Generation of vinyl radicals and their applications:

In radical reactions, the 'vinyl radical' formation is the principal step upon extrusion of the leaving group from vinyl halides.[11] Due to their high reactivity, vinyl radicals have been utilized in many valuable transformations in synthetic organic chemistry as well as in practical applications.[12,13] Since the pioneering work of Stork *et al*,[14] vinyl radical reactions have emerged as a versatile tool in synthetic organic chemistry.[12,13] Thermal vinyl radical generation from vinyl halides is traditionally carried out using tributyltin hydride (*n*-Bu_3SnH) and a radical initiator, such as AIBN.[9,15] Furthermore, the vinyl radical formation by electrochemical processes[16] or by photolysis of vinyl halides[17] is also well established in the literature. Though there are several other routes exists in literature for accessing this radical,[18] however, the photochemical processes are rare.[19]

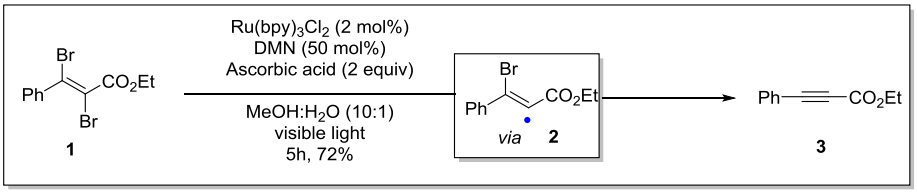

Scheme 2.1: Visible-light triggered synthesis of alkynes from *vic*-dibromoalkenes.

In 2011, Reiser *et al* have noticed reductive debromination[20] of *vic*-dibromoalkene **1** to corresponding alkyne **2** (Scheme 2.1), thus, they envisioned a visible-light triggered route to access vinyl radicals **2**. Typically, the photochemical activation of vinyl halides is difficult, requiring either an extended π-system or weak bonds as found in vinyl iodides (Scheme 2.2).[11]

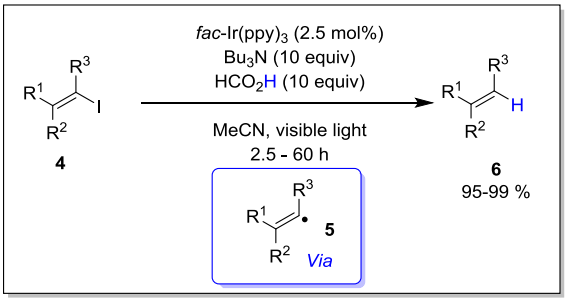

Scheme 2.2: Visible-light triggered synthesis of alkenes from vinyl-iodides.

Furthermore, they also found that α-bromochalcones **11** can be coupled with a broad variety of electron rich heteroarenes **12**[21] or alkenes **15**[22] give rise to polycyclic scaffolds (Schemes 2.3).

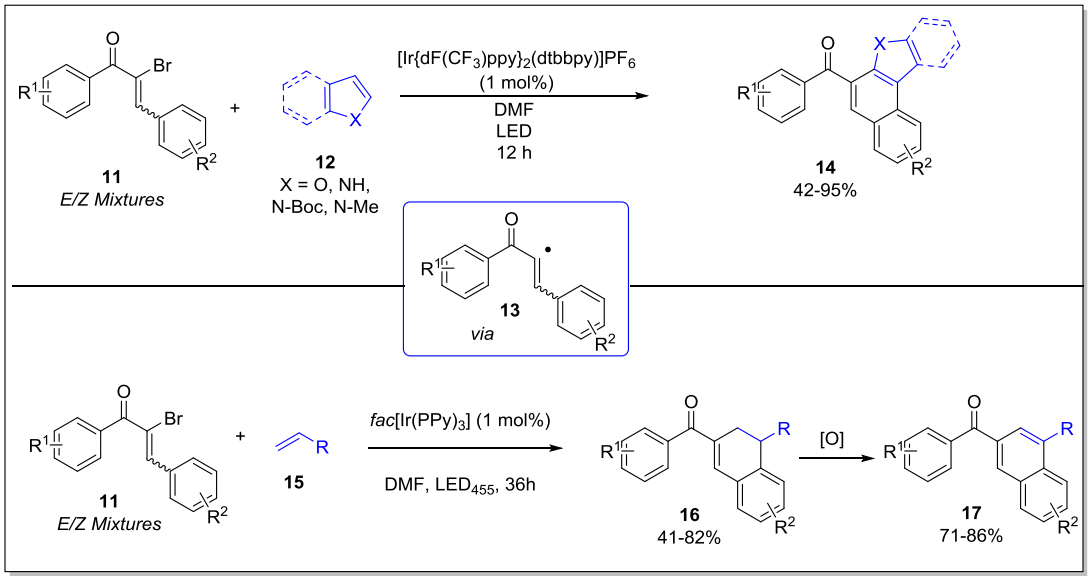

Scheme 2.3: Visible-light triggered synthesis polycyclic compounds from vinyl-bromides.

The vinyl radicals **13** were engaged in a cascade cyclization with heteroarenes in an intermolecular fashion forming novel scaffolds such as naphtho[2,1-*b*]furans, 3*H*-benzo[*e*]indoles and related heterocycles. The overall transformation is characterized by three-

fold C-H activation. The reaction was compatible to a broad variety of heteroarenes, ranging from furans, benzofurans to pyrroles, in protected or unprotected form, as well as indoles.

2.3 Conclusion and outlook:

The outlined work has been proved that the possibility of engaging vinyl-radical as a key intermediate in several organic transformations. In order to broaden the scope of C-X bond activation strategy, to understand reaction mechanisms in more details, and to highlight the importance of vinyl-radicals in organic synthesis, further work needs to be done.

2.4 References

[1] C. C. C. Johansson Seechurn, M. O. Kitching, T. J. Colacot, V. Snieckus, *Angew. Chem. Int. Ed.* **2012**, *51*, 5062.

[2] L. Li, C. Wang, R. Huang, M. R. Biscoe, *Nat. Chem.* **2013**, *5*, 607.

[3] K. Tamao, K. Sumitani, Y. Kiso, M. Zembayashi, A. Fujioka, S. Kodama, I. Nakajima, A. Minato, M. Kumada, *Bull. Chem. Soc. Jpn.* **1976**, *49*, 1958.

[4] a) N. Miyaura, A. Suzuki, *Chem. Rev.* **1995**, *95*, 2457; b) O. N. I. Maluenda, *Molecules* **2015**, *20*, 7528.

[5] C. Han, S. L. Buchwald, *J. Am. Chem. Soc.* **2009**, *131*, 7532.

[6] C. Vila, M. Giannerini, V. Hornillos, M. Fañanás-Mastral, B. L. Feringa, *Chem. Sci.* **2014**, *5*, 1361.

[7] a) J. C. Tellis, D. N. Primer, G. A. Molander, *Science* **2014**, *345*, 433; b) I. Ghosh, L. Marzo, A. Das, R. Shaikh, B. König, *Acc. Chem. Res.* **2016**, *49*, 1566.

[8] F. Alonso, I. P. Beletskaya, M. Yus, *Chem. Rev.* **2002**, *102*, 4009.

[9] I. Prediger, T. Weiss, O. Reiser, *Synthesis* **2008**, 2191.

[10] D. Solé, E. Peidró, J. Bonjoch, *Org. Lett.* **2000**, *2*, 2225.

[11] J. D. Nguyen, E. M. D'Amato, J. M. R. Narayanam, C. R. J. Stephenson, *Nat. Chem.* **2012**, *4*, 854.

[12] S. Z. Zard, *Radicals in organic synthesis* **2003**.

[13] P. Renaud, M. B. Sibi, *Radicals in organic synthesis* **2001**.

[14] G. Stork, M. Robert, *J. Am. Chem. Soc.* **1982**, *104*, 2321.

[15] a) D. P. Curran, D. Kim, C. Ziegler, *Tetrahedron* **1991**, *47*, 6189; b) D. P. Curran, D. Kim, H. T. Liu, W. Shen, *J. Am. Chem. Soc.* **1988**, *110*, 5900; c) D. P. Curran, W. Shen, *J. Am. Chem. Soc.* **1993**, *115*, 6051.

[16] A. J. Fry, M. Mitnick, *J. Am. Chem. Soc.* **1969**, *91*, 6207.

[17] M. U. Kahveci, M. Uygun, M. A. Tasdelen, W. Schnabel, W. D. Cook, Y. Yagci, *Macromolecules* **2009**, *42*, 4443.

[18] D. C. Lathbury, P. J. Parsons, I. Pinto, *J. Chem. Soc. Chem. Commun.* **1988**, 81.

[19] a) A. Cannillo, T. R. Schwantje, M. Bégin, F. Barabé, L. Barriault, *Org. Lett.* **2016**, *18*, 2592; b) J. Robertson, M. A. Peplow, J. Pillai, *Tetrahedron Lett.* **1996**, *37*, 5825.

[20] T. Maji, A. Karmakar, O. Reiser, *J. Org. Chem.* **2011**, *76*, 736.

[21] S. Paria, O. Reiser, *Adv. Synth. Catal.* **2014**, *356*, 557.

[22] S. Paria, V. Kais, O. Reiser, *Adv. Synth. Catal.* **2014**, *356*, 2853.

3 Visible-light promoted generation of α-ketoradicals from vinyl-bromides and molecular oxygen: An unprecedented synthesis of indenones and dihydroindeno[1,2-c]chromenes

3.1 Abstract:

Ortho-alkynylated α-bromocinnamates have been efficiently converted either to indenones or to dihydroindeno[1,2-c]chromenes by a visible-light mediated photocascade reaction with molecular oxygen. The one-step strategy features two key photochemical steps, i.e. molecular oxygen triggered unprecedented activation of vinyl bromides to generate α-ketoradicals and the *ortho*-hydroxylation of an arene moiety in the later step.

3.2 Introduction:

Visible-light photoredox catalysis not only offers unprecedented pathways to the established reactions but holds the promise to arrive at new bond forming transformations owing to the range of functional group compatibility under the mild reaction conditions.[1] In general, reduction potentials of the vinyl bromides are much higher than the typical photocatalysts in their excited states.[2,3,4] Thus, [Ru] or [Ir]-based photocatalysts generally do not possess a sufficient excited-state reduction potential for the SET process, and ultimately form a "vinyl radical" after bromide extrusion by an oxidative quenching cycle. In contrast, by employing the reductive quenching cycle in the presence of sacrificial electron donor such as amine for the activation of vinyl bromides only results in simple dehalogenations.[4,5]

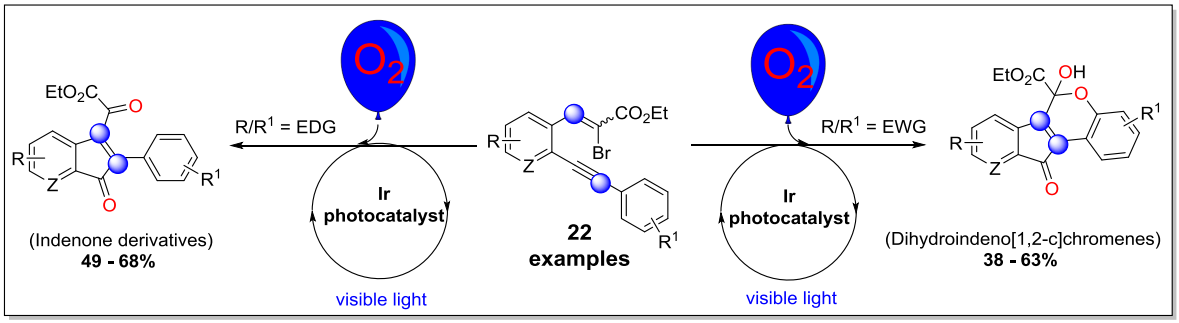

Scheme 3.1: Synthesis of Indenones and Dihydroindeno[1,2-c]chromenes.

This chapter has been published:

S. K. Pagire, P. Kreitmeier, O. Reiser, *Angew. Chem. Int. Ed.*, **2017**, *56*, 10928-10932;

Angew. Chem., **2017**, *129*, 11068-11072.

S.K.P., P.K., and O.R. wrote the manuscript.

Alternatively, the substrates can also be activated directly by energy transfer from the excited state photocatalysts.[6] In line with such an activation principle, we report here an unprecedented photochemical activation of vinyl bromides by employing *ortho*-alkynylated α-bromocinnamates **1** and molecular oxygen to give rise to indenones **2** or to dihydroindeno[1,2-c]chromenes **3** (Scheme 3.1), based on the electronic prerequisites of the substrates. As the key step in this process, the formation α-ketoradicals from the vinyl bromides is proposed, which is unambiguously supported by detailed mechanistic investigations and control experiments (*vide infra*).

3.3 Results and discussion:

We bagan our investigations by exposing **1a** (E_{red} = –1.38 V vs. SCE, see experimental section) in an oxygen atmosphere to irradiation with 5 mol % [Ir{dF(CF_3)ppy}$_2$(dtb-bpy)]PF_6[7] ($E_{Ir(IV)/Ir(III)*}$ = –0.89 V vs. SCE; excited state life-time (τ) = 2300 ns),[3] [dF(CF_3)ppy = 2-(2,4-difluorophenyl)-5-trifluoromethylpyridine, dtb-bpy = 4,4'-di-tert-butyl-2,2'-dipyridyl]) in anhydrous DMF with blue light (LED_{455}) indeed resulted in a fruitful transformation, leading to the formation of **2a** and **3a** in acceptable yields (Table 3.1, entry 1). In contrast, in the absence of oxygen, only *E/Z*-isomerization was observed (Table 3.1, entry 2), which is in accordance with the proposed activation (*vide infra*) of vinyl bromides **1** *via* a diradical intermediate generated by a triplet sensitization process.[8] Furthermore, other iridium photocatalysts such as [Ir(ppy)$_2$(dtb-bpy)]PF_6[9] ($E_{Ir(IV)/Ir(III)*}$ = –0.96 V vs. SCE, τ = 557 ns) [ppy = 2-phenylpyridine, dtb-bpy = 4,4'-di-tert-butyl-2,2'-dipyridyl] and neutral *fac*[Ir(ppy)$_3$][10] ($E_{Ir(IV)/Ir(III)*}$ = –1.73 V vs. SCE, τ = 1900 ns) [ppy = 2-phenylpyridine], gave a similar results, however, the product yields were comparatively lower (Table 3.1, entries 3, 4).

We emphasize, in all the cases, we noted a deep blood-red coloring of the reaction mixture during the course of the photo-irradiation, which probably blocking the photo-process. This could be explained by the incomplete conversion and long reaction time of the overall reactions. Lowering the catalyst concentration from 5 mol % to 1 mol % (Table 3.1, entry 5) gave almost the same results, suggesting that catalyst deactivation was not the limiting feature of the reaction. A significant enhancement in yield was observed upon carrying out the reaction at elevated temperature (60 °C), which was found to be the best parameter in combination with 2 mol % catalyst loading (Table 3.1, entry 6). Not surprisingly, in the absence of the iridium catalyst or light, no conversion of **1a** was observed (Table 3.1, entries 7, 8).

Next, by employing other photocatalysts such as $[Ru(bpy)_3Cl_2]$[11] ($E_{Ru(III)/Ru(II)^*}$ = –0.81 V vs. SCE, τ = 1100 ns) (bpy = 2,2'-bipyridine), Eosin Y,[12] and $[Cu(dap)_2Cl]$[13] ($E_{Cu(II)/Cu(I)^*}$ = –1.43 V vs. SCE, τ = 270 ns) [dap = 2,9-bis(*p*-anisyl)-1,10-phenanthroline], gave rise to low yields of **2a**/**3a** (Table 3.1, entries 9-11). As expected, a reductive quenching experiment by adding a tertiary amine as a sacrificial electron donor (e.g. diisopropylethylamine, DIPEA) (Table 3.1, entry 14), thus utilizing strong ground state reduction potentials of $[Ir\{dF(CF_3)ppy\}_2(dtb\text{-}bpy)]PF_6$ ($E_{Ir(III)/Ir(II)}$ = –1.37 V vs. SCE), only resulted in direct dehalogenation (99%).

3.4 Synthesis of 2a and 3a: Catalyst screening and reaction optimization

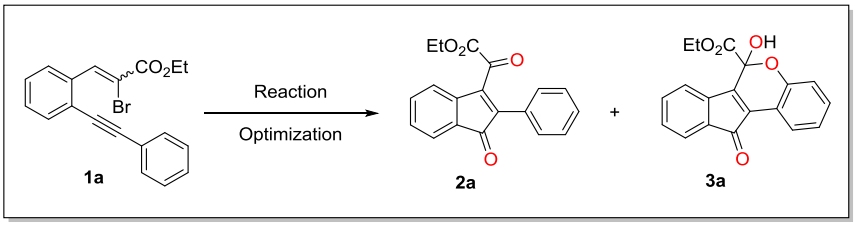

Entry	Photocatalyst (mol %)	Temperature (^oC)	Yield (%)[b] **2a**	**3a**
01	$[Ir\{dF(CF_3)ppy\}_2(dtb\text{-}bpy)]PF_6$ (5)	rt	16	41
02[c,d]	$Ir\{dF(CF_3)ppy\}_2(dtb\text{-}bpy)]PF_6$ (5), no O_2	rt	-	-
03	$[Ir(ppy)_2(dtb\text{-}bpy)]PF_6$ (5)	rt	10	22
04	*fac*$[Ir(ppy)_3]$ (5)	rt	14	33
05	$[Ir\{dF(CF_3)ppy\}_2(dtb\text{-}bpy)]PF_6$ (1)	rt	17	38
06	$[Ir\{dF(CF_3)ppy\}_2(dtb\text{-}bpy)]PF_6$ (2)	60	20	61
07	$[Ir\{dF(CF_3)ppy\}_2(dtb\text{-}bpy)]PF_6$ (1), dark	rt	-	-
08	No Catalyst	rt	-	-
09	$Ru(bpy)_3Cl_2$ (5)	rt	5	26
10	Eosin Y (5), 530 nm	rt	3	8
11	$[Cu(dap)_2Cl]$ (5), 530 nm	rt	-	-
12	Rose Bengal (5), 530 nm	rt	-	-
13	$ZnCl_2$/porphyrin (5), 530 nm	rt	-	-
14[e]	$r\{dF(CF_3)ppy\}_2(dtb\text{-}bpy)]PF_6$ (5), DIPEA	rt	-	-

Table 3.1: Reaction Conditions: [a] Substrate **1a** (0.5 mmol), photocatalyst (1-5 mol %), O_2, DMF, 72 h, rt, 60 ^oC, LED_{455}. [b] Isolated yields. [c] Under nitrogen. [d] *E*/*Z*-isomerization of **1a**, *Z*/*E* = 81:19 (before irradiation) to *Z*/*E* = 50:50 (after irradiation). [e] Dehalogenation product was identified by crude ^{1}H-NMR analysis.

3.5 Substrate scope:

By applying the optimized reaction conditions (Table 3.1, entry 6), a variety of *ortho*-alkynylated α-bromocinnamates **1** (mostly employed as *E/Z* mixtures) was subsequently examined (Table 3.2-3.4). To our surprise, a pronounced electronic effect was observed, which eventually determined the overall course of the reaction: Thus, α-bromocinnamates bearing +I (inductive donor) or +M (mesomeric/resonance donor) substituents yielded exclusively indenones **2b-k** (Table 3.2). In contrast, derivatives with only electron withdrawing substituents gave rise to dihydroindeno[1,2-c]chromenes **3b-h** (Table 3.3). However, an *ortho* substituent R^1 overrides the electronic preference (*cf.* **2l**, Table 3.2 and **3i**, Table 3.3). As expected, a mixture of both products **2** and **3** was observed for neutral or electronically unbiased substrates **1** (Table 3.4). Noteworthy, carrying out the reaction in a rotating film reactor dramatically enhanced the rate of the reaction (from 72 h / 60 °C to 24 h / 25 °C, See experimental section for more experimental details) due to the availability of larger surface area of the resulting reaction mixture that was exposed under the visible-light irradiation and to the oxygen atmosphere (*cf* Table 3.2-3.4). Furthermore, performing the reaction in the advanced micro(flow)reactor technique,[14] provides good yields also in a very short reaction times (Tables 3.2 and 3.3; also see the experimental section for detailed experimental set-ups).

3.5.1 Electron rich substrates:

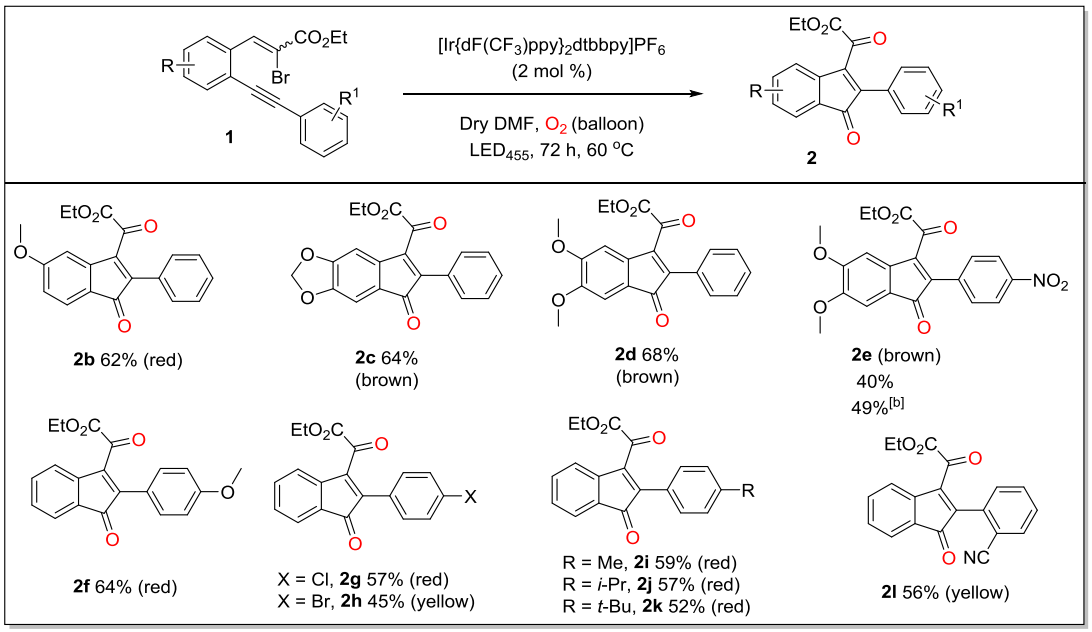

Table 3.2: Substrate scope: Electron rich systems.

3.5.2 Electron deficient substrates:

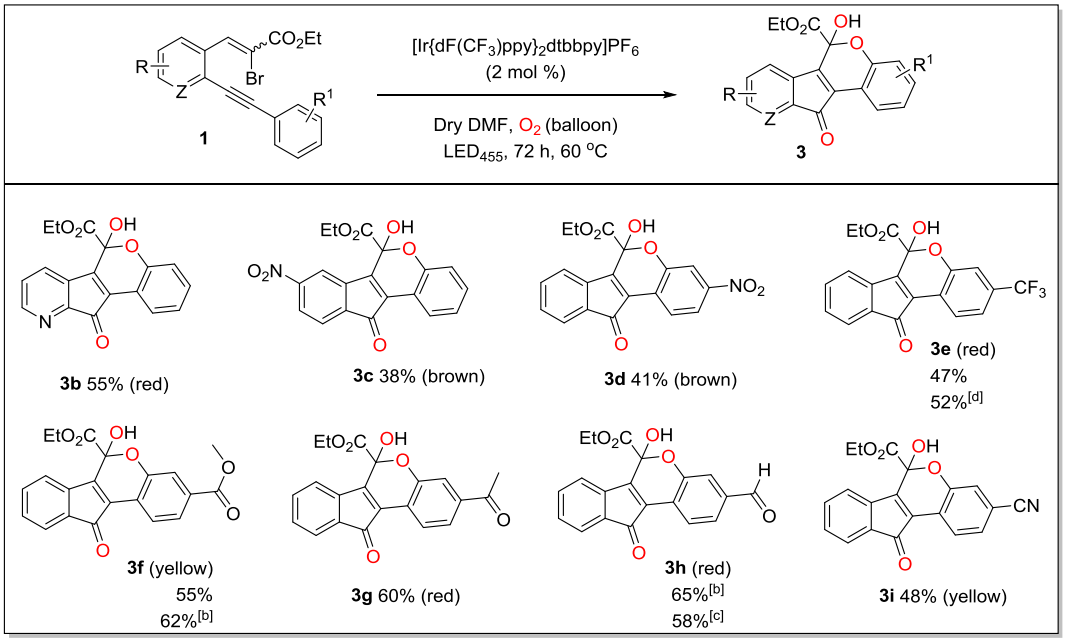

Table 3.3: Substrate scope: Electron deficient substrates.

3.5.3 Electron unbiased substrates:

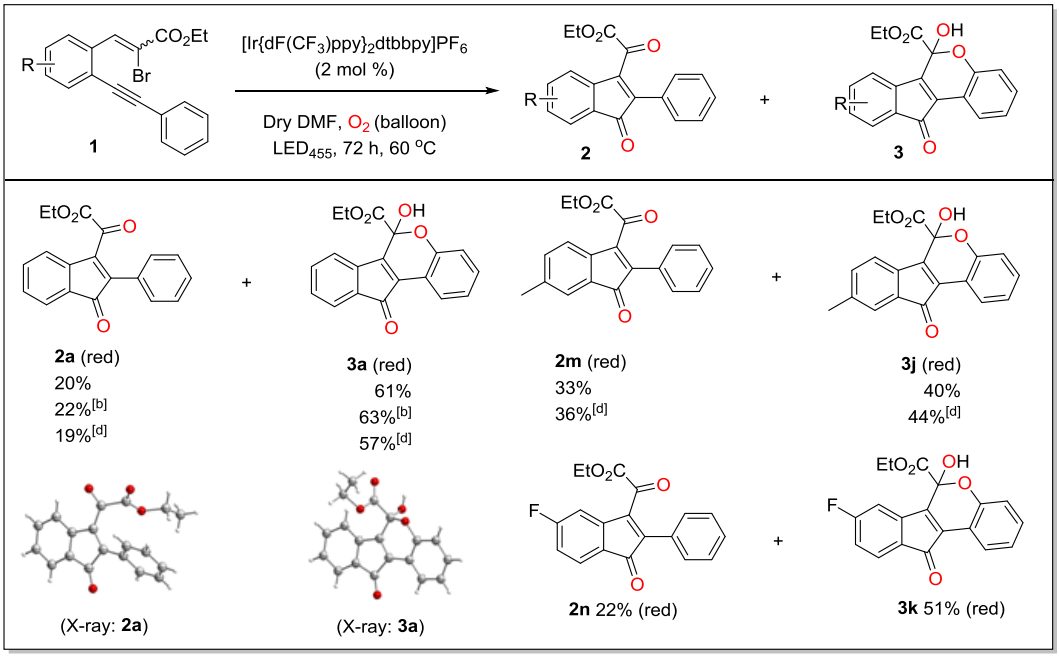

Table 3.4: Substrate scope: Electron unbiased substrates.

Tables 3.2-3.4: Reaction Conditions: [a] Substrate **1** (0.5 mmol, 1.0 equiv), photocatalyst (2 mol %), O_2 at 60 °C, in DMF, 72 h, LED_{455}, isolated yields of separated **2** and **3** are stated. [b] Reaction performed on rotating film reactor [c] 2.0 mmol scale reaction. [d] Reaction performed on micro(flow)reactor with 1 mol % photocatalyst, 40 min at room temperature (or 15 min at 60 °C). Compound color is mentioned in parentheses.

3.6 Proposed reaction mechanism:

As can be seen from the product structures; apparently, the mechanistic picture of this transformation looks complex and certainly points towards several unique photocatalytic steps (Figure 3.1). The Stern-Volmer or fluorescence quenching studies (see experimental section for more details) revealed that the starting material **1a** strongly interacts with the excited photocatalysts. As mentioned earlier, a direct photoelectron transfer from the Ir(III)-catalyst to **1** is thermodynamically unfavorable due to the large difference in reduction potentials of substrates **1** and the employed photocatalyst (e.g. **1a**: E_{red} = -1.38 V vs. SCE > **Ir-F**: -0.89 V vs. SCE).

By considering the experimental evidences, we propose the generation of a more stable diradical species **I*** (or a triplet excited state)[8,15] upon vinyl bromide **1** excitation by energy transfer from the excited *Ir(III)-catalyst. Noteworthy, the [2+2]-cycloaddition of **1** was not observed of these bromine centered diradicals in contrast to the non-brominated analog (Scheme 3.3). Instead, **I*** loses bromine radical (Br•) to form the subsequent vinyl radical **II**. Evidence for generation of **II** is found by carrying out a trapping experiment with TEMPO giving rise to **9** as well as the 5-*exo-trig* cyclization reaction of **4** to **5** (Scheme 3.2). In support, the ESR spectra also provides a broad signal of single radical species (*ge* = 1.984) under inert atmospheric conditions at low temperature (See experimental section for ESR spectra).

Surprisingly, a direct *5-exo*-dig or *6-endo*-dig cyclization of **II** was not feasible, probably due to two main reasons: either an unfavorable orientation of the reacting groups (see experimental section for the crystal structure of **1c**) or problem with the resulting radical termination. Nevertheless, the vinyl radical intermediate **II** is capable of adding on to the molecular oxygen gives rise to intermediate **III**, which should collapse to the α-ketoradical **IV** as a key intermediate. In support of this conclusion, the independent generation of **IV** from **8** by PET in the presence of oxygen indeed gives rise to **2a** and **3a** (Scheme 3.4). It should be noted that the conversion of **8** to **2a** and **3a** requires stoichiometric amounts of photocatalyst since the photoredox cycle cannot be closed in the absence of a sacrificial electron donor.

However, in the presence of DIPEA provides a direct reduced product. The α-ketoradical IV then undergoes 5-*endo-dig* cyclization[16] and eventually trapped by the second molecule of the molecular oxygen to access V. Finally, elimination of a water molecule subsequently leads to the desired indenones **2**. Evidently, an isotope labeling experiment with pure $^{18}O_2$ and a mixture of

$^{18/16}O_2$ proved that the oxygen atoms incorporated into the indenones **2** indeed originated from two different molecules of molecular oxygen (Scheme 3.6). Indenones **2** having electron accepting substituents in the aromatic ring undergoes a facile 6π-electrocyclization, leading to dihydroindeno[1,2-c]chromenes **3** (Scheme 3.5). Independent experiments under visible-light irradiation/photocatalyst or IV irradiation in the presence of oxygen (Scheme 3.5) with indenone **2** showed the possibility of the 6π-electrocyclization reaction.[17] Though, the yields obtained by the independent process were low as compared to starting from the corresponding compounds **1**.

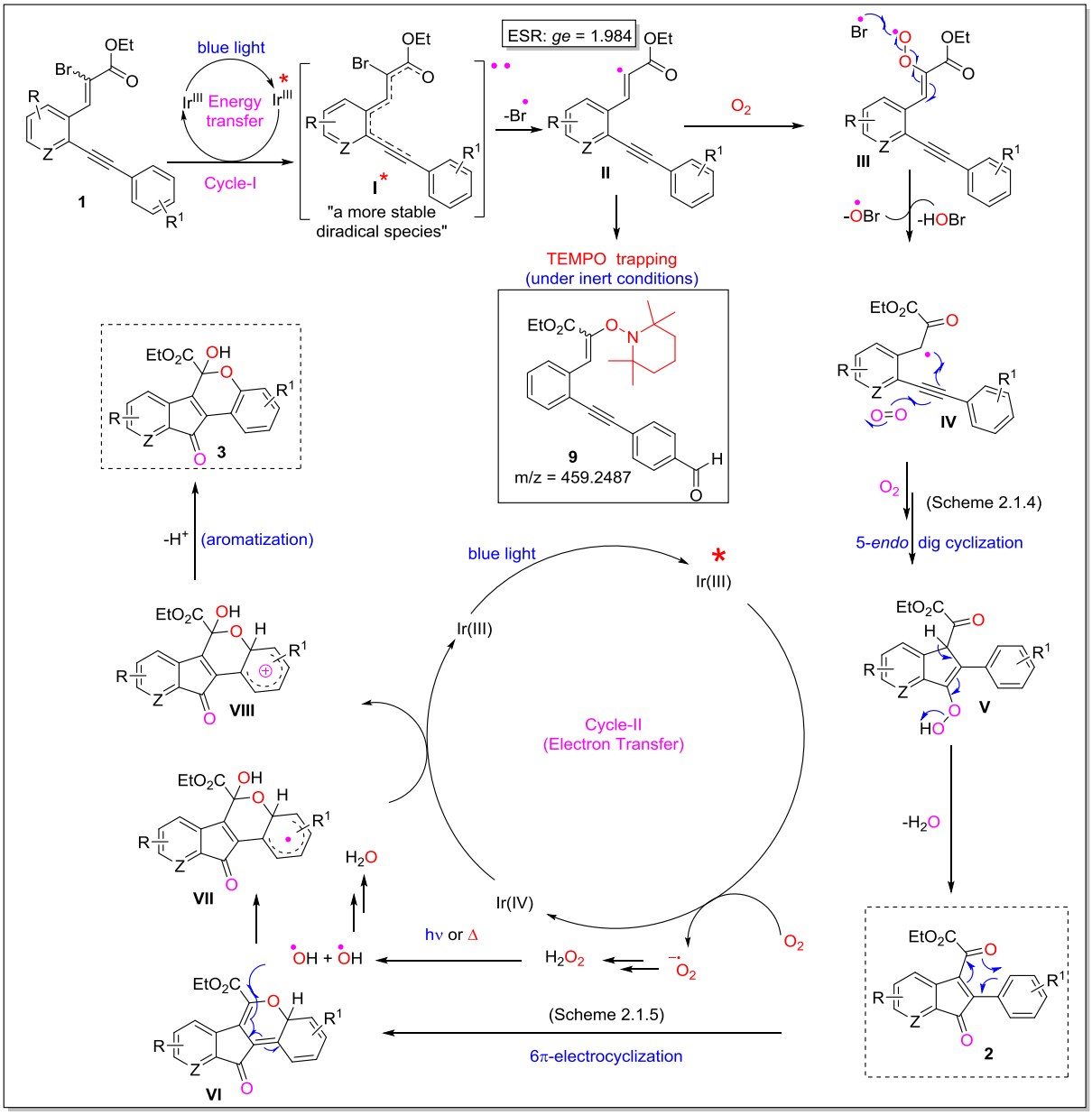

Figure 3.1: Proposed reaction mechanism.

3.7 Control experiments:

3.7.1 Without a double bond: The evidence for a vinyl radical formation

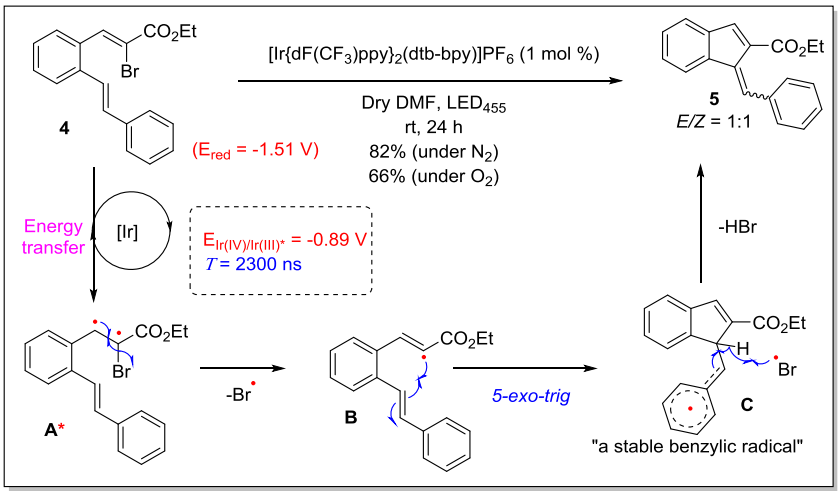

Scheme 3.2: Synthesis of indenones via vinyl radical intermediate.

3.7.2 Without a bromine: The evidence for a diradical formation

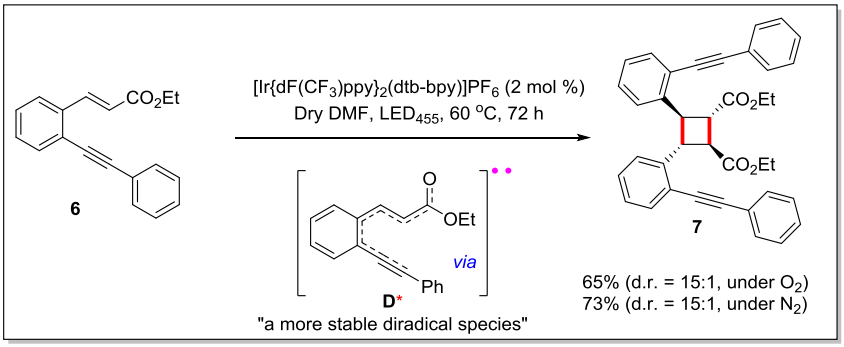

Scheme 3.3: Synthesis of cyclobutanes via diradical intermediate.

3.7.3 Direct synthesis of 2a and 3a: The evidence for α-ketoradical formation

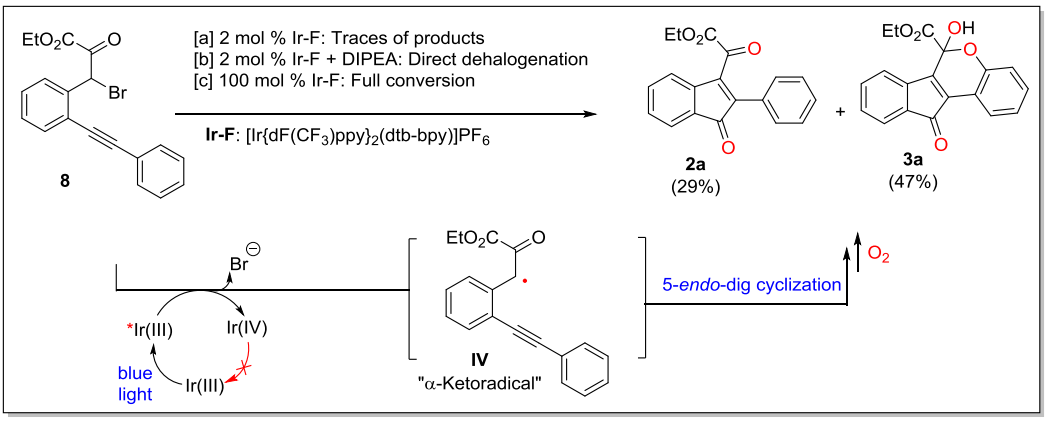

Scheme 3.4: Synthesis of **2a** and **3a** via α-ketoradical intermediate.

3.7.4 Direct synthesis of 3 from 2: An evidence for 6π-electrocyclization

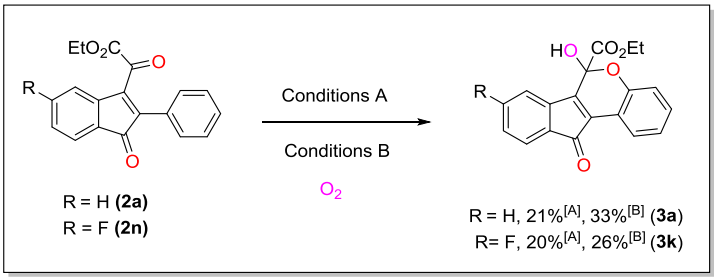

Scheme 3.5: Synthesis of **3a** / **3k** from **2a** / **2n** via 6π-electrocyclization.

Conditions A: Substrate **2** (0.25 mmol, 1.0 equiv), $[Ir\{dF(CF_3)ppy\}_2(dtb\text{-}bpy)]PF_6$ (2 mol %), O_2, at 60 °C, in DMF, 72 h, LED_{455}. **Conditions B:** Substrate **2** (0.25 mmol, 1.0 equiv), UV-Light (125 W Hg-lamp, λ > 300 nm), O_2, at 60 °C, in anhydrous DMF, 72 h.

3.7.5 Isotope labeling experiments:

The $^{18}O_2$ labeling experiments (Scheme 3.6, a) revealed that the termination of the electrocyclization by the introduction of a hydroxyl group also was ultimately derived from molecular oxygen. In addition, the mixed experiment (Scheme 3.6, b) disclosed the information of involvement of three different oxygen molecules (see also a detailed information in experimental section).[12,18]

a. Pure $^{18}O_2$ experiment:

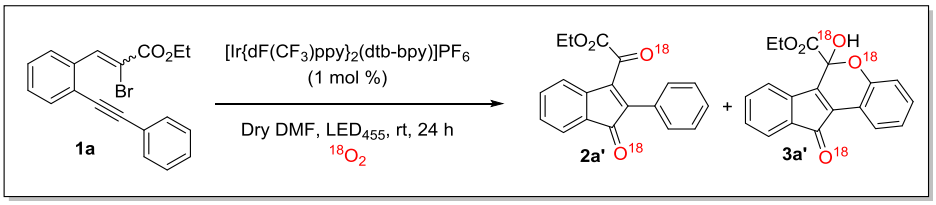

b. Mix $^{18}O_2$ / $^{16}O_2$ experiment:

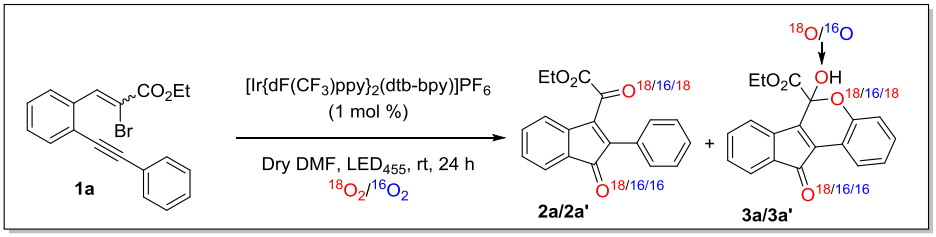

Scheme 3.6: Oxygen labeling experiments: Synthesis of **2a** / **2a**' and **3a** / **3a**'.

3.8 Conclusion:

To conclude, we have shown a novel strategy for the generation of α-ketoradicals from vinyl bromides and molecular oxygen by energy transfer process operated by an **Ir-F** photocatalyst under the mild reaction conditions. The resulting vinyl radical **II** from a diradical intermediate upon bromine extrusion could be engaged in a productive reaction cascades with up to three different oxygen molecules, leading to the complex molecular architectures in a single photochemical step. We emphasize here, this reaction could also be performed in the micro-flow or rotating film reactors in the short reaction time. Furthermore, the newly obtained tetracyclic compounds could also serve as valuable building blocks in medicinal chemistry. Since, these type of compounds having a heteroatom impregnated into the [6-5-6]-ABC skeleton are already advertised as taiwaniaquinoids related scaffolds by Panda *et al*,[19] which are closely related to the naturally occurring family of Taiwaniaquinoids possessing a common [6-5-6]-*abeo*-abietane carbon architecture with broad biological activities.[20] However, we admit that the electronic effect preference for electron deficient starting materials **1** to preferentially undergo the direct cyclization to **3** rather than to **2** has been unfortunately remained unclear at this point.

3.9 Experimental section:

3.9.1 General information:

Unless otherwise stated, all commercial chemical materials were used as received without further purification. All reactions were performed using common dry, inert atmosphere techniques. The blue light irradiation was done using blue light emitting diodes (700 mA, λ_{max} = 455 nm) produced by Oslon SSL. All the reactions were monitored by TLC and visualized by a dual short (254 nm) / long (366 nm) wavelength UV lamp. Analytical thin layer chromatography was performed on Merck TLC aluminum sheets silica gel 60 F 254. Purifications by column chromatography were performed on silica gel (0.063-0.200 mm). UV-Visible spectra were measured on Varian Cary 50 spectrophotometer. Melting points were recorded on Stanford Research Systems OptiMelt MPA 100 Automated melting point system. All products were characterized by appropriate techniques such as ^{1}H-NMR, ^{19}F-NMR, ^{31}P-NMR, ^{13}C-NMR, FT-IR and HRMS analysis. FT-IR (Cary 630) spectroscopy was carried out on a spectrometer, equipped with a Diamond Single Reflection ATR-System. NMR spectra were recorded on Bruker Avance 300, 400, or 600 MHz spectrometers. Chemical shifts for ^{1}H-NMR were reported as δ, parts per million, relative to the signal of $CHCl_3$ at 7.26 ppm. Chemical shifts for ^{13}C-NMR were reported as δ, parts per million, relative to the signal of $CHCl_3$ at 77.2 ppm and TMS as an internal standard. Coupling constants (*J*) are given in Hertz (Hz). The following notations indicate the multiplicity of the signals: s = singlet, bs = broad singlet, d = doublet, t = triplet, q = quartet, dd = doublet of doublets, td = triplet of doublets, and m = multiplet. Mass spectra were recorded at the Central Analytical Laboratory at the University of Regensburg on Agilent Technologies 6540 UHD Accurate-Mass Q-TOF LC/MS. THF was dried by distilling over KOH followed by stored on sodium metal wire under a nitrogen atmosphere. DMF was dried with distillation on calcium hydride then stored on activated molecular sieves (4 Å) under nitrogen. UV‑Visible and fluorescence measurements were performed with Varian Cary 50 UV/Vis-spectrophotometer and FluoroMax-4 spectrofluorometer, respectively. The ESR experiment was done on Magnettech MiniScope MS400 instrument having MW frequency 9.20-9.60 GHz (sensitivity: MS400: 8*10^9 Spins/0.1 mT) and Modulation Frequency 100 kHz (Field Modulation and Field stability was 5 μT – 0.7 mT and 1.5 μT/min, 15 μT/h, respectively). Electrochemical (cyclic voltammetry) studies were carried out under argon atmosphere. The measurements were performed in DMF containing 0.1 M tetra-*n*-butylammonium tetrafluoroborate using ferrocene/ferrocenium (Fc/Fc+) as an internal reference. A glassy carbon electrode (working electrode), platinum wire counter electrode, and Ag quasi-reference electrode were employed. (Note: this information is applicable to all the following chapters).

3.9.2 General procedure (GP-1) for Sonogashira coupling:

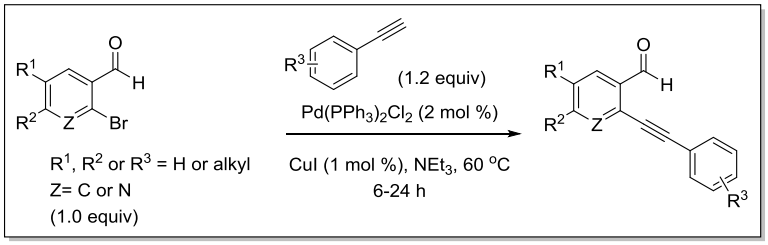

To a solution of the corresponding 2-bromobenzaldehyde derivative (2.00 mmol, 1.00 equiv), $PdCl_2$ $(PPh_3)_2$ (2.00 mol %), and CuI (1.00 mol %) in degassed NEt_3 (20 mL) was added the appropriate acetylene (2.40 mmol, 1.20 equiv). The resulting mixture was heated under nitrogen atmosphere at 60 °C for 6-24 h, gradually the reaction turned dark. The progress of the reaction was monitored by TLC. After complete consumption of the starting material, resulting mixture was diluted with 15 mL of EtOAc and filtered through the pad of celite. The filtrate was evaporated under reduced pressure and the pure compound was isolated through silica gel column chromatography using Hexanes/EtOAc as a solvent system.

2-(2-Phenylethynyl)benzaldehyde (S1a):

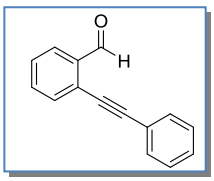

Following **GP-1**, **S1a** was prepared from 2-bromobenzaldehyde (5.0 g, 27.03 mmol). Purification of the crude product by column chromatography (Hexanes: EtOAc, 10:1, R_f = 0.53) afforded **S1a** as a brown oil (4.35 g, 78% yield).

^{1}H-NMR (300 MHz, $CDCl_3$): δ 10.66 (s, 1H), 7.95 (d, *J* = 7.8, 1H), 7.67 – 7.60 (m, 1H), 7.59 – 7.53 (m, 3H), 7.49 – 7.42 (m, 1H), 7.41 – 7.36 (m, 3H).

^{13}C-NMR (75 MHz, $CDCl_3$): δ 191.75, 135.84, 133.84, 133.25, 131.72, 129.12, 128.66, 128.57, 127.28, 126.91, 122.34, 96.37, 84.92.

The obtained data is in accordance with the literature data.[21]

5-Methoxy-2-(2-phenylethynyl)benzaldehyde (S1b):

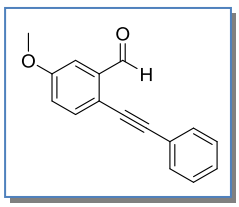

Following **GP-1**, **S1b** was prepared from 2-bromo-5-methoxybenzaldehyde (500 mg, 2.33 mmol). Purification of the crude product by column chromatography (Hexanes: EtOAc, 10:1, R_f = 0.51) afforded **S1b** as a brown solid (522 mg, 95% yield).

^{1}H-NMR (300 MHz, $CDCl_3$): δ 10.59 (s, 1H), 7.57 – 7.48 (m, 3H), 7.40 (d, *J* = 2.8 Hz, 1H), 7.35 (dd, *J* = 6.1, 2.6 Hz, 3H), 7.12 (dd, *J* = 8.6, 2.8 Hz, 1H), 3.85 (s, 3H).

^{13}C-NMR (75 MHz, $CDCl_3$): δ 191.63, 159.80, 137.19, 134.58, 131.54, 128.78, 128.53, 122.67, 121.76, 119.62, 109.82, 94.87, 84.86, 55.66.

The obtained data is in accordance with the literature data.[21]

4,5-Methylenedioxy-2-(2-phenylethynyl)benzaldehyde (S1c):

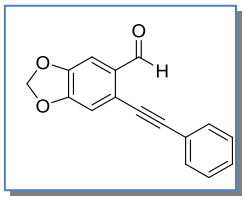

Following **GP-1**, **S1c** was prepared from 6-bromobenzo[d][1,3]dioxole-5-carbaldehyde (500 mg, 2.18 mmol). Purification of the crude product by column chromatography (Hexanes: EtOAc, 4:1, R_f = 0.58) afforded **S1c** as a white solid (540 mg, 99% yield).

^{1}H-NMR (300 MHz, $CDCl_3$): δ 10.49 (s, 1H), 7.60 – 7.48 (m, 2H), 7.42 – 7.32 (m, 4H), 7.03 (s, 1H), 6.09 (s, 2H).

^{13}C-NMR (75 MHz, $CDCl_3$): δ 190.08, 152.42, 148.73, 132.13, 131.60, 129.01, 128.55, 123.66, 122.33, 112.01, 106.11, 102.44, 95.16, 84.77.

The obtained data is in accordance with the literature data.[21]

4,5-Dimethoxy-2-(2-phenylethynyl)benzaldehyde (S1d):

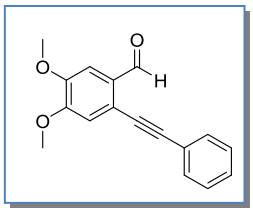

Following **GP-1**, **S1d** was prepared from 2-bromo-4,5-dimethoxybenzaldehyde (500 mg, 2.04 mmol). Purification of the crude product by column chromatography (Hexanes: EtOAc, 9:1, R_f = 0.49) afforded **S1d** as a brown solid (532 mg, 98% yield).

^{1}H-NMR (300 MHz, $CDCl_3$): δ 10.47 (s, 1H), 7.58 – 7.48 (m, 3H), 7.38 (s, 1H), 7.37 – 7.33 (m, 3H), 7.01 (s, *J* = 1H), 3.95 (s, 3H), 3.92 (s, 3H).

^{13}C-NMR (75 MHz, $CDCl_3$): δ 190.41, 153.61, 149.71, 131.56, 130.13, 128.90, 128.53, 122.46, 121.55, 114.26, 108.16, 94.99, 84.86, 56.21.

The obtained data is in accordance with the literature data.[21]

4,5-dimethoxy-2-((4-nitrophenyl)ethynyl)benzaldehyde (S1e):

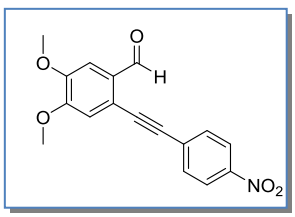

Following **GP-1**, **S1e** was prepared from 2-bromo-4,5-dimethoxybenzaldehyde (335 mg, 1.36 mmol). Purification of the crude product by column chromatography (Hexanes: EtOAc, 4:1, R_f = 0.29) afforded **S1e** as a yellow solid (378 mg, 89% yield).

^{1}H-NMR (300 MHz, $CDCl_3$): δ 10.46 (s, 1H), 8.30 – 8.20 (m, 2H), 7.73 – 7.64 (m, 2H), 7.44 (s, 1H), 7.08 (s, 1H), 4.01 (s, 3H), 3.98 (s, 3H).

^{13}C-NMR (75 MHz, $CDCl_3$): δ 189.79, 153.69, 150.51, 147.33, 132.29, 130.55, 129.35, 123.83, 119.92, 114.45, 108.56, 92.78, 90.06, 56.44, 56.26.

IR (neat, cm^{-1}): 2927, 1683, 1588, 1562, 1505, 1463, 1434, 1397, 1339, 1304, 1288, 1255, 1215, 1188, 1158, 1084, 1027, 994, 890, 871, 853, 824, 800, 775, 745, 684, 656.

HRMS (ESI): exact m/z calculated for $C_{17}H_{14}NO_5$ $(M+H)^+$: 312.0866; Found: 312.087 $(M+H)^+$.

Mp: 147-149 ^{o}C (decomposed).

2-(Phenylethynyl)nicotinaldehyde (S1f):

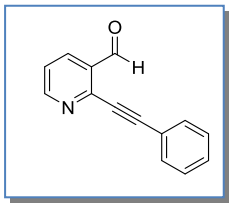

Following **GP-1**, **S1f** was prepared from 2-bromonicotinaldehyde (500 mg, 2.69 mmol). Purification of the crude product by column chromatography (Hexanes: EtOAc, 4:1, R_f = 0.32) afforded **S1f** as a brown solid (506 mg, 91% yield).

^{1}H-NMR (300 MHz, $CDCl_3$): δ 10.64 (s, 1H), 8.79 (s, 1H), 8.18 (dd, *J* = 7.9, 1.7 Hz, 1H), 7.67 – 7.56 (m, 2H), 7.44 – 7.31 (m, 4H).

^{13}C-NMR (75 MHz, $CDCl_3$): δ 190.81, 154.51, 146.06, 134.82, 132.20, 131.84, 129.89, 128.62, 123.28, 121.24, 96.07, 84.72.

The obtained data is in accordance with the literature data.[22]

5-nitro-2-(phenylethynyl)benzaldehyde (S1g):

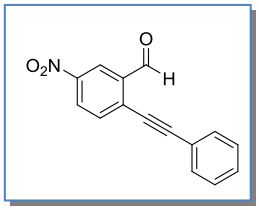

Following **GP-1**, **S1g** was prepared from 2-bromo-5-nitrobenzaldehyde (300 mg, 1.30 mmol). Purification of the crude product by column chromatography (Hexanes: EtOAc, 4:1, R_f = 0.47) afforded **S1g** as a yellow solid (281 mg, 86% yield).

^{1}H-NMR (300 MHz, $CDCl_3$): δ 10.63 (s, 1H), 8.73 (d, *J* = 2.4 Hz, 1H), 8.40 (dd, *J* = 8.5, 2.5 Hz, 1H), 7.81 (d, *J* = 8.5 Hz, 1H), 7.63 – 7.55 (m, 2H), 7.50 – 7.35 (m, 3H).

^{13}C-NMR (75 MHz, $CDCl_3$): δ 189.33, 147.23, 136.44, 134.39, 132.40, 132.02, 130.18, 128.77, 127.70, 122.65, 121.21, 101.69, 83.66.

The obtained data is in accordance with the literature data.[23]

4-Methyl-2-(2-phenylethynyl)benzaldehyde (S1h):

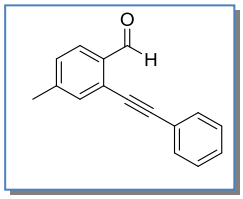

Following **GP-1**, **S1h** was prepared from 2-bromo-4-methylbenzaldehyde (500 mg, 2.51 mmol). Purification of the crude product by column chromatography (Hexanes: EtOAc, 10:1, R_f = 0.57) afforded **S1h** as a pale yellow solid (403 mg, 73% yield).

^{1}H-NMR (300 MHz, $CDCl_3$): δ 10.55 (s, 1H), 7.80 (d, *J* = 8.0 Hz, 1H), 7.55 – 7.47 (m, 2H), 7.40 (s, 1H), 7.37 – 7.30 (m, 3H), 7.19 (d, *J* = 7.9 Hz, 1H), 2.36 (s, 3H).

^{13}C-NMR (75 MHz, $CDCl_3$): δ 190.24, 143.79, 132.62, 132.52, 130.61, 128.61, 127.94, 127.46, 126.26, 125.79, 121.37, 94.80, 84.08, 20.54.

The obtained data is in accordance with the literature data.[21]

5-Fluoro-2-(2-phenylethynyl)benzaldehyde (S1i):

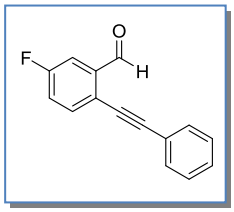

Following **GP-1**, **S1i** was prepared from 2-bromo-5-fluorobenzaldehyde (500 mg, 2.46 mmol). Purification of the crude product by column chromatography (Hexanes : EtOAc, 3:1, R_f = 0.39) afforded **S1i** as a pale yellow solid (480 mg, 87% yield).

^{1}H-NMR (300 MHz, $CDCl_3$): δ 10.57 (d, *J* = 3.2 Hz, 1H), 7.65 – 7.57 (m, 2H), 7.53 (ddd, *J* = 5.0, 3.8, 2.6 Hz, 2H), 7.39 – 7.35 (m, 3H), 7.31 – 7.23 (m, 1H).

^{13}C-NMR (75 MHz, $CDCl_3$): δ 190.49, 162.40 (d, *J* = 252.7 Hz), 137.77 (d, *J* = 6.7 Hz), 135.28 (d, *J* = 7.6 Hz), 131.67, 129.21, 128.60, 123.03 (d, *J* = 3.4 Hz), 122.13, 121.41 (d, *J* = 22.8 Hz), 113.72 (d, *J* = 23.0 Hz), 96.06, 83.85.

^{19}F-NMR (282 MHz, $CDCl_3$): δ -109.40.

The obtained data is in accordance with the literature data.[21]

3.9.3 Synthesis of 2-ethynylbenzaldehyde:[24,25]

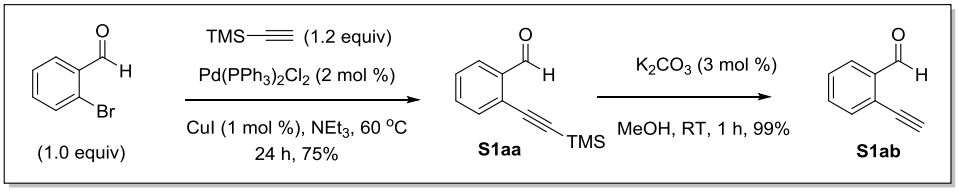

A dry round-bottomed flask was charged with 2-bromobenzaldehyde (10.0 g, 54.0 mmol, 1.00 equiv), CuI (0.103 g, 0.54 mmol, 0.01 equiv) and $[Pd(PPh_3)_2Cl_2]$ (0.759 g, 1.08 mmol, 0.02 equiv). 100 mL of NEt_3 and trimethylsilylacetylene (6.36 g, 64.08 mmol, 1.20 equiv) were added to the reaction mixture. The solution was degassed and allowed to stir at 60 ^oC for 24 h. The reaction mixture was then concentrated. The pure **S1aa** was isolated by flash column chromatography (10:1 Hexanes: EtOAc, R_f = 0.61) as a brown solid (8.89 g, 43.94 mmol, 75% yield); **S1aa** was then treated with K_2CO_3 (182 mg, 1.32 mmol, 3.00 mol %) in methanol (130 mL) for 1 h at room temperature. The pure compound **S1ab** was isolated through silica gel column chromatography (hexanes: EtOAc = 4:1, R_f = 0.46) as a white solid (5.67 g, 99% yield).

2-((trimethylsilyl)ethynyl)benzaldehyde (S1aa):

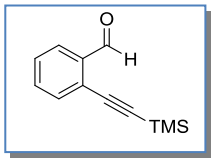

^{1}H-NMR (300 MHz, $CDCl_3$): δ 10.51 (s, 1H), 7.90 – 7.82 (m, 1H), 7.56 – 7.45 (m, 2H), 7.39 (m, 1H), 0.24 (s, 9H).

^{13}C-NMR (75 MHz, $CDCl_3$): δ 192.10, 136.37, 133.91, 133.72, 129.06, 127.09, 127.02, 102.64, 100.27, -0.19.

The obtained data is in accordance with the literature data.[24,25]

2-ethynylbenzaldehyde (S1ab):

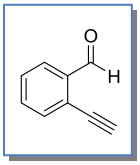

^{1}H-NMR (300 MHz, $CDCl_3$): δ 10.51 (s, 1H), 7.93 – 7.87 (m, 1H), 7.62 – 7.50 (m, 2H), 7.45 (t, *J* = 7.5 Hz, 1H), 3.42 (s, 1H).

^{13}C-NMR (75 MHz, $CDCl_3$): δ 191.47, 136.55, 133.93, 133.75, 129.25, 127.27, 125.51, 84.28, 79.21.

The obtained data is in accordance with the literature data.[24,25]

3.9.4 General procedure (GP-2) for Sonogashira coupling:

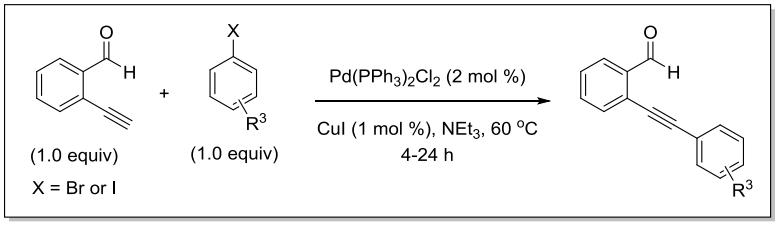

To the solution of appropriate halobenzene (iodo/bromo) derivatives (2.00 mmol, 1.00 equiv), $[Pd(PPh_3)_2Cl_2]$ (0.02 equiv), CuI (0.01 equiv) in degassed NEt_3 (20 mL), added the solution of 2-ethynylbenzaldehyde **S1ab** (2.00 mmol, 1.00 equiv). The mixture was stirred for 4-24 h at 60 ^oC. After completion of the reaction, the mixture was diluted with 15 mL of EtOAc and filtered through the pad of celite. The filtrate was evaporated under reduced pressure, and the pure compound was isolated through silica gel column chromatography using Hexanes/EtOAc as a solvent system.

2-((4-methoxyphenyl)ethynyl)benzaldehyde (S1j):

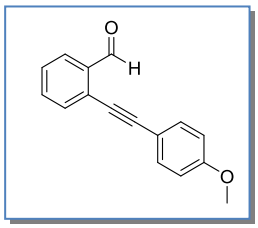

Following **GP-2**, **S1j** was prepared from 1-iodo-4-methoxybenzene (468 mg, 2.0 mmol). Purification of the crude product by column chromatography (Hexanes: EtOAc, 95:5, R_f = 0.3) afforded **S1j** as a white solid (387 mg, 82% yield).

^{1}H-NMR (300 MHz, $CDCl_3$): δ 10.65 (s, 1H), 7.97 – 7.90 (m, 1H), 7.65 – 7.56 (m, 2H), 7.55 – 7.46 (m, 3H), 7.46 – 7.38 (m, 1H), 6.94 – 6.88 (m, 2H), 3.84 (s, 3H).

^{13}C-NMR (75 MHz, $CDCl_3$): δ 191.94, 160.25, 135.64, 134.06, 133.82, 133.26, 133.06, 128.26, 127.22, 114.21, 96.62, 83.81, 55.38.

The obtained data is in accordance with the literature data.[26]

2-((4-chlorophenyl)ethynyl)benzaldehyde (S1k):

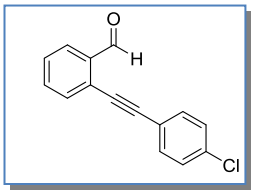

Following **GP-2**, **S1k** was prepared from 1-chloro-4-iodobenzene (476 mg, 2.0 mmol). Purification of the crude product by column chromatography (Hexanes: EtOAc, 9:1, R_f = 0.6) afforded **S1k** as a white solid (456 mg, 95% yield).

^{1}H-NMR (300 MHz, $CDCl_3$): δ 10.57 (s, 1H), 7.91 (ddd, *J* = 7.7, 1.3, 0.6 Hz, 1H), 7.62 – 7.51 (m, 2H), 7.48 – 7.39 (m, 3H), 7.35 – 7.28 (m, 2H).

^{13}C-NMR (75 MHz, $CDCl_3$): δ 191.53, 135.85, 135.21, 133.86, 133.26, 132.91, 128.91, 127.48, 126.43, 120.83, 95.09, 85.89.

The obtained data is in accordance with the literature data.[27]

2-((4-bromophenyl)ethynyl)benzaldehyde (S1l):

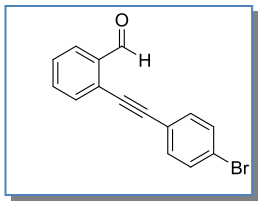

Following **GP-2**, **S1l** was prepared from 1-bromo-4-iodobenzene (565 mg, 2.0 mmol). Purification of the crude product by column chromatography (Hexanes: EtOAc, 9:1, R_f = 0.55) afforded **S1l** as a pale yellow solid (453 mg, 80% yield).

^{1}H-NMR (300 MHz, $CDCl_3$): δ 10.57 (s, 1H), 7.94 – 7.89 (m, 1H), 7.63 – 7.52 (m, 2H), 7.51 – 7.42 (m, 3H), 7.42 – 7.36 (m, 2H).

^{13}C-NMR (75 MHz, $CDCl_3$): δ 191.49, 135.87, 133.85, 133.26, 133.09, 131.87, 128.90, 127.50, 126.40, 123.47, 121.30, 95.14, 86.06.

The obtained data is in accordance with the literature data.[28]

2-(p-tolylethynyl)benzaldehyde (S1m):

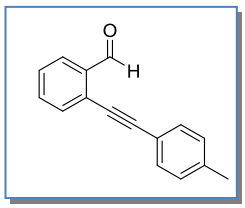

Following **GP-2**, **S1m** was prepared from 1-iodo-4-methylbenzene (436 mg, 2.0 mmol). Purification of the crude product by column chromatography (Hexanes: EtOAc, 9:1, R_f = 0.63) afforded **S1m** as a yellow solid (344 mg, 78% yield).

^{1}H-NMR (300 MHz, $CDCl_3$): δ 10.66 (s, 1H), 7.95 (dd, *J* = 7.8, 0.9 Hz, 1H), 7.60 (dtd, *J* = 9.1, 7.7, 1.3 Hz, 2H), 7.50 – 7.38 (m, 3H), 7.19 (d, *J* = 7.9 Hz, 2H), 2.39 (s, 3H).

^{13}C-NMR (75 MHz, $CDCl_3$): δ 191.89, 139.43, 135.76, 133.82, 133.17, 132.41, 131.62, 129.33, 128.45, 127.21, 119.26, 96.68, 84.34, 21.63.

The obtained data is in accordance with the literature data.[28]

2-((4-isopropylphenyl)ethynyl)benzaldehyde (S1n):

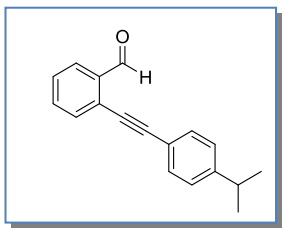

Following **GP-2**, **S1n** was prepared from 1-iodo-4-isopropylbenzene (492 mg, 2.0 mmol). Purification of the crude product by column chromatography (Hexanes: EtOAc, 95:5, R_f = 0.53) afforded **S1n** as a yellow viscous oil (461 mg, 93% yield).

^{1}H-NMR (300 MHz, $CDCl_3$): δ 10.64 (s, 1H), 7.92 (d, *J* = 9.7 Hz, 1H), 7.61 (ddd, *J* = 7.8, 1.4, 0.5 Hz, 1H), 7.54 (td, *J* = 7.5, 1.4 Hz, 1H), 7.50 – 7.45 (m, 2H), 7.44 – 7.37 (m, 1H), 7.25 – 7.20 (m, 2H), 2.91 (hept, *J* = 6.9 Hz, 1H), 1.24 (d, *J* = 6.9 Hz, 6H).

^{13}C-NMR (75 MHz, $CDCl_3$): δ 190.79, 149.19, 134.68, 132.72, 132.09, 130.65, 127.35, 126.09, 125.64, 118.54, 95.63, 83.18, 33.09, 22.70.

IR (neat, cm^{-1}): 2959, 2214, 1695, 1595, 1509, 1461, 1412, 1263, 1192, 1088, 1051, 1017, 834, 760, 700.

HRMS (ESI): exact m/z calculated for $C_{18}H_{17}O$ $(M+H)^+$: 249.1273; Found: 249.1268 $(M+H)^+$.

2-((4-(tert-butyl)phenyl)ethynyl)benzaldehyde (S1o):

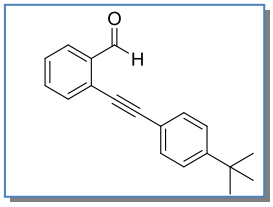

Following **GP-2**, **S1o** was prepared from 1-(tert-butyl)-4-iodobenzene (520 mg, 2.0 mmol). Purification of the crude product by column chromatography (Hexanes: EtOAc, 95:5, R_f = 0.59) afforded **S1o** as a white solid (445 mg, 85% yield).

^{1}H-NMR (300 MHz, $CDCl_3$): δ 10.69 (s, 1H), 7.96 (dd, *J* = 7.8, 0.9 Hz, 1H), 7.66 – 7.55 (m, 2H), 7.55 – 7.49 (m, 2H), 7.47 – 7.39 (m, 3H), 1.35 (s, 9H).

^{13}C-NMR (75 MHz, $CDCl_3$): δ 190.70, 151.39, 134.67, 132.68, 132.08, 130.37, 127.33, 126.08, 124.47, 118.20, 95.57, 83.24, 33.80, 30.05.

The obtained data is in accordance with the literature data.[29]

2-((2-formylphenyl)ethynyl)benzonitrile (S1p):

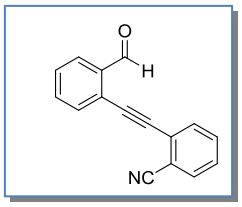

Following **GP-2**, **S1p** was prepared from 2-iodobenzonitrile (458 mg, 2.0 mmol). Purification of the crude product by column chromatography (Hexanes: EtOAc, 4:1, R_f = 0.51) afforded **S1p** as a white solid (291 mg, 63% yield).

^{1}H-NMR (300 MHz, $CDCl_3$): δ 10.65 (s, 1H), 7.94 (d, *J* = 7.7 Hz, 1H), 7.74 – 7.68 (m, 1H), 7.68 – 7.63 (m, 2H), 7.62 – 7.55 (m, 2H), 7.47 (m, 2H).

^{13}C-NMR (75 MHz, $CDCl_3$): δ 191.29, 136.15, 133.93, 133.86, 132.81, 132.61, 132.42, 129.66, 129.11, 127.55, 126.37, 125.26, 117.53, 115.39, 91.81, 91.29.

The obtained data is in accordance with the literature data.[30]

2-((4-nitrophenyl)ethynyl)benzaldehyde (S1q):

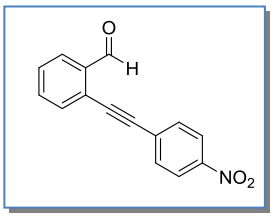

Following **GP-2**, **S1q** was prepared from 1-bromo-4-nitrobenzene (404 mg, 2.0 mmol). Purification of the crude product by column chromatography (Hexanes: EtOAc, 4:1, R_f = 0.5) afforded **S1q** as a yellow solid (386 mg, 77% yield).

^{1}H-NMR (300 MHz, $CDCl_3$): δ 10.58 (s, 1H), 8.27 – 8.20 (m, 2H), 7.99 – 7.93 (m, 1H), 7.74 – 7.67 (m, 2H), 7.63 (ddd, *J* = 9.1, 6.0, 1.2 Hz, 2H), 7.56 – 7.48 (m, 1H).

^{13}C-NMR (75 MHz, $CDCl_3$): δ 190.97, 147.47, 136.07, 133.94, 133.56, 132.48, 129.68, 129.17, 127.96, 125.18, 123.80, 93.82, 89.98.

The obtained data is in accordance with the literature data.[27]

2-((4-(trifluoromethyl)phenyl)ethynyl)benzaldehyde (S1r):

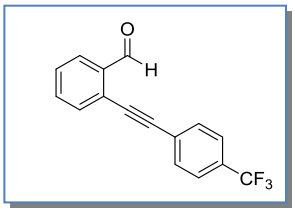

Following **GP-2**, **S1r** was prepared from 1-bromo-4-(trifluoromethyl)benzene (450 mg, 2.0 mmol). Purification of the crude product by column chromatography (Hexanes: EtOAc, 9:1, R_f = 0.61) afforded **S1r** as a light brown solid (383 mg, 70% yield).

^{1}H-NMR (300 MHz, $CDCl_3$): δ 10.59 (s, 1H), 7.93 (dt, *J* = 7.7, 3.8 Hz, 1H), 7.67 – 7.54 (m, 6H), 7.50 – 7.43 (m, 1H).

^{13}C-NMR (75 MHz, $CDCl_3$): δ 190.18, 134.93, 132.80, 132.36, 130.88, 128.16, 126.55, 124.49, 124.44, 124.39, 124.34, 93.49, 86.14.

^{19}F-NMR (282 MHz, $CDCl_3$): δ -63.35.

The obtained data is in accordance with the literature data.[28]

Methyl 4-((2-formylphenyl)ethynyl)benzoate (S1s):

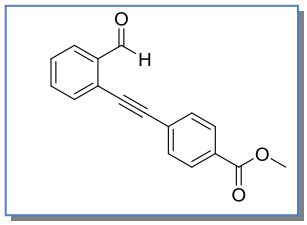

Following **GP-2**, **S1s** was prepared from methyl 4-iodobenzoate (524 mg, 2.0 mmol). Purification of the crude product by column chromatography (Hexanes: EtOAc, 9:1, R_f = 0.52) afforded **S1s** as a white solid (383 mg, 73% yield).

^{1}H-NMR (300 MHz, $CDCl_3$): δ 10.59 (s, 1H), 8.04 – 7.98 (m, 2H), 7.93 (dd, *J* = 8.0, 1.0 Hz, 1H), 7.65 – 7.53 (m, 4H), 7.46 (dt, *J* = 7.7, 3.9 Hz, 1H), 3.90 (s, 3H).

^{13}C-NMR (75 MHz, $CDCl_3$): δ 191.40, 166.41, 135.96, 133.89, 133.40, 131.64, 130.25, 129.69, 129.16, 127.55, 126.94, 126.11, 95.27, 87.68, 52.37.

IR (neat, cm^{-1}): 1717, 1689, 1590, 1558, 1542, 1508, 1438, 1402, 1393, 1261, 1191, 1144, 1105, 1014, 854, 824, 805, 763, 690.

HRMS (ESI): exact m/z calculated for $C_{17}H_{13}O_3$ $(M+H)^+$: 265.0859; Found: 265.0843 $(M+H)^+$.

Mp: 122-124 ^oC (decomposed).

2-((4-(2-methyl-1,3-dioxolan-2-yl)phenyl)ethynyl)benzaldehyde (S1t):

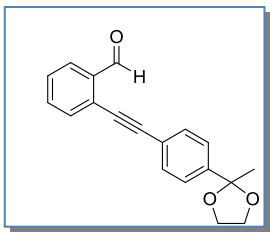

Following **GP-2**, **S1t** was prepared from 2-(4-iodophenyl)-2-methyl-1,3-dioxolane (580 mg, 2.0 mmol). Purification of the crude product by column chromatography (Hexanes: EtOAc, 4:1, R_f = 0.31) afforded **S1t** as a pale yellow solid (519 mg, 89% yield).

^{1}H-NMR (300 MHz, $CDCl_3$): δ 10.57 (s, 1H), 7.87 (dd, *J* = 7.8, 0.7 Hz, 1H), 7.56 (ddd, *J* = 8.0, 4.4, 1.0 Hz, 1H), 7.52 – 7.41 (m, 5H), 7.41 – 7.34 (m, 1H), 4.05 – 3.91 (m, 2H), 3.78 – 3.64 (m, 2H), 1.60 (s, 3H).

^{13}C-NMR (75 MHz, $CDCl_3$): δ 191.62, 144.45, 135.83, 133.80, 133.24, 131.62, 128.66, 127.28, 126.81, 125.58, 121.83, 108.54, 96.14, 85.04, 64.54, 27.46.

IR (neat, cm^{-1}): 2895, 1695, 1590, 1508, 1475, 1443, 1400, 1370, 1238, 1192, 1095, 1033, 945, 872, 818, 759, 707.

HRMS (ESI): exact m/z calculated for $C_{19}H_{17}O_3$ $(M+H)^+$: 293.1172; Found: 293.1188 $(M+H)^+$.

Mp: 75-77 ^oC (decomposed).

2-((4-(1,3-dioxolan-2-yl)phenyl)ethynyl)benzaldehyde (S1u):

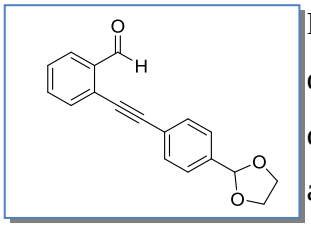

Following **GP-2**, **S1u** was prepared from 2-(4-bromophenyl)-1,3-dioxolane (458 mg, 2.0 mmol). Purification of the crude product by column chromatography (Hexanes: EtOAc, 4:1, R_f = 0.43) afforded **S1u** as a white solid (439 mg, 79% yield).

^{1}H-NMR (300 MHz, $CDCl_3$): δ 10.64 (s, 1H), 7.94 (dt, *J* = 14.0, 3.8 Hz, 1H), 7.69 – 7.35 (m, 7H), 5.83 (s, 1H), 4.19 – 3.96 (m, 4H).

^{13}C-NMR (75 MHz, $CDCl_3$): δ 191.67, 138.86, 135.85, 133.84, 133.28, 131.72, 128.75, 127.31, 126.70, 123.13, 103.17, 96.01, 85.41, 65.39.

IR (neat, cm^{-1}): 1692, 1595, 1561, 1509, 1476, 1449, 1386, 1267, 1203, 1166, 1073, 1017, 969, 939, 861, 827, 760, 704.

HRMS (ESI): exact m/z calculated for $C_{18}H_{15}O_3$ $(M+H)^+$: 279.1016; Found: 279.1006 $(M+H)^+$.

Mp: 60-62 ^oC (decomposed).

4-((2-formylphenyl)ethynyl)benzonitrile (S1v)

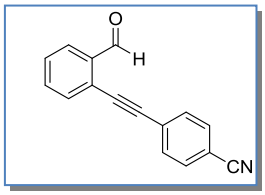

Following **GP-2**, **S1v** was prepared from 4-bromobenzonitrile (500 mg, 2.75 mmol). Purification of the crude product by column chromatography (Hexanes: EtOAc, 9:1, R_f = 0.31) afforded **S1v** as a pale yellow solid (514 mg, 81% yield).

^{1}H-NMR (300 MHz, $CDCl_3$): δ 10.59 (s, 1H), 7.97 (ddd, *J* = 7.7, 1.3, 0.6 Hz, 1H), 7.71 – 7.59 (m, 6H), 7.52 (tdd, *J* = 7.1, 1.7, 0.8 Hz, 1H).

^{13}C-NMR (75 MHz, $CDCl_3$): δ 191.07, 136.05, 133.92, 133.50, 132.24, 132.21, 129.54, 127.88, 127.22, 125.39, 118.33, 112.36, 94.10, 89.14.

The obtained data is in accordance with the literature data.[31]

(*E*)-2-styrylbenzaldehyde (S1w):[32]

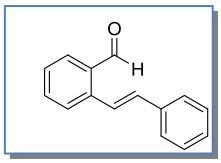

The mixture of 2-bromobenzaldehyde (1.0 g, 5.4 mmol), styrene (5.6 g, 54 mmol), potassium phosphate, (1.72 g, 8.1 mmol), $Pd(OAc)_2$ (0.121 g, 0.054 mmol) and *N*,*N*-dimethylacetamide (15 mL) was added to a 100 mL Schlenk flask under nitrogen atmosphere and stirred at 140 ^oC for 16 hours. Brine solution (60 mL) was added to the reaction mixture and extracted by ethyl acetate (30 mL x 3). The combined organic layer was dried over anhydrous Na_2SO_4. After the solvent was removed under reduced pressure, Purification of the crude product by column chromatography (Hexanes: EtOAc, 9:1, R_f = 0.33) afforded **S1w** as a pale yellow oil (0.785 g, 69% yield).

^{1}H-NMR (300 MHz, $CDCl_3$): δ 10.32 (s, 1H), 8.07 (d, *J* = 16.2 Hz, 1H), 7.85 (dd, *J* = 7.7, 1.3 Hz, 1H), 7.73 (d, *J* = 7.7 Hz, 1H), 7.59 (dt, *J* = 9.9, 2.1 Hz, 3H), 7.48 – 7.28 (m, 4H), 7.07 (d, *J* = 16.2 Hz, 1H).

^{13}C-NMR (75 MHz, $CDCl_3$): δ 192.83, 140.03, 136.99, 134.08, 133.86, 133.01, 132.50, 128.90, 128.44, 127.74, 127.28, 127.11, 124.87.

The obtained data is in accordance with the literature data.[32]

3.9.5 Bromination of triethyl phosphonoacetate:[33]

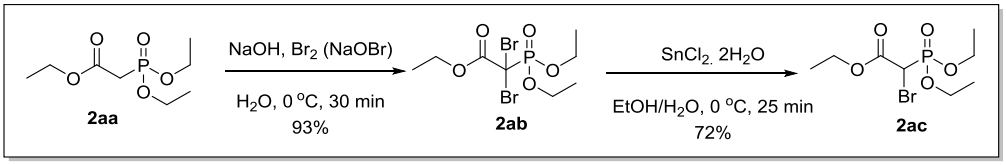

Triethyl dibromophosphonoacetate (2ab): A solution of sodium hydroxide (20 g, 500.0 mmol, 10.00 equiv) in H_2O (60 mL) was prepared in a 500-mL, three-necked, round-bottomed flask fitted with a thermometer and a dropping funnel. The solution was cooled to 0 ^oC in an ice-salt bath, and bromine (40 g, 12.81 mL, 250.0 mmol, 5.00 equiv) was slowly added with stirring over 25 min at a rate such that, the temperature did not exceed over 10 ^oC. Triethyl phosphonoacetate **2aa** (12 g, 53.5 mmol, 1.00 equiv) was added over 3 min to the freshly prepared, stirred sodium hypobromite (NaOBr) solution cooled in an ice-salt bath. Then the mixture was immediately extracted with chloroform (3 x 70 mL). The chloroform extracts were washed with water (2 **x** 20 mL) and dried over Na_2SO_4 and the solvent was removed *in vacuo*. The residue was partitioned between hexane (300 mL) and H_2O (2 **x** 5 ml), and the hexane extracts were again dried over Na_2SO_4. After removing the solvents *in vacuo* provided **2ab** 19.01 g (93%) as a pure product.

^{1}H-NMR (300 MHz, $CDCl_3$): δ 4.40-4.20 (m, 6H), 1.39-1.22 (m, 9H)

^{13}C-NMR (75 MHz, $CDCl_3$): δ 163.70, 66.39, 66.30, 64.56, 47.97, 45.86, 16.41, 16.34, 13.69.

^{31}P-NMR (121 MHz, $CDCl_3$): δ 8.34.

Triethyl Bromophosphonoacetate (2ac): To triethyl dibromophosphonoacetate **2ab** (18 g, 47 mmol, 1.00 equiv) dissolved in EtOH (50 mL) was added with cooling (ice bath) a solution of 9.56 g (42.40 mmol, 0.90 equiv) of $SnCl_2.2H_2O$ in H_2O (100 mL). The temperature was maintained below 10 ^oC. When the addition was complete (20 min), the reaction mixture was stirred for an additional 5 min at room temperature and then extracted with chloroform (3 x **7**5 mL). The chloroform extracts were dried over Na_2SO_4, and the solvent was removed in vacuo. The desired product was isolated by partitioning the crude residue between hexane (150 mL) and H_2O (4 **x** 50 mL). The aqueous fractions were combined and re-extracted with chloroform (3 x 75 mL). The chloroform extracts were dried over Na_2SO_4 and evaporated at reduced pressure to provide 10 g (72%) of pure triethyl bromophosphonoacetate **2ac**.

^{1}H-NMR (300 MHz, $CDCl_3$): δ 4.40 – 4.18 (m, 7H), 1.44 – 1.24 (m, 9H).

^{13}C-NMR (75 MHz, $CDCl_3$): δ 165.05, 64.67, 64.59, 63.11, 36.78, 34.85, 16.39, 16.31, 13.92.

^{31}P-NMR (121 MHz, $CDCl_3$): δ 13.17.

The obtained data is in accordance with the literature data.[33]

3.9.6 General procedure (GP-3) for the preparation of α-bromocinnamates:

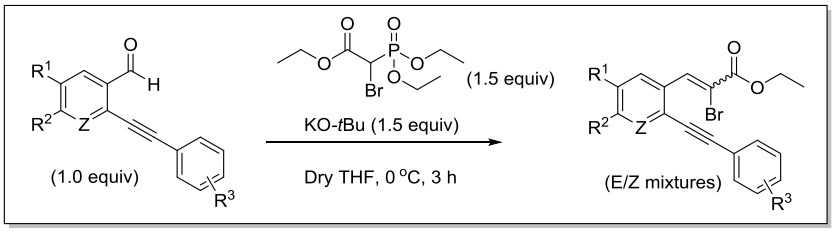

Potassium *tert*-butoxide (1.50 mmol, 1.50 equiv) was slowly added to triethyl bromophosphonoacetate **2ac** (1.50 mmol, 1.50 equiv) in anhydrous THF (15 mL) under a positive nitrogen atmosphere at 0 °C. The resulting mixture allowed stirring for 1 h, followed by slow addition of desired aldehyde **S1** (1.00 mmol, 1.00 equiv) in 3 mL THF over 5 min, the resulting mixture stirred under an inert atmosphere for 2 h at 0 °C. The progress of the reaction monitored by TLC analysis (staining with 2, 4-DNP / $KMnO_4$); after complete consumption of the starting material, the reaction was quenched by adding saturated ammonium chloride solution (10 mL) and extracted with ethyl acetate (10 mL x 3). Combined organic layer was washed with brine (20 mL), dried over anhydrous Na_2SO_4, and concentrated *in vacuo*. Purification of the crude product by silica gel column chromatography using Hexanes/EtOAc solvent system afforded pure *α*-bromocinnamates.

Ethyl 2-bromo-3-(2-(phenylethynyl)phenyl)acrylate (1a):

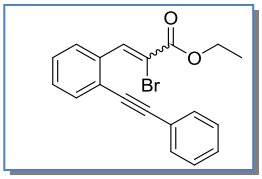

Following **GP-3**, **1a** was prepared from **S1a** (1.65 g, 8.0 mmol). Purification of the crude product by column chromatography (Hexanes: EtOAc, 95:5, R_f = 0.48) afforded **1a** as a yellow viscous oil (2.49 g, 88% yield, *Z:E* = 82:18).

^{1}H-NMR (300 MHz, $CDCl_3$, *Z* isomer, major): δ 8.76 (s, 1H), 8.20 – 8.13 (m, 1H), 7.63 – 7.50 (m, 3H), 7.44 – 7.27 (m, 5H), 4.38 (q, *J* = 7.1 Hz, 2H), 1.39 (t, *J* = 7.1 Hz, 3H).

^{13}C-NMR (75 MHz, $CDCl_3$, *Z* isomer, major): δ 163.20, 139.51, 135.66, 132.15, 131.61, 129.64, 128.85, 128.78, 128.47, 127.95, 124.66, 122.81, 115.07, 96.21, 87.09, 62.87, 14.28.

IR (neat, cm^{-1}): 2983, 2215, 1720, 1599, 1493, 1468, 1443, 1367, 1230, 1193, 1092, 1035, 985, 914, 871, 836, 752, 688, 630, 536, 497.

HRMS (ESI): exact m/z calculated for $C_{19}H_{16}BrO_2$ $(M+H)^+$: 355.0328; Found: 355.0331 $(M+H)^+$.

Ethyl 2-bromo-3-(5-methoxy-2-(phenylethynyl)phenyl)acrylate (1b):

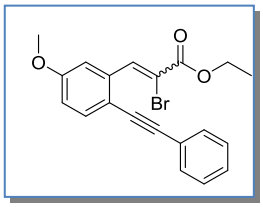

Following **GP-3**, **1b** was prepared from **S1b** (308 mg, 1.30 mmol). Purification of the crude product by column chromatography (Hexanes: EtOAc, 9:1, R_f = 0.32) afforded **1b** as a brown solid (466 mg, 93% yield. *Z:E* = 99:01).

^{1}H-NMR (300 MHz, $CDCl_3$, *Z* isomer, major): δ 8.75 (s, 1H), 7.76 (d, *J* = 2.6 Hz, 1H), 7.57 – 7.50 (m, 3H), 7.38 – 7.31 (m, 3H), 6.95 (dd, *J* = 8.6, 2.7 Hz, 1H), 4.38 (q, *J* = 7.1 Hz, 2H), 3.87 (s, 3H), 1.38 (t, *J* = 7.1 Hz, 3H).

^{13}C-NMR (75 MHz, $CDCl_3$, *Z* isomer, major): δ 163.15, 159.03, 139.32, 136.89, 133.43, 131.38, 128.40, 123.15, 117.09, 116.09, 115.13, 113.92, 94.76, 87.05, 62.90, 55.54, 14.26.

IR (neat, cm^{-1}): 2973, 1718, 1595, 1494, 1474, 1441, 1292, 1218, 1165, 1099, 1030, 902, 833, 752, 688, 720, 688.

HRMS (ESI): exact m/z calculated for $C_{20}H_{18}BrO_3$ $(M+H)^+$: 385.0434; Found: 385.0432 $(M+H)^+$.

Mp: 48-50 ^{o}C (decomposed).

Ethyl 2-bromo-3-(6-(phenylethynyl)benzo[d][1,3]dioxol-5-yl)acrylate (1c):

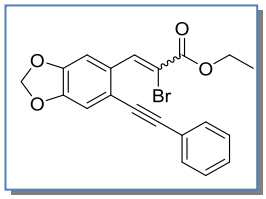

Following **GP-3**, **1c** was prepared from **S1c** (250 mg, 1.0 mmol). Purification of the crude product by column chromatography (Hexanes: EtOAc, 4:1, R_f = 0.62) afforded **1c** as a brown solid (369 mg, 92% yield, *Z:E* = 82:18).

^{1}H-NMR (300 MHz, $CDCl_3$, *Z* isomer, major): δ 8.79 (s, 1H), 7.86 (s, 1H), 7.59 – 7.49 (m, 2H), 7.39 – 7.31 (m, 3H), 7.03 (s, 1H), 6.06 (s, 2H), 4.36 (q, *J* = 7.1 Hz, 2H), 1.36 (t, *J* = 7.1 Hz, 3H).

^{13}C-NMR (75 MHz, $CDCl_3$, *Z* isomer, major): δ 163.35, 148.85, 147.67, 138.87, 131.44, 130.31, 128.63, 128.44, 122.83, 120.14, 112.99, 111.59, 108.61, 102.07, 95.49, 87.09, 62.79, 14.28.

IR (neat, cm^{-1}): 2981, 2906, 1706, 1598, 1503, 1476, 1455, 1393, 1358, 1329, 1248, 1219, 1135, 1033, 986, 932, 890, 748, 681, 573, 550, 505, 486.

HRMS (ESI): exact m/z calculated for $C_{20}H_{16}BrO_4$ $(M+H)^+$: 399.0226; Found: 399.0231 $(M+H)^+$.

Mp: 119-121 ^{o}C (decomposed).

Ethyl 2-bromo-3-(4,5-dimethoxy-2-(phenylethynyl)phenyl)acrylate (1d):

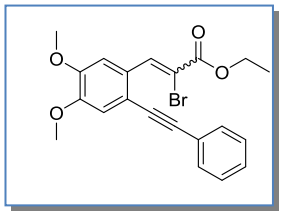

Following **GP-3**, **1d** was prepared from **S1d** (266 mg, 1.0 mmol). Purification of the crude product by column chromatography (Hexanes: EtOAc, 4:1, R_f = 0.52) afforded **1d** as a brown solid (377 mg, 91% yield, *Z:E* = 84:16).

^{1}H-NMR (300 MHz, $CDCl_3$, *Z* isomer, major): δ 8.82 (s, 1H), 7.98 (s, 1H), 7.59 – 7.49 (m, 2H), 7.40 – 7.30 (m, 3H), 7.06 (s, 1H), 4.35 (q, *J* = 7.1 Hz, 2H), 3.94 (s, 3H), 3.93 (s, 3H), 1.37 (t, *J* = 7.1 Hz, 3H).

^{13}C-NMR (75 MHz, $CDCl_3$, *Z* isomer, major): δ 163.41, 150.15, 148.63, 138.69, 131.41, 128.44, 122.93, 118.94, 114.01, 112.27, 111.16, 95.27, 87.12, 62.77, 56.05, 14.29.

IR (neat, cm^{-1}): 1703, 1592, 1506, 1463, 1335, 1291, 1254, 1209, 1167, 1091, 1029, 1001, 967, 892, 858, 759, 695, 635, 530, 503.

HRMS (ESI): exact m/z calculated for $C_{21}H_{20}BrO_4$ $(M+H)^+$: 415.0539; Found: 415.0539 $(M+H)^+$.

Mp: 80-82 ^oC.

Ethyl 2-bromo-3-(4,5-dimethoxy-2-((4-nitrophenyl)ethynyl)phenyl)acrylate (1e):

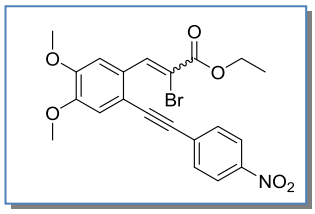

Following **GP-3**, **1e** was prepared from **S1e** (311 mg, 1.0 mmol). Purification of the crude product by column chromatography (Hexanes: EtOAc, 4:1, R_f = 0.33) afforded **1e** as a yellow solid (400 mg, 87% yield, *Z:E* = 99:01).

^{1}H-NMR (300 MHz, $CDCl_3$, *Z* isomer, major): δ 8.75 (s, 1H), 8.21 (d, *J* = 8.8 Hz, 2H), 7.96 (s, 1H), 7.67 (d, *J* = 8.8 Hz, 2H), 7.07 (s, 1H), 4.37 (q, *J* = 7.1 Hz, 2H), 3.95 (s, 3H), 3.95 (s, 3H), 1.38 (t, *J* = 7.1 Hz, 3H).

^{13}C-NMR (75 MHz, $CDCl_3$, *Z* isomer, major): δ 163.28, 150.17, 149.49, 147.03, 138.19, 131.99, 129.88, 129.31, 123.75, 117.36, 114.17, 112.85, 111.26, 93.30, 92.46, 62.90, 56.12, 14.34.

IR (neat, cm^{-1}): 2206, 1704, 1589, 1491, 1450, 1403, 1333, 1235, 1212, 1168, 1091, 1034, 987, 894, 850, 781, 748, 686, 581, 575, 503, 415.

HRMS (ESI): exact m/z calculated for $C_{21}H_{19}BrNO_6$ $(M+H)^+$: 460.039; Found: 460.0389 $(M+H)^+$.

Mp: 140-142 ^oC (decomposed).

Ethyl 2-bromo-3-(2-(phenylethynyl)pyridin-3-yl)acrylate (1f):

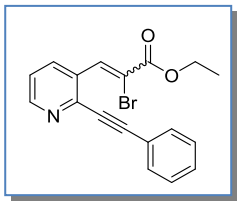

Following **GP-3**, **1f** was prepared from **S1f** (207 mg, 1.0 mmol). Purification of the crude product by column chromatography (Hexanes: EtOAc, 4:1, R_f = 0.6) afforded **1f** as a brown solid (316 mg, 89% yield, *Z:E* = 99:01)..

^{1}H-NMR (300 MHz, $CDCl_3$, *Z* isomer, major): δ 8.70 (s, 1H), 8.63 (dd, *J* = 4.8, 1.6 Hz, 1H), 8.47 (ddd, *J* = 8.1, 1.6, 0.6 Hz, 1H), 7.67 – 7.59 (m, 2H), 7.44 – 7.30 (m, 4H), 4.40 (q, *J* = 7.1 Hz, 2H), 1.40 (t, *J* = 7.1 Hz, 3H).

^{13}C-NMR (75 MHz, $CDCl_3$, *Z* isomer, major): δ 162.66, 150.51, 143.63, 137.05, 136.25, 132.29, 132.14, 129.57, 128.52, 122.18, 121.75, 117.33, 96.18, 86.54, 63.13, 14.24.

IR (neat, cm^{-1}): 2991, 2219, 1712, 1599, 1549, 1492, 1443, 1413, 1361, 1237, 1152, 1094, 1034, 988, 902, 861, 836, 806, 759, 688, 640, 545, 501.

HRMS (ESI): exact m/z calculated for $C_{18}H_{15}BrNO_2$ $(M+H)^+$: 356.0281; Found: 356.0285 $(M+H)^+$.

Mp: 78-80 ^oC

Ethyl 2-bromo-3-(5-nitro-2-(phenylethynyl)phenyl)acrylate (1g):

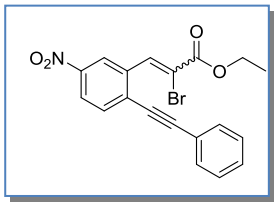

Following **GP-3**, **1g** was prepared from **S1g** (281 mg, 1.0 mmol). Purification of the crude product by column chromatography (Hexanes: EtOAc, 9:1, R_f = 0.47) afforded **1e** as a yellow solid (332 mg, 83% yield, *E:Z* = 95:05).

^{1}H-NMR (300 MHz, $CDCl_3$, *E* isomer, major): δ 8.19 (d, *J* = 2.2 Hz, 1H), 8.13 (dd, *J* = 8.5, 2.3 Hz, 1H), 7.68 (s, 1H), 7.63 (d, *J* = 8.5 Hz, 1H), 7.55 – 7.49 (m, 2H), 7.39 – 7.33 (m, 3H), 4.15 (q, *J* = 7.1 Hz, 2H), 1.10 (t, *J* = 7.1 Hz, 3H).

^{13}C-NMR (75 MHz, $CDCl_3$, *E* isomer, major): δ 162.84, 146.54, 138.42, 137.78, 132.65, 132.01, 129.72, 128.87, 128.66, 123.28, 123.16, 121.71, 117.00, 100.16, 85.91, 62.90, 13.70.

IR (neat, cm^{-1}): 2984, 2208, 1709, 1600, 1575, 1513, 1497, 1465, 1435, 1338, 1285, 1267, 1227, 1186, 1113, 1074, 1029, 983 912, 847, 823, 753, 735, 683, 658, 570, 531, 476, 418.

HRMS (ESI): exact m/z calculated for $C_{19}H_{14}BrNNaO_4$ $(M+Na)^+$: 421.9998; Found: 421.9999 $(M+Na)^+$.

Mp: 65-67 ^oC.

Ethyl 2-bromo-3-(4-methyl-2-(phenylethynyl)phenyl)acrylate (1h):

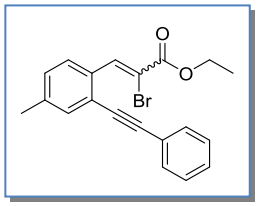

Following **GP-3**, **1h** was prepared from **S1h** (220 mg, 1.0 mmol). Purification of the crude product by column chromatography (Hexanes: EtOAc, 9:1, R_f = 0.56) afforded **1h** as a yellow oil (306 mg, 83% yield, *Z:E* = 80:20).

^{1}H-NMR (300 MHz, $CDCl_3$, *Z* isomer, major): δ 8.76 (s, 1H), 8.12 (d, *J* = 8.1 Hz, 1H), 7.57 – 7.50 (m, 2H), 7.41 (s, 1H), 7.37 – 7.31 (m, 3H), 7.20 (d, *J* = 8.1 Hz, 1H), 4.35 (q, *J* = 7.1 Hz, 2H), 2.35 (s, 3H), 1.36 (t, *J* = 7.1 Hz, 3H).

^{13}C-NMR (75 MHz, $CDCl_3$, *Z* isomer, major): δ 162.25, 139.05, 138.26, 131.66, 131.61, 131.46, 130.51, 127.85, 127.65, 127.63, 127.37, 126.84, 123.75, 121.80, 112.94, 94.78, 86.15, 61.70, 20.27, 13.21.

IR (neat, cm^{-1}): 2976, 2207, 1720, 1598, 1492, 1442, 1366, 1228, 1195, 1094, 1034, 982, 880, 841, 814, 752, 688.

HRMS (ESI): exact m/z calculated for $C_{20}H_{17}BrNaO_2$ $(M+Na)^+$: 391.0304; Found: 391.0307 $(M+Na)^+$.

Ethyl 2-bromo-3-(5-fluoro-2-(phenylethynyl)phenyl)acrylate (1i):

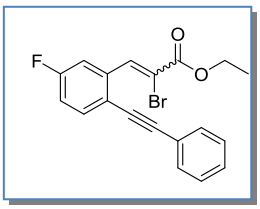

Following **GP-3**, **1i** was prepared from **S1i** (505 mg, 2.25 mmol). Purification of the crude product by column chromatography (Hexanes: EtOAc, 9:1, R_f = 0.38) afforded **1i** as a brown oil (756 mg, 90% yield, *Z:E* = 81:19).

^{1}H-NMR (300 MHz, $CDCl_3$, *Z* isomer, major): δ 8.72 (s, 1H), 7.94 (dd, *J* = 10.0, 2.7 Hz, 1H), 7.61 – 7.51 (m, 2H), 7.40 – 7.30 (m, 4H), 7.16 – 7.03 (m, 1H), 4.38 (q, *J* = 7.1 Hz, 2H), 1.39 (t, *J* = 7.1 Hz, 1H).

^{13}C-NMR (75 MHz, $CDCl_3$, *Z* isomer, major): δ 162.90, 160.04, 138.24, 137.69, 133.91, 132.53, 131.54, 129.24, 128.82, 128.48, 122.63, 117.21, 115.78, 95.87, 86.10, 63.02, 14.23.

^{19}F-NMR (282 MHz, $CDCl_3$): δ -110.10 (*Z*); -111.19 (*E*).

IR (neat, cm^{-1}): 2983, 1724, 1596, 1571, 1495, 1475, 1443, 1367, 1244, 1205, 1158, 1095, 1035, 989, 871, 822, 752, 722, 688, 638, 527, 495.

HRMS (ESI): exact m/z calculated for $C_{19}H_{15}BrFO_2$ $(M+H)^+$: 373.0234; Found: 373.0237 $(M+H)^+$.

Ethyl 2-bromo-3-(2-((4-methoxyphenyl)ethynyl)phenyl)acrylate (1j):

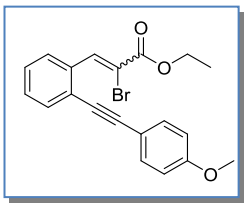

Following **GP-3**, **1j** was prepared from **S1j** (236 mg, 1.0 mmol). Purification of the crude product by column chromatography (Hexanes: EtOAc, 95:5, R_f = 0.3) afforded **1j** as a red solid (327 mg, 85% yield, *Z:E* = 73:27).

^{1}H-NMR (300 MHz, $CDCl_3$, *Z* isomer, major): δ 8.78 (s, 1H), 8.21 – 8.14 (m, 1H), 7.60 – 7.23 (m, 5H), 6.93 – 6.80 (m, 2H), 4.38 (q, *J* = 7.1 Hz, 2H), 3.81 (s, 3H), 1.39 (t, *J* = 7.1 Hz, 3H).

^{13}C-NMR (75 MHz, $CDCl_3$, *Z* isomer, major): δ 163.21, 160.27, 160.04, 139.62, 135.33, 134.07, 133.13, 131.91, 129.68, 128.81, 127.57, 125.13, 114.18, 114.12, 96.51, 85.98, 81.32, 73.07, 62.85, 55.33, 14.32.

IR (neat, cm^{-1}): 2980, 2211, 1714, 1605, 1569, 1509, 1461, 1287, 1243, 1175, 1090, 1025, 985, 889, 861, 824, 754, 689.

HRMS (ESI): exact m/z calculated for $C_{20}H_{17}BrNaO_3$ $(M+Na)^+$: 407.0253; Found: 407.0254 $(M+Na)^+$.

Mp: 95-97 ^oC (decomposed).

Ethyl 2-bromo-3-(2-((4-chlorophenyl)ethynyl)phenyl)acrylate (1k):

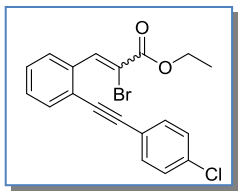

Following **GP-3**, **1k** was prepared from **S1k** (430 mg, 1.78 mmol). Purification of the crude product by column chromatography (Hexanes: EtOAc, 9:1, R_f = 0.6) afforded **1k** as a light brown solid (592 mg, 85% yield, *Z:E* = 91:09).

^{1}H-NMR (300 MHz, $CDCl_3$, *Z* isomer, major): δ 8.67 (s, 1H), 8.16 – 8.06 (m, 1H), 7.57 – 7.50 (m, 1H), 7.46 – 7.40 (m, 2H), 7.38 – 7.33 (m, 2H), 7.32 – 7.25 (m, 2H), 4.33 (q, *J* = 7.1 Hz, 2H), 1.34 (t, *J* = 7.1 Hz, 3H).

^{13}C-NMR (75 MHz, $CDCl_3$, *Z* isomer, major): δ 163.16, 139.35, 135.70, 134.80, 132.79, 132.14, 129.64, 128.87, 128.83, 128.16, 124.26, 121.30, 115.14, 94.97, 88.01, 62.89, 14.29.

IR (neat, cm^{-1}): 2972, 2927, 1723, 1614, 1489, 1389, 1231, 1085, 1034, 984, 863, 816, 750;

HRMS (ESI): exact m/z calculated for $C_{19}H_{14}BrClNaO_2$ $(M+Na)^+$: 410.9758; Found: 410.9758 $(M+Na)^+$.

Mp: 55-57 ^oC (decomposed).

Ethyl 2-bromo-3-(2-((4-bromophenyl)ethynyl)phenyl)acrylate (1l):

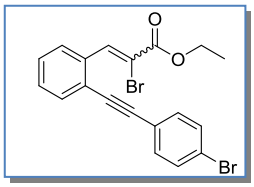

Following **GP-3**, **1l** was prepared from **S1l** (320 mg, 1.12 mmol). Purification of the crude product by column chromatography (Hexanes: EtOAc, 9:1, R_f = 0.52) afforded **1l** as a brown solid (445 mg, 91% yield, *Z:E* = 76:24).

^{1}H-NMR (300 MHz, $CDCl_3$, *Z* isomer, major): δ 8.71 (s, 1H), 8.19 – 8.12 (m, 1H), 8.18 – 8.11 (m, 1H), 7.61 – 7.56 (m, 1H), 7.53 – 7.47 (m, 2H), 7.44 – 7.37 (m, 4H), 4.38 (q, *J* = 7.1 Hz, 2H), 1.38 (t, *J* = 7.1 Hz, 3H).

^{13}C-NMR (75 MHz, $CDCl_3$, *Z* isomer, major): δ 163.15, 139.34, 135.71, 132.98, 132.14, 131.75, 129.64, 128.88, 128.19, 124.24, 123.05, 121.76, 115.16, 95.02, 88.19, 62.89, 14.30.

IR (neat, cm^{-1}): 2975, 2928, 1714, 1606, 1488, 1391, 1364, 1338, 1284, 1220, 1108, 1068, 1026, 1007, 885, 864, 815, 790, 745.

HRMS (ESI): exact m/z calculated for $C_{19}H_{14}Br_2NaO_2$ $(M+Na)^+$: 454.9253; Found: 454.9253 $(M+Na)^+$.

Mp: 58-60 ^oC (decomposed).

Ethyl 2-bromo-3-(2-(p-tolylethynyl)phenyl)acrylate (1m):

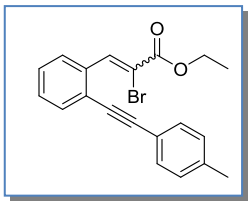

Following **GP-3**, **1m** was prepared from **S1m** (418 mg, 1.89 mmol). Purification of the crude product by column chromatography (Hexanes: EtOAc, 9:1, R_f = 0.56) afforded **1m** as a brown oil (623 mg, 89% yield, *Z:E* = 80:20).

^{1}H-NMR (300 MHz, $CDCl_3$, *Z* isomer, major): δ 8.75 (s, 1H), 8.18 – 8.10 (m, 1H), 7.61 – 7.54 (m, 1H), 7.42 (dd, *J* = 8.8, 5.8 Hz, 2H), 7.40 – 7.33 (m, 2H), 7.19 – 7.11 (m, 2H), 4.36 (q, *J* = 7.1 Hz, 2H), 1.37 (t, *J* = 7.1 Hz, 3H).

^{13}C-NMR (75 MHz, $CDCl_3$, *Z* isomer, major): δ 163.21, 139.59, 139.00, 135.54, 132.05, 131.51, 129.61, 129.22, 128.82, 127.72, 124.92, 119.74, 114.95, 96.50, 86.51, 62.83, 21.60, 14.29.

IR (neat, cm^{-1}): 2976, 2212, 1720, 1608, 1601, 1510, 1468, 1366, 1229, 1034, 982, 868, 839, 814, 756

HRMS (ESI): exact m/z calculated for $C_{20}H_{17}BrNaO_2$ $(M+Na)^+$: 391.0304; Found: 391.0311 $(M+Na)^+$.

Ethyl 2-bromo-3-(2-((4-isopropylphenyl)ethynyl)phenyl)acrylate (1n):

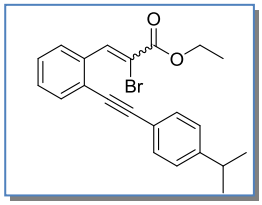

Following **GP-3**, **1n** was prepared from **S1n** (350 mg, 1.4 mmol). Purification of the crude product by column chromatography (Hexanes: EtOAc, 9:1, R_f = 0.43) afforded **1n** as a yellow viscous oil (473 mg, 84% yield, *Z:E* = 77:23).

^{1}H-NMR (300 MHz, $CDCl_3$, *Z* isomer, major): δ 8.75 (s, 1H), 8.18 – 8.08 (m, 1H), 7.62 – 7.53 (m, 1H), 7.52 – 7.43 (m, 2H), 7.41 – 7.34 (m, 2H), 7.26 – 7.16 (m, 2H), 4.37 (q, *J* = 7.1 Hz, 2H), 2.91 (hept, *J* = 6.9 Hz, 1H), 1.37 (t, *J* = 7.1 Hz, 3H), 1.24 (d, *J* = 6.9 Hz, 6H).

^{13}C-NMR (75 MHz, $CDCl_3$, *Z* isomer, major): δ 163.22, 149.89, 139.62, 135.57, 132.07, 131.63, 129.61, 128.82, 127.72, 126.61, 124.94, 120.11, 114.94, 96.53, 86.44, 62.84, 34.17, 23.83, 14.29.

IR (neat, cm^{-1}): 2959, 2214, 1722, 1610, 1509, 1464, 1412, 1334, 1230, 1092, 1036, 831, 752;

HRMS (ESI): exact m/z calculated for $C_{22}H_{21}BrNaO_2$ $(M+Na)^+$: 419.0617; Found: 419.0621 $(M+Na)^+$.

Ethyl 2-bromo-3-(2-((4-(tert-butyl)phenyl)ethynyl)phenyl)acrylate (1o):

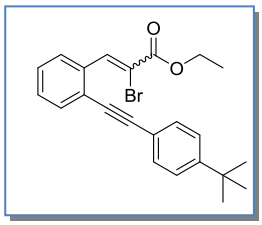

Following **GP-3**, **1o** was prepared from **S1o** (350 mg, 1.34 mmol). Purification of the crude product by column chromatography (Hexanes: EtOAc, 9:1, R_f = 0.32) afforded **1o** as a yellow oil (472 mg, 86% yield, *Z:E* = 80:20).

^{1}H-NMR (300 MHz, $CDCl_3$, *Z* isomer, major): δ 8.75 (s, 1H), 8.18 – 8.10 (m, 1H), 7.62 – 7.55 (m, 1H), 7.53 – 7.44 (m, 2H), 7.40 – 7.25 (m, 4H), 4.36 (q, *J* = 7.1 Hz, 2H), 1.37 (t, *J* = 7.1 Hz, 4H), 1.32 (s, 9H).

^{13}C-NMR (75 MHz, $CDCl_3$, *Z* isomer, major): δ 162.13, 151.04, 138.54, 134.51, 131.00, 130.28, 128.51, 127.74, 126.63, 124.38, 123.85, 118.71, 113.85, 95.39, 85.42, 61.75, 33.80, 30.11, 13.20.

IR (neat, cm^{-1}): 2960, 2214, 1722, 1609, 1508, 1466, 1392, 1364, 1247, 1191, 1088, 1028, 832, 800, 758, 699.

HRMS (ESI): exact m/z calculated for $C_{23}H_{24}BrO_2$ $(M+H)^+$: 411.0954; Found: 411.0955 $(M+H)^+$.

Ethyl 2-bromo-3-(2-((2-cyanophenyl)ethynyl)phenyl)acrylate (1p):

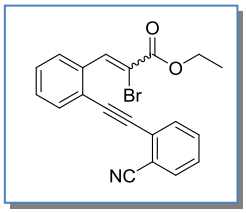

Following **GP-3**, **1p** was prepared from **S1p** (215 mg, 0.93 mmol). Purification of the crude product by column chromatography (Hexanes: EtOAc, 9:1, R_f = 0.27) afforded **1p** as a pale yellow solid (279 mg, 79% yield, *Z:E* = 85:15).

^{1}H-NMR (300 MHz, $CDCl_3$, *Z* isomer, major): δ 8.69 (s, 1H), 8.13 – 8.08 (m, 1H), 7.73 – 7.64 (m, 3H), 7.59 (tt, *J* = 7.7, 1.8 Hz, 1H), 7.50 – 7.38 (m, 3H), 4.38 (q, *J* = 7.1 Hz, 2H), 1.38 (t, *J* = 7.1 Hz, 3H).

^{13}C-NMR (75 MHz, $CDCl_3$, *Z* isomer, major): δ 163.13, 139.06, 136.15, 133.00, 132.72, 132.45, 132.41, 129.57, 128.95, 128.72, 126.73, 123.06, 117.38, 116.02, 115.10, 93.27, 91.53, 62.89, 14.23.

IR (neat, cm^{-1}): 2976, 2227, 1714, 1592, 1486, 1442, 1389, 1366, 1330, 1284, 1218, 1098, 1036, 980, 902, 874, 839, 753.

HRMS (ESI): exact m/z calculated for $C_{20}H_{15}BrNO_2$ $(M+H)^+$: 380.0281; Found: 380.0284 $(M+H)^+$.

Mp: 91-93 °C (decomposed).

Ethyl 2-bromo-3-(2-((4-nitrophenyl)ethynyl)phenyl)acrylate (1q):

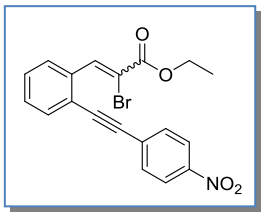

Following **GP-3**, **1q** was prepared from **S1q** (251 mg, 1.0 mmol). Purification of the crude product by column chromatography (Hexanes: EtOAc, 4:1, R_f = 0.47) afforded **1q** as a yellow solid (324 mg, 81% yield, *Z:E* = 99:01).

^{1}H-NMR (300 MHz, $CDCl_3$, *Z* isomer, major): δ 8.66 (s, 1H), 8.23 – 8.15 (m, 2H), 8.15 – 8.07 (m, 1H), 7.69 – 7.61 (m, 2H), 7.61 – 7.55 (m, 1H), 7.41 (pd, *J* = 7.4, 1.5 Hz, 2H), 4.35 (q, *J* = 7.1 Hz, 2H), 1.36 (t, *J* = 7.1 Hz, 3H).

^{13}C-NMR (75 MHz, $CDCl_3$, *Z* isomer, major): δ 163.07, 147.25, 138.98, 136.16, 132.45, 132.28, 129.01, 128.99, 123.75, 123.26, 115.59, 93.90, 92.12, 62.99, 14.30.

IR (neat, cm^{-1}): 2985, 2213, 1721, 1589, 1511, 1469, 1445, 1367, 1340, 1231, 1195, 1104, 1032, 849, 748, 684.

HRMS (ESI): exact m/z calculated for $C_{19}H_{14}BrNNaO_4$ $(M+Na)^+$: 421.9998; Found: 421.9997 $(M+Na)^+$.

Mp: 104-106 °C

Ethyl 2-bromo-3-(2-((4-(trifluoromethyl)phenyl)ethynyl)phenyl)acrylate (1r):

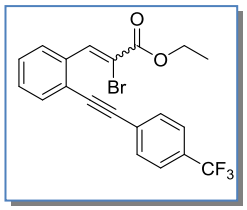

Following **GP-4**, **1r** was prepared from **S1r** (330 mg, 1.2 mmol). Purification of the crude product by column chromatography (Hexanes: EtOAc, 9:1, R_f = 0.67) afforded **1r** as a brown viscous oil (465 mg, 91% yield, *Z:E* = 76:24).

^{1}H-NMR (300 MHz, $CDCl_3$, *Z* isomer, major): δ 8.73 (s, 1H), 8.20 – 8.14 (m, 1H), 7.70 – 7.59 (m, 5H), 7.43 (tt, *J* = 8.9, 3.0 Hz, 1H), 7.36 – 7.30 (m, 1H), 4.39 (q, *J* = 7.1 Hz, 2H), 1.39 (t, *J* = 7.1 Hz, 3H).

^{13}C-NMR (75 MHz, $CDCl_3$, *Z* isomer, major): δ 162.05, 138.13, 134.90, 133.18, 131.25, 128.58, 127.85, 127.47, 126.48, 125.56, 124.33 (q, *J* = 3.8 Hz), 122.73, 114.30, 93.42, 88.25, 61.85, 13.20.

^{19}F-NMR (282 MHz, $CDCl_3$, *Z* isomer): δ -63.30.

IR (neat, cm^{-1}): 2962, 1722, 1612, 1470, 1404, 1319, 1251, 1165, 1122, 1062, 1014, 839, 800, 758, 697.

HRMS (ESI): exact m/z calculated for $C_{20}H_{14}BrF_3NaO_2$ $(M+Na)^+$: 445.0021; Found: 445.0024 $(M+Na)^+$.

Methyl 4-((2-(2-bromo-3-ethoxy-3-oxoprop-1-en-1-yl)phenyl)ethynyl)benzoate (1s):

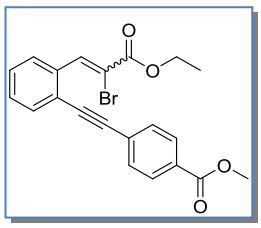

Following **GP-3**, **1s** was prepared from **S1s** (370 mg, 1.4 mmol). Purification of the crude product by column chromatography (Hexanes: EtOAc, 9:1, R_f = 0.26) afforded **1s** as a brown solid (509 mg, 88% yield, *Z:E* = 72:28).

^{1}H-NMR (300 MHz, $CDCl_3$, *Z* isomer, major): δ 8.68 (s, 1H), 8.15 – 8.09 (m, 1H), 8.02 – 7.96 (m, 2H), 7.60 – 7.52 (m, 3H), 7.41 – 7.34 (m, 2H), 4.34 (q, *J* = 7.1 Hz, 2H), 3.88 (s, 3H), 1.34 (t, *J* = 7.1 Hz, 3H).

^{13}C-NMR (75 MHz, $CDCl_3$, *Z* isomer, major): δ 166.48, 163.11, 139.21, 135.91, 132.31, 131.48, 129.66, 129.60, 128.91, 128.47, 128.01, 127.45, 123.96, 115.37, 95.20, 89.89, 62.93, 52.33, 14.30; **IR (neat, cm^{-1}):** 2958, 2926, 1715, 1704, 1602, 1462, 1447, 1428, 1271, 1244, 1189, 1105, 1031, 979, 959, 791, 886, 857, 838, 761, 749, 693.

HRMS (ESI): exact m/z calculated for $C_{21}H_{17}BrNaO_4$ $(M+Na)^+$: 435.0202; Found: 435.0209 $(M+Na)^+$.

Mp: 77-79 ^{o}C (decomposed).

Ethyl 3-(2-((4-acetylphenyl)ethynyl)phenyl)-2-bromoacrylate (1t):

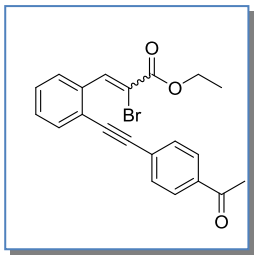

Following **GP-3**, **1t** was prepared from **S1t** (266 mg, 0.91 mmol). The crude product treated with aq. HCl (1 M, 10 mL) and reaction mixture was neutralized with saturated sodium bicarbonate solution. The crude product purified by column chromatography (Hexanes: EtOAc, 9:1, R_f = 0.13) afforded **1t** as a yellow solid (285 mg, 79% yield, *Z:E* = 85:15).

^{1}H-NMR (300 MHz, $CDCl_3$, *Z* isomer, major): δ 8.70 (s, 1H), 8.17 – 8.10 (m, 1H), 7.95 – 7.87 (m, 2H), 7.63 – 7.57 (m, 3H), 7.44 – 7.34 (m, 2H), 4.36 (q, *J* = 7.1 Hz, 2H), 2.58 (s, 3H), 1.37 (t, *J* = 7.1 Hz, 3H).

^{13}C-NMR (75 MHz, $CDCl_3$, *Z* isomer, major): δ 197.22, 163.05, 139.14, 136.50, 135.86, 132.31, 131.67, 129.67, 128.88, 128.52, 128.34, 127.58, 123.91, 115.31, 95.21, 90.22, 62.91, 26.66, 14.31.

IR (neat, cm^{-1}): 2973, 1722, 1683, 1598, 1557, 1468, 1424, 1402, 1259, 1217, 1109, 1028, 988, 955, 901, 868, 831, 753, 726.

HRMS (ESI): exact m/z calculated for $C_{21}H_{18}BrO_3$ $(M+H)^+$: 397.0434; Found: 397.044 $(M+H)^+$.

Mp: 89-91 ^{o}C (decomposed).

Ethyl 2-bromo-3-(2-((4-formylphenyl)ethynyl)phenyl)acrylate (1u):

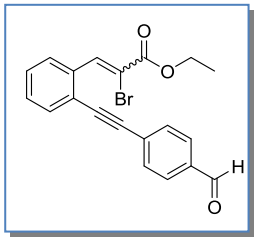

Following **GP-3**, **1u** was prepared from **S1u** (935 mg, 3.36 mmol). The crude product treated with aq. HCl (1 M, 10 mL) and reaction mixture was neutralized with saturated sodium bicarbonate solution. The crude product purified by column chromatography (Hexanes: EtOAc, 4:1, R_f = 0.6) afforded **2u** as a yellow solid (879 mg, 68% yield, *Z:E* = 80:20).

^{1}H-NMR (300 MHz, $CDCl_3$, *Z* isomer, major): δ 9.96 (s, 1H), 8.66 (s, 1H), 8.14 – 8.06 (m, 1H), 7.84 – 7.78 (m, 2H), 7.68 – 7.59 (m, 2H), 7.58 – 7.52 (m, 1H), 7.43 – 7.31 (m, 2H), 4.33 (q, *J* = 7.1 Hz, 2H), 1.33 (t, *J* = 7.1 Hz, 3H).

^{13}C-NMR (75 MHz, $CDCl_3$, *Z* isomer, major): ^{13}C δ 191.37, 163.06, 139.09, 135.98, 135.72, 132.38, 132.08, 129.64, 128.93, 128.69, 123.72, 115.43, 95.04, 90.91, 62.94, 14.30.

IR (neat, cm^{-1}): 2984, 2864, 1722, 1694, 1598, 1561, 1468, 1445, 1387, 1278, 1239, 1199, 1167, 1113, 1091, 1031, 987, 889, 822, 744, 689.

HRMS (ESI): exact m/z calculated for $C_{20}H_{16}BrO_3$ $(M+H)^+$: 383.0277; Found: 383.0279 $(M+H)^+$.

Mp 68-70 ^{o}C (decomposed).

Ethyl 2-bromo-3-(2-((4-cyanophenyl)ethynyl)phenyl)acrylate (1v):

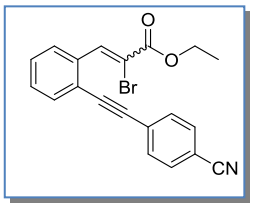

Following **GP-3**, **1v** was prepared from **S1v** (495 mg, 2.14 mmol). Purification of the crude product by column chromatography (Hexanes: EtOAc, 9:1, R_f = 0.42) afforded **1v** as a light brown solid (667 mg, 82% yield, *Z:E* = 70:30).

^{1}H-NMR (300 MHz, $CDCl_3$, *Z* isomer, major): δ 8.68 (s, 1H), 8.14 (dt, *J* = 4.4, 2.6 Hz, 1H), 7.69 – 7.58 (m, 5H), 7.43 (td, *J* = 7.0, 1.6 Hz, 1H), 7.36 – 7.29 (m, 1H), 4.38 (q, 7.1 Hz, 2H), 1.38 (t, *J* = 7.1 Hz, 3H).

^{13}C-NMR (75 MHz, $CDCl_3$, *Z* isomer): δ 163.07, 139.37, 139.03, 136.06, 132.39, 132.15, 132.05, 129.67, 128.62, 128.05, 127.69, 123.41, 118.43, 115.48, 111.94, 94.14, 91.26, 62.94, 14.28.

IR (neat, cm^{-1}): 2985, 2227, 1715, 1602, 1502, 1468, 1444, 1387, 1367, 1219, 1091, 1031, 984, 836, 753.

HRMS (ESI): exact m/z calculated for $C_{20}H_{15}BrNO_2$ $(M+H)^+$: 380.0281; Found: 380.0287 $(M+H)^+$.

Mp: 85-87 ^oC (decomposed).

Ethyl-2-bromo-3-(2-((*E*)-styryl)phenyl)acrylate (4):

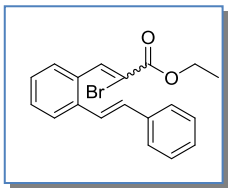

Following **GP-3**, **4** was prepared from **S1w** (416 mg, 2.00 mmol). Purification of the crude product by column chromatography (Hexanes: EtOAc, 9:1, R_f = 0.42) afforded **4** as a yellow oil (657 mg, 92% yield, *Z:E* = 77:23).

^{1}H-NMR (300 MHz, $CDCl_3$, *Z* isomer, major): δ 8.47 (s, 1H), 7.70 (ddd, *J* = 8.5, 5.5, 1.9 Hz, 1H), 7.59 – 7.51 (m, 2H), 7.46 – 7.30 (m, 2H), 7.29 – 7.18 (m, 1H), 7.06 (dd, *J* = 16.1, 2.3 Hz, 1H), 4.41 (q, *J* = 7.1 Hz, 2H), 1.42 (t, *J* = 7.1 Hz, 3H).

^{13}C-NMR (75 MHz, $CDCl_3$, *Z* isomer, major): δ 162.98, 140.84, 137.05, 136.67, 132.91, 132.35, 129.56, 129.22, 128.78, 128.15, 127.17, 126.82, 126.23, 125.64, 116.54, 62.87, 14.27;

IR (neat, cm^{-1}): 2981, 1719, 1608, 1493, 1472, 1447, 1390, 1366, 1327, 1234, 1218, 1201, 1092, 1031, 960, 860, 756, 689.

HRMS (ESI): exact m/z calculated for $C_{19}H_{18}BrO_2$ $(M+H)^+$: 357.0485; Found: 357.0485 $(M+H)^+$.

Ethyl (E)-3-(2-(phenylethynyl)phenyl)acrylate (6):

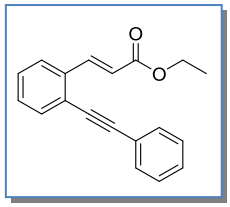

Following **GP-3**, **6** was prepared from **S1a** (412 mg, 2.0 mmol), triethylphosphonoacetate (672 mg, 3 mmol), and KO^t-Bu (336 mg, 3 mmol). Purification of the crude product by column chromatography (Hexanes: EtOAc, 95:05, R_f = 0.32) afforded **6** as a light yellow oil (518 mg, 94% yield, *E:Z* = 99:01).

^{1}H-NMR (300 MHz, $CDCl_3$, *E* isomer, major): δ 8.34 (d, *J* = 16.1 Hz, 1H), 7.69 – 7.53 (m, 4H), 7.43 – 7.29 (m, 5H), 6.58 (d, *J* = 16.1 Hz, 1H), 4.30 (q, *J* = 7.1 Hz, 2H), 1.37 (t, *J* = 7.1 Hz, 3H).

^{13}C-NMR (75 MHz, $CDCl_3$, *E* isomer, major): δ 166.93, 142.51, 135.78, 132.80, 131.69, 129.80, 128.74, 128.62, 128.51, 126.26, 124.09, 122.96, 119.84, 95.66, 87.15, 60.61, 14.40.

The obtained data is in accordance with the literature data.[34]

3.9.7 Reduction potentials of α-bromocinnamates:

The redox potentials of the *α*-bromocinnamates were measured in DMF containing 0.1 M tetra-*n*-butylammonium tetrafluoroborate as an electrolyte using ferrocene/ferrocenium (Fc/Fc+) as an internal reference. A glassy carbon electrode (working electrode), platinum wire counter electrode, and Ag quasi-reference electrode were employed. All values are given vs. Saturated Calomel Electrode (SCE). The scan rate was 50 mV S^{-1}.

α-Bromocinnamates	**Reduction potential (V)**
1a	-1.38
1b	-1.37
1c	-1.40
1d	-1.43
1e	-1.06
1f	-1.25
1g	-0.93
1h	-1.40
1i	-1.28
1j	-1.04
1k	-1.32
1l	-1.32
1m	-1.36
1n	-1.38
1o	-1.39
1p	-1.24
1q	-1.04
1r	-1.29
1s	-1.29
1t	-1.25
1u	-1.23
1v	-1.27
4	-1.51

Table 3.5: Redox potentials of the α-bromocinnamate ethyl esters vs SCE.

3.9.8 General procedure (GP-4) for visible-light photocatalysis:

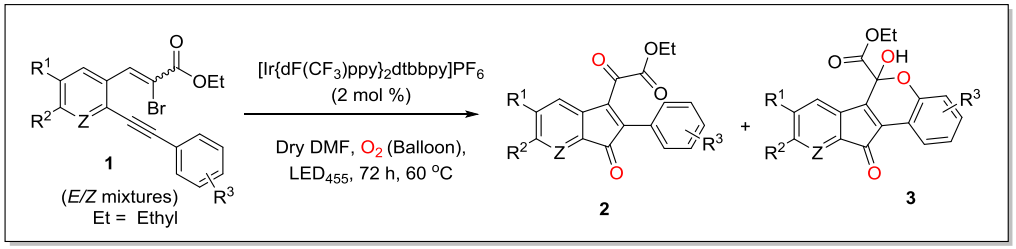

To a oven dried 10/25 mL three-necked flask was charged with **1** (0.50 mmol, 1.00 equiv) and $[Ir\{dF(CF_3)ppy\}_2(dtb\text{-}bpy)]PF_6$ (5.6 mg, 0.01 equiv, 1.00 mol %) in 3 mL anhydrous DMF. The reaction mixture was bubbled with oxygen balloon for 30 min, the flask was closed under positive oxygen atmosphere, and the reaction mixture was vigorously stirred (~1000 rpm) at 60 ^{o}C with internal irradiation of blue light (LED 455 nm). After 36 h, additional photocatalyst (5.6 mg, 1.00 mol %) was added to the reaction mixture under positive oxygen flow; after 72 h, distilled water (20 mL) was added to dilute the reaction mixture, the resulting dark red coloured mixture then transferred to the separatory funnel and extracted with ethyl acetate (3 x 10 mL). The combined organic layer was washed with brine (15 ml) and dried over Na_2SO_4. The residue was purified by flash column chromatography (SiO_2) with Hexanes/EtOAc as a solvent system.

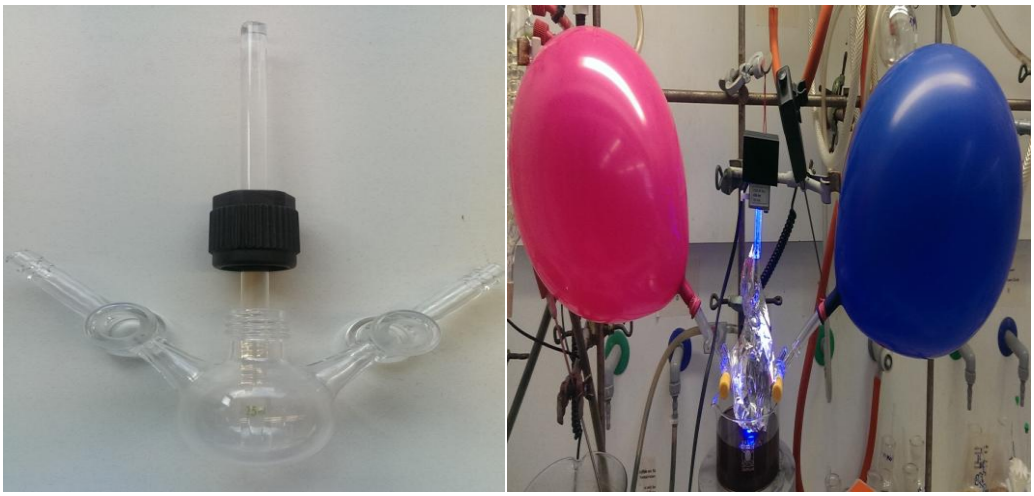

Figure 3.2: Reaction setup for photocatalytic oxidation reaction.

3.9.9 General procedure (GP-5): Photocatalysis with rotating film reactor:

A solution of 0.50 mmol **1** in 2 ml DMF and [Ir{dF(CF_3)ppy}$_2$(dtb-bpy)]PF_6 (5.6 mg, 0.01 equiv, 1.00 mol %) catalyst is slowly rotated in presence of oxygen atmosphere with an external irradiation of blue light for 24 h. Then distilled water (20 mL) was added to dilute the reaction mixture, the resulting dark red coloured mixture then transferred to the separatory funnel and extracted with ethyl acetate (3 x 10 mL). The combined organic layer was washed with brine (15 ml) and dried over Na_2SO_4. The resulting residue was purified by flash column chromatography (SiO_2) with Hexanes/EtOAc as solvent system.

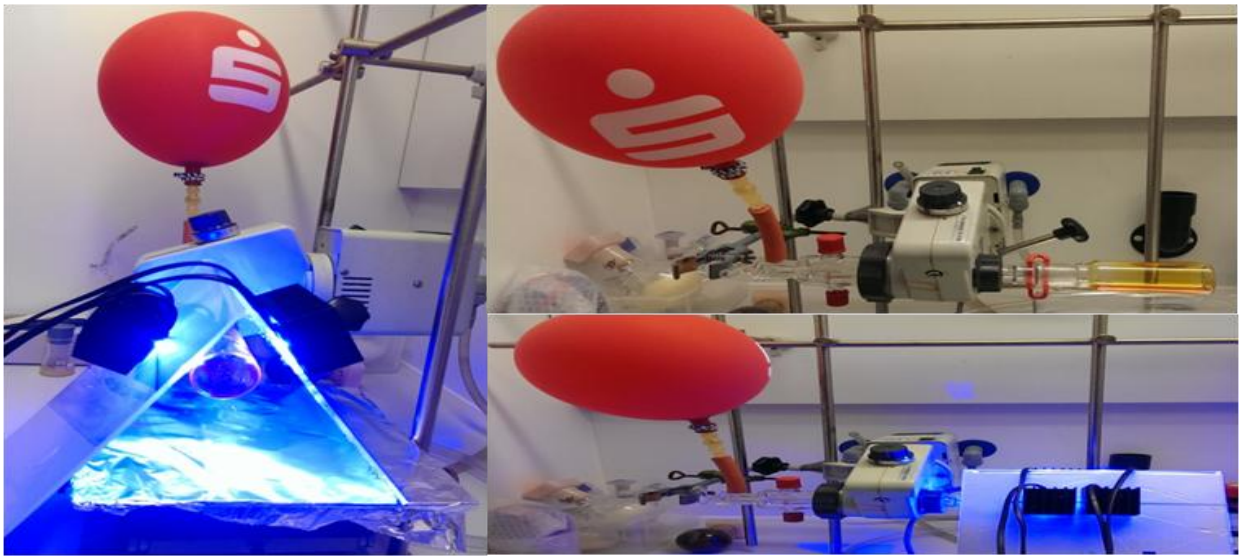

Figure 3.3: Rotating film reactor setup for photocatalytic oxidation reaction.

Ethyl 2-oxo-2-(1-oxo-2-phenyl-1*H*-inden-3-yl)acetate (2a):

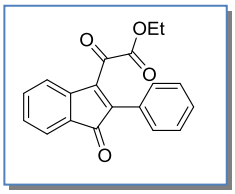

Following **GP-4**, **2a** was prepared from **1a** (177 mg, 0.50 mmol). Purification of the crude product by column chromatography (Hexanes: EtOAc, 9:1, R_f = 0.55) afforded **2a** as a light red solid (30 mg, 20% yield); **GP-5:** (33 mg, 22% yield).

^{1}H-NMR (300 MHz, $CDCl_3$): δ 7.56 (t, *J* = 6.6 Hz, 2H), 7.46 – 7.33 (m, 6H), 7.31 – 7.24 (m, 1H), 3.74 (q, *J* = 7.2 Hz, 2H), 0.94 (t, *J* = 7.2 Hz, 3H).

^{13}C-NMR (75 MHz, $CDCl_3$): δ 195.64, 186.22, 160.97, 143.62, 142.50, 141.92, 134.82, 130.44, 129.84, 129.57, 129.49, 129.19, 128.71, 124.42, 122.90, 62.66, 13.47.

IR (neat, cm^{-1}): 3059, 2923, 1722, 1661, 1594, 1564, 1445, 1371, 1285, 1247, 1209, 1180, 1106, 1083, 1039, 1010, 958, 909, 864, 847, 801, 784, 754, 719, 699, 673.

HRMS (ESI): exact m/z calculated for $C_{19}H_{15}O_4$ $(M+H)^+$: 307.0965; Found: 307.0969 $(M+H)^+$.

Mp: 98-100 ^oC (decomposed).

Ethyl 2-(5-methoxy-1-oxo-2-phenyl-1*H*-inden-3-yl)-2-oxoacetate (2b):

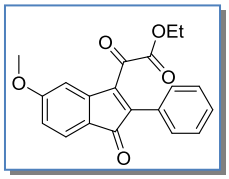

Following **GP-4**, **2b** was prepared from **1b** (192 mg, 0.50 mmol). Purification of the crude product by column chromatography (Hexanes: EtOAc, 9:1, R_f = 0.49) afforded **2b** as a light red solid (104 mg, 62% yield).

^{1}H-NMR (300 MHz, $CDCl_3$): δ 7.57 (d, *J* = 8.1 Hz, 1H), 7.47 – 7.37 (m, 5H), 7.16 (t, *J* = 9.3 Hz, 1H), 6.71 (dd, *J* = 8.1, 2.2 Hz, 1H), 3.88 (s, 3H), 3.76 (q, *J* = 7.2 Hz, 2H), 0.98 (t, *J* = 7.2 Hz, 3H).

^{13}C-NMR (75 MHz, $CDCl_3$): δ 193.68, 186.07, 165.32, 161.10, 145.26, 144.04, 141.48, 130.46, 129.92, 129.75, 128.64, 126.54, 121.79, 112.15, 111.05, 62.59, 55.96, 13.46.

IR (neat, cm^{-1}): 2926, 2854, 1739, 1706, 1689, 1665, 1597, 1544, 1526, 1491, 1468, 1447, 1431, 1368, 1340, 1286, 1259, 1213, 1172, 1107, 1081, 1042, 1016, 935, 879, 863, 846, 804, 781, 756, 734, 694, 666.

HRMS (ESI): exact m/z calculated for $C_{20}H_{17}O_5$ $(M+H)^+$: 337.1071; Found: 337.1076 $(M+H)^+$.

Mp: 88-90 ^oC (decomposed).

Ethyl 2-oxo-2-(5-oxo-6-phenyl-5*H*-indeno[5,6-d][1,3]dioxol-7-yl)acetate (2c):

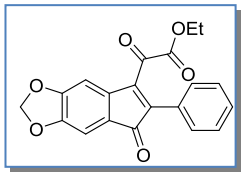

Following **GP-4**, **2c** was prepared from **1c** (200 mg, 0.50 mmol). Purification of the crude product by column chromatography (Hexanes: EtOAc, 9:1, R_f = 0.45) afforded **2c** as a dark brown solid (112 mg, 64% yield).

^{1}H-NMR (300 MHz, $CDCl_3$): δ 7.43 – 7.36 (m, 3H), 7.36 – 7.31 (m, 2H), 7.13 (s, 1H), 7.04 (s, 1H), 6.03 (s, 1H), 3.72 (q, *J* = 7.2 Hz, 2H), 0.95 (t, *J* = 7.2 Hz, 3H).

^{13}C-NMR (75 MHz, $CDCl_3$): δ 193.95, 185.96, 161.19, 152.79, 148.22, 142.15, 141.57, 139.57, 130.38, 129.80, 129.59, 128.63, 123.10, 105.86, 105.45, 102.50, 62.61, 13.45.

IR (neat, cm^{-1}): 2918, 1746, 1709, 1670, 1581, 1499, 1471, 1371, 1356, 1294, 1254, 1195, 1103, 1065, 1029, 1010, 928, 895, 874, 834, 787, 740, 694.

HRMS (ESI): exact m/z calculated for $C_{20}H_{15}O_6$ $(M+H)^+$: 351.0863; Found: 351.0868 $(M+H)^+$.

Mp: 114-116 ^oC (decomposed).

Ethyl 2-(5,6-dimethoxy-1-oxo-2-phenyl-1*H*-inden-3-yl)-2-oxoacetate (2d):

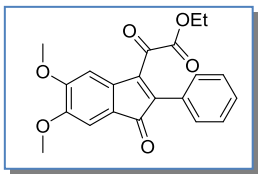

Following **GP-4**, **2d** was prepared from **1d** (207 mg, 0.50 mmol). Purification of the crude product by column chromatography (Hexanes: EtOAc, 9:1, R_f = 0.43) afforded **2d** as a dark brown solid (124 mg, 68% yield).

^{1}H-NMR (300 MHz, $CDCl_3$): δ 7.46 – 7.40 (m, 3H), 7.39 – 7.35 (m, 2H), 7.21 (s, 1H), 7.18 (s, 1H), 3.98 (s, 3H), 3.91 (s, 3H), 3.75 (q, *J* = 7.2 Hz, 2H), 0.97 (t, *J* = 7.2 Hz, 3H**).**

^{13}C-NMR (75 MHz, $CDCl_3$): δ 194.76, 186.25, 161.23, 153.85, 149.42, 142.25, 141.86, 137.70, 130.32, 129.78, 128.62, 121.33, 108.06, 107.04, 62.57, 56.53, 56.38, 13.45.

IR (neat, cm^{-1}): 2976, 2942, 1743, 1700, 1659, 1580, 1486, 1467, 1443, 1414, 1368, 1352, 1292, 1238, 1219, 1192, 1128, 1089, 1037, 1020, 893, 790, 754, 729, 695.

HRMS (ESI): exact m/z calculated for $C_{21}H_{19}O_6$ $(M+H)^+$: 367.1176; Found: 367.1179 $(M+H)^+$.

Mp: 148-150 ^oC (decomposed).

Ethyl 2-(5,6-dimethoxy-2-(4-nitrophenyl)-1-oxo-1*H*-inden-3-yl)-2-oxoacetate (2e):

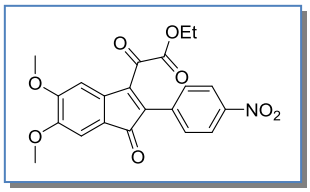

Following **GP-4**, **1e** was prepared from **1e** (230 mg, 0.50 mmol). Purification of the crude product by column chromatography (Hexanes: EtOAc, 4:1, R_f = 0.19) afforded **1e** as a dark brown solid (82 mg, 40% yield); (decomposed); **GP-5:** (100 mg, 49% yield).

^{1}H-NMR (600 MHz, $CDCl_3$): δ 8.27 (d, *J* = 8.7 Hz, 2H), 7.55 (d, *J* = 8.7 Hz, 2H), 7.20 (s, 1H), 7.16 (s, 1H), 3.99 (s, 3H), 3.93 (s, 3H), 3.88 (q, *J* = 7.2 Hz, 2H), 1.07 (t, *J* = 7.2 Hz, 3H).

^{13}C-NMR (151 MHz, $CDCl_3$): δ 193.48, 185.48, 160.62, 154.12, 150.16, 148.33, 144.61, 138.46, 136.91, 136.04, 130.53, 123.61, 121.19, 108.35, 107.34, 63.02, 56.60, 56.45, 13.57.

IR (neat, cm^{-1}): 2925, 2854, 1743, 1709, 1689, 1581, 1520, 1497, 1460, 1343, 1297, 1259, 1219, 1132, 1102, 1038, 1012, 865, 847, 800, 782, 763, 736, 692.

HRMS (ESI): exact m/z calculated for $C_{21}H_{18}NO_8$ $(M+H)^+$: 412.1027; Found: 412.1028 $(M+H)^+$.

Mp: 130-132 ^oC

Ethyl 2-(2-(4-methoxyphenyl)-1-oxo-1*H*-inden-3-yl)-2-oxoacetate (2f):

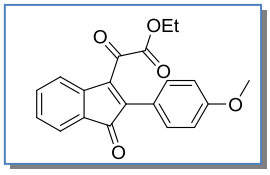

Following **GP-4**, **2f** was prepared from **1j** (192 mg, 0.50 mmol). Purification of the crude product by column chromatography (Hexanes: EtOAc, 9:1, R_f = 0.51) afforded **2f** as a red solid (107 mg, 64% yield).

^{1}H-NMR (300 MHz, $CDCl_3$): δ 7.58 – 7.54 (m, 2H), 7.42 (td, *J* = 7.6, 1.1 Hz, 1H), 7.38 – 7.32 (m, 2H), 7.29 – 7.21 (m, 1H), 6.95 – 6.89 (m, 2H), 3.82 (q, , *J* = 7.2 Hz, 2H), 3.81 (s, 3H), 0.99 (t, *J* = 7.2 Hz, 3H).

^{13}C-NMR (75 MHz, $CDCl_3$): δ 196.20, 186.31, 161.73, 161.31, 142.86, 141.79, 141.74, 134.84, 131.62, 129.20, 129.11, 124.31, 122.66, 122.20, 114.31, 62.62, 55.47, 13.54.

IR (neat, cm^{-1}): 2957, 2927, 2848, 1734, 1715, 1672, 1597, 1505, 1556, 1370, 1344, 1290, 1246, 1172, 1107, 1041, 1021, 948, 909, 853, 831, 814, 790, 750, 730, 711, 654.

HRMS (ESI): exact m/z calculated for $C_{20}H_{17}O_5$ $(M+H)^+$: 337.1071; Found: 337.1072 $(M+H)^+$.

Mp: 70-72 ^oC (decomposed).

Ethyl 2-(2-(4-chlorophenyl)-1-oxo-1*H*-inden-3-yl)-2-oxoacetate (2g):

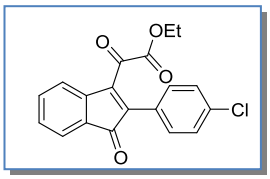

Following **GP-4**, **2g** was prepared from **1k** (194 mg, 0.50 mmol). Purification of the crude product by column chromatography (Hexanes: EtOAc, 9:1, R_f = 0.49) afforded **2g** as a light red solid (97 mg, 57% yield).

^{1}H-NMR (300 MHz, $CDCl_3$): δ 7.56 (ddd, *J* = 13.2, 6.8, 3.9 Hz, 2H), 7.43 (td, *J* = 7.5, 1.2 Hz, 1H), 7.40 – 7.26 (m, 5H), 3.84 (q, *J* = 7.2 Hz, 2H), 1.01 (t, *J* = 7.2 Hz, 3H).

^{13}C-NMR (75 MHz, $CDCl_3$): δ 195.27, 185.92, 160.87, 143.98, 142.29, 140.35, 136.81, 134.93, 131.06, 129.70, 129.06, 129.02, 127.97, 124.55, 122.99, 62.87, 13.53.

IR (neat, cm^{-1}): 2959, 2918, 2850, 1718, 1691, 1591, 1544, 1488, 1456, 1397, 1370, 1346, 1300, 1255, 1213, 1174, 1099, 1035, 1002, 949, 905, 729, 792, 754, 729, 706, 658.

HRMS (ESI): exact m/z calculated for $C_{19}H_{14}ClO_4$ $(M+H)^+$: 341.0575; Found: 341.058 $(M+H)^+$.

Mp: 105-107 ^oC (decomposed).

Ethyl 2-(2-(4-bromophenyl)-1-oxo-1*H*-inden-3-yl)-2-oxoacetate (2h):

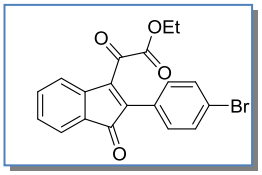

Following **GP-4**, **2h** was prepared from **1l** (217 mg, 0.50 mmol). Purification of the crude product by column chromatography (Hexanes: EtOAc, 9:1, R_f = 0.5) afforded **2h** as a yellow solid (87 mg, 45% yield).

^{1}H-NMR (300 MHz, $CDCl_3$): δ 7.60 – 7.51 (m, 4H), 7.44 (td, *J* = 7.5, 1.1 Hz, 1H), 7.30 (td, *J* = 7.6, 0.9 Hz, 1H), 7.26 – 7.21 (m, 2H), 3.85 (q, *J* = 7.2 Hz, 2H), 1.01 (t, *J* = 7.2 Hz, 3H).

^{13}C-NMR (75 MHz, $CDCl_3$): δ 195.18, 185.92, 160.86, 144.01, 142.29, 140.39, 134.94, 131.97, 131.23, 129.71, 129.07, 128.40, 125.15, 124.56, 123.00, 62.89, 13.53.

IR (neat, cm^{-1}): 2975, 2929, 1717, 1675, 1595, 1575, 1486, 1453, 1392, 1376, 1151, 1253, 1214, 1151, 1105, 1039, 1008, 847, 834, 795, 751, 729, 703, 679, 659.

HRMS (ESI): exact m/z calculated for $C_{19}H_{13}BrNaO_4$ $(M+Na)^+$: 406.9889; Found: 406.9894 $(M+Na)^+$.

Mp: 98-100 ^oC (decomposed).

Ethyl 2-oxo-2-(1-oxo-2-(*p*-tolyl)-1*H*-inden-3-yl)acetate (2i):

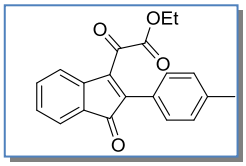

Following **GP-4**, **2i** was prepared from **1m** (184 mg, 0.50 mmol). Purification of the crude product by column chromatography (Hexanes: EtOAc, 9:1, R_f = 0.53) afforded **2i** as a red viscous oil (94 mg, 59% yield).

^{1}H-NMR (300 MHz, $CDCl_3$): δ 7.58 – 7.52 (m, 2H), 7.40 (td, *J* = 7.6, 1.0 Hz, 1H), 7.23 (dt, *J* = 12.0, 7.7 Hz, 5H), 3.76 (q, *J* = 7.2 Hz, 2H), 2.34 (s, 3H), 0.94 (t, *J* = 7.2 Hz, 3H).

^{13}C-NMR (75 MHz, $CDCl_3$): δ 195.88, 186.29, 161.12, 142.84, 142.66, 142.10, 141.03, 134.79, 129.85, 129.44, 129.29, 129.23, 126.77, 124.33, 122.76, 62.59, 21.55, 13.44.

IR (neat, cm^{-1}): 2975, 2932, 2873, 1719, 1675, 1596, 1509, 1459, 1374, 1286, 1244, 1179, 1104, 1040, 1010, 909, 855, 791, 752, 727, 710.

HRMS (ESI): exact m/z calculated for $C_{20}H_{17}O_4$ $(M+H)^+$: 321.1121; Found: 321.1122 $(M+H)^+$.

Ethyl 2-(2-(4-isopropylphenyl)-1-oxo-1*H*-inden-3-yl)-2-oxoacetate (2j):

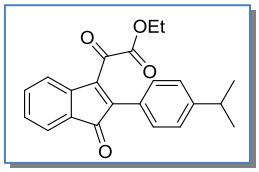

Following **GP-4**, **2j** was prepared from **1n** (198 mg, 0.50 mmol). Purification of the crude product by column chromatography (Hexanes: EtOAc, 9:1, R_f = 0.5) afforded **2j** as a red solid (99 mg, 57% yield).

^{1}H-NMR (300 MHz, $CDCl_3$): δ 7.61 (dd, *J* = 6.6, 1.1 Hz, 2H), 7.46 (td, *J* = 7.6, 1.1 Hz, 1H), 7.37 – 7.25 (m, 5H), 3.78 (q, *J* = 7.2 Hz, 2H), 2.94 (hept, *J* = 6.9 Hz, 1H), 1.25 (d, *J* = 6.9 Hz, 6H), 0.94 (t, *J* = 7.2 Hz, 3H).

^{13}C-NMR (75 MHz, $CDCl_3$): δ 195.93, 186.28, 161.15, 151.86, 142.89, 142.70, 142.20, 134.79, 129.98, 129.29, 129.25, 127.16, 126.89, 126.59, 124.34, 122.80, 62.55, 34.19, 23.76, 13.40.

IR (neat, cm^{-1}): 2964, 2927, 2871, 1742, 1714, 1678, 1596, 1502, 1457, 1368, 1288, 1244, 1210, 1179, 1105, 1037, 1011, 948, 907, 850, 797, 752, 717, 654.

HRMS (ESI): exact m/z calculated for $C_{22}H_{20}NaO_4$ $(M+Na)^+$: 371.1254; Found: 371.1257 $(M+H)^+$.

Mp: 76-78 ^{o}C (decomposed).

Ethyl 2-(2-(4-(*tert*-butyl)phenyl)-1-oxo-1*H*-inden-3-yl)-2-oxoacetate (2k):

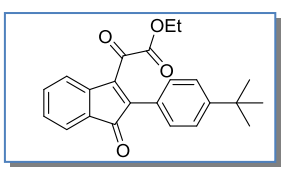

Following **GP-4**, **2k** was prepared from **1o** (205 mg, 0.50 mmol). Purification of the crude product by column chromatography (Hexanes: EtOAc, 9:1, R_f = 0.51) afforded **2k** as a red solid (94 mg, 52% yield).

^{1}H-NMR (300 MHz, $CDCl_3$): δ 7.60 – 7.55 (m, 2H), 7.46 – 7.39 (m, 3H), 7.33 – 7.21 (m, 3H), 3.73 (q, *J* = 7.2 Hz, 2H), 1.28 (s, 9H), 0.89 (t, *J* = 7.2 Hz, 3H**).**

^{13}C-NMR (75 MHz, $CDCl_3$): δ 195.97, 186.27, 161.16, 154.08, 142.93, 142.70, 142.19, 134.80, 129.70, 129.30, 129.26, 126.79, 125.76, 124.37, 122.82, 62.56, 34.97, 31.12, 13.39.

IR (neat, cm^{-1}): 2958, 2927, 2864, 1741, 1713, 1684, 1596, 1502, 1458, 1396, 1365, 1288, 1246, 1218, 1178, 1117, 1097, 1042, 1009, 952, 906, 856, 800, 756, 722, 657.

HRMS (ESI): exact m/z calculated for $C_{23}H_{23}O_4$ $(M+H)^+$: 363.1591; Found: 363.1597 $(M+H)^+$.

Mp: 73-75 ^oC (decomposed).

Ethyl 2-(2-(2-cyanophenyl)-5,6-dimethoxy-1-oxo-1*H*-inden-3-yl)-2-oxoacetate (2l):

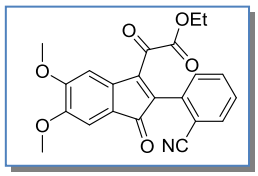

Following **GP-4**, **2l** was prepared from **1p** (190 mg, 0.50 mmol). Purification of the crude product by column chromatography (Hexanes: EtOAc, 4:1, R_f = 0.4) afforded **2l** as a yellow solid (92 mg, 56% yield).

^{1}H-NMR (300 MHz, $CDCl_3$): δ 7.79 (dd, *J* = 7.7, 0.9 Hz, 1H), 7.73 – 7.63 (m, 3H), 7.54 (dtd, *J* = 12.8, 7.6, 1.3 Hz, 2H), 7.38 (ddd, *J* = 8.4, 6.8, 0.8 Hz, 2H), 3.83 (q, *J* = 7.2 Hz, 2H), 1.10 (t, *J* = 7.2 Hz, 3H**).**

^{13}C-NMR (75 MHz, $CDCl_3$): δ 193.60, 184.84, 160.88, 146.23, 141.73, 139.15, 134.95, 133.33, 133.27, 132.55, 131.12, 130.31, 130.05, 128.92, 124.96, 124.02, 117.25, 113.31, 62.88, 13.60;

IR (neat, cm^{-1}): 2929, 2225, 1719, 1687, 1597, 1562, 1544, 1487, 1376, 1286, 1257, 1209, 1177, 1094, 1031, 1008, 852, 754, 719, 692.

HRMS (ESI): exact m/z calculated for $C_{20}H_{14}NO_4$ $(M+H)^+$: 332.0917; Found: 332.0919 $(M+H)^+$. Mp 115-117 ^oC (decomposed).

Ethyl 2-(6-methyl-1-oxo-2-phenyl-1*H*-inden-3-yl)-2-oxoacetate (2m):

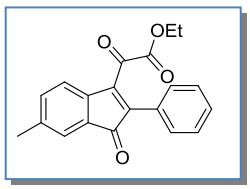

Following **GP-4**, **2m** was prepared from **1h** (184 mg, 0.50 mmol). Purification of the crude product by column chromatography (Hexanes: EtOAc, 9:1, R_f = 0.48) afforded **2m** as a red viscous oil (53 mg, 33% yield); (GP-7, Setup-B, 58 mg, 36% yield).

^{1}H-NMR (300 MHz, $CDCl_3$): δ 7.36 (m, 7H), 7.22 (m, 1H), 3.74 (q, *J* = 7.2 Hz, 2H), 2.34 (s, 3H), 0.94 (t, *J* = 7.2 Hz, 3H.

^{13}C-NMR (75 MHz, $CDCl_3$): δ 194.92, 185.26, 160.01, 142.84, 140.33, 138.85, 138.71, 133.79, 129.21, 128.73, 128.66, 128.49, 127.60, 124.33, 121.68, 61.55, 20.33, 12.40.

IR (neat, cm^{-1}): 2925, 1734, 1715, 1673, 1595, 1476, 1444, 1371, 1255, 1218, 1114, 1042, 1024, 938, 885, 860, 835, 791, 753, 737, 695.

HRMS (ESI): exact m/z calculated for $C_{20}H_{17}O_4$ $(M+H)^+$: 321.1121; Found: 321.1125 $(M+H)^+$.

Ethyl 2-(5-fluoro-1-oxo-2-phenyl-1*H*-inden-3-yl)-2-oxoacetate (2n):

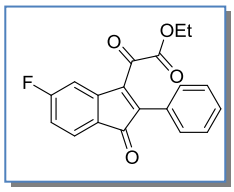

Following **GP-4**, **2n** was prepared from **1i** (186 mg, 0.50 mmol). Purification of the crude product by column chromatography (Hexanes: EtOAc, 9:1, R_f = 0.46) afforded **2n** as a light red solid (35 mg, 22% yield).

^{1}H-NMR (300 MHz, $CDCl_3$): δ 7.59 (dd, *J* = 8.1, 5.1 Hz, 1H), 7.46 – 7.32 (m, 6H), 6.98 – 6.90 (m, 1H), 3.74 (q, *J* = 7.2 Hz, 2H), 0.96 (t, *J* = 7.2 Hz, 3H).

^{13}C-NMR (75 MHz, $CDCl_3$): δ 193.71, 185.82, δ 166.89 (d, *J* = 257.0 Hz), 160.95, 145.64 (d, *J* = 10.6 Hz), 143.52, 141.42, 130.79, 129.94, 129.28, 128.76, 126.36 (d, *J* = 10.2 Hz), 125.06, 115.40 (d, *J* = 23.3 Hz), 111.98 (d, *J* = 26.6 Hz), 62.73, 13.45.

^{19}F-NMR (282 MHz, $CDCl_3$): δ -101.28.

IR (neat, cm^{-1}): 2923, 2852, 1742, 1720, 1676, 1597, 1461, 1444, 1371, 1254, 1214, 1174, 1103, 1072, 1037, 1016, 950, 868, 838, 822, 804, 788, 753, 732, 693, 657.

HRMS (ESI): exact m/z calculated for $C_{19}H_{12}FO_4$ $(M+H)^+$: 325.0871; Found: 325.0878 $(M+H)^+$.

Mp: 104-106 ^oC (decomposed).

Ethyl 6-hydroxy-11-oxo-6,11-dihydroindeno[1,2-c]chromene-6-carboxylate (3a):

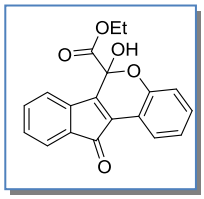

Following **GP-4**, **3a** was prepared from **1a** (177 mg, 0.50 mmol). Purification of the crude product by column chromatography (Hexanes: EtOAc, 4:1, R_f = 0.37) afforded **3a** as a red solid (98 mg, 61% yield). **GP-5:** (101 mg, 63% yield).

^{1}H-NMR (300 MHz, $CDCl_3$): δ 8.18 (dd, *J* = 7.7, 1.5 Hz, 1H), 7.55 – 7.50 (m, 1H), 7.38 – 7.20 (m, 3H), 7.07 (td, *J* = 7.6, 1.2 Hz, 1H), 6.99 (dd, *J* = 8.2, 0.8 Hz, 1H), 6.91 (dd, *J* = 4.3, 3.5 Hz, 1H), 5.22 (bs, 1H), 4.38 (q, *J* = 7.1 Hz, 2H), 1.25 (t, *J* = 7.1 Hz, 3H).

^{13}C-NMR (75 MHz, $CDCl_3$): δ 194.28, 168.52, 150.70, 142.27, 140.80, 134.16, 131.31, 130.37, 129.13, 126.75, 124.64, 123.69, 122.55, 120.12, 116.25, 114.84, 93.79, 64.15, 13.94.

IR (neat, cm^{-1}): 3341, 2972, 1744, 1703, 1624, 1594, 1562, 1490, 1457, 1370, 1293, 1263, 1232, 1214, 1169, 1122, 1091, 1057, 1032, 994, 854, 746, 708, 680.

HRMS (ESI): exact m/z calculated for $C_{19}H_{15}O_5$ $(M+H)^+$: 323.0914; Found: 323.0917 $(M+H)^+$.

Mp: 157-159 ^oC (decomposed).

Ethyl 6-hydroxy-11-oxo-6,11-dihydrochromeno[3',4':3,4]cyclopenta[1,2-b]pyridine-6-carboxylate (3b):

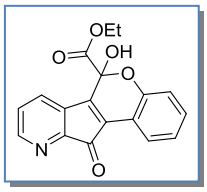

Following **GP-4**, **3b** was prepared from **1f** (178 mg, 0.50 mmol). Purification of the crude product by column chromatography (Hexanes: EtOAc, 4:1, R_f = 0.26) afforded **3b** as a red solid (88 mg, 55% yield).

^{1}H-NMR (300 MHz, $CDCl_3$): δ 8.52 (d, *J* = 4.1 Hz, 1H), 8.25 (dd, *J* = 7.7, 1.5 Hz, 1H), 7.40 – 7.28 (m, 2H), 7.23 (dd, *J* = 7.5, 5.1 Hz, 1H), 7.13 (dd, *J* = 10.9, 4.2 Hz, 1H), 7.05 (d, *J* = 7.6 Hz, 1H), 5.33 (bs, 1H), 4.42 (q, *J* = 7.1 Hz, 2H), 1.29 (t, *J* = 7.1 Hz, 3H).

^{13}C-NMR (151 MHz, $CDCl_3$): δ 192.77, 167.95, 151.12, 150.94, 149.20, 140.41, 136.85, 131.13, 126.75, 126.29, 125.98, 125.06, 122.80, 116.43, 113.91, 93.47, 64.26, 13.96.

IR (neat, cm^{-1}): 3399, 2956, 2922, 2852, 1762, 1735, 1576, 1460, 1415, 1367, 1329, 1296, 1256, 1222, 1173, 1147, 1133, 1106, 1063, 1029, 1011, 977, 948, 912, 889, 848, 801, 756, 720, 701, 677, 657.

HRMS (ESI): exact m/z calculated for $C_{18}H_{14}NO_5$ $(M+H)^+$: 324.0866; Found: 324.0873 $(M+H)^+$.

Mp: 147-149 ^{o}C (decomposed).

Ethyl 6-hydroxy-8-nitro-11-oxo-6,11-dihydroindeno[1,2-c]chromene-6-carboxylate (3c):

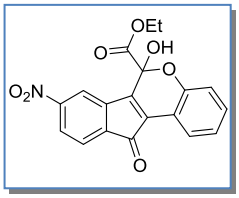

Following **GP-4**, **3c** was prepared from **1g** (200 mg, 0.50 mmol). Purification of the crude product by column chromatography (Hexanes: EtOAc, 4:1, R_f = 0.42) afforded **3c** as a brown solid (69 mg, 38% yield);

^{1}H-NMR (600 MHz, $CDCl_3$): δ 8.18 (dd, *J* = 7.9, 1.6 Hz, 2H), 7.70 (dd, *J* = 12.5, 4.8 Hz, 2H), 7.37 – 7.32 (m, 1H), 7.11 (dd, *J* = 11.0, 4.1 Hz, 1H), 7.03 (d, *J* = 8.2 Hz, 1H), 5.17 (s, 1H), 4.42 (q, *J* = 7.1 Hz, 2H), 1.28 (t, *J* = 7.1 Hz, 3H).

^{13}C-NMR (151 MHz, $CDCl_3$): δ 191.77, 167.67, 151.76, 151.06, 142.51, 140.69, 135.51, 131.50, 129.05, 125.15, 124.93, 123.73, 122.85, 116.54, 114.77, 114.01, 93.61, 64.50, 13.97.

IR (neat, cm^{-1}): 3393, 3099, 2921, 2852, 1755, 1713, 1612, 1591, 1536, 1449, 1375, 1341, 1305, 1256, 1217, 1122, 1084, 1067, 1040, 1002, 951, 898, 869, 843, 827, 791, 763, 735, 719, 687.

HRMS (ESI): exact m/z calculated for $C_{19}H_{17}N_2O_7$ $(M+NH_4)^+$: 385.103; Found: 385.103 $(M+NH_4)^+$.

Mp: 202-204 ^{o}C (decomposed).

Ethyl 6-hydroxy-3-nitro-11-oxo-6,11-dihydroindeno[1,2-c]chromene-6-carboxylate (3d):

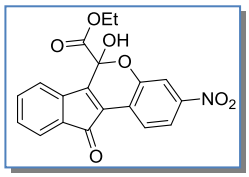

Following **GP-4**, **3d** was prepared from **1q** (200 mg, 0.50 mmol). Purification of the crude product by column chromatography (Hexanes: EtOAc, 4:1, R_f = 0.3) afforded **3d** as a dark brown solid (75 mg, 41% yield).

^{1}H-NMR (600 MHz, $CDCl_3$): δ 8.35 (d, *J* = 8.5 Hz, 1H), 7.95 (dd, *J* = 8.5, 2.2 Hz, 1H), 7.86 (d, *J* = 2.2 Hz, 1H), 7.60 (d, *J* = 7.1 Hz, 1H), 7.41 (td, *J* = 7.7, 1.0 Hz, 1H), 7.36 – 7.33 (m, 1H), 7.00 (d, *J* = 7.3 Hz, 1H), 5.32 (s, 1H), 4.41 (q, *J* = 7.1 Hz, 2H), 1.26 (t, *J* = 7.1 Hz, 3H).

^{13}C-NMR (75 MHz, $CDCl_3$): δ 193.08, 167.72, 150.76, 148.30, 145.76, 139.78, 134.53, 131.18, 130.38, 124.94, 124.17, 121.04, 120.63, 117.68, 111.85, 94.16, 64.64, 13.94.

IR (neat, cm^{-1}): 3466, 2924, 2854, 1759, 1701, 1587, 1517, 1457, 1417, 1378, 1339, 1295, 1252, 1228, 1161, 1127, 1084, 1066, 1040, 1010, 951, 851, 833, 799, 774, 753, 739, 711, 683.

HRMS (ESI): exact m/z calculated for $C_{19}H_{17}N_2O_7$ $(M+NH_4)^+$: 385.103; Found: 385.1034 $(M+NH_4)^+$.

Mp: 175-177 ^oC (decomposed).

Ethyl 6-hydroxy-11-oxo-3-(trifluoromethyl)-6,11-dihydroindeno[1,2-c]chromene-6-carboxylate (3e):

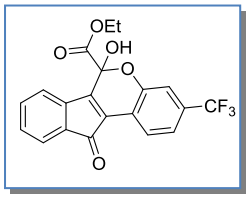

Following **GP-4**, **3e** was prepared from **1r** (211 mg, 0.50 mmol). Purification of the crude product by column chromatography (Hexanes: EtOAc, 4:1, R_f = 0.48) afforded **3e** as a red solid (91 mg, 47% yield), (GP-7, Setup B: 100 mg, 52% yield).

^{1}H-NMR (300 MHz, $CDCl_3$): δ 8.24 (d, *J* = 8.0 Hz, 1H), 7.54 – 7.49 (m, 1H), 7.33 (td, *J* = 7.7, 1.2 Hz, 1H), 7.29 – 7.24 (m, 2H), 7.21 (d, *J* = 4.0 Hz, 1H), 6.92 (d, *J* = 7.1 Hz, 1H), 5.30 (bs, 1H), 4.34 (q, *J* = 7.1 Hz, 2H), 1.21 (t, *J* = 7.1 Hz, 2H).

^{13}C-NMR (75 MHz, $CDCl_3$): δ 193.56, 168.03, 150.56, 144.38, 140.16, 134.34, 132.02, 131.58, 131.21, 129.83, 125.60, 125.40, 124.99, 123.95, 120.63, 119.21 (q, *J* = 7.7 Hz), 117.87, 113.47 (q, *J* = 8.5 Hz), 93.97, 64.42, 13.91.

^{19}F-NMR (282 MHz, $CDCl_3$): δ -63.39.

IR (neat, cm^{-1}): 3339, 2925, 1765, 1698, 1619, 1593, 1562, 1509, 1456, 1424, 1389, 1325, 1254, 1219, 1166, 1114, 1066, 1053, 997, 939, 875, 853, 833, 801, 769, 748, 716, 701, 682, 659.

HRMS (ESI): exact m/z calculated for $C_{20}H_{13}F_3NaO_5$ $(M+H)^+$: 413.0607; Found: 413.0609 $(M+H)^+$.

Mp: 145-147 ^oC (decomposed).

6-ethyl 3-methyl 6-hydroxy-11-oxo-6,11-dihydroindeno[1,2-c]chromene-3,6-dicarboxylate (3f):

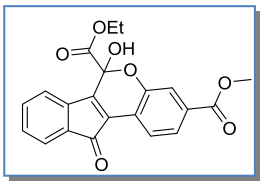

Following **GP-4**, **3f** was prepared from **1s** (206 mg, 0.50 mmol). Purification of the crude product by column chromatography (Hexanes: EtOAc, 4:1, R_f = 0.25) afforded **3f** as a yellow solid (104 mg, 55% yield); **GP-5:** (116 mg, 62% yield).

^{1}H-NMR (300 MHz, $CDCl_3$): δ 8.24 (d, *J* = 8.1 Hz, 1H), 7.73 (dd, *J* = 8.1, 1.6 Hz, 1H), 7.65 (d, *J* = 1.4 Hz, 1H), 7.58 – 7.53 (m, 1H), 7.37 (td, *J* = 7.7, 1.2 Hz, 1H), 7.32 – 7.28 (m, 1H), 6.97 (d, *J* = 7.1 Hz, 1H), 5.26 (bs, 1H), 4.38 (q, *J* = 7.1 Hz, 2H), 3.91 (s, 3H), 1.24 (t, *J* = 7.1 Hz, 3H).

^{13}C-NMR (75 MHz, $CDCl_3$): δ 193.69, 168.15, 166.38, 150.46, 144.53, 140.29, 134.31, 131.42, 131.29, 129.77, 126.00, 124.42, 123.90, 123.67, 120.64, 118.84, 117.37, 93.89, 64.30, 52.37, 13.93.

IR (neat, cm^{-1}): 3356, 2955, 2927, 1746, 1721, 1701, 1603, 1558, 1491, 1458, 1434, 1416, 1370, 1285, 1254, 1219, 1136, 1095, 1056, 1000, 927, 888, 855, 836, 803, 761, 734, 710, 686.

HRMS (ESI): exact m/z calculated for $C_{21}H_{17}O_7$ $(M+H)^+$: 381.0969; Found: 381.0968 $(M+H)^+$.

Mp: 156-158 ^oC (decomposed).

Ethyl 3-acetyl-6-hydroxy-11-oxo-6,11-dihydroindeno[1,2-c]chromene-6-carboxylate (3g):

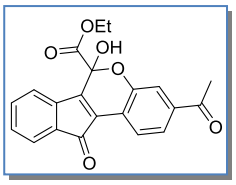

Following **GP-4**, **3g** was prepared from **1t** (198 mg, 0.50 mmol). Purification of the crude product by column chromatography (Hexanes: EtOAc, 4:1, R_f = 0.2) afforded **3g** as a red solid (109 mg, 60% yield).

^{1}H-NMR (600 MHz, $CDCl_3$): δ 8.28 (d, *J* = 8.0 Hz, 1H), 7.67 (dd, *J* = 8.0, 1.6 Hz, 1H), 7.59 – 7.56 (m, 2H), 7.40 – 7.36 (m, 1H), 7.30 (t, *J* = 7.4 Hz, 1H), 6.97 (d, *J* = 7.3 Hz, 1H), 5.21 (s, 1H), 4.39 (q, *J* = 7.1 Hz, 2H), 2.59 (s, 3H), 1.25 (t, *J* = 7.1 Hz, 1H).

^{13}C-NMR (151 MHz, $CDCl_3$): δ 197.00, 193.61, 168.23, 150.66, 144.64, 140.37, 138.15, 134.30, 131.36, 129.81, 126.01, 124.63, 123.91, 122.56, 120.63, 118.95, 115.95, 93.87, 64.36, 26.70, 13.92.

IR (neat, cm^{-1}): 3216, 2924, 2854, 1743, 1716, 1686, 1664, 1602, 1557, 1457, 1413, 1357, 1319, 1277, 1248, 1232, 1181, 1160, 1092, 1066, 1044, 1012, 967, 921, 884, 850, 825, 798, 757, 736, 710, 691.

HRMS (ESI): exact m/z calculated for $C_{21}H_{17}O_6$ $(M+H)^+$: 365.102; Found: 365.1026 $(M+H)^+$.

Mp: 176-178 ^oC (decomposed).

Ethyl 3-formyl-6-hydroxy-11-oxo-6,11-dihydroindeno[1,2-c]chromene-6-carboxylate (3h):

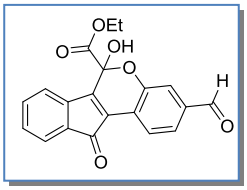

Following **GP-4**, **3h** was prepared from **1u** (764 mg, 2.0 mmol). Purification of the crude product by column chromatography (Hexanes: EtOAc, 4:1, R_f = 0.24) afforded **3h** as a brown red solid (404 mg, 58% yield); **GP-5:** (113 mg, 65% yield on 0.50 mmol scale).

^{1}H-NMR (300 MHz, $CDCl_3$): δ 9.90 (s, 1H), 8.30 (d, *J* = 7.9 Hz, 1H), 7.56 – 7.50 (m, 2H), 7.44 (d, *J* = 1.3 Hz, 1H), 7.34 (td, *J* = 7.7, 1.2 Hz, 1H), 7.30 – 7.21 (m, 1H), 6.95 (d, *J* = 7.1 Hz, 1H), 5.38 (bs, 1H), 4.35 (q, *J* = 7.1 Hz, 2H), 1.21 (t, *J* = 7.1 Hz, 3H).

^{13}C-NMR (75 MHz, $CDCl_3$): δ 193.49, 191.35, 167.99, 151.03, 145.31, 140.11, 137.32, 134.40, 131.27, 130.03, 125.79, 125.09, 124.42, 123.99, 120.85, 120.33, 116.43, 93.97, 64.39, 13.93.

IR (neat, cm^{-1}): 3412, 2925, 2853, 1757, 1740, 1695, 1602, 1557, 1509, 1458, 1424, 1375, 1322, 1274, 1234, 1172, 1145, 1089, 1068, 1043, 1001, 956, 916, 882, 850, 830, 798, 771, 753, 731, 715, 675.

HRMS (ESI): exact m/z calculated for $C_{20}H_{15}O_6$ $(M+H)^+$: 351.0863; Found: 351.0867 $(M+H)^+$.

Mp: 172-174 ^oC (decomposed).

Ethyl 3-cyano-6-hydroxy-11-oxo-6,11-dihydroindeno[1,2-c]chromene-6-carboxylate (3i):

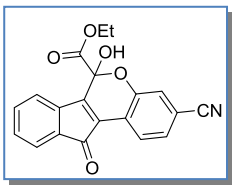

Following **GP-4**, **3i** was prepared from **1v** (190 mg, 0.50 mmol). Purification of the crude product by column chromatography (Hexanes: EtOAc, 4:1, R_f = 0.26) afforded **3i** as a yellow solid (83 mg, 48% yield).

^{1}H-NMR (600 MHz, $CDCl_3$): δ 8.29 (d, *J* = 8.0 Hz, 1H), 7.59 – 7.57 (m, 1H), 7.39 (td, *J* = 7.7, 1.1 Hz, 1H), 7.35 (dd, *J* = 8.0, 1.5 Hz, 1H), 7.34 – 7.31 (m, 1H), 7.25 (d, *J* = 1.4 Hz, 1H), 6.98 (d, *J* = 7.3 Hz, 1H), 5.31 (bs, 1H), 4.40 (q, *J* = 7.1 Hz, 2H), 1.26 (t, *J* = 7.1 Hz, 3H).

^{13}C-NMR (151 MHz, $CDCl_3$): δ 193.16, 167.77, 150.46, 145.20, 139.89, 134.43, 131.19, 130.16, 126.23, 125.22, 125.19, 124.07, 120.85, 119.68, 119.15, 118.29, 112.91, 93.98, 64.55, 13.91.

IR (neat, cm^{-1}): 3370, 2922, 2852, 2233, 1749, 1719, 1602, 1547, 1457, 1412, 1311, 1289, 1265, 1244, 1146, 1134, 1092, 1054, 1001, 859, 826, 796, 774, 755, 734, 713, 685.

HRMS (ESI): exact m/z calculated for $C_{20}H_{14}NO_5$ $(M+H)^+$: 348.0866; Found: 348.0867 $(M+H)^+$.

Mp: 131-133 ^oC (decomposed).

Ethyl 6-hydroxy-9-methyl-11-oxo-6,11-dihydroindeno[1,2-c]chromene-6-carboxylate (3j):

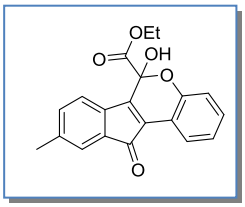

Following **GP-4**, **3j** was prepared from **1h** (184 mg, 0.50 mmol). Purification of the crude product by column chromatography (Hexanes: EtOAc, 4:1, R_f = 0.53) afforded **3j** as a red solid (67 mg, 40% yield); (GP-7, Setup B, 73 mg, 44% yield).

^{1}H-NMR (600 MHz, $CDCl_3$): δ 8.17 (dd, *J* = 7.7, 1.4 Hz, 1H), 7.35 (s, 1H), 7.28 – 7.23 (m, 1H), 7.12 (d, *J* = 7.4 Hz, 1H), 7.06 (dd, *J* = 10.9, 4.1 Hz, 1H), 6.98 (d, *J* = 8.2 Hz, 1H), 6.80 (d, *J* = 7.4 Hz, 1H), 5.08 (bs, 1H), 4.36 (q, *J* = 7.1 Hz, 2H), 2.34 (s, 3H), 1.25 (t, *J* = 7.1 Hz, 3H**).**

^{13}C-NMR (75 MHz, $CDCl_3$): δ 194.56, 168.59, 150.53, 142.67, 139.59, 137.90, 134.02, 131.69, 130.07, 126.17, 124.84, 124.48, 122.50, 119.93, 116.20, 115.02, 93.79, 64.10, 21.47, 13.95.

IR (neat, cm^{-1}): 3374, 2924, 2854, 1740, 1704, 1606, 1443, 1366, 1260, 1230, 1213, 1127, 1100, 1056, 1033, 1000, 902, 861, 845, 827, 786, 749, 724, 696.

HRMS (ESI): exact m/z calculated for $C_{20}H_{17}O_5$ $(M+H)^+$: 337.1071; Found: 337.1077 $(M+H)^+$.

Mp: 140-142 ^oC (decomposed).

Ethyl 8-fluoro-6-hydroxy-11-oxo-6,11-dihydroindeno[1,2-c]chromene-6-carboxylate (3k):

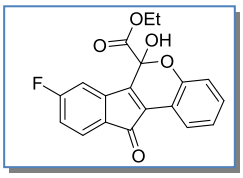

Following **GP-4**, **3k** was prepared from **1i** (186 mg, 0.50 mmol). Purification of the crude product by column chromatography (Hexanes: EtOAc, 4:1, R_f = 0.4) afforded **3k** as a red solid (86 mg, 51% yield).

^{1}H-NMR (600 MHz, $CDCl_3$): δ 8.17 (dd, *J* = 7.7, 1.5 Hz, 1H), 7.52 (dd, *J* = 8.0, 5.1 Hz, 1H), 7.32 – 7.27 (m, 1H), 7.07 (td, *J* = 7.6, 0.9 Hz, 1H), 6.99 (d, *J* = 8.2 Hz, 1H), 6.90 – 6.84 (m, 1H), 6.64 (dd, *J* = 8.1, 2.1 Hz, 1H), 5.10 (bs, 1H), 4.38 (q, *J* = 7.1, 2H), 1.26 (t, *J* = 7.1 Hz, 3H).

^{13}C-NMR (151 MHz, $CDCl_3$): δ 192.41, 168.21, 166.40 (d, *J* = 179.1 Hz), 150.94, 144.00 (d, *J* = 10.23 Hz), 139.95 (d, *J* = 2.78 Hz, 130.81, 128.32, 127.13, 125.51 (d, *J* = 10.1 Hz), 124.81, 122.64, 116.30, 114.63, 114.51 (*J* = 8.5 Hz), 109.09 (d, *J* = 26.22 Hz), 93.69, 64.27, 13.94.

^{19}F-NMR (282 MHz, $CDCl_3$): δ -103.41.

IR (neat, cm^{-1}): 3412, 2923, 2853, 1763, 1702, 1590, 1461, 1361, 1237, 1220, 1191, 1147, 1121, 1094, 1061, 1035, 1007, 972, 946, 875, 857, 840, 816, 784, 757, 728, 709.

HRMS (ESI): exact m/z calculated for $C_{19}H_{13}FNaO_5$ $(M+Na)^+$: 363.0639; Found: 363.064 $(M+Na)^+$.

Mp: 117-119 ^oC (decomposed).

Ethyl 1-benzylidene-1H-indene-2-carboxylate (5):

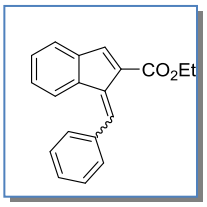

Following **GP-4**, **5** was prepared from **4** (178 mg, 0.50 mmol) and [Ir{dF(CF$_3$)ppy}$_2$(dtb-bpy)]PF$_6$ (5.6 mg, 1 mol %) in DMF (2 mL) under nitrogen atmosphere. Purification of the crude product by column chromatography (Hexanes: EtOAc, 9:1, R_f = 0.61) afforded **5** as a yellow oil (113 mg, *E/Z* = 1:1, 82% yield).

^{1}H-NMR (300 MHz, CDCl$_3$, isolated isomer): δ 8.35 (s, 1H), 7.93 – 7.87 (m, 1H), 7.82 (d, *J* = 7.9 Hz, 1H), 7.78 (s, 1H), 7.59 – 7.46 (m, 2H), 7.42 – 7.27 (m, 4H), 7.21 (s, 1H), 4.10 (q, *J* = 7.1 Hz, 2H), 0.99 (t, *J* = 7.1 Hz, 3H).

^{13}C-NMR (75 MHz, CDCl$_3$, isolated isomer): δ 168.78, 141.69, 138.80, 134.33, 131.60, 130.87, 129.65, 129.59, 128.60, 128.19, 128.03, 127.82, 127.40, 127.06, 126.72, 61.08, 13.74.

IR (neat, cm^{-1}): 2980, 1711, 1629, 1595, 1490, 1444, 1365, 1274, 1212, 1193, 1134, 1086, 1016, 894, 863, 762, 747, 697.

HRMS (ESI): exact m/z calculated for $C_{19}H_{16}O_2$ $(M)^+$: 276.1145; Found: $(M)^+$: 276.1146.

Diethyl (1*S*,2*S*,3*R*,4*R*)-3,4-bis(2-(phenylethynyl)phenyl)cyclobutane-1,2-dicarboxylate (7):

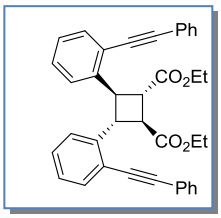

Following **GP-4**, **7** was prepared from **6** (138 mg, 0.50 mmol). Purification of the crude product by column chromatography (Hexanes: EtOAc, 9:1, R_f = 0.37) afforded **7** as a pale yellow oil [89 mg, 65% yield (under oxygen); 99 mg, 73% yield (under nitrogen)].

^{1}H-NMR (300 MHz, CDCl$_3$): δ 7.66 (d, *J* = 7.2 Hz, 1H), 7.52 – 7.41 (m, 3H), 7.37 – 7.30 (m, 3H), 7.27 (td, *J* = 7.6, 1.4 Hz, 1H), 7.14 (td, *J* = 7.5, 1.2 Hz, 1H), 4.55 – 4.51 (m, 1H), 4.02 (q, *J* = 7.1 Hz, 2H), 3.57 – 3.52 (m, 1H), 1.12 (t, *J* = 7.1 Hz, 3H).

^{13}C-NMR (75 MHz, CDCl$_3$): δ 172.71, 142.06, 132.60, 131.79, 129.00, 128.41, 127.08, 127.02, 123.39, 123.05, 93.65, 88.00, 61.05, 45.52, 45.03, 14.20.

IR (neat, cm^{-1}): 2925, 2854, 1723, 1598, 1493, 1443, 1368, 1318, 1201, 1157, 1095, 1027, 914, 855, 752, 689.

EI-MS: exact m/z calculated for $C_{38}H_{33}O_4$ $(M+H)^+$: 553.2373; Found: 553.2382 $(M+Na)^+$.

3.9.10 General procedure (GP-6) for 6π-electrocyclization:

a. Visible-light photocatalysis:

A solution of **2** (0.25 mmol and 2 mol % photocatalyst in 1 mL DMF) irradiated with blue light (λmax = 455 nm) in presence of oxygen atmosphere for 72 h at 60 ^{o}C. The distilled water (20 mL) was added to dilute the reaction mixture, the resulting red coloured mixture then transferred to the separatory funnel and extracted with ethyl acetate (3 x 10 mL). The combined organic layer was washed with brine (15 mL) and dried over Na_2SO_4. The purification by flash column chromatography (SiO_2) with Hexanes/EtOAc afforded **3**. (Note: we have also conducted these experiments in presence of stoichiometric amount of water (for a hydroxyl source), but we did not get any improvement in the yields).

b. UV-light experiment:

Followed the same procedure as mentioned above without adding a photocatalyst. The UV-light irradiation was done by Philips HPK 125 instrument (125 W Hg-lamp, λ =300 nm).

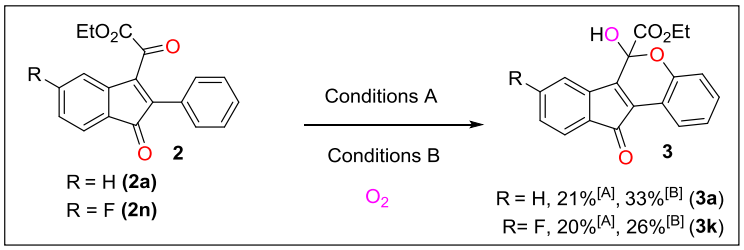

Conditions A: Substrate **2** (0.25 mmol, 1.0 equiv), $[Ir\{dF(CF_3)ppy\}_2(dtb\text{-}bpy)]PF_6$ (2 mol %), O_2, at 60 ^{o}C, in DMF, 72 h, LED_{455}. **Conditions B:** Substrate **2** (0.25 mmol, 1.0 equiv), UV-Light (125 W Hg-lamp, λ > 300 nm), O_2, at 60 ^{o}C, in DMF, 72 h.

3.9.11 General procedure (GP-7): Photocatalysis with micro(flow)reactor:

a. Micro(flow)reactor setup-A:

A solution of **1a** (177 mg, 0.50 mmol) in 5 mL DMF and [Ir{dF(CF_3)ppy}$_2$(dtb-bpy)]PF_6 (5.6 mg, 0.01 equiv, 1.00 mol %) catalyst is pumped through a tee and mixed with a pulsed stream of oxygen to produce a segmented liquid-gas suspension, which flows through a glass flow reactor (LTF-V, channel diameter 1 mm, total volume 1.7 ml, Little Things Factory). The glass reactor is illuminated by 8 blue LED_{455}. After 40 min, the distilled water (10 mL) was added to dilute the reaction mixture, the resulting dark red coloured mixture then transferred to the separatory funnel and extracted with ethyl acetate (3 x 10 mL). The combined organic layer was washed with brine (10 mL) and dried over Na_2SO_4. The residue was purified by flash column chromatography (SiO_2) with Hexanes/EtOAc as the solvent system to give **2a** (25.5 mg, 17%) and **3a** (68 mg, 43%). The yields are low here, therefore we switched to the advanced micro(flow)reactor setup available in our department (see, setup-B).[14]

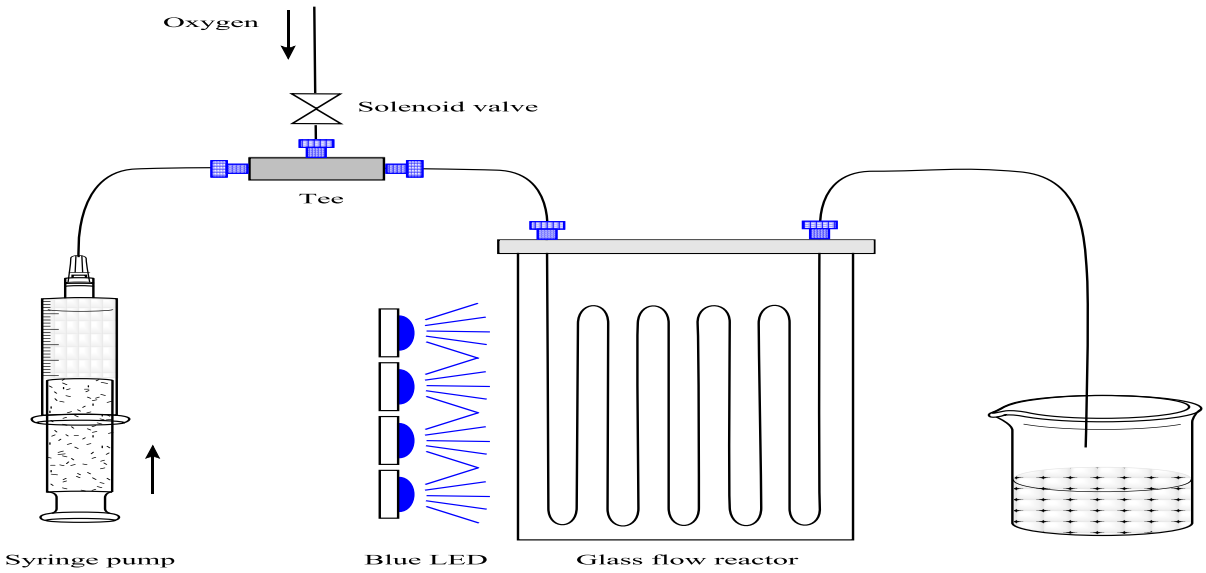

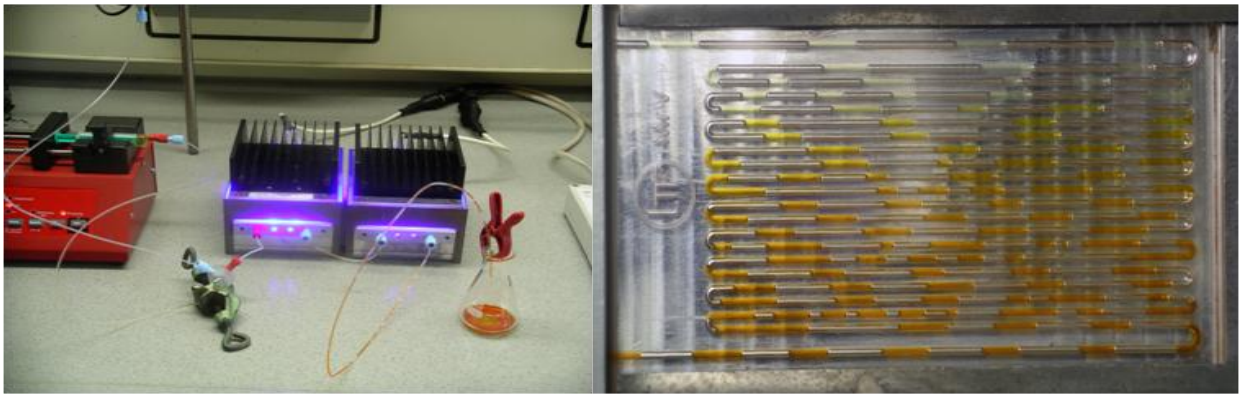

Figure 3.4: Micro(flow)reaction (gas-liquid phase) setup for photocatalytic oxidation reaction.

Flow rate liquid phase: 0.020 mL/min

Oxygen: a 0.1 sec. pulse every 10 seconds to produce a liquid/gas segmented flow with a liquid-gas ratio of approx 1:2 (V/V).

Estimated residence time: 35-40 min.

Reaction Temperature: 20-23 ^{o}C

b. Micro(flow)reactor setup-B:[14] A solution of **1a** (177 mg, 0.50 mmol) in 2 mL DMF and [Ir{dF(CF_3)ppy}$_2$(dtb-bpy)]PF_6 (5.6 mg, 0.01 equiv, 1.00 mol %) catalyst is pumped through a tee (BOLA, F 731-02) by HPLC (Bischoff dosage pump 2250; P_{HPLC} = 40 bar) via a capillary (for back-pressure build-up; Bischoff PEEK capillary 1021903PK; BPR = 12 bar) and subsequently mixed with a pulsed stream of oxygen (oxygen supply: Linde 4.6; oxygen pressure = 30 bar), to produce a segmented liquid-gas suspension, which flows through a FEP capillary.

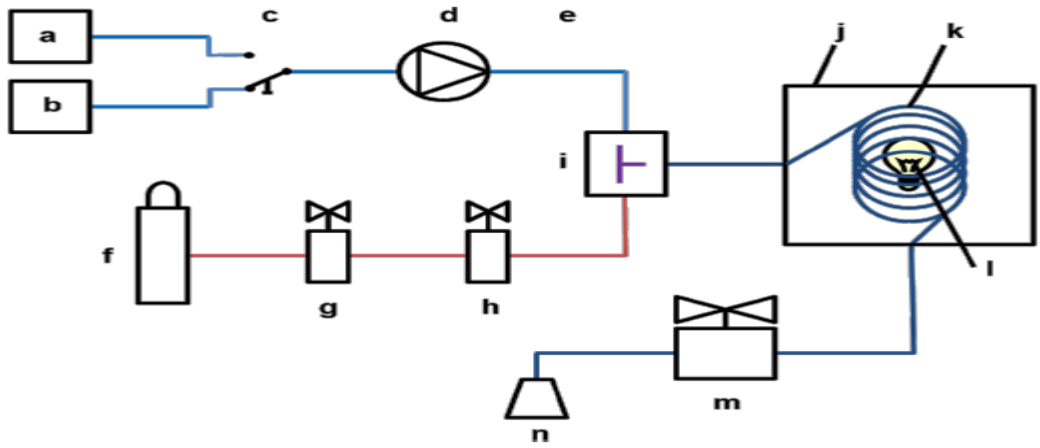

Figure 3.5: Schematic representation of Micro(flow)reaction (gas-liquid phase) setup.

Figure 3.5: Schematic illustration of the reactor setup: [a] solvent reservoir, [b] substrate solution, [c] T valve (BOLA, F 731-02), [d] HPLC pump (Bischoff dosage pump 2250), [e] capillary (for back-pressure build-up; Bischoff PEEK capillary 1021903PK), [f] oxygen supply (Linde 4.6, upto 200 bar), [g] pressure reducing valve (GO regulator, TeamTrade, PR11I11ACW-111), [h] mass flow controller (Brooks SLA 5850), [i] T mixer (IDEX, P-727 or P-632), [j] thermostat bath, [k] FEP capillary, [l] LED light source (24 × Cree Xlamp MK-R, blue light, 700 mA), [m] back-pressure regulator (IDEX, P-763, 100 psi), [n] collecting vessel.

The reactor heated to 60 ^{o}C (Note: the yields were low at room temperature conditions, therefore we have performed this reaction at 60 ^{o}C) and illuminated by 24 blue LED$_s$. After 15 min, the distilled water (10 mL) was added to dilute the reaction mixture, the resulting dark red coloured mixture then transferred to the separatory funnel and extracted with ethyl acetate (3 x 10 mL). The combined organic layer was washed with brine (10 mL) and dried over Na_2SO_4. The residue

was purified by flash column chromatography (SiO_2) with Hexanes/EtOAc as the solvent system to give **2a** (28 mg, 19%) and **3a** (90 mg, 57%).

Flow rate liquid phase: 0.025 ml/min

Oxygen: a 0.1 sec. pulse every 5 seconds to produce a liquid/gas segmented flow with a liquid-gas ratio of approx 1:1 (V/V).

Estimated residence time: 15 min.

Reaction Temperature: 60 ^{o}C.

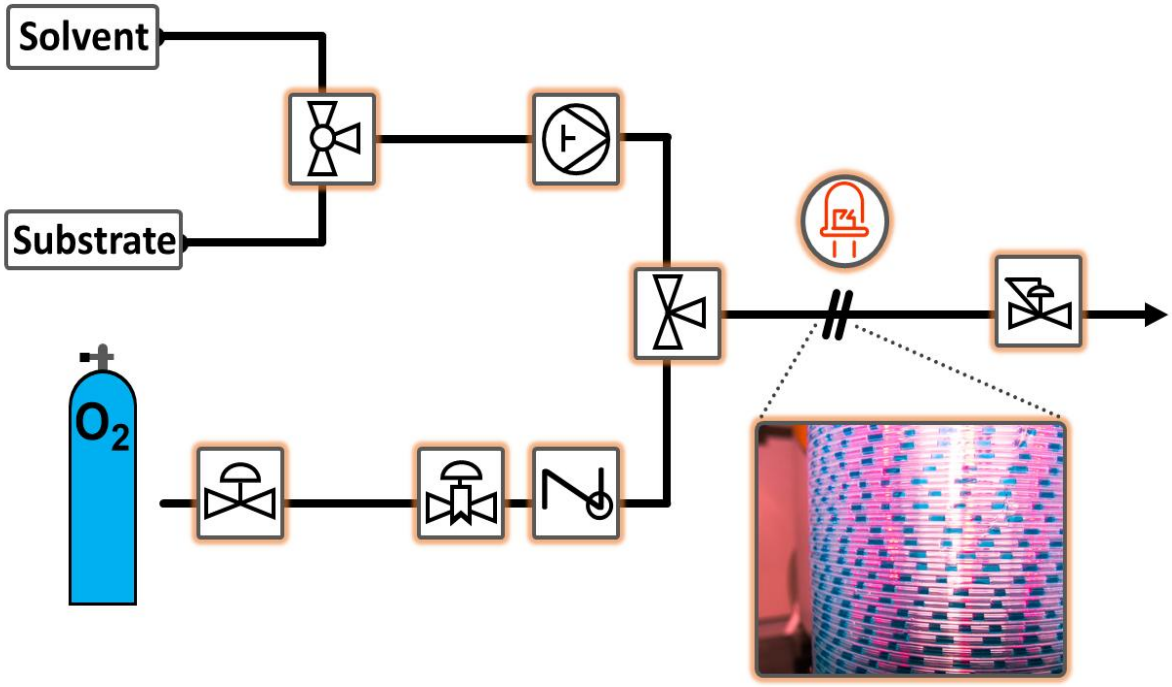

Figure 3.6: Simplified Micro(flow)reaction (gas-liquid phase) setup.

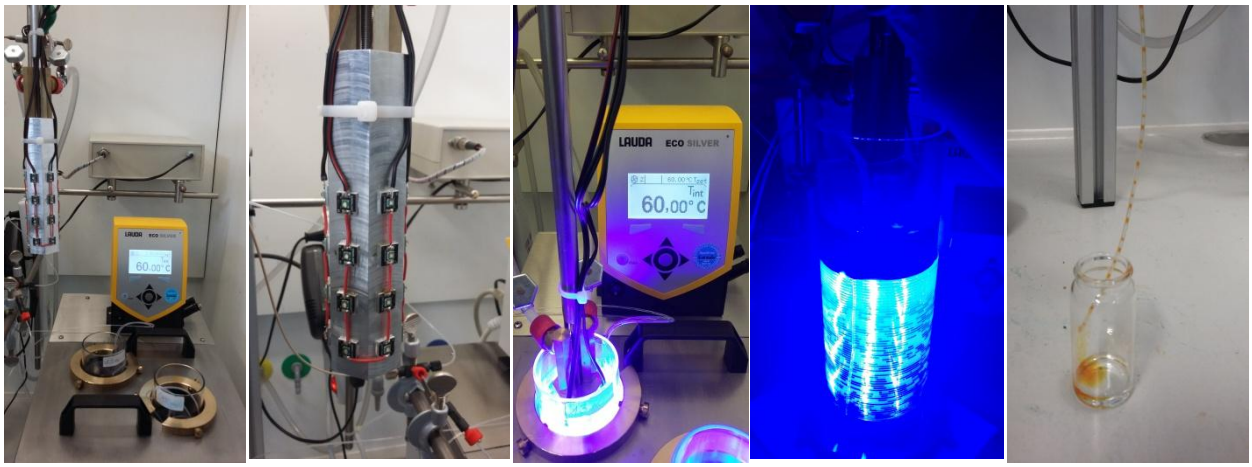

Figure 3.7: Some original photographs taken of the micro(flow)reactor setup during the experiments.

3.9.12 Oxygen labeling experiments:

a. Pure $^{18}O_2$ experiment:

An oven dried 10 mL Schlenk tube equipped with a rubber septum and a magnetic stir bar was charged with [Ir{dF(CF_3)ppy}$_2$(dtb-bpy)]PF_6 (1 mol %), α-bromocinnamate **1a** (0.25 mmol, 1.0 equiv). The flask was purged with a stream of nitrogen and 1.0 mL of dry DMF was added via syringe. The resultant mixture was degassed by the freeze-pump-thaw procedure (3 cycles). Followed by pure $^{18}O_2$ was transferred to the reaction. The tube was sealed and externally irradiated with blue light. After 24 h of irradiation oxygen labeled compounds **2a** and **3a** were detected by HRMS analysis. Crude mixtures were submitted to the HRMS analysis.

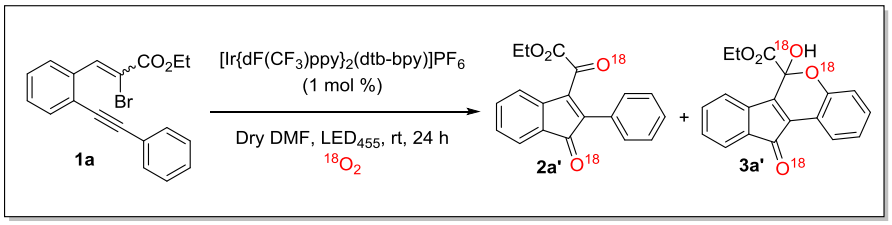

Scheme 3.7: Pure $^{18}O_2$ labeling experiment.

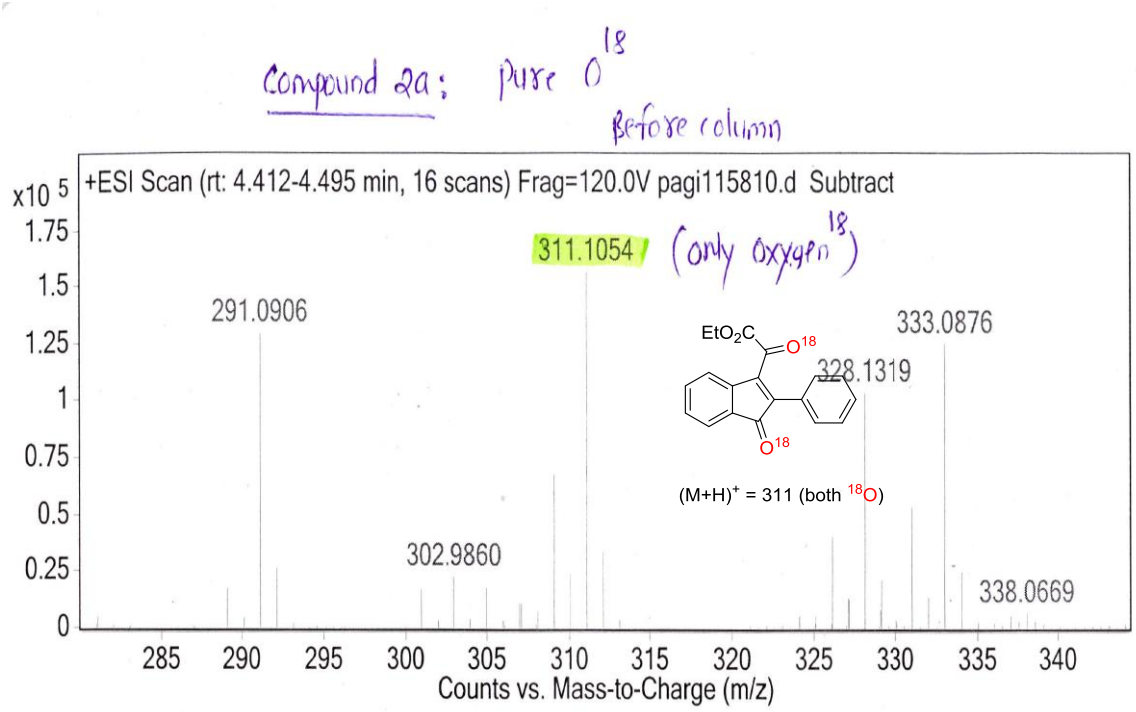

(i) HRMS Spectra of 2a': crude reaction mixture submitted for HRMS analysis

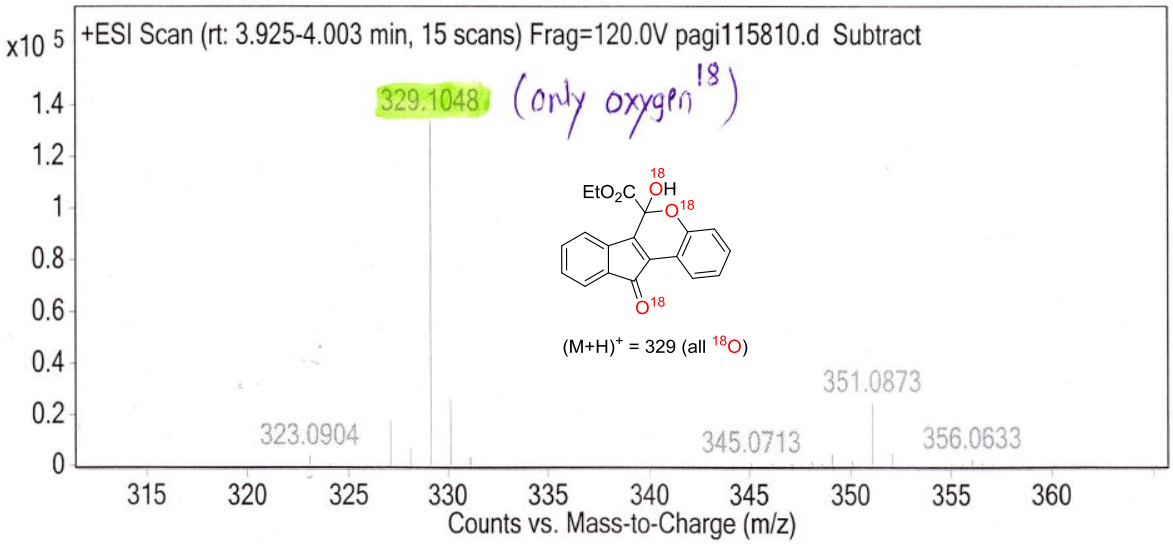

(ii) HRMS Spectra of 3a': crude reaction mixture submitted for HRMS analysis

b. Mix $^{18}O_2/^{16}O_2$ experiment: Followed the same procedure as described above: Herein, approximately half of the pure $^{18}O_2$ was transferred into the reaction mixture containing $^{16}O_2$.

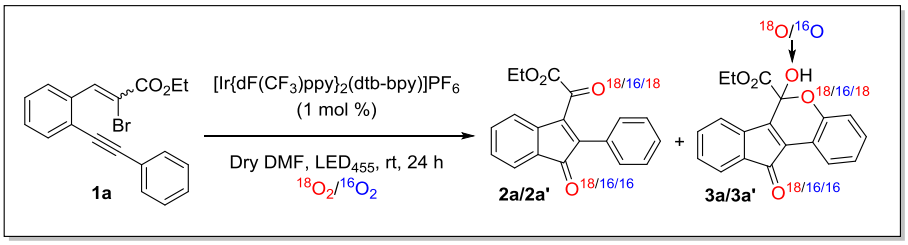

Scheme 3.8: Mix $^{18}O_2$ / $^{16}O_2$ labeling experiment.

Compound **2a**: Possible oxygen isotope incorporations

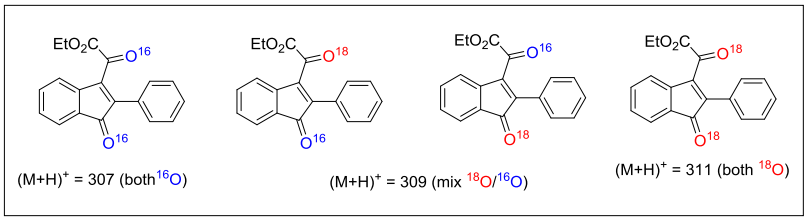

Figure 3.8: Possible oxygen incorporations in **2a/2a'.**

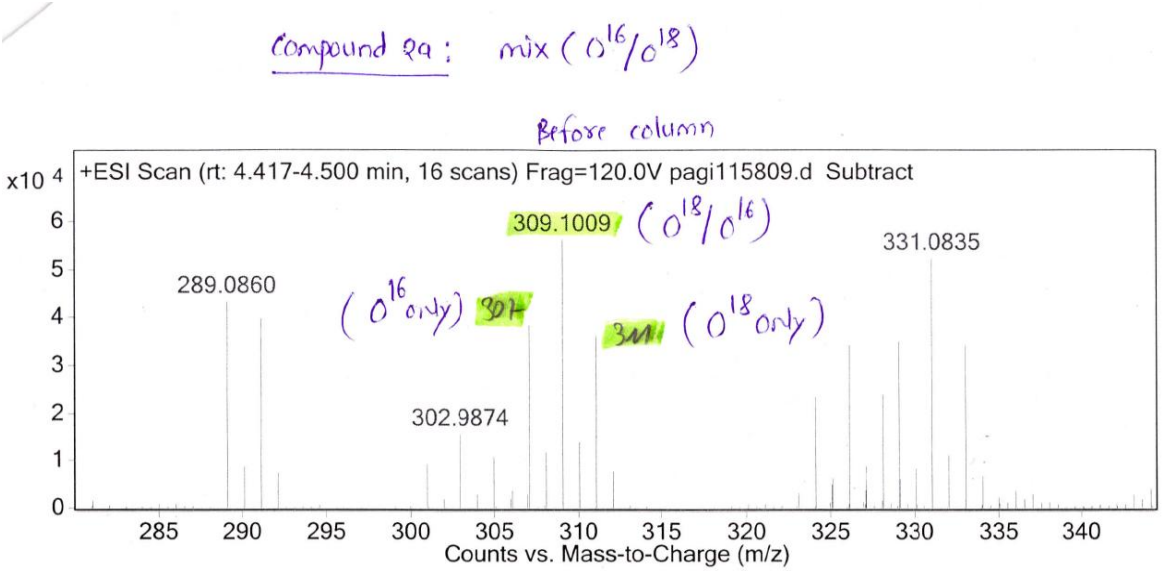

(iii) HRMS Spectra of 2a/2a': crude reaction mixture submitted for HRMS analysis.

Compound **3a**: Possible oxygen isotope incorporations

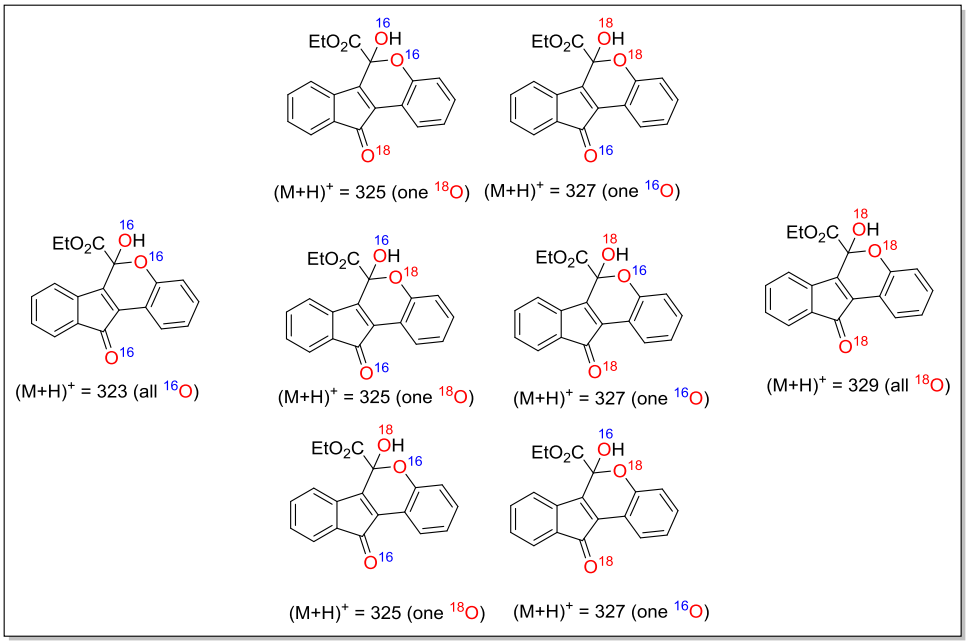

Figure 3.9: Possible oxygen incorporations in **3a/3a'.**

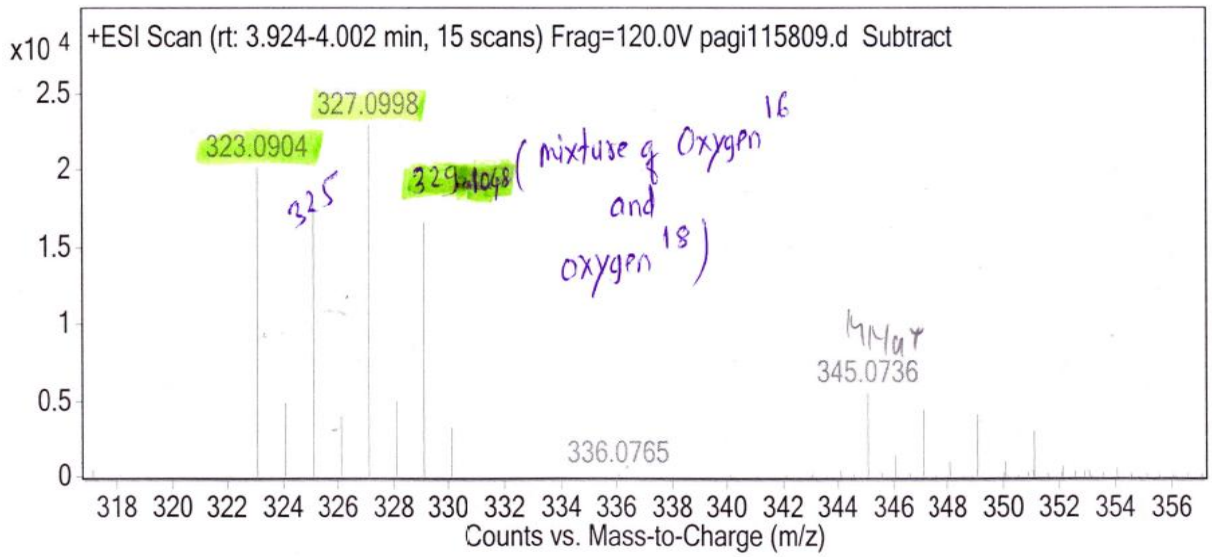

(iv) HRMS Spectra of 3a/3a': crude reaction mixture submitted for HRMS analysis.

3.9.13 Stern-Volmer luminescence quenching experiments:

Stern-Volmer luminescence intensities were recorded using a FluoroMax-4 spectrofluorometer. All solutions were excited at (λ_{ex} = 450 nm) and the emissions (λ_{em}) were recorded in the range of 452-750 nm.

a. Figure 2.1.10:

To a degassed DMF in quartz cuvettes, capped with septa, was introduced a stock solution of an [Ir(dF(CF$_3$)ppy)$_2$(dtb-bpy)PF$_6$] photocatalyst (148.56 µM) under nitrogen (inert) atmosphere. This blank [Ir]-catalyst solution was excited by blue light (λ_{ex} = 450 nm) at 20 ^{o}C (Figure 3.10, A). The maximum emission was recorded at λ_{em} = 476 nm with an intensity of 1.7 x 10^6 (red colour plot, Figure 3.10, A). Strong changes in the luminescence intensities of [Ir(dF(CF$_3$)ppy)$_2$(dtb-bpy)PF$_6$] was observed upon successive addition of **1a** in DMF. In the inset, Stern-Volmer plots are shown.

From the plot A, the following data was obtained:
(1) Stern-Volmer constant (*Ksv*) = $Kq\,T_0$ = 968.1 ± 8.304
(2) The fluorescence lifetime (T_0) = 2300 ns[3]

b. Figure 2.1.10:

To a non-degassed DMF in quartz cuvettes, capped with septa, was introduced a stock solution of an [Ir(dF(CF$_3$)ppy)$_2$(dtb-bpy)PF$_6$] photocatalyst under air. The resulting blank Ir-catalyst solution was excited by blue light (λ_{ex} = 450 nm) at 20 ^{o}C (Figure 3.10, B). The maximum emission was recorded at λ_{em} = 476 nm with an intensity of 1.0 x 10^6 (red colour plot, Figure 3.10, B). In this case, the intensity is slightly lower for the photocatalyst as compared to Figure 3.10, A (under nitrogen). This is due to the quenching of the oxygen molecule present in the air. The oxygen quenching is also called as collision quenching typically occurred by physical energy transfer processes (or non-radiative transitions). However, the oxygen quenching is not as strong as the substrate **1a** with the photocatalyst. Which is proved upon further addition of **1a** to the [Ir(dF(CF$_3$)ppy)$_2$(dtb-bpy)PF$_6$] photocatalyst solution under air at 20 ^{o}C (Figure 3.10, B). This experiment suggests, the starting material interacts strongly with the excited photocatalyst irrespective of the presence of oxygen molecule in the solution. In the inset, Stern-Volmer plots are shown.

From the plot B, the following data was obtained:

(1) Stern-Volmer constant (*Ksv*) = $Kq\,T_0 = 287.0 \pm 9.032$

(2) The fluorescence lifetime (T_0) = 2300 ns[3]

c. Figure 2.1.10:

The separate oxygen quenching experiment was conducted by successive addition of an approximate amount of oxygen to the catalyst solutions at every 5 min until the solution gets saturated with oxygen (red line). After this, further quenching did not takes place. The resulting quenching spectra are shown in (Figure 3.10, C). Although, the quenching with oxygen was not as strong as the starting material but it suggested that, the oxygen molecule also takes part in the catalytic cycle.

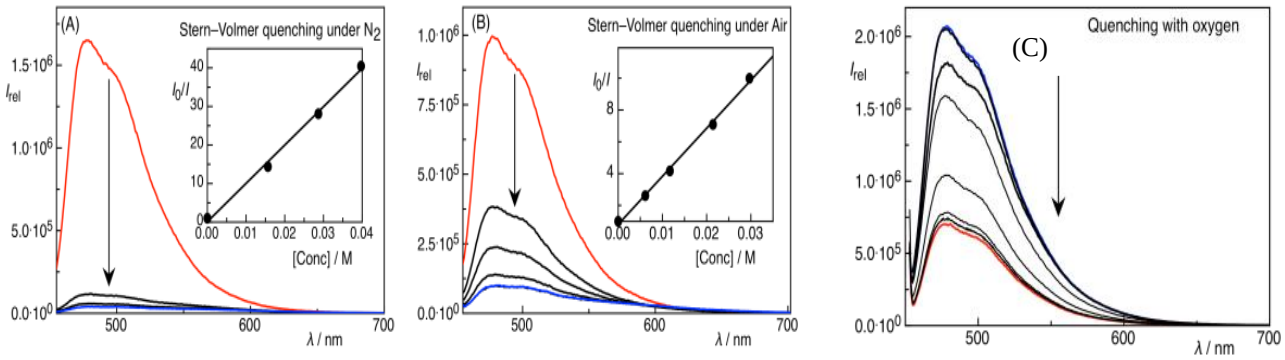

Figure 3.10: [A] Fluorescence quenching of the [Ir{dF(CF_3)ppy}$_2$(dtb-bpy)]PF_6 upon successive addition of **1a** under nitrogen in DMF at rt.

[B] Fluorescence quenching of the [Ir{dF(CF_3)ppy}$_2$(dtb-bpy)]PF_6 upon successive addition of **1a** under air in DMF at rt (in the insets, Stern-Volmer plots are shown).

[C] Fluorescence quenching of the [Ir{dF(CF_3)ppy}$_2$(dtb-bpy)]PF_6 upon successive addition of oxygen in DMF.

3.9.14 ESR spectra of a vinyl radical:

A solution of **1a** (0.10 mmol) and [Ir{dF(CF_3)ppy}$_2$(dtb-bpy)]PF_6 (5 mol %) was irradiated at 455 nm under inert atmosphere at low temperature (using liquid nitrogen) in DMF (0.3 mL). After 10 min of irradiation, a vinyl radical was detected (Figure 3.11) having *g*-factor (*ge*) = 1.984, which corresponds to the single electron. The instrument details are given below:

Magnettech MiniScope MS400

Power Consumption: ca. 500 VA

Microwave (MW) Power: 100 µW-50 mW (10 µW-100 mW optional)

Sensitivity MS400: 8*109 Spins/0.1 mT

MW Frequency: 9,20-9,60 GHz

Field Homogeneity: ± 5 µT sample area

Field Range: 50 – 450 mT (optional 50 – 600 mT with water cooling)

Field Sweep: 0 – 400 mT (optional 0 – 550 mT with water cooling)

Sweep Time: 12 s – 34 min

Field Stability: 1.5 µT/min, 15 µT/h

Field Modulation: 5 µT – 0.7 mT

Modulation Frequency: 100 kHz

Resonator rectangular: TE102

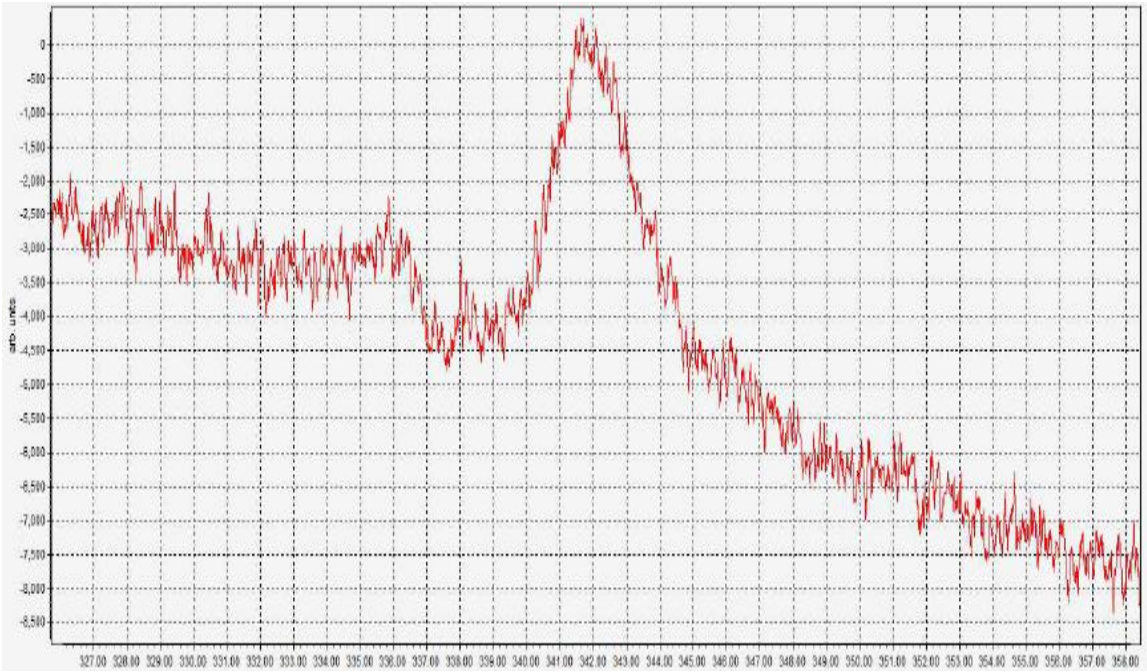

Figure 3.11: ESR spectra for vinyl radical of **1a.**

3.9.15 Experimental procedure to trap a vinyl radical with TEMPO:

An oven dried 10 mL Schlenk tube equipped with a rubber septum and a magnetic stir bar was charged with [Ir{dF(CF_3)ppy}$_2$(dtb-bpy)]PF_6 (2 mol %), α-bromocinnamate **1u** (0.10 mmol, 1.0 equiv) and TEMPO (0.3 mmol, 3.0 equiv). The flask was purged with a stream of nitrogen and 1.0 mL of dry DMF was added via syringe. The resultant mixture was degassed by the freeze-pump-thaw procedure (3 cycles). The tube was sealed with an internal blue light irradiation set up. After 12 h of irradiation, TEMPO trapped compound **9** was detected by mass spectra; $(M+H)^+$: 460.2487 ($C_{29}H_{34}NO_4$).

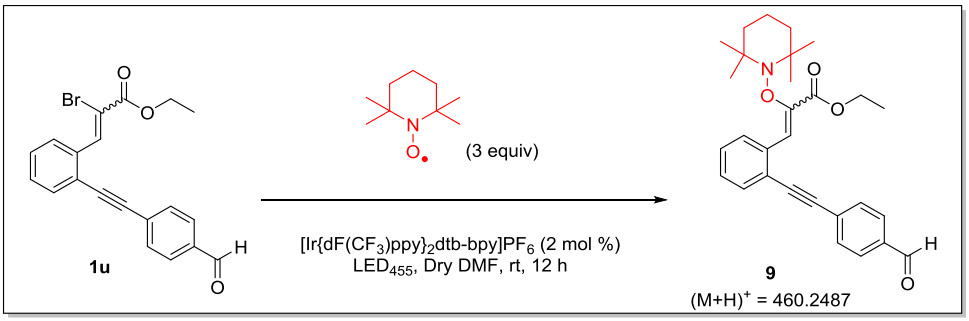

Scheme 3.9: TEMPO trapping experiment.

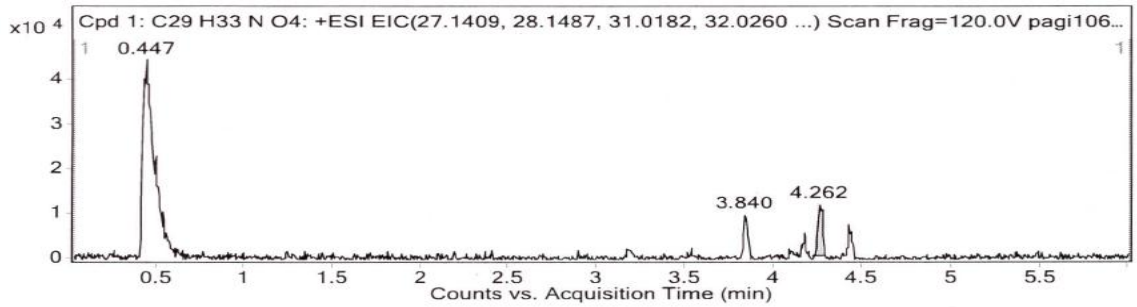

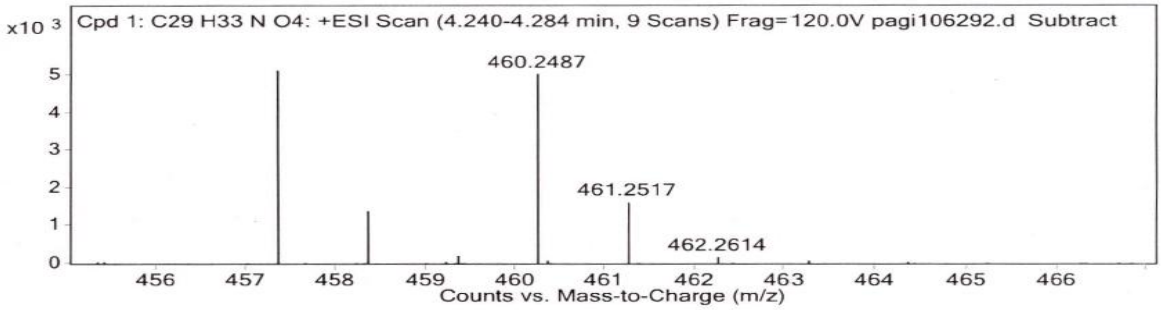

MS Spectrum Peak List

m/z	*Calc m/z*	Diff(ppm)	z	Abund	Formula	Ion
413.3239				8224.47		
460.2487	460.2482	1.03	1	5028.32	C29H34NO4	(M+H)+
461.2517	461.2516	0.41	1	1633.94	C29H34NO4	(M+H)+
462.2614	462.2545	14.76	1	180.1	C29H34NO4	(M+H)+

3.9.16 Synthesis of starting material precursors:[35]

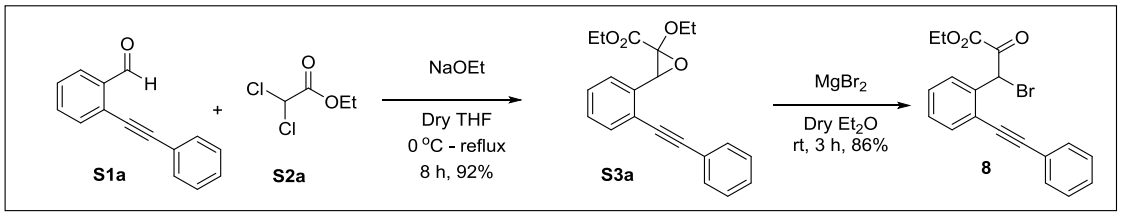

a. Synthesis of ethyl 2-ethoxy-3-(2-(phenylethynyl)phenyl)oxirane-2-carboxylate (S3a):

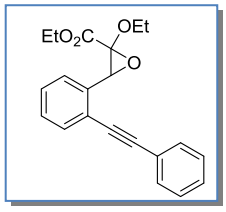

To a solution of sodium ethoxide, made by dissolving 0.222 g of sodium (9.64 mmol) in 7 ml of anhydrous ethanol, was added a solution of **S1a** (1.00 g, 4.84 mmol) and ethyl dichloroacetate **S2a** (0.890 ml, 7.26 mmol) in THF (13 ml) at 0 °C via cannula. The suspension was then heated at reflux for 8 h. After removing all the solvent *in vacuo*, the residue was diluted with CH_2Cl_2 (30 ml) and washed with saturated NH_4Cl (20 mL). The aqueous layer was extracted with CH_2Cl_2 (3 x 20 ml). The combined organic layers were dried (Na_2SO_4) and the solvents were evaporated *in vacuo*. Purification of the crude product by column chromatography (Hexanes: EtOAc, 9:1, R_f = 0.29) afforded **S3a** as a light yellow oil (1.50 g, 92% yield, *dr* = 5.18:1).

^{1}H-NMR (300 MHz, $CDCl_3$, major isomer): δ 7.56 – 7.51 (m, 1H), 7.52 – 7.44 (m, 2H), 7.41 – 7.29 (m, 6H), 4.87 (s, 1H), 4.35 (q, *J* = 7.1 Hz, 2H), 3.85 (q, *J* = 7.1 Hz, 2H), 1.30 (t, *J* = 7.1 Hz, 3H), 1.14 (t, *J* = 7.1 Hz, 3H).

^{13}C-NMR (75 MHz, $CDCl_3$, major isomer): δ 167.28, 134.59, 131.83, 131.58, 128.71, 128.52, 128.29, 128.09, 126.88, 123.01, 122.71, 95.09, 86.41, 83.21, 64.38, 63.13, 62.49, 15.17, 14.22.

b. Synthesis of ethyl 3-bromo-2-oxo-3-(2-(phenylethynyl)phenyl)propanoate (8):

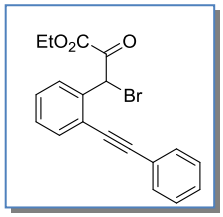

To a solution of **S3a** (0.336 g, 1.00 mmol) in Et_2O (10 ml) was added magnesium bromide (0.368 g, 2.00 mmol) in portions at room temperature for 3 h. Deionized water (20 ml) was then added and the organic layer was separated. The aqueous layer was extracted with Et_2O (3 x 20 ml). The combined organic layers were dried (Na_2SO_4) and concentrated *in vacuo*. Purification of the crude product by column chromatography (Hexanes: EtOAc, 9:1, R_f = 0.19) afforded **8** as a yellow oil (319 mg, 86% yield).

^{1}H-NMR (300 MHz, $CDCl_3$): δ 7.62 – 7.54 (m, 4H), 7.45 – 7.33 (m, 5H), 6.90 (s, 1H), 4.30 (qd, *J* = 7.1, 4.1 Hz, 2H), 1.28 (t, *J* = 7.1 Hz, 3H).

^{13}C-NMR (75 MHz, $CDCl_3$): δ 184.51, 159.99, 135.08, 132.52, 131.82, 130.41, 129.46, 129.24, 129.09, 128.64, 123.15, 122.61, 96.23, 86.21, 63.35, 48.49, 14.01.

3.9.17 Synthesis of 2a and 3a from 8:

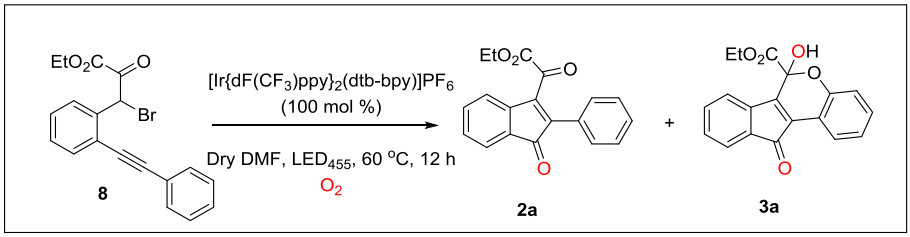

An oven dried 10 mL Schlenk tube equipped with a magnetic stir bar was charged with [Ir{dF(CF_3)ppy}$_2$(dtb-bpy)]PF_6 (56 mg, 100 mol %), **8** (18.5 mg, 0.05 mmol, 1.0 equiv). The flask was purged with a stream of oxygen and 1.0 mL of dry DMF (1 mL) was added via syringe. The resultant mixture was bubbled by oxygen. Then, the tube was sealed under positive oxygen atmosphere and irradiated with blue light for 12 h. After complete consumption of the starting material (analyzed by TLC), the reaction mixture was diluted with EtOAc (10 mL) and transferred to the separatory funnel. This mixture was then washed with water (3 x 10 mL) and with brine solution (10 mL). The combined brine and water fractions were again washed with EtOAc (3 x 10 mL). The combined organic layers were dried over Na_2SO_4 and concentrated *in vacuo*. Purification of the crude product by column chromatography (Hexanes: EtOAc, 9:1) afforded **2a** (4.1 mg, 27% yield) and **3a** (7.6 mg, 47% yield).

3.10 Representative UV-Visible spectra in dilute acetonitrile:

a. Compound **3a**: (red colour)

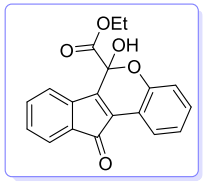

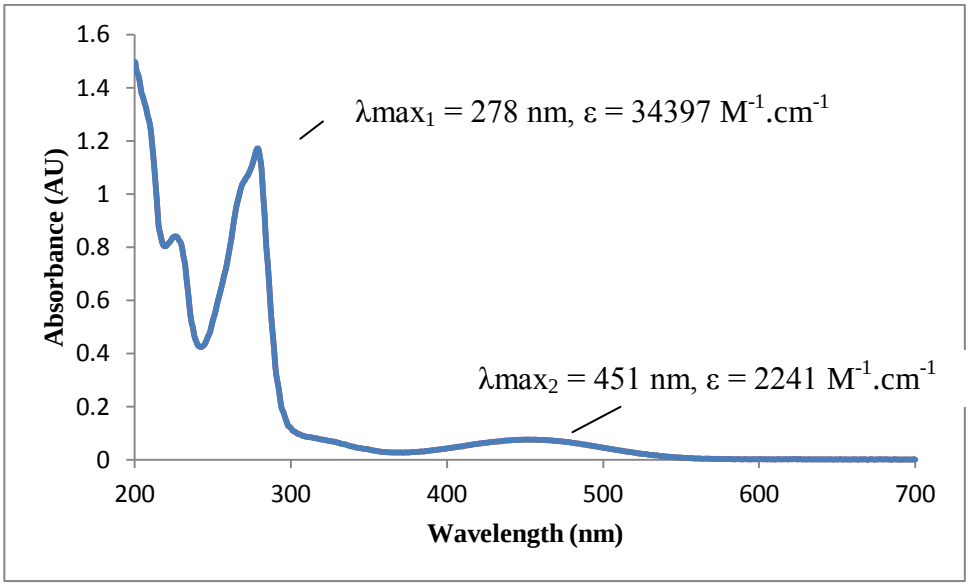

b. Compound **3c**: (dark brown colour)

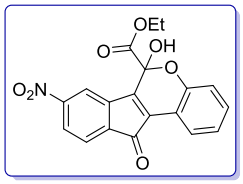

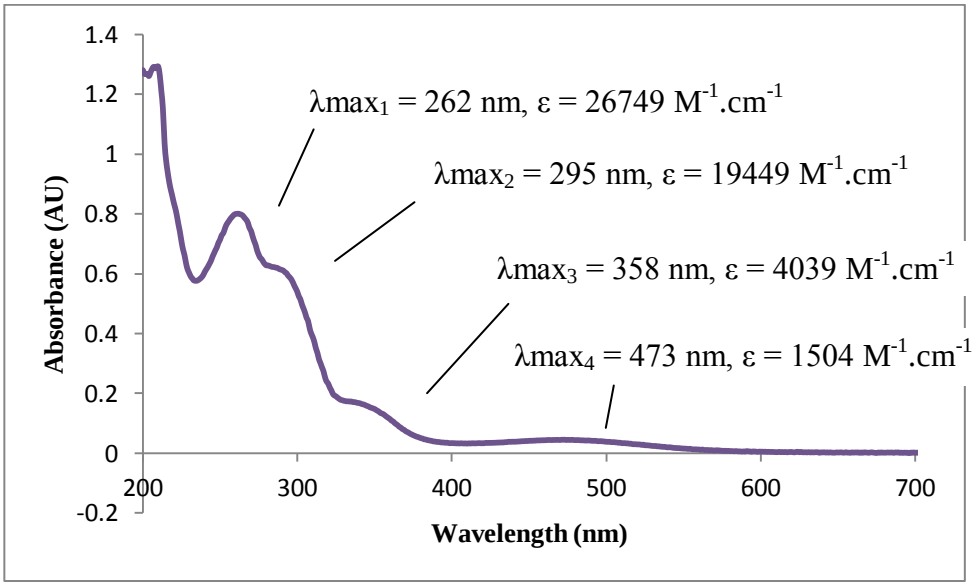

c. Compound **2b**: (light red colour)

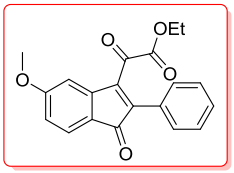

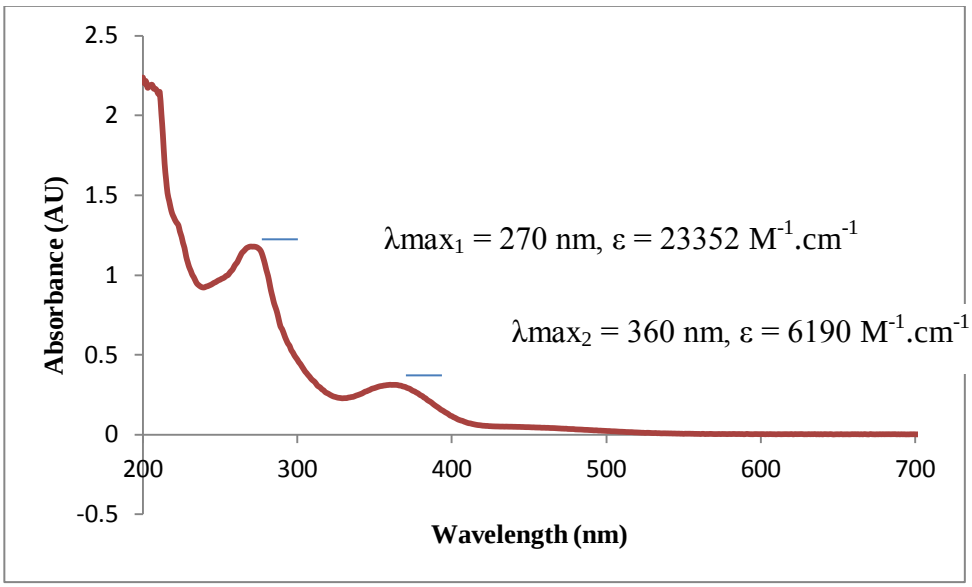

d. Compound **2e**: (violet colour)

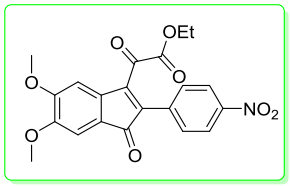

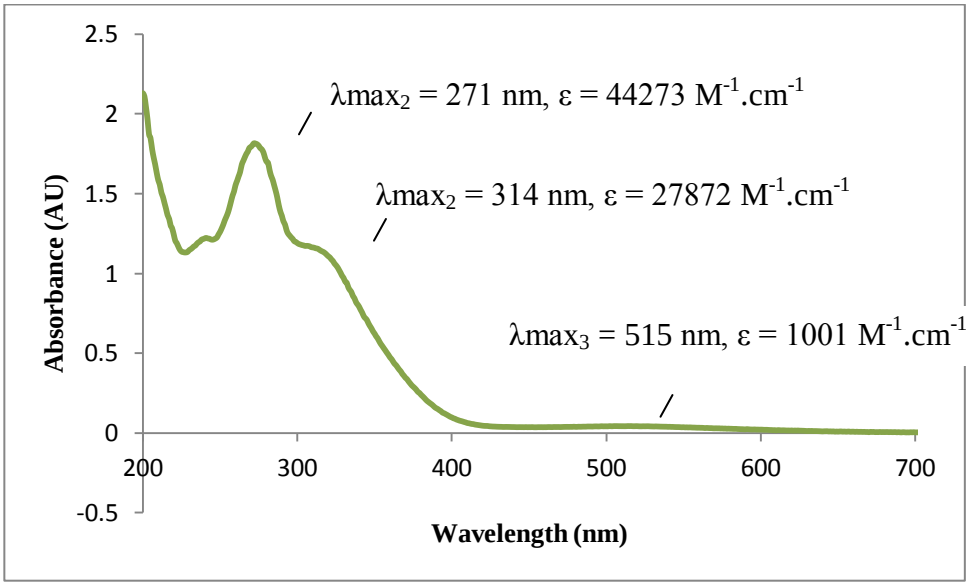

3.11 NMR spectra:

^{1}H-NMR: **S1a**

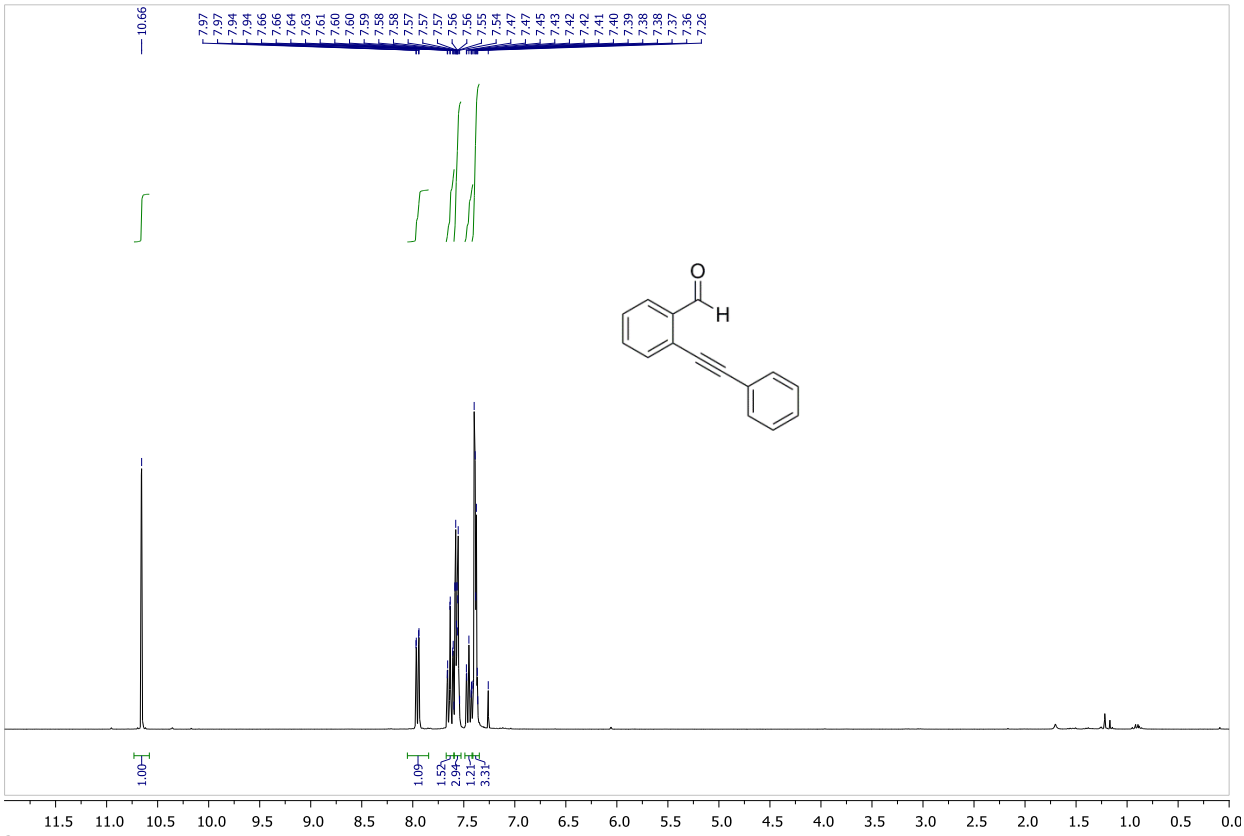

^{13}C-NMR: **S1a**

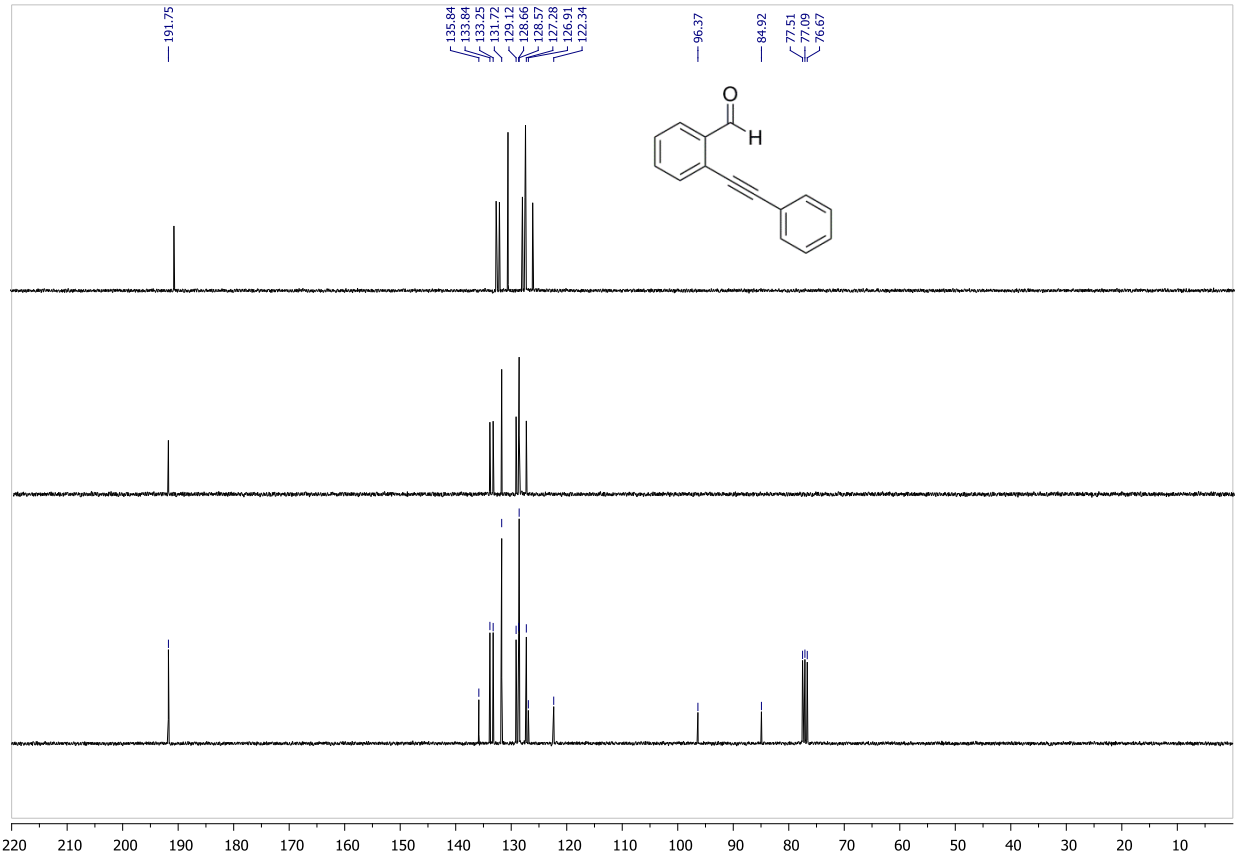

^{1}H-NMR: **S1b**

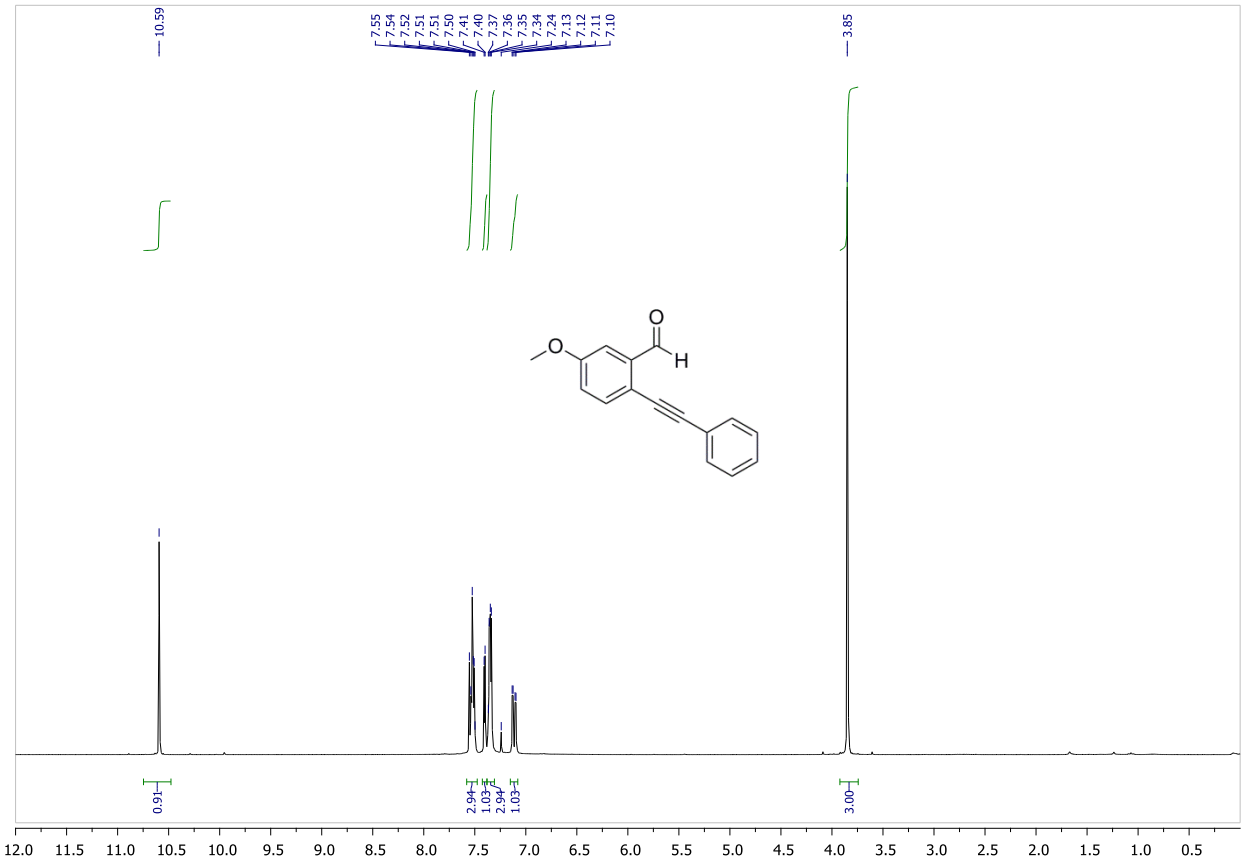

^{13}C-NMR: **S1b**

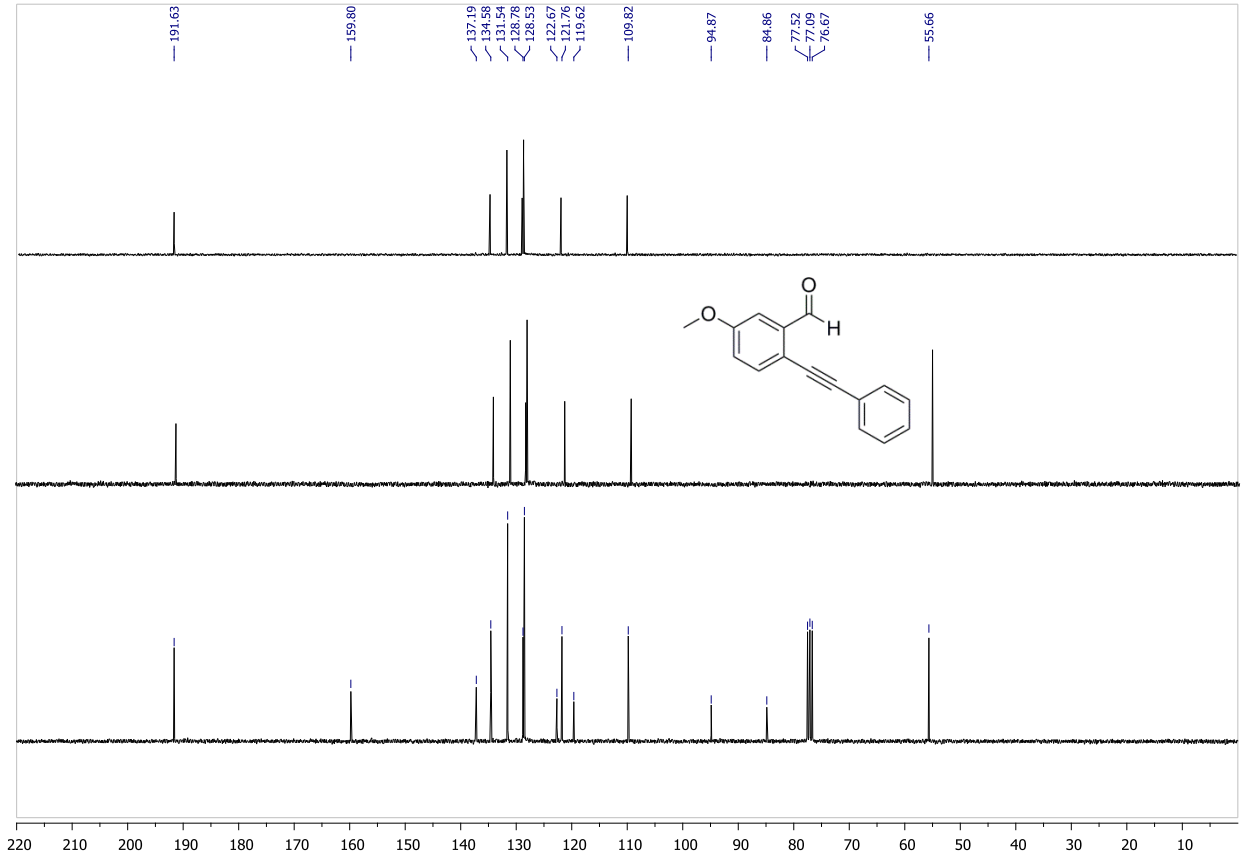

^{1}H-NMR: **S1c**

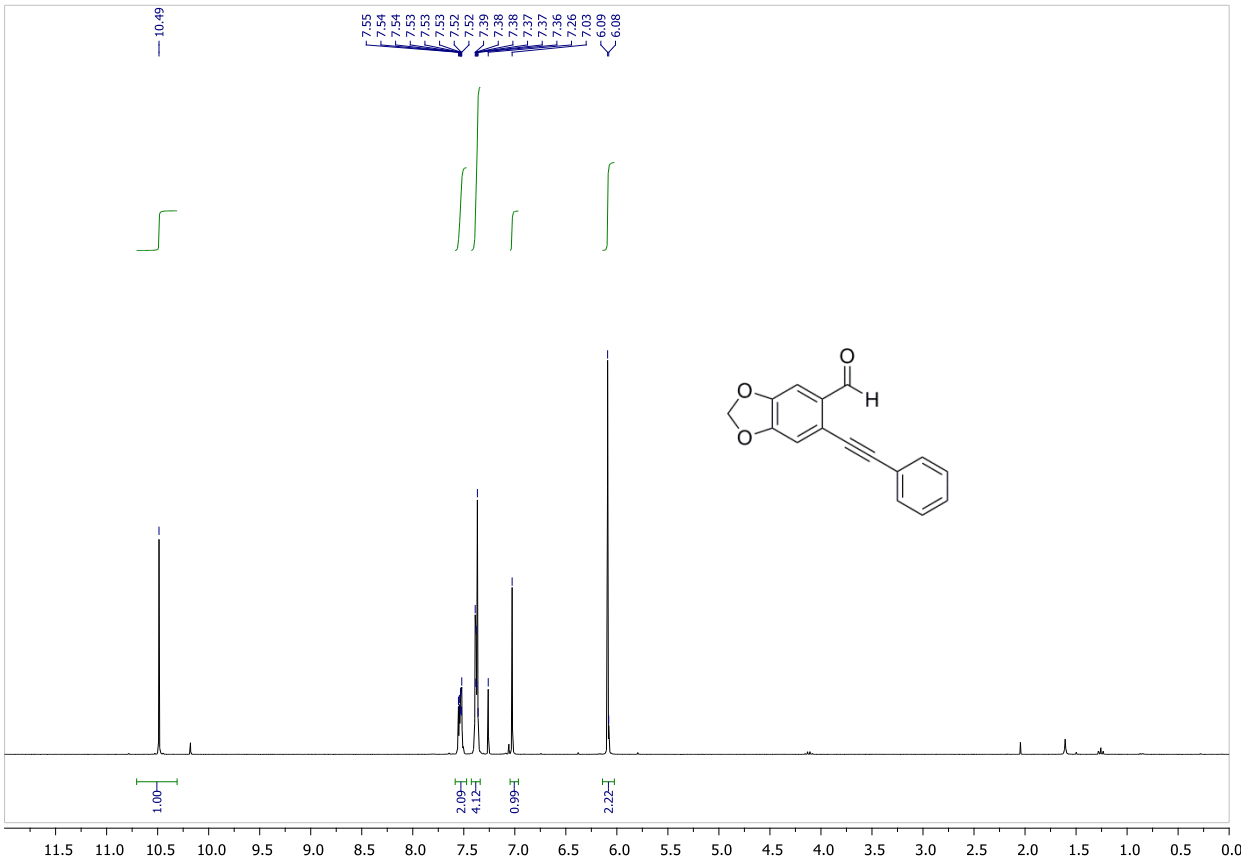

^{13}C-NMR: **S1c**

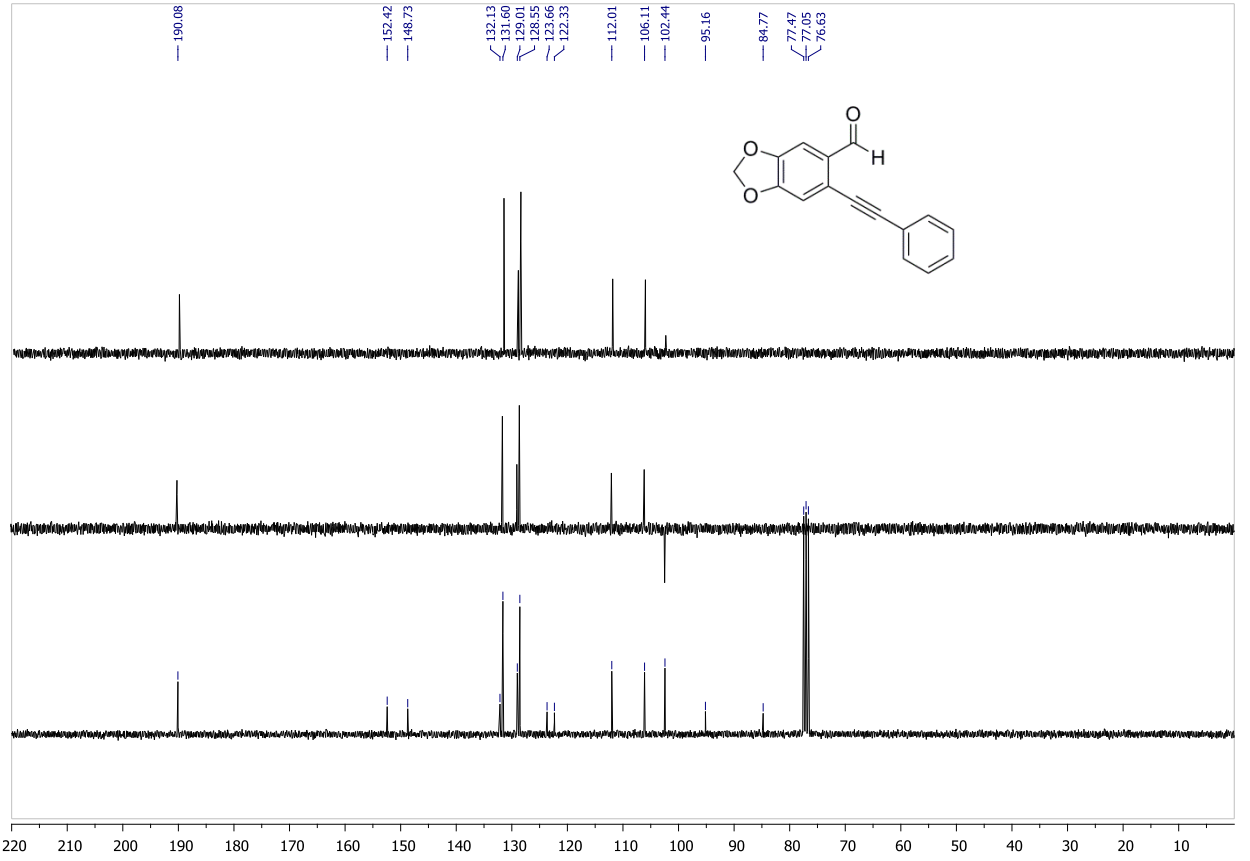

^{1}H-NMR: **S1d**

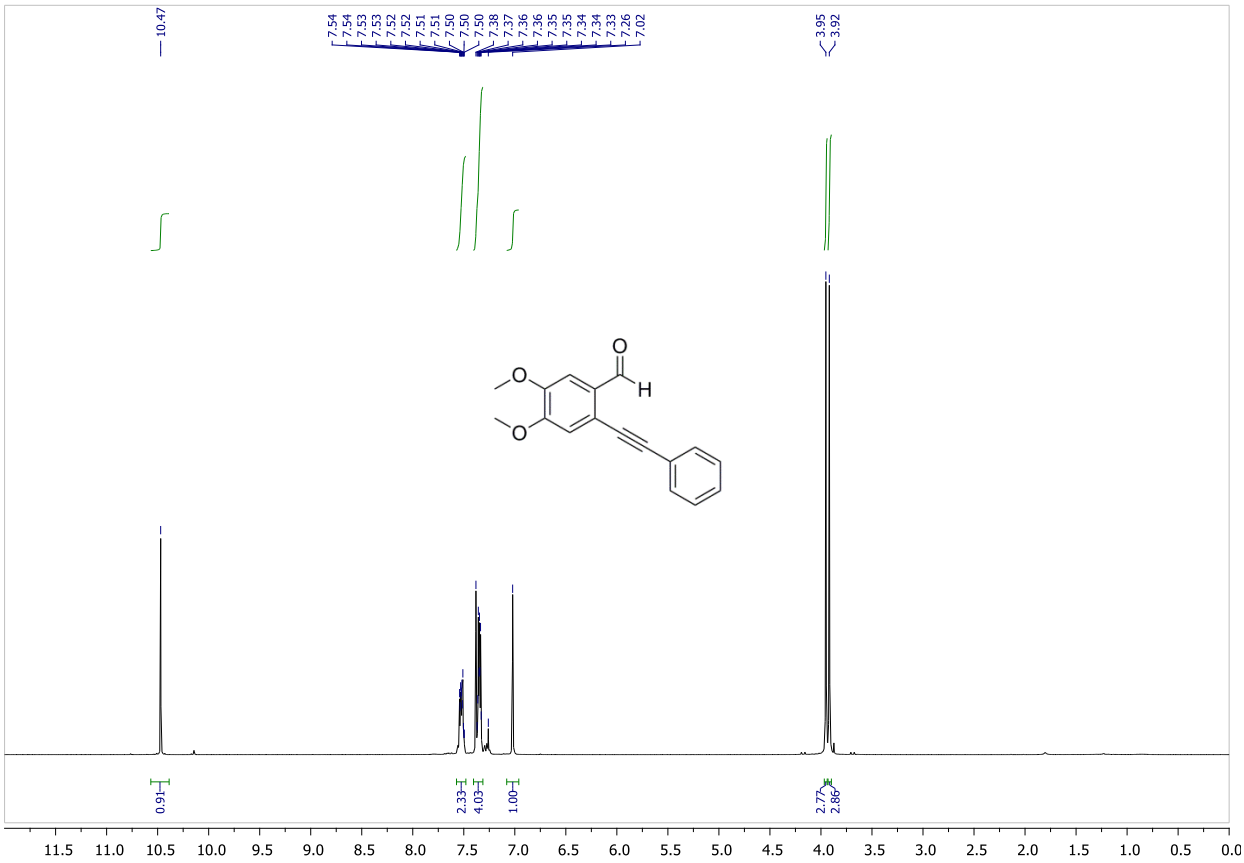

^{13}C-NMR: **S1d**

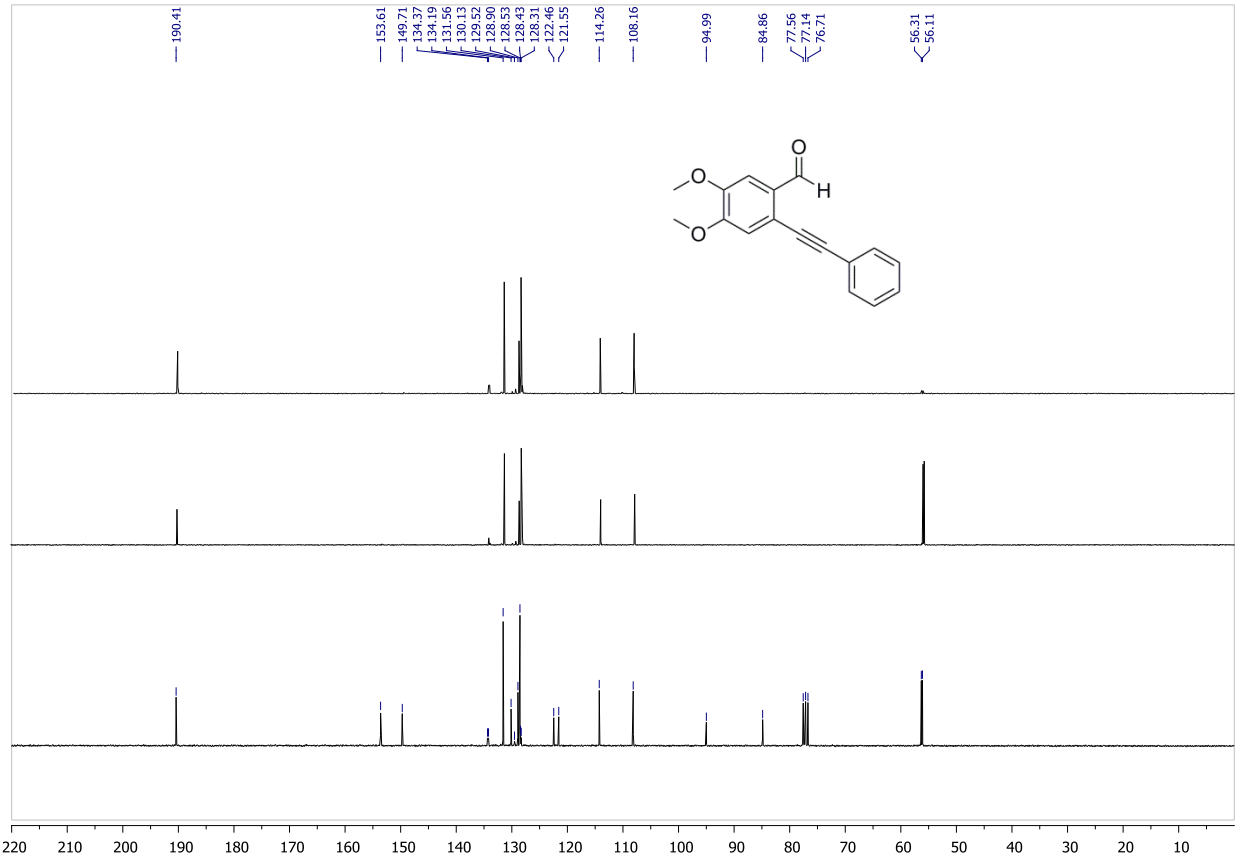

^{1}H-NMR: **S1e**

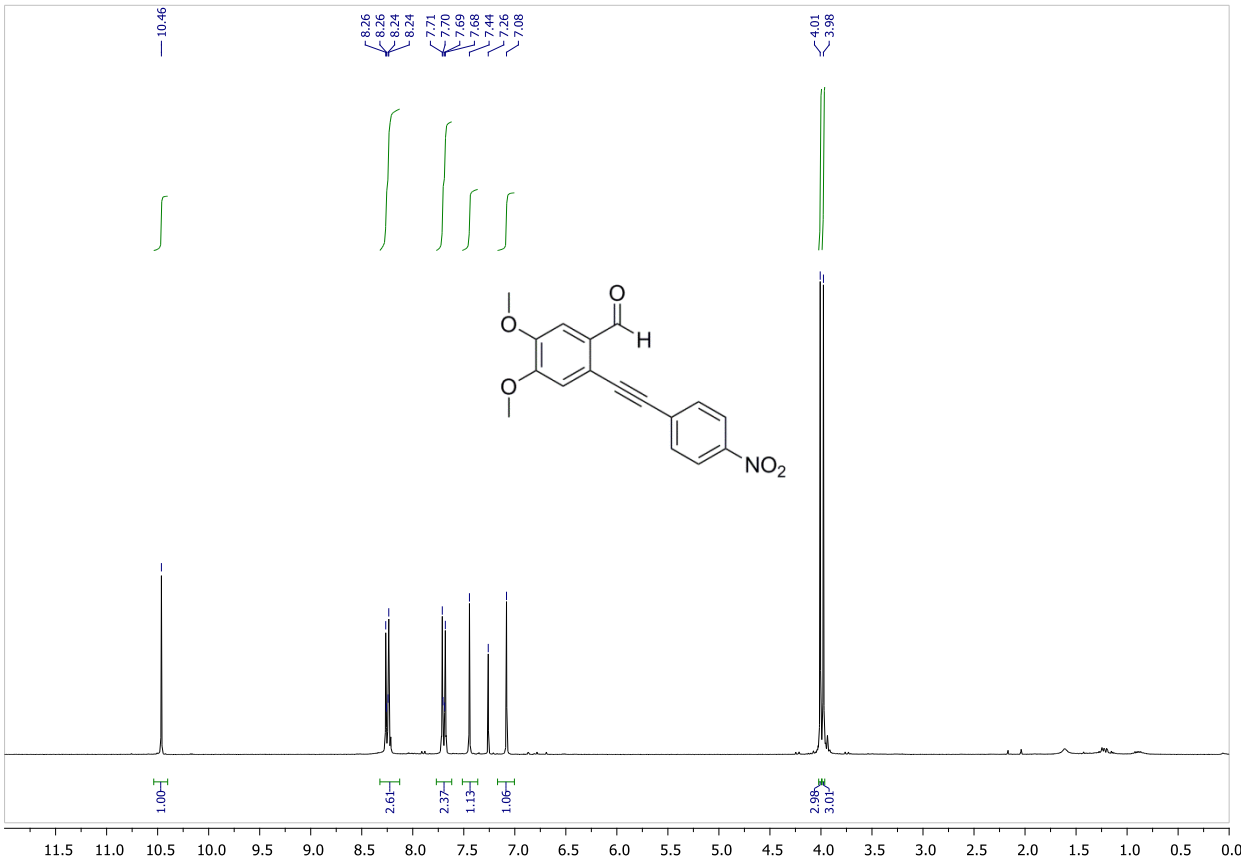

^{13}C-NMR: **S1e**

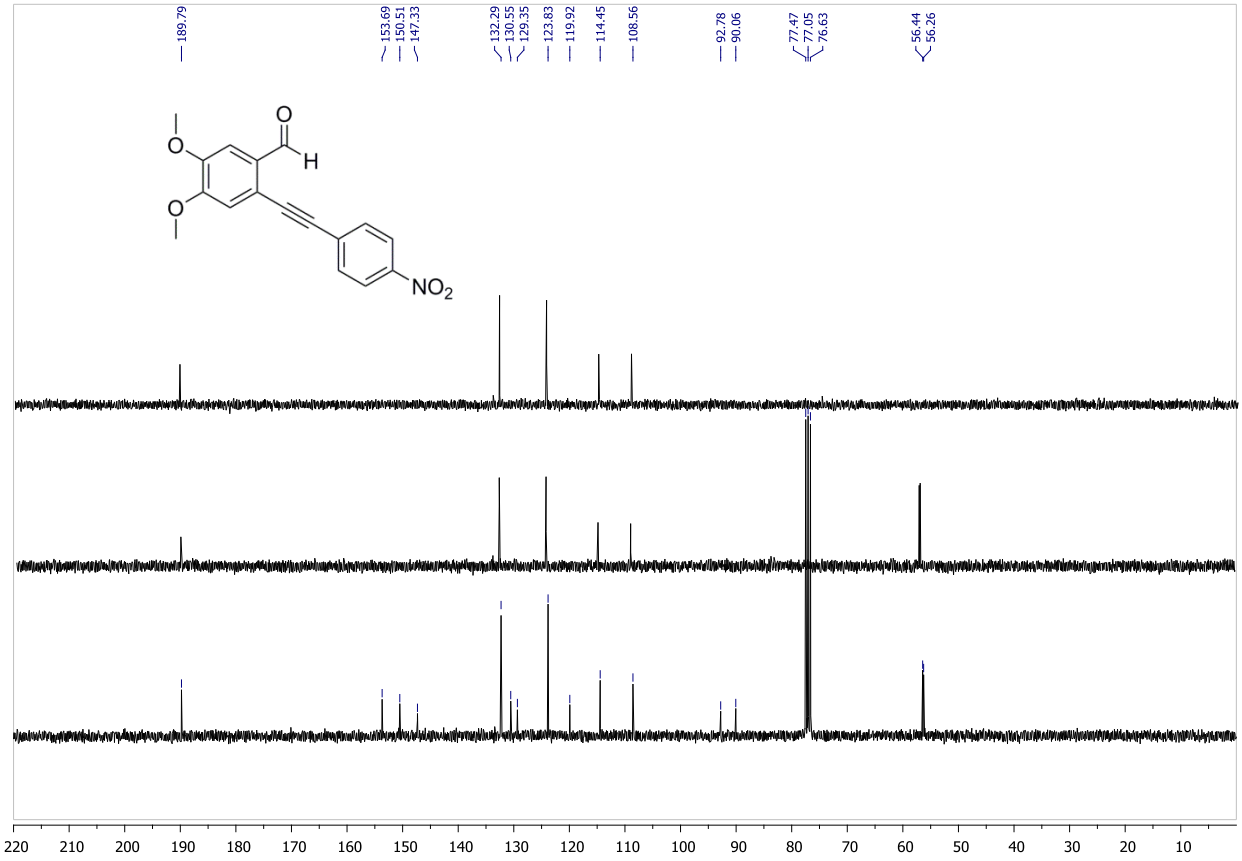

^{1}H-NMR: **S1f**

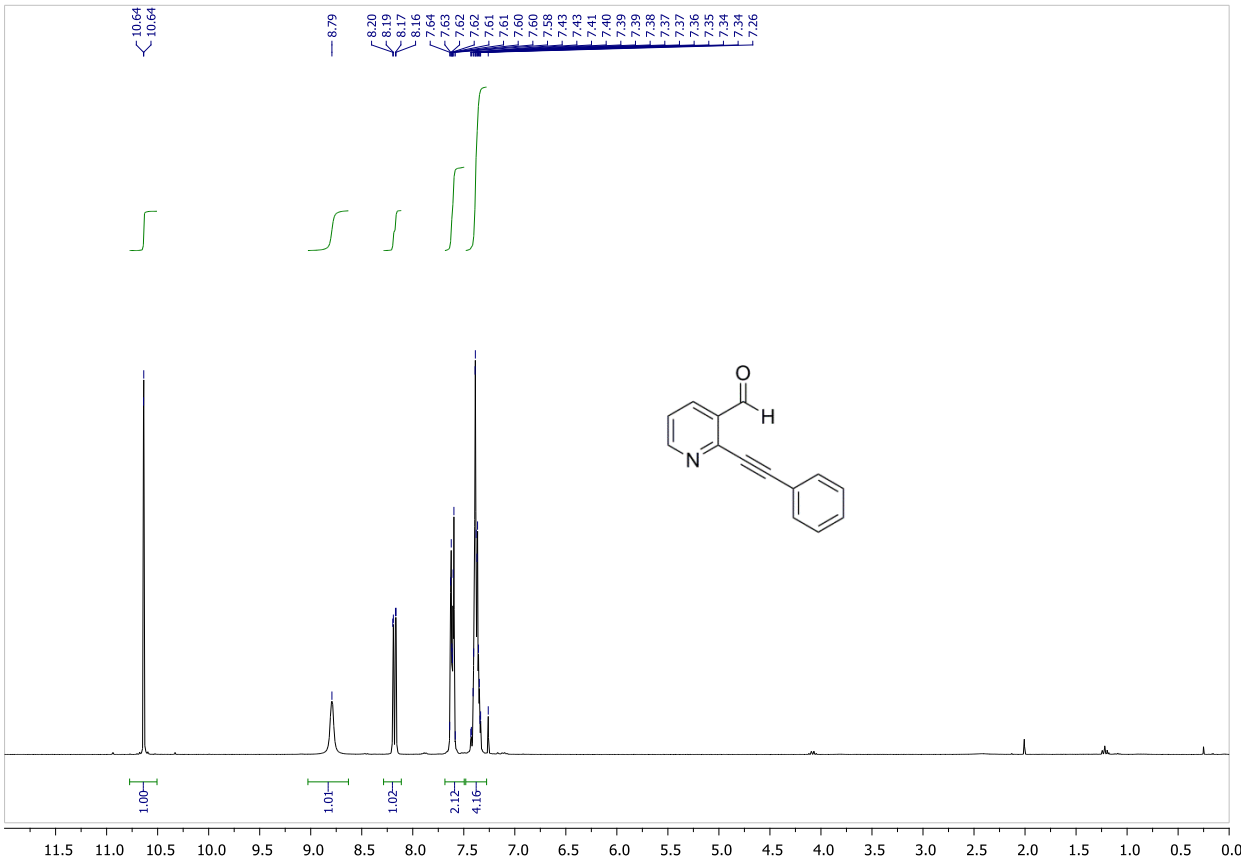

^{13}C-NMR: **S1f**

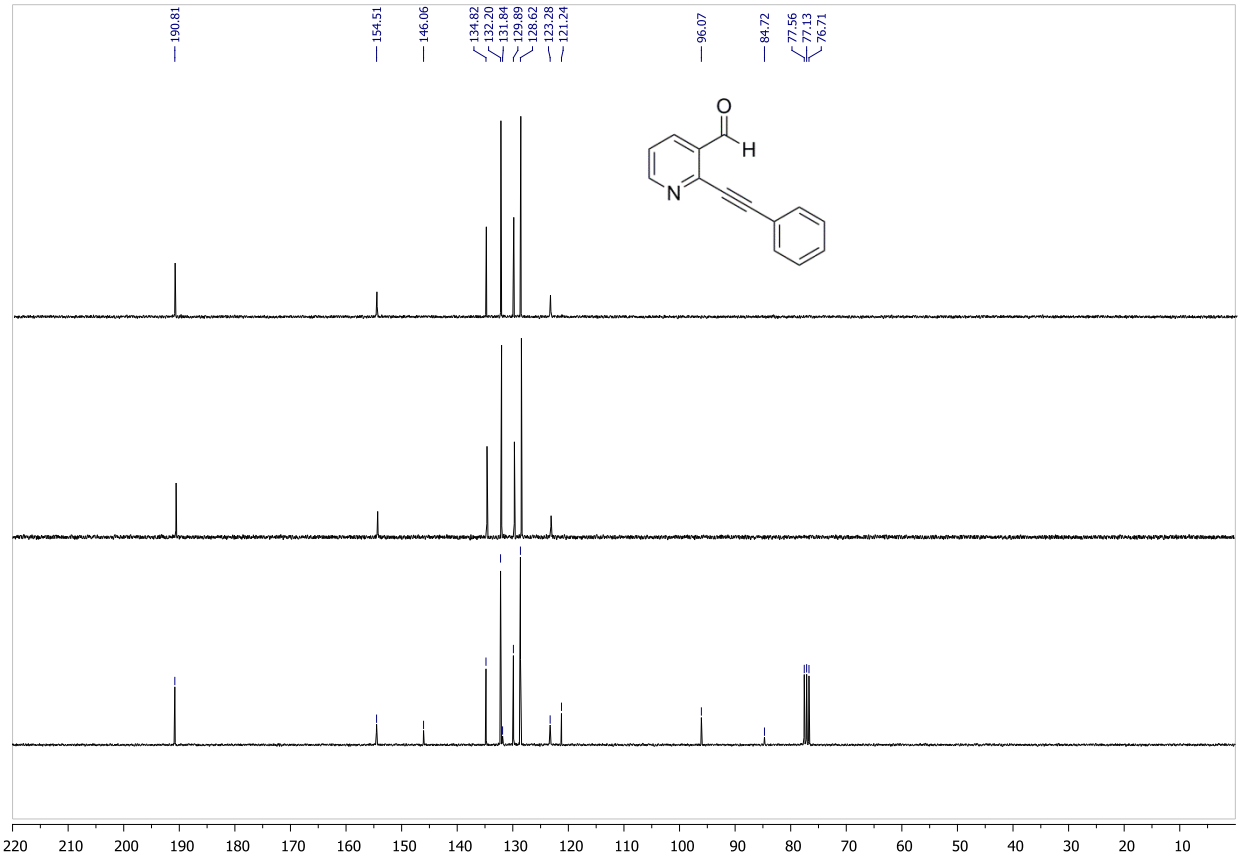

^{1}H-NMR: **S1g**

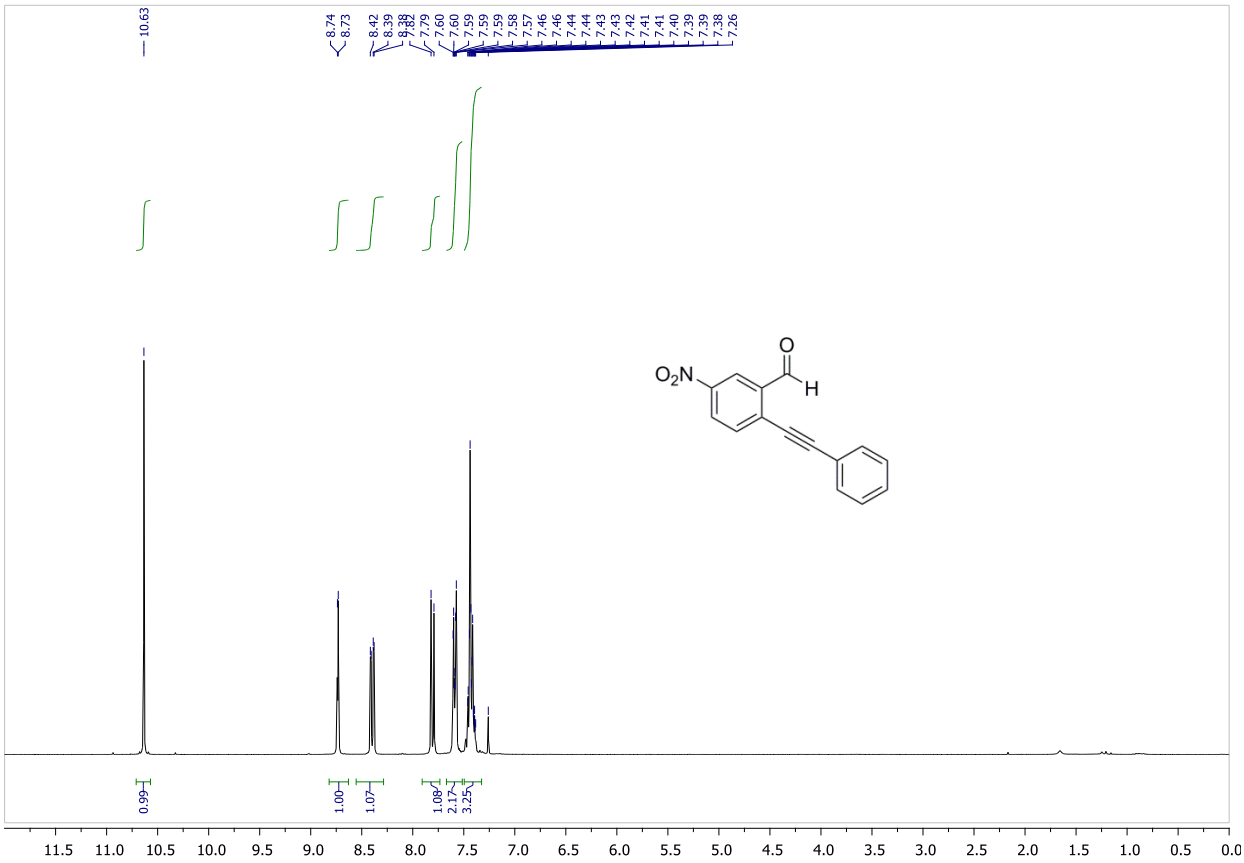

^{13}C-NMR: **S1g**

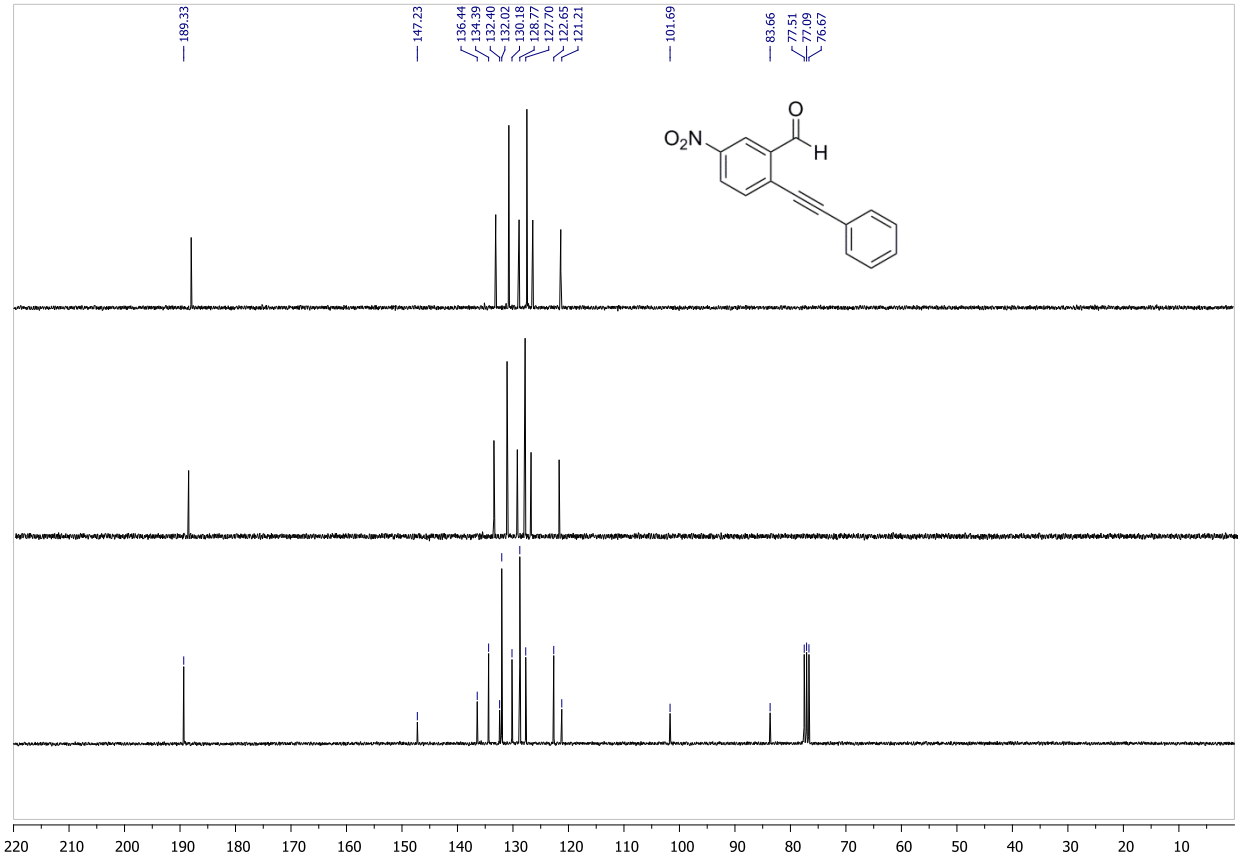

^{1}H-NMR: **S1h**

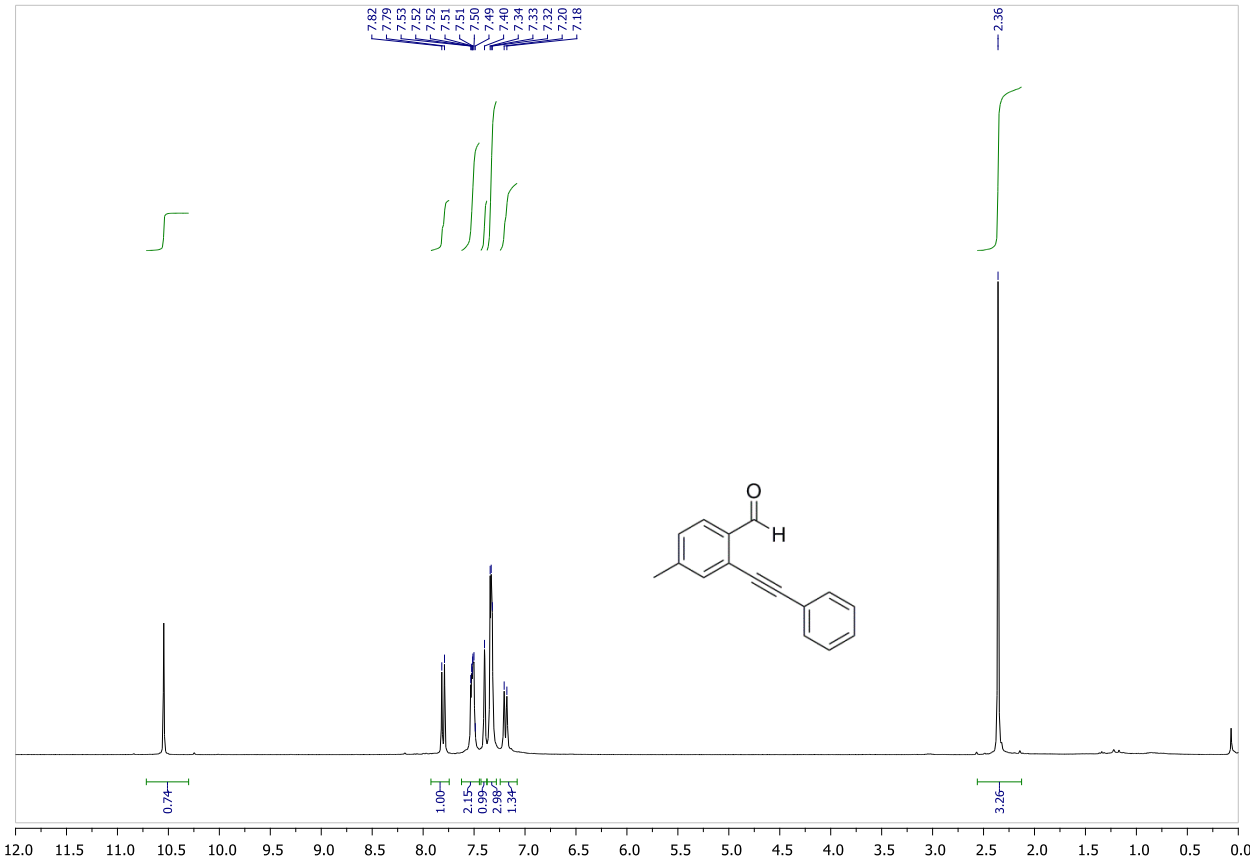

^{13}C-NMR: **S1h**

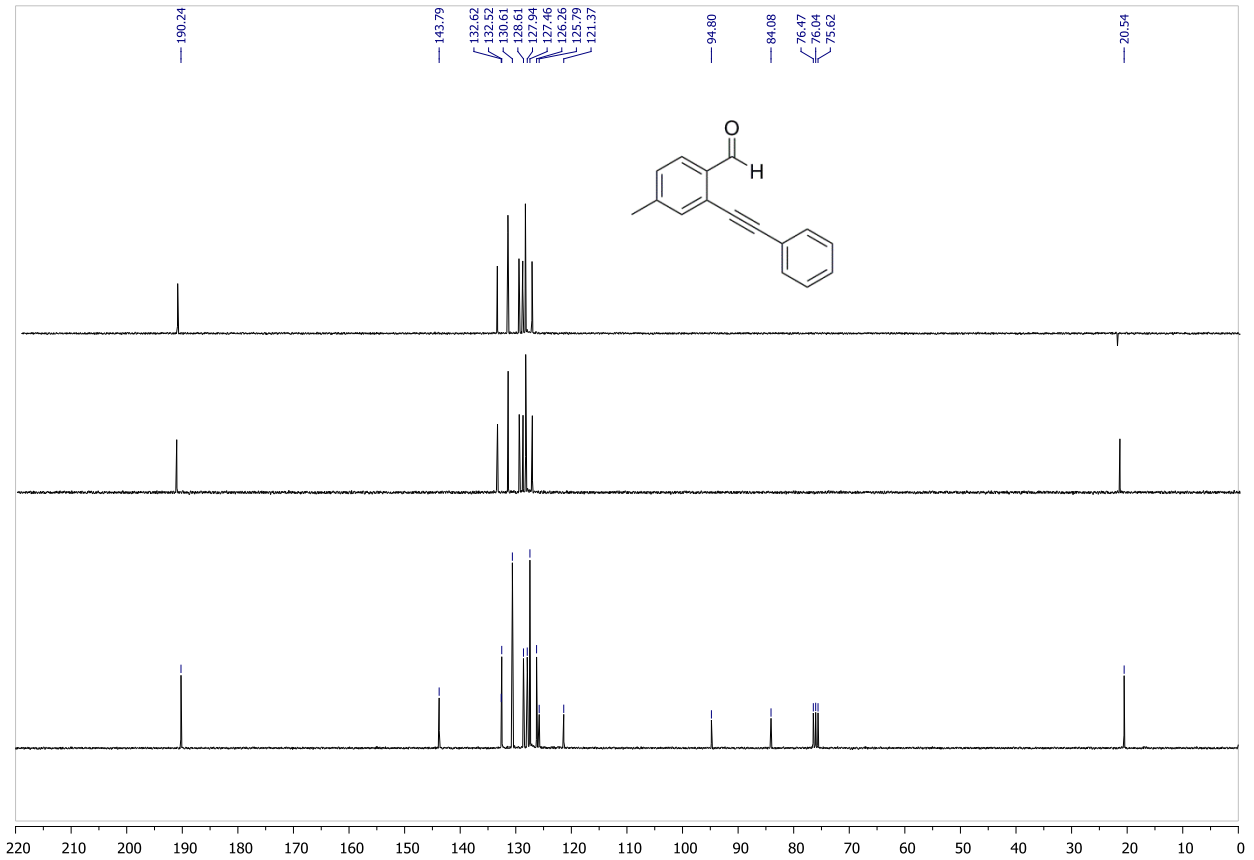

^{1}H-NMR: **S1i**

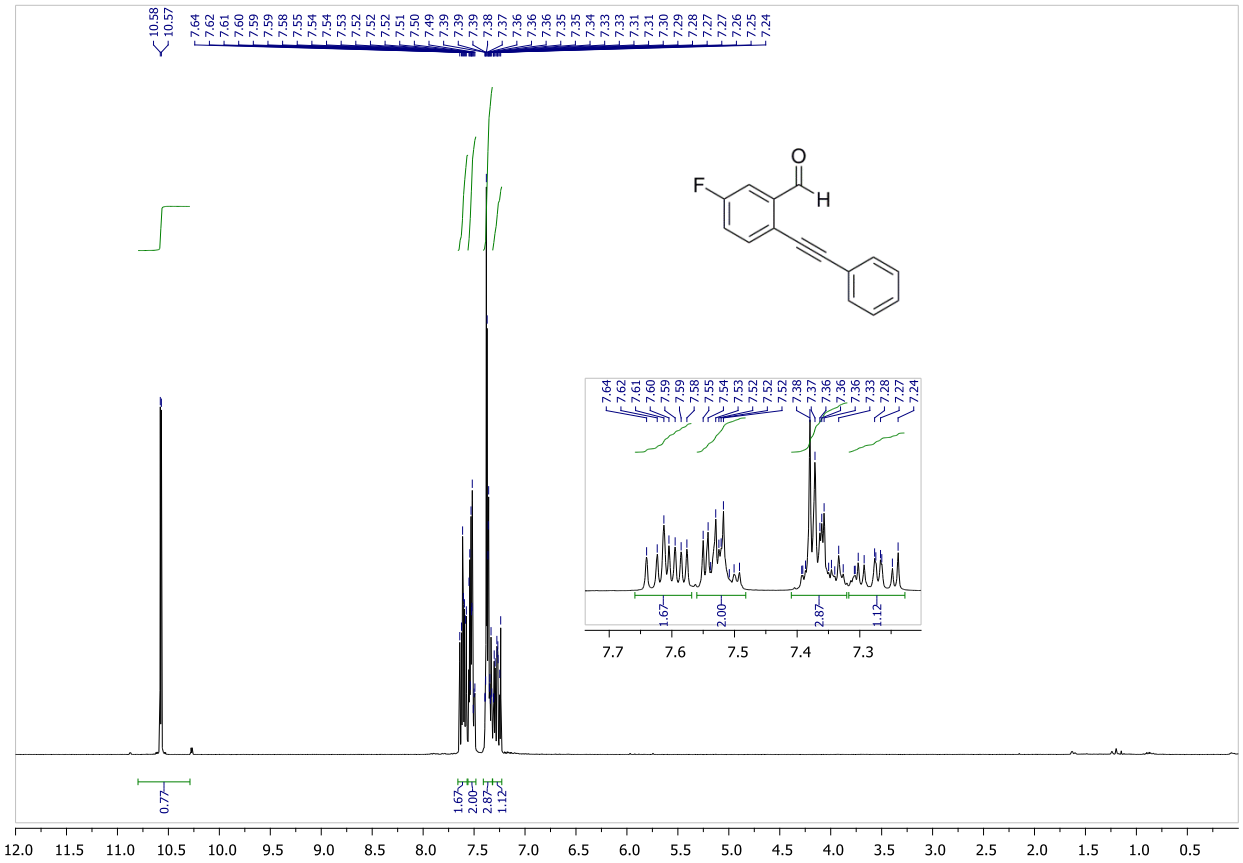

^{13}C-NMR: **S1i**

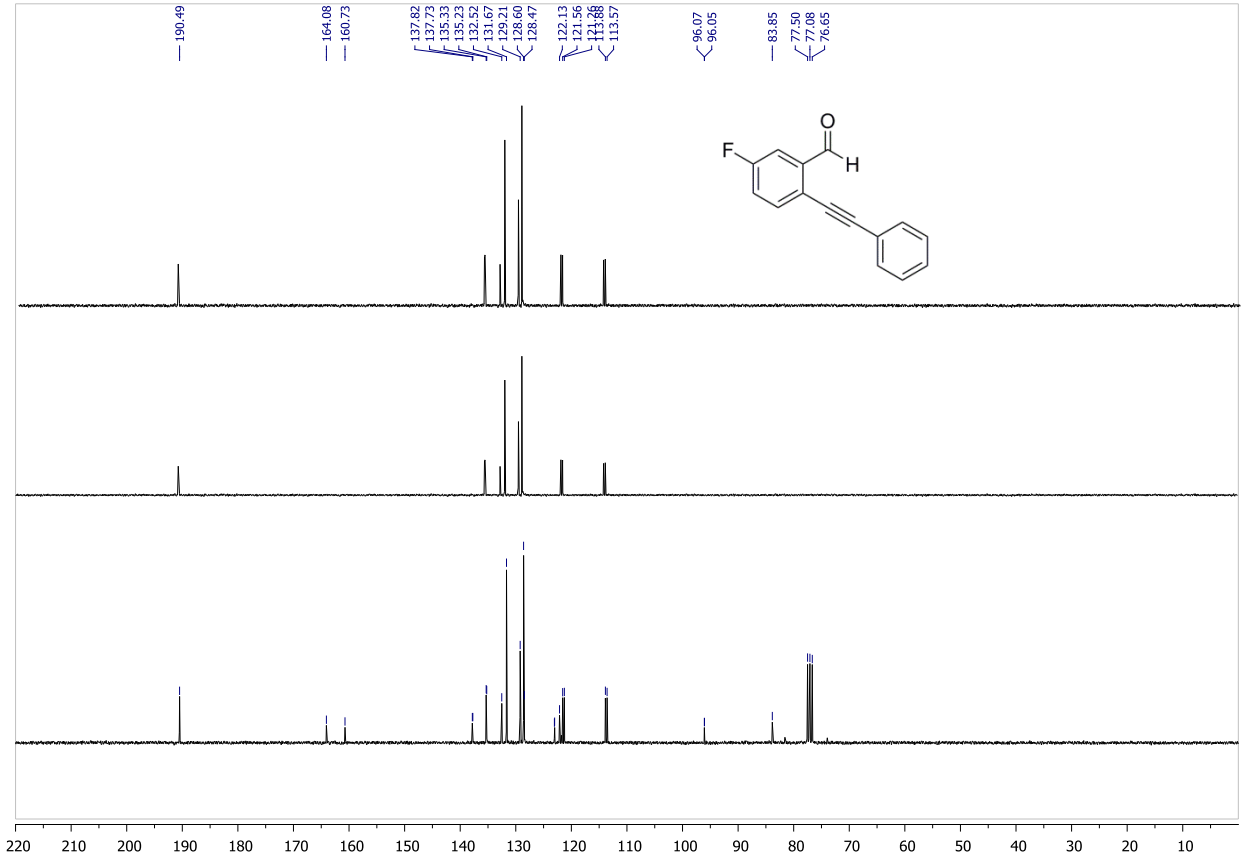

^{19}F-NMR: **S1i**

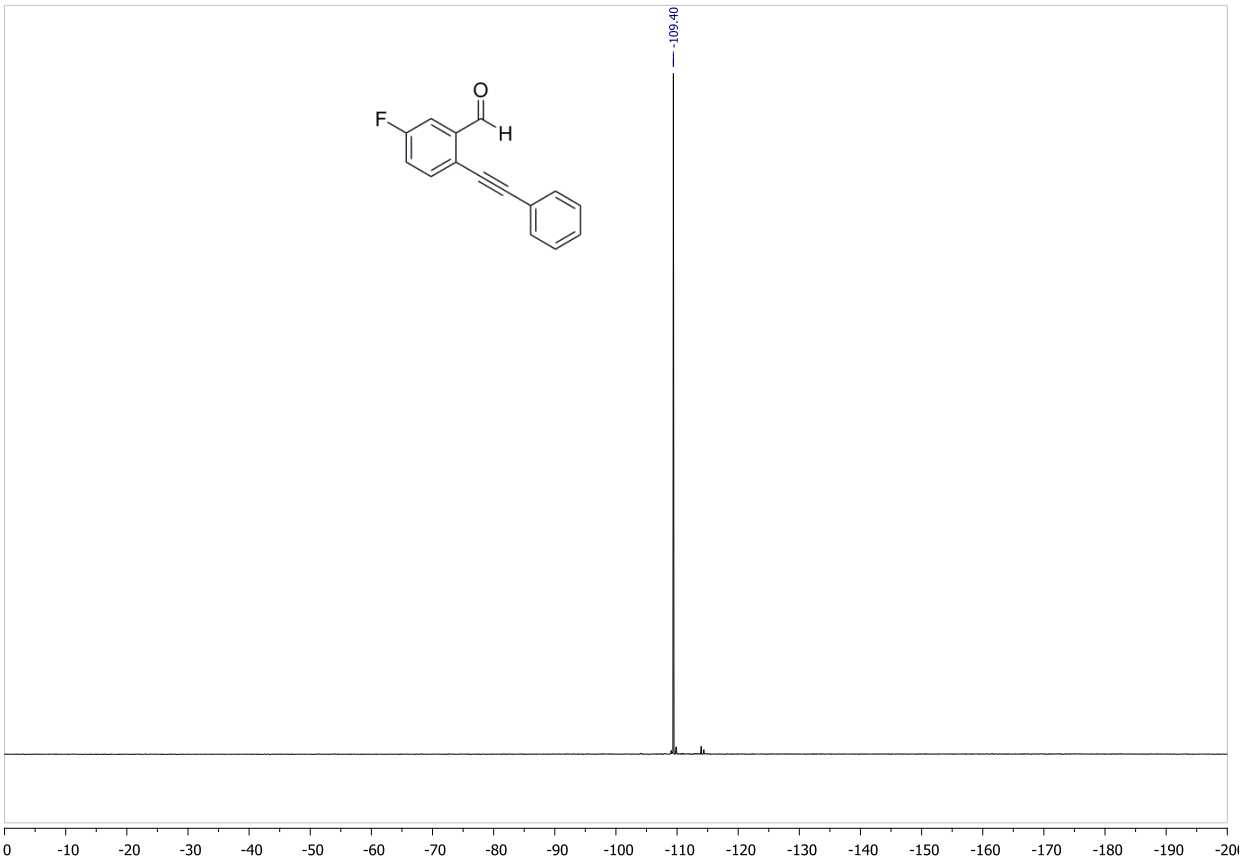
-109.40
F
O
H
0
-10
-20
-30
-40
-50
-60
-70
-80
-90
-100
-110
-120
-130
-140
-150
-160
-170
-180
-190

^{1}H-NMR: **S1j**

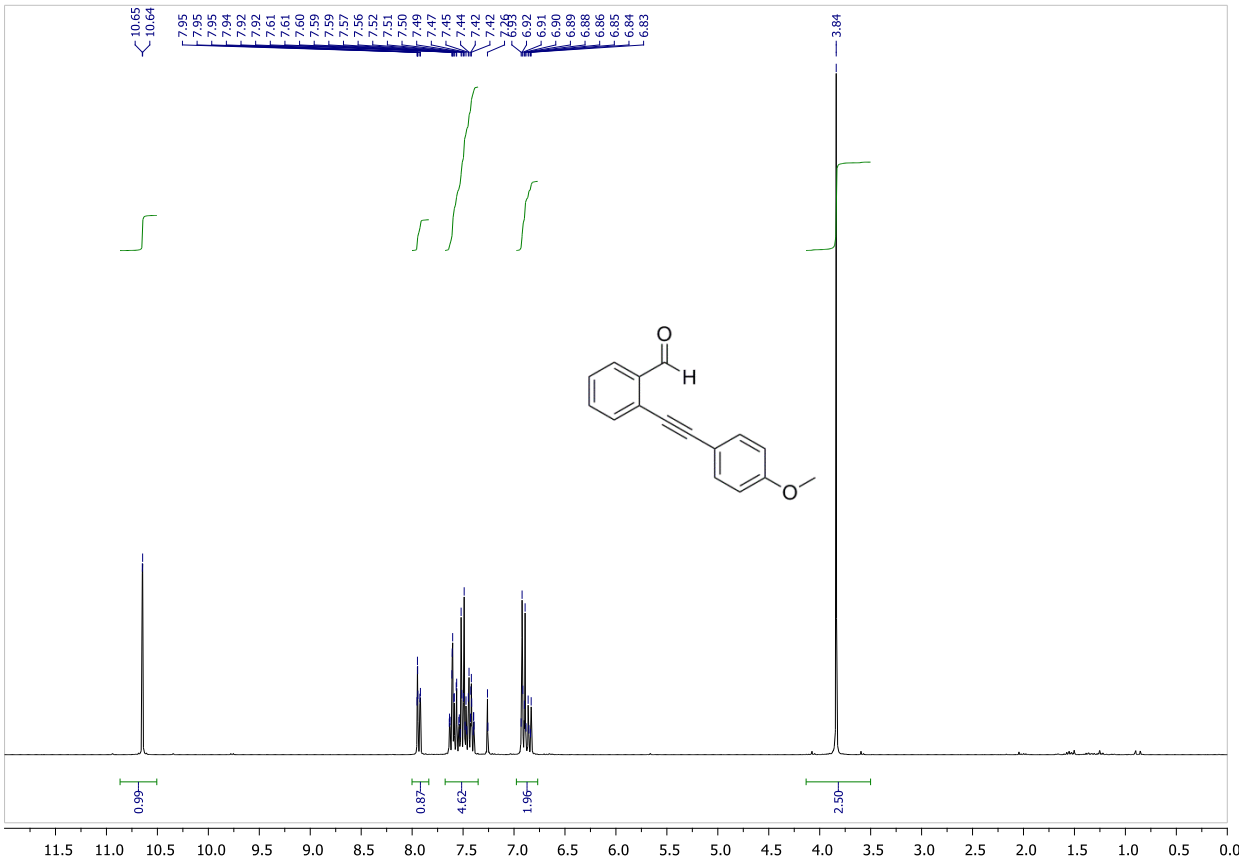

^{13}C-NMR: **S1j**

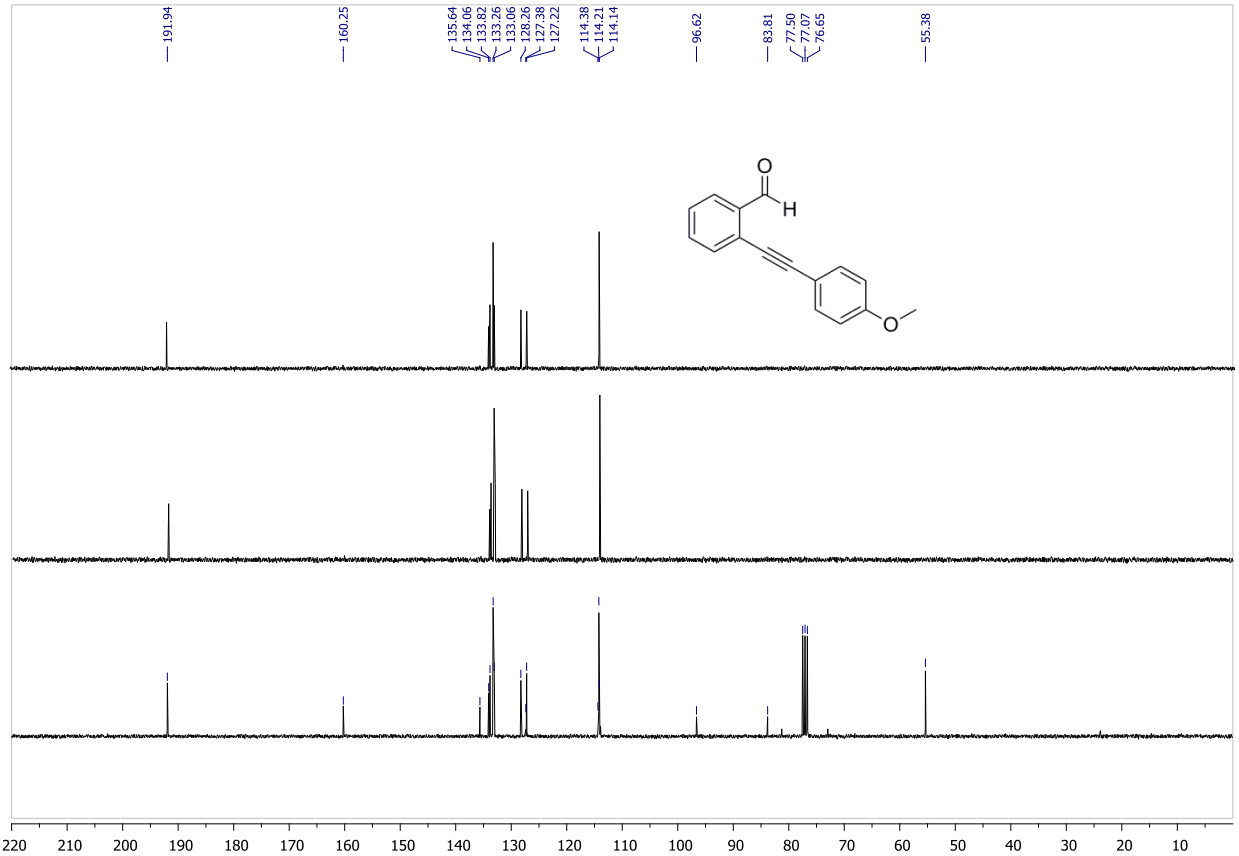

^{1}H-NMR: **S1k**

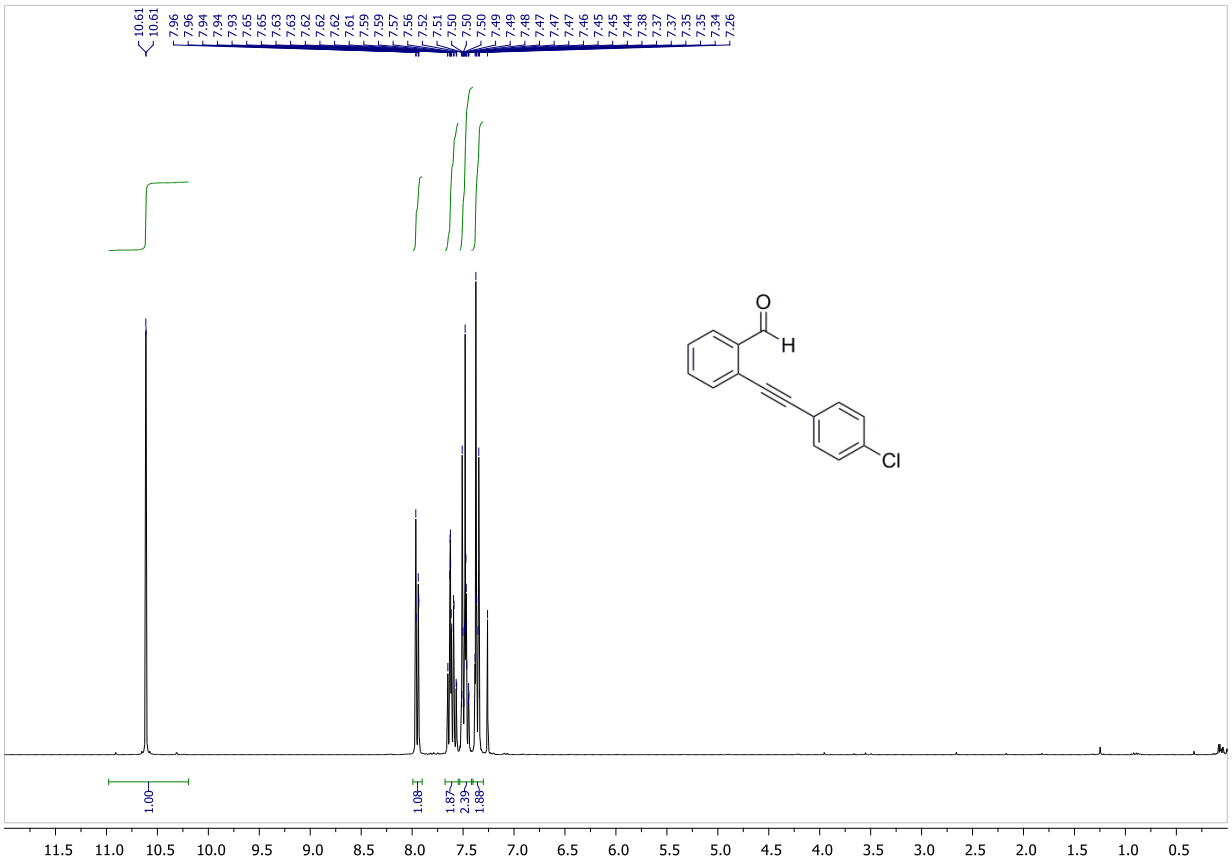

^{13}C-NMR: **S1k**

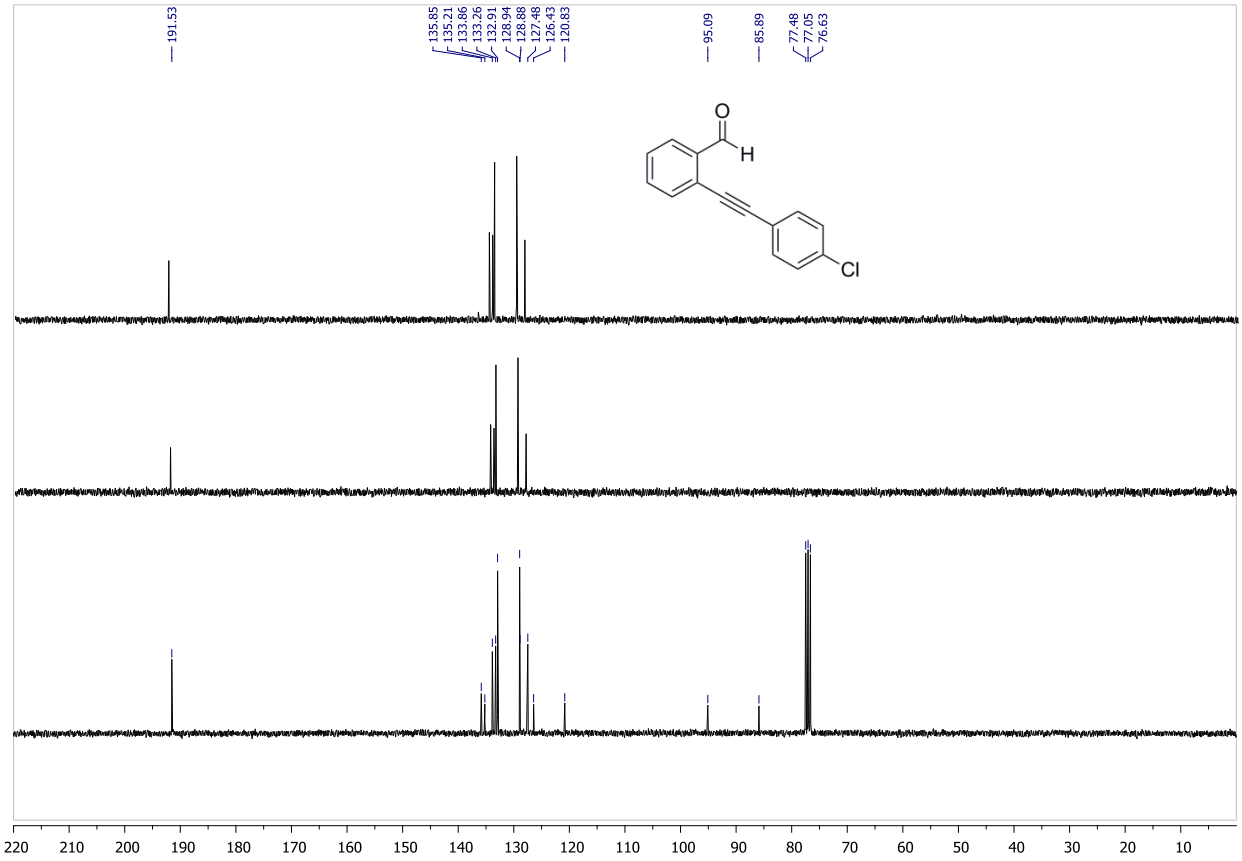

^{1}H-NMR: **S1l**

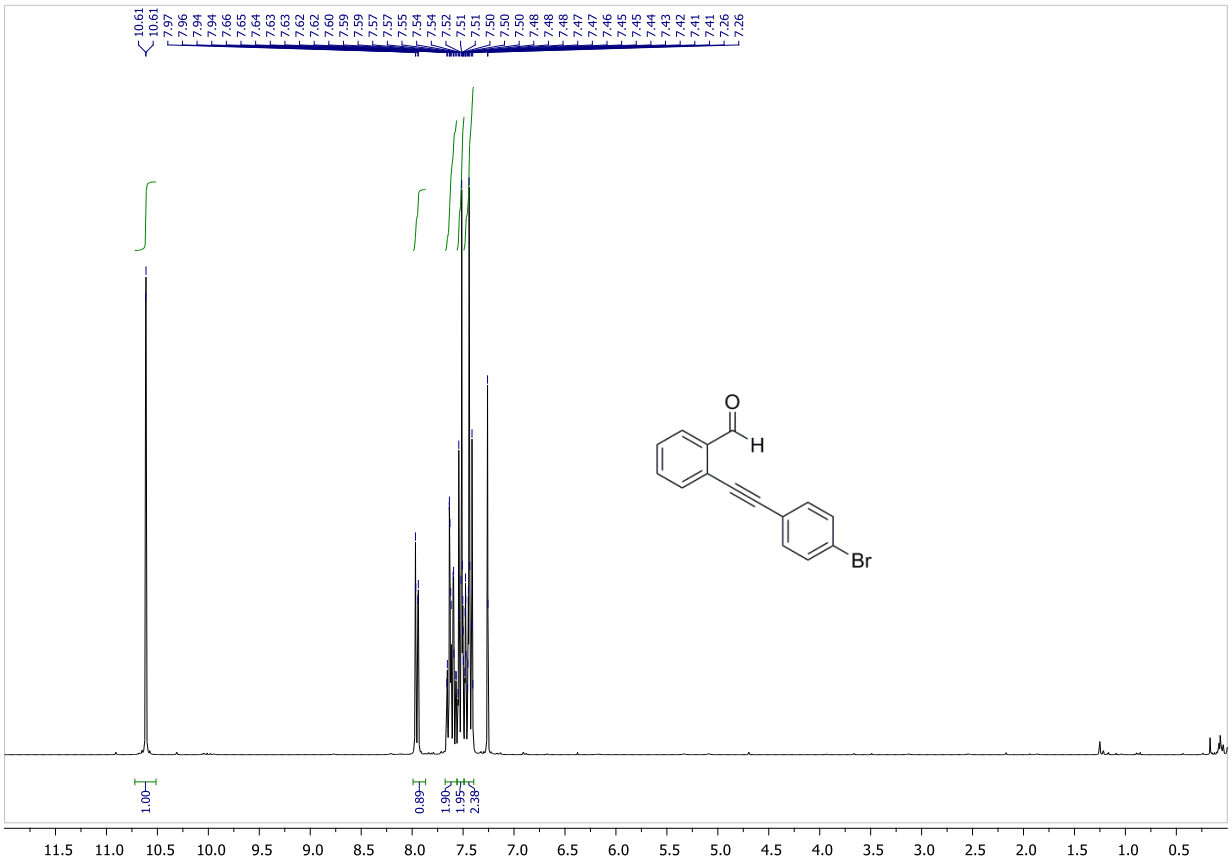

^{13}C-NMR: **S1l**

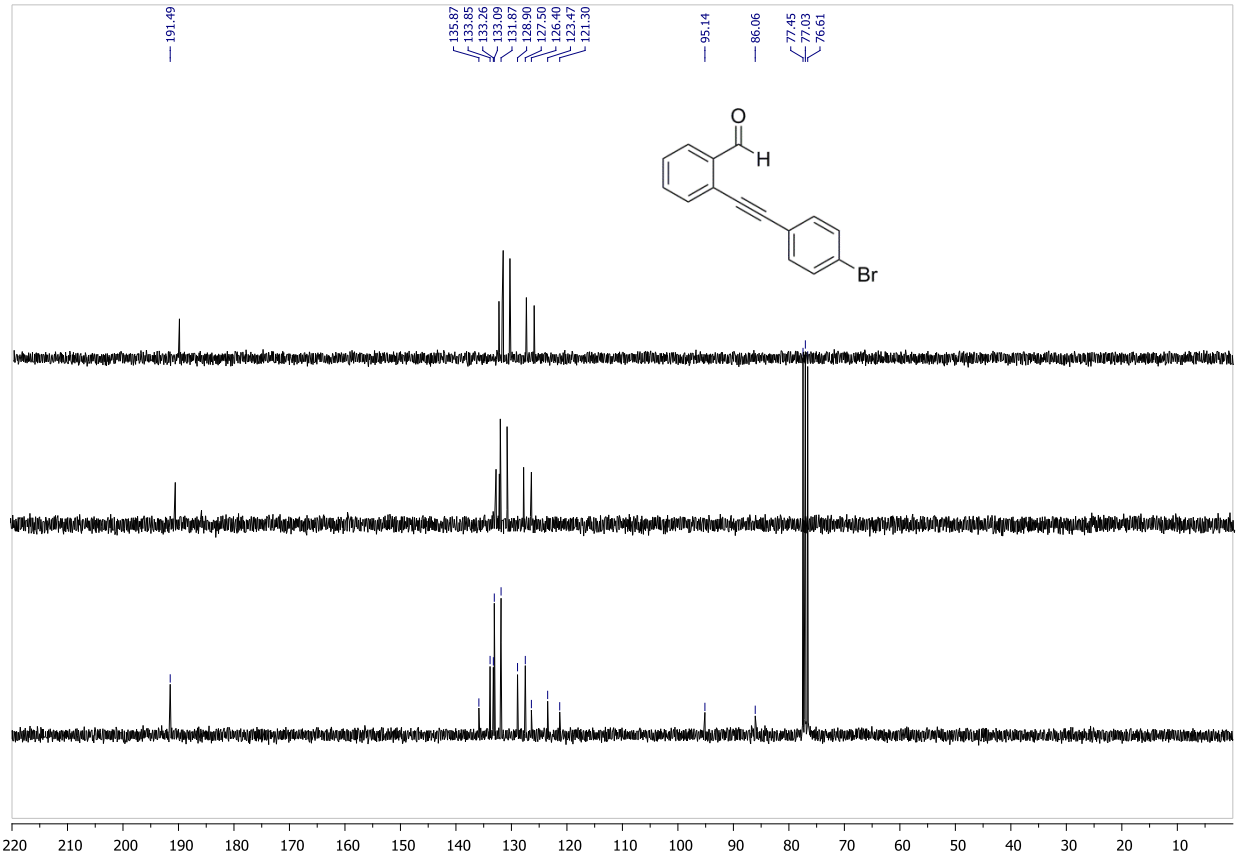

^{1}H-NMR: **S1m**

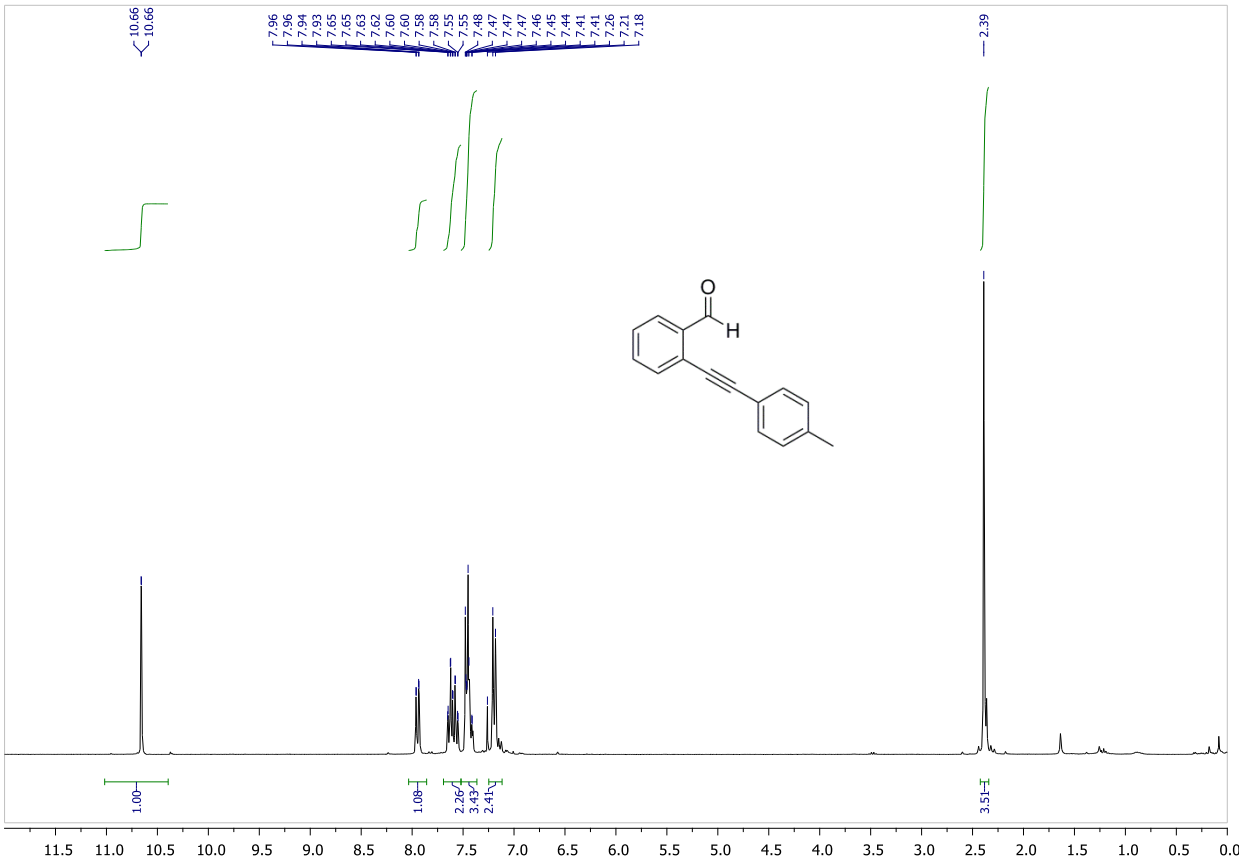

^{13}C-NMR: **S1m**

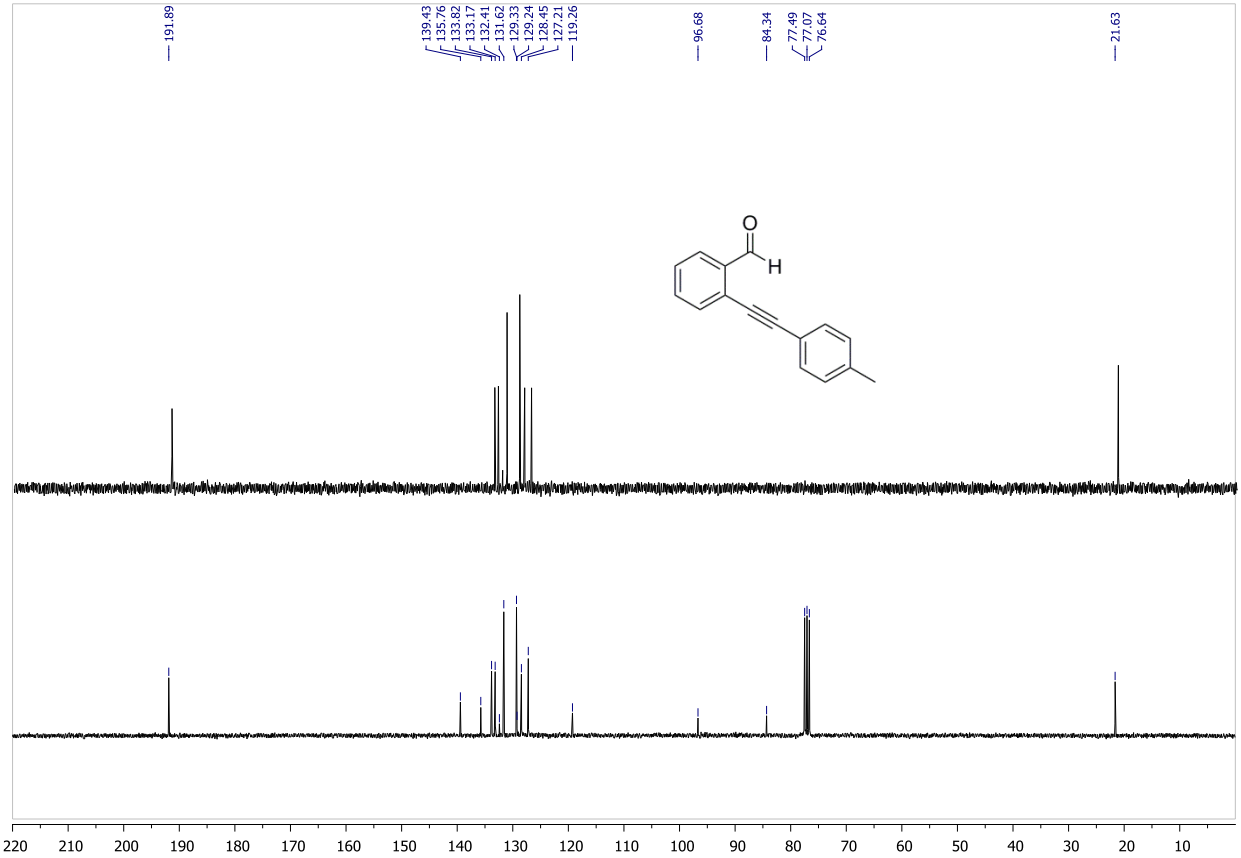

^{1}H-NMR: **S1n**

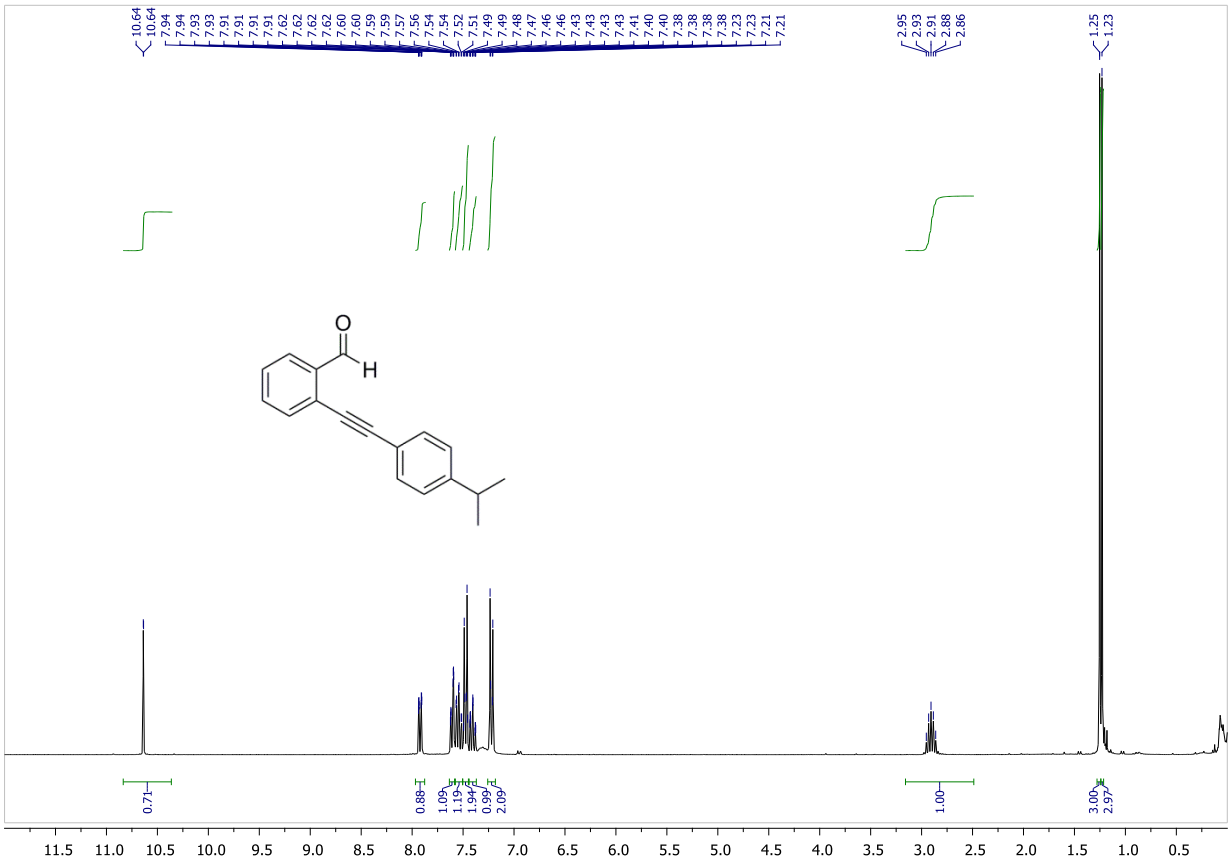

^{13}C-NMR: **S1n**

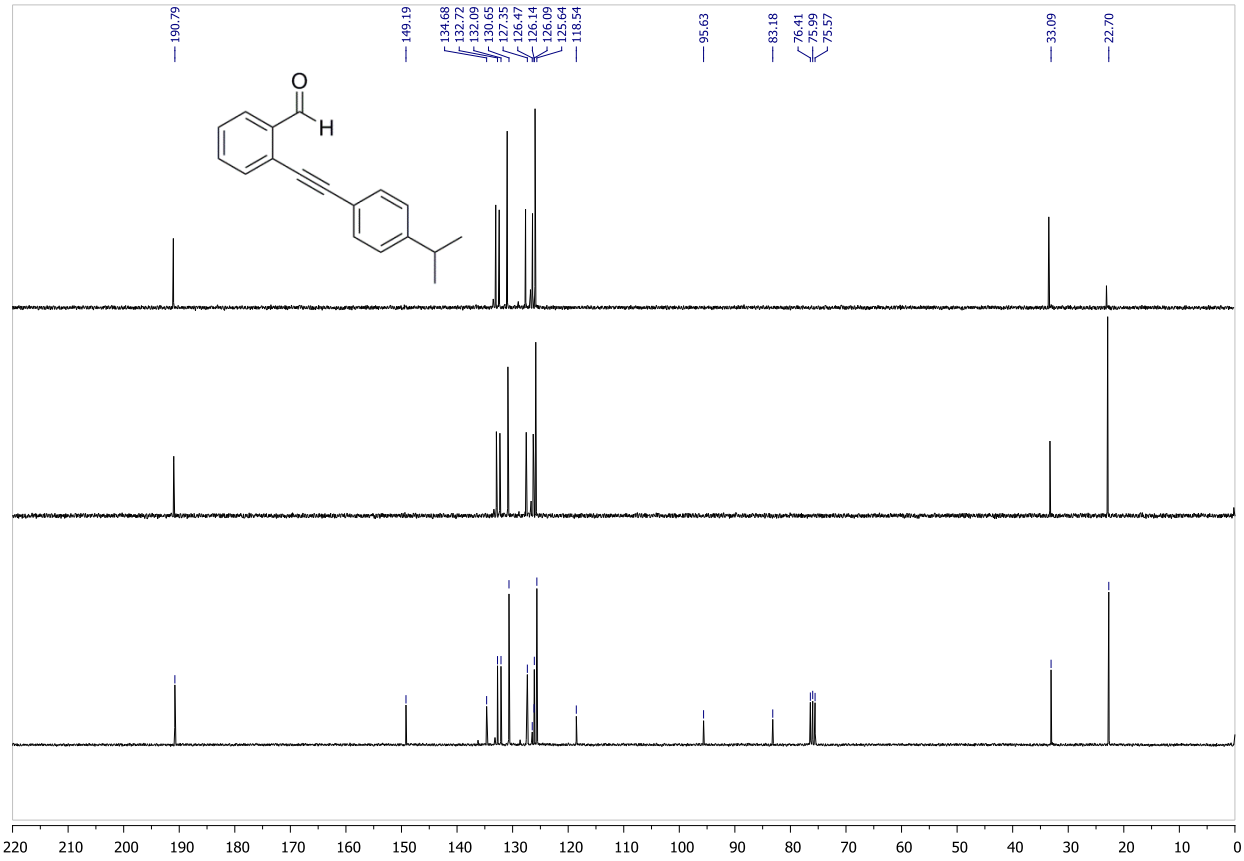

^{1}H-NMR: **S1o**

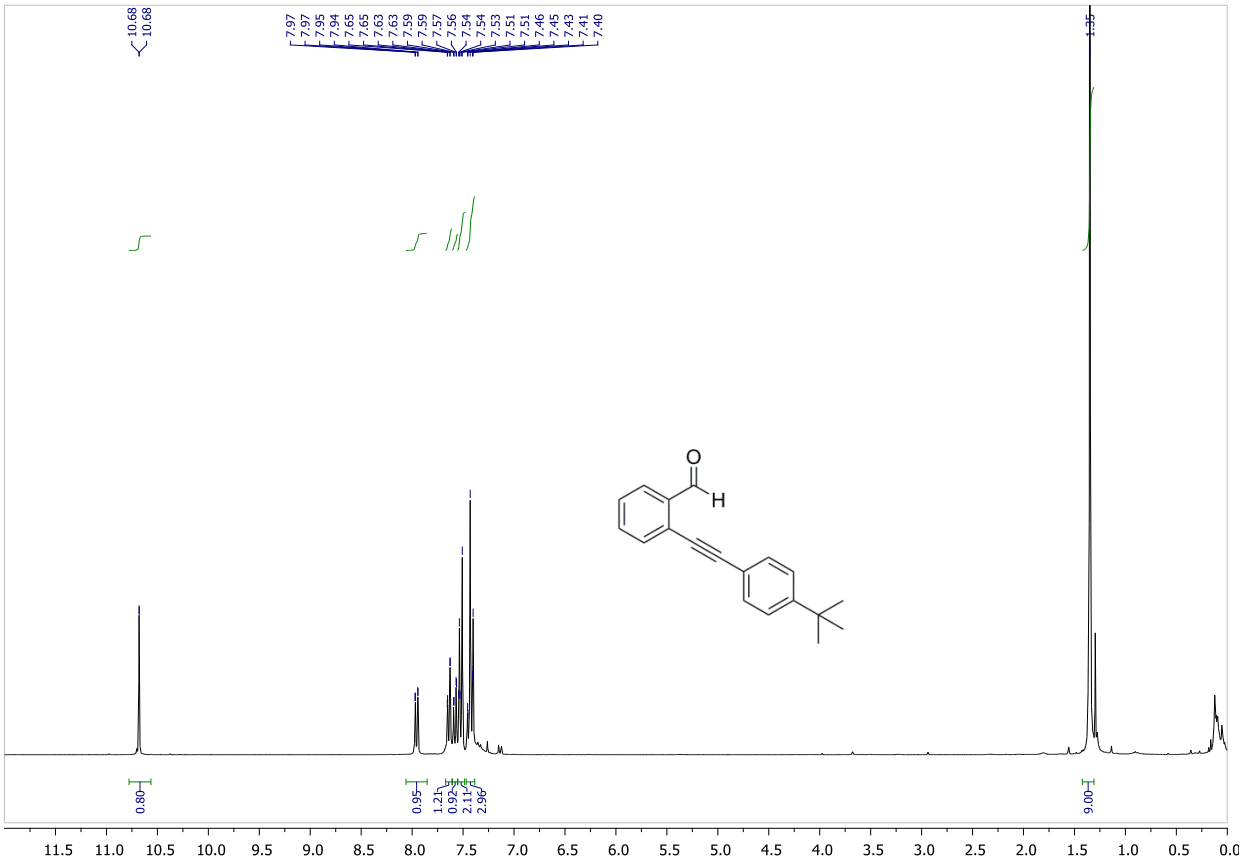

^{13}C-NMR: **S1o**

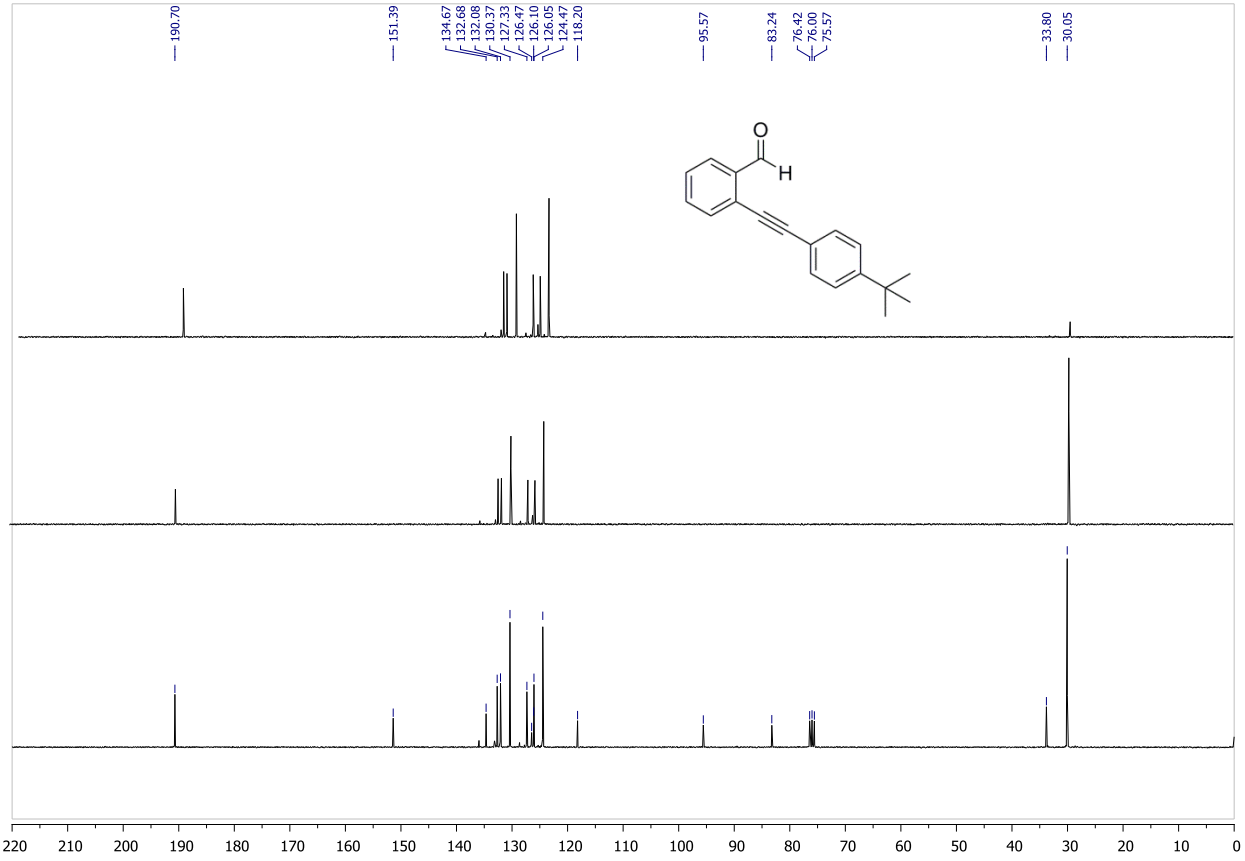

^{1}H-NMR: **S1p**

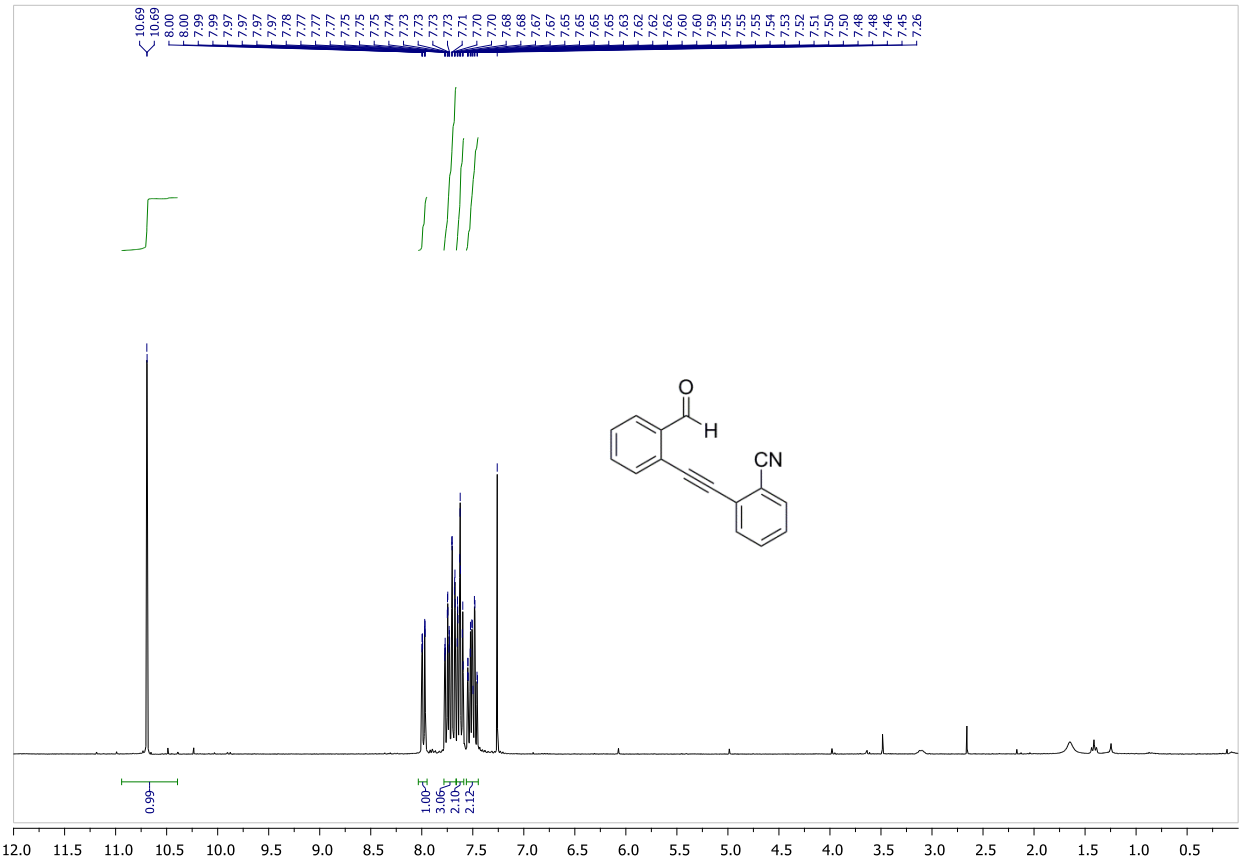

^{13}C-NMR: **S1p**

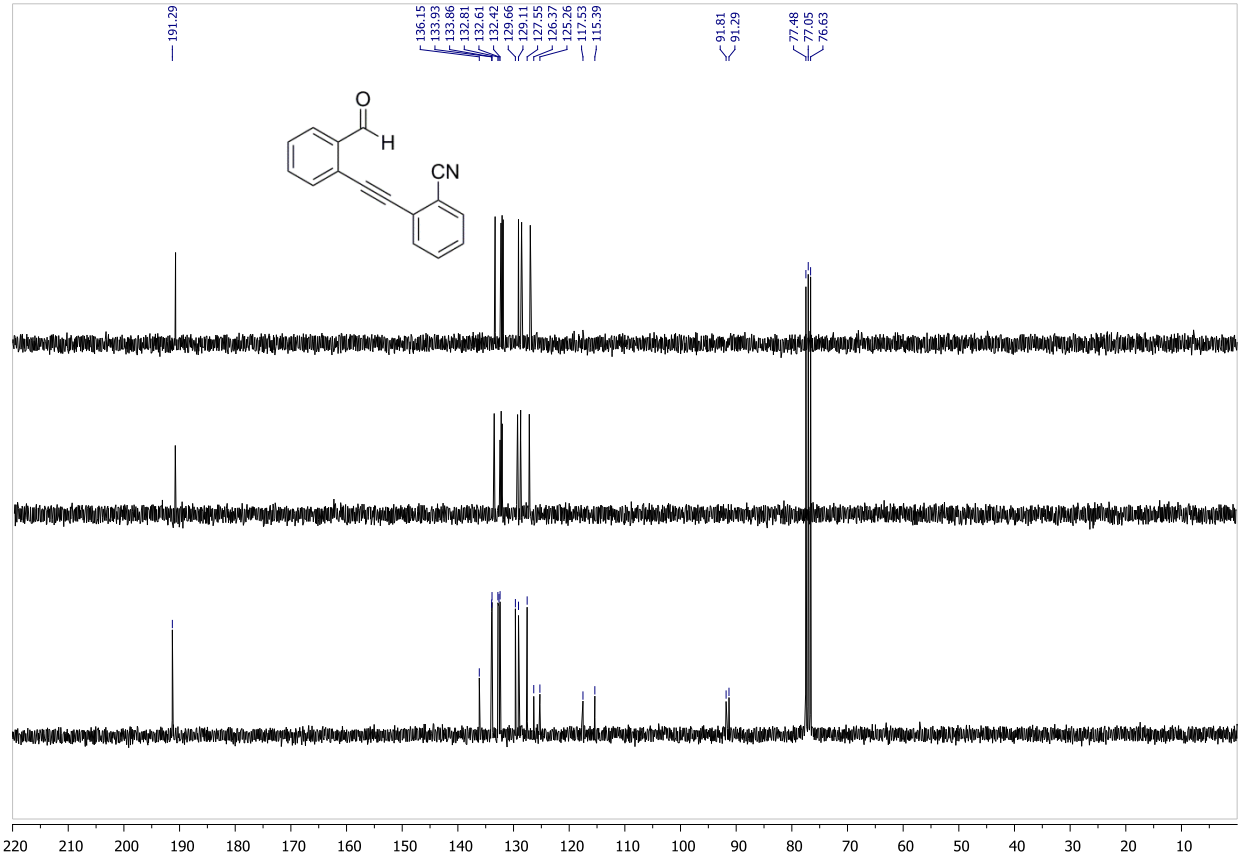

^{1}H-NMR: **S1q**

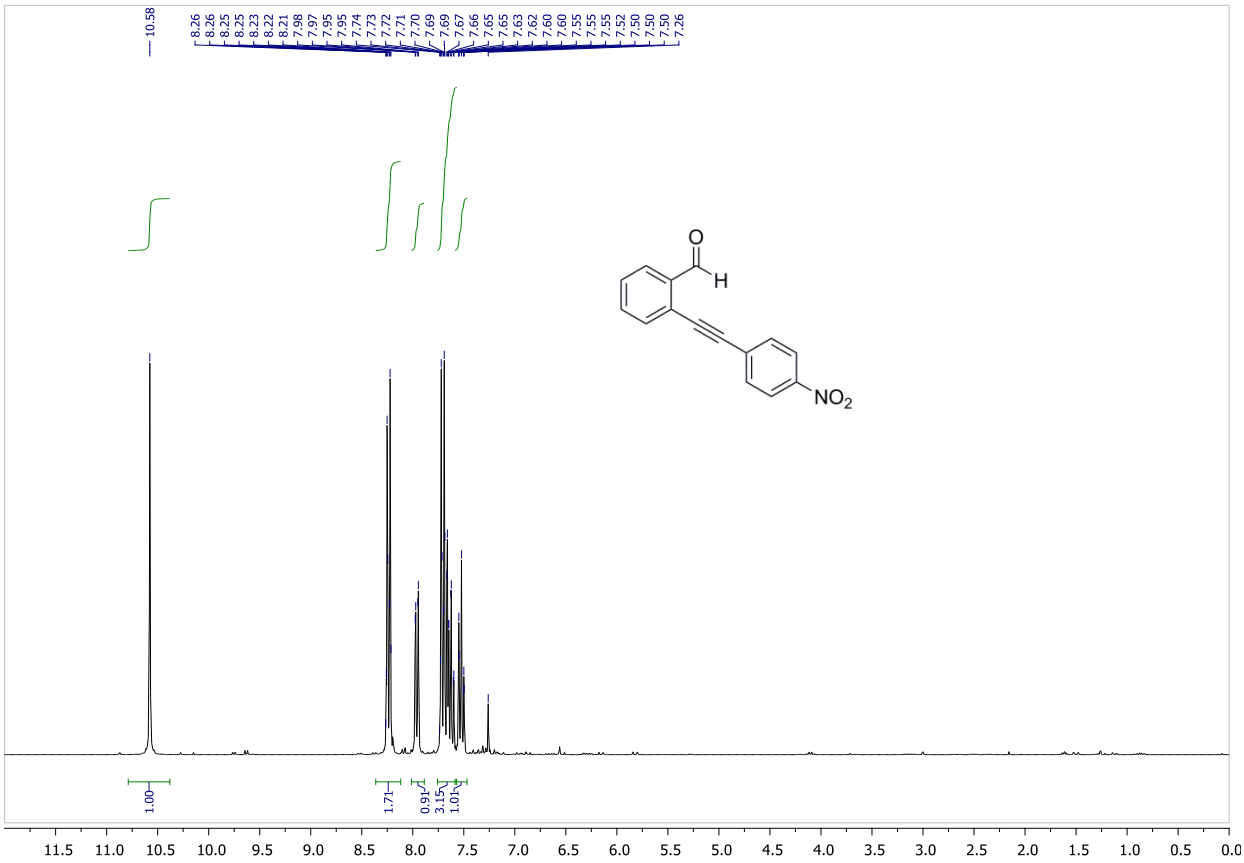

^{13}C-NMR: **S1q**

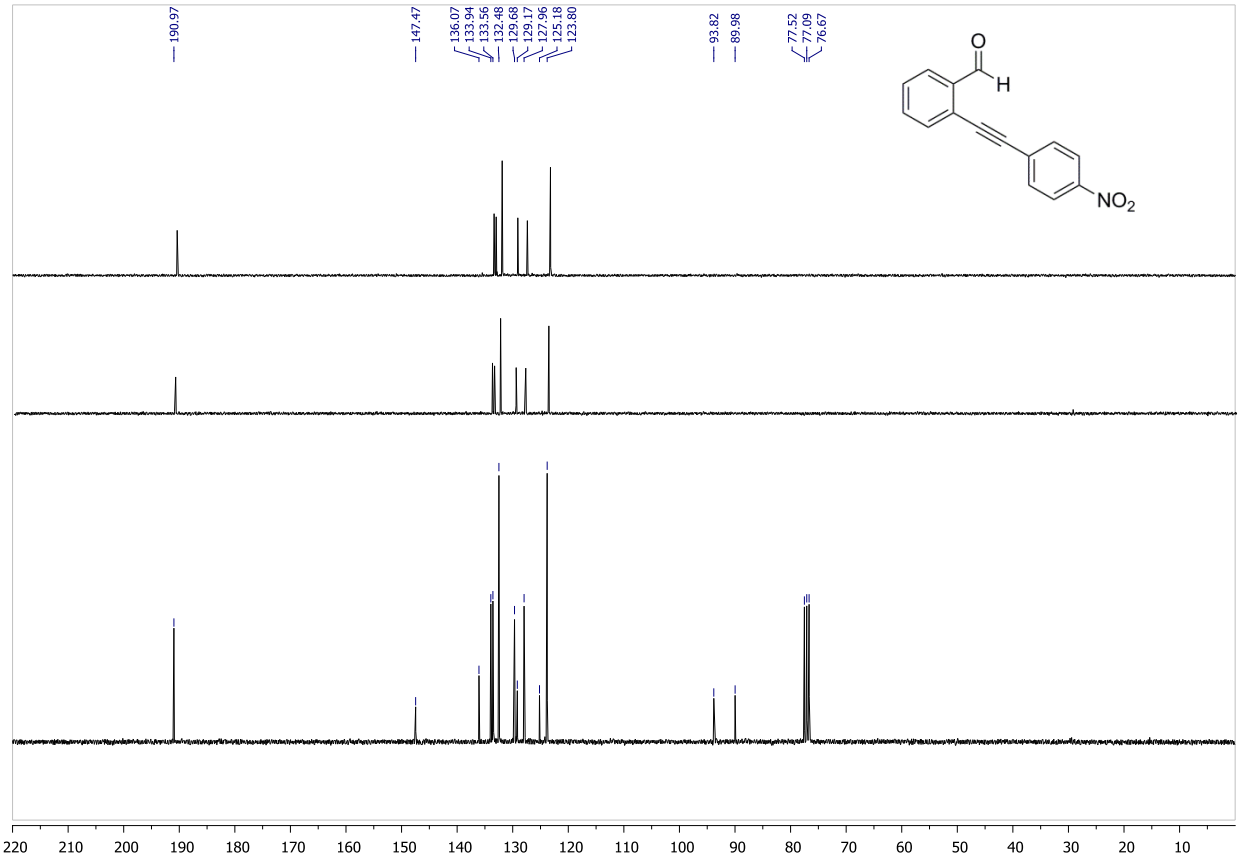

^{1}H-NMR: **S1r**

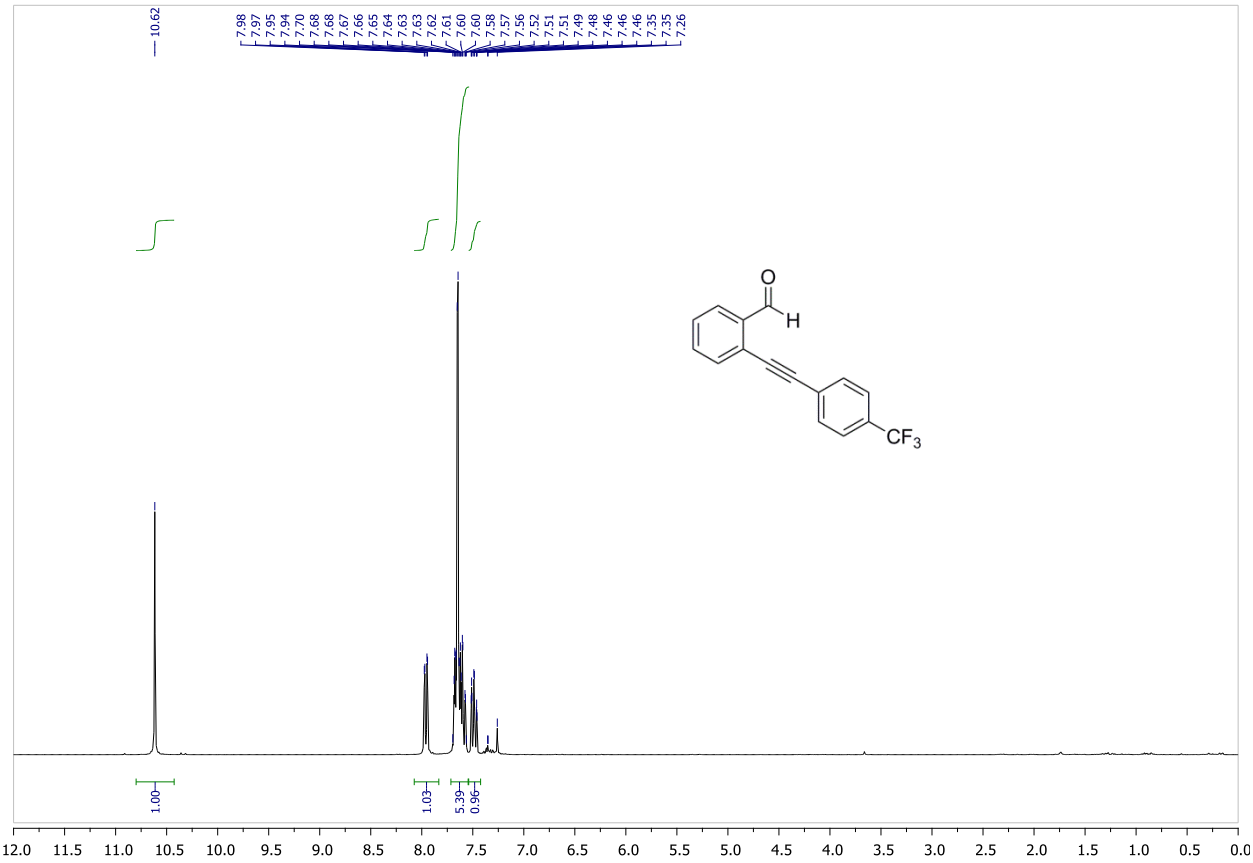

^{13}C-NMR: **S1r**

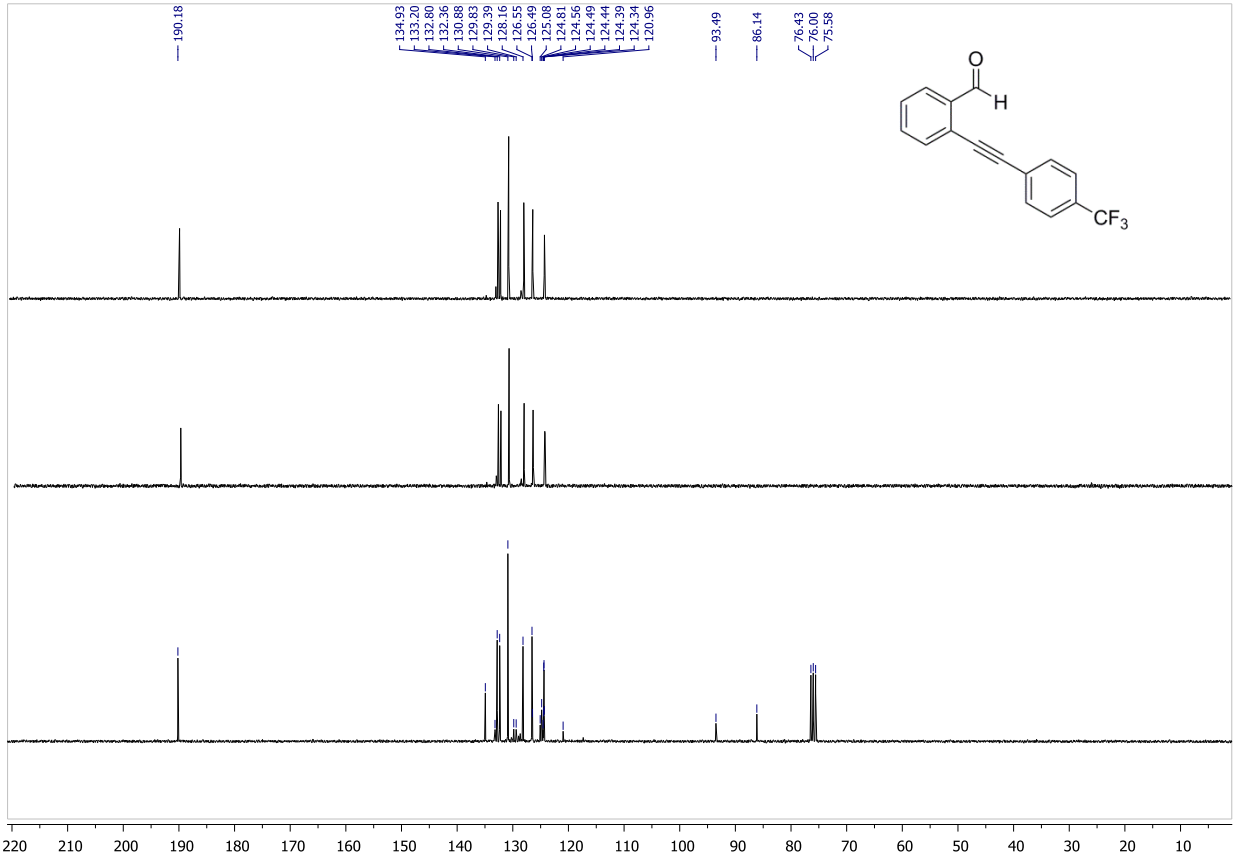

^{19}F-NMR: **S1r**

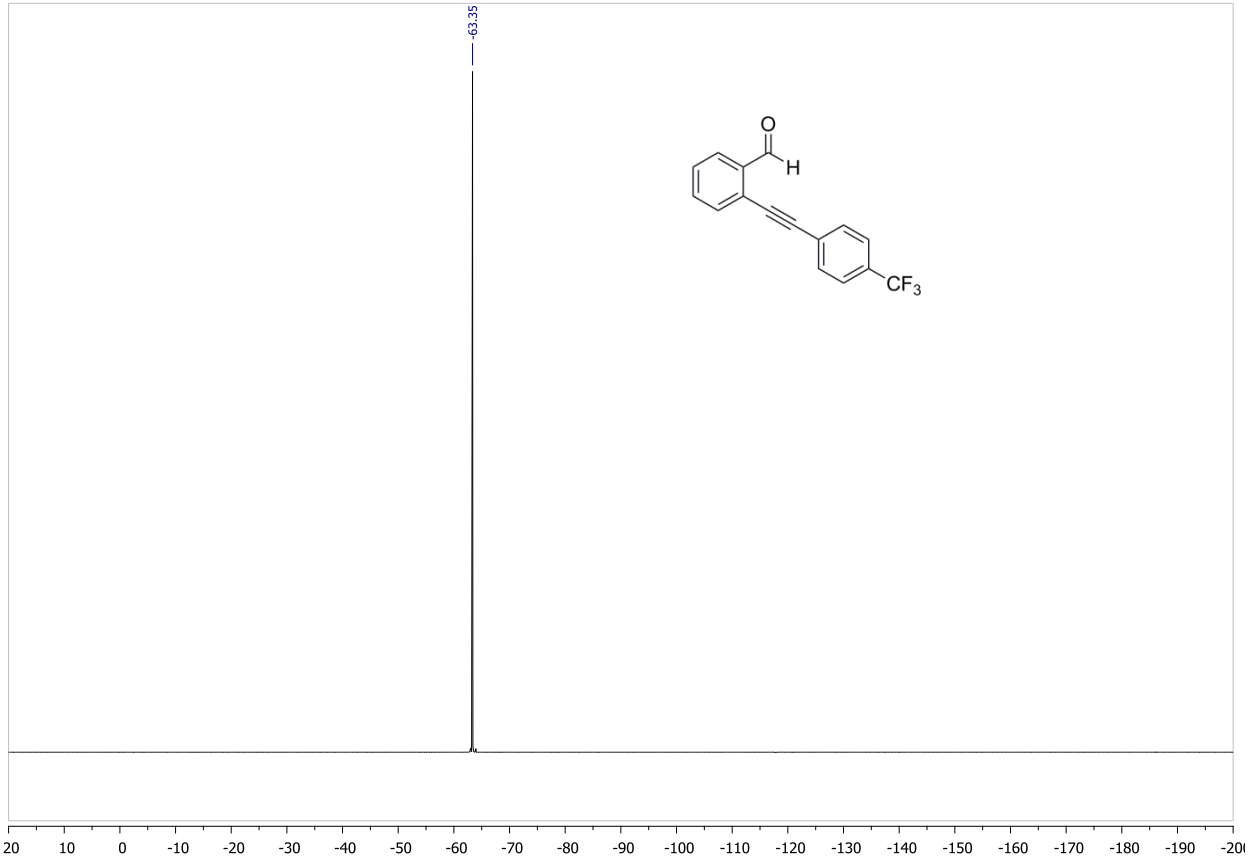
-63.35
O
H
CF3
20
10
0
-10
-20
-30
-40
-50
-60
-70
-80
-90
-100
-110
-120
-130
-140
-150
-160
-170
-180
-190

^{1}H-NMR: **S1s**

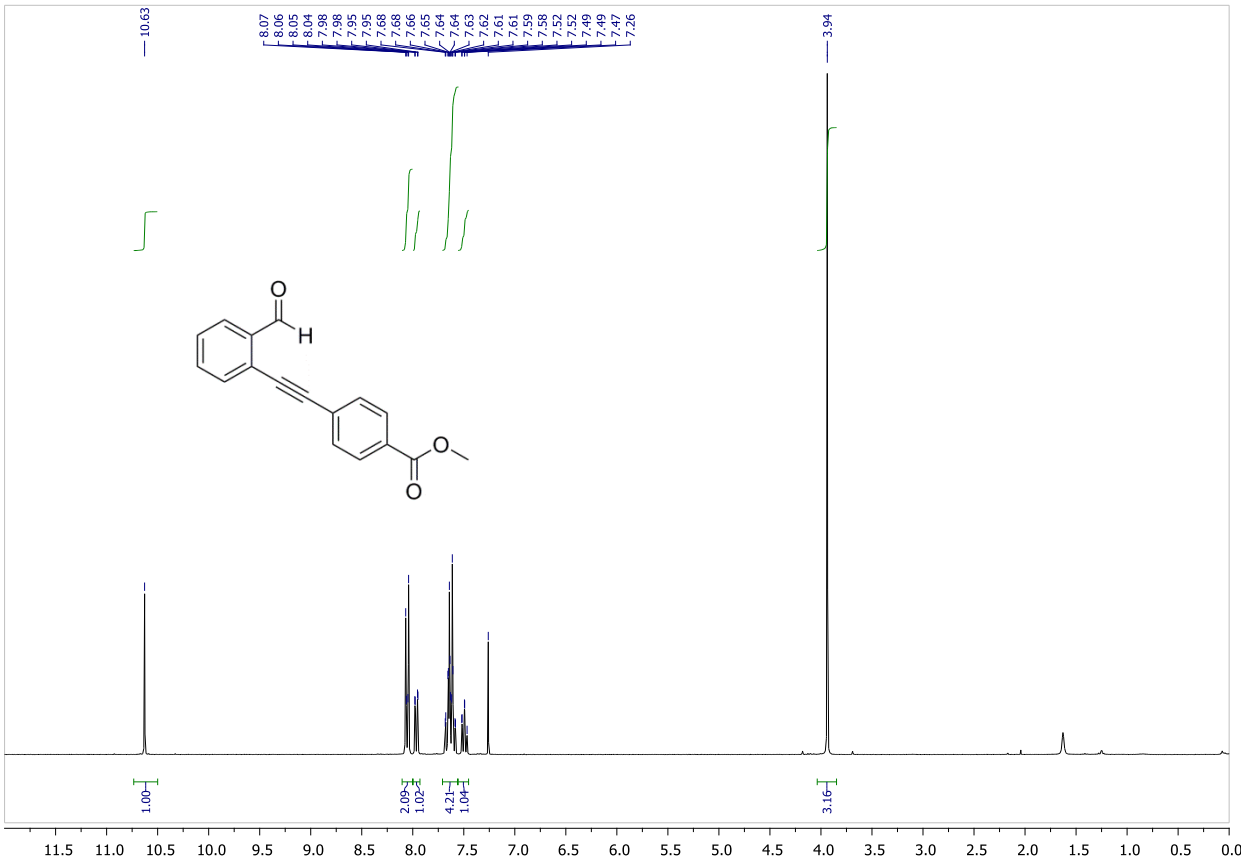

^{13}C-NMR: **S1s**

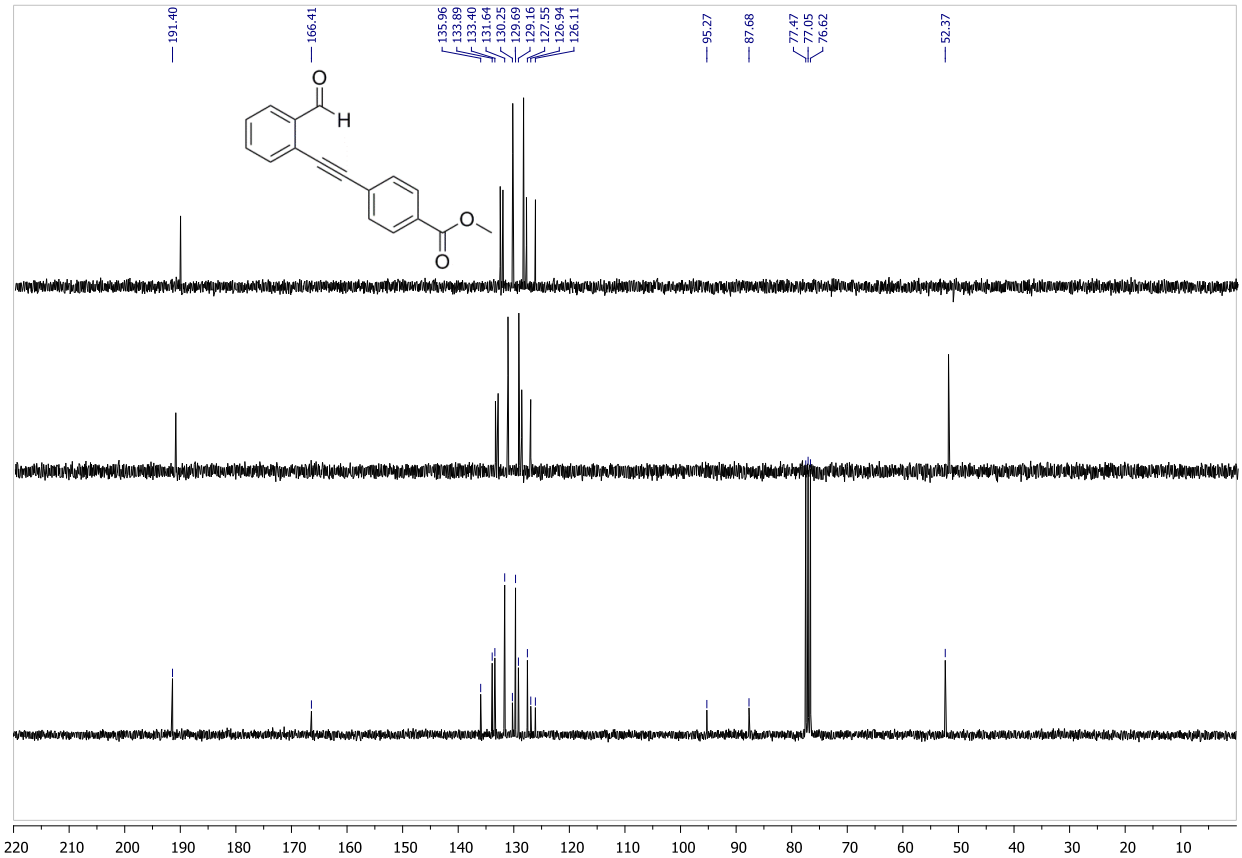

^{1}H-NMR: **S1t**

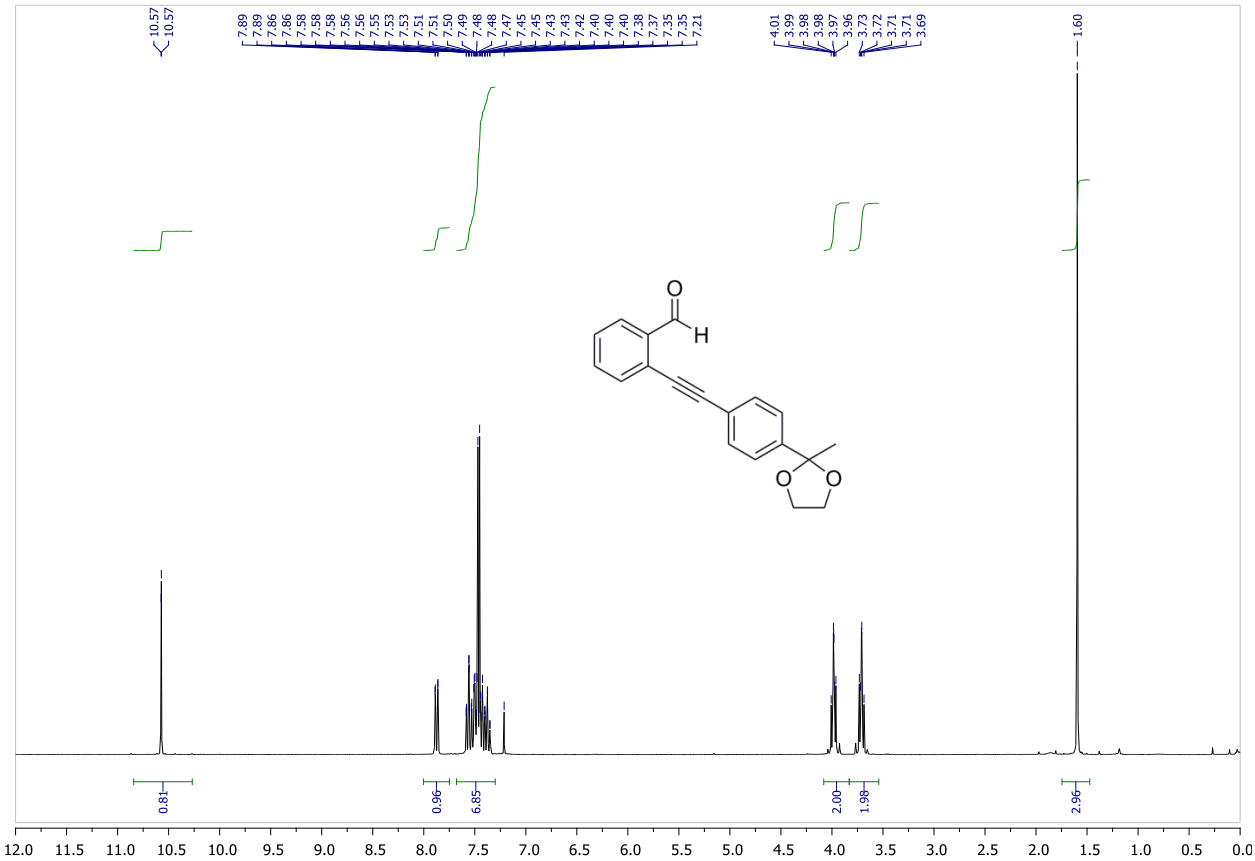

^{13}C-NMR: **S1t**

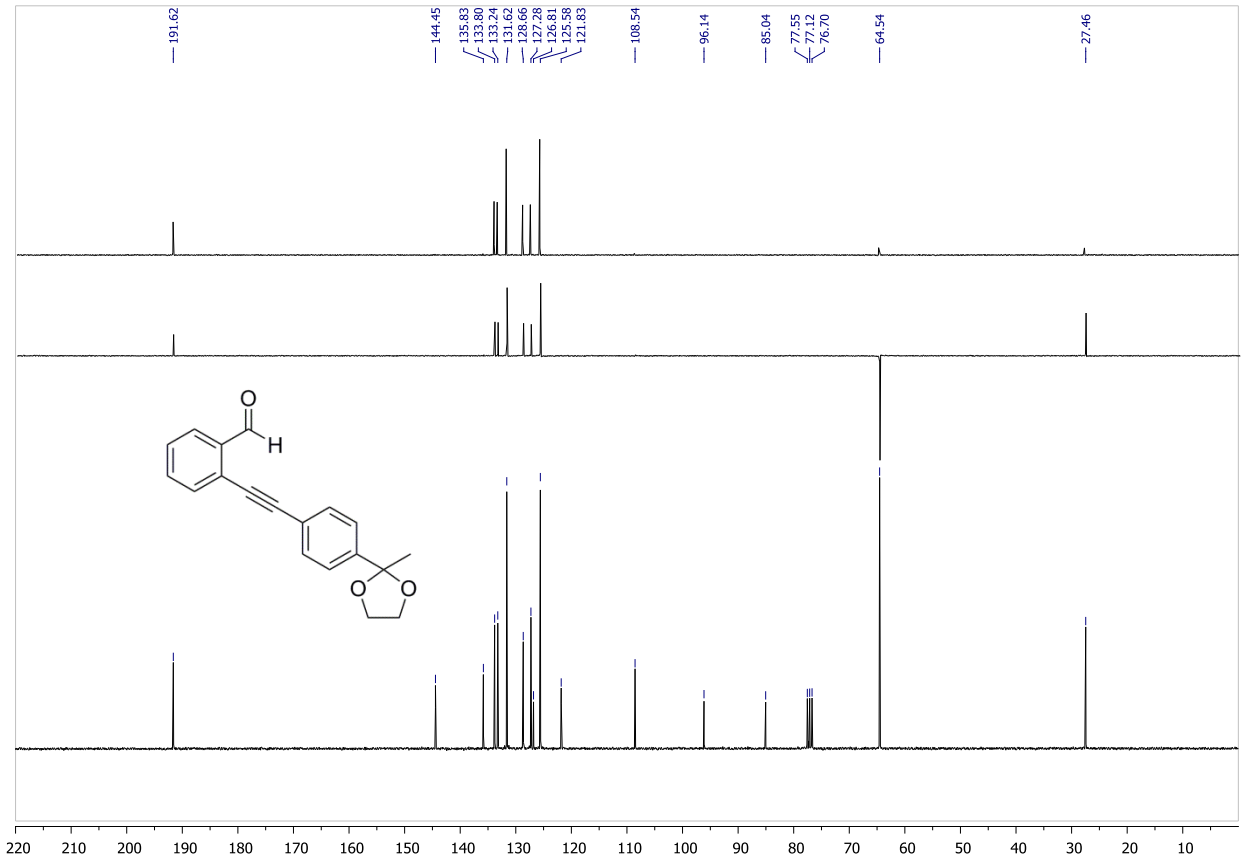

^{1}H-NMR: **S1u**

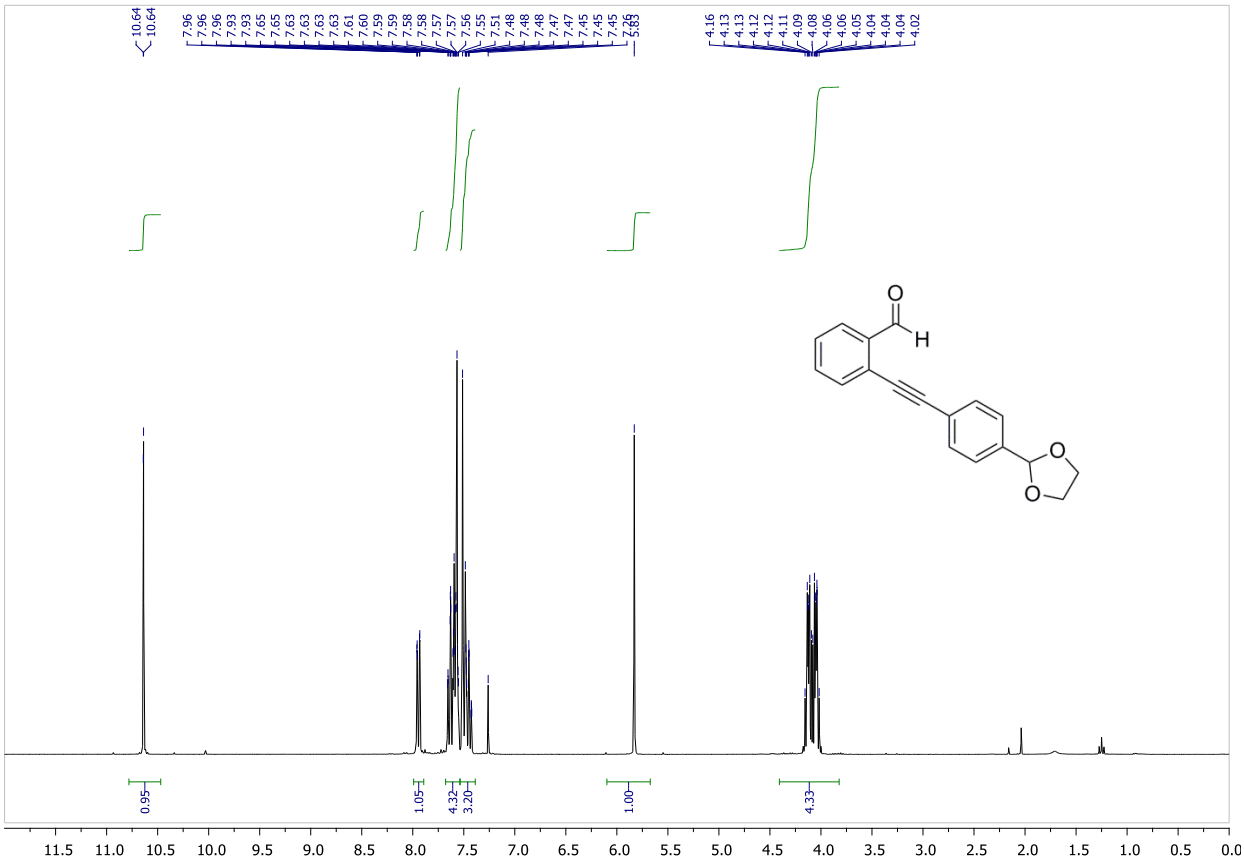

^{13}C-NMR: **S1u**

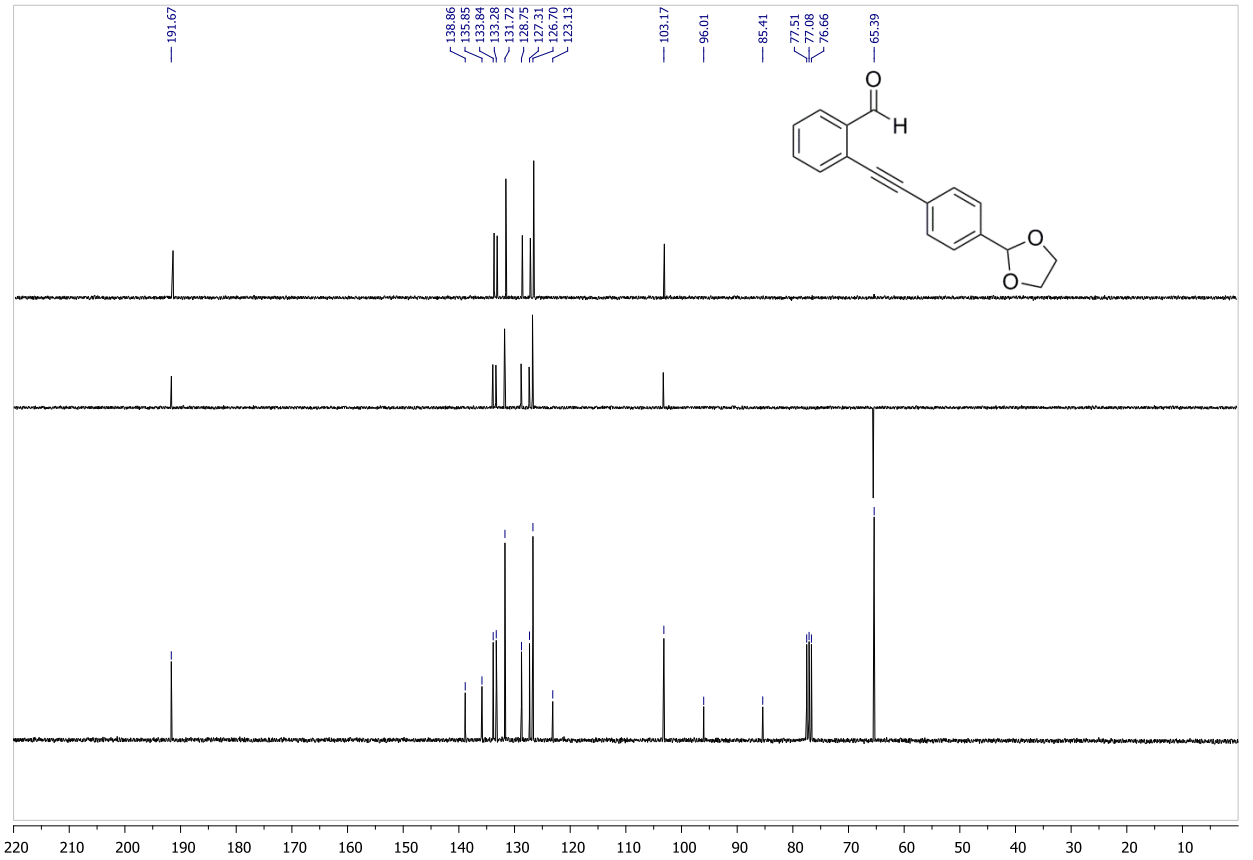

^{1}H-NMR: **S1v**

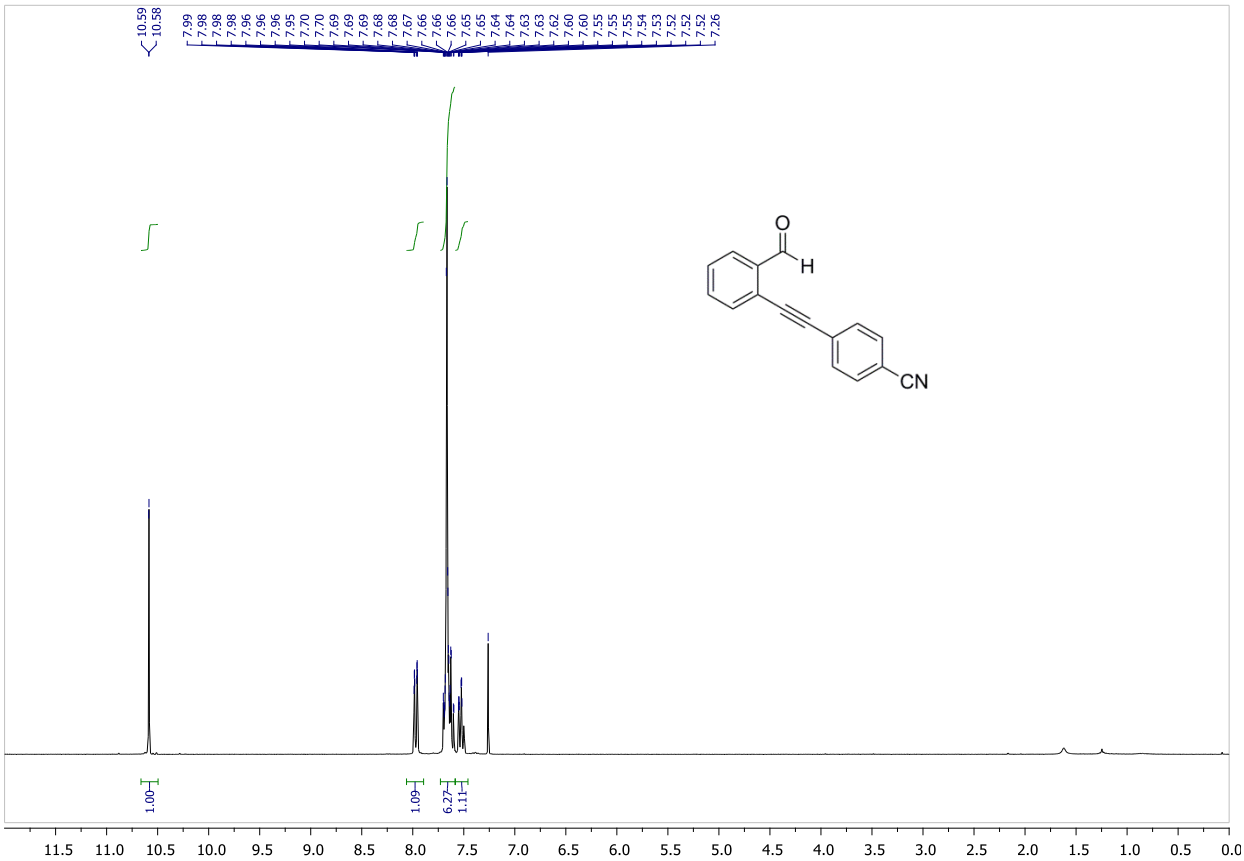

^{13}C-NMR: **S1v**

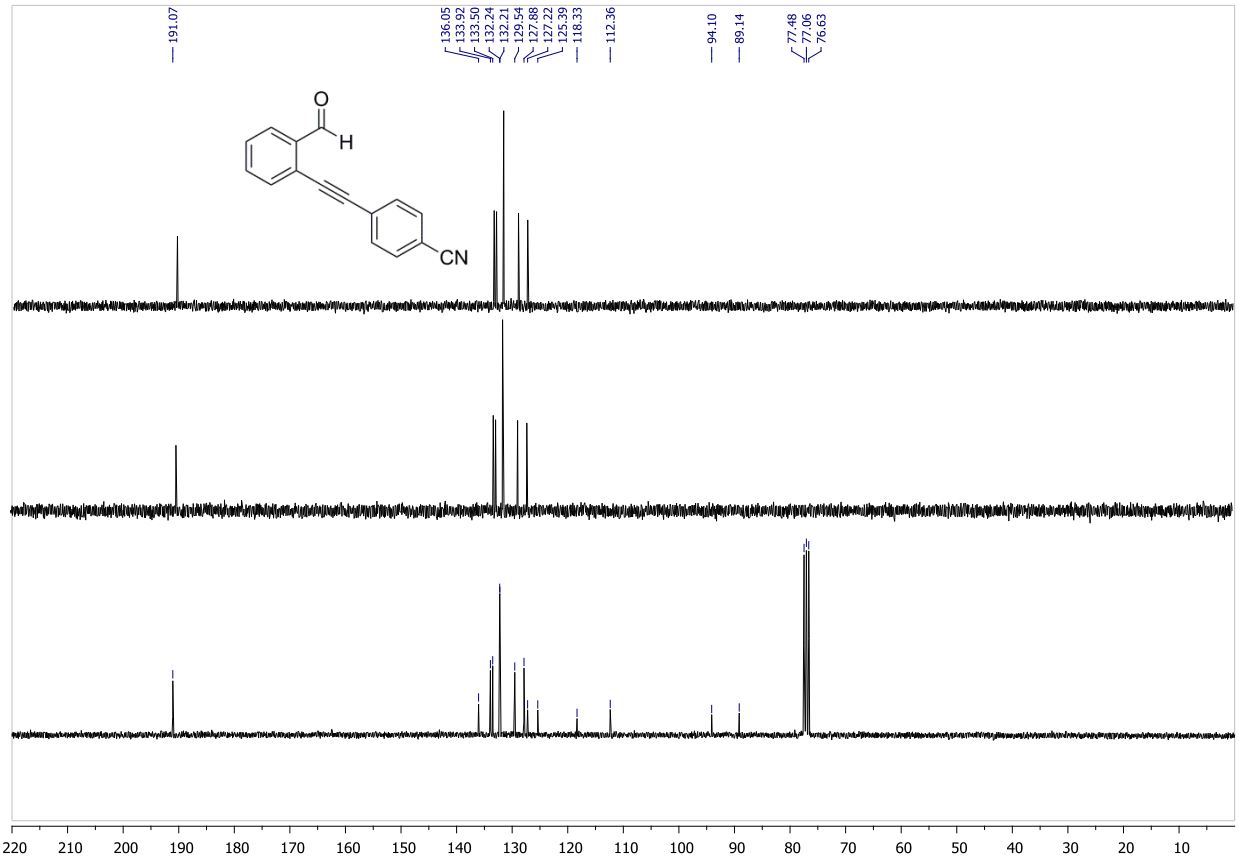

^{1}H-NMR: **S1w**

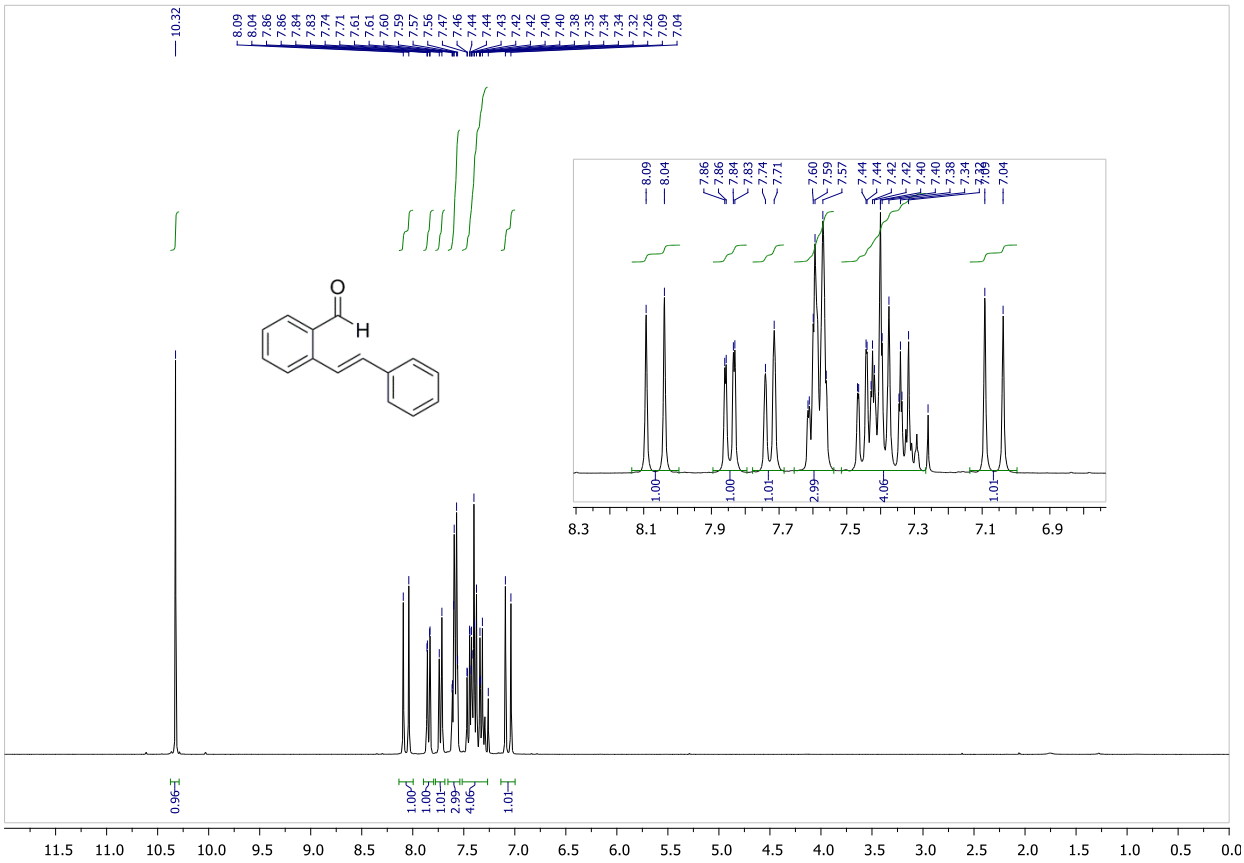

^{13}C-NMR: **S1w**

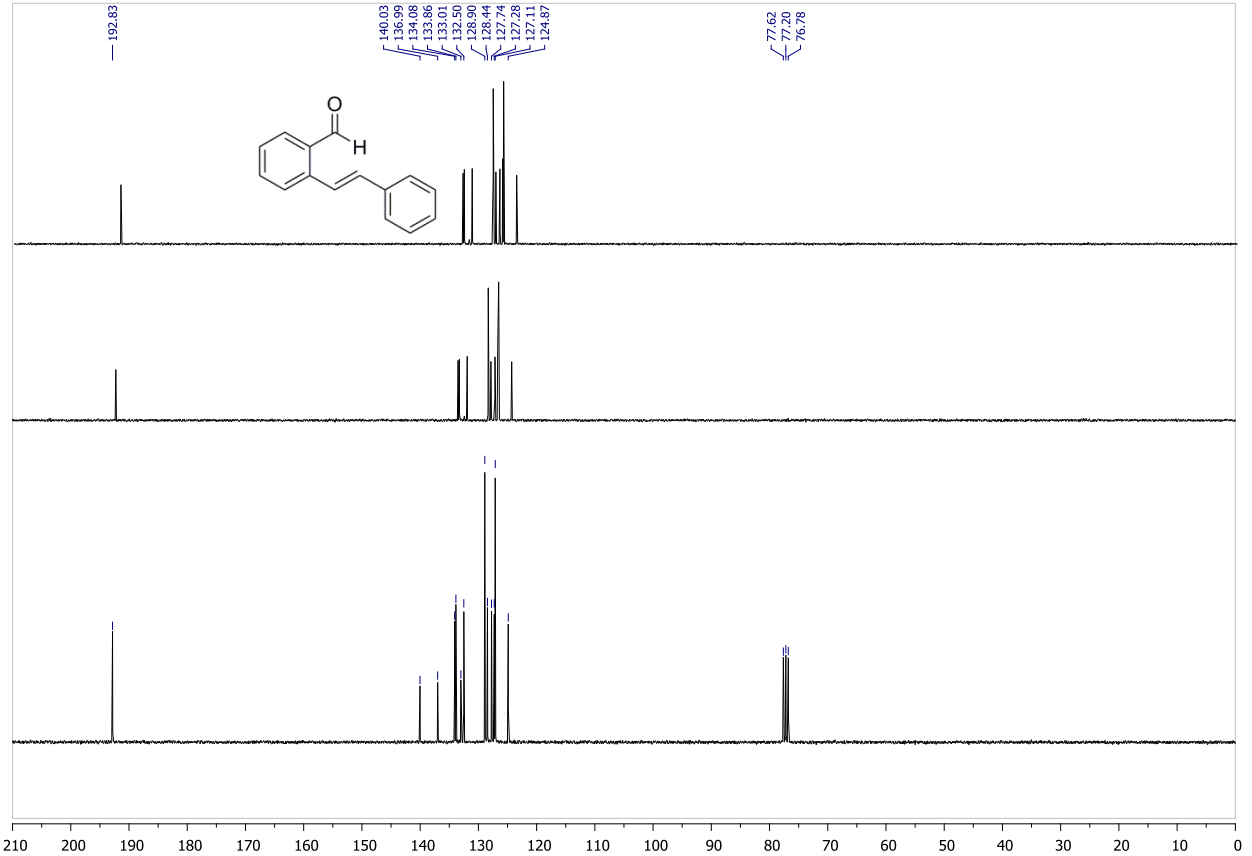

^{1}H-NMR: **S1aa**

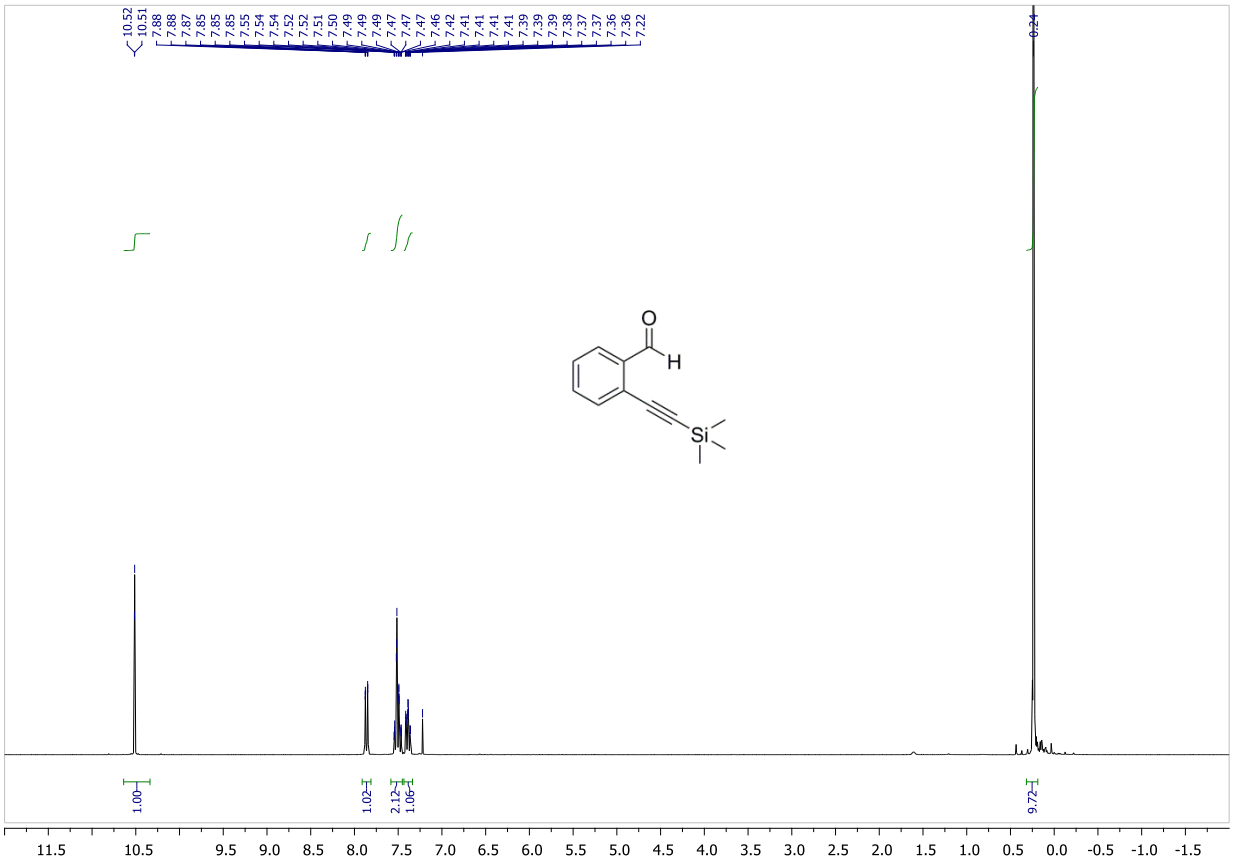

^{13}C-NMR: **S1aa**

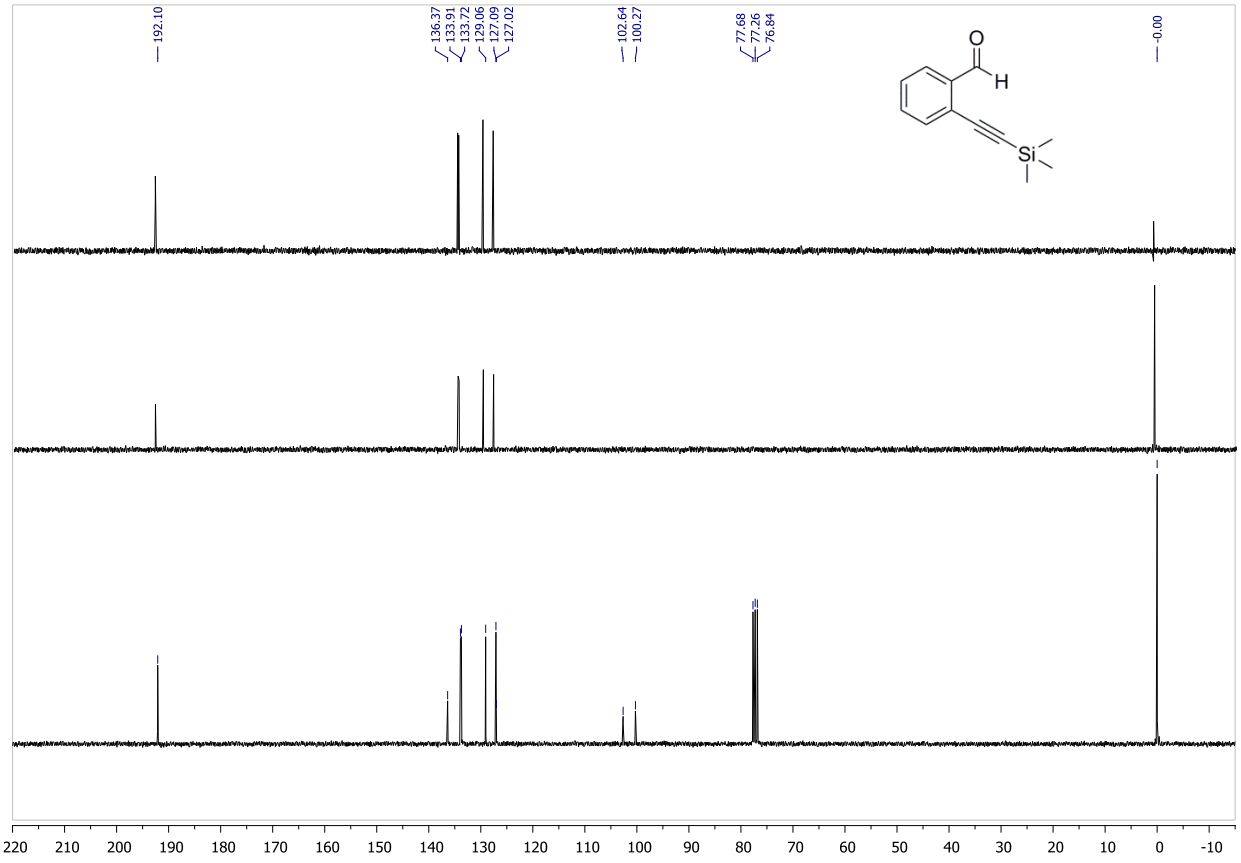

^{1}H-NMR: **S1ab**

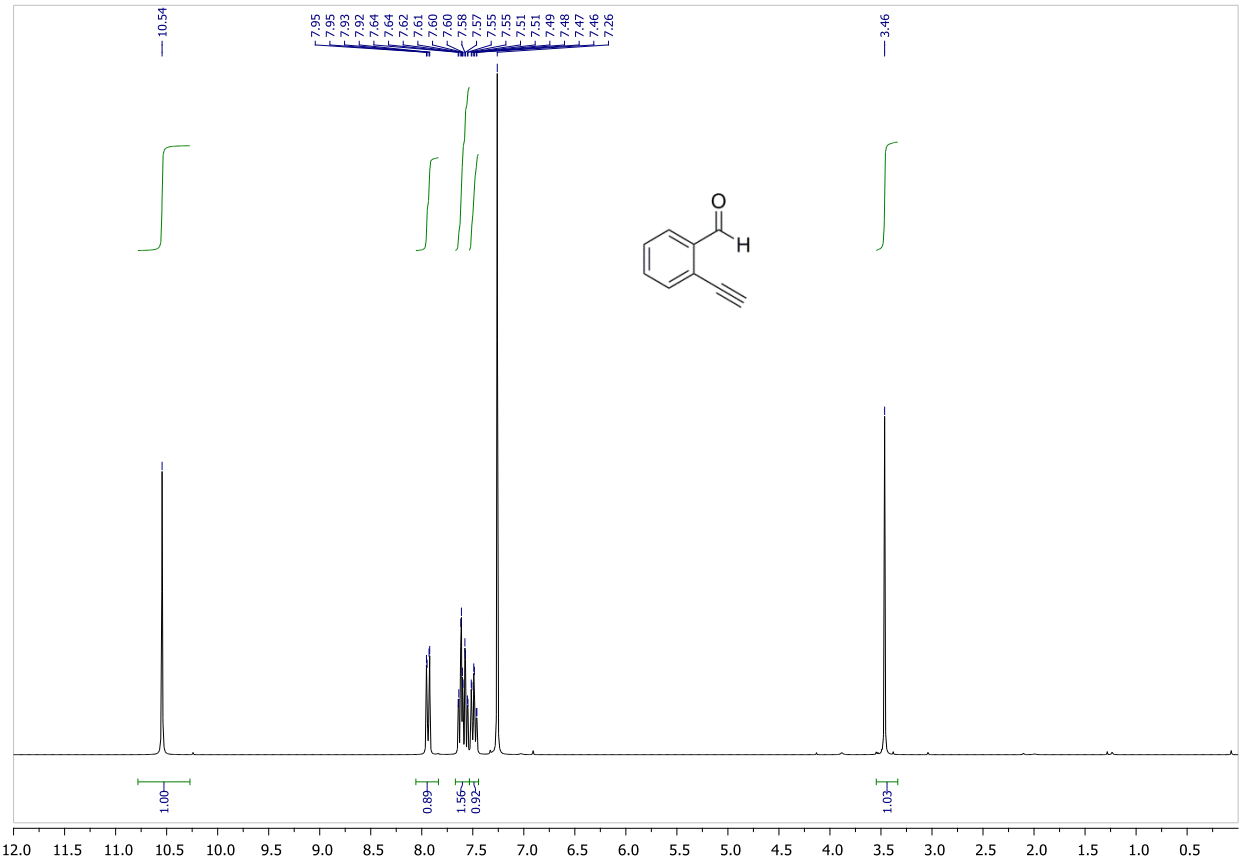

^{13}C-NMR: **S1ab**

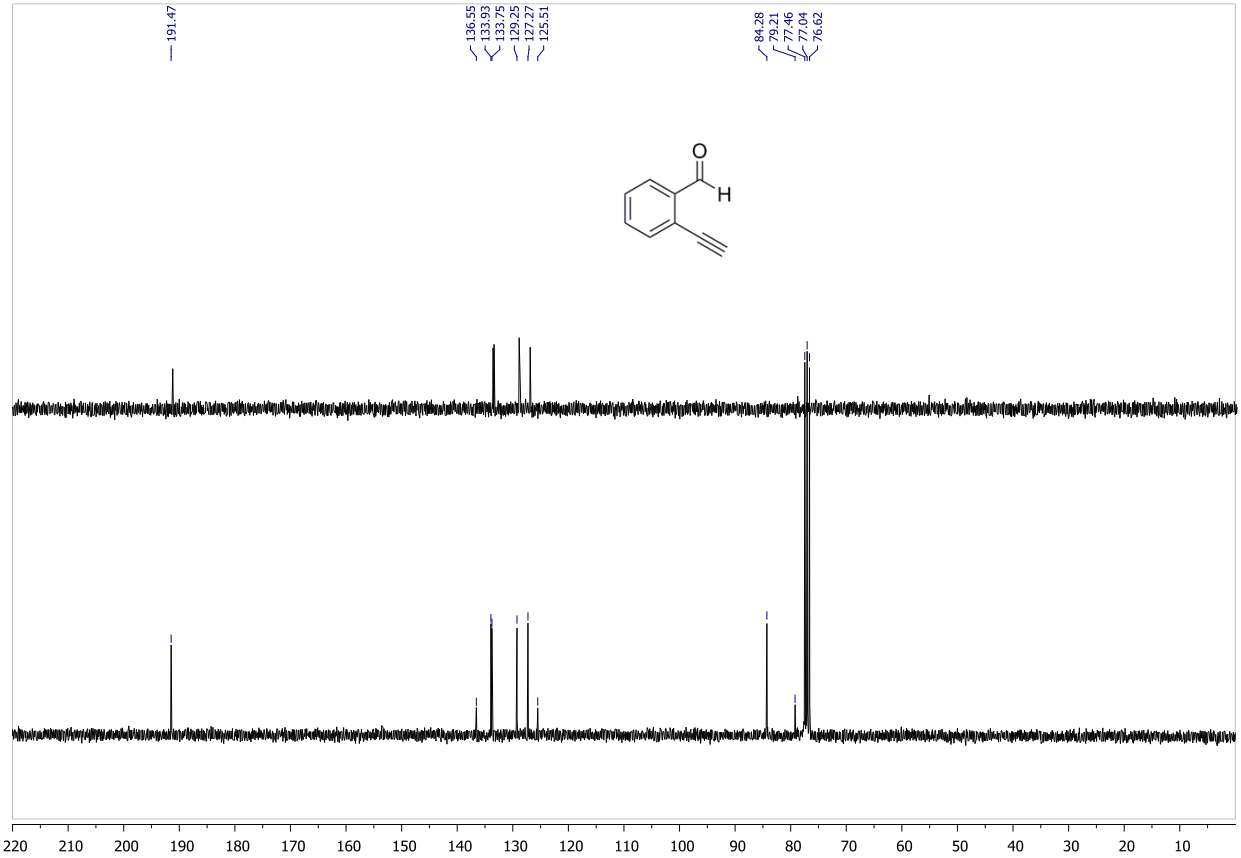

^{1}H-NMR: **2ab**

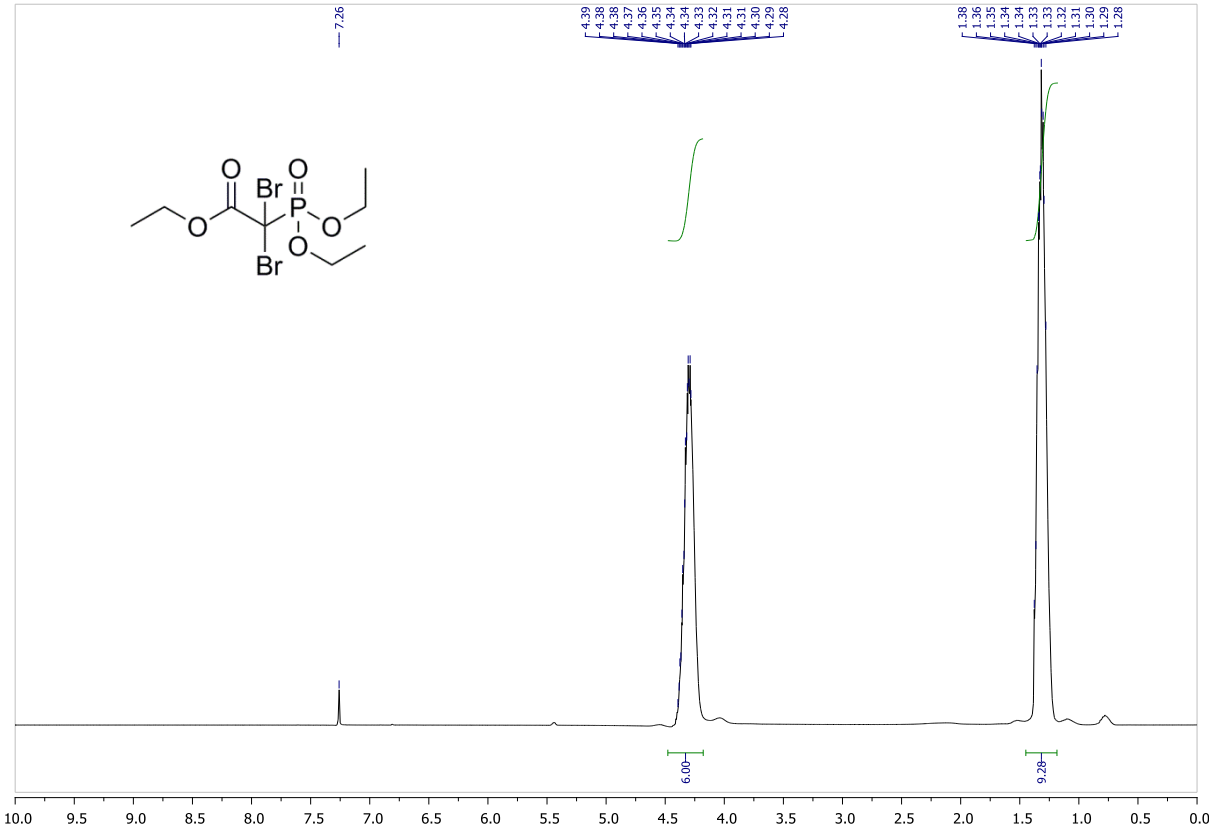

^{13}C-NMR: **2ab**

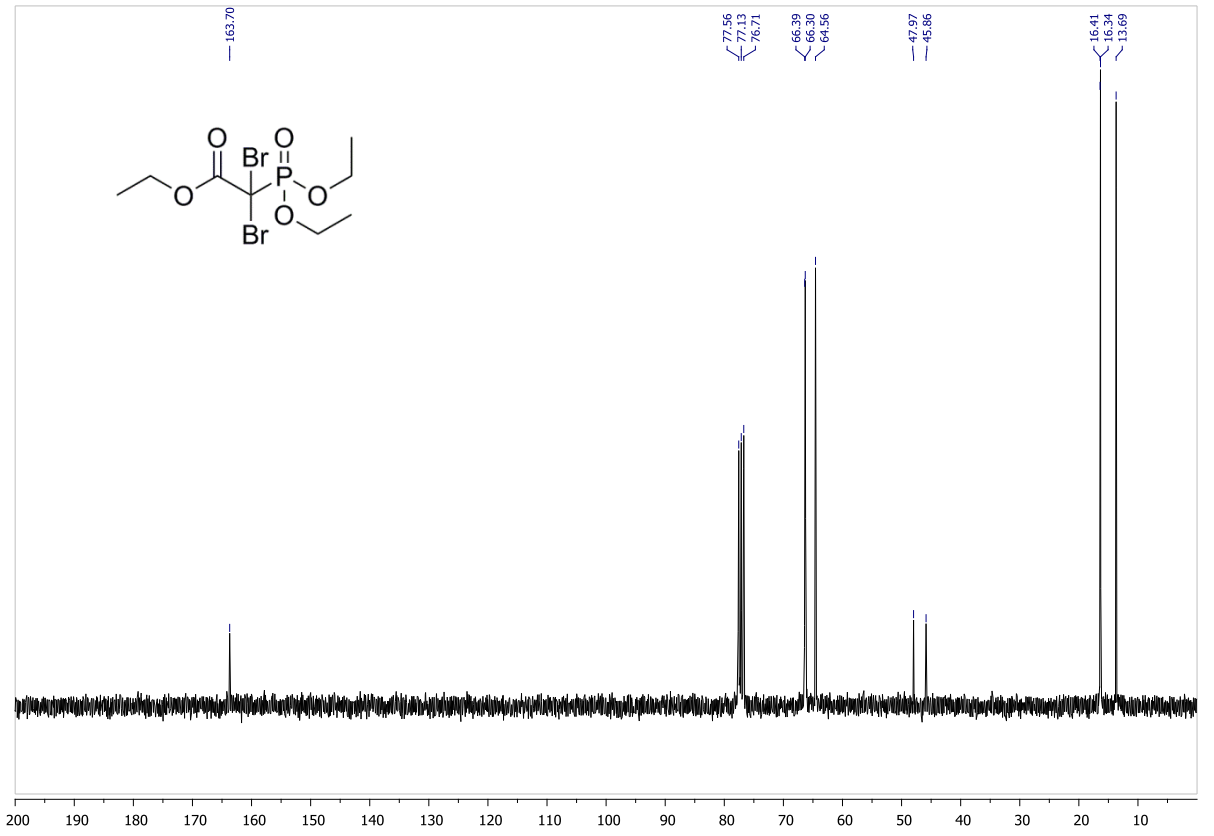

^{31}P-NMR: **2ab**

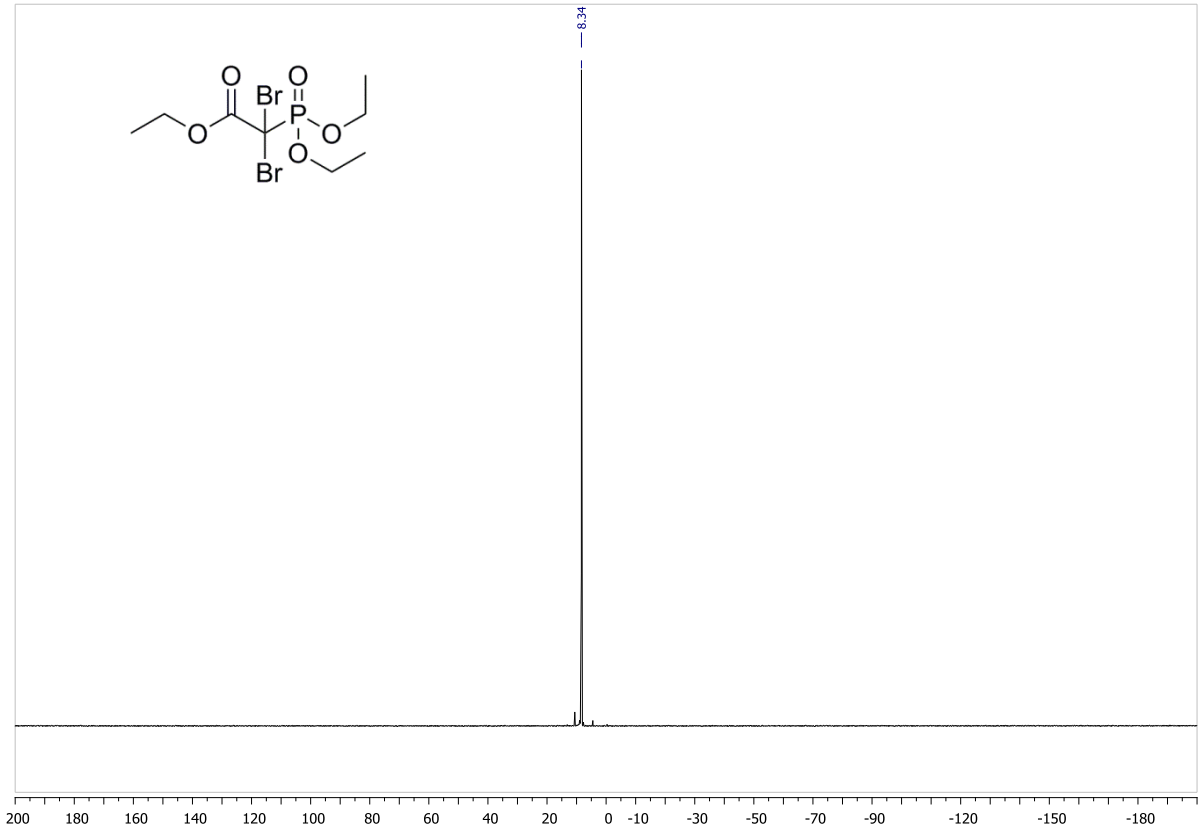

^{1}H-NMR: **2ac**

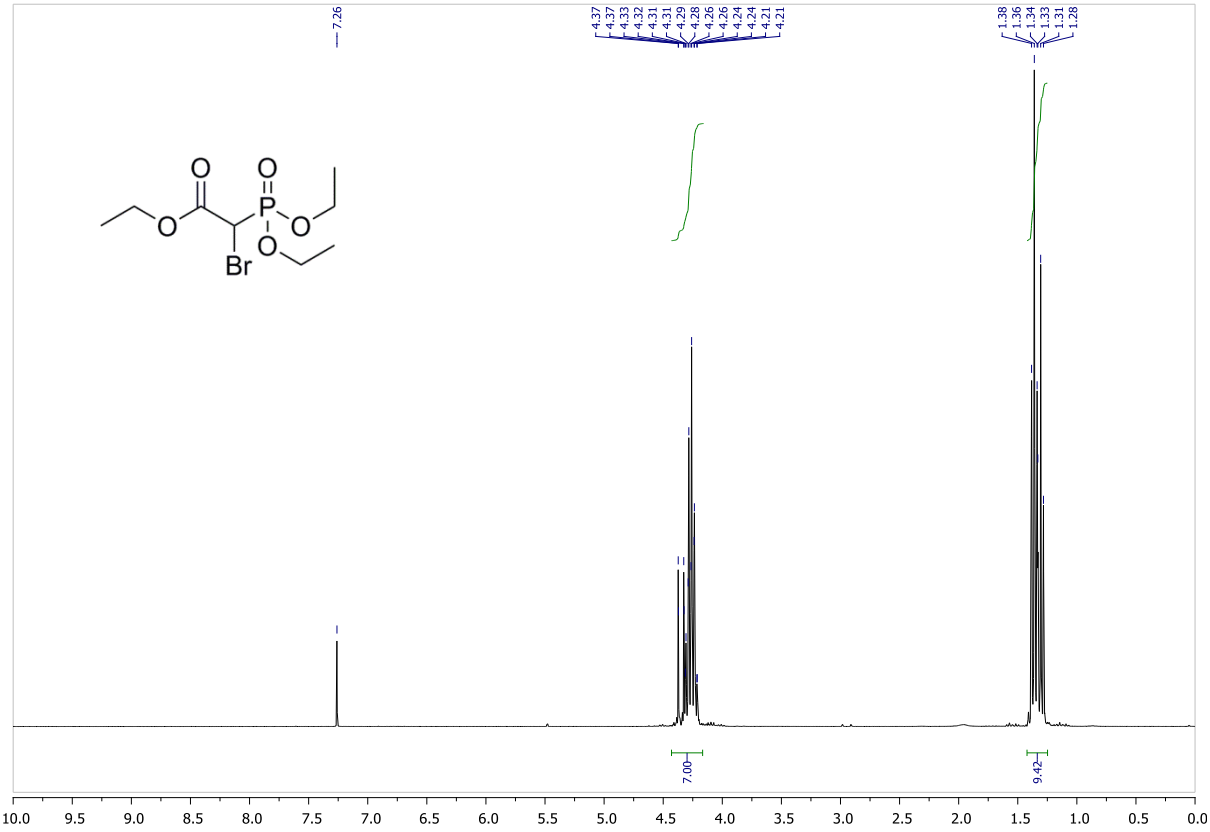

^{13}C-NMR: **2ac**

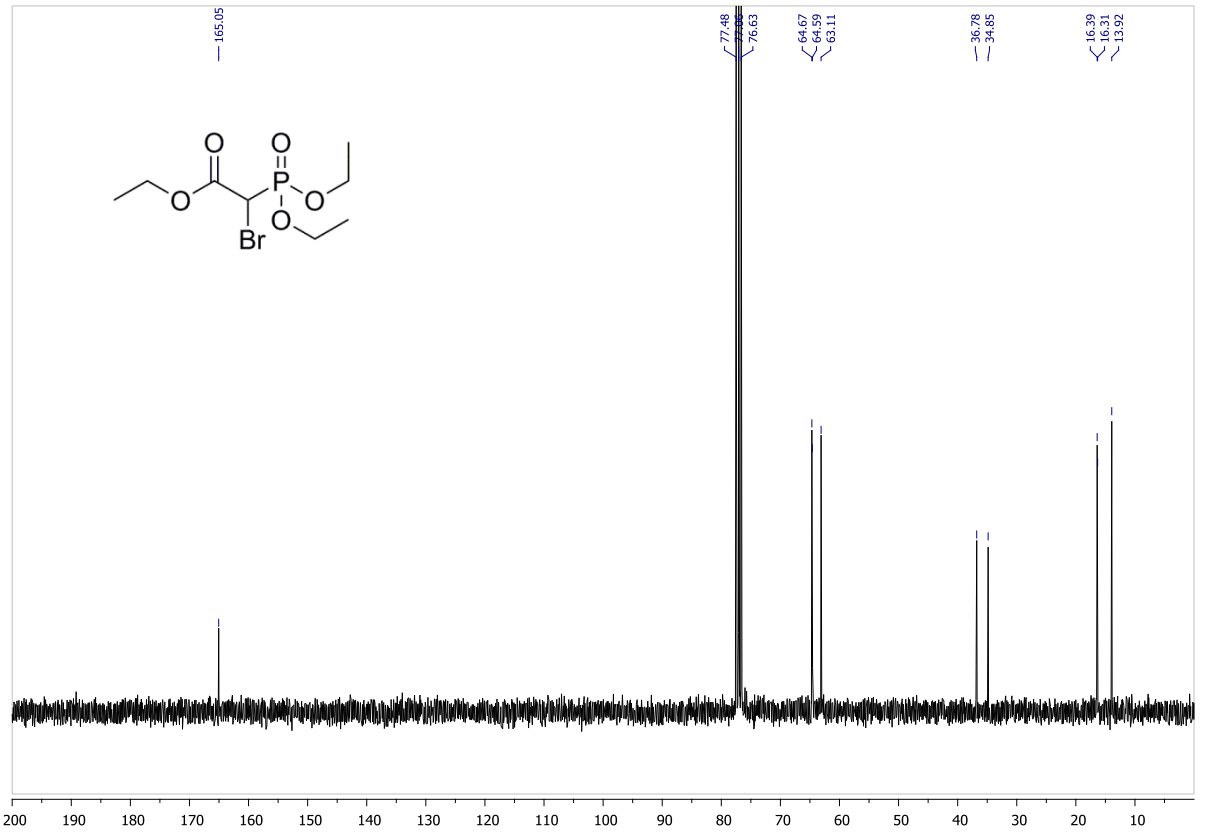

^{31}P-NMR: **2ac**

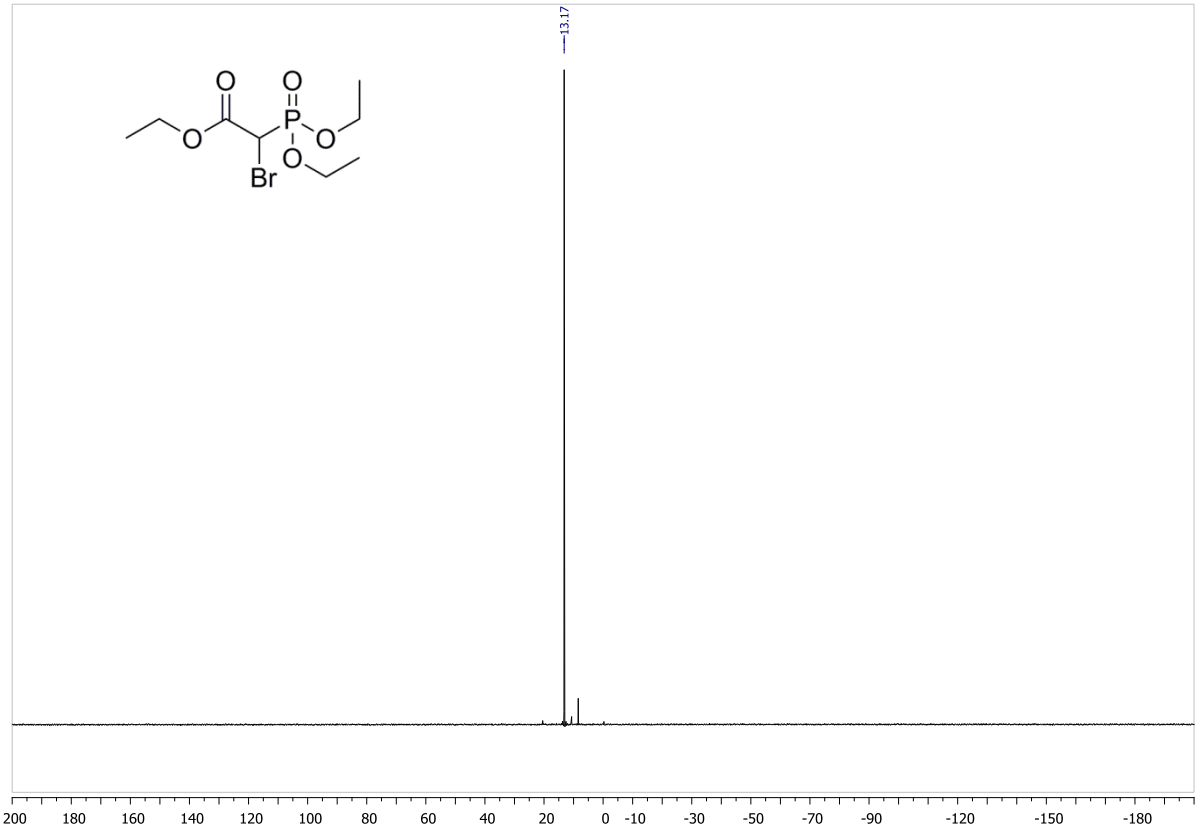
13.17
O
O
P
O
O
O
Br
200
180
160
140
120
100
80
60
40
20
0
-10
-30
-50
-70
-90
-120
-150
-180

^{1}H-NMR: **1a**

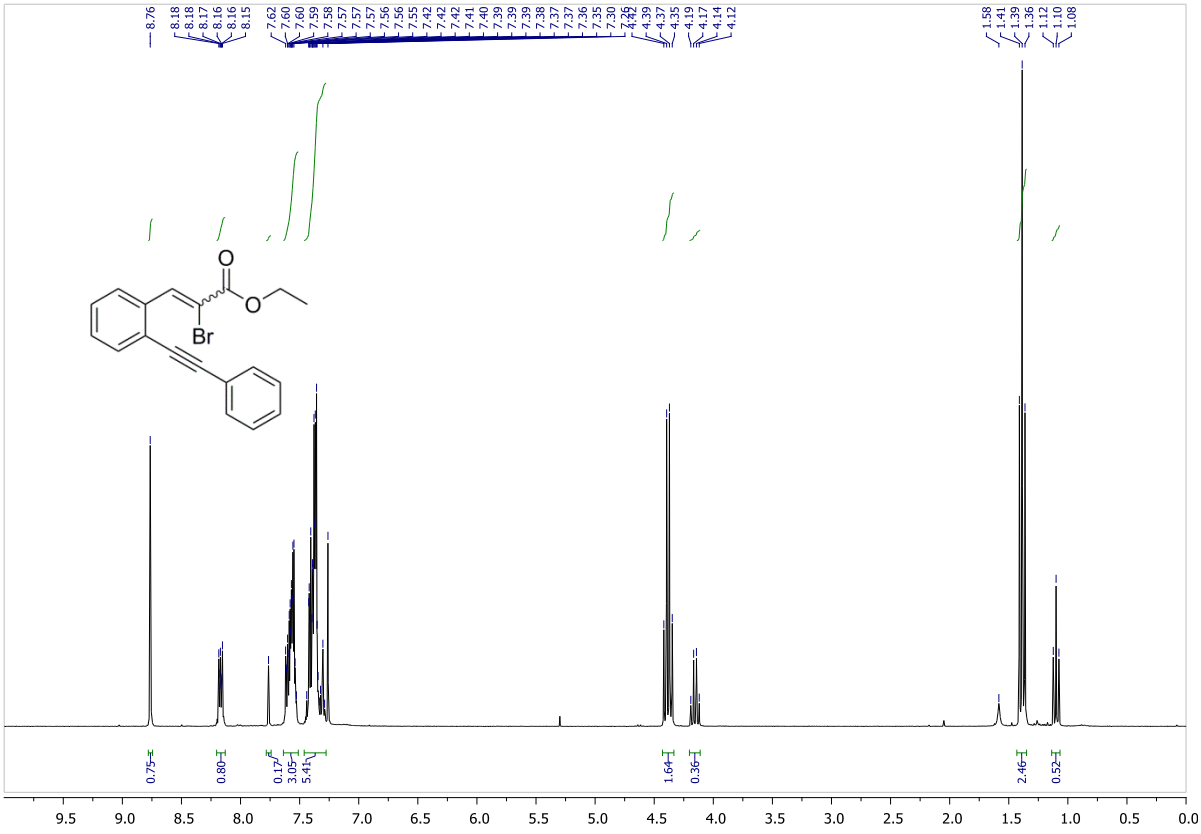

^{13}C-NMR: **1a**

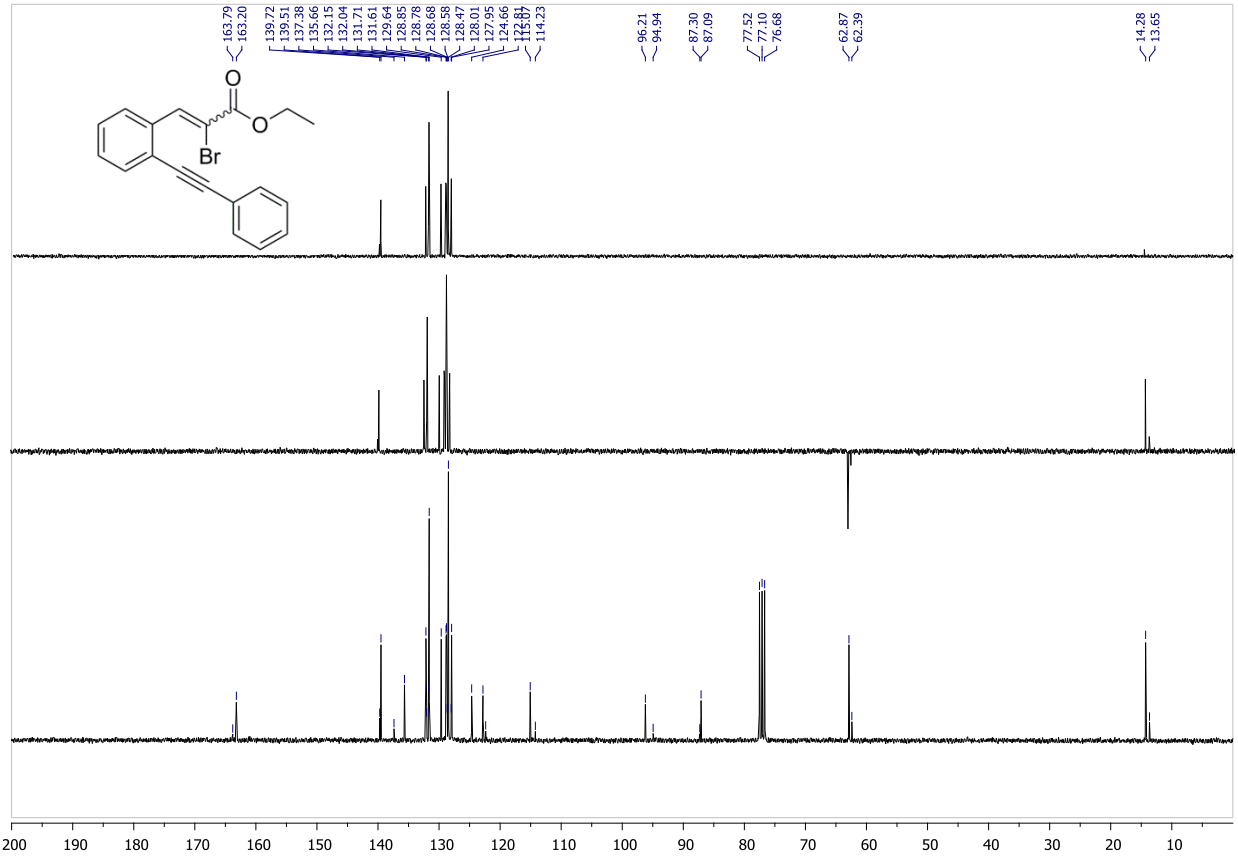

^{1}H-NMR: **1b**

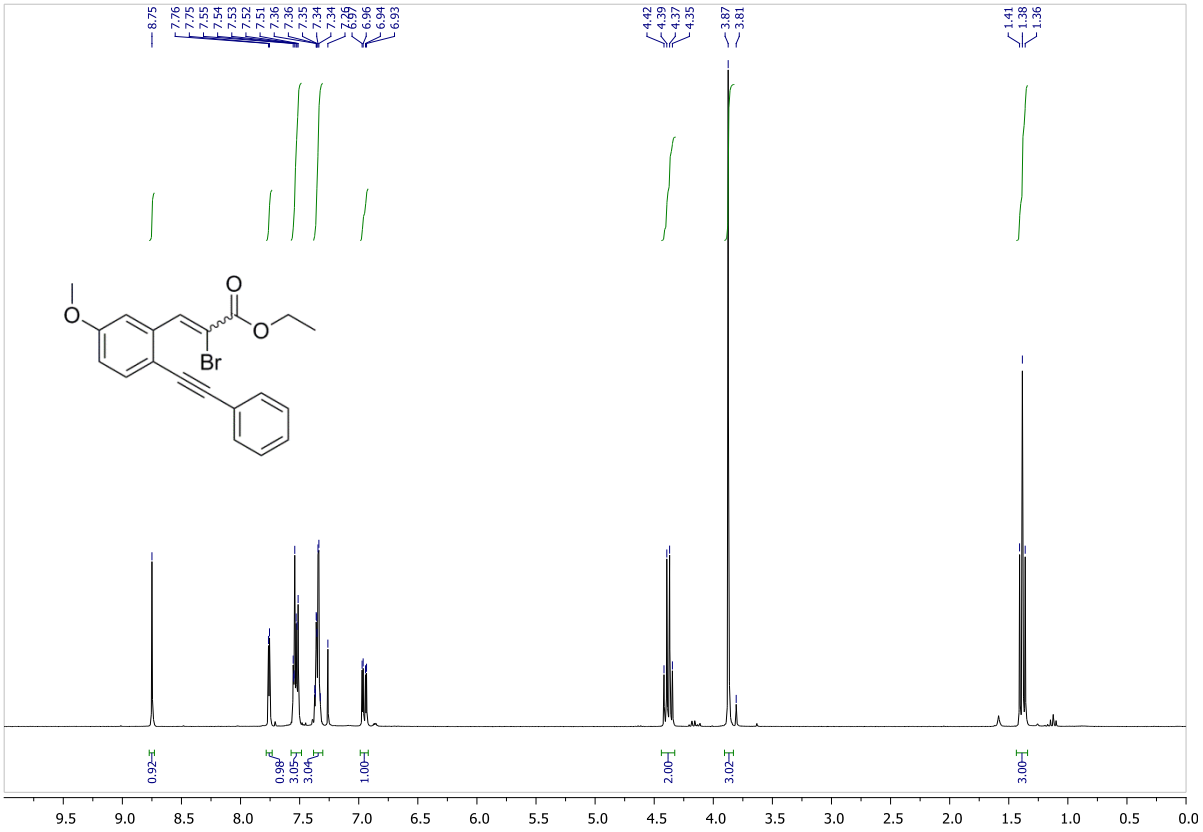

^{13}C-NMR: **1b**

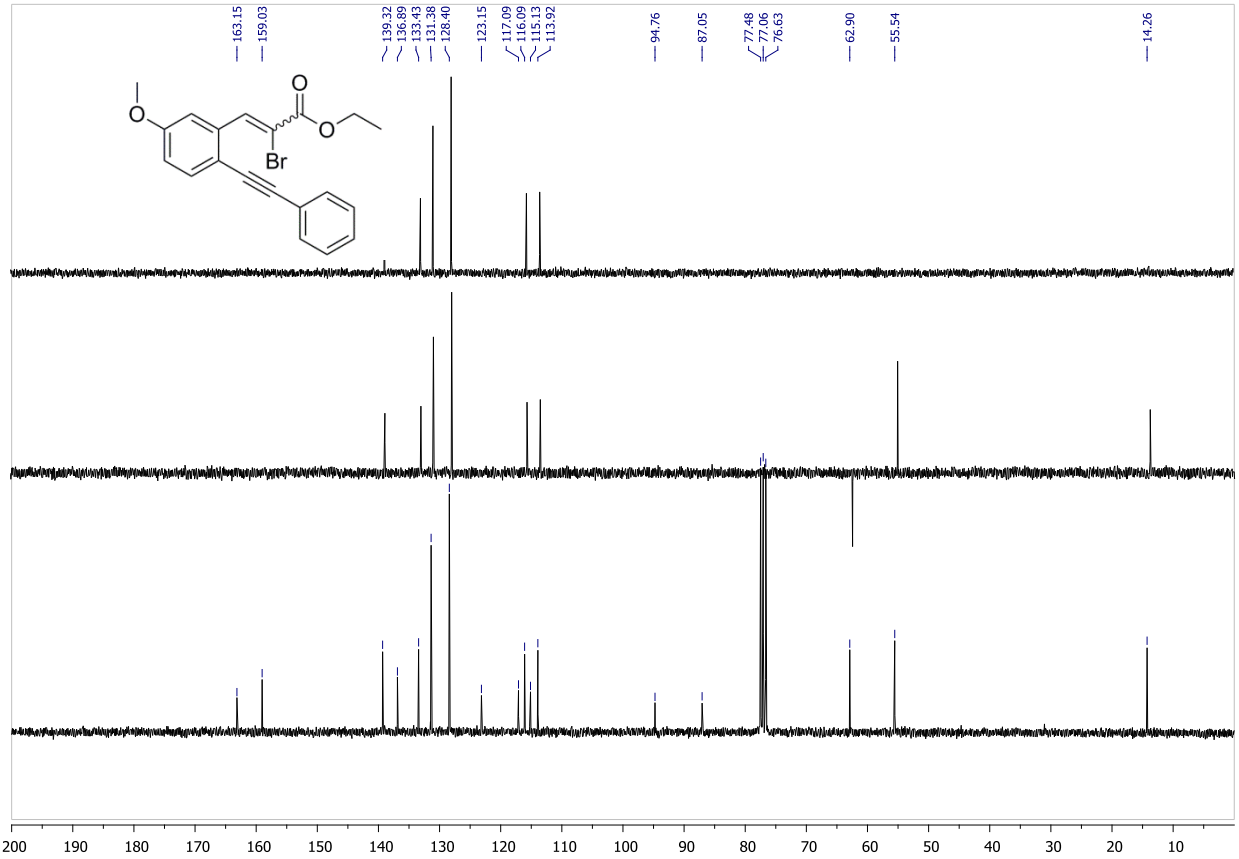

^{1}H-NMR: **1c**

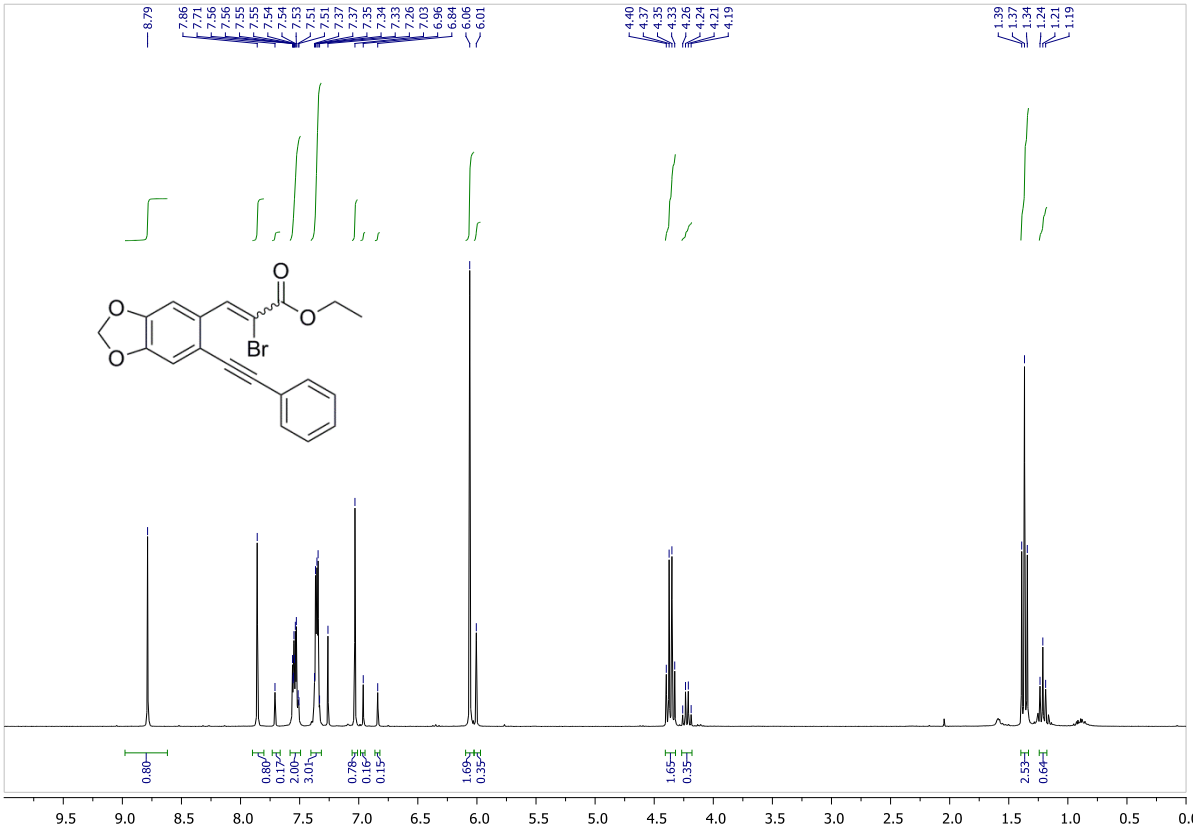

^{13}C-NMR: **1c**

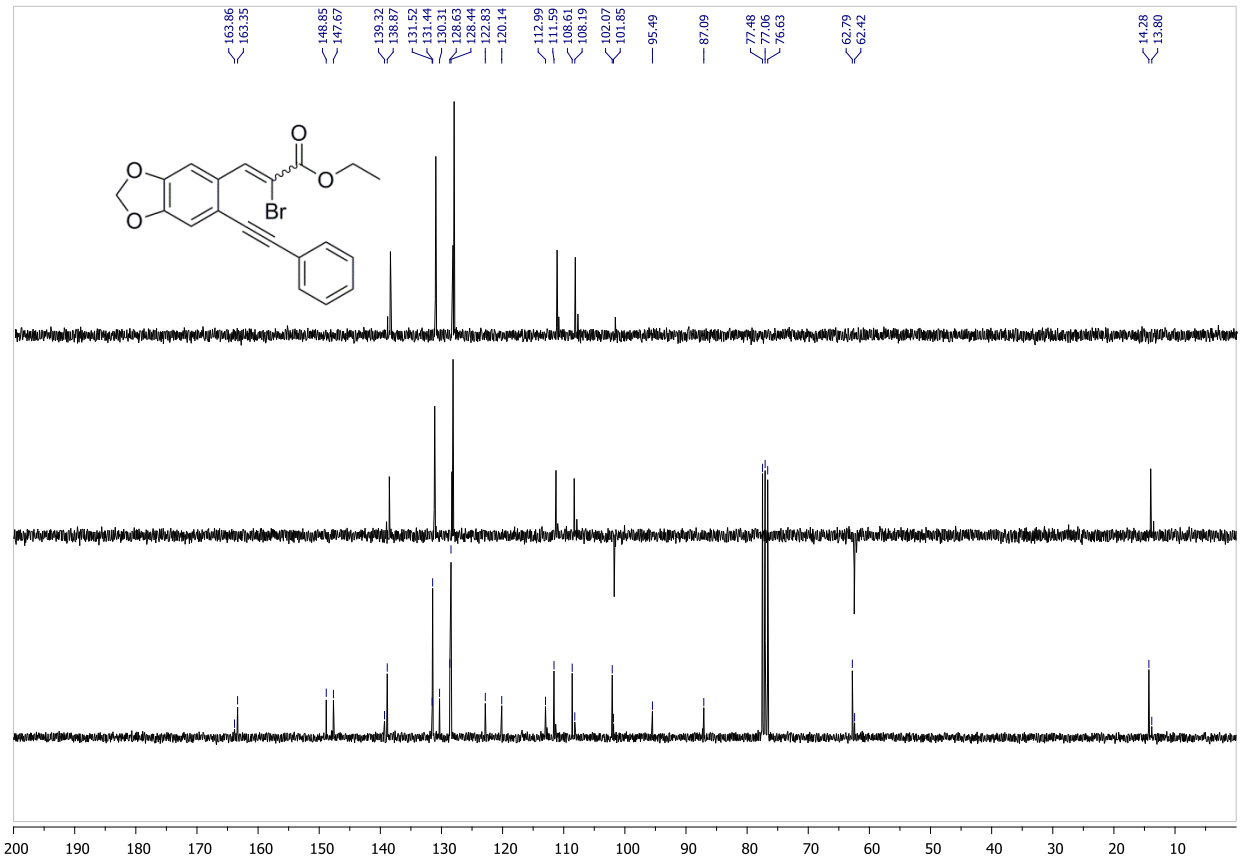

^{1}H-NMR: **1d**

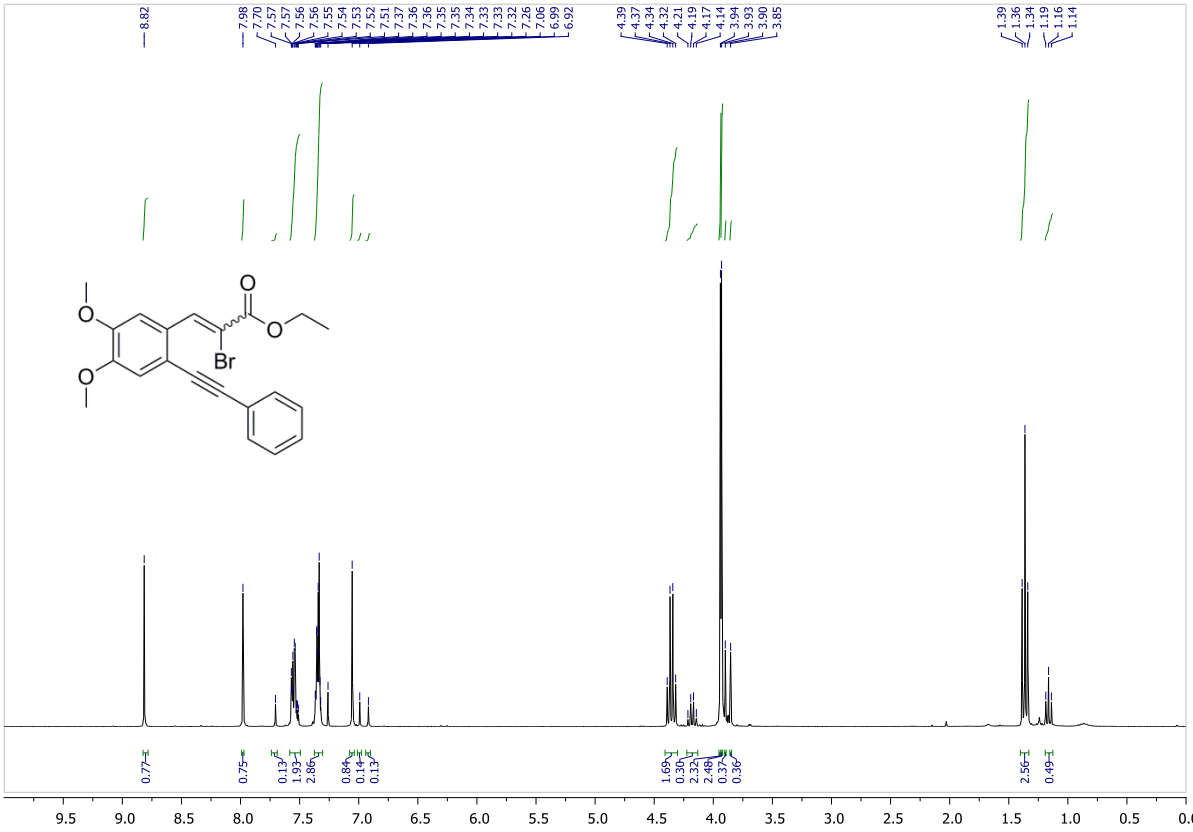

^{13}C-NMR: **1d**

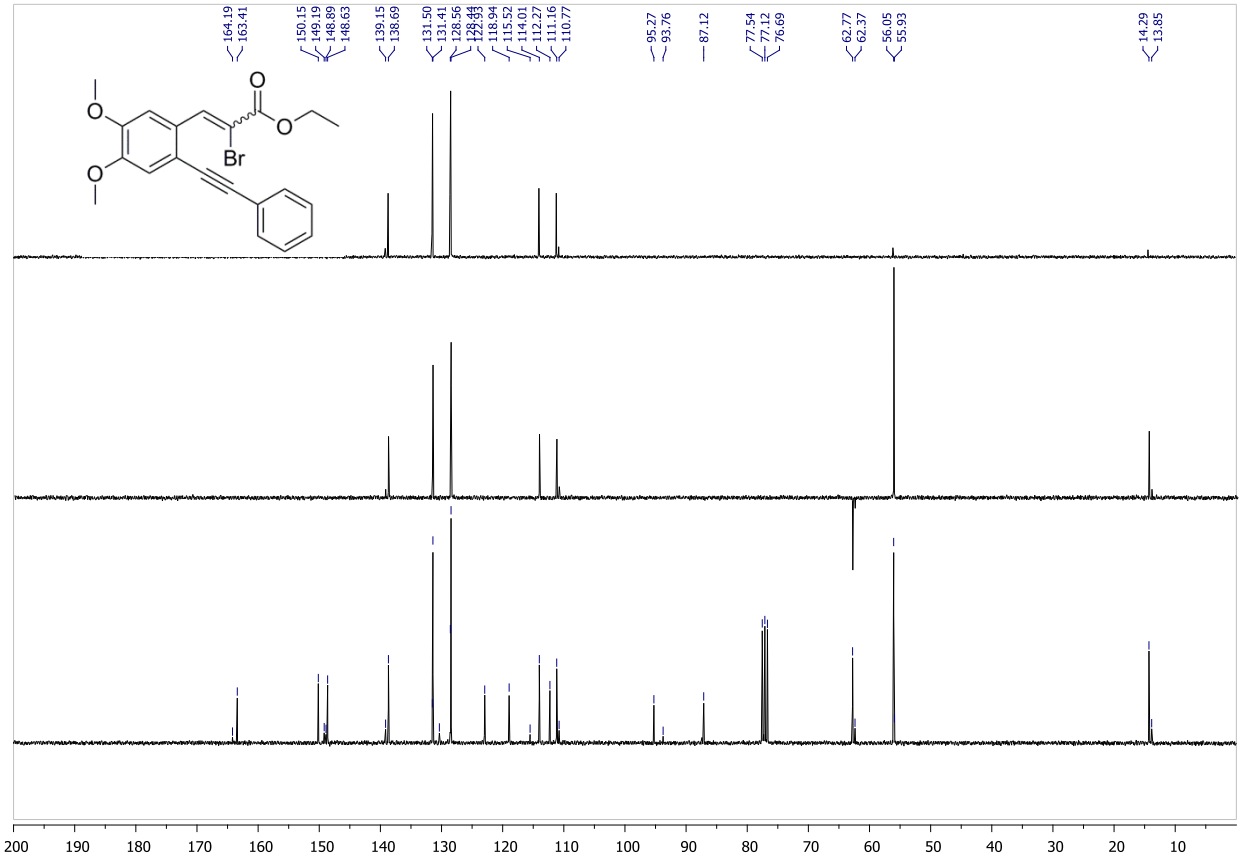

^{1}H-NMR: **1e**

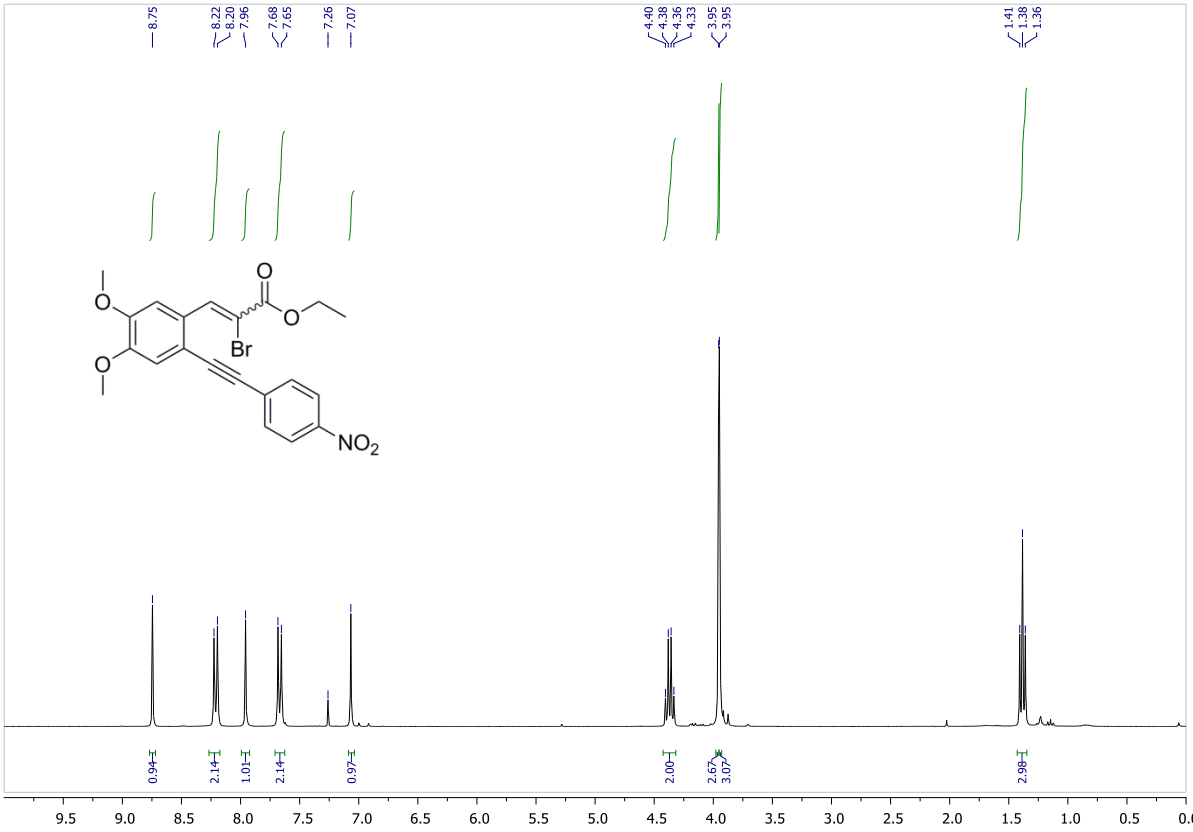

^{13}C-NMR: **1e**

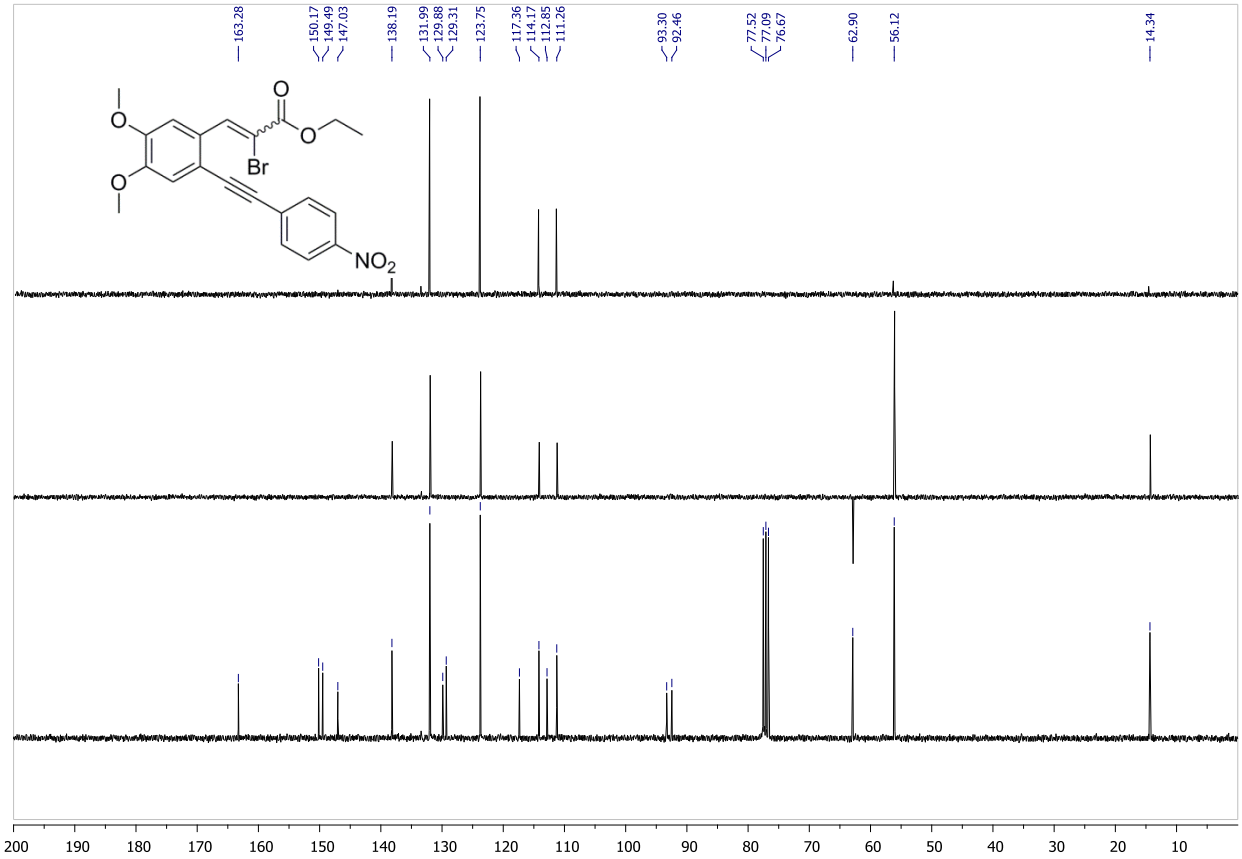

^{1}H-NMR: **1f**

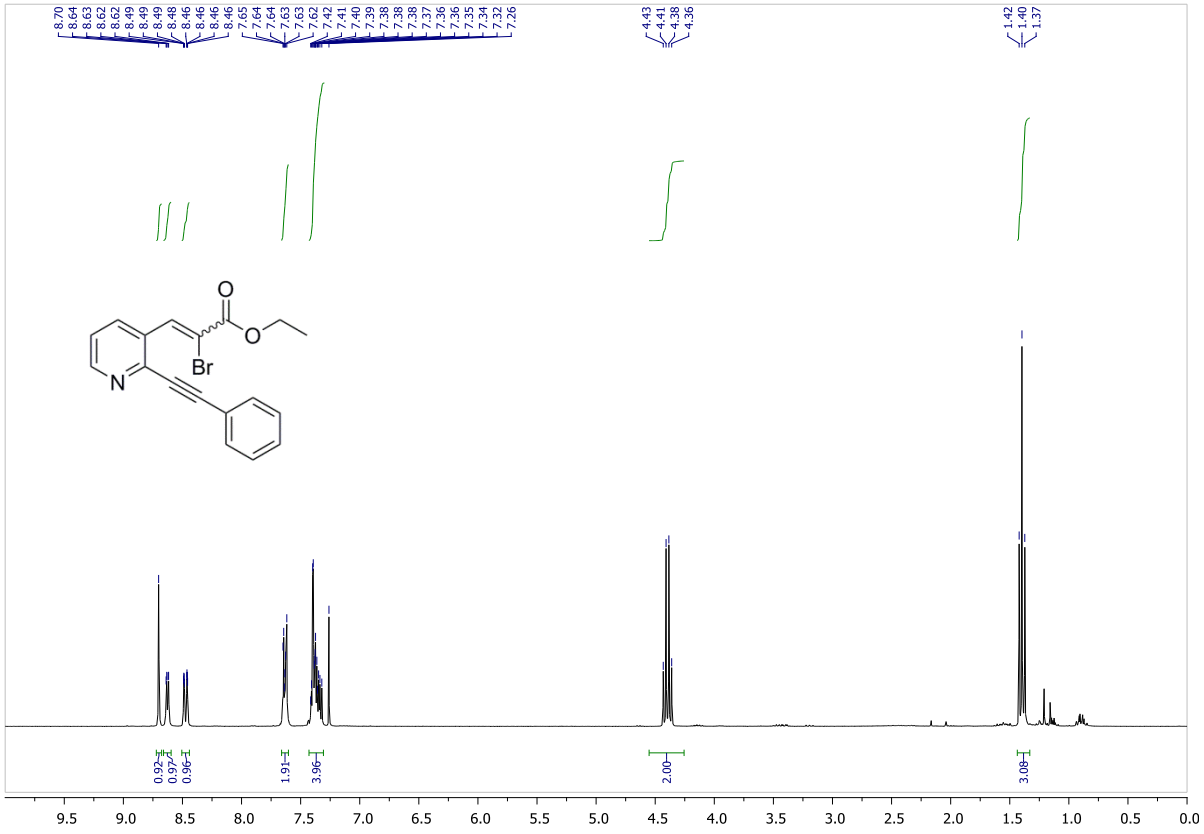

^{13}C-NMR: **1f**

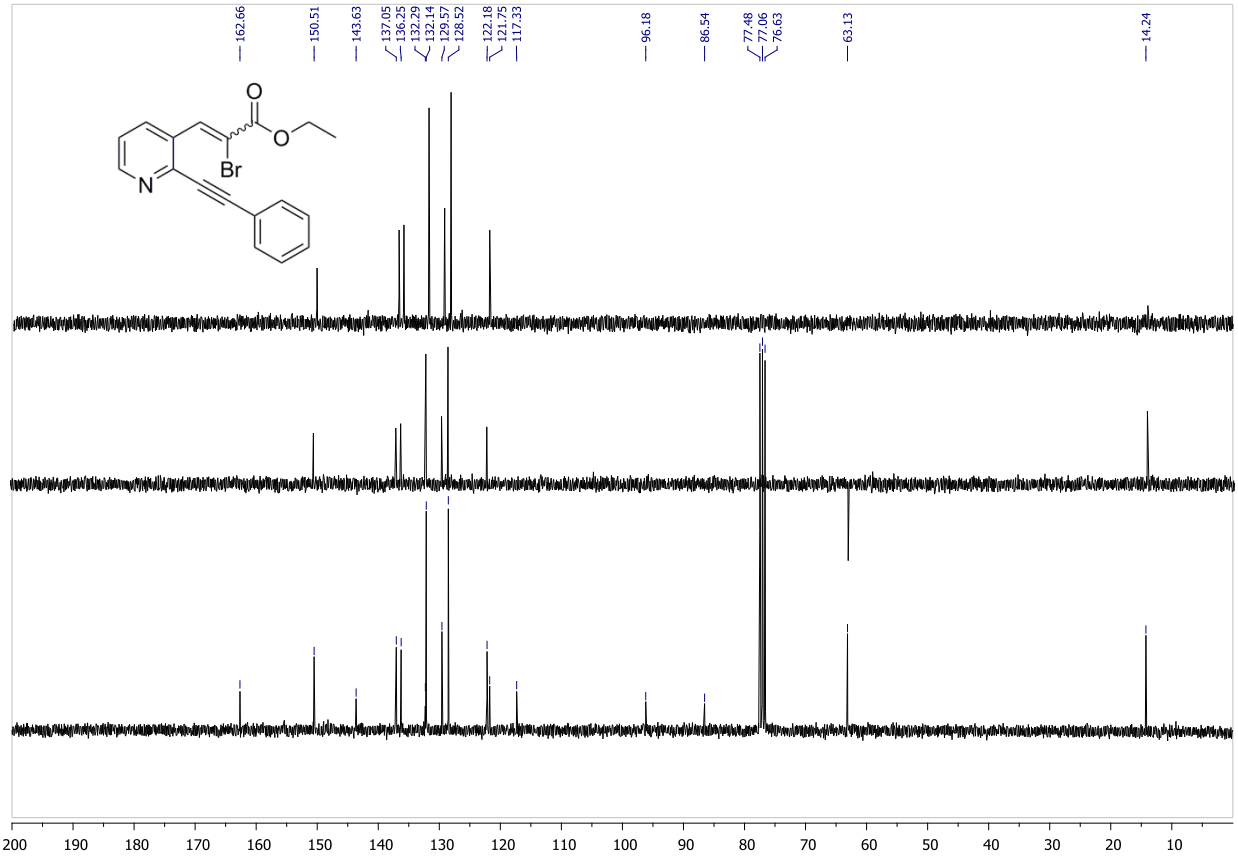

^{1}H-NMR: **1g**

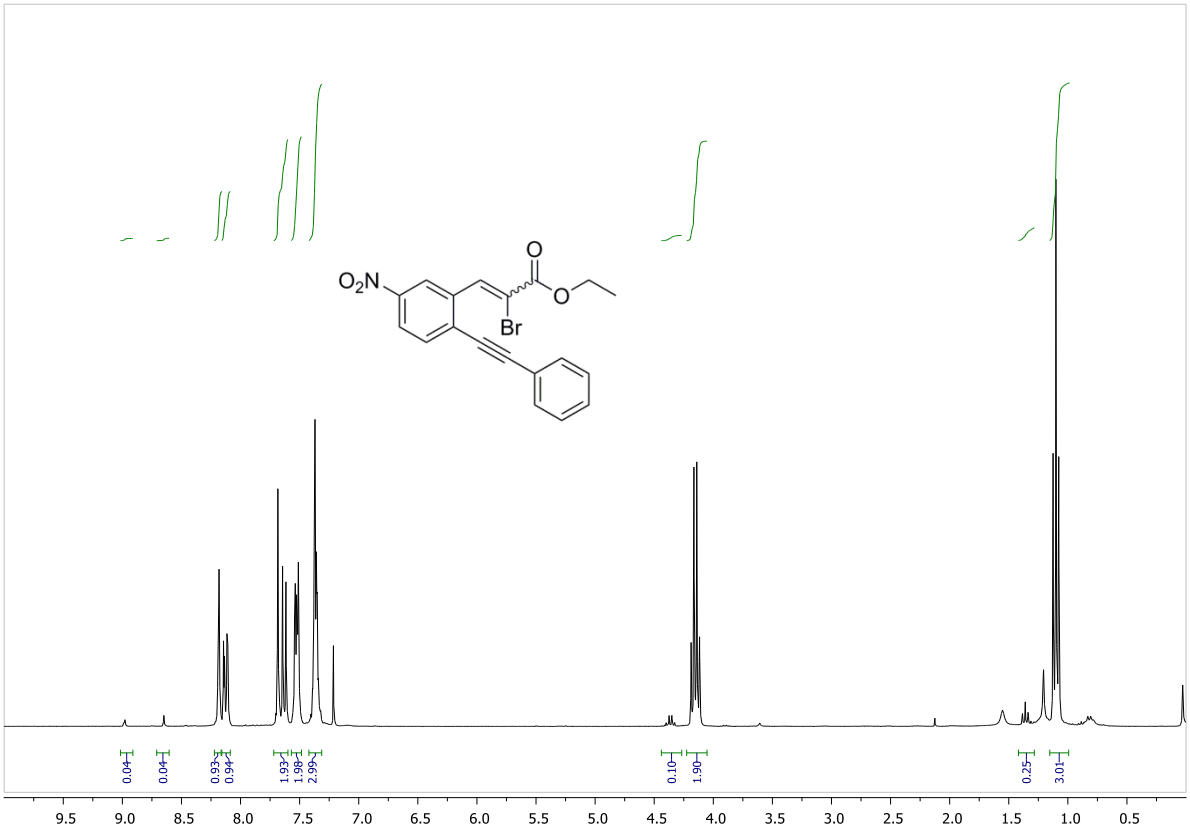

^{13}C-NMR: **1g**

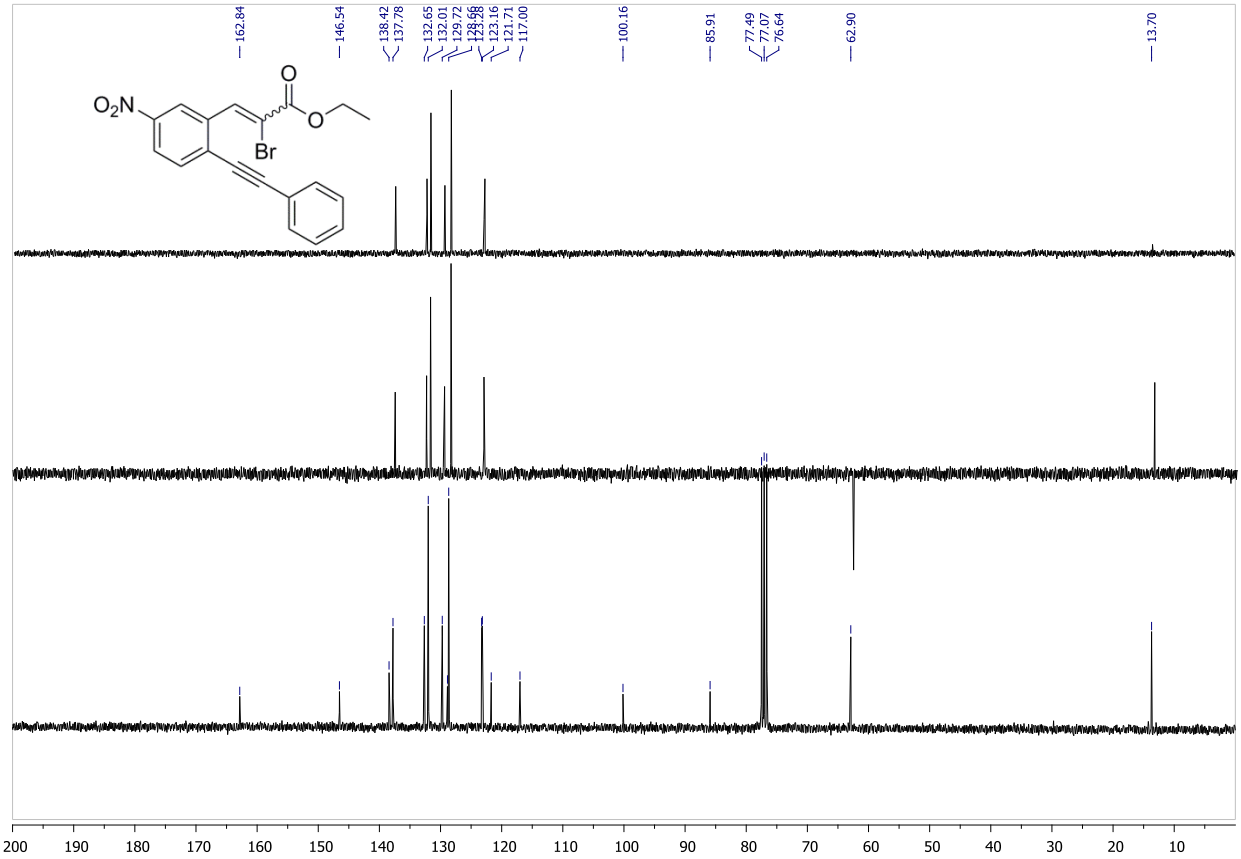

^{1}H-NMR: **1h**

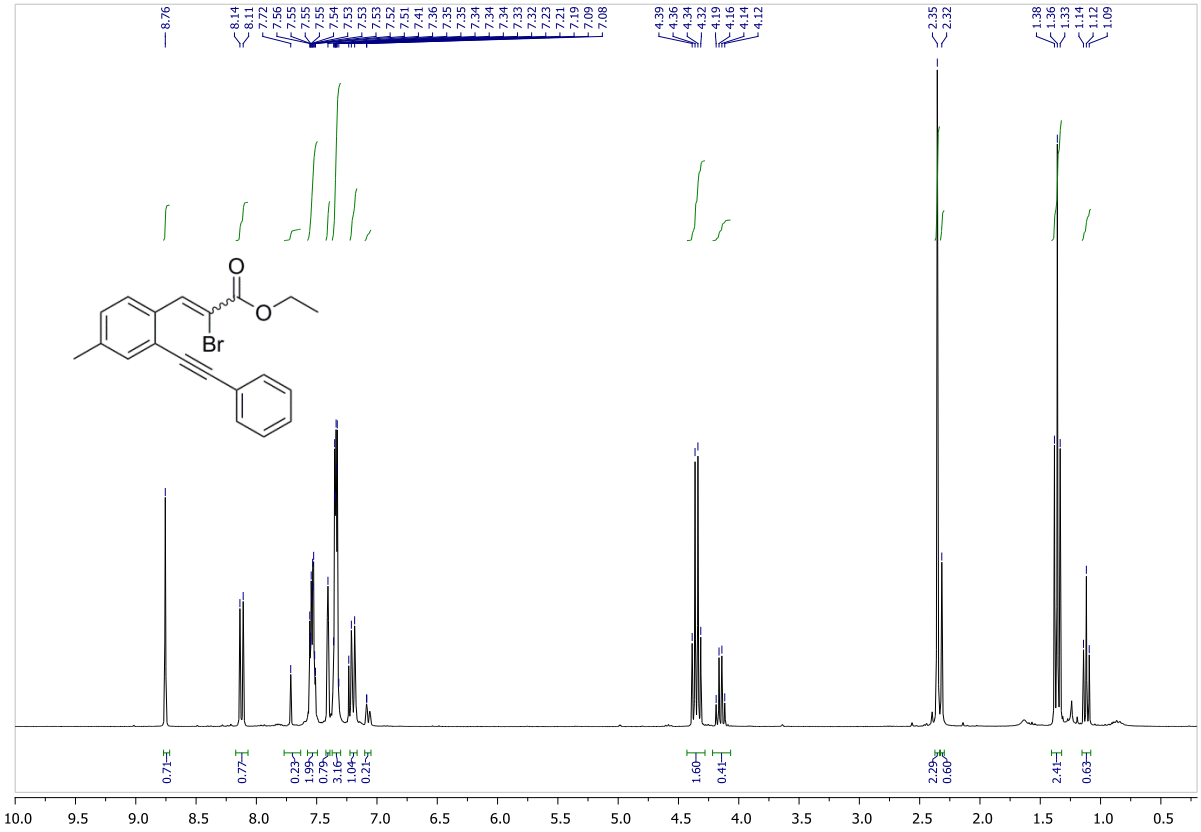

^{13}C-NMR: **1h**

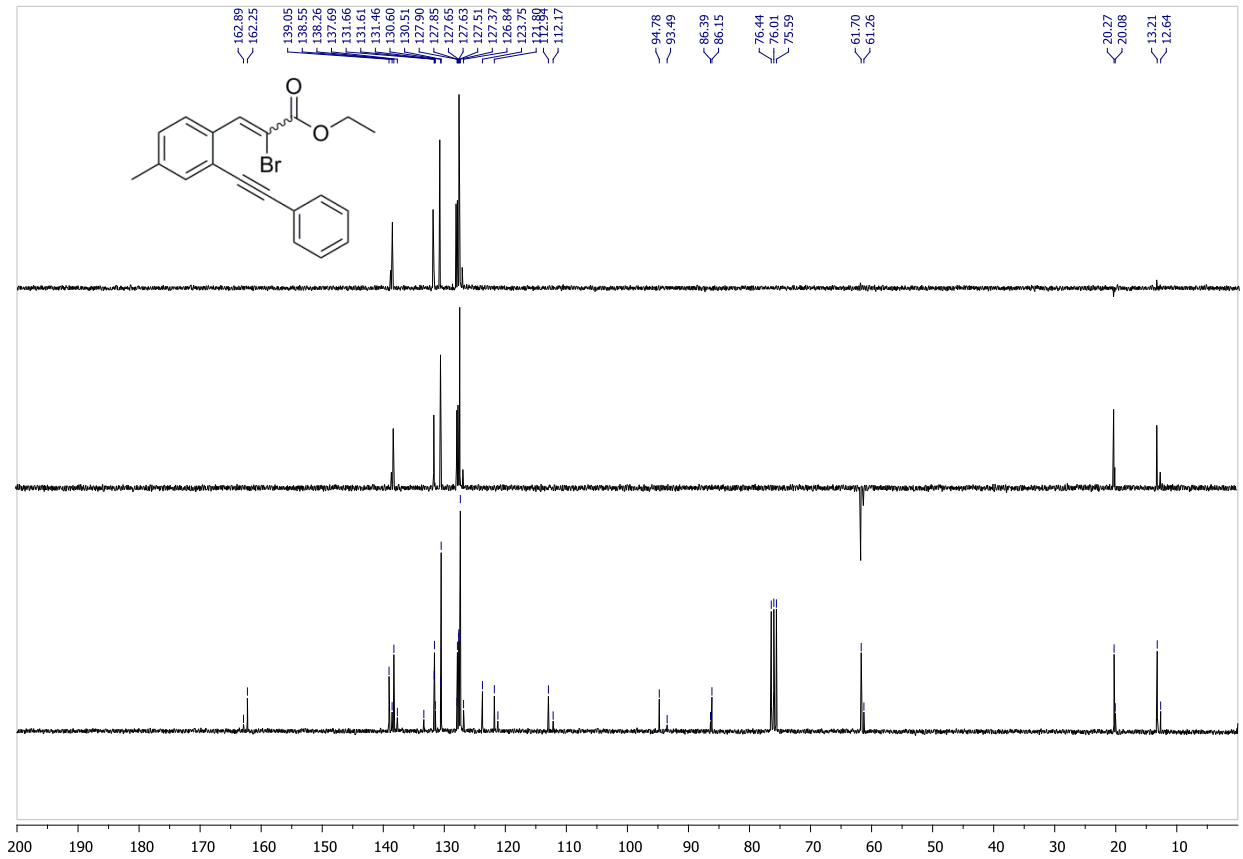

^{1}H-NMR: **1i**

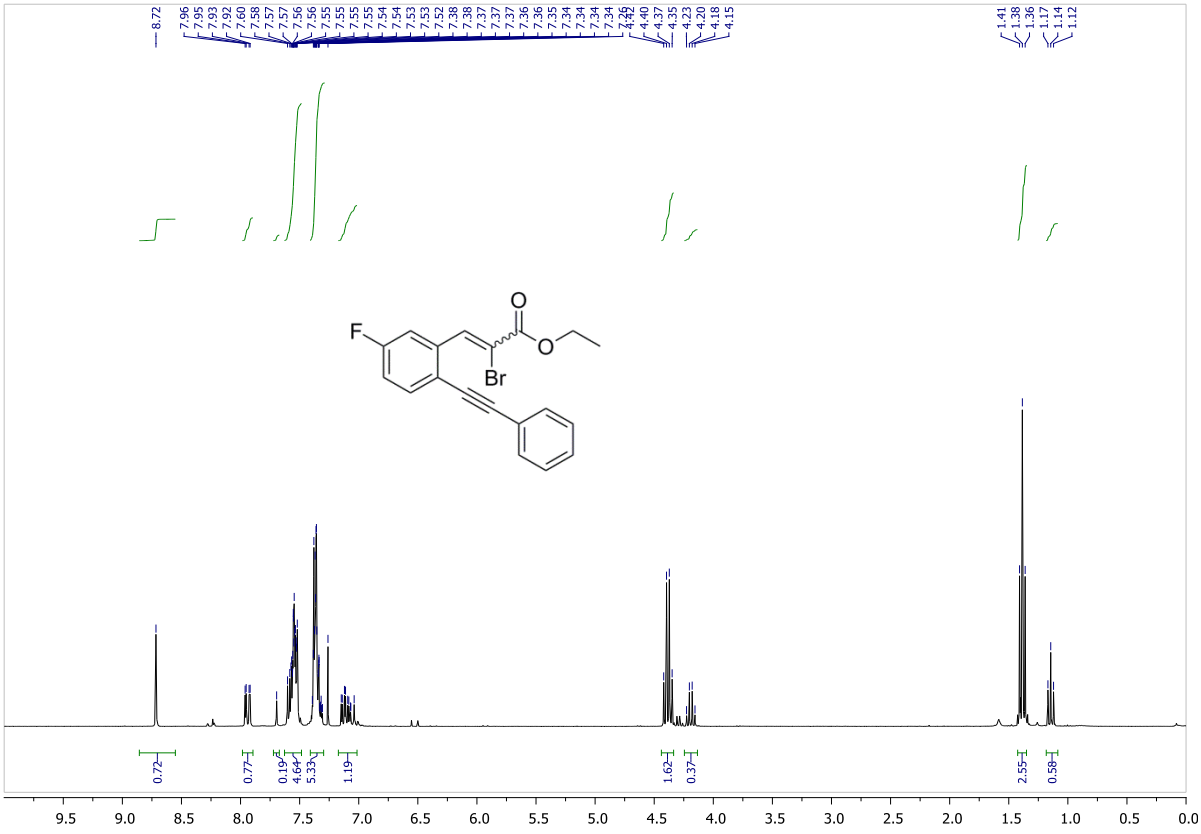

^{13}C-NMR: **1i**

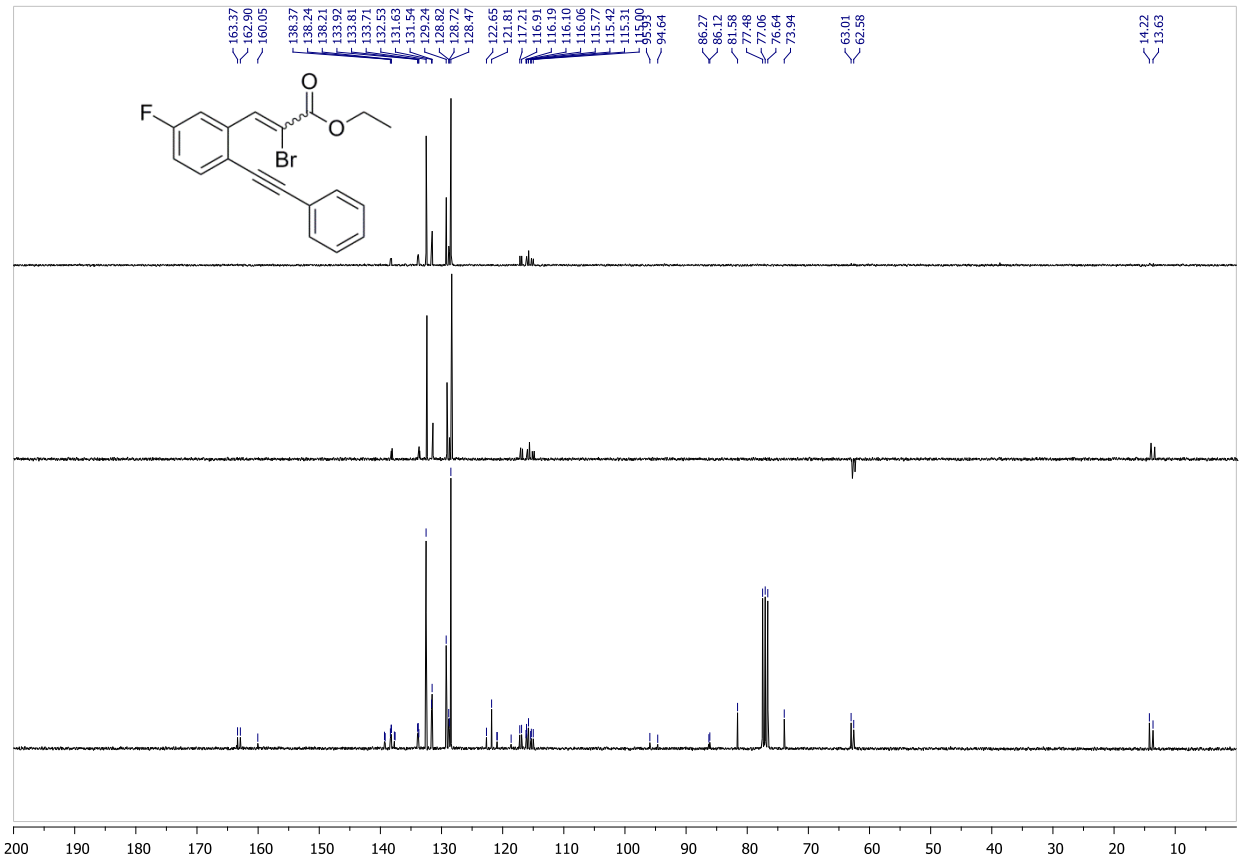

^{1}H-NMR: **1j**

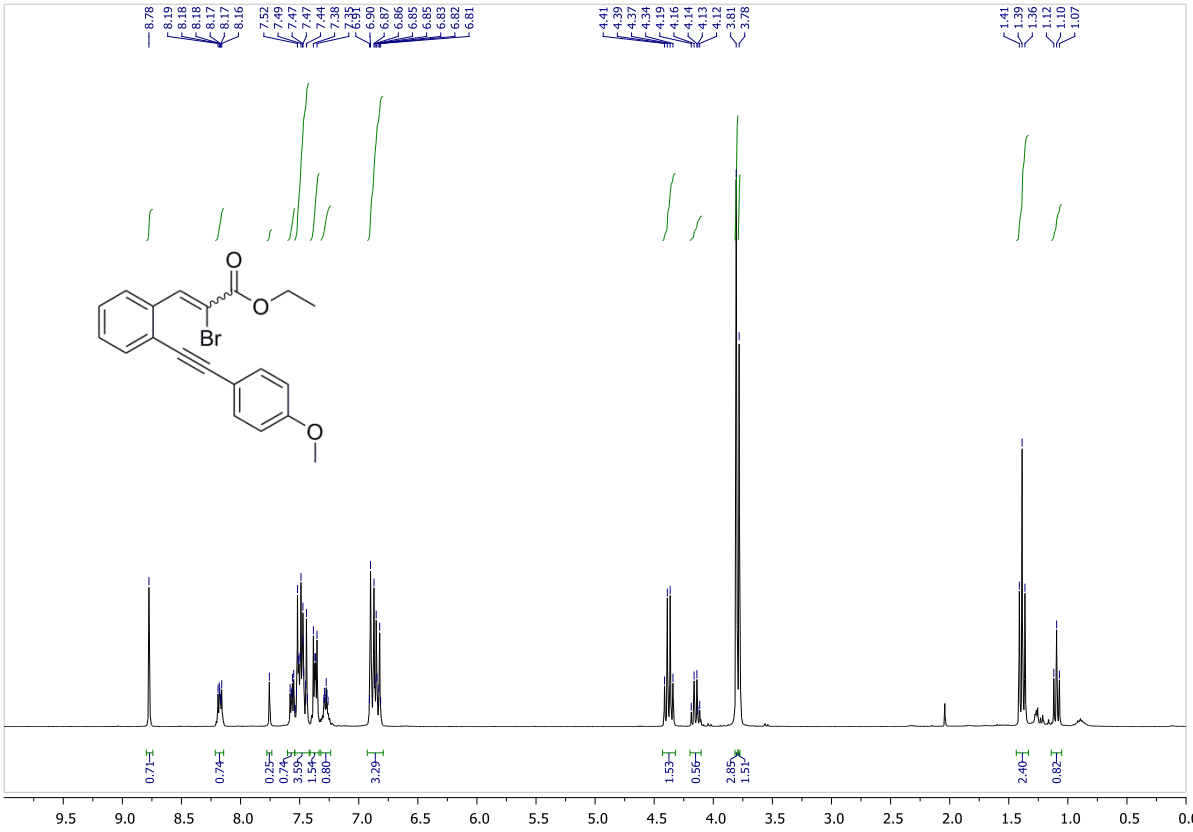

^{13}C-NMR: **1j**

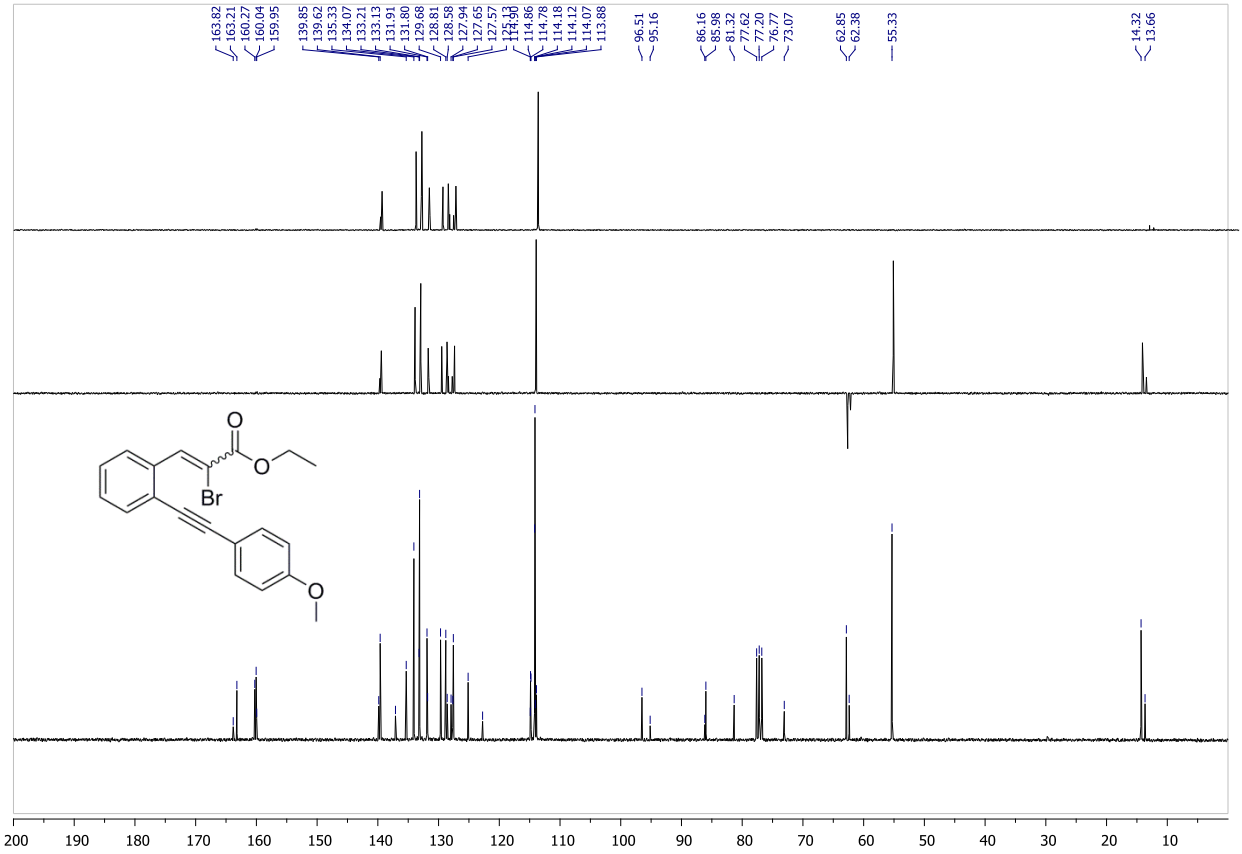

^{1}H-NMR: **1k**

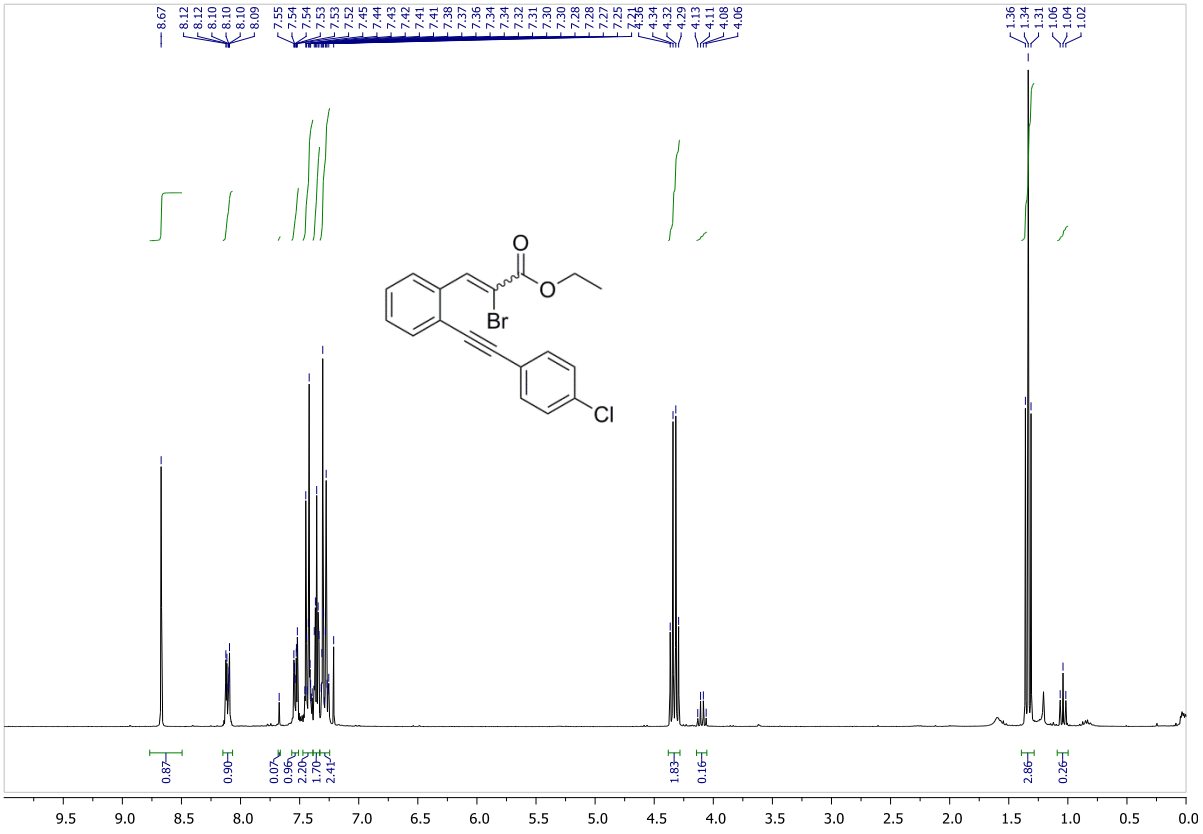

^{13}C-NMR: **1k**

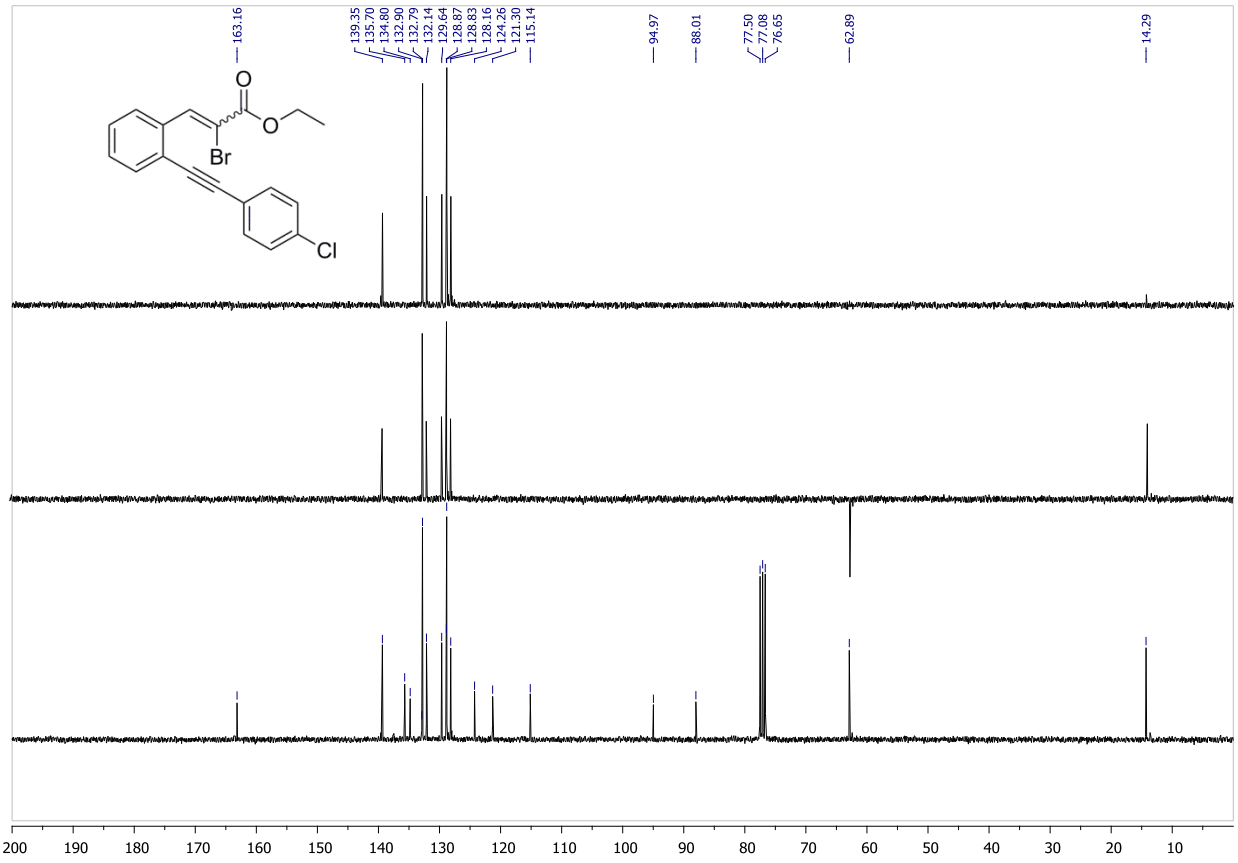

^{1}H-NMR: **1l**

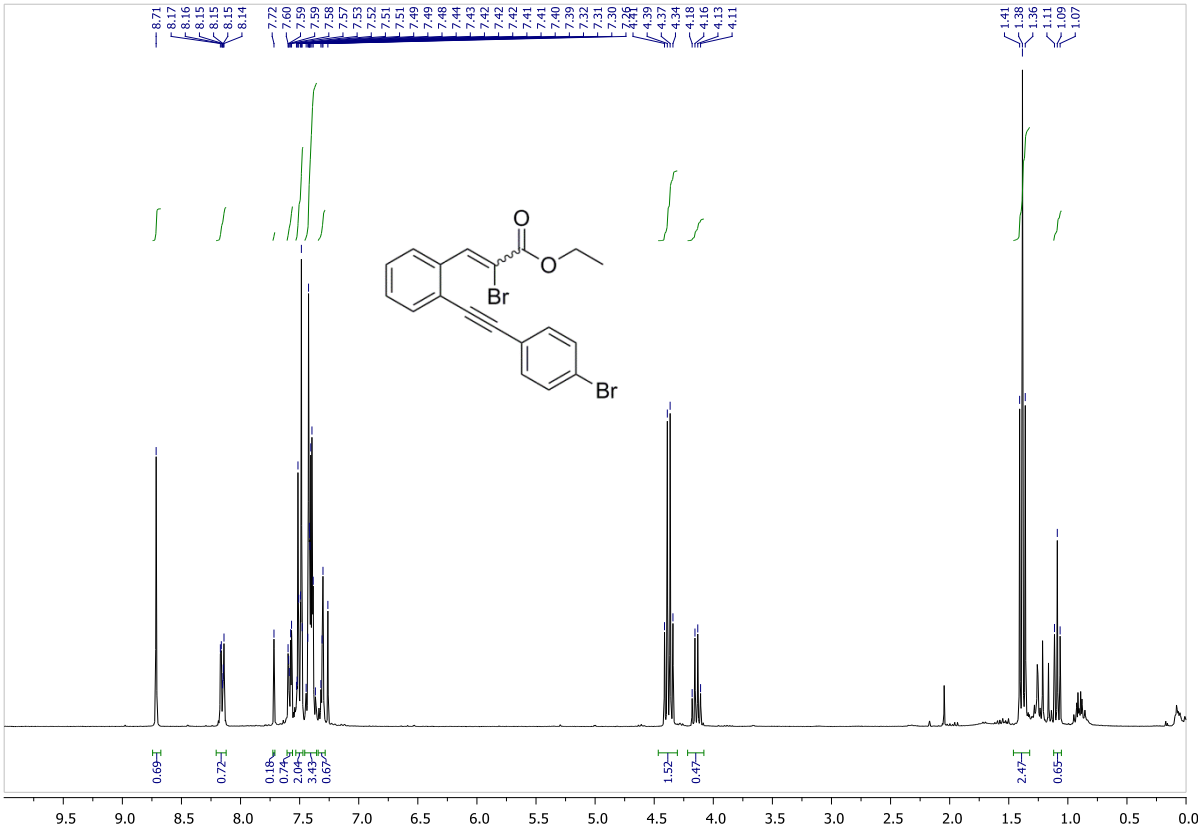

^{13}C-NMR: **1l**

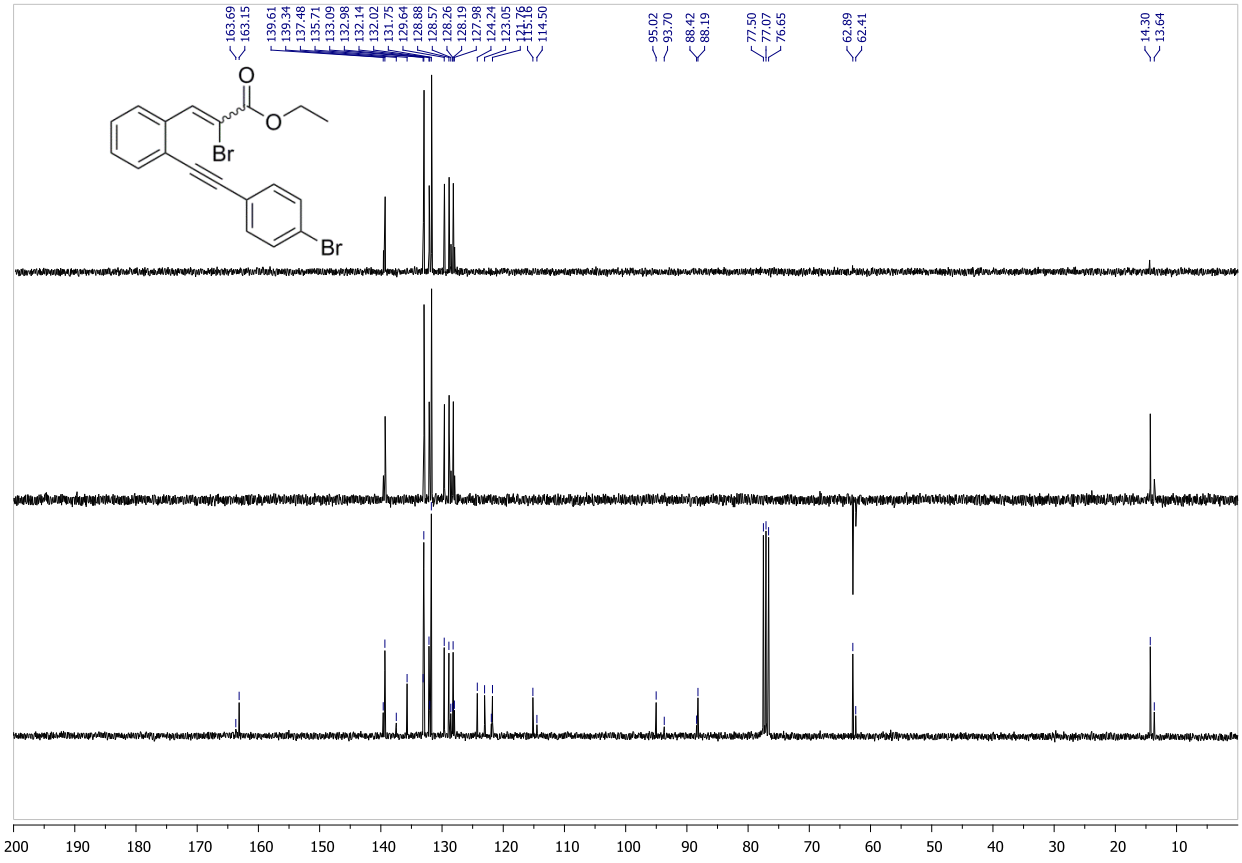

^{1}H-NMR: **1m**

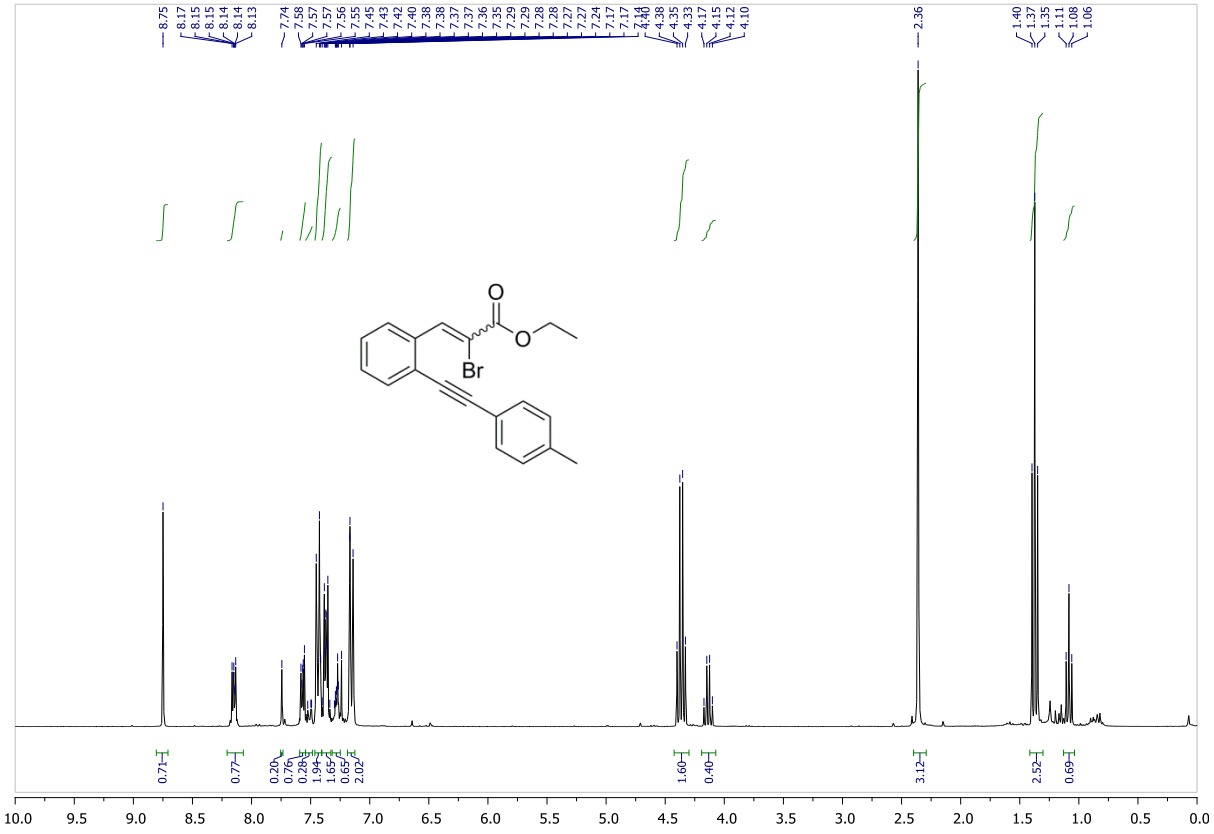

^{13}C-NMR: **1m**

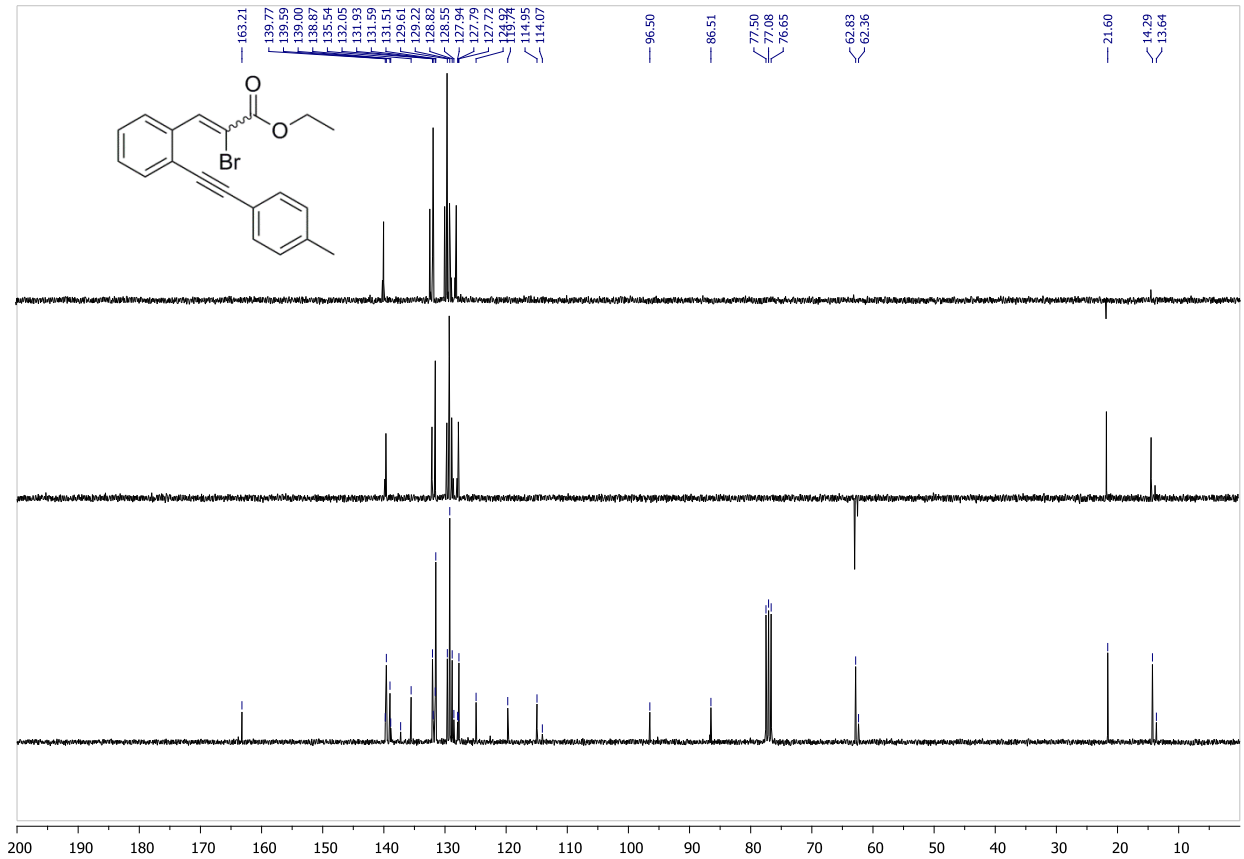

^{1}H-NMR: **1n**

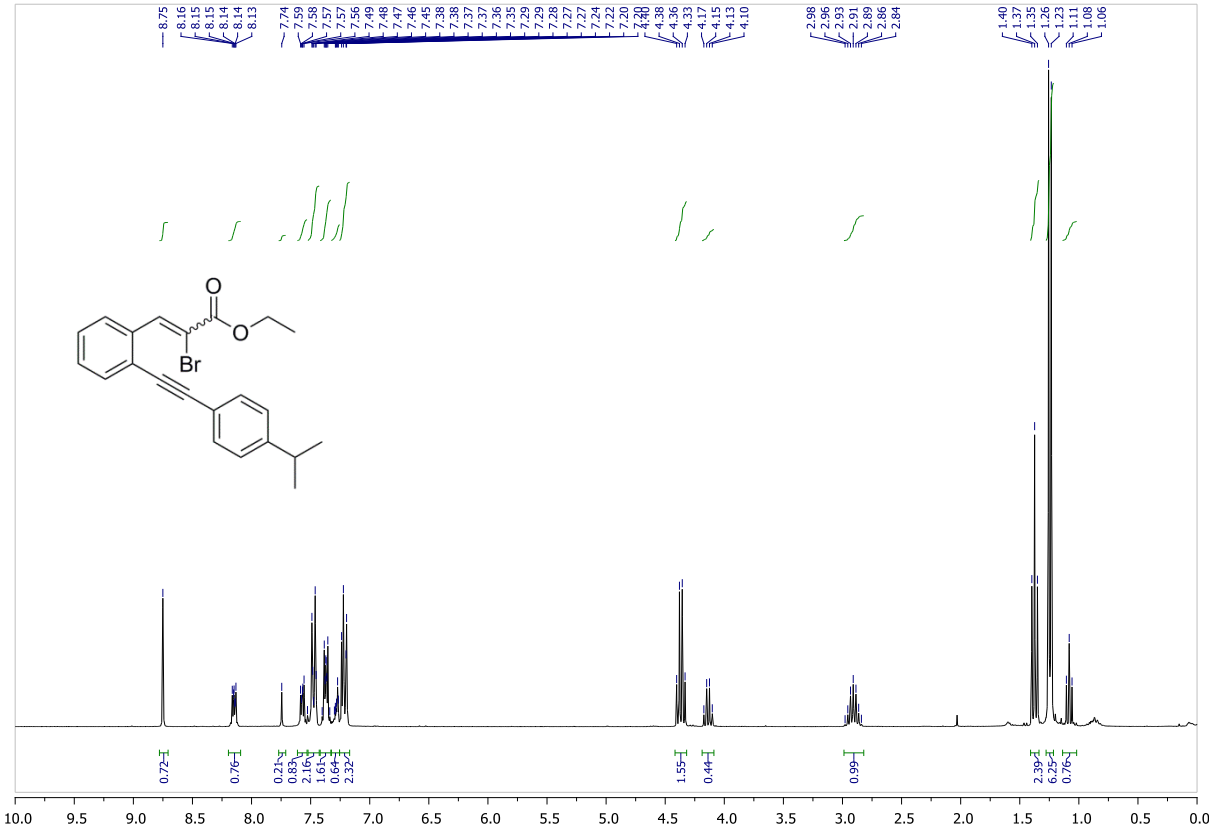

^{13}C-NMR: **1n**

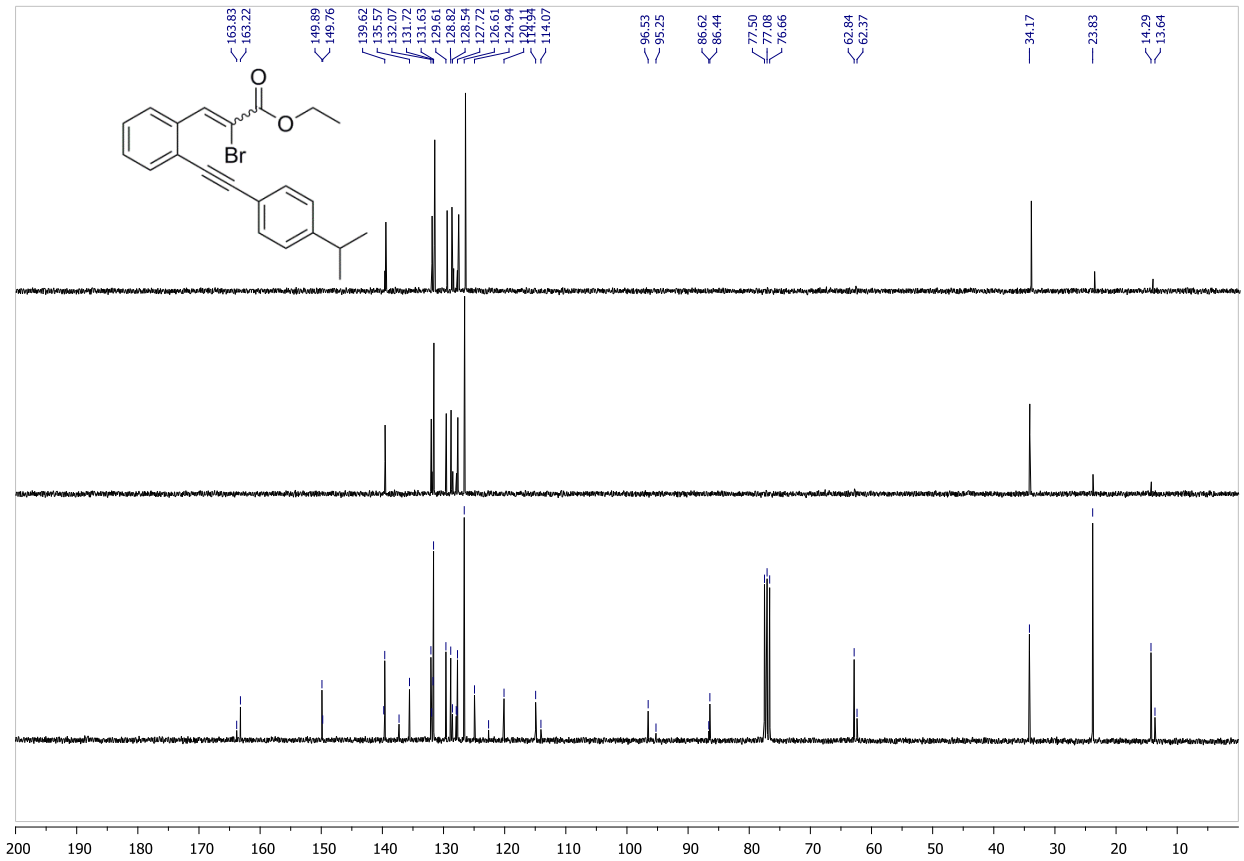

^{1}H-NMR: **1o**

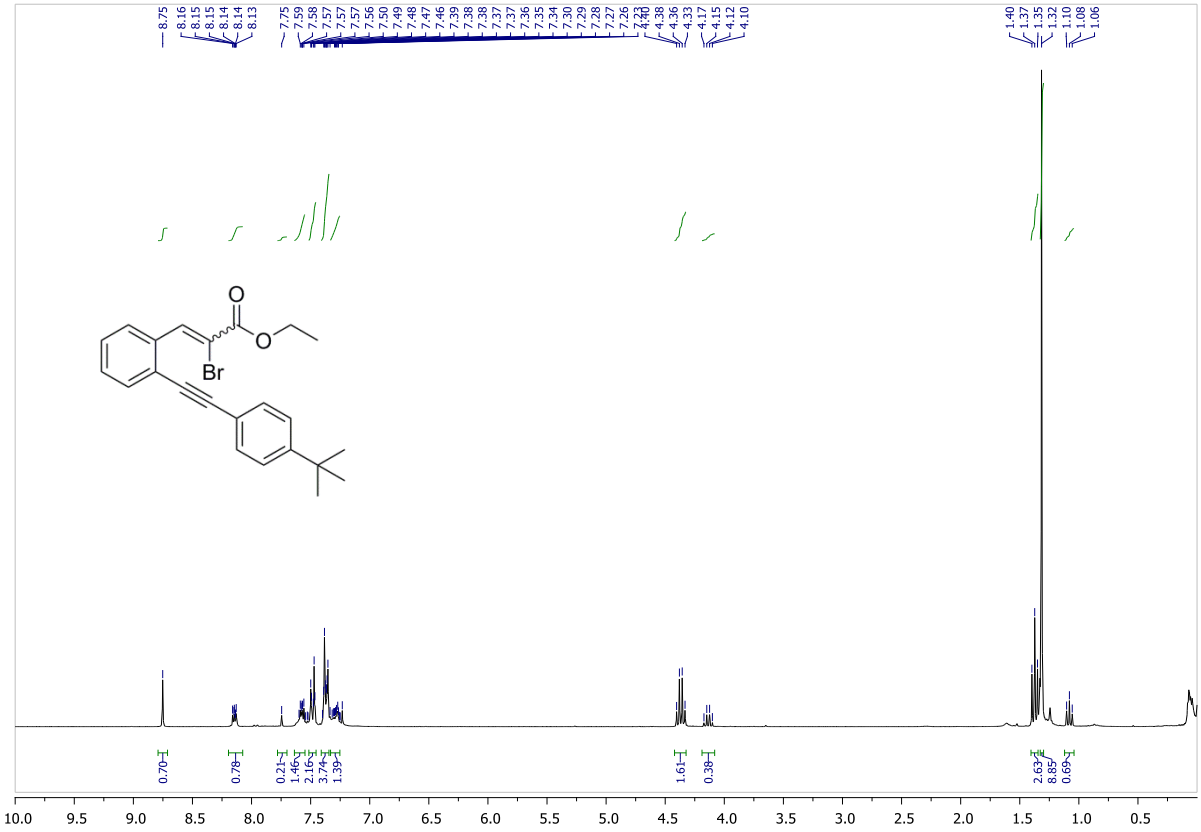

^{13}C-NMR: **1o**

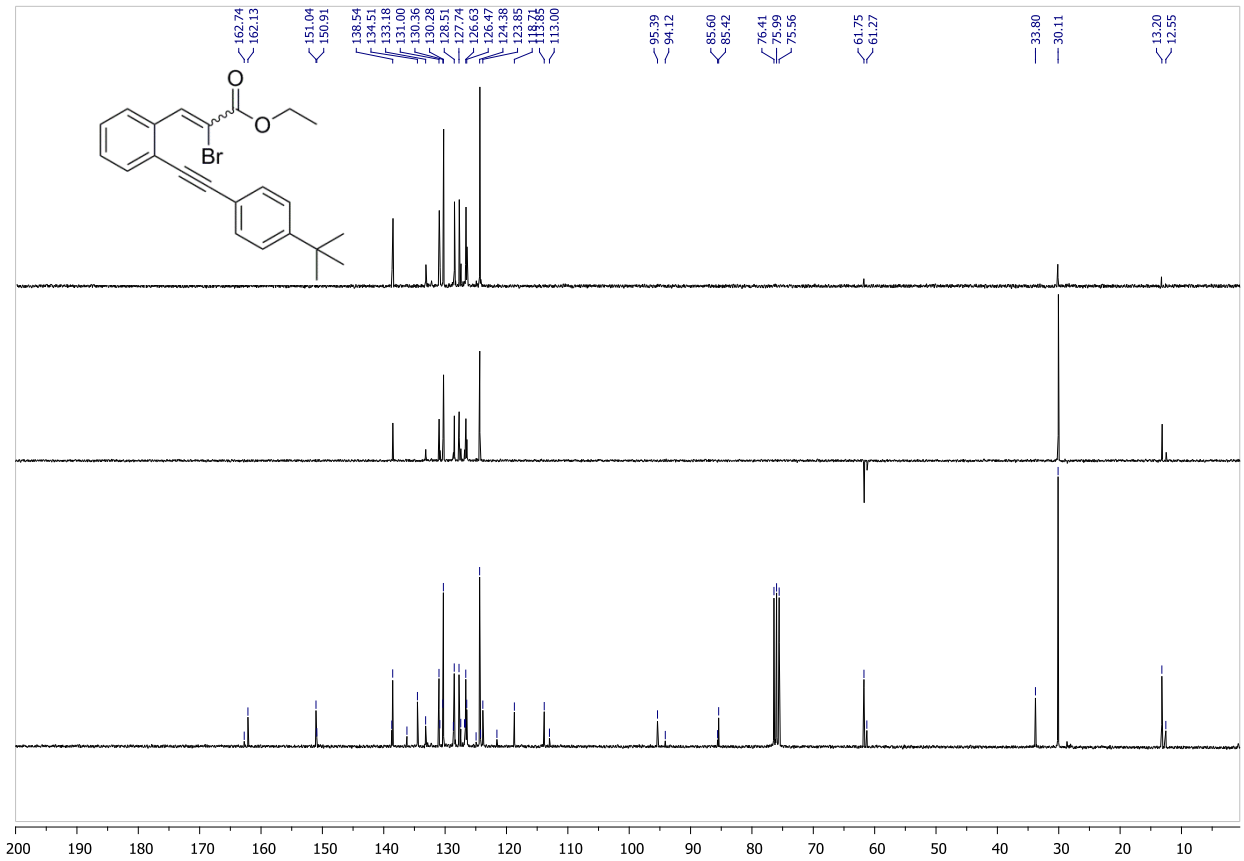

^{1}H-NMR: **1p**

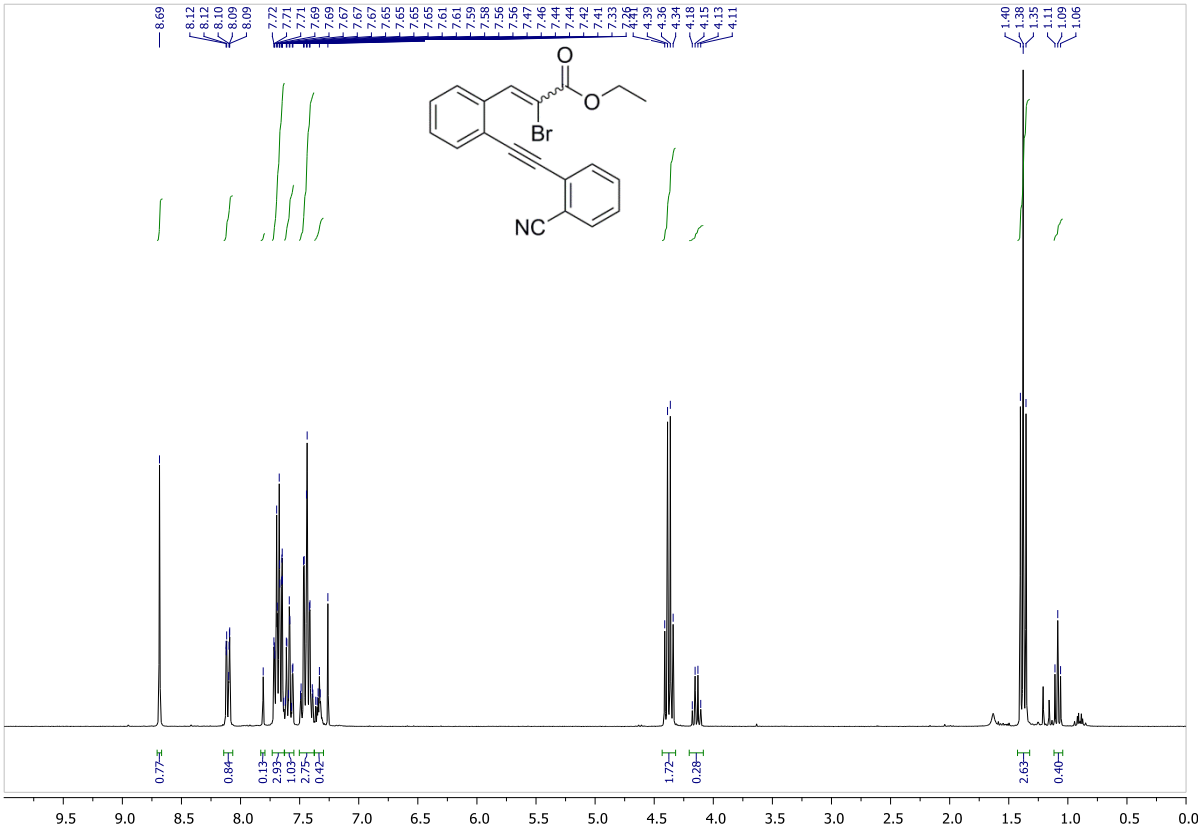

^{13}C-NMR: **1p**

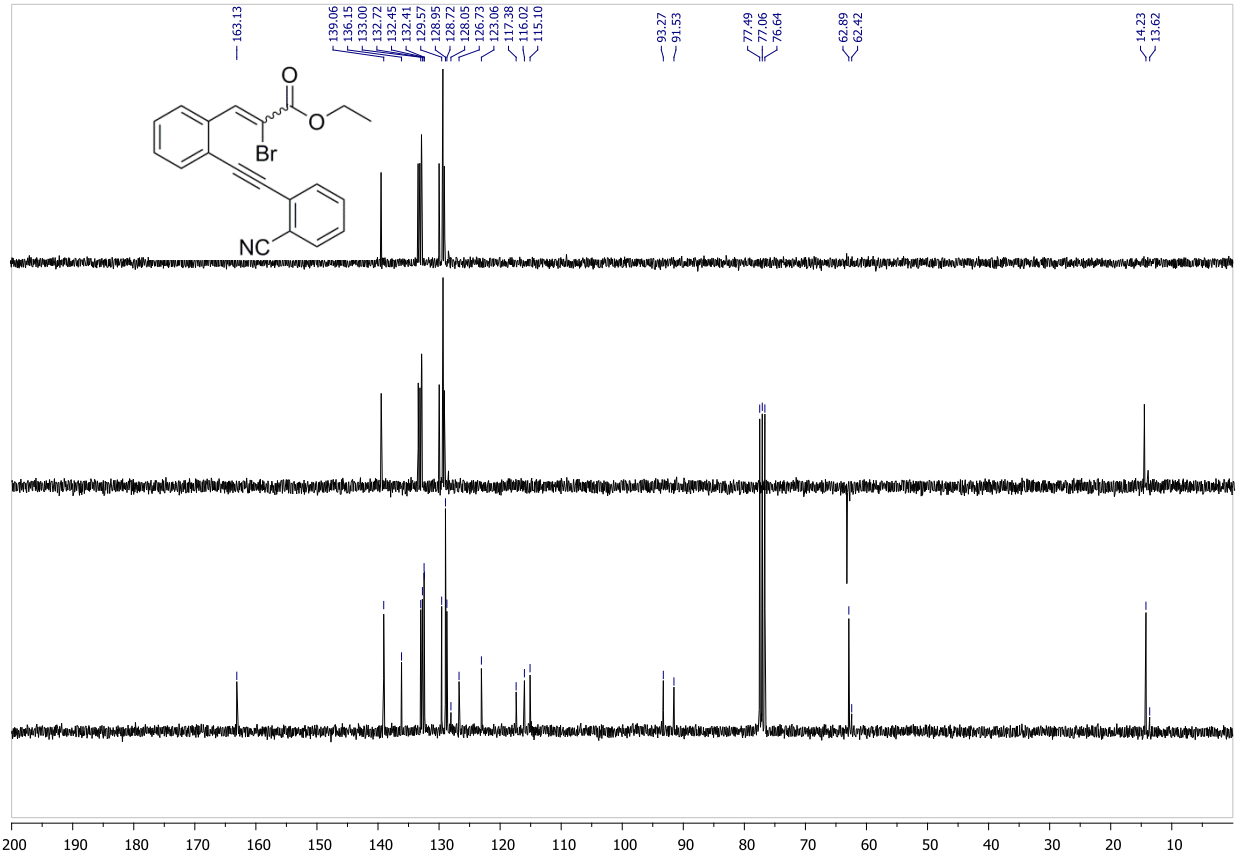

^{1}H-NMR: **1q**

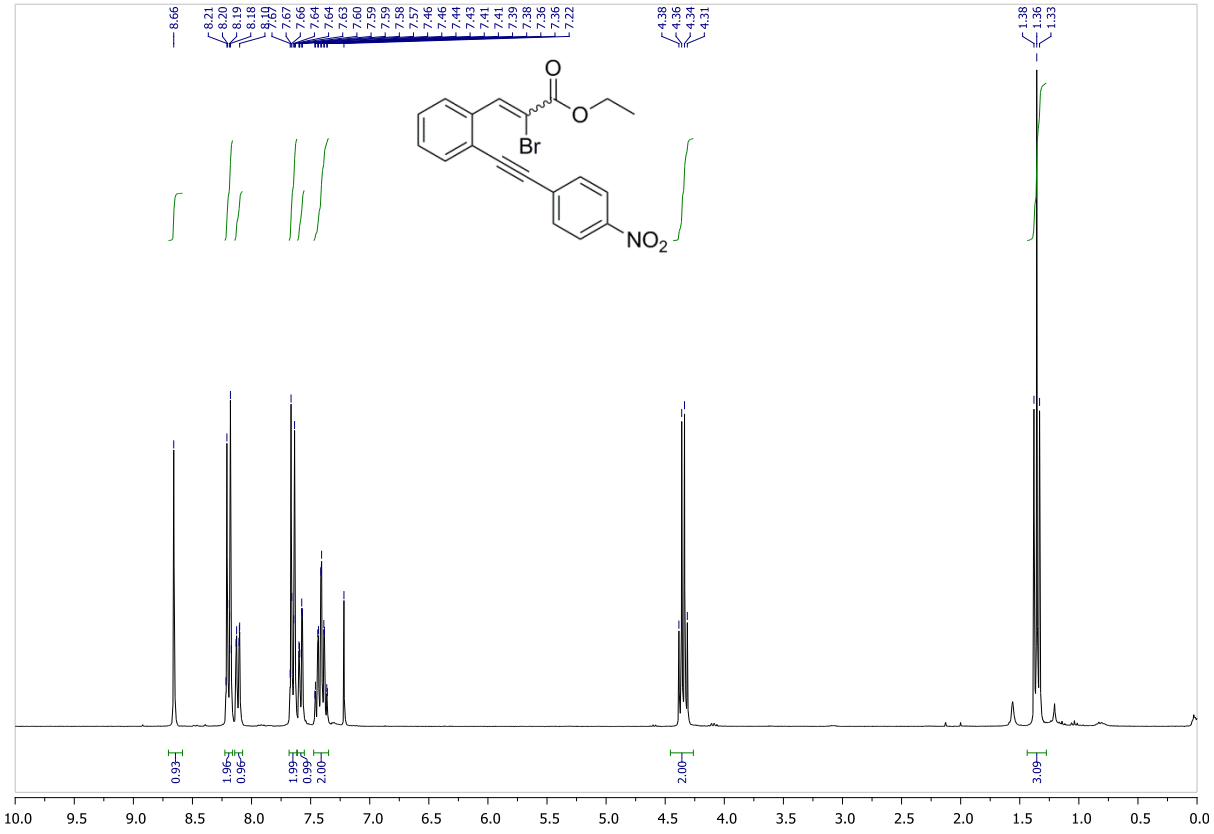

^{13}C-NMR: **1q**

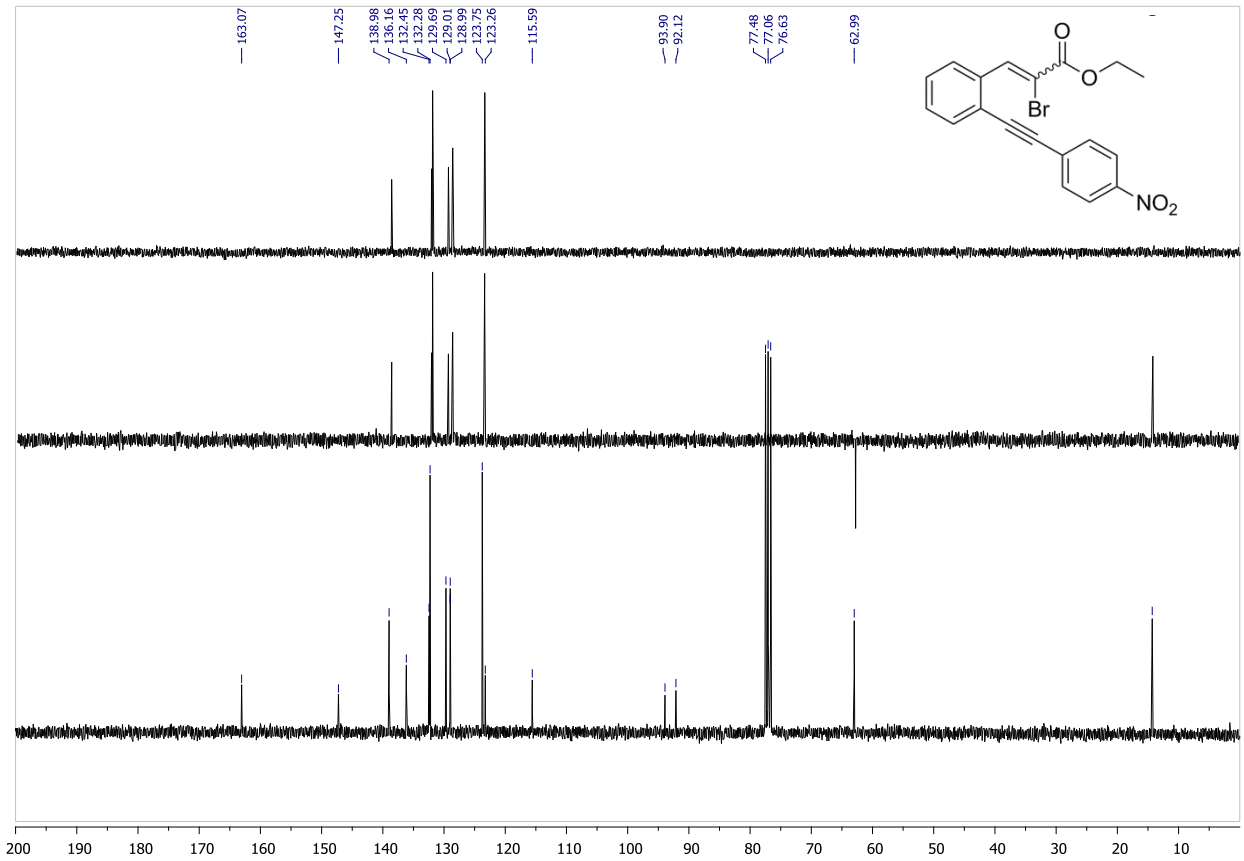

^{1}H-NMR: **1r**

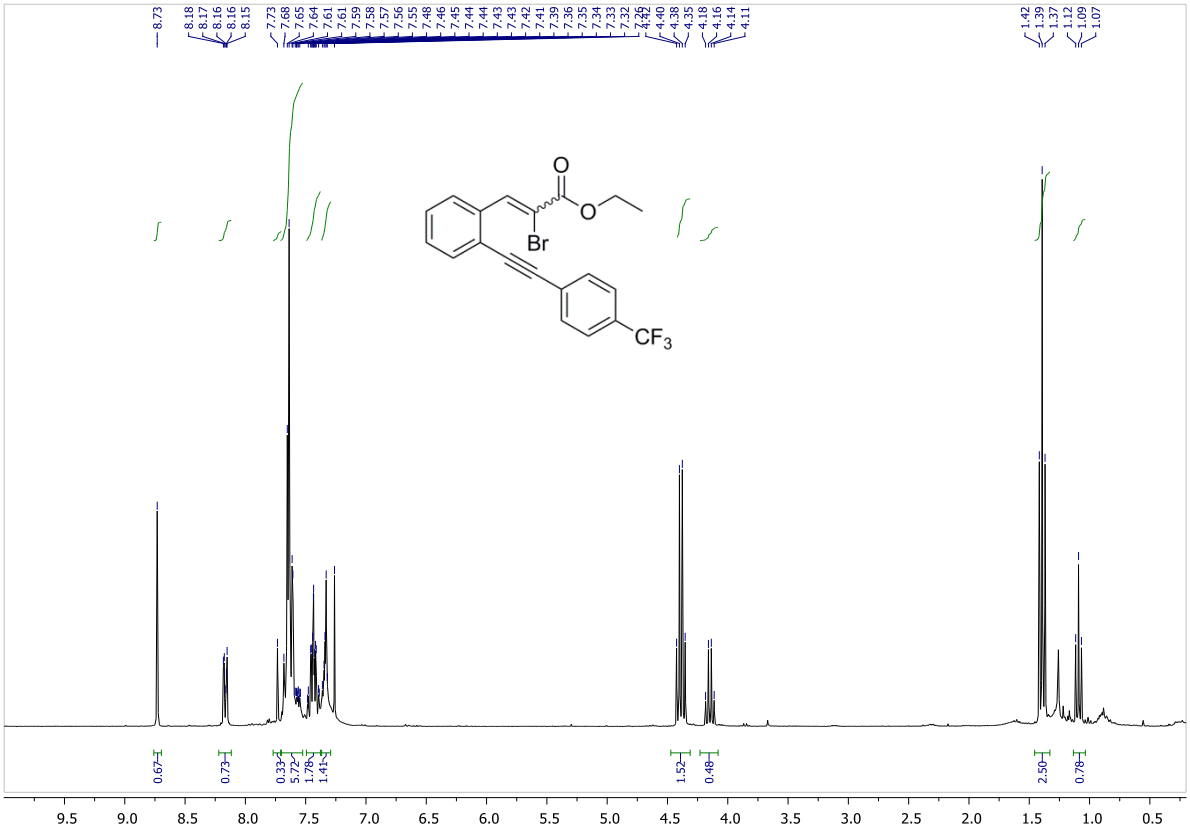

^{13}C-NMR: **1r**

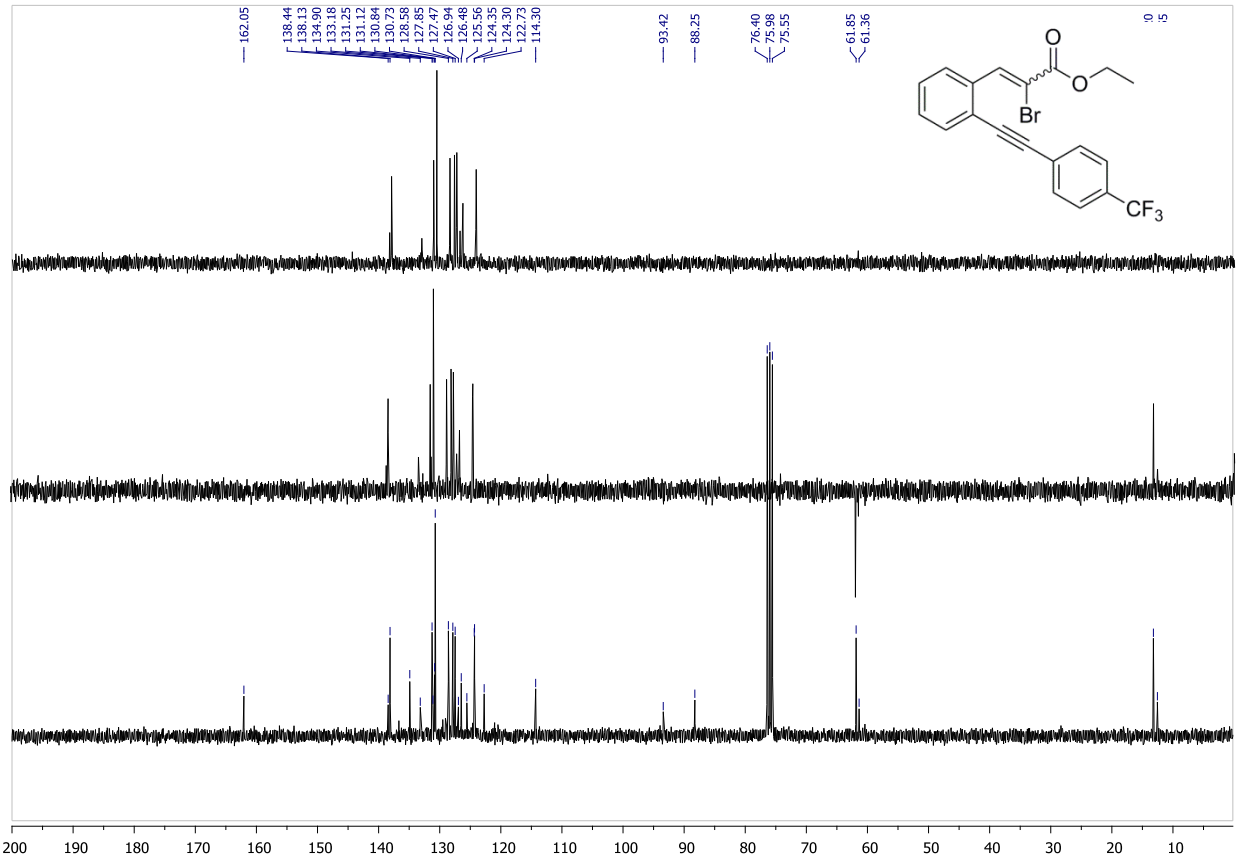

^{19}F-NMR: **1r**

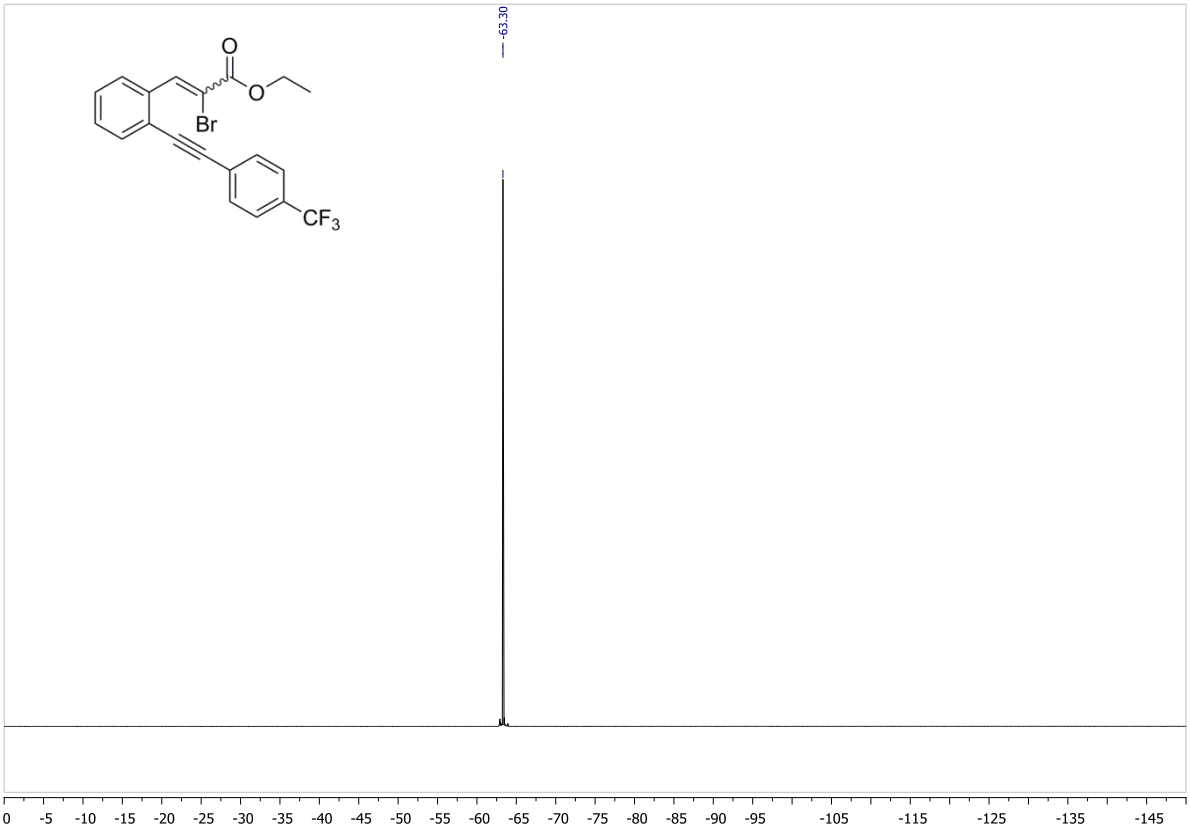
-63.30
O
O
Br
CF3
0 -5 -10 -15 -20 -25 -30 -35 -40 -45 -50 -55 -60 -65 -70 -75 -80 -85 -90 -95 -105 -115 -125 -135 -145

^{1}H-NMR: **1s**

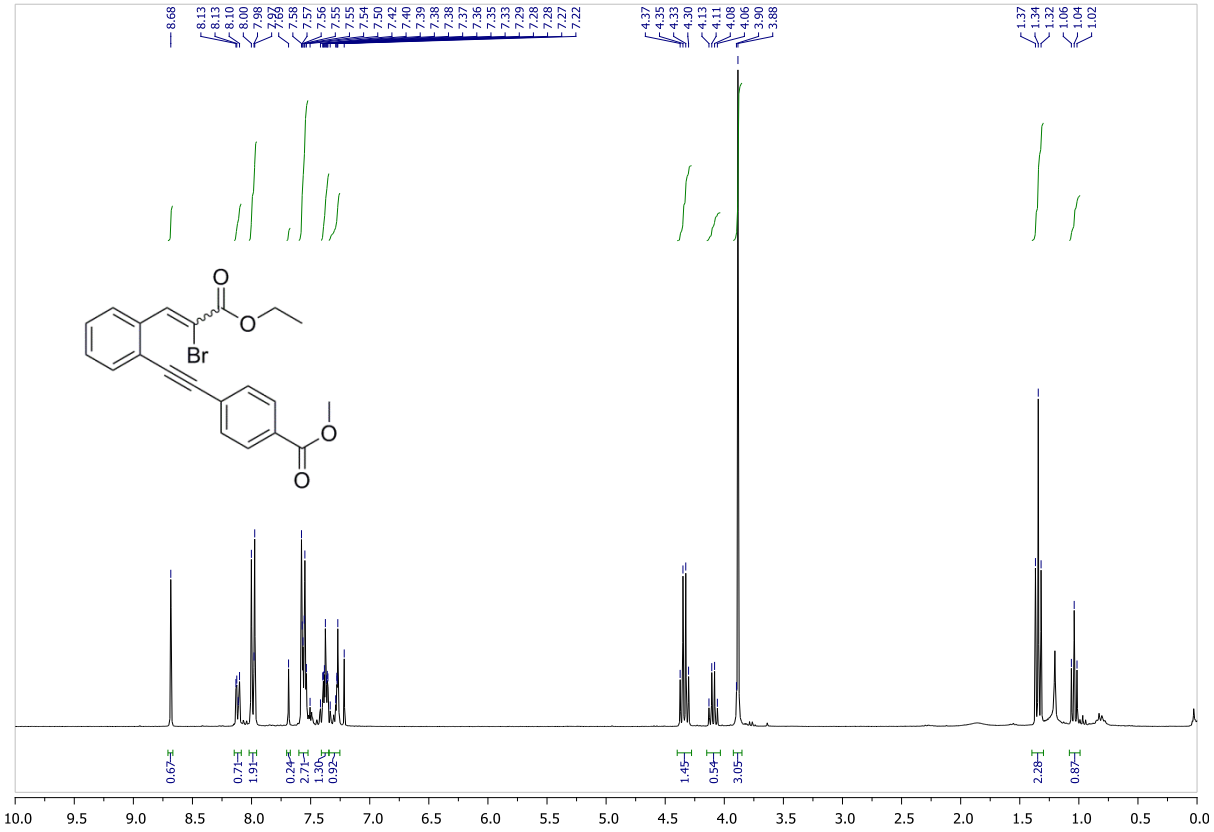

^{13}C-NMR: **1s**

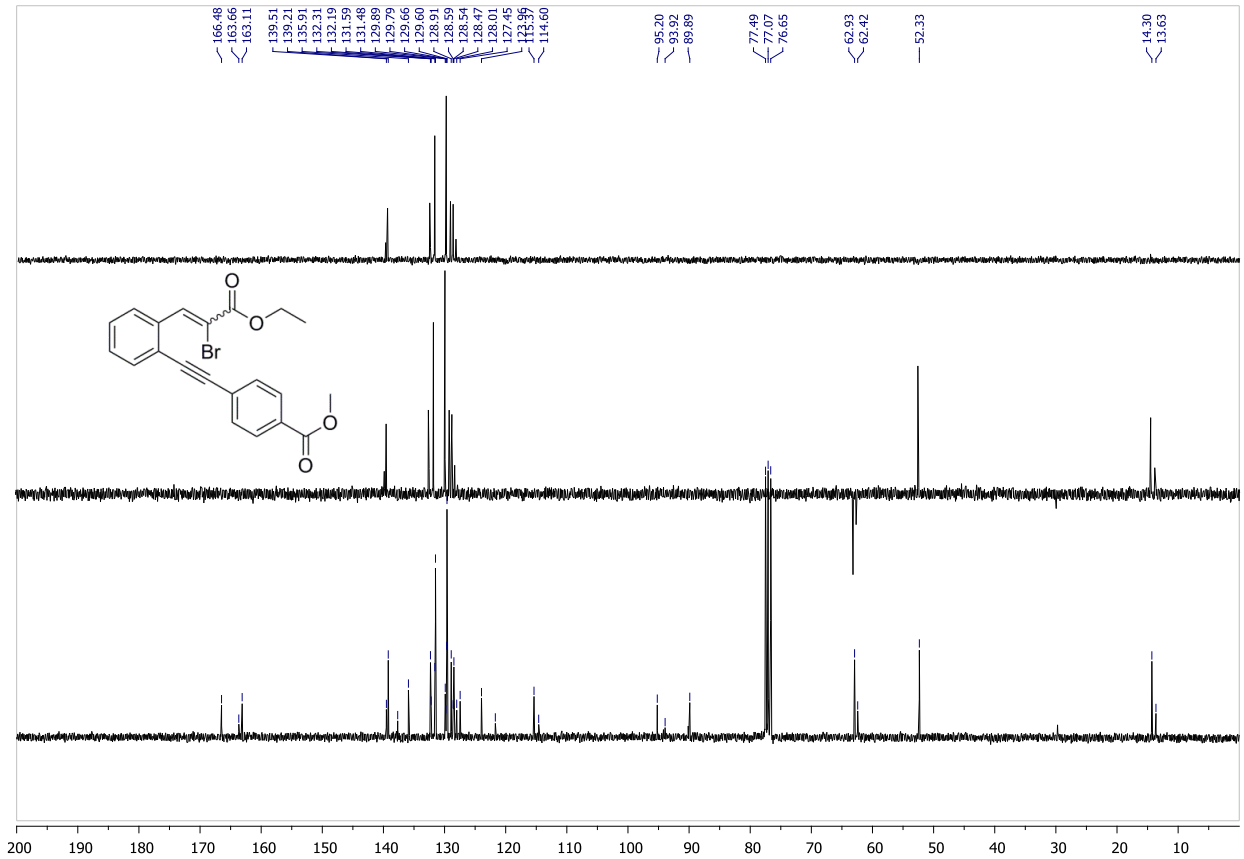

^{1}H-NMR: **1t**

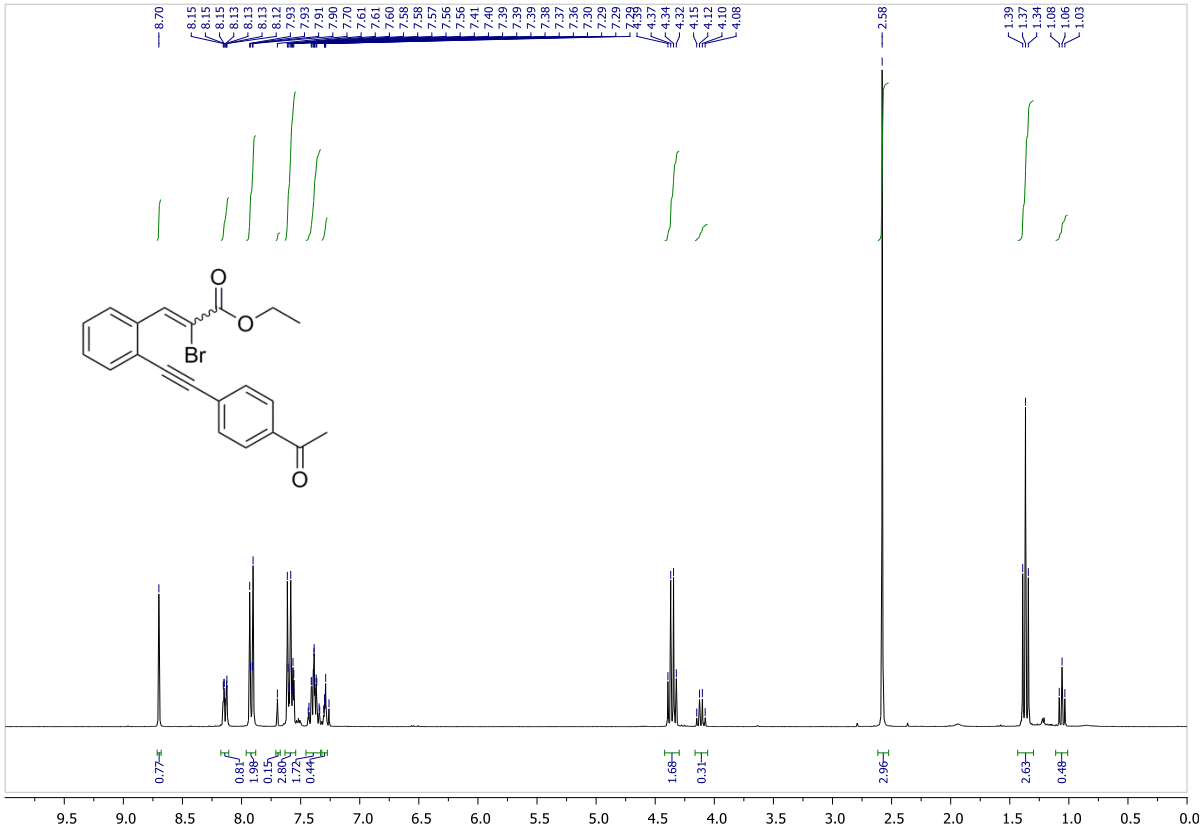

^{13}C-NMR: **1t**

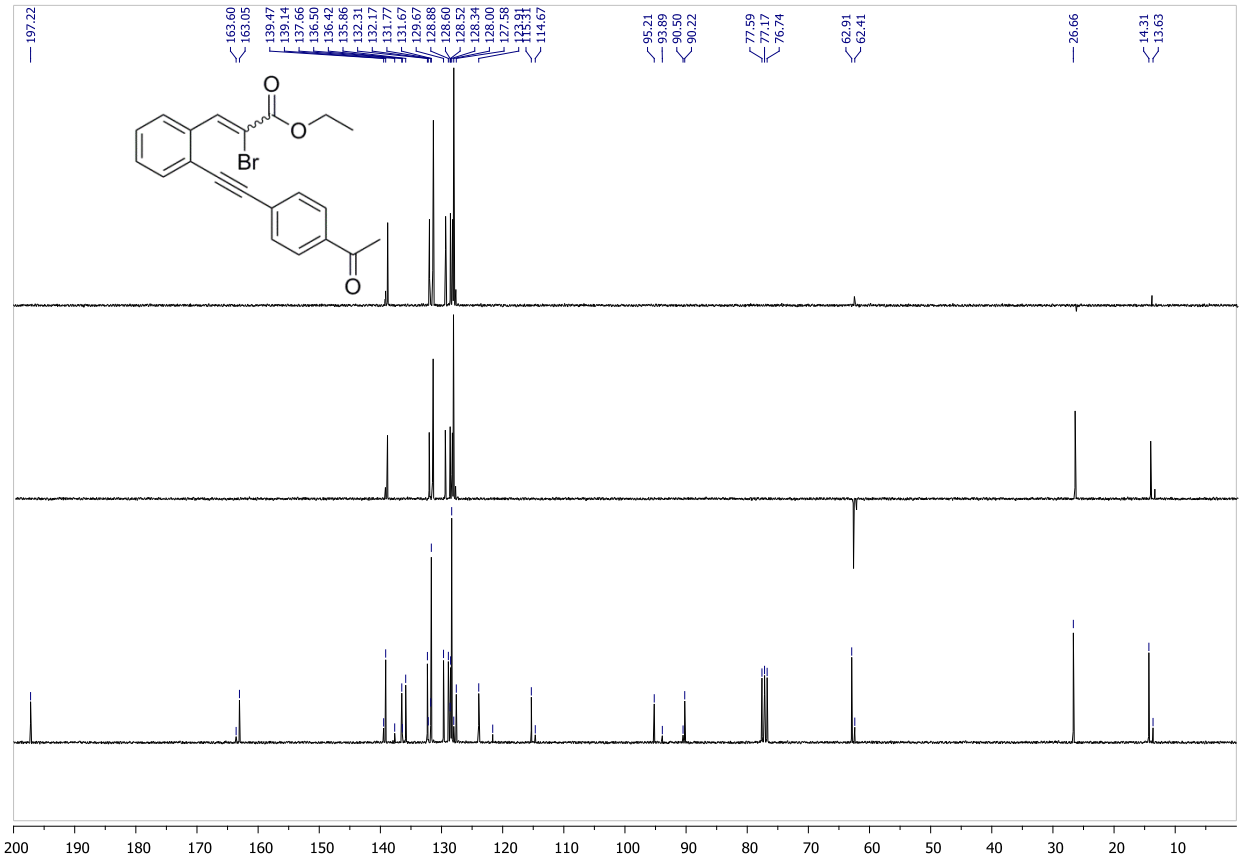

^{1}H-NMR: **1u**

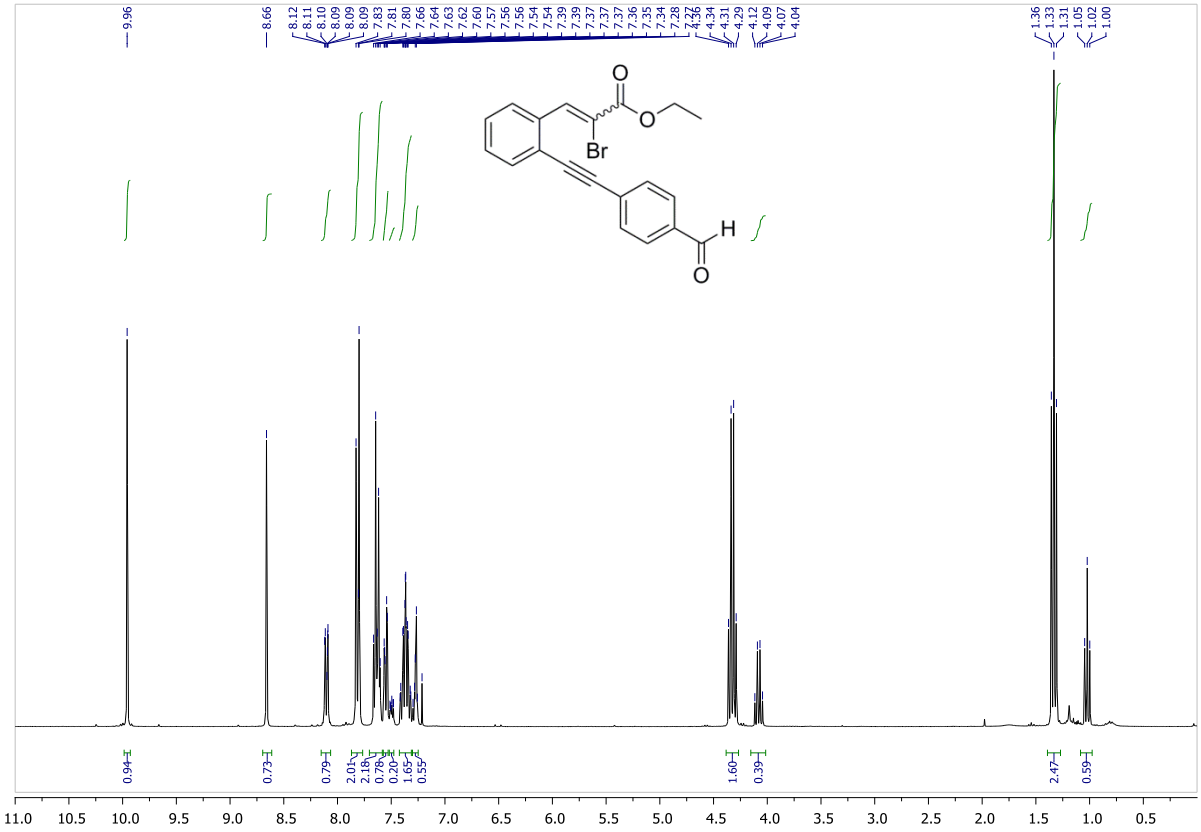

^{13}C-NMR: **1u**

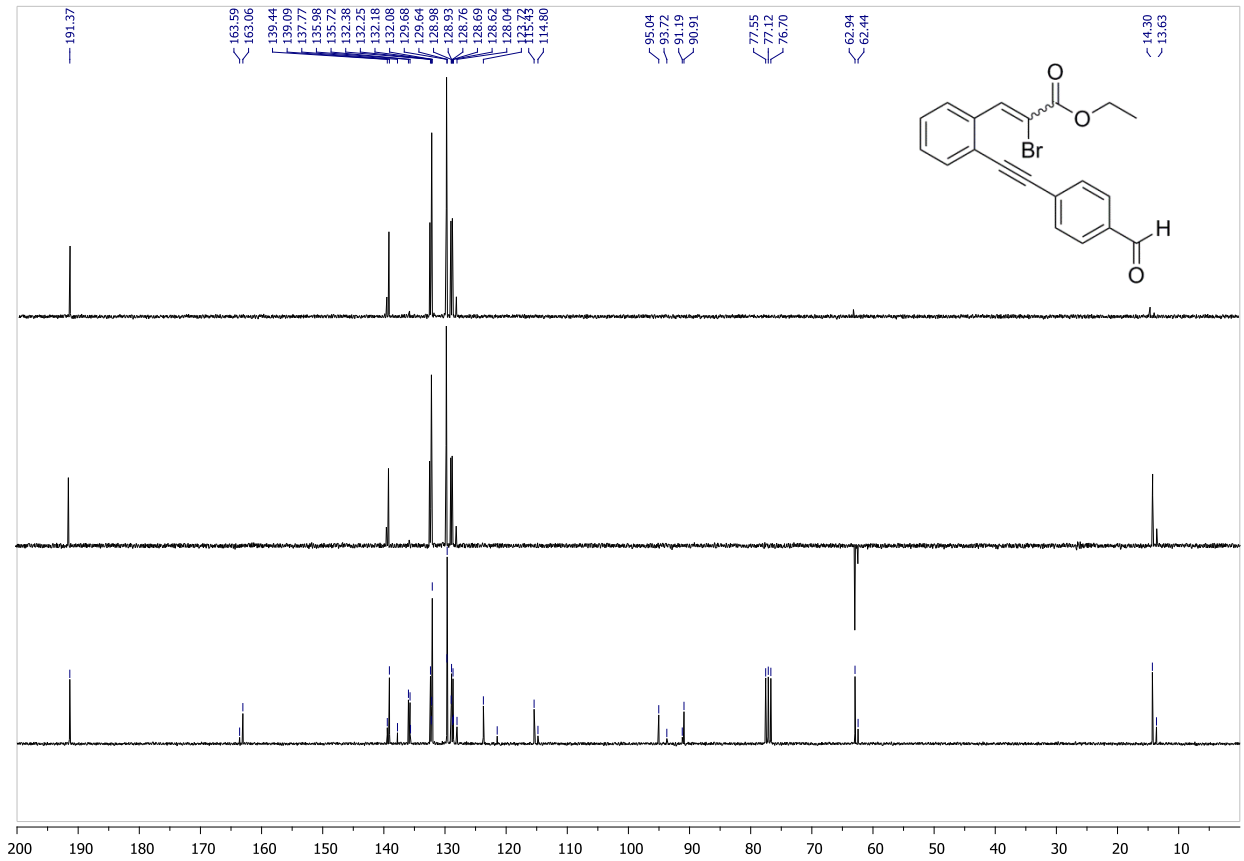

^{1}H-NMR: **1v**

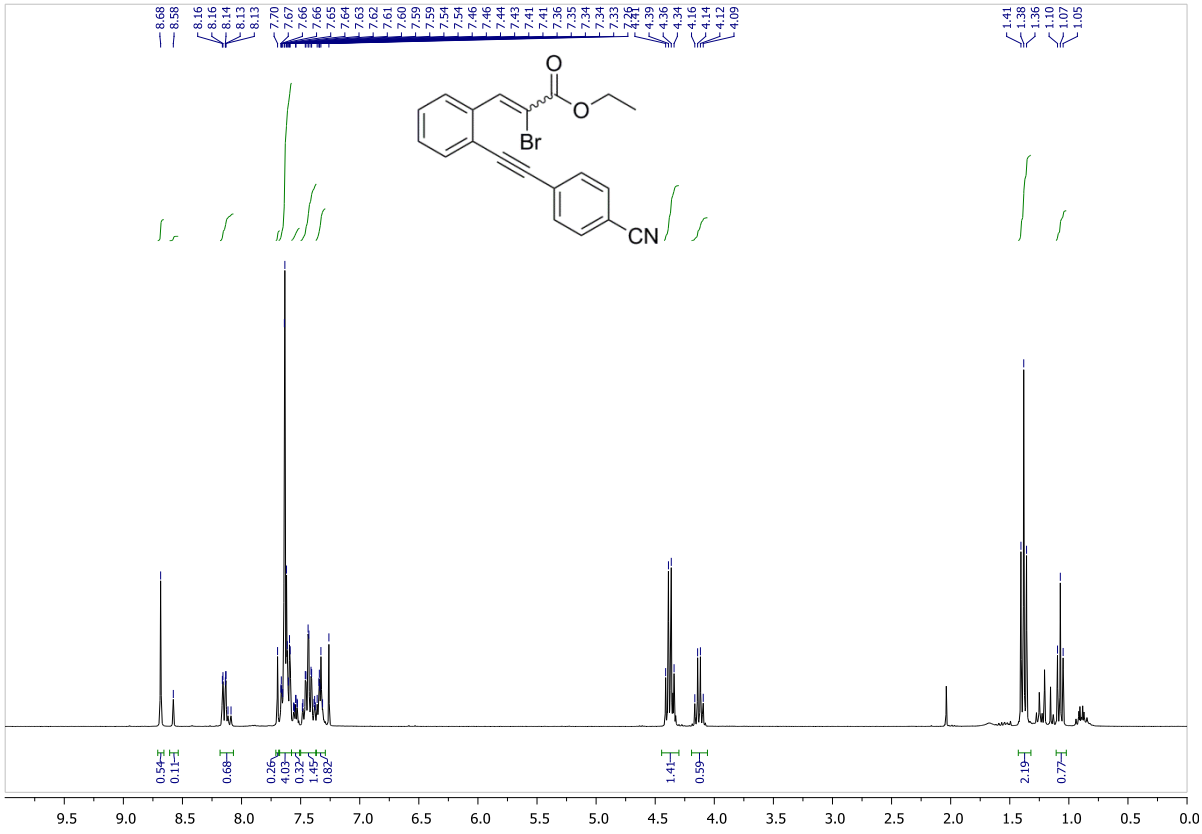

^{13}C-NMR: **1v**

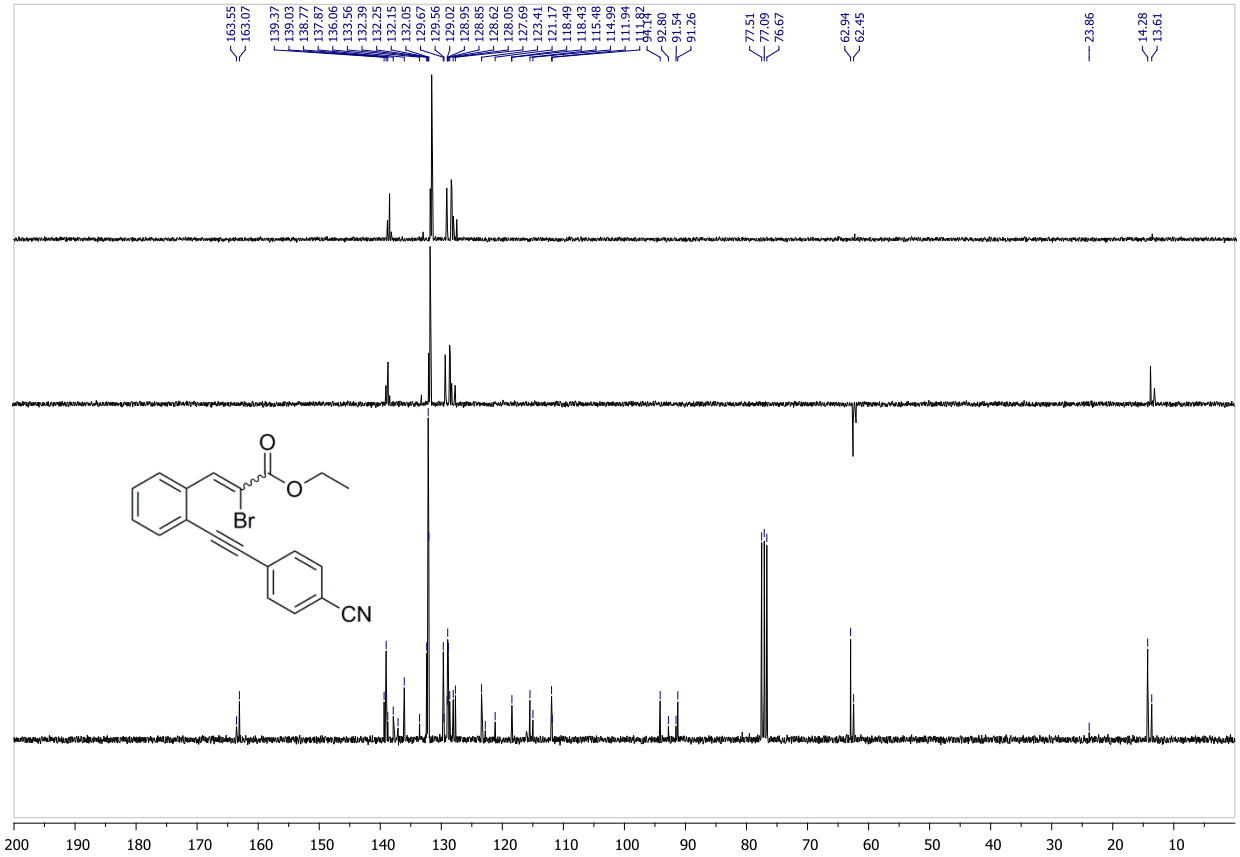

^{1}H-NMR: **4**

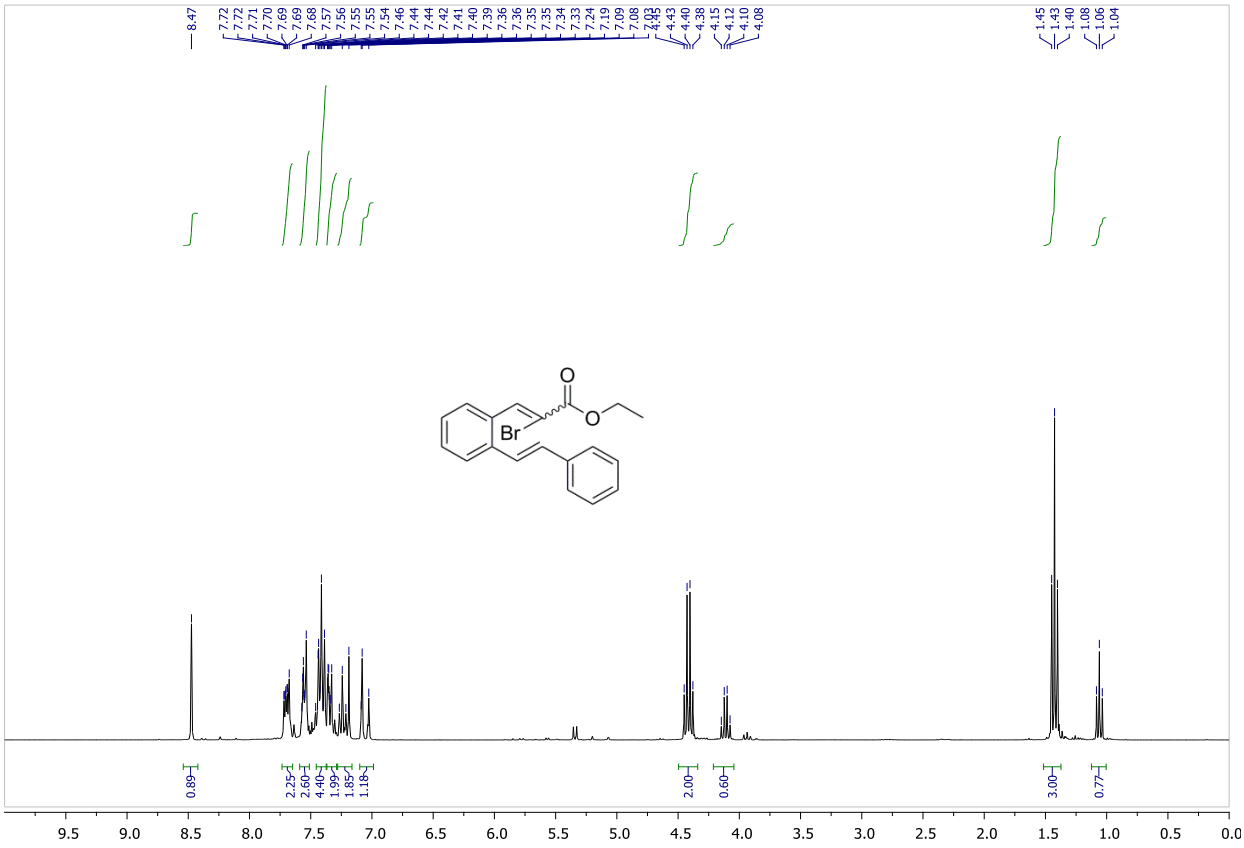

^{13}C-NMR: **4**

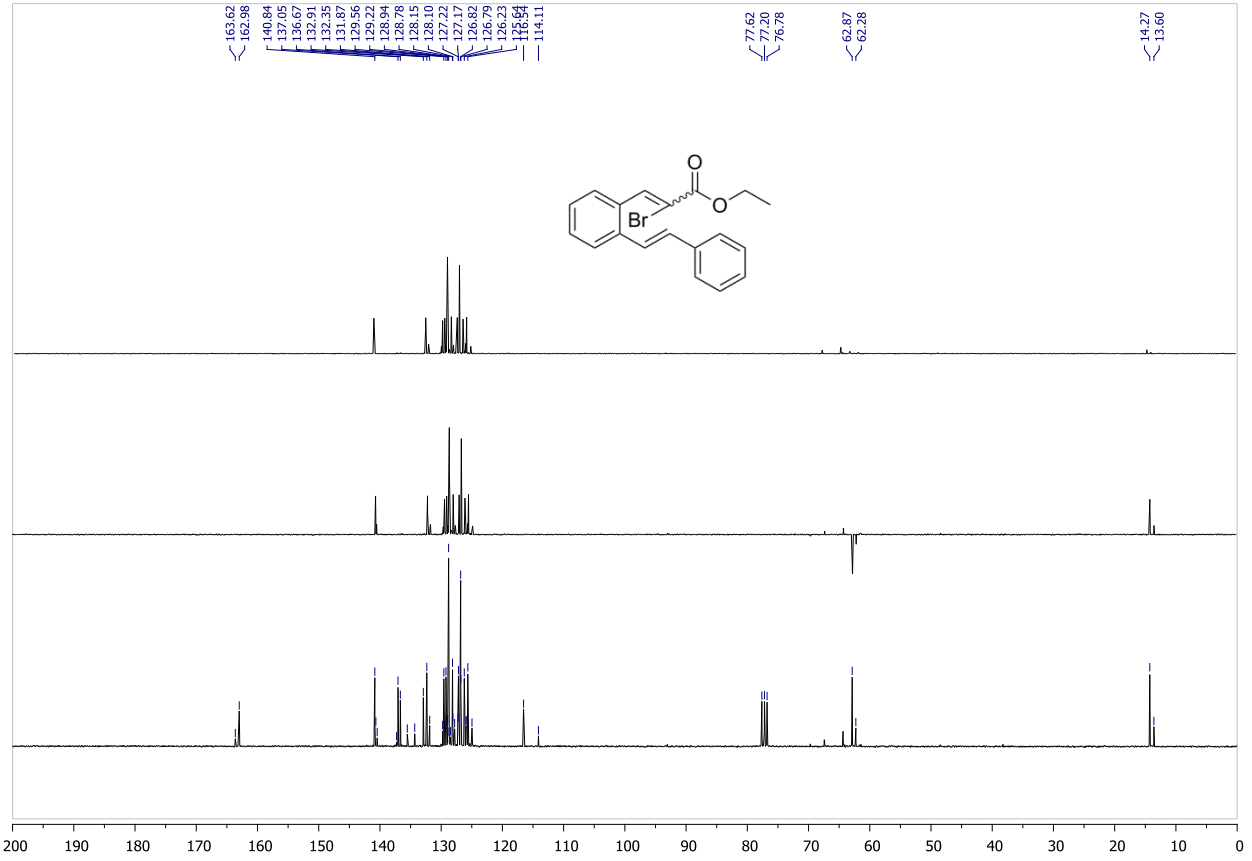

^{1}H-NMR: **6**

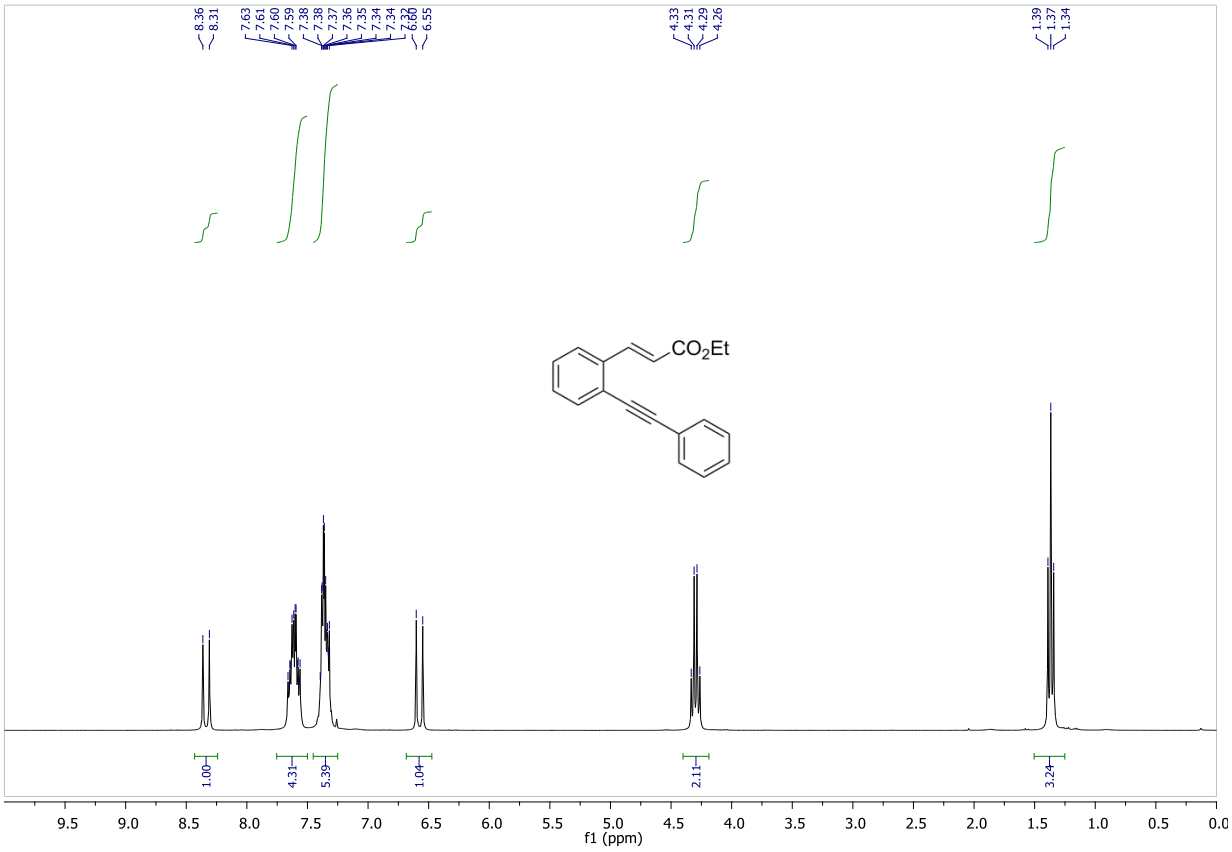

^{13}C-NMR: **6**

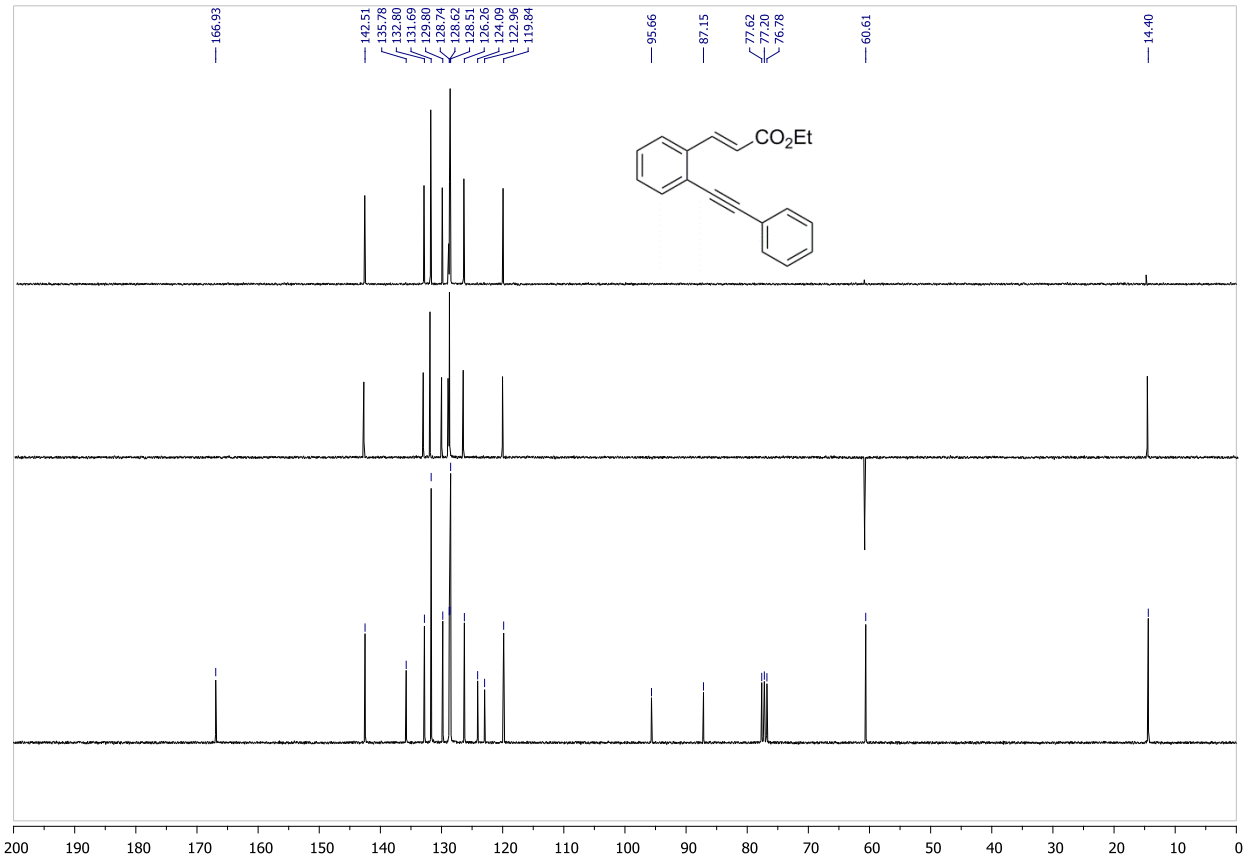

^{1}H-NMR: **2a**

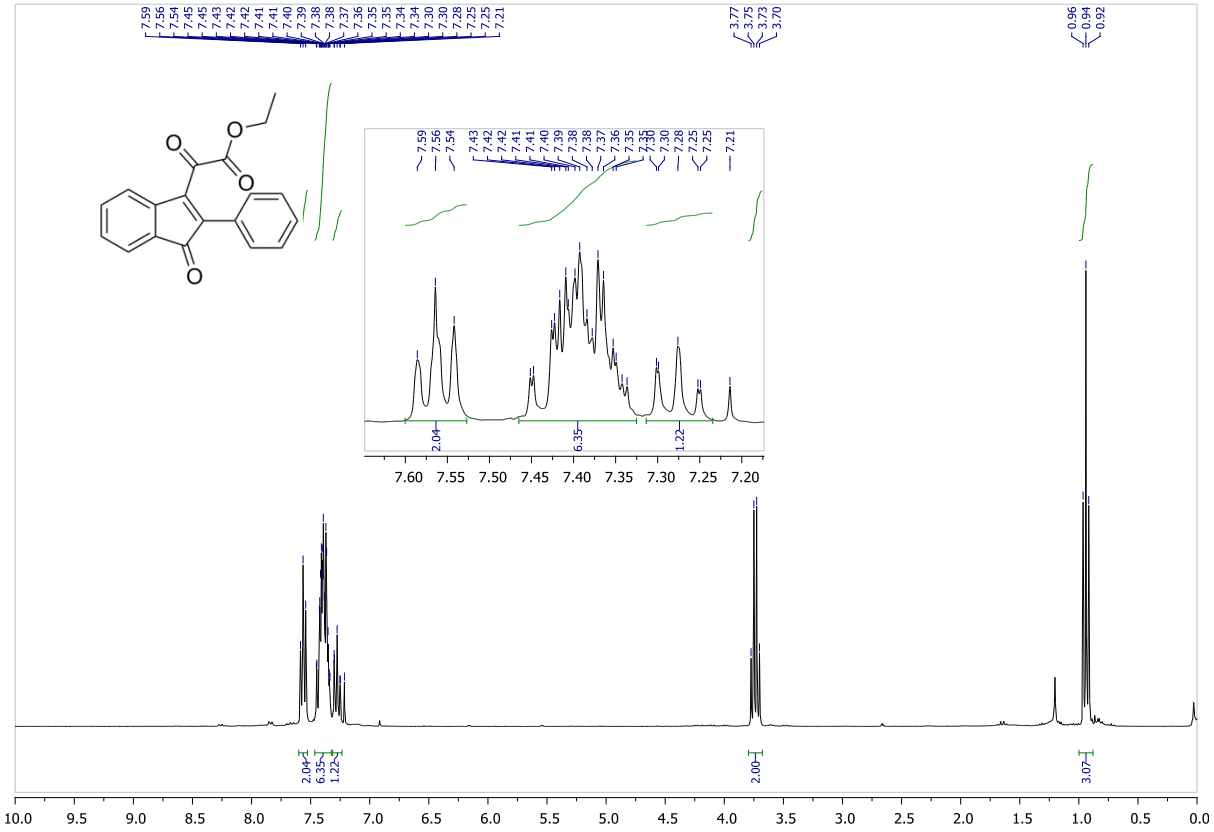

^{13}C-NMR: **2a**

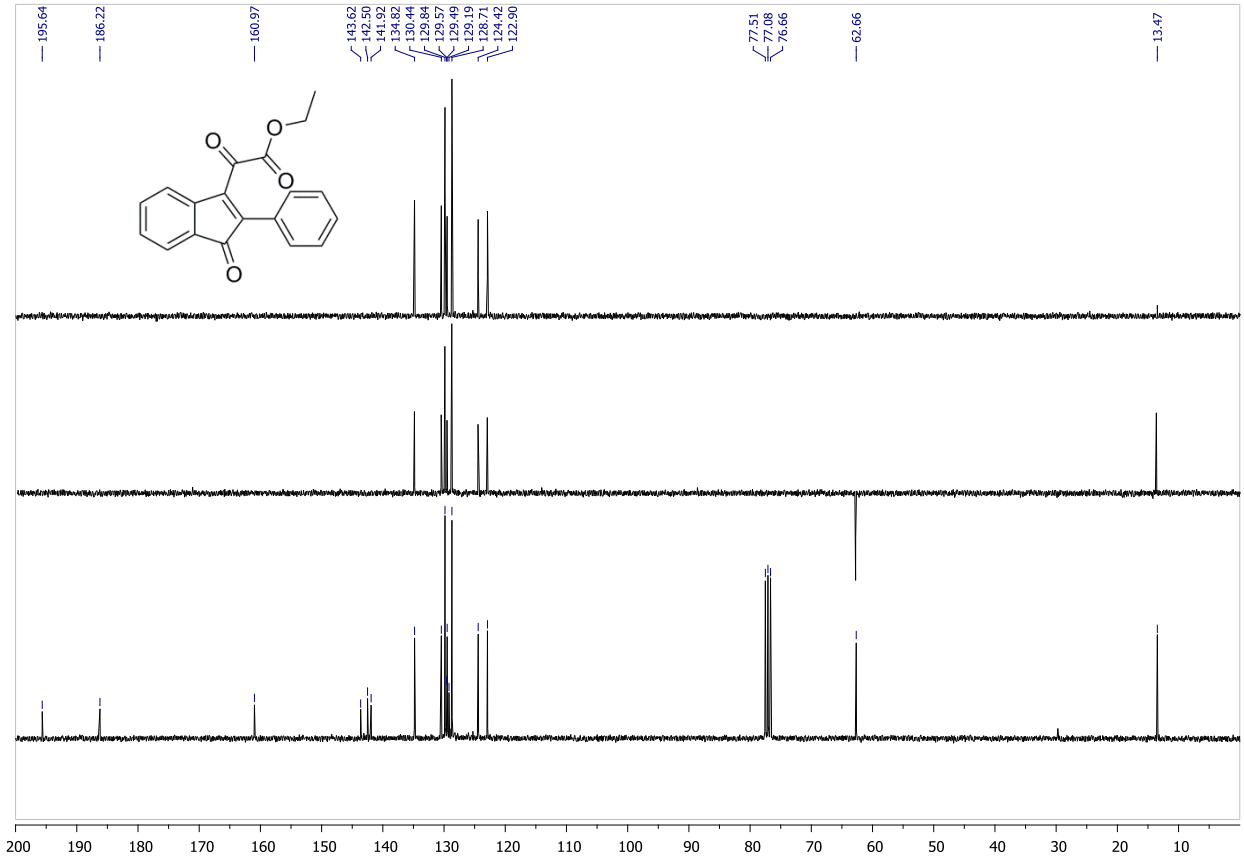

^{1}H-NMR: **2b**

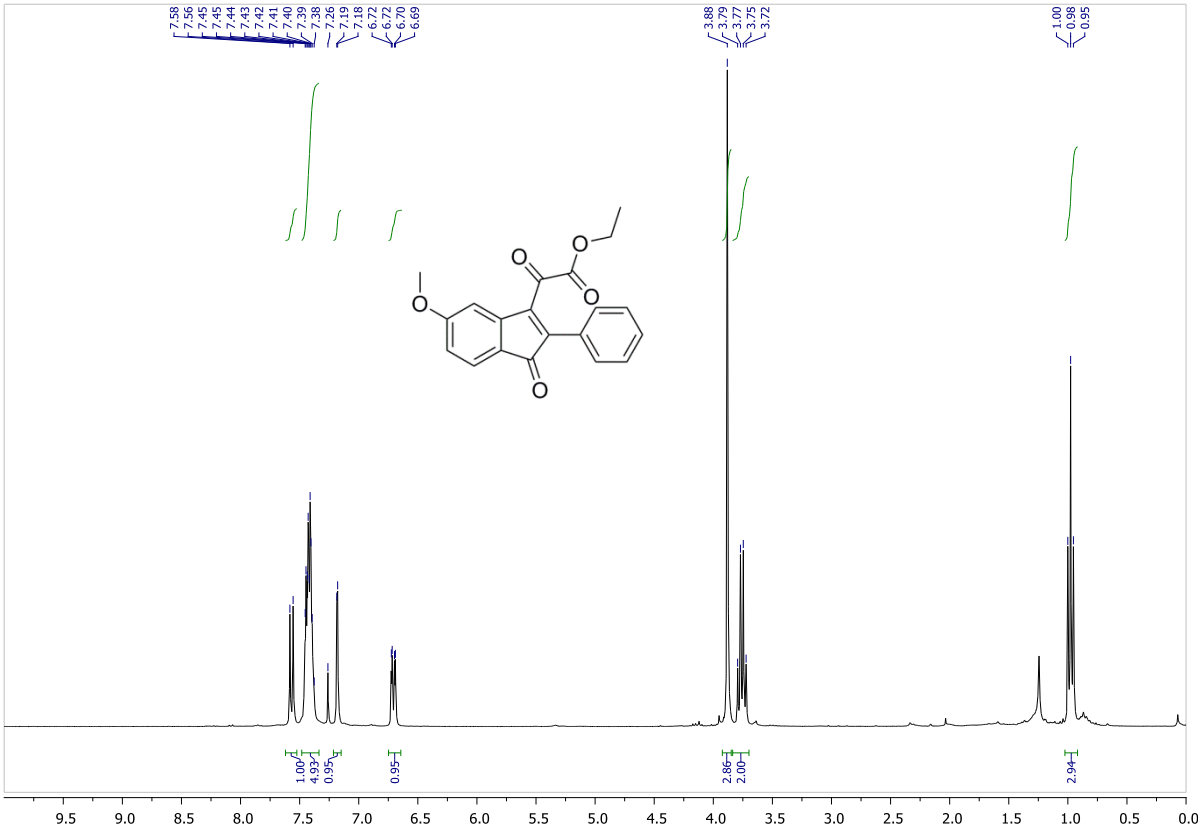

^{13}C-NMR: **2b**

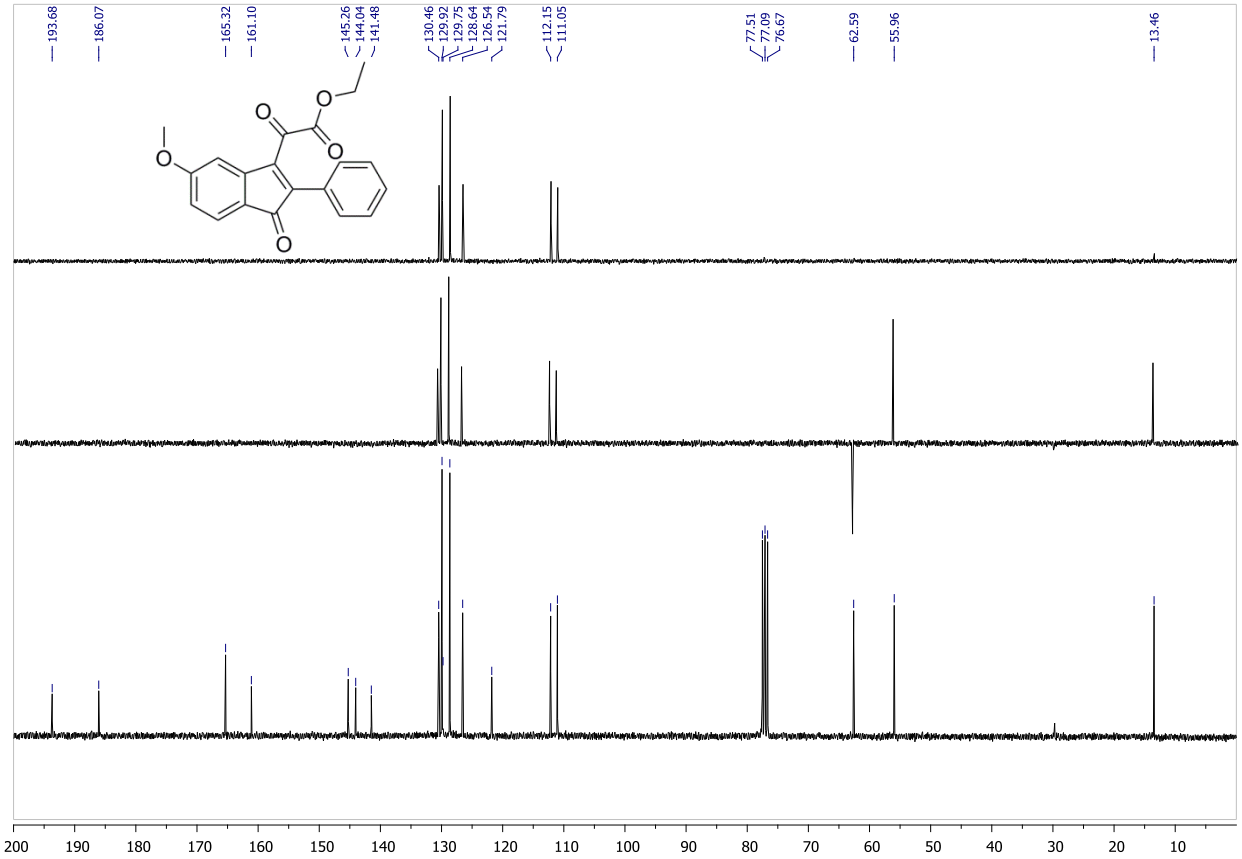

^{1}H-NMR: **2c**

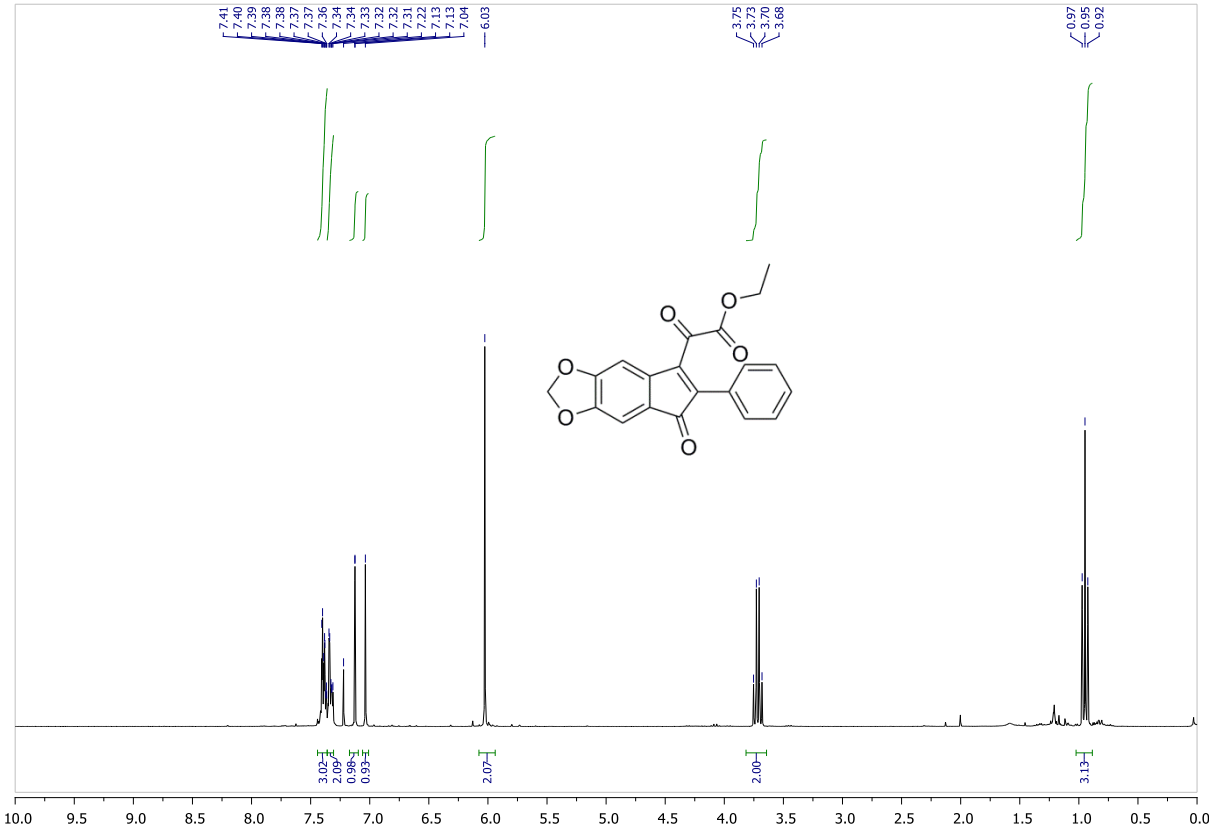

^{13}C-NMR: **2c**

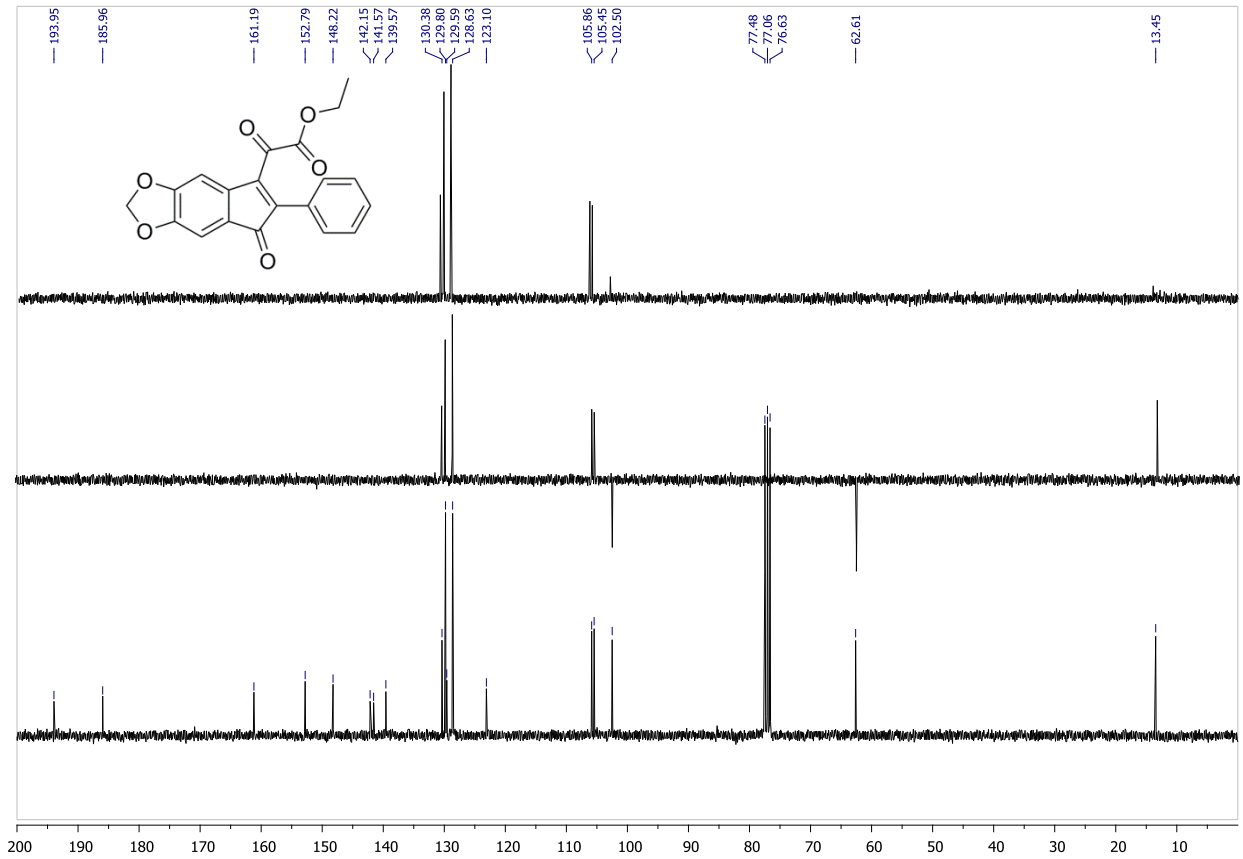

^{1}H-NMR: **2d**

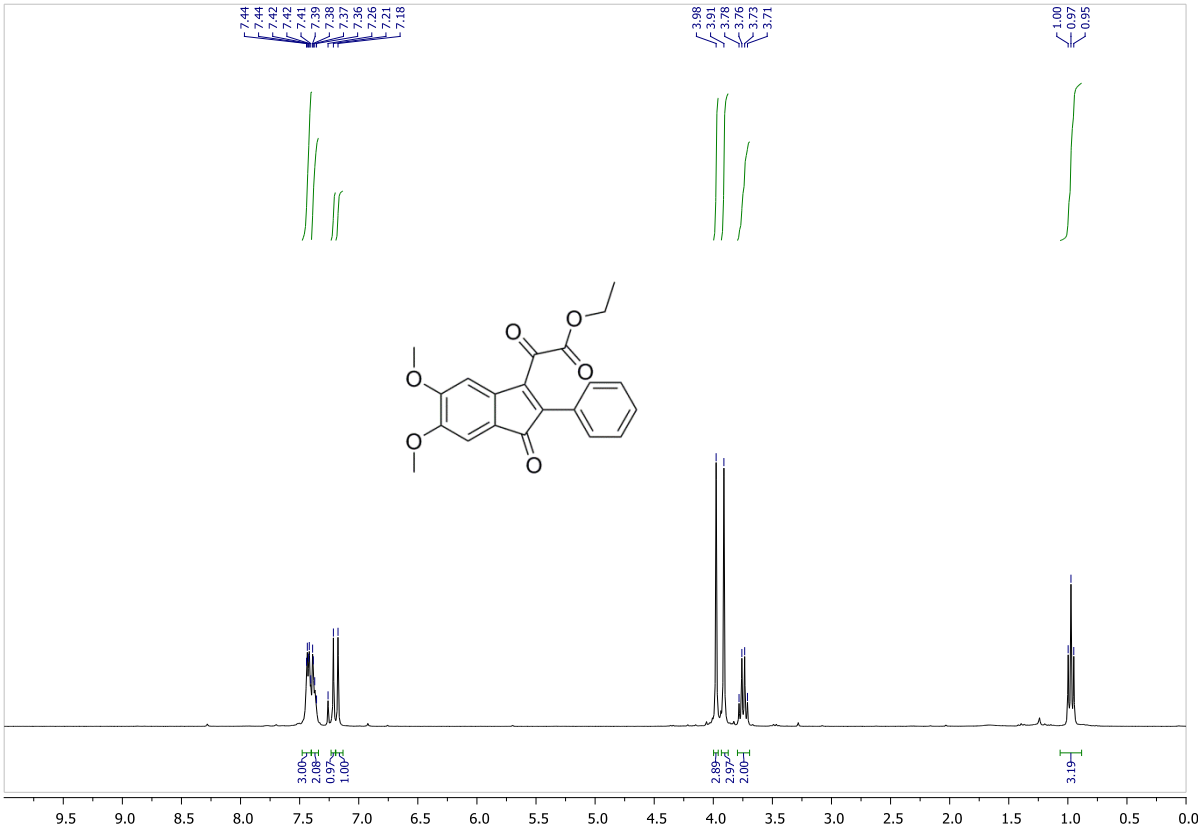

^{13}C-NMR: **2d**

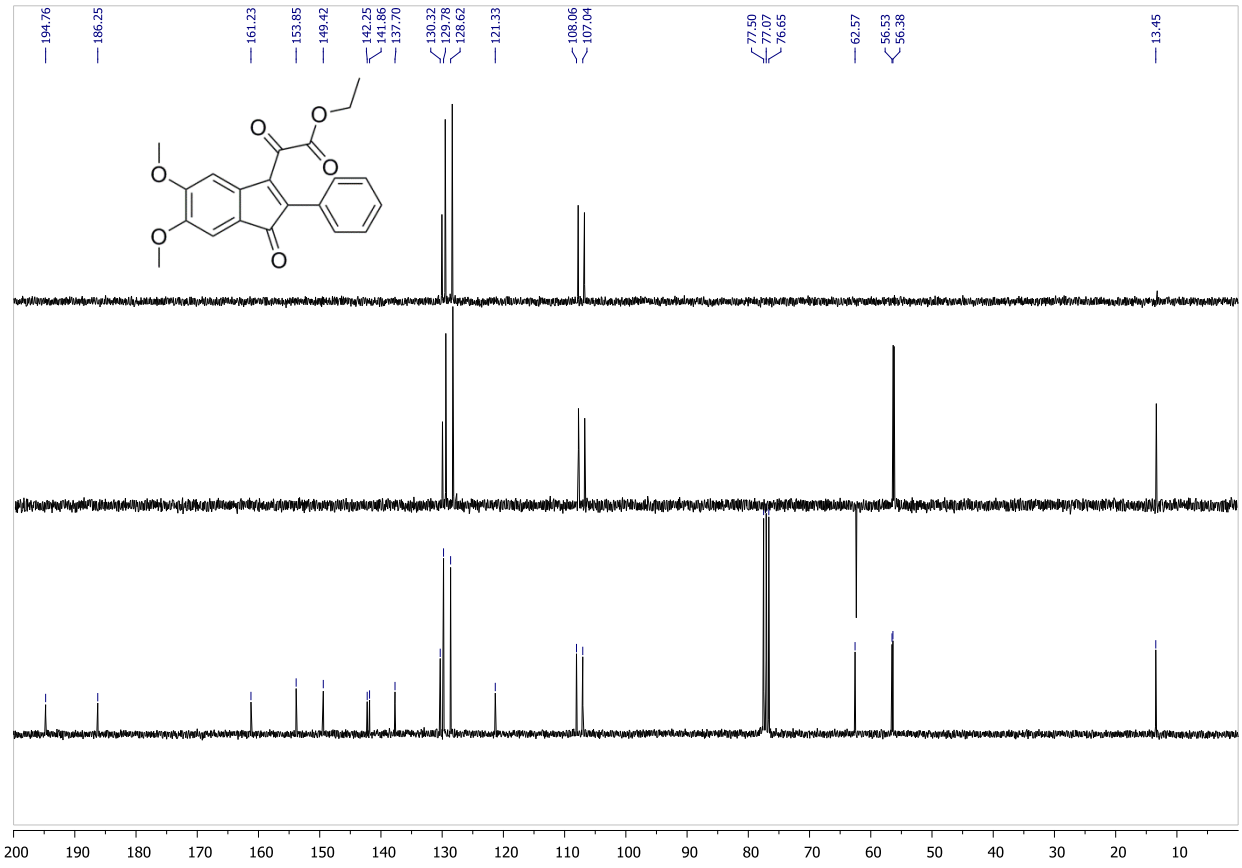

^{1}H-NMR: **2e**

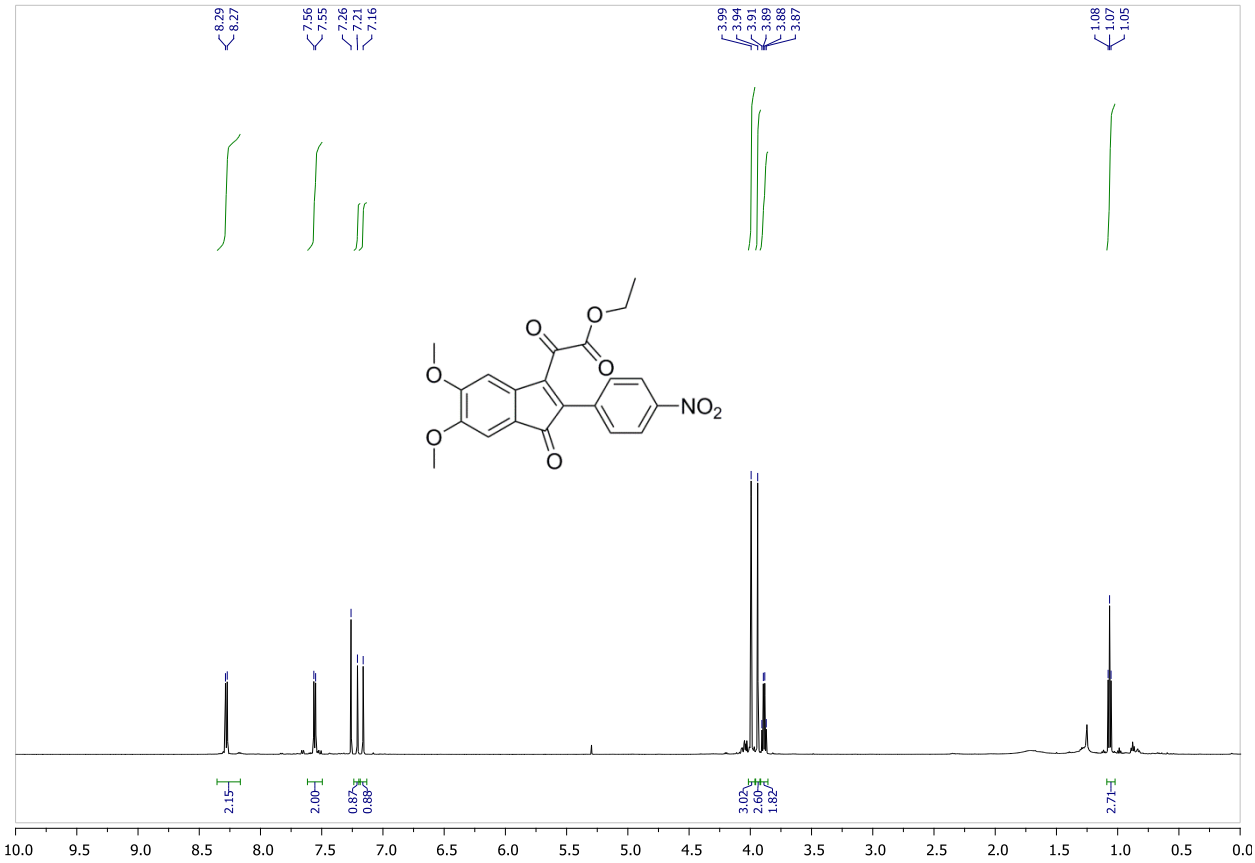

^{13}C-NMR: **2e**

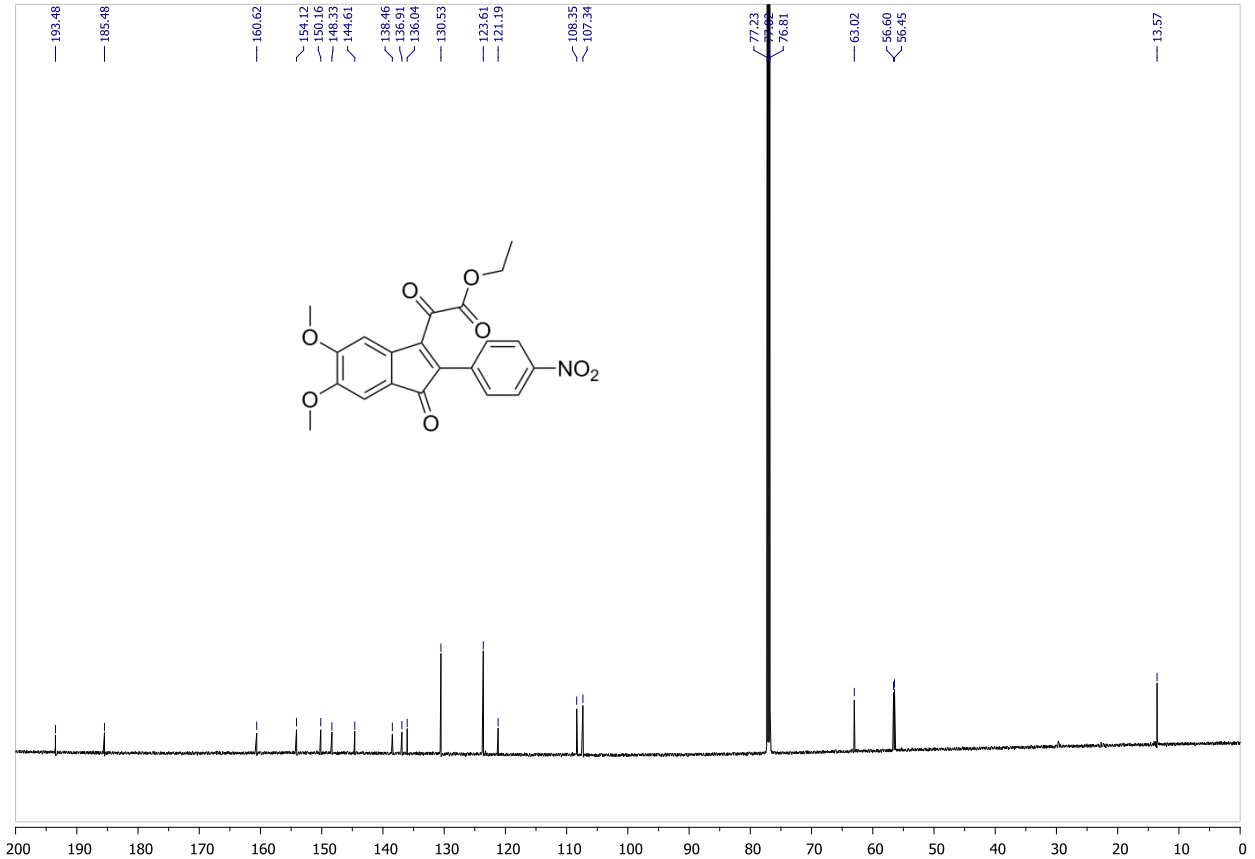

^{1}H-NMR: **2f**

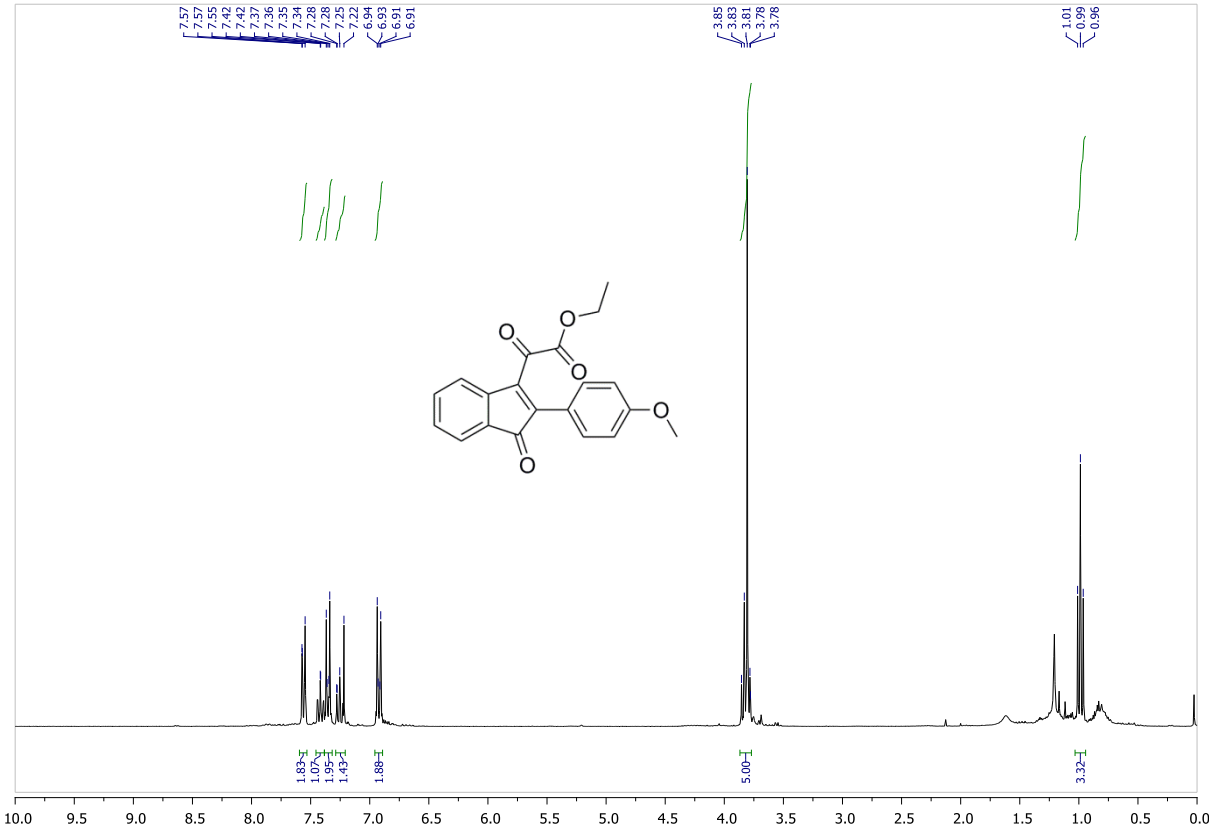

^{13}C-NMR: **2f**

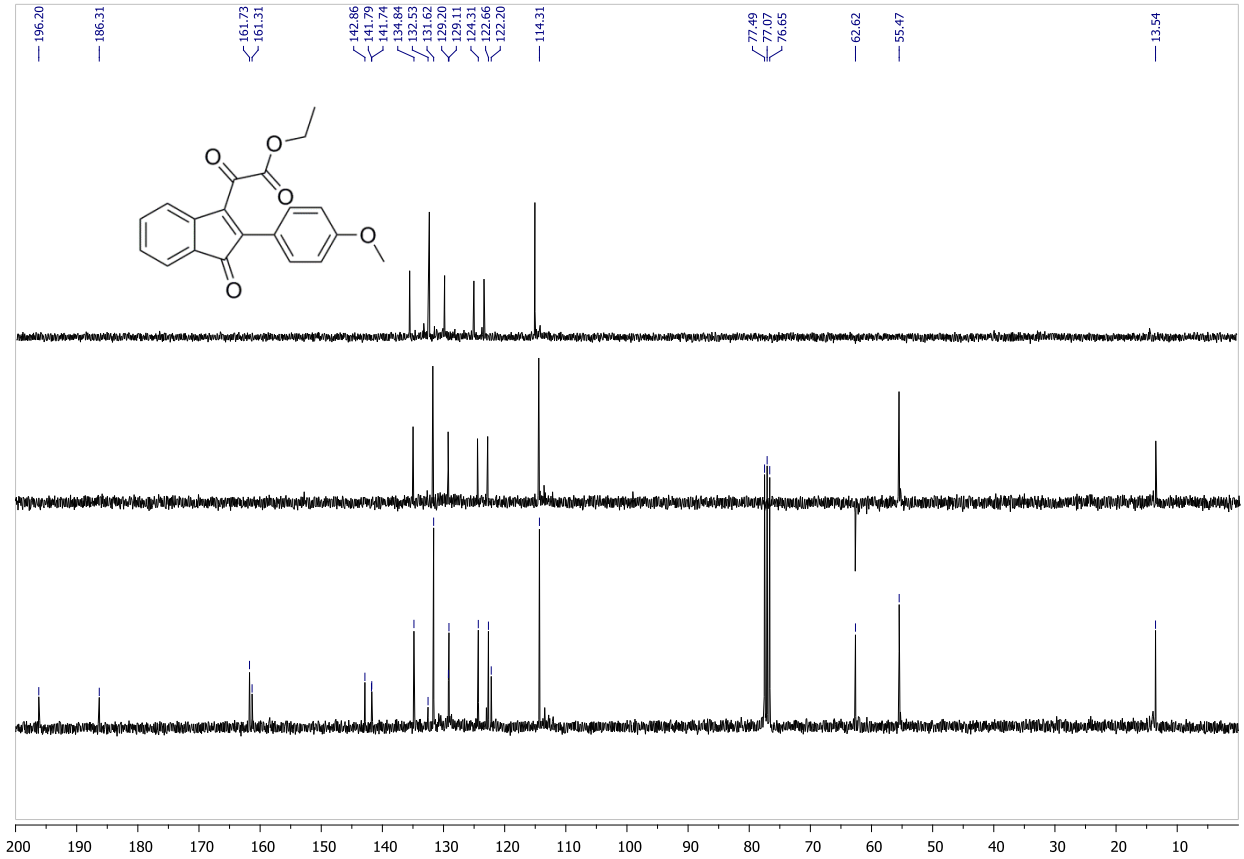

^{1}H-NMR: **2g**

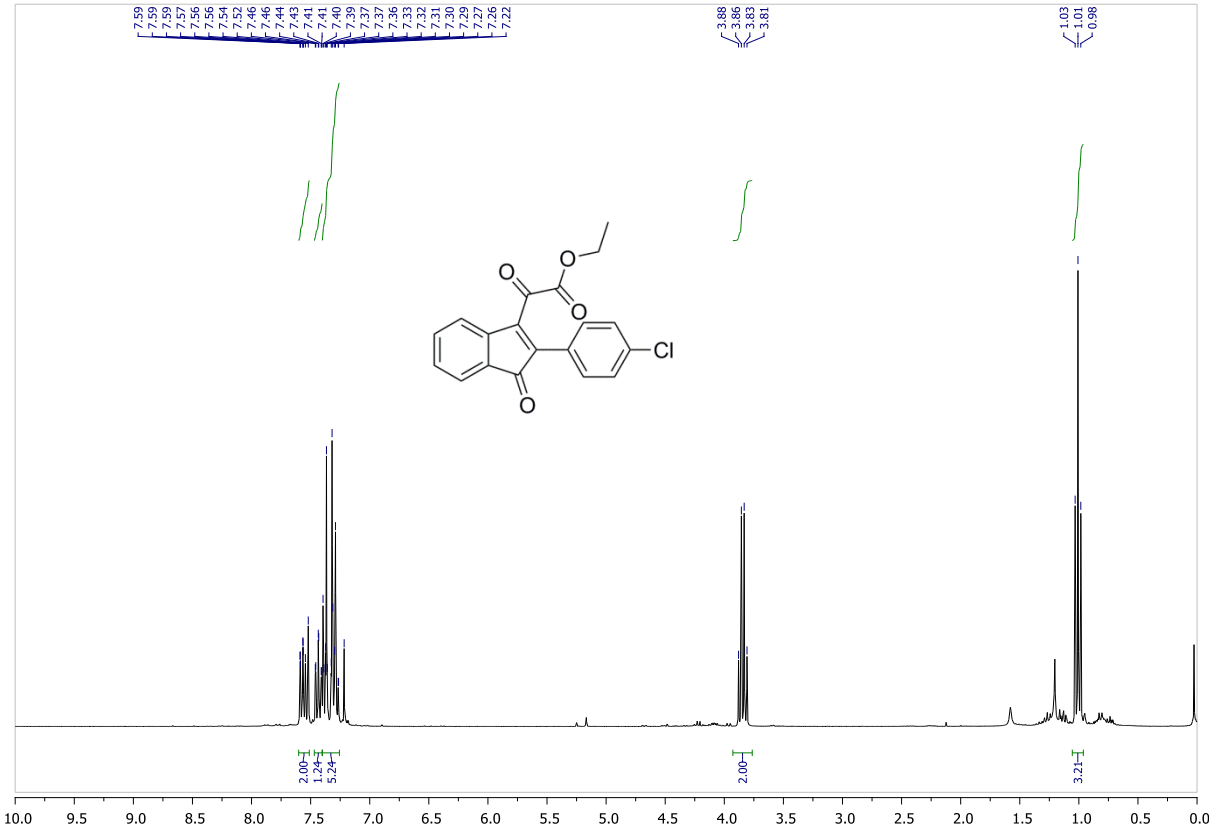

^{13}C-NMR**: 2g**

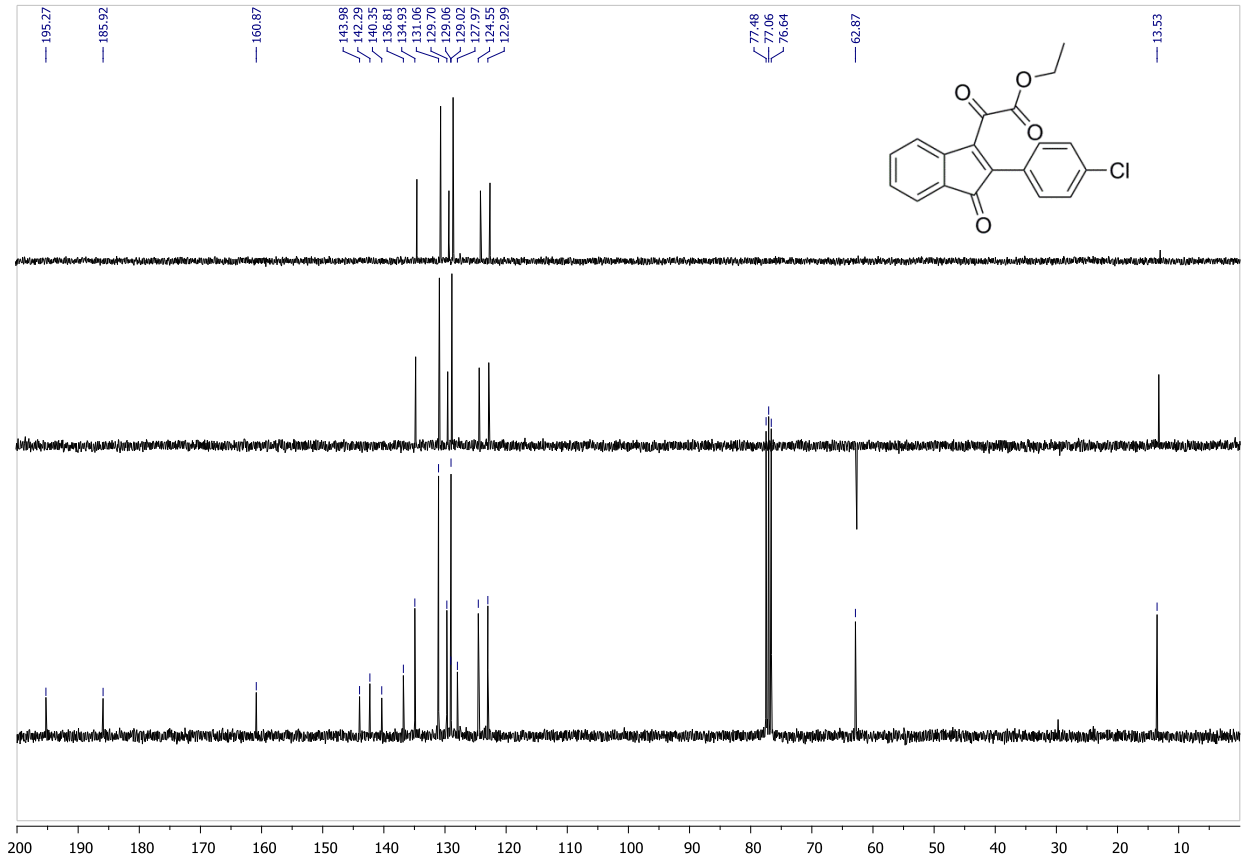

^{1}H-NMR**: 2h**

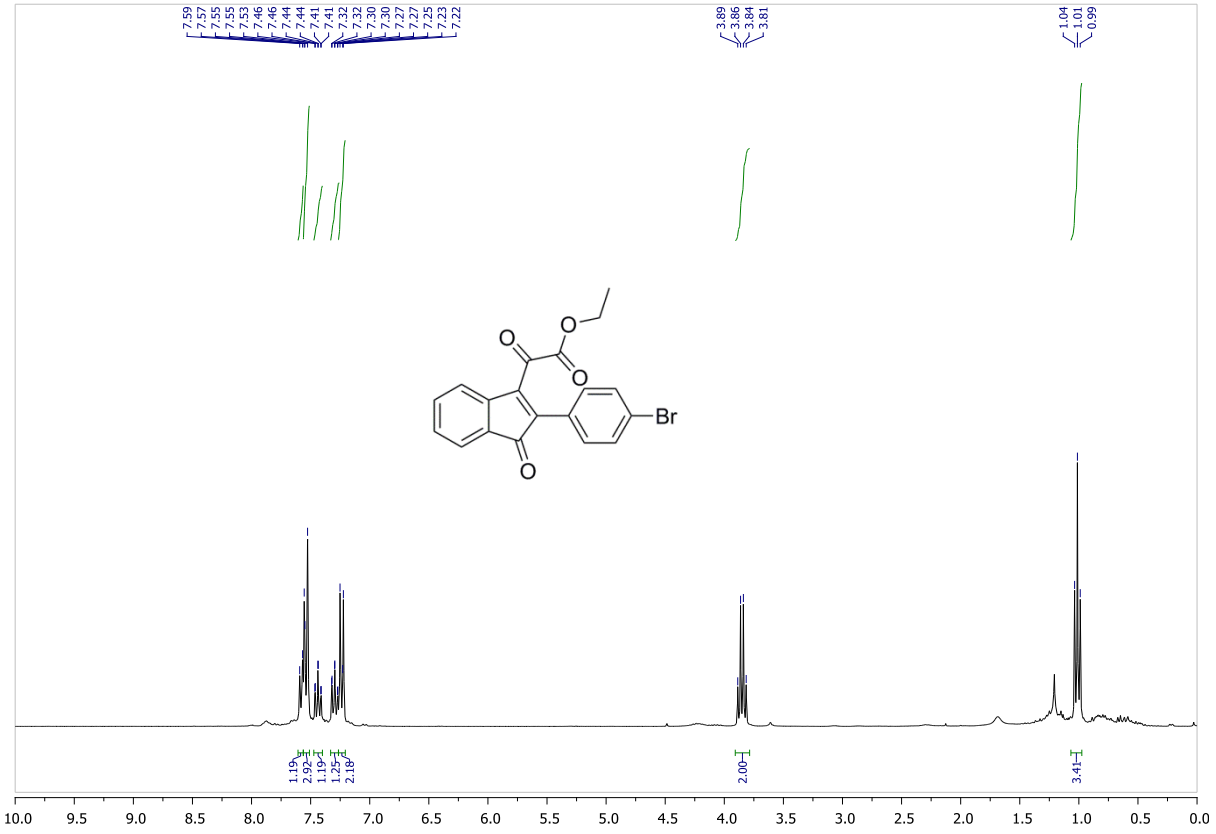

^{13}C-NMR: **2h**

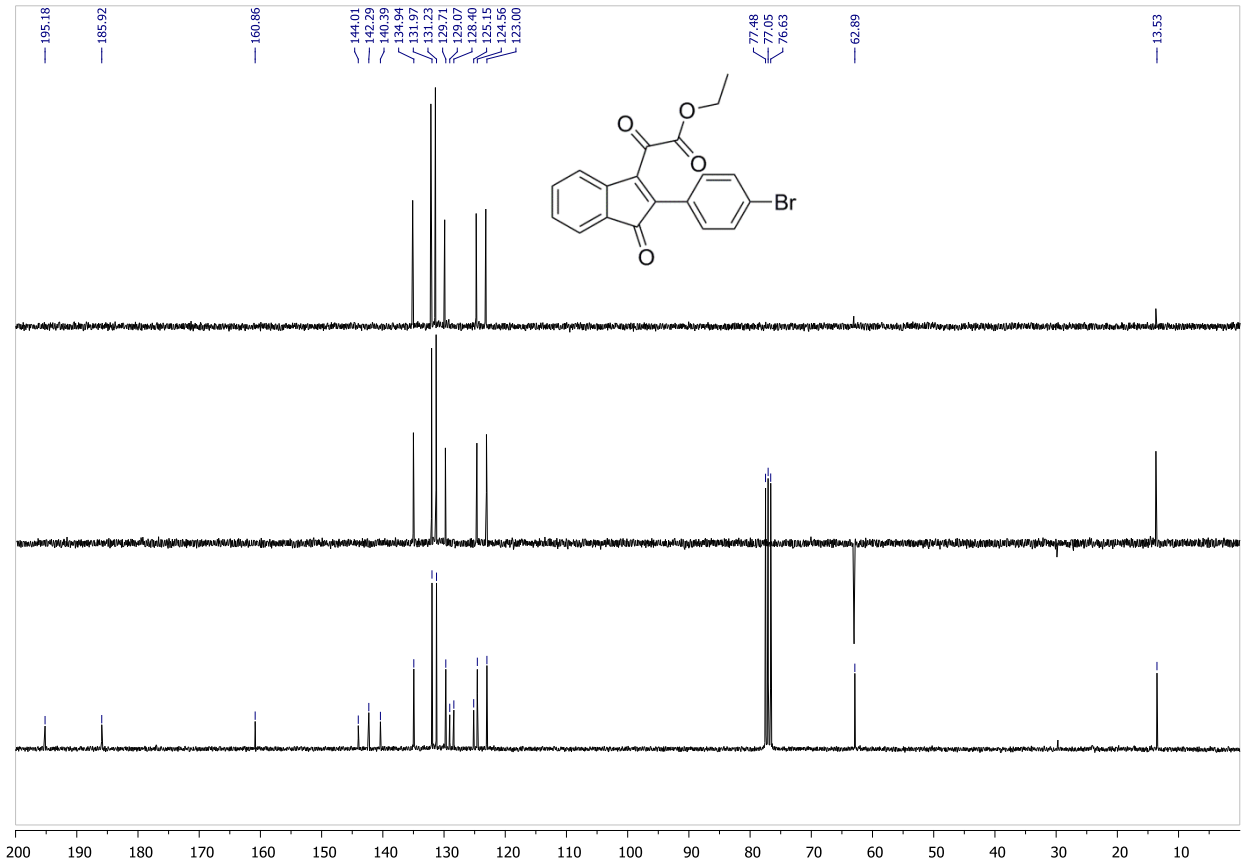

^{1}H-NMR: **2i**

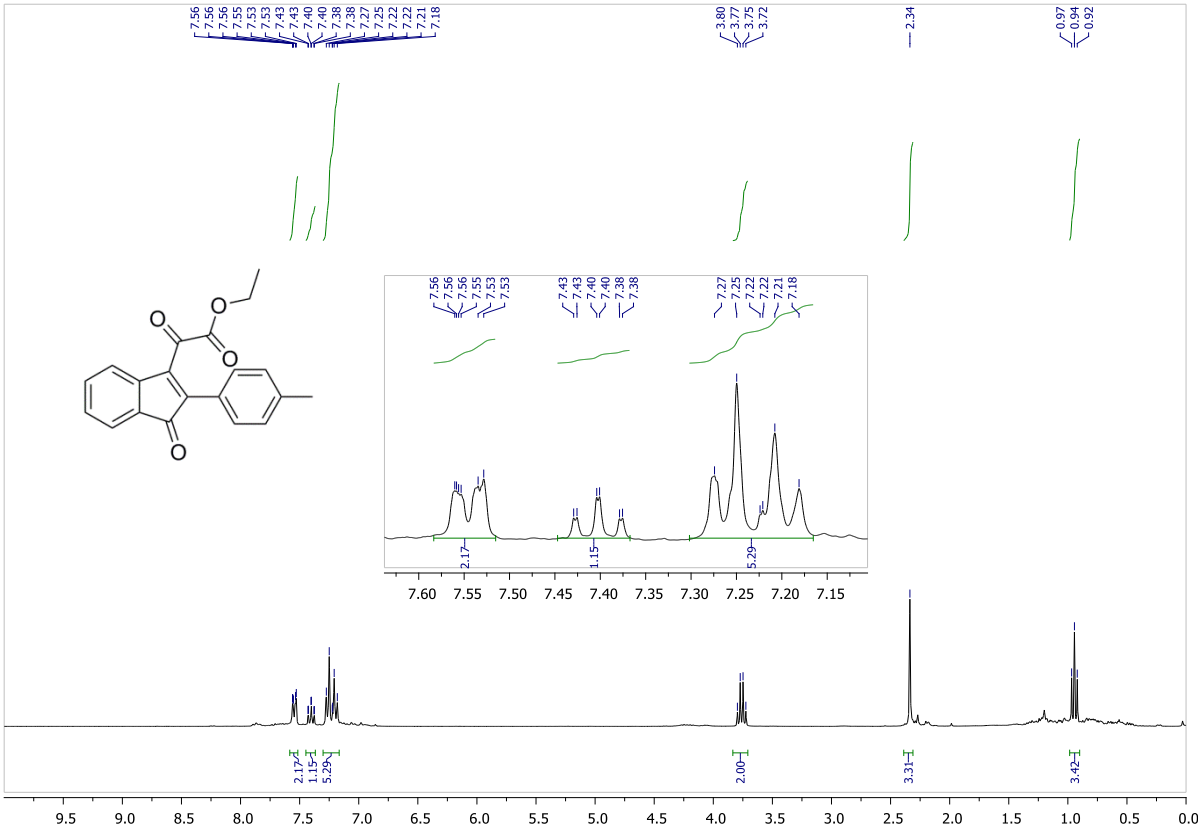

^{13}C-NMR: **2i**

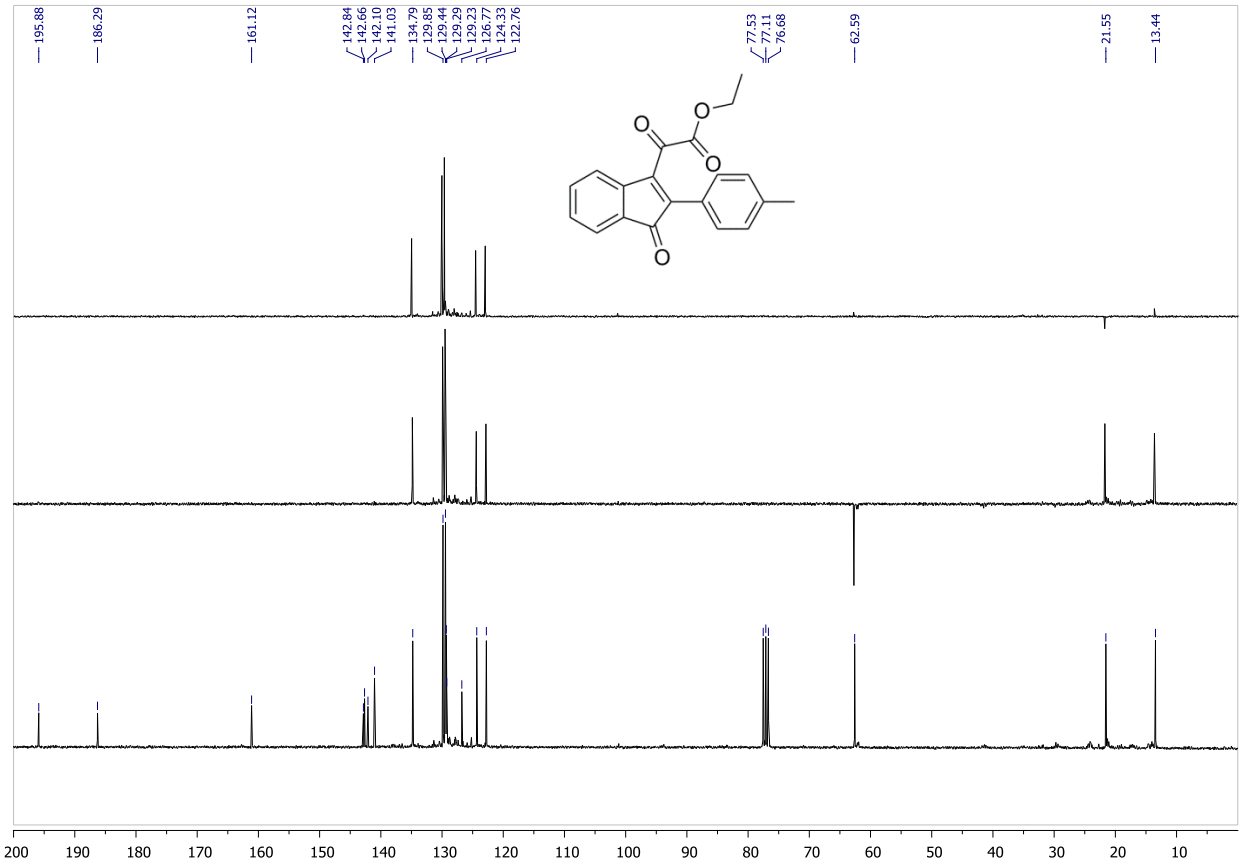

^{1}H-NMR: **2j**

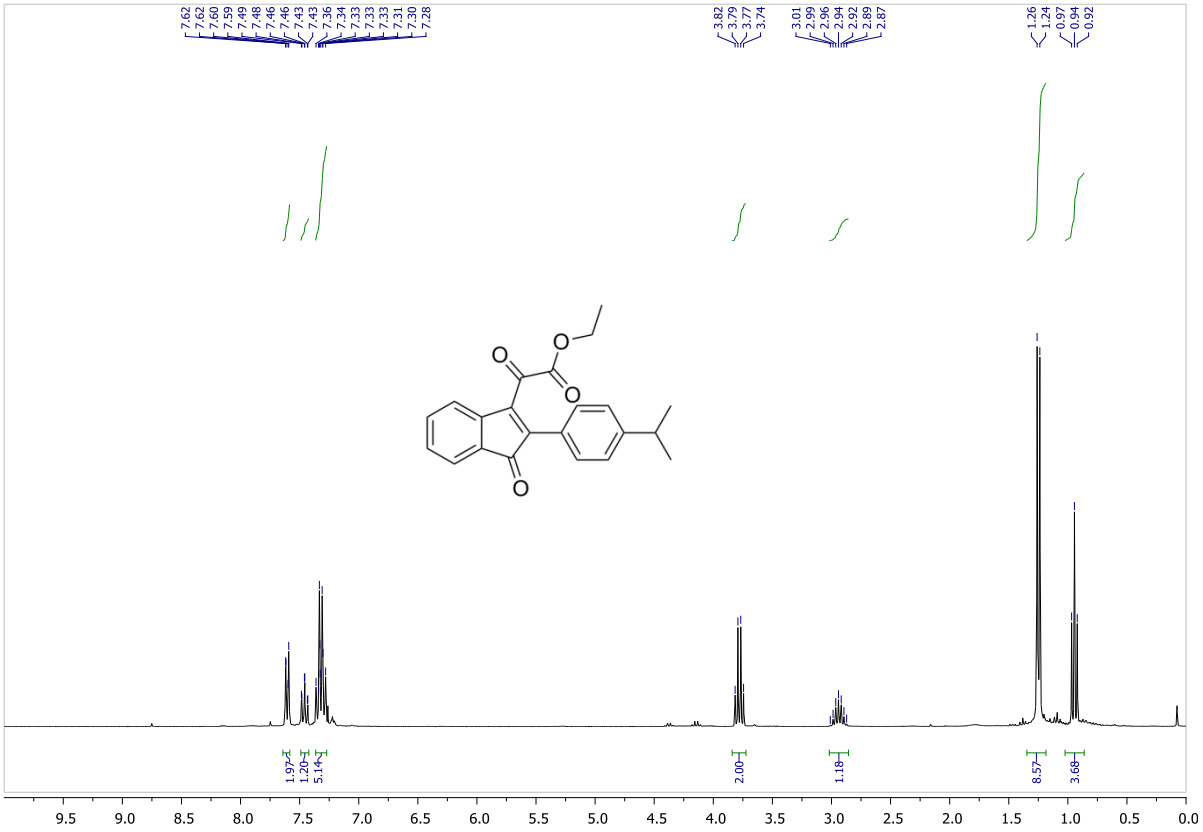

^{13}C-NMR: **2j**

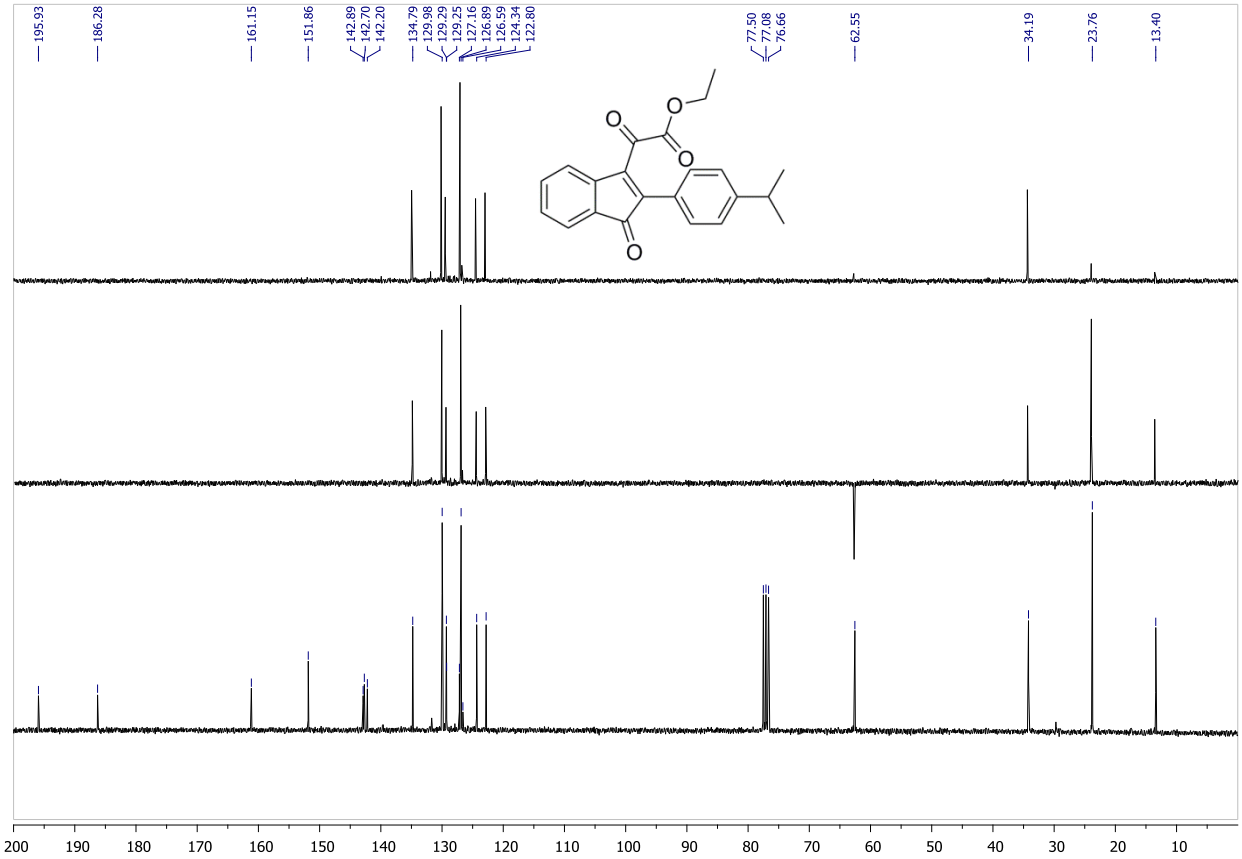

^{1}H-NMR: **2k**

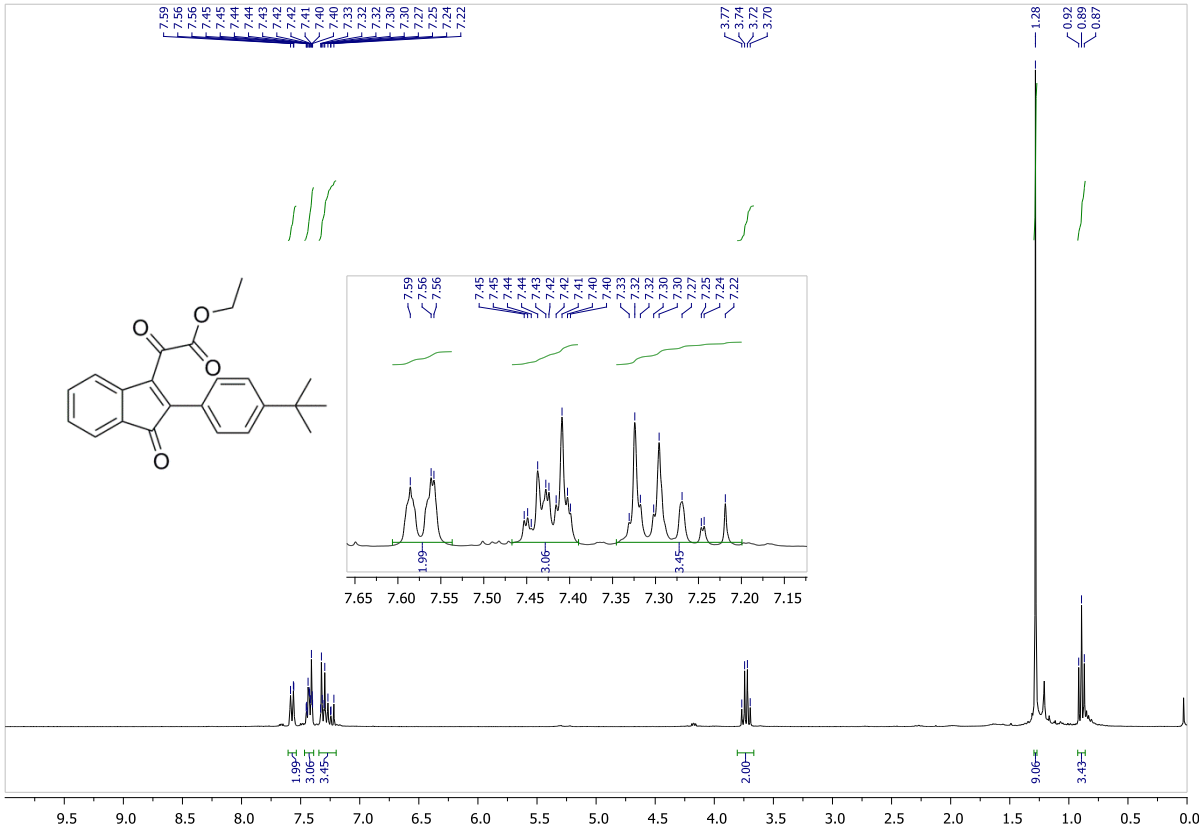

^{13}C-NMR: **2k**

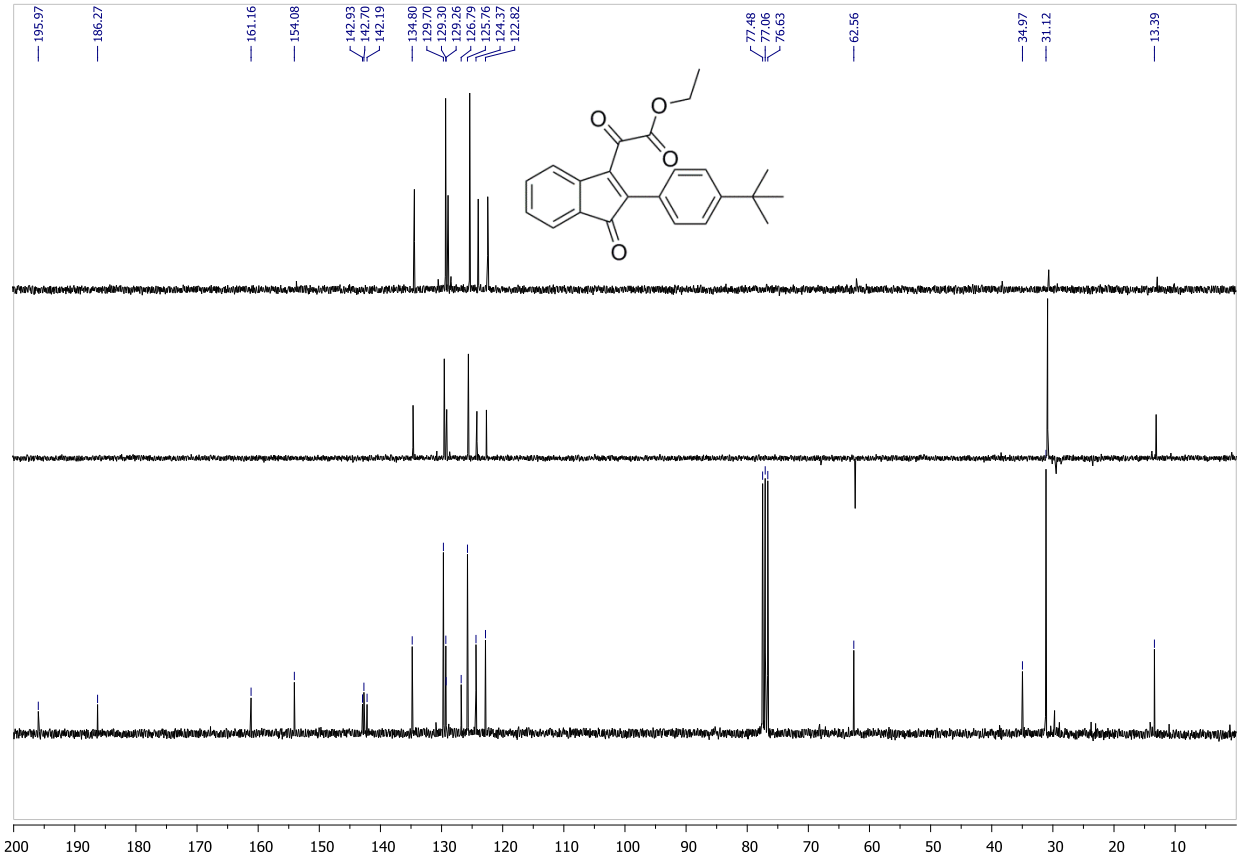

^{1}H-NMR: **2l**

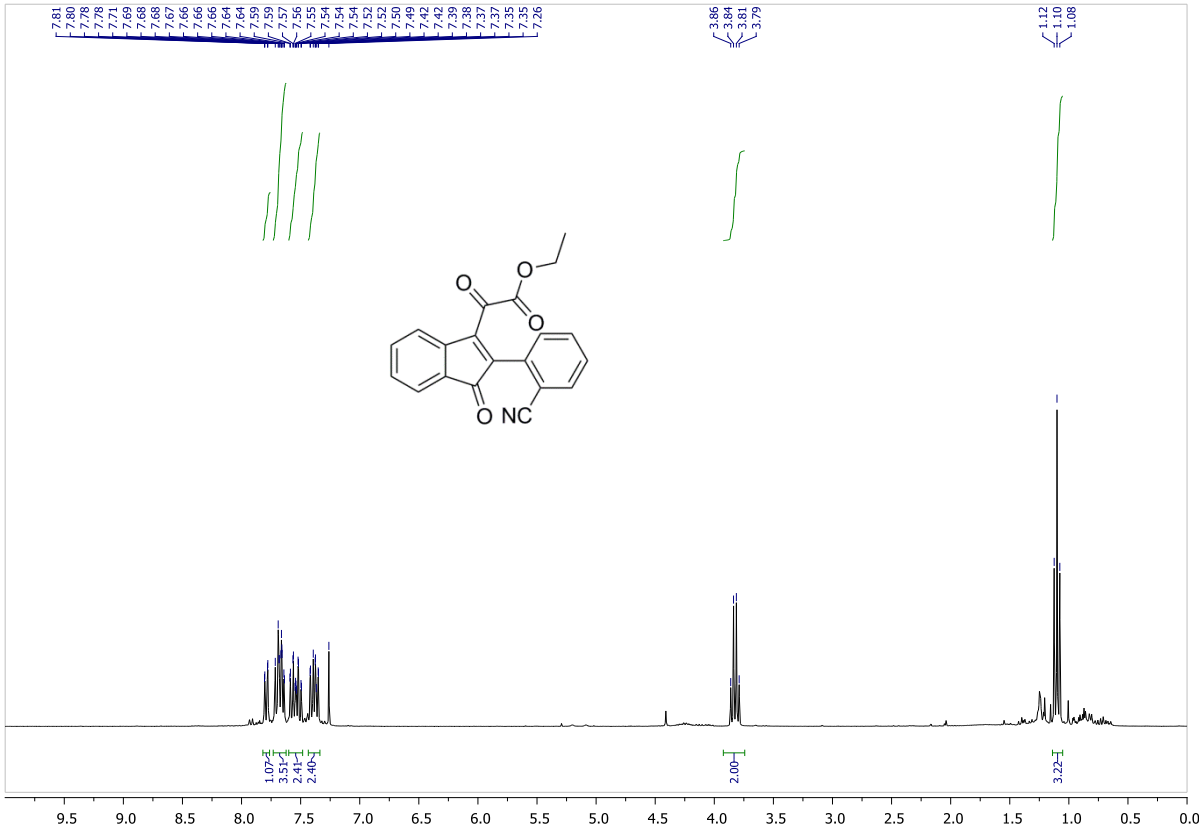

^{13}C-NMR: **2l**

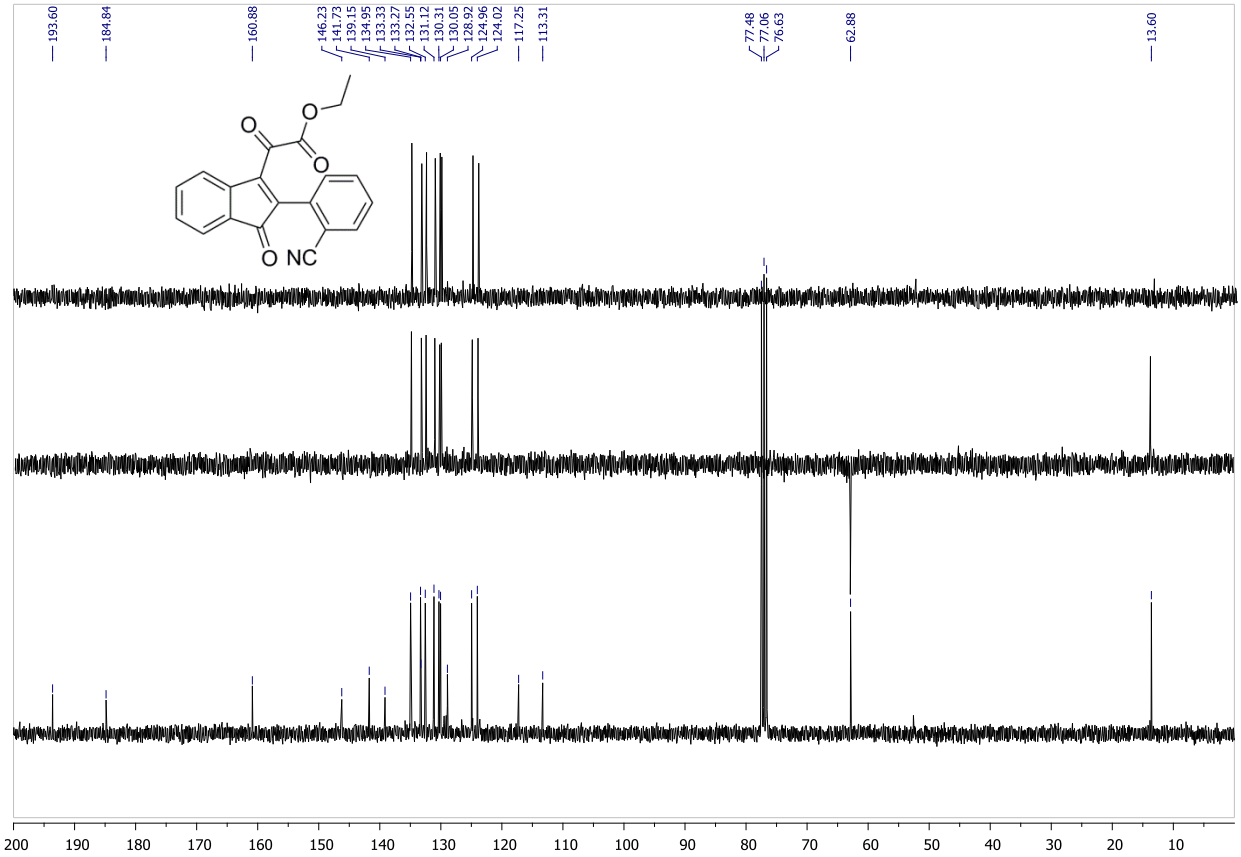

^{1}H-NMR: **2m**

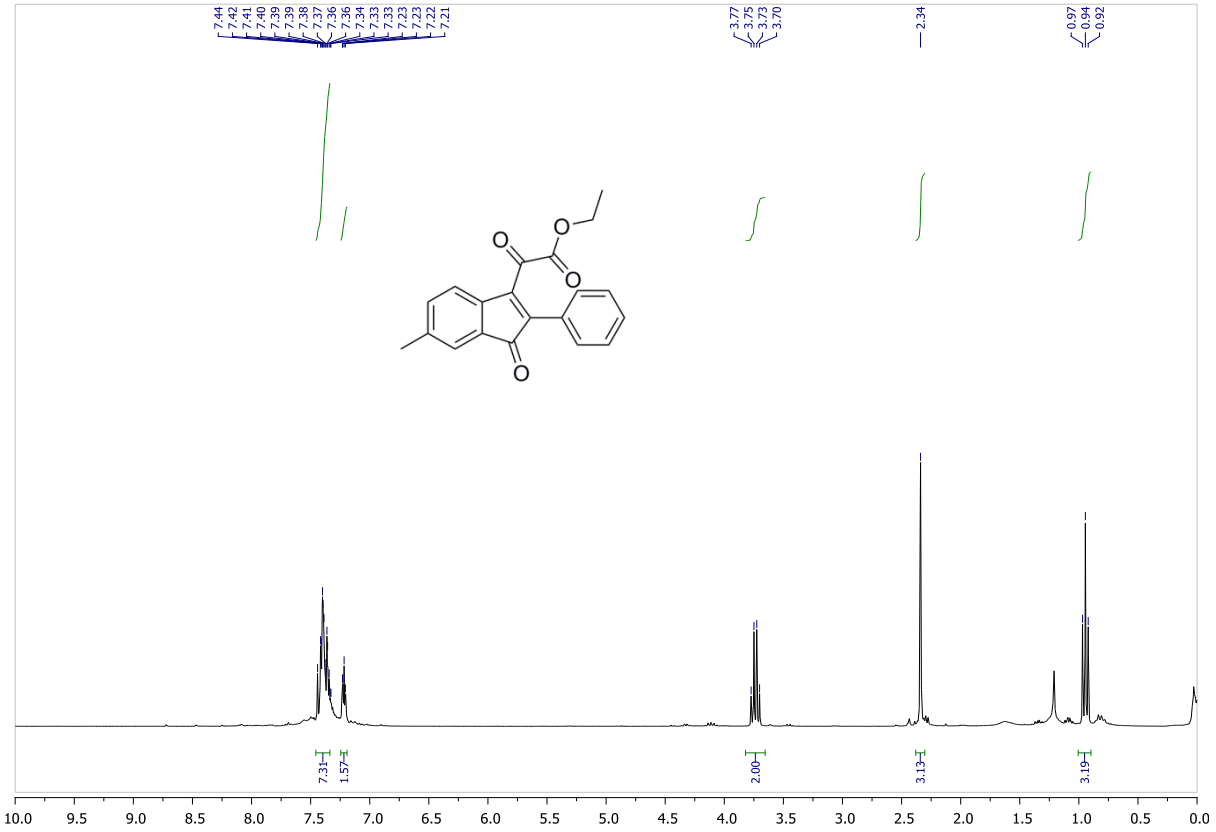

^{13}C-NMR: **2m**

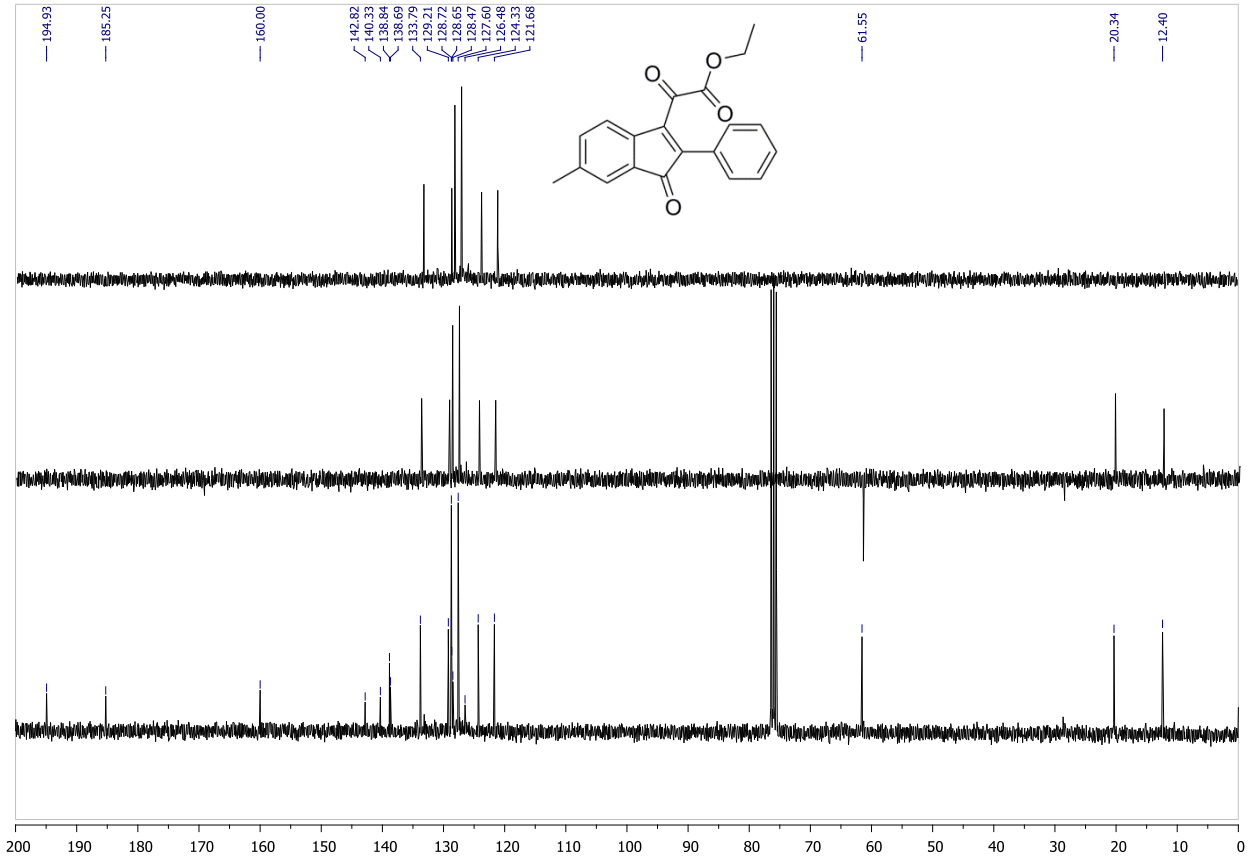

^{1}H-NMR: **2n**

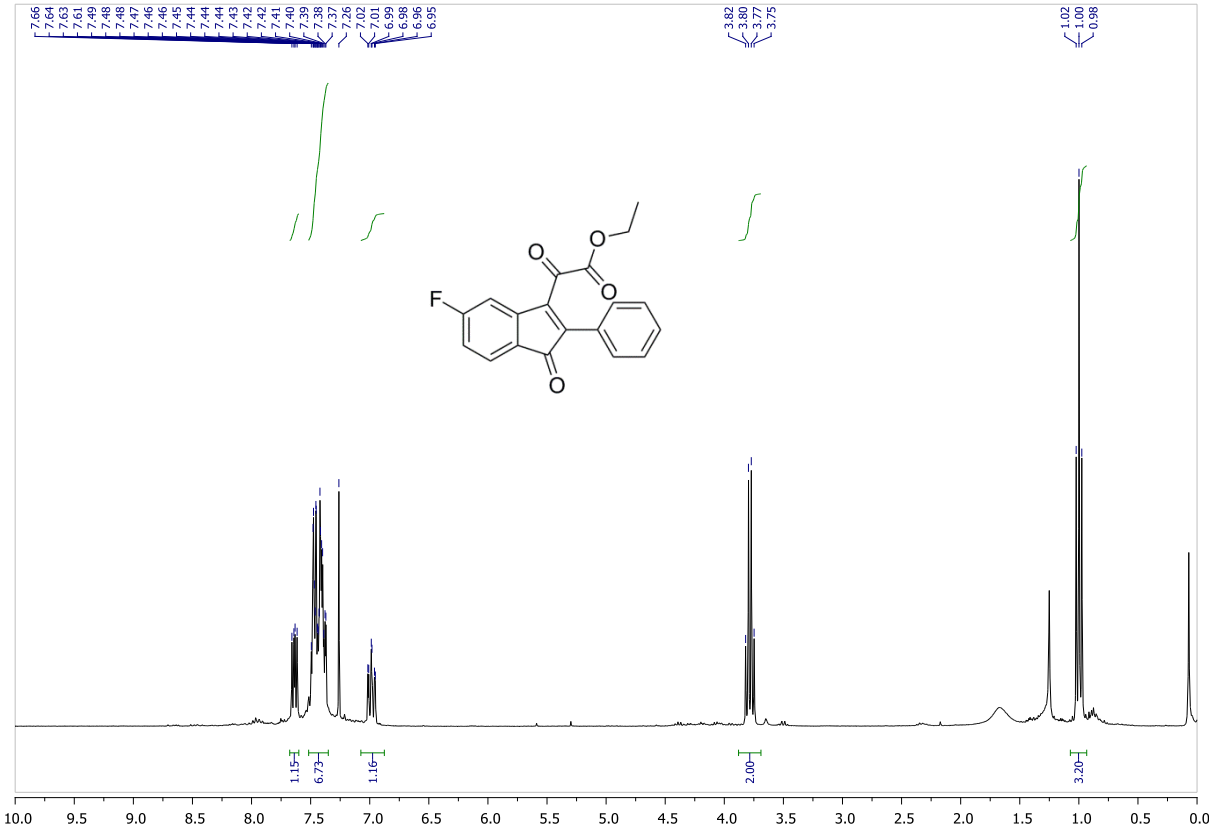

^{13}C-NMR: **2n**

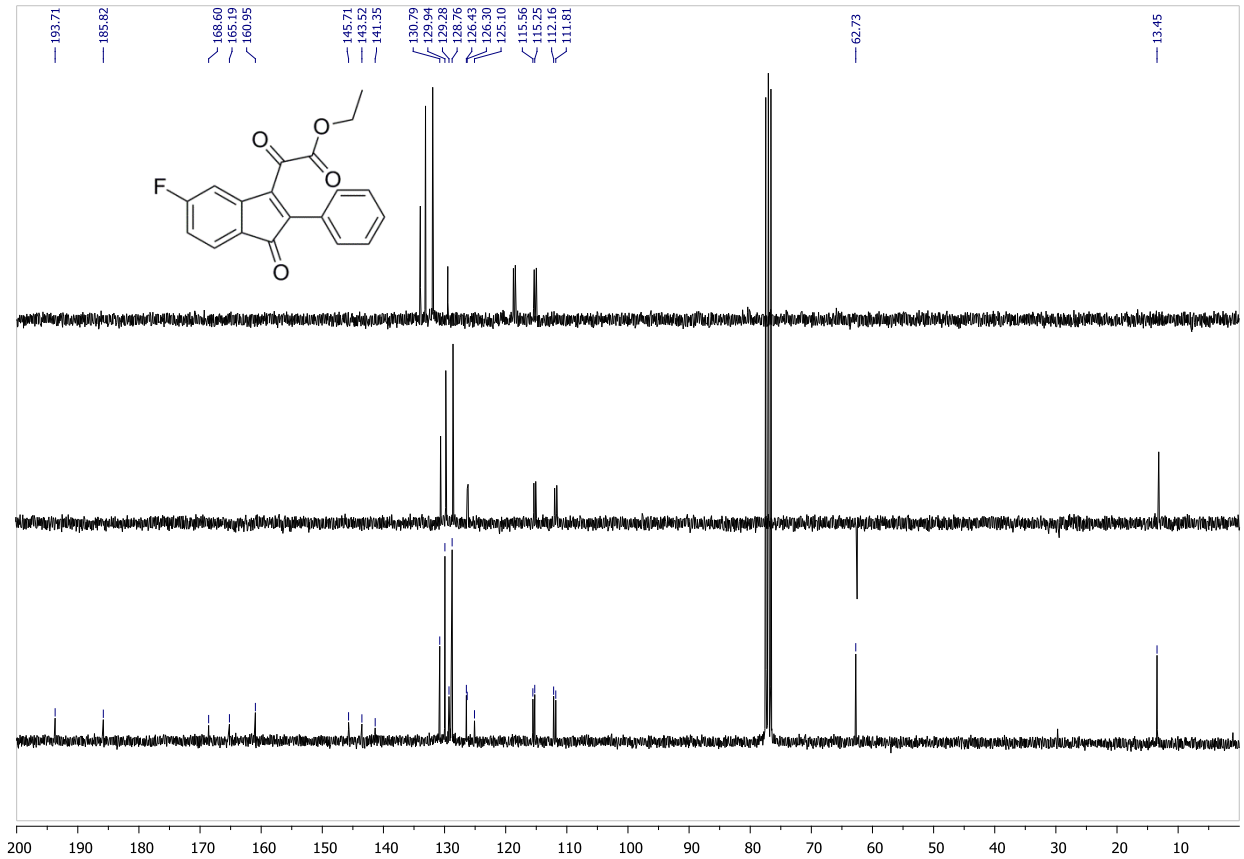

^{19}F-NMR: **2n**

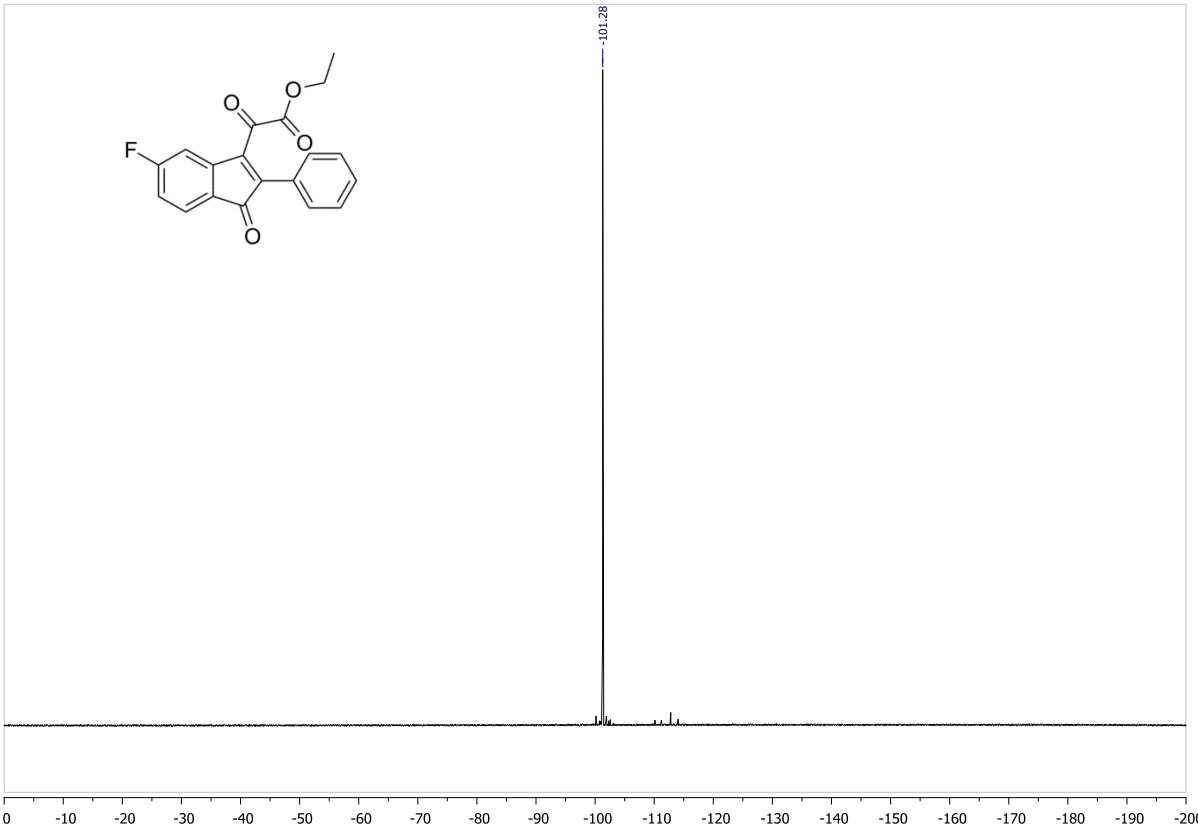
-101.28
F
O
O
O
O
0
-10
-20
-30
-40
-50
-60
-70
-80
-90
-100
-110
-120
-130
-140
-150
-160
-170
-180
-190

^{1}H-NMR: **3a**

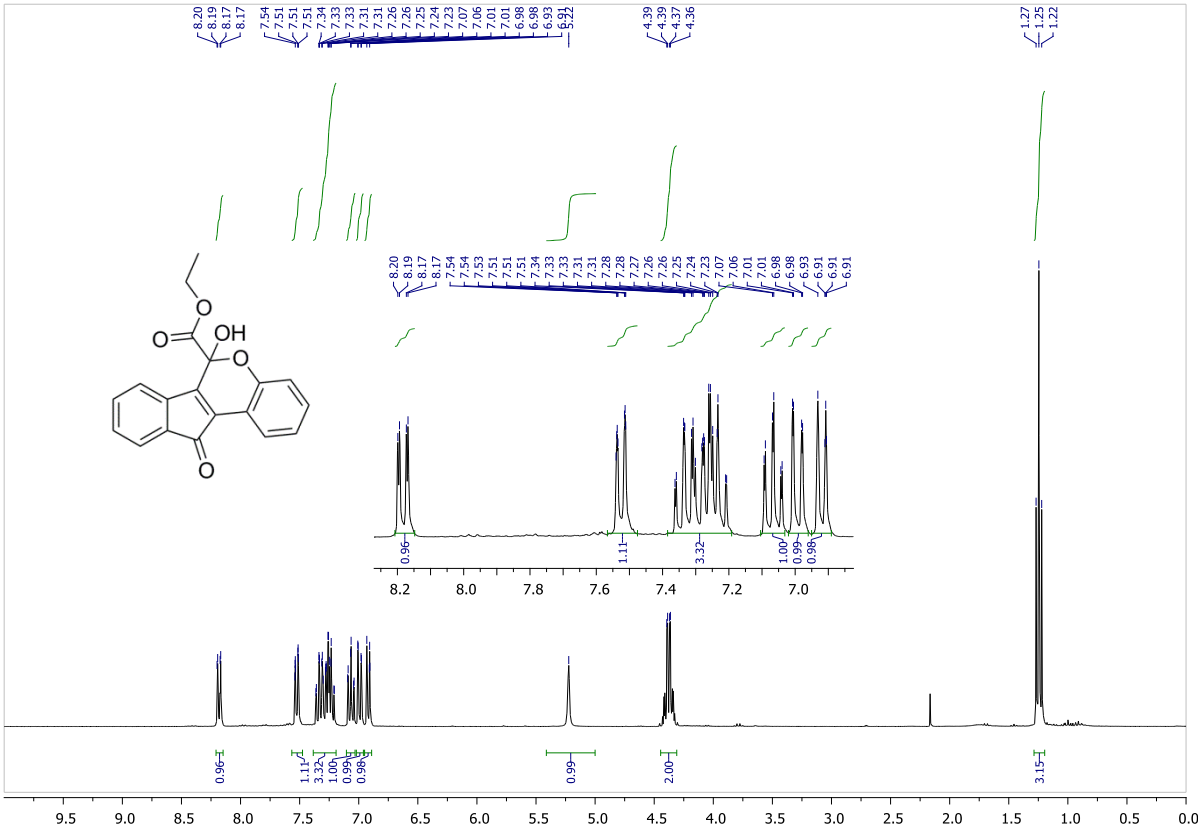

^{13}C-NMR: **3a**

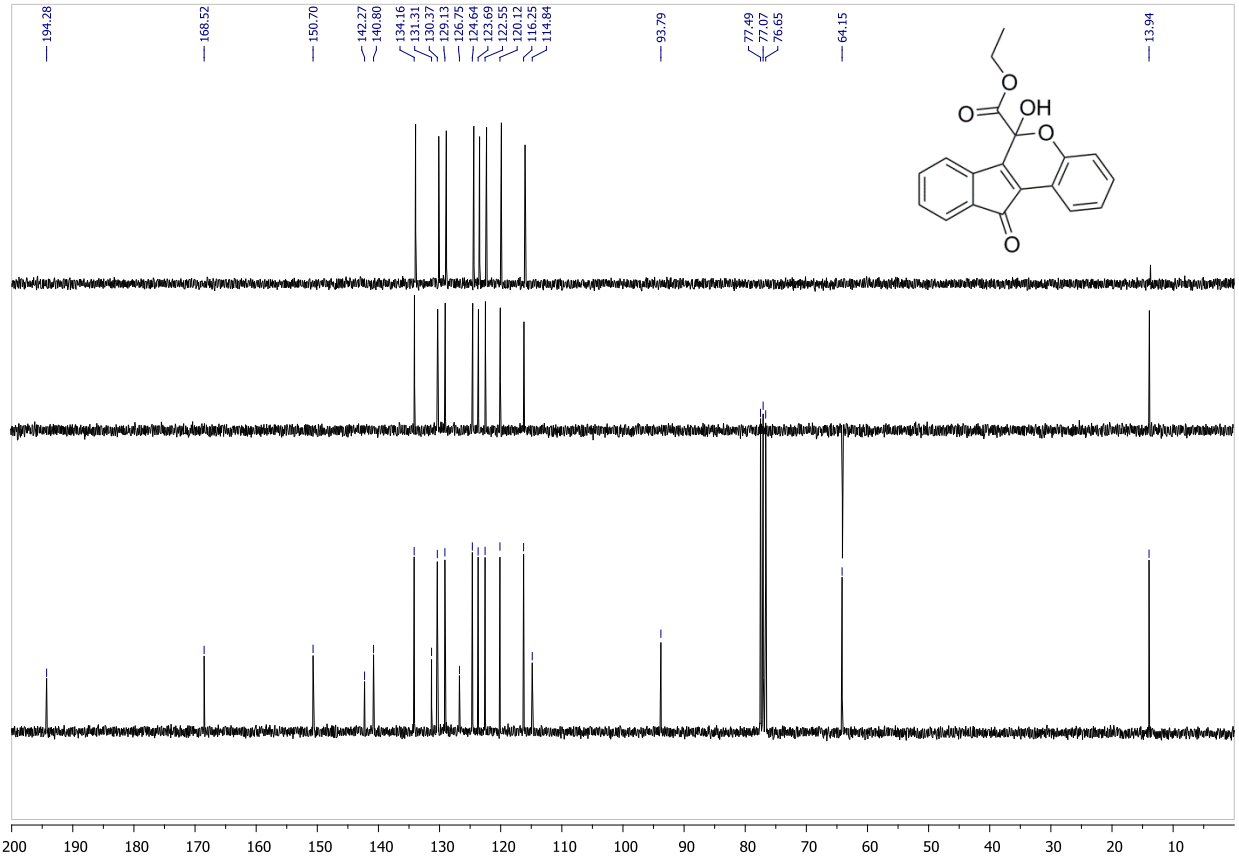

^{1}H-NMR: **3b**

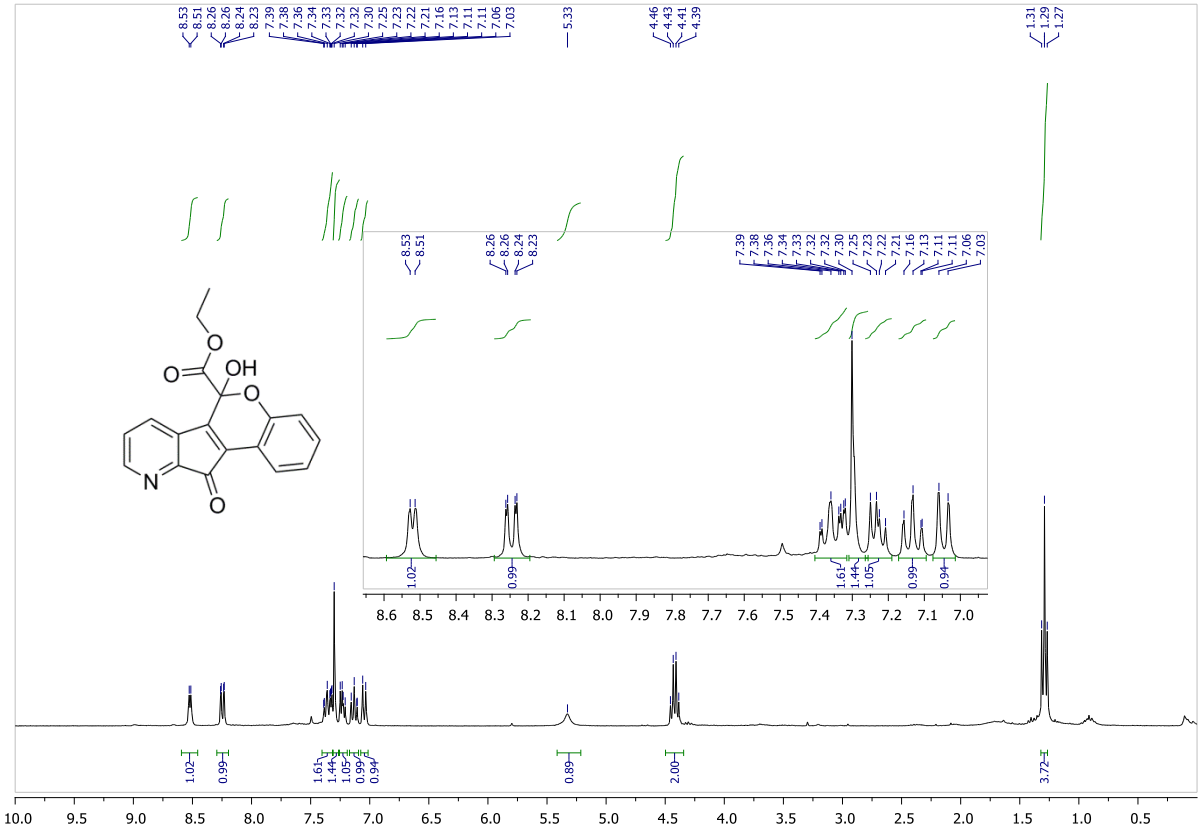

^{13}C-NMR: **3b**

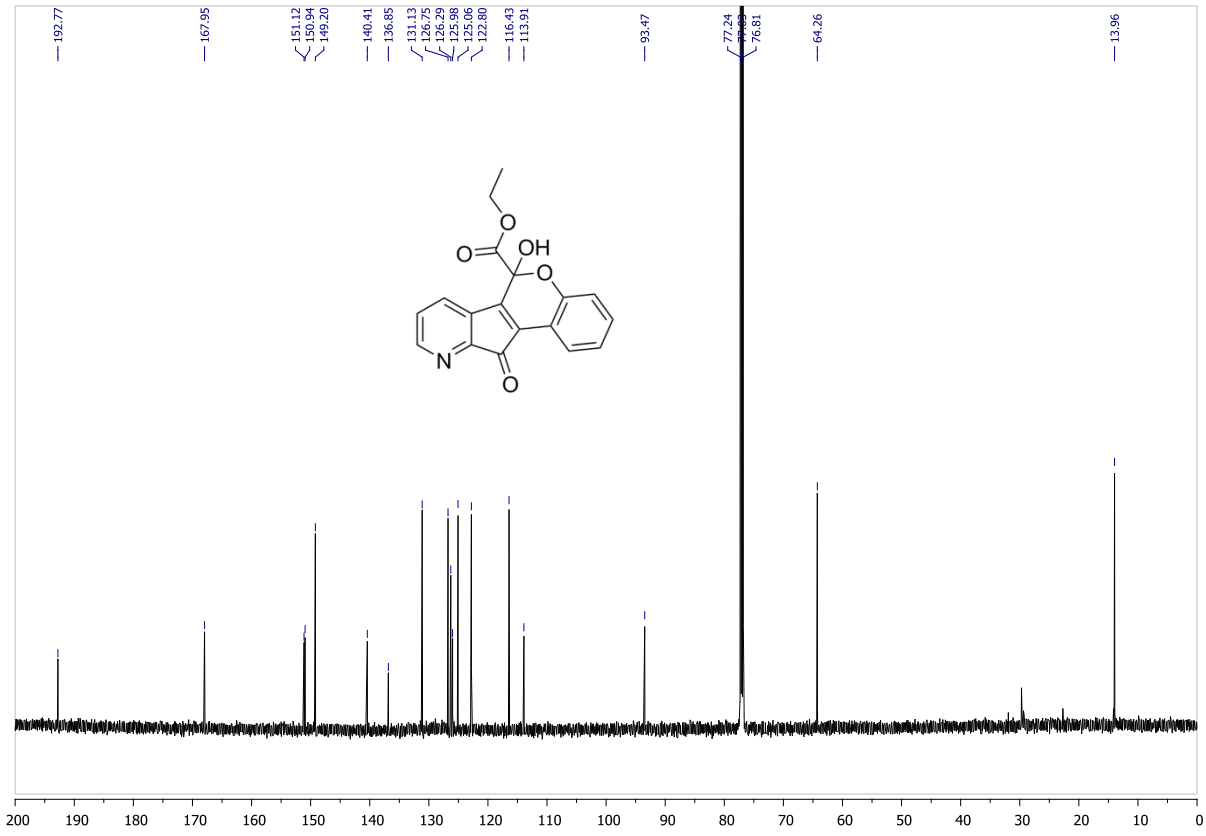

^{1}H-NMR: **3c**

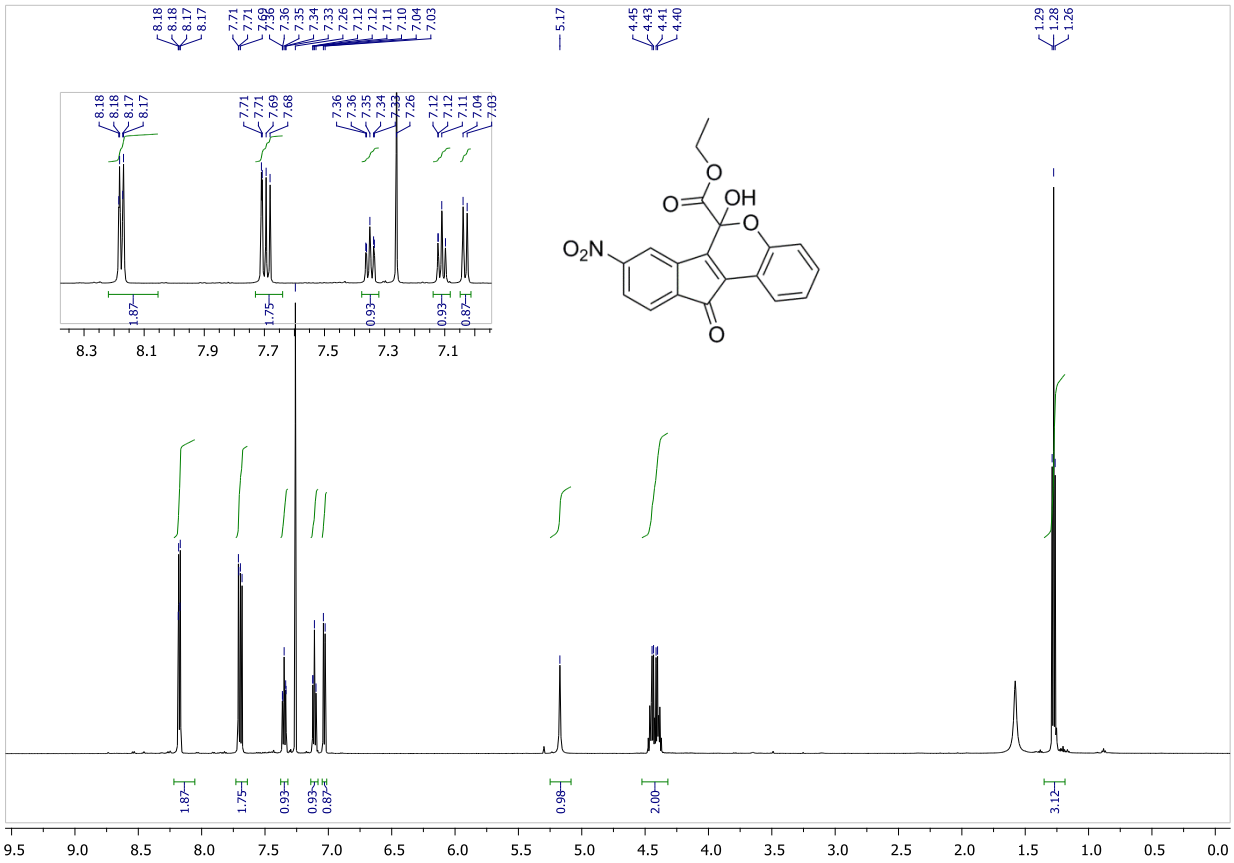

^{13}C-NMR: **3c**

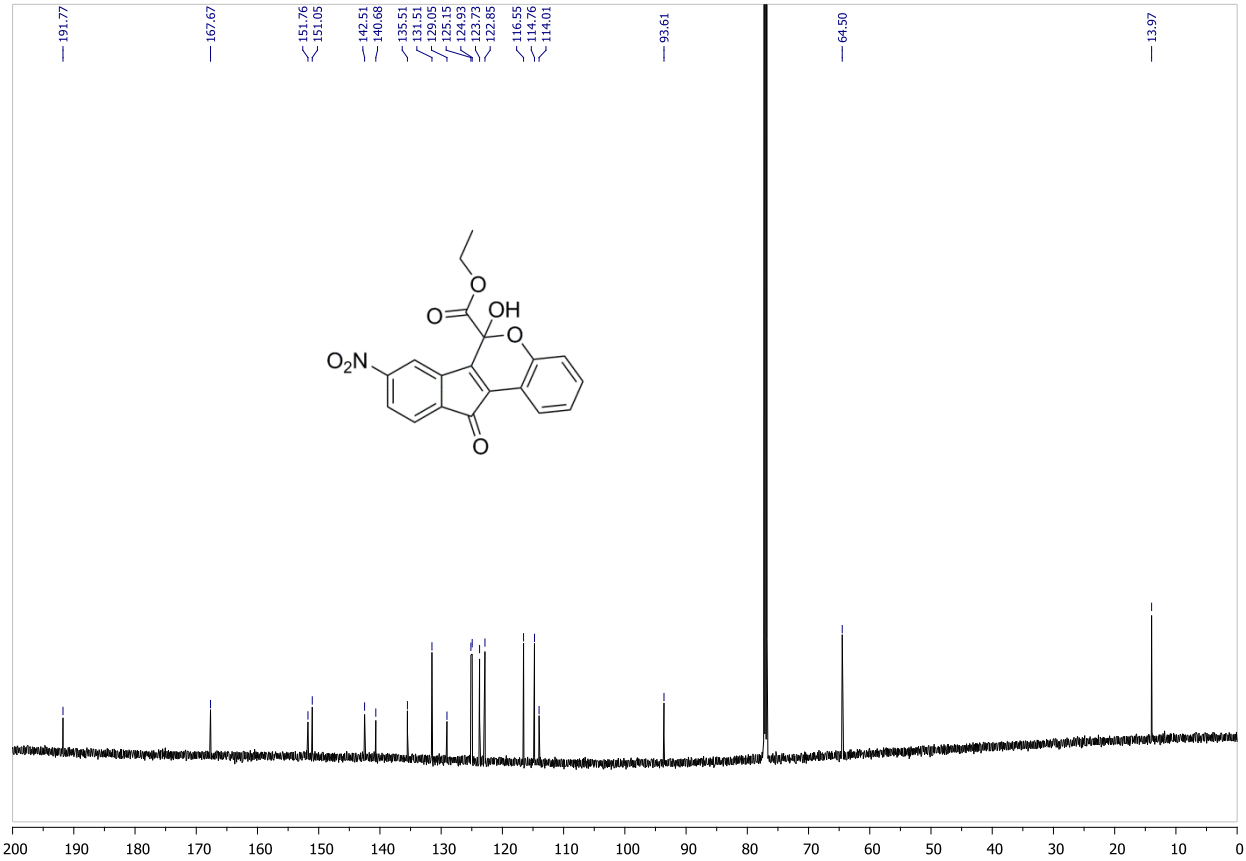

^{1}H-NMR: **3d**

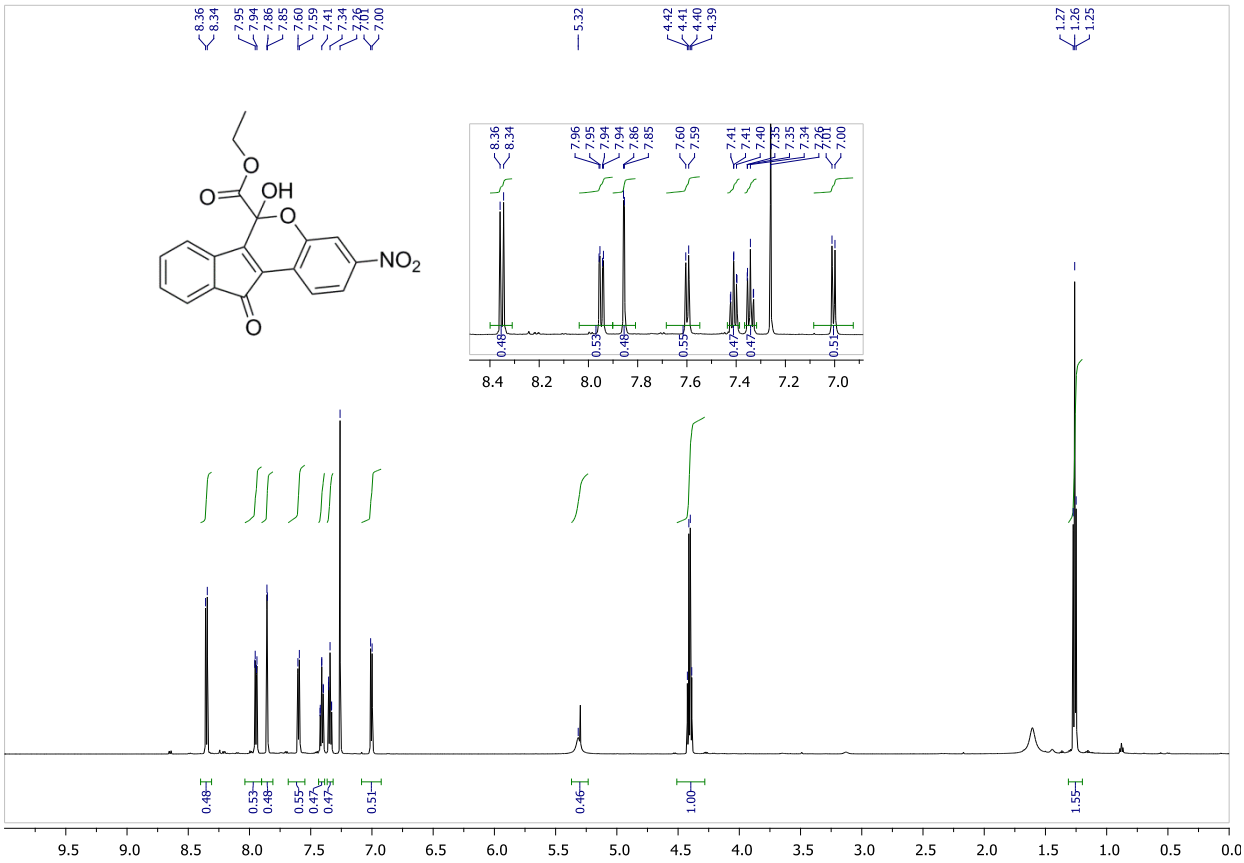

^{13}C-NMR: **3d**

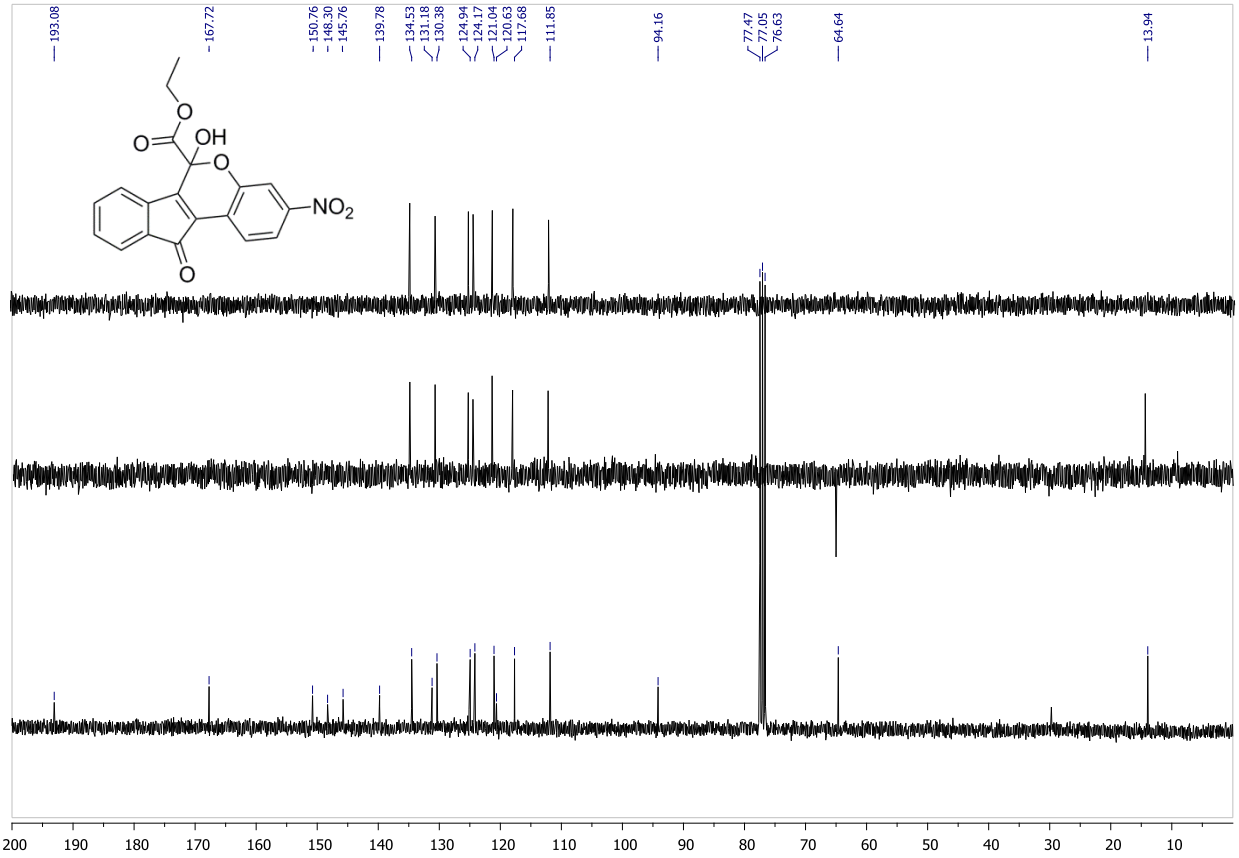

^{1}H-NMR: **3e**

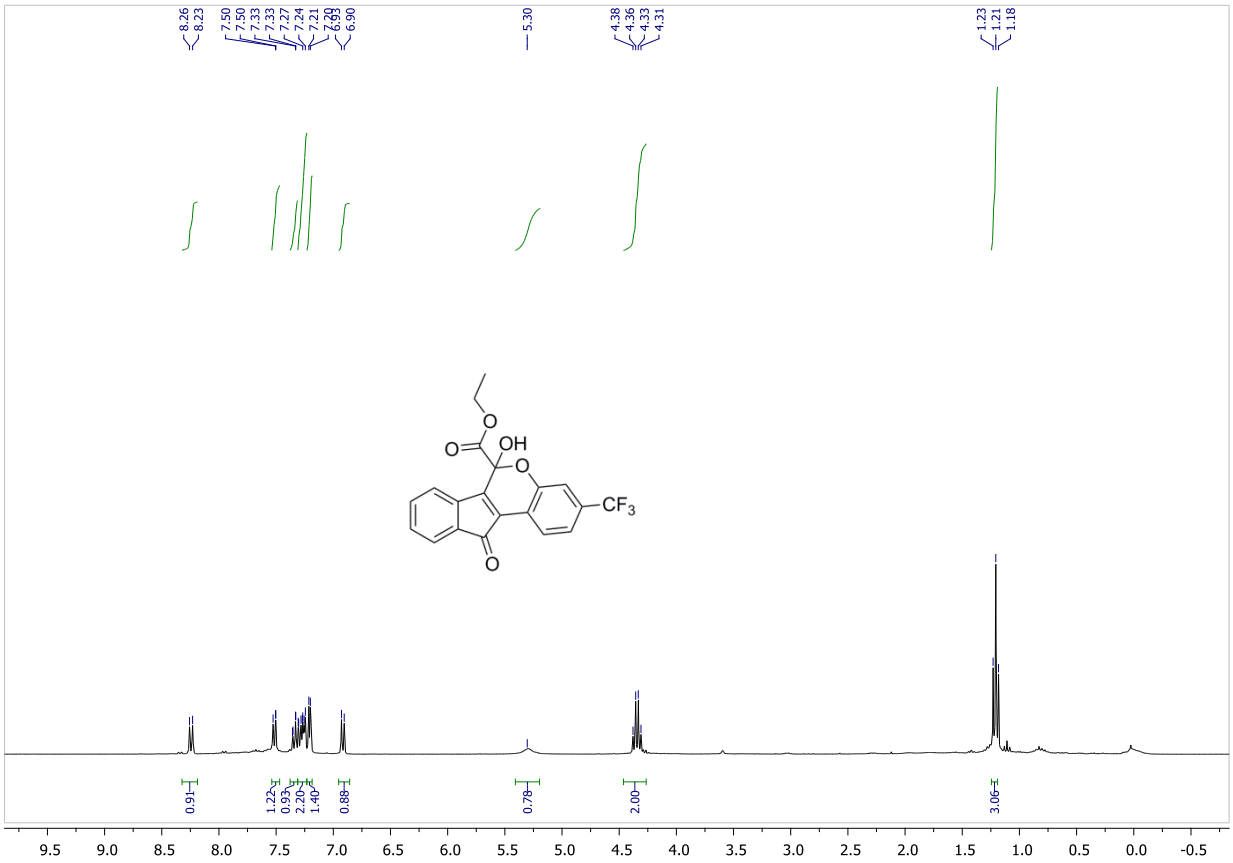

^{13}C-NMR: **3e**

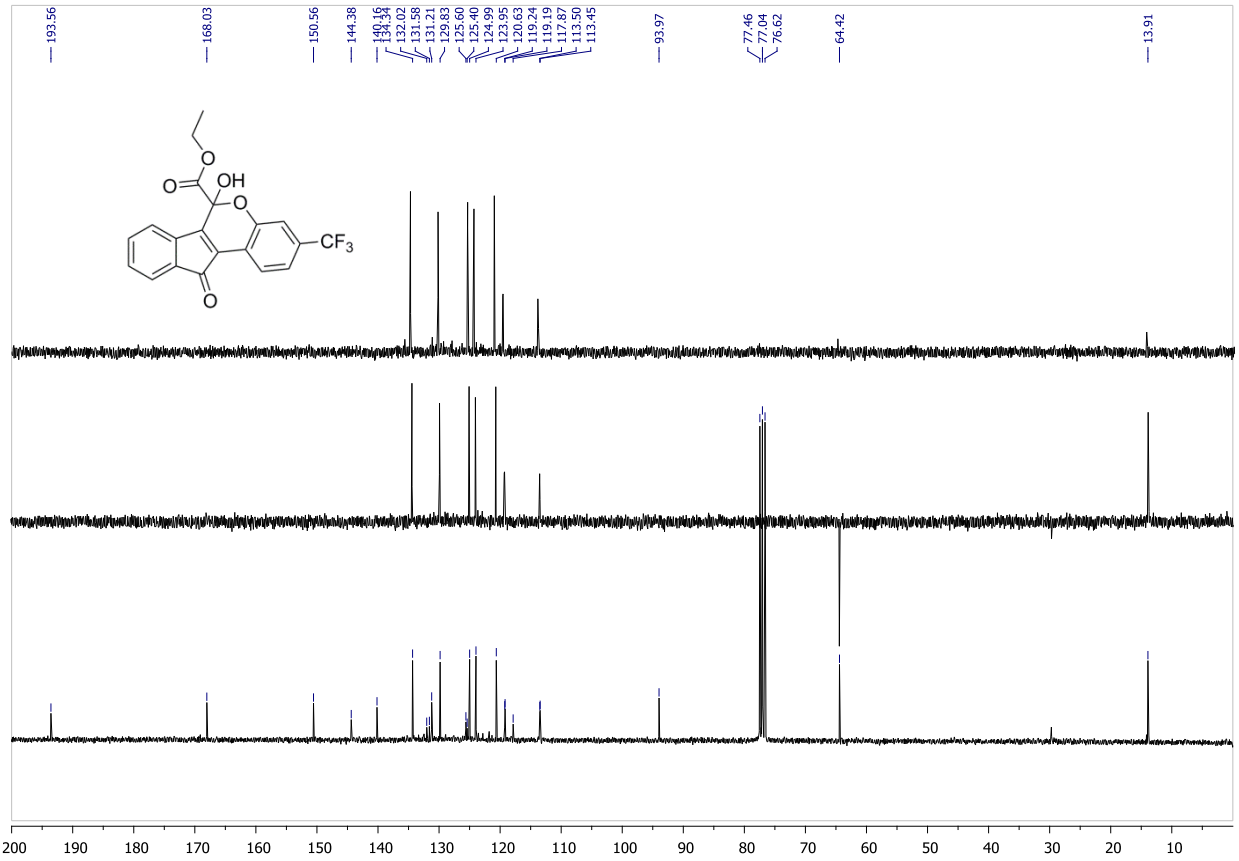

^{19}F-NMR: **3e**

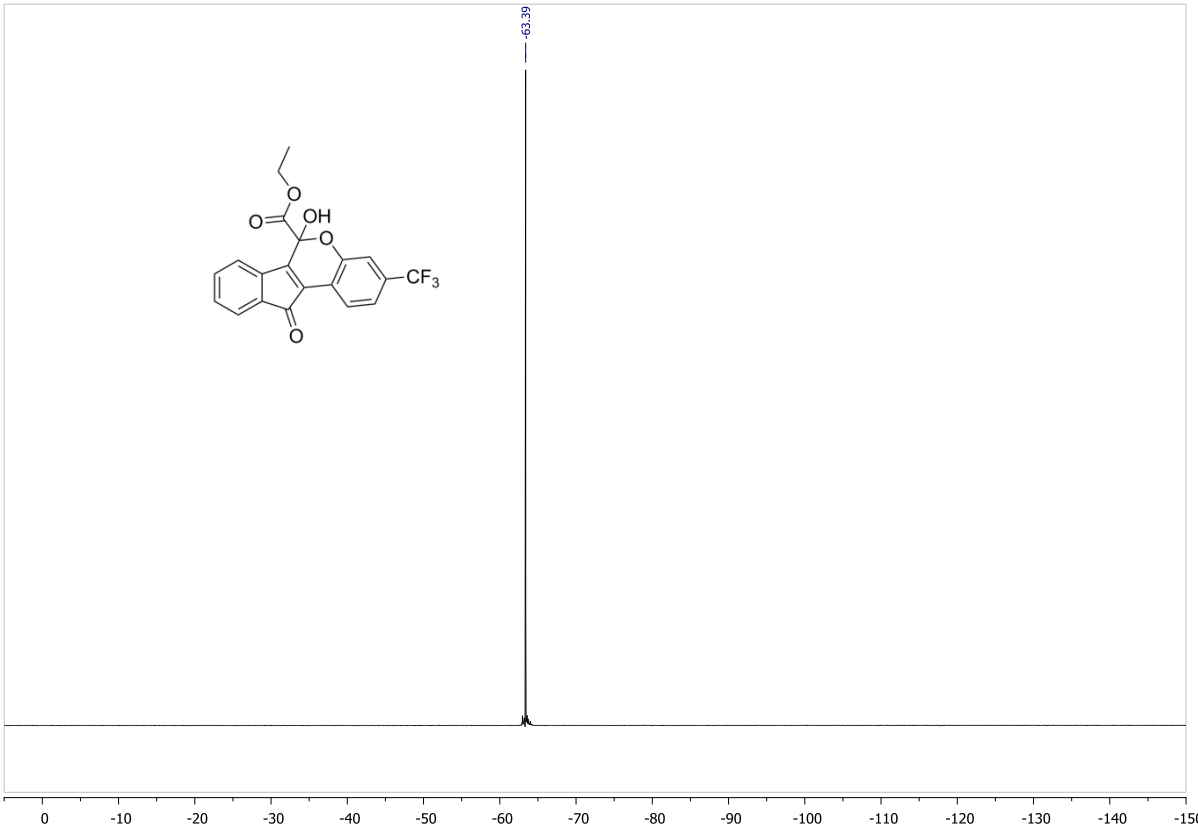

^{1}H-NMR: **3f**

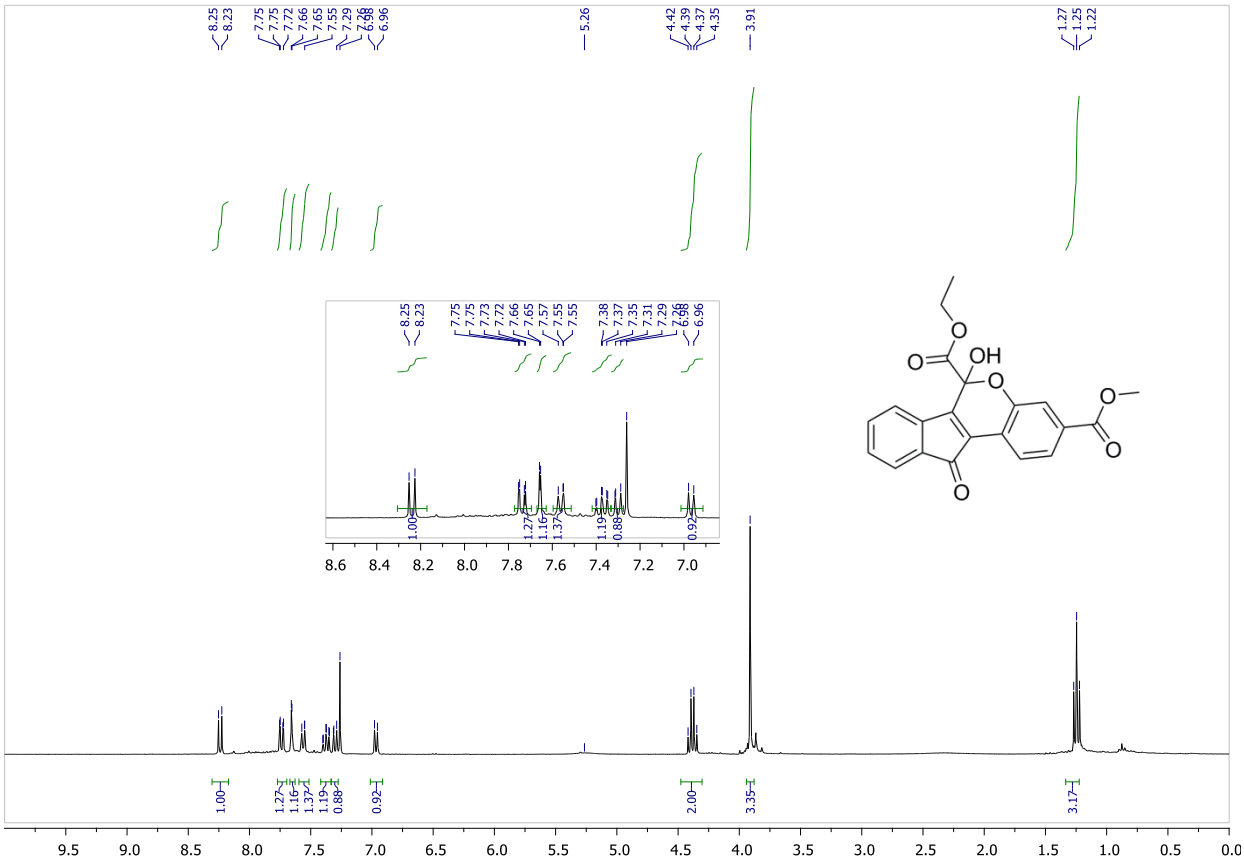

^{13}C-NMR: **3f**

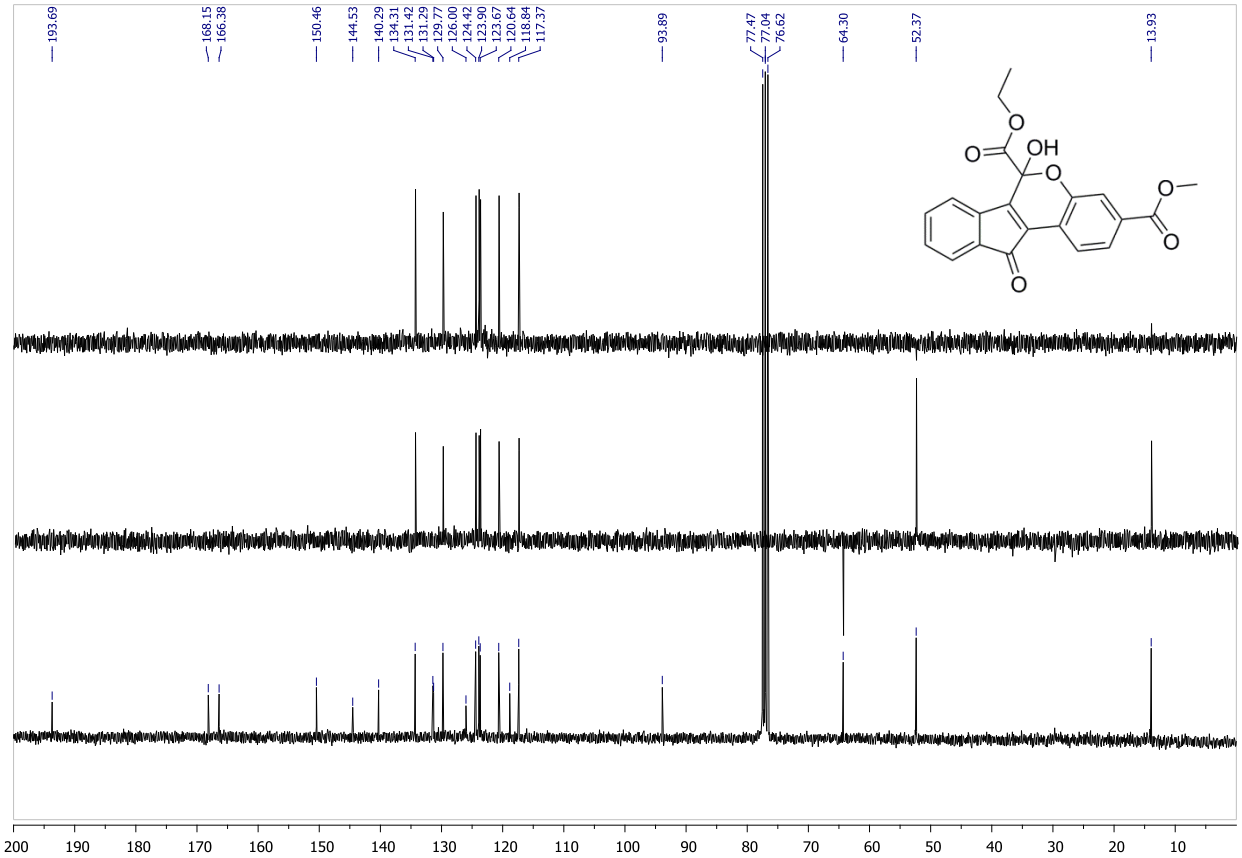

^{1}H-NMR: **3g**

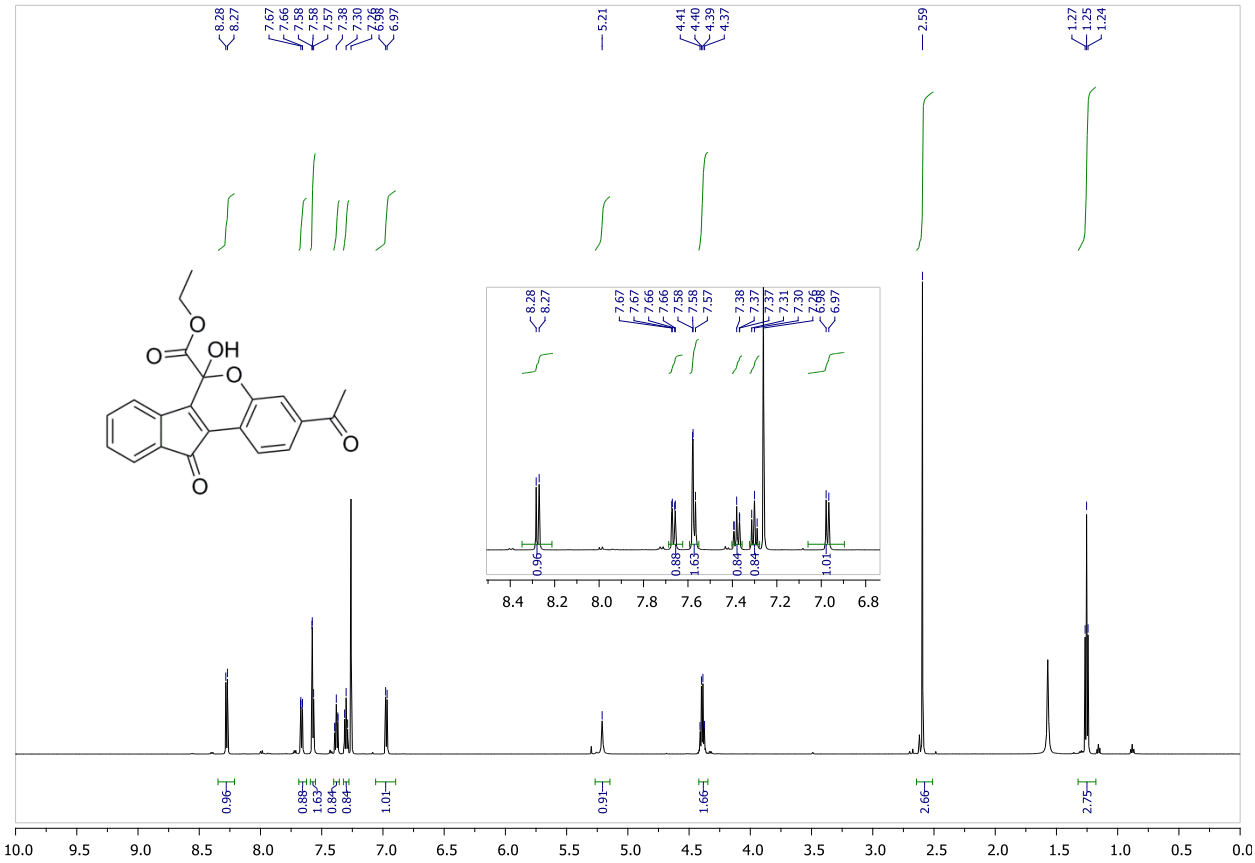

^{13}C-NMR: **3g**

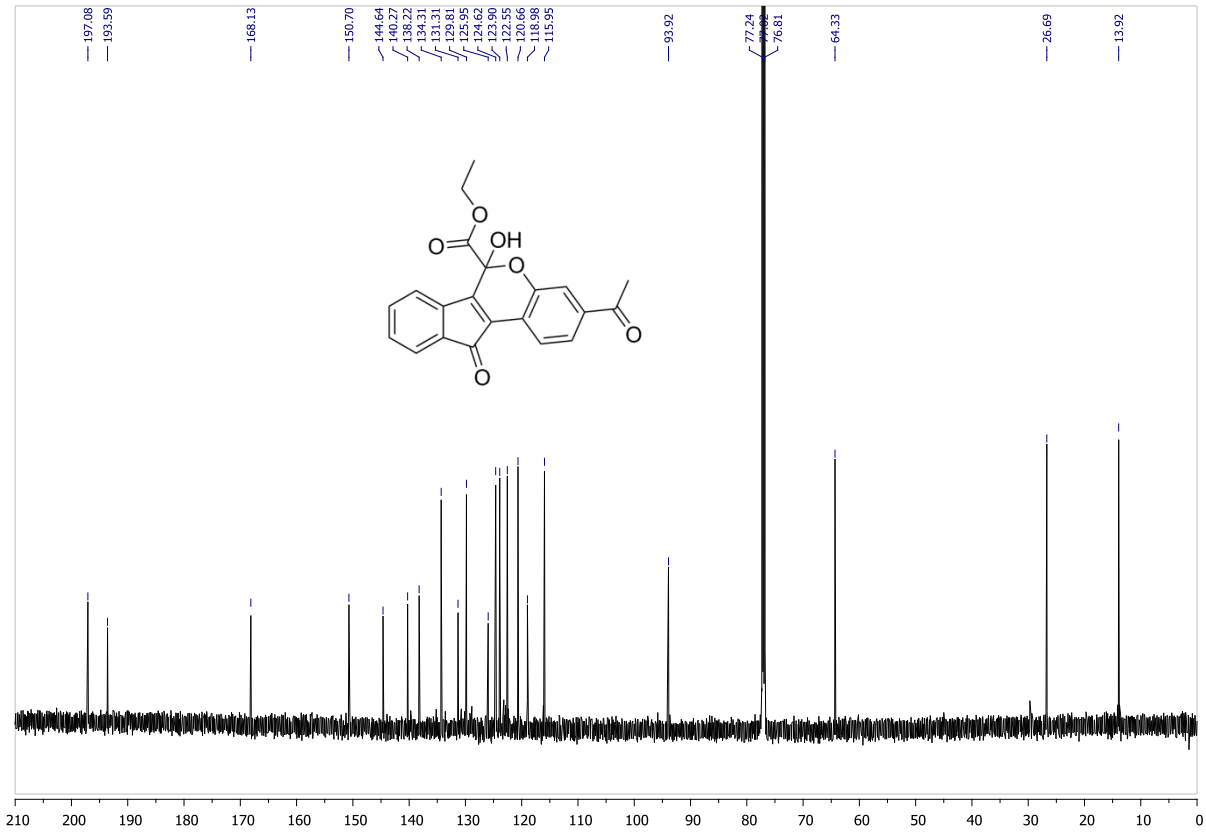

^{1}H-NMR: **3h**

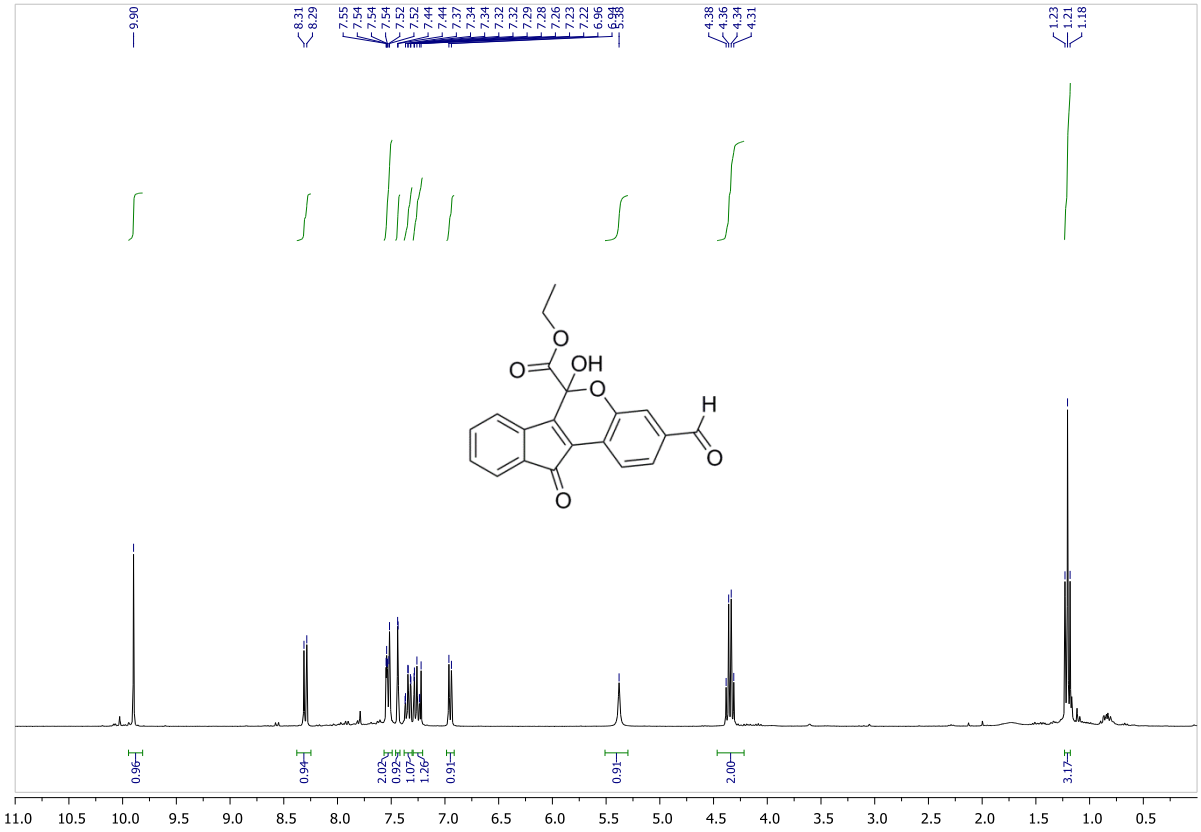

^{13}C-NMR: **3h**

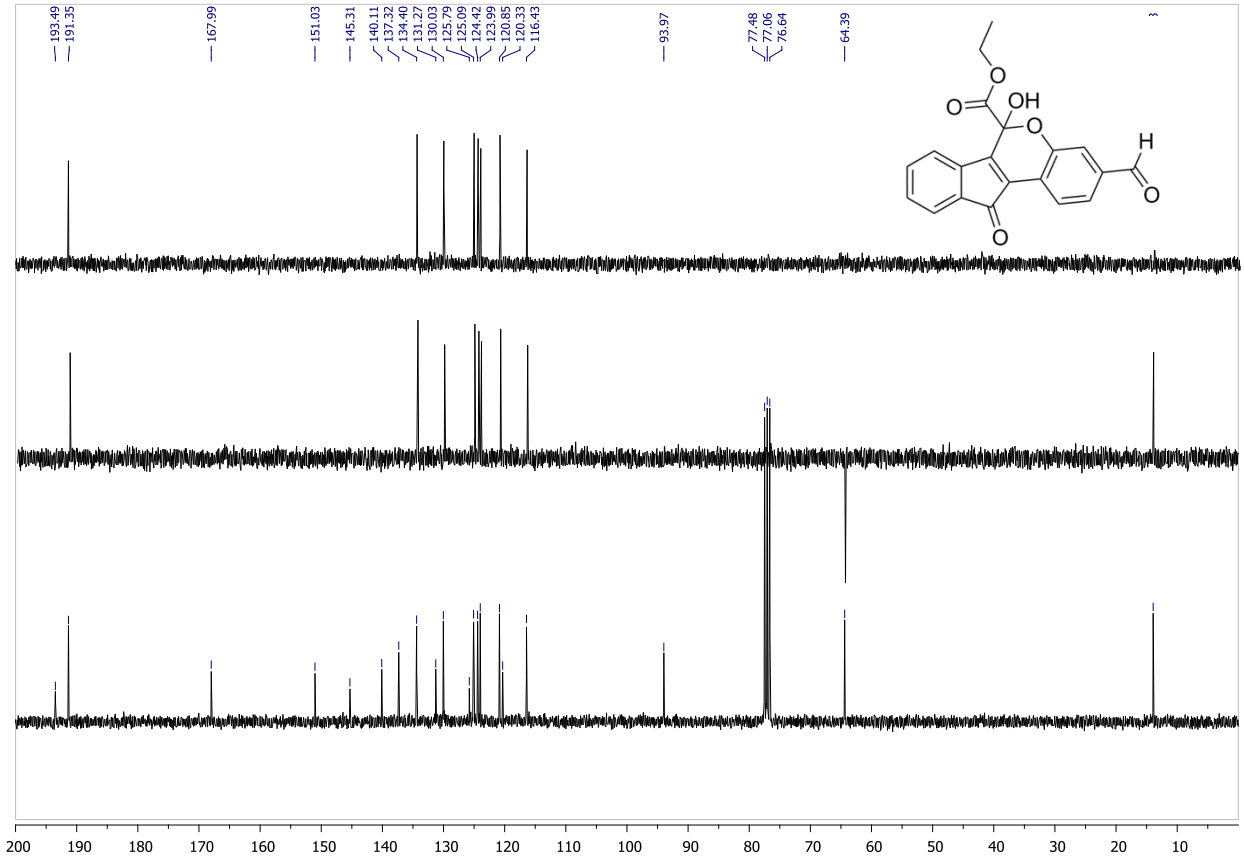

^{1}H-NMR: **3i**

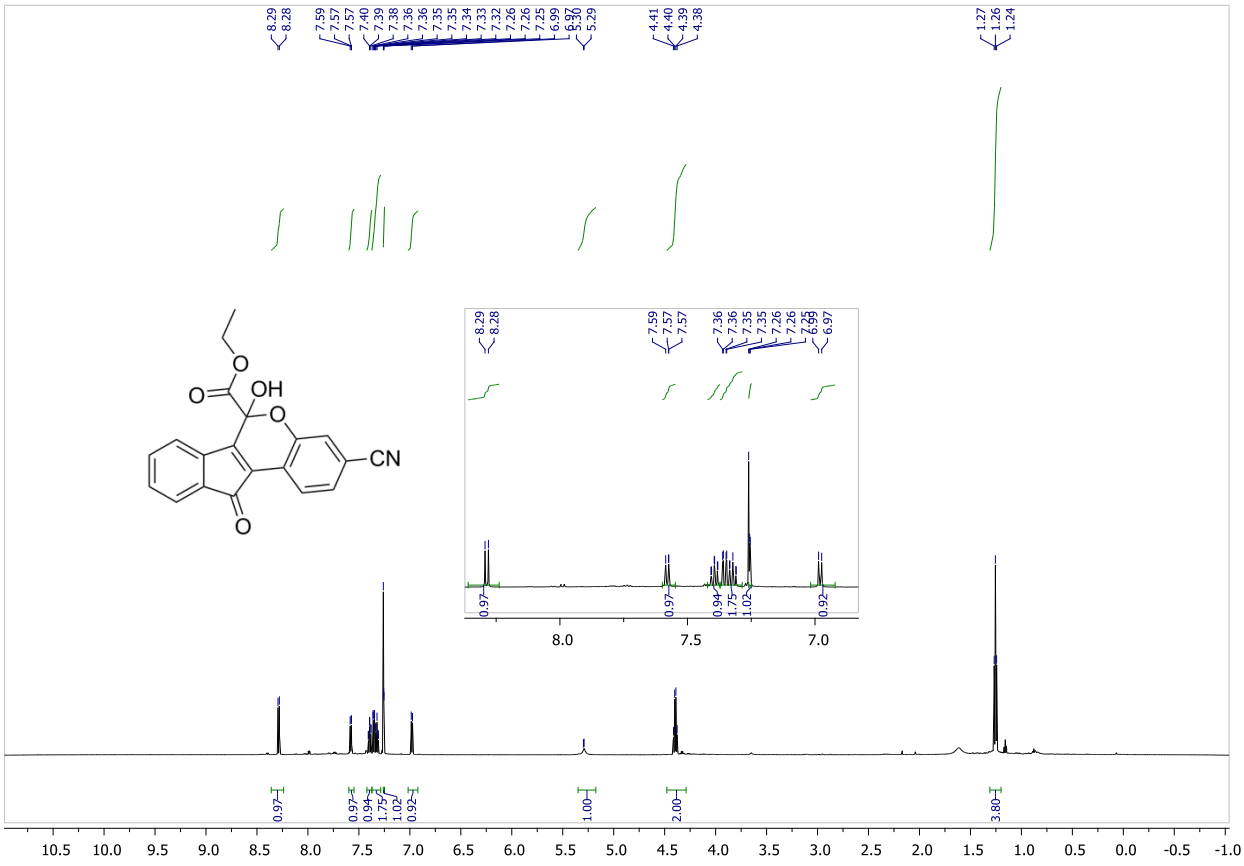

^{13}C-NMR**: 3i**

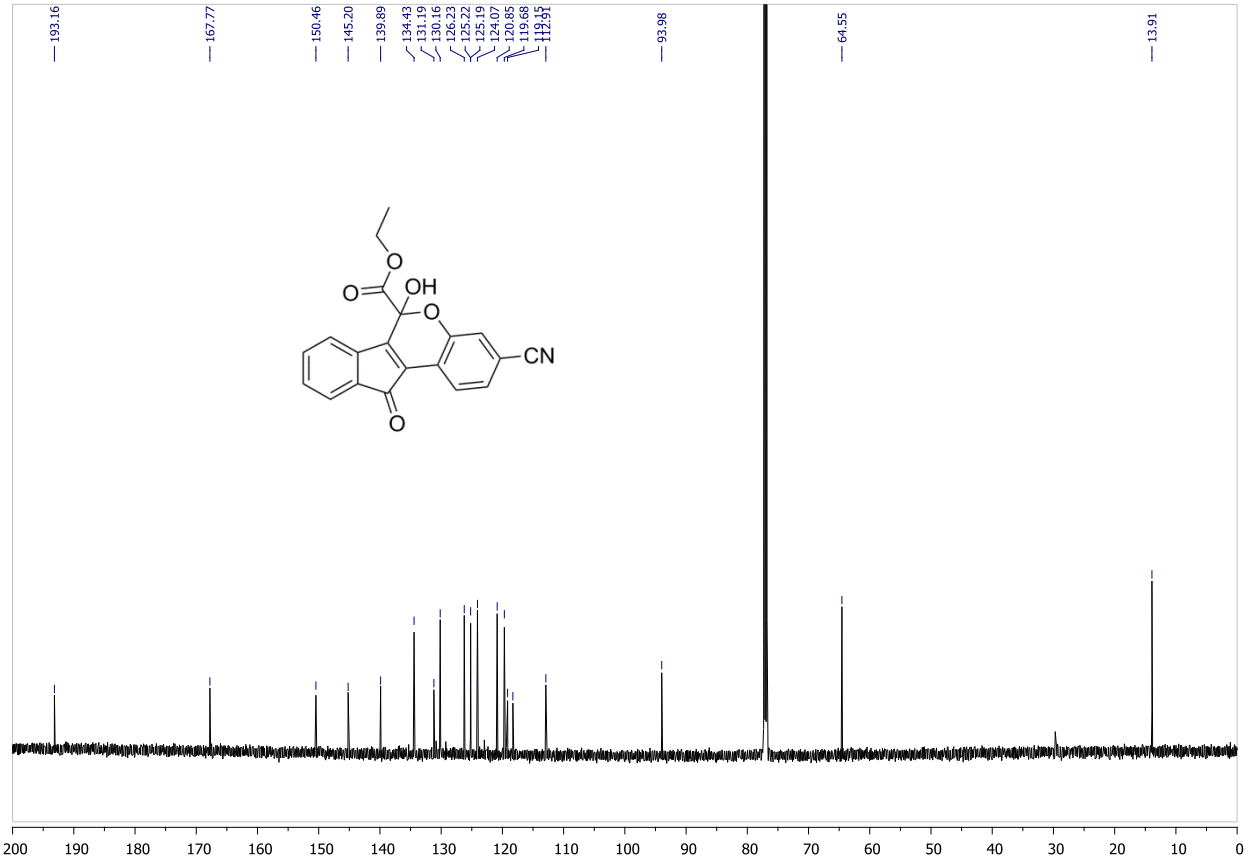

^{1}H-NMR: **3j**

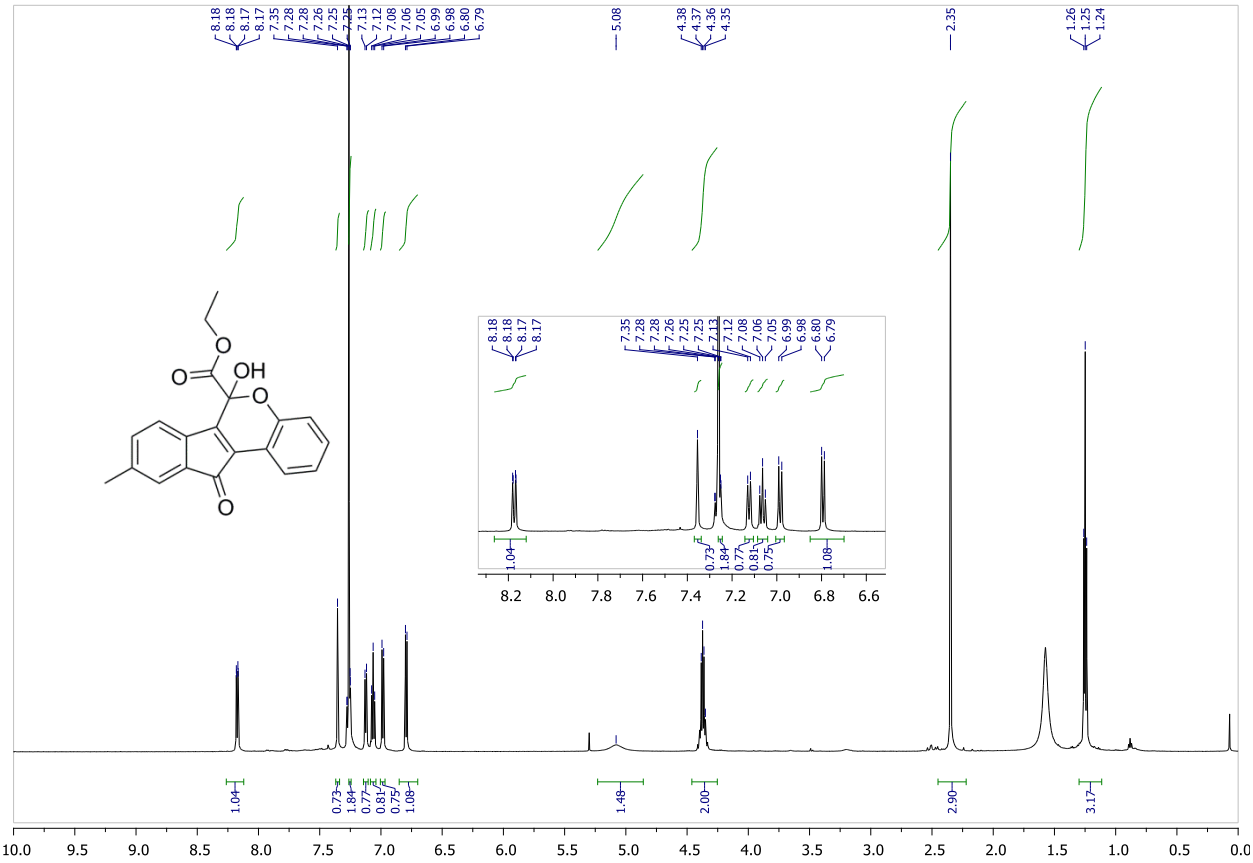

^{13}C-NMR: **3j**

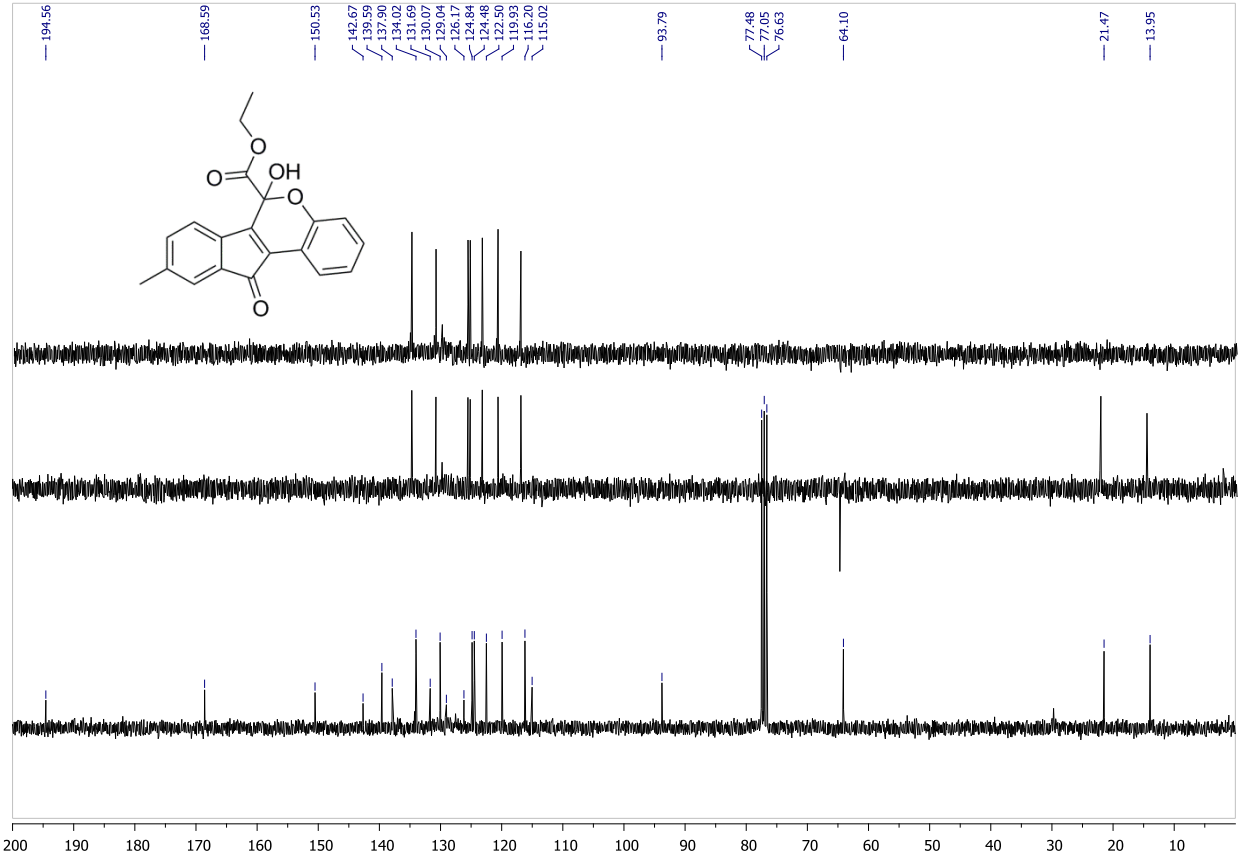

^{1}H-NMR: **3k**

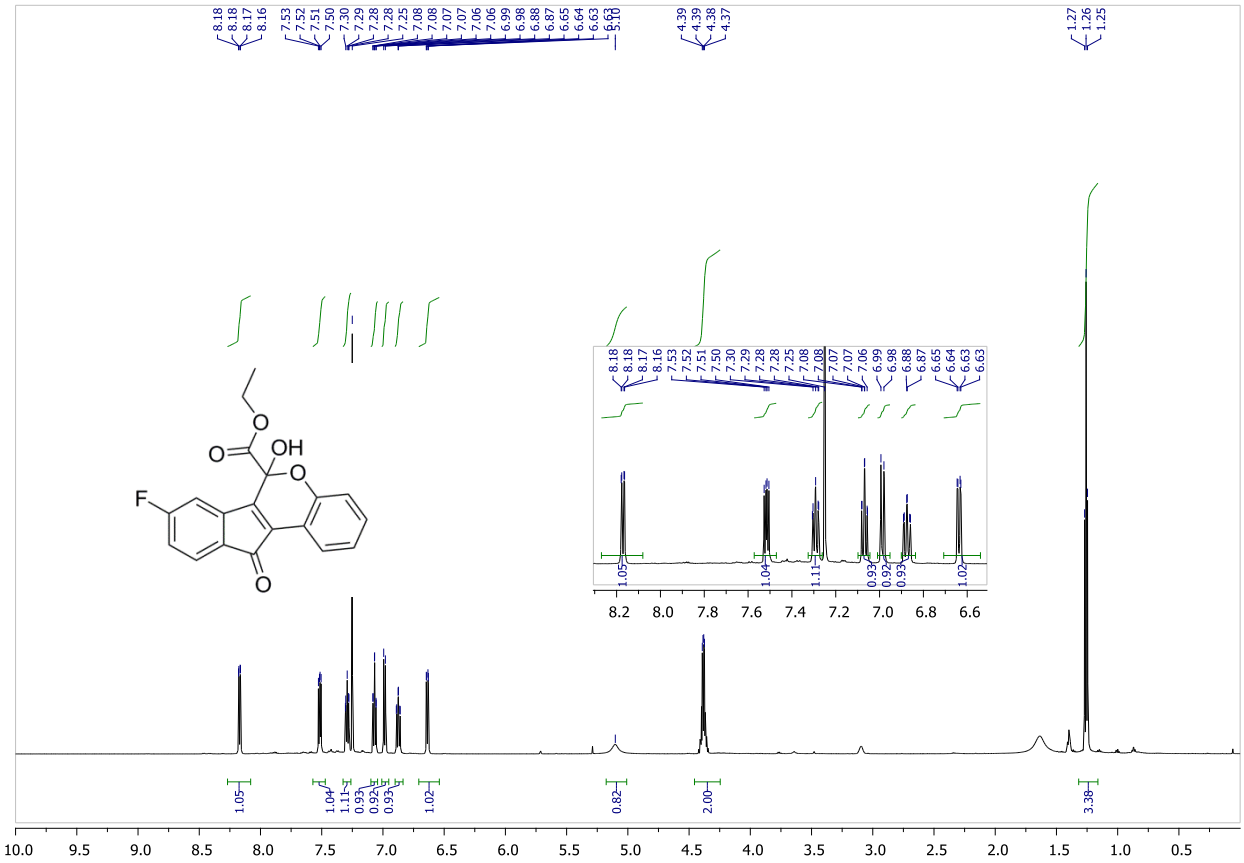

^{13}C-NMR: **3k**

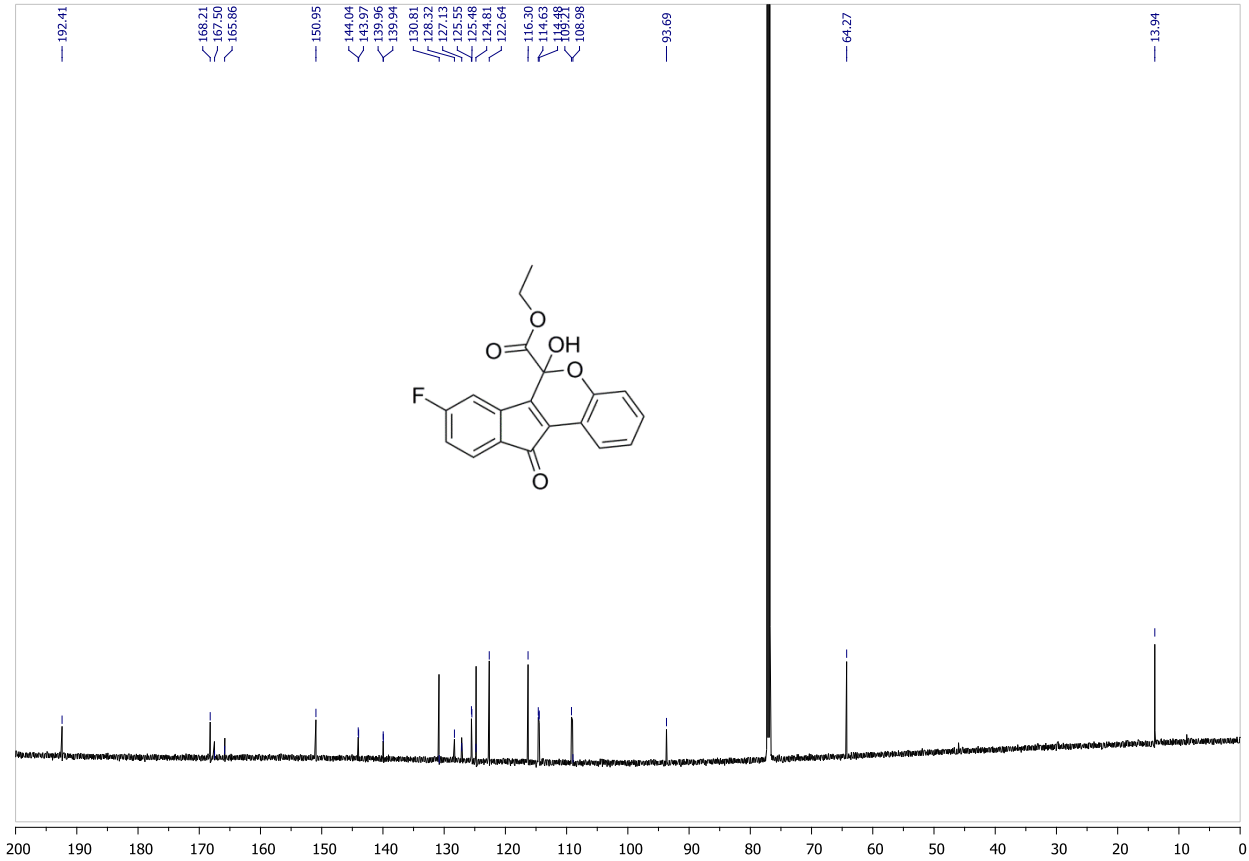

^{19}F-NMR: **3k**

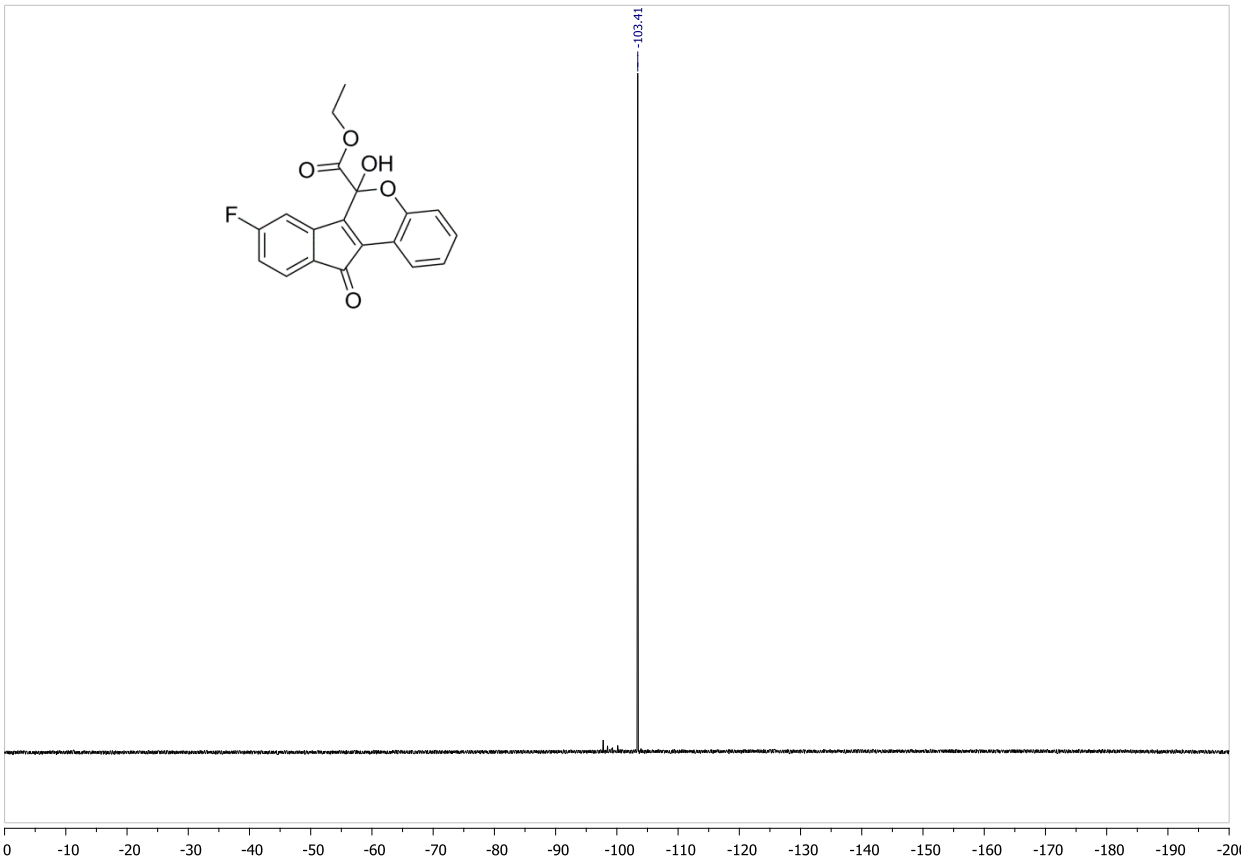
-103.41
O
O
OH
O
F
O
0
-10
-20
-30
-40
-50
-60
-70
-80
-90
-100
-110
-120
-130
-140
-150
-160
-170
-180
-190

^{1}H-NMR: **5**

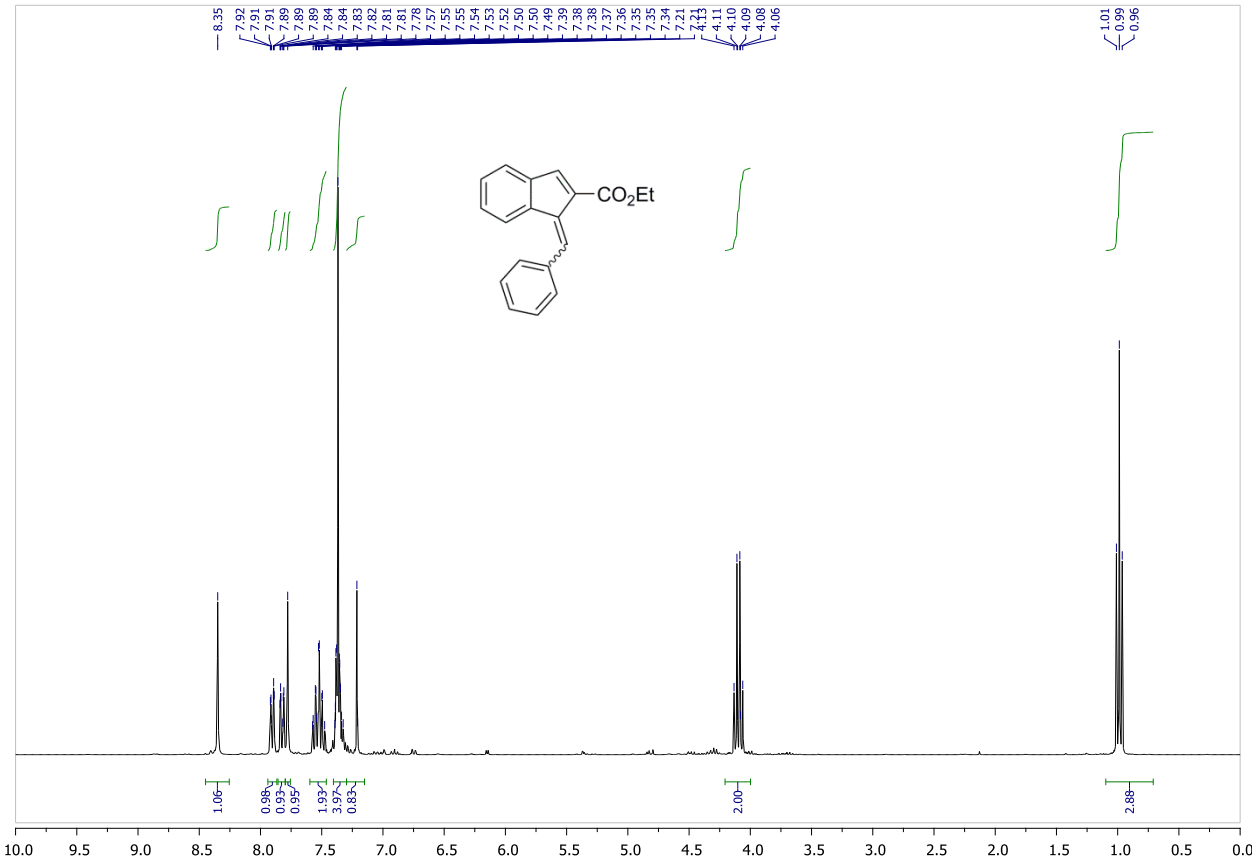

^{13}C-NMR: **5**

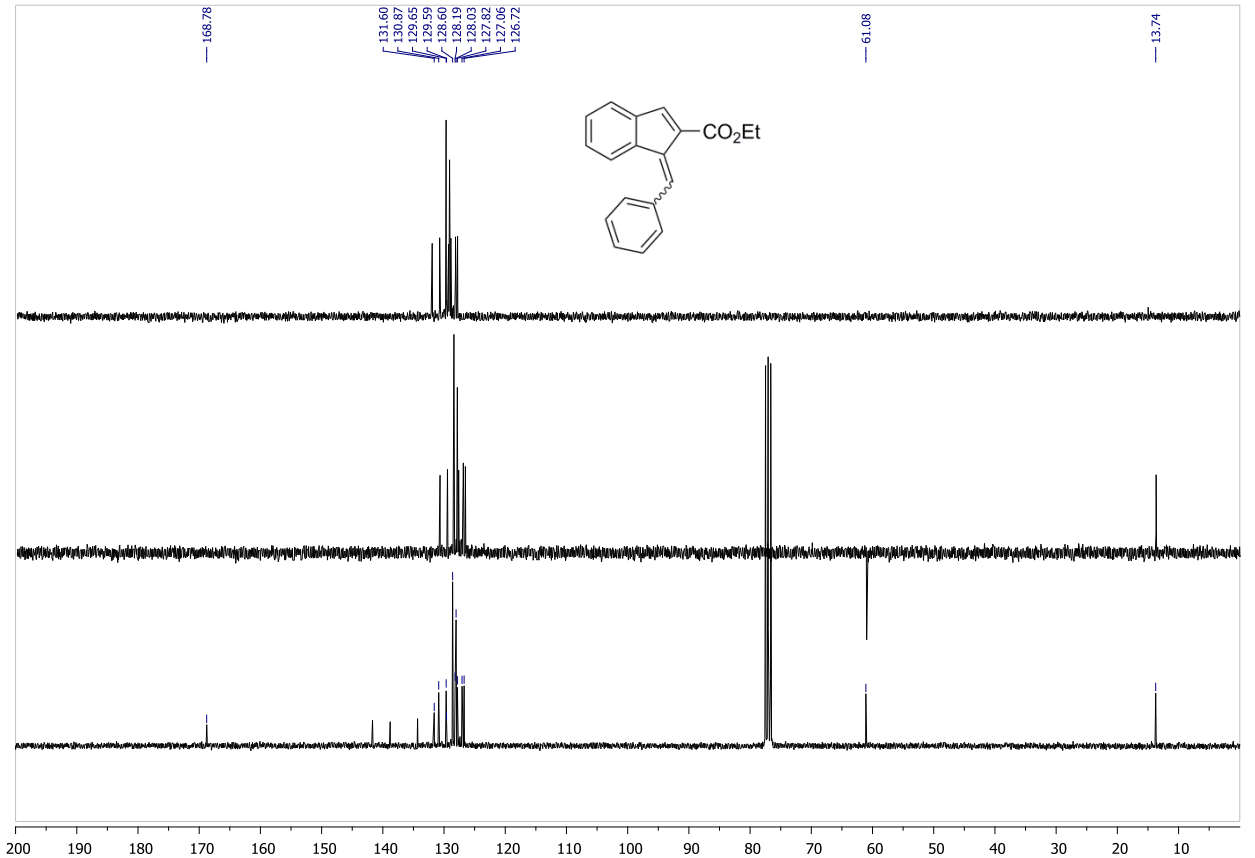

^{1}H-NMR: **7**

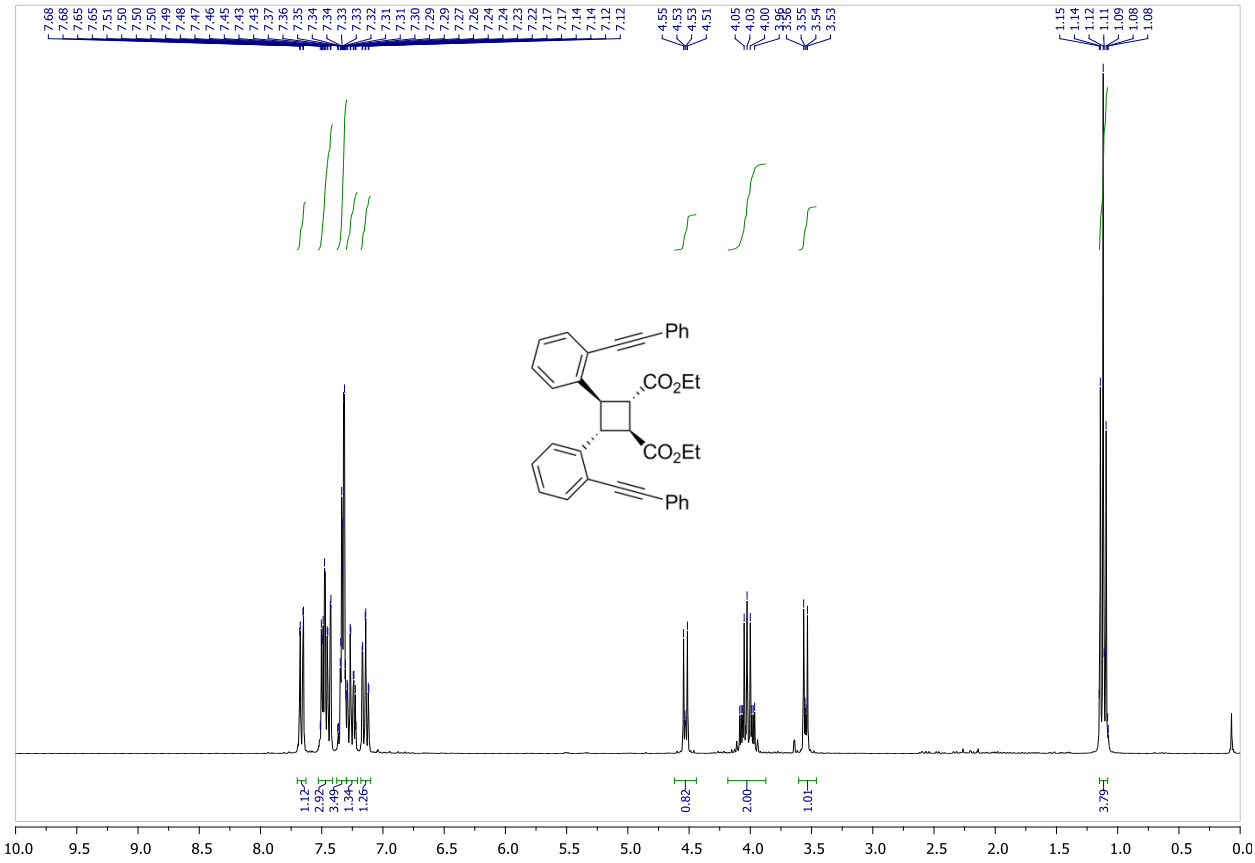

^{13}C-NMR: **7**

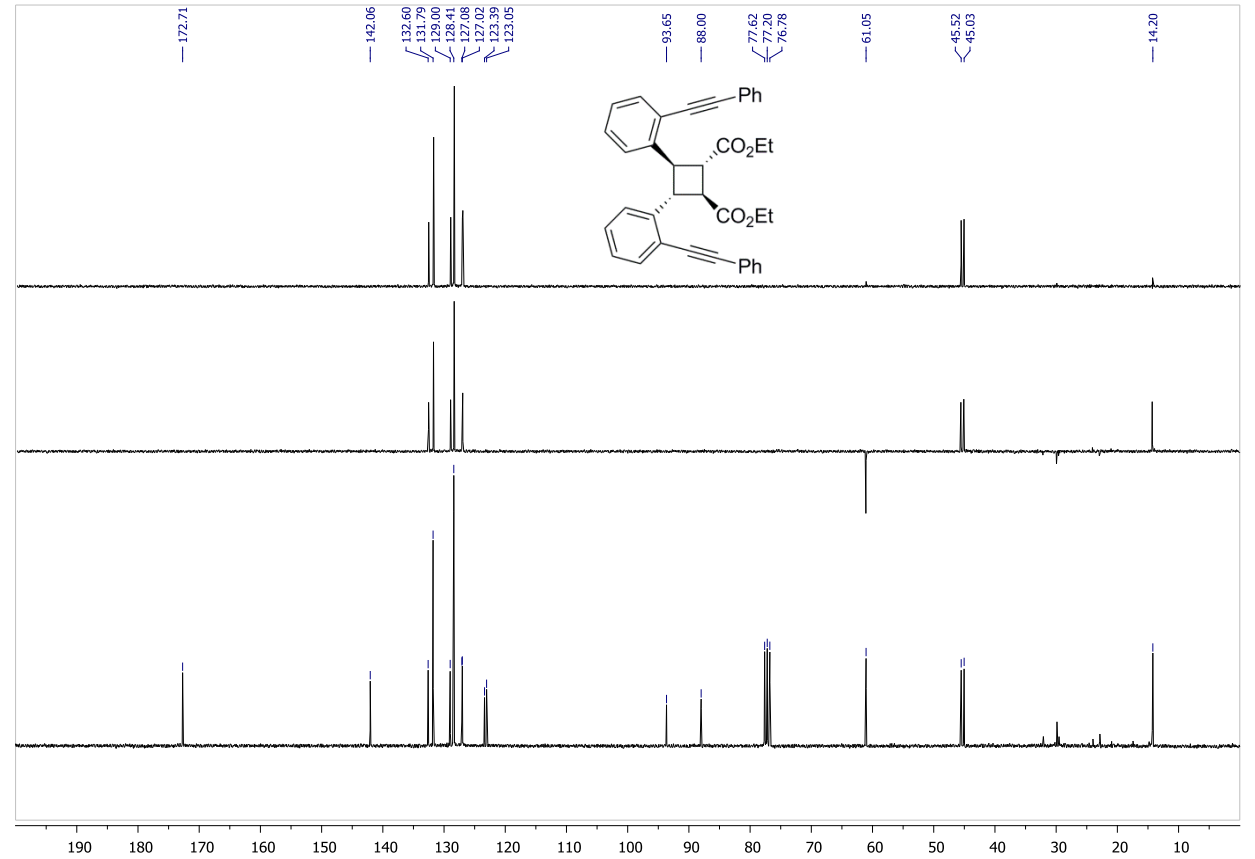

^{1}H-NMR: **S3a**

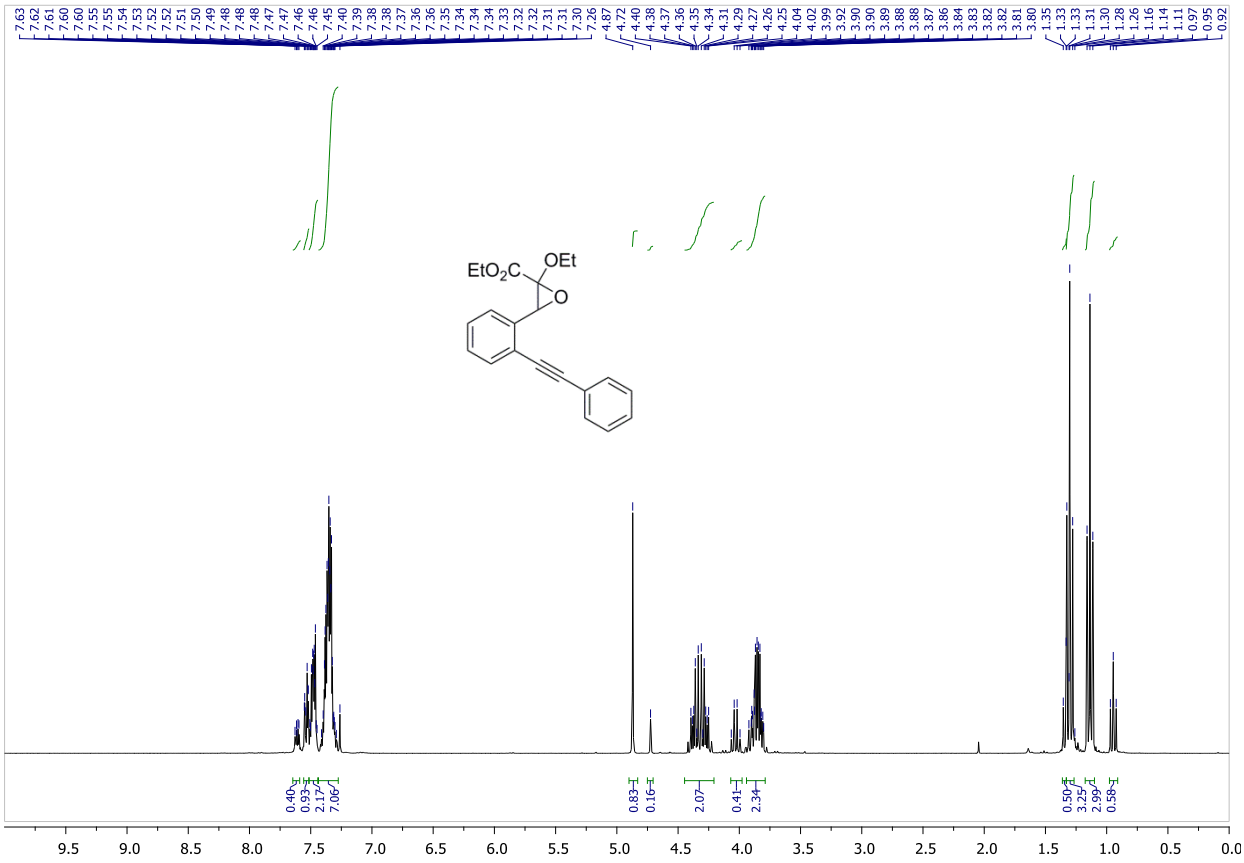

^{13}C-NMR: **S3a**

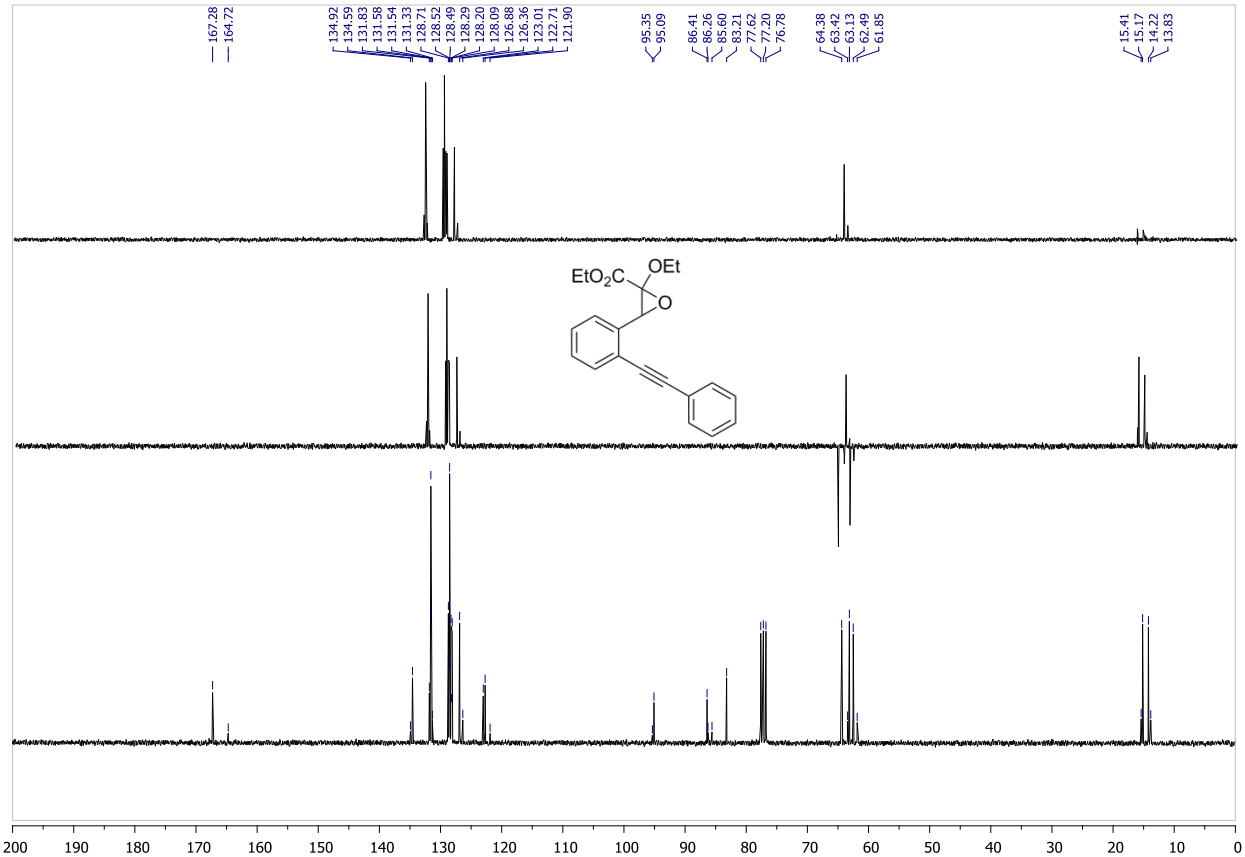

^{1}H-NMR: **8**

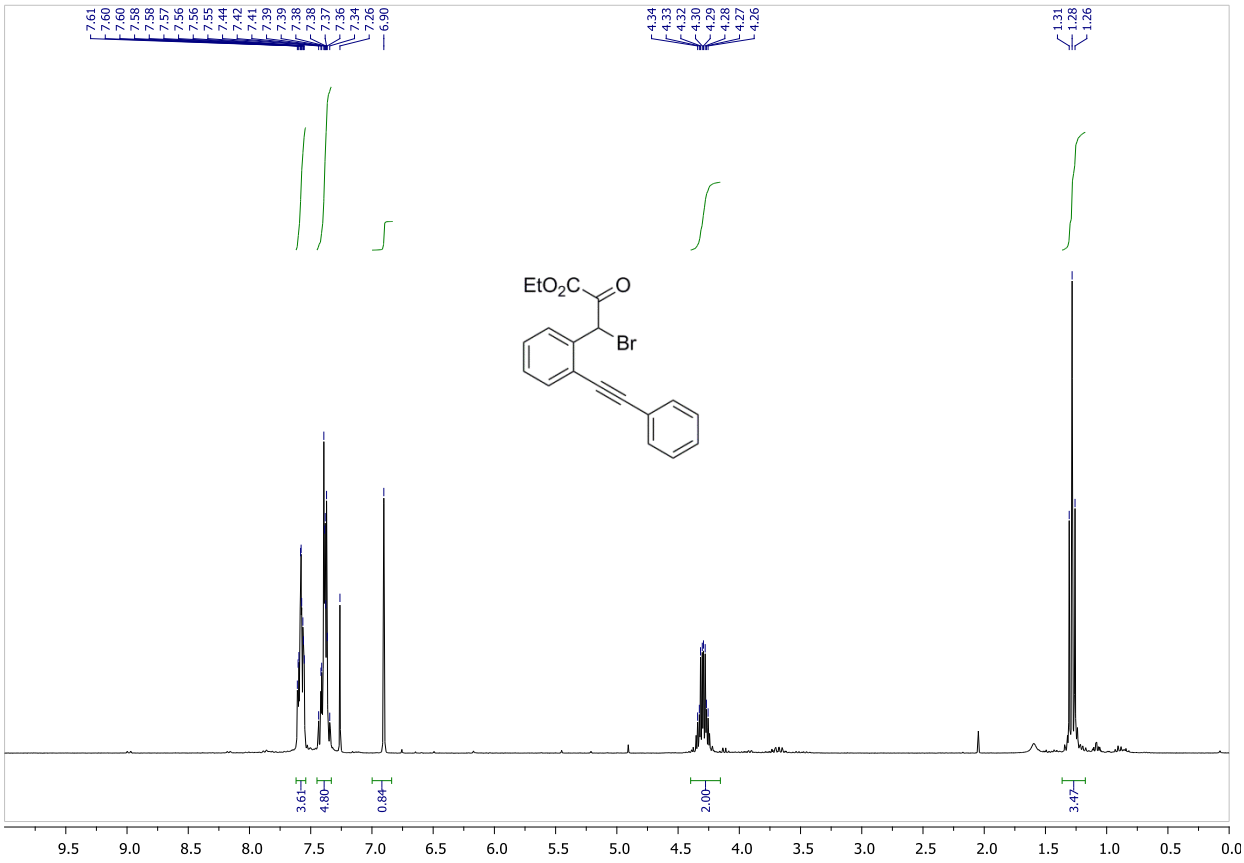

^{13}C-NMR: **8**

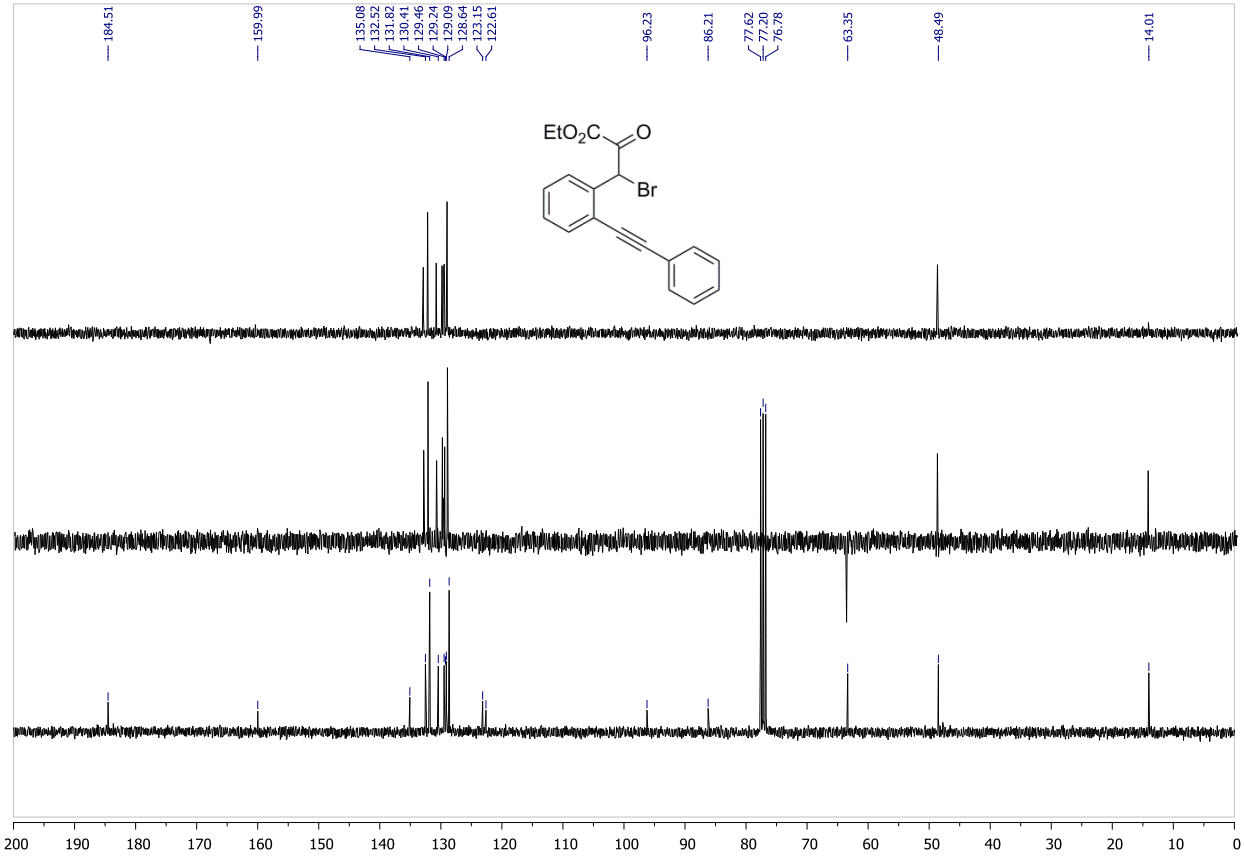

3.12 Crystal data: 3a

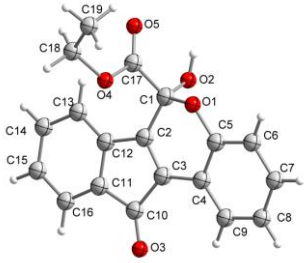

Figure 3.12: Single-crystal X-ray structure of **3a**

The recrystallization was done by DCM/pentane diffusion method.

Crystal Data. $C_{19}H_{14}O_5$, M_r = 322.30, triclinic, P-1 (No. 2), a = 7.8329(2) Å, b = 8.2722(2) Å, c = 11.4374(2) Å, α = 92.787(2)°, β = 95.928(2)°, γ = 93.919(2)°, V = 734.24(3) Å^3, T = 123.01(10) K, Z = 2, Z' = 1, μ(CuK$_\alpha$) = 0.882, 13287 reflections measured, 2918 unique (R_{int} = 0.0276) which were used in all calculations. The final wR_2 was 0.0902 (all data) and R_1 was 0.0343 (I = 2(I)).

Compound	3a
Formula	$C_{19}H_{14}O_5$
$D_{calc.}$/ g cm^{-3}	1.458
μ/mm^{-1}	0.882
Formula Weight	322.30
Colour	red
Shape	prism
Max Size/mm	0.19
Mid Size/mm	0.16
Min Size/mm	0.09
T/K	123.01(10)
Crystal System	triclinic
Space Group	P-1
a/Å	7.8329(2)
b/Å	8.2722(2)
c/Å	11.4374(2)
α/°	92.787(2)
β/°	95.928(2)
γ/°	93.919(2)
V/Å^3	734.24(3)
Z	2
Z'	1
Θ_{min}/°	3.892
Θ_{max}/°	73.635
Measured Refl.	13287
Independent Refl.	2918
Reflections Used	2647
R_{int}	0.0276
Parameters	219
Restraints	0
Largest Peak	0.274
Deepest Hole	-0.203
GooF	1.036
wR_2 (all data)	0.0902
wR_2	0.0874
R_1 (all data)	0.0378
R_1	0.0343

Table 3.6: Fractional Atomic Coordinates (×10^4) and Equivalent Isotropic Displacement Parameters (Å^2×10^3) for **3a**. U_{eq} is defined as 1/3 of the trace of the orthogonalized U_{ij}.

Atom	x	y	z	U_{eq}
O2	5114.3(11)	9349.3(10)	3258.0(8)	26.3(2)
O1	5717.4(11)	8469(1)	1384.9(8)	26.0(2)
O3	4811.8(11)	2719.3(10)	2868.4(8)	27.8(2)
O4	9190.9(11)	8485.5(10)	2366.5(9)	29.1(2)
O5	8291.9(12)	10767.7(11)	3167.9(9)	35.3(2)
C4	4173.3(15)	5815.8(14)	1380.4(11)	22.8(3)
C2	6206.7(15)	6818.2(14)	3058.6(11)	21.9(2)
C5	4462.1(15)	7315.3(14)	881.5(11)	23.2(3)
C11	6660.6(15)	4623.7(14)	4214.5(11)	23.4(3)
C3	5215.3(15)	5586.3(14)	2472.3(11)	22.4(3)
C12	7109.9(15)	6290.2(14)	4155.3(11)	22.7(3)
C10	5451.2(15)	4081.5(14)	3145.2(11)	23.2(3)
C17	8027.6(16)	9404.8(14)	2756.3(11)	23.7(3)
C1	6216.0(15)	8501.3(14)	2632.3(11)	22.9(3)
C6	3585.0(16)	7656.4(15)	-182.3(11)	26.3(3)

Atom	x	y	z	U_{eq}
C16	7279.8(16)	3764.5(15)	5150.2(12)	26.2(3)
C9	2954.1(16)	4666.8(15)	787.9(12)	25.9(3)
C13	8190.0(16)	7120.1(15)	5043.4(11)	26.0(3)
C14	8829.0(17)	6251.7(16)	5996.7(11)	28.0(3)
C15	8385.3(17)	4613.4(16)	6050.7(12)	28.4(3)
C7	2385.0(16)	6491.3(16)	-754.9(12)	27.6(3)
C8	2065.6(16)	5002.3(16)	-273.3(12)	28.0(3)
C18	10968.9(16)	9214.0(16)	2471.8(13)	29.6(3)
C19	11264.1(17)	10284.7(16)	1483.8(13)	31.2(3)

Table 3.7: Anisotropic Displacement Parameters (×10⁴) **3a**. The anisotropic displacement factor exponent takes the form: $-2\pi^2[h^2a^{*2} \times U_{11} + \ldots + 2hka^* \times b^* \times U_{12}]$

Atom	U_{11}	U_{22}	U_{33}	U_{23}	U_{13}	U_{12}
O2	23.4(4)	17.1(4)	39.0(5)	3.4(3)	5.3(4)	3.0(3)
O1	26.1(4)	20.8(4)	29.8(5)	5.6(3)	-1.4(4)	-2.9(3)
O3	26.5(5)	18.1(4)	38.5(5)	3.9(3)	1.8(4)	0.6(3)
O4	20.0(4)	20.7(4)	47.0(6)	2.2(4)	5.5(4)	0.6(3)
O5	28.5(5)	25.5(5)	50.7(6)	-7.1(4)	6.7(4)	-4.3(4)
C4	18.6(6)	21.0(6)	29.5(6)	2.3(5)	3.8(5)	3.1(4)
C2	18.3(5)	19.7(6)	28.5(6)	3.1(5)	4.5(5)	2.5(4)
C5	19.5(6)	20.1(5)	30.1(6)	0.9(5)	2.7(5)	2.0(4)
C11	19.9(6)	20.7(6)	30.4(6)	2.7(5)	5.2(5)	3.0(4)
C3	18.7(6)	18.8(5)	30.6(6)	4.0(5)	4.9(5)	2.2(4)
C12	19.8(6)	21.0(6)	28.6(6)	4.4(5)	5.5(5)	3.9(4)
C10	19.4(6)	20.0(6)	31.4(6)	3.9(5)	6.3(5)	2.9(4)
C17	22.6(6)	19.6(6)	28.7(6)	4.2(5)	0.6(5)	0.8(5)
C1	20.3(6)	19.5(6)	28.6(6)	3.5(4)	0.2(5)	1.3(4)
C6	24.4(6)	24.2(6)	31.1(7)	4.4(5)	3.3(5)	5.1(5)
C16	25.3(6)	21.9(6)	32.9(7)	6.5(5)	6.6(5)	4.6(5)
C9	22.1(6)	21.4(6)	34.3(7)	1.6(5)	3.8(5)	0.8(5)
C13	25.8(6)	22.2(6)	30.1(6)	2.1(5)	4.0(5)	1.3(5)
C14	26.8(6)	30.4(6)	26.5(6)	0.9(5)	2.1(5)	2.0(5)
C15	29.0(7)	29.8(6)	27.8(6)	6.9(5)	4.5(5)	6.5(5)
C7	22.7(6)	30.9(6)	29.3(6)	1.0(5)	0.2(5)	7.3(5)
C8	20.5(6)	27.5(6)	35.2(7)	-2.9(5)	0.9(5)	1.5(5)
C18	18.7(6)	28.3(6)	41.7(7)	7.3(5)	1.1(5)	0.3(5)
C19	24.0(6)	31.2(7)	39.0(7)	6.1(6)	4.0(5)	2.5(5)

Table 3.8: Bond Lengths in Å for **3a**.

Atom	Atom	Length/Å
O2	C1	1.3822(15)
O1	C5	1.3822(14)
O1	C1	1.4382(15)
O3	C10	1.2150(15)
O4	C17	1.3240(15)
O4	C18	1.4700(15)
O5	C17	1.1966(15)
C4	C5	1.4045(17)
C4	C3	1.4476(17)
C4	C9	1.3979(17)
C2	C3	1.3449(17)
C2	C12	1.4754(17)
C2	C1	1.4972(16)
C5	C6	1.3853(18)

Atom	Atom	Length/Å
C11	C12	1.4059(16)
C11	C10	1.4979(18)
C11	C16	1.3782(18)
C3	C10	1.5071(16)
C12	C13	1.3763(18)
C17	C1	1.5477(16)
C6	C7	1.3889(18)
C16	C15	1.4021(19)
C9	C8	1.3854(19)
C13	C14	1.4028(18)
C14	C15	1.3819(19)
C7	C8	1.3912(19)
C18	C19	1.4961(19)

Table 3.9: Bond Angles in ° for **3a**.

Atom	**Atom**	**Atom**	**Angle/°**
C5	O1	C1	119.16(9)
C17	O4	C18	116.30(10)
C5	C4	C3	116.00(11)
C9	C4	C5	118.56(11)
C9	C4	C3	125.42(11)
C3	C2	C12	111.33(10)
C3	C2	C1	121.11(11)
C12	C2	C1	127.42(11)
O1	C5	C4	121.55(11)
O1	C5	C6	116.95(11)
C6	C5	C4	121.34(11)
C12	C11	C10	107.99(11)
C16	C11	C12	121.75(12)
C16	C11	C10	130.24(11)
C4	C3	C10	130.40(11)
C2	C3	C4	121.54(11)
C2	C3	C10	108.05(11)
C11	C12	C2	107.40(11)
C13	C12	C2	132.08(11)
C13	C12	C11	120.51(12)
O3	C10	C11	127.61(11)
O3	C10	C3	127.20(12)
C11	C10	C3	105.19(10)
O4	C17	C1	111.83(10)
O5	C17	O4	125.99(12)
O5	C17	C1	122.18(11)
O2	C1	O1	111.67(10)
O2	C1	C2	107.65(10)
O2	C1	C17	110.40(10)
O1	C1	C2	110.96(10)
O1	C1	C17	102.64(9)
C2	C1	C17	113.55(10)
C5	C6	C7	118.93(12)
C11	C16	C15	117.55(11)
C8	C9	C4	120.43(12)
C12	C13	C14	118.03(12)
C15	C14	C13	121.27(12)
C14	C15	C16	120.90(12)
C6	C7	C8	120.79(12)
C9	C8	C7	119.94(12)
O4	C18	C19	111.71(11)

Table 3.10: Hydrogen Fractional Atomic Coordinates (×10⁴) and Equivalent Isotropic Displacement Parameters (Å²×10³) for **3a**. U_{eq} is defined as 1/3 of the trace of the orthogonalised U_{ij}.

Atom	x	y	z	U_{eq}
H2	5331	10350	3205	39
H6	3801	8671	-515	32
H16	6969	2639	5184	31
H9	2733	3649	1115	31
H13	8494	8248	5012	31
H14	9581	6801	6617	34
H15	8835	4055	6707	34
H7	1775	6714	-1484	33
H8	1239	4216	-672	34
H18A	11772	8341	2473	36
H18B	11215	9859	3230	36
H19A	11001	9654	731	47
H19B	12470	10717	1566	47
H19C	10515	11185	1506	47

3.13 Crystal data: 2a

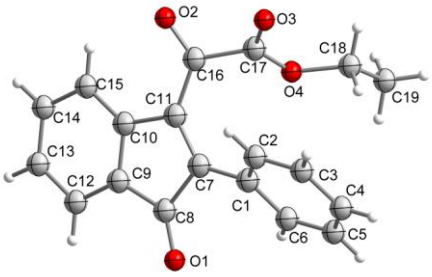

Figure 3.13: Single-crystal X-ray structure of **2a.**

The recrystallization was done by DCM/pentane diffusion method.

Crystal Data. $C_{19}H_{14}O_4$, M_r = 306.30, monoclinic, C2/c (No. 15), a = 15.1845(4) Å, b = 14.3496(4) Å, c = 13.6636(4) Å, β = 98.670(3)°, α = γ = 90°, V = 2943.16(15) Å^3, T = 122.99(10) K, Z = 8, Z' = 1, μ(MoK$_\alpha$) = 0.097, 20923 reflections measured, 3647 unique (R_{int} = 0.0294) which were used in all calculations. The final wR_2 was 0.1310 (all data) and R_1 was 0.0441 (I = 2(I)).

Compound	**2a**
Formula	$C_{19}H_{14}O_4$
$D_{calc.}$/ g cm^{-3}	1.383
μ/mm^{-1}	0.097
Formula Weight	306.30
Colour	red
Shape	prism
Max Size/mm	0.58
Mid Size/mm	0.26
Min Size/mm	0.21
T/K	122.99(10)
Crystal System	monoclinic
Space Group	C2/c
a/Å	15.1845(4)
b/Å	14.3496(4)
c/Å	13.6636(4)
α/°	90
β/°	98.670(3)
γ/°	90
V/Å^3	2943.16(15)
Z	8
Z'	1
Θ_{min}/°	3.215
Θ_{max}/°	29.177
Measured Refl.	20923
Independent Refl.	3647
Reflections Used	3103
R_{int}	0.0294
Parameters	209
Restraints	0
Largest Peak	0.317
Deepest Hole	-0.312
GooF	1.127
wR_2 (all data)	0.1310
wR_2	0.1268
R_1 (all data)	0.0519
R_1	0.0441

Table 3.11: Fractional Atomic Coordinates (×10^4) and Equivalent Isotropic Displacement Parameters (Å^2×10^3) for **2a**. U_{eq} is defined as 1/3 of the trace of the orthogonalised U_{ij}.

Atom	**x**	**y**	**z**	U_{eq}
O4	7910.6(7)	3065.3(7)	7356.8(7)	19.3(2)
O2	6230.7(7)	2022.1(7)	5981.4(9)	24.4(3)
O3	8109.4(7)	2177.2(8)	6045.2(8)	24.5(3)
O1	5916.8(8)	6055.1(8)	6312.5(9)	28.5(3)
C2	8000.2(10)	4442.8(10)	5537.2(10)	18.3(3)
C10	5213.3(9)	3729.1(10)	6150.2(10)	17.6(3)
C16	6641.2(9)	2741.1(10)	6182.1(10)	17.1(3)
C11	6197.6(9)	3653.7(9)	6168.9(10)	16.0(3)
C9	4994.7(10)	4672.2(10)	6206.3(10)	19.3(3)
C14	3681.1(10)	3359.5(12)	6143.8(11)	25.1(3)
C17	7651.7(10)	2640.8(10)	6502.1(11)	17.7(3)
C12	4132.7(10)	4971.4(11)	6229.1(11)	23.5(3)
C15	4554.2(10)	3061.5(11)	6114.9(11)	21.3(3)
C3	8873.1(10)	4728.8(10)	5549.9(11)	21.2(3)
C1	7489.4(9)	4820.0(9)	6209.1(10)	17.4(3)

Atom	x	y	z	U_{eq}
C5	8736.3(11)	5781.1(11)	6884.5(12)	24.8(3)
C6	7862(1)	5504.6(10)	6876.1(11)	21.4(3)
C18	8866.6(10)	3037.9(11)	7718.2(11)	23.1(3)
C8	5825.8(10)	5221.5(10)	6253.2(10)	19.8(3)
C7	6570.0(9)	4516.9(10)	6213.7(10)	17.4(3)
C13	3471.9(10)	4296.3(12)	6200.2(11)	26.5(3)
C4	9246.0(11)	5394.6(11)	6224.4(12)	25.0(3)
C19	8992.8(13)	3322.4(15)	8783.1(13)	36.7(4)

Table 3.12: Anisotropic Displacement Parameters (×10^4) **2a**. The anisotropic displacement factor exponent takes the form: $-2\pi^2[h^2a^{*2} \times U_{11} + \ldots + 2hka^* \times b^* \times U_{12}]$

Atom	U_{11}	U_{22}	U_{33}	U_{23}	U_{13}	U_{12}
O4	19.9(5)	19.8(5)	17.6(5)	0.3(4)	1.2(4)	1.0(4)
O2	24.5(6)	17.3(5)	32.1(6)	-4.0(4)	6.6(5)	-2.8(4)
O3	23.7(5)	23.5(6)	26.1(6)	-4.6(4)	2.7(4)	7.2(4)
O1	35.2(6)	16.3(5)	33.9(6)	-3.3(4)	4.6(5)	3.9(4)
C2	23.5(7)	15.0(6)	15.9(6)	1.4(5)	1.2(5)	0.1(5)
C10	19.4(7)	20.1(7)	13.1(6)	0.8(5)	2.1(5)	2.7(5)
C16	20.8(7)	15.8(6)	15.3(6)	-0.8(5)	4.6(5)	0.0(5)
C11	18.5(6)	16.8(7)	12.9(6)	-1.1(5)	2.8(5)	1.4(5)
C9	22.3(7)	21.9(7)	13.6(6)	-0.3(5)	2.2(5)	4.0(5)
C14	19.1(7)	34.3(8)	21.9(7)	3.4(6)	3.1(6)	-1.8(6)
C17	21.3(7)	13.4(6)	18.5(7)	2.3(5)	3.3(5)	1.3(5)
C12	25.5(8)	27.7(8)	17.3(7)	0.8(6)	3.4(6)	9.4(6)
C15	21.5(7)	23.2(7)	19.2(7)	1.2(6)	2.6(5)	-0.8(6)
C3	23.9(7)	20.2(7)	20.6(7)	2.1(5)	6.6(6)	0.8(6)
C1	21.3(7)	13.7(6)	17.0(6)	1.9(5)	2.0(5)	-0.1(5)
C5	30.1(8)	21.2(7)	22.8(7)	-3.6(6)	2.9(6)	-7.5(6)
C6	27.3(8)	17.9(7)	19.4(7)	-2.4(5)	5.0(6)	-1.5(6)
C18	19.6(7)	24.7(7)	23.8(7)	4.2(6)	-1.1(6)	0.0(6)
C8	25.9(7)	17.9(7)	15.6(7)	-0.9(5)	2.8(5)	4.0(6)
C7	21.4(7)	16.1(6)	14.3(6)	-0.6(5)	2.0(5)	1.9(5)
C13	20.3(7)	39.2(9)	20.3(7)	3.2(6)	4.4(6)	7.1(6)
C4	23.7(7)	25.1(8)	26.3(8)	1.2(6)	4.4(6)	-5.6(6)
C19	33.6(9)	44.0(11)	28.9(9)	-8.6(8)	-7.4(7)	0.1(8)

Table 3.13: Bond Lengths in Å for **2a**.

Atom	Atom	Length/Å
O4	C17	1.3233(18)
O4	C18	1.4618(18)
O2	C16	1.2152(17)
O3	C17	1.2025(18)
O1	C8	1.2054(19)
C2	C3	1.385(2)
C2	C1	1.397(2)
C10	C11	1.4949(19)
C10	C9	1.398(2)
C10	C15	1.381(2)
C16	C11	1.4714(19)
C16	C17	1.538(2)
C11	C7	1.3592(19)
C9	C12	1.382(2)
C9	C8	1.481(2)
C14	C15	1.399(2)

Atom	Atom	Length/Å
C14	C13	1.386(2)
C12	C13	1.391(2)
C3	C4	1.388(2)
C1	C6	1.400(2)
C1	C7	1.4632(19)
C5	C6	1.384(2)
C5	C4	1.389(2)
C18	C19	1.495(2)
C8	C7	1.5232(19)

Table 3.14: Bond Angles in ° for **2a**

Atom	Atom	Atom	Angle/°
C17	O4	C18	115.69(11)
C3	C2	C1	120.14(13)
C9	C10	C11	108.31(12)
C15	C10	C11	131.90(13)
C15	C10	C9	119.77(13)
O2	C16	C11	122.31(13)
O2	C16	C17	116.14(12)
C11	C16	C17	121.48(12)
C16	C11	C10	121.29(12)
C7	C11	C10	110.05(12)
C7	C11	C16	128.61(13)
C10	C9	C8	108.04(12)
C12	C9	C10	122.36(14)
C12	C9	C8	129.59(14)
C13	C14	C15	121.61(15)
O4	C17	C16	111.02(12)
O3	C17	O4	126.50(14)
O3	C17	C16	122.29(13)
C9	C12	C13	117.68(15)
C10	C15	C14	118.15(14)
C2	C3	C4	120.41(14)
C2	C1	C6	119.31(13)
C2	C1	C7	120.82(13)
C6	C1	C7	119.86(13)
C6	C5	C4	120.51(14)
C5	C6	C1	119.97(14)
O4	C18	C19	107.24(13)
O1	C8	C9	128.26(14)
O1	C8	C7	125.65(14)
C9	C8	C7	106.08(12)
C11	C7	C1	131.41(13)
C11	C7	C8	107.50(12)
C1	C7	C8	121.08(12)
C14	C13	C12	120.44(14)
C3	C4	C5	119.64(14)

Table 3.15: Hydrogen Fractional Atomic Coordinates ($\times 10^4$) and Equivalent Isotropic Displacement Parameters ($Å^2 \times 10^3$) for **2a**. U_{eq} is defined as 1/3 of the trace of the orthogonalised U_{ij}.

Atom	x	y	z	U_{eq}
H2	7748	3989	5071	22
H14	3221	2909	6124	30
H12	3996	5616	6263	28
H15	4690	2418	6072	26
H3	9219	4467	5094	25
H5	8990	6239	7345	30
H6	7515	5779	7323	26
H18A	9188	3471	7332	28
H18B	9101	2401	7652	28
H13	2873	4478	6219	32
H4	9846	5585	6235	30
H19A	8784	3964	8836	55
H19B	9626	3284	9059	55
H19C	8651	2906	9152	55

3.14 Crystal data: 1c

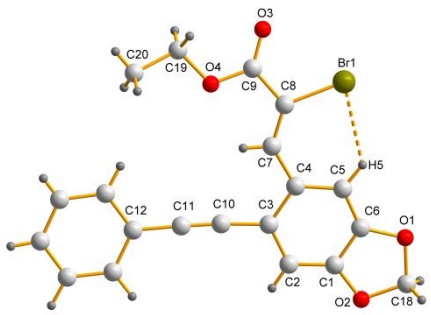

Figure 3.14: Single-crystal X-ray structure of **1c.**

The recrystallization was done by DCM/pentane diffusion method.

Crystal Data. $C_{20}H_{15}BrO_4$, M_r = 399.23, monoclinic, Ia (No. 9), a = 7.3822(2) Å, b = 24.5362(5) Å, c = 9.3974(2) Å, β = 103.349(3)°, α = γ = 90°, V = 1656.17(7) Å^3, T = 123.01(10) K, Z = 4, Z' = 1, μ(Cu K$_\alpha$) = 3.580, 12765 reflections measured, 3047 unique (R_{int} = 0.0326) which were used in all calculations. The final wR_2 was 0.0612 (all data) and R_1 was 0.0248 (I > 2(I)).

Compound	**1c**
Formula	$C_{20}H_{15}BrO_4$
$D_{calc.}$/ g cm^{-3}	1.601
μ/mm^{-1}	3.580
Formula Weight	399.23
Colour	clear colourless
Shape	prism
Size/mm^3	0.11×0.07×0.03
T/K	123.01(10)
Crystal System	monoclinic
Flack Parameter	-0.043(13)
Hooft Parameter	-0.007(7)
Space Group	Ia
a/Å	7.3822(2)
b/Å	24.5362(5)
c/Å	9.3974(2)
α/°	90
β/°	103.349(3)
γ/°	90
V/Å^3	1656.17(7)
Z	4
Z'	1
Wavelength/Å	1.54184
Radiation type	Cu K$_\alpha$
Θ_{min}/°	3.603
Θ_{max}/°	73.488
Measured Refl.	12765
Independent Refl.	3047
Reflections Used	2883
R_{int}	0.0326
Parameters	286
Restraints	50
Largest Peak	0.224
Deepest Hole	-0.347
GooF	1.041
wR_2 (all data)	0.0612
wR_2	0.0593
R_1 (all data)	0.0277
R_1	0.0248

Table 3.16: Fractional Atomic Coordinates (×10^4) and Equivalent Isotropic Displacement Parameters (Å^2×10^3) for **1c**. U_{eq} is defined as 1/3 of the trace of the orthogonalised U_{ij}.

Atom	**x**	**y**	**z**	U_{eq}
Br(1)	-1031.5(7)	9520.1(2)	-254.3(6)	43.23(15)
O(4)	-883(4)	7888.4(10)	66(2)	22.0(6)
O(1)	3031(4)	10455(1)	4381(3)	25.1(5)
C(2)	4242(6)	9080.5(16)	5341(4)	21.8(7)
O(3)	-2058(4)	8475.3(11)	-1747(3)	29.6(6)
C(20)	-1376(7)	6923.1(15)	-84(5)	25.7(9)
O(2)	5033(4)	10005.9(11)	6291(3)	26.3(5)
C(3)	3120(5)	8785.6(15)	4179(4)	21.4(7)
C(11)	3433(5)	7720.7(15)	4359(4)	22.3(7)
C(7)	809(5)	8717.2(14)	1831(4)	19.5(7)
C(8)	-335(5)	8821.9(13)	547(4)	21.6(8)

Atom	x	y	z	U_{eq}
C(4)	1893(5)	9056.8(14)	2994(4)	20.1(7)
C(10)	3267(5)	8203.3(15)	4233(4)	22.0(7)
C(5)	1805(5)	9632.3(14)	3007(4)	21.6(7)
C(13)	4820(6)	6945.2(17)	5871(5)	25.1(9)
C(16)	3246(7)	6219.4(19)	3718(5)	31.8(10)
C(19)	-1672(6)	7449.6(15)	-920(4)	23.5(8)
C(15)	4348(7)	6033.0(16)	5023(6)	34.9(12)
C(17)	2923(6)	6769(2)	3467(5)	27.9(9)
C(18)	4294(6)	10529.7(15)	5773(5)	26.2(8)
C(12)	3713(5)	7142.6(13)	4558(4)	20.3(8)
C(14)	5143(7)	6396.7(18)	6093(5)	29.6(9)
C(9)	-1198(6)	8387.7(14)	-508(4)	21.7(9)
C(6)	2916(5)	9900.9(14)	4147(4)	21.3(7)
C(1)	4097(5)	9636.2(14)	5299(4)	20.9(7)

Table 3.17: Anisotropic Displacement Parameters (×10^4) **1c**. The anisotropic displacement factor exponent takes the form: $-2\pi^2[h^2a^{*2} \times U_{11} + \ldots + 2hka^* \times b^* \times U_{12}]$

Atom	U_{11}	U_{22}	U_{33}	U_{23}	U_{13}	U_{12}
Br(1)	64.5(3)	18.58(16)	33.7(2)	4.7(2)	-15.06(17)	-0.5(3)
O(4)	25.6(14)	17.8(11)	19.6(16)	-3.4(9)	-0.8(13)	-3.6(10)
O(1)	28.1(15)	17.5(12)	26.7(14)	-2(1)	0.2(11)	-0.8(11)
C(2)	19.8(18)	23.4(17)	21.4(16)	4.4(15)	2.7(13)	0.7(15)
O(3)	36.3(17)	28.8(14)	19.2(13)	0.4(11)	-2.6(11)	2.2(12)
C(20)	30(3)	18.8(15)	26(2)	-3.0(16)	0.2(16)	-3.9(16)
O(2)	27.5(14)	20.6(11)	26.1(13)	-3.4(10)	-3.2(10)	-1.9(10)
C(3)	20.6(19)	20.4(16)	23.7(19)	1.6(15)	6.1(14)	0.1(15)
C(11)	21(2)	22.0(17)	22.8(16)	-1.4(14)	2.6(12)	-0.8(14)
C(7)	20(2)	13.7(15)	24.9(18)	0.5(12)	4.6(14)	0.1(12)
C(8)	25(2)	13.4(16)	25.0(19)	2.6(13)	3.0(15)	0.7(13)
C(4)	18.9(18)	20.4(16)	20.5(16)	-0.4(13)	3.3(14)	-0.8(14)
C(10)	19.5(19)	23.7(17)	21.2(16)	1.9(15)	1.4(13)	1.0(15)
C(5)	22.5(19)	19.7(16)	22.5(17)	1.1(13)	4.8(14)	0.2(14)
C(13)	23(2)	28(2)	22(2)	-0.7(16)	-1.2(16)	-2.7(16)
C(16)	37(3)	25(2)	34(2)	-13.0(18)	9.0(18)	-10.7(18)
C(19)	23(2)	22.2(18)	21.1(19)	-6.7(14)	-2.1(16)	-2.5(15)
C(15)	40(3)	16.3(16)	51(3)	3.6(17)	17(2)	-0.1(16)
C(17)	28(2)	34(2)	19.3(19)	-3.7(17)	1.2(16)	-4.1(17)
C(18)	27(2)	21.4(17)	27.2(19)	-5.2(15)	0.4(17)	-4.5(16)
C(12)	20(2)	19.7(15)	21(2)	2.6(15)	3.5(17)	1.7(15)
C(14)	29(2)	27(2)	31(2)	9.7(16)	1.8(16)	1.5(17)
C(9)	19(2)	24.1(15)	22(3)	0.3(13)	5(2)	1.7(15)
C(6)	22.6(19)	17.5(16)	23.4(18)	0.2(14)	4.8(14)	-1.4(14)
C(1)	17.6(19)	23.0(16)	22.4(16)	-4.4(13)	5.0(14)	-4.2(15)

Table 3.18: Bond Lengths in Å for **1c**.

Atom	Atom	Length/Å
Br(1)	C(8)	1.894(3)
O(4)	C(19)	1.452(4)
O(4)	C(9)	1.337(4)
O(1)	C(18)	1.432(5)
O(1)	C(6)	1.377(4)
C(2)	C(3)	1.409(5)
C(2)	C(1)	1.368(5)
O(3)	C(9)	1.210(5)
C(20)	C(19)	1.502(5)
O(2)	C(18)	1.437(5)
O(2)	C(1)	1.368(4)

Atom	Atom	Length/Å
C(3)	C(4)	1.427(5)
C(3)	C(10)	1.433(5)
C(11)	C(10)	1.194(5)
C(11)	C(12)	1.439(4)
C(7)	C(8)	1.328(5)
C(7)	C(4)	1.458(5)
C(8)	C(9)	1.494(5)
C(4)	C(5)	1.414(5)
C(5)	C(6)	1.360(5)
C(13)	C(12)	1.399(6)
C(13)	C(14)	1.374(6)

Atom	Atom	Length/Å
C(16)	C(15)	1.383(7)
C(16)	C(17)	1.379(7)
C(15)	C(14)	1.371(6)
C(17)	C(12)	1.400(5)
C(6)	C(1)	1.385(5)

Table 3.19: Bond Angles in ° for **1c**.

Atom	Atom	Atom	Angle/°
C(9)	O(4)	C(19)	114.5(3)
C(6)	O(1)	C(18)	106.0(3)
C(1)	C(2)	C(3)	117.5(4)
C(1)	O(2)	C(18)	105.6(3)
C(2)	C(3)	C(4)	121.3(3)
C(2)	C(3)	C(10)	117.3(3)
C(4)	C(3)	C(10)	121.5(3)
C(10)	C(11)	C(12)	177.4(4)
C(8)	C(7)	C(4)	134.0(3)
C(7)	C(8)	Br(1)	126.4(3)
C(7)	C(8)	C(9)	123.3(3)
C(9)	C(8)	Br(1)	110.3(3)
C(3)	C(4)	C(7)	117.3(3)
C(5)	C(4)	C(3)	118.8(3)
C(5)	C(4)	C(7)	124.0(3)
C(11)	C(10)	C(3)	176.4(4)
C(6)	C(5)	C(4)	118.0(3)
C(14)	C(13)	C(12)	121.2(4)
C(17)	C(16)	C(15)	121.2(4)
O(4)	C(19)	C(20)	108.4(3)
C(14)	C(15)	C(16)	120.0(4)
C(16)	C(17)	C(12)	119.2(4)
O(1)	C(18)	O(2)	108.1(3)
C(13)	C(12)	C(11)	119.5(3)
C(13)	C(12)	C(17)	118.6(3)
C(17)	C(12)	C(11)	121.9(3)
C(15)	C(14)	C(13)	119.7(4)
O(4)	C(9)	C(8)	112.2(3)
O(3)	C(9)	O(4)	123.7(3)
O(3)	C(9)	C(8)	124.1(3)
O(1)	C(6)	C(1)	109.5(3)
C(5)	C(6)	O(1)	127.4(3)
C(5)	C(6)	C(1)	123.0(3)
C(2)	C(1)	O(2)	128.1(4)
C(2)	C(1)	C(6)	121.4(4)
O(2)	C(1)	C(6)	110.5(3)

Table 3.20: Hydrogen Fractional Atomic Coordinates (×10⁴) and Equivalent Isotropic Displacement Parameters (Å²×10³) for **1c**. U_{eq} is defined as 1/3 of the trace of the orthogonalised U_{ij}.

Atom	x	y	z	U_{eq}
H(20A)	-1890(70)	6670(20)	-710(60)	25(11)
H(18A)	3630(60)	10680(17)	6410(50)	22(10)
H(15)	4560(80)	5680(20)	5230(60)	41(14)
H(19A)	-1010(60)	7446(16)	-1690(50)	20(10)
H(2)	5040(60)	8911(17)	6080(50)	16(10)
H(14)	5940(80)	6240(20)	6980(60)	43(15)
H(17)	2230(70)	6920(20)	2600(60)	36(13)
H(20B)	-120(130)	6860(30)	240(90)	90(30)
H(13)	5250(90)	7200(20)	6610(70)	54(16)
H(19B)	-2990(70)	7531(17)	-1220(50)	21(10)
H(18B)	5230(80)	10740(20)	5500(60)	38(13)
H(5)	1040(80)	9840(20)	2260(60)	39(13)
H(7)	920(60)	8367(18)	1940(50)	19(10)
H(20C)	-1990(80)	6930(30)	640(70)	60(18)
H(16)	2800(80)	6000(20)	3090(60)	45(16)

3.15 References:

[1] a) D. Ravelli, S. Protti, M. Fagnoni, *Chem. Rev.* **2016**, *116*, 9850; b) O. Reiser, *Acc. Chem. Res.* **2016**, *49*, 1990; c) N. A. Romero, D. A. Nicewicz, *Chem. Rev.* **2016**, *116*, 10075; d) M. H. Shaw, J. Twilton, D. W. C. MacMillan, *J. Org. Chem.* **2016**, *81*, 6898; e) T. P. Yoon, M. A. Ischay, J. Du, *Nat. Chem.* **2010**, *2*, 527.

[2] a) H. G. Roth, N. A. Romero, D. A. Nicewicz, *Synlett* **2016**, *27*, 714; b) S. Paria, O. Reiser, *Adv. Synth. Catal.* **2014**, *356*, 557.

[3] C. K. Prier, D. A. Rankic, D. W. C. MacMillan, *Chem. Rev.* **2013**, *113*, 5322.

[4] S. K. Pagire, O. Reiser, *Green Chem.* **2017**, *19*, 1721-1725.

[5] T. Maji, A. Karmakar, O. Reiser, *J. Org. Chem.* **2011**, *76*, 736.

[6] a) S. K. Han, T.-M. Hwang, Y. Yoon, J.-W. Kang, *Chemosphere* **2011**, *84*, 1095; b) Z. Lu, T. P. Yoon, *Angew. Chem. Int. Ed.* **2012**, *51*, 10329; c) E. Brachet, T. Ghosh, I. Ghosh, B. König, *Chem. Sci.* **2015**, *6*, 987; d) M. Wrighton, J. Markham, *J. Phys. Chem.* **1973**, *77*, 3042; e) W. L. Dilling, *Chem. Rev.* **1969**, *69*, 845; f) N. J. Turro, *J. Chem. Educ.* **1966**, *43*, 13.

[7] M. S. Lowry, J. I. Goldsmith, J. D. Slinker, R. Rohl, R. A. Pascal, G. G. Malliaras, S. Bernhard, *Chem. Mater.* **2005**, *17*, 5712.

[8] J. B. Metternich, R. Gilmour, *J. Am. Chem. Soc.* **2015**, *137*, 11254.

[9] J. D. Slinker, A. A. Gorodetsky, M. S. Lowry, J. Wang, S. Parker, R. Rohl, S. Bernhard, G. G. Malliaras, *J. Am. Chem. Soc.* **2004**, *126*, 2763.

[10] J. Sun, W. Wu, J. Zhao, *Chem. Eur. J.* **2012**, *18*, 8100.

[11] F. Teplý, *Collect. Czech. Chem. Commun.* **2011**, *76*, 859.

[12] D. P. Hari, B. Konig, *Chem. Comm.* **2014**, *50*, 6688.

[13] a) J. M. Kern, J. P. Sauvage, *J. Chem. Soc. Chem. Commun.* **1987**, 546; b) S. Paria, O. Reiser, *ChemCatChem* **2014**, *6*, 2477; c) S. K. Pagire, S. Paria, O. Reiser, *Org. Lett.* **2016**, *18*, 2106; d) M. Pirtsch, S. Paria, T. Matsuno, H. Isobe, O. Reiser, *Chem. Eur. J.* **2012**, *18*, 7336.

[14] J. Schachtner, P. Bayer, A. Jacobi von Wangelin, *Beilstein J. Org. Chem.* **2016**, *12*, 1798.

[15] R. K. Mohamed, S. Mondal, K. Jorner, T. F. Delgado, V. V. Lobodin, H. Ottosson, I. V. Alabugin, *J. Am. Chem. Soc.* **2015**, *137*, 15441.

[16] a) K. Gilmore, I. V. Alabugin, *Chem. Rev.* **2011**, *111*, 6513; b) I. V. Alabugin, K. Gilmore, M. Manoharan, *J. Am. Chem. Soc.* **2011**, *133*, 12608; c) J. E. Baldwin, *J. C. S. Chem. Comm.* **1976**, 734.

[17] a) O. Anamimoghadam, M. D. Symes, C. Busche, D.-L. Long, S. T. Caldwell, C. Flors, S. Nonell, L. Cronin, G. Bucher, *Org. Lett.* **2013**, *15*, 2970; b) A. C. Hernandez-Perez, S. K. Collins, *Acc. Chem. Res.* **2016**, *49*, 1557; c) S. Parisien-Collette, A. C. Hernandez-Perez, S. K. Collins, *Org. Lett.* **2016**, *18*, 4994; d) O. Kikuchi, *Tetrahedron Lett.* **1981**, *22*, 859.

[18] a) Y. Cheng, J. Yang, Y. Qu, P. Li, *Org. Lett.* **2012**, *14*, 98; b) D. C. Fabry, M. Rueping, *Acc. Chem. Res.* **2016**, *49*, 1969; c) S. K. Han, T.-M. Hwang, Y. Yoon, J.-W. Kang, *Chemosphere* **2011**, *84*, 1095; d) S. Zhu, A. Das, L. Bui, H. Zhou, D. P. Curran, M. Rueping, *J. Am. Chem. Soc.* **2013**, *135*, 1823.

[19] a) R. Singh, G. Panda, *Org. Biomol. Chem.* **2011**, *9*, 4782; b) R. Singh, M. K. Parai, G. Panda, *Org. Biomol. Chem.* **2009**, *7*, 1858.

[20] a) G. Majetich, J. M. Shimkus, *J. Nat. Prod.* **2010**, *73*, 284; b) G. Liang, Y. Xu, I. B. Seiple, D. Trauner, *J. Am. Chem. Soc.* **2006**, *128*, 11022.

[21] J. H. Park, S. V. Bhilare, S. W. Youn, *Org. Lett.* **2011**, *13*, 2228.

[22] A. K. Verma, V. Rustagi, T. Aggarwal, A. P. Singh, *J. Org. Chem.* **2010**, *75*, 7691.

[23] N. A. Markina, R. Mancuso, B. Neuenswander, G. H. Lushington, R. C. Larock, *ACS Comb. Sci.* **2011**, *13*, 265.

[24] Y. Luan, K. S. Barbato, P. N. Moquist, T. Kodama, S. E. Schaus, *J. Am. Chem. Soc.* **2015**, *137*, 3233.

[25] K. Yoshida, H. Shida, H. Takahashi, A. Yanagisawa, *Chem. Eur. J.* **2011**, *17*, 344.

[26] S. Zhu, H. Huang, Z. Zhang, T. Ma, H. Jiang, *J. Org. Chem.* **2014**, *79*, 6113.

[27] M. Dell'Acqua, D. Facoetti, G. Abbiati, E. Rossi, *Synthesis* **2010**, *2010*, 2367.

[28] G. Mariaule, G. Newsome, P. Y. Toullec, P. Belmont, V. Michelet, *Org. Lett.* **2014**, *16*, 4570.

[29] R. R. Jha, R. K. Saunthwal, A. K. Verma, *Org. Biomol. Chem.* **2014**, *12*, 552.

[30] A. Mukherjee, R.-S. Liu, *Org. Lett.* **2011**, *13*, 660.

[31] V. Reddy, A. S. Jadhav, R. Vijaya Anand, *Org. Biomol. Chem.* **2015**, *13*, 3732.

[32] Y. Hu, Z. Shen, H. Huang, *ACS Catal.* **2016**, *6*, 6785.

[33] C. E. McKenna, L. A. Khawli, *J. Org. Chem.* **1986**, *51*, 5467.

[34] S. Mondal, R. K. Mohamed, M. Manoharan, H. Phan, I. V. Alabugin, *Org. Lett.* **2013**, *15*, 5650.

[35] M. A. Calter, N. Li, *Org. Lett.* **2011**, *13*, 3686.

4 Photosensitized regioselective [2+2]-cycloaddition of cinnamates and related alkenes

4.1 Abstract:

A facile, mild and efficient method for the synthesis of substituted cyclobutane derivatives from cinnamates, chalcones, and styrenes has been developed by using a visible-light energy transfer mode. This reaction access a broad range of substituted 4-membered carbocycles in high yields with reasonable regio- and diastereoselectivities without providing external additives. We believe that the excellent regioselectivity is observed due to strong π-π-stacking between two distinct arene groups, whereas diastereoselectivity depends on the electronic effects or *ortho*-substitution of the arene moieties. The efficiency of the presented method is also demonstrated with the formal synthesis of the natural product (±)-Tanegool.

4.2 Introduction:

Strained 4-membered carbocycles are valuable structural building blocks, which commonly features in natural products (Figure 4.1). In general, they are found in insects, microbial species, and the plant kingdom, most of them possess a broad range of biological activities with potential therapeutic uses.[1] In particular, cinnamic acid derived dimers, such as truxinic acid, piperarborenine D, or Sagerinic acid derivatives are particularly important class due to their attractive biological activities (Figure 4.1).[2] In addition, the styrene-based naturally occurring cyclobutanes such as Endiandrin A, di-*O*-methylendiandrin A, Magnosalin (*trans*) or Andamanicin (*cis*) are typically used as anti-inflammatory agents, which potently bind to glucocorticoid receptors (GR).[3] As a consequence, various atom economic methods have been established for the synthesis of cyclobutanes.[4,5] In general, the [2+2]-cycloadditions of alkenes by thermal methods is uncommon,[6] whereas photochemical approaches under UV-irradiation have been established from decades.[7] Recently, visible-light photocatalysis approach has been extensively applied for this transformation.[8]

This chapter has been published:

S. K. Pagire, A. Hossain, L. Traub, S. Kerres, O. Reiser, *Chem. Commun.* **2017**; **DOI**: 10.1039/C7CC06710K. This work has been featured as a cover page of a journal**.**

S.K.P. and O.R. wrote the manuscript.

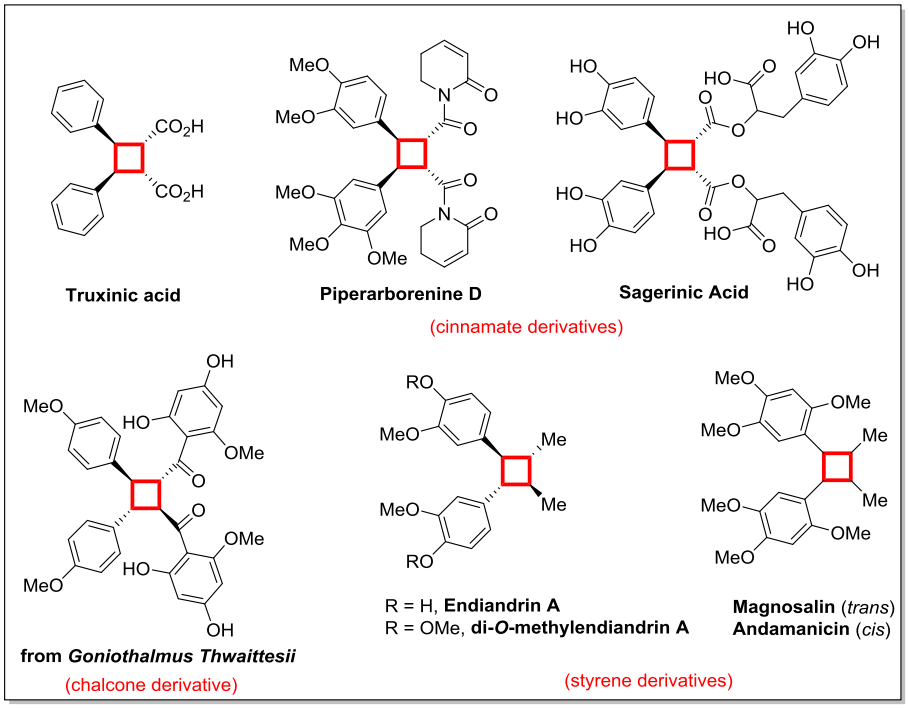

Figure 4.1: Representative biologically active cyclobutanes.

In particular, the group of Yoon has established the visible-light mediated methods for the synthesis of a wide range of cyclobutanes derivatives from different olefins.[9,10] Despite the enormous development of visible-light mediated [2+2]-cycloaddition reactions, surprisingly the cycloaddition of cinnamates or styrenes has not been achieved efficiently so far.[11] This is being summarized in a recent review with the following statement: *Only if rendered intramolecular and only if the reacting centres are spatially close is a [2+2] photocycloaddition with cinnamates and other* β*-arylacrylic acid derivatives possible*.[4]

Though, a number of indirect approaches have been developed for such substrates, which however requiring additional synthetic steps or additives: for instance, Yoon and co-workers have presented a stepwise method for photocycloaddition of desired cyclobutanes. They introduced a cleavable redox auxiliary for α–β-unsaturated carbonyl compounds, which upon dimerization under visible-light provides intermediate cyclobutanes, and subsequent cleavage of the auxiliary affords the aimed cyclobutane carboxamides, esters, or thioesters.[12] Despite its importance, this method requires nevertheless extra steps for the introduction and cleavage of such redox auxiliary. In 2015, Beeler *et al* developed an UV-light mediated flow-technique for the dimerization of cinnamates to afford ester-substituted cyclobutanes with the introduction of a thiourea derived catalyst (Scheme 4.2, top).[13]

4.3 Initial findings: Chemoselective [2+2] cycloaddition

In recent times, we have presented that α-bromocinnamates can be activated either by direct electron transfer[14] or by a dual energy- and electron transfer photocascade[15] process.[16] In particular, the latter process of α-bromocinnamate activation[16] is supposed to be initiated via a stabilized diradical species through energy transfer from the excited [Ir]-photocatalyst. This eventually cleaves off to a vinyl radical upon bromine extrusion in the presence of oxygen. Notably, in the absence of oxygen only *E/Z*-isomerisation product was observed, and in particular, no [2+2]-cycloadduct(s) could be isolated.

With reference to previous chapter 3, Scheme 3.3 (see also a mechanistic discussion from both these chapters), when **1p** was subjected under the standard reaction conditions, to our surprise, we only observed a [2+2]-cycloaddition product **2p** (Scheme 4.1) of the α,β-unsaturated double bonds. Unexpectedly, the triple bonds do not interfere with the diradical (A*) involved, providing only the chemoselective cycloadditions. Initially, we were assuming a direct intramolecular cyclization of diradical on the triple bond should be the more feasible pathway. However, a photosensitized [2+2]-cycloaddition of α,β-unsaturated bonds was turned out to be a dominating pathway. We later noticed that such cycloaddition reactions of corresponding cinnamate derivatives were not explored in the literature.[4]

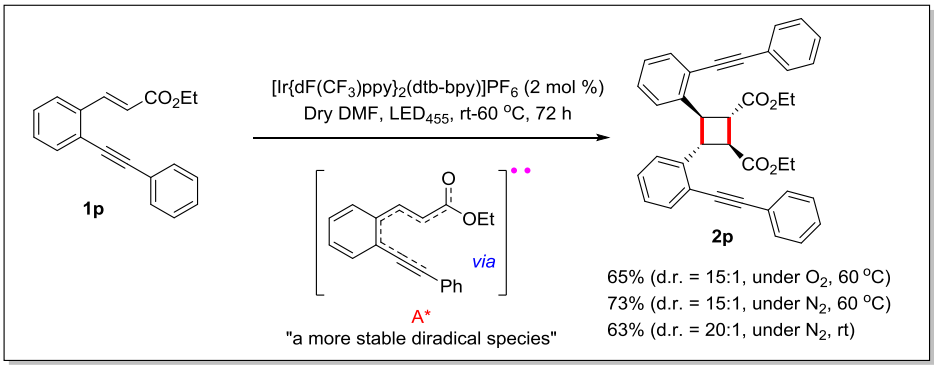

Scheme 4.1: Chemoselective [2+2] cycloaddition.

Accordingly, we questioned about the utilization of such diradicals for simple cinnamates, and indeed, we present here the possibility of a energy transfer protocol for [2+2]-cycloadditions. By this method, not only the synthesis of ester-substituted cyclobutanes are

accessed but the chalcones and styrenes derived cyclobutanes also synthesized in good to excellent yields and selectivities (Scheme 4.2, bottom).

4.4 Beeler's work: Combining UV-light and a thiourea catalyst

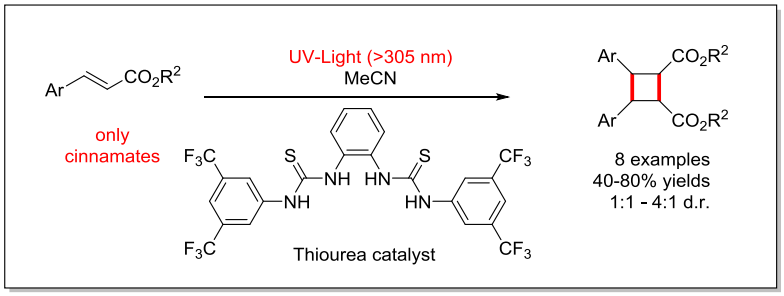

4.5 This work: Visible-light photoredox catalysis

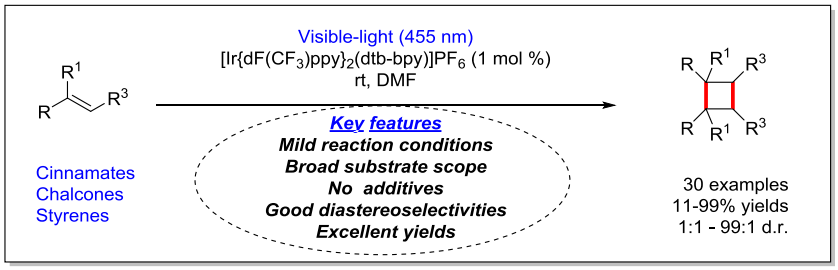

Scheme 4.2: Representative synthesis of cyclobutanes by UV-light and visible light photocatalysis.

In principle, the direct photoinduced electron transfer (PET) to cinnamates is thermodynamically unfavourable owing to its high reduction potential (e.g. –1.79 V vs SCE for **1a**)[17] by typical photocatalysts[18] including $[Ru(bpy)_3]Cl_2$] (–0.81 V vs SCE)[19] or $[Ir\{dF(CF_3)ppy\}_2(dtb\text{-}bpy)]PF_6$ (**Ir-F**: –0.89 V vs SCE).[20] Alternatively, visible-light triggered photoredox catalyzed cycloadditions of these types of unsaturated carbonyl compounds is only feasible by triplet-sensitization or energy transfer mode.[21] Noteworthy, the efficiency of energy transfer is solely independent of the redox potentials of the reacting substrates, which depends on the excited state lifetime of the photocatalysts. Thus, long-lived excited state photocatalysts typically provide better results.

4.6 Results and discussion:

Considering these facts, we began our photochemical experiments by exploring [2+2]-photocycloaddition of ethyl cinnamate **1a** with the $[Ir\{dF(CF_3)ppy\}_2(dtb\text{-}bpy)]PF_6$ photocatalyst, which having longer excited state lifetime (τ = 2300 ns)[20] under an oxygen atmosphere with blue light (Table 4.1, entry 1). Pleasantly, only head-to-head (δ-truxinate, *trans*) **2a** and (β-truxinate, *cis*) **3a** isomers were obtained in a 9:1 ratio and 63% yield. The use of neutral *fac*$[Ir(ppy)_3]$ (τ = 1900 ns, entry 2) and $[Ir(ppy)_2(dtb\text{-}bpy)]PF_6$ (τ = 557 ns, entry 3) gave lower yields.

4.7 Synthesis of 2a and 3a: Catalyst screening and reaction optimization

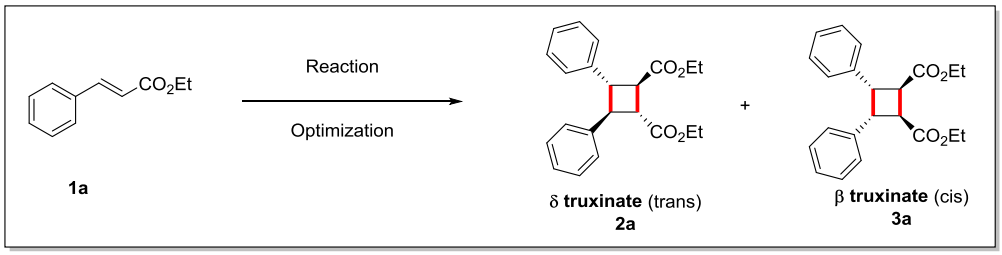

Entry	Photocatalyst (1.0 mol %)	Atmosphere	Yield (%)[b]	d.r. (δ/β)[c]
01	$[Ir\{dF(CF_3)ppy\}_2(dtb\text{-}bpy)]PF_6$	O_2	63	9:1
02	*fac*$[Ir(ppy)_3]$	O_2	44	9:1
03	$[Ir(ppy)_2(dtb\text{-}bpy)]PF_6$	O_2	18	9:1
04	$[Cu(dap)_2Cl]$	O_2	traces	-
05	$[Ru(bpy)_3Cl_2]$	O_2	traces	-
06	$[Ir\{dF(CF_3)ppy\}_2(dtb\text{-}bpy)]PF_6$	N_2	96	9:1
07[d,e]	$[Ir\{dF(CF_3)ppy\}_2(dtb\text{-}bpy)]PF_6$	N_2	78	ND[f]
08	Rose bengal, 530 nm	N_2	-	-
09	No catalyst	N_2	NR[g]	-
10	$[Ir\{dF(CF_3)ppy\}_2(dtb\text{-}bpy)]PF_6$ no light	N_2	NR[g]	-

Table 4.1: Reaction conditions: [a] Ethyl cinnamate **1a** (1.0 mmol), photocatalyst (1.0 mol %), dry DMF (2 mL), $LED_{455,}$ 72 h, LED_{455}, room temperature. [b] Isolated yields. [c] Determined by crude ^{1}H-NMR analysis. [d] 0.5 mol % photocatalyst used. [e] Reaction time was 84 h. [f] d.r. not determined. [g] No reaction. [h] The optimizations are done by *Santosh K. Pagire* and *Asik Hossain*.

While $[Cu(dap)_2Cl]$[22] (τ = 270 ns) and $[Ru(bpy)_3Cl_2]$, (τ = 1100 ns) did not provide any product under the identical conditions (Table 4.1, entry 4, 5). Lowering the catalyst concentration to 0.5 mol% (Table 4.1, entry 7) gave lower, but still respectable yields (78%). No reaction was observed in the presence of the typical triplet sensitizer rose bengal, highlighting the importance of the [Ir]-photocatalyst (Table 4.1, entry 8). The control experiments suggested the importance of both, [Ir]-photocatalyst and visible-light together (Table 4.1, entries 9, 10). Obviously, the best catalyst (**Ir-F**, Table 4.1, entry 1) was selected for next optimizations: Gratifyingly, the cycloaddition proceeded much more efficiently under nitrogen (N_2) atmosphere (Table 4.1, entry 6), giving rise to **2a**/**3a** (9:1) in 96% yield.

4.8 Substrate scope: Cinnamates and Chalcones

Having identified the best conditions (Table 4.1, entry 6), next, the substrate scope was examined. With the standard conditions, methyl cinnamate (**1b**) provided **2b/3b** in 89% yield and 10:1 diastereoselectivity, also improving the literature report that yielded the desired cycloadduct in lower yields and selectivity (60%; up to 4:1, Scheme 4.2).[13] Similarly, the cycloaddition of β-methyl ethyl cinnamate (**1c**) provides solely the δ-diastereomer **2c** in 88% yield. Moreover, *para*-substituted cinnamates with electron donating substituents (+I/+M) or weak acceptors (–I/–M) groups afford the thermodynamically favored *all-trans* substituted cyclobutanes in good yields and diastereoselectivities (**2d/3d** to **2h/3h,** Table 4.2).

In contrast, strong electron withdrawing groups decrease the diastereoselectivity to a great extent, most likely due to the destabilisation of the radical species formed as intermediates (see the mechanistic discussion). Notably, substitution in *ortho*-position of the arene moiety dramatically enhances the diastereoselectivity up to 20:1 (Table 4.2 and Scheme 4.1; **2n/3n** and **2p/3p**, respectively). Furthermore, relevant for naturally occurring cyclobutanes (*cf.* Figure 4.1), di- or tri-arylsubstituted cinnamates can also be engaged in photodimerization, providing cyclobutanes **2l/3l** and **2m/3m** in reasonable yields and diastereoselectivities. In particular, the isolated δ-isomer (**3l**) has already been recognized as a critical intermediate for the synthesis of lignane natural product (±)-Tanegool.[4,23] Moreover, Furan, thiophene, and *N*-Boc-pyrrole substituted cinnamates were also suitable substrates,[4,24] providing the desired head-to-head dimers **2q-s**/**3q-s** in good yields, however, with low diastereoselectivity (~1.7:1). Interestingly, for the first two substrates, the unexpected head-to-tail dimers **4q**, **4r** could also be detected in minute amounts (see ^{1}H-NMR in the ESI), whereas, in the case of

the pyrrole derivative, only the head-to-head cycloaddition product **2s**/**3s** was obtained. The limitation of our method was observed for the indole derivative, it only gave corresponding cycloadduct product **2t** in 11% yield (Table 4.2).

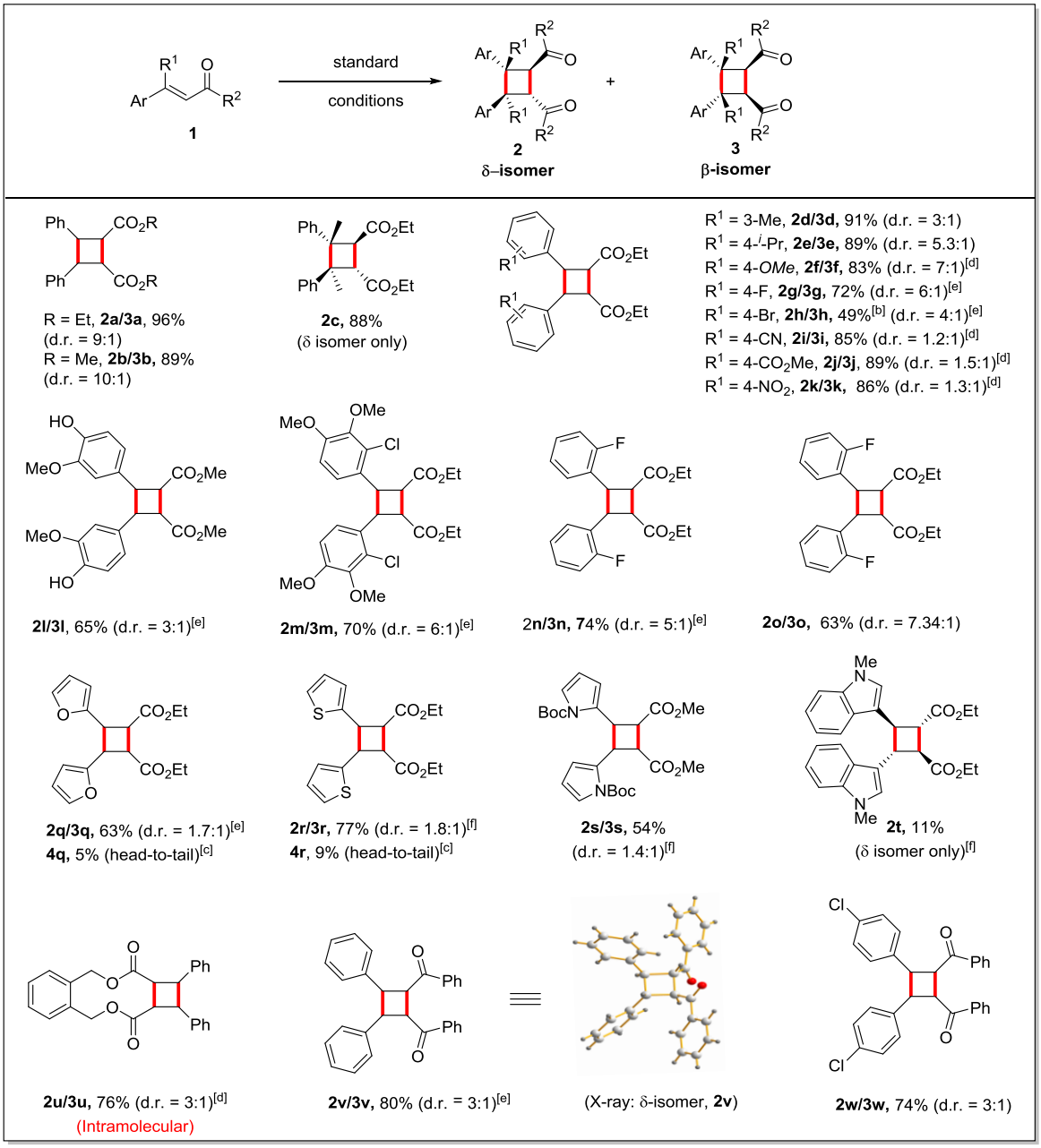

Table 4.2: Reaction conditions: [a] Substrate **1** (1.0 mmol), [Ir{dF(CF_3)ppy}$_2$(dtb-bpy)]PF_6 (1.0 mol %), dry DMF (2 mL), LED_{455}, 72 h, LED_{455}, room temperature, the diastereomeric ratios were determined either by crude ^{1}H-NMR analysis or on the basis of yield of isolated products. [b] Reaction time was 96 h. [c] Head-to-tail products were detected by ^{1}H-NMR analysis. [d] These compounds are isolated by *Lukas Traub*. [e] These compounds are isolated by *Asik Hossain*. [f] These compounds are isolated by *Sabine Kerres*.

Due to the fast *cis/trans* isomerization process (or relaxation of the excited state), the [2+2] photocycloaddition reactions of chalcones are relatively rare.[25] Nevertheless, we were pleased to notice that chalcones also efficiently underwent a complete dimerization under the standard conditions, providing the desired products (**2v/3v** and **2w/3w**) in good yields with 3:1 diastereoselectivity. In addition, the δ-isomer of **2v** could also be isolated and unambiguously characterised by single X-ray crystallography (Table 4.2), confirming the stereochemistry of a major isomer. Unfortunately, the attempted photodimerization of corresponding sulfone, cyano, or nitro substituted alkenes only led to the *E/Z*-isomerization of the starting materials, and no cyclobutanes could be detected.

4.9 Substrate scope: Styrenes

Having established a protocol for α-β-unsaturated carbonyl compounds, next, we explored the intermolecular [2+2] photo-dimerization of styrenes **5** by triplet sensitization,[21] given the importance of the resulting cyclobutanes for biologically active molecules (*cf.* Figure 4.1). In literature, the intermolecular styrene cycloadditions by photochemical alkene oxidation were already reported under visible-light conditions, but they require the electron rich systems to obtain desired products.[10,26] Pleasingly, in our case (Table 4.3), a range of electronically unbiased styrenes **5a,c-e**, but also the nitro-substituted styrene **5b** provided the corresponding head-to-head cycloadducts **6** in excellent yields. Surprisingly, the corresponding 1,2-diphenyl ethene (*E*-Stilbene) only undergoes *cis/trans* isomerization.

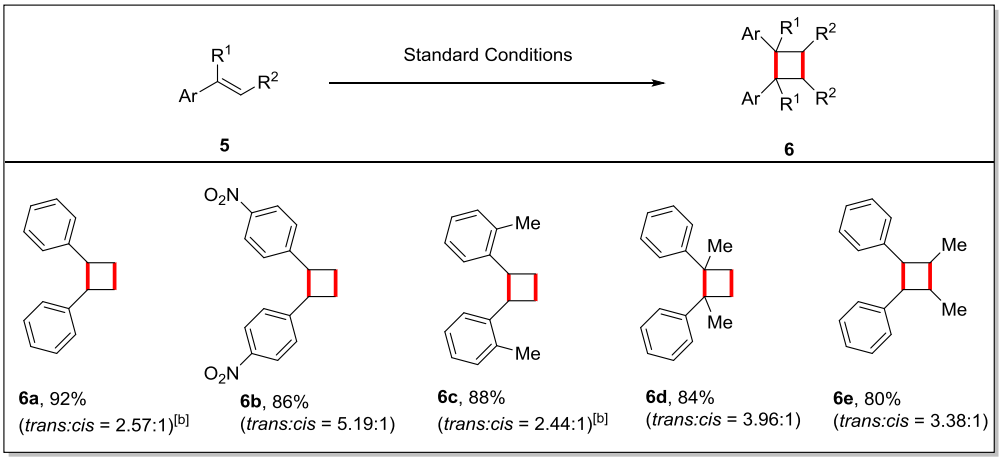

Table 4.3: Reaction conditions: [a] Unless otherwise stated, the identical conditions from Table 4.2 were used. [b] These compounds are isolated by *Asik Hossain.*

4.10 [2+2] cross-cycloaddition of cinnamates

The selective synthesis of unsymmetrical cyclobutanes derivatives is a long-standing problem in organic synthesis and only a few protocols are known.[27] In line with our strategy, we next questioned if two electronically differentiated cinnamates would allow cross-cycloaddition beyond the statistically assumed distribution of possible products (Table 4.4). Indeed, in all cases tested the expected cross-coupling products were obtained; however, no acceptable bias towards the cross-coupled cinnamates was observed.

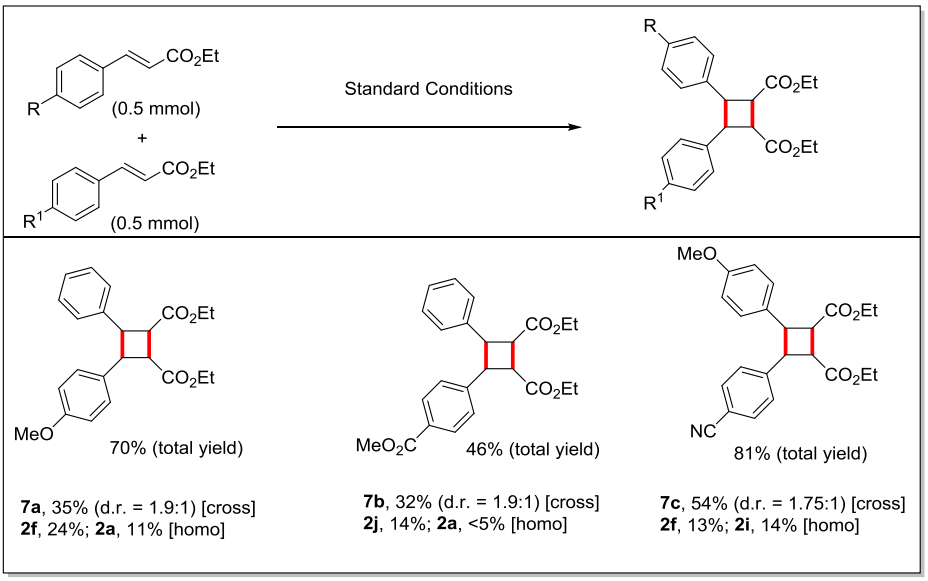

Table 4.4: Reaction conditions: [a] Substrate **1** (1.0 mmol, in total), [Ir{dF(CF$_3$)ppy}$_2$(dtb-bpy)]PF$_6$ (1.0 mol %), dry DMF (2 mL), LED$_{455,}$ 72 h, LED$_{455}$, room temperature, the diastereomeric ratios were determined either by crude ^{1}H-NMR analysis or on the basis of yield of isolated products. [b] All the cross-cycloaddition reactions were performed by *Lukas Traub.*

4.11 Proposed reaction mechanism

Following the underlying principle put forward by Haag and co-workers for the cycloaddition of cinnamates,[28] we, therefore, propose that the method described here should also proceed by energy transfer mode through diradical formation (Figure 4.2).[29] The visible-light excitation of the [Ir]-photocatalyst forms the excited Ir*, which transfers triplet-energy to the substrate **1** to form the activated diradical (triplet) species **1***, followed by coupling with **1** to give rise to **A**. In full agreement with the experimental outcomes, we reasoned, the regioselective (head-to-head) product formation is only possible due to the strong π-π

stacking of an arene moiety. However, the stereoselectivity is dependent on the stabilization of the adjacent benzylic radicals (Figure 4.2, **A**), being more influential for electron donating substituted substrates, which consequently undergo slower ring (as compared to the electron withdrawing substituents) closure that enables equilibrating **A** to the sterically most favourable all-trans arrangements.

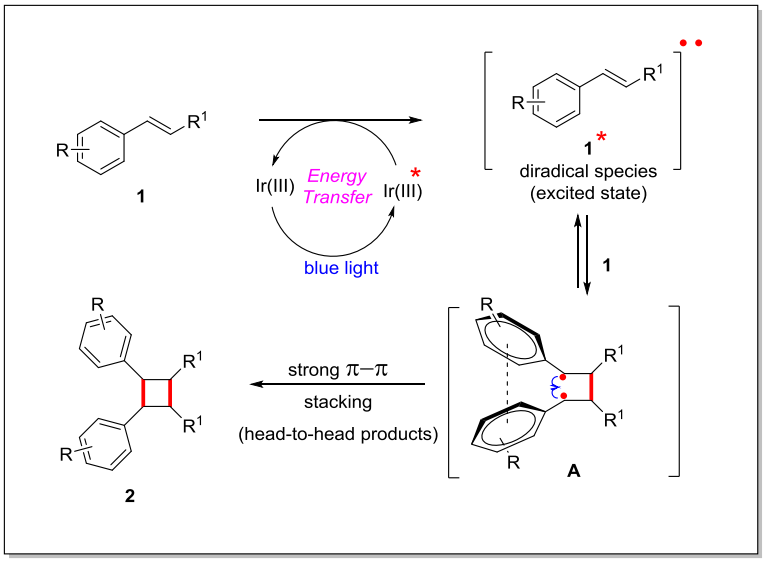

Figure 4.2: Proposed reaction mechanism.

4.12 Conclusion:

To summarize, we have developed for the first time an efficient strategy for homo-cycloaddition of cinnamates, styrenes, and chalcones which offers a range of substituted cyclobutanes in excellent yields with moderate to good diastereoselectivities under the sustainable reaction conditions. In addition, we have also shown that cross-cycloaddition also possible with an appropriate combination of the reactants. Moreover, the scope of this strategy was extended by carrying out the intramolecular and chemoselective synthesis of cyclobutanes. Finally, the value of this method highlighted with the formal synthesis of lignane natural product (±)-Tanegool.

4.13 Experimental section:

4.13.1 General procedure (GP-1) for visible-light photocatalysis:

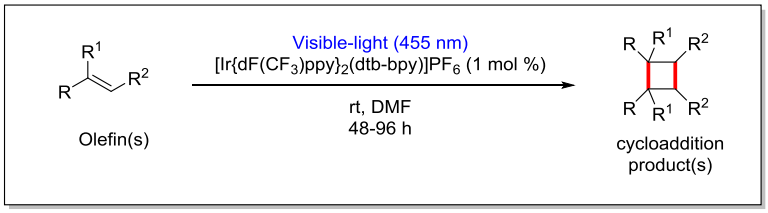

An oven dried 10 mL schlenk flask was charged with olefin (1.00 mmol, 1.00 equiv) and $[Ir\{dF(CF_3)ppy\}_2(dtb\text{-}bpy)]PF_6$ (11.22 mg, 0.01 equiv, 1.0 mol %) in 2.0 mL anhydrous DMF. The resulting suspension was deoxygenated by three freeze-pump-thaw cycles. The reaction mixture was irradiated with blue light emitting diode (LED, λ_{max} = 455 nm) at room temperature for 72 h. Then the reaction mixture was saturated with brine (15 mL) and extracted with ethyl acetate (3 x 20 mL). After drying the combined organic layers on Na_2SO_4, the resulting solution was concentrated *in vacuo*. Purification by silica-gel column chromatography using hexanes and ethyl acetate as eluents afforded cycloaddition product(s).

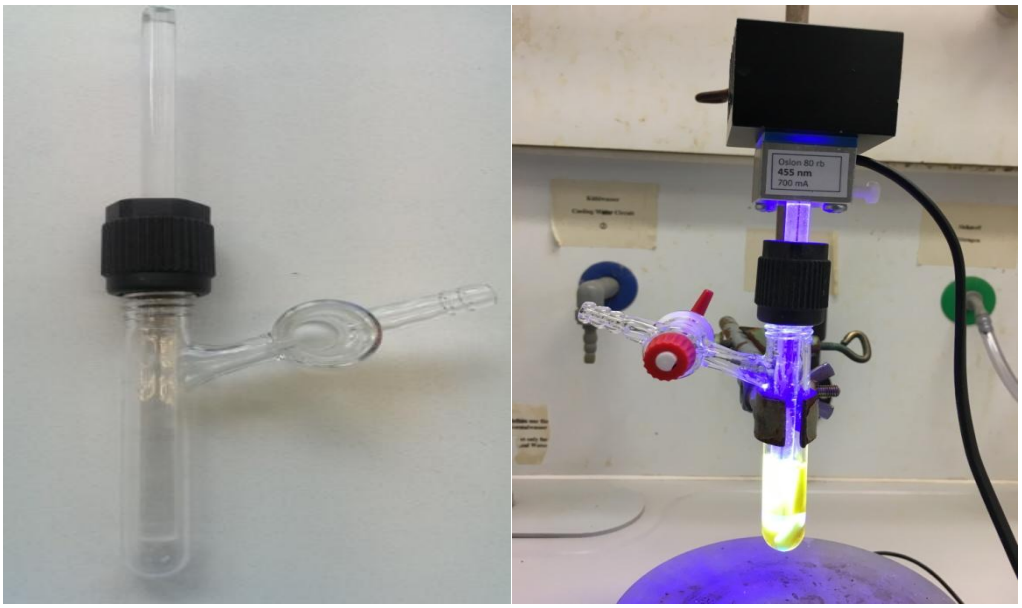

Figure 4.3: Experimental set-up the cycloaddition reaction.

Diethyl (1*R*,2*R*,3*S*,4*S*)-3,4-diphenylcyclobutane-1,2-dicarboxylate (2a):

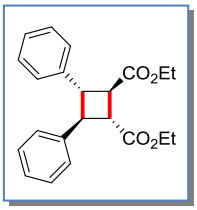

Following **GP-1**, **2a** was prepared from ethyl cinnamate **1a** (176.2 mg, 1.0 mmol, 1.00 equiv) and [Ir{dF(CF$_3$)ppy}$_2$(dtb-bpy)]PF$_6$ (11.22 mg, 0.01 equiv, 1.0 mol %) in dry DMF (2 mL). The crude product was purified by column chromatography (silica gel, hexanes–EtOAc, 9:1, R_f = 0.43) to afford **2a** as a colourless oil (153 mg, 87% yield).

^{1}H-NMR (300 MHz, CDCl$_3$): δ 7.45 – 7.06 (m, 10H), 4.22 (q, *J* = 7.1 Hz, 4H), 3.79 (d, *J* = 9.6 Hz, 2H), 3.48 (d, *J* = 9.5 Hz, 2H), 1.29 (t, *J* = 7.1 Hz, 6H).

^{13}C-NMR (75 MHz, CDCl3): δ 172.72, 141.31, 128.73, 127.19, 126.97, 61.13, 47.09, 44.95, 14.37.

IR (neat, cm^{-1}): 3030, 2981, 2936, 1723, 1602, 1496, 1449, 1416, 1388, 1368, 1317, 1198, 1156, 1095, 1030, 856, 751, 696.

EI-MS: exact m/z calculated for $C_{22}H_{24}O_4$ $(M)^+$: 352.16691; Found: 352.16799 $(M)^+$.

Diethyl (1*R*,2*S*,4*S*)-3,4-diphenylcyclobutane-1,2-dicarboxylate (3a):

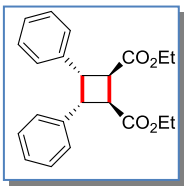

Following **GP-1**, **3a** was prepared from ethyl cinnamate **1a** (176.2 mg, 1.0 mmol, 1.00 equiv) and [Ir{dF(CF$_3$)ppy}$_2$(dtb-bpy)]PF$_6$ (11.22 mg, 0.01 equiv, 1.0 mol %) in dry DMF (2 mL). The crude product was purified by column chromatography (silica gel, hexanes–EtOAc, 9:1, R_f = 0.39) to afford **3a** as a colourless oil (17 mg, 9% yield).

^{1}H-NMR (300 MHz, CDCl$_3$): δ 7.37 – 7.15 (m, 4H), 7.12 – 6.95 (m, 4H), 6.94 – 6.85 (m, 2H), 4.40 – 4.32 (m, 2H), 4.16 (q, *J* = 7.1 Hz, 4H), 3.78 (m, 2H), 1.23 (t, *J* = 7.1 Hz, 6H).

^{13}C-NMR (75 MHz, CDCl$_3$): δ 172.65, 138.88, 128.15, 127.98, 126.47, 61.16, 45.00, 43.61, 14.39.

IR (neat, cm^{-1}): 3030, 2981, 2935, 1725, 1602, 1496, 1449, 1267, 1196, 1158, 1095, 1062, 1015, 856, 749, 696.

EI-MS: exact m/z calculated for $C_{22}H_{24}O_4$ $(M)^+$: 352.16691; Found: 352.16799 $(M)^+$.

Dimethyl (1*R*,2*R*,3*S*,4*S*)-3,4-diphenylcyclobutane-1,2-dicarboxylate (2b):

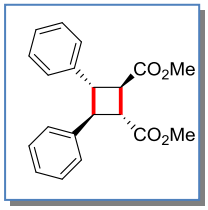

Following **GP-1**, **2b** was prepared from methyl cinnamate **1b** (162.2 mg, 1.0 mmol, 1.00 equiv) and [Ir{dF(CF$_3$)ppy}$_2$(dtb-bpy)]PF$_6$ (11.22 mg, 0.01 equiv, 1.0 mol %) in dry DMF (2 mL). The crude product was purified by column chromatography (silica gel, hexanes–EtOAc, 9:1, R_f = 0.40) to afford **2b** as a white solid (131 mg, 81% yield).

^{1}H-NMR (300 MHz, CDCl$_3$): δ 7.40 – 7.22 (m, 10H), 3.78 (m, 2H), 3.75 (s, 6H), 3.56 – 3.50 (m, 2H).

^{13}C-NMR (75 MHz, CDCl$_3$): δ 173.12, 141.08, 128.77, 127.29, 126.96, 52.34, 47.47, 44.53;

IR (neat, cm^{-1}): 3031, 2950, 2923, 2853, 1725, 1602, 1496, 1433, 1313, 1281, 1200, 1167, 1115, 1023, 1006, 905, 775, 753, 733, 696.

HRMS (ESI): exact m/z calculated for $C_{20}H_{21}O_4$ $(M+H)^+$: 325.1434; Found: 325.1443 $(M+H)^+$.

Mp: 69-71 ^{o}C (decomposed).

Dimethyl (1*R*,2*S*,4*S*)-3,4-diphenylcyclobutane-1,2-dicarboxylate (3b):

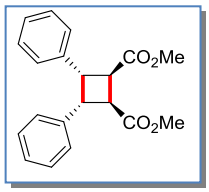

Following **GP-1**, **3b** was prepared from methyl cinnamate **1b** (162.2 mg, 1.0 mmol, 1.00 equiv) and [Ir{dF(CF$_3$)ppy}$_2$(dtb-bpy)]PF$_6$ (11.22 mg, 0.01 equiv, 1.0 mol %) in dry DMF (2 mL). The crude product was purified by column chromatography (silica gel, hexanes–EtOAc, 9:1, R_f = 0.36) to afford **3b** as a colourless oil (13 mg, 8% yield).

^{1}H-NMR (300 MHz, CDCl$_3$): δ 7.15 – 7.01 (m, 6H), 6.95 – 6.89 (m, 4H), 4.41 (dd, *J* = 3.9, 2.3 Hz, 2H), 3.86 (dt, *J* = 3.3, 0.9 Hz, 2H), 3.76 (s, 6H).

^{13}C-NMR (75 MHz, CDCl$_3$): δ 173.13, 138.61, 128.17, 127.92, 126.54, 52.36, 45.08, 43.39.

IR (neat, cm^{-1}): 3029, 2951, 2923, 1726, 1602, 1496, 1434, 1367, 1270, 1200, 1163, 1062, 1029, 967, 748, 695.

HRMS (ESI): exact m/z calculated for $C_{20}H_{21}O_4$ $(M+H)^+$: 325.1434; Found: 325.1443 $(M+H)^+$.

Diethyl (1*S*,2*S*,3*S*,4*S*)-3,4-dimethyl-3,4-diphenylcyclobutane-1,2-dicarboxylate (2c):

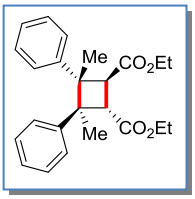

Following **GP-1**, **2c** was prepared from ethyl (*E*)-3-phenylbut-2-enoate **1c** (190.2 mg, 1.0 mmol, 1.00 equiv) and [Ir{dF(CF$_3$)ppy}$_2$(dtb-bpy)]PF$_6$ (11.22 mg, 0.01 equiv, 1.0 mol %) in dry DMF (2 mL). The crude product was purified by column chromatography (silica gel, hexanes–EtOAc, 9:1, R_f = 0.56) to afford **2c** as a colourless oil (167 mg, 88% yield).

^{1}H-NMR (300 MHz, CDCl$_3$): δ 7.45 – 7.27 (m, 6H), 7.21 (dd, *J* = 7.7, 1.7 Hz, 4H), 5.92 (d, *J* = 1.3 Hz, 2H), 4.01 (q, *J* = 7.1 Hz, 4H), 2.19 (d, *J* = 1.4 Hz, 6H), 1.09 (t, *J* = 7.1 Hz, 6H).
^{13}C-NMR (75 MHz, CDCl$_3$): δ 166.08, 155.57, 141.00, 128.03, 127.87, 126.95, 117.90, 59.90, 27.31, 14.10.
IR (neat, cm^{-1}): 2979, 2937, 1722, 1705, 1638, 1600, 1575, 1492, 1441, 1373, 1273, 1227, 1155, 1095, 1075, 1043, 954, 912, 860, 766, 696.
EI-MS: exact m/z calculated for $C_{24}H_{28}O_4$ $(M)^+$: 380.19821; Found: 380.19819 $(M)^+$.

Diethyl (1*S*,2*S*,3*R*,4*R*)-3,4-di-*m*-tolylcyclobutane-1,2-dicarboxylate (2d):

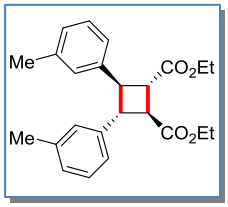

Following **GP-1**, **2d** was prepared from ethyl (*E*)-3-(*m*-tolyl)acrylate **1d** (190.2 mg, 1.0 mmol, 1.00 equiv) and [Ir{dF(CF$_3$)ppy}$_2$(dtb-bpy)]PF$_6$ (11.22 mg, 0.01 equiv, 1.0 mol %) in dry DMF (2 mL). The crude product was purified by column chromatography (silica gel, hexanes–EtOAc, 9:1, R_f = 0.49) to afford **2d** as a colourless oil (130 mg, 68% yield).

^{1}H-NMR (300 MHz, CDCl$_3$): δ 7.24 (t, *J* = 7.5 Hz, 2H), 7.18 – 7.05 (m, 6H), 4.24 (q, *J* = 7.1 Hz, 4H), 3.82 – 3.71 (m, 2H), 3.49 – 3.41 (m, 2H), 2.37 (s, 6H), 1.31 (t, *J* = 7.1 Hz, 6H).
^{13}C-NMR (75 MHz, CDCl$_3$): δ 172.79, 141.29, 138.29, 128.58, 127.91, 127.66, 124.08, 61.06, 46.95, 45.02, 21.58, 14.35.
IR (neat, cm^{-1}): 2980, 2924, 2870, 1725, 1606, 1589, 1489, 1460, 1445, 1410, 1385, 1368, 1310, 1197, 1156, 1095, 1021, 857, 778, 698.
EI-MS: exact m/z calculated for $C_{24}H_{28}O_4$ $(M)^+$: 380.19821; Found: 380.19819 $(M)^+$.

Diethyl (1*R*,2*S*,4*S*)-3,4-di-*m*-tolylcyclobutane-1,2-dicarboxylate (3d):

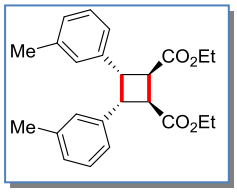

Following **GP-1**, **3d** was prepared from ethyl (*E*)-3-(*m*-tolyl)acrylate **1d** (190.2 mg, 1.0 mmol, 1.00 equiv) and [Ir{dF(CF_3)ppy}$_2$(dtb-bpy)]PF_6 (11.22 mg, 0.01 equiv, 1.0 mol %) in dry DMF (2 mL). The crude product was purified by column chromatography (silica gel, hexanes–EtOAc, 9:1, R_f = 0.43) to afford **3d** as a colourless oil (43 mg, 23% yield).

^{1}H-NMR (300 MHz, $CDCl_3$): δ 7.24 – 6.83 (m, 6H), 6.77 – 6.67 (m, 2H), 4.34 (dd, *J* = 3.9, 2.3 Hz, 2H), 4.20 (q, *J* = 7.1 Hz, 4H), 3.85 – 3.78 (m, 2H), 2.19 (s, 6H), 1.29 (t, *J* = 7.1 Hz, 6H).

^{13}C-NMR (75 MHz, $CDCl_3$): δ 172.71, 138.82, 137.51, 128.87, 127.92, 127.13, 125.00, 61.09, 44.91, 43.64, 21.49, 14.38.

IR (neat, cm^{-1}): 2979, 2924, 2856, 1727, 1606, 1589, 1489, 1460, 1446, 1372, 1349, 1300, 1274, 1198, 1159, 1095, 1066, 1024, 878, 857, 776, 698.

EI-MS: exact m/z calculated for $C_{24}H_{28}O_4$ $(M)^+$: 380.19821; Found: 380.19819 $(M)^+$.

Diethyl (1*S*,2*S*,3*R*,4*R*)-3,4-bis(4-isopropylphenyl)cyclobutane-1,2-dicarboxylate (2e):

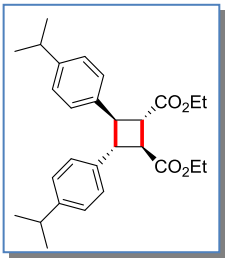

Following **GP-1**, **2e** was prepared from ethyl (*E*)-3-(4-isopropylphenyl)acrylate **1e** (218.3 mg, 1.0 mmol, 1.00 equiv) and [Ir{dF(CF_3)ppy}$_2$(dtb-bpy)]PF_6 (11.22 mg, 0.01 equiv, 1.0 mol %) in dry DMF (2 mL). The crude product was purified by column chromatography (silica gel, hexanes–EtOAc, 9:1, R_f = 0.52) to afford **2e** as a colourless oil (163 mg, 75% yield).

^{1}H-NMR (300 MHz, $CDCl_3$): δ 7.32 – 7.26 (m, 4H), 7.24 – 7.18 (m, 4H), 4.23 (q, *J* = 7.1 Hz, 4H), 3.84 – 3.73 (m, 2H), 3.48 – 3.40 (m, 2H), 2.92 (m, 2H), 1.31 (t, *J* = 7.1 6H), 1.27 (d, *J* = 6.9 Hz, 12H).

^{13}C-NMR (75 MHz, $CDCl_3$): δ 172.83, 147.67, 138.82, 126.93, 126.71, 61.03, 46.70, 45.11, 33.88, 24.11, 14.37.

IR (neat, cm^{-1}): 2960, 2931, 2871, 1726, 1513, 1461, 1409, 1366, 1316, 1263, 1199, 1156, 1097, 1033, 1017, 824.

EI-MS: exact m/z calculated for $C_{28}H_{36}O_4$ $(M)^+$: 436.26081; Found: 436.25936 $(M)^+$.

Diethyl (1*R*,2*S*,4*S*)-3,4-bis(4-isopropylphenyl)cyclobutane-1,2-dicarboxylate (3e):

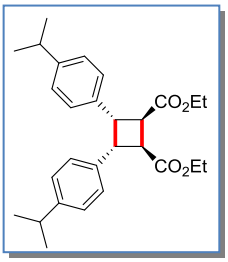

Following **GP-1**, **3e** was prepared from ethyl (*E*)-3-(4-isopropylphenyl)acrylate **1e** (218.3 mg, 1.0 mmol, 1.00 equiv) and [Ir{dF(CF$_3$)ppy}$_2$(dtb-bpy)]PF$_6$ (11.22 mg, 0.01 equiv, 1.0 mol %) in dry DMF (2 mL). The crude product was purified by column chromatography (silica gel, hexanes–EtOAc, 9:1, R_f = 0.46) to afford **3e** as a colourless oil (31 mg, 14% yield).

^{1}H-NMR (300 MHz, CDCl$_3$): δ 7.23 – 6.90 (m, 4H), 6.88 – 6.78 (m, 4H), 4.42 – 4.26 (m, 2H), 4.19 (q, *J* = 7.1 Hz, 4H), 3.85 – 3.78 (m, 2H), 2.88 – 2.60 (m, 2H), 1.28 (t, *J* = 7.1 Hz, 6H), 1.12 (d, *J* = 7.0 Hz, 12H).

^{13}C-NMR (75 MHz, CDCl$_3$): δ 172.81, 146.95, 136.29, 127.89, 126.03, 61.06, 44.75, 43.62, 33.92, 33.74, 29.88, 24.16, 24.09, 14.39.

IR (neat, cm^{-1}): 2959, 2925, 2855, 1727, 1606, 1513, 1461, 1373, 1265, 1191, 1158, 1097, 1056, 1017, 827.

EI-MS: exact m/z calculated for $C_{28}H_{36}O_4$ $(M)^+$: 436.26081; Found: 436.25936 $(M)^+$.

Diethyl (1*R*,2*R*,3*S*,4*S*)-3,4-bis(4-methoxyphenyl)cyclobutane-1,2-dicarboxylate (2f):

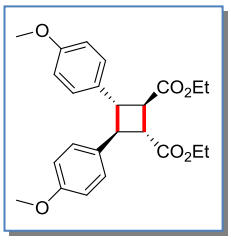

Following **GP-1**, **2f** was prepared from ethyl (*E*)-3-(4-methoxyphenyl)acrylate **1f** (206.2 mg, 1.0 mmol, 1.00 equiv) and [Ir{dF(CF$_3$)ppy}$_2$(dtb-bpy)]PF$_6$ (11.22 mg, 0.01 equiv, 1.0 mol %) in dry DMF (2 mL). The crude product was purified by column chromatography (silica gel, hexanes–EtOAc, 5:1, R_f = 0.40) to afford **2f** as a colourless oil (122 mg, 59% yield) and a mixture of **2f/3f** as yellow oil (49 mg, 27% yield, 1:0.84 d.r.).

^{1}H-NMR (300 MHz, CDCl$_3$, mixture of both isomers): δ 7.24 – 7.17 (m, 2H), 6.88 – 6.81 (m, 4H), 6.66 (d, *J* = 8.8 Hz, 2H), 4.29 (dd, *J*=4.0, 2.2, 1H), 4.19 (qd, *J*=7.1, 1.6, 4H), 3.79 (s, 3H), 3.77 (d, *J* =1.4 Hz, 1H), 3.76 – 3.72 (m, 1H), 3.71 (d, *J* = 2.2 Hz, 2H), 3.64 – 3.59 (m, 1H), 3.39 – 3.34 (m, 1H), 1.27 (td, *J* = 7.1, 4.5 Hz, 6H).

^{1}H-NMR (300 MHz, CDCl$_3$, *trans* isomer): δ 7.21 – 7.13 (m, 2H), 6.85 – 6.74 (m, 2H), 6.85 – 6.76 (m, 2H), 4.14 (q, *J* = 7.1, 2H), 3.77 – 3.70 (m, 6H), 3.61 – 3.54 (m, 1H), 3.36 – 3.28 (m, 1H), 1.21 (t, *J* = *7.1* Hz, 6H).

^{13}C-NMR (75 MHz, $CDCl_3$, *trans* isomer): δ 172.71, 158.67, 133.38, 127.95, 113.99, 77.38, 77.06, 76.74, 60.94, 55.29, 46.94, 45.01, 14.27.

IR (neat, cm^{-1}): 2982, 2836, 1722, 1610, 1513, 1461, 1245, 1033, 826, 731.

HRMS (ESI): exact m/z calculated for mixture: $C_{24}H_{28}O_6$ $(M+H)^+$: 413.1959; Found: 413.1959 $(M+H)^+$; For *trans*: exact m/z calculated for $C_{24}H_{28}O_6$ $(M+H)^+$: 413.1959; Found: 413.1959 $(M+H)^+$; For *cis*: exact m/z calculated for $C_{24}H_{28}O_6$ $(M+H)^+$: 413.1959; Found: 413.1961 $(M+H)^+$.

Diethyl-3,4-bis(4-fluorophenyl)cyclobutane-1,2-dicarboxylate (2g/3g):

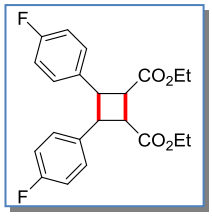

Following **GP-1**, **2g/3g** was prepared from ethyl (*E*)-3-(4-fluorophenyl)acrylate **1g** (194.2 mg, 1.0 mmol, 1.00 equiv) and [Ir{dF(CF_3)ppy}$_2$(dtb-bpy)]PF_6 (11.22 mg, 0.01 equiv, 1.0 mol %) in dry DMF (2 mL). The crude product was purified by column chromatography (silica gel, hexanes–EtOAc, 9:1, R_f = 0.20 (*trans*), R_f = 0.17 (*cis*) to afford mixture of **2g/3g** as a white solid (139 mg, 72% yield; d.r. = 6:1).

^{1}H-NMR (300 MHz, $CDCl_3$, major isomer): δ 7.39 – 7.12 (m, 4H), 7.01 (t, *J* = 8.6 Hz, 4H), 4.20 (q, *J* = 7.1 Hz, 4H), 3.75 – 3.55 (m, 2H), 3.47 – 3.31 (m, 2H), 1.27 (t, *J* = 7.1 Hz, 6H).

^{13}C-NMR (75 MHz, $CDCl_3$, major isomer): δ 172.52, 162.12 (d, $^1J_{C\text{-}F}$ = 245.5 Hz), 136.78 (d, $^4J_{C\text{-}F}$ = 3.1 Hz), 128.51 (d, $^3J_{C\text{-}F}$ = 8.0 Hz), 115.68 (d, $^2J_{C\text{-}F}$ = 21.4 Hz), 61.29, 46.78, 45.05, 14.38.

^{19}F-NMR (282 MHz, $CDCl_3$): δ -115.85.

IR (neat, cm^{-1}): 2989, 2944, 1718, 1601, 1509, 1473, 1447, 1393, 1368, 1300, 1215, 1196, 1155, 1109, 1033, 1015, 965, 870, 824, 791, 671.

EI-MS: exact m/z calculated for $C_{22}H_{22}O_4F_2$ $(M)^+$: 388.14807; Found: 388.14844 $(M)^+$.

Mp: 60-62 ^{o}C (decomposed).

Diethyl-3,4-bis(4-bromophenyl)cyclobutane-1,2-dicarboxylate (2h/3h):

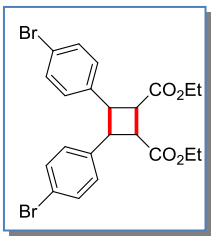

Following **GP-1**, **2h/3h** was prepared from ethyl (*E*)-3-(4-bromophenyl)acrylate **1h** (255.1 mg, 1.0 mmol, 1.00 equiv) and [Ir{dF(CF_3)ppy}$_2$(dtb-bpy)]PF_6 (11.22 mg, 0.01 equiv, 1.0 mol %) in dry DMF (2 mL). The crude product was purified by column chromatography (silica gel, hexanes–EtOAc, 9:1, R_f = 0.20 (*trans*), R_f = 0.17 (*cis*) to afford mixture of **2h/3h** as a white solid (125 mg, 49% yield; d.r. = 4:1).

^{1}H-NMR (300 MHz, $CDCl_3$, major isomer): δ 7.48 – 7.41 (m, 4H), 7.18 – 7.11 (m, 4H), 4.20 (q, *J* = 7.1 Hz, 4H), 3.66 – 3.58 (m, 2H), 3.42 – 3.34 (m, 2H), 1.26 (t, *J* = 7.1 Hz, 6H).
^{13}C-NMR (75 MHz, $CDCl_3$, major isomer): δ 172.35, 139.85, 131.96, 128.69, 121.32, 61.38, 46.73, 44.73, 14.39.
IR (neat, cm^{-1}): 2985, 2937, 1717, 1588, 1486, 1394, 1364, 1315, 1294, 1273, 1195, 1159, 1111, 1070, 1006, 962, 864, 812, 755, 702.
EI-MS: exact m/z calculated for $C_{22}H_{22}O_4Br_2$ $(M)^+$: 507.98498; Found: 507.98582 $(M)^+$.
Mp: 92-94 °C (decomposed).

Diethyl-3,4-bis(4-cyanophenyl)cyclobutane-1,2-dicarboxylate (2i/3i):

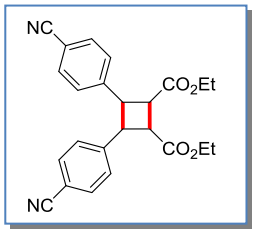

Following **GP-1**, **2i/3i** was prepared from ethyl (*E*)-3-(4-cyanophenyl)acrylate **1i** (201.2 mg, 1.0 mmol, 1.00 equiv) and $[Ir\{dF(CF_3)ppy\}_2(dtb\text{-}bpy)]PF_6$ (11.22 mg, 0.01 equiv, 1.0 mol %) in dry DMF (2 mL). The crude product was purified by column chromatography (silica gel, hexanes–EtOAc, 5:1, R_f = 0.20) to afford a mixture of **2i/3i** as a white solid (171 mg, 85% yield, 1.15:1 d.r.).

^{1}H-NMR (400 MHz, $CDCl_3$, *trans* isomer): δ 7.68 – 7.58 (m, 2H), 7.38 (d, *J* = 8.3 Hz, 2H), 4.22 (qd, *J* = 7.1 Hz, 1.6, 2H), 3.87 – 3.74 (m, 1H), 3.59 – 3.40 (m, 1H), 1.27 (t, *J* = 7.1 Hz, 3H).
^{13}C-NMR (101 MHz, $CDCl_3$, *trans* isomer): δ 172.71, 158.67, 133.38, 127.95, 113.99, 77.38, 77.06, 76.74, 60.94, 55.29, 46.94, 45.01, 14.27.
IR (neat, cm^{-1}): 3064, 2989, 2229, 1715, 1607, 1506, 1372, 1312, 1200, 1163, 1014, 828;
HRMS (ESI): exact m/z calculated for $C_{24}H_{22}N_2O_4$ $(M+H)^+$: 403.1652; Found: 403.1652 $(M+H)^+$.
Mp: 121-122 °C (decomposed).

Diethyl (1*S*,2*S*,3*R*,4*R*)-3,4-bis(4-(methoxycarbonyl)phenyl)cyclobutane-1,2-dicarboxylate (2j):

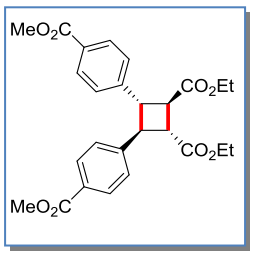

Following **GP-1**, **2j** was prepared from methyl (*E*)-4-(3-ethoxy-3-oxoprop-1-en-1-yl)benzoate **1j** (234.3 mg, 1.0 mmol, 1.00 equiv) and $[Ir\{dF(CF_3)ppy\}_2(dtb\text{-}bpy)]PF_6$ (11.22 mg, 0.01 equiv, 1.0 mol %) in dry DMF (2 mL). The crude product was purified by column chromatography (hexanes–EtOAc, 5:1) to afford **2j** as colourless oil (130 mg, 56% yield).

^{1}H-NMR (400 MHz, $CDCl_3$): δ 7.71 (d, 2H), 6.94 (d, *J* = 8.4 Hz, 2H), 4.42 (dd, *J* = 3.9, 2.2, 2H), 4.16 (q, *J* = 7.1 Hz, 2H), 3.84 (d, *J* = 1.6 Hz, 1H), 3.78 (s, 3H), 1.23 (t, *J* = 7.1 Hz, 3H).
^{13}C-NMR (75 MHz, $CDCl_3$): δ 172.13, 166.79, 145.80, 130.07, 129.18, 126.85, 77.47, 77.05, 76.63, 61.30, 52.17, 46.79, 44.52, 14.22.
IR (neat, cm^{-1}): 2952, 1718, 1610, 1435, 1159, 1275, 1193, 1103, 1018, 965, 857, 768, 701.
HRMS (ESI): exact m/z calculated for $C_{26}H_{28}O_8$ $(M+H)^+$: 469.1857; Found: 469.1862 $(M+H)^+$.

Diethyl (1*R*,2*S*,3*R*,4*S*)-3,4-bis(4-(methoxycarbonyl)phenyl)cyclobutane-1,2-dicarboxylate (3j):

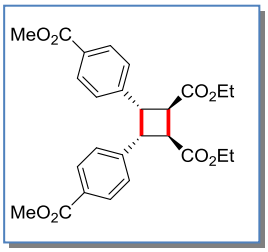

Following **GP-1**, **3j** was prepared from methyl (*E*)-4-(3-ethoxy-3-oxoprop-1-en-1-yl)benzoate **1j** (234.3 mg, 1.0 mmol, 1.00 equiv) and [Ir{dF(CF_3)ppy}$_2$(dtb-bpy)]PF_6 (11.22 mg, 0.01 equiv, 1.0 mol %) in dry DMF (2 mL). The crude product was purified by column chromatography (silica gel, hexanes–EtOAc, 5:1) to afford **3j** as colourless oil (79 mg, 34% yield).

^{1}H-NMR (400 MHz, $CDCl_3$): δ = 7.71 (d, 2H), 6.94 (d, *J* = 8.4 Hz, 2H), 4.42 (dd, *J* = 3.9 Hz, 2.2, 1H), 4.16 (q, *J* =7.1 Hz, 2H), 3.84 (d, *J* = 1.6 Hz, 1H), 3.78 (s, 3H), 1.23 (t, *J* = 7.1 Hz, 3H).
^{13}C-NMR (75 MHz, $CDCl_3$): δ 172.13, 166.79, 145.80, 130.07, 129.18, 126.85, 77.47, 77.05, 76.63, 61.30, 52.17, 46.79, 44.52, 14.22.
IR (neat, cm^{-1}): 2952, 1718, 1610,1435, 1159, 1275, 1193, 1103, 1018, 965, 857, 768, 701.
HRMS (ESI): exact m/z calculated for $C_{26}H_{28}O_8$ $(M+H)^+$: 469.1857; Found: 469.1860 $(M+H)^+$.

Diethyl (1*S*,2*S*,3*R*,4*R*)-3,4-bis(4-nitrophenyl)cyclobutane-1,2-dicarboxylate (2k):

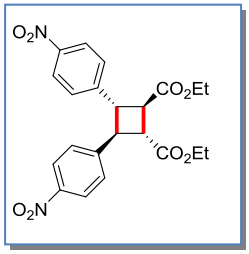

Following **GP-1**, **2k** was prepared from ethyl (*E*)-3-(4-nitrophenyl)acrylate **1k** (221.2 mg, 1.0 mmol, 1.00 equiv) and [Ir{dF(CF_3)ppy}$_2$(dtb-bpy)]PF_6 (11.22 mg, 0.01 equiv, 1.0 mol %) in dry DMF (2 mL). The crude product was purified by column chromatography (silica gel, hexanes–EtOAc, 10:1, R_f = 0.2) to afford **2k** as a orange viscous oil (115 mg, 49% yield).

^{1}H-NMR (400 MHz, $CDCl_3$): δ 8.24 – 8.16 (m, 2H), 7.45 (d, *J* = 8.7 Hz, 2H), 4.24 (qd, *J* = 7.1 Hz, 1.4, 2H), 3.90 – 3.81 (m, 1H), 3.53 – 3.43 (m, 1H), 1.33 – 1.23 (m, 3H).

^{13}C-NMR (101 MHz, $CDCl_3$): δ 171.61, 147.50, 147.34, 127.72, 124.17, 77.38, 77.07, 76.75, 61.62, 46.36, 44.60, 14.22.

IR (neat, cm^{-1}): 2982, 2937, 1722, 1603, 1517, 1342, 1200, 1159, 1111, 1014, 854, 746.

HRMS (ESI): exact m/z calculated for $C_{22}H_{22}N_2O_8$ $(M+H)^+$: 443.1449; Found: 443.1457 $(M+H)^+$.

Diethyl (1*R*,2*S*,3*R*,4*S*)-3,4-bis(4-nitrophenyl)cyclobutane-1,2-dicarboxylate (3k):

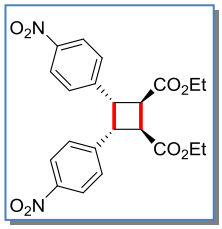

Following **GP-1**, **3k** was prepared from ethyl (*E*)-3-(4-nitrophenyl)acrylate **1k** (221.2 mg, 1.0 mmol, 1.00 equiv) and [Ir{dF(CF_3)ppy}$_2$(dtb-bpy)]PF_6 (11.22 mg, 0.01 equiv, 1.0 mol %) in dry DMF (2 mL). The crude product was purified by column chromatography (silica gel, hexanes–EtOAc, 10:1, R_f = 0.15) to afford **3k** with impurities of **2k** as orange oil. (87 mg, 37% yield).

^{1}H-NMR (400 MHz, $CDCl_3$): δ 8.01 (d, *J* = 8.8 Hz, 2H), 7.11 (d, *J* = 8.7 Hz, 2H), 4.57 (d, *J* = 6.2 Hz, 1H), 4.24 (q, *J* =7.1 Hz, 2H), 3.86 (dd, *J* = 3.7, 2.4 Hz, 1H), 1.30 (t, *J* = 7.1 Hz, 3H).

IR (neat, cm^{-1}): 2982, 2937, 1722, 1603, 1517, 1342, 1200, 1159, 1111, 1014, 854, 746.

HRMS (ESI): exact m/z calculated for $C_{22}H_{22}N_2O_8$ $(M+H)^+$: 443.1449; Found: 443.1455 $(M+H)^+$.

Dimethyl-3,4-bis(4-hydroxy-3-methoxyphenyl)cyclobutane-1,2-dicarboxylate (2l/3l):

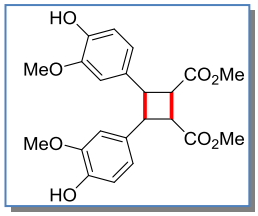

Following **GP-1**, **2l/3l** was prepared from methyl (*E*)-3-(4-hydroxy-3-methoxyphenyl)acrylate **1l** (208.2 mg, 1.0 mmol, 1.00 equiv) and [Ir{dF(CF_3)ppy}$_2$(dtb-bpy)]PF_6 (11.22 mg, 0.01 equiv, 1.0 mol %) in dry DMF (2 mL). The crude product was purified by column chromatography (silica gel, hexanes–EtOAc, 1:1, R_f = 0.20) to afford mixture of **2l/3l** as a colourless oil (135 mg, 65% yield; d.r. = 2.94:1).

^{1}H-NMR (300 MHz, $CDCl_3$, major isomer): δ 6.86 (d, *J* = 8.2 Hz, 2H), 6.82 – 6.74 (m, 4H), 5.65 (bs, 2H), 3.84 (s, 6H), 3.74 (s, 6H), 3.61 – 3.53 (m, 2H), 3.45 – 3.38 (m, 2H).

^{13}C-NMR (75 MHz, $CDCl_3$, major isomer): δ 173.28, 146.70, 144.89, 133.08, 119.71, 114.57, 109.48, 56.01, 52.36, 47.98, 44.61.

IR (neat, cm^{-1}): 3433, 2952, 2844, 1721, 1602, 1514, 1434, 1264, 1235, 1200, 1156, 1121, 1028, 851, 812, 766, 733, 700.

HRMS (ESI): exact m/z calculated for $C_{22}H_{25}O_8$ $(M+H)^+$: 417.1544; Found: 417.1546 $(M+H)^+$.

Diethyl-3,4-bis(2-chloro-3,4-dimethoxyphenyl)cyclobutane-1,2-dicarboxylate (2m/3m):

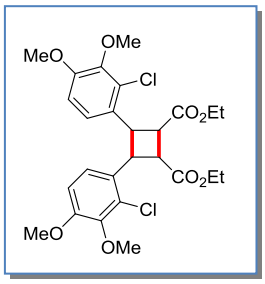

Following **GP-1**, **2m/3m** was prepared from ethyl (*E*)-3-(2-chloro-3,4-dimethoxyphenyl)acrylate **1m** (270.7 mg, 1.0 mmol, 1.00 equiv) and [Ir{dF(CF_3)ppy}$_2$(dtb-bpy)]PF_6 (11.22 mg, 0.01 equiv, 1.0 mol %) in dry DMF (2 mL). The crude product was purified by column chromatography (silica gel, hexanes–EtOAc, 4:1, R_f = 0.16 (trans), R_f = 0.14 (cis) to afford mixture of **2m/3m** as a yellow solid (189 mg, 70% yield; d.r. = 6:1).

^{1}H-NMR (300 MHz, $CDCl_3$, major isomer): δ 7.26 (d, *J* = 8.7 Hz, 2H), 6.85 (d, *J* = 8.7 Hz, 2H), 4.23 – 4.19 (m, 2H), 4.16 (q, *J* = 7.1 Hz, 4H), 3.84 (s, 6H), 3.81 (s, 6H), 3.41 – 3.24 (m, 2H), 1.24 (t, *J* = 7.1 Hz, 6H).

^{13}C-NMR (75 MHz, $CDCl_3$, major isomer): δ 172.57, 152.89, 145.37, 130.94, 128.54, 123.17, 110.82, 61.18, 60.62, 56.15, 45.45, 43.21, 14.25.

IR (neat, cm^{-1}): 2934, 2839, 1721, 1594, 1490, 1462, 1439, 1420, 1294, 1267, 1205, 1176, 1149, 1036, 1012, 980, 841, 807, 774, 710, 666.

HRMS (ESI): exact m/z calculated for $C_{26}H_{31}Cl_2O_8$ $(M+H)^+$: 541.1390; Found: 541.1403 $(M+H)^+$.

Mp: 125-127 ^oC (decomposed).

Diethyl-3,4-bis(2-fluorophenyl)cyclobutane-1,2-dicarboxylate (2n/3n):

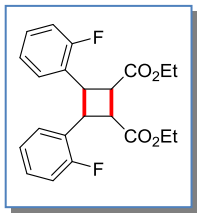

Following **GP-1**, **2n/3n** was prepared from ethyl (*E*)-3-(2-fluorophenyl)acrylate **1n** (194.2 mg, 1.0 mmol, 1.00 equiv) and [Ir{dF(CF_3)ppy}$_2$(dtb-bpy)]PF_6 (11.22 mg, 0.01 equiv, 1.0 mol %) in dry DMF (2 mL). The crude product was purified by column chromatography (silica gel, hexanes–EtOAc, 9:1, R_f = 0.25 (trans), R_f = 0.20 (cis) to afford mixture of **2n/3n** as a white solid (143 mg, 74% yield; d.r. = 5:1).

^{1}H-NMR (300 MHz, $CDCl_3$, major isomer): δ 7.42 (td, *J* = 7.5, 1.7 Hz, 2H), 7.23 (tdd, *J* = 7.2, 5.1, 1.8 Hz, 2H), 7.13 (tt, *J* = 9.0, 4.5 Hz, 2H), 7.06 – 6.98 (m, 2H), 4.20 (q, *J* = 7.1 Hz, 4H), 4.13 – 4.04 (m, 2H), 3.53 – 3.43 (m, 2H), 1.26 (t, *J* = 7.1 Hz, 6H).

^{13}C-NMR (75 MHz, $CDCl_3$, major isomer): δ 172.35, 160.98 (d, $^{1}J_{C\text{-}F}$ = 246.2 Hz), 128.90 (d, $^{3}J_{C\text{-}F}$ = 8.3 Hz), 128.43 (d, $^{3}J_{C\text{-}F}$ = 4.7 Hz), 127.57 (d, $^{2}J_{C\text{-}F}$ = 15.1 Hz), 124.46 (d, $^{4}J_{C\text{-}F}$ = 3.6 Hz), 115.55 (d, $^{2}J_{C\text{-}F}$ = 22.0 Hz), 61.21, 44.84, 40.09, 14.29.

^{19}F-NMR (282 MHz, $CDCl_3$): δ -116.94.

IR (neat, cm^{-1}): 2988, 2944, 1719, 1602, 1509, 1472, 1446, 1393, 1368, 1302, 1216, 1196, 1156, 1107, 1034, 1015, 965, 826, 807, 768, 731, 671.

EI-MS: exact m/z calculated for $C_{22}H_{22}O_4F_2$ $(M)^+$: 388.14807; Found: 388.14844 $(M)^+$.

Mp: 57-59 ^{o}C (decomposed).

Diethyl-3,4-bis(2-cyanophenyl)cyclobutane-1,2-dicarboxylate (2o/3o):

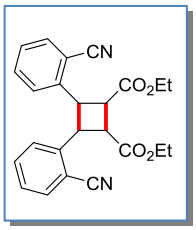

Following **GP-1**, **2o/3o** was prepared from ethyl (*E*)-3-(2-cyanophenyl)acrylate **1o** (201.2 mg, 1.0 mmol, 1.00 equiv) and [Ir{dF(CF_3)ppy}$_2$(dtb-bpy)]PF_6 (11.22 mg, 0.01 equiv, 1.0 mol %) in dry DMF (2 mL). The crude product was purified by column chromatography (silica gel, hexanes–EtOAc, 85:15, R_f = 0.40) to afford mixture of **2o/3o** as a white solid (127 mg, 63% yield; d.r. = 7.34:1).

^{1}H-NMR (300 MHz, $CDCl_3$, major isomer): δ 7.79 (d, *J* = 7.5 Hz, 2H), 7.73 – 7.65 (m, 2H), 7.59 (dd, *J* = 7.8, 1.1 Hz, 2H), 7.42 – 7.35 (m, 2H), 4.22 (q, *J* = 7.1 Hz, 4H), 4.20 – 4.15 (m, 2H), 3.63 – 3.50 (m, 2H), 1.27 (t, *J* = 7.1 Hz, 6H).

^{13}C-NMR (75 MHz, $CDCl_3$, major isomer): δ 171.46, 142.92, 133.83, 133.18, 128.34, 127.67, 117.63, 112.49, 61.74, 14.22.

IR (neat, cm^{-1}): 2988, 2931, 2222, 1715, 1597, 1473, 1446, 1369, 1320, 1255, 1218, 1193, 1169, 1122, 1103, 1023, 970, 853, 769, 728, 676.

EI-MS: exact m/z calculated for $C_{24}H_{22}N_2O_4$ $(M)^+$: 402.15607; Found: 402.15624 $(M)^+$.

Mp: 110-112 ^{o}C (decomposed).

Diethyl (1*S*,2*S*,3*R*,4*R*)-3,4-bis(2-(phenylethynyl)phenyl)cyclobutane-1,2-dicarboxylate (2p):

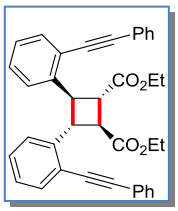

Following **GP-1**, **2p** was prepared from ethyl (*E*)-3-(2-(phenylethynyl)phenyl)acrylate **1p** (276.3 mg, 1.0 mmol, 1.00 equiv). Purification of the crude product by column chromatography (Hexanes: EtOAc, 9:1, R_f = 0.37) afforded **2p** as a pale yellow oil (174 mg, 63% yield; d.r. = 20:1).

^{1}H-NMR (300 MHz, $CDCl_3$): δ 7.66 (d, *J* = 7.2 Hz, 1H), 7.52 – 7.41 (m, 3H), 7.37 – 7.30 (m, 3H), 7.27 (td, *J* = 7.6, 1.4 Hz, 1H), 7.14 (td, *J* = 7.5, 1.2 Hz, 1H), 4.55 – 4.51 (m, 1H), 4.02 (q, *J* = 7.1 Hz, 2H), 3.57 – 3.52 (m, 1H), 1.12 (t, *J* = 7.1 Hz, 3H).

^{13}C-NMR (75 MHz, $CDCl_3$): δ 172.71, 142.06, 132.60, 131.79, 129.00, 128.41, 127.08, 127.02, 123.39, 123.05, 93.65, 88.00, 61.05, 45.52, 45.03, 14.20.

IR (neat, cm^{-1}): 2925, 2854, 1723, 1598, 1493, 1443, 1368, 1318, 1201, 1157, 1095, 1027, 914, 855, 752, 689.

EI-MS: exact m/z calculated for $C_{38}H_{33}O_4$ $(M+H)^+$: 553.2373; Found: 553.2382 $(M+H)^+$.

Diethyl 3,4-di(furan-2-yl)cyclobutane-1,2-dicarboxylate (2r/3r) and diethyl 2,4-di(furan-2-yl)cyclobutane-1,3-dicarboxylate (2q/3q/4q):

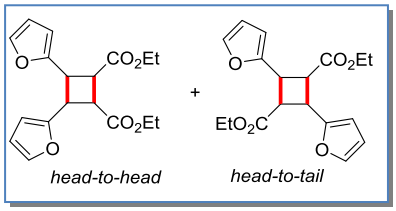

Following **GP-1**, **2q/3q/4q** was prepared from ethyl (*E*)-3-(furan-2-yl)acrylate **1r** (166.2 mg, 1.0 mmol, 1.00 equiv) and $[Ir\{dF(CF_3)ppy\}_2(dtb\text{-}bpy)]PF_6$ (11.22 mg, 0.01 equiv, 1.0 mol %) in dry DMF (2 mL). The crude product was purified by column chromatography (silica gel, hexanes–EtOAc, 5:1, R_f = 0.4-0.2) to afford **4q** as orange oil (27 mg, 16% yield) and a mixture of **2r/3r/4r** as orange oil. (88 mg, 53% yield).

^{1}H-NMR (300 MHz, $CDCl_3$, *trans* isomer): δ 7.36 (dd, *J* = 1.8, 0.8 Hz, 1H), 6.30 (dd, *J* = 3.2, 1.9 Hz, 1H), 6.16 (dd, *J* = 3.2, 0.7 Hz, 1H), 4.18 (qd, *J* =7.1, 0.6 Hz, 2H), 3.82 – 3.72 (m, 1H), 3.53 – 3.44 (m, 1H), 1.25 (t, *J* = 7.1, 3H).

^{1}H-NMR (300 MHz, $CDCl_3$, *cis* isomer): δ = 7.22 (dd, *J* = 1.8, 0.8 Hz, 1H), 6.20 (dd, *J* = 3.2, 1.8 Hz, 1H), 5.94 (d, *J* = 2.8 Hz, 1H), 4.25 (dd, *J* = 3.8, 2.2, 1H), 4.18 (qd, *J* = 7.1, 1.5 Hz, 2H), 3.85 (dd, *J* = 3.7, 2.2, 1H), 1.26 (td, *J* =7.1, 3.6 Hz, 3H).

^{13}C-NMR (101 MHz, $CDCl_3$, *trans* isomer): δ 171.88, 153.36, 142.17, 110.37, 106.58, 77.35, 77.03, 76.71, 61.08, 43.37, 39.44, 14.19.

IR (neat, cm^{-1}): 2982, 2941, 1800, 1726, 1372, 1200, 1096, 1014, 924, 738.

HRMS (ESI): ***trans***: exact m/z calculated for $C_{18}H_{20}O_6$ $(M+H)^+$: 333.1338; Found: 333.1334 $(M+H)^+$; ***cis***: exact m/z calculated for $C_{18}H_{20}O_6$ $(M+H)^+$: 333.1338; Found: 333.1336 $(M+H)^+$; **head-to-tail conformer**: exact m/z calculated for $C_{18}H_{20}O_6$ $(M+H)^+$: 333.1338; Found: 333.1335 $(M+H)^+$.

Diethyl-3,4-di(thiophen-2-yl)cyclobutane-1,2-dicarboxylate (2r/3r, 4r):

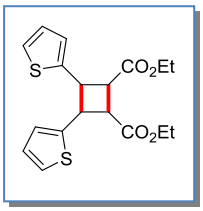

Following **GP-1**, **2r/3r, 4r** was prepared from methyl (*E*)-3-(thiophen-2-yl)acrylate (188 mg, 1.0 mmol, 1.00 equiv) and [Ir{dF(CF$_3$)ppy}$_2$(dtb-bpy)]PF$_6$ (11.22 mg, 0.01 equiv, 1.0 mol %) in dry DMF (2 mL). The crude product was purified by column chromatography (silica gel, hexanes–EtOAc, 5:1, R_f = 0.58) to afford mixture of **2r/3r, 4r** as a yellow oil (145.1 mg, 77% yield; d.r. = 1.8:1).

^{1}H-NMR (300 MHz, CDCl$_3$): δ 7.21 (dd, *J* = 4.2, 2.1 Hz, 2H, *trans*), 7.09 (dd, *J* = 5.1, 1.1 Hz, 1H, *cis*), 7.04 (dd, *J* = 4.9, 0.8 Hz, 0.2H, head-to-tail conformer), 7.00 – 6.93 (m, 4H, *trans*), 6.85 (dd, *J* = 5.0, 3.5 Hz, 1H, *cis*), 6.81 (dd, *J* = 5.1, 3.6 Hz, 0.2H, head-to-tail conformer), 6.73 (dd, *J* = 3.5, 1.0 Hz, 1H, *cis*), 4.52 (dd, *J* = 3.9, 2.2 Hz, 1H, *cis*), 4.26 – 4.13 (m, 7H, *trans/cis*), 3.88 – 3.82 (m, 2H, *trans*), 3.79 (dd, *J* = 3.7, 2.2 Hz, 1H, *cis*), 3.48 – 3.36 (m, 2H, *trans*), 1.29 (t under t, *J* = 7.1, 3.8 Hz, 10H, *trans/cis*), 0.96 (t under t, *J* = 7.1, 4.9 Hz, 0.9H, head-to-tail conformer).

^{13}C-NMR (75 MHz, CDCl$_3$, *trans*/*cis* isomer, head-to-tail conformer): δ 172.57, 171.76, 171.68, 170.27, 143.92, 141.83, 141.35, 138.63, 127.08, 126.66, 126.62, 126.47, 126.39, 125.46, 125.33, 124.86, 124.62, 124.50, 124.39, 77.55, 77.13, 76.70, 61.23, 61.19, 60.80, 46.06, 45.85, 44.71, 44.63, 43.47, 42.30, 41.39, 41.02, 14.24, 14.21, 13.86.

IR (neat, cm^{-1}): 3108, 2981, 1722, 1442, 1371, 1297, 1192, 1036, 849, 790, 693.

HRMS (ESI): ***trans***: exact m/z calculated for $C_{18}H_{21}S_2O_4$ $(M+H)^+$: 365.0876; Found: 365.0880 $(M+H)^+$; ***cis***: exact m/z calculated for $C_{18}H_{21}S_2O_4$ $(M+H)^+$: 365.0876; Found: 365.0880 $(M+H)^+$; **head-to-tail conformer**: exact m/z calculated for $C_{18}H_{21}S_2O_4$ $(M+H)^+$: 365.0876; Found: 365.0880 $(M+H)^+$.

Dimethyl-3,4-bis(1-(*tert*-butoxycarbonyl)-1*H*-pyrrol-2-yl)cyclobutane-1,2-dicarboxylate (2s/3s):

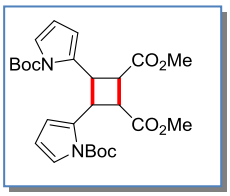

Following **GP-1**, **2s/3s** was prepared from methyl *tert*-butyl (*E*)-2-(3-methoxy-3-oxoprop-1-en-1-yl)-1*H*-pyrrole-1-carboxylate **1s** (263.3 mg, 1.0 mmol, 1.00 equiv) and [Ir{dF(CF_3)ppy}$_2$(dtb-bpy)]PF_6 (11.22 mg, 0.01 equiv, 1.0 mol %) in dry DMF (2 mL). The crude product was purified by column chromatography (silica gel, hexanes–EtOAc, 5:1, R_f = 0.28) to afford mixture of **2s/3s** as a yellow oil (137.5 mg, 54% yield; d.r. = 1.38:1).

^{1}H-NMR (300 MHz, $CDCl_3$, *trans* isomer): δ 7.10 (dd, *J* = 3.3, 1.7 Hz, 2H), 5.98 (t, *J* = 3.4 Hz, 2H), 5.77 (dd, *J* = 3.4, 1.7 Hz, 2H), 5.02 – 4.92 (m, 2H), 3.71 (s, 6H), 3.60 – 3.54 (m, 2H), 1.53 (s, 18H).

^{1}H-NMR (300 MHz, $CDCl_3$, *cis* isomer): 7.13 (dd, *J* = 3.3, 1.8 Hz, 2H), 6.29 (dd, *J* = 3.3, 1.7 Hz, 2H), 6.09 (t, *J* = 3.4 Hz, 2H), 4.46 – 4.40 (m, 2H), 3.68 (s, 6H), 3.34 – 3.27 (m, 2H), 1.52 (s, 18H).

^{13}C-NMR (75 MHz, $CDCl_3$, *trans/cis* isomer): δ 172.84, 172.79, 149.12, 148.96, 135.31, 133.30, 121.72 (*cis*), 121.64, 111.84 (*cis*), 110.98, 110.26 , 109.61, 83.52, 83.42, 51.99, 51.97 (*cis*), 45.33 (*cis*), 44.05, 40.49 (*cis*), 38.44, 27.97, 27.92.

IR (neat, cm^{-1}): 2981, 1733, 1435, 1319, 1159, 1125, 1066, 846, 723.

HRMS (ESI): trans: exact m/z calculated for $C_{26}H_{35}N_2O_8$ $(M+H)^+$: 503.2388; Found: 503.2390 $(M+H)^+$; **cis**: exact m/z calculated for $C_{26}H_{35}N_2O_8$ $(M+H)^+$: 503.2388; Found: 503.2390 $(M+H)^+$.

Diethyl (1*S*,3*R*)-3,4-bis(1-methyl-1*H*-indol-3-yl)cyclobutane-1,2-dicarboxylate (2t):

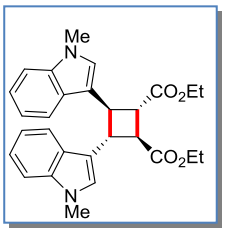

Following **GP-1**, **2t** was prepared from methyl (*E*)-3-(1-methyl-1*H*-indol-3-yl)acrylate **1t** (233.1 mg, 1.0 mmol, 1.00 equiv) and [Ir{dF(CF_3)ppy}$_2$(dtb-bpy)]PF_6 (11.22 mg, 0.01 equiv, 1.0 mol %) in dry DMF (2 mL). The crude product was purified by column chromatography (silica gel, hexanes–EtOAc, 5:1, R_f = 0.23) to afford mixture of **2t** as a yellow oil (51.6 mg, 11% yield).

^{1}H-NMR (300 MHz, $CDCl_3$): δ 7.69 (dd, *J* = 8.0, 0.6 Hz, 1H), 7.38 – 7.04 (m, 4H), 4.32 – 4.14 (m, 3H), 3.74 (s, *J* = 6.6 Hz, 3H), 3.63 – 3.57 (m, 1H), 1.29 (t, *J* = 7.1 Hz, 3H).

^{13}C-NMR (75 MHz, $CDCl_3$): δ 173.41, 137.40, 127.02, 126.54, 121.73, 119.89, 119.01, 115.51, 109.33, 77.52, 77.09, 76.67, 60.92, 45.88, 39.83, 32.72, 14.30.

IR (neat, cm^{-1}): 3049, 2978, 2929, 1710, 1613, 1550, 1472, 1371, 1315, 1244, 1203, 1177, 1036, 834, 738.

HRMS (ESI): exact m/z calculated for $C_{28}H_{30}N_2O_4Na$ $(M+Na)^+$: 481.2098; Found: 481.2104 $(M+Na)^+$.

1,2-diphenyl-1,2,2a,5,10,12a-hexahydrobenzo[c]cyclobuta[h][1,6]dioxecine-3,12-dione (2u/3u):

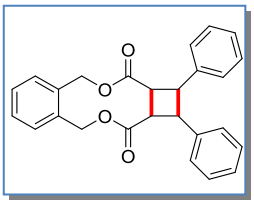

Following **GP-1**, **2u/3u** was prepared from 1,2-phenylenebis(methylene) (2*E*,2'*E*)-bis(3-phenylacrylate) **1u** (398.5 mg, 1.0 mmol, 1.00 equiv) and [Ir{dF(CF_3)ppy}$_2$(dtb-bpy)]PF_6 (11.22 mg, 0.01 equiv, 1.0 mol %) in dry DMF (2 mL). The crude product was purified by column chromatography (silica gel, hexanes–EtOAc, 5:1, R_f = 0.3) to afford the major diastereomer of **2u** as white solid (168 mg, 42% yield) and a mixture of both diastereomers of **2u/3u** as colorless oil. (142 mg, 35% yield 1:1.36 d.r.).

^{1}H-NMR (400 MHz, $CDCl_3$, major isomer): δ 7.48 – 7.38 (m, 2H), 7.14 – 7.01 (m, 3H), 6.91 (dd, *J* = 5.2, 3.2 Hz, 2H), 5.27 (dd, *J* = 109.2, 12.2 Hz, 2H), 4.46 (dd, *J* = 3.8, 2.3 Hz, 1H), 3.81 (dd, *J* = 3.8, 2.3 Hz, 1H).

^{13}C-NMR (101 MHz, $CDCl_3$, major isomer): δ 171.47, 138.25, 135.22, 131.58, 129.27, 128.09, 127.75, 126.45, 67.66, 44.31, 43.71.

IR (neat, cm^{-1}): 3027, 2060, 2963, 1730, 1498, 1446, 1256, 1185, 1163, 1048, 1018, 839, 749, 697.

HRMS (ESI) major isomer: exact m/z calculated for $C_{26}H_{22}O_4$ $(M+H)^+$: 399.1591; Found: 399.1590 $(M+H)^+$. **Minor isomer:** exact m/z calculated for $C_{26}H_{22}O_4$ $(M+H)^+$: 399.1591; Found: 399.1588 $(M+H)^+$.

Mp: 153–154 °C (decomposed).

3,4-diphenylcyclobutane-1,2-diyl)bis(phenylmethanone) (2v/3v):

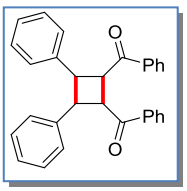

Following **GP-1**, **2v/3v** was prepared from (*E*)-chalcone **1v** (208.2 mg, 1.0 mmol, 1.00 equiv) and [Ir{dF(CF_3)ppy}$_2$(dtb-bpy)]PF_6 (11.22 mg, 0.01 equiv, 1.0 mol %) in dry DMF (2 mL). The crude product was purified by column chromatography (silica gel, hexanes–EtOAc, 9:1, R_f = 0.30 (*trans*), R_f = 0.15

(*cis*) to afford mixture of **2v/3v** as a white solid (167 mg, 80% yield; d.r. = 3:1).

^{1}H-NMR (300 MHz, $CDCl_3$, major isomer): δ 7.81 (dt, *J* = 8.5, 1.7 Hz, 4H), 7.48 – 7.40 (m, 2H), 7.33 – 7.17 (m, 14H), 4.63 – 4.57 (m, 2H), 3.99 – 3.93 (m, 2H).

^{13}C-NMR (75 MHz, $CDCl_3$, major isomer): δ 199.20, 141.55, 135.70, 133.63, 129.00, 128.86, 128.69, 127.58, 127.37, 48.07, 47.79.

IR (neat, cm^{-1}): 2925, 1741, 1663, 1595, 1579, 1491, 1448, 1381, 1293, 1273, 1208, 1178, 1154, 1075, 1020, 985, 910, 857, 802, 775, 749, 689, 661.

HRMS (ESI): exact m/z calculated for $C_{30}H_{25}O_2$ $(M+H)^+$: 417.1849; Found: 417.1848 $(M+H)^+$.

Mp: 54-56 ^oC (decomposed).

3,4-bis(4-chlorophenyl)cyclobutane-1,2-diyl)bis(phenylmethanone) (2w/3w):

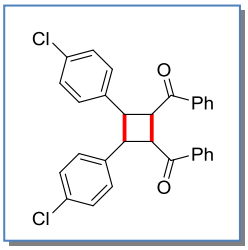

Following **GP-1**, **2w/3w** was prepared from (*E*)-3-(4-chlorophenyl)-1-phenylprop-2-en-1-one **1w** (242.7 mg, 1.0 mmol, 1.00 equiv) and $[Ir\{dF(CF_3)ppy\}_2(dtb\text{-}bpy)]PF_6$ (11.22 mg, 0.01 equiv, 1.0 mol %) in dry DMF (2 mL). The crude product was purified by column chromatography [silica gel, hexanes–EtOAc, 9:1, R_f = 0.28 (*trans*); R_f = 0.17 (*cis*)] to afford mixture of **2w/3w** as a white solid (179 mg, 74% yield; d.r. = 3:1).

^{1}H-NMR (300 MHz, $CDCl_3$, major isomer): δ 7.85 – 7.78 (m, 4H), 7.49 (ddd, *J* = 6.9, 2.4, 1.2 Hz, 2H), 7.39 – 7.18 (m, 12H), 4.61 – 4.53 (m, 2H), 3.92 – 3.85 (m, 2H).

^{13}C-NMR (75 MHz, $CDCl_3$, major isomer): δ 198.78, 139.71, 135.45, 133.88, 133.29, 129.10, 128.93, 128.86, 128.83, 47.57, 47.47.

IR (neat, cm^{-1}): 3058, 2927, 1733, 1670, 1636, 1594, 1579, 1559, 1488, 1446, 1403, 1373, 1316, 1296, 1275, 1230, 1210, 1179, 1089, 1043, 1012, 934, 912, 859, 821, 701, 685.

HRMS (ESI): exact m/z calculated for $C_{30}H_{23}Cl_2O_2$ $(M+H)^+$: 485.1070; Found: 485.1069 $(M+H)^+$.

Mp: 119-121 ^oC (decomposed).

1,2-diphenylcyclobutane (6a):

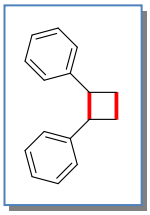

Following **GP-1**, **6a** was prepared from styrene **5a** (104.1 mg, 1.0 mmol, 1.00 equiv) and [Ir{dF(CF_3)ppy}$_2$(dtb-bpy)]PF_6 (11.22 mg, 0.01 equiv, 1.0 mol %) in dry DMF (2 mL). The crude product was purified by column chromatography (silica gel, hexanes–EtOAc, 95:5, R_f = 0.45) to afford *cis/trans* mixture of **6a** as a colourless oil (95 mg, 92% yield; *trans/cis* = 2.57:1).

^{1}H-NMR (300 MHz, $CDCl_3$): δ 7.43 – 7.24 (m, 7H, *trans/cis*), 7.22 – 7.00 (m, 3H, *trans/cis*), 4.11 (ddd, *J* = 5.6, 3.9, 2.2 Hz, 2H, *cis*), 3.73 – 3.61 (m, 2H, *trans*), 2.55 (ddd, *J* = 6.5, 4.2, 2.6 Hz, 2H, *trans/cis*), 2.47 – 2.33 (m, 4H, *trans/cis*), 2.31 – 2.16 (m, 4H, *trans/cis*).
^{13}C-NMR (75 MHz, $CDCl_3$): δ 144.71 (*trans*), 141.62 (*cis*), 128.47 (*trans*), 128.08 (*cis*), 127.80 (*cis*), 126.78 (*trans*), 126.25 (*trans*), 125.67 (*cis*), 48.02 (*trans*), 45.41 (*cis*), 26.10 (*trans*), 24.34 (*cis*).
IR (neat, cm^{-1}): 3059, 3026, 2940, 2866, 1685, 1600, 1493, 1446, 1028, 749, 694.
EI-MS: exact m/z calculated for $C_{16}H_{16}$ $(M)^+$: 208.12465; Found: 208.12450 $(M)^+$.

1,2-bis(4-nitrophenyl)cyclobutane (6b):

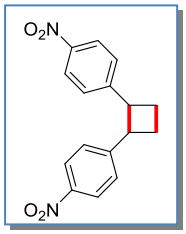

Following **GP-1**, **6b** was prepared from 1-nitro-4-vinylbenzene **5b** (149.1 mg, 1.0 mmol, 1.00 equiv) and [Ir{dF(CF_3)ppy}$_2$(dtb-bpy)]PF_6 (11.22 mg, 0.01 equiv, 1.0 mol %) in dry DMF (2 mL). The crude product was purified by column chromatography (silica gel, hexanes–EtOAc, 9:1, R_f = 0.26) to afford *cis/trans* mixture of **6b** as a pale yellow solid (128 mg, 86% yield; *trans/cis* = 5.19:1).

^{1}H-NMR (300 MHz, $CDCl_3$): δ 8.21 – 8.11 (m, 4H, *trans*), 8.01 – 7.90 (m, 4H, *cis*), 7.42 – 7.31 (m, 4H, *trans*), 7.14 – 7.05 (m, 4H, *cis*), 4.26 – 4.17 (m, 2H, *cis*), 3.77 – 3.62 (m, 2H, *trans*), 2.54 – 2.36 (m, 4H, *trans/cis*), 2.34 – 2.15 (m, 4H, *trans/cis*).
^{13}C-NMR (75 MHz, $CDCl_3$): δ 151.05 (*trans*), 146.84 (*cis*), 128.56 (*cis*), 127.52 (*trans*), 124.06 (*trans*), 123.48 (*cis*), 47.82 (*trans*), 45.22 (*cis*), 25.92 (*trans*), 24.14 (*cis*).
The obtained data is in accordance with literature data.[30]

1,2-di-*o*-tolylcyclobutane (6c):

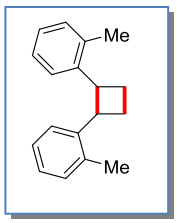

Following **GP-1**, **6c** was prepared from 1-methyl-2-vinylbenzene **5c** (118.1 mg, 1.0 mmol, 1.00 equiv) and [Ir{dF(CF_3)ppy}$_2$(dtb-bpy)]PF_6 (11.22 mg, 0.01 equiv, 1.0 mol %) in dry DMF (2 mL). The crude product was purified by column chromatography (silica gel, hexanes–EtOAc, 95:5, R_f = 0.43) to afford *cis/trans* mixture of **6c** as a colourless liquid (104 mg, 88% yield; *trans/cis* = 2.44:1).

^{1}H-NMR (300 MHz, $CDCl_3$): δ 7.28 – 6.93 (m, 10H, *trans/cis*), 4.26 – 4.17 (m, 2H, *cis*), 3.97 – 3.85 (m, 2H, *trans*), 2.55 – 2.35 (m, 4H, *trans*), 2.30 (s, 3H, *trans*), 2.10 (s, 3H, *cis*), 1.96 (dd, *J* = 13.7, 9.1 Hz, 1H, *cis*).

^{13}C-NMR (75 MHz, $CDCl_3$): δ 142.35 (*trans*), 139.80 (*cis*), 136.38 (*cis*), 136.08 (*trans*), 130.17 (*trans*), 129.86 (*cis*), 126.83 (*cis*), 126.14 (*trans*), 126.09 (*trans*), 125.98 (*trans*), 125.86 (*cis*), 125.43 (*cis*), 43.33 (*trans*), 41.67 (*cis*), 27.09 (*trans*), 24.97 (*cis*), 19.96 (*trans*), 19.83 (*cis*).

IR (neat, cm^{-1}): 3019, 2965, 2943, 1686, 1602, 1488, 1458, 1378, 1031, 734.

EI-MS: exact m/z calculated for $C_{18}H_{20}$ $(M)^+$: 236.15595; Found: 236.15646 $(M)^+$.

1,2-dimethyl-1,2-diphenylcyclobutane (6d):

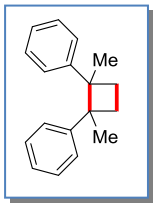

Following **GP-1**, **6d** was prepared from prop-1-en-2-ylbenzene **5d** (118.1 mg, 1.0 mmol, 1.00 equiv) and [Ir{dF(CF_3)ppy}$_2$(dtb-bpy)]PF_6 (11.22 mg, 0.01 equiv, 1.0 mol %) in dry DMF (2 mL). The crude product was purified by column chromatography (silica gel, hexanes–EtOAc, 95:05, R_f = 0.57) to afford *cis/trans* mixture of **6d** as a colourless oil (99 mg, 84% yield; *trans/cis* = 3.96:1).

^{1}H-NMR (300 MHz, $CDCl_3$): δ 7.42 – 7.36 (m, 6H, *trans*), 7.36 – 7.16 (m, 4H, *trans*), 7.03 (d, *J* = 4.3 Hz, 6H, *cis*), 6.97 – 6.89 (m, 4H, *cis*), 2.90 – 2.73 (m, 2H, *trans*), 2.68 (dd, *J* = 11.8, 6.3 Hz, 2H, *cis*), 2.15 – 2.01 (m, 2H, *cis*), 1.85 – 1.70 (m, 2H, *trans*), 1.65 (s, 3H, *cis*), 1.17 (s, 3H, *trans*).

^{13}C-NMR (75 MHz, $CDCl_3$): δ 147.44 (*trans*), 147.25 (*cis*), 128.20 (*trans*), 127.45 (*cis*), 126.79 (*trans*), 126.59 (*cis*), 125.81 (*trans*), 125.13 (*cis*), 49.25 (*trans*), 37.00 (*cis*), 29.78 (*cis*), 27.33 (*trans*), 27.00 (*trans*), 26.28 (*cis*).

IR (neat, cm^{-1}): 2926, 1457, 1421, 1263, 1094, 1029, 895, 804, 733, 703.

EI-MS: exact m/z calculated for $C_{18}H_{20}$ $(M)^+$: 236.15595; Found: 236.15563 $(M)^+$.

3,4-dimethylcyclobutane-1,2-diyl)dibenzene (6e):

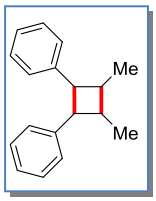

Following **GP-1**, **6e** was prepared from (*E*)-prop-1-en-1-ylbenzene **5e** (118.1 mg, 1.0 mmol, 1.00 equiv) and [Ir{dF(CF_3)ppy}$_2$(dtb-bpy)]PF_6 (11.22 mg, 0.01 equiv, 1.0 mol %) in dry DMF (2 mL). The crude product was purified by column chromatography (silica gel, hexanes–EtOAc, 95:05, R_f = 0.59) to afford *cis/trans* mixture of **6e** as a colourless oil (94 mg, 80% yield; *trans/cis* = 3.38:1).

^{1}H-NMR (300 MHz, $CDCl_3$): δ 7.39 – 7.13 (m, 10H, *trans*), 7.13 – 6.90 (m, 10H, *cis*), 3.56 – 3.52 (m, 2H, *cis*), 2.99 – 2.90 (m, 2H, *trans*), 1.91 (td, *J* = 9.4, 3.9 Hz, 2H, *cis*), 1.55 (s, 3H, *cis*), 1.26 (s, 3H, *trans*), 1.23 – 1.18 (m, 2H, *trans*).

^{13}C-NMR (75 MHz, $CDCl_3$): δ 143.86 (*trans*), 128.48 (*trans*), 128.22 (*cis*), 127.83 (*cis*), 127.00 (*trans*), 126.24 (*trans*), 125.58 (*cis*), 52.83 (*trans*), 43.32 (*trans*), 19.15 (*trans*).

IR (neat, cm^{-1}): 3058, 2955, 2923, 2861, 1494, 1453, 1261, 1094, 1029, 803, 749, 698.

EI-MS: exact m/z calculated for $C_{18}H_{20}$ $(M)^+$: 236.15595; Found: 236.15556 $(M)^+$.

Diethyl 3-(4-methoxyphenyl)-4-phenylcyclobutane-1,2-dicarboxylate (7a):

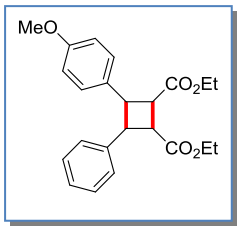

Following **GP-1**, **7a** was prepared from ethyl cinnamate **1a** (88.1 mg, 0.5 mmol, 1.00 equiv), ethyl-3-(4-methoxyphenyl)acrylate **1f** (103.1 mg, 0.5 mmol, 1.00 equiv) and [Ir{dF(CF_3)ppy}$_2$(dtb-bpy)]PF_6 (11.22 mg, 0.02 equiv, 2.0 mol %) in dry DMF (2 mL). The crude product was purified by column chromatography (silica gel, hexanes–EtOAc, 5:1, R_f = 0.3) to afford the desired product **7a** as colorless oil (67 mg, 35% yield), product **2f** as yellow oil (46 mg, 24% yield) and product **2a** (21 mg, 11% yield) as colorless oil.

^{1}H-NMR (400 MHz, $CDCl_3$): δ 7.35 – 7.26 (m, 5H), 7.26 – 7.21 (m, 3H), 6.89 – 6.83 (m, 2H), 4.19 (qt, *J* = 10.8, 5.4 Hz, 4H), 3.79 (s, 3H), 3.76 – 3.63 (m, 2H), 3.47 – 3.35 (m, 2H), 1.27 (td, *J* = 7.1, 3.3 Hz, 6H).

^{13}C-NMR (101 MHz, $CDCl_3$): δ 172.70, 172.63, 158.71, 141.27, 133.33, 128.59, 128.01, 127.01, 126.81, 114.02, 77.37, 77.05, 76.73, 61.00, 60.96, 55.30, 47.27, 46.67, 45.27, 44.60, 14.26.

IR (neat, cm^{-1}): 2982, 1722, 1610, 1513, 1457, 1249, 1178, 1033, 828, 701.

HRMS (ESI): exact m/z calculated for $C_{23}H_{26}O_5$ $(M+H)^+$: 383.1859; Found: 383.1586 $(M+H)^+$.

Diethyl 3-(4-(methoxycarbonyl)phenyl)-4-phenylcyclobutane-1,2-dicarboxylate (7b):

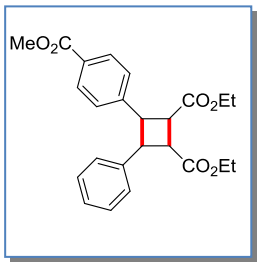

Following **GP-1**, **7b** was prepared from ethyl cinnamate **1a** (88.1 mg, 0.5 mmol, 1.00 equiv), methyl-4-(3-ethoxy-3-oxoprop-1-en-1-yl)benzoate **1j** (117.1 mg, 0.5 mmol, 1.00 equiv) and $[Ir\{dF(CF_3)ppy\}_2(dtb\text{-}bpy)]PF_6$ (11.22 mg, 0.02 equiv, 2.0 mol %) in dry DMF (2 mL). The crude product was purified by column chromatography (silica gel, hexanes–EtOAc, 5:1, R_f = 0.4-0.1) to afford the desired product **7b** (76 mg, 32% yield, 1.9:1 d.r.) and product **2j** (25 mg, 14% yield) as colorless oils.

^{1}H-NMR (400 MHz, $CDCl_3$): δ 7.99 (d, *J* = 8.3 Hz, 2H), 7.32 (ddd, *J* = 19.6, 15.8, 7.8 Hz, 7H), 4.26 – 4.16 (m, 4H), 3.90 (s, 3H), 3.84 – 3.71 (m, 2H), 3.51 – 3.41 (m, 2H), 1.33 – 1.22 (m, 6H).

^{13}C-NMR (101 MHz, $CDCl_3$): δ 172.13, 166.79, 145.82, 130.08, 129.49, 129.22, 127.71, 126.85, 77.36, 77.04, 76.73, 61.29, 52.15, 52.03, 46.82, 44.90, 44.56, 43.24, 14.23.

IR (neat, cm^{-1}): 2952, 1718, 1610, 1435, 1275, 1185, 1103, 1017, 965, 857, 767, 705.

HRMS (ESI): exact m/z calculated for $C_{24}H_{26}O_6$ $(M+H)^+$: 411.1808; Found: 411.1807 $(M+H)^+$.

Diethyl 3-(4-cyanophenyl)-4-(4-methoxyphenyl)cyclobutane-1,2-dicarboxylate (7c):

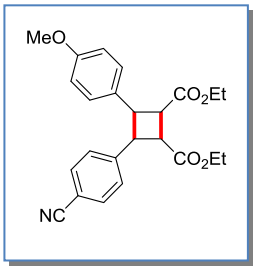

Following **GP-1**, **7c** was prepared from ethyl-3-(4-methoxyphenyl)acrylate **1f** (103.1 mg, 0.5 mmol, 1.00 equiv), ethyl-3-(4-cyanophenyl)acrylate **1i** (100.6 mg, 0.5 mmol, 1.00 equiv) and $[Ir\{dF(CF_3)ppy\}_2(dtb\text{-}bpy)]PF_6$ (11.22 mg, 0.02 equiv, 2.0 mol %) in dry DMF (2 mL). The crude product was purified by column chromatography (silica gel, hexanes–EtOAc, 5:1, R_f = 0.4-0.1) to afford the desired product **7c** (111.3 mg, 54% yield, d.r. 1.75:1) and product **2f** (26.4 mg, 13% yield, 99:1 d.r.) as white solids and product **2i** (17 mg, 14% yield, 90:1 d.r.) as colorless oil.

^{1}H-NMR (400 MHz, $CDCl_3$): δ 7.63 – 7.55 (m, 2H), 7.38 (d, *J* = 8.1 Hz, 2H), 7.24 – 7.16 (m, 2H), 6.90 – 6.85 (m, 2H), 4.20 (p, *J* = 7.2 Hz, 4H), 3.80 (s, 3H), 3.77 – 3.56 (m, 2H), 3.44 – 3.38 (m, 2H), 1.27 (dd, *J* = 13.4, 7.1, 6H).

^{13}C-NMR (101 MHz, $CDCl_3$): δ 172.3, 172.2, 159.0, 146.6, 132.5, 132.4, 127.9, 127.6, 118.8, 114.2, 110.9, 77.4, 77.1, 76.8, 61.3, 61.2, 55.3, 46.9, 46.7, 45.4, 44.0, 14.2.

IR (neat, cm^{-1}): 2981, 2937, 2840, 229, 1718, 1610, 1513, 1245, 1178, 114, 1036, 828.

HRMS (ESI): exact m/z calculated for $C_{24}H_{25}NO_5$ $(M+H)^+$: 408.1811; Found: 408.1805 $(M+H)^+$.

Mp: 54-56 °C (decomposed).

4.14 NMR spectra:

^{1}H-NMR: **2a/3a** (mixture, before separation)

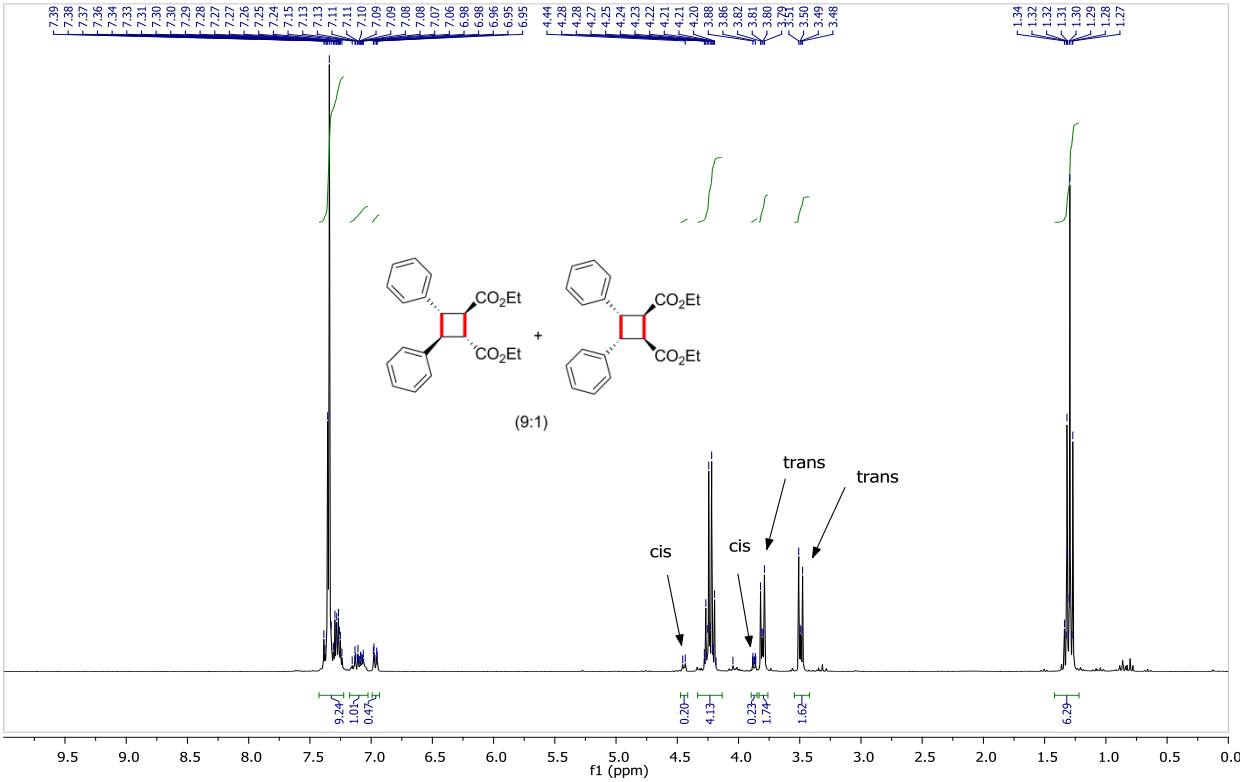

^{13}C-NMR: **2a/3a** (mixture, before separation)

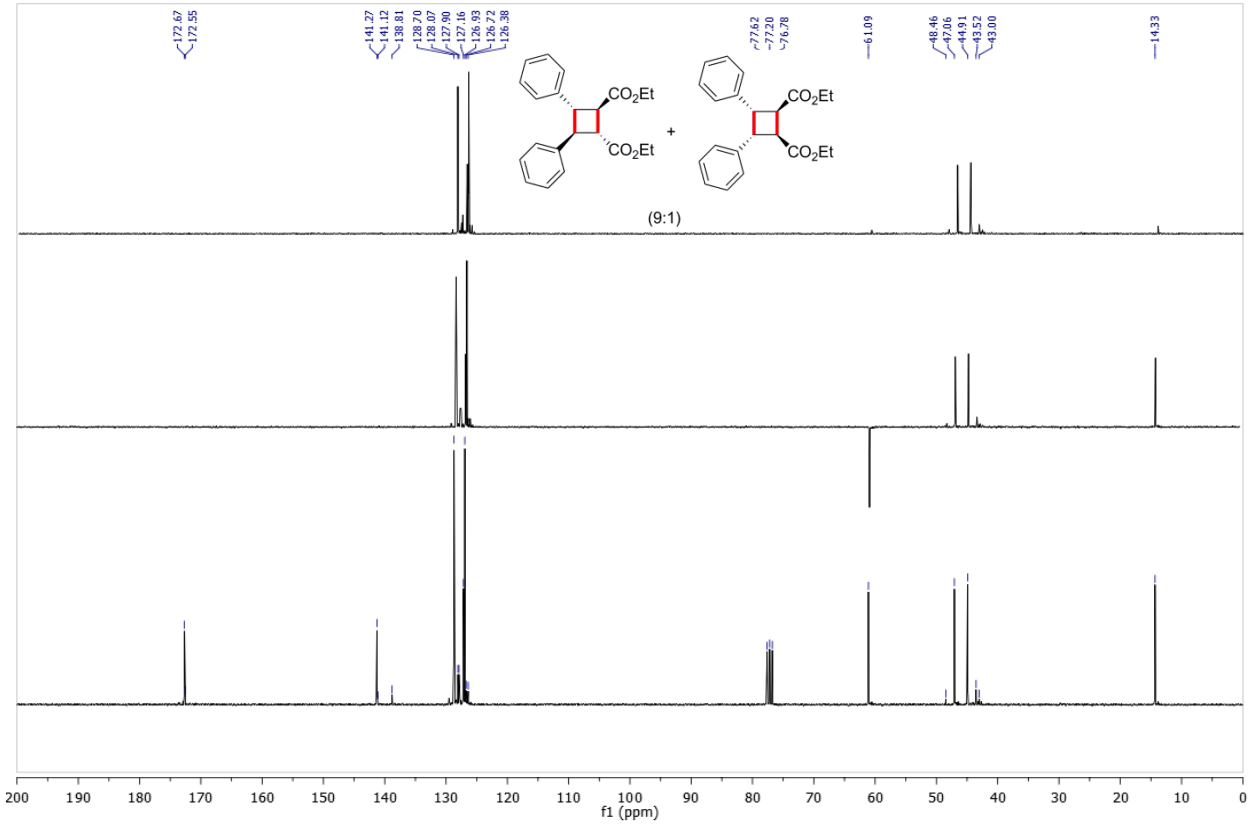

^{1}H-NMR: **2a** (*trans*, after separation)

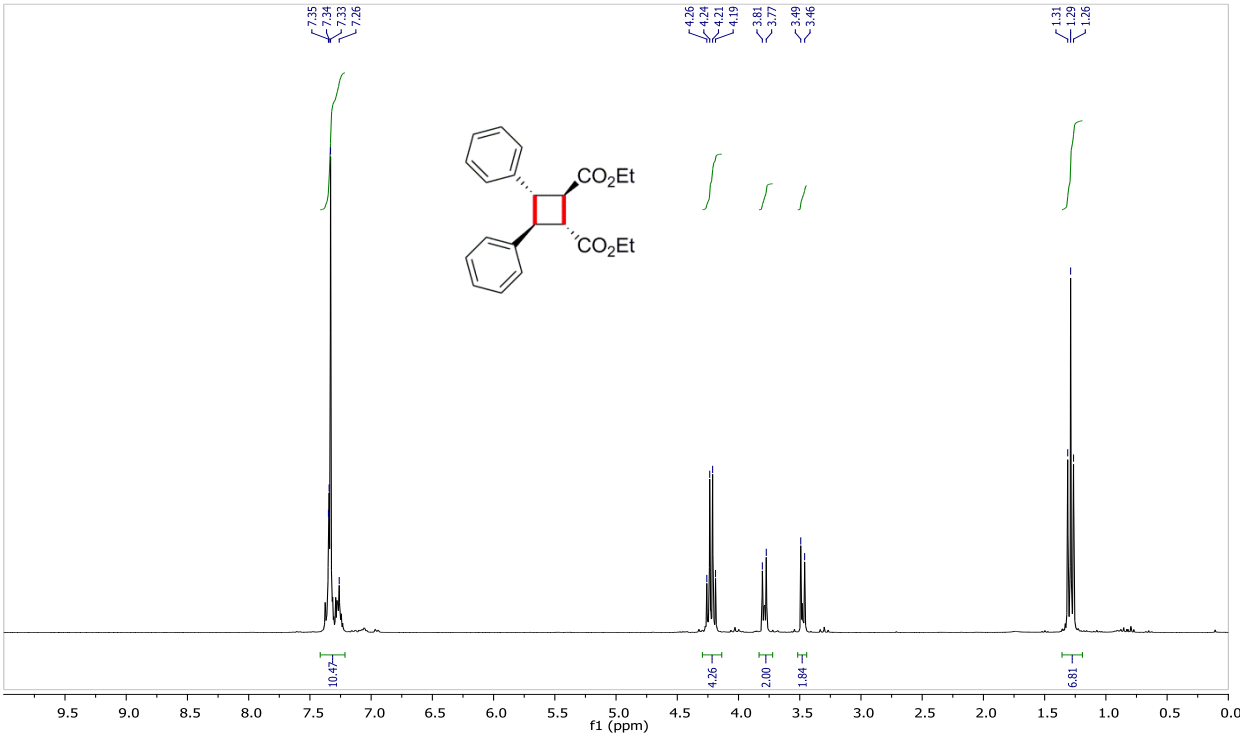

^{13}C-NMR: **2a** (*trans*, after separation)

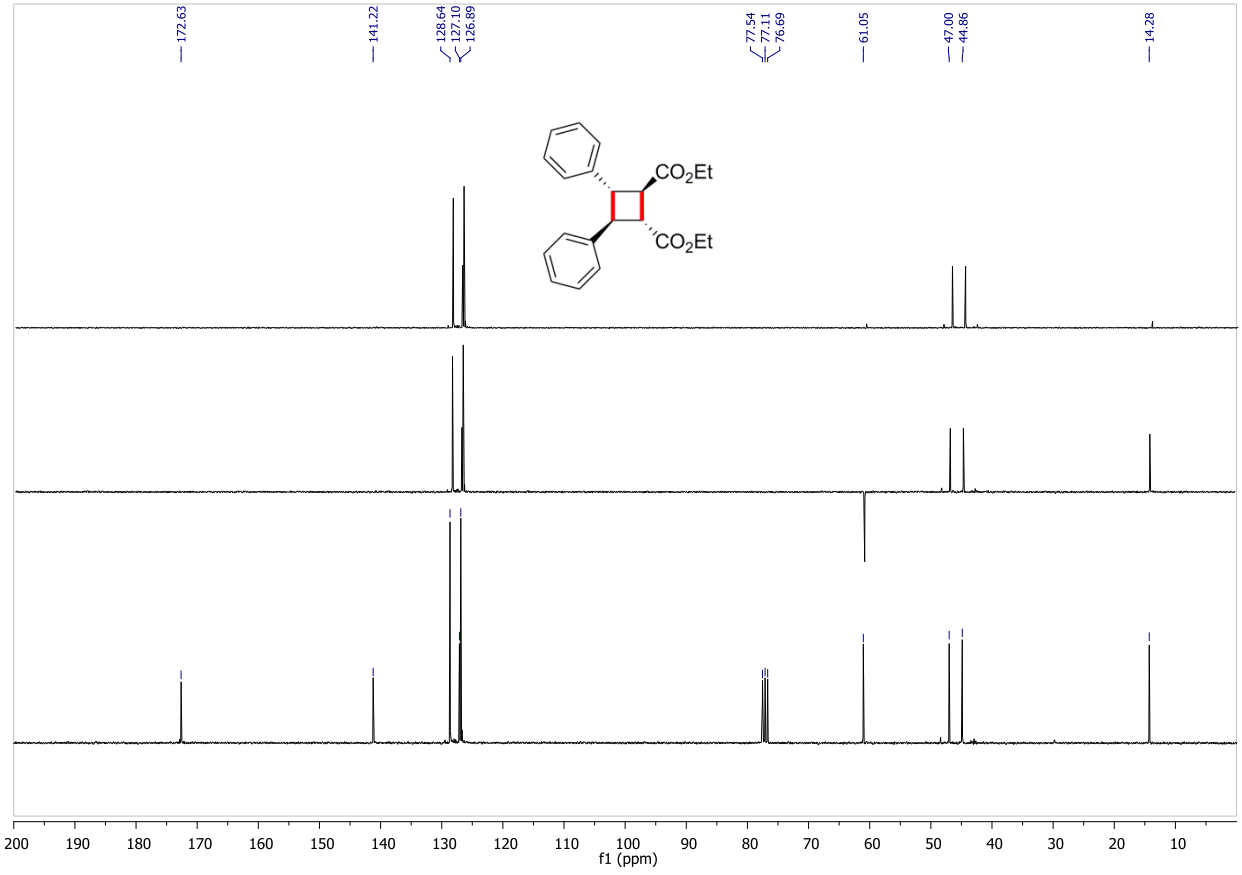

^{1}H-NMR: **3a** (*cis*, after separation)

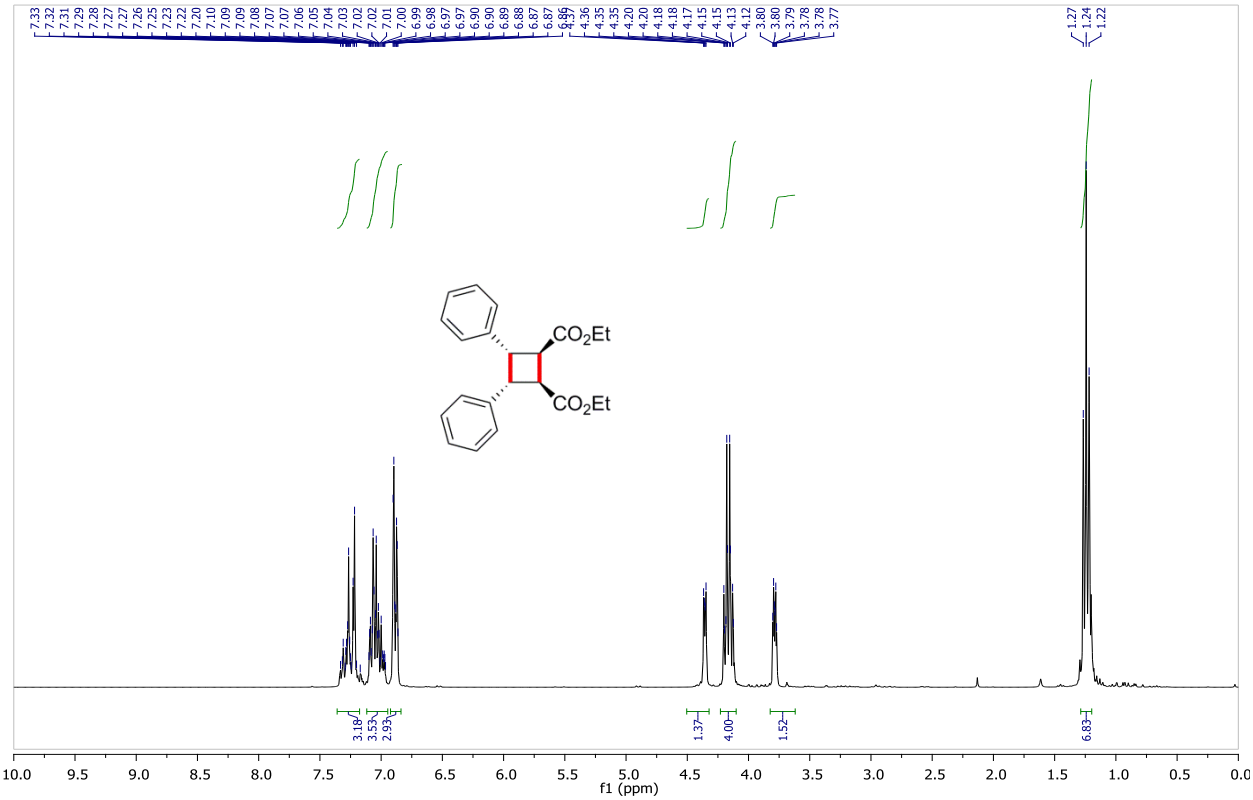

^{13}C-NMR: **3a** (*cis*, after separation)

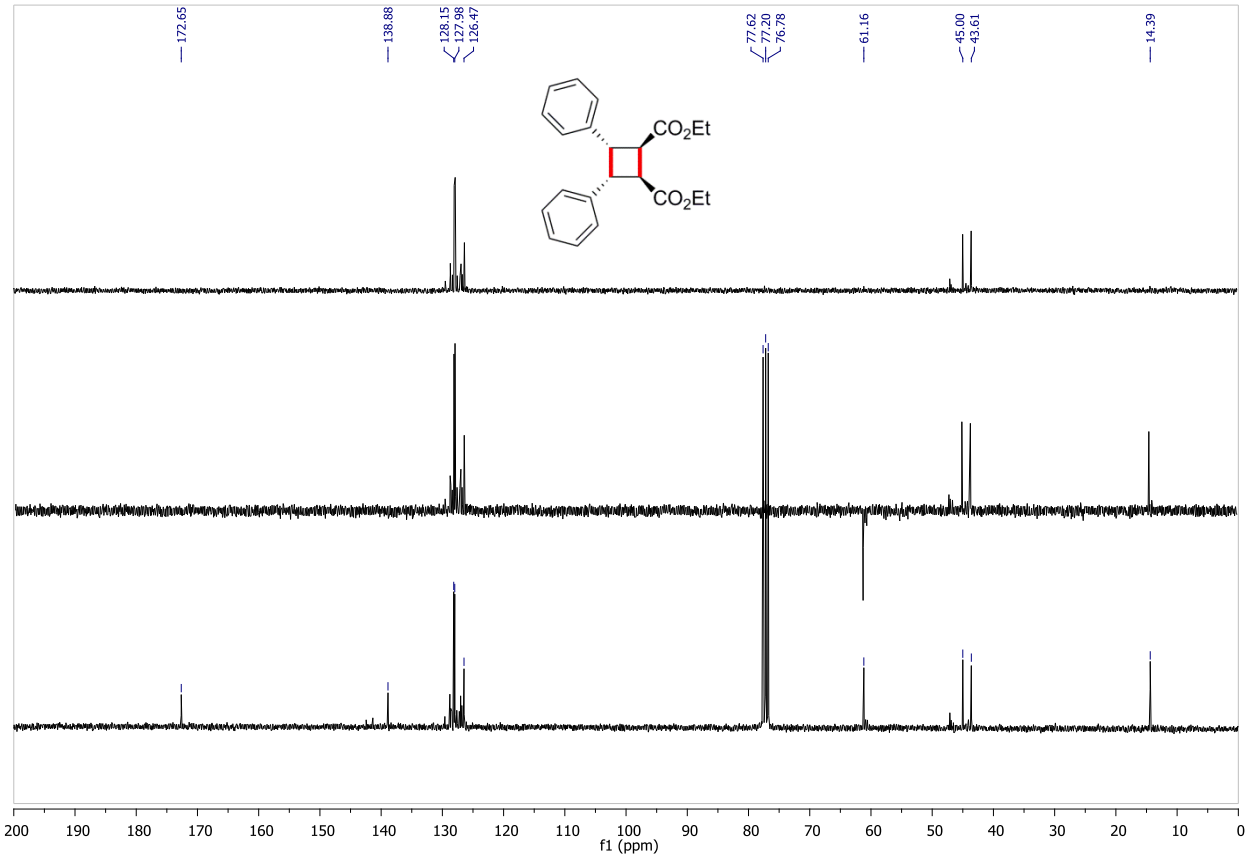

^{1}H-NMR: **2b** (*trans*, after separation)

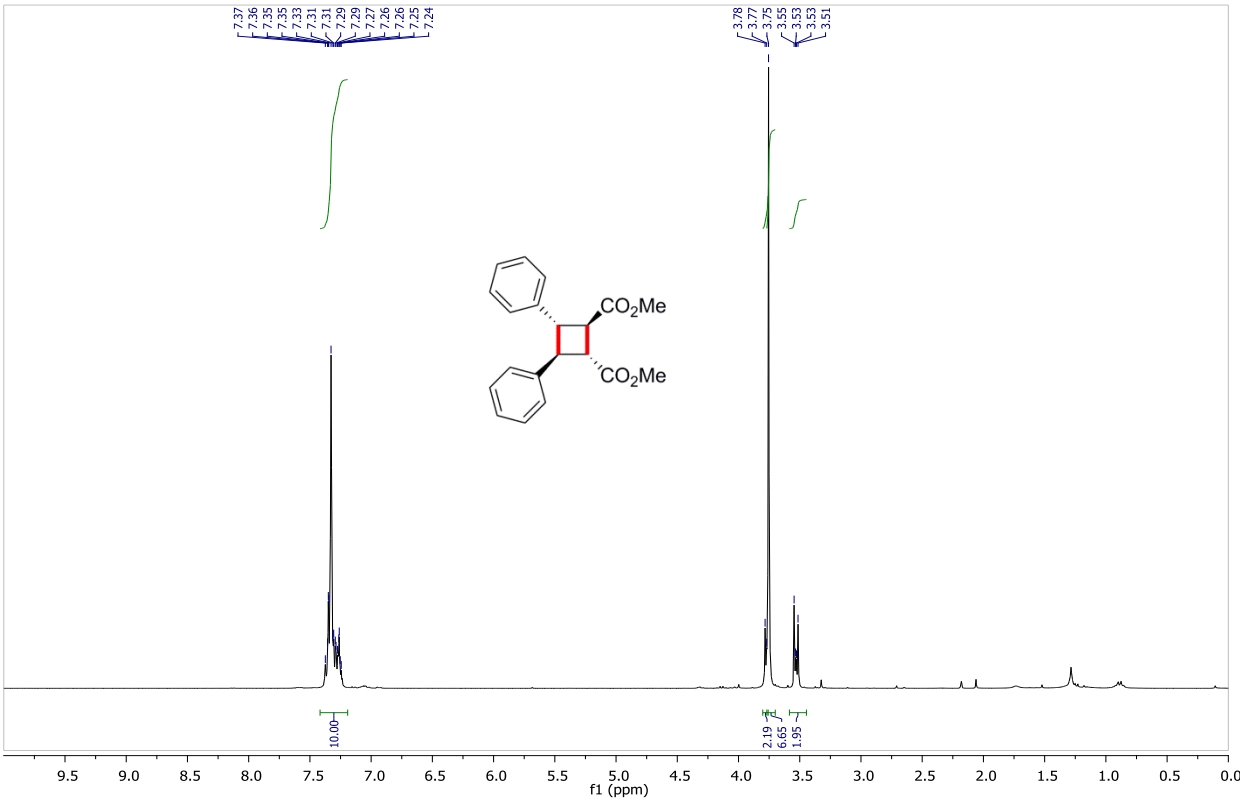

^{13}C-NMR: **2b** (*trans*, after separation)

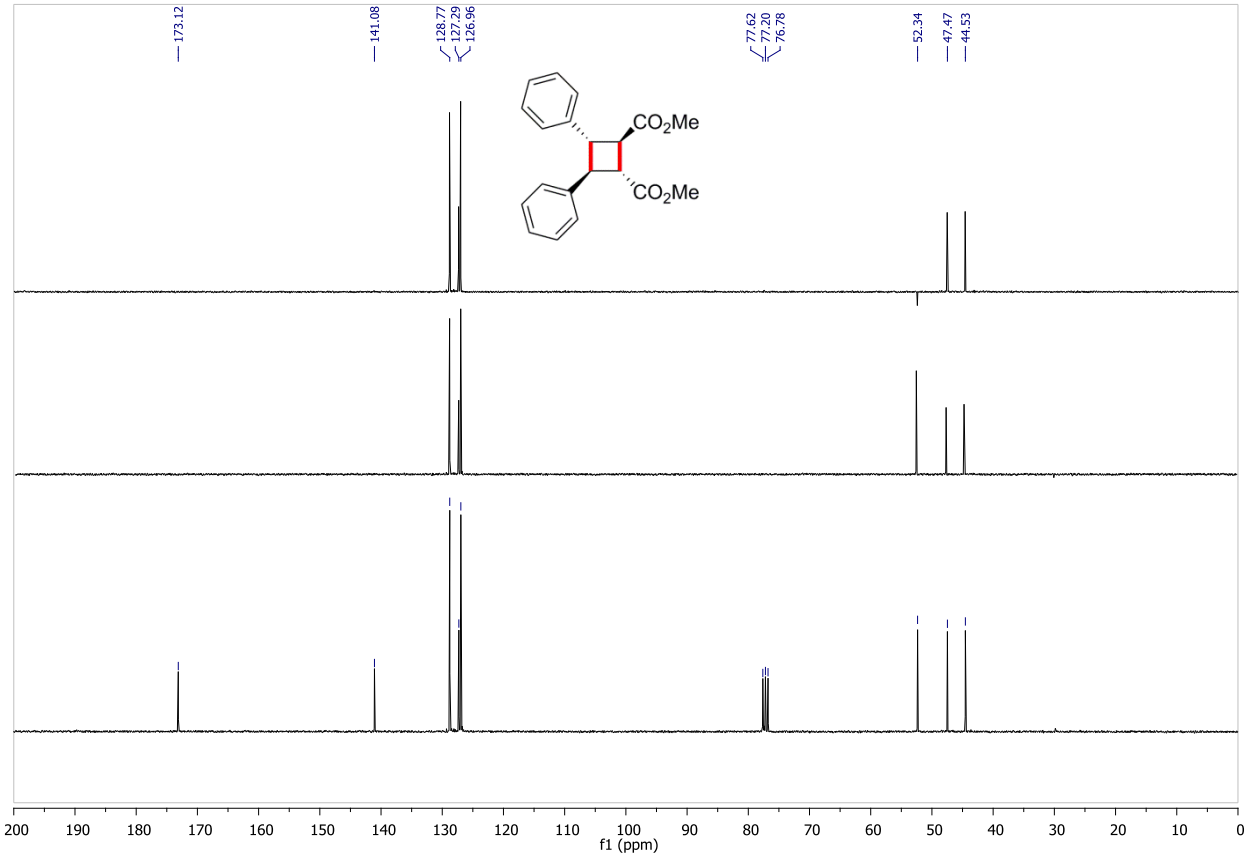

^{1}H-NMR: **3b** (*cis*, after separation)

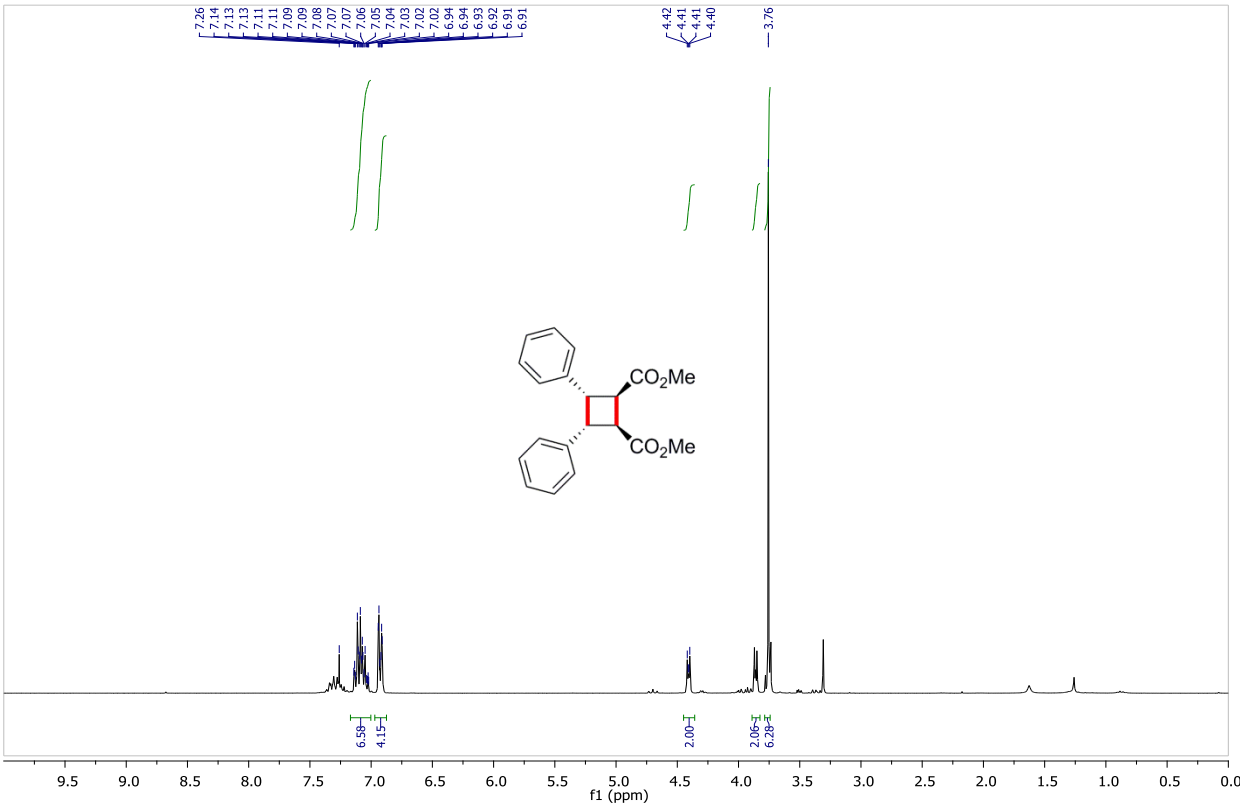

^{13}C-NMR: **3b** (*cis*, after separation)

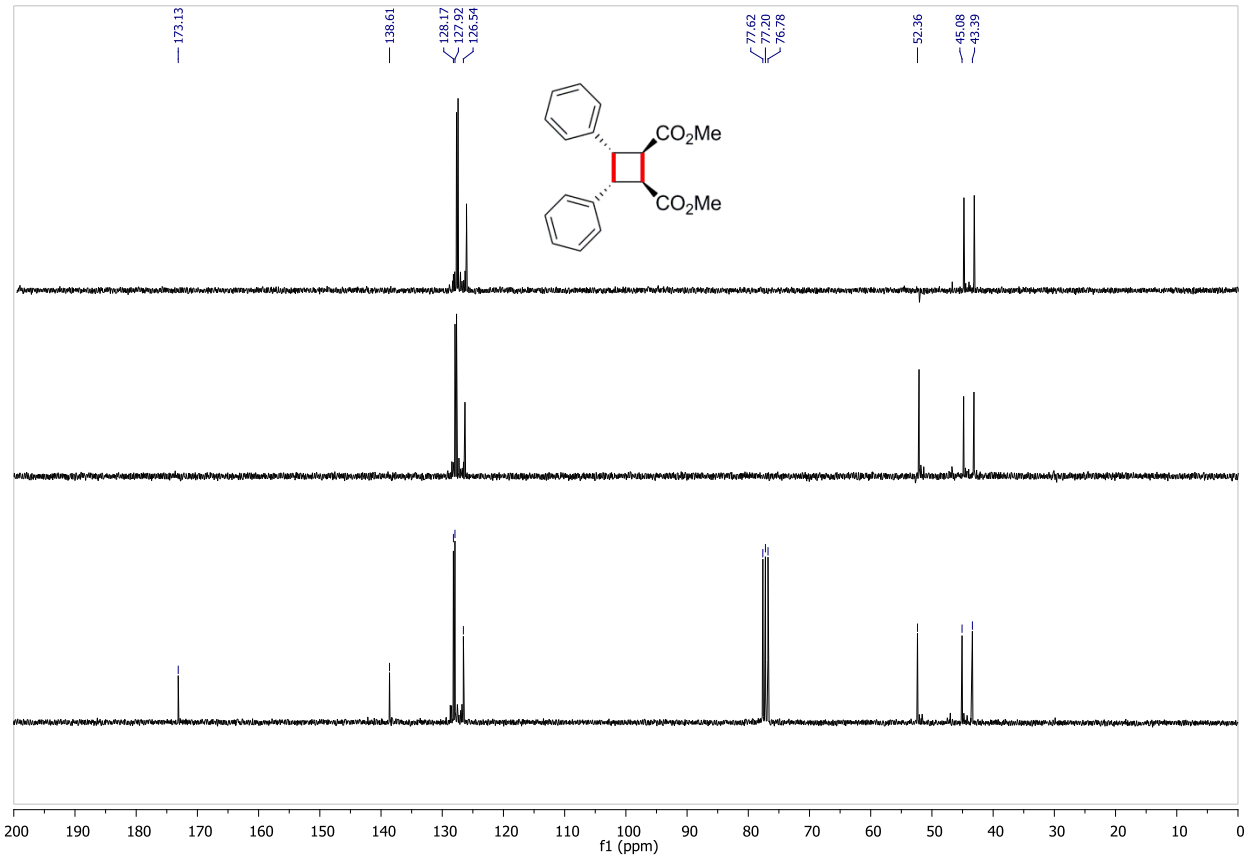

^{1}H-NMR: **2c** (*trans*, isomer only)

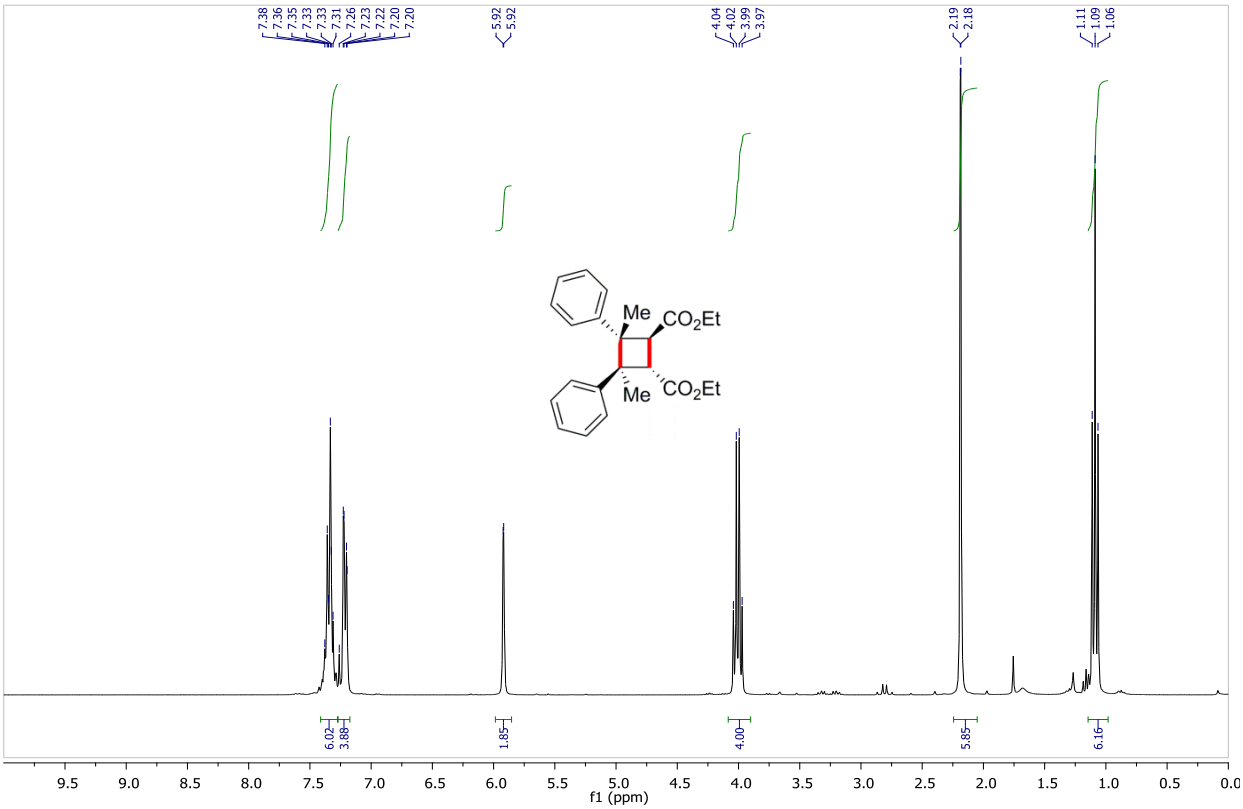

^{13}C-NMR: **2c** (*trans*, isomer only)

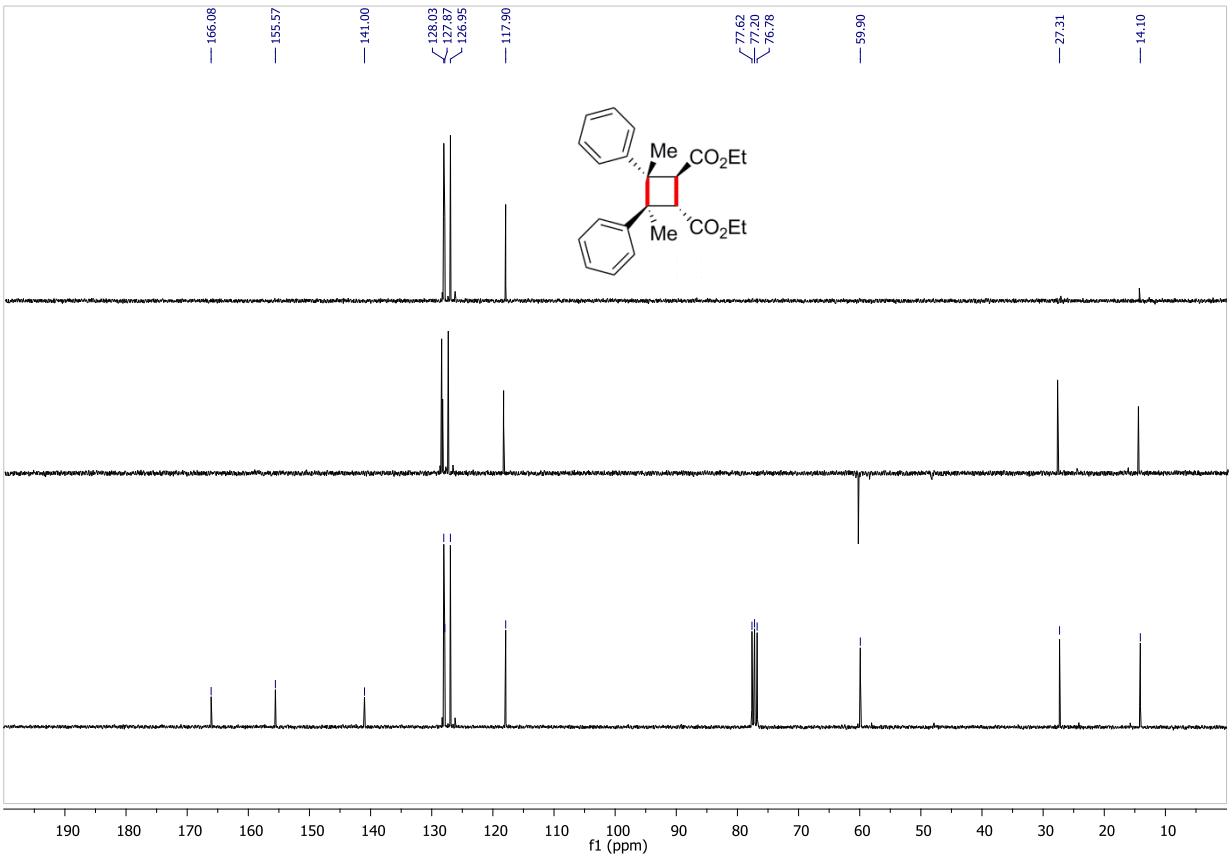

^{1}H-NMR: **2d/3d** (mixture, before separation)

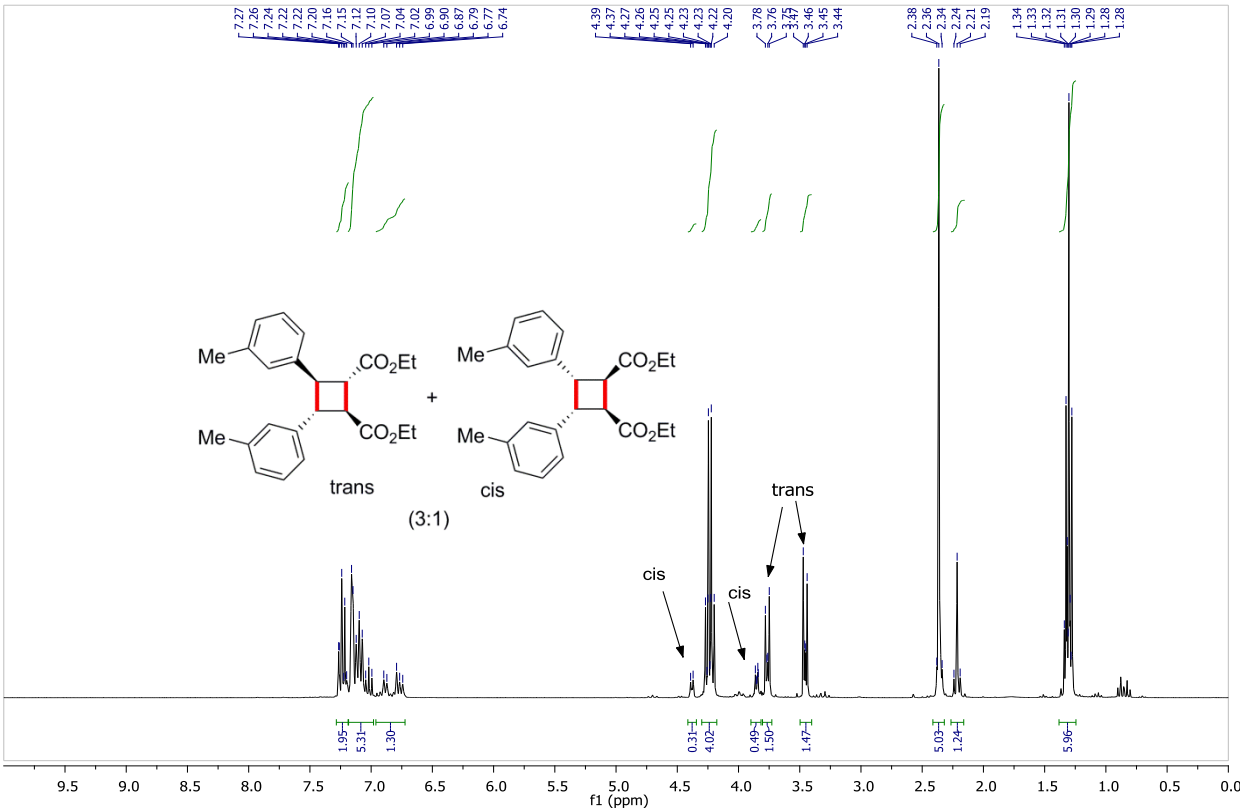

^{13}C-NMR: **2d/3d** (mixture, before separation)

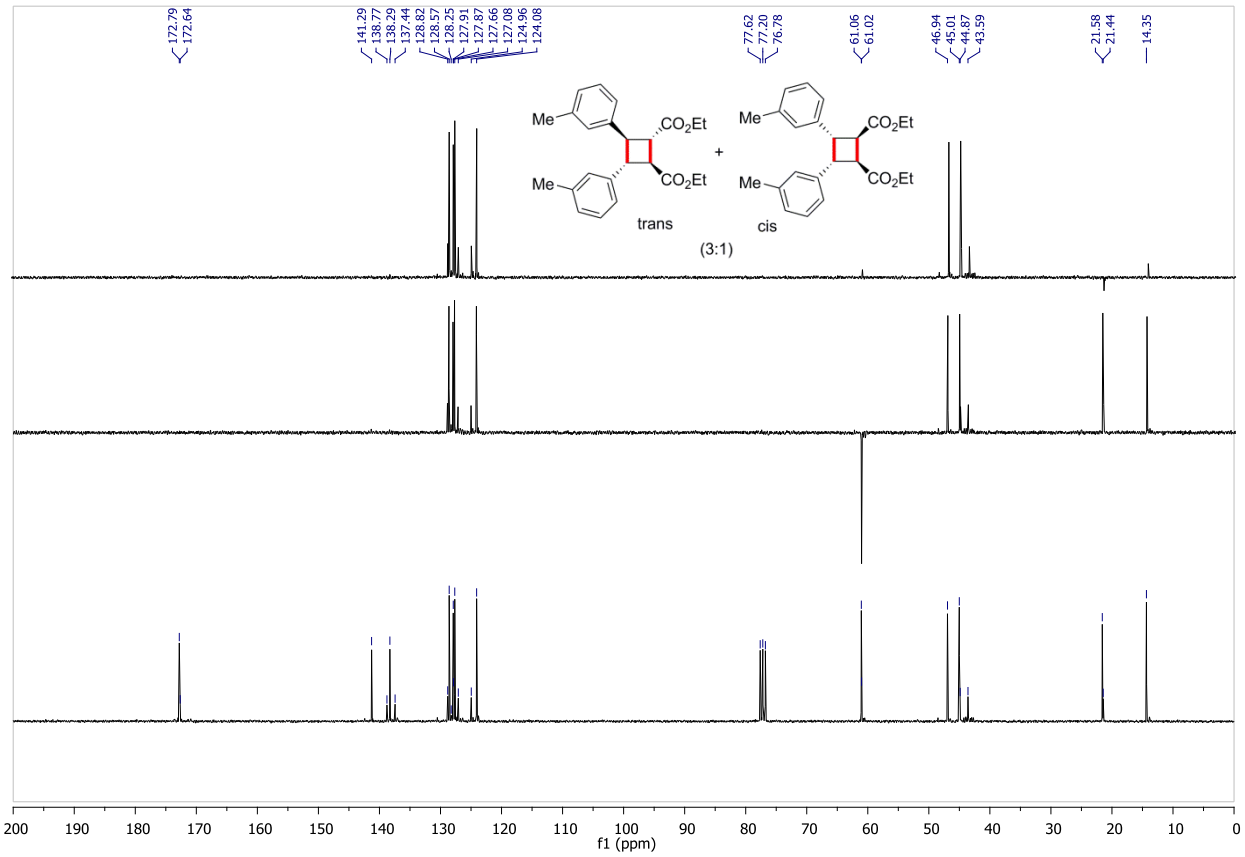

^{1}H-NMR: **2d** (*trans*, after separation)

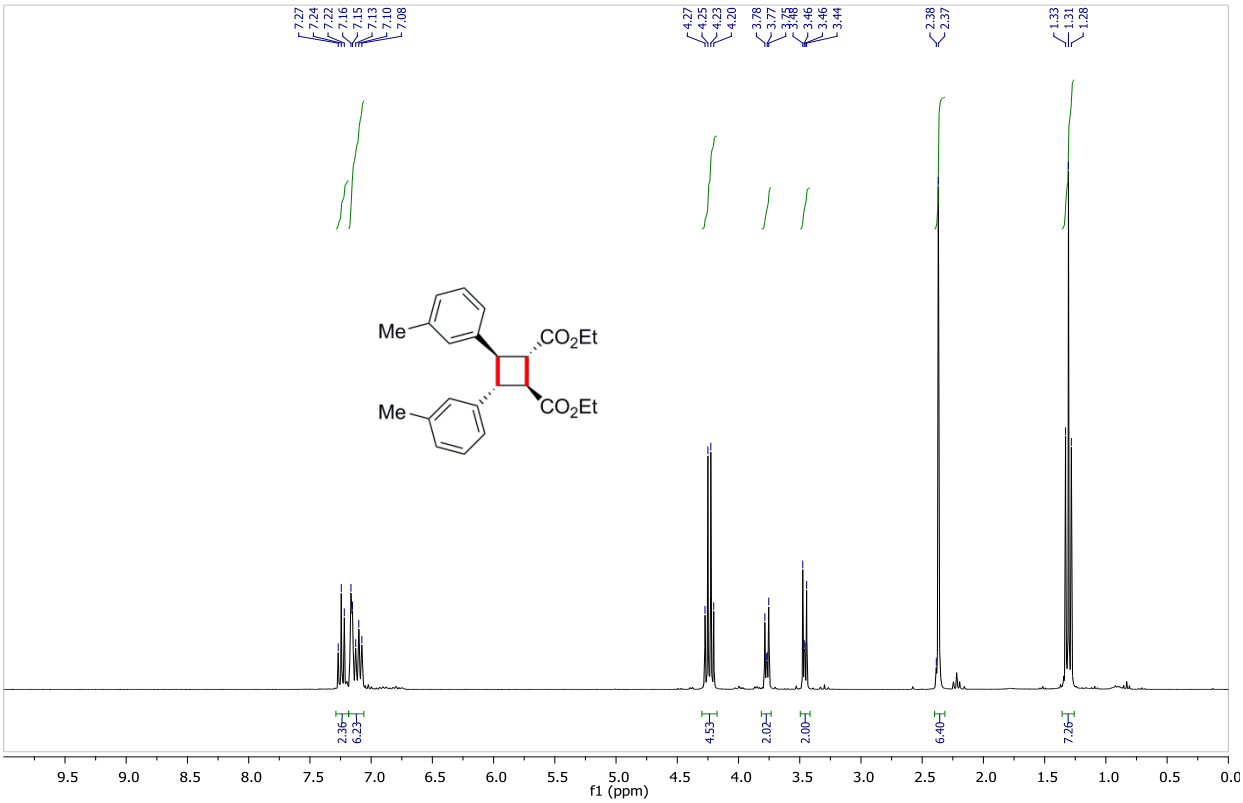

^{13}C-NMR: **2d** (*trans*, after separation)

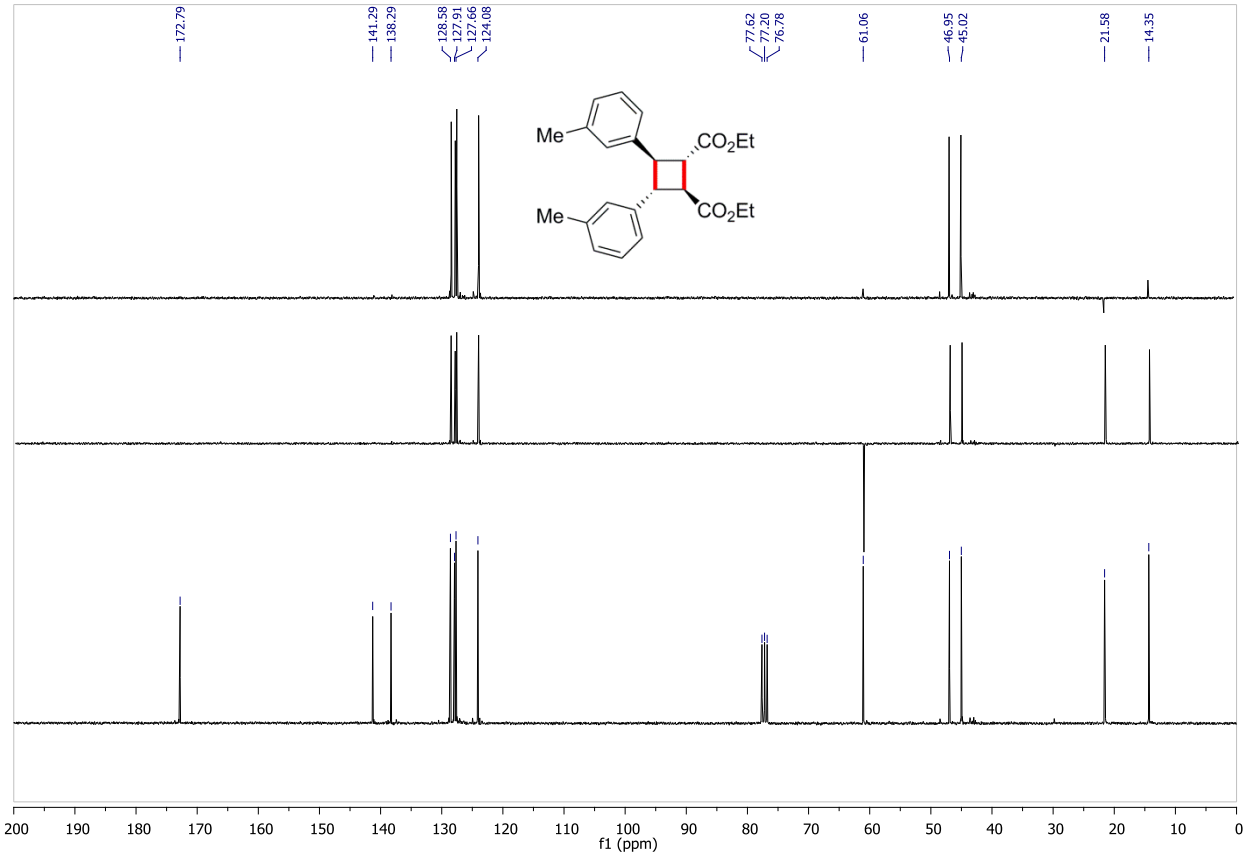

^{1}H-NMR: **3d** (*cis*, after separation)

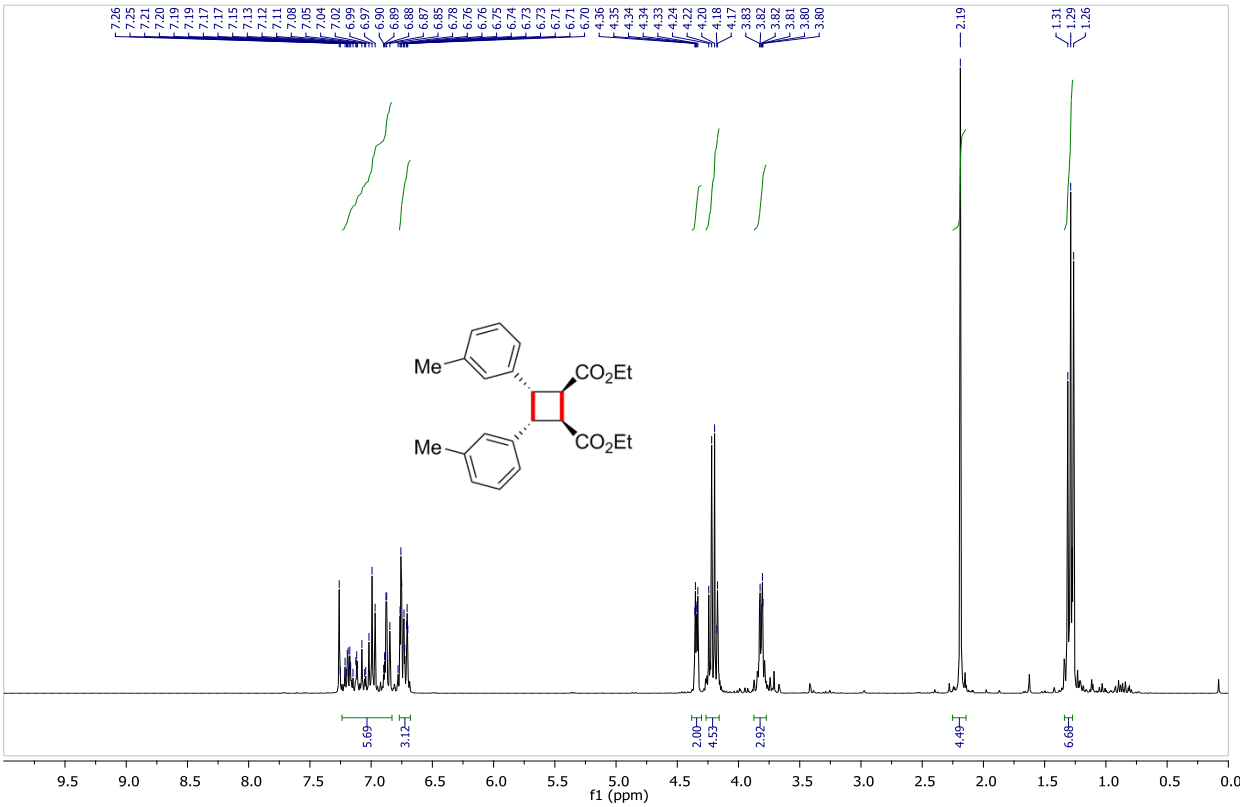

^{13}C-NMR: **3d** (*cis*, after separation)

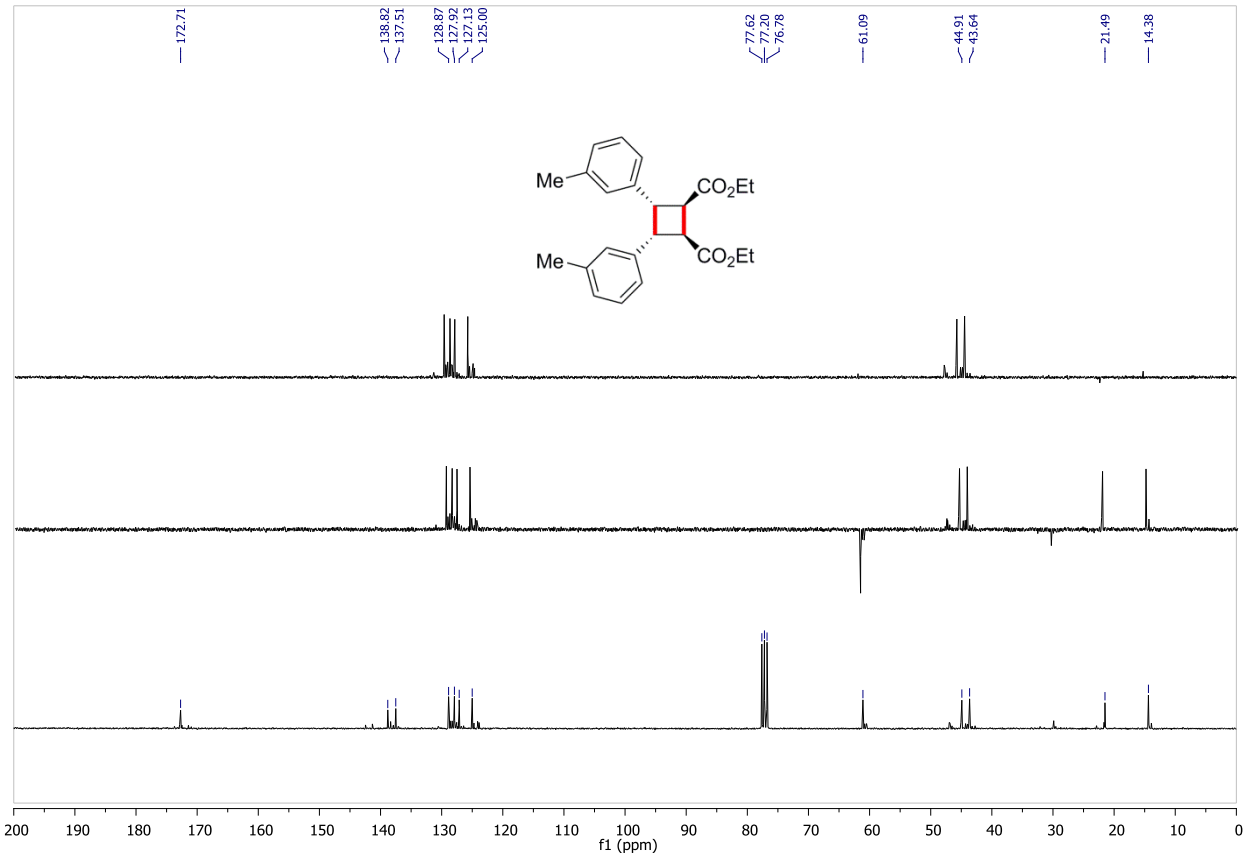

^{1}H-NMR: **2e/3e** (mixture, before separation)

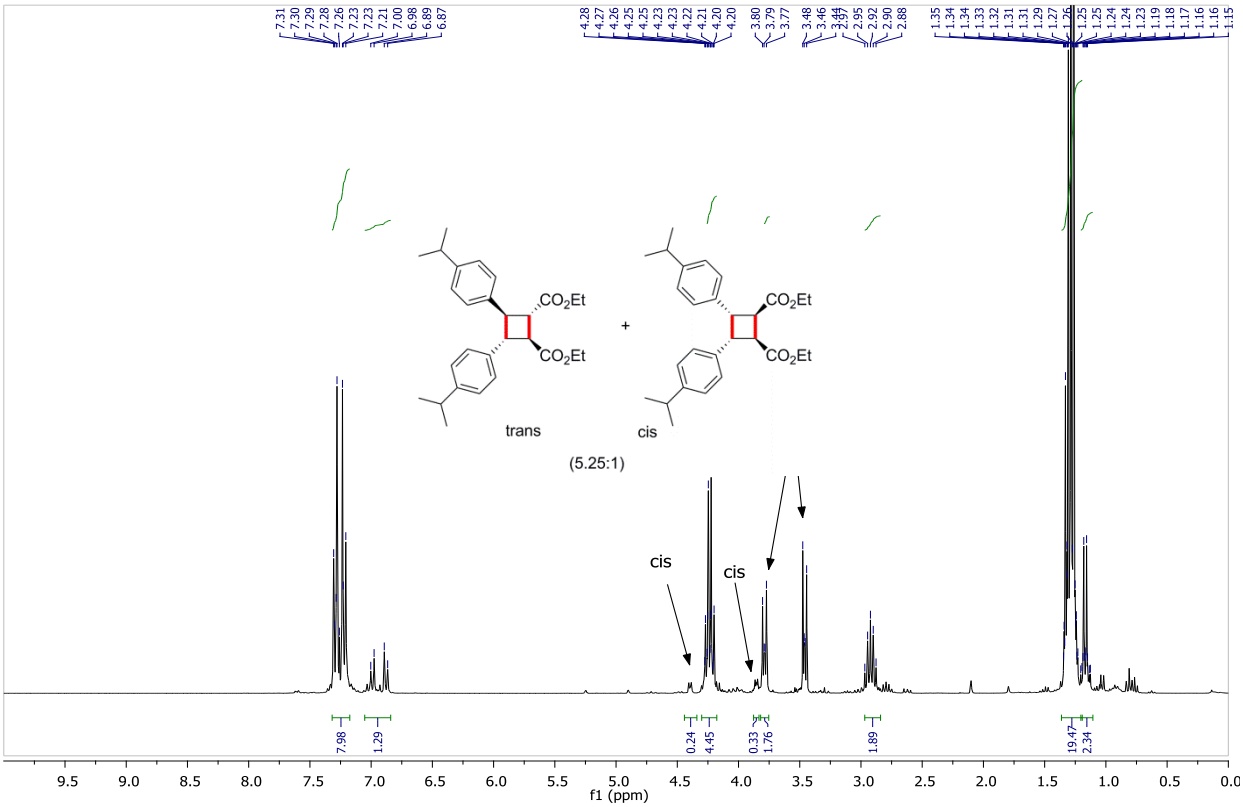

^{13}C-NMR: **2e/3e** (mixture, before separation)

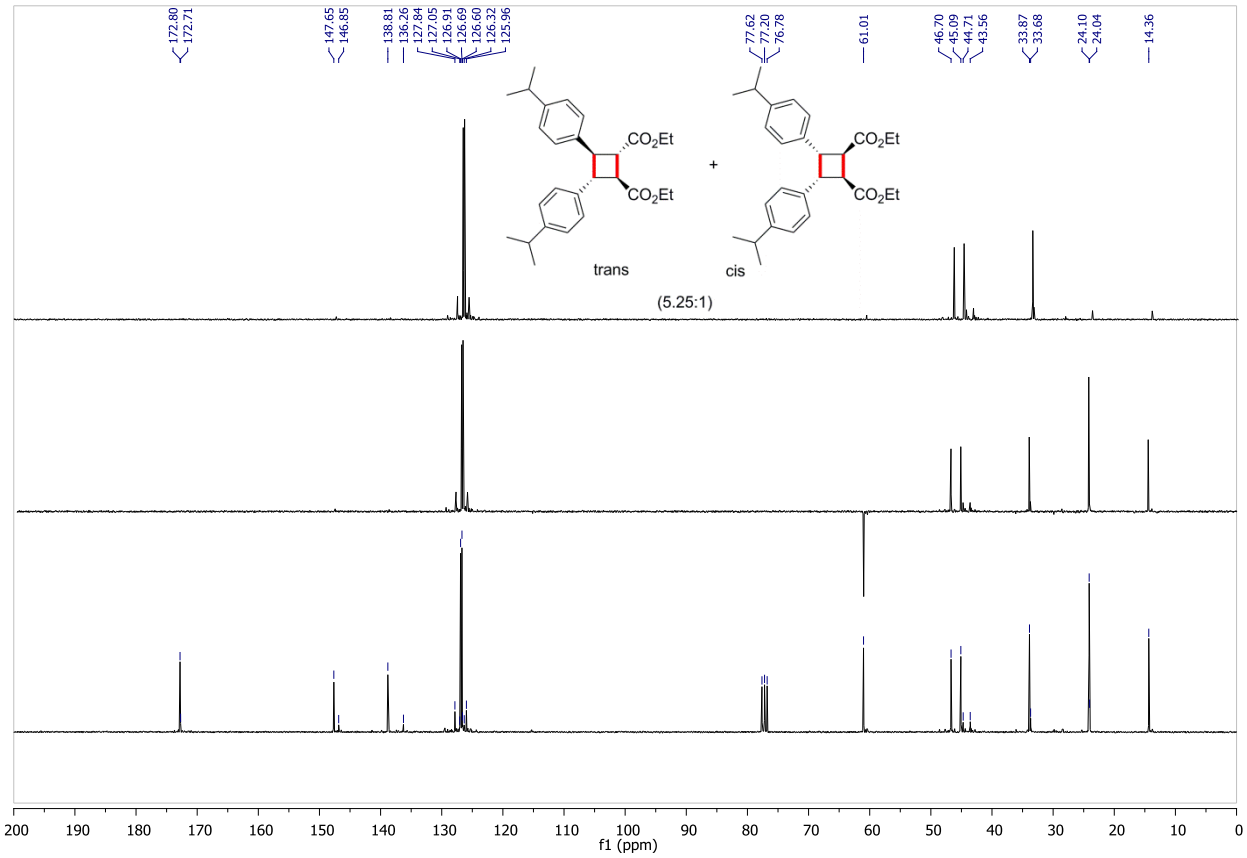

^{1}H-NMR: **2e** (*trans*, after separation)

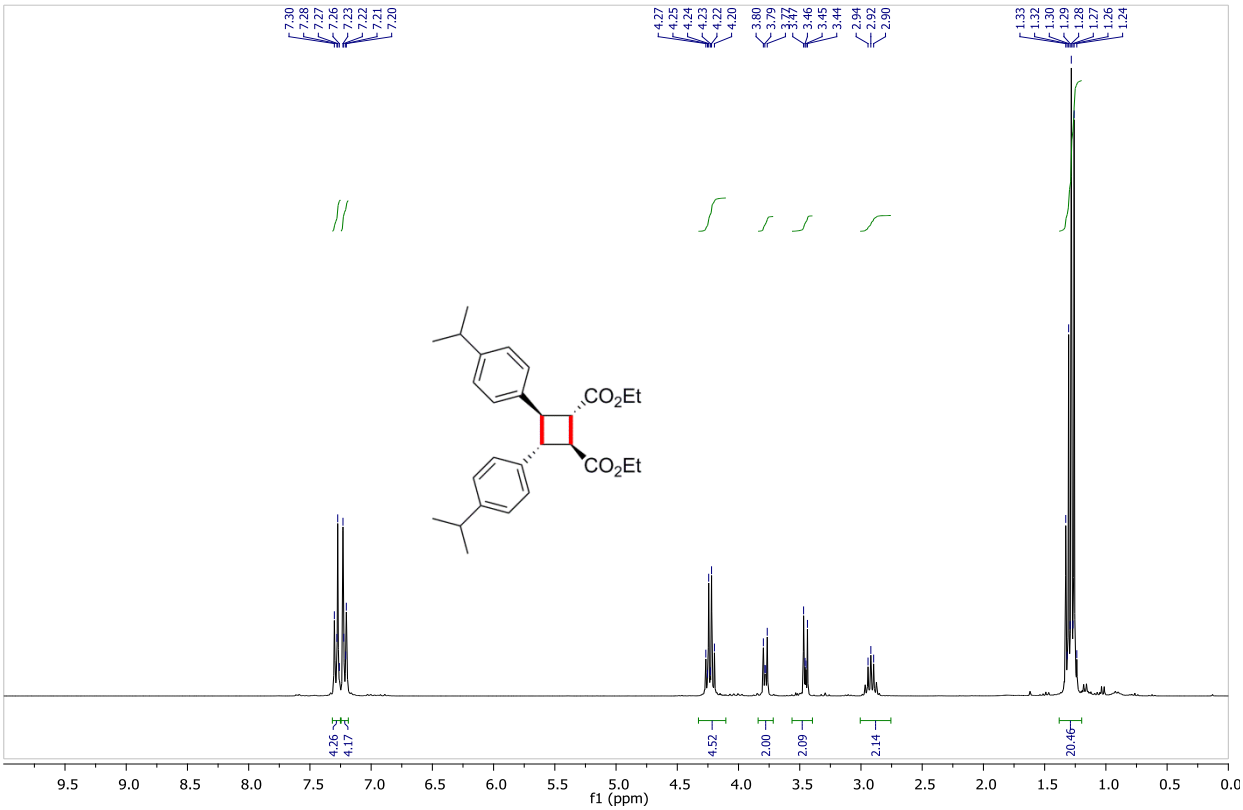

^{13}C-NMR: **2e** (*trans*, after separation)

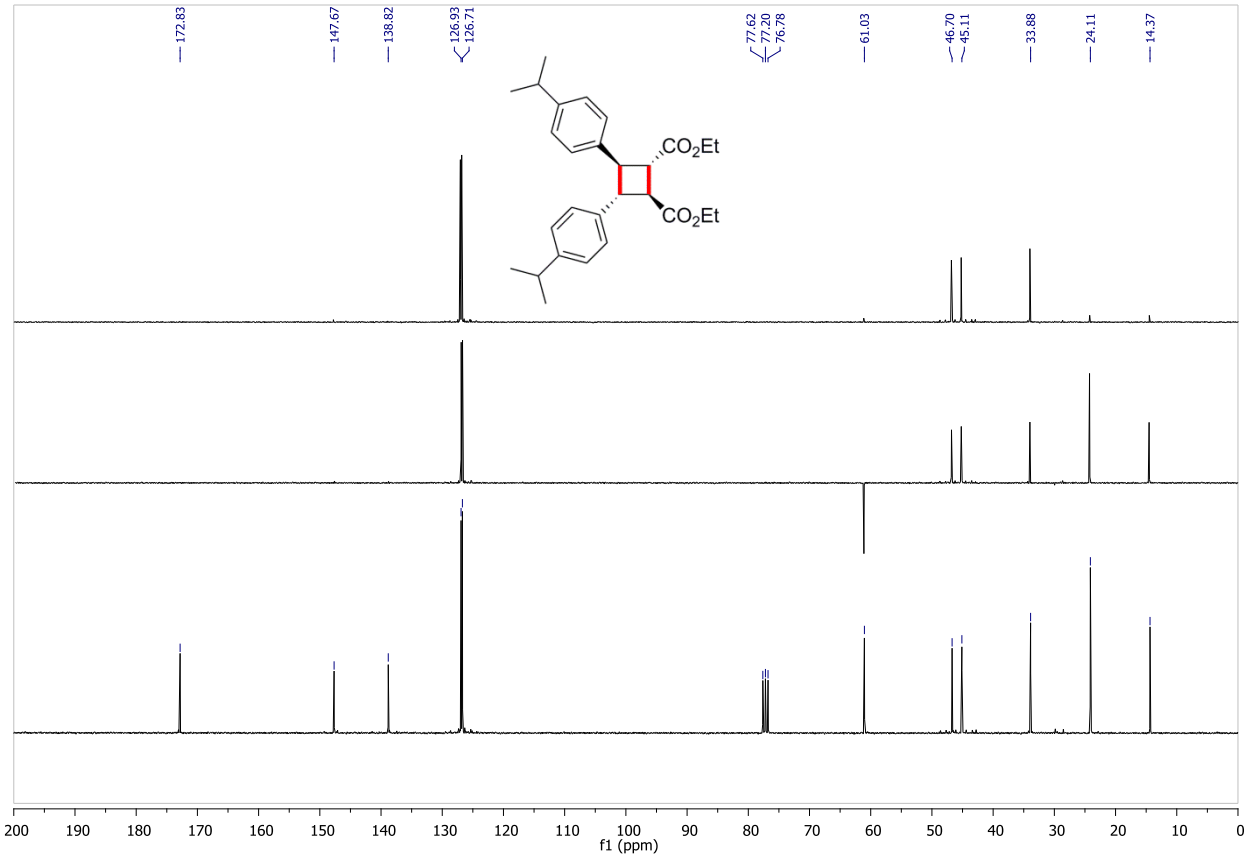

^{1}H-NMR: **3e** (*cis*, after separation)

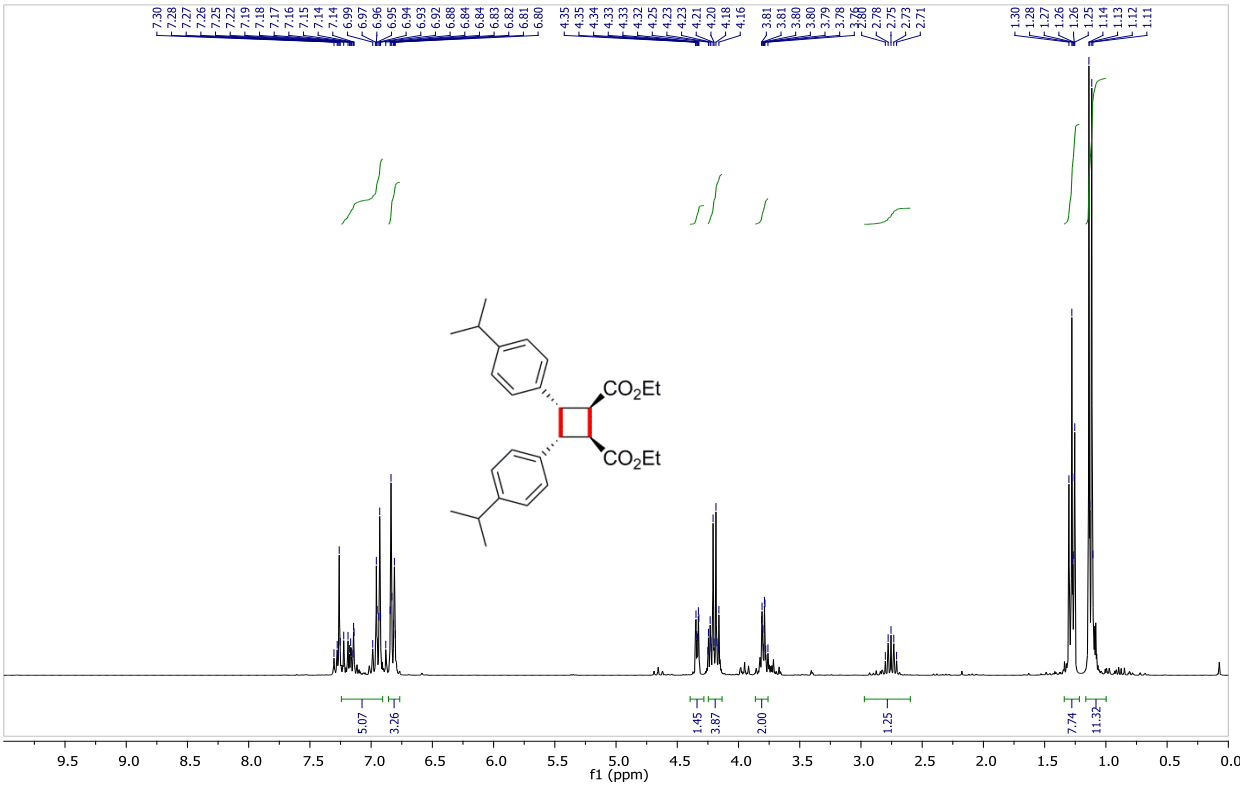

^{13}C-NMR: **3e** (*cis*, after separation)

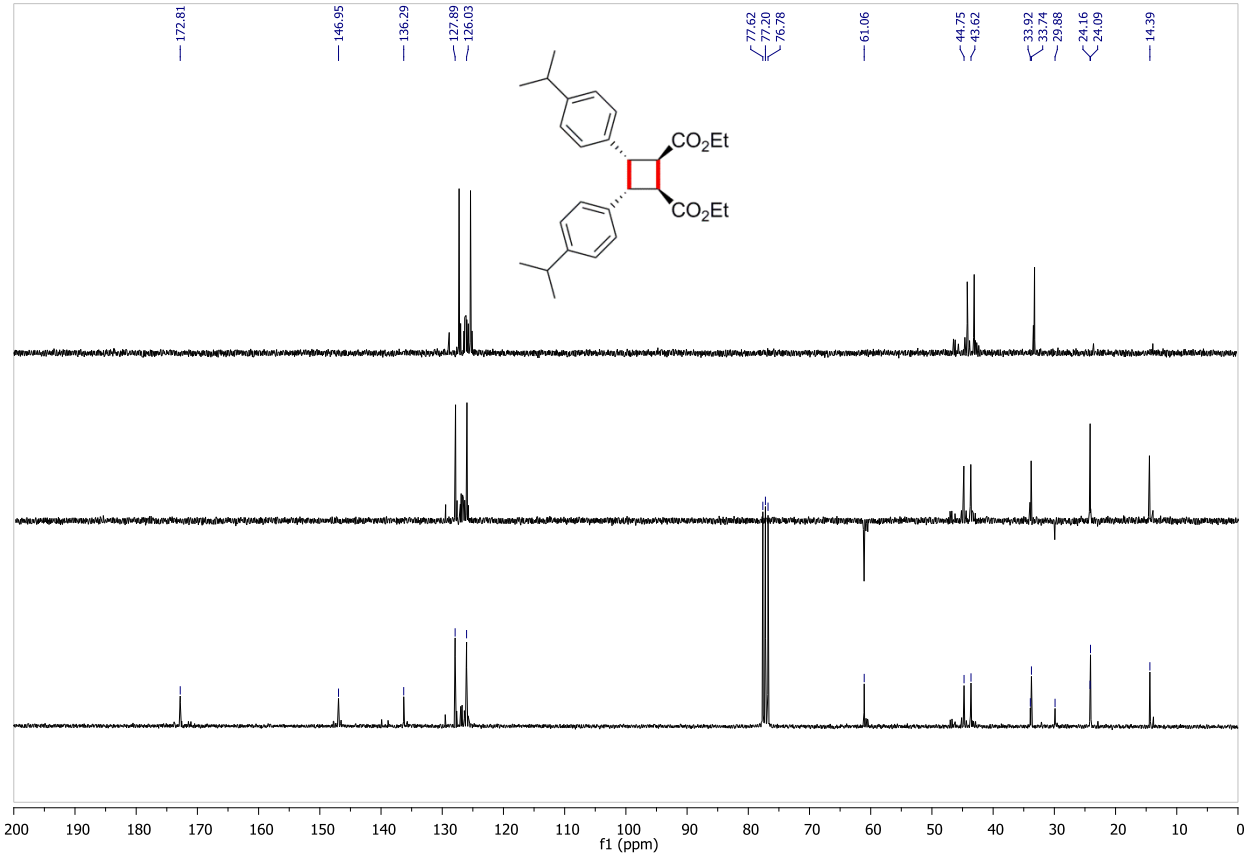

^{1}H-NMR: **2f** (*mixture*, before seperation)

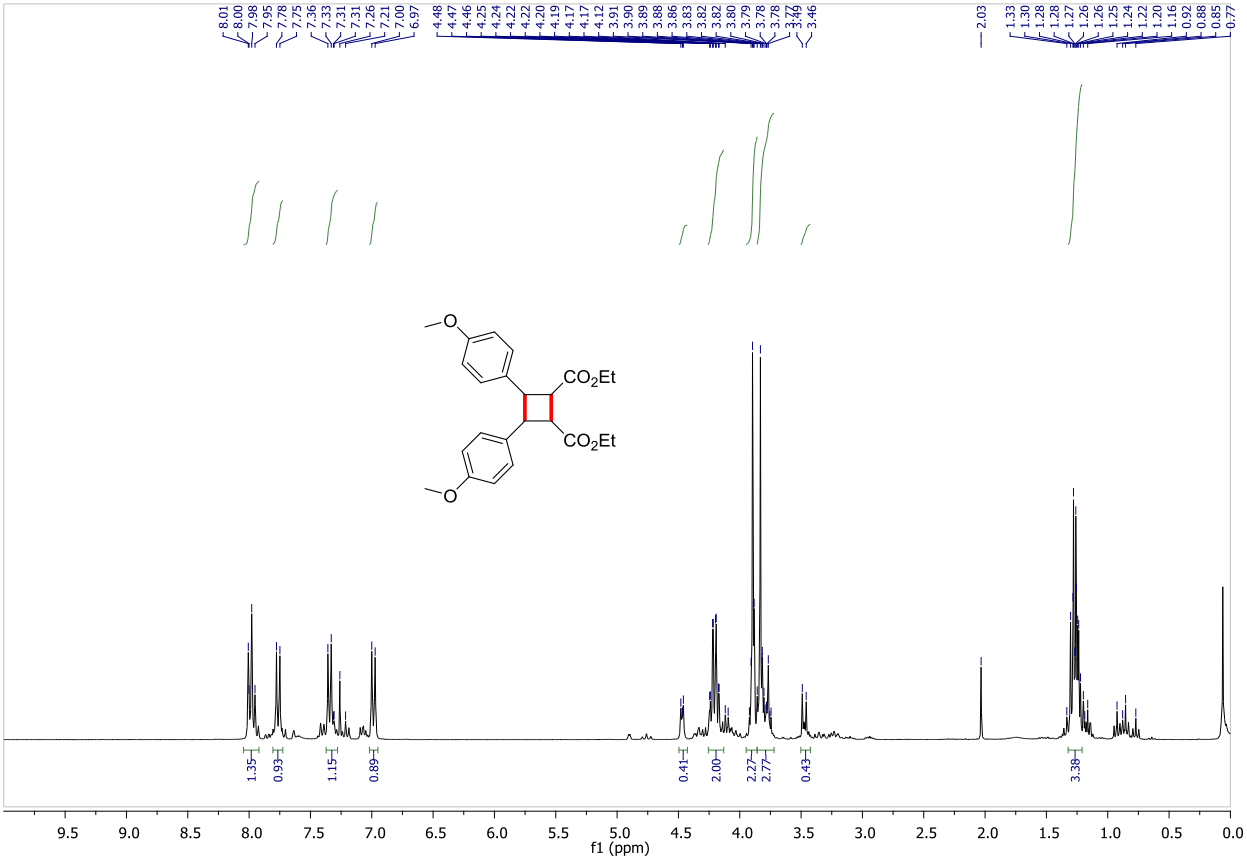

^{1}H-NMR: **2f** (*trans*, after seperation)

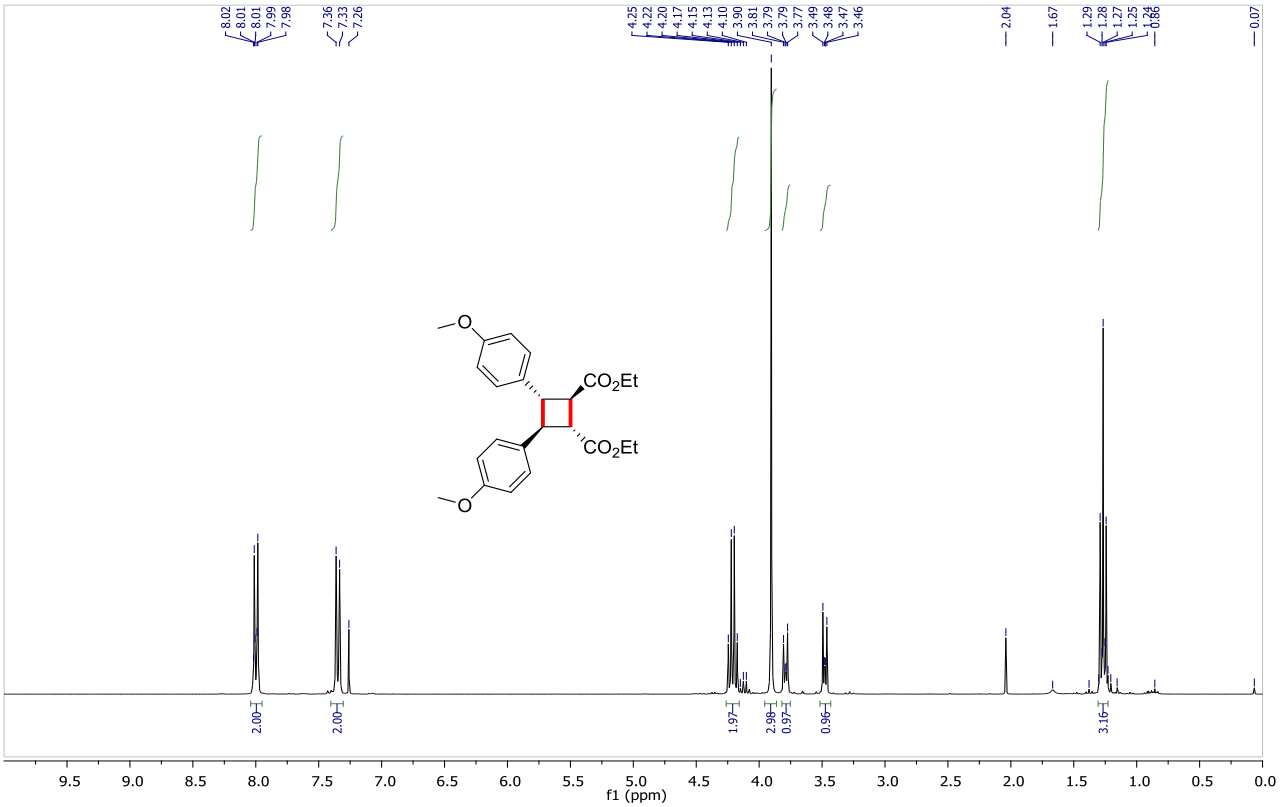

^{13}C-NMR: **2f** (*trans*, after separation)

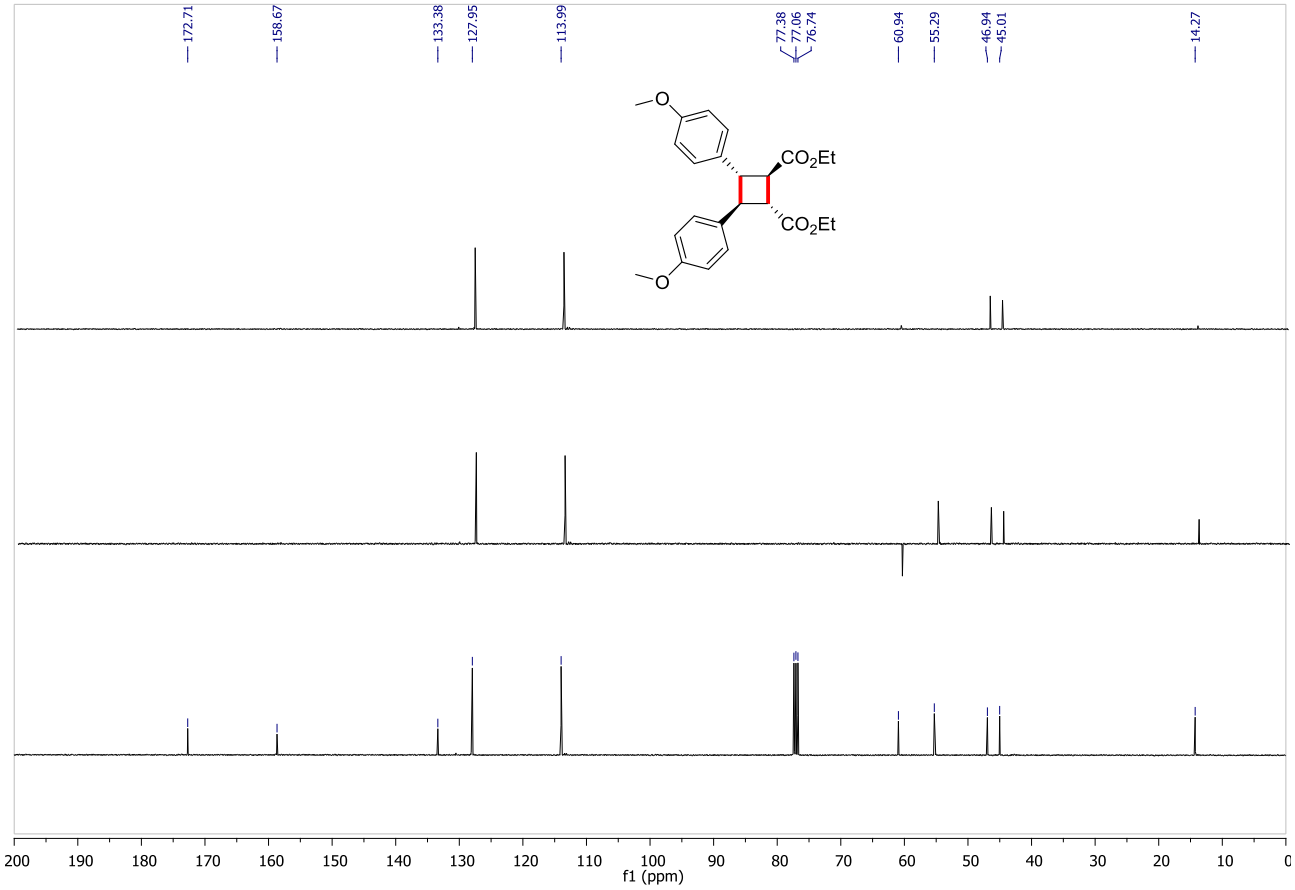

^{1}H-NMR: **2g** (*trans*, after separation)

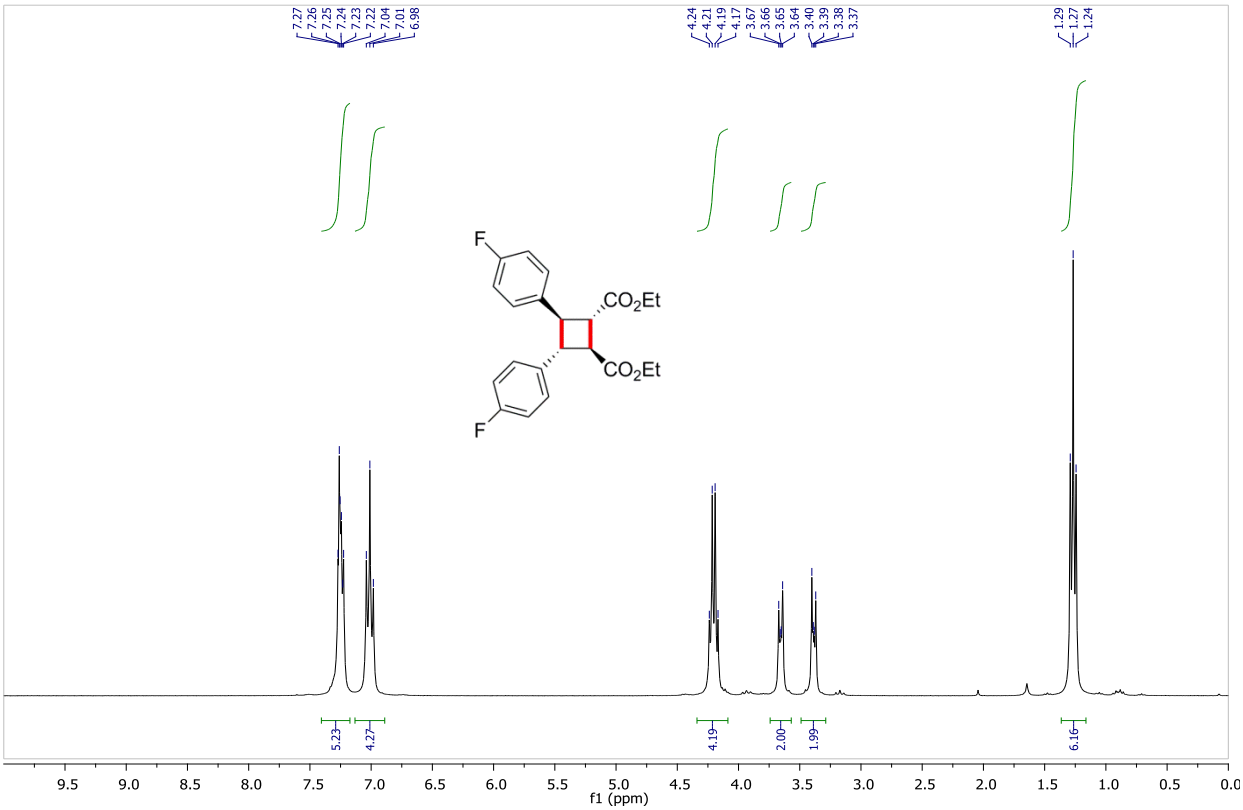

^{13}C-NMR: **2g** (*trans*, after separation)

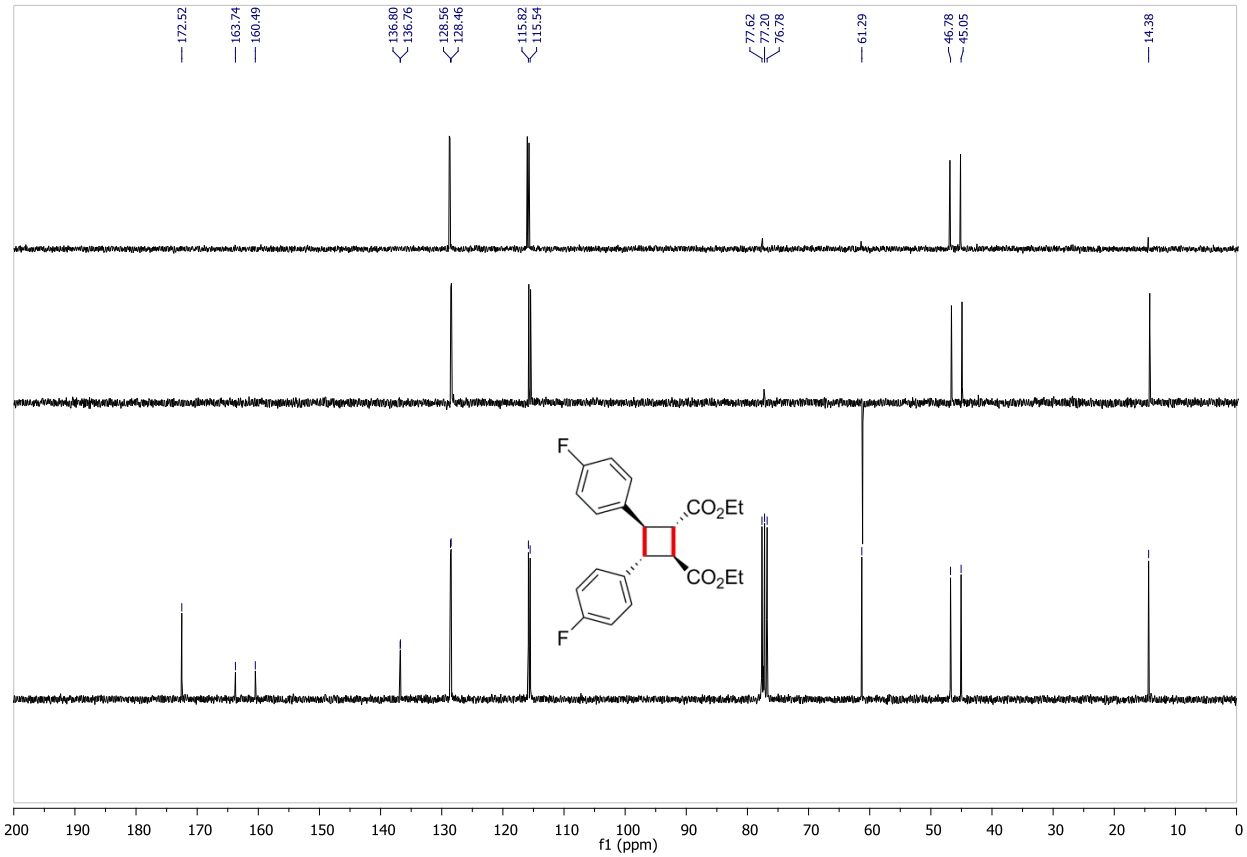

^{19}F-NMR: **2g** (*trans*, after separation)

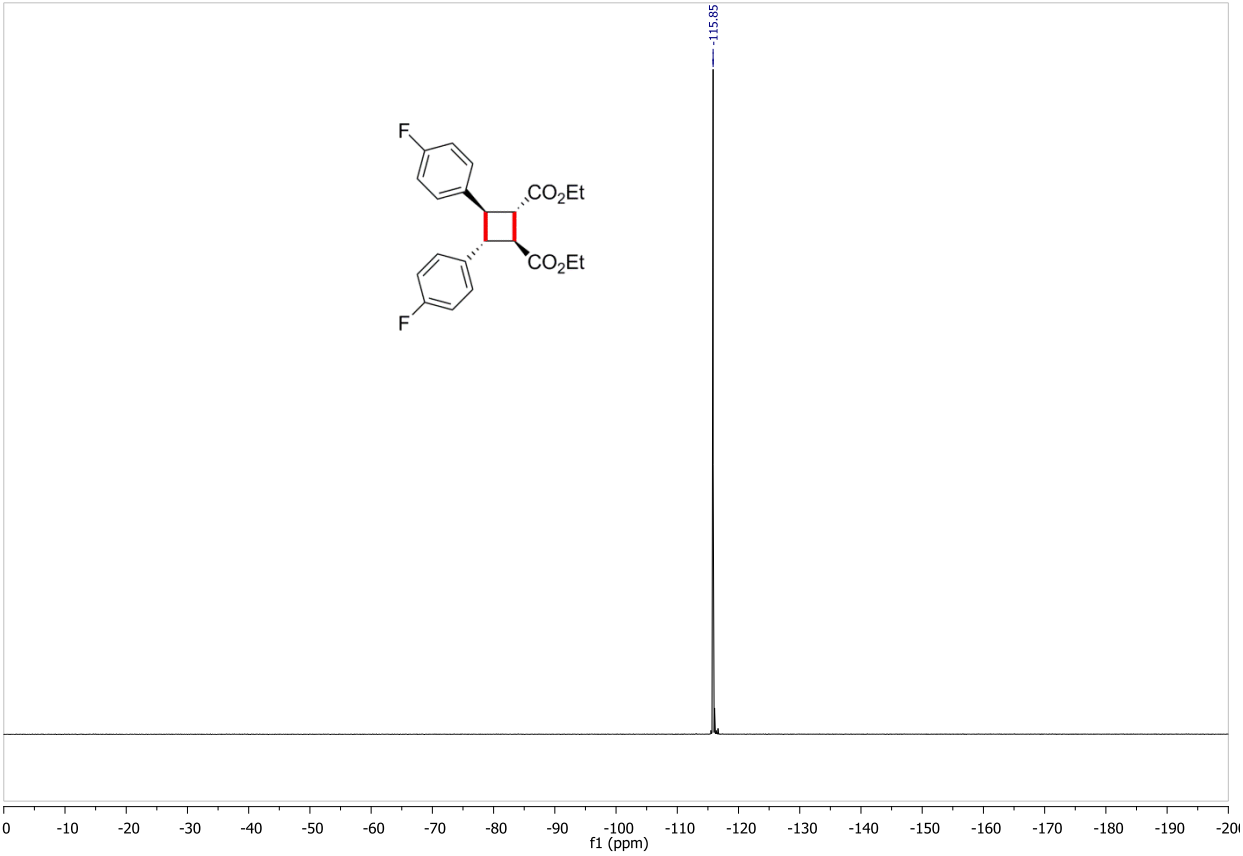

^{1}H-NMR: **2h** (*trans*, after separation)

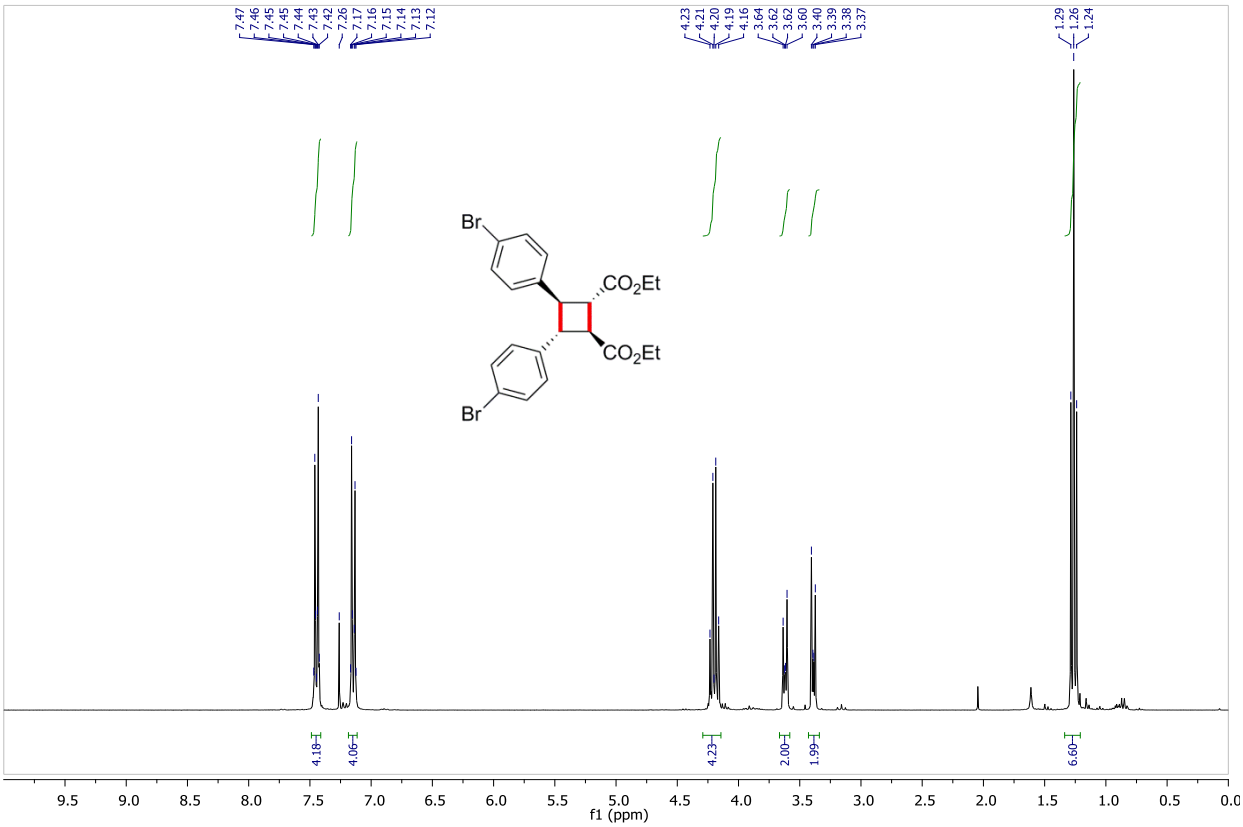

^{13}C-NMR: **2h**(*trans*, after separation)

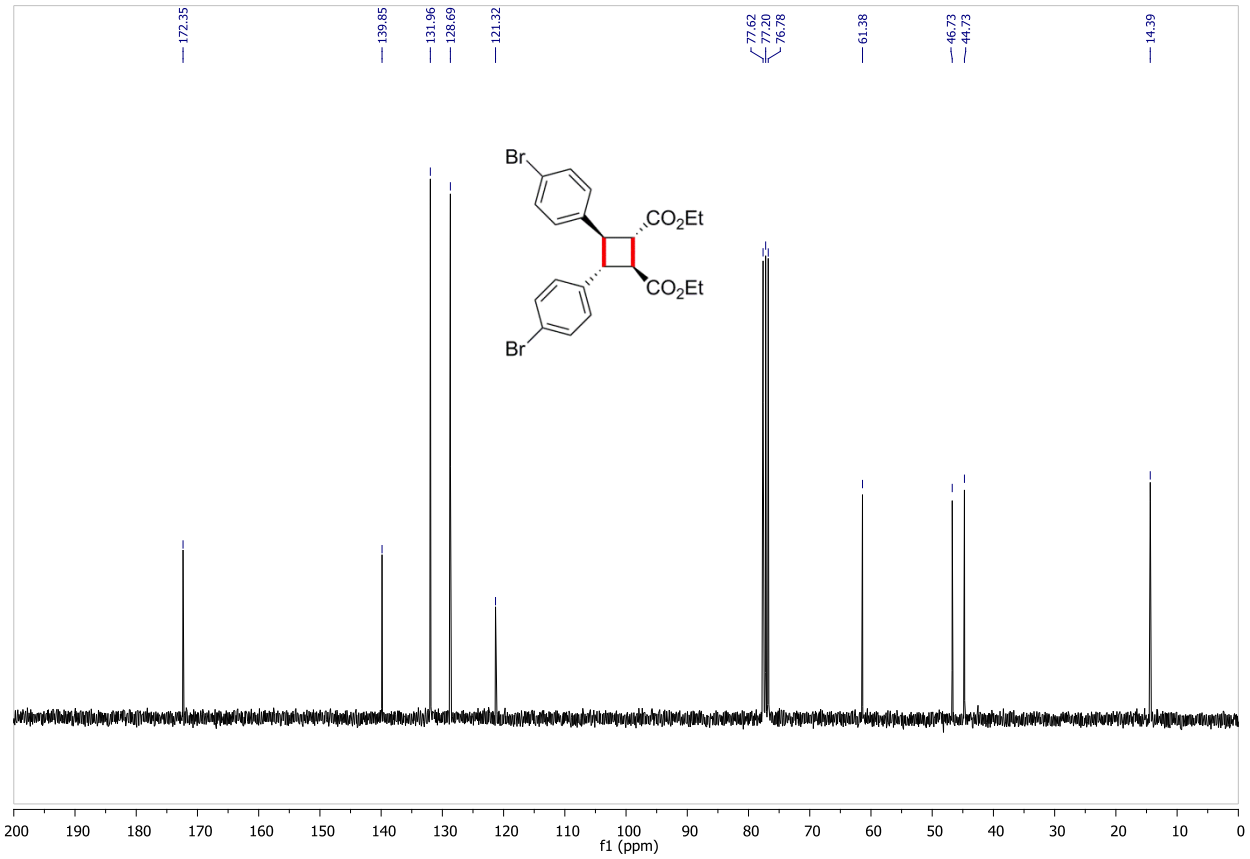

^{1}H-NMR: **2i/3i** (*mixture*, before separation)

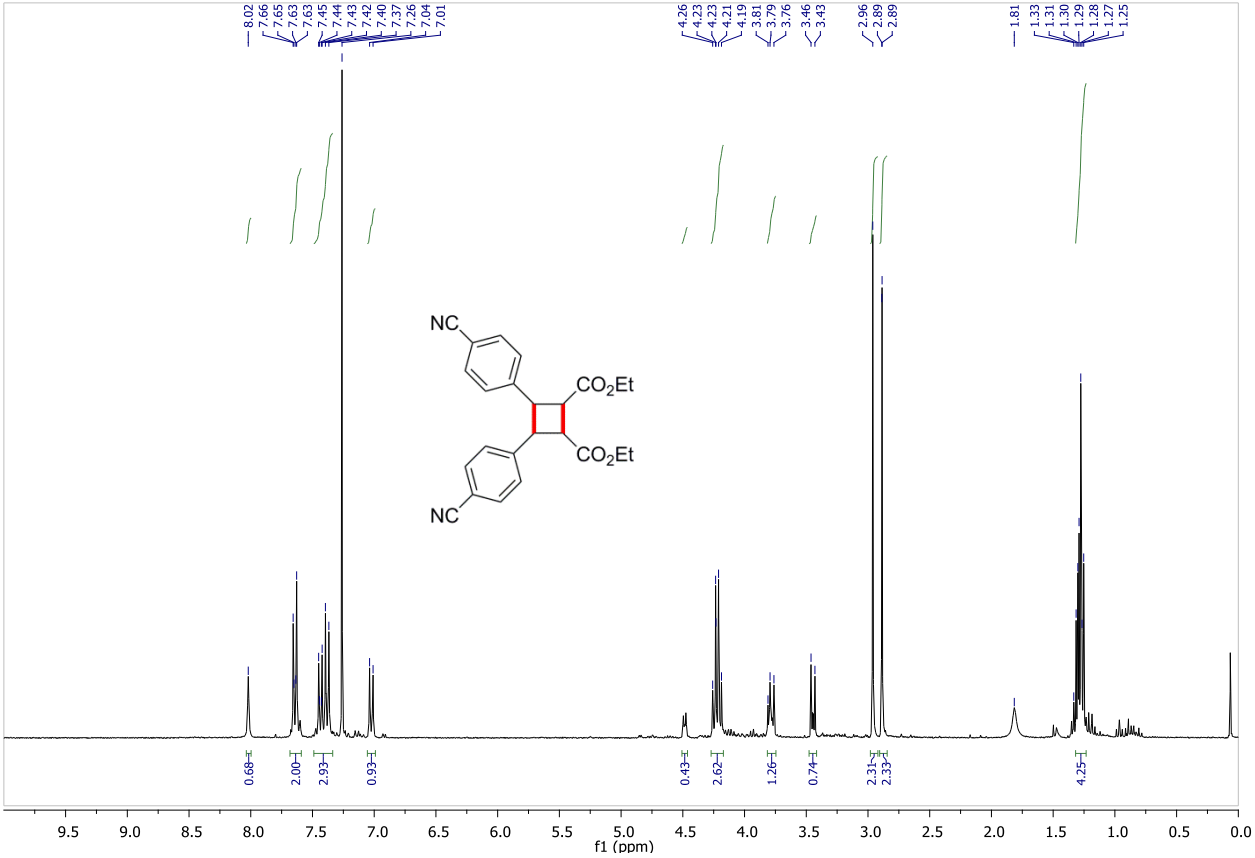

^{1}H-NMR: **2i** (*trans*, after separation)

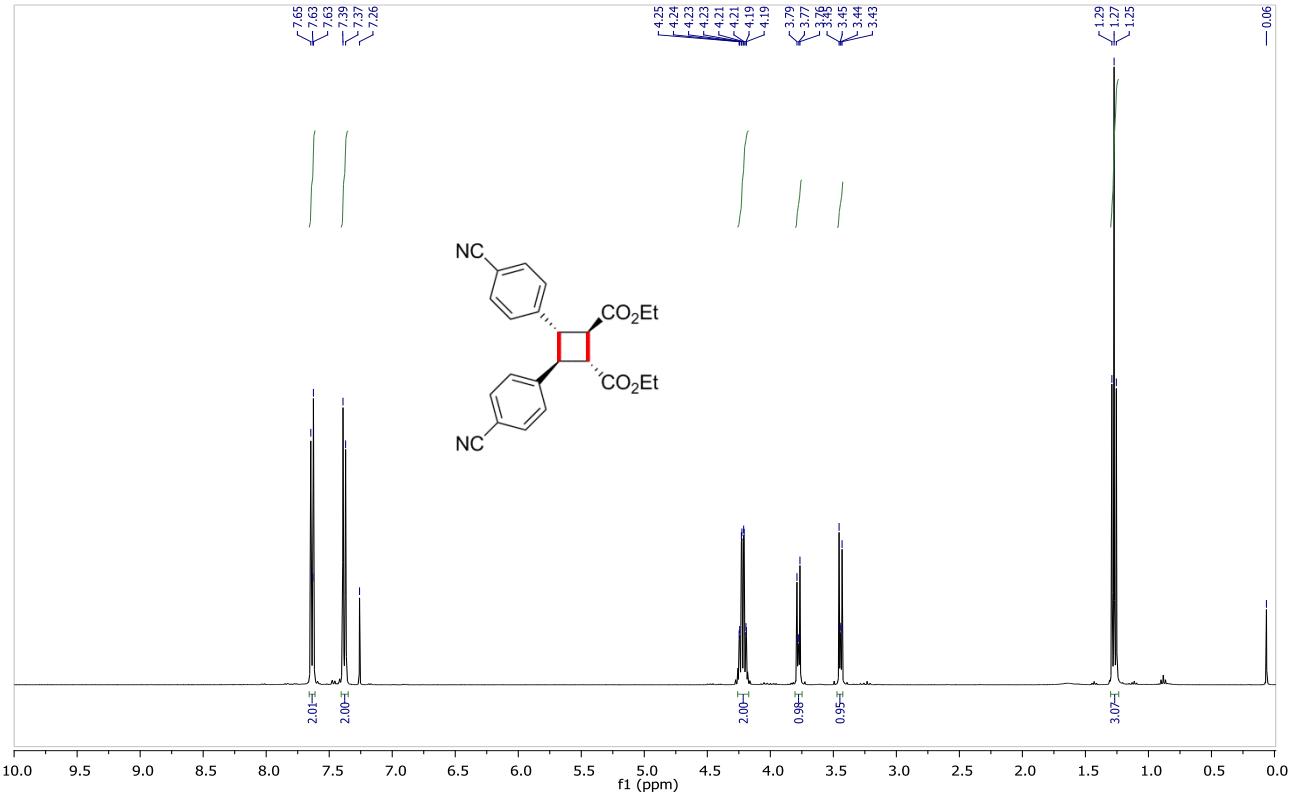

^{13}C-NMR: **2i** (*trans*, after separation)

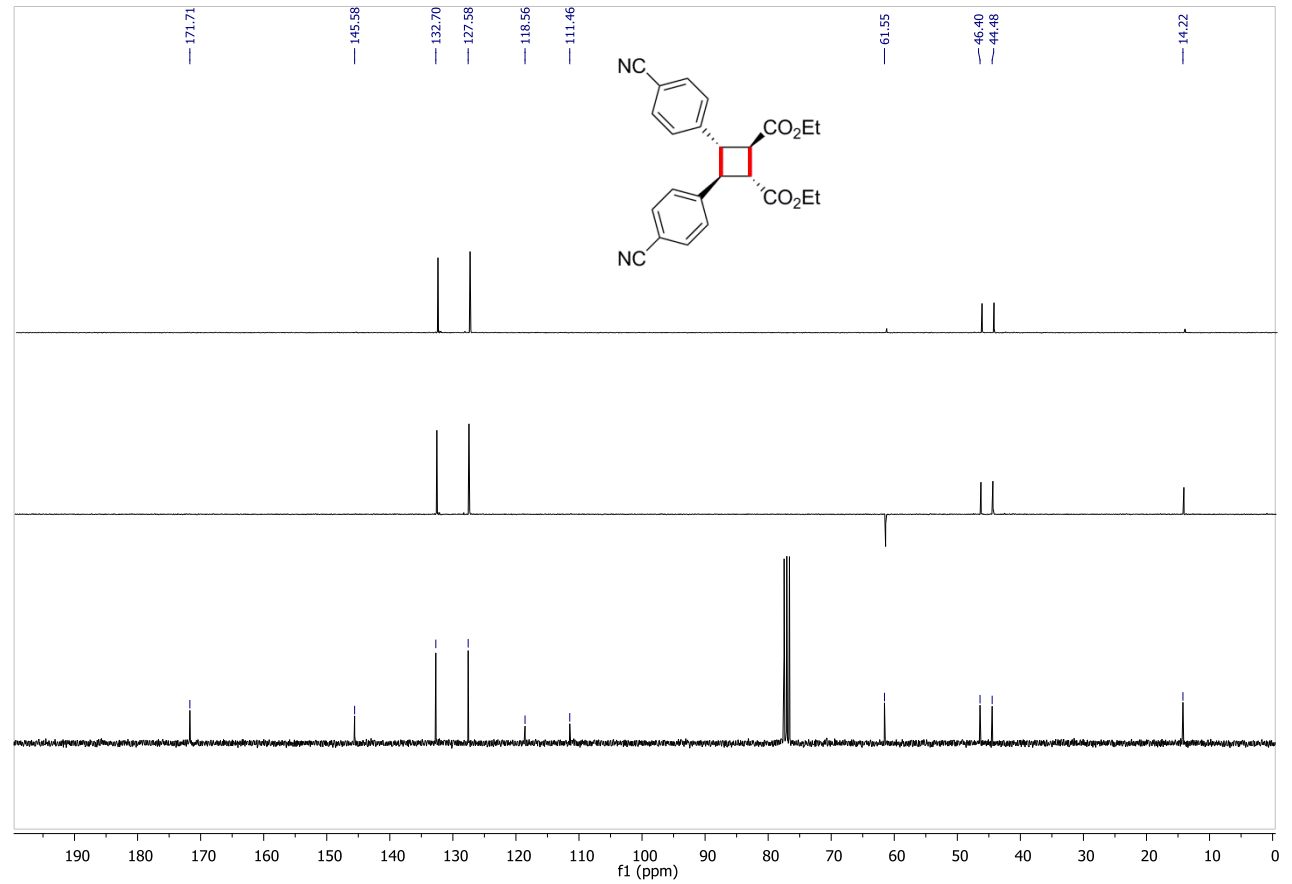

^{1}H-NMR: **2j** (*trans*, after separation)

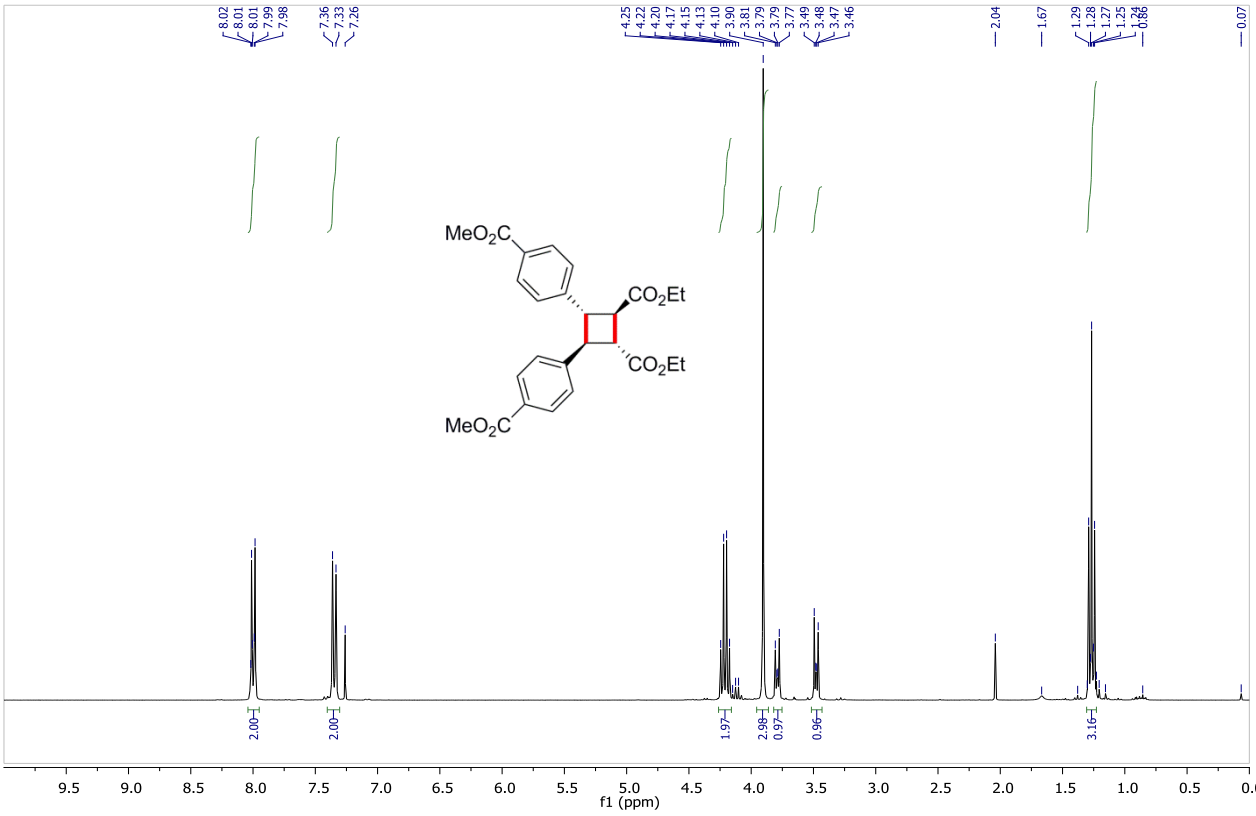

^{13}C-NMR: **2j** (*trans*, after separation)

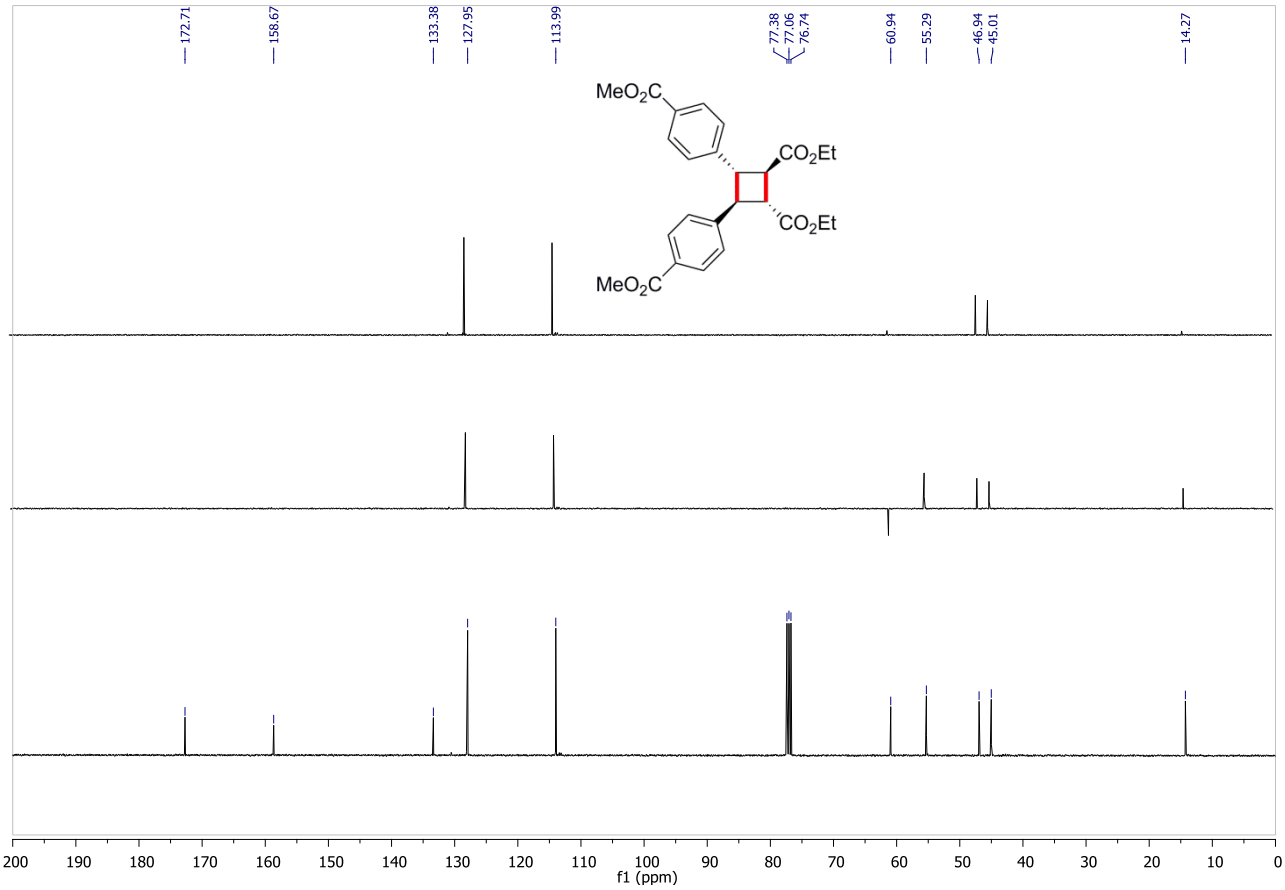

^{1}H-NMR: **3j** (*cis*, after separation)

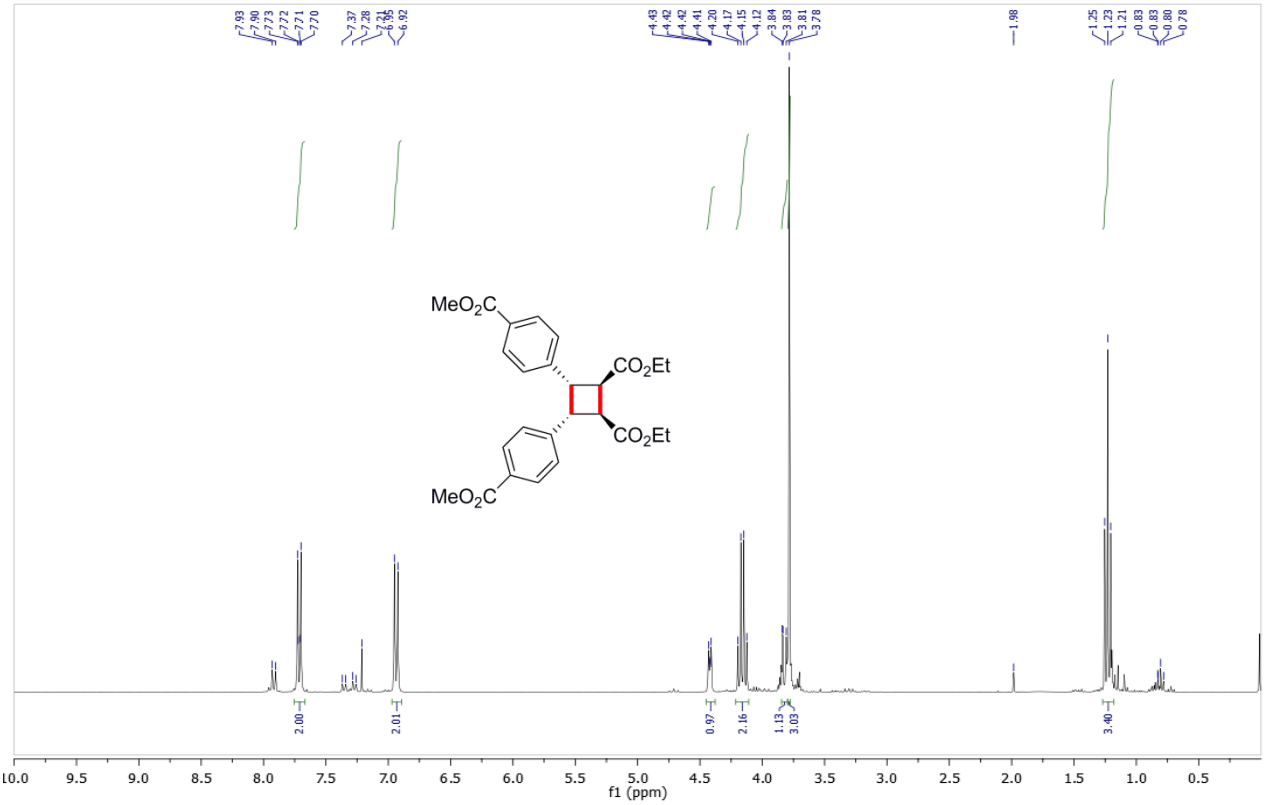

^{13}C-NMR: **3j** (*cis*, after separation)

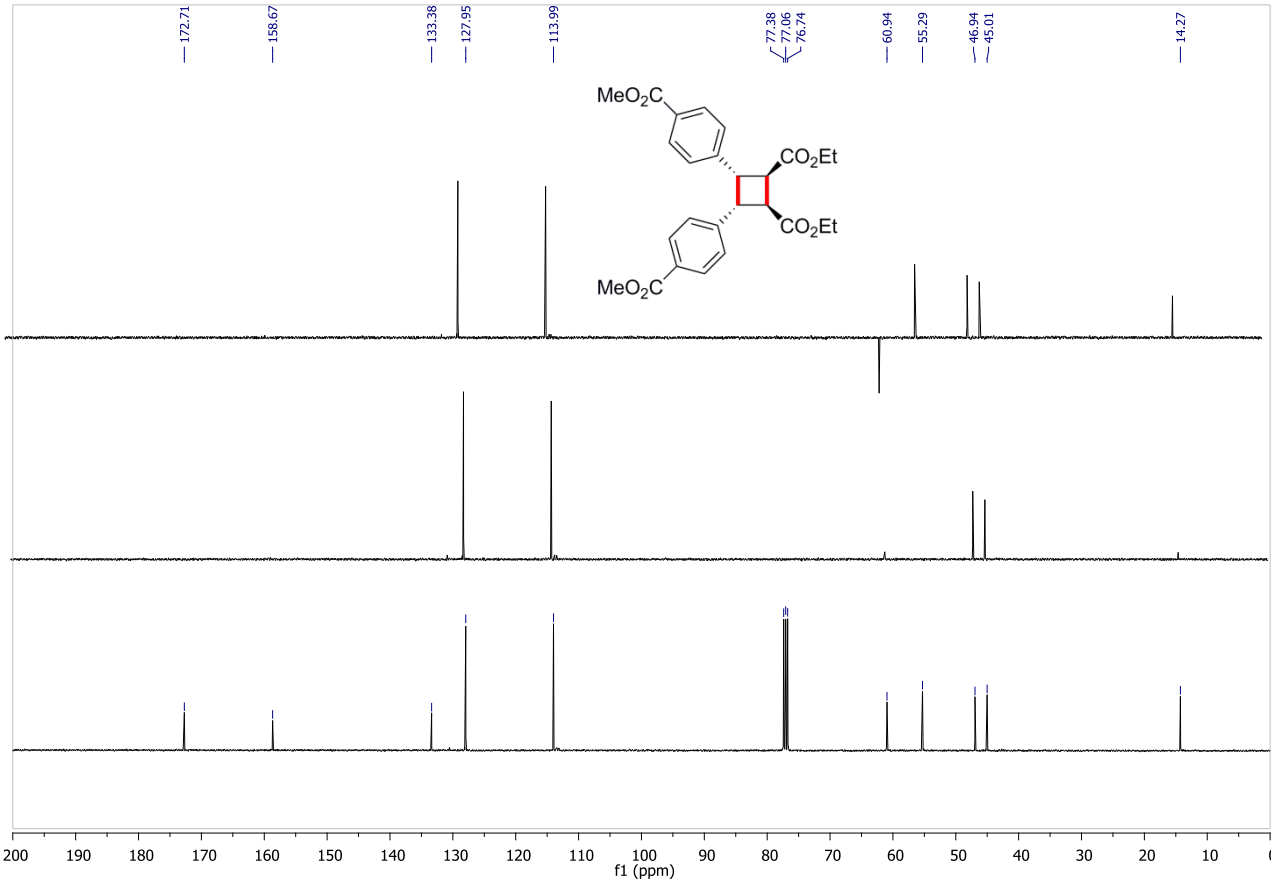

^{1}H-NMR: **2k** (*trans*, after separation)

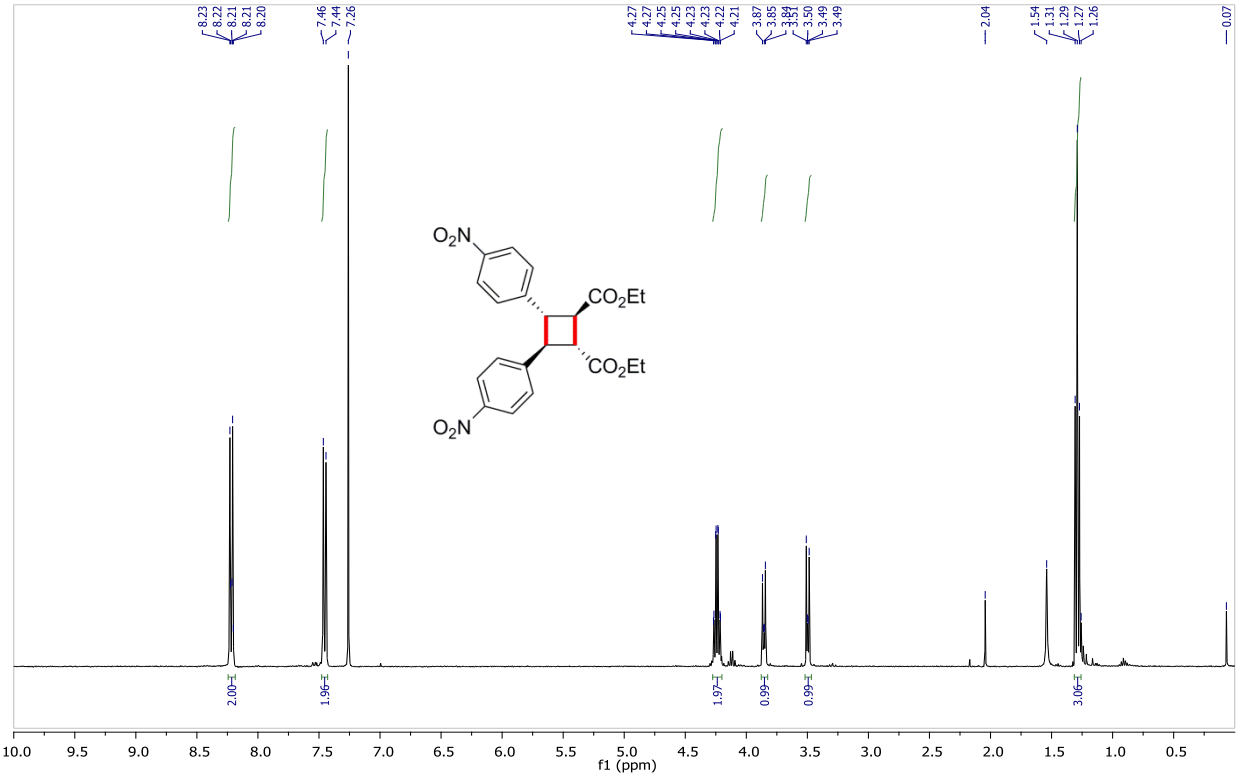

^{13}C-NMR: **2k** (*trans*, after separation)

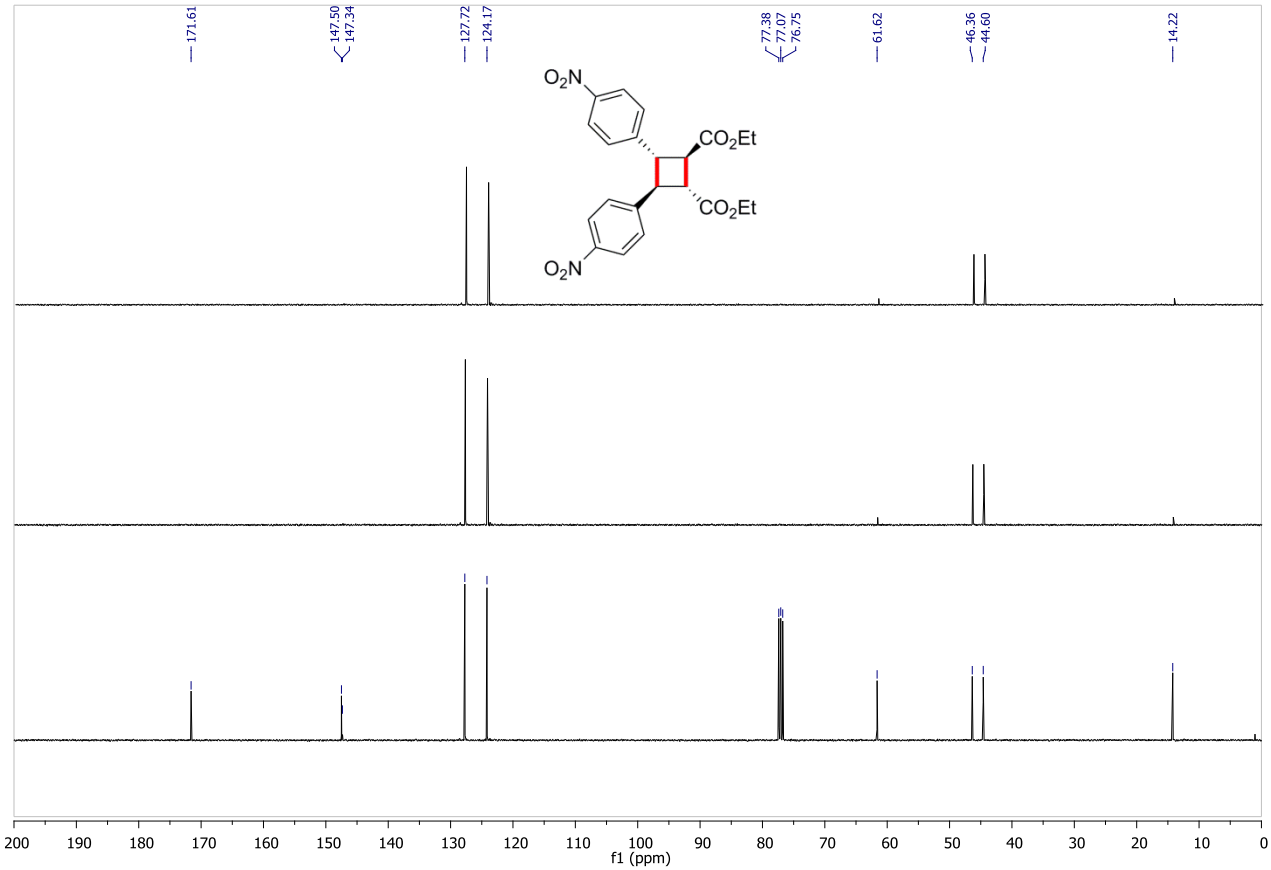

^{1}H-NMR: **3k** (*cis*, after separation)

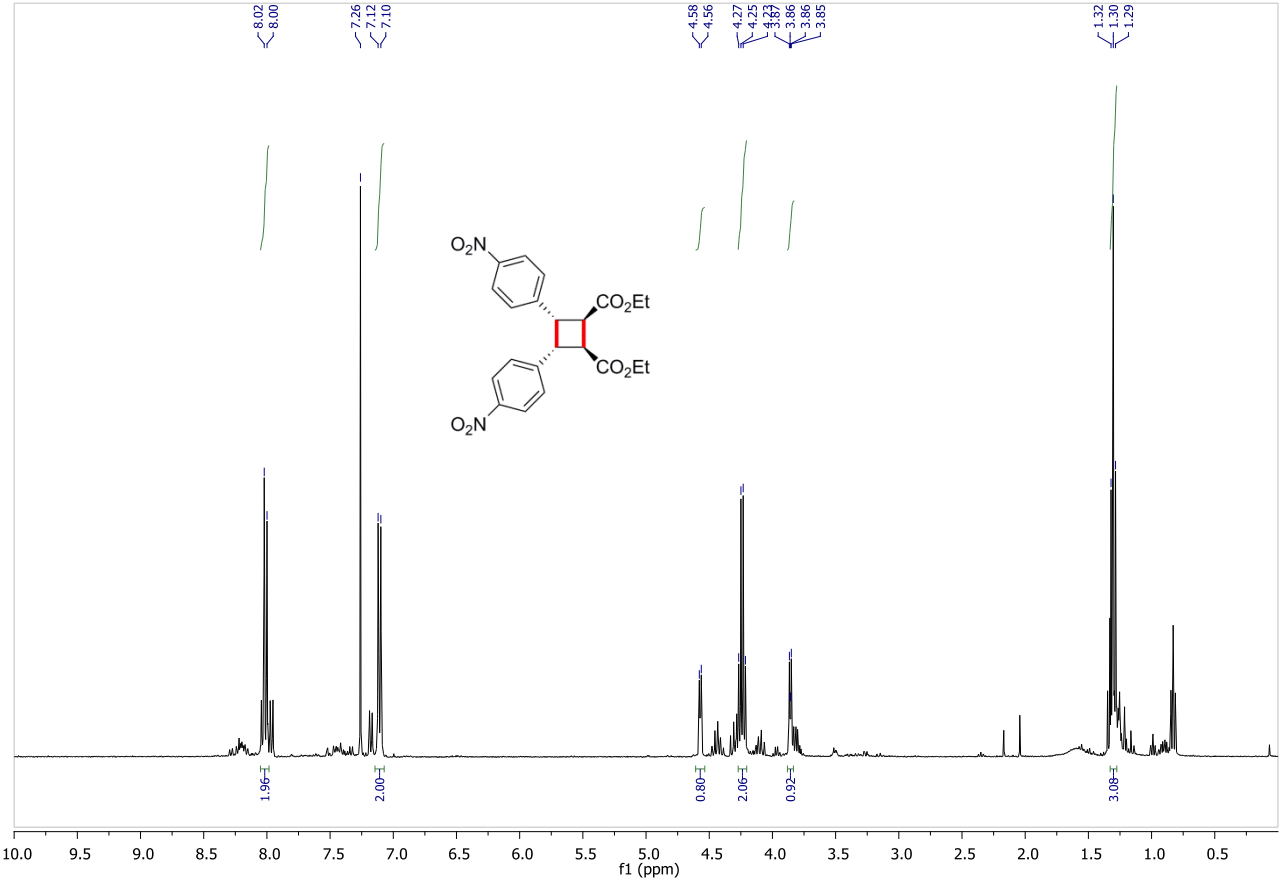

^{1}H-NMR: **2l** (*trans*, after separation)

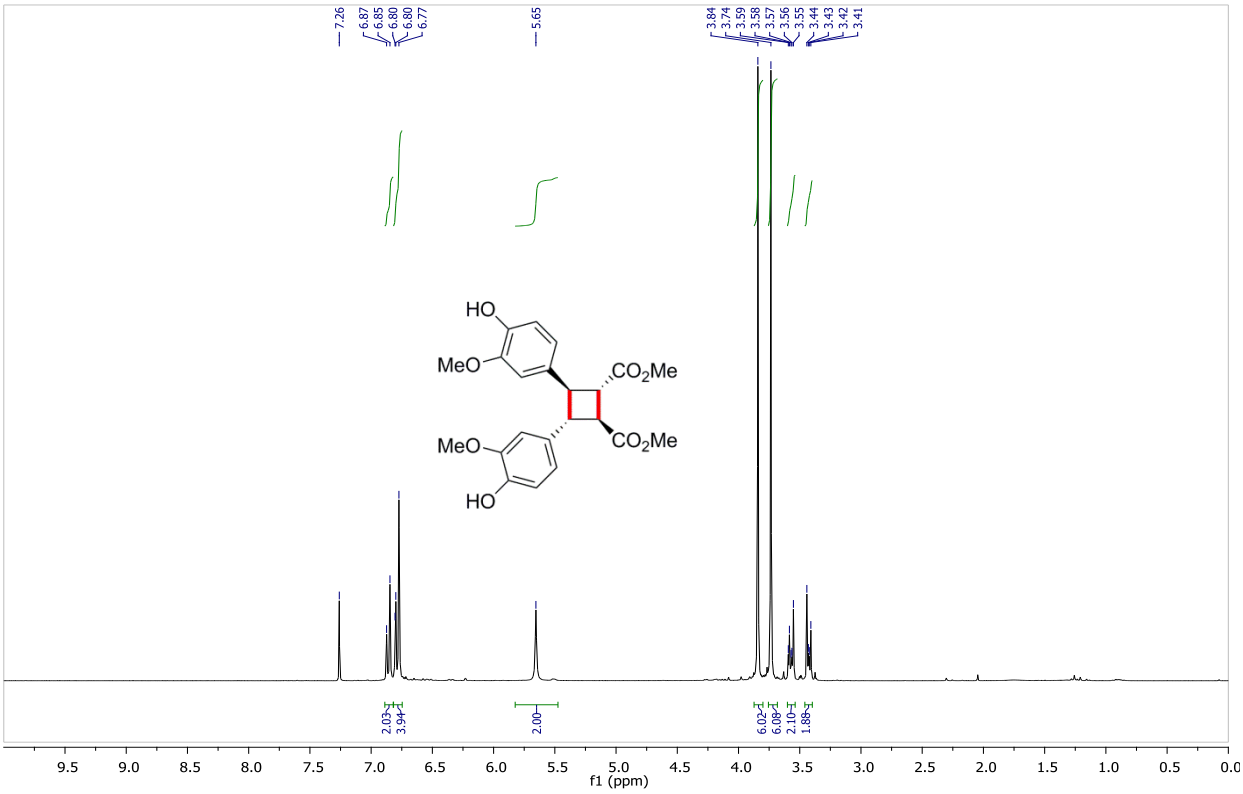

^{13}C-NMR: **2l** (*trans*, after separation)

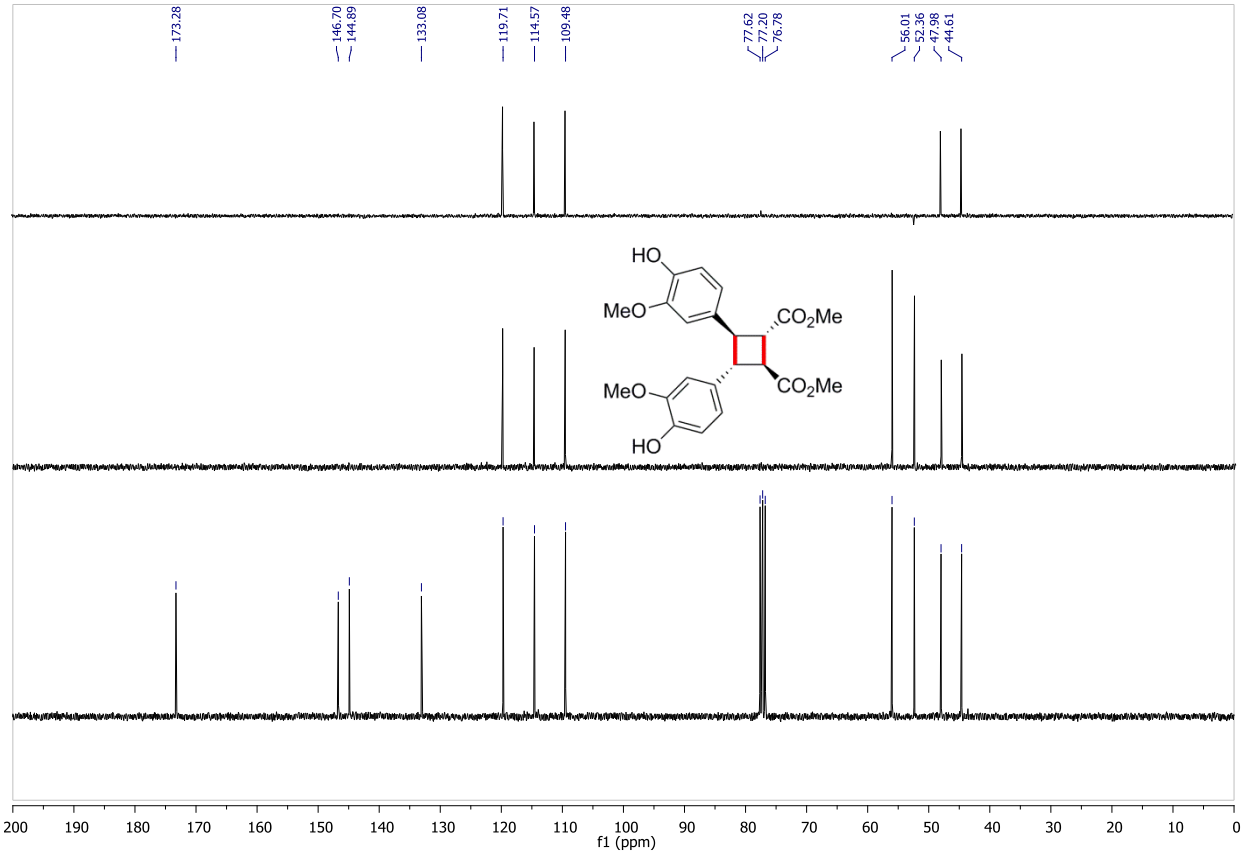

^{1}H-NMR: **2m** (*trans*, after separation)

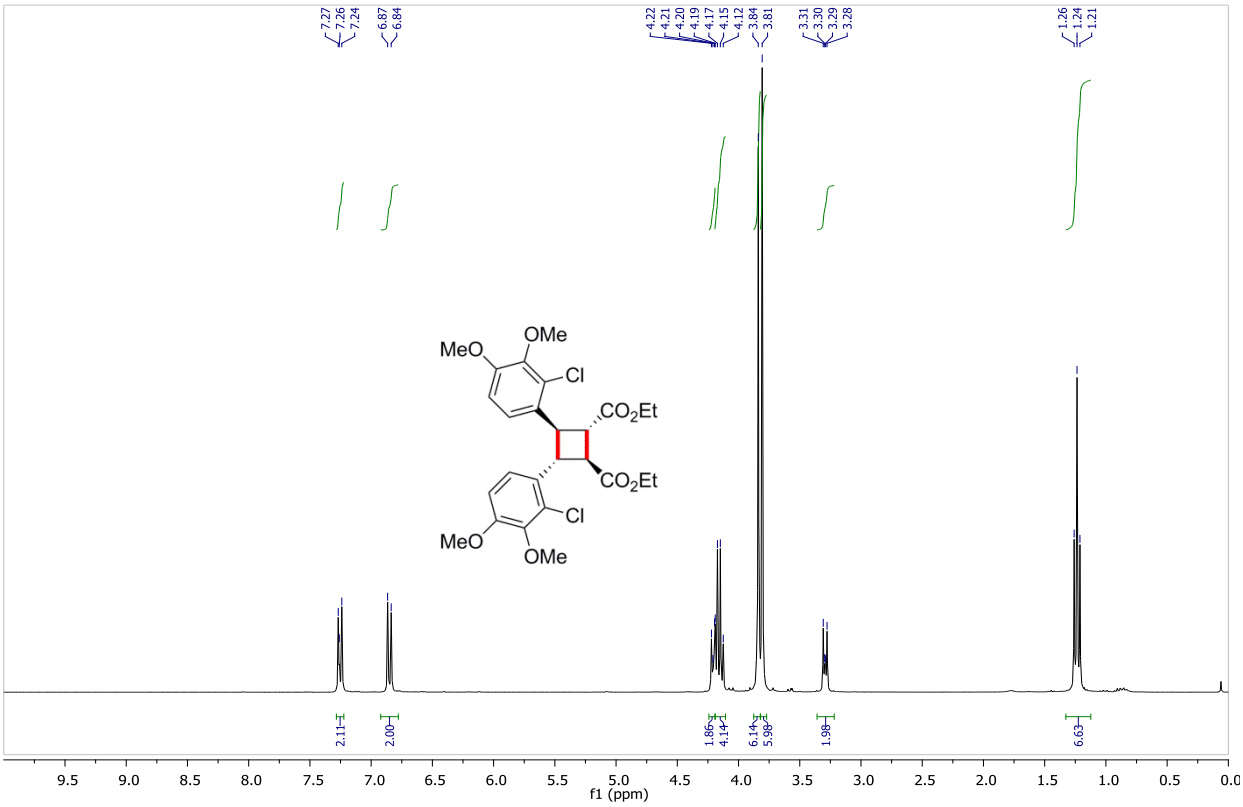

^{13}C-NMR: **2m** (*trans*, after separation)

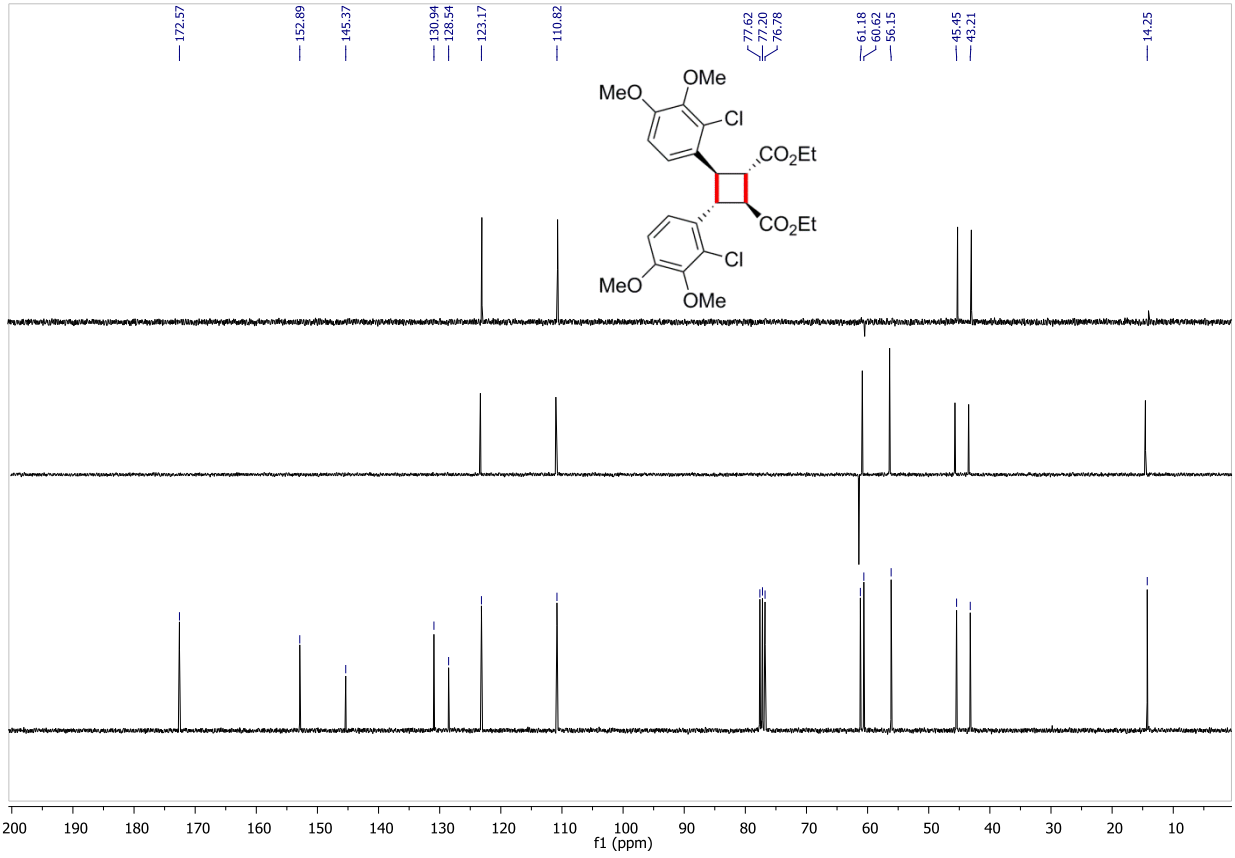

^{1}H-NMR: **2n** (*trans*, after separation)

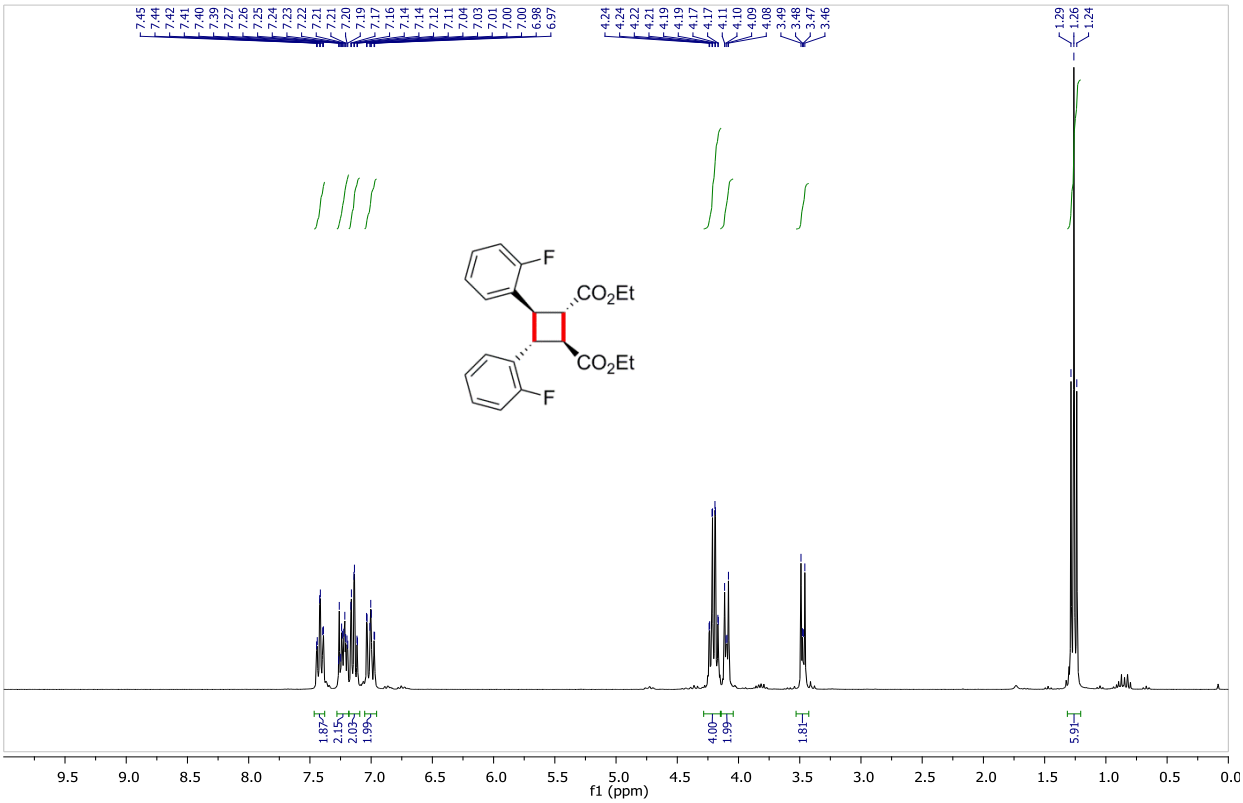

^{13}C-NMR: **2n** (*trans*, after separation)

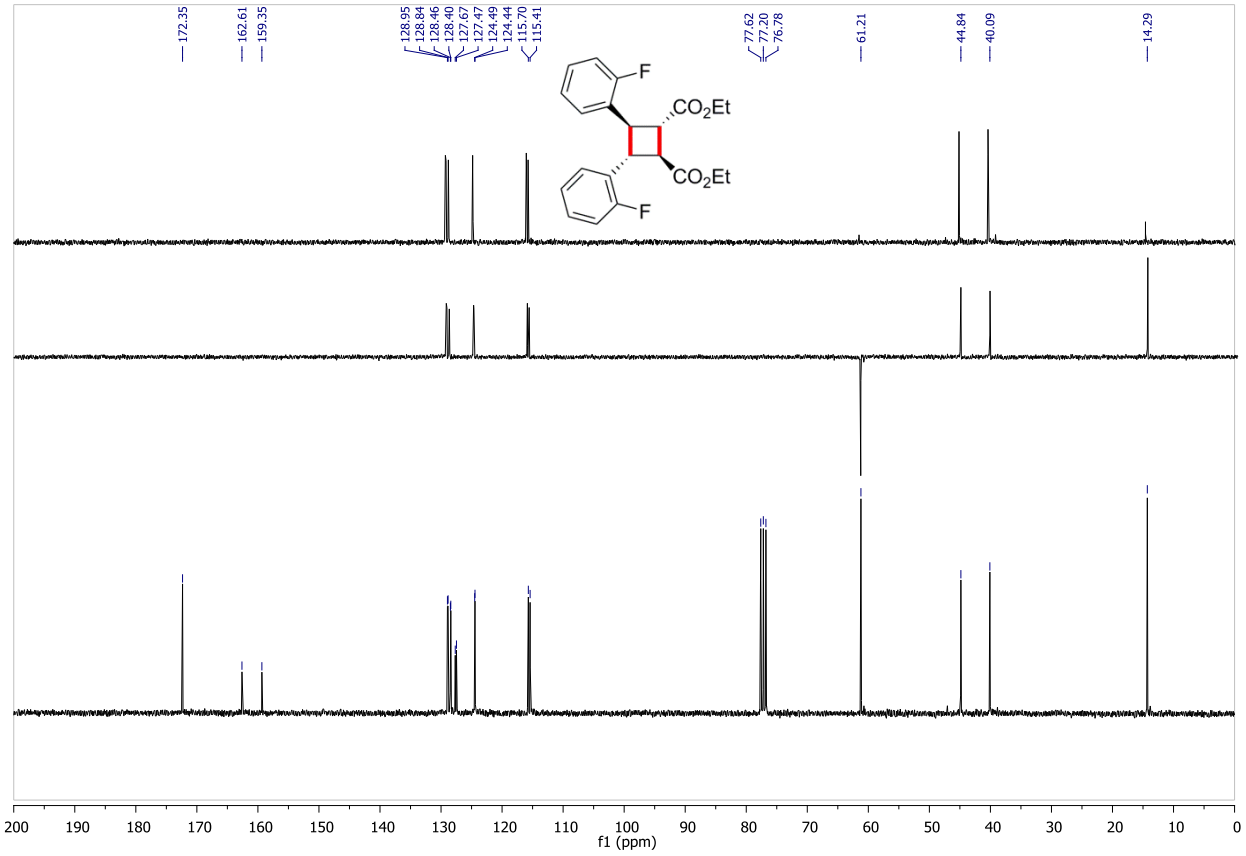

^{19}F-NMR: **2n** (*trans*, after separation)

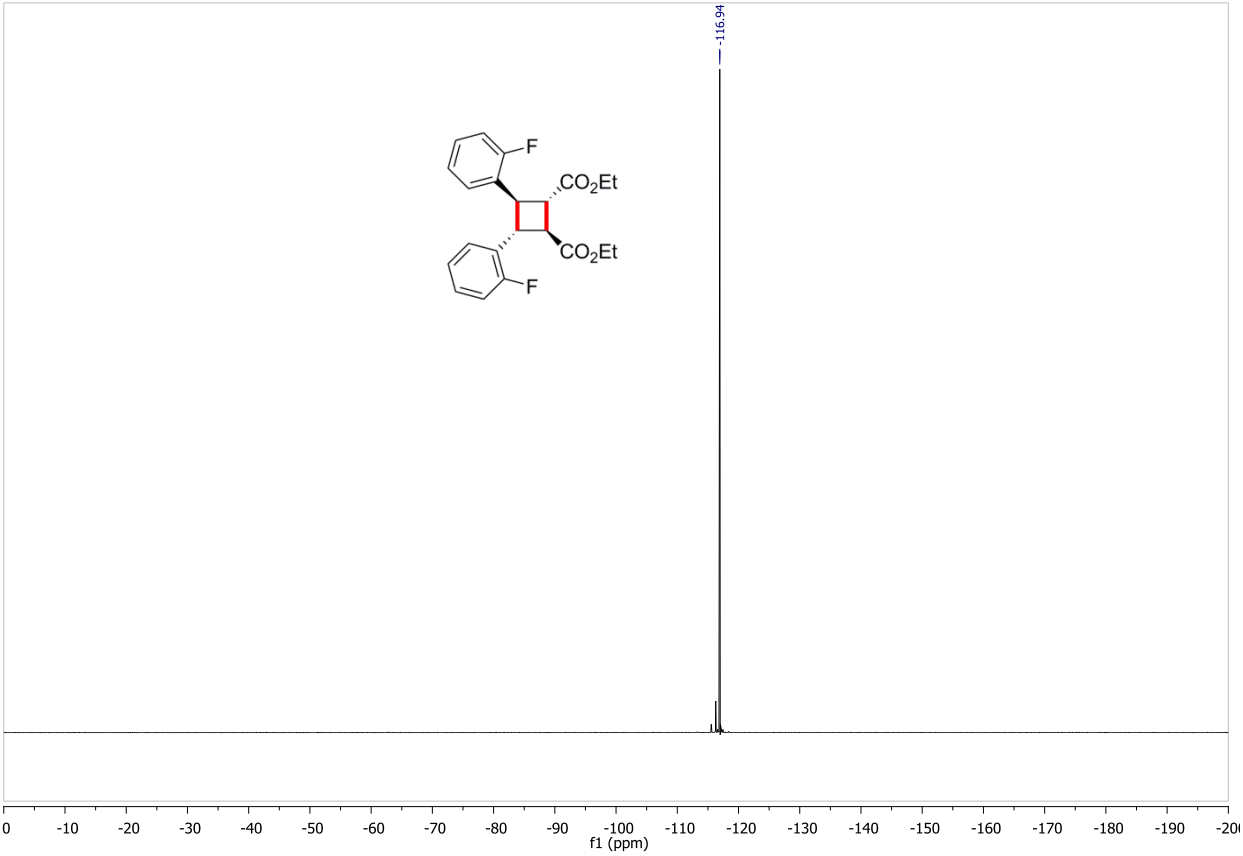

^{1}H-NMR: **2o** (*trans*, after separation)

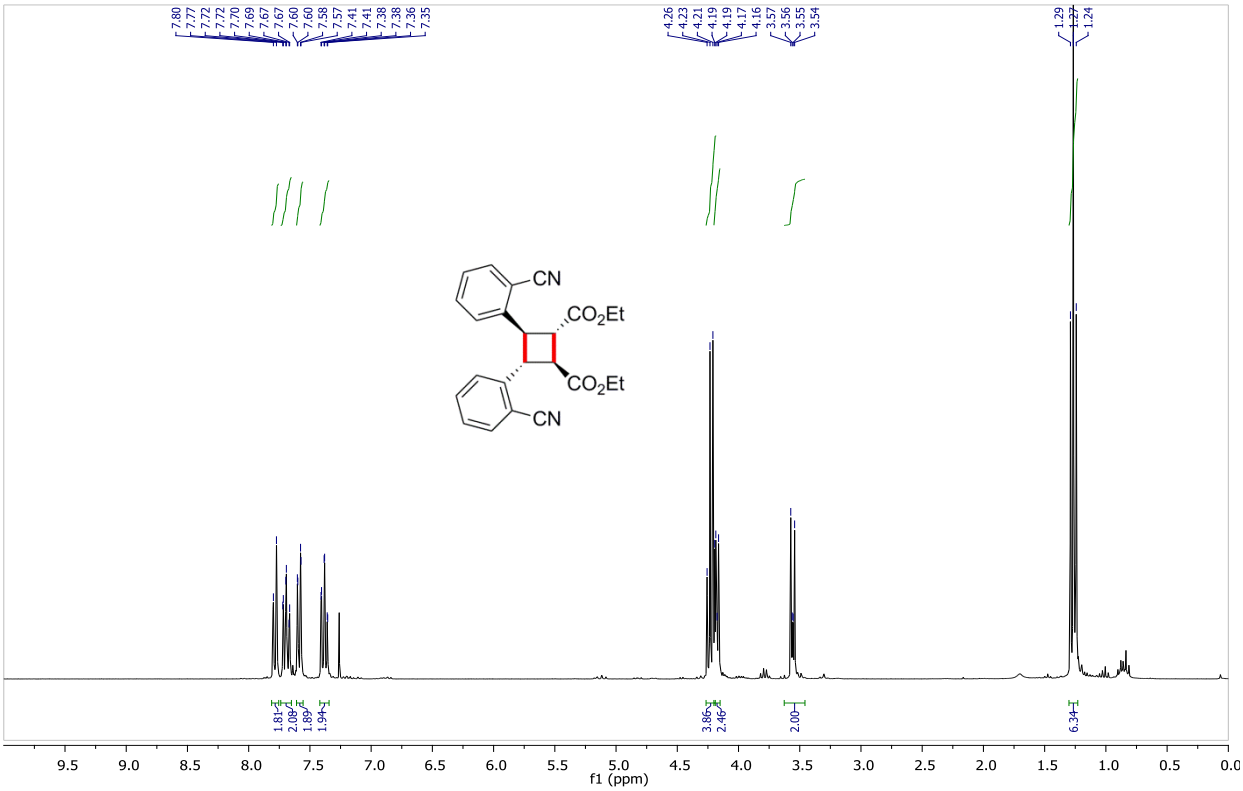

^{13}C-NMR: **2o** (*trans*, after separation)

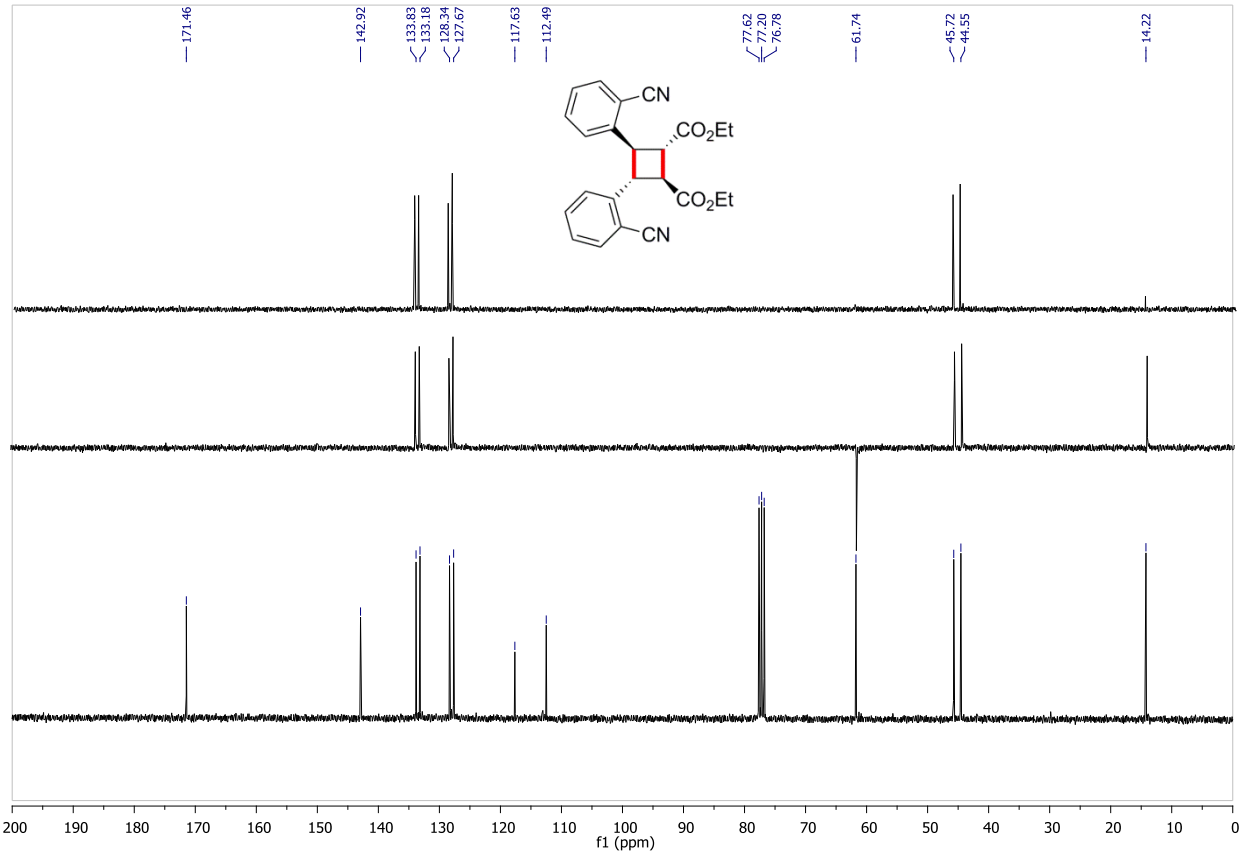

^{1}H-NMR: **2p** (*trans*, after separation)

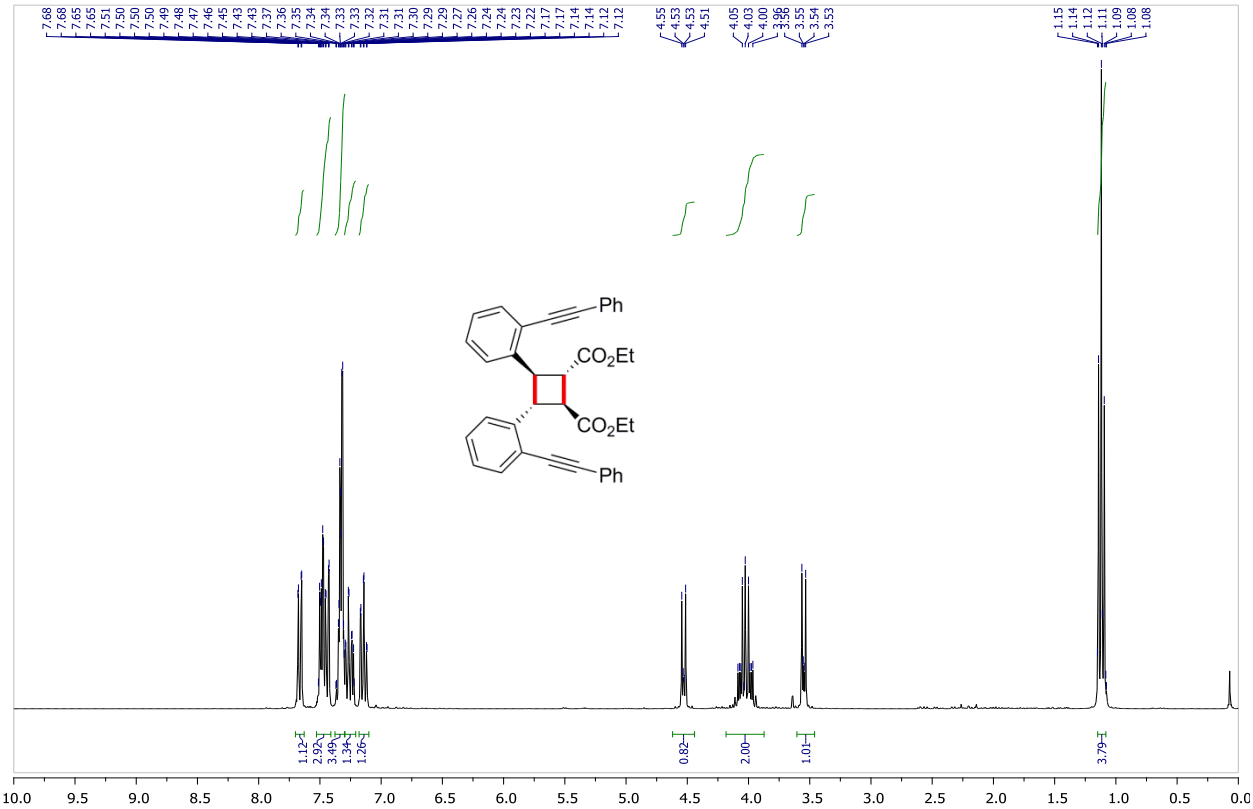

^{13}C-NMR: **2p** (*trans*, after separation)

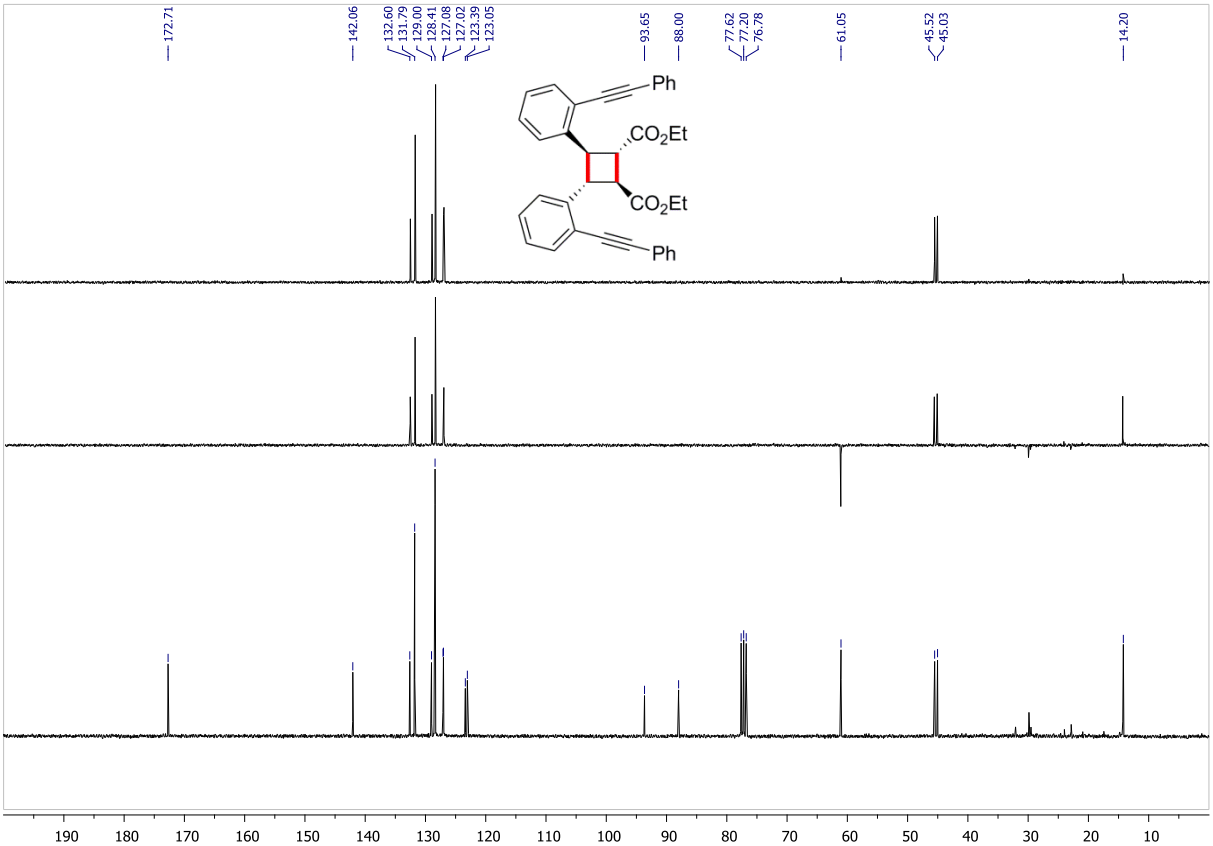

^{1}H-NMR: **2q/3q/4q** (*mixture*, before separation)

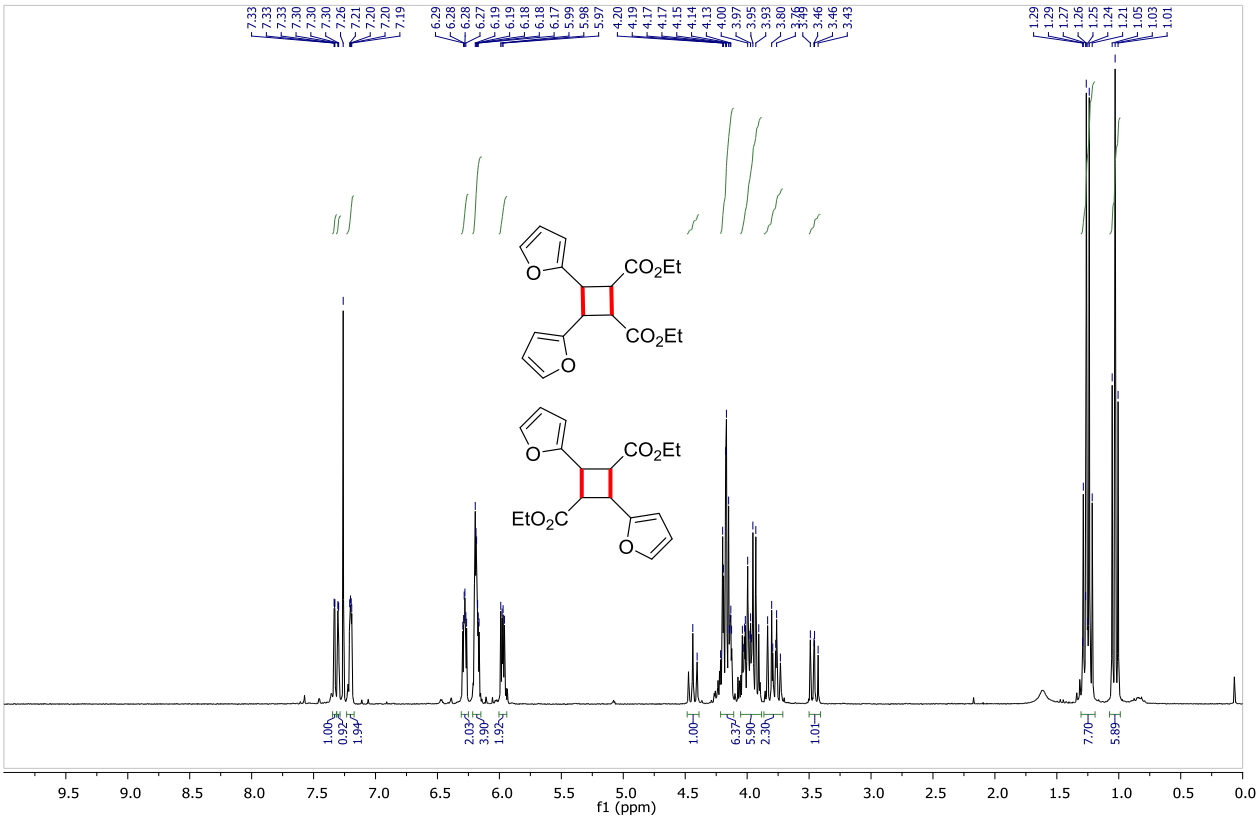

^{1}H-NMR: **2q/3q** (*mixture*, after separation)

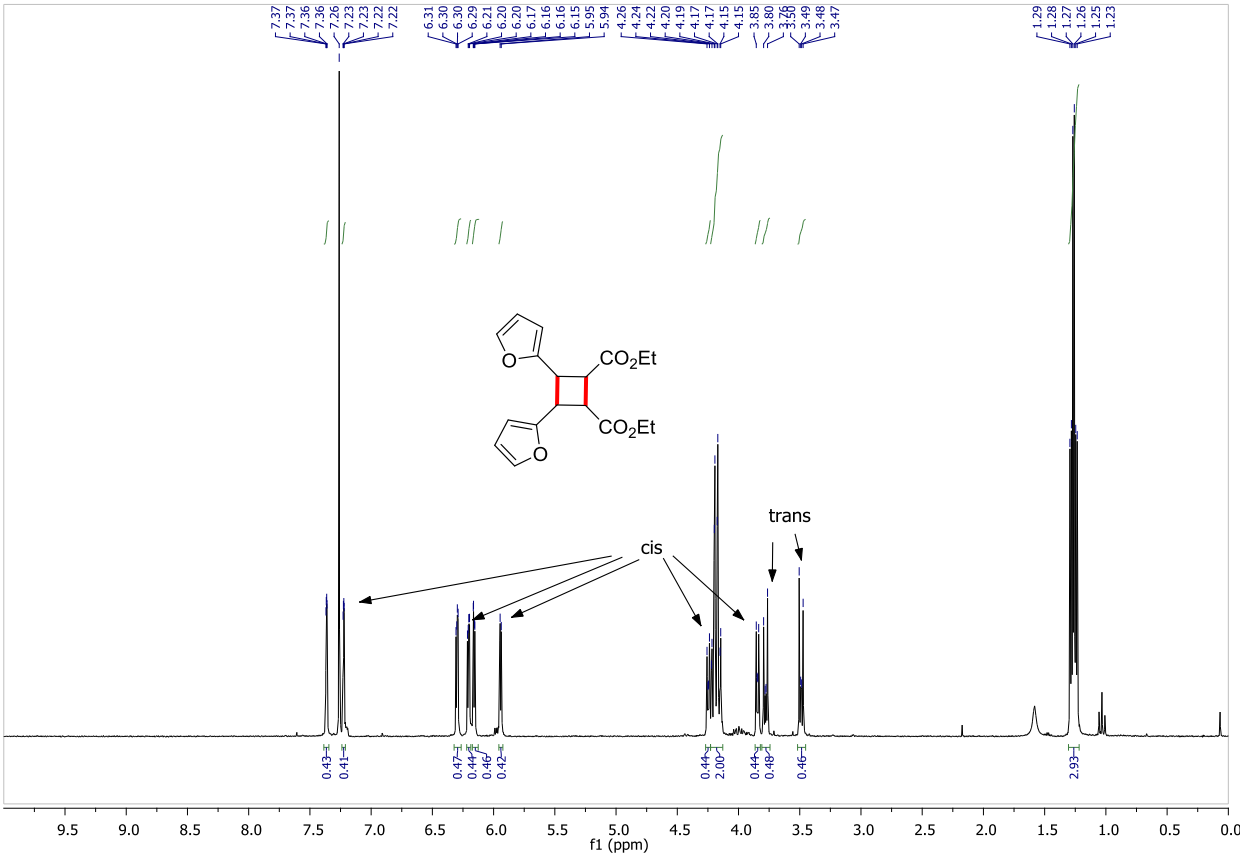

^{1}H-NMR: **2q** (*trans*, after separation)

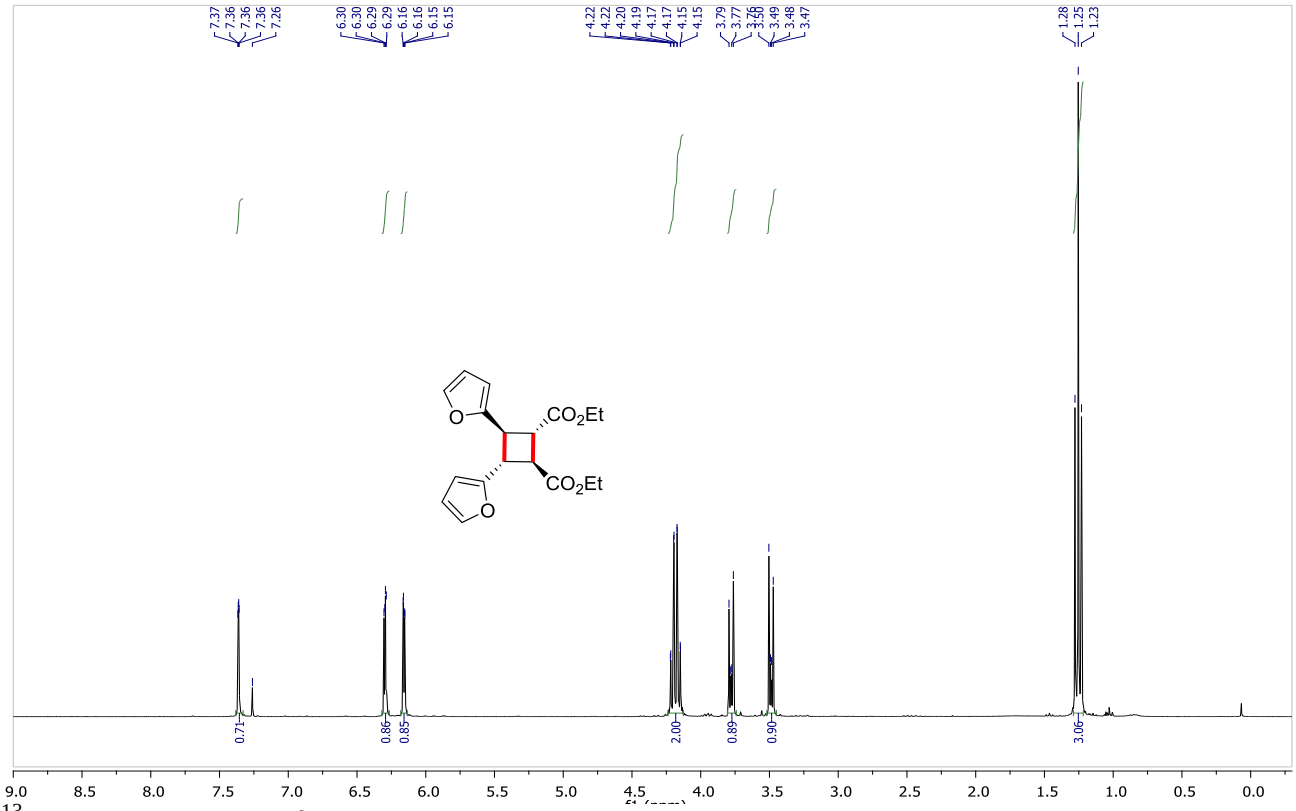

^{13}C-NMR: **2q** (*trans*, after separation)

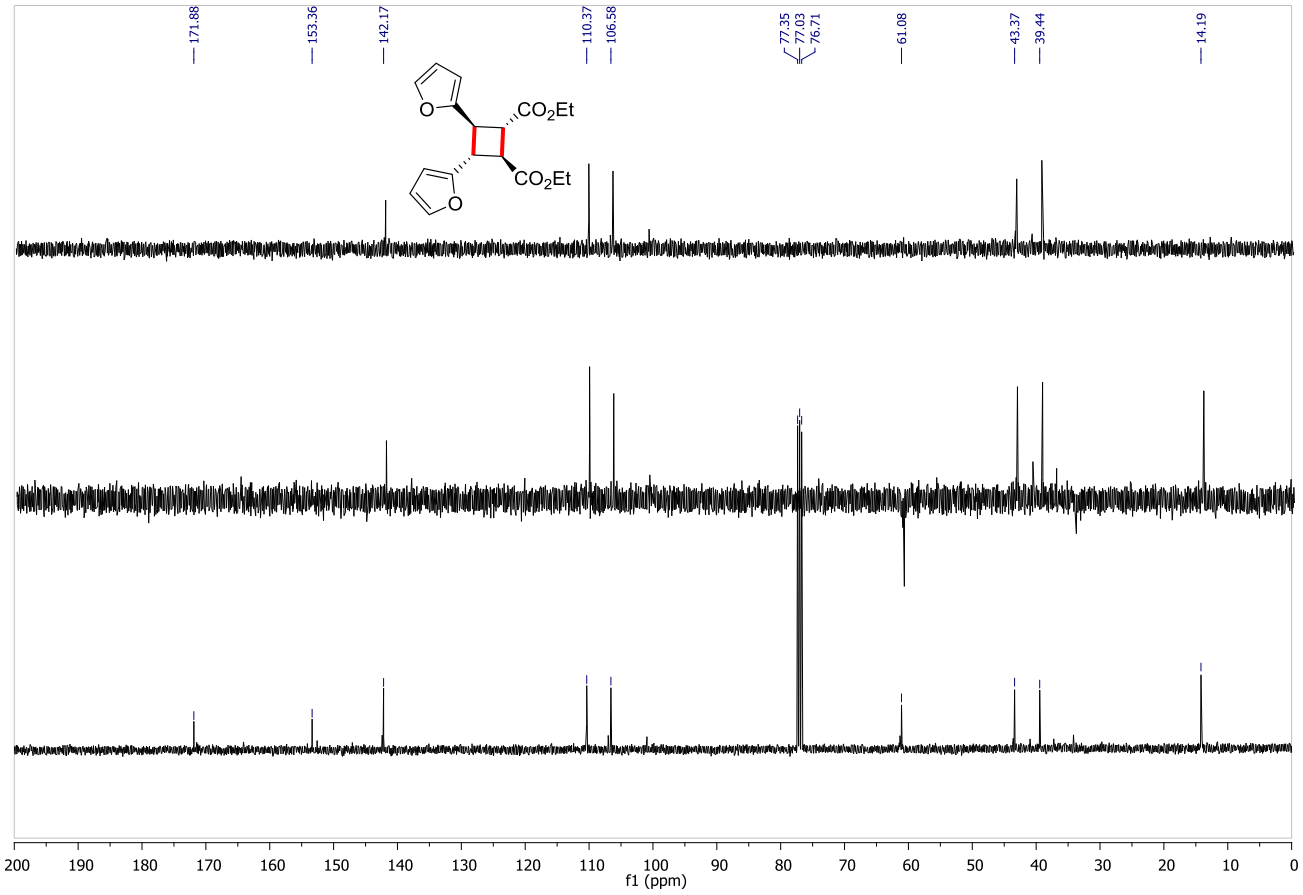

^{1}H-NMR: **2r/3r, 4r**

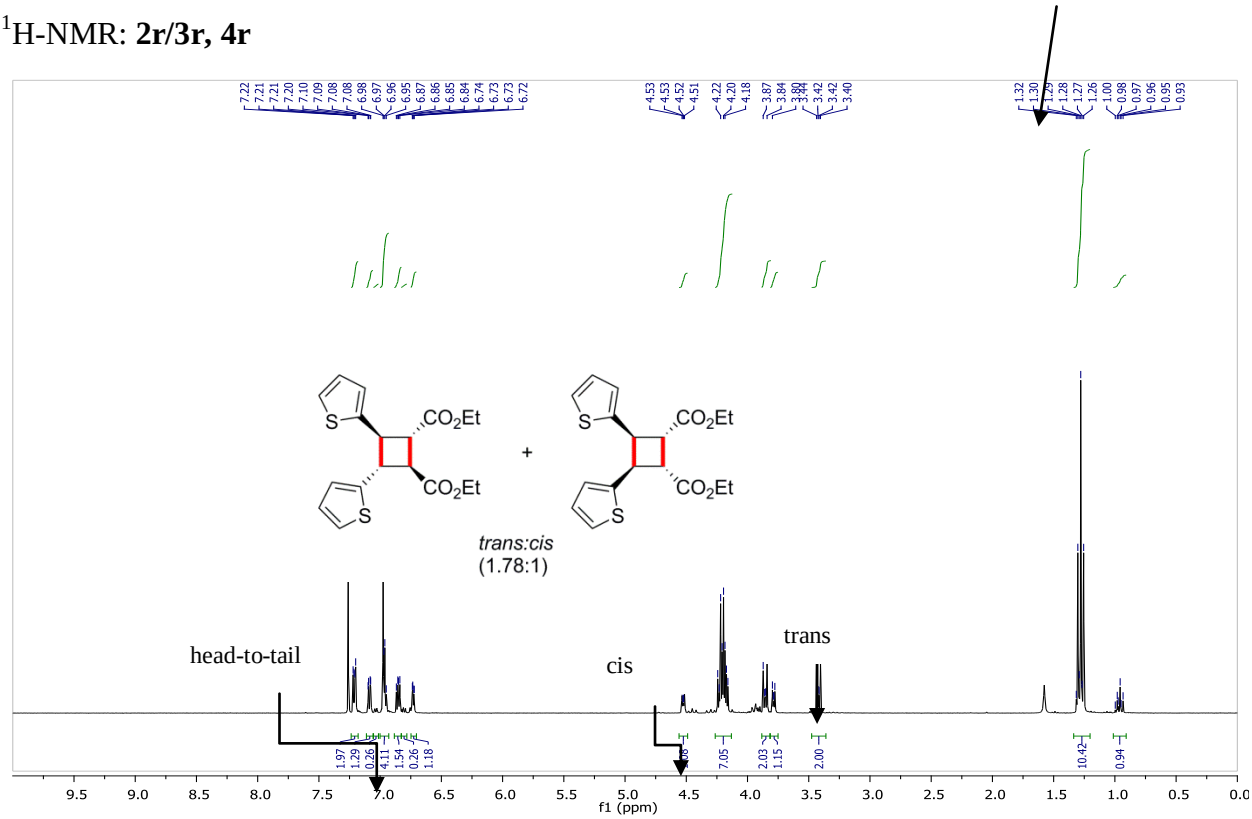

^{13}C-NMR: **2r/3r, 4r**

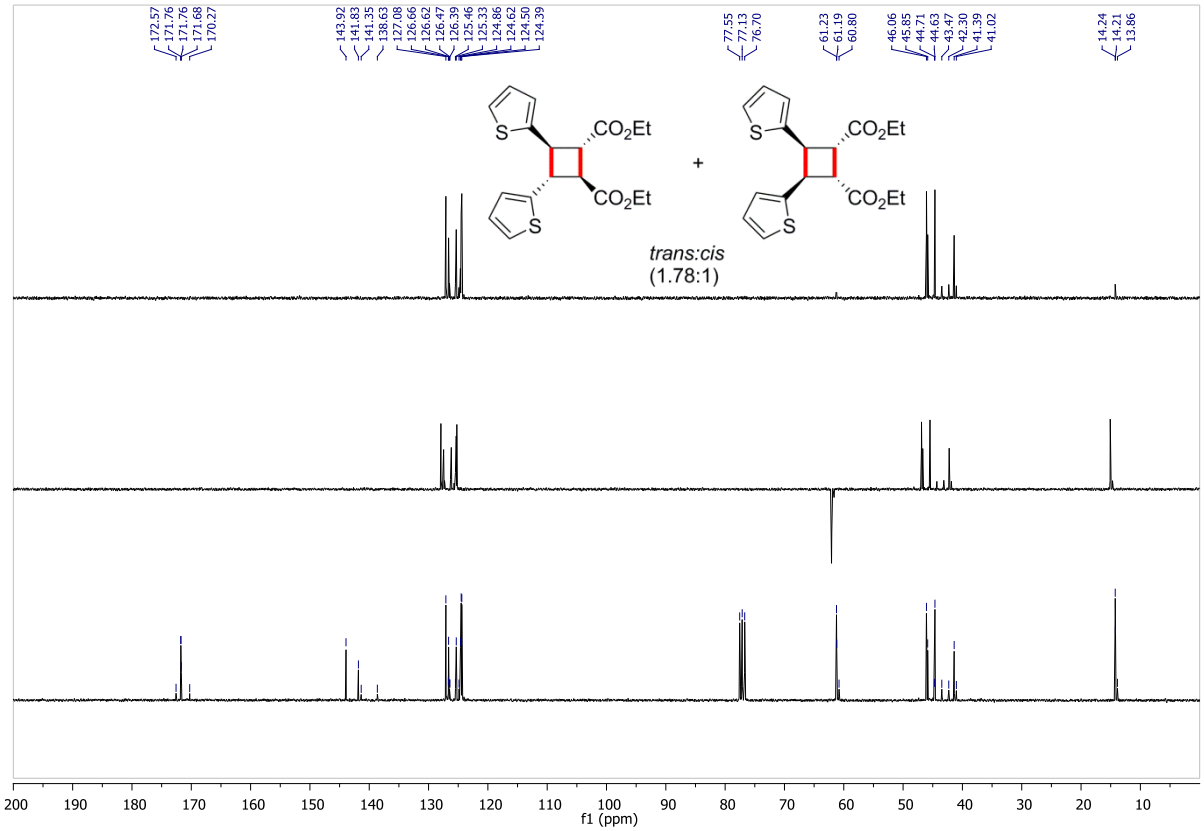

^{1}H-NMR: **2s/3s**

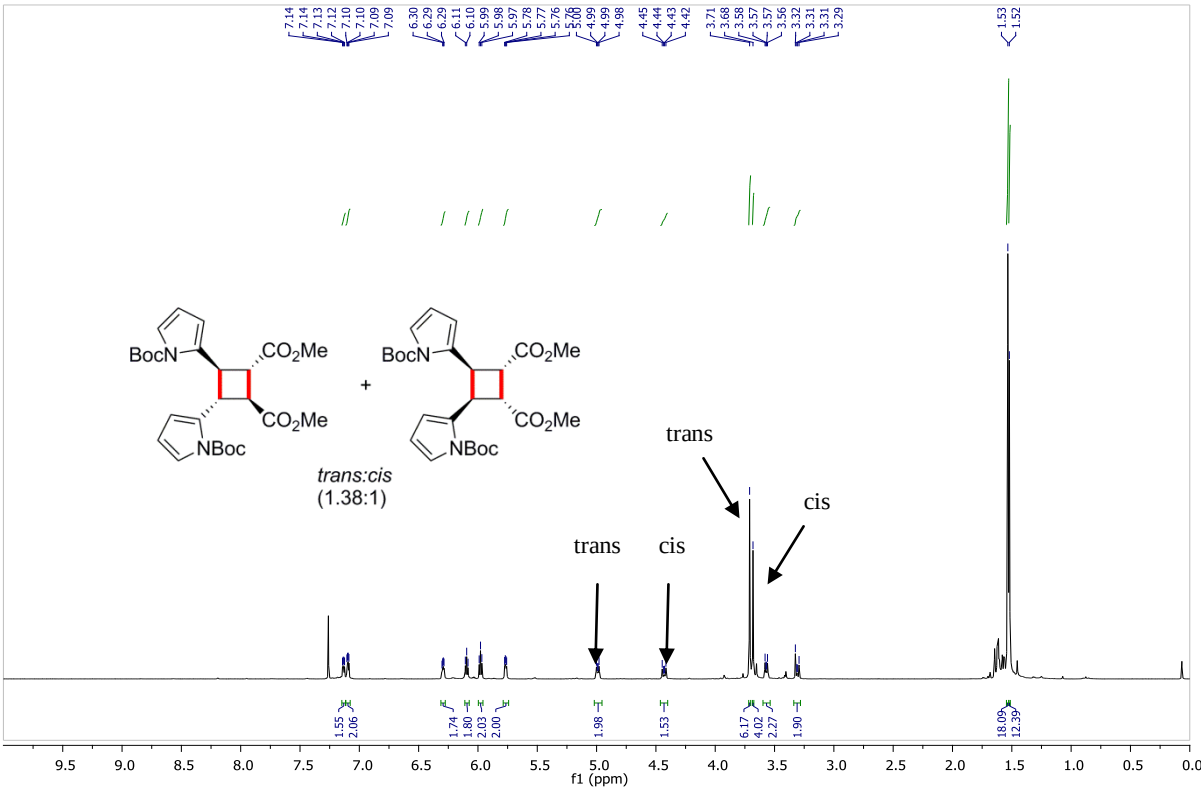

^{13}C-NMR: **2s/3s**

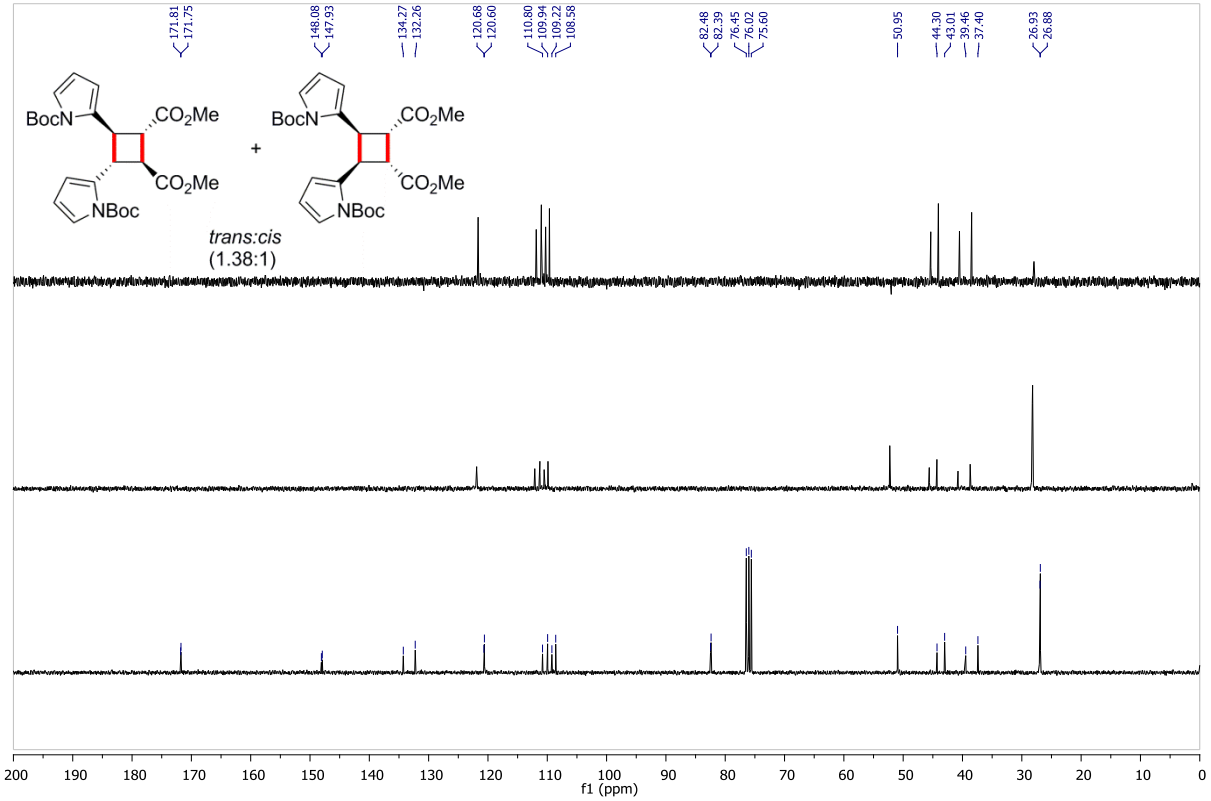

^{1}H-NMR: **2t** (*trans*, after separation)

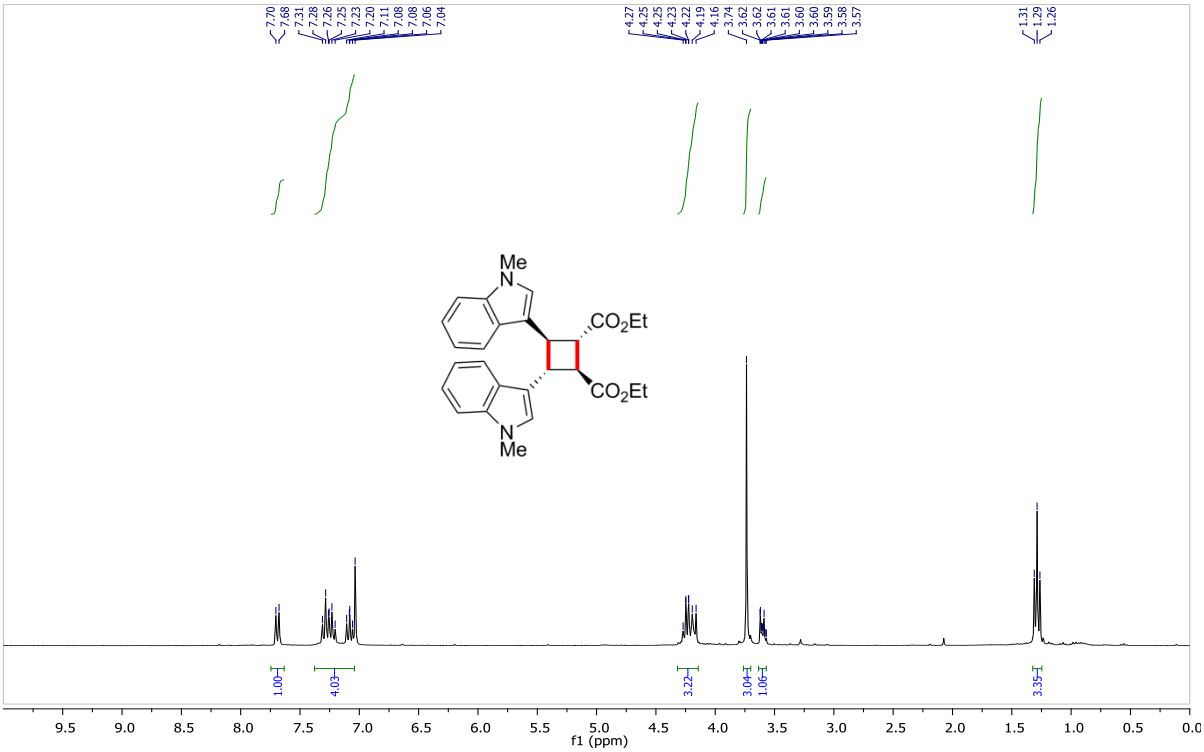

^{13}C-NMR: **2t** (*trans*, after separation)

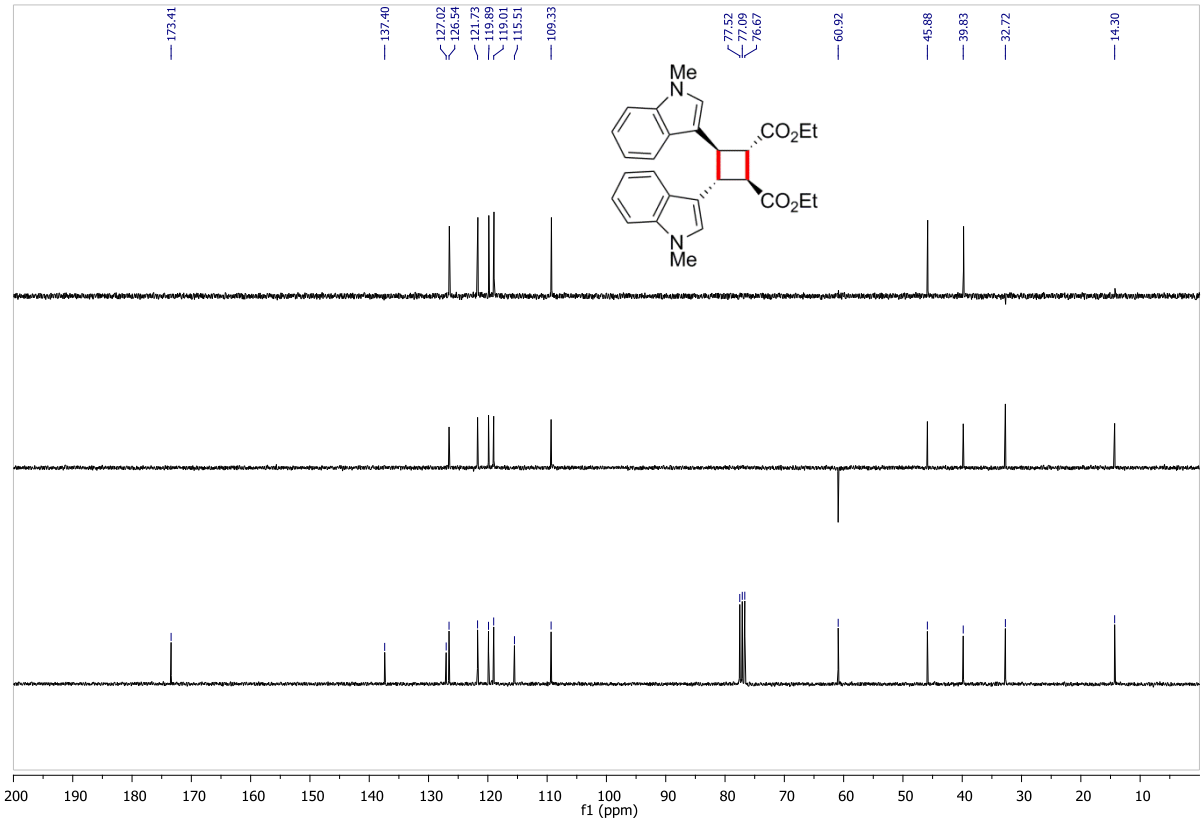

^{1}H-NMR: **2u/3u** (*cis*/*trans*)

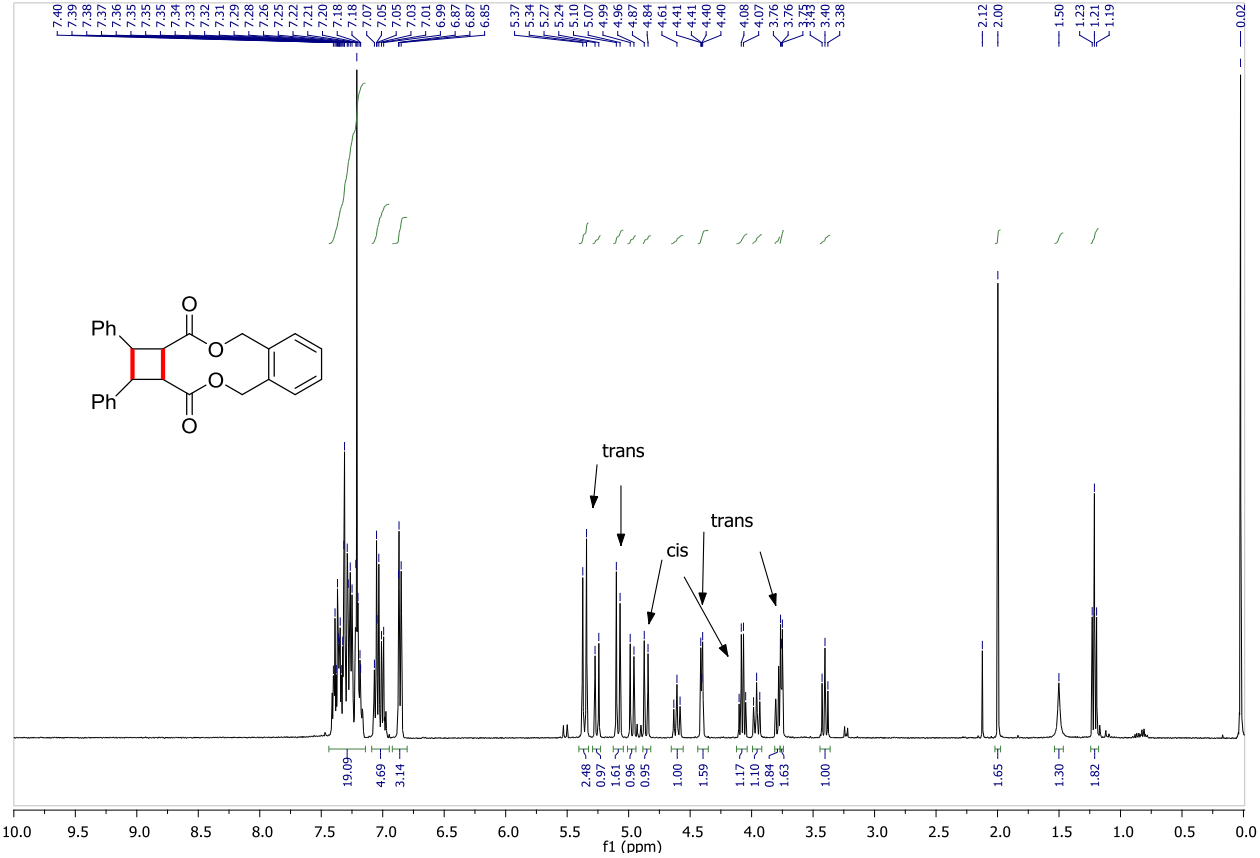

^{1}H-NMR: **2u** (*major isomer*)

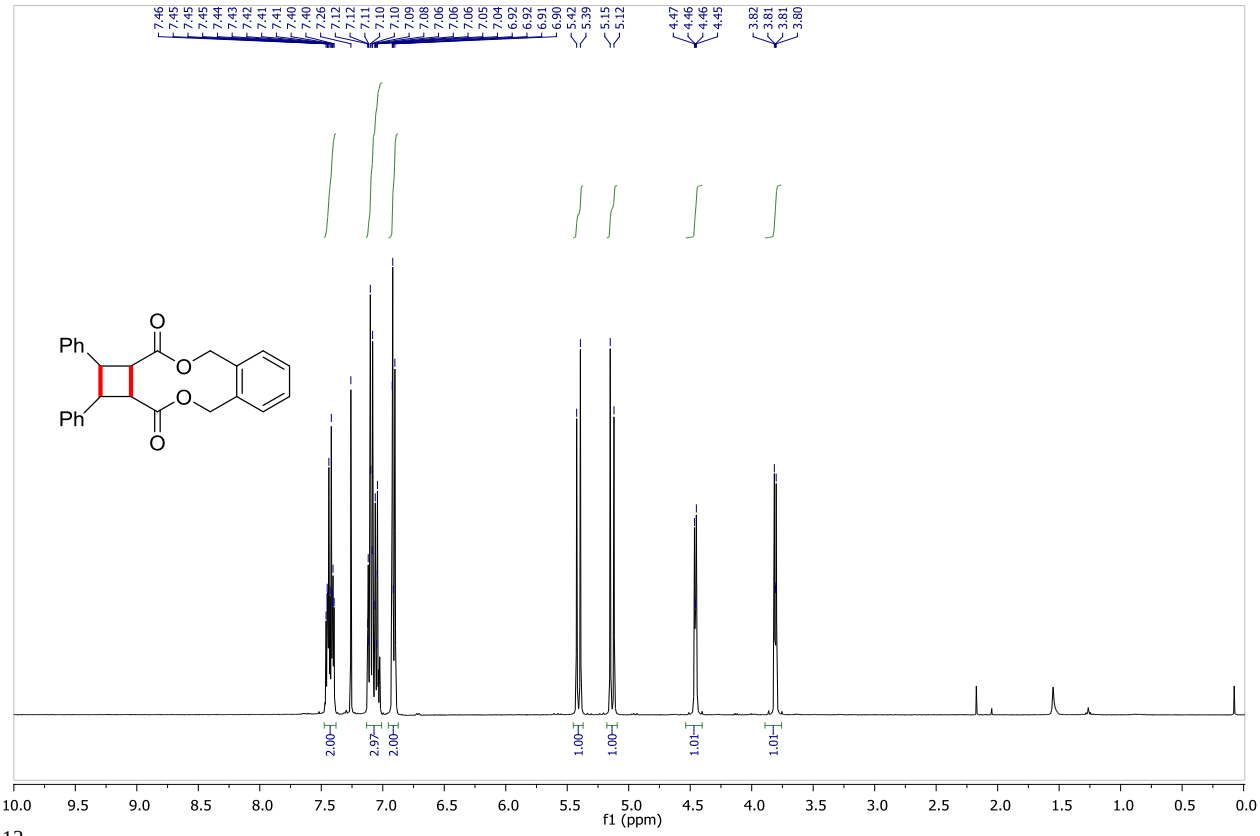

^{13}C-NMR: **2u** (*major isomer*)

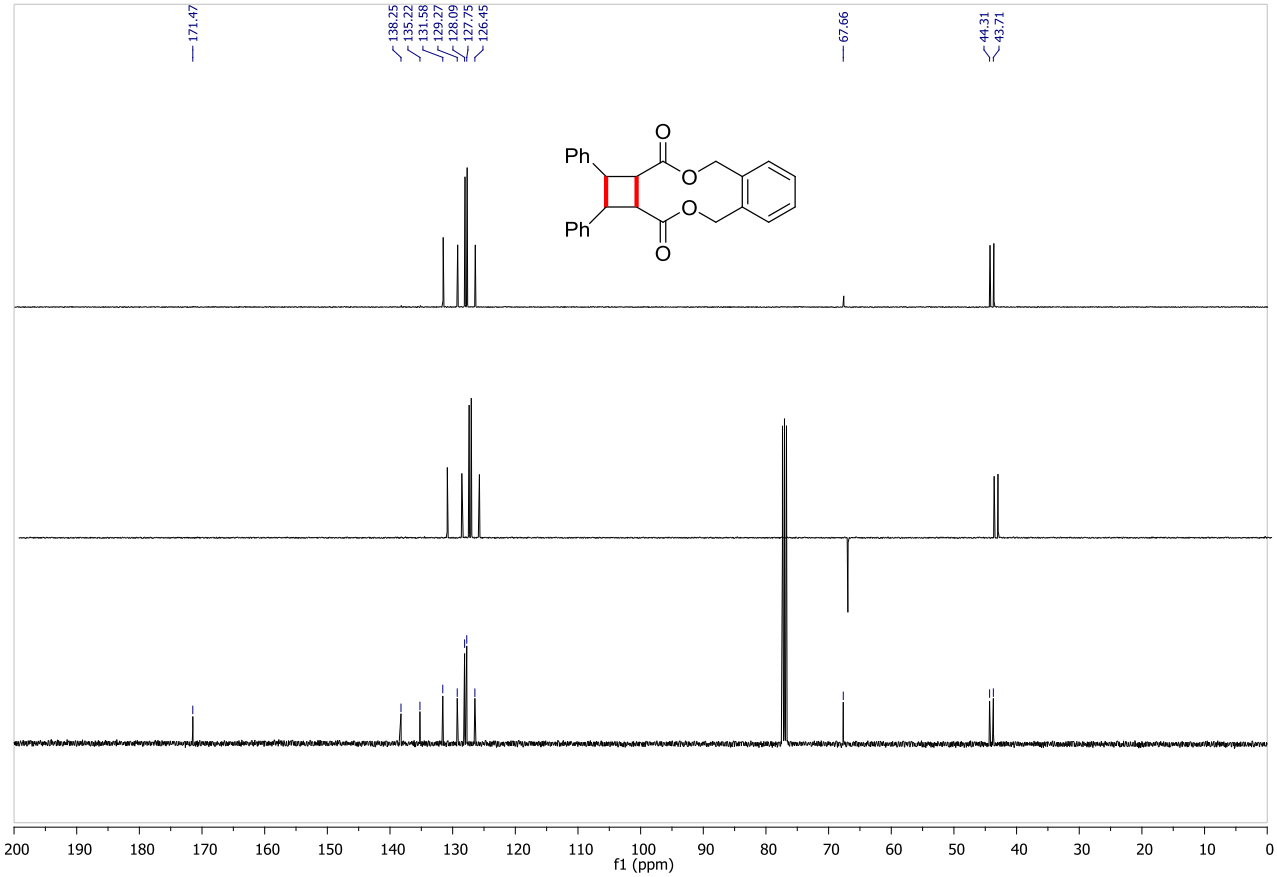

^{1}H-NMR: **2v** (*trans*, after separation)

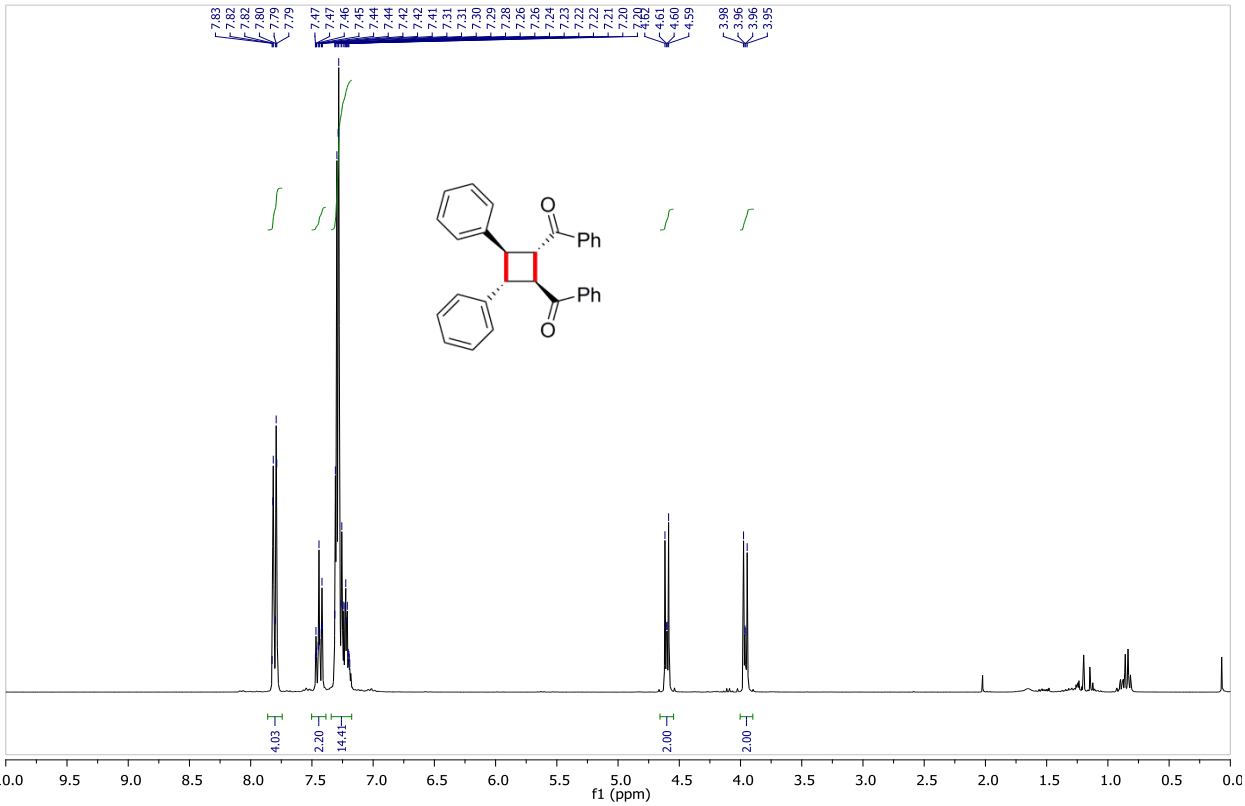

^{13}C-NMR: **2v** (*trans*, after separation)

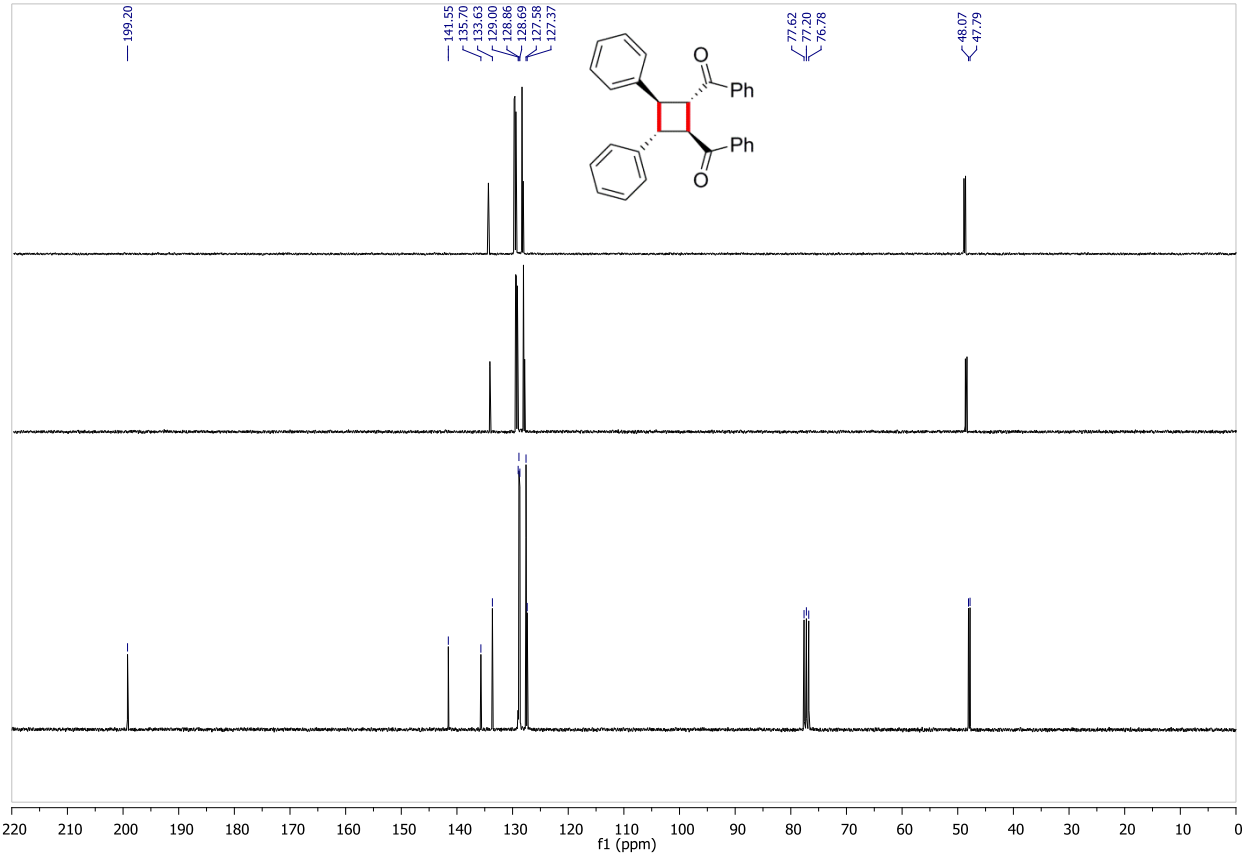

^{1}H-NMR: **2w** (*trans*, after separation)

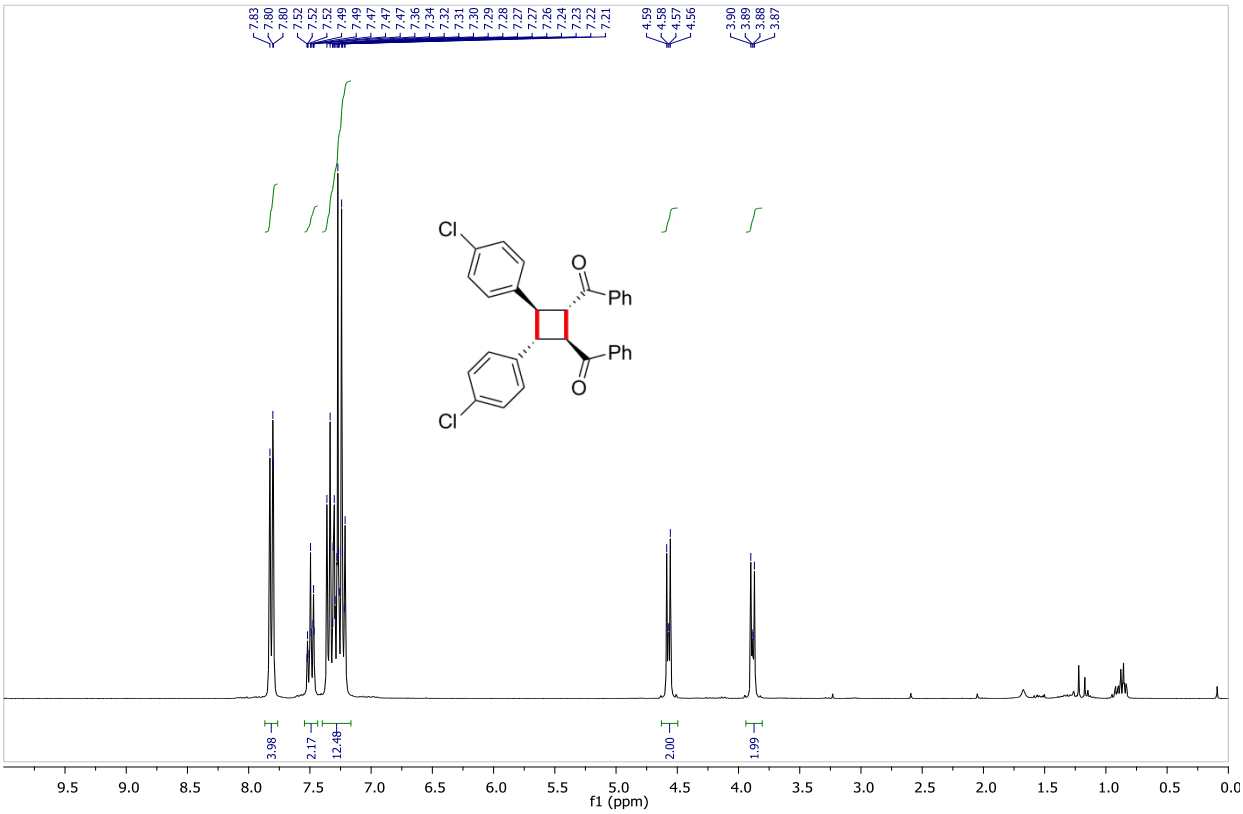

^{13}C-NMR: **2w** (*trans*, after separation)

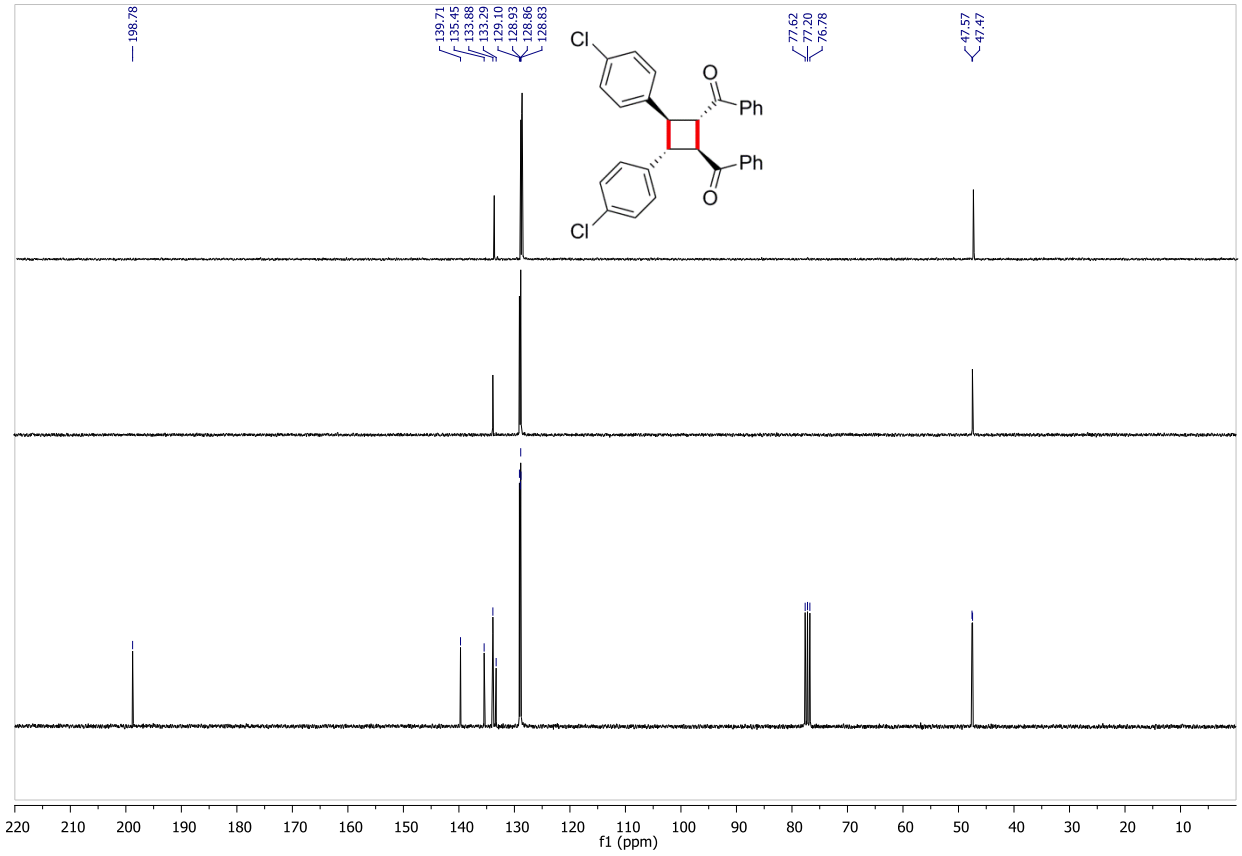

^{1}H-NMR: **6a** (*cis*/*trans*)

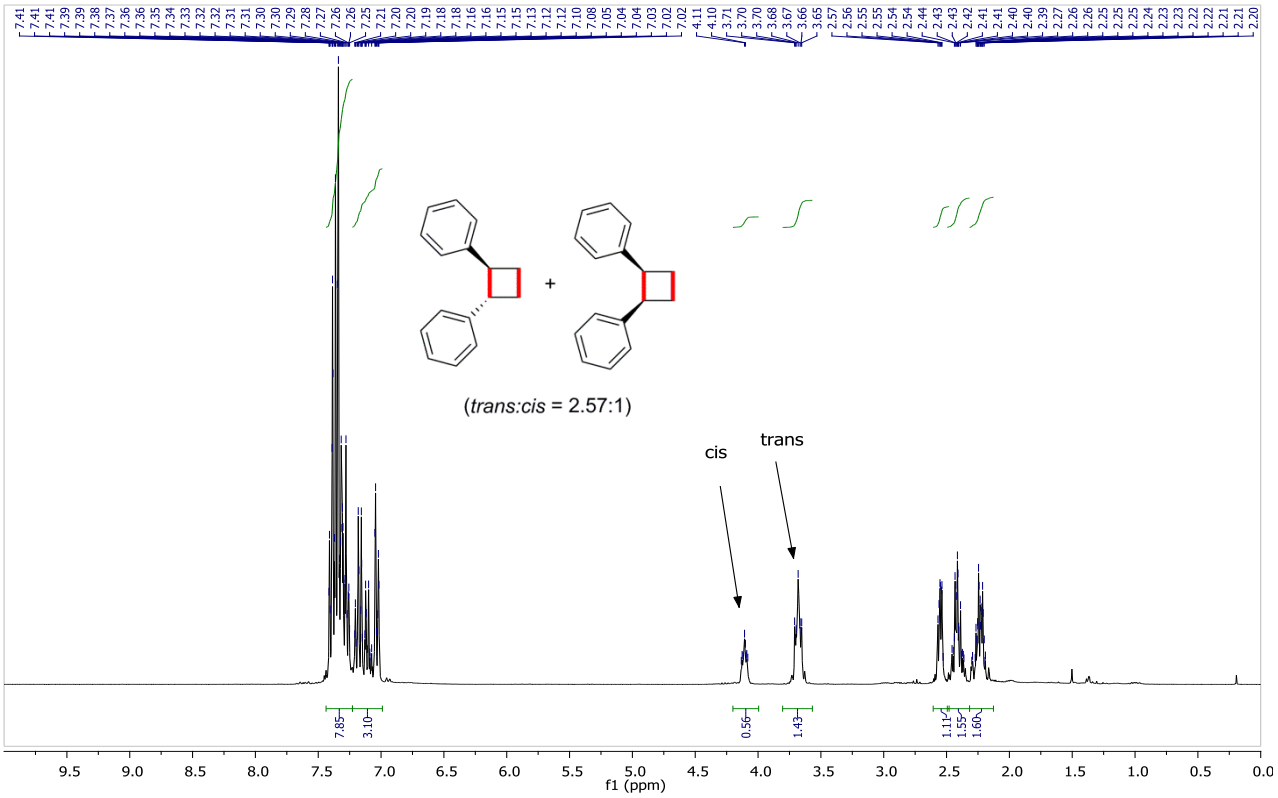

^{13}C-NMR: **6a** (*cis*/*trans*)

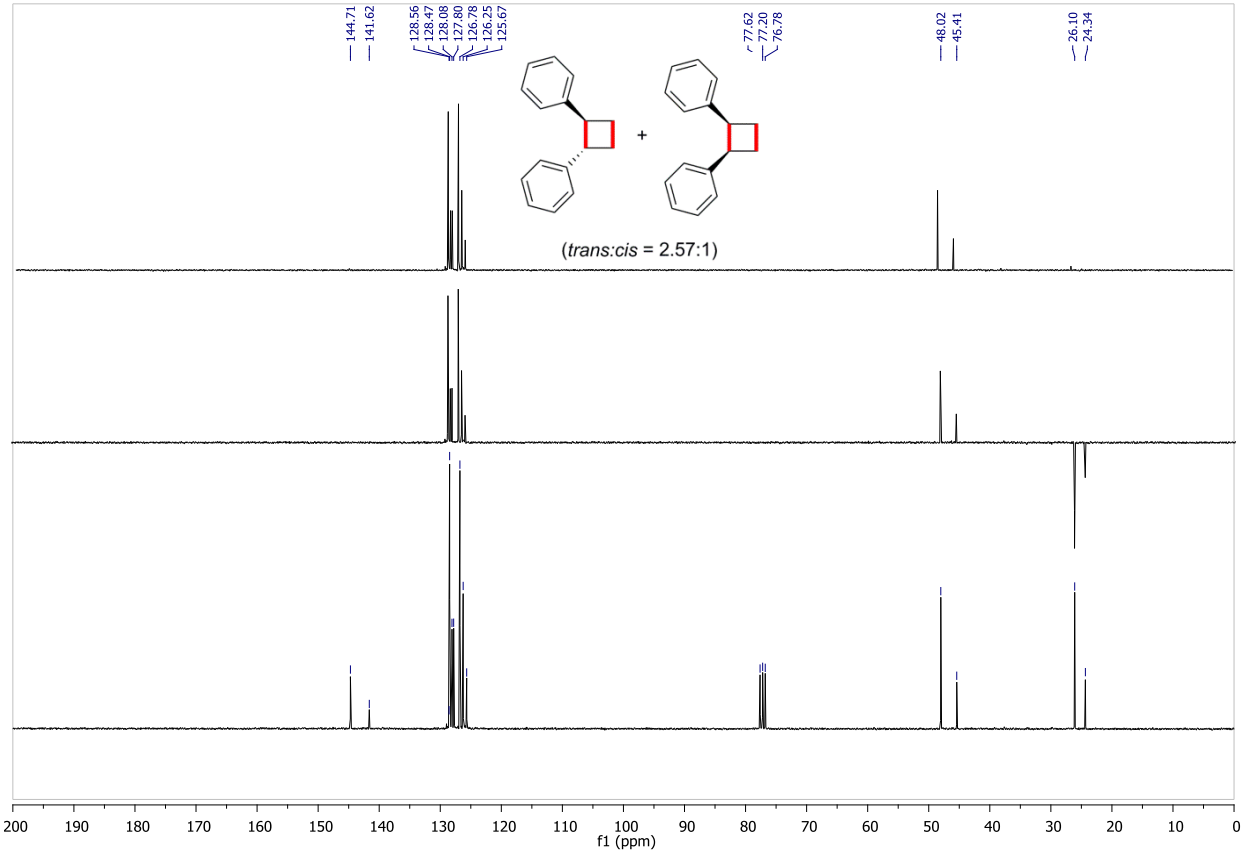

^{1}H-NMR: **6b** (*cis*/*trans*)

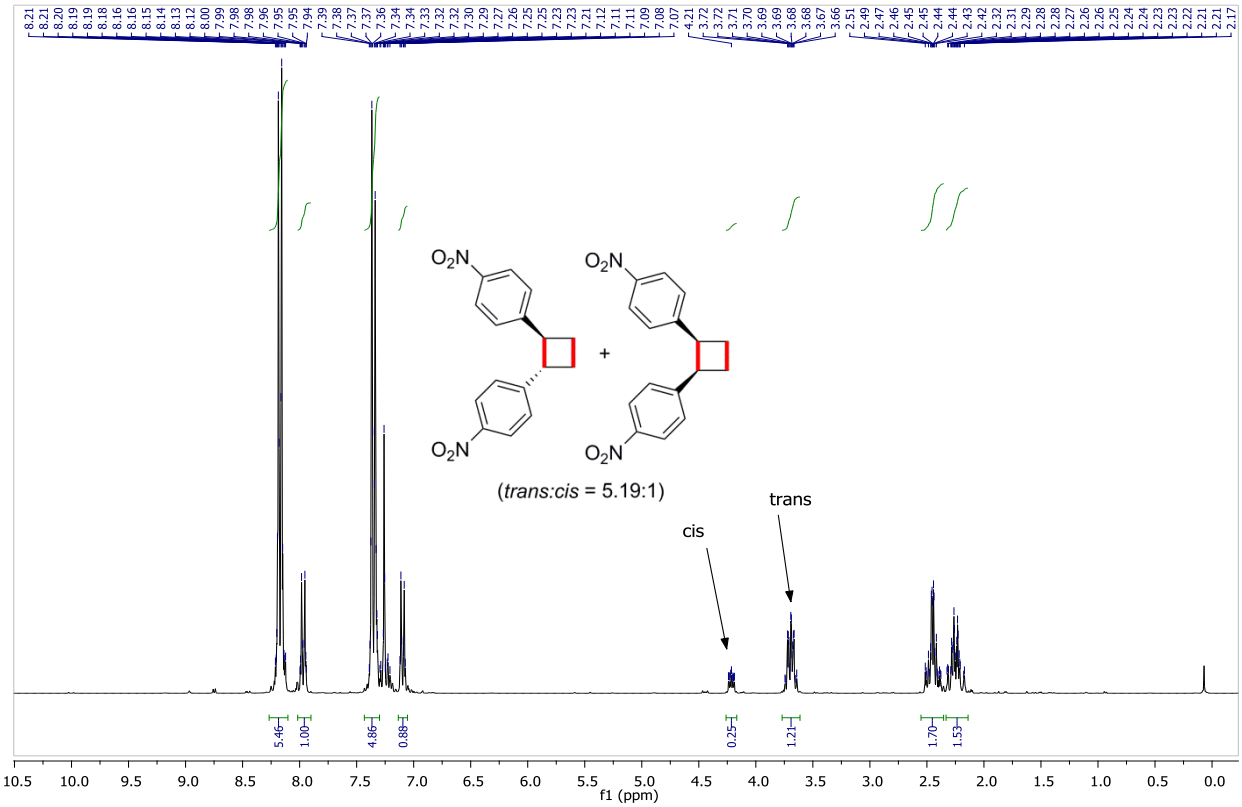

^{13}C-NMR: **6b** (*cis*/*trans*)

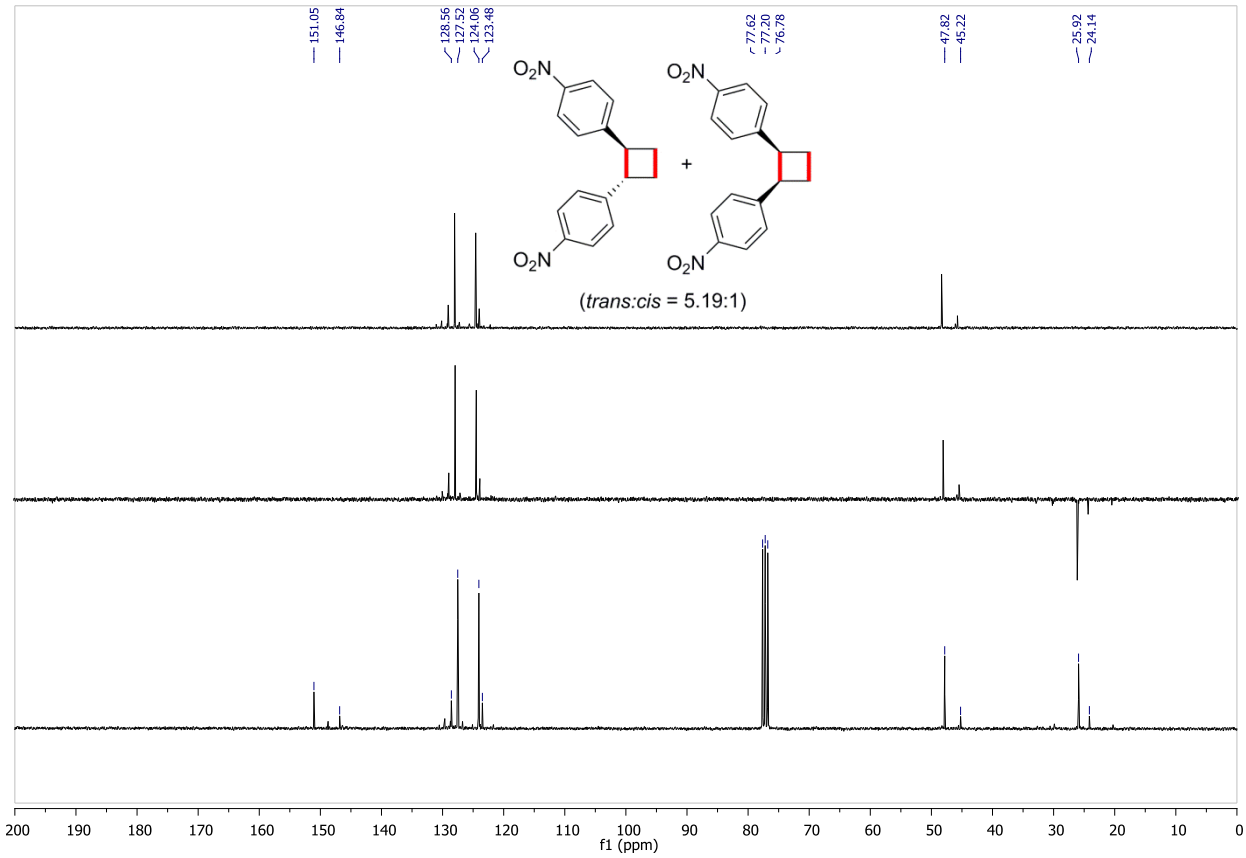

^{1}H-NMR: **6c** (*cis*/*trans*)

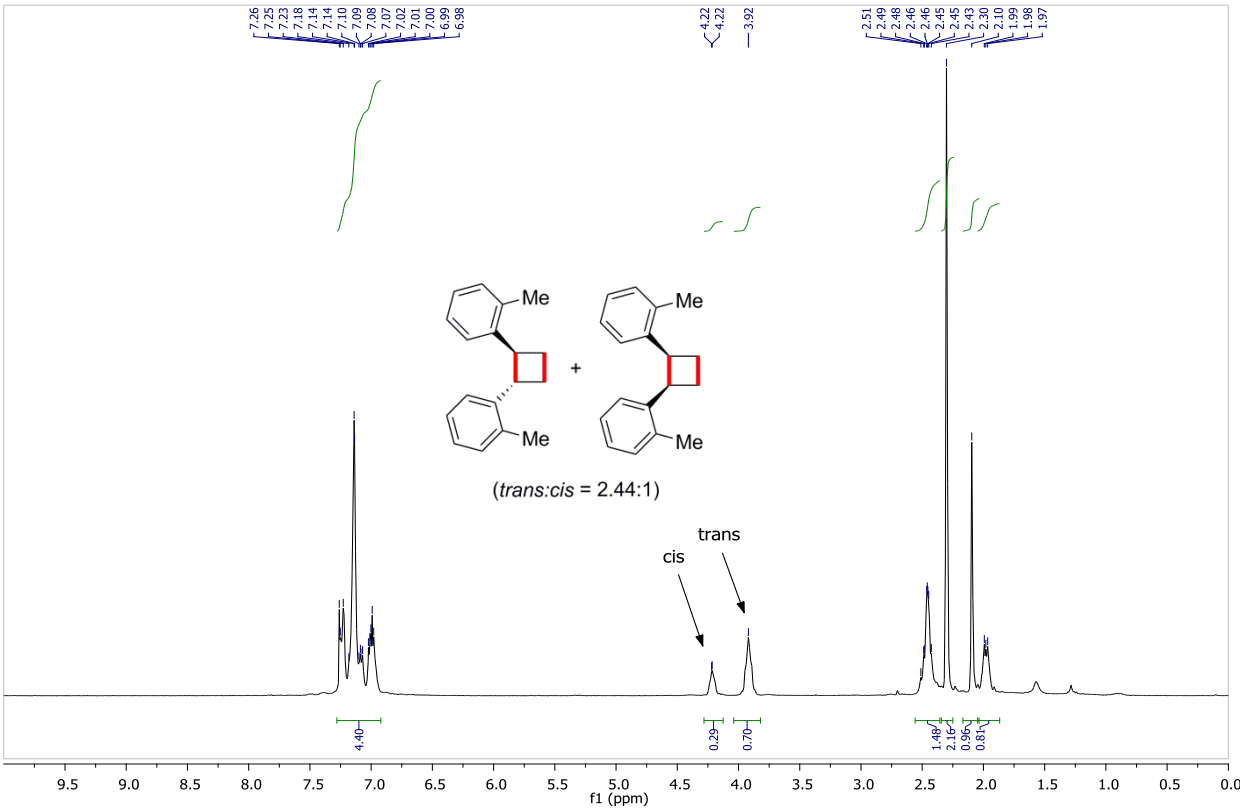

^{13}C-NMR: **6c** (*cis*/*trans*)

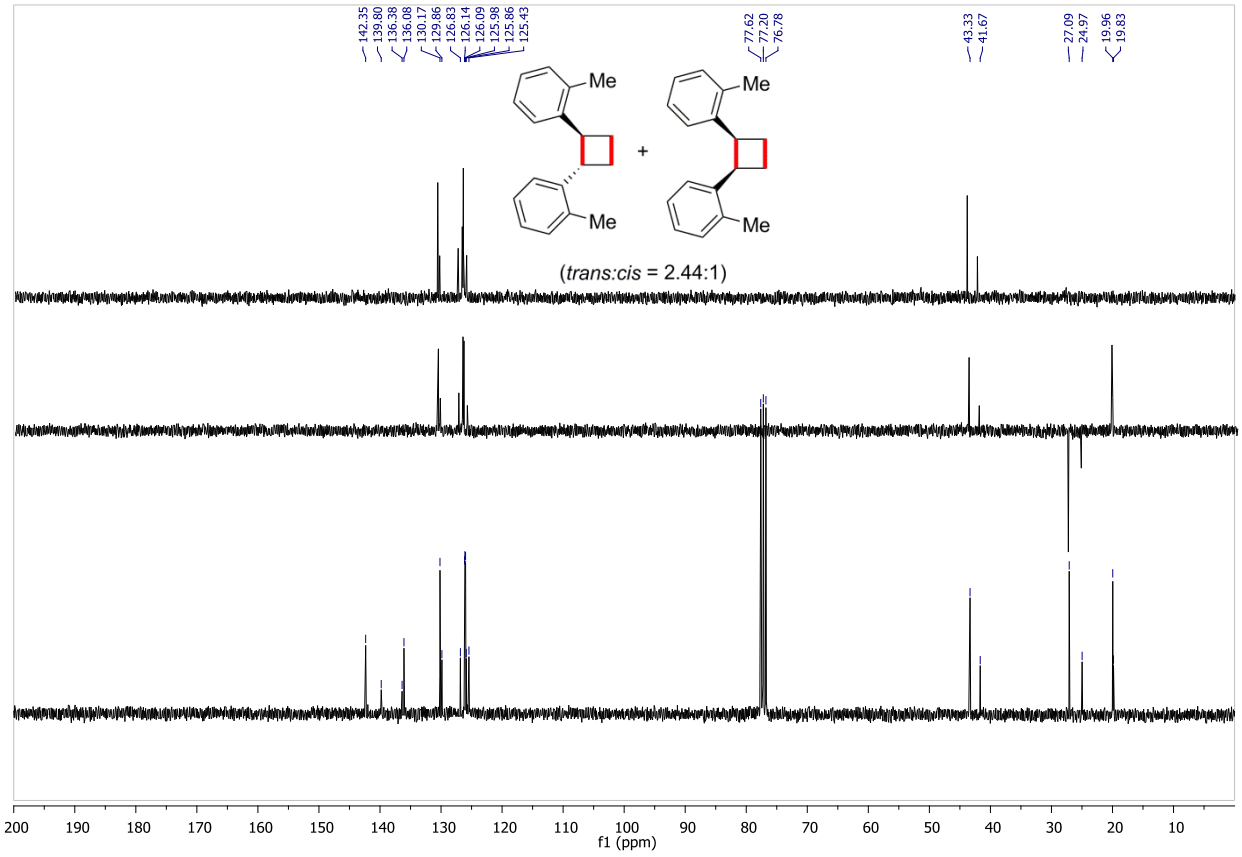

^{1}H-NMR: **6d** (*cis*/*trans*)

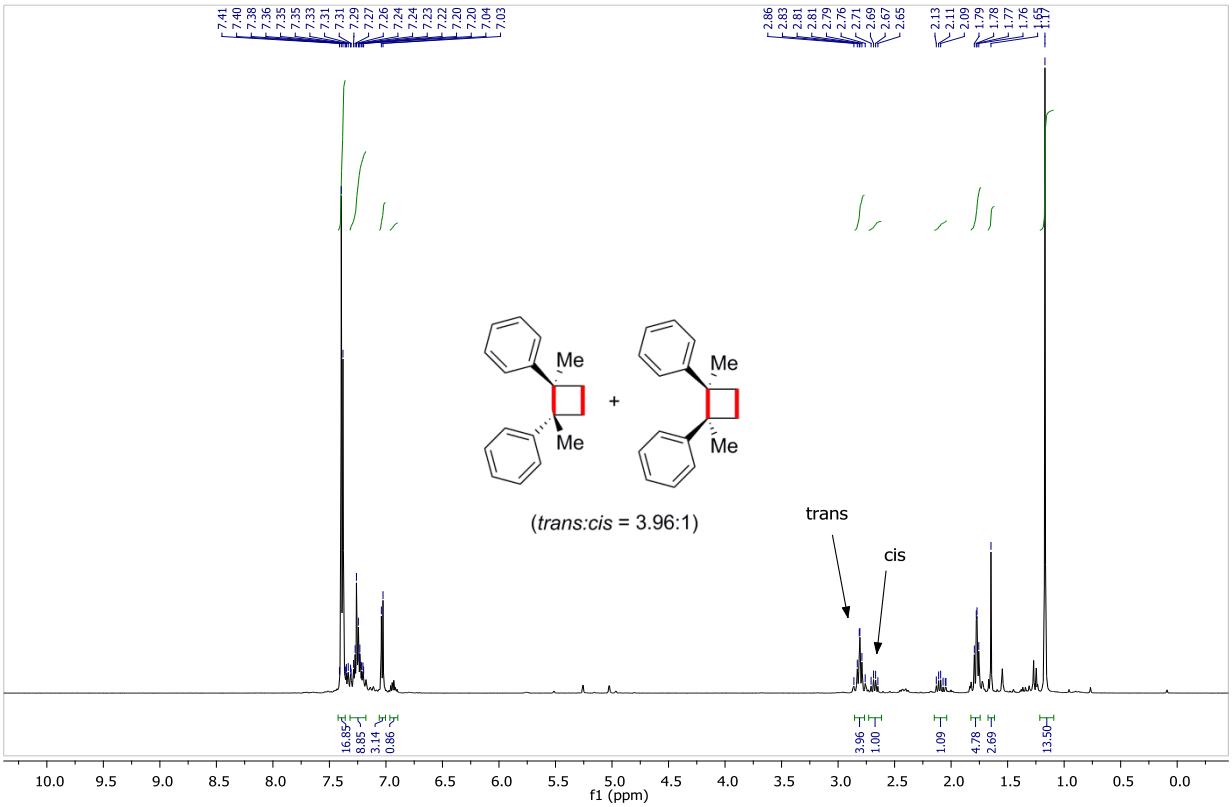

^{13}C-NMR: **6d** (*cis*/*trans*)

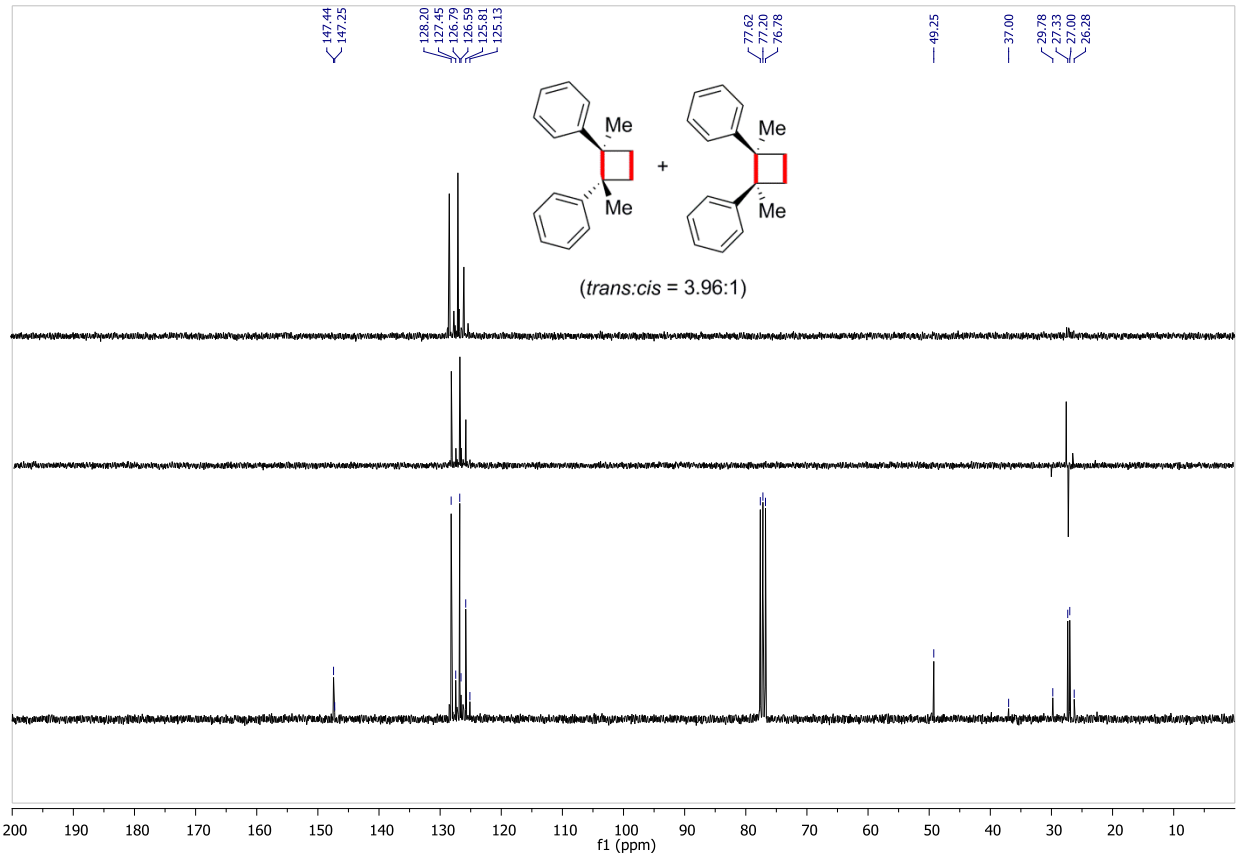

^{1}H-NMR: **6e** (*cis*/*trans*)

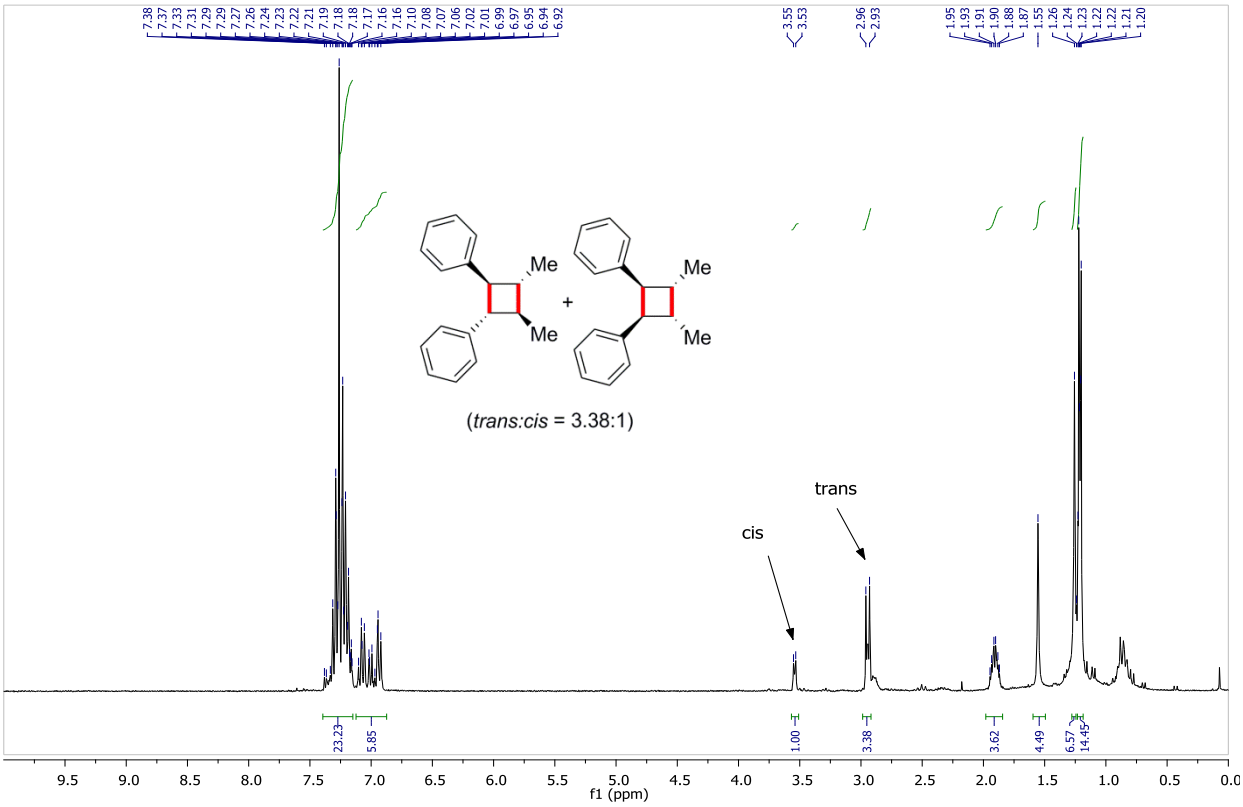

^{13}C-NMR: **6e** (*cis*/*trans*)

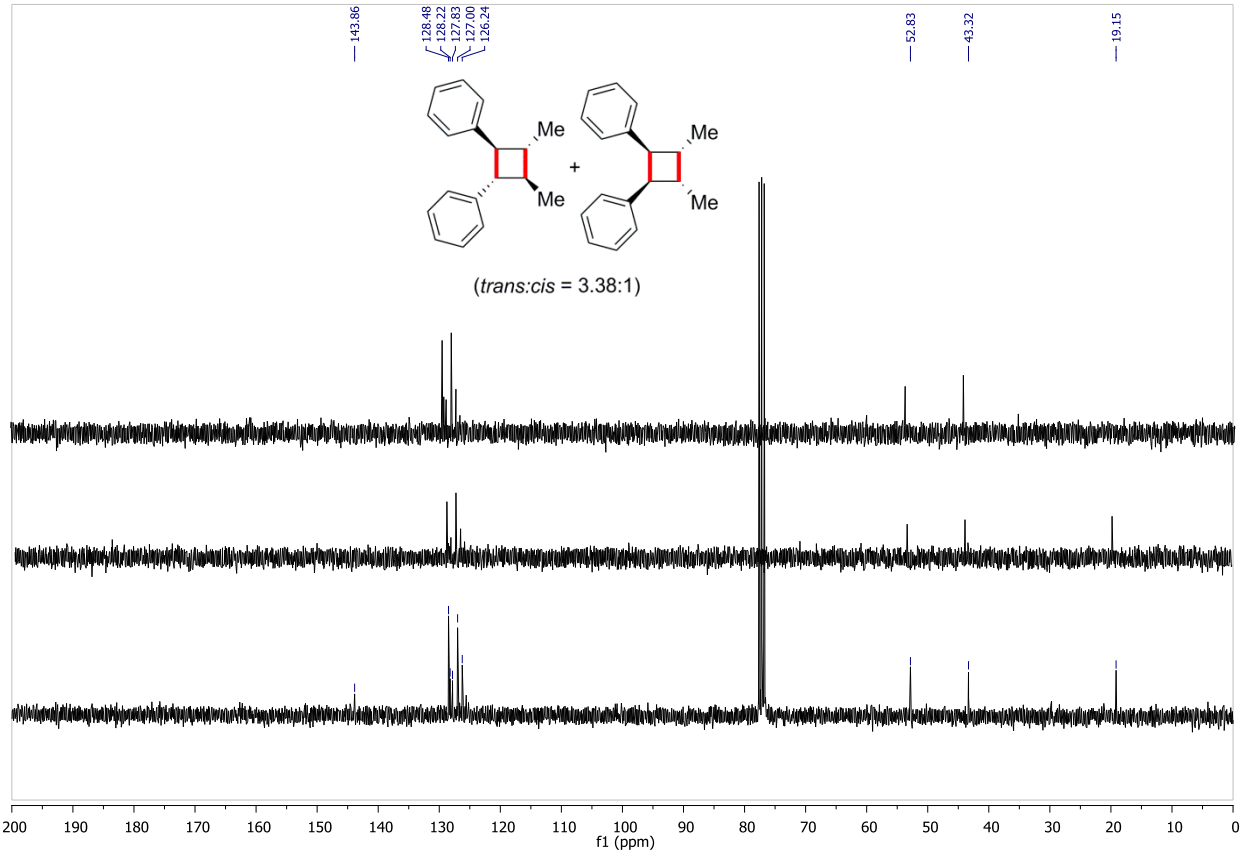

^{1}H-NMR: **7a** (*trans*)

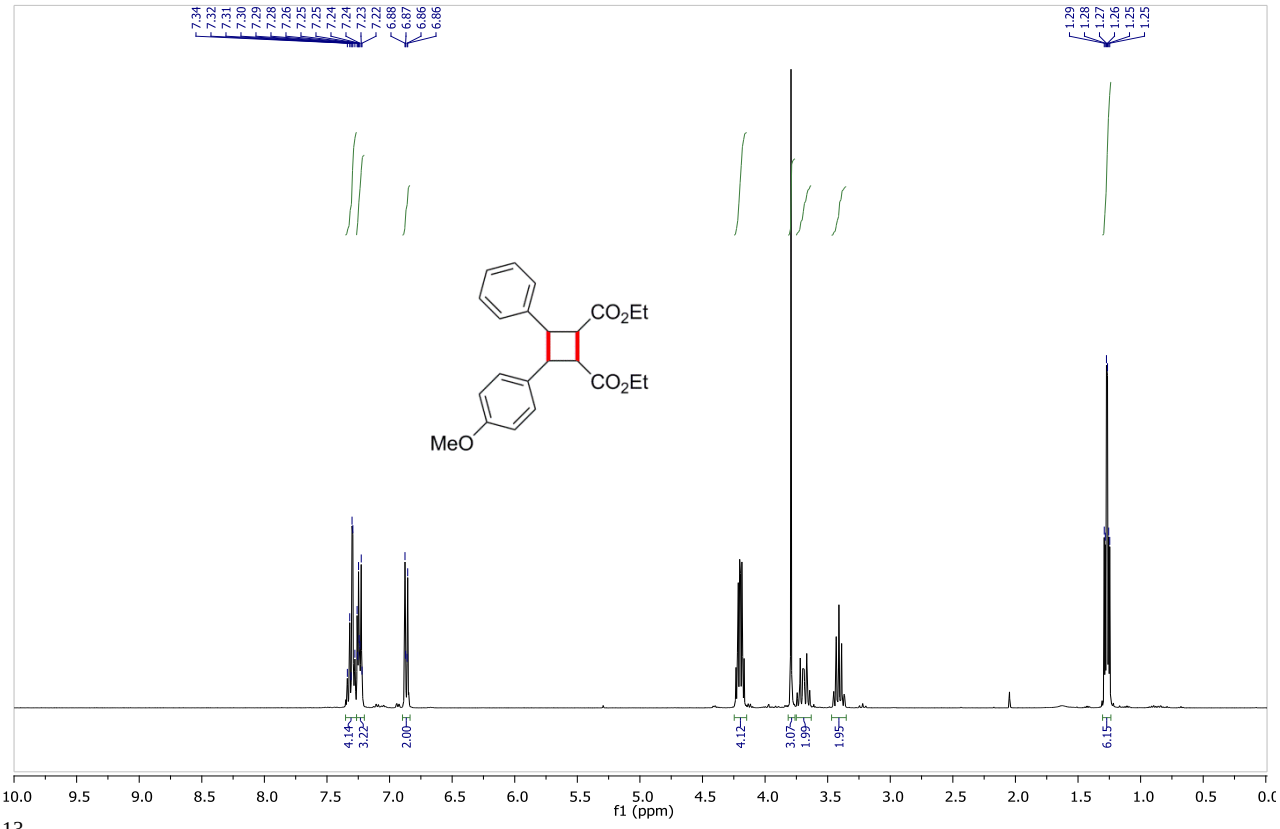

^{13}C-NMR: **7a** (*trans*)

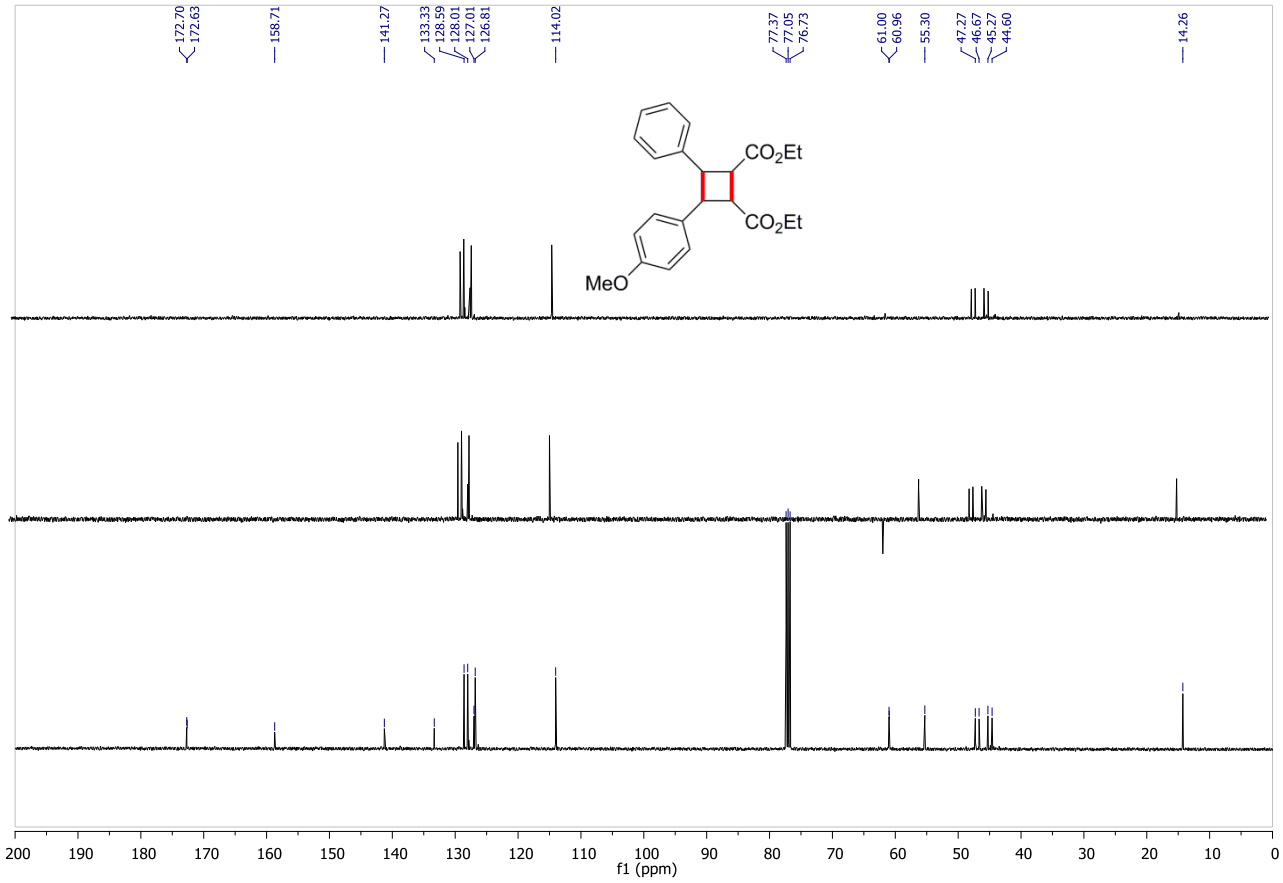

^{1}H-NMR: **7b** (*trans*)

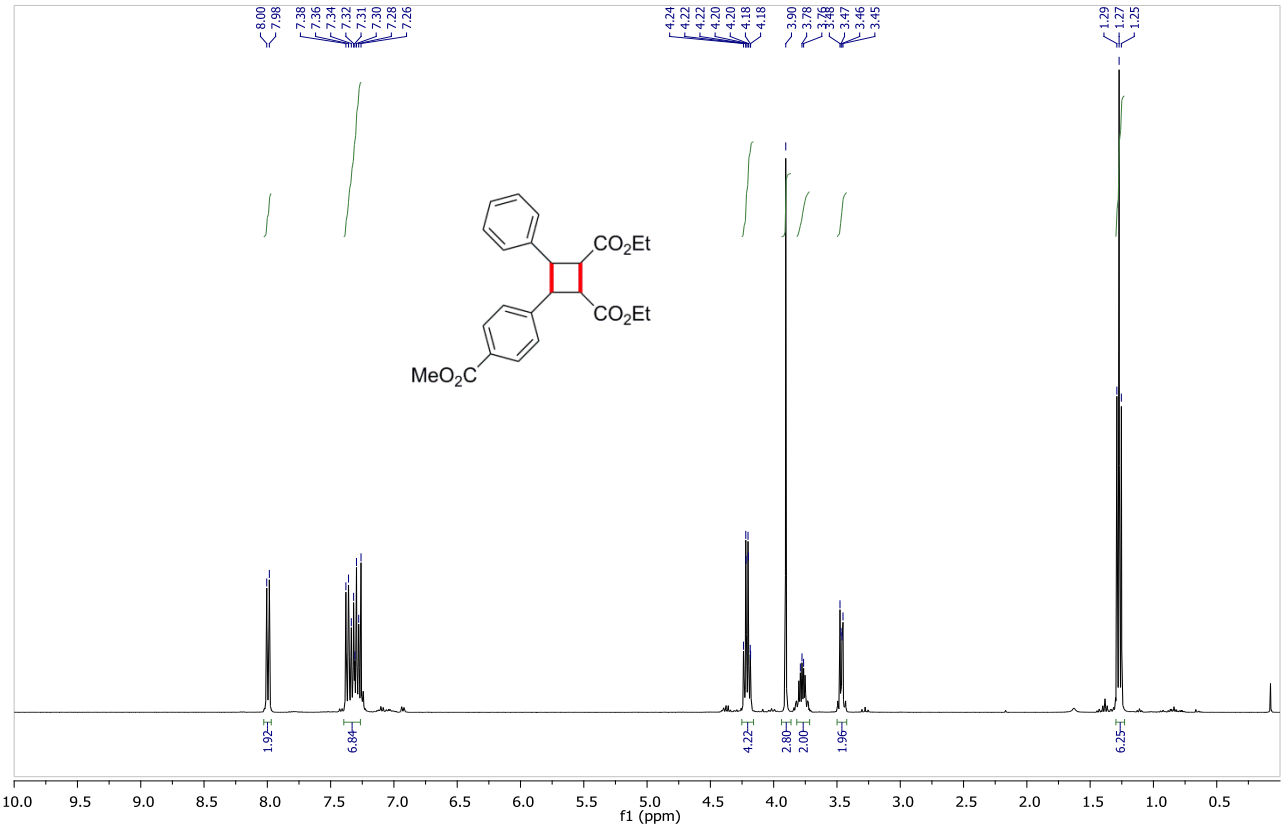

^{13}C-NMR: **7b** (*trans*)

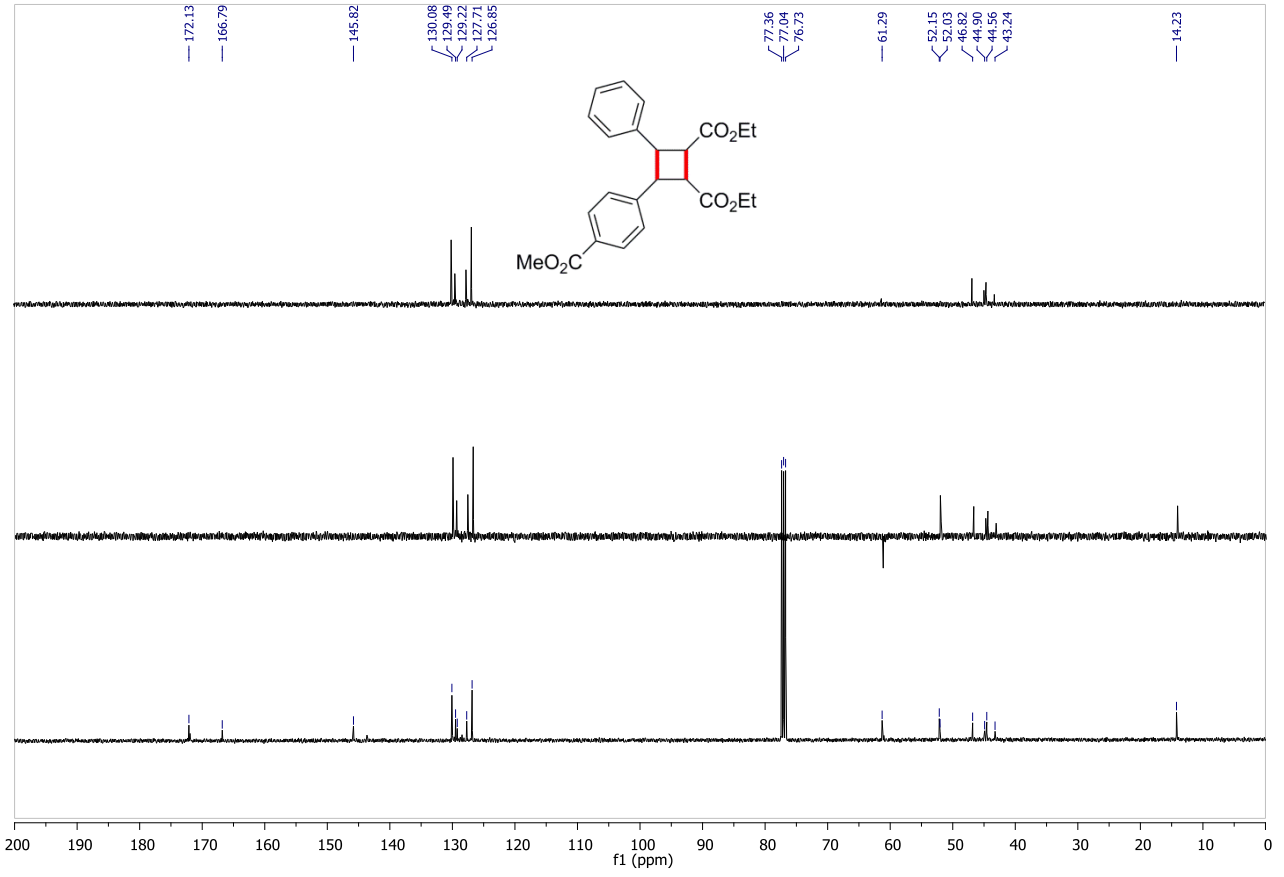

^{1}H-NMR: **7c** (*trans*)

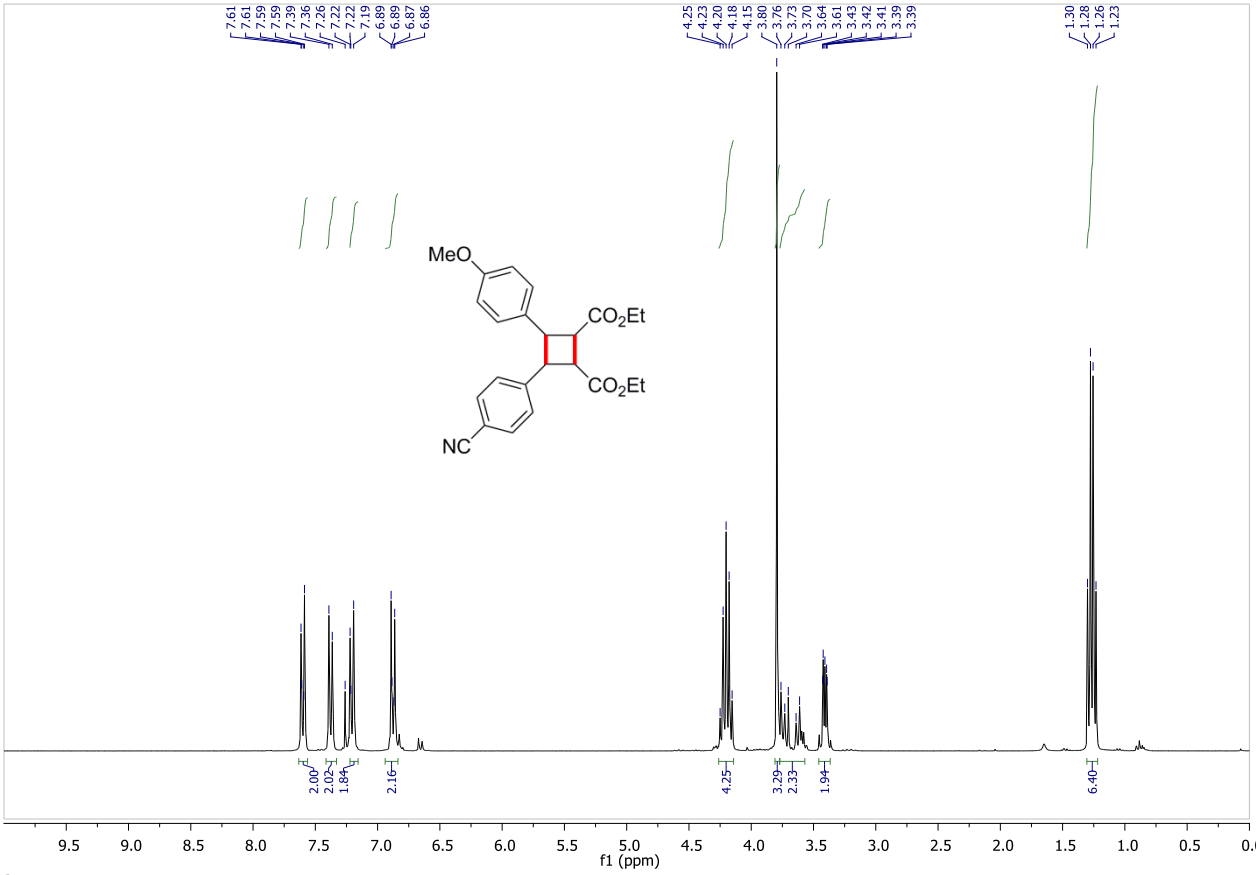

^{13}C-NMR: **7c** (*trans*)

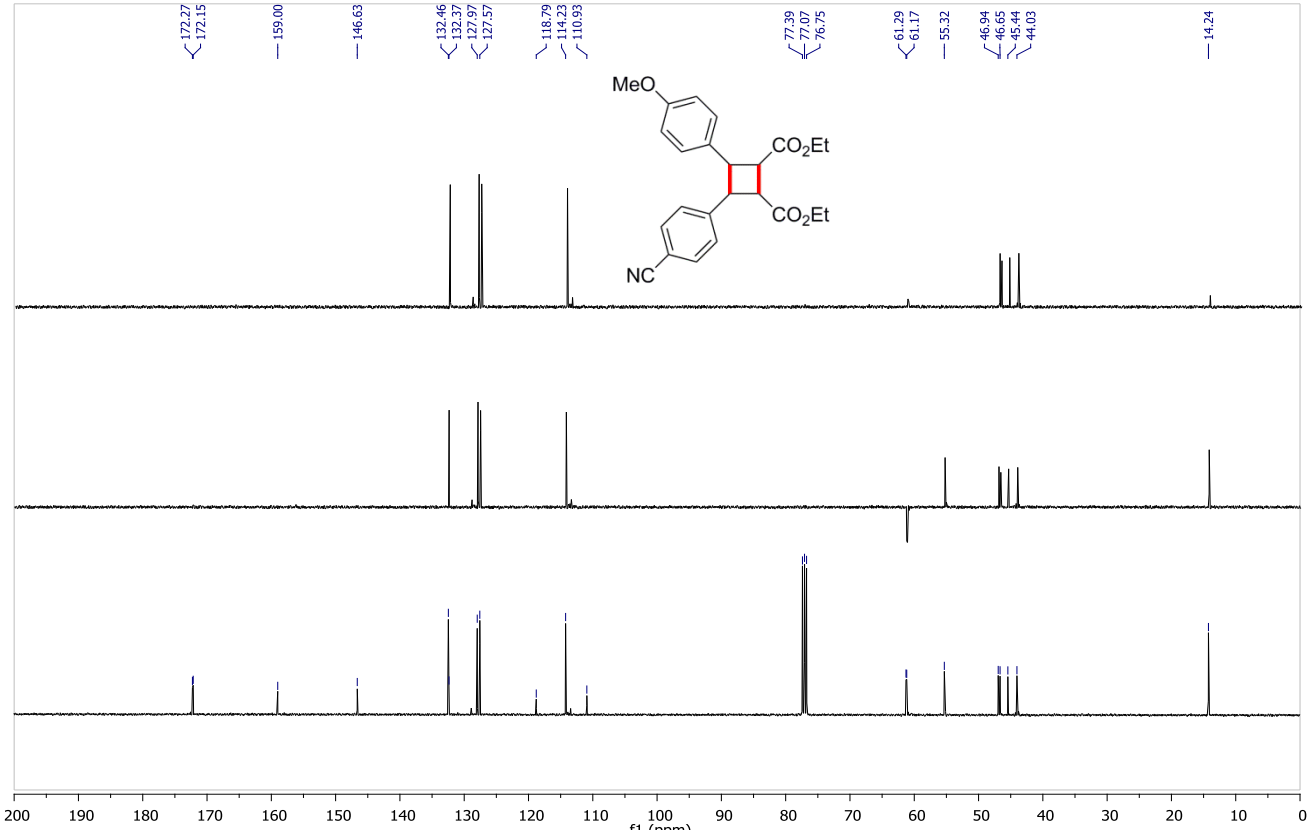

4.15 Crystal data for 2v:

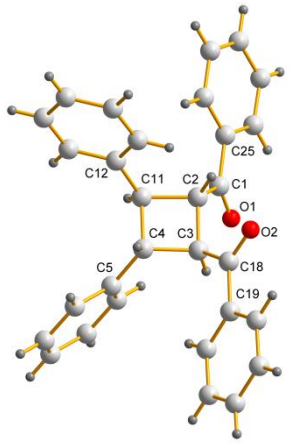

Figure 4.4: Crystal structure of **2v**

Experimental: Single clear colourless prism-shaped crystals of (**2v**) were obtained by recrystallisation from DCM/pentane. A suitable crystal (0.27×0.10×0.07) mm³ was selected and mounted on a MITIGEN holder with inert oil on a SuperNova, Single source at offset, Atlas diffractometer. The crystal was kept at T = 123.01(10) K during data collection. Using **Olex2** (Dolomanov et al., 2009), the structure was solved with the Sheldrick, 2015) structure solution program, using the None methods solution method. The model was refined with version of **olex2.refine** (Bourhis et al., 2015) using Gauss-Newton minimisation.

Crystal Data. $C_{30}H_{24}O_2$, M_r = 416.52, monoclinic, $P2_1/c$ (No. 14), a = 10.8157(1) Å, b = 9.5942(1) Å, c = 21.1289(2) Å, β = 91.349(1)°, $\alpha = \gamma = 90°$, V = 2191.90(4) Å³, T = 123.01(10) K, Z = 4, Z' = 1, μ(Cu K_α) = 0.606, 49002 reflections measured, 4378 unique (R_{int} = 0.0317) which were used in all calculations. The final wR_2 was 0.0873 (all data) and R_1 was 0.0338 (I≥σ(I)).

Compound	**2v**
Formula	$C_{30}H_{24}O_2$
$D_{calc.}$/ g cm^{-3}	1.2621
μ/mm^{-1}	0.606
Formula Weight	416.52
Colour	clear colourless
Shape	prism
Size/mm³	0.27×0.10×0.07
T/K	123.01(10)
Crystal System	monoclinic
Space Group	$P2_1/c$
a/Å	10.8157(1)
b/Å	9.5942(1)
c/Å	21.1289(2)
α/°	90
β/°	91.349(1)
γ/°	90
V/Å³	2191.90(4)
Z	4
Z'	1
Wavelength/Å	1.54184
Radiation type	Cu K_α
Θ_{min}/°	4.09
Θ_{max}/°	73.59
Measured Refl.	49002
Independent Refl.	4378
Reflections Used	4034
R_{int}	0.0317
Parameters	288
Restraints	0
Largest Peak	0.2557
Deepest Hole	-0.1984
GooF	1.0479
wR_2 (all data)	0.0873
wR_2	0.0849
R_1 (all data)	0.0367
R_1	0.0338

Table 4.5: Fractional Atomic Coordinates (×10⁴) and Equivalent Isotropic Displacement Parameters (Å²×10³) for **2v**. U_{eq} is defined as 1/3 of the trace of the orthogonalised U_{ij}.

Atom	x	y	z	U_{eq}
O(1)	2124.4(7)	9112.5(8)	5945.5(4)	30.51(19)
O(2)	3233.2(8)	5262.6(9)	5034.9(4)	33.1(2)
C(5)	2024.0(9)	5363.4(11)	7158.8(5)	21.1(2)
C(3)	2450.1(9)	6193.2(11)	5986.1(5)	21.3(2)
C(2)	3542.5(9)	7222.2(11)	6008.6(5)	21.5(2)
C(4)	2909.1(9)	5523.5(11)	6626.5(5)	21.2(2)
C(19)	1440.8(10)	4123.2(11)	5377.4(5)	23.1(2)
C(12)	5194.4(9)	6212.8(11)	6843.0(5)	22.7(2)
C(25)	4214.1(10)	9794.1(11)	5880.2(5)	24.9(2)
C(11)	3900.2(9)	6717.2(11)	6695.6(5)	21.7(2)
C(6)	2020.8(10)	4149.0(11)	7516.7(5)	26.6(2)
C(1)	3206.6(10)	8745.5(11)	5943.8(5)	23.1(2)
C(10)	1213.5(10)	6430.8(12)	7316.3(5)	25.2(2)
C(18)	2427.1(10)	5206.7(11)	5428.6(5)	23.2(2)
C(20)	1478.8(11)	3171.3(12)	4875.0(5)	29.1(2)
C(24)	491.7(10)	4021.5(11)	5808.6(5)	25.2(2)
C(23)	-399(1)	2981.9(12)	5739.6(5)	28.8(2)
C(13)	5925.2(10)	5643.5(12)	6376.5(5)	28.5(2)
C(9)	411.4(10)	6272.1(13)	7815.1(5)	29.2(2)
C(17)	5649.6(11)	6219.6(12)	7464.6(5)	28.5(2)
C(7)	1217.1(11)	3995.9(13)	8017.1(5)	31.0(3)
C(26)	5453.0(11)	9473.6(13)	6000.3(6)	31.0(3)
C(15)	7534.3(11)	5116.4(12)	7142.4(6)	32.7(3)
C(8)	412.5(10)	5050.6(14)	8166.3(5)	30.7(3)
C(30)	3893.3(11)	11146.9(12)	5698.1(6)	30.7(2)
C(16)	6816.0(11)	5669.8(13)	7611.5(6)	33.6(3)
C(22)	-357.8(11)	2057.6(12)	5239.8(6)	32.0(3)
C(14)	7088.7(11)	5110.7(13)	6524.8(6)	32.6(3)
C(21)	581.6(12)	2156.7(13)	4807.0(6)	34.0(3)
C(29)	4795.9(12)	12149.4(13)	5628.4(6)	35.9(3)
C(28)	6025.4(12)	11824.5(13)	5752.0(6)	36.4(3)
C(27)	6351.6(11)	10494.8(14)	5941.9(6)	37.5(3)

Table 4.6: Anisotropic Displacement Parameters (×10⁴) **2v**. The anisotropic displacement factor exponent takes the form: $-2\pi^2[h^2a^{*2} \times U_{11} + \ldots + 2hka^* \times b^* \times U_{12}]$

Atom	U_{11}	U_{22}	U_{33}	U_{23}	U_{13}	U_{12}
O(1)	22.7(4)	25.6(4)	43.2(5)	1.1(3)	0.3(3)	-1.3(3)
O(2)	34.5(4)	36.5(5)	28.6(4)	-8.0(4)	9.9(3)	-6.4(3)
C(5)	19.4(5)	22.6(5)	21.3(5)	-3.8(4)	-0.3(4)	-1.6(4)
C(3)	19.3(5)	21.1(5)	23.7(5)	-1.4(4)	1.9(4)	-0.1(4)
C(2)	18.8(5)	22.2(5)	23.4(5)	-1.3(4)	2.0(4)	-0.4(4)
C(4)	20.7(5)	19.8(5)	23.3(5)	-0.2(4)	2.5(4)	-1.2(4)
C(19)	24.4(5)	22.2(5)	22.6(5)	0.8(4)	-3.3(4)	1.2(4)
C(12)	21.6(5)	21.3(5)	25.3(5)	-4.7(4)	0.2(4)	2.2(4)
C(25)	25.8(5)	24.4(5)	24.4(5)	-2.1(4)	0.6(4)	1.4(4)
C(11)	20.9(5)	21.7(5)	22.6(5)	-1.7(4)	2.9(4)	-1.3(4)
C(6)	30.1(6)	22.3(5)	27.3(5)	-1.8(4)	0.6(4)	-0.4(4)
C(1)	22.6(5)	24.3(5)	22.4(5)	-0.2(4)	0.0(4)	-0.3(4)
C(10)	24.1(5)	26.2(5)	25.4(5)	0.9(4)	2.4(4)	1.3(4)
C(18)	23.4(5)	24.3(5)	22.0(5)	1.0(4)	0.4(4)	1.5(4)

Atom	U_{11}	U_{22}	U_{33}	U_{23}	U_{13}	U_{12}
C(20)	33.9(6)	27.5(6)	25.9(5)	-0.6(5)	1.1(4)	-1.6(4)
C(24)	24.3(5)	25.1(5)	26.2(5)	-0.3(4)	-1.2(4)	-1.3(4)
C(23)	24.5(5)	29.1(6)	32.7(6)	-1.8(4)	-0.8(4)	3.2(5)
C(13)	24.7(5)	33.1(6)	27.4(5)	2.8(4)	-2.4(4)	-1.9(4)
C(9)	22.5(5)	38.7(6)	26.6(5)	3.3(5)	2.4(4)	-2.9(5)
C(17)	29.4(6)	31.9(6)	24.4(5)	-5.6(5)	0.9(4)	3.6(4)
C(7)	35.7(6)	31.0(6)	26.2(5)	-9.7(5)	1.1(5)	5.2(4)
C(26)	25.7(6)	27.2(6)	39.8(6)	-2.3(4)	-0.4(5)	8.4(5)
C(15)	23.7(6)	28.9(6)	45.1(7)	-1.1(4)	-7.2(5)	8.8(5)
C(8)	24.3(6)	45.8(7)	22.0(5)	-9.2(5)	2.3(4)	0.2(5)
C(30)	30.0(6)	27.1(6)	34.8(6)	0.5(5)	-1.2(5)	4.3(5)
C(16)	33.9(6)	36.4(6)	30.1(6)	-7.1(5)	-8.8(5)	10.0(5)
C(22)	33.0(6)	25.8(6)	36.6(6)	-7.6(5)	-8.2(5)	2.0(5)
C(14)	24.8(6)	33.5(6)	39.5(6)	3.8(5)	0.2(5)	-1.3(5)
C(21)	43.9(7)	28.0(6)	29.7(6)	-4.3(5)	-3.9(5)	-5.7(5)
C(29)	42.1(7)	24.6(6)	40.9(7)	-3.6(5)	-0.1(5)	7.6(5)
C(28)	35.3(6)	32.5(6)	41.5(7)	-12.8(5)	0.2(5)	6.9(5)
C(27)	25.8(6)	38.5(7)	48.1(7)	-6.4(5)	-3.0(5)	10.4(6)

Table 4.7: Bond Lengths in Å for **2v**.

Atom	Atom	Length/Å
O(1)	C(1)	1.2224(13)
O(2)	C(18)	1.2204(13)
C(5)	C(4)	1.5018(14)
C(5)	C(6)	1.3890(15)
C(5)	C(10)	1.3935(15)
C(3)	C(2)	1.5396(14)
C(3)	C(4)	1.5681(14)
C(3)	C(18)	1.5108(14)
C(2)	C(11)	1.5699(14)
C(2)	C(1)	1.5114(14)
C(4)	C(11)	1.5732(14)
C(19)	C(18)	1.4916(15)
C(19)	C(20)	1.4016(15)
C(19)	C(24)	1.3919(15)
C(12)	C(11)	1.5066(14)
C(12)	C(13)	1.3896(15)
C(12)	C(17)	1.3919(15)
C(25)	C(1)	1.4915(15)
C(25)	C(26)	1.3923(16)
C(25)	C(30)	1.3952(16)
C(6)	C(7)	1.3923(16)
C(10)	C(9)	1.3890(15)
C(20)	C(21)	1.3796(17)
C(24)	C(23)	1.3919(15)
C(23)	C(22)	1.3805(17)
C(13)	C(14)	1.3872(16)
C(9)	C(8)	1.3871(17)
C(17)	C(16)	1.3955(17)
C(7)	C(8)	1.3761(18)
C(26)	C(27)	1.3876(17)
C(15)	C(16)	1.3799(19)
C(15)	C(14)	1.3805(17)
C(30)	C(29)	1.3807(17)
C(22)	C(21)	1.3862(18)
C(29)	C(28)	1.3846(18)
C(28)	C(27)	1.3807(18)

Table 4.8: Bond Angles in ° for **2v**.

Atom	Atom	Atom	Angle/°
C(6)	C(5)	C(4)	120.22(9)
C(10)	C(5)	C(4)	121.29(9)
C(10)	C(5)	C(6)	118.47(10)
C(4)	C(3)	C(2)	90.51(7)
C(18)	C(3)	C(2)	115.11(8)
C(18)	C(3)	C(4)	114.53(8)
C(11)	C(2)	C(3)	90.17(7)
C(1)	C(2)	C(3)	115.76(8)
C(1)	C(2)	C(11)	115.83(8)
C(3)	C(4)	C(5)	119.59(8)
C(11)	C(4)	C(5)	116.74(8)
C(11)	C(4)	C(3)	89.02(7)
C(20)	C(19)	C(18)	118.39(10)
C(24)	C(19)	C(18)	122.58(9)
C(24)	C(19)	C(20)	119.03(10)
C(13)	C(12)	C(11)	121.39(9)
C(17)	C(12)	C(11)	119.99(10)
C(17)	C(12)	C(13)	118.46(10)
C(26)	C(25)	C(1)	122.45(10)
C(30)	C(25)	C(1)	118.35(10)
C(30)	C(25)	C(26)	119.19(10)
C(4)	C(11)	C(2)	89.22(7)
C(12)	C(11)	C(2)	119.85(8)
C(12)	C(11)	C(4)	114.40(8)
C(7)	C(6)	C(5)	120.77(11)
C(2)	C(1)	O(1)	120.43(9)
C(25)	C(1)	O(1)	120.50(10)
C(25)	C(1)	C(2)	119.07(9)
C(9)	C(10)	C(5)	120.55(10)
C(3)	C(18)	O(2)	120.34(9)
C(19)	C(18)	O(2)	120.15(10)
C(19)	C(18)	C(3)	119.46(9)
C(21)	C(20)	C(19)	120.37(11)
C(23)	C(24)	C(19)	120.06(10)
C(22)	C(23)	C(24)	120.37(11)
C(14)	C(13)	C(12)	120.86(11)
C(8)	C(9)	C(10)	120.39(11)
C(16)	C(17)	C(12)	120.39(11)
C(8)	C(7)	C(6)	120.39(11)
C(27)	C(26)	C(25)	120.06(11)
C(14)	C(15)	C(16)	119.38(11)
C(7)	C(8)	C(9)	119.43(10)
C(29)	C(30)	C(25)	120.37(11)
C(15)	C(16)	C(17)	120.47(11)
C(21)	C(22)	C(23)	119.87(11)
C(15)	C(14)	C(13)	120.44(11)
C(22)	C(21)	C(20)	120.29(11)
C(28)	C(29)	C(30)	120.09(11)
C(27)	C(28)	C(29)	120.03(11)
C(28)	C(27)	C(26)	120.24(12)

Table 4.9: Hydrogen Fractional Atomic Coordinates (×10⁴) and Equivalent Isotropic Displacement Parameters (Å²×10³) for **2v**. U_{eq} is defined as 1/3 of the trace of the orthogonalised U_{ij}.

Atom	x	y	z	U_{eq}
H(3)	1656.4(9)	6672.0(11)	6030.4(5)	25.6(3)
H(2)	4175.4(9)	6957.9(11)	5706.7(5)	25.8(3)
H(4)	3318.9(9)	4632.5(11)	6545.1(5)	25.5(3)
H(11)	3645.4(9)	7405.0(11)	7009.7(5)	26.0(3)
H(6)	2561.7(10)	3429.9(11)	7420.9(5)	31.9(3)
H(10)	1209.7(10)	7256.4(12)	7085.6(5)	30.2(3)
H(20)	2112.4(11)	3223.9(12)	4585.9(5)	34.9(3)
H(24)	452.6(10)	4648.7(11)	6143.1(5)	30.3(3)
H(23)	-1025.4(10)	2909.6(12)	6031.9(5)	34.5(3)
H(13)	5630.6(10)	5619.4(12)	5959.6(5)	34.2(3)
H(9)	-129.6(10)	6989.0(13)	7914.1(5)	35.1(3)
H(17)	5173.7(11)	6592.9(12)	7784.0(5)	34.3(3)
H(7)	1224.2(11)	3176.0(13)	8252.0(5)	37.1(3)
H(26)	5678.5(11)	8574.2(13)	6119.9(6)	37.1(3)
H(15)	8311.3(11)	4750.6(12)	7241.4(6)	39.2(3)
H(8)	-125.8(10)	4945.5(14)	8499.8(5)	36.8(3)
H(30)	3067.0(11)	11374.7(12)	5623.2(6)	36.8(3)
H(16)	7111.2(11)	5676.4(13)	8028.5(6)	40.3(3)
H(22)	-959.1(11)	1369.8(12)	5193.6(6)	38.4(3)
H(14)	7571.7(11)	4747.2(13)	6205.9(6)	39.2(3)
H(21)	607.2(12)	1536.6(13)	4469.2(6)	40.7(3)
H(29)	4577.7(12)	13044.0(13)	5498.3(6)	43.1(3)
H(28)	6631.7(12)	12502.3(13)	5707.0(6)	43.7(3)
H(27)	7176.5(11)	10282.8(14)	6030.9(6)	45.0(3)

4.16 References

[1] a) V. M. Dembitsky, *J. Nat. Med.* **2008**, *62*, 1; b) V. M. Dembitsky, *Phytomedicine* **2014**, *21*, 1559; c) J. C. Namyslo, D. E. Kaufmann, *Chem. Rev.* **2003**, *103*, 1485; d) A. Sergeiko, V. V. Poroikov, L. O. Hanus, V. M. Dembitsky, *Open Med. Chem. J.* **2008**, *2*, 26.

[2] a) R. D. Hartley, W. H. Morrison III, F. Balza, G. H. Neil Towers, *Phytochemistry* **1990**, *29*, 3699; b) M. Krauze-Baranowska, *Acta Pol. Pharm.* **2002**, *59*, 403.

[3] R. A. Davis, A. R. Carroll, S. Duffy, V. M. Avery, G. P. Guymer, P. I. Forster, R. J. Quinn, *J. Nat. Prod.* **2007**, *70*, 1118.

[4] S. Poplata, A. Troster, Y.-Q. Zou, T. Bach, *Chem. Rev.* **2016**, *116*, 9748.

[5] a) Y. Xu, M. L. Conner, M. K. Brown, *Angew. Chem., Int. Ed.* **2015**, *54*, 11918; b) M. B. Boxer, H. Yamamoto, *Org. Lett.* **2005**, *7*, 3127; c) G.-J. Duan, J.-B. Ling, W.-P. Wang, Y.-C. Luo, P.-F. Xu, *Chem. Commun.* **2013**, *49*, 4625; d) K. Sakai, T. Kochi, F. Kakiuchi, *Org. Lett.* **2013**, *15*, 1024; e) F. Kleinbeck, F. D. Toste, *J. Am. Chem. Soc.* **2009**, *131*, 9178; f) G. Alberti, A. Bernard, A. Frongia, P. Piras, F. Secci, M. Spiga, *Synlett* **2006**, 2241.

[6] M. W. Smith, P. S. Baran, *Science* **2015**, *349*, 925.

[7] D. M. Schultz, T. P. Yoon, *Science* **2014**, *343*, 1239176.

[8] a) M. H. Shaw, J. Twilton, D. W. C. MacMillan, *J. Org. Chem.* **2016**, *81*, 6898; b) O. Reiser, *Acc. Chem. Res.* **2016**, *49*, 1990; c) M. Majek, A. Jacobi von Wangelin, *Acc. Chem. Res.* **2016**, *49*, 2316; d) M. D. Kärkäs, J. A. Porco, C. R. J. Stephenson, *Chem. Rev.* **2016**, *116*, 9683; e) D. Ravelli, S. Protti, M. Fagnoni, *Chem. Rev.* **2016**, *116*, 9850; f) J.-R. Chen, X.-Q. Hu, L.-Q. Lu, W.-J. Xiao, *Acc. Chem. Res.* **2016**, *49*, 1911; g) N. Hoffmann, *Eur. J. Org. Chem.* **2017**, *2017*, 1982; h) D. Menigaux, P. Belmont, E. Brachet, *Eur. J. Org. Chem.* **2017**, *2017*, 2008.

[9] a) T. P. Yoon, M. A. Ischay, J. Du, *Nat. Chem.* **2010**, *2*, 527; b) M. A. Ischay, M. E. Anzovino, J. Du, T. P. Yoon, *J. Am. Chem. Soc.* **2008**, *130*, 12886; c) J. Du, T. P. Yoon, *J. Am. Chem. Soc.* **2009**, *131*, 14604; d) T. P. Yoon, *Acc. Chem. Res.* **2016**, *49*, 2307; e) T. R. Blum, Z. D. Miller, D. M. Bates, I. A. Guzei, T. P. Yoon, *Science* **2016**, *354*, 1391; f) J. Du, K. L. Skubi, D. M. Schultz, T. P. Yoon, *Science* **2014**, *344*, 392; g) M. A. Ischay, Z. Lu, T. P. Yoon, *J. Am. Chem. Soc.* **2010**, *132*, 8572; h) K. L. Skubi, T. R. Blum, T. P. Yoon, *Chem. Rev.* **2016**, *116*, 10035; i) S. Lin, S. D. Lies, C. S. Gravatt, T. P. Yoon, *Org. Lett.* **2017**, *19*, 368; j) M. A. Cismesia, T. P. Yoon, *Chem. Sci.* **2015**, *6*, 5426.

[10] M. A. Ischay, M. S. Ament, T. P. Yoon, *Chem. Sci.* **2012**, *3*, 2807.

[11] a) S. Karthikeyan, V. Ramamurthy, *J. Org. Chem.* **2007**, *72*, 452; b) N. Nguyen, A. R. Clements, M. Pattabiraman, *New J. Chem.* **2016**, *40*, 2433.

[12] E. L. Tyson, E. P. Farney, T. P. Yoon, *Org. Lett.* **2012**, *14*, 1110.

[13] R. Telmesani, S. H. Park, T. Lynch-Colameta, A. B. Beeler, *Angew. Chem., Int. Ed.* **2015**, *54*, 11521.

[14] a) S. K. Pagire, O. Reiser, *Green Chem.* **2017**, *19*, 1721; b) S. Paria, V. Kais, O. Reiser, *Adv. Synth. Catal.* **2014**, *356*, 2853; c) S. Paria, O. Reiser, *Adv. Synth. Catal.* **2014**, *356*, 557.

[15] a) A. Hossain, S. K. Pagire, O. Reiser, *Synlett* **2017**, *28*, 1707; b) J. Xuan, X.-D. Xia, T.-T. Zeng, Z.-J. Feng, J.-R. Chen, L.-Q. Lu, W.-J. Xiao, *Angew. Chem., Int. Ed.* **2014**, *53*, 5653.

[16] S. K. Pagire, P. Kreitmeier, O. Reiser, *Angew. Chem., Int. Ed.* **2017**, *56*, 10928.

[17] I. Fussing, M. Gullu, O. Hammerich, A. Hussain, M. F. Nielsen, J. H. P. Utley, *J. Chem. Soc., Perkin Trans. 2* **1996**, 649.

[18] H. Roth, N. Romero, D. Nicewicz, *Synlett* **2016**, *27*, 714.

[19] F. Teplý, *Collect. Czech. Chem. Commun.* **2011**, *76*, 859.

[20] C. K. Prier, D. A. Rankic, D. W. C. MacMillan, *Chem. Rev.* **2013**, *113*, 5322.

[21] Z. Lu, T. P. Yoon, *Angew. Chem., Int. Ed.* **2012**, *51*, 10329.

[22] a) D. B. Bagal, G. Kachkovskyi, M. Knorn, T. Rawner, B. M. Bhanage, O. Reiser, *Angew. Chem., Int. Ed.* **2015**, *54*, 6999; b) M. Knorn, T. Rawner, R. Czerwieniec, O. Reiser, *ACS Catal.* **2015**, *5*, 5186; c) S. K. Pagire, S. Paria, O. Reiser, *Org. Lett.* **2016**, *18*, 2106; d) T. Rawner, M. Knorn, E. Lutsker, A. Hossain, O. Reiser, *J. Org. Chem.* **2016**, *81*, 7139; e) S. Paria, O. Reiser, *ChemCatChem* **2014**, *6*, 2477.

[23] A. K. F. Albertson, J.-P. Lumb, *Angew. Chem., Int. Ed.* **2015**, *54*, 2204.

[24] M. D'Auria, G. Piancatelli, A. Vantaggi, *J. Chem. Soc., Perkin Trans. 1* **1990**, 2999.

[25] F. Toda, K. Tanaka, M. Kato, *J. Chem. Soc., Perkin Trans. 1* **1998**, 1315.

[26] a) R. Li, B. C. Ma, W. Huang, L. Wang, Di Wang, H. Lu, K. Landfester, K. A. I. Zhang, *ACS Catal.* **2017**, *7*, 3097; b) M. Riener, D. A. Nicewicz, *Chem. Sci.* **2013**, *4*, 2625.

[27] a) W. R. Gutekunst, P. S. Baran, *J. Am. Chem. Soc.* **2011**, *133*, 19076; b) W. R. Gutekunst, P. S. Baran, *J. Org. Chem.* **2014**, *79*, 2430; c) J. He, Q. Shao, Q. Wu, J.-Q. Yu, *J. Am. Chem. Soc.* **2017**, *139*, 3344; d) R. Liu, M. Zhang, T. P. Wyche, G. N. Winston-McPherson, T. S. Bugni, W. Tang, *Angew. Chem., Int. Ed.* **2012**, *51*, 7503; e) R. A. Panish, S. R. Chintala, J. M. Fox, *Angew. Chem., Int. Ed.* **2016**, *55*, 4983.

[28] D. Haag, H.-D. Scharf, *J. Org. Chem.* **1996**, *61*, 6127.

[29] J. B. Metternich, R. Gilmour, *J. Am. Chem. Soc.* **2015**, *137*, 11254.

[30] J. H. Schauble, E. H. Freed, M. D. Swerdloff, *J. Org. Chem.* **1971**, *36*, 1302.

5 Tandem cyclization of vinyl radicals: A sustainable approach to indolines utilizing visible-light photocatalysis

5.1 Abstract:

A tin-free strategy for the synthesis of substituted indolines has been demonstrated generating vinyl radicals utilizing the reductive quenching cycle operated by visible-light-promoted photocatalysis. This method offers a robust, mild, and high yielding route to a broad range of indoline derivatives containing different electronic functionalities. The resultant 2,3-disubstituted indolines features as valuable precursors for the synthesis of a number of biologically active molecules, which is demonstrated with the formal synthesis of representative examples, such as Furoindolines or Tryptamines etc.

5.2 Introduction:

Indoles are a one of the commonly occurred prevalent structural entities in a range of bioactive natural products, drug candidates, pharmaceutical, alkaloids, and functional materials.[1] In particular, 2,3-disubstituted indoles are a valuable class of organic compounds, which exhibit a remarkable biological activities.[2] For example, FGIN-1-27 (**1**, Figure 5.1) is recognized as an agonist anxiolytic drug candidate, which potently and specifically binds to the glial mitochondrial diazepam binding receptor complex (*K*i = 4.4 nM).[3] Whereas, the 2-phenyl tryptamine derivative **2** is a high-affinity and selective antagonist of the human 5-HT_{2A} receptor (*K*i = 2.7 nM).[4] Furthermore, the 2-arylindole-3-acetamide derivative **3** was identified as a FPP-competitive inhibitor of farnesyl protein transferase (IC_{50} = 31 nM)[5] and 2-(3,5-dimethylphenyl)tryptamine derivatives such as **4** exhibit incredible affinity for the gonadotropin-releasing hormone (GnRH-antagonist).[6] In turn, a number of elegant synthetic approaches targeting this class of indoles have been established over the years.[7,8] Among them, the tandem radical cyclization via hydrogen translocation strategy (Scheme 5.2) pioneered by Parson and co-workers[9] offers an efficient and direct approach to 2,3-disubstituted benzodihydrofurans and indolines with the desired 3-acetic acid side chain,[10,11] and subsequently, 2-arylindolin-3-ylacetic acid esters **7** (Table 5.1-5.2).

This chapter has been published:

S. K. Pagire, O. Reiser, *Green Chem.* **2017**, *19*, 1721-1725.

S.K.P. and O.R. wrote the manuscript.

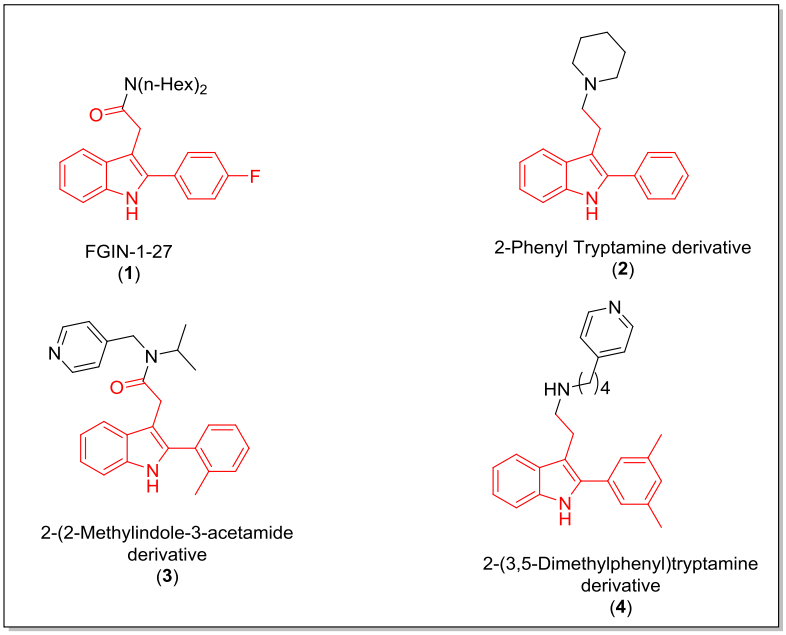

Figure 5.1 Representative biologically active 2-arylindoles.

However, the protocols that were demonstrated for the tandem radical cyclization suffers through harsh reaction conditions: the high reaction temperatures (> 100 °C) and the use of super-stoichiometric Bu_3SnH (1.4 to 2 equiv)/AIBN (0.5 equiv) (Scheme 5.2), which is non-practical from a sustainable point of view, especially for the late-stage synthesis of pharmaceutically active compounds on industrial scale.

Alternatively, visible-light photoredox catalysis offers a mild and benign route for such transformations. The low catalyst loading (0.3 mol %, see results and discussion) and unlimited source of clean light energy certainly hold promise for the future developments. Utilizing this technology, we intended to develop a complementary method towards 2,3-disubstituted indolines, which not only overcome the shortcomings of employing toxic reagents in large amounts but also opens new doors in organic synthesis.

Typically, visible-light induced activation of vinyl halides and their applications in organic transformations has not been widely explored and only few examples are known.[12,13,14] This is mainly due to their high redox potentials, which generally require a strongly reducing photocatalysts. This is mostly possible in the reductive quenching cycle to successfully generate a vinyl radical under extrusion of halide. However, the high reactivity such vinyl radicals results overall in simple reductions with efficient quenching by the sacrificial electron donor present. For example, our efforts to engage α-bromochalcones or α-bromocinnamates in a visible-light mediated C-C bond forming reactions with heteroarenes using *fac*[$Ir(ppy)_3$] or

$[Ir\{dF(CF_3)ppy\}_2(dtb\text{-}bpy)]PF_6$ in combination with amines (such as DIPEA or NEt_3) as sacrificial electron donor were unsuccessful. Instead, a vinyl bromide reduction was efficiently taking place in quantitative yields (>95%), but no coupling products could be isolated (Scheme 5.1).[13,14] Nevertheless, we questioned that vinyl radicals generated from α-bromocinnamate derivatives by photoredox catalysis in the reductive quenching cycle might readily undergo hydrogen translocation from a suitable H-donor being present in the substrate itself instead of external reduction. This way, the productive C-C bond forming process should be possible (Scheme 5.2).[15]

5.2.1 Previous attempts: Direct dehalogenation products

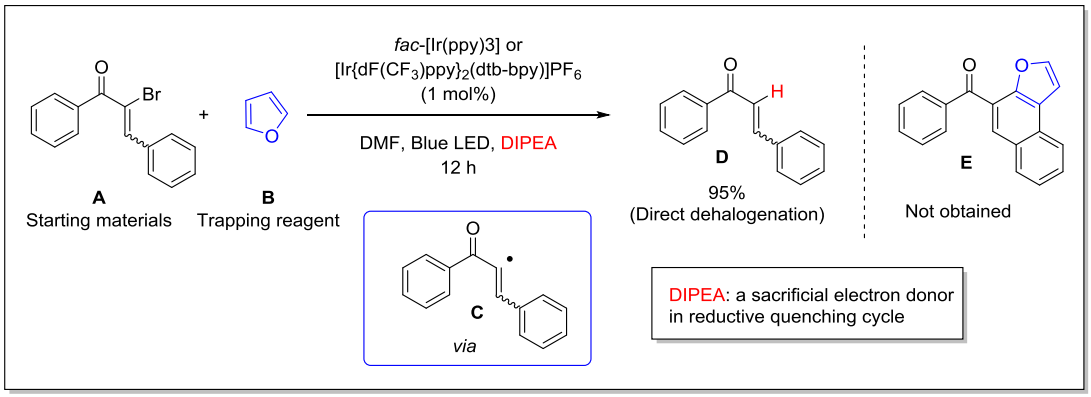

Scheme 5.1: Unsuccessful attempts of C-C bond formations utilizing reductive quenching cycles.

5.2.2 This attempt: Successful 1,6-HAT process

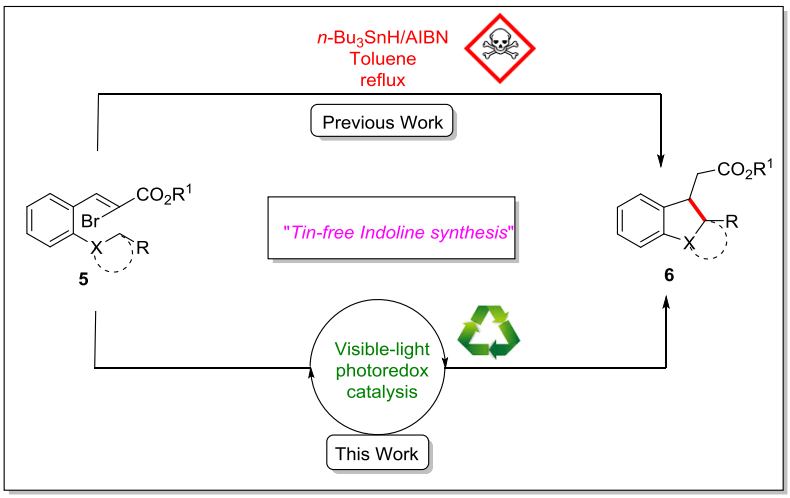

Scheme 5.2: Successful tandem cyclization via 1,6-hydrogen atom translocation (HAT) strategy.

5.3 Results and discussion:

Our interpretation was confirmed when α-bromocinnamate **7a** did not give any cyclized product upon utilizing oxidative quenching conditions employing with $[Ir\{dF(CF_3)ppy\}_2(dtb\text{-}bpy)]PF_6$ (Ir^{4+}/Ir^{*3+} = –0.89 V vs. SCE)[16] or $[Ir(ppy)_2(dtb\text{-}bpy)]PF_6$ (Ir^{4+}/Ir^{*3+} = –0.96 V vs. SCE)[17] as photocatalysts[18] in DMF under blue light (λmax = 455 nm) irradiation (Table 5.1, entry 1, 2).

5.4 Synthesis of 8a: Catalyst screening and reaction optimization

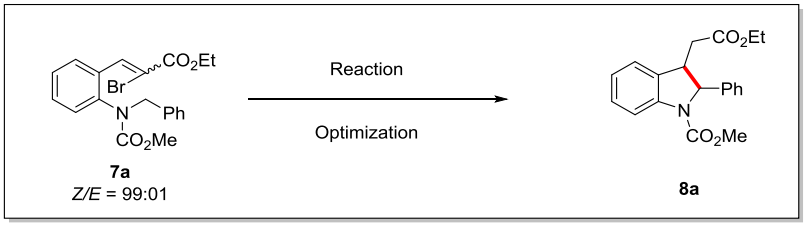

Entry	Photocatalyst (mol %), additive, solvent	Time (h)	Ratio **8a** (*cis*/*trans*)[b]	Yield (%)[c]
01[a]	$[Ir\{dF(CF_3)ppy\}_2(dtb\text{-}bpy)]PF_6$ (5), DMF	72	-	-
02	$[Ir(ppy)_2(dtb\text{-}bpy)]PF_6$ (5), DMF	72	-	-
03	$[Cu(dap)_2Cl]$ (5), DMF	72	-	NR[d]
04	*fac*$[Ir(ppy)_3]$ (5), DMF	72	-	-[e]
05[f]	*fac*$[Ir(ppy)_3]$ (5), DIPEA, DMF	36	81:19	71
06	$[Ir(ppy)_2(dtb\text{-}bpy)]PF_6$ (5), DIPEA, DMF	36	67:33	76
07	$[Ir\{dF(CF_3)ppy\}_2(dtb\text{-}bpy)]PF_6$ (5), DIPEA, DMF	36	71:29	15
08	$[Ir(ppy)_2(dtb\text{-}bpy)]PF_6$ (1), DIPEA, DMF	36	67:33	71
09	$[Ir(ppy)_2(dtb\text{-}bpy)]PF_6$ (1), DIPEA, MeCN	36	76:24	82
10	$[Ir(ppy)_2(dtb\text{-}bpy)]PF_6$ (0.3), DIPEA, MeCN	48	76:24	78
11	$[Ir(ppy)_2(dtb\text{-}bpy)]PF_6$ (0.1), DIPEA, MeCN	48	76:24	59
12	$[Ir(ppy)_2(dtb\text{-}bpy)]PF_6$ (0.1), DIPEA, MeCN	72	76:24	61
13	No Catalyst, DIPEA, MeCN	48	-	NR[d]
14	$[Ir(ppy)_2(dtb\text{-}bpy)]PF_6$ (0.3), no light, DIPEA, MeCN	48	-	NR[d]

Table 5.1: Reaction conditions: [a] Oxidative quenching (entries 1-4): Substrate **7a** (0.5 mmol), photocatalyst (5 mol %), anhydrous DMF (2 mL), LED_{455}, 72 h, room temperature. [b] *Cis/trans ratio* was determined by ^{1}H-NMR. [c] Isolated yields. [d] No reaction (starting material recovered). [e] *E/Z*-isomerization. [f] Reductive quenching (entries 5-13): Substrate **7a** (0.5 mmol), photocatalyst (0.1-5 mol %), DIPEA (1.1 mmol), anhydrous DMF or MeCN (2.0 mL), LED_{455}, room temperature, 36 h-72 h.

This is in accordance with the cyclic voltammetry measurements, suggesting that **7a** (–1.50 V vs. SCE, see experimental section) has a considerably higher reduction potential. Also, no reaction of **7a** occurred with [Cu(dap)$_2$Cl] (Cu^{2+}/Cu^{*+} = –1.43 V vs. SCE) under the identical reactions conditions (Table 5.1, entry 3).[19] By employing even more stronger reducing *fac*[Ir(ppy)$_3$] photocatalyst (Ir^{4+}/Ir^{*3+} = –1.73 V vs. SCE),[20] only resulted a simple *E/Z* isomerization of **7a**, however, no C-C bond formation takes place with the vinyl radical which might have generated in the reaction media (Table 5.1, entry 4), although the reducing power of the *fac*[Ir(ppy)$_3$] catalyst should have been now sufficient.

Next, we switched to the reductive quenching cycle: Surprisingly, irradiating **7a** in the presence of sacrificial electron donor DIPEA (2.2 equiv) and *fac*[Ir(ppy)$_3$] (5 mol %, Ir^{3+}/Ir^{2+} = –2.13 V vs. SCE) in DMF smoothly provided the desired product **8a** in 71% yields (Table 5.1, entry 5), favoring the direct cyclization over the expected debromination. Notably, the [Ir(ppy)$_2$(dtb-bpy)]PF_6 (Ir^{3+}/Ir^{2+} = –1.51 V vs. SCE) is subsequently found to be a suitable photocatalyst in the reductive quenching cycle (Table 5.1, entry 6). As expected, lower yield was observed with the [Ir{dF(CF$_3$)ppy}$_2$(dtb-bpy)]PF_6 photocatalyst since it's the reduction potential (Ir^{3+}/Ir^{2+} = –1.37 V vs. SCE) apparently too low to allow an efficient conversion of **7a** to **8a** (Table 5.1, entry 7). The *cis*-diastereomer of **8a** was formed predominantly with moderate selectivity (2:1 to 4:1), which was nevertheless without consequence of the aimed subsequent aromatization of **8** to indoles.

Having identified the suitable catalyst b [Ir(ppy)$_2$(dtb-bpy)]PF_6 for this conversion, further optimization enabled the synthesis of **8a** with improved yield by switching to the acetonitrile as a solvent (Table 5.1, entry 9). To our delight, the catalyst concentration could also be lowered to 0.3 mol % (Table 5.1, entry 10), though the reaction time needed to be elongated (from 36 h to 48 h). Whereas, further lowering the catalyst loading to 0.1 mol % gave inferior results even if the reaction time was prolonged from 36 h to 72 h (Table 5.1, entries 11, 12). In the absence of catalyst or light, no product formation is observed confirming the process is indeed driven by visible-light photocatalyst (Table 5.1, entries 13, 14).

5.5 Substrate scope

Having identified the best reaction conditions (Table 5.1, entry 10), we proceeded to expand the synthesis of various 2-aryl substituted indolin-3-ylacetic acid derivatives (Table 5.2). Gratifyingly, both electron rich and withdrawing substituents in the aryl moiety gave good results. However, a nitro substituent in **7k** did not provide the desired cyclization product, nevertheless, which has already been noted to be incompatible in some photoredox processes before.[13,14] Notably, the thiomethyl indoline derivative **8h** was smoothly formed in 89% yield by the photocatalytic method, contrasting the initiation by classical methods (*n*-Bu_3SnH/AIBN), which is known to reduce these type of thioethers.[21] The *cis/trans* isomers of **8b** were separated by recrystallization method and the *cis* diastereomer was clearly analyzed by single crystal X-ray analysis (Table 5.2). Evidently, the *cis*-diastereomers of **8** are kinetically more favoured and thus formed preferentially (*cis*/*trans* ~3:1) over the thermodynamically more favourable *trans*-diastereomers.

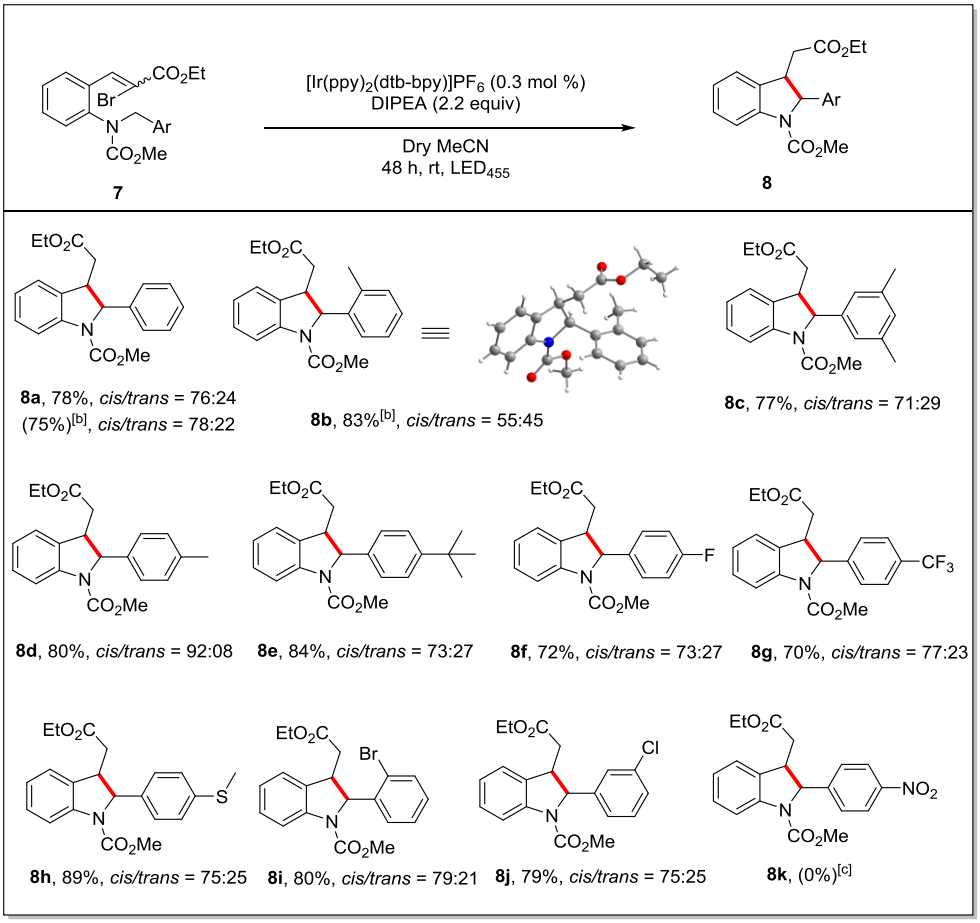

Table 5.2: Reaction conditions: [a] Substrate **7** (0.5 mmol), $[Ir(ppy)_2(dtb\text{-}bpy)]PF_6$ (0.3 mol %), anhydrous MeCN (2 mL), LED_{455}, 48 h, rt. [b] 3.0 mmol scale. [c] Complete conversion but expected product was not observed.

5.6 Proposed reaction mechanism:

A plausible reaction mechanism is presented in Figure 5.2. It is known that Ir(III) photoredox catalysts efficiently generate the oxidizing excited state *Ir(III) upon blue-light irradiation. Being highly oxidizing in nature in the excited state, *Ir(III) undergoes single electron reduction by the readily available sacrificial electron donor DIPEA to form even more stronger ground state reductant Ir(II). A facile single electron transfer (SET) to **7** from Ir(II) gives rise to the key vinyl radical intermediate **I** with the extrusion of bromide, thus completing the [Ir]-catalytic cycle. The resulting vinyl radical **I** is converted to the nucleophilic α-amino radical species **II** upon 1,6-H atom translocation (HAT). This stable α-amino radical undergoes a facile *5-exo*-trig ring closure to form α-alkyl radical intermediate **III**. Subsequent protonation from oxidized DIPEA finally provides the desired indoline **8**. Evidently, the possibility of a final proton transfer from the solvent was excluded by carrying out reactions in deuterated solvents (e.g. MeCN-d^3 and DMF-d^7), for which no deuterium incorporated product was observed, pointing towards the important role of the DIPEA besides initiating the reductive quenching cycle.[22]

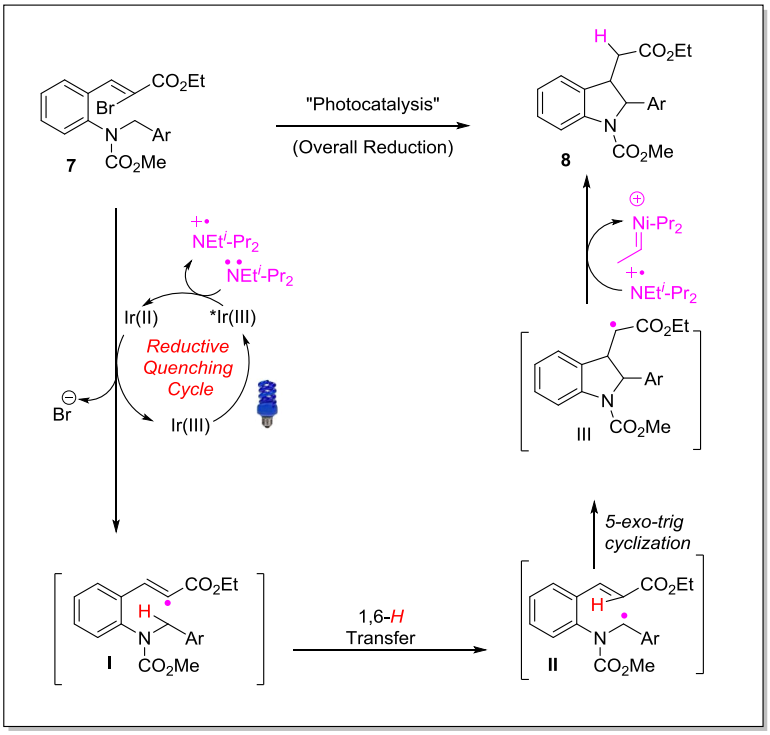

Figure 5.2: Proposed reaction mechanism.

5.7 Applications:

Next, we intended for the manipulation of **8** to show the applications of the title transformation (Scheme 5.3). A facile oxidation of indolines **8a** and **8b** to corresponding 2,3-disubstituted indoles took place with DDQ in toluene under microwave irradiation at 120 ^{o}C.[11] The resulting product was directly subjected to the carbamate deprotection with Bu_4NF, which provided **9a** and **9b** in 60-63 % yields (over two steps),[23] which also completed the formal synthesis of the desired drug candidates **3** and **11**.[5,8] In addition, **9a** was reduced with $LiAlH_4$ to form **10**,[24] which is a valuable intermediate for the synthesis of a number of other biologically active molecules, e.g. tryptamine **2**[25] and furoindolines **12**.[26]

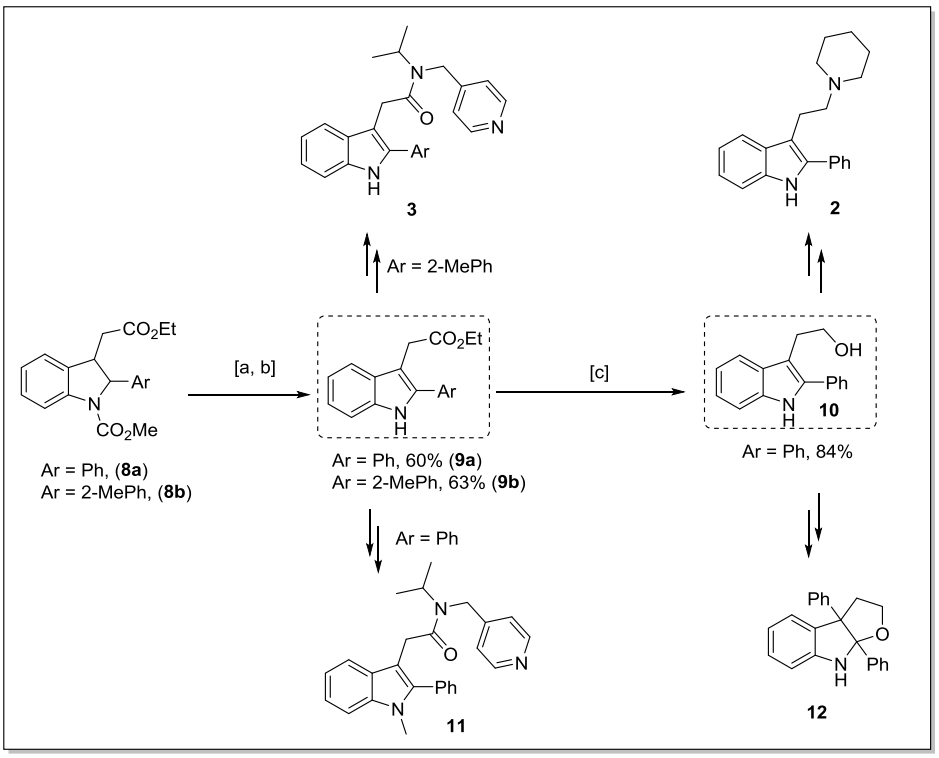

Scheme 5.3: Reaction conditions: [a] **8a** or **8b** (2.0 mmol), DDQ (4.0 mmol), toluene (15 mL), microwave irradiation, 120 ^{o}C, 10 h; then, [b] Bu_4NF (10 mmol), THF (20 mL), rt, 24 h. [c] **9a** (0.716 mmol), $LiAlH_4$ (1.04 mmol), anhydrous THF (4 mL), rt, 10 h.

5.8 Conclusions:

In summary, we have successfully utilized visible-light mediated reductive quenching activation mode for the C-C bond formations with vinyl bromides. By using this method, 2,3-disubstituted indole derivatives was efficiently synthesized from readily accessed *ortho*-amino α-bromocinnamates. Notably, the reaction was also proceeded efficiently even with the very low (0.3 mol %) catalyst loading. Thus, this method certainly opens a new door in replacing the previously reported procedure that required super-stoichiometric amounts of toxic reagents. Furthermore, the resulting 2,3-indolines could be efficiently converted to the biologically active indole derivatives.

5.9 Experimental section:

5.9.1 Synthesis of starting material precursor:[11]

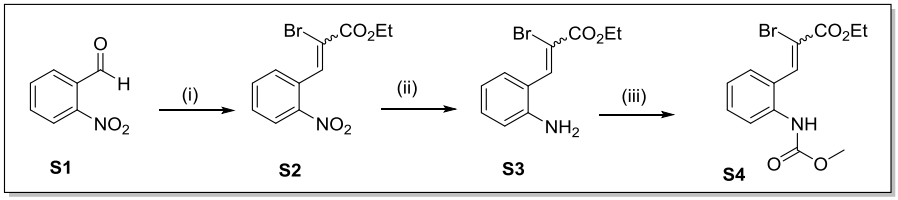

Reagents and conditions: (i) KO^{t}Bu (1.5 equiv), triethyl-α-bromophosphonoacetate (1.5 equiv), THF, 0 °C - rt, 3 h, 94% (**S2**); (ii) Fe-powder (3.5 equiv), EtOH/HCl, reflux, 3 h, 83% (S**3**); (iii) Methyl chloroformate (1.5 equiv), ^{i}Pr$_2$Et (3.0 equiv), CH_2Cl_2, 0 °C - rt, 12 h, 87% (**S4**).

Ethyl 2-bromo-3-(2-nitrophenyl)acrylate (S2):

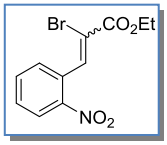

Potassium *tert*-butoxide (22.28 g, 198.5 mmol, 1.50 equiv) was slowly added to triethyl-α-bromophosphonoacetate (60.30 g, 198.5 mmol, 1.50 equiv) in anhydrous THF (250 mL) under positive nitrogen atmosphere at 0 ^{o}C. The resulting mixture allowed to stir for 1 h, followed by slow addition of 2-nitrobenzaldehyde **S1** (20.00 g, 132.3 mmol, 1.00 equiv) to the reaction mixture, resulting mixture stirred further for 2 h at 0 ^{o}C under inert atmosphere. The progress of the reaction was monitored by TLC analysis (staining with 2, 4-DNP / $KMnO_4$); after complete consumption of the starting material, reaction was quenched by adding saturated ammonium chloride solution (100 mL), and extracted with ethyl acetate (3 x 150 mL). Combined organic phases were washed with brine (100 mL), dried over anhydrous Na_2SO_4, and concentrated *in vacuo*. Purification of the crude product by column chromatography (silica gel, hexanes–EtOAc, 4:1, R_f = 0.49) afforded **2a** as a yellow solid (37.33 g, 94% yield).

^{1}H-NMR (300 MHz, $CDCl_3$): δ = 8.46 (s, 1H), 8.19 (dd, *J* = 8.2, 1.0 Hz, 1H), 7.75 – 7.68 (m, 1H), 7.65 – 7.54 (m, 2H), 4.36 (q, *J* = 7.1 Hz, 2H), 1.38 (t, *J* = 7.1 Hz, 3H).

^{13}C-NMR (75 MHz, $CDCl_3$): δ = 162.3, 146.9, 139.2, 133.7, 131.2, 130.9, 129.9, 124.8, 117.3, 63.1, 14.1.

The obtained data is in accordance with the literature data.[11]

Ethyl 3-(2-aminophenyl)-2-bromoacrylate (S3):

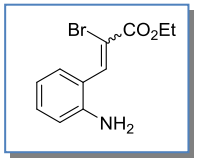

Ethyl 2-bromo-3-(2-nitrophenyl)acrylate **S2** (35.00 g, 116.62 mmol, 1.00 equiv) was dissolved under reflux in EtOH (150 mL) in a three-necked-flask, which equipped with a cooling condensor and a dropping funnel. Then Fe-powder (22.80 g, 408.1 mmol, 3.5 equiv) and 37% aq. HCl (90 mL) were added by a dropping funnel over 2 h under reflux, and the resulting mixture was refluxed for an additional hour. The mixture was concentrated on a rotary evaporator. Saturated $NaHCO_3$ (200 mL) was then added to adjust the pH of the aqueous layer to 8, and then aqueous layer was extracted with CH_2Cl_2 (3 × 150 mL). The combined organic phases were dried over Na_2SO_4, filtered, and concentrated *in vacuo*. Purification of the crude product by column chromatography (silica gel, hexanes–EtOAc, 9:1, R_f = 0.60) afforded **S3** as a pale yellow solid (26.00 g, 83% yield).

^{1}H-NMR (300 MHz, $CDCl_3$): δ 8.16 (s, 1H), 7.73 – 7.57 (m, 1H), 7.23 – 7.16 (m, 1H), 6.81 (t, *J* = 7.6 Hz, 1H), 6.73 (dd, *J* = 8.1, 0.6 Hz, 1H), 4.34 (q, *J* = 7.1 Hz, 2H), 3.70 (bs, 1H), 1.38 (t, *J* = 7.1 Hz, 3H).

^{13}C-NMR (75 MHz, $CDCl_3$): δ 162.2, 143.9, 136.4, 129.9, 128.3, 118.8, 117.2, 115.0, 114.6, 61.8, 13.2.

The obtained data is in accordance with the literature data.[11]

Ethyl 2-bromo-3-(2-((methoxycarbonyl)amino)phenyl)acrylate (S4):

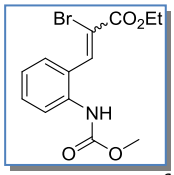

To a solution of **S4** (25.00 g, 92.93 mmol, 1.0 equiv) in CH_2Cl_2 (150 mL) was added ^{i}Pr$_2$Et (36.03 g, 278.81 mmol, 3 equiv) followed by methylchloroformate (13.17 g, 139.39 mmol, 1.5 equiv) a 0 ^{o}C. The mixture was then stirred at room temperature for 10 h, subsequently diluted with EtOAc (100 mL) and saturated NH_4Cl (100 mL). This mixture was additionally extracted with EtOAc (2 × 100 mL). And the combined organic phases were washed with brine (100 mL), dried over Na_2SO_4, filtered, and concentrated *in vacuo*. Purification of the crude product by column chromatography (silica gel, hexanes–EtOAc, 4:1, R_f = 0.60) afforded a pale yellow solid **S4** (26.50 g, 87% yield).

^{1}H-NMR (300 MHz, $CDCl_3$): δ 8.15 (s, 1H), 7.85 (d, *J* = 7.7 Hz, 1H), 7.56 (d, *J* = 7.7 Hz, 1H,), 7.39 (dt, *J* = 7.8, 1.3 Hz, 1H), 7.16 (dt, *J* = 7.6, 0.9 Hz, 1H,), 7.01 (d, *J* = 8.0 Hz, 1H), 6.23 (s, 1H), 4.39 (q, *J* = 7.1 Hz, 2H), 4.15 (s, 3H), 1.38 (t, *J* = 7.1 Hz, 3H,).

^{13}C-NMR (75 MHz, $CDCl_3$): δ 162.6, 154.1, 137.5, 135.5, 130.3, 129.0, 125.7, 123.9, 121.9, 118.4, 63.1, 52.6, 14.2.

The obtained data is in accordance with the literature data.[11]

5.9.2 General procedure (GP-1) for *N*-benzylation:

$ArCH_2Br$ (1.5 mmol, 1.5 equiv) was added to a solution of **S4** (0.328 g, 1.0 mmol, 1.0 equiv), K_2CO_3 (0.415 g, 3.0 mmol, 3.0 equiv) and tetrabutylammonium bromide (0.161 g, 0.5 mmol, 0.5 equiv) in MeCN (60 mL). The mixture was stirred at room temperature for a further 48 h. Then reaction mixture was diluted with EtOAc (50 mL), washed with brine solution (50 mL), and extracted with EtOAc (3 × 50 mL). The combined organic phases were dried over Na_2SO_4, filtered, and concentrated *in vacuo*. Purification of the crude product by column chromatography (silica gel, hexanes–EtOAc, 9:1) afforded **7**.

Ethyl 3-(2-(benzyl(methoxycarbonyl)amino)phenyl)-2-bromoacrylate (7a):

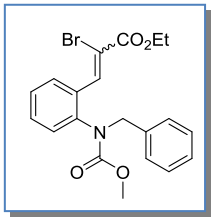

Following **GP-1**, **7a** was prepared from **S4** (5 g, 15.23 mmol, 1.00 equiv), benzyl bromide or (bromomethyl)benzene (3.90 g, 22.85 mmol, 1.5 equiv), K_2CO_3 (6.30 g, 45.69 mmol, 3.00 equiv), and tetrabutylammonium bromide (2.45 g, 7.61 mmol, 0.5 equiv) in MeCN (150 mL). Purification of the crude product by column chromatography (silica gel, hexanes–EtOAc, 9:1, R_f = 0.43) afforded **7a** as a pale yellow oil (5.90 g, *Z:E* = 99:01, 93% yield).

^{1}H-NMR (300 MHz, $CDCl_3$, *Z*-isomer): δ 7.79 (d, *J* = 5.4 Hz, 1H), 7.70 (s, 1H), 7.40 – 7.29 (m, 2H), 7.27 – 7.21 (m, 3H), 7.20 (s, 2H), 7.09 – 7.02 (m, 1H), 4.75 (s, 2H), 4.30 (q, *J* = 7.1 Hz, 2H), 3.63 (s, 3H), 1.36 (t, *J* = 7.1 Hz, 3H).

^{13}C-NMR (75 MHz, $CDCl_3$, *Z*-isomer): δ 162.68, 155.98, 140.41, 138.29, 136.85, 133.18, 130.41, 129.94, 129.08, 128.50, 128.27, 127.82, 127.23, 116.34, 62.80, 54.59, 53.25, 14.21.

The obtained data is in accordance with the literature data.[11]

Ethyl 2-bromo-3-(2-((methoxycarbonyl)(2-methylbenzyl)amino)phenyl)acrylate (7b):

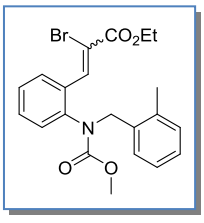

Following **GP-1**, **7b** was prepared from **S4** (5.00 g, 15.23 mmol, 1.00 equiv), 2-Methylbenzyl bromide (4.23 g, 22.85 mmol, 1.5 equiv), K_2CO_3 (6.30 g, 45.69 mmol, 3.00 equiv), and tetrabutylammonium bromide (2.45 g, 7.61 mmol, 0.5 equiv) in MeCN (150 mL). Purification of the crude product by column chromatography (silica gel, hexanes–EtOAc, 9:1, R_f = 0.51) afforded **7b** as a pale yellow solid (6.19 g, *Z:E* = 89:11, 94% yield).

^{1}H-NMR (300 MHz, $CDCl_3$, *Z*-isomer): δ 7.76 (d, *J* = 6.5 Hz, 1H), 7.68 (s, 1H), 7.38 – 7.26 (m, 2H), 7.15 – 6.97 (m, 5H), 5.05 – 4.70 (m, 2H), 4.30 (q, *J* = 7.1 Hz, 2H), 3.63 (s, 3H), 2.14 (s, 3H), 1.36 (t, *J* = 7.1 Hz, 3H).

^{13}C-NMR (75 MHz, $CDCl_3$, *Z*-isomer): δ 162.66, 155.82, 140.24, 138.09, 136.78, 134.57, 133.48, 130.46, 130.40, 129.84, 128.25, 127.99, 127.26, 125.99, 116.16, 62.77, 53.27, 51.60, 19.19, 14.24.

IR (neat, cm^{-1}): 2981, 2951, 1700, 1598, 1569, 1480, 1453, 1438, 1373, 1289, 1265, 1185, 1126, 1101, 1035, 1011, 977, 910, 893, 866, 781, 756, 736, 663.

HRMS (ESI): exact m/z calculated for $C_{21}H_{23}BrNO_4$ $(M+H)^+$: 432.0805; Found: 432.081 $(M+H)^+$.

Mp: 64-66 ^oC (decomposed).

Ethyl 2-bromo-3-(2-((3,5-dimethylbenzyl)(methoxycarbonyl)amino)phenyl)acrylate (7c):

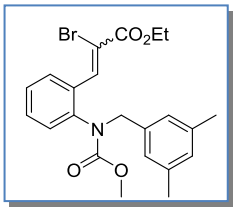

Following **GP-1**, **7c** was prepared from **S4** (0.328 g, 1.0 mmol, 1.00 equiv), 1-(bromomethyl)-3,5-dimethylbenzene (0.298 g, 1.5 mmol, 1.5 equiv), K_2CO_3 (0.415 g, 3.0 mmol, 3.00 equiv), and tetrabutylammonium bromide (0.161 g, 0.5 mmol, 0.5 equiv) in MeCN (60 mL). Purification of the crude product by column chromatography (silica gel, hexanes–EtOAc, 9:1, R_f = 0.46) afforded **7c** as a pale yellow syrup (0.405 g, *Z:E* = 82:18, 91% yield).

^{1}H-NMR (300 MHz, $CDCl_3$, *Z*-isomer): δ 7.78 (s, 2H), 7.33 (m, 2H), 7.08 (d, *J* = 7.2 Hz, 1H), 6.85 (s, 1H), 6.78 (s, 2H), 4.79 – 4.62 (m, 2H), 4.29 (q, *J* = 7.1, 2H), 3.62 (s, 3H), 2.22 (s, 6H), 1.35 (t, *J* = 7.1 Hz, 3H).

^{13}C-NMR (75 MHz, $CDCl_3$, *Z*-isomer): δ 171.09, 162.64, 155.94, 140.62, 138.29, 137.93, 136.72, 133.18, 130.39, 129.87, 129.43, 128.28, 127.14, 126.79, 115.88, 62.73, 54.54, 53.17, 21.24, 14.18.

IR (neat, cm^{-1}): 2984, 2953, 1700, 1599, 1485, 1443, 1376, 1288, 1249, 1215, 1136, 1106, 1021, 991, 849, 761, 715.

HRMS (ESI): exact m/z calculated for $C_{22}H_{25}BrNO_4$ $(M+H)^+$: 446.0961; Found: 446.0968 $(M+H)^+$.

Ethyl 2-bromo-3-(2-((methoxycarbonyl)(4-methylbenzyl)amino)phenyl)acrylate (7d):

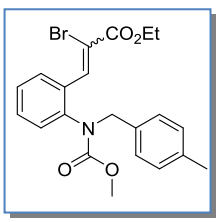

Following **GP-1**, **7d** was prepared from **S4** (0.328 g, 1.0 mmol, 1.00 equiv), 1-(bromomethyl)-4-methylbenzene (0.278 g, 1.5 mmol, 1.5 equiv), K_2CO_3 (0.415 g, 3.0 mmol, 3.00 equiv), and tetrabutylammonium bromide (0.161 g, 0.5 mmol, 0.5 equiv) in MeCN (60 mL). Purification of the crude product by column chromatography (silica gel, hexanes–EtOAc, 9:1, R_f = 0.40) afforded **7d** as a colourless viscous oil (0.396 g, *Z:E* = 99:01, 92% yield).

^{1}H-NMR (300 MHz, $CDCl_3$, *Z*-isomer): δ 7.77 (d, *J* = 10.5 Hz, 1H), 7.69 (s, 1H), 7.41 – 7.29 (m, 2H), 7.04 (s, 4H), 4.72 (m, 2H), 4.29 (q, *J* = 7.1, 2H), 3.62 (s, 3H), 2.29 (s, 3H), 1.36 (t, *J* = 7.1, 3H).

^{13}C-NMR (75 MHz, $CDCl_3$, *Z*-isomer): δ 162.66, 155.93, 140.46, 138.29, 137.46, 133.80, 133.23, 130.42, 129.90, 129.17, 129.04, 128.31, 127.18, 116.18, 62.75, 54.31, 53.20, 21.17, 14.20.

IR (neat, cm^{-1}): 2983, 2953, 1702, 1617, 1598, 1514, 1482, 1443, 1376, 1317, 1292, 1234, 1215, 1188, 1134, 1102, 1036, 990, 902, 844, 711, 761, 660.

HRMS (ESI): exact m/z calculated for $C_{21}H_{23}BrNO_4$ $(M+H)^+$: 432.0805; Found: 432.0811 $(M+H)^+$.

Ethyl 2-bromo-3-(2-((4-(tert-butyl)benzyl)(methoxycarbonyl)amino)phenyl)acrylate (7e):

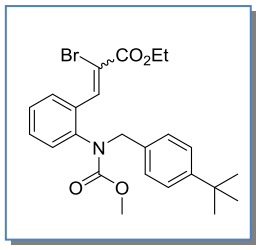

Following **GP-1**, **7e** was prepared from **S4** (0.328 g, 1.0 mmol, 1.00 equiv), 1-(bromomethyl)-4-(tert-butyl)benzene (0.340 g, 1.5 mmol, 1.5 equiv), K_2CO_3 (0.415 g, 3.0 mmol, 3.00 equiv), and tetrabutylammonium bromide (0.161 g, 0.5 mmol, 0.5 equiv) in MeCN (60 mL). Purification of the crude product by column chromatography (silica gel, hexanes–EtOAc, 9:1, R_f = 0.43) afforded **7e** as a colourless viscous oil (0.427 g, *Z:E* = 99:01, 90% yield).

^{1}H-NMR (300 MHz, $CDCl_3$, *Z*-isomer): δ 7.86 – 7.75 (m, 2H), 7.42 – 7.32 (m, 2H), 7.31 – 7.22 (m, 3H), 7.14 (m, 2H), 4.72 (s, 2H), 4.30 (q, *J* = 7.1Hz, 2H), 3.63 (s, 3H), 1.37 (t, *J* = 7.1Hz, 3H), 1.28 (s, 9H).

^{13}C-NMR (75 MHz, $CDCl_3$, *Z*-isomer): δ 162.65, 155.93, 150.62, 140.63, 138.24, 133.75, 133.16, 130.43, 129.88, 128.75, 128.34, 127.18, 126.90, 125.33, 116.16, 62.75, 54.28, 53.20, 34.50, 31.32, 14.23.

IR (neat, cm^{-1}): 2956, 2906, 2868, 1704, 1617, 1598, 1481, 1444, 1377, 1318, 1293, 1232, 1189, 1135, 1104, 1038, 983, 904, 850, 760, 671, 657.

HRMS (ESI): exact m/z calculated for $C_{24}H_{29}BrNO_4$ $(M+H)^+$: 474.1274; Found: 474.1282 $(M+H)^+$.

Ethyl 2-bromo-3-(2-((4-fluorobenzyl)(methoxycarbonyl)amino)phenyl)acrylate (7f):

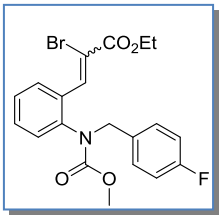

Following **GP-1**, **7f** was prepared from **S4** (0.328 g, 1.0 mmol, 1.00 equiv), 1-(bromomethyl)-4-fluorobenzene (0.284 g, 1.5 mmol, 1.5 equiv), K_2CO_3 (0.415 g, 3.0 mmol, 3.00 equiv), and tetrabutylammonium bromide (0.161 g,

0.5 mmol, 0.5 equiv) in MeCN (60 mL). Purification of the crude product by column chromatography (silica gel, hexanes–EtOAc, 9:1, R_f = 0.52) afforde **7f** as a colourless viscous oil (0.384 g, *Z:E* = 99:01, 88% yield).

^{1}H-NMR (300 MHz, $CDCl_3$, *Z*-isomer): δ 7.77 (d, *J* = 6.0 Hz, 1H), 7.67 (s, 1H), 7.38 – 7.27 (m, 2H), 7.20 – 7.08 (m, 2H), 7.05 – 6.99 (m, 1H), 6.94 – 6.85 (m, 2H), 4.83 – 4.57 (m, 1H), 4.26 (q, *J* = 7.1Hz, 2H), 3.59 (s, 3H), 1.32 (t, *J* = 7.1Hz, 3H).

^{13}C-NMR (75 MHz, $CDCl_3$, *Z*-isomer): δ 163.98, 162.58, 160.71, 155.92, 140.25, 138.13, 134.16, 133.14, 132.77 (d, *J* = 3.2 Hz), 130.87 (d, *J* = 8.1 Hz), 130.48, 130.01, 128.33, 62.81, 53.81, 53.24, 14.14.

^{19}F-NMR (282 MHz, $CDCl_3$, *Z*-isomer: δ -114.76, ***E*-isomer:** δ -115.25).

IR (neat, cm^{-1}): 2983, 2954, 1702, 1602, 1509, 1482, 1445, 1376, 1215, 1189, 1157, 1135, 1095, 1035, 1016, 983, 902, 839, 756, 656.

HRMS (ESI): exact m/z calculated for $C_{20}H_{20}BrFNO_4$ $(M+H)^+$: 436.0554; Found: 436.0562 $(M+H)^+$.

Ethyl 2-bromo-3-(2-((methoxycarbonyl)(4-(trifluoromethyl)benzyl)amino)phenyl)acrylate (7g):

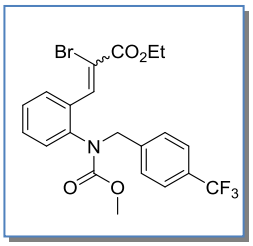

Following **GP-1**, **7g** was prepared from **S4** (0.328 g, 1.0 mmol, 1.00 equiv), 1-(bromomethyl)-4-(trifluoromethyl)benzene (0.359 g, 1.5 mmol, 1.5 equiv), K_2CO_3 (0.415 g, 3.0 mmol, 3.00 equiv), and tetrabutylammonium bromide (0.161 g, 0.5 mmol, 0.5 equiv) in MeCN (60 mL). Purification of the crude product by column chromatography (silica gel, hexanes–EtOAc, 9:1, R_f = 0.33) afforded **7g** as a pale yellow viscous oil (0.418 g, *Z:E* = 95:05, 86% yield).

^{1}H-NMR (300 MHz, $CDCl_3$, *Z*-isomer): δ 7.81 – 7.72 (m, 2H), 7.49 (d, *J* = 8.1 Hz, 2H), 7.40 – 7.27 (m, 4H), 7.05 (d, *J* = 6.6 Hz, 1H), 4.77 (s, 2H), 4.27 (q, *J* = 7.1 Hz, 2H), 3.62 (s, 3H), 1.32 (t, *J* = 7.1 Hz, 3H).

^{13}C-NMR (75 MHz, $CDCl_3$, *Z*-isomer): δ 162.48, 155.98, 140.91, 140.24, 137.97, 133.03, 130.55, 130.11, 129.71, 129.32, 128.19, 127.48, 125.43 (q, *J* = 3.7 Hz), 124.05 (q, *J* = 272.07 Hz), 122.25, 116.61, 62.84, 54.15, 53.35, 14.06.

^{19}F-NMR (282 MHz, $CDCl_3$, *Z*-isomer): δ -63.03.

IR (neat, cm^{-1}): 2956, 1704, 1619, 1598, 1483, 1446, 1421, 1378, 1322, 1301, 1253, 1236, 1190, 1161, 1111, 1064, 1037, 1018, 985, 906, 852, 820, 760, 660.

HRMS (ESI): exact m/z calculated for $C_{21}H_{20}BrF_3NO_4$ $(M+H)^+$: 486.0522; Found: 486.0528 $(M+H)^+$.

Ethyl 2-bromo-3-(2-((methoxycarbonyl)(4-(methylthio)benzyl)amino)phenyl)acrylate (7h):

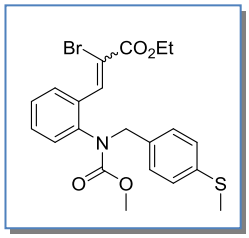

Following **GP-1**, **7h** was prepared from **S4** (0.328 g, 1.0 mmol, 1.00 equiv), (4-(bromomethyl)phenyl)(methyl)sulfane (0.326 g, 1.5 mmol, 1.5 equiv), K_2CO_3 (0.415 g, 3.0 mmol, 3.00 equiv), and tetrabutylammonium bromide (0.161 g, 0.5 mmol, 0.5 equiv) in MeCN (60 mL). Purification of the crude product by column chromatography (silica gel, hexanes–EtOAc, 9:1, R_f = 0.49) afforded **7h** as a pale yellow viscous oil (0.441 g, *Z:E* = 91:09, 95% yield).

^{1}H-NMR (300 MHz, $CDCl_3$, *Z*-isomer): δ 7.79 (d, *J* = 5.9 Hz, 1H), 7.71 (s, 1H), 7.41 – 7.28 (m, 2H), 7.18 – 6.99 (m, 5H), 4.81 – 4.59 (m, 2H), 4.28 (q, *J* = 7.1 Hz, 2H), 3.61 (s, 3H), 2.43 (s, 3H), 1.35 (t, *J* = 7.1 Hz, 3H).

^{13}C-NMR (75 MHz, $CDCl_3$, *Z*-isomer): δ 162.60, 155.94, 140.38, 138.21, 138.09, 133.56, 133.14, 130.46, 129.98, 129.62, 128.35, 127.60, 127.28, 126.76, 126.40, 116.34, 62.83, 54.13, 53.24, 14.20.

IR (neat, cm^{-1}): 2982, 2952, 2922, 1701, 1618, 1597, 1570, 1482, 1442, 1376, 1234, 1215, 1188, 1135, 1092, 1035, 1016, 983, 840, 804, 759, 656.

HRMS (ESI): exact m/z calculated for $C_{21}H_{23}BrNO_4S$ $(M+H)^+$: 464.0526; Found: 464.0536 $(M+H)^+$.

Ethyl 2-bromo-3-(2-((2-bromobenzyl)(methoxycarbonyl)amino)phenyl)acrylate (7i):

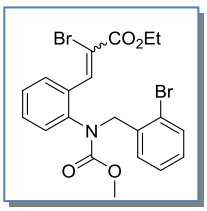

Following **GP-1**, **7i** was prepared from **S4** (0.328 g, 1.0 mmol, 1.00 equiv), 1-bromo-2-(bromomethyl)benzene (0.375 g, 1.5 mmol, 1.5 equiv), K_2CO_3 (0.415 g, 3.0 mmol, 3.00 equiv), and tetrabutylammonium bromide (0.161 g, 0.5 mmol, 0.5 equiv) in MeCN (60 mL). Purification of the crude product by column chromatography (silica gel, hexanes–EtOAc, 9:1, R_f = 0.31) afforded **7i** as a pale yellow solid (0.462 g, *Z:E* = 99:01, 93% yield).

^{1}H-NMR (300 MHz, $CDCl_3$, *Z*-isomer): δ 7.90 (d, *J* = 10.5 Hz, 1H), 7.88 – 7.75 (m, 1H), 7.48 (d, *J* = 7.9 Hz, 1H), 7.40 – 7.32 (m, 3H), 7.24 (t, *J* = 7.1 Hz, 1H), 7.19 – 7.07 (m, 2H), 4.99 (s, 2H), 4.35 (q, *J* = 7.1 Hz, 2H), 3.79 (s, 3H), 1.40 (t, *J* = 7.1 Hz, 3H).

^{13}C-NMR (75 MHz, $CDCl_3$, *Z*-isomer): δ 162.73, 155.92, 140.09, 138.07, 136.03, 133.17, 132.93, 131.27, 130.41, 129.89, 129.37, 128.20, 127.55, 127.32, 124.19, 116.30, 62.83, 53.68, 53.40, 14.25.

IR (neat, cm^{-1}): 2976, 2952, 1707, 1614, 1596, 1569, 1440, 1378, 1297, 1250, 1213, 1189, 1140, 1105, 1026, 983, 896, 875, 782, 752, 653.

HRMS (ESI): exact m/z calculated for $C_{20}H_{20}Br_2NO_4$ $(M+H)^+$: 495.9754; Found: 495.9756 $(M+H)^+$.

Mp: 58-60 ^oC (decomposed).

Ethyl 2-bromo-3-(2-((3-chlorobenzyl)(methoxycarbonyl)amino)phenyl)acrylate (7j):

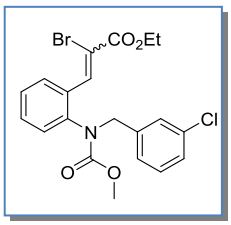

Following **GP-1**, **7j** was prepared from **S4** (0.328 g, 1.0 mmol, 1.00 equiv), 1-(bromomethyl)-3-chlorobenzene (0.308 g, 1.5 mmol, 1.5 equiv), K_2CO_3 (0.415 g, 3.0 mmol, 3.00 equiv), and tetrabutylammonium bromide (0.161 g, 0.5 mmol, 0.5 equiv) in MeCN (60 mL). Purification of the crude product by column chromatography (silica gel, hexanes–EtOAc, 9:1, R_f = 0.36) afforded **7j** as a pale yellow oil (0.402 g, *Z:E* = 99:01, 89% yield).

^{1}H-NMR (300 MHz, $CDCl_3$, *Z*-isomer): δ 7.73 (d, *J* = 6.7 Hz, 1H), 7.69 (s, 1H), 7.36 – 7.23 (m, 2H), 7.20 – 7.05 (m, 3H), 6.99 (m, 2H), 4.65 (m, 1H), 4.24 (q, *J* = 7.1 Hz, 2H), 3.56 (s, 3H), 1.29 (t, *J* = 7.1 Hz, 1H).

^{13}C-NMR (75 MHz, $CDCl_3$, *Z*-isomer): δ 162.50, 155.90, 140.21, 138.88, 137.95, 134.27, 133.05, 130.55, 130.03, 129.79, 129.04, 128.21, 128.04, 127.43, 127.19, 116.46, 62.86, 54.07, 53.32, 14.19.

The obtained data is in accordance with the literature data.[11]

Ethyl 2-bromo-3-(2-((methoxycarbonyl)(4-nitrobenzyl)amino)phenyl)acrylate (7k):

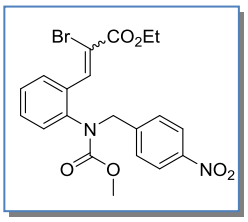

Following **GP-1**, **7k** was prepared from **S4** (0.209 g, 0.5 mmol, 1.00 equiv), 1-(bromomethyl)-4-nitrobenzene (0.324 g, 1.5 mmol, 1.5 equiv), K_2CO_3 (0.415 g, 3.0 mmol, 3.00 equiv), and tetrabutylammonium bromide (0.161 g, 0.5 mmol, 0.5 equiv) in MeCN (60 mL). Purification of the crude product by column chromatography (silica gel, hexanes–EtOAc, 9:1, R_f = 0.32) afforded **7k** as a pale yellow oil (0.407 g, *Z:E* = 99:01, 88% yield).

^{1}H-NMR (300 MHz, $CDCl_3$, *Z*-isomer): δ 8.07 (d, *J* = 8.7 Hz, 2H), 7.74 (d, *J* = 7.4 Hz, 2H), 7.42 – 7.28 (m, 4H), 7.05 (d, *J* = 6.8 Hz, 1H), 4.79 (s, 2H), 4.26 (q, *J* = 7.1 Hz, 2H), 3.62 (s, 3H), 1.32 (t, *J* = 7.1 Hz, 3H).

^{13}C-NMR (75 MHz, $CDCl_3$, *Z*-isomer): δ 162.45, 155.99, 147.45, 144.24, 140.04, 137.89, 132.94, 130.66, 130.21, 129.82, 128.21, 127.68, 123.74, 116.65, 62.98, 53.93, 53.51, 14.12.

The obtained data is in accordance with the literature data.[11]

5.9.3 Reduction potentials:

Redox potentials of the α-bromocinnamates were measured by cyclic voltammetry in acetonitrile (MeCN) containing tetrabutylammonium tetrafluoroborate (0.1 M) as a supporting electrolyte. All values are given vs. Saturated Calomel Electrode (SCE). The scan rate was 50 mV S^{-1}.

α-Bromocinnamates	**Reduction potential (V)**
7a	-1.50
7b	-1.48
7c	-1.47
7d	-1.51
7e	-1.52
7f	-1.51
7g	-1.50
7h	-1.48
7i	-1.45
7j	-1.50
7k	-1.19

Table 5.3: Reduction potentials of the α-bromocinnamate ethyl esters vs SCE.

5.9.4. General procedure (GP-2) for photocatalysis:

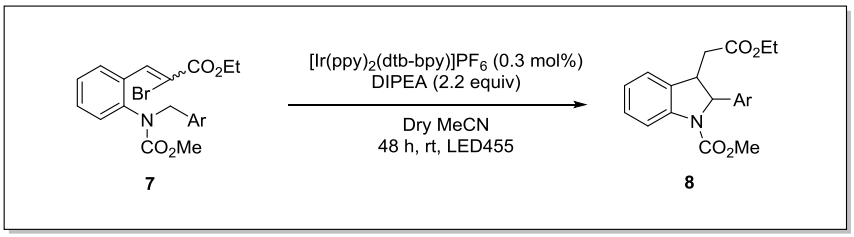

An oven dried 10 mL schlenk flask was charged with **7** (0.50 mmol, 1.00 equiv) and $[Ir(ppy)_2(dtb\text{-}bpy)]PF_6$ (1.37 mg, 0.003 equiv, 0.3 mol %) in anhydrous MeCN (2.0 mL). Then, anhydrous DIPEA (0.191 mL, 1.1 mmol, 2.2 equiv) was added and the resulting suspension was deoxygenated by three freeze-pump-thaw cycles. The resulting reaction mixture was irradiated with blue light emitting diode (LED, λ_{max} = 455 nm) at room temperature for 48 h. After completion of reaction mixture, the crude mixture was filtered and washed with ethyl acetate. The crude residue was concentrated *in vacuo*. Purification of the crude product by column chromatography on silica gel by using hexanes and ethyl acetate afforded the pure product **8**.

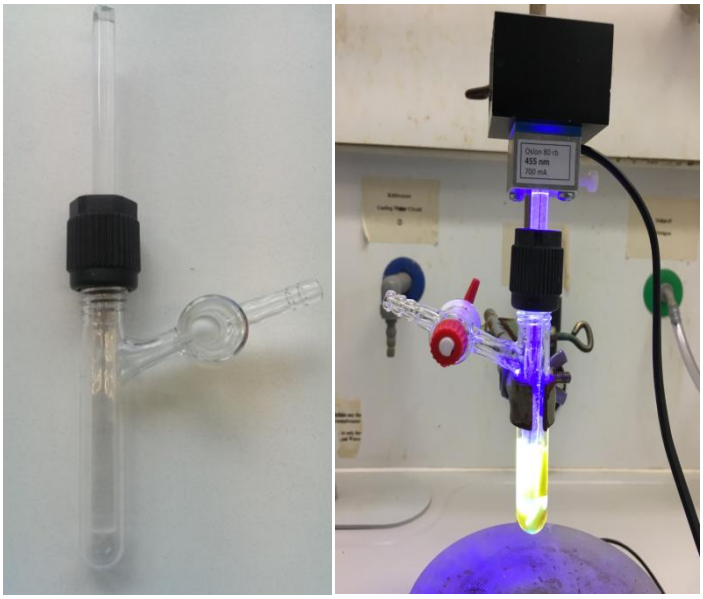

Figure 5.3: Experimental set-up for photochemical reaction.

Methyl 3-(2-ethoxy-2-oxoethyl)-2-phenylindoline-1-carboxylate (8a):

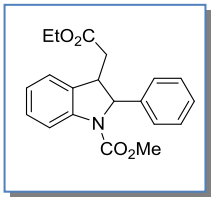

Following **GP-2**, **8a** was prepared from **7a** (1.254 g, 3.0 mmol, 1.00 equiv), $[Ir(ppy)_2(dtb\text{-}bpy)]PF_6$ (8.22 mg, 0.003 equiv, 0.3 mol %) and DIPEA (1.146 mL, 1.1 mmol, 2.2 equiv) in MeCN (10 mL). Purification of the crude product by column chromatography (silica gel, hexanes–EtOAc, 9:1, R_f = 0.46) afforded **8a** as a white solid (0.773 g, *cis / trans* = 78:22, 75% yield).

^{1}H-NMR (300 MHz, $CDCl_3$, *cis* isomer): δ 7.87 (s, 1H), 7.37 – 7.09 (m, 4H), 7.05 – 6.85 (m, 4H), 5.58 (d, *J* = 9.6 Hz, 1H), 4.23 (td, *J* = 10.0, 4.9 Hz, 1H), 4.09 – 3.99 (dq, *J* = 7.2 Hz, 2H), 3.63 (s, 3H), 2.70 – 2.49 (m, 1H), 1.97 (dd, *J* = 17.4, 10.2 Hz, 1H), 1.16 (t, *J* = 7.1 Hz, 3H).

^{1}H-NMR (300 MHz, $CDCl_3$, *trans* isomer): δ 7.29 – 7.07 (m, 5H), 7.03 – 6.92 (m, 4H), 5.17 (s, 1H), 4.23 (ddd, *J* = 12.1, 8.5, 3.5 Hz, 1H), 4.19 – 4.10 (m, 1H), 4.04 (dq, *J* = 7.1 Hz, 2H), 2.56 (d, *J* = 4.9 Hz, 1H), 1.97 (dd, *J* = 17.4, 10.2 Hz, 1H), 1.21 (t, *J* = 7.2 Hz, 3H).

^{13}C-NMR (75 MHz, $CDCl_3$, *cis* isomer): δ 172.23, 153.51, 138.26, 128.63, 128.39, 127.92, 127.46, 126.93, 125.29, 123.42, 123.11, 114.56, 66.40, 60.67, 52.65, 41.18, 34.20, 14.16.

^{13}C-NMR (75 MHz, $CDCl_3$, *trans* isomer): δ 171.53, 147.41, 141.00, 128.34, 138.21, 130.62, 128.53, 128.34, 128.12, 127.46, 127.00, 125.29, 115.02, 60.84, 52.71, 41.00, 33.97, 14.24.

The obtained data is in accordance with the literature data.[11]

Methyl 3-(2-ethoxy-2-oxoethyl)-2-(o-tolyl)indoline-1-carboxylate (8b):

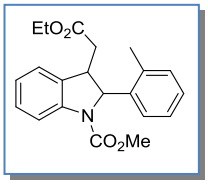

Following **GP-2**, **8b** was prepared from **7b** (1.296 g, 3.0 mmol, 1.00 equiv), $[Ir(ppy)_2(dtb\text{-}bpy)]PF_6$ (8.22 mg, 0.003 equiv, 0.3 mol %) and DIPEA (1.146 mL, 1.1 mmol, 2.2 equiv) in MeCN (10 mL). Purification of the crude product by column chromatography (silica gel, hexanes–EtOAc, 9:1, R_f = 0.48) afforded **8b** as a white solid (0.879 g, *cis / trans* = 55:45, 83% yield).

^{1}H-NMR (300 MHz, $CDCl_3$, *cis* isomer): δ 7.86 (bs, 1H), 7.35 – 7.23 (m, 3H), 7.01 (dt, *J* = 11.9, 5.8 Hz, 4H), 5.89 (d, *J* = 10.1 Hz, 1H), 4.37 (dt, *J* = 17.3, 8.6 Hz, 1H),, 4.01 (q, *J* = 7.1 Hz, 2H), 3.66 (s, 3H), 3.53 (td, *J* = 7.0, 1.9 Hz, 1H), 2.74 (qd, *J* = 15.4, 7.1 Hz, 1H), 2.45 (s, 3H), 1.13 (t, *J* = 7.2 Hz, 3H).

^{1}H-NMR (300 MHz, $CDCl_3$, *trans* isomer): δ 7.20 – 7.06 (m, 7H), 6.89 (dd, *J* = 14.8, 7.6 Hz, 2H), 5.41 (s, 1H), 4.13 (q, *J* = 7.1 Hz, 2H), 3.69 (s, 3H), 2.54 (dd, *J* = 17.1, 5.9 Hz, 1H), 2.46 (s, 3H), 2.25 – 2.12 (m, 1H), 1.31 – 1.25 (m, 1H), 1.20 (t, *J* = 7.1 Hz, 3H).

^{13}C-NMR (75 MHz, $CDCl_3$, *cis* isomer): δ 172.09, 153.48, 140.59, 136.84, 132.74, 130.63, 128.28, 127.75, 126.50, 126.23, 125.05, 124.21, 123.08, 114.61, 61.39, 60.60, 52.63, 41.57, 35.10, 19.49, 14.09.

^{13}C-NMR (75 MHz, $CDCl_3$, *trans* isomer): δ 171.26, 153.61, 142.95, 135.81, 134.44, 130.49, 128.69, 127.35, 125.97, 125.90, 123.68, 123.26, 122.86, 114.90, 65.06, 61.39, 52.72, 46.01, 40.42, 19.37, 14.16.

IR (neat, cm^{-1}): 2955, 1705, 1599, 1483, 1461, 1440, 1376, 1346, 1329, 1308, 1274, 1248, 1156, 1138, 1054, 1020, 746.

HRMS (ESI): exact m/z calculated for $C_{21}H_{24}NO_4$ $(M+H)^+$: 354.17; Found: 354.1708 $(M+H)^+$.
Mp: 51-53 ^oC (decomposed).

Methyl 2-(3,5-dimethylphenyl)-3-(2-ethoxy-2-oxoethyl)indoline-1-carboxylate (8c):

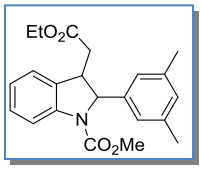

Following **GP-2**, **8c** was prepared from **7c** (0.223 g, 0.5 mmol, 1.00 equiv), $[Ir(ppy)_2(dtb\text{-}bpy)]PF_6$ (1.37 mg, 0.003 equiv, 0.3 mol %) and DIPEA (0.191 mL, 1.1 mmol, 2.2 equiv) in MeCN (1.5 mL). Purification of the crude product by column chromatography (silica gel, hexanes–EtOAc, 9:1, R_f = 0.53) afforded **8c** as a pale yellow solid (0.141 g, *cis* / *trans* = 71:29, 77% yield).

^{1}H-NMR (300 MHz, $CDCl_3$, *cis* isomer): δ 7.84 (bs, 1H), 7.35 – 7.22 (m, 2H), 7.08 – 6.96 (m, 2H), 6.87 (dd, *J* = 25.7, 9.0 Hz, 2H), 5.56 (d, *J* = 10.0 Hz, 1H), 4.19 (ddd, *J* = 9.5, 4.7, 1.5 Hz, 1H), 4.11 (qd, *J* = 7.2, 1.9 Hz, 2H), 3.69 (s, 3H), 2.71 – 2.62 (m, 1H), 2.19 (s, 6H), 2.09 – 1.97 (m, 1H), 1.25 – 1.19 (t, *J* = 7.2 Hz, 3H).
^{1}H-NMR (300 MHz, $CDCl_3$, *trans* isomer): δ 7.51 – 7.39 (m, 1H), 7.14 (d, *J* = 7.4 Hz, 2H), 6.60 (s, 4H), 5.18 (d, *J* = 1.9 Hz, 1H), 4.19 (q, *J* = 7.1 Hz, 2H), 3.98 (s, 3H), 3.55 (dd, *J* = 10.5, 4.0 Hz, 1H), 2.58 (d, *J* = 4.9 Hz, 1H), 2.27 (d, *J* = 6.8 Hz, 1H), 2.24 (s, 6H), 1.29 – 1.23 (m, 3H).
^{13}C-NMR (75 MHz, $CDCl_3$, *cis* isomer): δ 172.35, 153.58, 142.44, 138.10, 137.76, 129.63, 129.20, 128.55, 128.27, 124.55, 123.45, 123.26, 123.03, 114.56, 66.32, 60.63, 52.63, 41.26, 34.25, 21.35, 14.23.
^{13}C-NMR (75 MHz, $CDCl_3$, *trans* isomer): δ 171.42, 153.84, 143.04, 138.44, 138.20, 132.13, 131.23, 130.90, 128.16, 124.81, 124.43, 122.93, 122.74, 115.03, 68.07, 61.21, 60.38, 40.99, 29.74, 21.39, 18.90.
IR (neat, cm^{-1}): 2956, 2920, 1709, 1601, 1484, 1461, 1384, 1338, 1308, 1264, 1248, 1174, 1138, 1057, 1022, 850, 766, 750, 718, 679.
HRMS (ESI): exact m/z calculated for $C_{22}H_{26}NO_4$ $(M+H)^+$: 368.1856; Found: 368.1864 $(M+H)^+$.
Mp: 69-71 ^oC (decomposed).

Methyl 3-(2-ethoxy-2-oxoethyl)-2-(p-tolyl)indoline-1-carboxylate (8d):

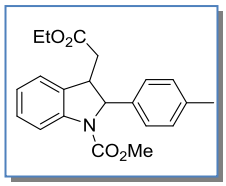

Following **GP-2**, **8d** was prepared from **7d** (0.216 g, 0.5 mmol, 1.00 equiv), $[Ir(ppy)_2(dtb\text{-}bpy)]PF_6$ (1.37 mg, 0.003 equiv, 0.3 mol %) and DIPEA (0.191 mL, 1.1 mmol, 2.2 equiv) in MeCN (1.5 mL). Purification of the crude product by column chromatography (silica gel, hexanes–EtOAc, 9:1, R_f = 0.33) afforded **8d** as a white solid (0.141 g, *cis / trans* = 92:08, 80% yield).

^{1}H-NMR (300 MHz, $CDCl_3$, *cis* isomer, major): δ 7.82 (bs, 1H), 7.30 – 7.19 (m, 1H), 7.01 – 6.91 (m, 4H), 6.83 (d, *J* = 8.0 Hz, 2H), 5.55 (d, *J* = 9.6 Hz, 1H), 4.19 (ddd, *J* = 14.3, 9.5, 6.1 Hz, 1H), 4.06 (q, *J* = 7.1 Hz, 2H), 3.63 (s, 3H), 2.59 (dt, *J* = 17.4, 4.1 Hz, 1H), 2.24 (s, 3H), 2.00 (dd, *J* = 17.4, 10.1 Hz, 1H), 1.16 (t, *J* = 7.1 Hz, 3H).

^{13}C-NMR (75 MHz, $CDCl_3$, *cis* isomer, major): δ 172.28, 153.54, 137.52, 135.19, 129.29, 129.07, 128.28, 126.82, 123.40, 123.04, 114.56, 66.23, 60.66, 52.65, 41.01, 34.19, 21.17, 14.17.

IR (neat, cm^{-1}): 2955, 2929, 1706, 1598, 1513, 1482, 1460, 1377, 1339, 1304, 1269, 1250, 1167, 1155, 1136, 1111, 1053, 1021, 999, 809, 766, 743.

HRMS (ESI): exact m/z calculated for $C_{21}H_{24}NO_4$ $(M+H)^+$: 354.17; Found: 354.1709 $(M+H)^+$.

Mp: 93-95 ^oC (decomposed).

Methyl 2-(4-(*tert*-butyl)phenyl)-3-(2-ethoxy-2-oxoethyl)indoline-1-carboxylate (8e):

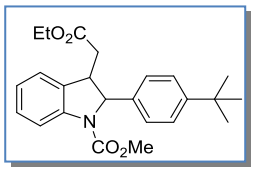

Following **GP-2**, **8e** was prepared from **7e** (0.236 g, 0.5 mmol, 1.00 equiv), $[Ir(ppy)_2(dtb\text{-}bpy)]PF_6$ (1.37 mg, 0.003 equiv, 0.3 mol %) and DIPEA (0.191 mL, 1.1 mmol, 2.2 equiv) in MeCN (1.5 mL). Purification of the crude product by column chromatography (silica gel, hexanes–EtOAc, 9:1, R_f = 0.84) afforded **8e** as a pale yellow solid (0.166 g, *cis / trans* = 73:27, 84% yield).

^{1}H-NMR (300 MHz, $CDCl_3$, *cis* isomer): δ 7.78 (bs, 1H), 7.30 – 7.12 (m, 3H), 7.03 – 6.91 (m, 2H), 6.86 (d, *J* = 8.3 Hz, 2H), 5.56 (d, *J* = 9.5 Hz, 1H), 4.27 – 4.12 (m, 1H), 4.12 – 3.98 (m, 2H), 3.64 (s, 3H), 2.74 – 2.48 (m, 1H), 2.01 (dd, *J* = 17.4, 10.0 Hz, 1H), 1.21 (s, 9H), 1.15 (t, *J* = 7.1 Hz, 3H).

^{1}H-NMR (300 MHz, $CDCl_3$, *trans* isomer): δ 7.16 (d, *J* = 8.4 Hz, 3H), 7.08 (dd, *J* = 7.4, 5.1 Hz, 3H), 6.98 – 6.92 (m, 2H), 5.16 (s, 1H), 4.27 – 4.12 (m, 1H), 4.12 – 3.98 (m, 2H), 3.64 (s, 3H), 3.54 – 3.44 (m, 1H), 2.74 – 2.48 (m, 1H), 1.25 (t, *J* = 7.1 Hz, 3H), 1.22 (s, *J* = 1.1 Hz, 9H).

^{13}C-NMR (75 MHz, $CDCl_3$, *cis* isomer): δ 172.33, 153.56, 150.63, 135.01, 128.25, 126.60,

125.49, 125.19, 123.37, 123.27, 123.03, 114.60, 66.19, 60.58, 52.64, 41.16, 34.47, 31.30, 29.73, 14.17.

^{13}C-NMR (75 MHz, $CDCl_3$, *trans* isomer): δ 171.56, 153.87, 150.17, 139.12, 132.19, 128.55, 126.25, 125.31, 125.27, 124.94, 123.27, 115.09, 67.92, 60.81, 52.73, 41.93, 34.15, 31.37, 29.73, 14.25.

IR (neat, cm^{-1}): 2958, 2868, 1708, 1600, 1512, 1483, 1440, 1380, 1267, 1159, 1138, 1055, 1019, 927, 832, 812, 764, 747.

HRMS (ESI): exact m/z calculated for $C_{24}H_{30}NO_4$ $(M+H)^+$: 396.2169; Found: 396.2179 $(M+H)^+$.

Mp: 43-45 °C (decomposed).

Methyl 3-(2-ethoxy-2-oxoethyl)-2-(4-fluorophenyl)indoline-1-carboxylate (8f):

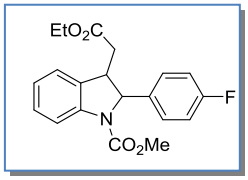

Following **GP-2**, **8f** was prepared from **7f** (0.218 g, 0.5 mmol, 1.00 equiv), $[Ir(ppy)_2(dtb\text{-}bpy)]PF_6$ (1.37 mg, 0.003 equiv, 0.3 mol %) and DIPEA (0.191 mL, 1.1 mmol, 2.2 equiv) in MeCN (1.5 mL). Purification of the crude product by column chromatography (silica gel, hexanes–EtOAc, 9:1, R_f = 0.49) afforded **8f** as a white solid (0.128 g, *cis / trans* = 73:27, 72% yield).

^{1}H-NMR (300 MHz, $CDCl_3$, *cis* isomer): δ 7.82 (bs, 1H), 7.25 (ddd, *J* = 6.2, 3.3, 1.2 Hz, 1H), 7.05 – 6.81 (m, 5H), 5.59 (d, *J* = 9.6 Hz, 1H), 4.26 – 4.19 (m, 1H), 4.04 (q, *J* = 7.1 Hz, 2H), 3.64 (s, 3H), 2.69 – 2.62 (m, 1H), 1.96 (dd, *J* = 17.5, 10.5 Hz, 1H), 1.16 (t, *J* = 7.1 Hz, 3H).

^{1}H-NMR (300 MHz, $CDCl_3$, *trans* isomer): δ 7.56 (s, 1H), 7.28 – 7.23 (m, 1H), 7.13 (dd, *J* = 13.6, 6.6 Hz, 1H), 7.05 – 6.81 (m, 5H), 5.15 (s, 1H), 4.15 (q, *J* = 7.1 Hz, 1H), 3.64 (s, 3H), 3.46 (t, *J* = 7.3 Hz, 1H), 2.61 (d, *J* = 4.7 Hz, 1H), 1.24 (m, 1H), 1.22 (t, *J* = 7.1 Hz, 3H).

^{19}F-NMR (282 MHz, $CDCl_3$): δ -114.71 (***cis***), -115.70 (***trans***).

^{13}C-NMR (75 MHz, $CDCl_3$, *cis* isomer): δ 172.11, 163.97, 160.71, 153.42, 134.15 (d, *J* = 3.63 Hz), 128.66 (d, *J* = 8.4 Hz), 128.45, 123.47, 123.23, 115.44, 115.16, 114.63, 65.73, 60.75, 52.70, 41.04, 34.11, 29.71, 14.16.

^{13}C-NMR (75 MHz, $CDCl_3$, *trans* isomer): δ 171.63, 163.97, 160.71, 153.42, 134.15 (d, *J* = 3.63 Hz), 131.65, 128.66 (d, *J* = 8.4 Hz), 127.03, 124.85, 115.60, 115.32, 115.08, 61.67, 60.88, 50.20, 40.90, 35.71, 29.67, 14.24.

IR (neat, cm^{-1}): 2956, 2930, 2855, 1705, 1602, 1509, 1483, 1441, 1378, 1309, 1269, 1220, 1176, 1158, 1096, 1054, 1019, 824, 748.

HRMS (ESI): exact m/z calculated for $C_{20}H_{21}FNO_4$ $(M+H)^+$: 358.1449; Found: 358.1458 $(M+H)^+$.

Mp: 46-48 ^oC (decomposed).

Methyl 3-(2-ethoxy-2-oxoethyl)-2-(4-(trifluoromethyl)phenyl)indoline-1-carboxylate (8g):

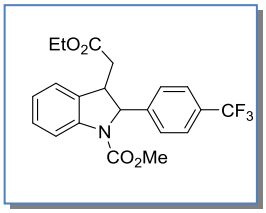

Following **GP-2**, **8g** was prepared from **7g** (0.243 g, 0.5 mmol, 1.00 equiv), $[Ir(ppy)_2(dtb\text{-}bpy)]PF_6$ (1.37 mg, 0.003 equiv, 0.3 mol %) and DIPEA (0.191 mL, 1.1 mmol, 2.2 equiv) in MeCN (1.5 mL). Purification of the crude product by column chromatography (silica gel, hexanes–EtOAc, 9:1, R_f = 0.37) afforded **8g** as a white solid (0.142 g, *cis / trans* = 77:23, 70% yield);

^{1}H-NMR (300 MHz, $CDCl_3$, *cis* isomer): δ 7.83 (bs, 1H), 7.46 (dd, *J* = 14.2, 8.1 Hz, 1H), 7.34 – 7.22 (m, 2H), 7.10 (d, *J* = 8.0 Hz, 2H), 7.06 – 6.95 (m, 2H), 5.66 (d, *J* = 9.7 Hz, 1H), 4.27 (td, *J* = 10.2, 4.7 Hz, 1H), 4.03 (q, *J* = 7.1 Hz, 2H), 3.64 (s, 3H), 2.69 – 2.58 (m, 1H), 2.00 – 1.85 (m, 1H), 1.15 (t, *J* = 7.1, Hz, 3H).

^{1}H-NMR (300 MHz, $CDCl_3$, *trans* isomer): δ 7.59 (s, 1H), 7.57 – 7.47 (m, 1H), 7.39 – 7.22 (m, 2H), 7.16 (d, *J* = 4.7 Hz, 2H), 7.02 – 6.96 (m, 2H), 5.24 (s, 1H), 4.16 (q, *J* = 7.1 Hz, 2H), 3.95 (s, 1H), 3.64 (s, 3H), 3.52 – 3.41 (m, 1H), 2.61 (d, *J* = 4.8 Hz, 1H), 1.23 (t, *J* = 7.1 Hz, 1H).

^{19}F-NMR (282 MHz, $CDCl_3$): δ -63.01 (***trans***), -63.09 (***cis***).

^{13}C-NMR (75 MHz, $CDCl_3$, *cis* isomer): δ 171.97, 153.33, 142.35, 130.34, 129.91, 128.61, 127.44, 125.38 (q, *J* = 3.8 Hz), 123.85 (q, *J* = 273.42 Hz), 123.63, 123.50, 123.40, 114.67, 65.91, 60.83, 52.81, 41.00, 34.17, 29.72, 14.07.

IR (neat, cm^{-1}): 2957, 2930, 2855, 1709, 1619, 1600, 1484, 1442, 1379, 1322, 1274, 1255, 1163, 1110, 1064, 1017, 839, 818, 748,664.

HRMS (ESI): exact m/z calculated for $C_{21}H_{21}F_3NO_4$ $(M+H)^+$: 408.1417; Found: 408.1428 $(M+H)^+$.

Mp: 49-51 ^oC (decomposed).

Methyl 3-(2-ethoxy-2-oxoethyl)-2-(4-(trifluoromethyl)phenyl)indoline-1-carboxylate (8h):

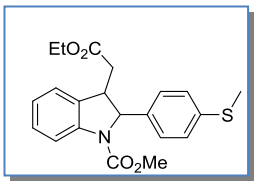

Following **GP-2**, **8h** was prepared from **7h** (0.232 g, 0.5 mmol, 1.00 equiv), $[Ir(ppy)_2(dtb\text{-}bpy)]PF_6$ (1.37 mg, 0.003 equiv, 0.3 mol %) and DIPEA (0.191 mL, 1.1 mmol, 2.2 equiv) in MeCN (1.5 mL). Purification of the crude product by column chromatography (silica gel, hexanes–EtOAc, 9:1, R_f = 0.53) afforded **8h** as a white solid (0.171 g, *cis / trans* = 75:25, 89% yield).

^{1}H-NMR (300 MHz, $CDCl_3$, *cis* isomer): δ 7.81 (bs, 1H), 7.17 – 7.08 (m, 2H), 7.07 – 6.96 (m, 3H), 6.87 (d, *J* = 8.3 Hz, 2H), 5.55 (d, *J* = 9.6 Hz, 1H), 4.26 – 4.17 (m, 1H), 4.05 (q, *J* = 7.1 Hz, 2H), 3.64 (s, 3H), 2.67 – 2.59 (m, 1H), 2.39 (s, 3H), 2.01 (dd, *J* = 17.5, 10.2 Hz, 1H), 1.17 (t, *J* = 7.1 Hz, 3H).

^{1}H-NMR (300 MHz, $CDCl_3$, *trans* isomer): δ 7.28 – 7.18 (m, 1H), 7.17 – 7.07 (m, 3H), 7.07 – 6.92 (m, 4H), 5.13 (s, 1H), 4.15 (q, *J* = 7.1 Hz, 2H), 3.64 (s, 3H), 3.45 (dd, *J* = 16.9, 10.2 Hz, 1H), 2.57 (d, *J* = 4.9 Hz, 1H), 2.42 (s, 3H), 1.26 (dd, *J* = 9.4, 4.9 Hz, 1H), 1.21 (t, *J* = 7.1 Hz, 2H).

^{13}C-NMR (75 MHz, $CDCl_3$, *cis* isomer): δ 172.20, 153.46, 138.05, 135.03, 128.37, 127.46, 126.83, 126.25, 125.88, 123.43, 123.14, 114.58, 66.05, 60.73, 52.70, 41.08, 34.13, 15.58, 14.18.

^{13}C-NMR (75 MHz, $CDCl_3$, *trans* isomer): δ 171.45, 150.95, 137.36, 134.35, 128.59, 127.40, 126.77, 126.36, 126.30, 123.37, 122.73, 115.06, 66.52, 60.86, 52.77, 40.95, 29.71, 15.85, 14.25.

IR (neat, cm^{-1}): 2975, 2955, 2922, 1707, 1599, 1483, 1459, 1438, 1378, 1349, 1309, 1270, 1246, 1181, 1157, 1136, 1090, 1053, 1018, 968, 928, 839, 806, 745, 680.

HRMS (ESI): exact m/z calculated for $C_{21}H_{24}NO_4S$ $(M+H)^+$: 386.1421; Found: 386.1424 $(M+H)^+$.

Mp: 65-67 ^oC (decomposed).

Methyl 2-(2-bromophenyl)-3-(2-ethoxy-2-oxoethyl)indoline-1-carboxylate (8i):

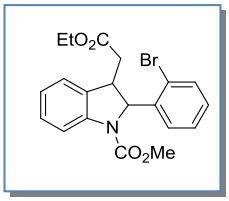

Following **GP-2**, **8i** was prepared from **7i** (0.249 g, 0.5 mmol, 1.00 equiv), $[Ir(ppy)_2(dtb\text{-}bpy)]PF_6$ (1.37 mg, 0.003 equiv, 0.3 mol %) and DIPEA (0.191 mL, 1.1 mmol, 2.2 equiv) in MeCN (1.5 mL). Purification of the crude product by column chromatography (silica gel, hexanes–EtOAc, 9:1, R_f = 0.30) afforded **8i** as a pale yellow syrup (0.167 g, *cis / trans* = 79:21, 80% yield).

^{1}H-NMR (300 MHz, $CDCl_3$, *cis* isomer): δ 7.83 (bs, 1H), 7.28 – 7.12 (m, 4H), 7.03 – 6.91 (m, 3H), 5.59 (d, *J* = 9.7 Hz, 1H), 4.33 – 4.19 (m, 1H), 4.04 (q, *J* = 7.1 Hz, 2H), 3.63 (s, 3H), 2.63 – 2.53 (m, 1H), 1.97 (dd, *J* = 17.5, 10.2 Hz, 1H), 1.15 (t, *J* = 7.1 Hz, 3H).

^{1}H-NMR (300 MHz, $CDCl_3$, *trans* isomer): δ 7.47 (m, 1H), 7.28 – 7.12 (m, 4H), 7.03 – 6.91 (m, 3H), 4.70 (s, 1H), 4.15 (q, *J* = 7.1 Hz, 1H), 3.63 (s, 3H), 3.54 – 3.45 (m, 1H), 2.66 – 2.61 (m, 1H), 1.27 – 1.22 (m, 1H), 1.21 (t, *J* = 7.1 Hz, 3H).

^{13}C-NMR (75 MHz, $CDCl_3$, *cis* isomer): δ 172.23, 153.51, 138.25, 128.63, 128.38, 127.92, 127.45, 126.93, 125.29, 123.98, 123.42, 123.11, 114.56, 66.40, 60.67, 52.65, 41.00, 34.20, 14.16.

^{13}C-NMR (75 MHz, $CDCl_3$, *trans* isomer): δ 171.58, 152.96, 138.14, 131.98, 130.39, 128.87, 128.08, 128.04, 127.33, 124.53, 123.97, 123.34, 115.05, 66.44, 60.83, 52.77, 41.00, 29.70, 14.24.

IR (neat, cm^{-1}): 2958, 2922, 2851, 1708, 1596, 1575, 1482, 1439, 1378, 1334, 1307, 1269, 1252, 1176, 1136, 1080, 1053, 1021, 933, 793, 766, 749, 757.

HRMS (ESI): exact m/z calculated for $C_{20}H_{21}BrNO_4$ $(M+H)^+$: 418.0621; Found: 418.0624 $(M+H)^+$.

Methyl 2-(3-chlorophenyl)-3-(2-ethoxy-2-oxoethyl)indoline-1-carboxylate (8j):[11]

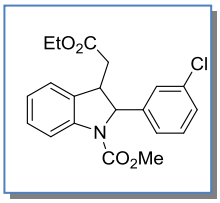

Following **GP-2**, **8j** was prepared from **7j** (0.226 g, 0.5 mmol, 1.00 equiv), $[Ir(ppy)_2(dtb\text{-}bpy)]PF_6$ (1.37 mg, 0.003 equiv, 0.3 mol %) and DIPEA (0.191 mL, 1.1 mmol, 2.2 equiv) in MeCN (1.5 mL). Purification of the crude product by column chromatography (silica gel, hexanes–EtOAc, 9:1, R_f = 0.33) afforded **8j** as a white solid (0.147 g, *cis* / *trans* = 75:25, 79% yield).

^{1}H-NMR (300 MHz, $CDCl_3$, *cis* isomer): δ 7.83 (s, 1H), 7.29 – 7.18 (m, 2H), 7.20 – 7.14 (m, 1H), 7.10 (dd, *J* = 10.1, 5.4 Hz, 1H), 7.02 – 6.95 (m, 2H), 6.83 (d, *J* = 7.4 Hz, 1H), 5.56 (d, *J* = 9.6 Hz, 1H), 4.30 – 4.21 (m, 1H), 4.11 – 4.03 (q, *J* = 7.1 Hz, 2H), 3.65 (s, 3H), 2.66 (dd, *J* = 9.1, 3.3 Hz, 1H), 1.94 (dd, *J* = 17.5, 10.6 Hz, 1H), 1.18 (t, *J* = 7.1 Hz, 3H).

^{1}H-NMR (300 MHz, $CDCl_3$, *trans* isomer): δ 7.75 (s, 1H), 7.30 – 7.17 (m, 3H), 7.14 – 7.04 (m, 2H), 7.04 – 6.92 (m, 2H), 5.15 (s, 1H), 4.21 – 4.12 (q, *J* = 7.1 Hz, 2H), 3.65 (s, 3H), 3.48 (t, *J* = 7.3 Hz, 1H), 2.63 (dd, *J* = 9.0, 2.7 Hz, 1H), 1.25 (dd, *J* = 7.1, 5.4 Hz, 1H), 1.25 – 1.21 (t, *J* = 7.1 Hz, 3H).

^{13}C-NMR (75 MHz, $CDCl_3$, *cis* isomer): δ 172.13, 153.36, 140.43, 134.25, 129.99, 129.79, 128.54, 128.16, 127.68, 127.26, 125.56, 124.94, 123.32, 114.65, 65.92, 60.91, 52.80, 41.08, 34.16, 14.17.

5.9.5 General procedure (GP-3) for aromatization and deprotection of indolines:

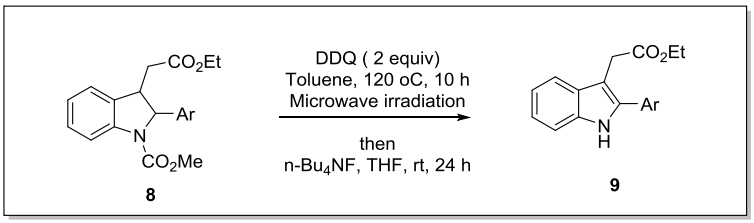

A solution of indoline **8** (2 mmol, 1.0 equiv) and DDQ (4 mmol, 2.0 equiv) in toluene (15 mL) was placed in a sealed vessel in a microwave and irradiated at 120 °C for 10 h. After completion of the reaction, the solvent was removed and the residue was washed with saturated $NaHCO_3$ (15 mL) solution, and extracted with CH_2Cl_2 (3 × 20 mL). The combined organic phases were dried over Na_2SO_4, filtered, and concentrated *in vacuo*. The crude product was dissolved in THF (20 mL) and treated with Bu_4NF (10 mmol, 5 equiv) for 24 h at room temperature. After complete conversion of the starting material, the reaction mixture was concentrated *in vacuo*. Purification of the crude product by column chromatography (silica gel, hexanes–EtOAc) afforded **9** as a pure compound.

Ethyl 2-(2-phenyl-1*H*-indol-3-yl)acetate (9a):

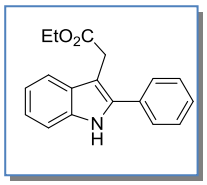

Following **GP-3**, **9a** was prepared from **8a** (0.678 g, 2.0 mmol, 1.00 equiv). Purification of the crude product by column chromatography (silica gel, hexanes–EtOAc, 9:1, R_f = 0.35) afforded **8a** as a pale yellow oil (0.335 g, 60% yield).

^{1}H-NMR (300 MHz, $CDCl_3$): δ 8.18 (bs, 1H), 7.72 – 7.64 (m, 3H), 7.53 – 7.44 (m, 2H), 7.44 – 7.34 (m, 2H), 7.27 – 7.12 (m, 2H), 4.19 (q, *J* = 7.1 Hz, 2H), 3.85 (s, 2H), 1.27 (t, *J* = 7.1 Hz, 3H).

^{13}C-NMR (75 MHz, $CDCl_3$): δ 172.29, 136.19, 135.75, 132.43, 129.07, 128.97, 128.28, 128.08, 122.57, 120.05, 119.38, 110.88, 105.76, 60.91, 31.21, 14.26.

The obtained data is in accordance with the literature data.[27]

Ethyl 2-(2-(o-tolyl)-1*H*-indol-3-yl)acetate (9b):

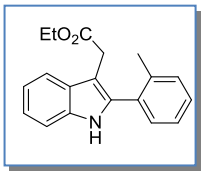

Following **GP-3**, **9b** was prepared from **8b** (0.706 g, 2.0 mmol, 1.00 equiv). Purification of the crude product by column chromatography (silica gel, hexanes–EtOAc, 9:1, R_f = 0.36) afforded **9b** as a pale yellow oil (0.369 g, 63% yield).

^{1}H-NMR (300 MHz, $CDCl_3$): δ 8.10 (bs, 1H), 7.69 (dd, *J* = 11.5, 4.3 Hz, 1H), 7.46 – 7.15 (m, 7H), 4.10 (q, *J* = 7.1 Hz, 2H), 3.64 (s, 2H), 2.27 (s, 3H), 1.25 – 1.18 (t, *J* = 7.1 Hz, 3H).

^{13}C-NMR (75 MHz, $CDCl_3$): δ 172.12, 137.91, 136.04, 135.61, 131.81, 131.22, 130.36, 128.88, 128.17, 125.72, 122.14, 119.82, 119.20, 110.87, 106.53, 60.71, 31.01, 20.07, 14.23.

IR (neat, cm^{-1}): 3355; 2978, 2925, 1717, 1486, 1456, 1367, 1306, 1265, 1238, 1175, 1155, 1110, 1026, 943, 740, 693.

HRMS (ESI): exact m/z calculated for $C_{19}H_{20}NO_4$ $(M+H)^+$: 293.1410 Found: 293.1417 $(M+H)^+$.

5.9.6 Reduction of indole esters with $LiAlH_4$:

2-(2-phenyl-1*H*-indol-3-yl)ethan-1-ol (10):

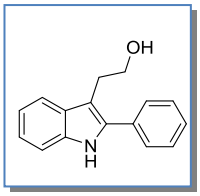

To a stirred suspension of $LiAlH_4$ (0.040 g, 1.04 mmol) in dry THF (4 mL) was added **9a** (0.200 g, 0.716 mmol) slowly at 0 ^{o}C. The resulting solution was stirred at room temperature for 10 h. The reaction mixture was quenched by using wet Na_2SO_4 and diluted with EtOAc (20 mL), filtered through pad of celite and concentrated under reduced pressure to give crude alcohol **10**. Purification of the crude product by column chromatography (silica gel, hexanes–EtOAc, 9:1, R_f = 0.13) afforded **10** as a pale yellow solid (0.206 g, 84% yield).

^{1}H-NMR (300 MHz, $CDCl_3$): δ 8.20 (bs, 1H), 7.68 – 7.56 (m, 3H), 7.51 – 7.41 (m, 2H), 7.41 – 7.32 (m, 2H), 7.17 (m, 2H), 3.95 (t, *J* = 6.7 Hz, 2H), 3.16 (t, *J* = 6.7 Hz, 2H).

^{13}C-NMR (75 MHz, $CDCl_3$): δ 135.92, 132.87, 129.18, 128.95, 128.18, 127.90, 122.49, 119.84, 119.16, 110.96, 108.86, 63.01, 28.06.

The obtained data is in accordance with the literature data.[28]

5.10 NMR spectra:

^{1}H-NMR: **7a**

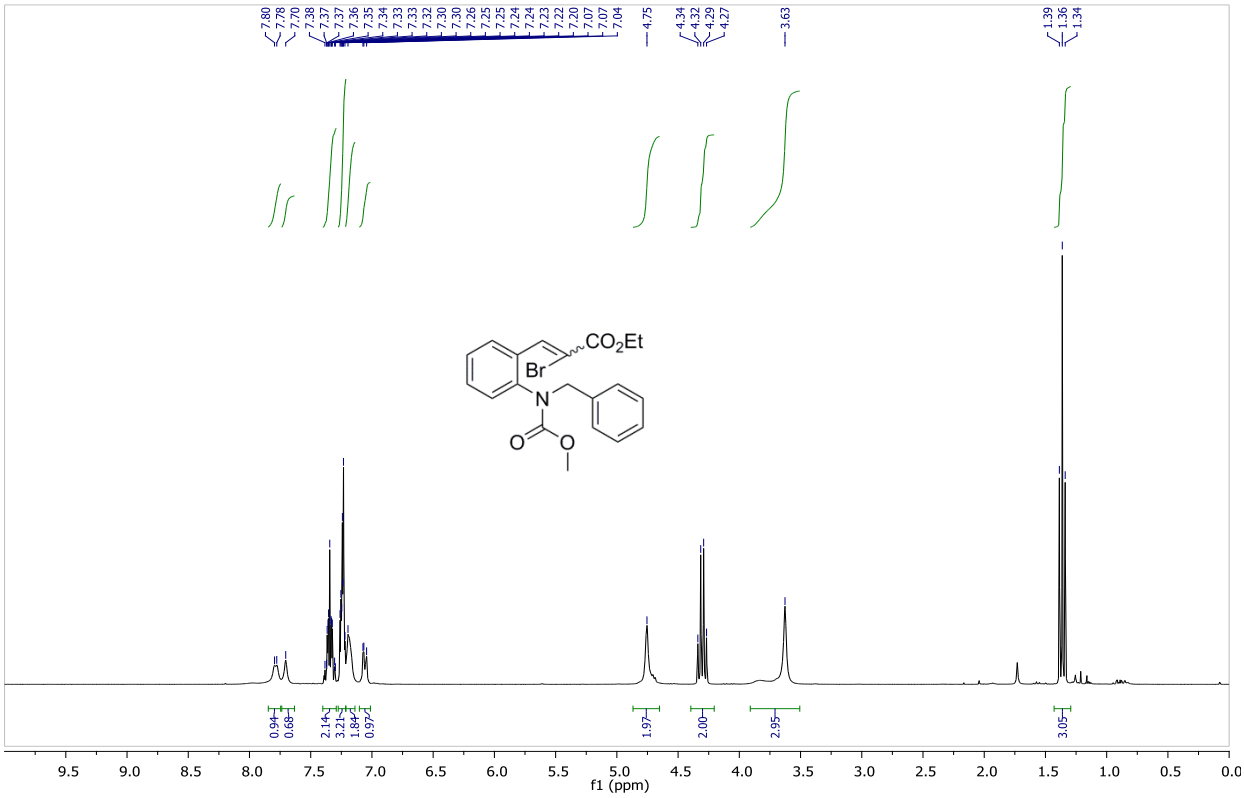

^{13}C-NMR: **7a**

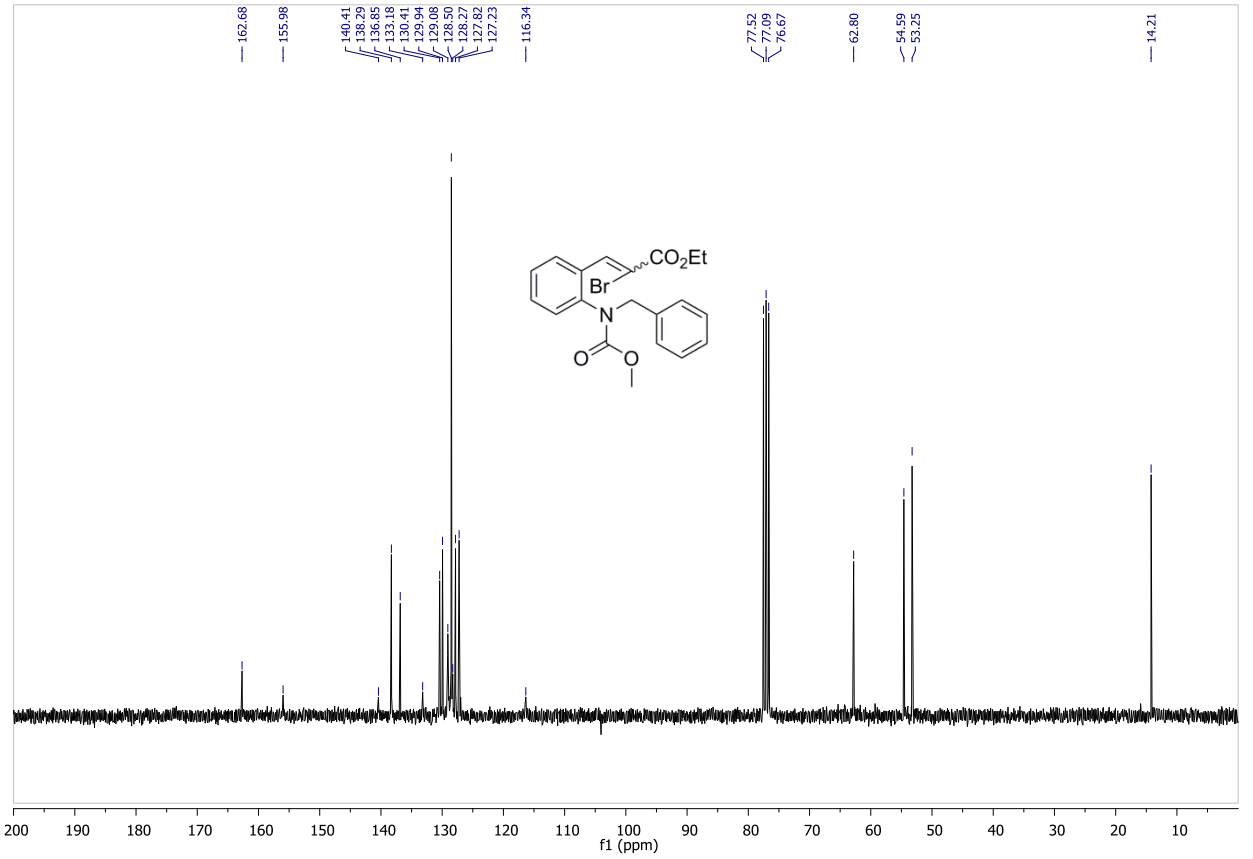

^{1}H-NMR: **7b**

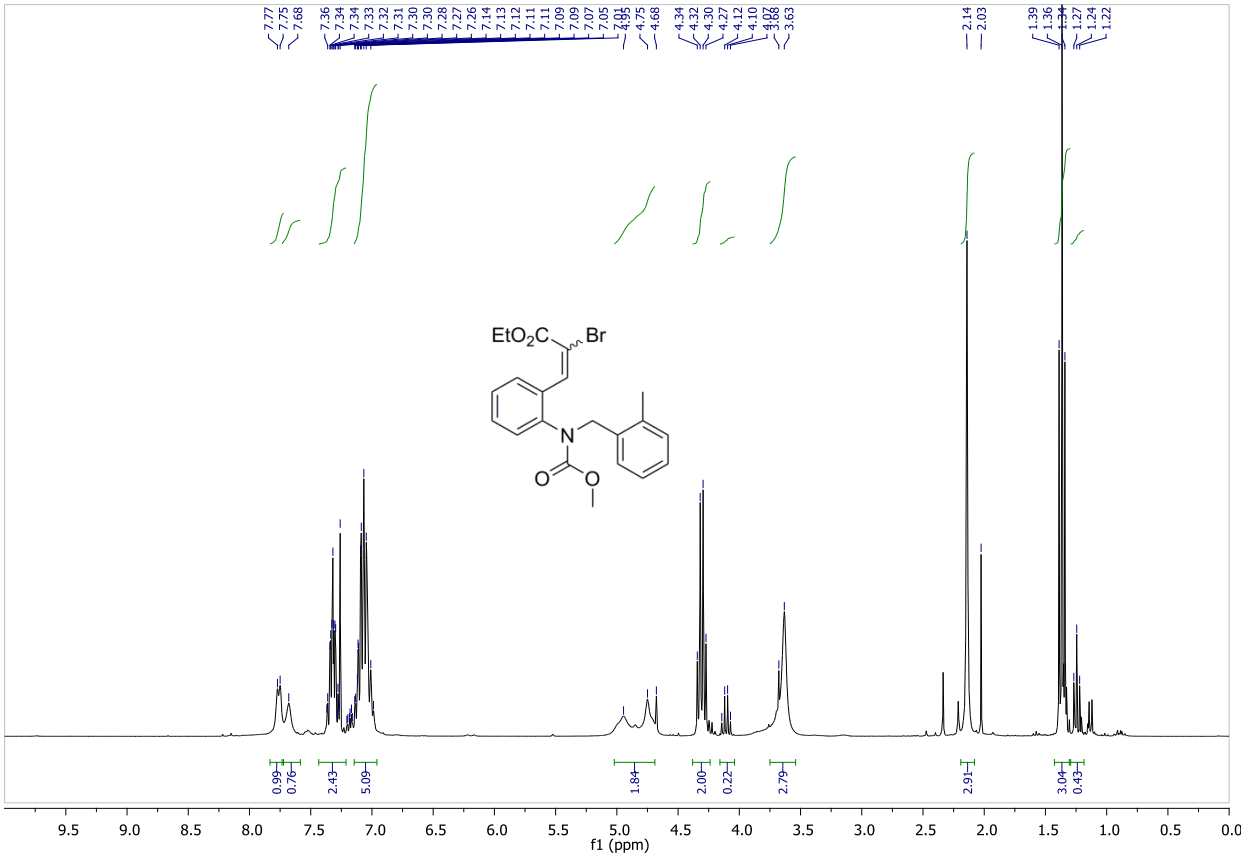

^{13}C-NMR: **7b**

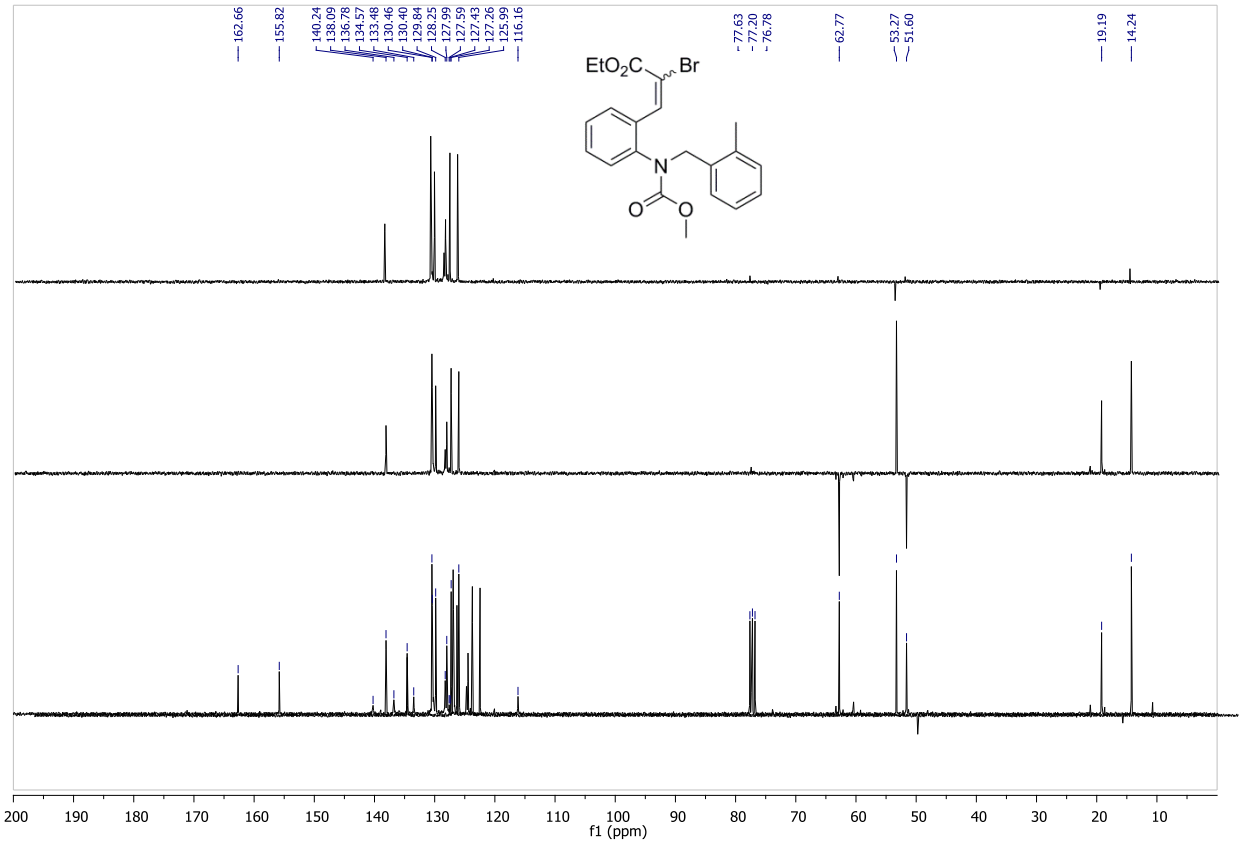

^{1}H-NMR: **7c**

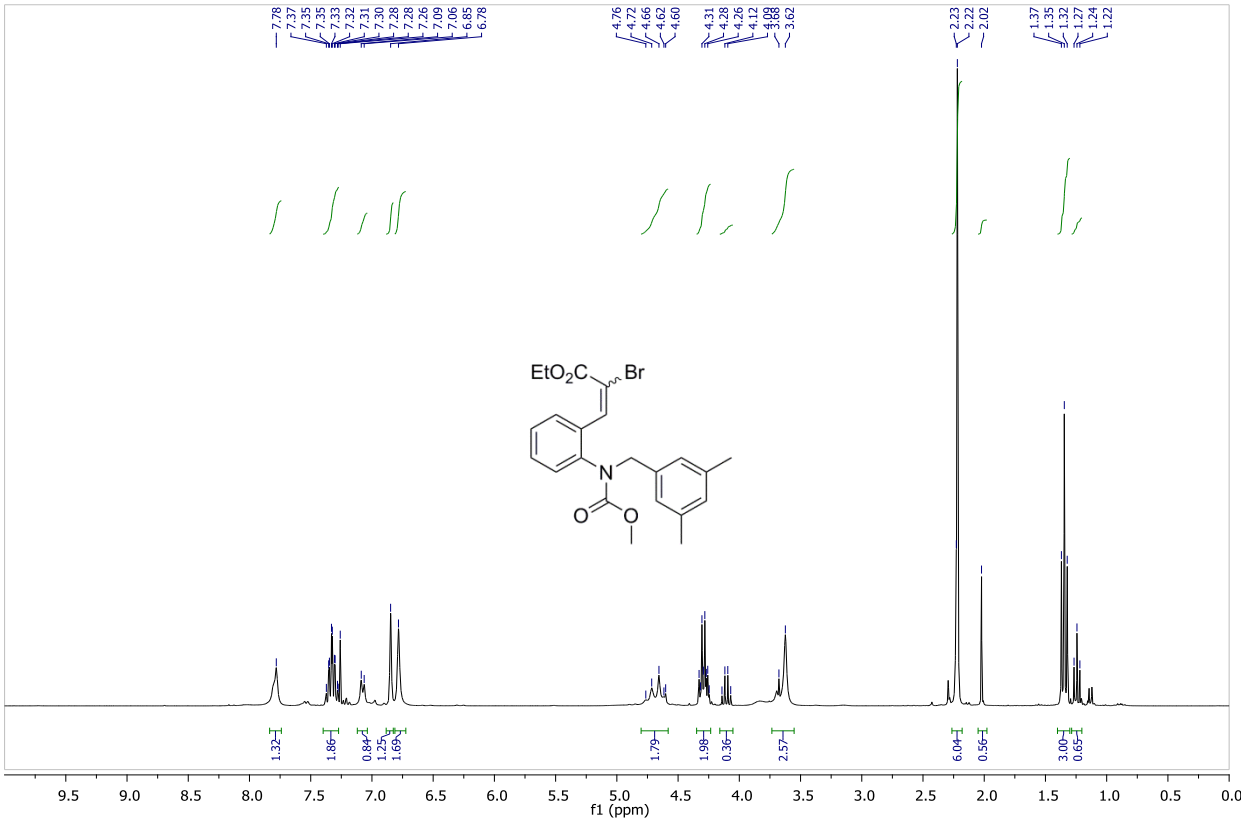

^{13}C-NMR: **7c**

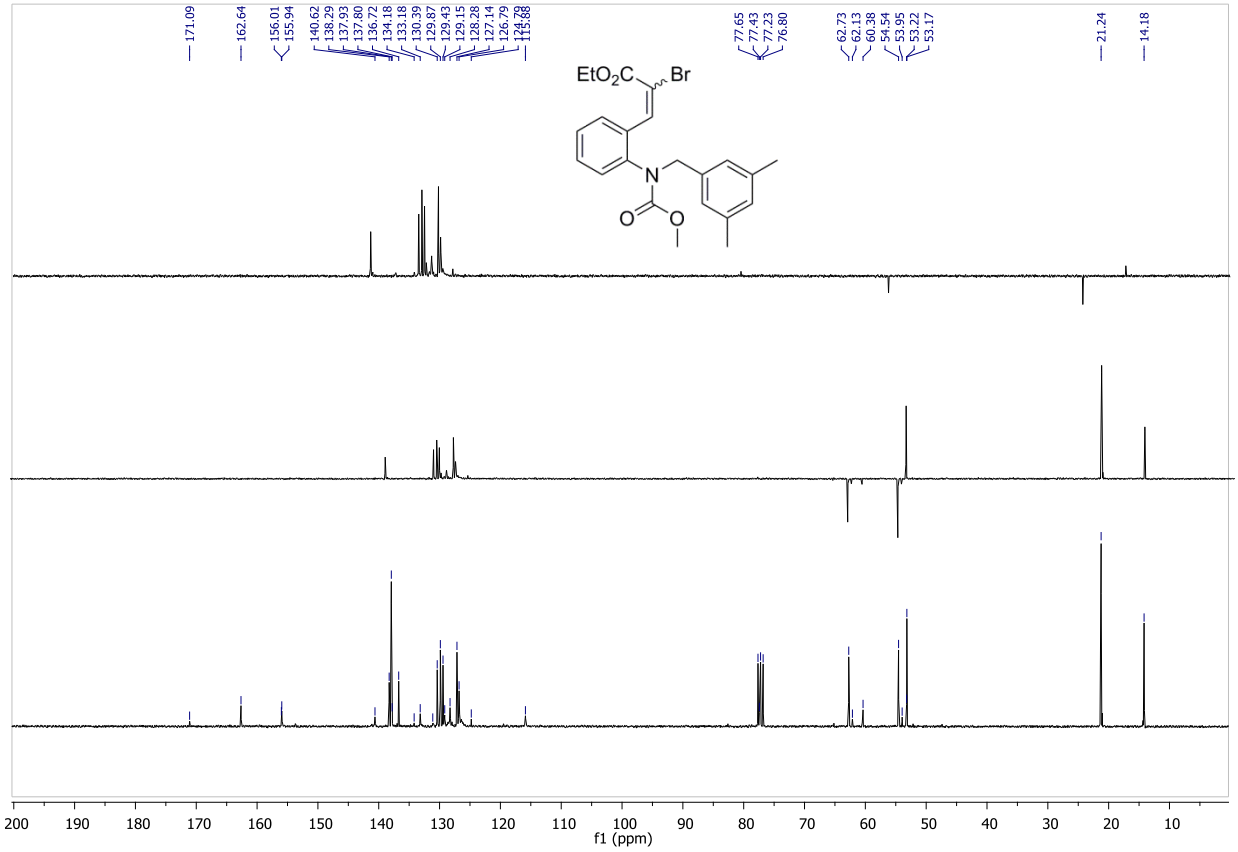

^{1}H-NMR: **7d**

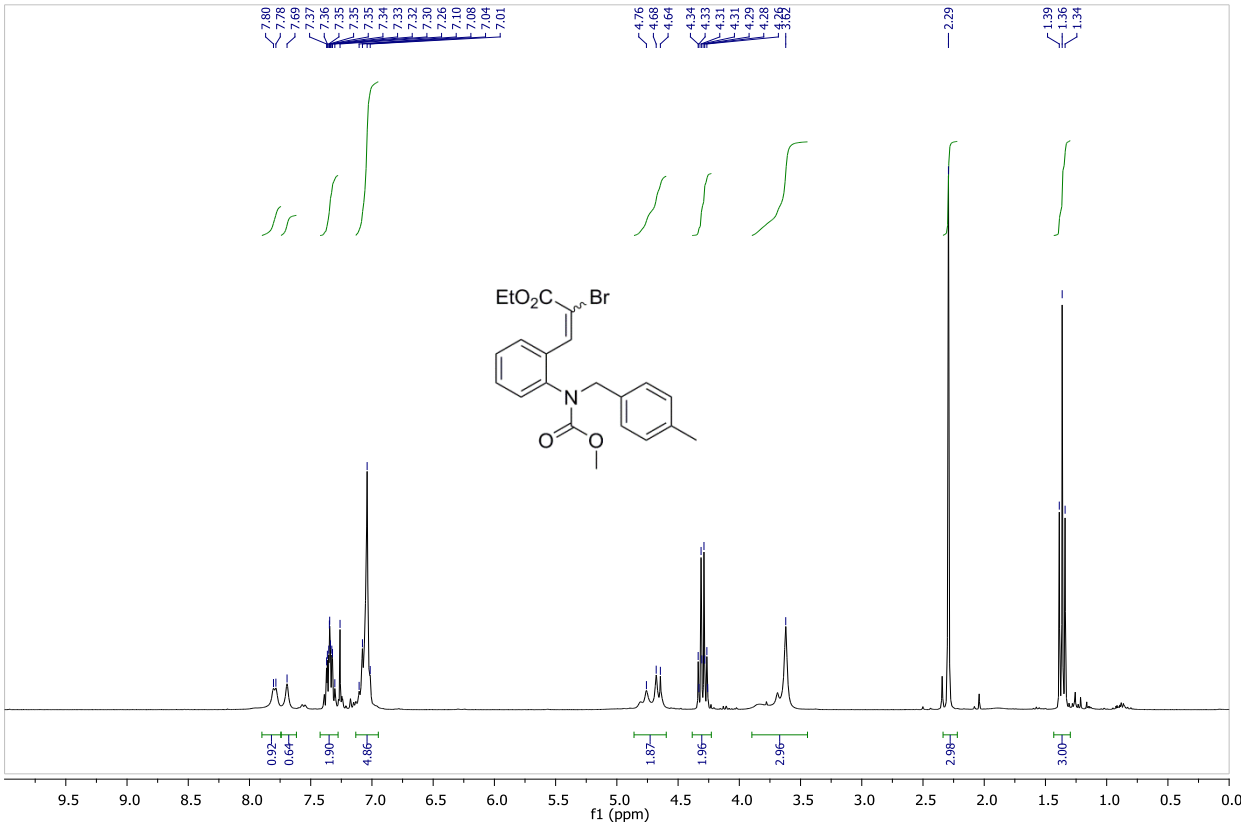

^{13}C-NMR: **7d**

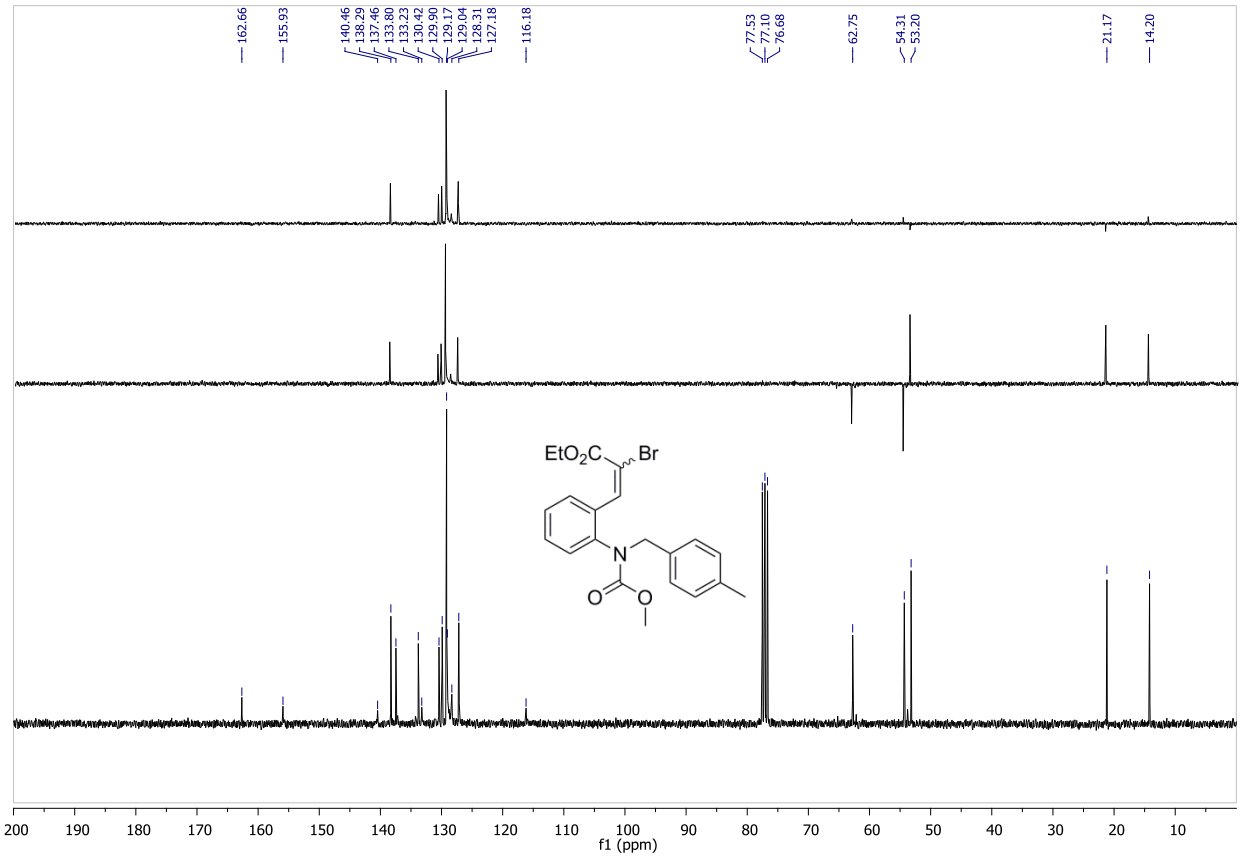

^{1}H-NMR: **7e**

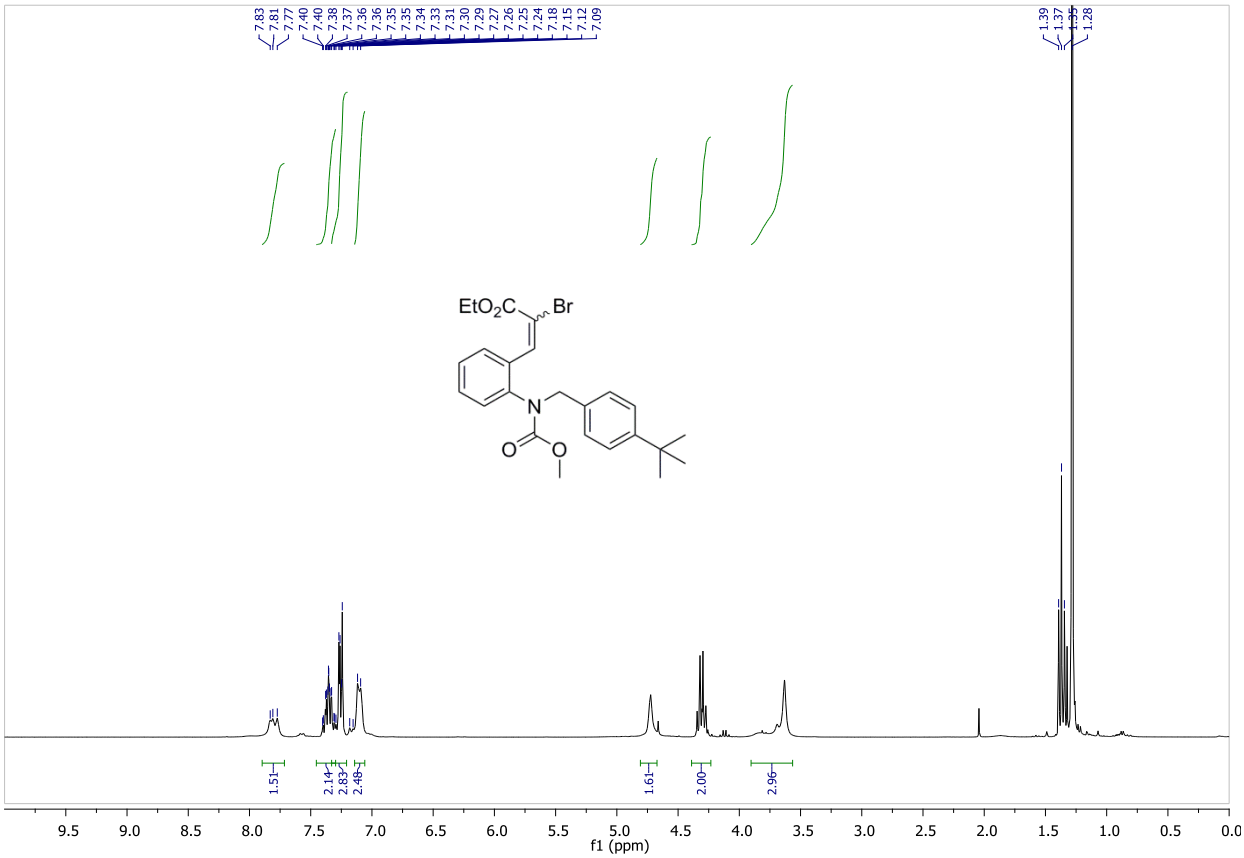

^{13}C-NMR: **7e**

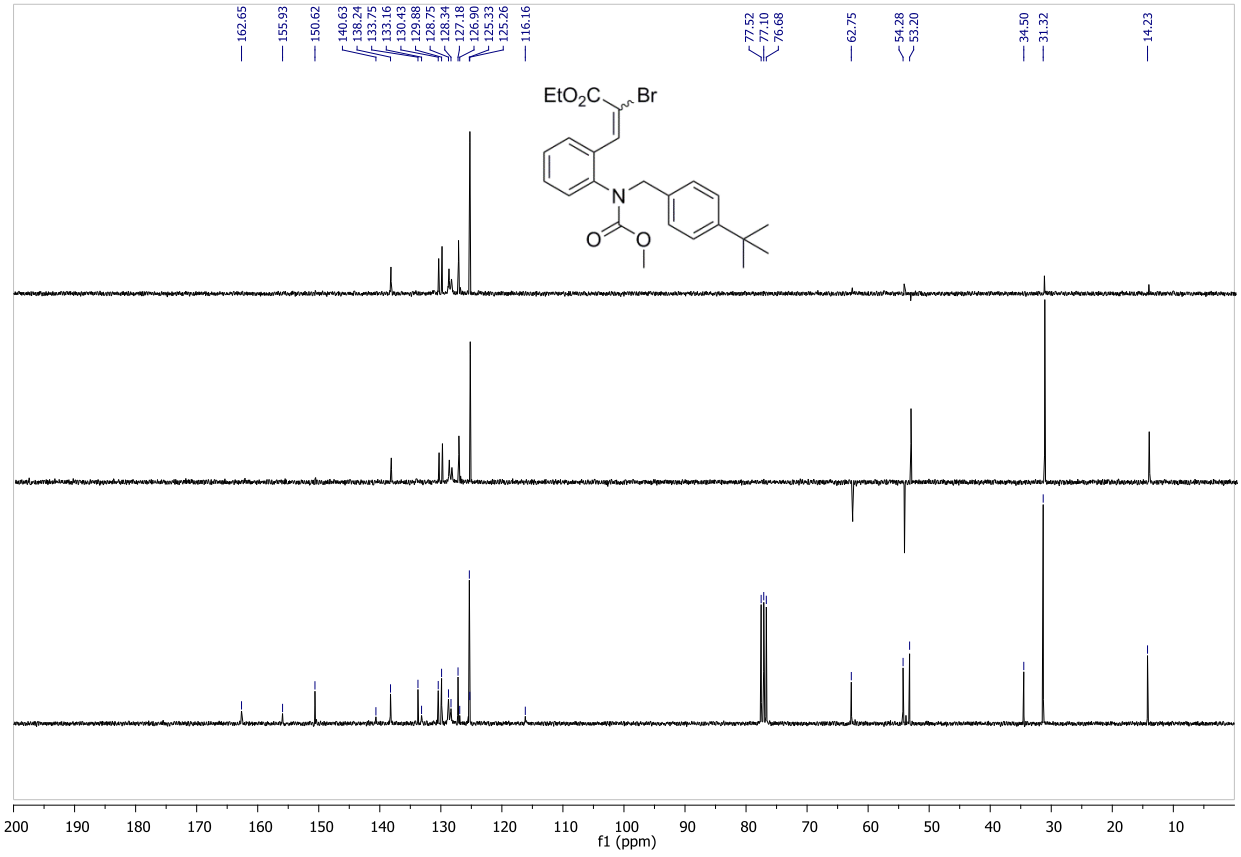

^{1}H-NMR: **7f**

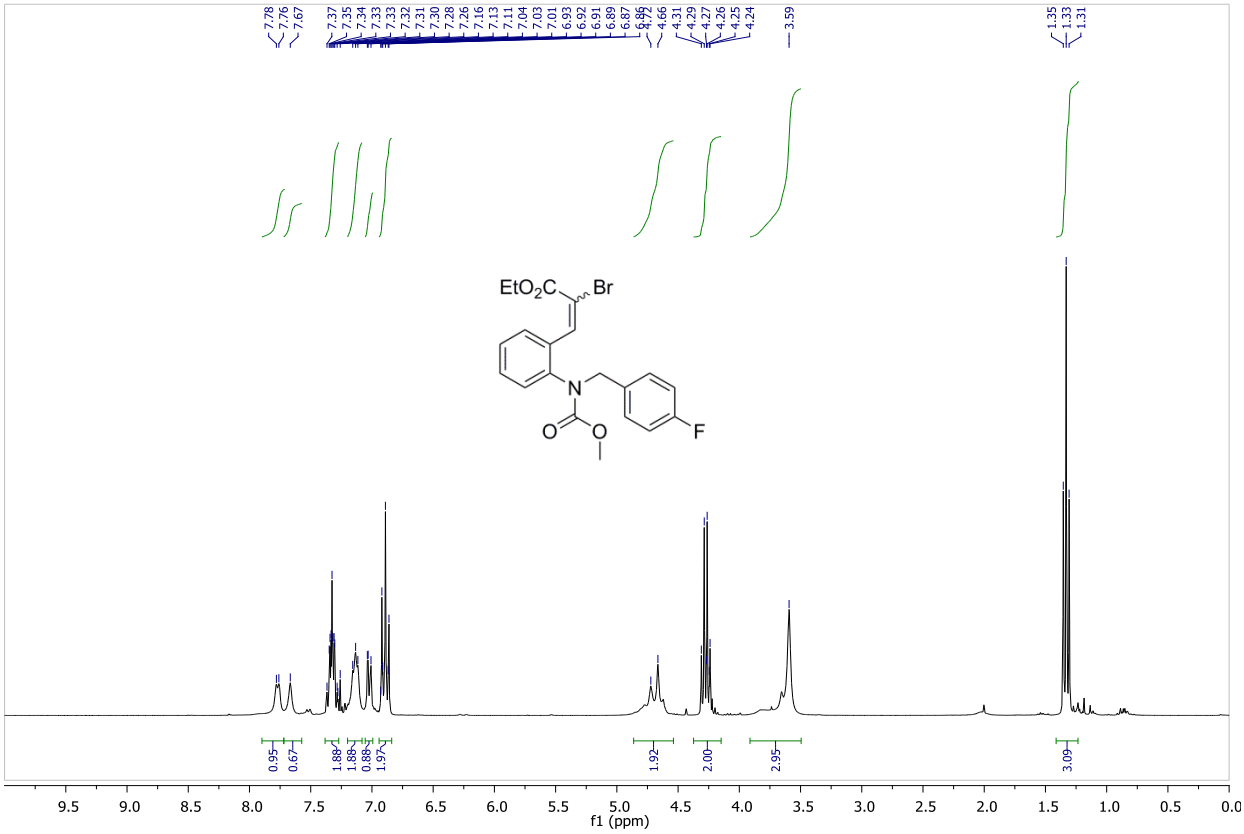

^{13}C-NMR: **7f**

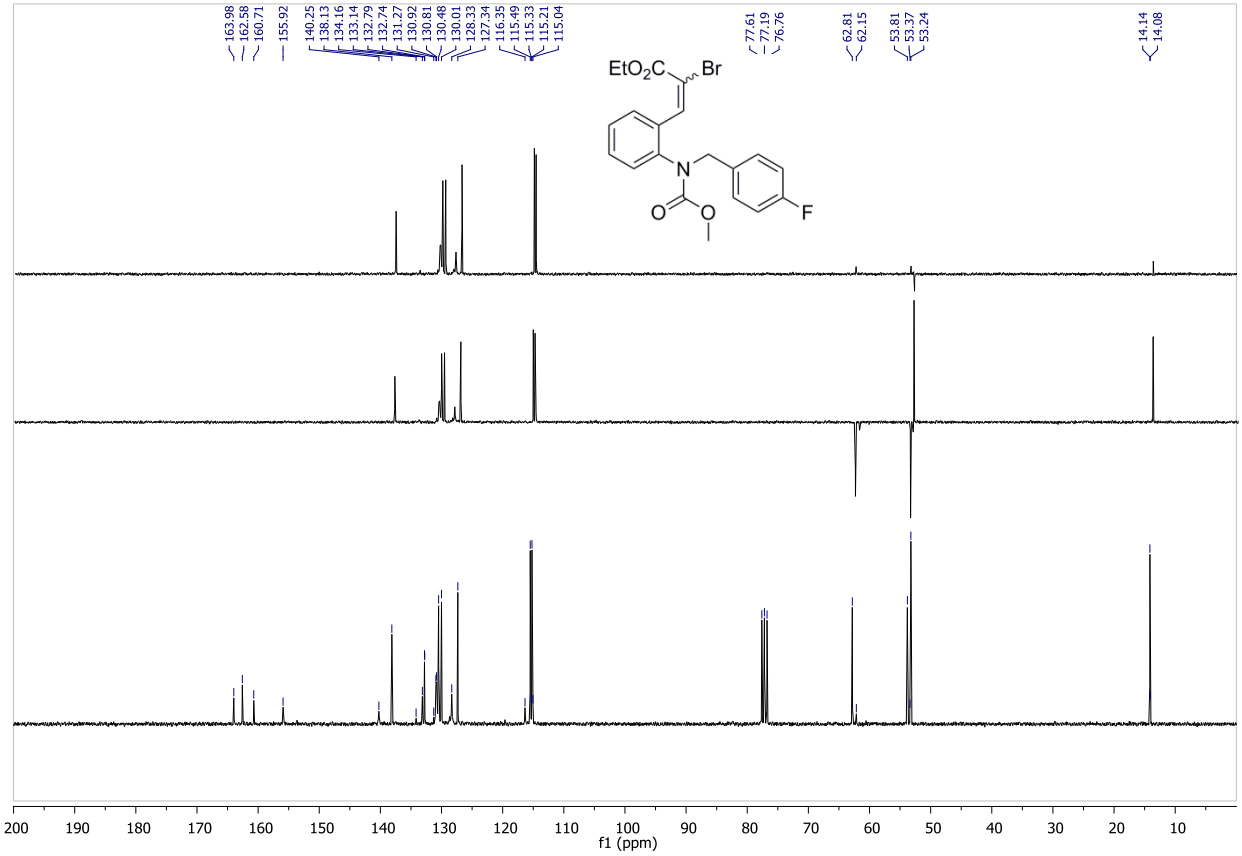

^{19}F-NMR: **7f**

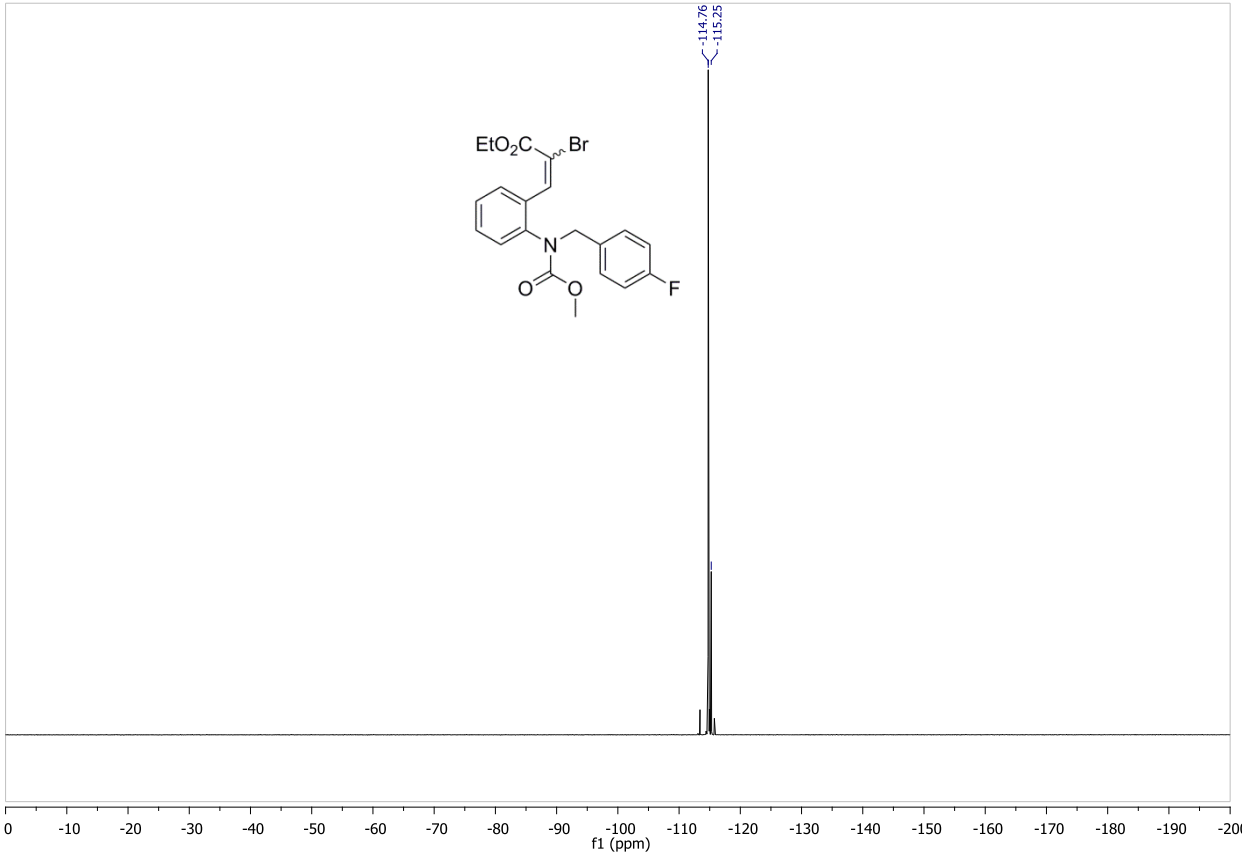
-114.76
-115.25
EtO2C
Br
N
O
O
F
0
-10
-20
-30
-40
-50
-60
-70
-80
-90
-100
-110
-120
-130
-140
-150
-160
-170
-180
-190
f1 (ppm)

^{1}H-NMR: **7g**

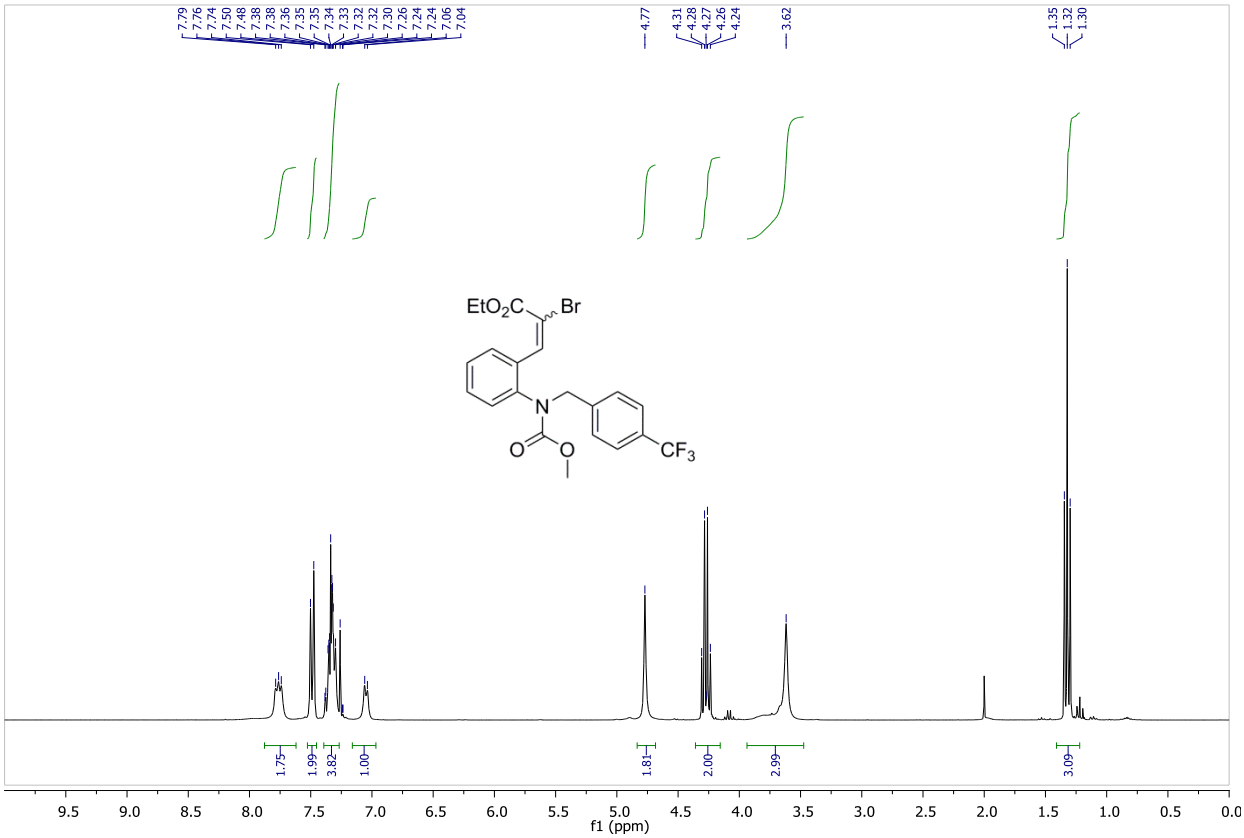

^{13}C-NMR: **7g**

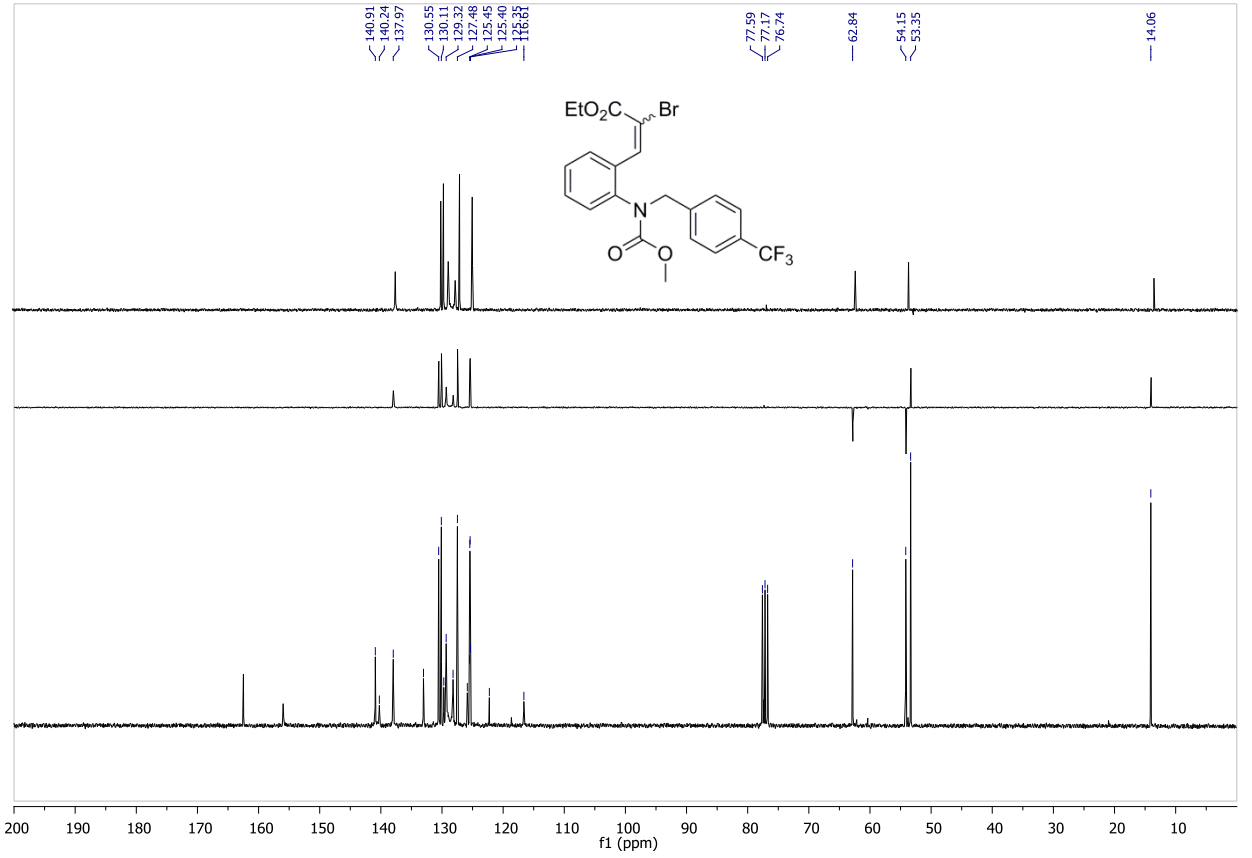

^{19}F-NMR: **7g**

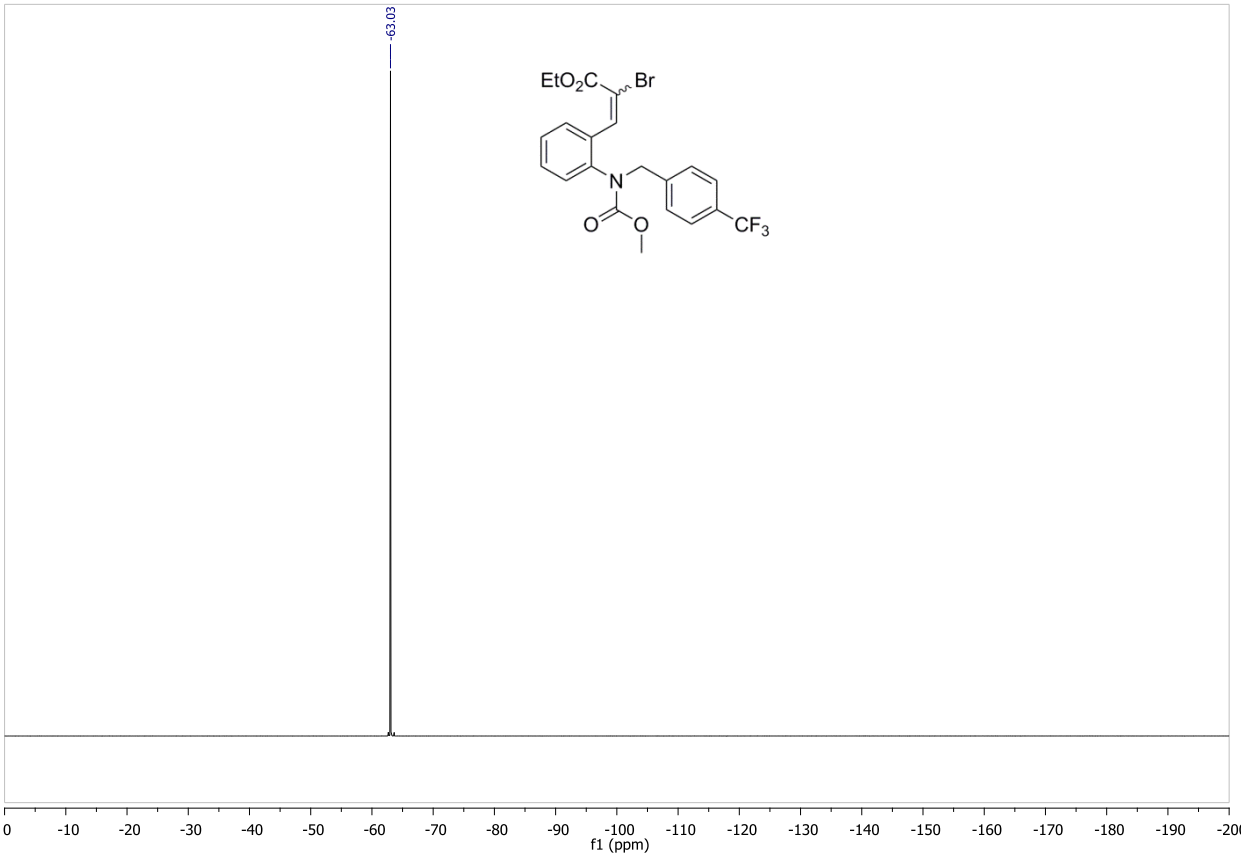
-63.03
EtO2C
Br
N
O
O
CF3
0
-10
-20
-30
-40
-50
-60
-70
-80
-90
-100
-110
-120
-130
-140
-150
-160
-170
-180
-190
f1 (ppm)

^{1}H-NMR: **7h**

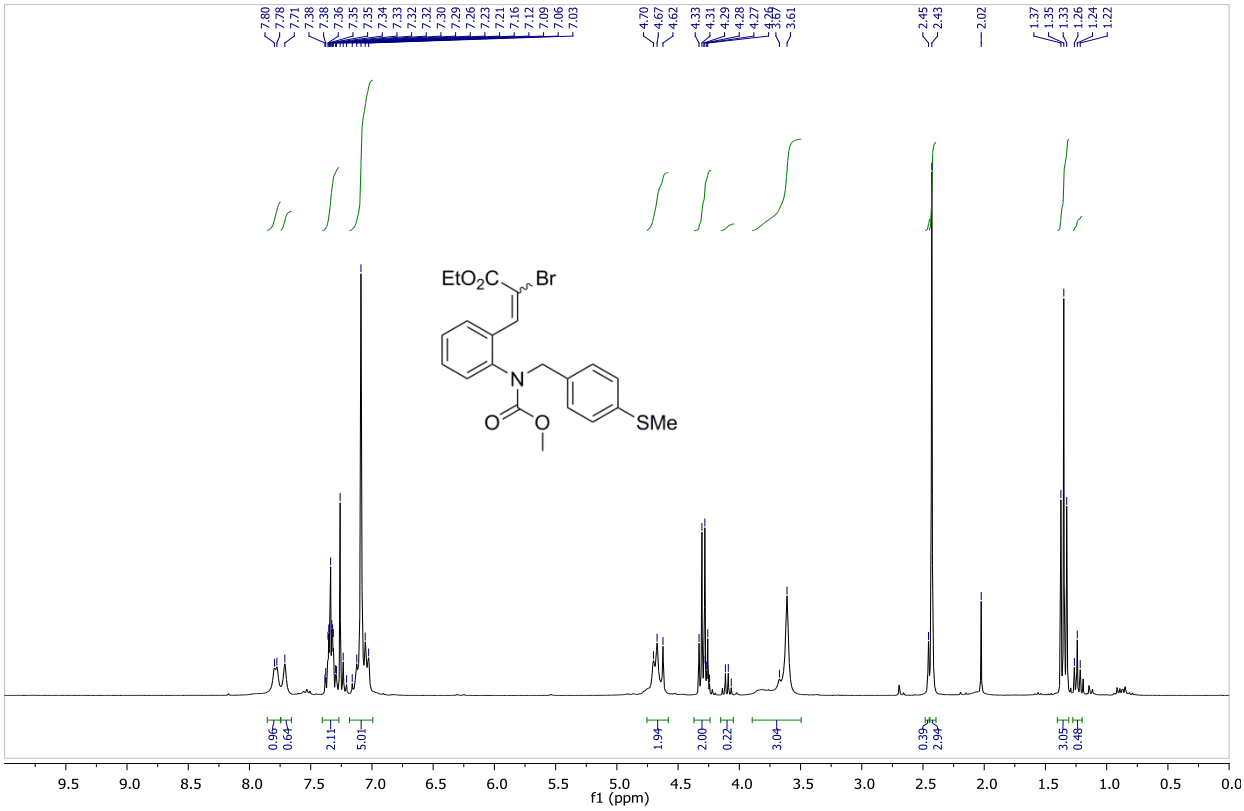

^{13}C-NMR: **7h**

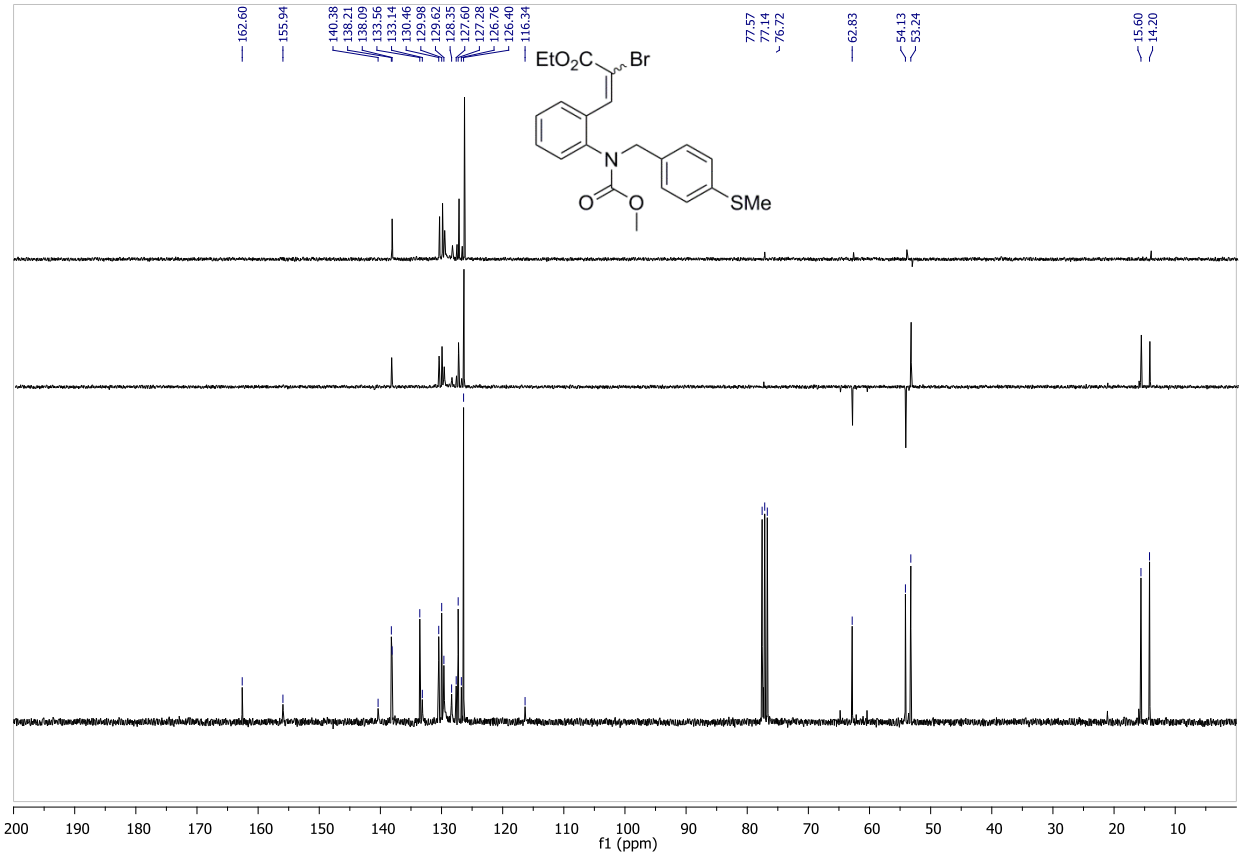

^{1}H-NMR: **7i**

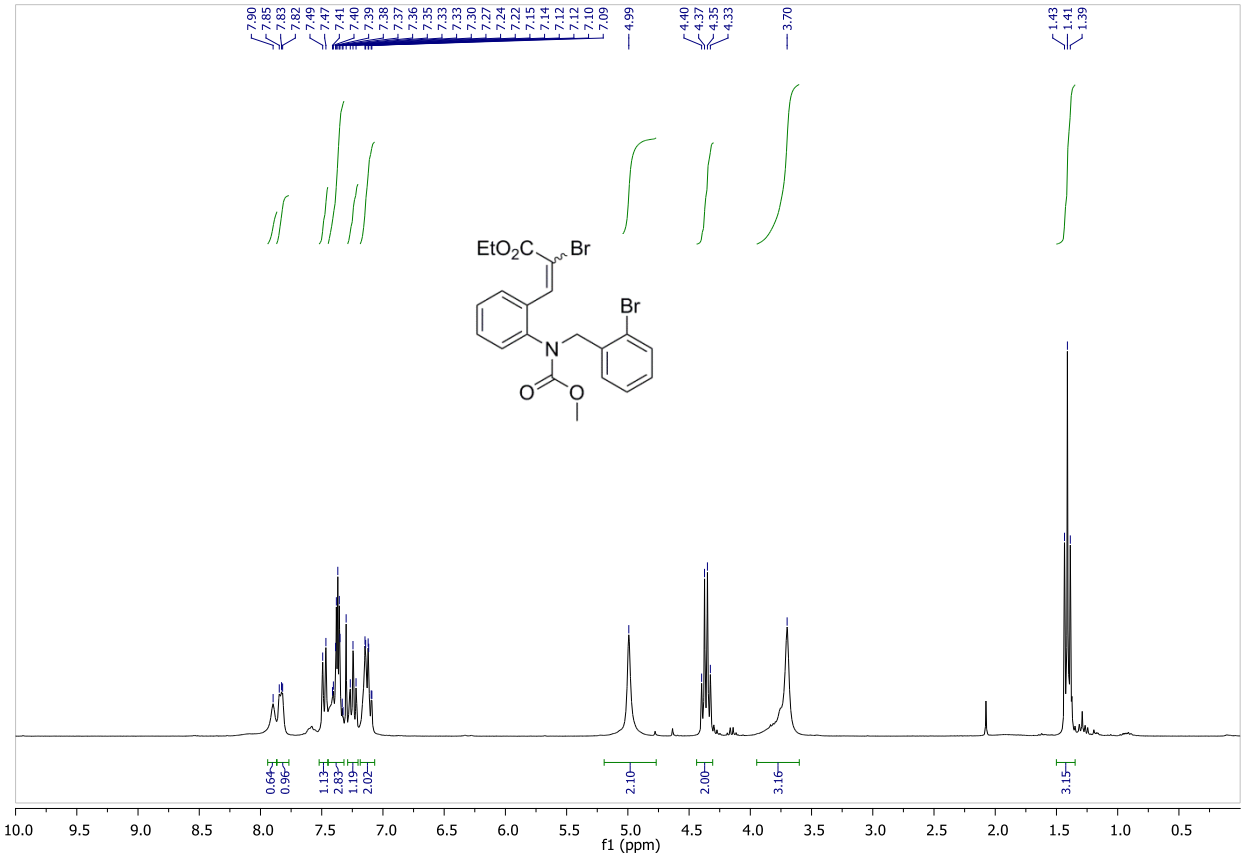

^{13}C-NMR: **7i**

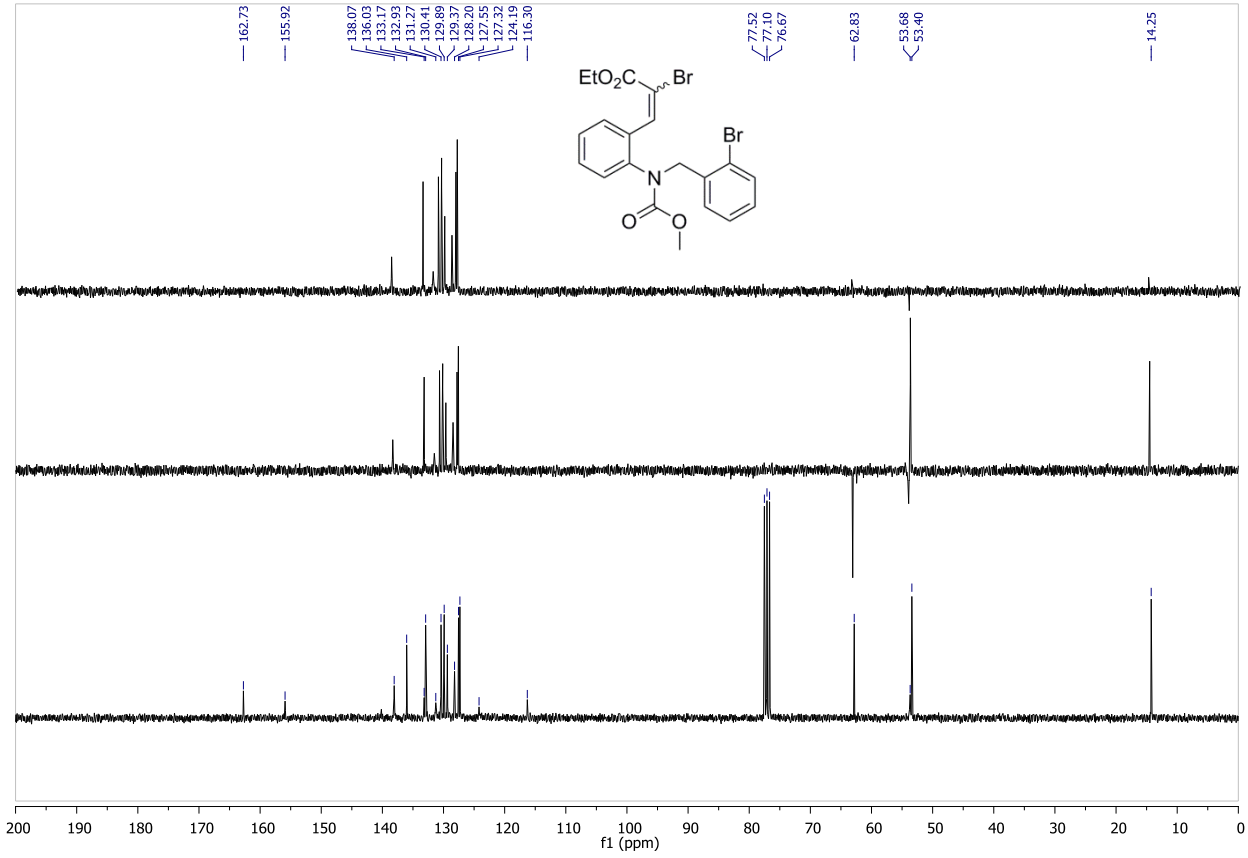

^{1}H-NMR: **7j**

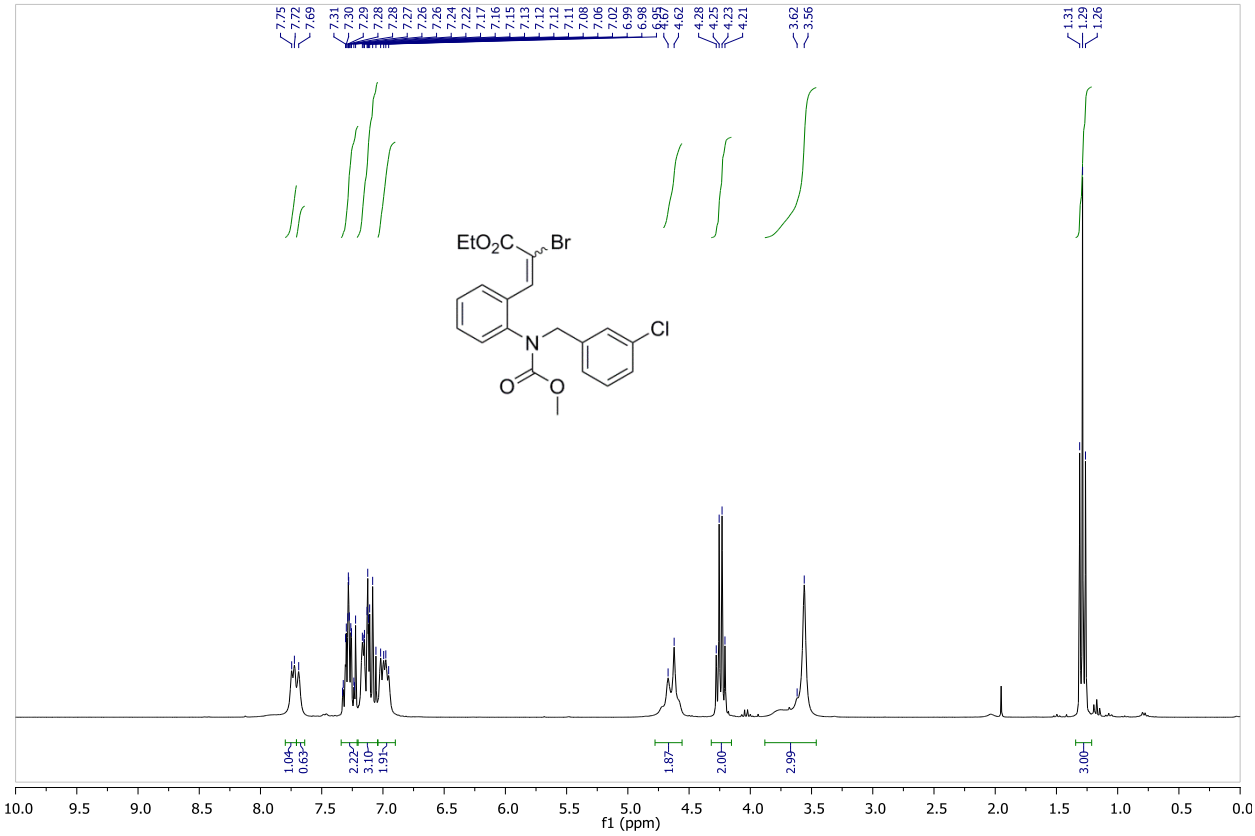

^{13}C-NMR: **7j**

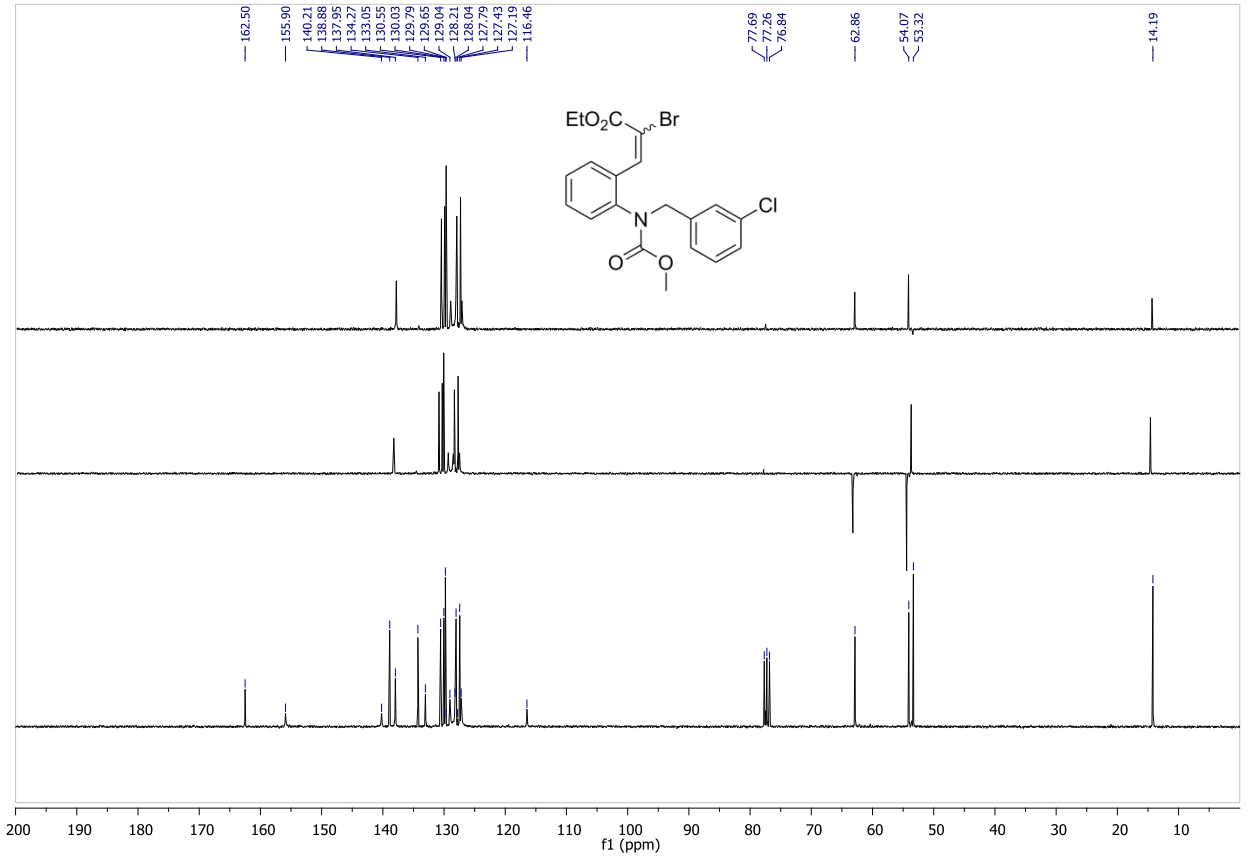

^{1}H-NMR: **7k**

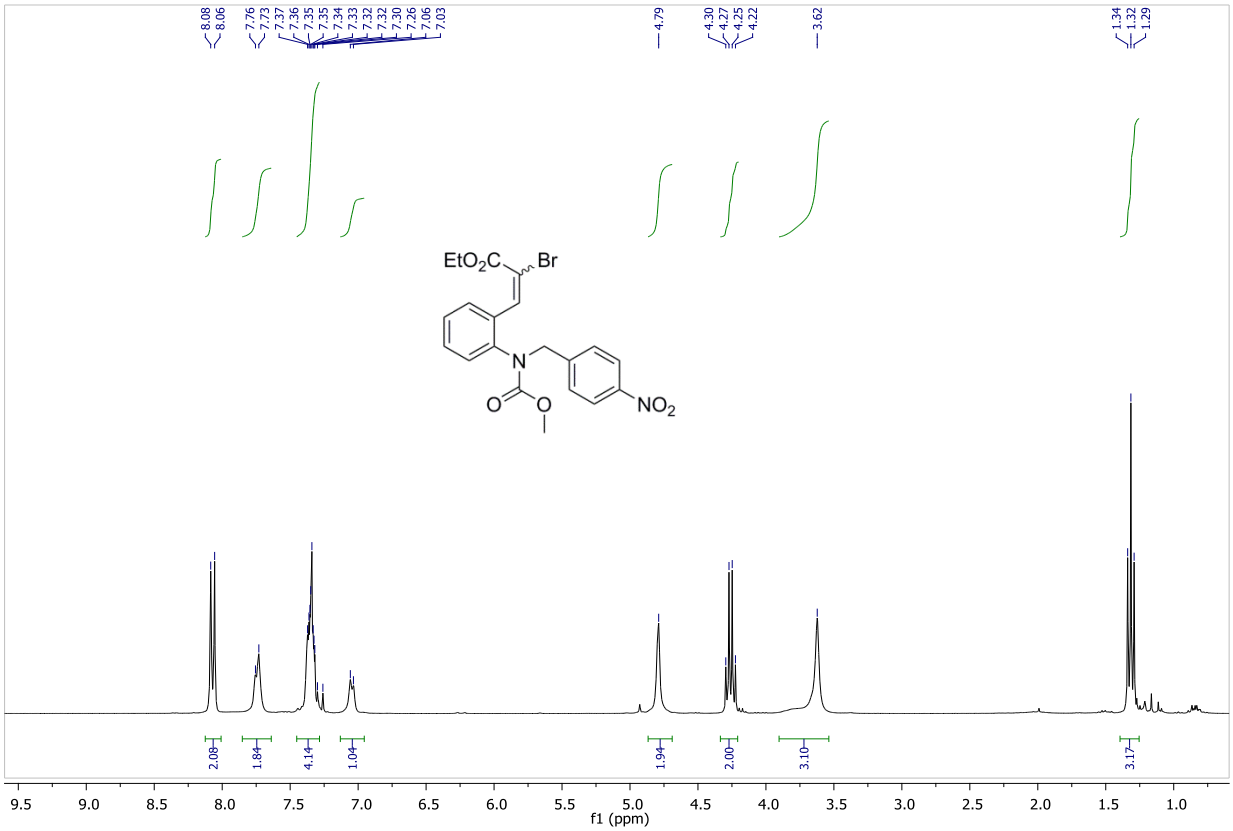

^{13}C-NMR: **7k**

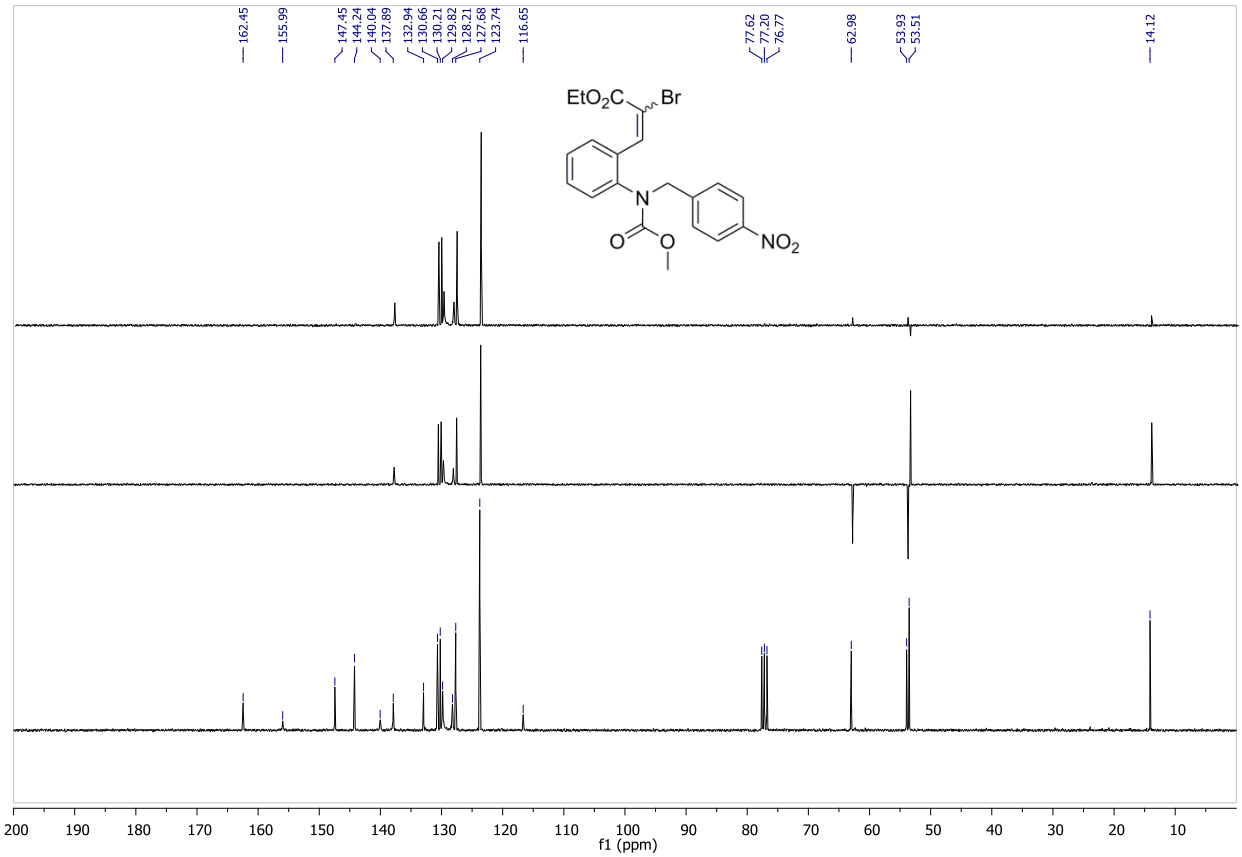

^{1}H-NMR: **8a**

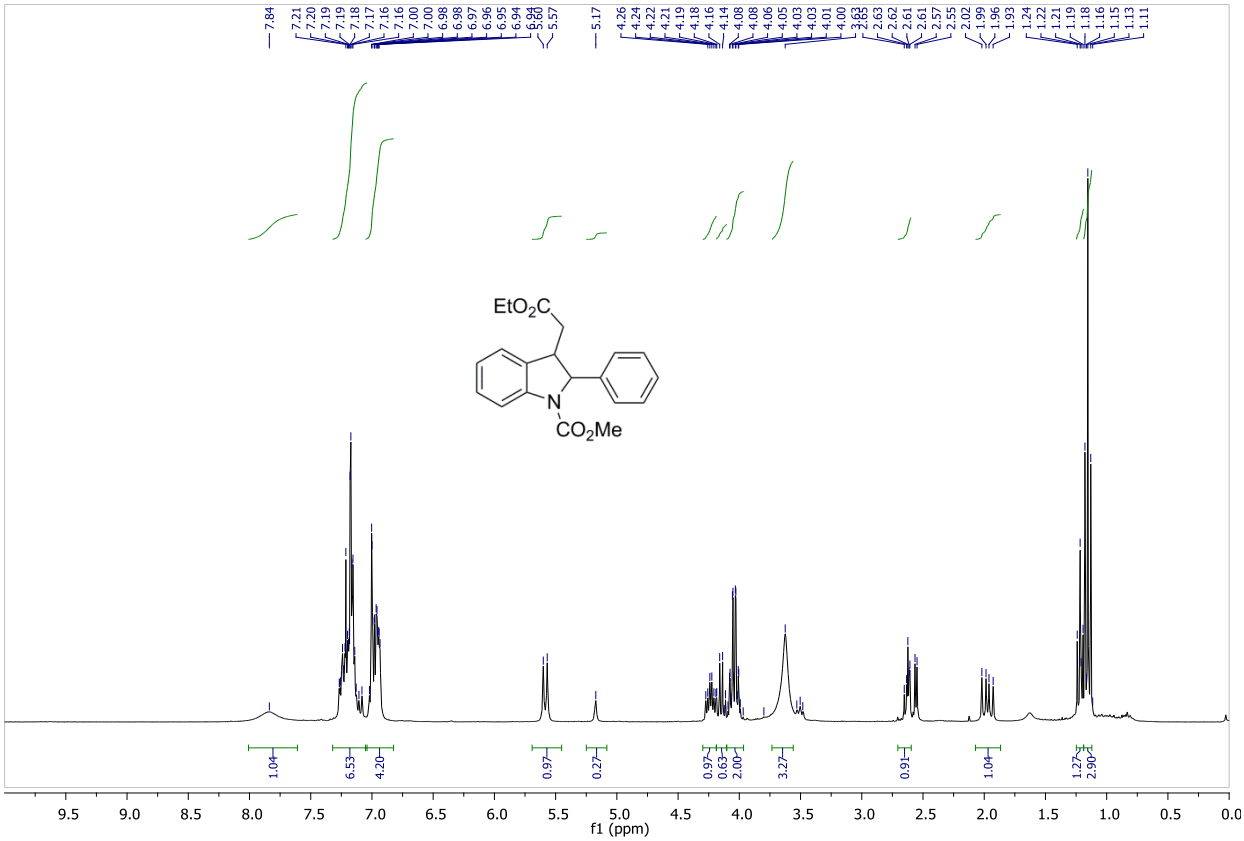

^{13}C-NMR: **8a**

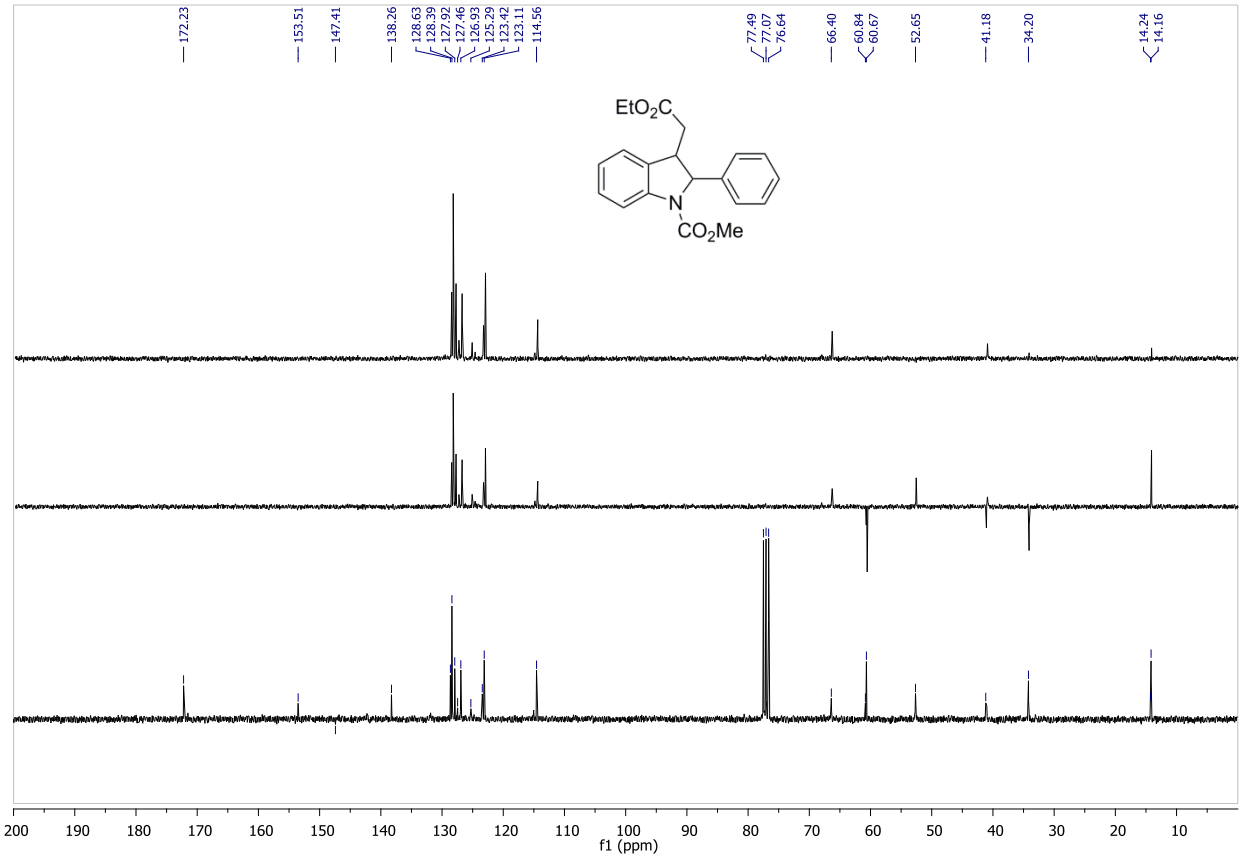

^{1}H-NMR: **8b**

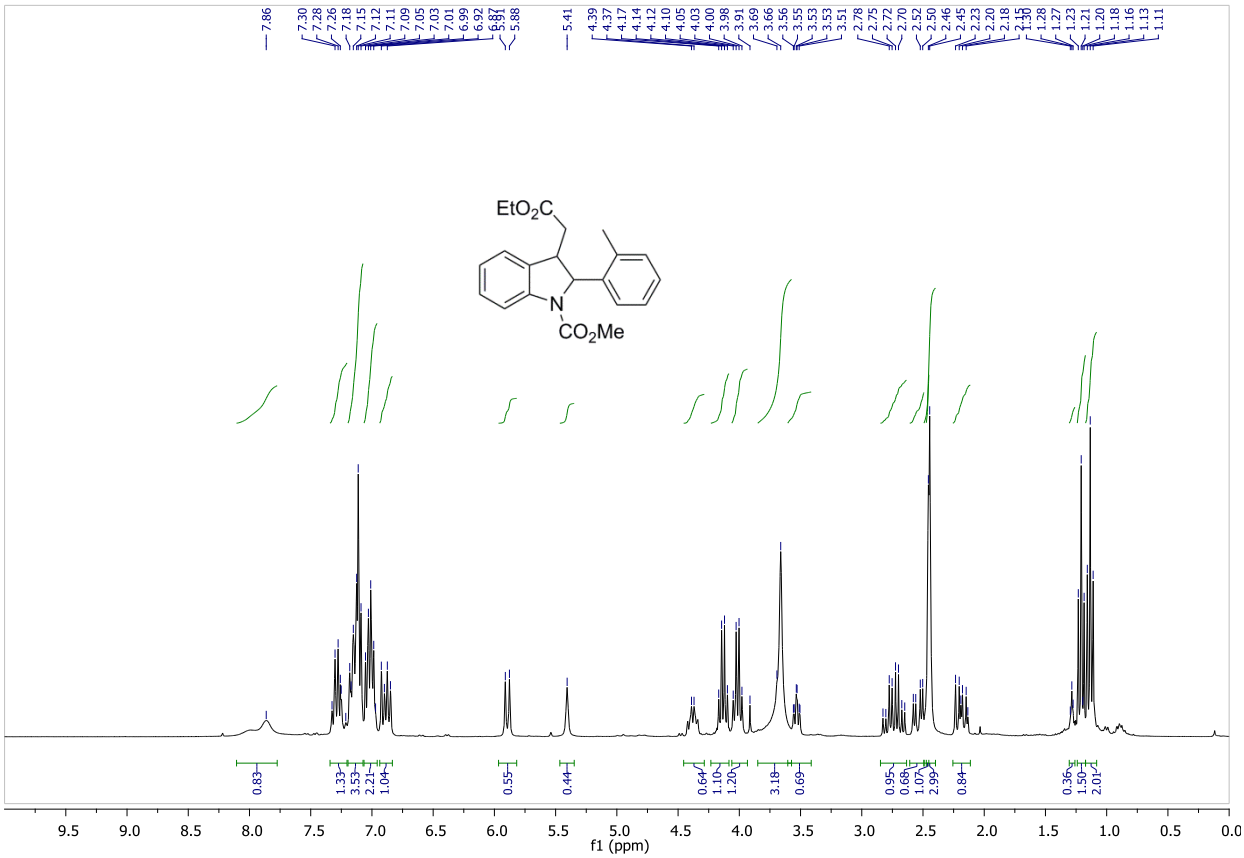

^{13}C-NMR: **8b**

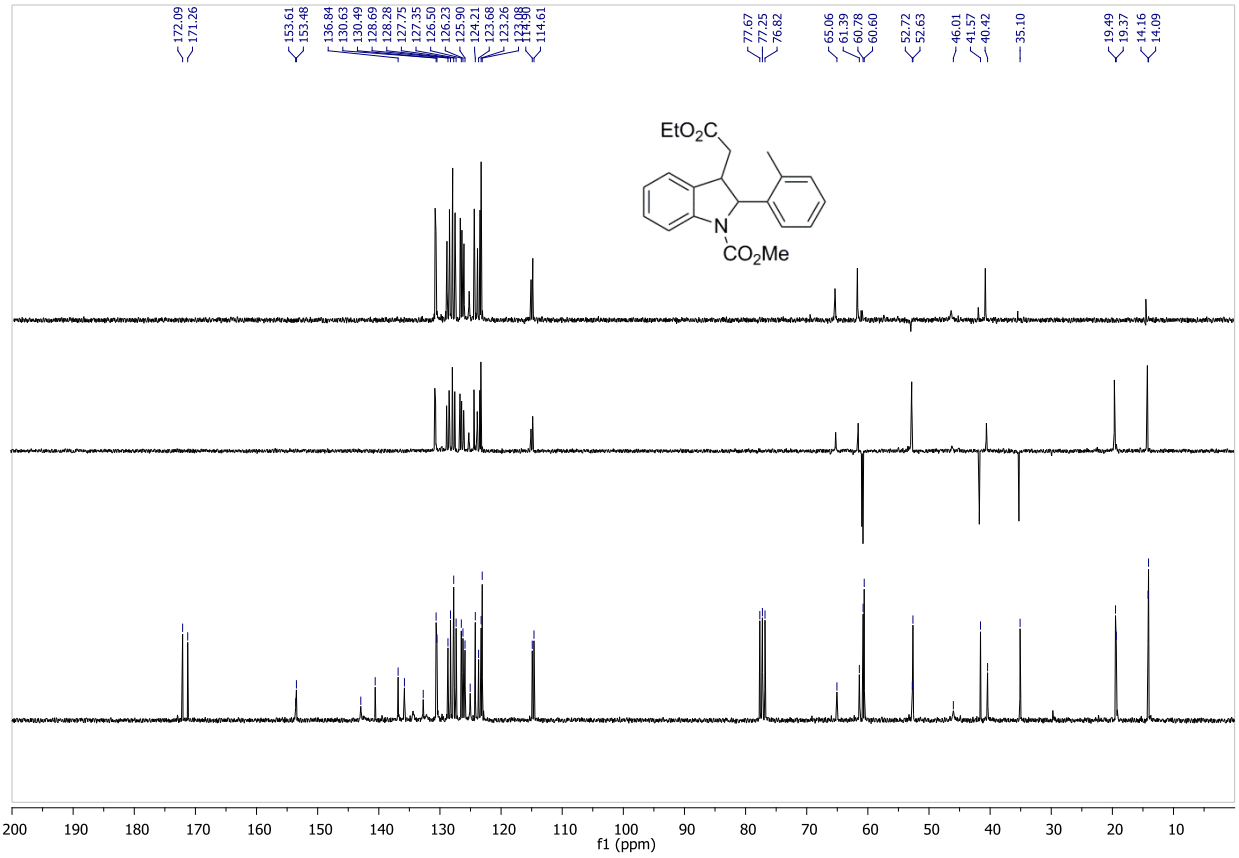

^{1}H-NMR: **8c**

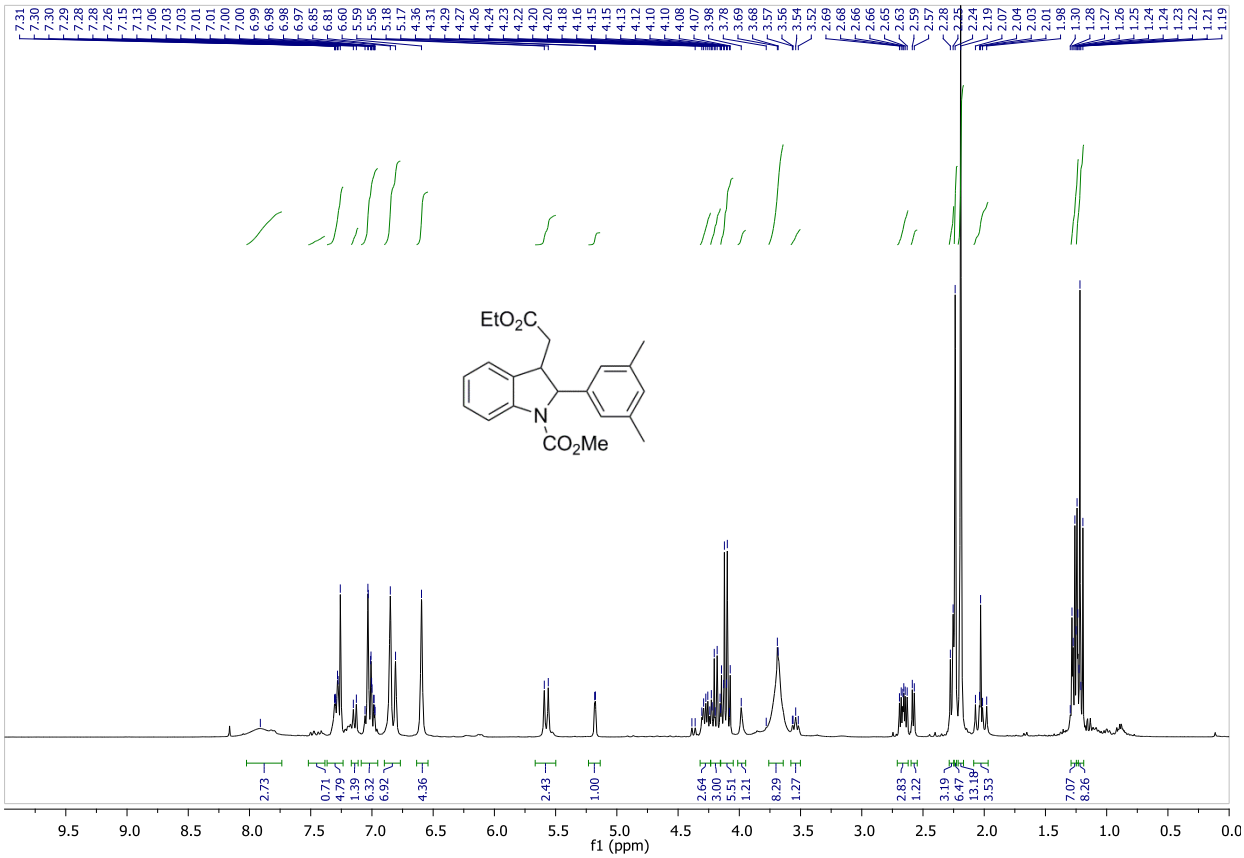

^{13}C-NMR: **8c**

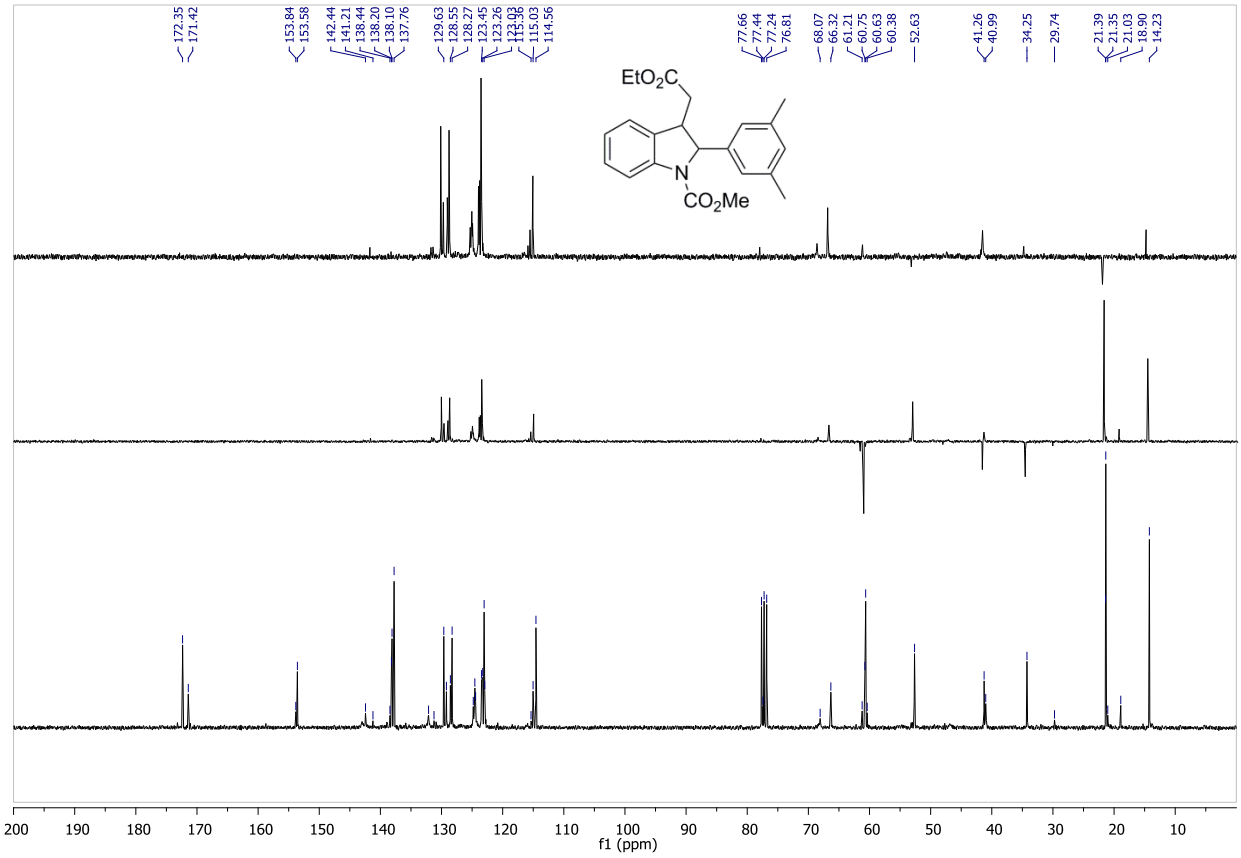

^{1}H-NMR: **8d**

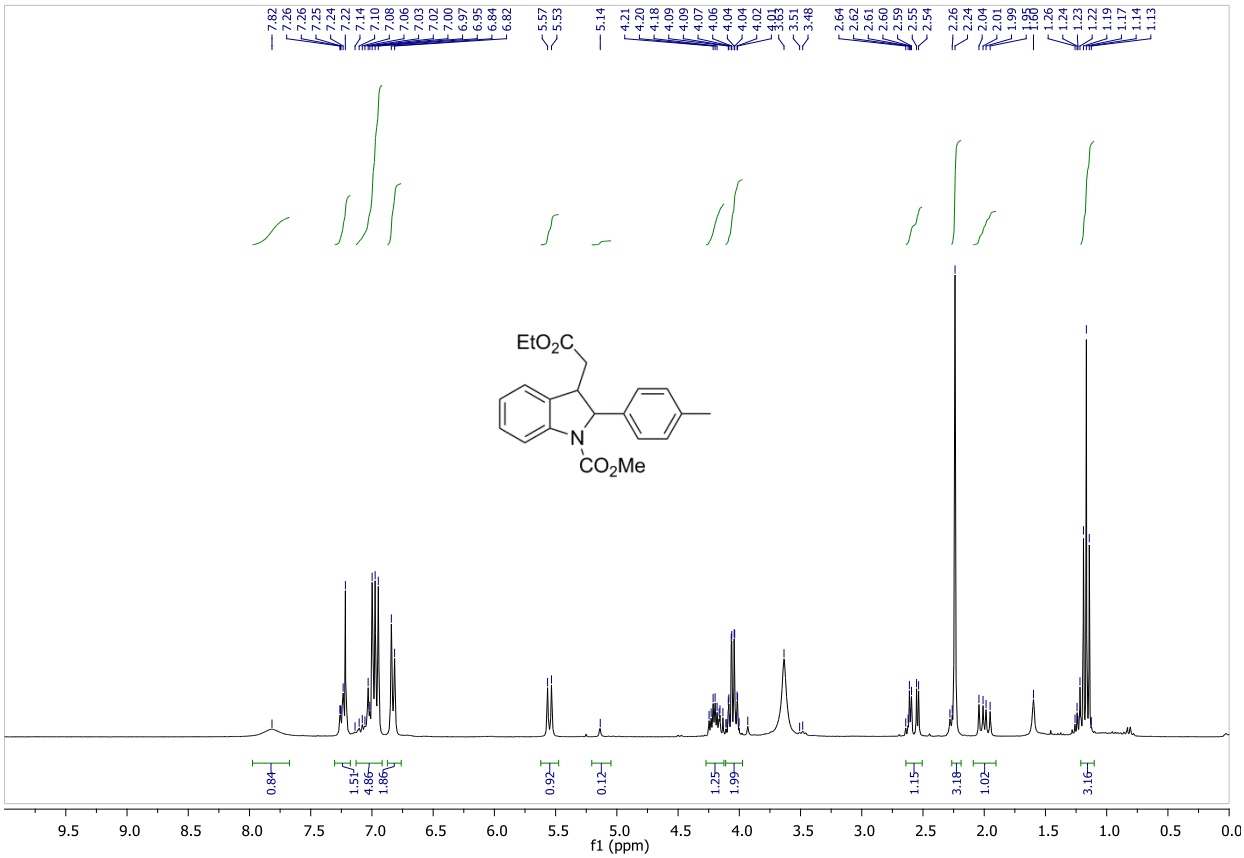

^{13}C-NMR: **8d**

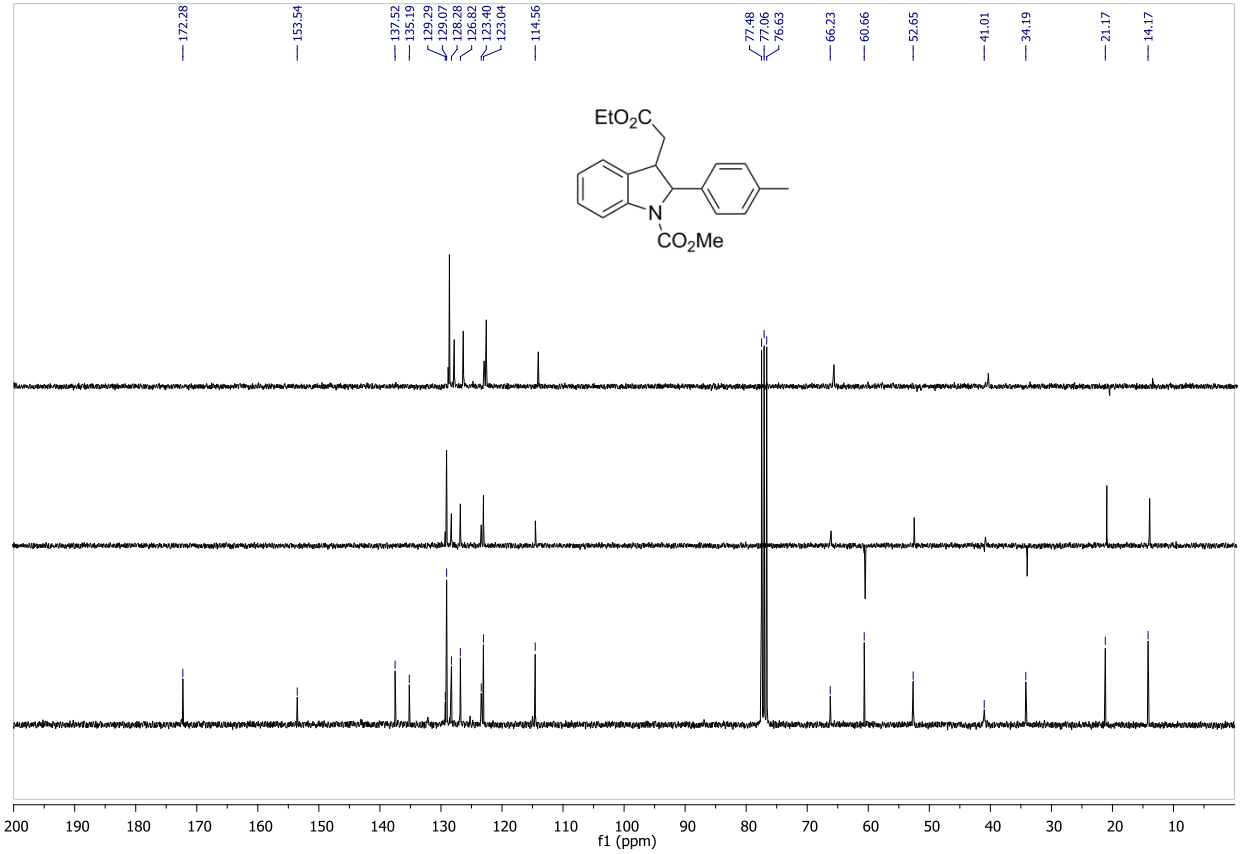

^{1}H-NMR: **8e**

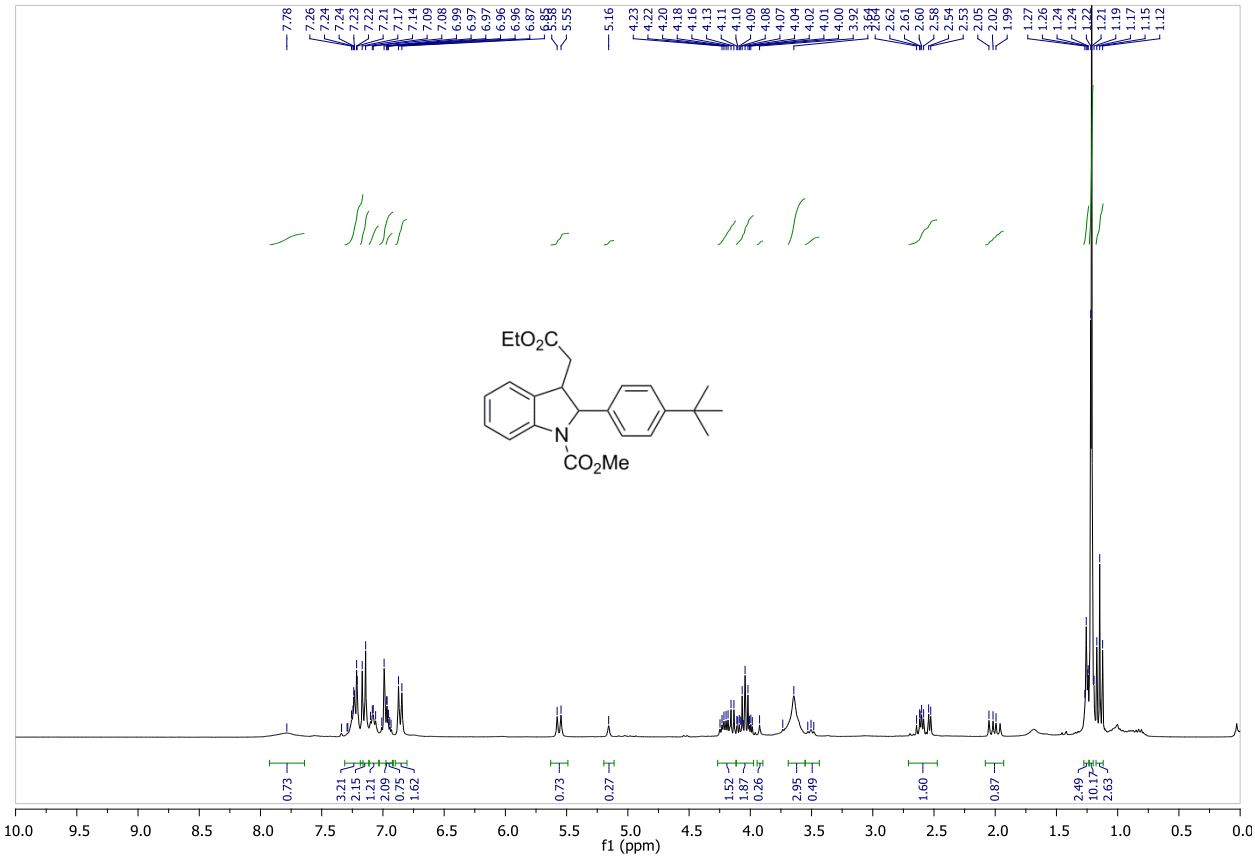

^{13}C-NMR: **8e**

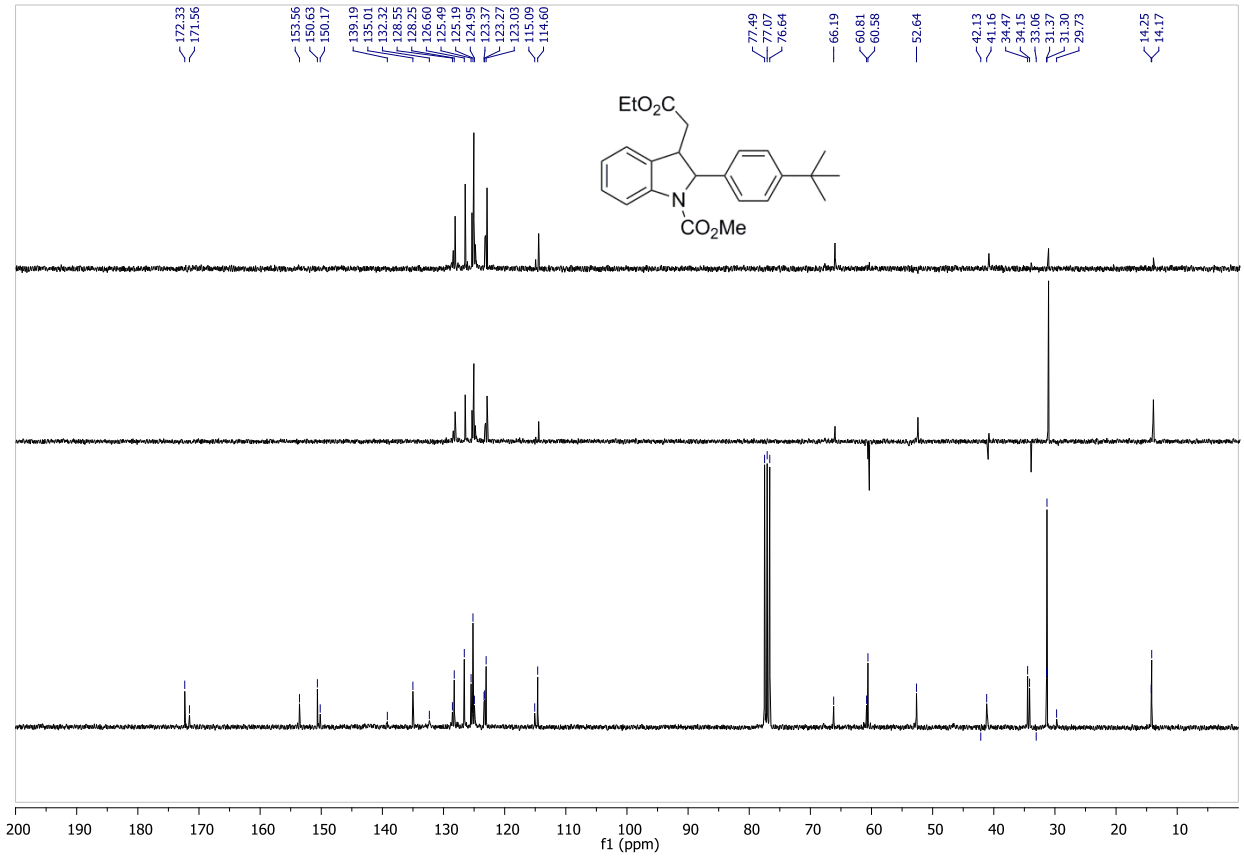

^{1}H-NMR: **8f**

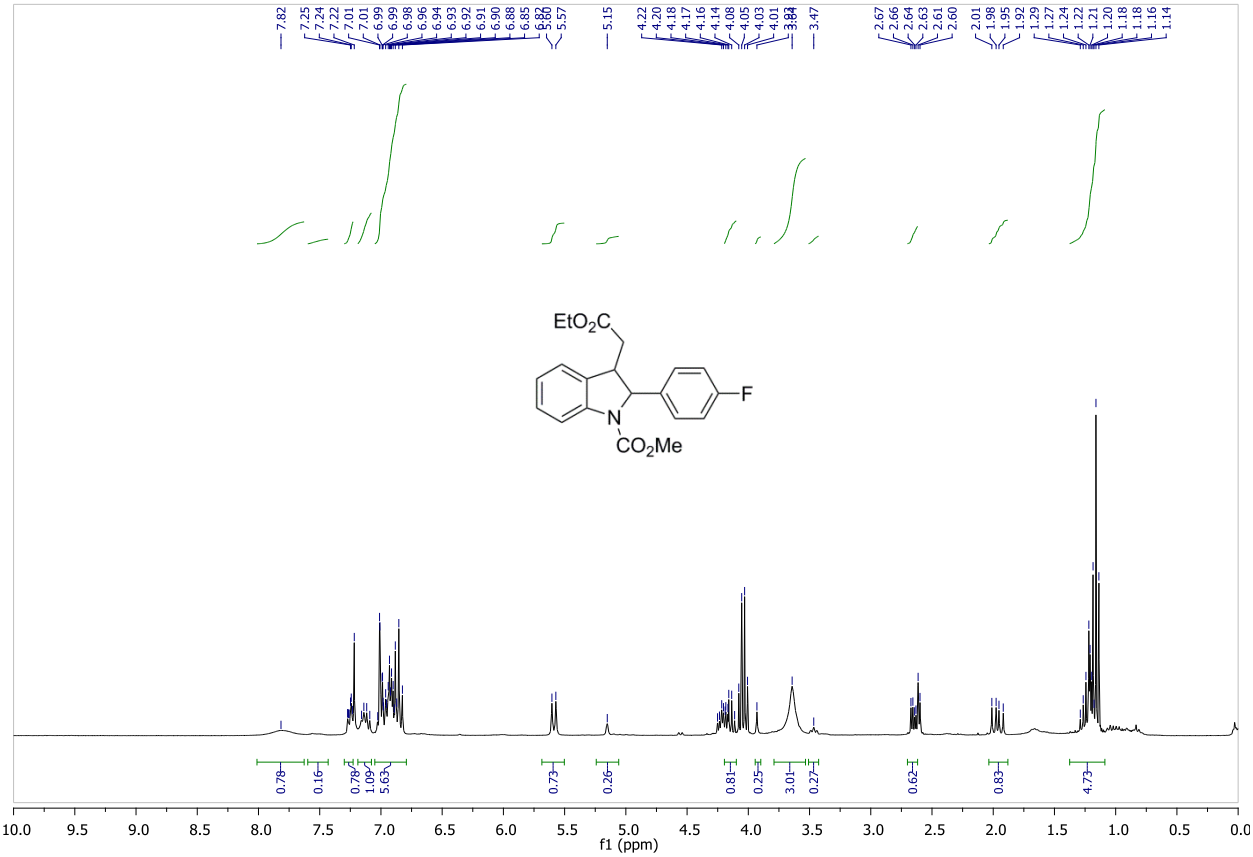

^{13}C-NMR: **8f**

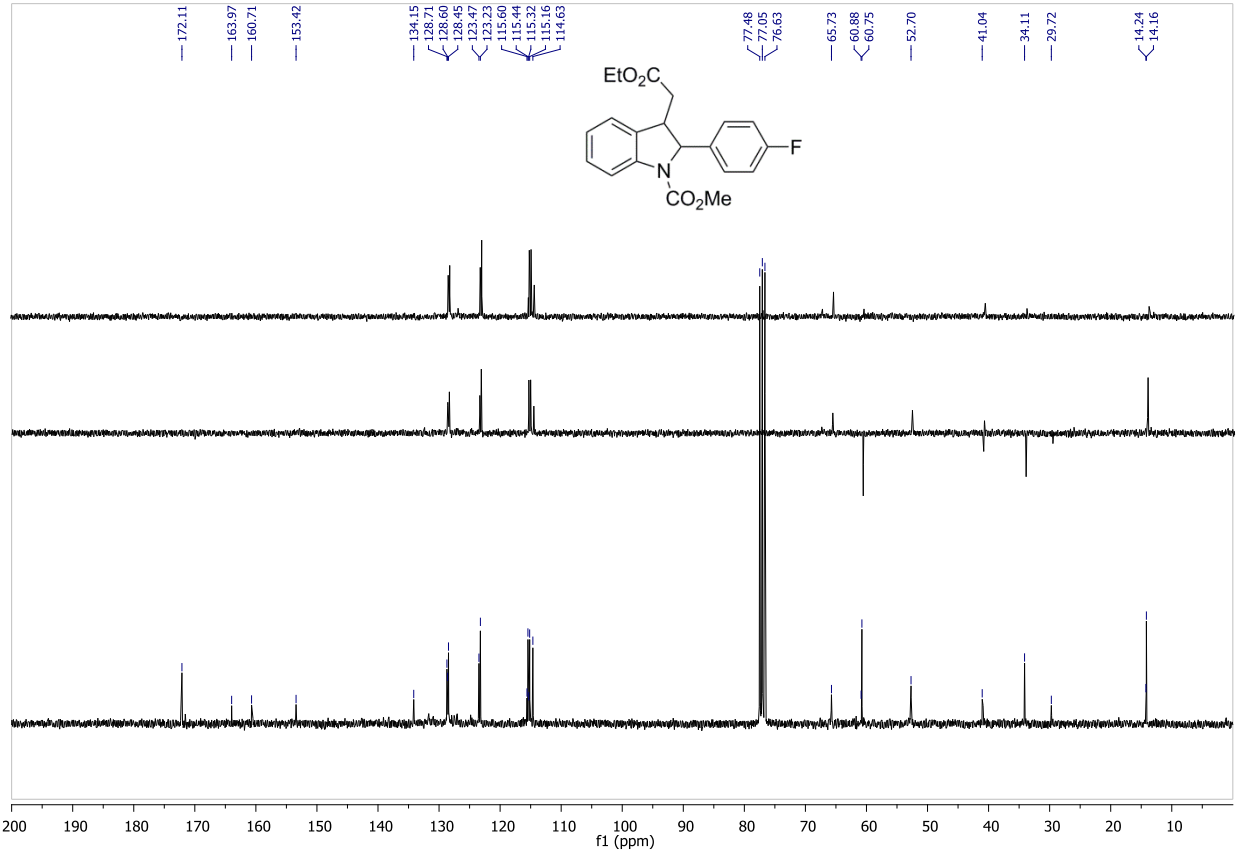

^{19}F-NMR: **8f**

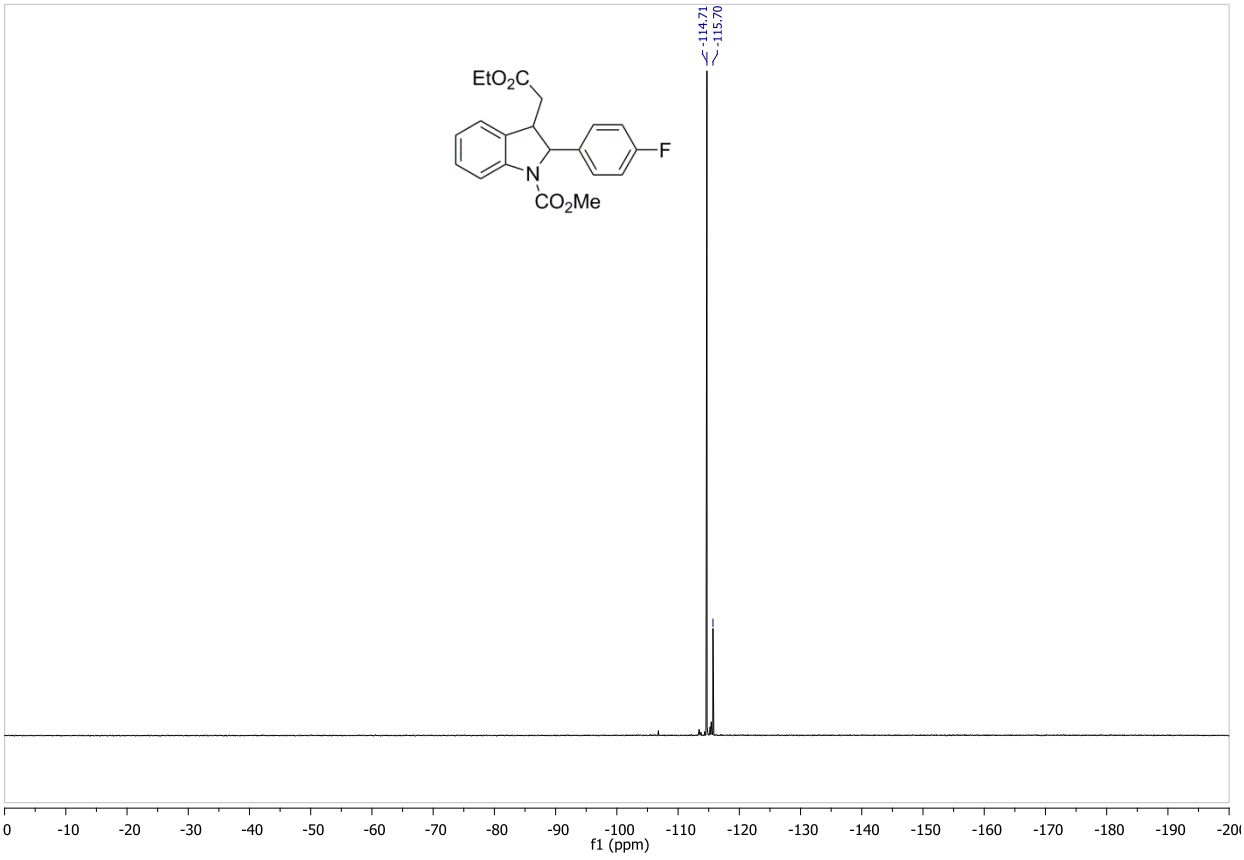
-114.71
-115.70
EtO2C
F
N
CO2Me
0
-10
-20
-30
-40
-50
-60
-70
-80
-90
-100
-110
-120
-130
-140
-150
-160
-170
-180
-190
f1 (ppm)

^{1}H-NMR: **8g**

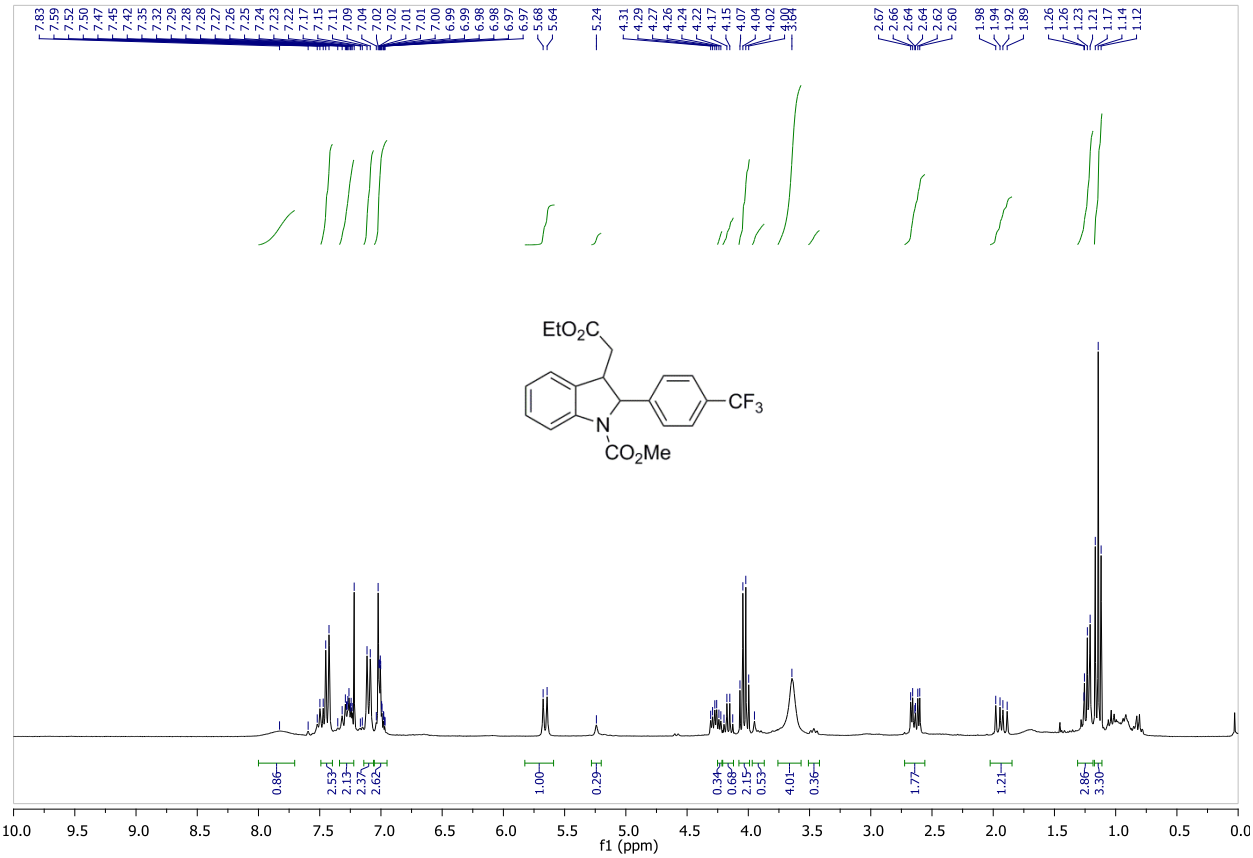

^{13}C-NMR: **8g**

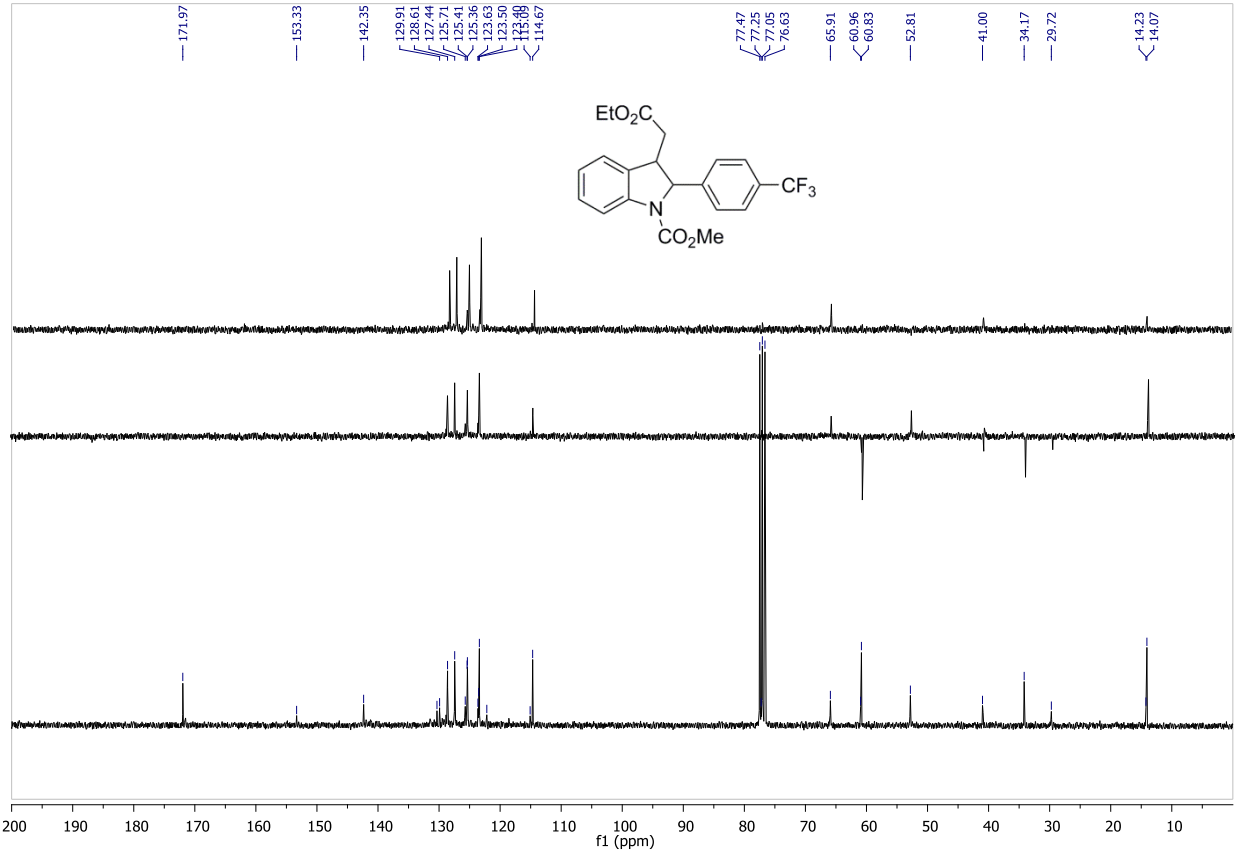

^{19}F-NMR: **8g**

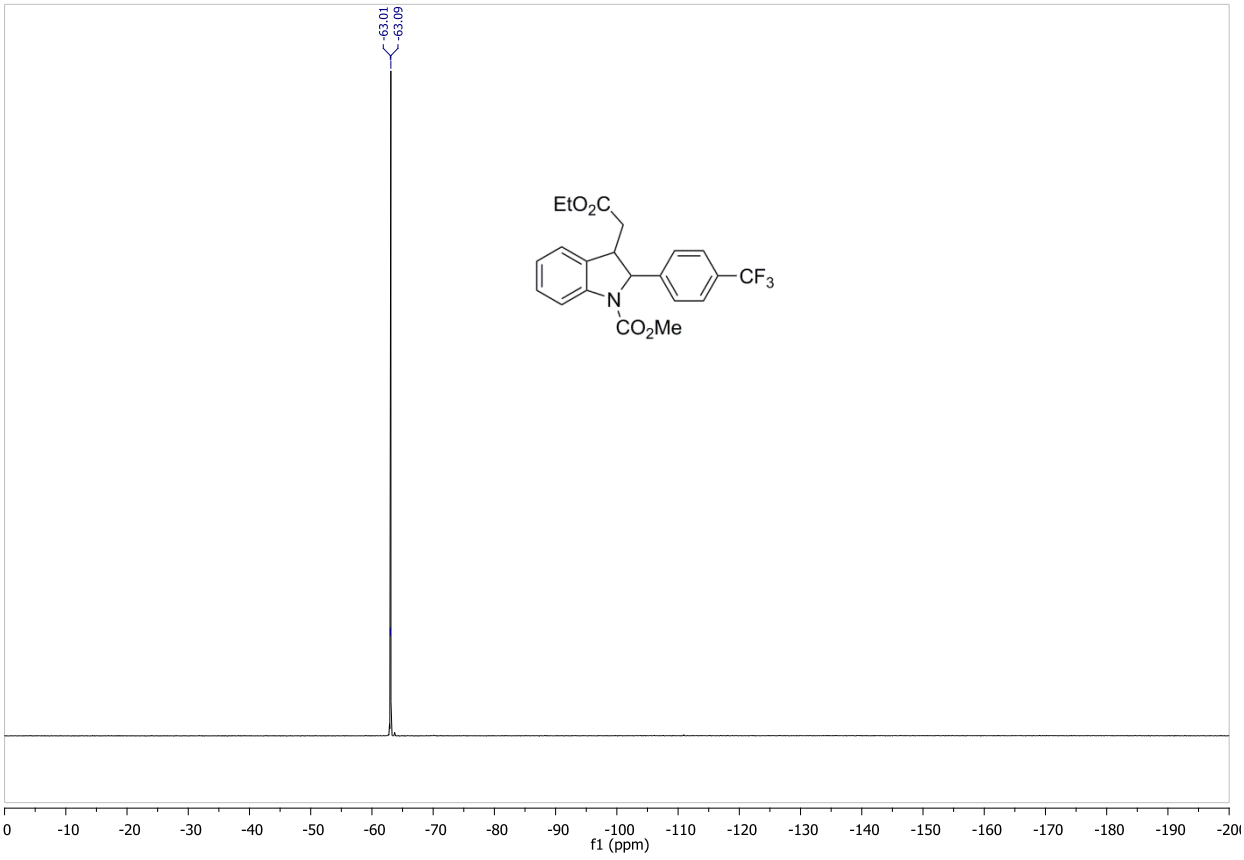
-63.01
-63.09
EtO2C
CF3
N
CO2Me
0
-10
-20
-30
-40
-50
-60
-70
-80
-90
-100
-110
-120
-130
-140
-150
-160
-170
-180
-190
f1 (ppm)

^{1}H-NMR: **8h**

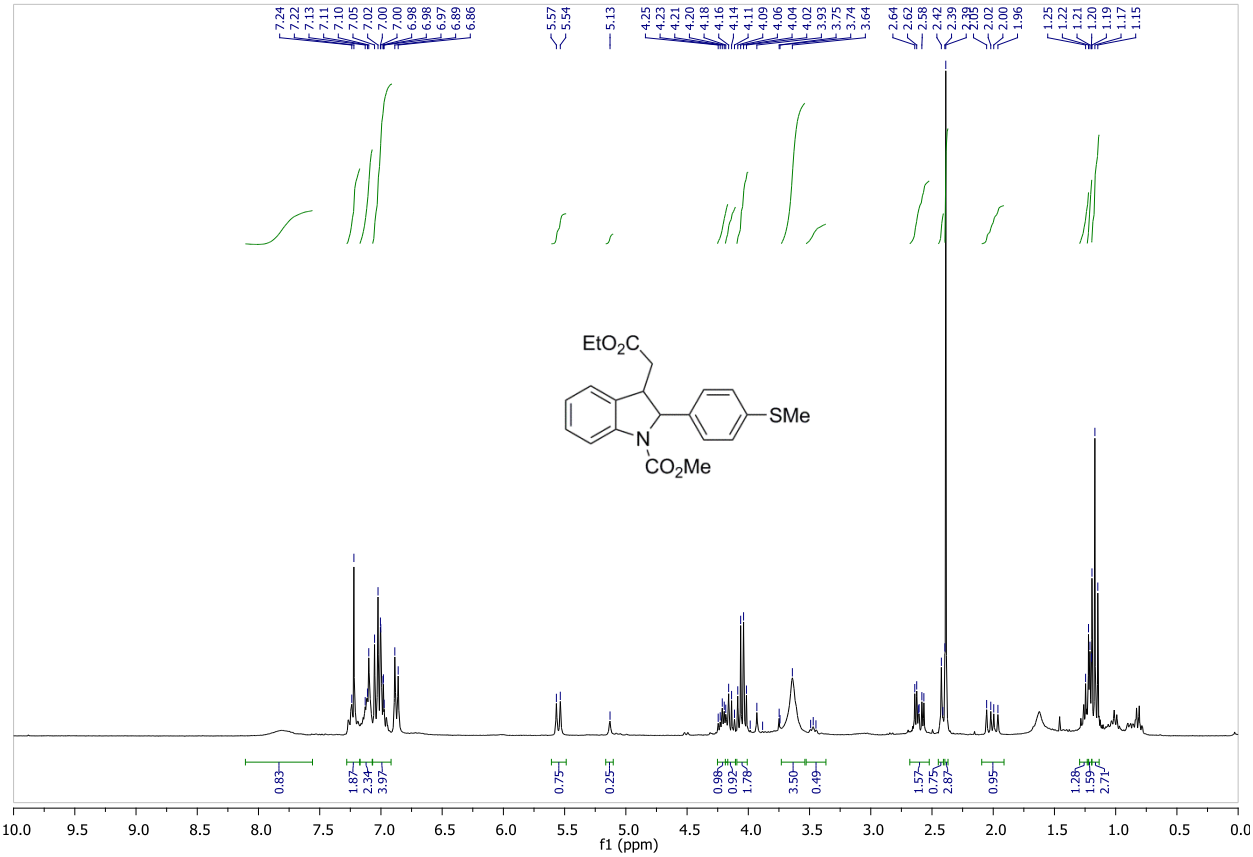

^{13}C-NMR: **8h**

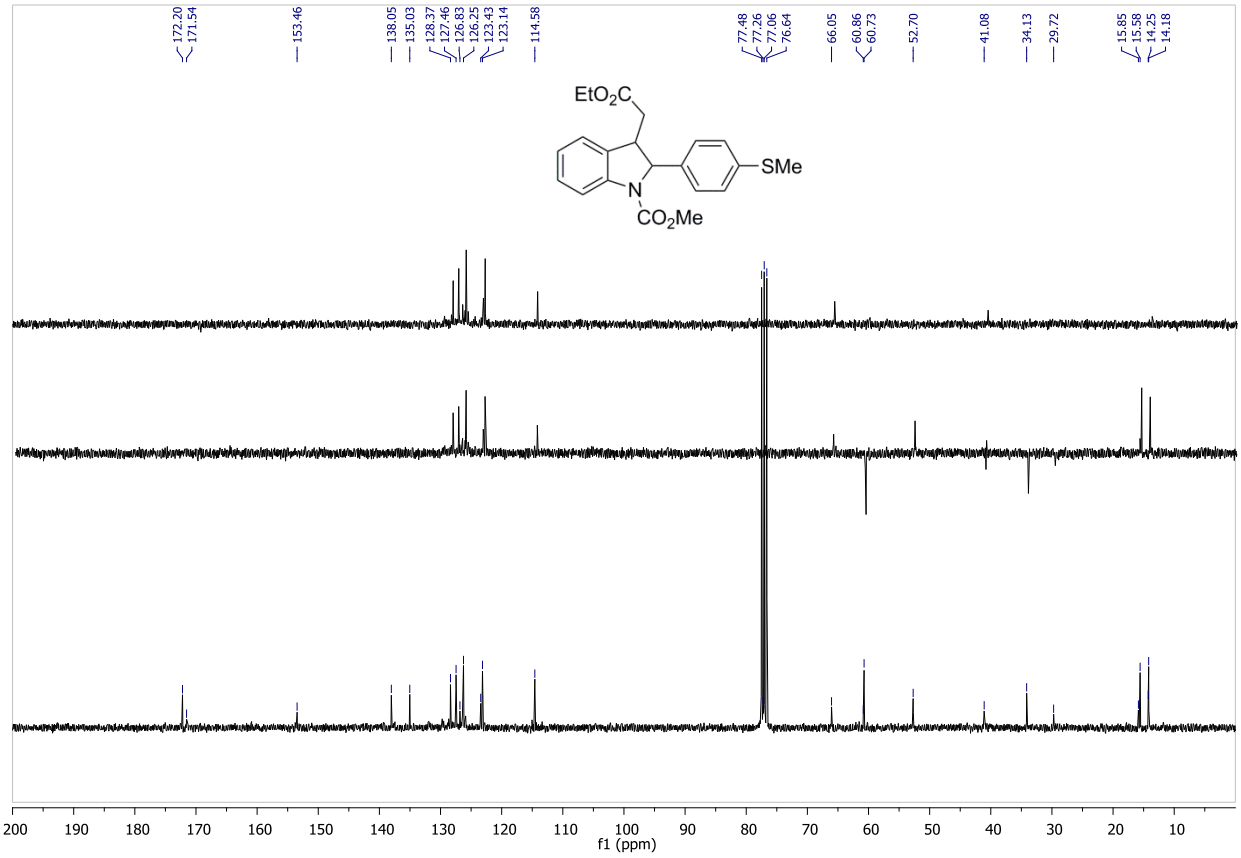

^{1}H-NMR: **8i**

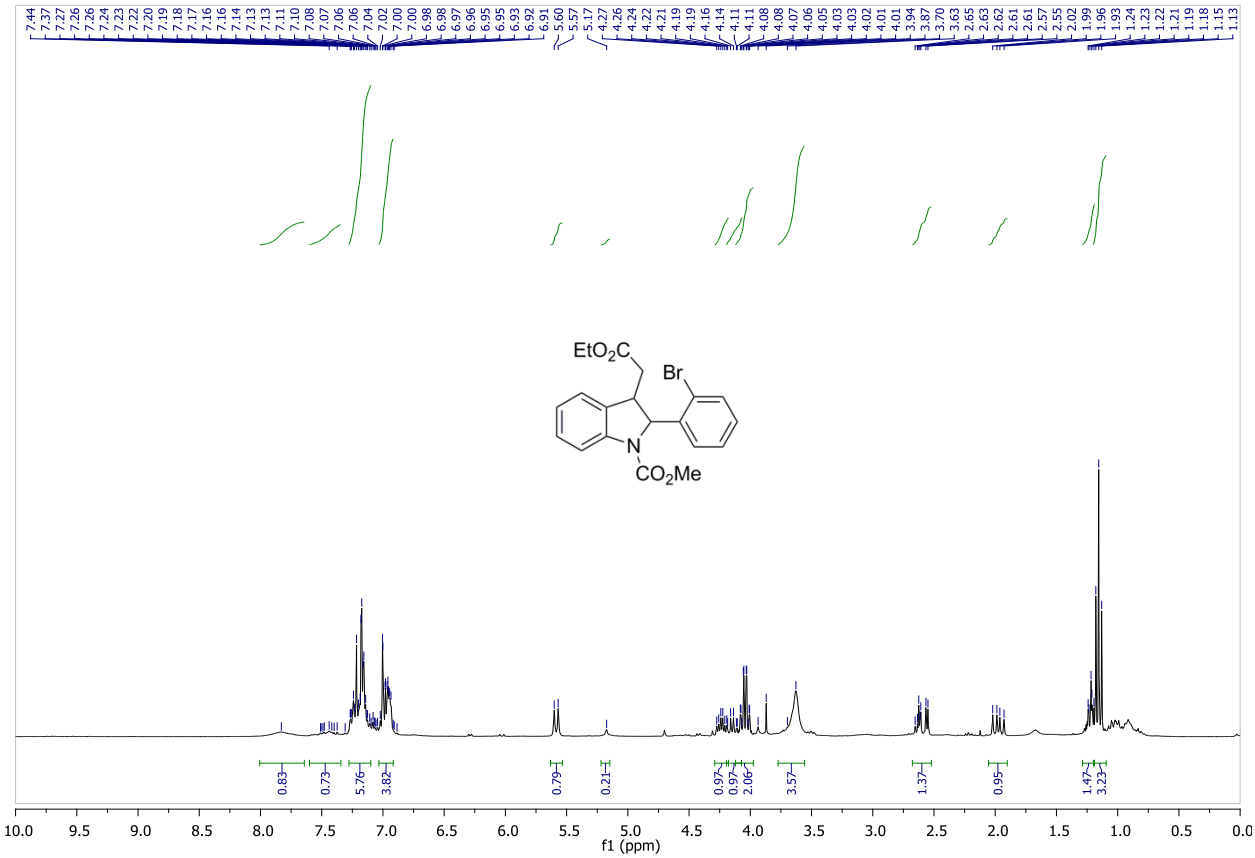

^{13}C-NMR: **8i**

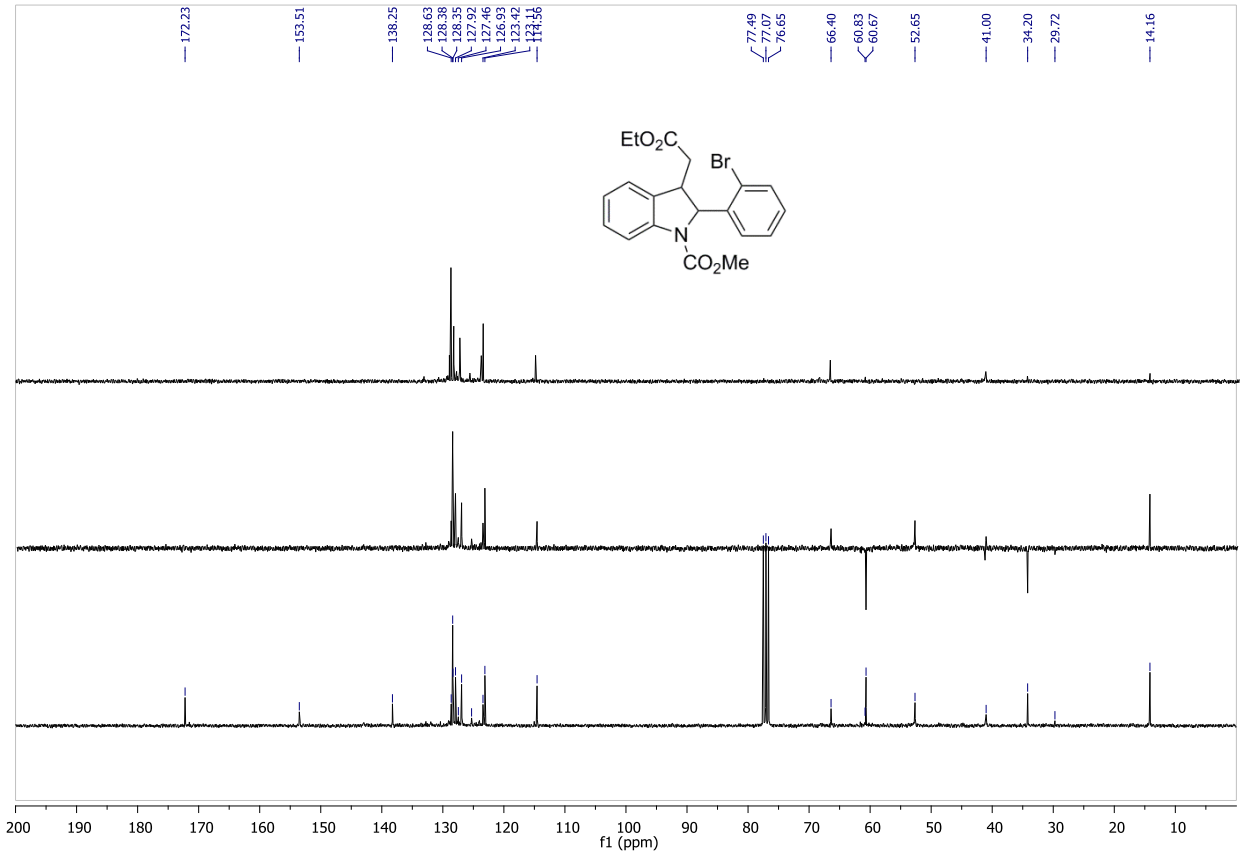

^{1}H-NMR: **8j**

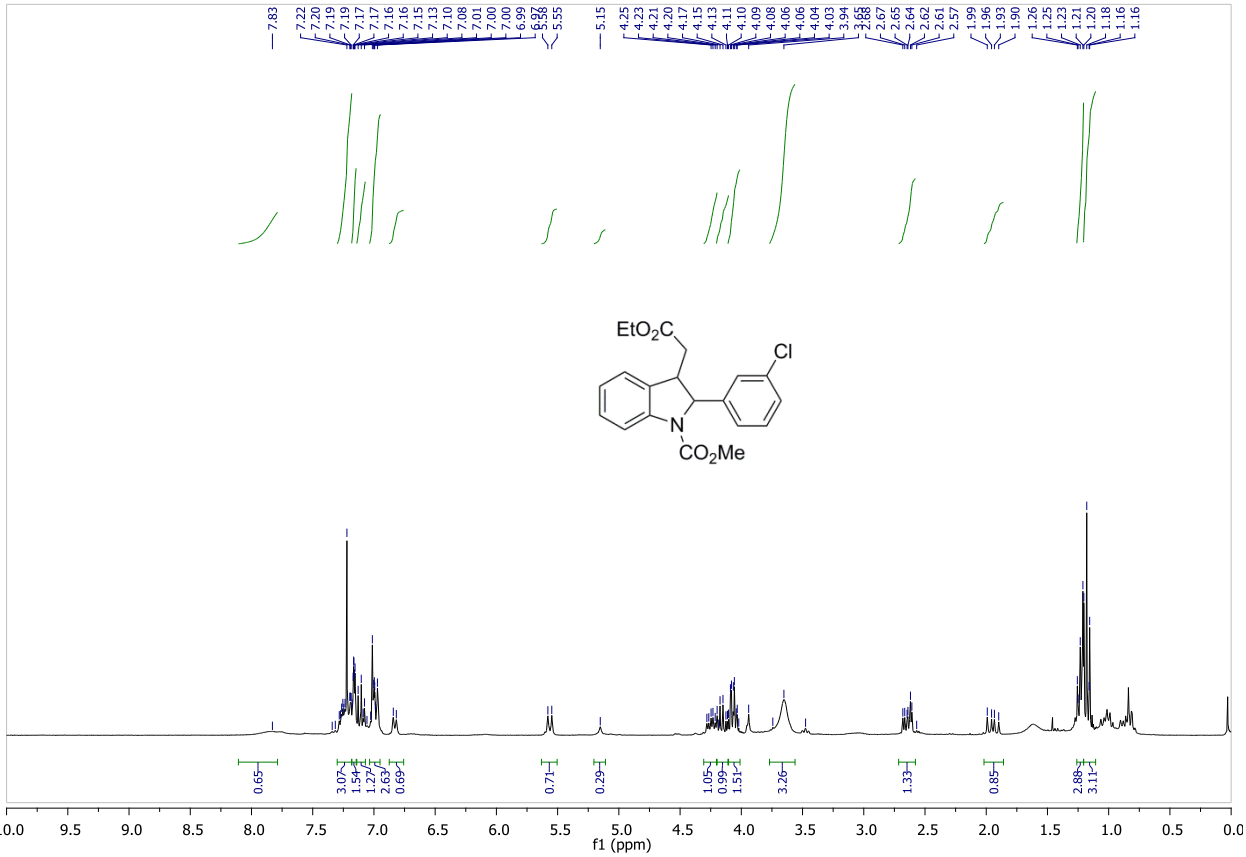

^{13}C-NMR: **8j**

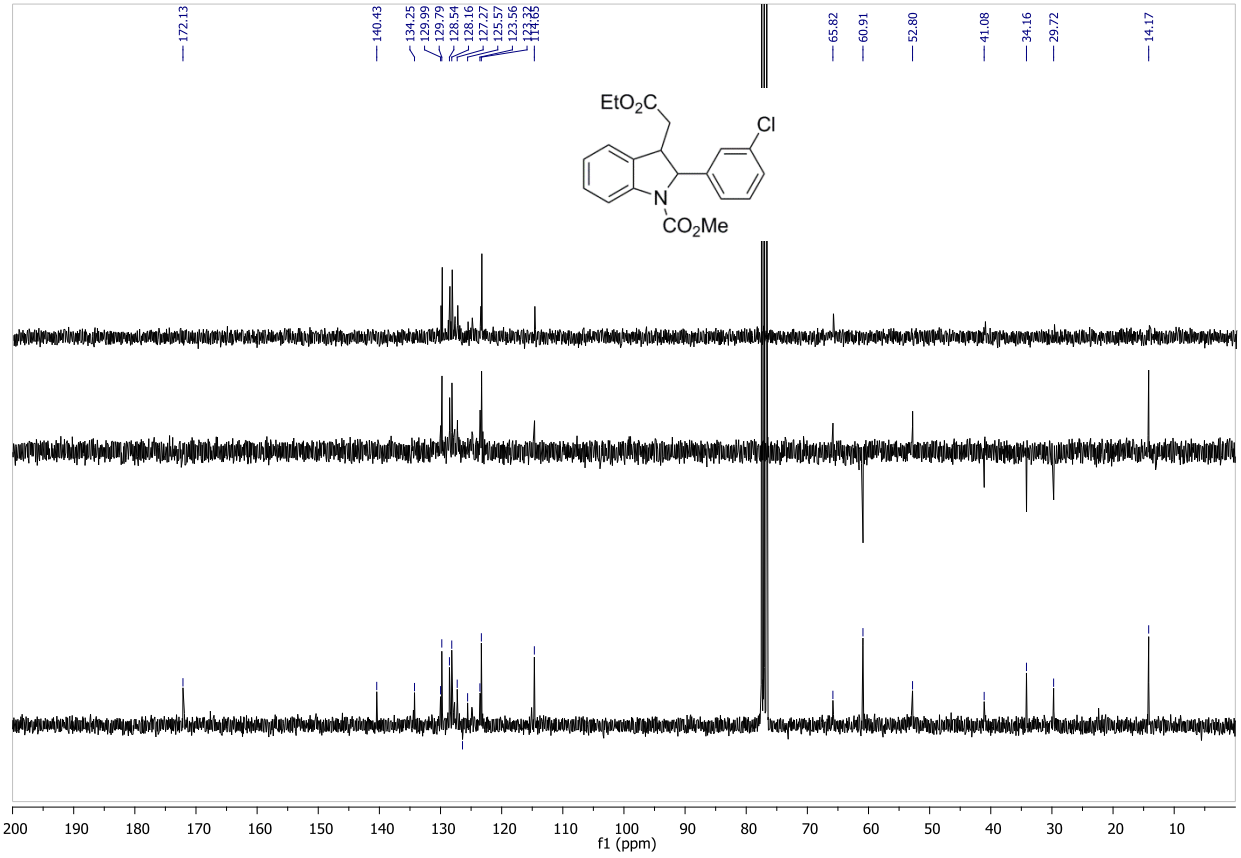

^{1}H-NMR: **9a**

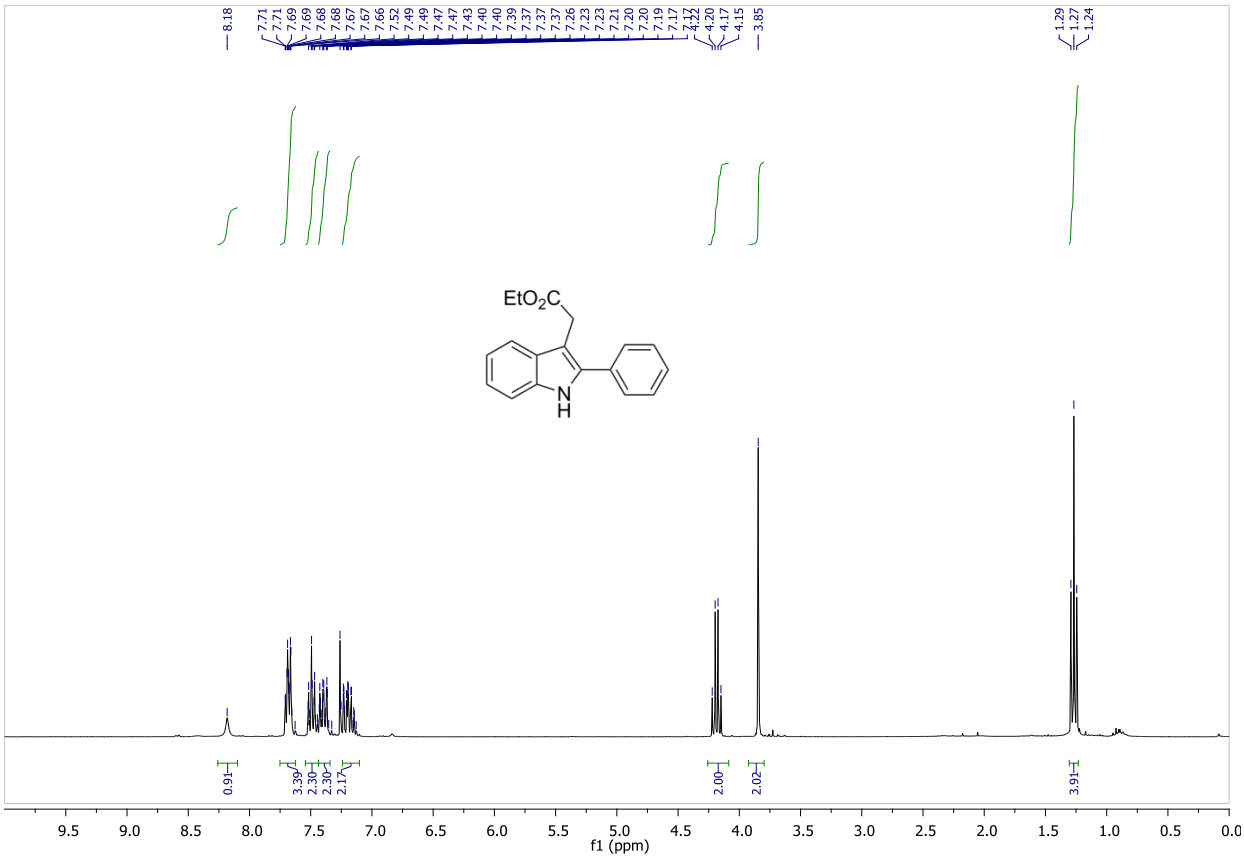

^{13}C-NMR: **9a**

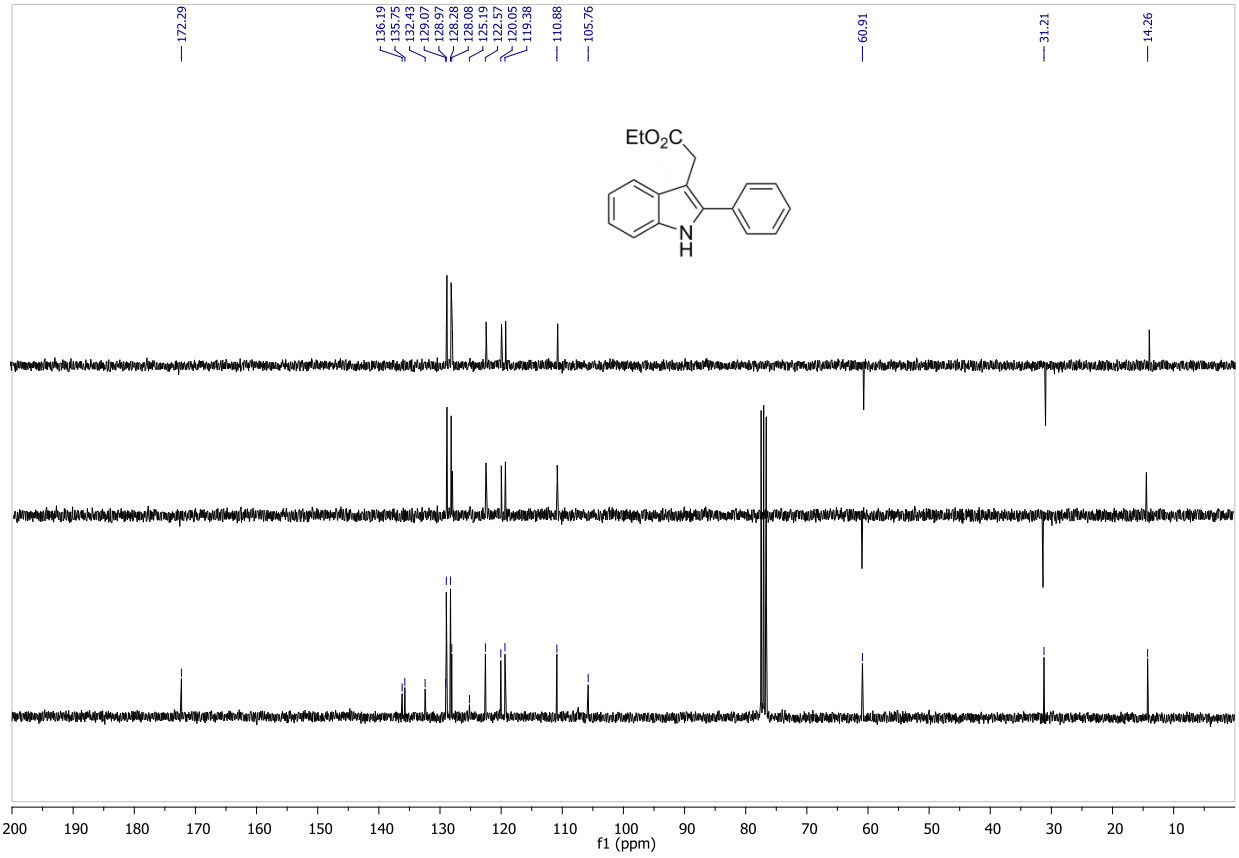

^{1}H-NMR: **9b**

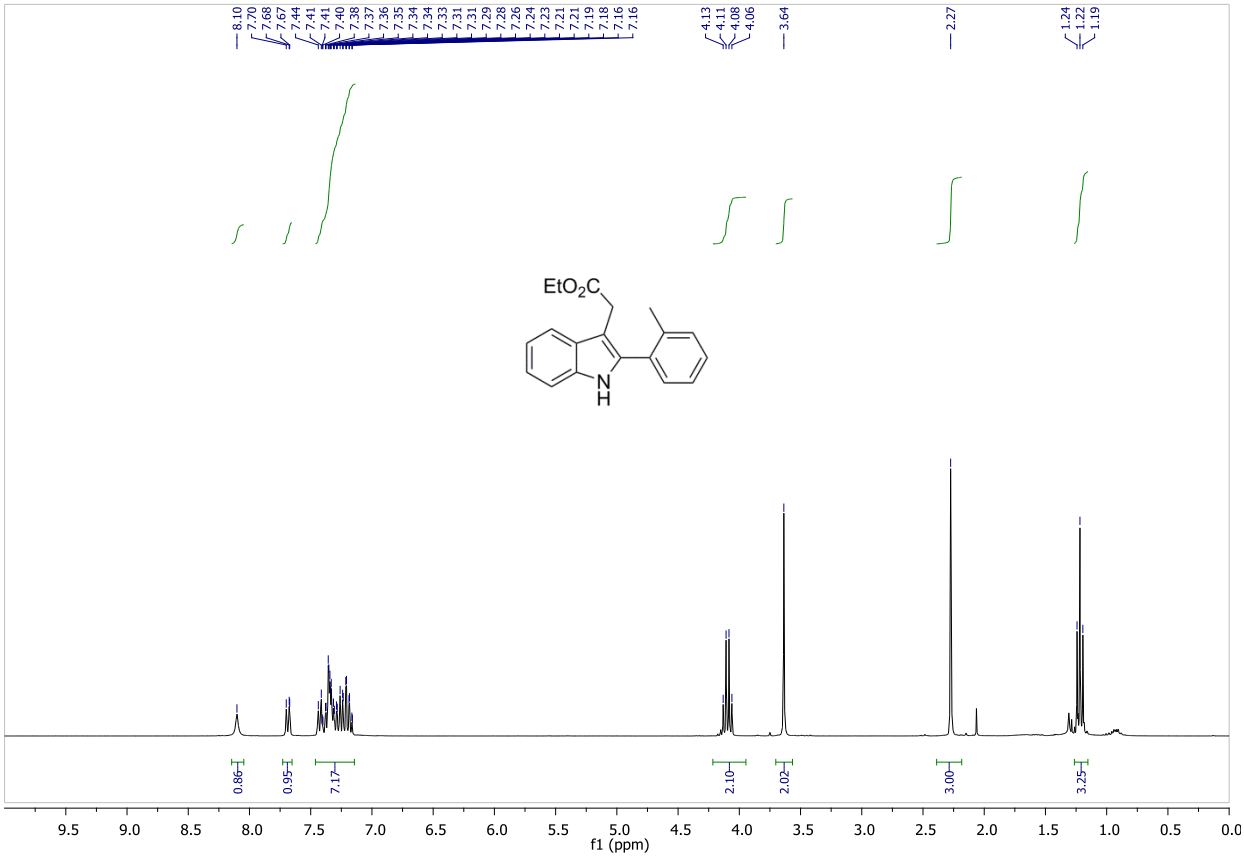

^{13}C-NMR: **9b**

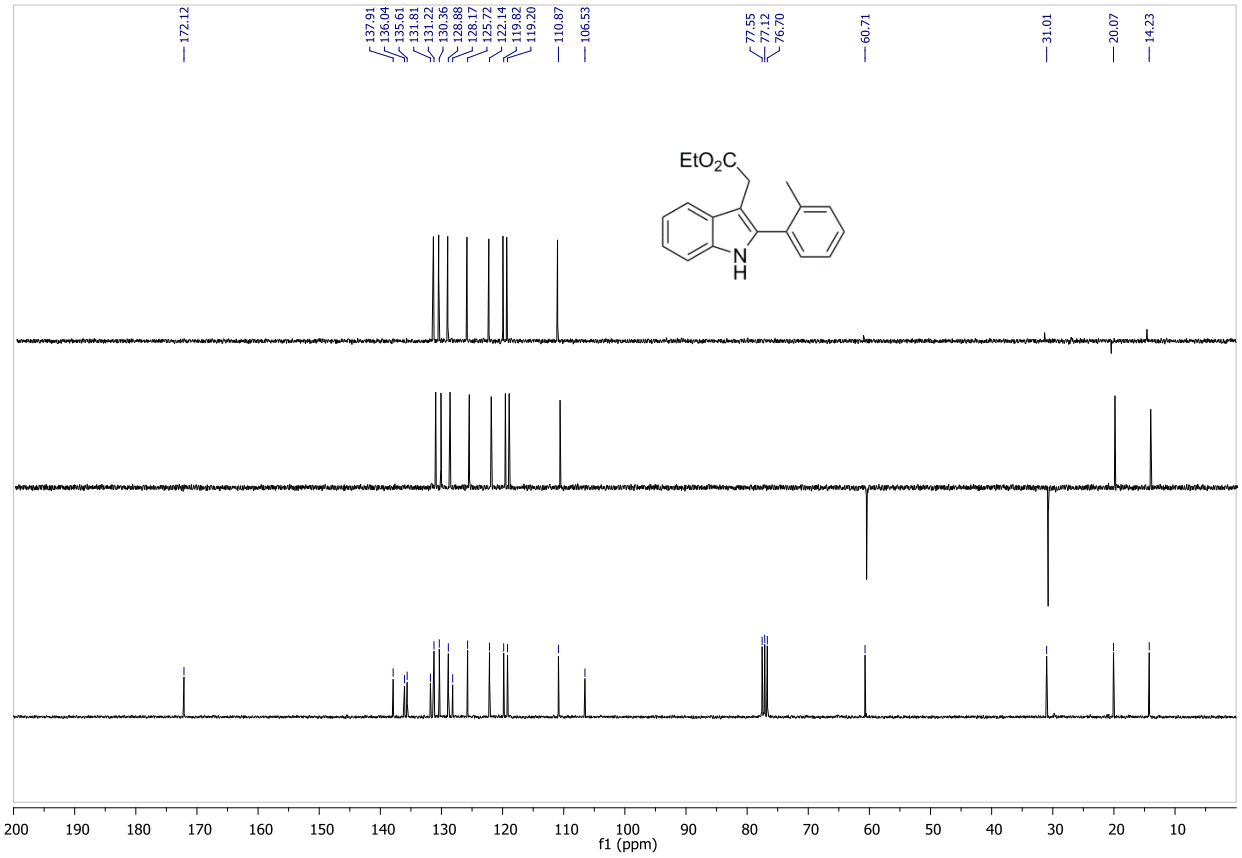

^{1}H-NMR: **10**

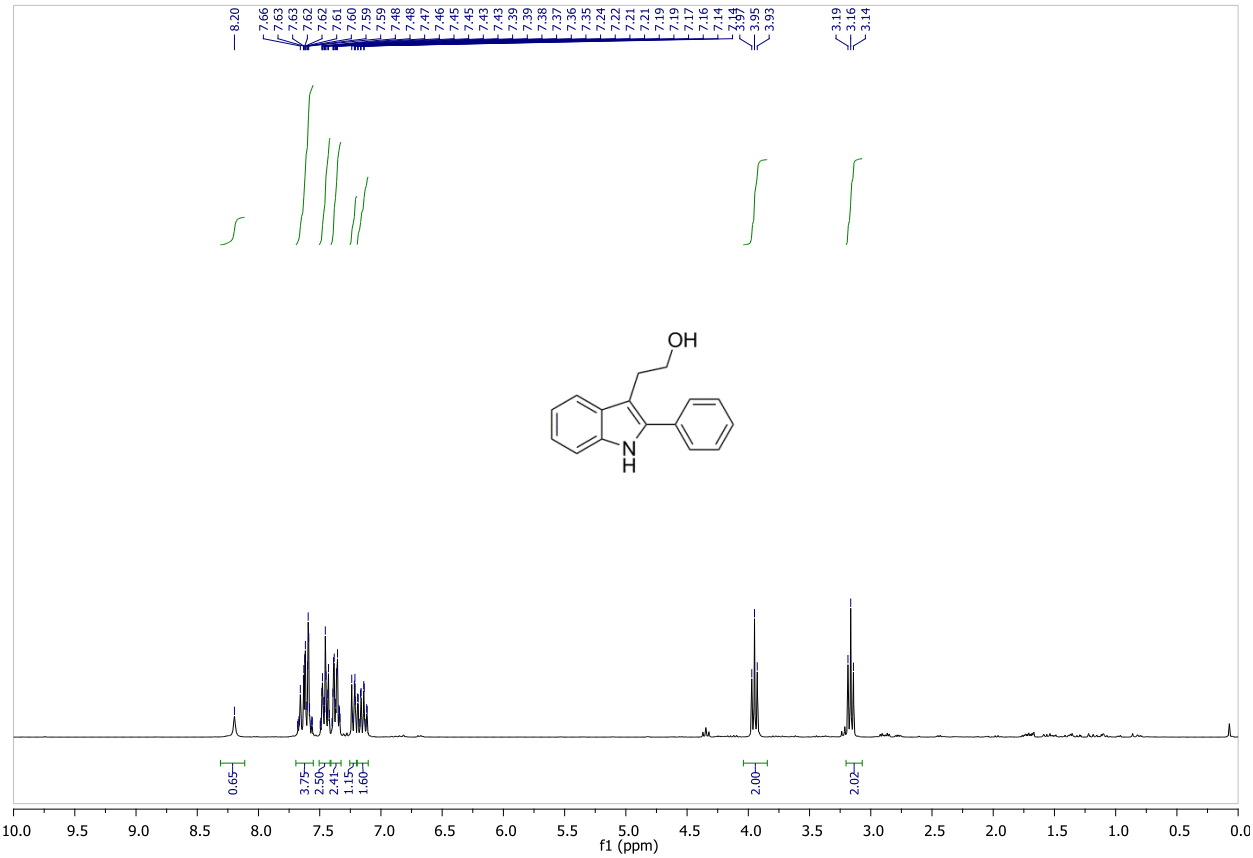

^{13}C-NMR: **10**

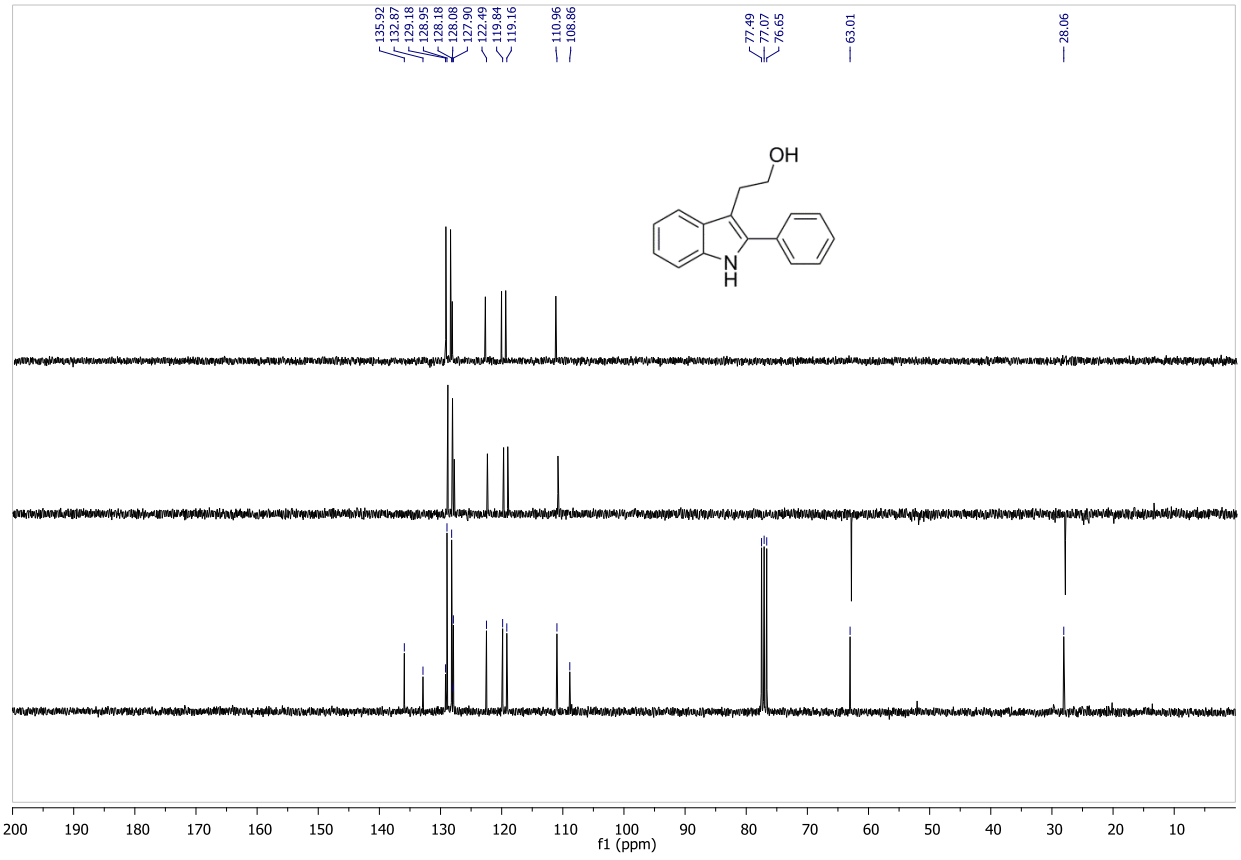

5.11 Crystal data: 8b

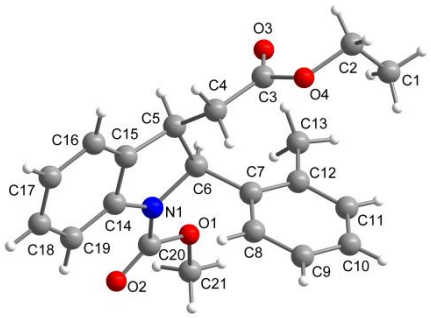

Figure 5.4: Single-crystal X-ray crystallographic analysis of **8b.**

Crystal data. $C_{21}H_{23}NO_4$, M_r = 353.40, monoclinic, $P2_1/c$ (No. 14), a = 10.2857(2) Å, b = 22.5658(4) Å, c = 7.71479(14) Å, β = 97.8249(18)°, α = γ = 90°, V = 1773.97(6) Å^3, T = 123.01(10) K, Z = 4, Z' = 1, μ(CuK_α) = 0.742, 15306 reflections measured, 3706 unique (R_{int} = 0.0331) which were used in all calculations. The final wR_2 was 0.1167 (all data) and R_1 was 0.0422 (I > 2(I)).

Compound	**8b**
Formula	$C_{21}H_{23}NO_4$
$D_{calc.}$/ g cm^{-3}	1.323
μ/mm^{-1}	0.742
Formula weight	353.40
Colour	clear colourless
Shape	irregular
Size/mm^3	0.30×0.14×0.10
T/K	123.01(10)
Crystal system	monoclinic
Space group	$P2_1/c$
a/Å	10.2857(2)
b/Å	22.5658(4)
c/Å	7.71479(14)
α/°	90
β/°	97.8249(18)
γ/°	90
V/Å^3	1773.97(6)
Z	4
Z'	1
Wavelength/Å	1.54184
Radiation type	CuK_α
Θ_{min}/°	3.918
Θ_{max}/°	76.327
Measured refl.	15306
Independent refl.	3706
Reflections used	3222
R_{int}	0.0331
Parameters	248
Restraints	0
Largest peak	0.602
Deepest hole	-0.278
GooF	1.034
wR_2 (all data)	0.1167
wR_2	0.1101
R_1 (all data)	0.0487
R_1	0.0422

Table 5.4: Fractional atomic coordinates (×10^4) and equivalent isotropic displacement parameters (Å^2×10^3) for **8b**. U_{eq} is defined as 1/3 of the trace of the orthogonalised U_{ij}.

Atom	**x**	**y**	**z**	U_{eq}
O(4)	2038.1(10)	7329.3(4)	2472.2(14)	28.1(2)
O(2)	3276.6(11)	5048.7(5)	408.5(13)	30.5(2)
O(3)	3679.0(11)	7940.0(5)	3639.7(15)	31.4(3)
O(1)	3913.0(19)	4509.9(10)	2840.1(19)	26.5(6)
N(1)	4081.2(11)	6984.5(5)	2883.9(15)	23.0(2)
C(7)	2808.4(13)	6117.5(6)	3630.0(18)	21.6(3)
C(15)	5459.3(14)	6982.9(6)	3221.3(17)	22.6(3)
C(8)	3399.3(14)	6099.6(6)	5368.2(18)	24.2(3)
C(20)	3306.9(14)	7462.3(6)	3057.8(18)	23.6(3)

Atom	x	y	z	U_{eq}
C(12)	1541.8(14)	5884.5(6)	3188.7(18)	23.8(3)
C(6)	3556.6(13)	6395.2(6)	2268.5(17)	21.6(3)
C(3)	3937.9(14)	4993.7(6)	1817.9(19)	25.5(3)
C(14)	5935.6(14)	6445.4(6)	2675.8(17)	23.0(3)
C(4)	4973.4(14)	5419.5(6)	2623.4(18)	23.7(3)
C(9)	2782.3(15)	5836.9(6)	6660.8(18)	26.0(3)
C(5)	4817.7(13)	6048.8(6)	1898.4(17)	22.1(3)
C(16)	6301.2(15)	7422.4(7)	3978.6(19)	27.0(3)
C(11)	927.3(15)	5629.4(6)	4515(2)	27.7(3)
C(19)	7273.3(14)	6339.0(7)	2864.5(19)	28.6(3)
C(10)	1541.4(15)	5596.9(6)	6226.4(19)	28.6(3)
C(13)	812.5(15)	5911.0(7)	1353(2)	30.6(3)
C(17)	7646.0(15)	7308.0(7)	4152(2)	32.1(3)
C(18)	8134.5(15)	6777.9(7)	3601(2)	33.2(3)
C(21)	1125.6(16)	7803.7(7)	2589(3)	37.9(4)
C(2)	3024.9(17)	4030.4(7)	2189(2)	36.3(4)
C(1)	1657.3(18)	4166.4(8)	2492(2)	41.2(4)
O(1A)	3390(20)	4726(7)	3131(15)	31(4)

Table 5.5: Anisotropic displacement parameters (×10^4) **8b**. The anisotropic displacement factor exponent takes the form: $-2\pi^2[h^2a^{*2} \times U_{11} + \ldots + 2hka^* \times b^* \times U_{12}]$

Atom	U_{11}	U_{22}	U_{33}	U_{23}	U_{13}	U_{12}
O(4)	24.6(5)	20.4(5)	38.9(6)	-0.4(4)	2.8(4)	4.1(4)
O(2)	39.4(6)	28.6(5)	23.3(5)	2.3(4)	3.7(4)	-1.1(4)
O(3)	34.0(6)	21.1(5)	38.3(6)	-4.5(4)	2.0(5)	1.7(4)
O(1)	29.6(9)	20.6(9)	28.6(6)	4.7(5)	0.9(6)	-0.7(7)
N(1)	22.9(6)	18.7(5)	27.8(6)	0.4(4)	4.3(4)	-0.2(4)
C(7)	23.7(6)	16.9(6)	24.6(6)	0.6(5)	5.1(5)	3.0(5)
C(15)	24.3(7)	23.3(6)	20.6(6)	3.3(5)	4.5(5)	-0.1(5)
C(8)	25.6(7)	21.5(6)	25.4(7)	-0.6(5)	3.3(5)	1.6(5)
C(20)	27.0(7)	20.8(6)	23.3(6)	1.9(5)	4.4(5)	1.9(5)
C(12)	24.5(7)	20.7(6)	25.9(7)	0.0(5)	2.7(5)	0.9(5)
C(6)	23.4(6)	18.2(6)	23.0(6)	0.5(5)	2.6(5)	0.8(5)
C(3)	31.2(7)	22.4(7)	23.7(6)	0.3(5)	7.0(5)	1.5(5)
C(14)	24.6(7)	23.3(6)	21.6(6)	2.3(5)	4.7(5)	-0.6(5)
C(4)	26.7(7)	21.3(6)	23.6(6)	0.6(5)	5.1(5)	2.5(5)
C(9)	33.9(8)	22.4(6)	21.7(6)	0.5(5)	3.7(5)	4.1(5)
C(5)	24.1(7)	21.5(6)	21.3(6)	1.3(5)	5.1(5)	1.1(5)
C(16)	30.3(7)	24.5(7)	26.4(7)	-0.5(5)	4.2(6)	-2.9(5)
C(11)	27.3(7)	24.5(7)	32.2(7)	0.0(5)	7.2(6)	-2.6(5)
C(19)	26.4(7)	29.1(7)	31.0(7)	2.4(6)	6.6(6)	2.3(6)
C(10)	36.6(8)	23.5(7)	27.9(7)	2.7(5)	12.4(6)	-1.0(6)
C(13)	26.0(7)	35.5(8)	29.0(7)	2.3(6)	-0.4(6)	-3.0(6)
C(17)	28.1(8)	33.6(8)	33.6(8)	0.3(6)	0.5(6)	-7.9(6)
C(18)	22.7(7)	39.2(8)	37.2(8)	4.7(7)	3.0(6)	-1.0(6)
C(21)	27.4(8)	26.7(7)	58.9(10)	-3.8(7)	3.3(7)	7.4(6)
C(2)	41.1(9)	29.7(8)	37.8(8)	1.0(6)	4.1(7)	0.1(7)
C(1)	40.9(9)	43.3(10)	39.4(9)	6.2(7)	4.9(7)	-0.9(7)
O(1A)	41(9)	17(6)	34(6)	-11(4)	5(5)	10(6)

Table 5.6: Bond lengths in Å for **8b**.

Atom	Atom	Length/Å	Atom	Atom	Length/Å
O(4)	C(20)	1.3554(18)	O(3)	C(20)	1.2096(18)
O(4)	C(21)	1.4346(17)	O(1)	C(3)	1.349(2)
O(2)	C(3)	1.2080(18)	O(1)	C(2)	1.460(2)

Atom	Atom	Length/Å
N(1)	C(15)	1.4059(18)
N(1)	C(20)	1.3579(18)
N(1)	C(6)	1.4883(16)
C(7)	C(8)	1.3954(19)
C(7)	C(12)	1.4032(19)
C(7)	C(6)	1.5194(18)
C(15)	C(14)	1.394(2)
C(15)	C(16)	1.392(2)
C(8)	C(9)	1.386(2)
C(12)	C(11)	1.398(2)
C(12)	C(13)	1.5106(19)
C(6)	C(5)	1.5735(18)

Atom	Atom	Length/Å
C(3)	C(4)	1.5045(19)
C(3)	O(1A)	1.368(14)
C(14)	C(5)	1.5150(19)
C(14)	C(19)	1.385(2)
C(4)	C(5)	1.5267(18)
C(9)	C(10)	1.385(2)
C(16)	C(17)	1.395(2)
C(11)	C(10)	1.386(2)
C(19)	C(18)	1.397(2)
C(17)	C(18)	1.386(2)
C(2)	C(1)	1.489(2)
C(2)	O(1A)	1.748(14)

Table 5.7: Bond angles in ° for **8b**.

Atom	Atom	Atom	Angle/°
C(20)	O(4)	C(21)	114.98(12)
C(3)	O(1)	C(2)	117.35(12)
C(15)	N(1)	C(6)	111.68(11)
C(20)	N(1)	C(15)	125.02(12)
C(20)	N(1)	C(6)	123.29(12)
C(8)	C(7)	C(12)	119.39(13)
C(8)	C(7)	C(6)	118.75(12)
C(12)	C(7)	C(6)	121.86(12)
C(14)	C(15)	N(1)	109.46(12)
C(16)	C(15)	N(1)	129.04(13)
C(16)	C(15)	C(14)	121.49(13)
C(9)	C(8)	C(7)	121.44(13)
O(4)	C(20)	N(1)	110.02(12)
O(3)	C(20)	O(4)	124.24(13)
O(3)	C(20)	N(1)	125.74(14)
C(7)	C(12)	C(13)	122.60(13)
C(11)	C(12)	C(7)	118.31(13)
C(11)	C(12)	C(13)	119.08(13)
N(1)	C(6)	C(7)	110.11(11)
N(1)	C(6)	C(5)	103.28(10)
C(7)	C(6)	C(5)	115.35(11)
O(2)	C(3)	O(1)	123.80(14)

Atom	Atom	Atom	Angle/°
O(2)	C(3)	C(4)	125.90(13)
O(2)	C(3)	O(1A)	118.2(6)
O(1)	C(3)	C(4)	110.13(12)
O(1A)	C(3)	C(4)	108.6(5)
C(15)	C(14)	C(5)	110.75(12)
C(19)	C(14)	C(15)	120.27(13)
C(19)	C(14)	C(5)	128.98(13)
C(3)	C(4)	C(5)	114.19(11)
C(10)	C(9)	C(8)	119.36(13)
C(14)	C(5)	C(6)	103.57(10)
C(14)	C(5)	C(4)	111.62(11)
C(4)	C(5)	C(6)	116.33(11)
C(15)	C(16)	C(17)	117.41(14)
C(10)	C(11)	C(12)	121.76(14)
C(14)	C(19)	C(18)	119.07(14)
C(9)	C(10)	C(11)	119.68(13)
C(18)	C(17)	C(16)	121.74(14)
C(17)	C(18)	C(19)	120.01(14)
O(1)	C(2)	C(1)	110.70(17)
C(1)	C(2)	O(1A)	84.3(8)
C(3)	O(1A)	C(2)	100.1(10)

Table 5.8: Torsion angles in ° for **8b**.

Atom	Atom	Atom	Atom	Angle/°
O(2)	C(3)	C(4)	C(5)	22.3(2)
O(2)	C(3)	O(1A)	C(2)	60.6(13)
O(1)	C(3)	C(4)	C(5)	-162.43(16)
N(1)	C(15)	C(14)	C(5)	0.37(15)
N(1)	C(15)	C(14)	C(19)	179.68(12)
N(1)	C(15)	C(16)	C(17)	-179.52(13)
N(1)	C(6)	C(5)	C(14)	10.34(13)
N(1)	C(6)	C(5)	C(4)	133.18(12)
C(7)	C(8)	C(9)	C(10)	-1.3(2)
C(7)	C(12)	C(11)	C(10)	-0.7(2)
C(7)	C(6)	C(5)	C(14)	-109.84(12)

Atom	Atom	Atom	Atom	Angle/°
C(7)	C(6)	C(5)	C(4)	13.01(16)
C(15)	N(1)	C(20)	O(4)	174.21(12)
C(15)	N(1)	C(20)	O(3)	-5.5(2)
C(15)	N(1)	C(6)	C(7)	112.70(12)
C(15)	N(1)	C(6)	C(5)	-11.00(14)
C(15)	C(14)	C(5)	C(6)	-6.97(14)
C(15)	C(14)	C(5)	C(4)	-132.88(12)
C(15)	C(14)	C(19)	C(18)	-0.3(2)
C(15)	C(16)	C(17)	C(18)	-0.2(2)
C(8)	C(7)	C(12)	C(11)	-1.4(2)
C(8)	C(7)	C(12)	C(13)	177.27(13)
C(8)	C(7)	C(6)	N(1)	-49.23(16)
C(8)	C(7)	C(6)	C(5)	67.14(16)
C(8)	C(9)	C(10)	C(11)	-0.9(2)
C(20)	N(1)	C(15)	C(14)	-171.75(13)
C(20)	N(1)	C(15)	C(16)	8.5(2)
C(20)	N(1)	C(6)	C(7)	-68.43(16)
C(20)	N(1)	C(6)	C(5)	167.87(12)
C(12)	C(7)	C(8)	C(9)	2.4(2)
C(12)	C(7)	C(6)	N(1)	130.23(13)
C(12)	C(7)	C(6)	C(5)	-113.41(14)
C(12)	C(11)	C(10)	C(9)	1.9(2)
C(6)	N(1)	C(15)	C(14)	7.09(15)
C(6)	N(1)	C(15)	C(16)	-172.61(13)
C(6)	N(1)	C(20)	O(4)	-4.51(18)
C(6)	N(1)	C(20)	O(3)	175.78(13)
C(6)	C(7)	C(8)	C(9)	-178.12(12)
C(6)	C(7)	C(12)	C(11)	179.16(12)
C(6)	C(7)	C(12)	C(13)	-2.2(2)
C(3)	O(1)	C(2)	C(1)	-80.0(2)
C(3)	C(4)	C(5)	C(6)	65.10(15)
C(3)	C(4)	C(5)	C(14)	-176.36(11)
C(14)	C(15)	C(16)	C(17)	0.8(2)
C(14)	C(19)	C(18)	C(17)	0.9(2)
C(4)	C(3)	O(1A)	C(2)	-147.6(5)
C(5)	C(14)	C(19)	C(18)	178.91(13)
C(16)	C(15)	C(14)	C(5)	-179.90(12)
C(16)	C(15)	C(14)	C(19)	-0.6(2)
C(16)	C(17)	C(18)	C(19)	-0.6(2)
C(19)	C(14)	C(5)	C(6)	173.80(14)
C(19)	C(14)	C(5)	C(4)	47.89(19)
C(13)	C(12)	C(11)	C(10)	-179.43(13)
C(21)	O(4)	C(20)	O(3)	-0.1(2)
C(21)	O(4)	C(20)	N(1)	-179.86(13)
C(2)	O(1)	C(3)	O(2)	-0.3(3)
C(2)	O(1)	C(3)	C(4)	-175.73(18)
C(1)	C(2)	O(1A)	C(3)	-123.4(10)
O(1A)	C(3)	C(4)	C(5)	-126.8(10)

Table 5.9: Hydrogen fractional atomic coordinates ($\times 10^4$) and equivalent isotropic displacement parameters ($Å^2 \times 10^3$) for **8b**. U_{eq} is defined as 1/3 of the trace of the orthogonalised U_{ij}.

Atom	x	y	z	U_{eq}
H(8)	4225	6268	5666	29
H(6)	2964	6444	1171	26
H(4A)	5827	5270	2436	28
H(4B)	4952	5433	3876	28
H(9)	3198	5822	7809	31
H(5)	4819	6032	629	27
H(16)	5980	7779	4354	32
H(11)	84	5478	4241	33
H(19)	7594	5980	2506	34
H(10)	1122	5415	7079	34
H(13A)	673	6317	1009	46
H(13B)	-19	5715	1321	46
H(13C)	1320	5717	564	46
H(17)	8230	7595	4651	39
H(18)	9036	6715	3721	40
H(21A)	1303	8119	1819	57
H(21B)	1216	7948	3769	57
H(21C)	248	7661	2256	57
H(2AA)	3311	3664	2781	44
H(2AB)	3050	3976	947	44
H(2BC)	3147	4002	967	44
H(2BD)	3426	3700	2866	44
H(1A)	1647	4257	3706	62
H(1B)	1107	3829	2174	62
H(1C)	1336	4501	1791	62

5.12 References:

[1] a) A. J. Kochanowska-Karamyan, M. T. Hamann, *Chem. Rev.* **2010**, *110*, 4489; b) S. A. Patil, R. Patil, D. D. Miller, *Future Med. Chem.* **2012**, *4*, 2085; c) N. K. Kaushik, N. Kaushik, P. Attri, N. Kumar, C. H. Kim, A. K. Verma, E. H. Choi, *Molecules* **2013**, *18*, 6620; d) M. Ishikura, T. Abe, T. Choshi, S. Hibino, *Nat. Prod. Rep.* **2013**, *30*, 694; e) F. R. de Sa Alves, E. J. Barreiro, C. A. M. Fraga, *MINI-Rev. Med. Chem.* **2009**, *9*, 782; f) B. Costall, S. J. Gunning, R. J. Naylor, M. B. Tyers, *Br. J. Pharmac.* **1987**, *91*, 263; g) R. K. Cady, J. K. Wendt, J. R. Kirchner, J. D. Sargent, J. F. Rothrock, H. Skaggs, *Lancet* **1988**, *1*, 1309; h) C. Schultz, A. Link, M. Leost, D. W. Zaharevitz, R. Gussio, E. A. Sausville, L. Meijer, C. Kunick, *J. Med. Chem.* **1999**, *42*, 2909.

[2] T. Opatz, D. Ferenc, *Org. Lett.* **2006**, *8*, 4473.

[3] a) A. P. Kozikowski, D. Ma, J. Brewer, S. Sun, E. Costa, E. Romeo, A. Guidotti, *J. Med. Chem.* **1993**, *36*, 2908; b) J. Auta, E. Romeo, A. Kozikowski, D. Ma, E. Costa, A. Guidotti, *J. Pharm. Exp. Ther.* **1993**, *265*, 649.

[4] a) G. I. Stevenson, A. L. Smith, S. Lewis, S. G. Michie, J. G. Neduvelil, S. Patel, R. Marwood, S. Patel, J. L. Castro, *Bioorg. Med. Chem. Lett.* **2000**, *10*, 2697; b) A. L. Smith, G. I. Stevenson, S. Lewis, S. Patel, J. L. Castro, *Bioorg. Med. Chem. Lett.* **2000**, *10*, 2693.

[5] B. W. Trotter, A. G. Quigley, W. C. Lumma, J. T. Sisko, E. S. Walsh, C. S. Hamann, R. G. Robinson, H. Bhimnathwala, D. G. Kolodin, W. Zheng, C. A. Buser, H. E. Huber, R. B. Lobell, N. E. Kohl, T. M. Williams, S. L. Grahama, C. J. Dinsmore, *Bioorg. Med. Chem. Lett.* **2001**, *11*, 865.

[6] P. Lin, M. Parikh, J.-L. Lo, Y. T. Yang, K. Cheng, R. G. Smith, M. H. Fisher, M. J. Wyvratt, M. T. Goulet, *Bioorg. Med. Chem. Lett.* **2001**, *11*, 1077.

[7] a) A. Arcadi, S. Cacchi, G. Fabrizi, F. Marinelli, *Synlett* **2000**, 394; b) S. Cacchi, G. Fabrizi, L. M. Parisi, *Synthesis* **2004**, 1889; c) D. F. Taber, P. K. Tirunahari, *Tetrahedron* **2011**, *67*, 7195; d) F. J. E. Fischer, *Ber. Dtsch. Chem. Ges.* **1883**, *16*, 2241; e) G. R. Humphrey, J. T. Kuethe, *Chem. Rev.* **2006**, *106*, 2875; f) M. Inman, C. J. Moody, *Chem. Sci.* **2013**, *4*, 29; g) M. Tobisu, H. Fujihara, K. Koh, N. Chatani, *J. Org. Chem.* **2010**, *75*, 4841; h) R. Vicente, *Org. Biomol. Chem.* **2011**, *9*, 6469.

[8] S. J. Lee, H.-A. Seo, C.-H. Cheon, *Adv. Synth. Catal.* **2016**, *358*, 1566.

[9] G. M. Allan, A. F. Parsons, J.-F. Pons, *Synlett* **2002**, *2002*, 1431.

[10] H. Lin, A. Schall, O. Reiser, *Synlett* **2005**, 2603.

[11] I. Prediger, T. Weiss, O. Reiser, *Synthesis* **2008**, 2191.

[12] a) T. Maji, A. Karmakar, O. Reiser, *J. Org. Chem.* **2011**, *76*, 736; b) J. D. Nguyen, E. M. D'Amato, J. M. R. Narayanam, C. R. J. Stephenson, *Nat. Chem.* **2012**, *4*, 854.

[13] S. Paria, V. Kais, O. Reiser, *Adv. Synth. Catal.* **2014**, *356*, 2853.

[14] S. Paria, O. Reiser, *Adv. Synth. Catal.* **2014**, *356*, 557.

[15] S. K. Pagire, O. Reiser, *Green Chem.* **2017**, *19*, 1721.

[16] M. S. Lowry, J. I. Goldsmith, J. D. Slinker, R. Rohl, R. A. Pascal, G. G. Malliaras, S. Bernhard, *Chem. Mater.* **2005**, *17*, 5712.

[17] J. D. Slinker, A. A. Gorodetsky, M. S. Lowry, J. Wang, S. Parker, R. Rohl, S. Bernhard, G. G. Malliaras, *J. Am. Chem. Soc.* **2004**, *126*, 2763.

[18] C. K. Prier, D. A. Rankic, D. W. C. MacMillan, *Chem. Rev.* **2013**, *113*, 5322.

[19] a) S. K. Pagire, S. Paria, O. Reiser, *Org. Lett.* **2016**, *18*, 2106; b) S. Paria, O. Reiser, *ChemCatChem* **2014**, *6*, 2477; c) O. Reiser, *Acc. Chem. Res.* **2016**, *49*, 1990.

[20] J. Sun, W. Wu, J. Zhao, *Chem. Eur. J.* **2012**, *18*, 8100.

[21] a) C. G. Gutierrez, R. A. Stringham, T. Nitasaka, K. G. Glasscock, *J. Org. Chem.* **1980**, *45*, 3393; b) C. P. Alexis, J. M. Uribe, J. D. Beller, G. Godjoian, C. G. Gutierrez, *Phosphorus, Sulfur Silicon Relat. Elem.* **1996**, *119*, 93.

[22] I. Ghosh, B. König, *Angew. Chem. Int. Ed.* **2016**, *55*, 7676.

[23] U. Jacquemard, V. Bénéteau, M. Lefoix, S. Routier, J.-Y. Mérour, G. Coudert, *Tetrahedron* **2004**, *60*, 10039.

[24] T. Goto, Y. Natori, K. Takeda, H. Nambu, S. Hashimoto, *Tetrahedron: Asymmetry* **2011**, *22*, 907.

[25] L. Zheng, R. Hua, *Chem. Eur. J.* **2014**, *20*, 2352.

[26] C. Liu, W. Zhang, L.-X. Dai, S.-L. You, *Org. Lett.* **2012**, *14*, 4525.

[27] X. Wang, D. V. Gribkov, D. Sames, *J. Org. Chem.* **2007**, *72*, 1476.

[28] C. Liu, W. Zhang, L.-X. Dai, S.-L. You, *Org. Lett.* **2012**, *14*, 4525.

6 One step synthesis of triquinacenes from vinyl-chlorides and acetylenes: A surprising discovery in visible-light photocatalysis

6.1 Abstract:

The unprecedented synthesis of Triquinacenes is demonstrated from readily available *ortho*-alkynylated α-halocinnamates and acetylenes under the visible-light conditions.

6.2 Introduction:

The core structure (i.e. the three adjacent five membered rings) is a well-known scaffold called Triquinacenes,[1] which was first synthesized by R. B. Woodward in 1964,[2] being suspected for quite a long time to have "homoaromatic" properties.[3] Since then, several protocols targeting to construct the Triquinacene backbone and its subsequent transformations to the related molecules have been appeared.[4] Along these lines, Meijere *et al* have detailed attempts to prepare the strained polyquinene acepentalene from triquinacenes derivatives and has successfully reported the preparation of dihydroacepentalenediide.[5] Furthermore, he also studied their ions in gas phase.[6]

However, the synthesis of triquinacenes and their derivatives have not been established by photochemical methods till date. Having inspired with our previous exciting photochemical reaction outcomes with *ortho*-alkynylated α-halocinnamates and molecular oxygen (Chapter 3), which led us to the unprecedented formation of indenones and taiwaniaquinoid related scaffolds via a highly reactive vinyl radical species.[7] Herein, we aimed to engage these vinyl radicals in simple C-C bond forming reactions with alkynes in the absence of oxygen, which consequently provided incredibly complex product structures called Triquinacenes.

This chapter is unpublished:

S. K. Pagire, V. Adiyala, J. Yedoyan, O. Reiser, *work in progress*.

6.3 Results and discussion:

We began our investigations by reacting **1a** with **2a** by using $[Ir\{dF(CF_3)ppy\}_2(dtb\text{-}bpy)]PF_6$[8] ($E_{Ir(IV)/Ir(III)^*}$ = –0.89 V vs. SCE)[9] under blue light in wet DMF.

6.4 Synthesis of 3a: Catalyst screening and reaction optimization

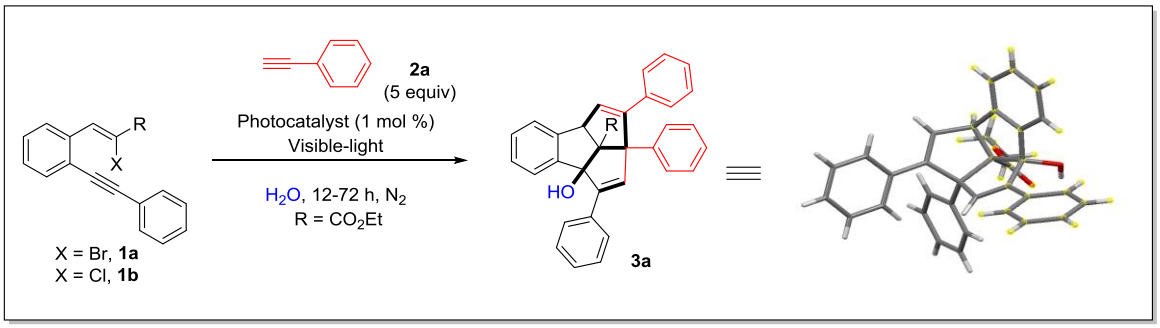

Entry	X	Photocatalyst	Solvent	H_2O (equiv)	Temp (^oC)	Yield (%)[b]
1	Br	Ir-F	wet DMF	0	rt	19
2	Br	Ir-F	dry DMF	0	rt	traces
3	Br	Ir-F	wet DMF	2	rt	22
4	Br	Ir-F	wet DMSO	2	rt	0
5	Br	Ir-F	wet DCM	2	rt	0
6	Br	Ir-F	wet MeCN	2	rt	traces
7	**Br**	***fac*-Ir(ppy)$_3$**	**wet DMF**	**2**	**rt**	**26**
8	Br	*fac*-Ir(ppy)$_3$	Phenyl acetylene	2	rt	0
9	Cl	*fac*-Ir(ppy)$_3$	wet MeCN	2	rt	25
10	**Cl**	***fac*-Ir(ppy)$_3$**	**wet DMF**	**2**	**rt**	**33**
11	Cl	No catalyst	wet DMF	2	rt	0
12[c]	Cl	*fac*-Ir(ppy)$_3$	wet DMF	2	rt	0
13	Cl	*fac*-Ir(ppy)$_3$	wet DMF	5	rt	17
14	Cl	*fac*-Ir(ppy)$_3$	wet DMF	10	rt	traces
15[d]	Cl	*fac*-Ir(ppy)$_3$	wet DMF	2	rt	29
16[e]	Cl	*fac*-Ir(ppy)$_3$	wet DMF	2	rt	20

Tables 6.1: Reaction Conditions: [a] Substrate **1a/1b** (0.5 mmol, 1.0 equiv), photocatalyst (1 mol %), rt-60 ^oC, solvent(s) (2 mL), H_2O (0-40 equiv), 12-72 h, LED_{455}, under N_2 [b] isolated. [c] Dark reaction. [d] 1.5 mol % photocatalyst. [e] 2.0 mol % photocatalyst, (Note: the extra catalyst was insoluble and blocked the way in the micro-reactor capillary during the reaction). [f] All these optimizations were done by *Santosh K. Pagire* and *Vidyasagar Adiyala*. [g] Isolation, crystallization, and single X-ray of **3a** were done by *Julietta Yedoyan*.

This indeed gave **3a** in 19% yields at room temperature conditions. We later identified the product structure by the single X-ray crystal analysis, and immediately realized that the water molecule is involved in the process, which should have stem from the wet DMF since we have not added any extra water for this attempt. This conclusion is further supported by the dry DMF experiment: In absence of water, thus dissolving **1a** and **2a** in anhydrous DMF solution under nitrogen atmosphere provides only traces of product **3a**, indicating the need of water as an external nucleophile to introduce a hydroxyl group (Table 6.1, entry 2). In a subsequent attempt, 2 equiv of distilled water was added, which also slightly better results (Table 6.1, entry 3). Other solvents, such as DMSO, DCM or MeCN do not provide any products (Table 6.1, entries 4-6). Switching to the strong [Ir]-photocatalyst, *fac*[Ir(ppy)$_3$][10] ($E_{Ir(IV)/Ir(III)*}$ = –1.73 V vs. SCE (Table 6.1, entry 7) slightly improved the yields (26%). However, no product formation was occurred with phenyl acetylene (2 mL) as a neat solvent (Table 6.1, entry 8).

In all cases, we noted a deep red colouring of the solution in the course of the reaction, probably blocking the photo-process, which could explain the incomplete conversion and long reaction time of the overall transformation. To our delight, a significant increase in yield was observed upon replacing α-bromocinnamates **1a** with α-chlorocinnamates **1b**, which might be due to the higher electronegativity and high oxidising power of chlorine compared to the bromine. Of course, this conclusion further needs to be analyzed and confirmed by carrying out several control experiments and spectroscopic investigations, such as CV-measurements etc. At the moment, we are beginners to utilize vinyl-chlorides as a starting material for organic synthesis, thus more studies are desired in this topic. This would probably shine the light into the dark corners which are currently invisible.

For instance, we found (Table 6.1, entry 10) as an optimal condition for further investigations, though product yields are still unsatisfactory (33%). In the absence of the iridium catalyst or visible-light, no conversion of **1b** was observed, which again indicated the process is driven by visible-light photocatalysis (Table 6.1, entries 11, 12). To our surprise, increasing the catalyst loading does not assist in increasing the yields (Table 6.1, entries 13, 14), which probably due to the insolubility of extra catalyst, and in turn, it was also blocking the flow of the reaction mixture under the light.

6.5 Proposed reaction mechanism:

We again noticed the unique photochemistry associated with such *ortho*-alkynylated α-halocinnamate activation under visible-light. The mechanistic picture of this transformation is straightforward, though the compound structure of **3a** is complex (Figure 6.1). Initially, a direct photoelectron transfer (PET) from the excited Ir(III)*-catalyst to **1a** should occur, to generate a first vinyl radical **I** by kicking out a chlorine anion with concurrent oxidation of excited *Ir(III) to Ir(IV). The vinyl radical **I** then undergoes a favorable *5-exo*-dig cyclization to form second vinyl radical **II**, which adds to the first phenyl acetylene **2a** molecule to form third vinyl radical **III**. This radical then undergoes *5-exo*-trig ring closure to access the benzylic radical **IV**. The relatively stable benzylic radical then adds to the second phenyl acetylene molecule to provide fourth vinyl radical intermediate **V**, which ultimately undergoes *5-exo*-trig ring closure to access another stable benzylic (as well as tertiary and allylic) radical **VI**. The resulting stable radical **VI** should undergo back electron transfer to Ir(IV), thus completing the catalytic cycle with the concurrent formation of the benzylic cation **VII**. Finally, this carbocation **VII** gets trapped by the nucleophilic water present in the reaction media to access the final triquinacene scaffold **3a**.

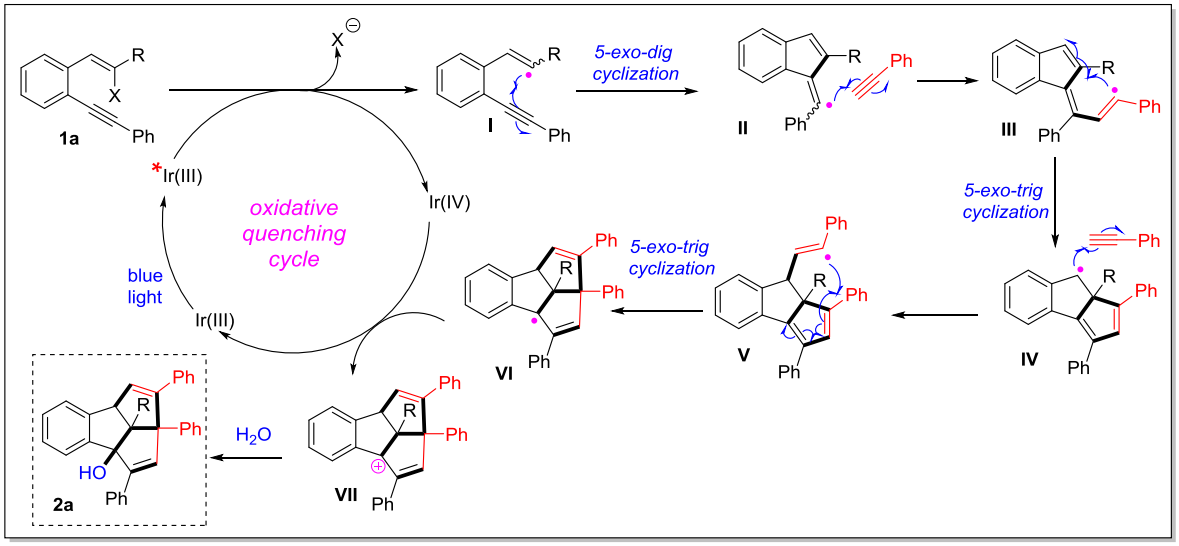

Figure 6.1: Proposed reaction mechanism for the synthesis of **3a**.

6.6 Conclusion:

In summary, we have shown for the first time, a visible-light mediated cascade of C-C bond formations with vinyl chlorides and phenyl acetylenes. Noteworthy, this process involves four highly reactive vinyl radical intermediates, which was engaged in a productive reaction cascades with two phenyl acetylene molecules, leading to complex molecular designs in a single photochemical step under the mild reaction conditions. We emphasize here, this reaction could also be performed in the micro-flow reactors in the short reaction time. Arguably, the single step synthesis of these types of complex architectures is certainly impossible to accomplish by employing other methods at this moment.

Despite the spectacular structure of the obtained product, we found that this reaction is very tricky and unfortunately suffers with several reproducibility problems. These compounds are less stable on the column which explains the product formation with lower yields although the conversion was 100%. This unfortunately put us on the back seat at this moment. In order to push this project to the conclusion, further investigations needs to be done. In particular, the acid catalyzed ring opening experiments and physical studies might give us some insightful information of the overall process.

Nevertheless, we made a range of electronically differentiated starting materials (See experimental section for representative examples) in order to understand the electronic influence on the reaction and their outcomes. Thus the broadening of substrate scope, further understanding the reaction mechanisms by trapping the carbocation by other nucleophiles (such as MeOH or labeled H_2O^{18}) or changing the trapping reagents is currently underway, and hopefully we will see these results in a reputed journal within the next few months.

6.7 Experimental Section:

6.7.1 General procedure (GP-1): Sonogashira coupling

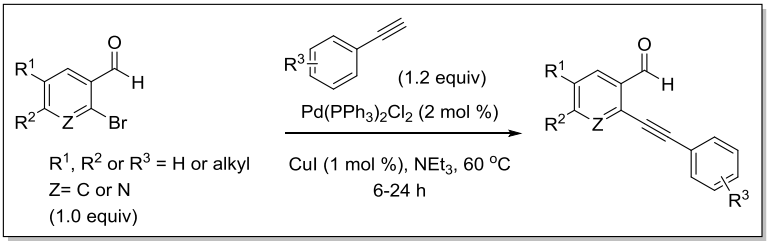

[Note: see the experimental section of Chapter 3 for detailed information about these coupling compounds**].**

To a solution of the corresponding 2-bromobenzaldehyde derivative (2.00 mmol, 1.00 equiv), $PdCl_2$ $(PPh_3)_2$ (2.00 mol %), and CuI (1.00 mol %) in degassed NEt_3 (20 mL) was added the appropriate acetylene (60 mmol, 1.20 equiv). The resulting mixture was heated under nitrogen atmosphere at 60 °C for 6-24 h, gradually the reaction turned dark. The progress of the reaction was monitored by TLC. After complete consumption of the starting material, resulting mixture was diluted with 15 mL of EtOAc and filtered through the pad of celite. The filtrate was evaporated under reduced pressure and the pure compound was isolated through silica gel column chromatography using Hexanes/EtOAc as a solvent system.

6.7.2 General procedure (GP-2) for the preparation of α-chlorocinnamate derivatives:

This experimental procedure is known in the literature:[11] To a solution of aldehydes **S1** (3.0 mmol, these compounds are directly adopted from chapter 2.1) and α-chloroacetate (3.6 mmol) in DCM (20 mL) under a nitrogen atmosphere was added $TiCl_4$ (3.6 mmol, 1.0 M solution in DCM) in drops for 10 minutes. The mixture was then stirred at room temperature for 30-45 min. To this was added Et_3N (6.0 mmol) in drops over a period of 10 minutes while maintaining the reaction temperature below 30 °C with external water bath. The resulting brown mixture was then stirred at room temperature for next 2–5 h (controlled by TLC). When the reaction was completed (Hexanes:EtOAc = 9:1), the mixture was diluted with DCM (30 mL) and washed with 1.0 N aqueous HCl (20 mL), water, and brine. The organic phase was dried over Na_2SO_4. The solvent was removed under reduced pressure and the crude product was passed through a plug of silica to afford the desired (*Z*)-α-chlorocinnamates **1**.

Ethyl 2-chloro-3-(2-(phenylethynyl)phenyl)acrylate (1a):

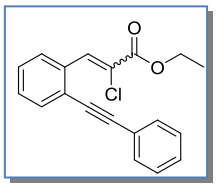

Following GP-2, **1a** was prepared from **S1a** (618 mg, 3.00 mmol). The crude product was purified by column chromatography (Hexanes: EtOAc, 9:1, R_f = 0.6) afforded **1a** as a brown solid (883 mg, 95% yield, *Z:E* = 99:01).

^{1}H-NMR (300 MHz, $CDCl_3$, *Z* isomer, major): δ 8.56 (s, 1H), 8.29 – 8.14 (m, 1H), 7.69 – 7.52 (m, 3H), 7.47 – 7.30 (m, 5H), 4.39 (q, *J* = 7.1 Hz, 2H), 1.40 (t, *J* = 7.1 Hz, 3H).

^{13}C-NMR (75 MHz, $CDCl_3$, *Z* isomer, major): δ 163.35, 135.33, 134.65, 132.29, 131.69, 129.76, 129.29, 128.86, 128.55, 128.23, 125.03, 123.68, 122.89, 96.28, 87.17, 62.75, 14.35.

IR (neat, cm^{-1}): 2985, 2902, 1712, 1598, 1492, 1467, 1443, 1390, 1363, 1233, 1194, 1111, 1091, 1043, 1043, 994, 904, 861, 835, 753, 684.

HRMS (ESI): exact m/z calculated for $C_{19}H_{15}ClNaO_2$ $(M+Na)^+$: 333.0653; Found: 333.0654 $(M+Na)^+$.

Ethyl 2-chloro-3-(5-methoxy-2-(phenylethynyl)phenyl)acrylate (1b):

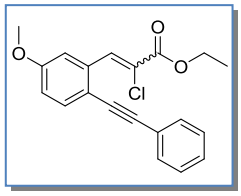

Following GP-2, **1b** was prepared from **S1b** (622 mg, 2.63 mmol). Purification of the crude product by column chromatography (Hexanes: EtOAc, 9:1, R_f = 0.50) afforded **1b** as a brown solid (860 mg, 96% yield. *Z:E* = 99:01).

^{1}H-NMR (300 MHz, $CDCl_3$, *Z* isomer, major): δ 8.48 (s, 1H), 7.73 (d, *J* = 2.6 Hz, 1H), 7.61 – 7.41 (m, 3H), 7.35 – 7.25 (m, 3H), 6.99 – 6.80 (m, 1H), 4.30 (q, *J* = 7.1 Hz, 2H), 3.83 (s, 3H), 1.34 (t, *J* = 7.1 Hz, 3H).

^{13}C-NMR (75 MHz, $CDCl_3$, *Z* isomer, major): δ 163.35, 159.32, 135.99, 135.27, 133.57, 131.52, 128.55, 123.82, 123.29, 117.50, 116.20, 114.49, 94.85, 87.19, 62.83, 55.64, 14.39.

IR (neat, cm^{-1}): 2974, 2933, 2839, 1718, 1594, 1560, 1495, 1463, 1442, 1391, 1368, 1319, 1293, 1276, 1222, 1165, 1097, 1030, 851, 832, 753, 689.

HRMS (ESI): exact m/z calculated for $C_{20}H_{18}ClO_3$ $(M+H)^+$: 341.0939; Found: 341.0941 $(M+H)^+$.

Ethyl 2-chloro-3-(6-(phenylethynyl)benzo[d][1,3]dioxol-5-yl)acrylate (1c):

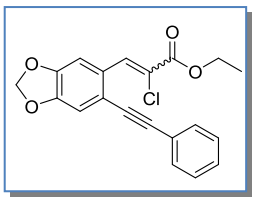

Following **GP-2**, **1c** was prepared from **S1c** (320 mg, 1.29 mmol). Purification of the crude product by column chromatography (Hexanes: EtOAc, 9:1, R_f = 0.39) afforded **1c** as a brown solid (472 mg, 92% yield, *Z:E* = 99:01).

^{1}H-NMR (300 MHz, $CDCl_3$, *Z* isomer, major): δ 8.55 (s, 1H), 7.84 (s, 1H), 7.60 – 7.51 (m, 2H), 7.39 – 7.32 (m, 3H), 7.03 (s, 1H), 6.05 (s, 2H), 4.36 (q, *J* = 7.1 Hz, 2H), 1.37 (t, *J* = 7.1 Hz, 3H).

^{13}C-NMR (75 MHz, $CDCl_3$, *Z* isomer, major): δ 163.58, 148.95, 148.04, 134.89, 131.58, 129.61, 128.77, 128.58, 122.97, 121.78, 120.45, 111.75, 109.07, 102.21, 95.50, 87.24, 62.71, 14.41.

IR (neat, cm^{-1}): 2954, 2920, 2852, 1703, 1594, 1497, 1470, 1442, 1392, 1353, 1329, 1271, 1239, 1221, 1139, 1032, 998, 926, 904, 860, 756, 721, 693, 671.

HRMS (ESI): exact m/z calculated for $C_{20}H_{15}ClNaO_4$ $(M+Na)^+$: 377.0551; Found: 377.0553 $(M+Na)^+$.

Ethyl 2-chloro-3-(5-nitro-2-(phenylethynyl)phenyl)acrylate (1d):

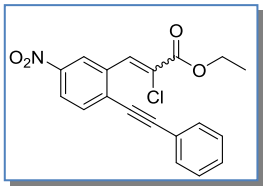

Following GP-2, **1d** was prepared from **S1g** (419 mg, 1.67 mmol). Purification of the crude product by column chromatography (Hexanes: EtOAc, 9:1, R_f = 0.49) afforded **1d** as a yellow solid (533 mg, 90% yield, *Z:E* = 95:05).

^{1}H-NMR (300 MHz, $CDCl_3$, *Z* isomer, major): δ 9.00 (d, *J* = 2.3 Hz, 1H), 8.43 (s, 1H), 8.17 (dt, *J* = 9.0, 4.5 Hz, 1H), 7.73 – 7.66 (m, 1H), 7.58 – 7.51 (m, 2H), 7.42 – 7.32 (m, 3H), 4.36 (q, *J* = 7.1 Hz, 2H), 1.40 – 1.33 (t, *J* = 7.1 Hz, 3H).

^{13}C-NMR (75 MHz, $CDCl_3$, *E* isomer, major): δ 162.73, 146.88, 135.88, 133.10, 132.98, 132.08, 131.14, 129.96, 128.82, 126.39, 124.32, 124.20, 121.85, 101.45, 85.89, 63.19, 14.37.

IR (neat, cm^{-1}): 2923, 2851, 2209, 1739, 1713, 1598, 1516, 1492, 1461, 1442, 1367, 1338, 1267, 1229, 1072, 1035, 995, 911, 847, 827, 753, 740, 684.

HRMS (ESI): exact m/z calculated for $C_{19}H_{14}ClNNaO_4$ $(M+Na)^+$: 378.0504; Found: 378.0504 $(M+Na)^+$.

Ethyl 2-chloro-3-(4-methyl-2-(phenylethynyl)phenyl)acrylate (1e):

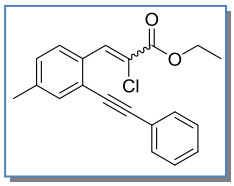

Following GP-2, **1e** was prepared from **S1h** (412 mg, 1.87 mmol). Purification of the crude product by column chromatography (Hexanes: EtOAc, 9:1, R_f = 0.44) afforded **1e** as a yellow solid (582 mg, 96% yield, *Z:E* = 92:08).

^{1}H-NMR (300 MHz, $CDCl_3$, *Z* isomer, major): δ δ 8.53 (s, 1H), 8.17 – 8.10 (m, 1H), 7.59 – 7.49 (m, 2H), 7.42 (d, *J* = 7.3 Hz, 1H), 7.38 – 7.30 (m, 3H), 7.26 – 7.16 (m, 1H), 4.35 (q, *J* = 7.1 Hz, 2H), 2.35 (s, 3H), 1.39 – 1.33 (t, *J* = 7.1 Hz, 3H).

^{13}C-NMR (75 MHz, $CDCl_3$, *Z* isomer, major): δ 163.53, 140.27, 135.22, 132.85, 131.87, 131.70, 129.26, 129.23, 128.81, 128.56, 125.16, 123.00, 122.75, 95.91, 87.34, 62.68, 21.43, 14.38.

IR (neat, cm^{-1}): 2977, 2928, 2907, 1711, 1595, 1491, 1474, 1439, 1393, 1367, 1282, 1233, 1198, 1151, 1114, 1043, 993, 910, 867, 817, 750, 685.

HRMS (ESI): exact m/z calculated for $C_{20}H_{17}ClNaO_2$ $(M+Na)^+$: 347.0809; Found: 347.0812 $(M+Na)^+$.

6.7.3 General procedure (GP-3) for the preparation of Triquinacenes:

To a oven dried 10 mL Schlenk flask was charged with **1** (0.50 mmol, 1.00 equiv) and *fac*-[Ir(ppy)$_3$] (3.3 mg, 0.01 equiv, 1.00 mol %) in 2 mL anhydrous DMF. The reaction mixture was degassed with freeze-pump thaw cycles (3x), then the phenyl acetylene (2.5 mmol, 5 equiv) was added under the positive nitrogen atmosphere, and the reaction mixture was vigorously stirred (~1000 rpm) at rt with an internal irradiation of blue light (LED 455 nm). After 72 h, distilled water (20 mL) was added to dilute the reaction mixture, the resulting dark red coloured mixture then transferred to the separatory funnel and extracted with ethyl acetate (3 x 10 mL). The combined organic layer was washed with brine (15 ml) and dried over Na_2SO_4. The residue was purified by flash column chromatography (SiO_2) with Hexanes/EtOAc as a solvent system.

Ethyl (2a^1*R*,4a*R*,8b*R*)-8b-hydroxy-1,2a,3-triphenyl-4a,8b-dihydropentaleno[1,6-ab]indene-2a^1(2a*H*)-carboxylate (3a):

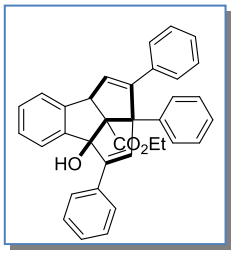

Following **GP-3**, **3a** was prepared from **1a** (155 mg, 0.50 mmol). Purification of the crude product by column chromatography (Hexanes: EtOAc, 4:1, R_f = 0.42) afforded **3a** as a yellow solid (80 mg, 29% yield).

^{1}H-NMR (400 MHz, $CDCl_3$): δ 7.79 – 7.74 (m, 2H), 7.33 (ddd, *J* = 10.1, 7.7, 2.3 Hz, 5H), 7.29 – 7.21 (m, 6H), 7.16 (dt, *J* = 7.0, 3.3 Hz, 3H), 7.11 (dd, *J* = 6.6, 3.6 Hz, 3H), 7.05 – 6.99 (m, 2H), 6.46 – 6.30 (m, 2H), 5.31 (d, *J* = 2.7 Hz, 1H), 4.90 (s, 1H), 3.60 – 3.38 (m, 2H), 1.07 – 0.90 (t, *J* = 7.1 Hz, 3H).

^{13}C-NMR (101 MHz, $CDCl_3$): δ 171.28, 147.10, 142.76, 142.29, 141.16, 134.41, 133.20, 132.25, 128.38, 128.27, 128.02, 127.29, 127.25, 126.57, 126.47, 126.39, 124.20, 123.00, 96.72, 80.63, 73.84, 60.54, 55.79, 12.90.

6.8 NMR spectra:

^{1}H-NMR: **1a**

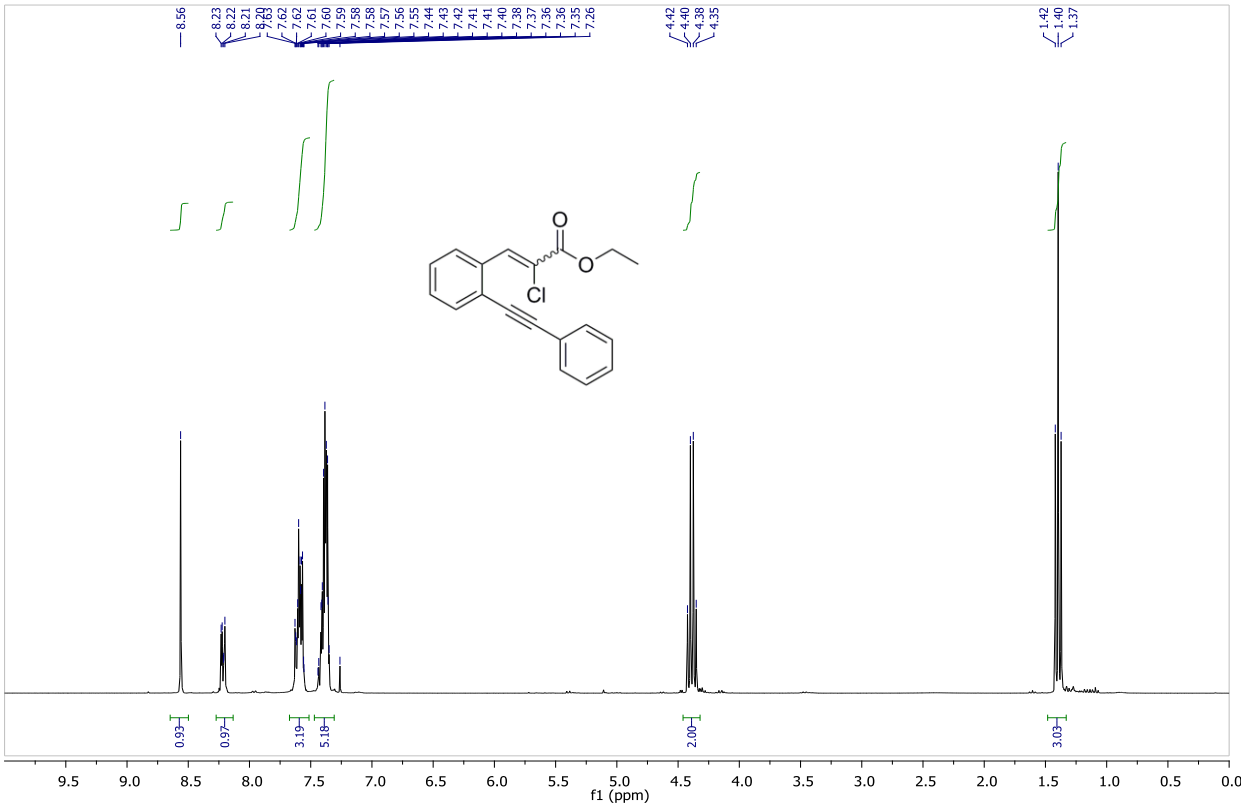

^{13}C-NMR: **1a**

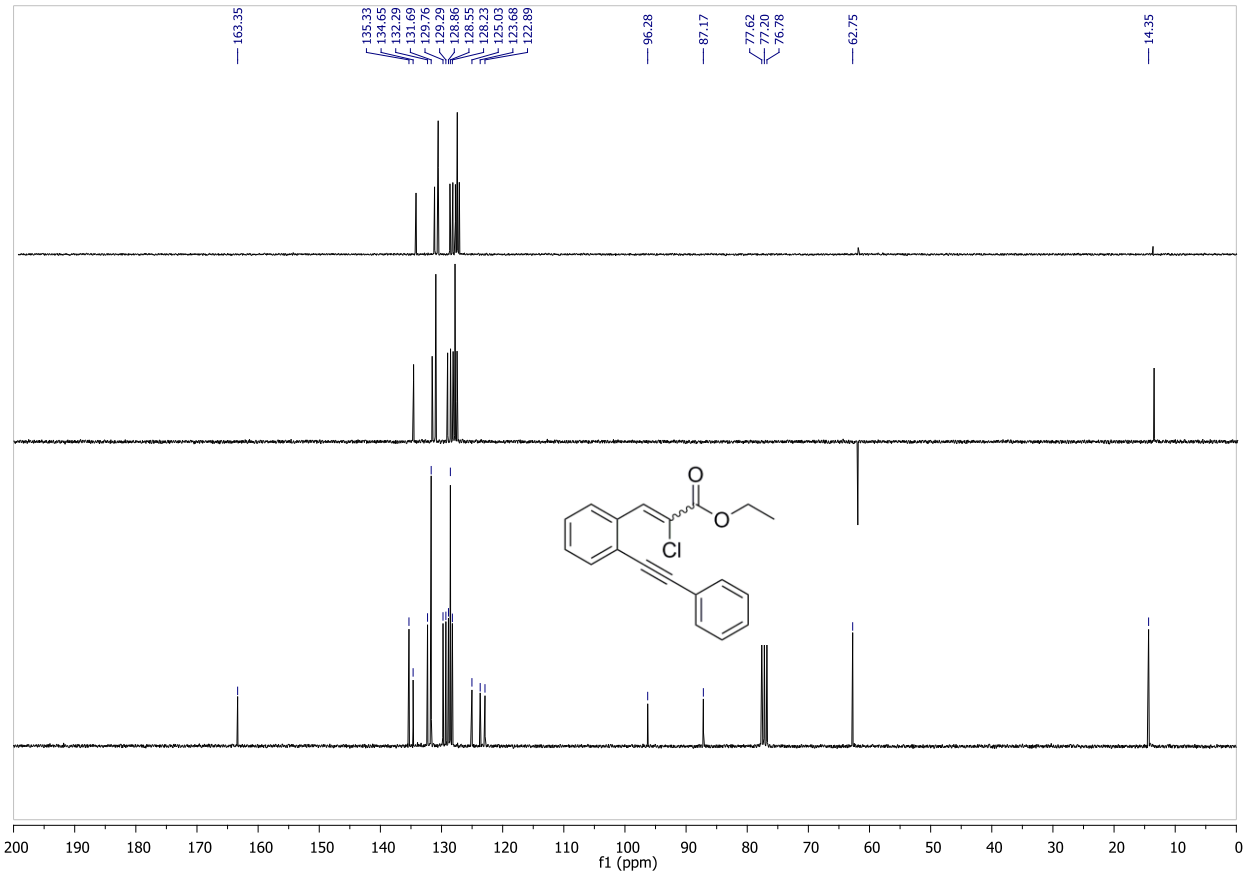

^{1}H-NMR: **1b**

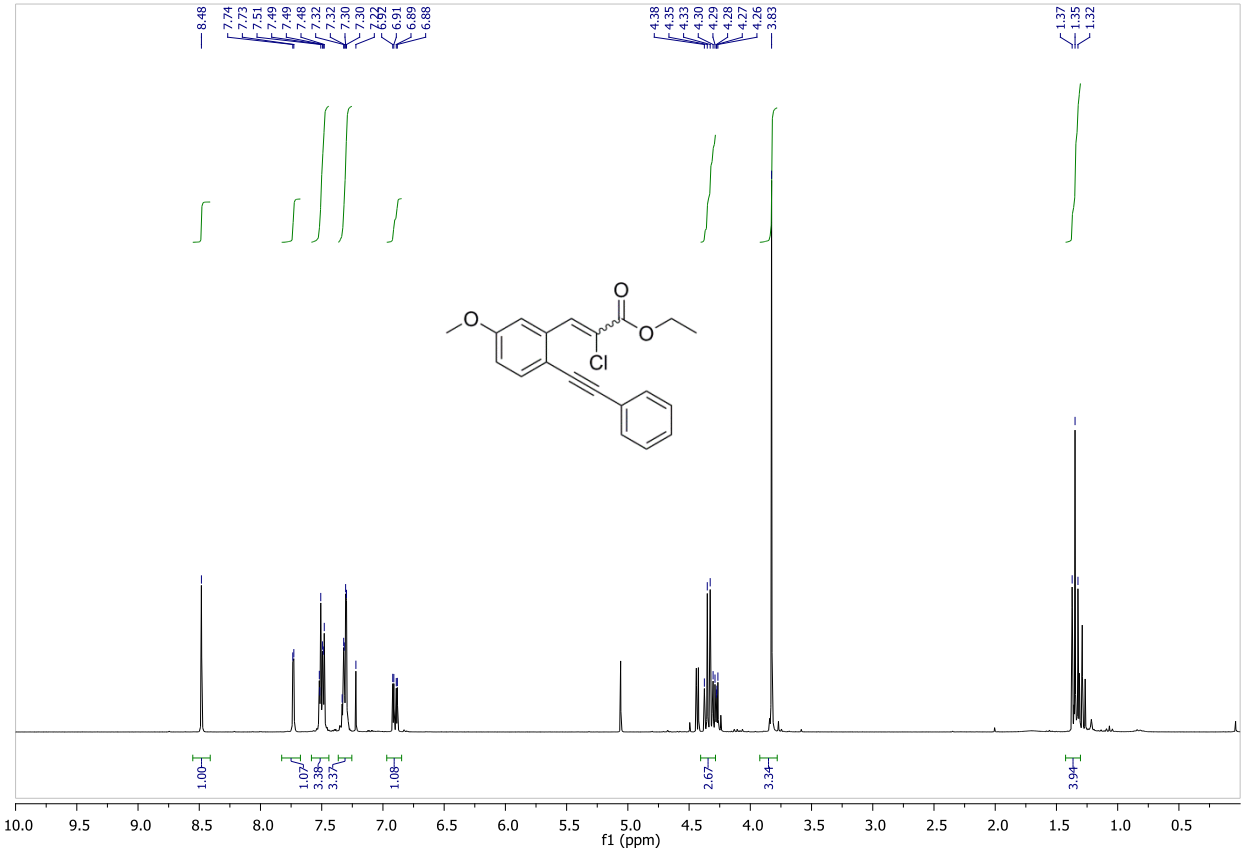

^{13}C-NMR: **1b**

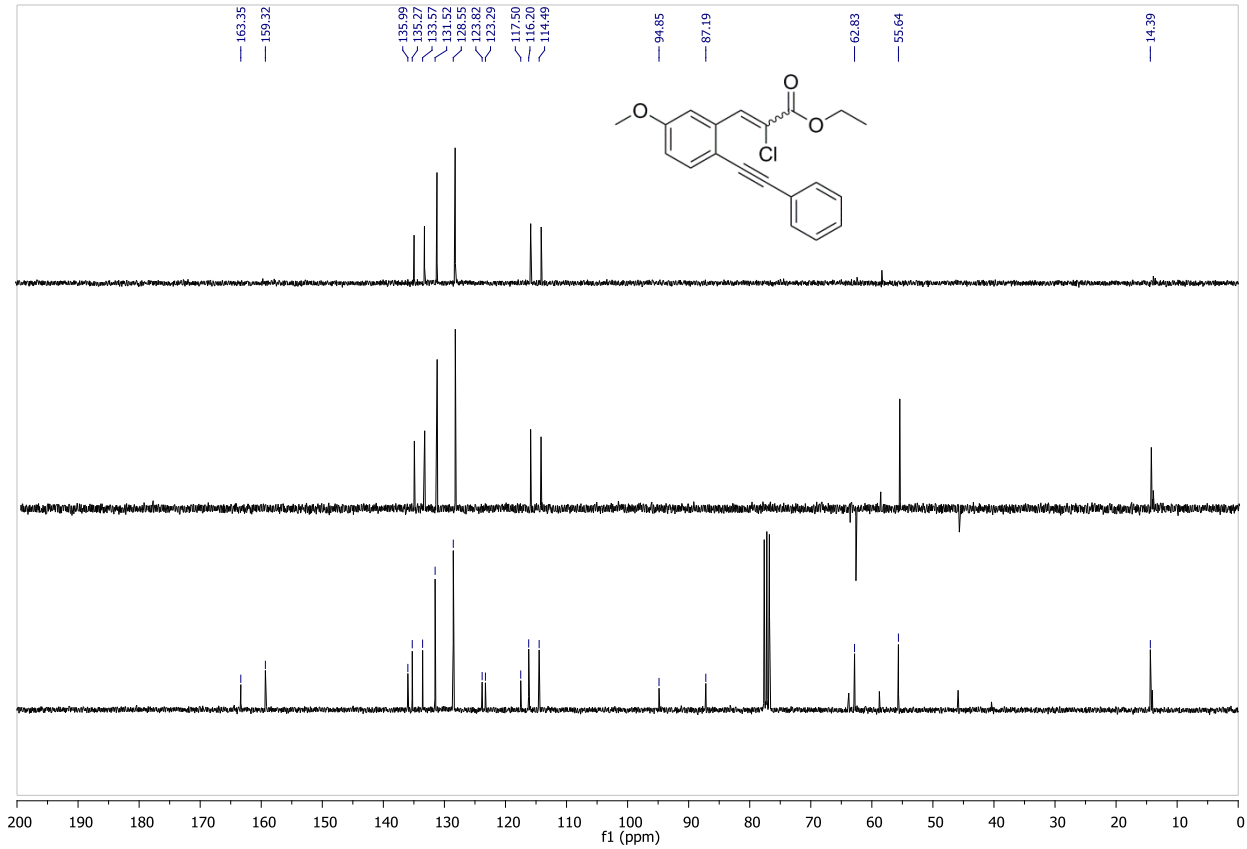

^{1}H-NMR: **1c**

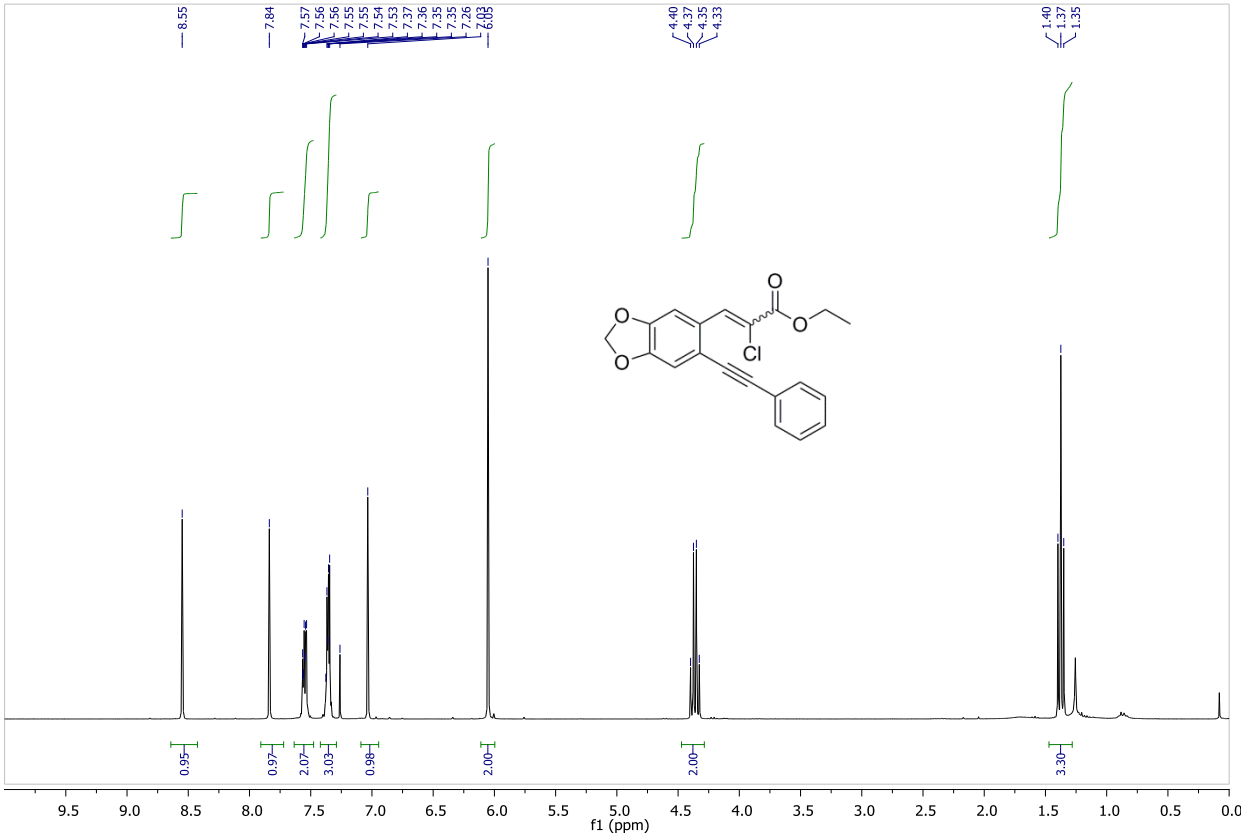

^{13}C-NMR: **1c**

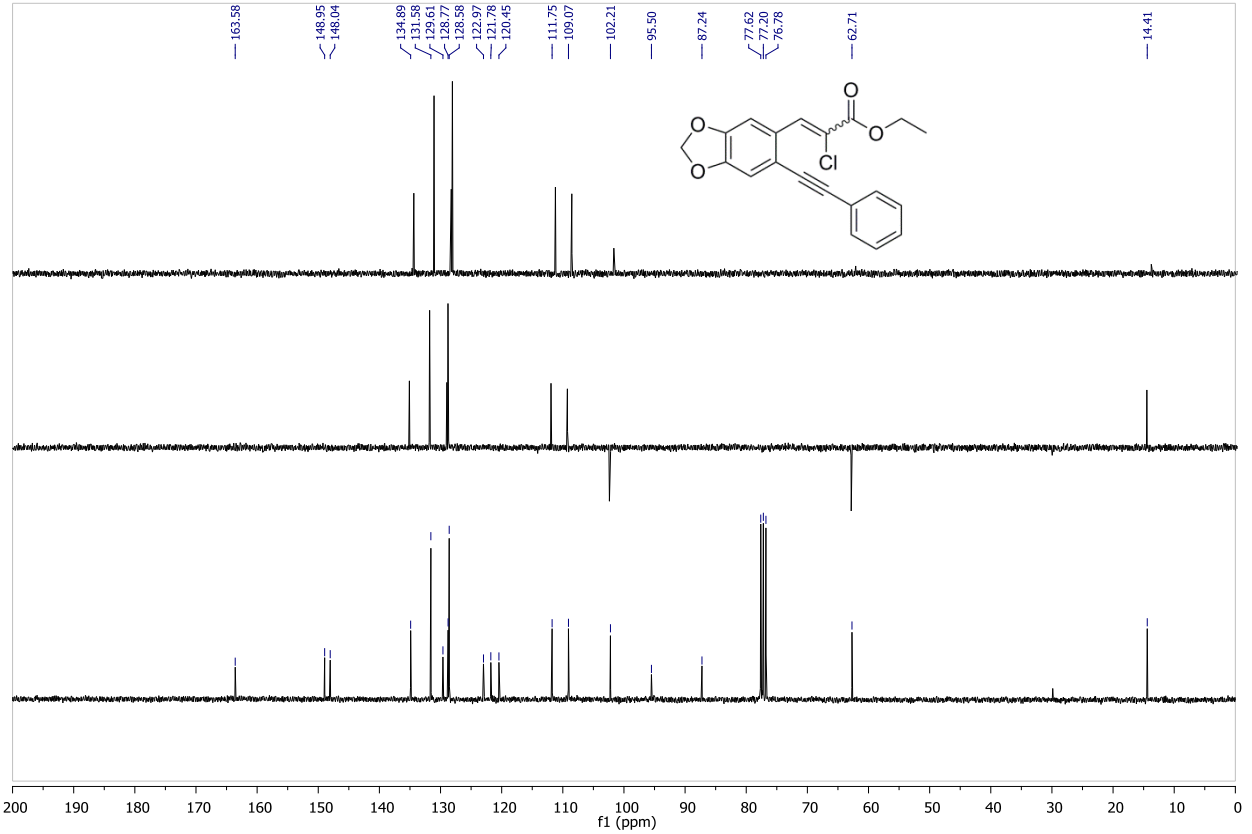

^{1}H-NMR: **1d**

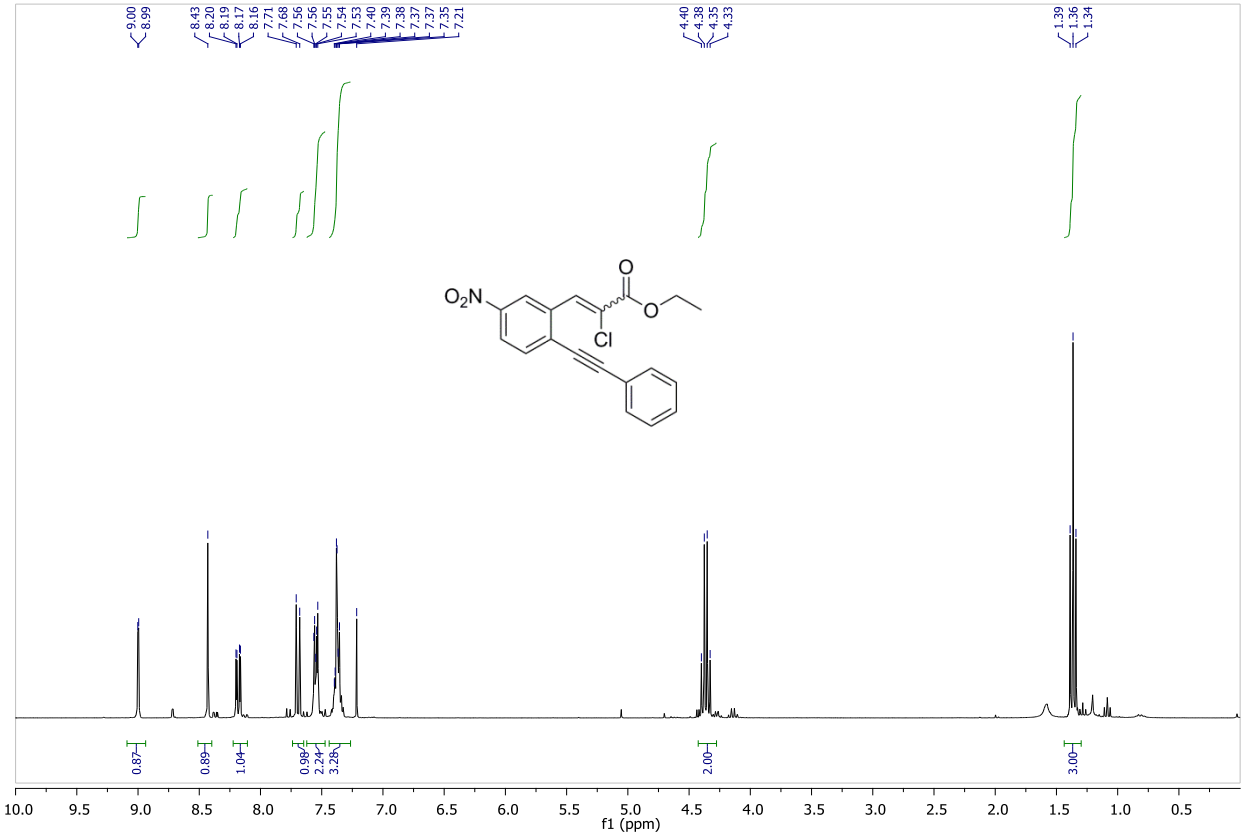

^{13}C-NMR: **1d**

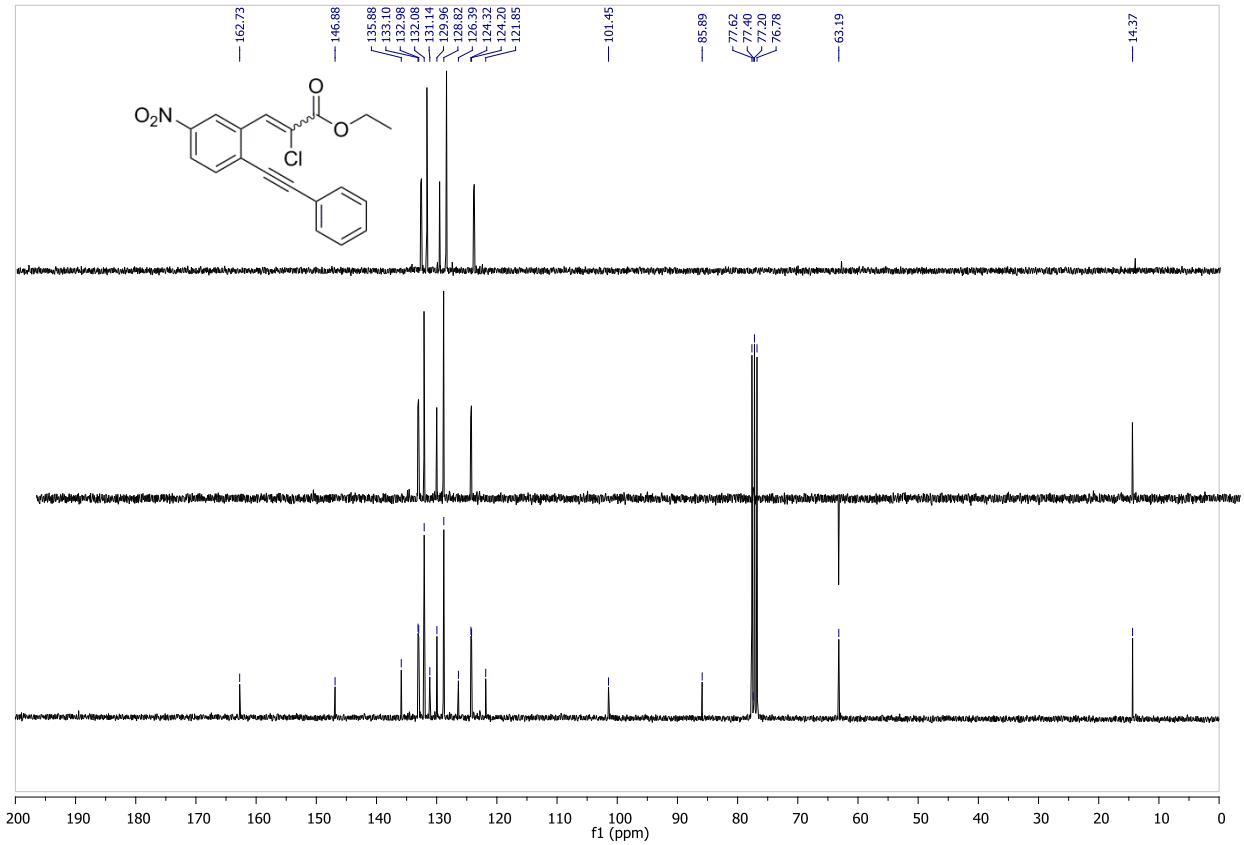

^{1}H-NMR: **1e**

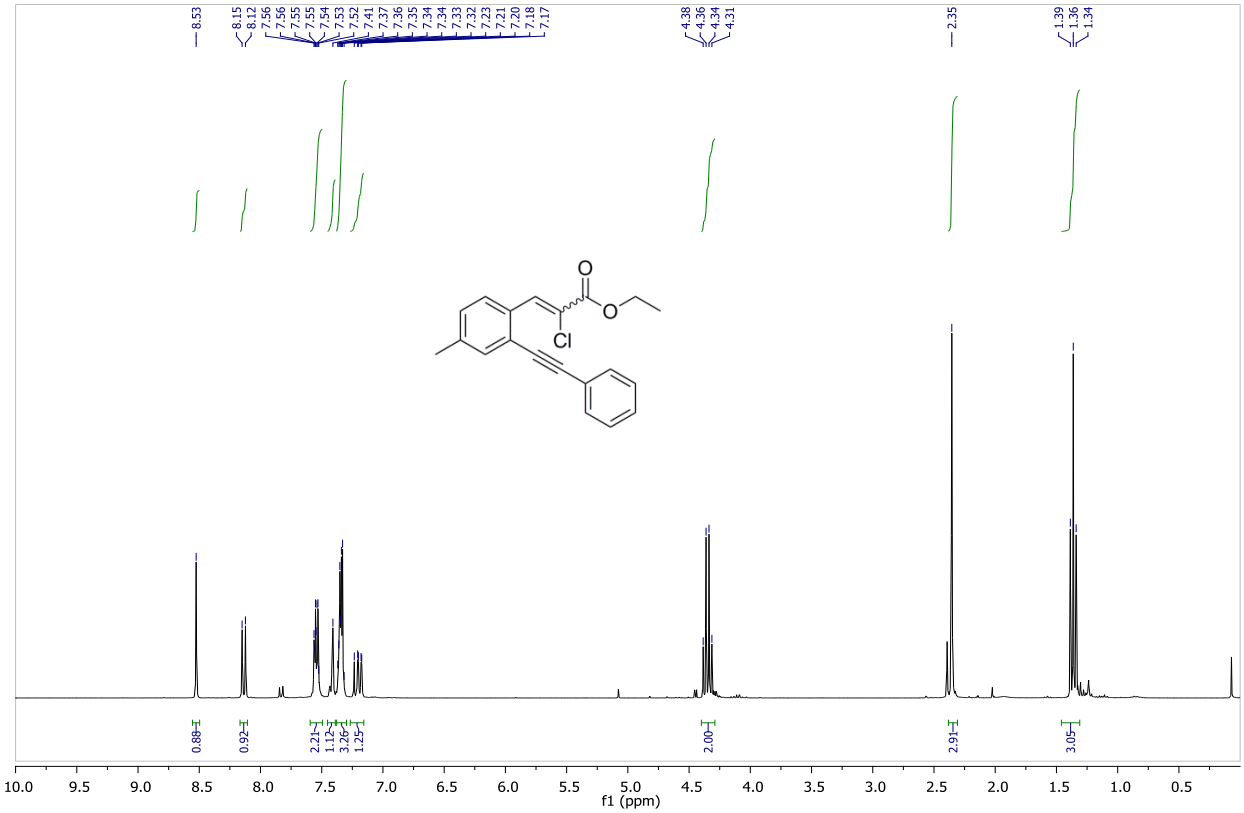

^{13}C-NMR: **1e**

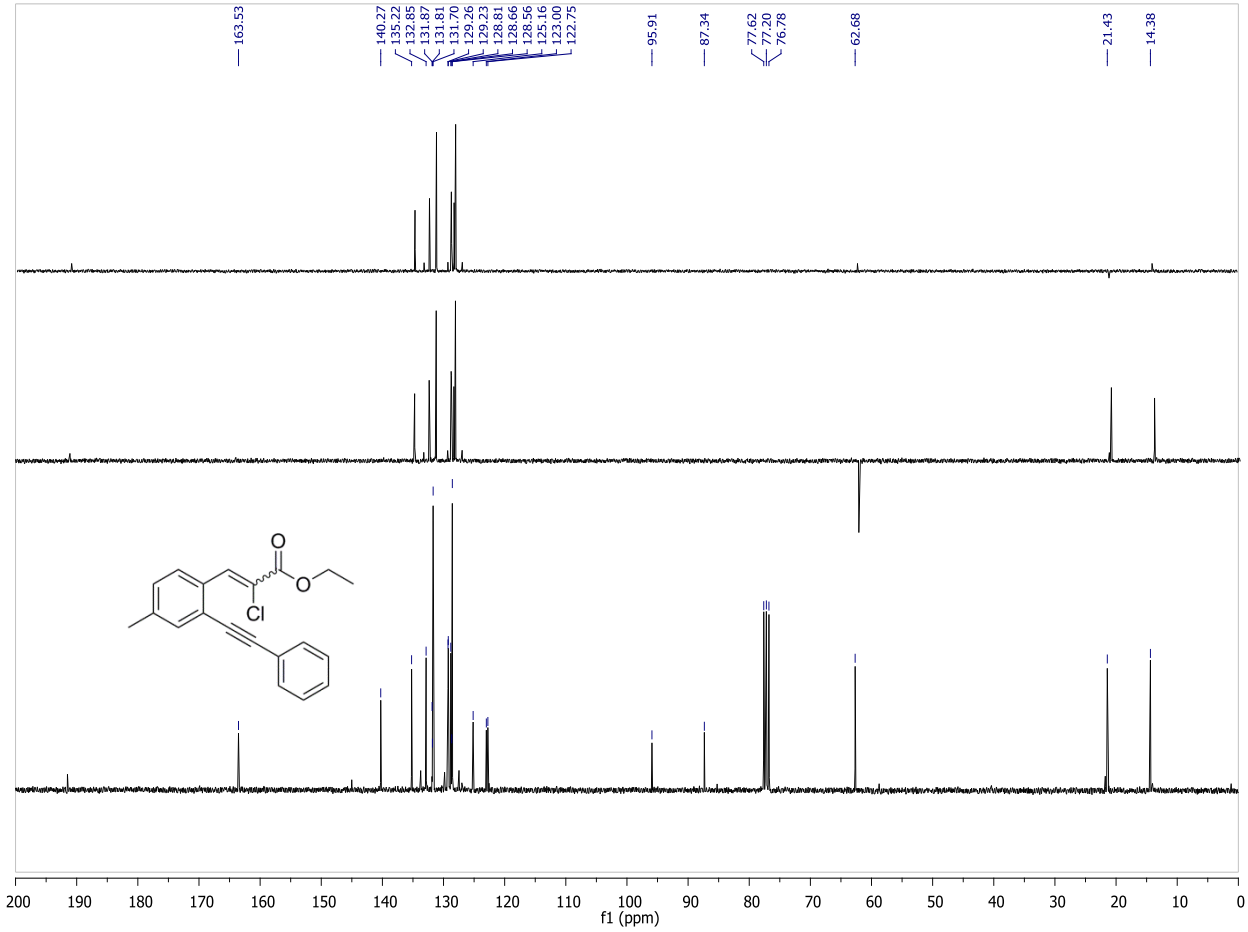

^{1}H-NMR: **3a**

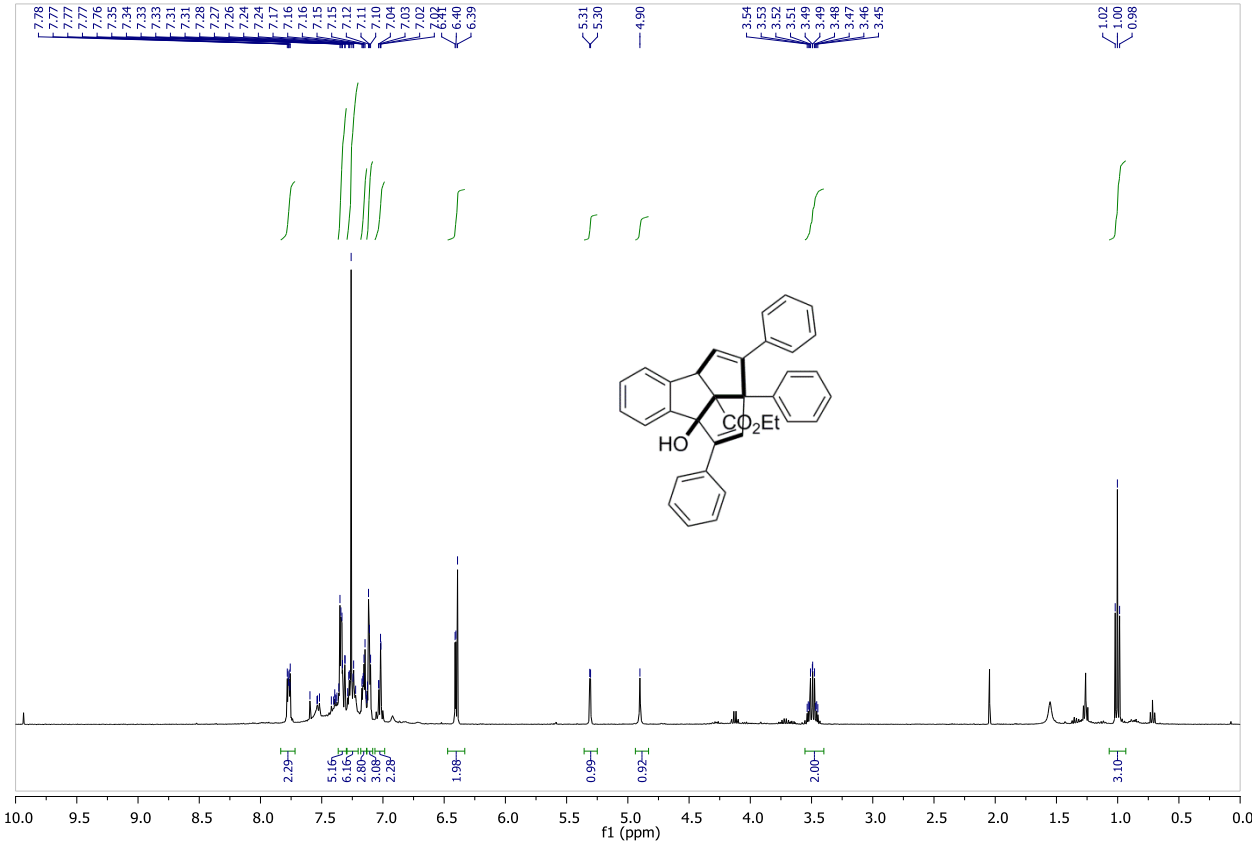

^{13}C-NMR: **3a**

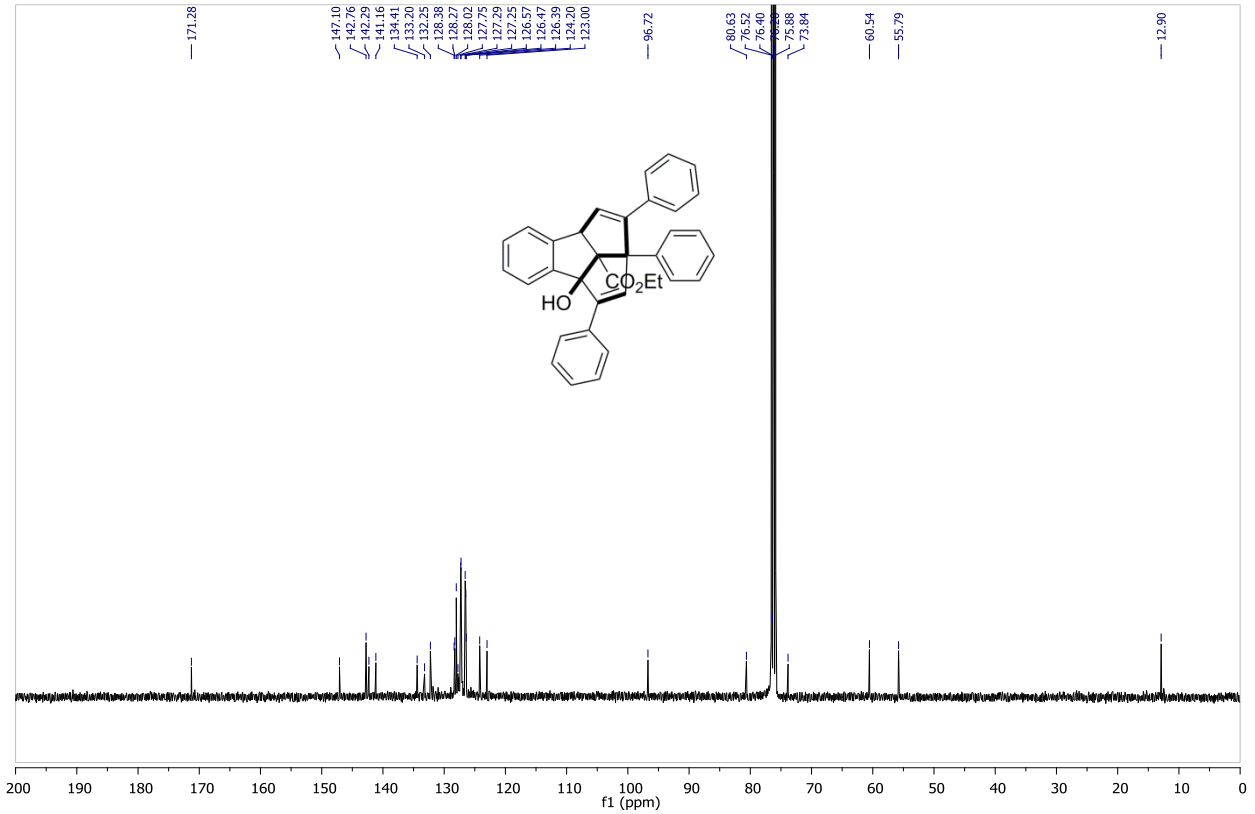

6.9 Crystal data of 3a:

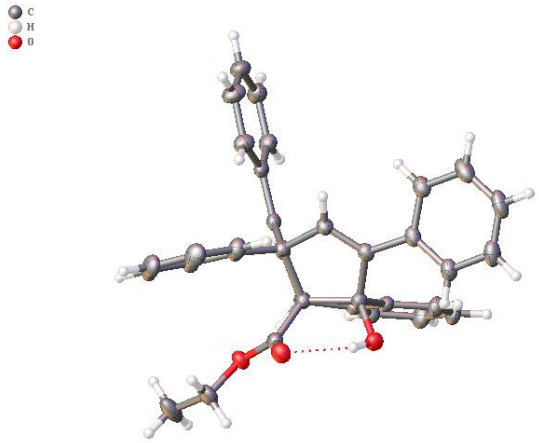

Figure: 6.3: Single crystal structure of **3a**

Experimental: Single clear yellow prism-shaped crystals of (**3A**) were obtained by recrystallisation from DCM/Pentane diffusion method. A suitable crystal (0.22×0.15×0.09) mm³ was selected and mounted on a MITIGEN holder oil on a SuperNova, Single source at offset, Atlas diffractometer. The crystal was kept at T = 297.77(10) K during data collection. Using **Olex2** (Dolomanov et al., 2009), the structure was solved with the **ShelXT** (Sheldrick, 2015) structure solution program, using the Intrinsic Phasing solution method. The model was refined with version 2016/6 of **ShelXL** (Sheldrick, 2015) using Least Squares minimisation.

Crystal Data. $C_{35}H_{28}O_3$, M_r = 496.57, triclinic, P-1 (No. 2), a = 9.2067(3) Å, b = 10.1106(4) Å, c = 15.1256(5) Å, α = 79.025(3)°, β = 86.455(2)°, γ = 65.654(3)°, V = 1259.08(8) Å³, T = 297.77(10) K, Z = 2, Z' = 1, μ(CuK_α) = 0.648, 33922 reflections measured, 5040 unique (R_{int} = 0.0527) which were used in all calculations. The final wR_2 was 0.1051 (all data) and R_1 was 0.0387 (I > 2(I)).

Compound	**3a**
Formula	$C_{35}H_{28}O_3$
$D_{calc.}$/ g cm^{-3}	1.310
μ/mm^{-1}	0.648
Formula Weight	496.57
Colour	clear yellow
Shape	prism
Size/mm³	0.22×0.15×0.09
T/K	297.77(10)
Crystal System	triclinic
Space Group	P-1
a/Å	9.2067(3)
b/Å	10.1106(4)
c/Å	15.1256(5)
α/°	79.025(3)
β/°	86.455(2)
γ/°	65.654(3)
V/Å³	1259.08(8)
Z	2
Z'	1
Wavelength/Å	1.54184
Radiation type	CuK_α
Θ_{min}/°	4.882
Θ_{max}/°	73.705
Measured Refl.	33922
Independent Refl.	5040
Reflections Used	4210
R_{int}	0.0527
Parameters	345
Restraints	0
Largest Peak	0.273
Deepest Hole	-0.191
GooF	1.030
wR_2 (all data)	0.1051
wR_2	0.0981
R_1 (all data)	0.0481
R_1	0.0387

Table 6.2: Fractional Atomic Coordinates (×10⁴) and Equivalent Isotropic Displacement Parameters (Å²×10³) for **3a**. U_{eq} is defined as 1/3 of the trace of the orthogonalised U_{ij}.

Atom	x	y	z	U_{eq}
O(3)	4471.6(11)	8349.4(10)	6783.9(7)	28.2(2)
O(1)	2641.2(10)	5712.3(10)	8144.4(6)	28.1(2)
O(2)	2914.2(11)	6677.4(11)	6714.0(6)	30.8(2)
C(5)	5430.2(15)	5577.8(13)	8775.2(8)	22.3(3)
C(3)	3451.1(15)	6136.7(14)	7473.1(9)	24.2(3)
C(6)	5937.7(14)	6778.5(14)	8889.0(9)	23.3(3)
C(11)	6341.8(15)	4328.5(13)	7424.6(8)	26(3)
C(4)	5136.4(14)	5808.6(13)	7747.3(8)	22.0(3)
C(7)	6171.2(14)	7543.2(13)	8064.5(9)	23.3(3)
C(9)	7052.3(15)	6291.6(14)	6676.9(8)	23.6(3)
C(12)	5502.6(15)	3527.9(13)	7037.3(9)	24.5(3)
C(19)	8769.4(15)	2033.5(14)	8276.7(9)	24.7(3)
C(18)	7322.6(15)	3416.5(13)	8281.4(9)	23.2(3)
C(25)	6782.1(15)	4079.7(14)	8991.8(9)	23.4(3)
C(10)	7347.2(15)	4869.1(14)	6756.4(8)	23.4(3)
C(26)	7944.4(16)	7039.4(15)	6088.9(9)	25.8(3)
C(13)	4806.7(16)	2705.9(14)	7609.7(10)	28.6(3)
C(8)	5690.7(15)	7066.6(13)	7277.0(9)	22.8(3)
C(32)	6715.8(17)	8644.4(15)	8038.3(10)	29.9(3)
C(17)	5347.8(17)	3658.4(15)	6112.1(10)	30.6(3)
C(27)	7284.0(18)	8566.4(16)	5764.0(9)	30.8(3)
C(35)	6205.9(16)	7118.2(15)	9691.9(9)	28.6(3)
C(20)	9106.4(17)	1263.0(15)	7560.7(10)	31.5(3)
C(24)	9871.0(16)	1470.2(15)	8992.6(10)	30.4(3)
C(31)	9491.2(17)	6207.6(17)	5833.3(9)	30.7(3)
C(22)	11558.4(17)	-543.9(16)	8280.3(11)	35.7(3)
C(34)	6732.0(18)	8230.4(16)	9663.3(10)	33.9(3)
C(21)	10492.6(19)	-9.0(16)	7563.3(11)	37.6(3)
C(14)	3944.4(18)	2063.6(16)	7265.8(11)	35.2(3)
C(33)	7006(19)	8971.9(16)	8843.7(10)	34.9(3)
C(15)	3789.3(19)	2209.7(16)	6345.0(11)	37.6(3)
C(28)	8156(2)	9216.8(18)	5200.7(10)	37.5(3)
C(23)	11241.8(17)	190.2(16)	8999.5(11)	34.9(3)
C(16)	4501.0(19)	2997.2(17)	5767.5(10)	36.8(3)
C(30)	10351.7(19)	6865.2(19)	5276(1)	37.5(4)
C(29)	9682(2)	8372.7(19)	4957.7(10)	40.0(4)
C(2)	1073.9(17)	5834.1(18)	7902.3(11)	38.5(4)
C(1)	416(2)	5233(2)	8717.2(14)	54.5(5)

Table 6.3: Anisotropic Displacement Parameters (×10⁴) **3a**. The anisotropic displacement factor exponent takes the form: $-2\pi^2[h^2a^{*2} \times U_{11} + \ldots + 2hka^* \times b^* \times U_{12}]$

Atom	U_{11}	U_{22}	U_{33}	U_{23}	U_{13}	U_{12}
O(3)	27.3(5)	24.7(5)	30.5(5)	-0.8(4)	-6(4)	-10.0(4)
O(1)	22.8(4)	33.7(5)	30.4(5)	-5.0(4)	6(4)	-14.9(4)
O(2)	29.8(5)	35.9(5)	28.6(5)	-4.6(4)	-3.0(4)	-15.3(4)
C(5)	23.8(6)	24.9(6)	21.3(6)	-5.5(5)	3.7(5)	-12.8(5)
C(3)	24.8(6)	22.2(6)	27.4(7)	-7.2(5)	2.2(5)	-10.5(5)
C(6)	21.3(6)	23.2(6)	26.5(7)	-7.1(5)	2.6(5)	-9.5(5)
C(11)	24.8(6)	22.6(6)	21.5(6)	-6.0(5)	3.7(5)	-10.9(5)
C(4)	23.1(6)	22.8(6)	22.8(6)	-6.0(5)	3.1(5)	-11.5(5)
C(7)	22.0(6)	21.3(6)	26.3(7)	-6.1(5)	6(5)	-8.1(5)

Atom	U_{11}	U_{22}	U_{33}	U_{23}	U_{13}	U_{12}
C(9)	24.6(6)	28.7(6)	20.1(6)	-4.7(5)	0.4(5)	-13.3(5)
C(12)	26.5(6)	21.6(6)	26.9(7)	-6.8(5)	1.8(5)	-10.5(5)
C(19)	26.2(6)	22.2(6)	27.5(7)	-3.6(5)	4.6(5)	-12.7(5)
C(18)	25.7(6)	23.2(6)	24.2(6)	-3.6(5)	2.9(5)	-14.2(5)
C(25)	25.9(6)	24.5(6)	22.2(6)	-3.1(5)	1.6(5)	-13.3(5)
C(10)	24.6(6)	26.9(6)	20.3(6)	-6.1(5)	3.4(5)	-11.8(5)
C(26)	31.6(7)	33.1(7)	19.8(6)	-5.9(5)	1.5(5)	-20.1(6)
C(13)	34.5(7)	26.7(6)	27.5(7)	-5.7(5)	6(5)	-15.3(6)
C(8)	23.1(6)	21.4(6)	24.1(6)	-2.7(5)	1.0(5)	-10.1(5)
C(32)	36.1(7)	26.0(6)	30.5(7)	-4.1(5)	2.7(6)	-16.4(6)
C(17)	38.2(7)	30.9(7)	27.2(7)	-6.1(5)	0.6(6)	-18.2(6)
C(27)	36.3(7)	34.3(7)	27.8(7)	-3.5(6)	0.3(6)	-21.4(6)
C(35)	33.9(7)	29.4(7)	25.8(7)	-6.6(5)	2.8(5)	-15.8(6)
C(20)	34.7(7)	29.5(7)	26.7(7)	-5.8(5)	2.5(6)	-9.7(6)
C(24)	31.8(7)	27.2(7)	34.4(8)	-8.8(6)	0.3(6)	-12.6(6)
C(31)	34.9(7)	38.9(7)	26.8(7)	-11.3(6)	5.7(6)	-21.9(6)
C(22)	30.2(7)	26.2(7)	44.9(9)	-6.9(6)	4.7(6)	-6.3(6)
C(34)	45.2(8)	34.5(7)	30.3(8)	-10.9(6)	-0.2(6)	-22.3(7)
C(21)	41.2(8)	30.4(7)	34.5(8)	-10.8(6)	7.2(6)	-6.8(6)
C(14)	40.3(8)	30.9(7)	42.1(9)	-7.1(6)	2.1(6)	-22.1(6)
C(33)	47.2(8)	30.8(7)	37.0(8)	-8.7(6)	1.1(7)	-25.0(7)
C(15)	42.8(8)	34.1(8)	44.2(9)	-12.5(6)	-5.8(7)	-20.8(7)
C(28)	52.1(9)	42.3(8)	28.9(8)	1.0(6)	-3.4(7)	-32.7(7)
C(23)	31.4(7)	29.6(7)	42.7(9)	-4.6(6)	-5.5(6)	-11.7(6)
C(16)	47.3(9)	37.5(8)	30.0(8)	-8.7(6)	-5.4(6)	-19.7(7)
C(30)	39.5(8)	57.8(10)	30.5(8)	-18.8(7)	11.1(6)	-31.9(7)
C(29)	53.7(9)	60.9(10)	26.0(7)	-8.1(7)	8.0(7)	-44.6(9)
C(2)	24.4(7)	47.7(9)	46.1(9)	-2.9(7)	-3.8(6)	-19.3(6)
C(1)	29.2(8)	65.3(11)	65.6(12)	13.5(9)	-3.2(8)	-26.4(8)

Table 6.4: Bond Lengths in Å for **3a**.

Atom	Atom	Length/Å
O(3)	C(8)	1.4259(15)
O(1)	C(3)	1.3325(15)
O(1)	C(2)	1.4606(16)
O(2)	C(3)	1.2124(16)
C(5)	C(6)	1.5096(17)
C(5)	C(4)	1.5512(18)
C(5)	C(25)	1.5026(17)
C(3)	C(4)	1.5141(18)
C(6)	C(7)	1.3913(18)
C(6)	C(35)	1.3855(19)
C(11)	C(4)	1.5972(16)
C(11)	C(12)	1.5322(18)
C(11)	C(18)	1.5325(18)
C(11)	C(10)	1.5060(17)
C(4)	C(8)	1.5906(16)
C(7)	C(8)	1.5186(18)
C(7)	C(32)	1.3906(18)
C(9)	C(10)	1.3315(18)
C(9)	C(26)	1.4842(17)
C(9)	C(8)	1.5263(17)
C(12)	C(13)	1.3954(18)
C(12)	C(17)	1.391(2)
C(19)	C(18)	1.4821(17)
C(19)	C(20)	1.3987(19)
C(19)	C(24)	1.396(2)
C(18)	C(25)	1.3359(18)
C(26)	C(27)	1.4032(19)
C(26)	C(31)	1.3976(19)
C(13)	C(14)	1.388(2)
C(32)	C(33)	1.389(2)
C(17)	C(16)	1.392(2)
C(27)	C(28)	1.3929(19)
C(35)	C(34)	1.3889(19)
C(20)	C(21)	1.389(2)
C(24)	C(23)	1.385(2)
C(31)	C(30)	1.3851(19)
C(22)	C(21)	1.379(2)
C(22)	C(23)	1.382(2)
C(34)	C(33)	1.387(2)
C(14)	C(15)	1.382(2)
C(15)	C(16)	1.386(2)
C(28)	C(29)	1.380(2)
C(30)	C(29)	1.385(2)
C(2)	C(1)	1.477(2)

Table 6.5: Bond Angles in ° for **3a**.

Atom	Atom	Atom	Angle/°
C(3)	O(1)	C(2)	115.85(11)
C(6)	C(5)	C(4)	104.86(10)
C(25)	C(5)	C(6)	111.21(10)
C(25)	C(5)	C(4)	104.23(10)
O(1)	C(3)	C(4)	112.91(11)
O(2)	C(3)	O(1)	123.48(12)
O(2)	C(3)	C(4)	123.55(11)
C(7)	C(6)	C(5)	111.92(11)
C(35)	C(6)	C(5)	127.07(12)
C(35)	C(6)	C(7)	120.98(12)
C(12)	C(11)	C(4)	113.39(10)
C(12)	C(11)	C(18)	112.79(10)
C(18)	C(11)	C(4)	102.95(10)
C(10)	C(11)	C(4)	102.53(9)
C(10)	C(11)	C(12)	114.01(10)
C(10)	C(11)	C(18)	110.19(10)
C(5)	C(4)	C(11)	106.55(10)
C(5)	C(4)	C(8)	107.13(10)
C(3)	C(4)	C(5)	115.07(10)
C(3)	C(4)	C(11)	109.35(10)
C(3)	C(4)	C(8)	112.17(10)
C(8)	C(4)	C(11)	106.05(9)
C(6)	C(7)	C(8)	112.00(11)
C(32)	C(7)	C(6)	119.99(12)
C(32)	C(7)	C(8)	127.94(12)
C(10)	C(9)	C(26)	124.58(12)
C(10)	C(9)	C(8)	111.71(11)
C(26)	C(9)	C(8)	123.70(11)
C(13)	C(12)	C(11)	120.35(12)
C(17)	C(12)	C(11)	121.13(11)
C(17)	C(12)	C(13)	118.45(12)
C(20)	C(19)	C(18)	122.17(12)
C(24)	C(19)	C(18)	120.28(12)
C(24)	C(19)	C(20)	117.54(12)
C(19)	C(18)	C(11)	1265(11)
C(25)	C(18)	C(11)	111.80(11)
C(25)	C(18)	C(19)	125.56(12)
C(18)	C(25)	C(5)	114.23(12)
C(9)	C(10)	C(11)	115.54(11)
C(27)	C(26)	C(9)	122.36(12)
C(31)	C(26)	C(9)	119.63(12)
C(31)	C(26)	C(27)	118.00(12)
C(14)	C(13)	C(12)	120.91(13)
O(3)	C(8)	C(4)	115.08(10)
O(3)	C(8)	C(7)	106.74(10)
O(3)	C(8)	C(9)	112.17(10)
C(7)	C(8)	C(4)	103.55(10)
C(7)	C(8)	C(9)	115.33(10)
C(9)	C(8)	C(4)	103.91(10)
C(33)	C(32)	C(7)	118.96(13)
C(12)	C(17)	C(16)	120.61(13)
C(28)	C(27)	C(26)	120.35(14)
C(6)	C(35)	C(34)	118.88(13)
C(21)	C(20)	C(19)	120.94(14)
C(23)	C(24)	C(19)	121.43(13)
C(30)	C(31)	C(26)	121.23(14)
C(21)	C(22)	C(23)	119.74(13)
C(33)	C(34)	C(35)	120.35(13)
C(22)	C(21)	C(20)	120.33(14)
C(15)	C(14)	C(13)	120.09(13)
C(34)	C(33)	C(32)	120.81(13)
C(14)	C(15)	C(16)	119.70(14)
C(29)	C(28)	C(27)	120.59(15)
C(22)	C(23)	C(24)	120.02(14)
C(15)	C(16)	C(17)	120.22(14)
C(29)	C(30)	C(31)	120.11(14)
C(28)	C(29)	C(30)	119.72(13)
O(1)	C(2)	C(1)	107.64(13)

Table 6.6: Hydrogen Fractional Atomic Coordinates (×10⁴) and Equivalent Isotropic Displacement Parameters (Å²×10³) for **3a**. U_{eq} is defined as 1/3 of the trace of the orthogonalised U_{ij}.

Atom	x	y	z	U_{eq}
H(3)	3929.5	8101.39	6496.57	42
H(5)	4477.29	5631.33	9120.53	27
H(25)	7206.1	3651.12	9570.53	28
H(10)	81262	4250.49	6421.57	28
H(13)	4922.14	2586.78	8229.98	34
H(32)	6885.36	9153.66	7490.06	36
H(17)	5814.08	4192.14	5720.01	37
H(27)	6258.63	9147.34	5925.67	37
H(35)	6036.49	6610.12	10240.64	34
H(20)	8391.86	1607.5	7076.1	38
H(24)	9679.82	1965.28	9475.11	37
H(31)	9951.3	5193.7	6041.13	37
H(22)	12486.49	-1395.34	8279.72	43
H(34)	6903.82	8479.11	10196.65	41
H(21)	10703.46	-502.66	7079.11	45
H(14)	3470.46	1534.19	7655.52	42
H(33)	7380.39	9697.53	8833.23	42
H(15)	3209.95	1781.52	6114.03	45
H(28)	7705.68	10229.09	4986.49	45
H(23)	11949.53	-175.37	9488.33	42
H(16)	4412.75	3084.34	5147.9	44
H(30)	11381.28	6293.42	5115.46	45
H(29)	10257.25	8814.21	4581.66	48
H(2A)	1169.51	5279.93	7428.03	46
H(2B)	375.72	6858.99	7687.54	46
H(1A)	-613.69	5291.41	8576.23	82
H(1B)	314.49	5796.87	9179.34	82
H(1C)	1118.67	4221.43	8925.79	82

6.10 References:

[1] a) A. Gupta, J. Cook, U. Weiss, *Tetrahedron Lett.* **1988**, *29*, 2535; b) S. H. Bertz, G. Lannoye, J. M. Cook, *Tetrahedron Lett.* **1985**, *26*, 4695; c) A. K. Gupta, G. S. Lannoye, G. Kubiak, J. Schkeryantz, S. Wehrli, J. M. Cook, *J. Am. Chem. Soc.* **1989**, *111*, 2169.

[2] R. B. Woodward, T. Fukunaga, R. C. Kelly, *J. Am. Chem. Soc.* **1964**, 3162.

[3] S. P. Verevkin, H.-D. Beckhaus, C. Rüchardt, R. Haag, S. I. Kozhushkov, T. Zywietz, A. de Meijere, H. Jiao, P. v. R. Schleyer, *J. Am. Chem. Soc.* **1998**, *120*, 11130.

[4] a) J. W. Baum, C. D. Gutsche, *J. Org. Chem.* **1968**, *33*, 4312; b) Pierre Deslongchamps, Ukken Ouseph Cheriyan, Yvon Lambert, Jean-Claude Mercier, Luc Ruest, Robert Russo, Pierre Soucy, *Can. J. Chem.* **1978**, *56*, 1687.

[5] H. Butenschön, A. de Meijere, *Tetrahedron Lett.* **1983**, *24*, 4563.

[6] A. de Meijere, *Int. J. Mass Spec. Ion Phys.* **1982**, *44*, 277.

[7] S. K. Pagire, P. Kreitmeier, O. Reiser, *Angew. Chem., Int. Ed.* **2017**, *56*, 10928.

[8] M. S. Lowry, J. I. Goldsmith, J. D. Slinker, R. Rohl, R. A. Pascal, G. G. Malliaras, S. Bernhard, *Chem. Mater.* **2005**, *17*, 5712.

[9] C. K. Prier, D. A. Rankic, D. W. C. MacMillan, *Chem. Rev.* **2013**, *113*, 5322.

[10] J. Sun, W. Wu, J. Zhao, *Chem. Eur. J.* **2012**, *18*, 8100.

[11] J. K. Augustine, A. Bombrun, S. Venkatachaliah, A. Jothi, *Org. Biomol. Chem.* **2013**, *11*, 8065.

7 Shining visible-light on sulfonyl chlorides: Versatile applications in organic synthesis

7.1 Introduction:

Recently, sulfonyl chlorides have been recognized as cheapest, commercially available, biocompatible, and stable starting materials in the construction of C-C or C-S bonds.[1] In principle, the sulfonyl chlorides known to undergo the loss of SO_2 group to trigger the C-C bond formation in visible-light photocatalysis.[2,3–5] For instance, trifluoromethyl sulfonyl chloride or aryl sulfonyl chloride directly forms a trifluoromethyl[3,5] or aryl radicals[4] upon SO_2 extrusion under the oxidative quenching cycle providing corresponding C-CF_3 or C-aryl products, respectively. For aryl radical generations, diazonium salts used as alternative coupling partners in visible-light photocatalysis.[6] However, diazonium salts suffer from various disadvantages, such as: explosive in nature, unstable at ambient conditions, expensive, difficult to store for longer periods of time even at low temperatures, functionalized derivatives are not commercially available, and it should be freshly prepared prior to use.

Secondly, a few examples concerning the construction of C-S bond are also known.[7,8] Oxidative quenching is one of the principal SET processes in the activation of sulfonyl chlorides. In this process, the excited-state photocatalyst is quenched by the sulfonyl chloride, giving rise to sulfonyl radical with the extrusion of a chloride.[7] Notably, other sulfonyl sources such as aryl or alkyl sulfinates,[9] sulfonyl hydrazides[10] or sulfinic acids[11] are also known to provide the identical sulfonyl radicals; however, most of these reagents are commercially not available, thus it needs to synthesize in the laboratory before starting the desired reaction, which ultimately calls for additional synthetic/purification steps.

All in all, having identified the advantage of using sulfonyl chlorides over aryl diazonium salts or other sulfonyl sources, synthetic community turned their attention towards sulfonyl chlorides, and indeed, a number of synthetic methods have been established over the period of time, which are recently summarized by Natarajan *et al* in their excellent review article.[12]

7.2 References:

[1] a) H. Jiang, Y. Cheng, Y. Zhang, S. Yu, *Eur. J. Med. Chem.* **2013**, *2013*, 5485; b) G. Li, X. Lv, K. Guo, Y. Wang, S. Yang, L. Yu, Y. Yu, J. Wang, *Org. Chem. Front.* **2017**, *4*, 1145; c) Y. Wang, X. Zhang, H. Liu, H. Chen, D. Huang, *Org. Chem. Front.* **2017**, *4*, 31; d) A. Hfaiedh, H. Ben Ammar, J.-F. Soulé, H. Doucet, *Org. Biomol. Chem.* **2016**, *14*, 4947.

[2] a) P. Natarajan, A. Bala, S. K. Mehta, K. K. Bhasin, *Tetrahedron* **2016**, *72*, 2521; b) X.-J. Tang, W. R. Dolbier, *Angew. Chem., Int. Ed.* **2015**, *54*, 4246; c) L. Gu, C. Jin, J. Liu, H. Ding, B. Fan, *Chem. Comm.* **2014**, *50*, 4643; d) L. Gu, C. Jin, W. Wang, Y. He, G. Yang, G. Li, *Chem. Comm.* **2017**, *53*, 4203; e) C. Liu, B. Zhang, *RSC Adv.* **2015**, *5*, 61199; f) M. Baar, S. Blechert, *Chem. Eur. J.* **2015**, *21*, 526; g) X. Li, D. Liang, W. Huang, H. Zhou, Z. Li, B. Wang, Y. Ma, H. Wang, *Tetrahedron* **2016**, *72*, 8442; h) J.-D. Xia, G.-B. Deng, M.-B. Zhou, W. Liu, P. Xie, J.-H. Li, *Synlett* **2012**, *23*, 2707.

[3] D. A. Nagib, D. W. C. MacMillan, *Nature* **2011**, *480*, 224.

[4] G.-B. Deng, Z.-Q. Wang, J.-D. Xia, P.-C. Qian, R.-J. Song, M. Hu, L.-B. Gong, J.-H. Li, *Angew. Chem., Int. Ed.* **2013**, *52*, 1535.

[5] D. B. Bagal, G. Kachkovskyi, M. Knorn, T. Rawner, B. M. Bhanage, O. Reiser, *Angew. Chem., Int. Ed.* **2015**, *54*, 6999.

[6] D. P. Hari, B. Konig, *Chem. Comm.* **2014**, *50*, 6688.

[7] S. K. Pagire, S. Paria, O. Reiser, *Org. Lett.* **2016**, *18*, 2106.

[8] a) M. Chen, Z.-T. Huang, Q.-Y. Zheng, *Org. Biomol. Chem.* **2014**, *12*, 9337; b) X. Liu, T. Cong, P. Liu, P. Sun, *Org. Biomol. Chem.* **2016**, *14*, 9416; c) Z. Zhang, X.-J. Tang, W. R. Dolbier, *Org. Lett.* **2016**, *18*, 1048; d) X.-F. Xia, S.-L. Zhu, D. Wang, Y.-M. Liang, *Adv. Synth. Catal.* **2017**, *359*, 859.

[9] a) A. U. Meyer, K. Straková, T. Slanina, B. König, *Chem. Eur. J.* **2016**, *22*, 8694; b) A. U. Meyer, A. Wimmer, B. Konig, *Angew. Chem., Int. Ed.* **2017**, *56*, 409.

[10] T. Taniguchi, A. Idota, H. Ishibashi, *Org. Biomol. Chem.* **2011**, *9*, 3151.

[11] N. Taniguchi, *J. Org. Chem.* **2015**, *80*, 7797.

[12] R. Chaudhary, P. Natarajan, *ChemistrySelect* **2017**, *2*, 6458.

8 Synthesis of β-hydroxysulfones from sulfonyl chlorides and alkenes utilizing visible-light photocatalytic sequences

8.1 Abstract:

The synthesis of β-hydroxysulfones from sulfonyl chlorides and styrenes has been achieved in high yields by a visible light mediated Atom Transfer Radical Addition (ATRA)-like process utilizing *fac*[Ir(ppy)$_3$] as photoredox catalyst. Moreover, this process could also be combined with the visible light mediated synthesis of trifluoromethylated sulfonyl chlorides via an ATRA reaction between unactivated alkenes and CF_3SO_2Cl utilizing [Cu(dap)$_2$Cl] as photoredox catalyst, signifying the opportunity of sequential photoredox processes.

8.2 Introduction:

The β-hydroxysulfone is a privileged scaffold that has been utilized for numerous pharmaceutical drug candidates, fine chemicals, and as a valuable precursor in the synthesis of a variety of biologically active molecules.[1] For example, the anticancer drug bicalutamide and antifungal agents, for instance, Sch42427 and SSY726 attribute a β-hydroxysulfone moiety.[2] Recently, quite a lot of advancements for the synthesis of β-hydroxysulfones have been reported.

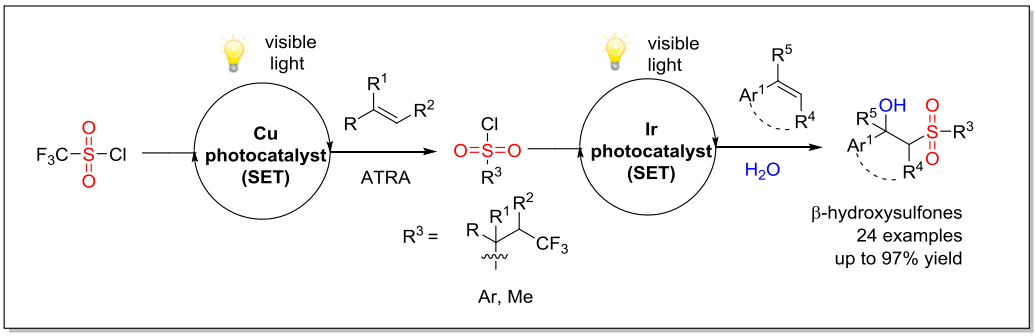

Scheme 8.1: Sequential [Cu]- and [Ir] catalyzed method for the synthesis of β-hydroxysulfones.

This Chapter has been published:

S. K. Pagire, S. Paria, O. Reiser, *Org. Lett.* **2016**, *18*, 2106-2109.

S.K.P. and O.R. wrote the manuscript.

For instance, the opening of epoxides with sulfinate salts,[3] chemical or bio-reduction of β-ketosulfones,[4] and the addition of organometallic reagents to carbonyl compounds.[5]

A range of techniques utilizing the addition of sulfonic acid derivatives to styrenes have been particularly developed towards the intention compounds.[6,7] Given the broad accessibility of sulfonyl chlorides, a few of them like *p*-toluenesulfonyl chloride (TsCl) being industrially produced on ton scale, this compound set appears to be striking for the direct synthesis of β-hydroxysulfones. However, to the best of our information, this has not been accessed yet by photochemical methods.[8] Almost from a last decade, visible-light induced photoredox catalysis has been proved a fascinating field in organic synthesis, offering a non-polluting, endlessly clean source of energy, naturally abundant, with exceptional applications in organic synthesis.[9,10]
We present here the [Ir]-catalyzed, visible-light mediated ATRA-like reaction for the synthesis of β-hydroxysulfone from sulfonyl chlorides and styrenes, featuring sustainable and cost-effective reaction conditions, high yields and superb regioselectivity. Moreover, since trifluoromethylated sulfonyl chlorides can be achieved by a copper-catalyzed, visible light mediated ATRA reaction between CF_3SO_2Cl and alkenes (*vide infra*),[11] we showcase the sequential exploitation of two photoredox processes for the synthesis of the aimed compounds, fetching together two diverse photo-reactions.

As a first step, we tested the viability of developing a photochemical ATRA-like reaction between sulfonyl chlorides to β-hydroxysulfones. Sulfinic acid salts[12] and especially sulfonyl chlorides[13] have been utilized previously in photoredox processes signifying that the generation of sulfonyl radicals by single electron transfer (SET) should be possible.

8.3 Results and discussion:

Consequently, using α-methyl styrene **1a** and 4-nitrobenzenesulfonyl chloride **2a** as model, we screened various photoredox catalysts under visible light irradiation in aqueous solvents, targeted the formation of hydroxysulfone **3a**. Starting with $[Ru(bpy)_3Cl_2]$ (bpy = bipyridine; E = -0.81 V versus SCE) as catalyst under blue light irradiation (λ_{max} = 455 nm), we quickly realized that a mixture of acetonitrile and water, ensuring both, solubility of reagents and catalyst as well as

having a supply for introduction of the hydroxyl group is necessary (Table 8.1, entries 1-6). The best ratio of acetonitrile / water was found to be 5:1 (Table 8.1, entry 5) giving rise to **3a** in 90% yield. Substituting $[Ru(bpy)_3Cl_2]$ with $[Cu(dap)_2Cl]$[14] (dap = 2,9-bis(*p*-anisyl)-1,10-phenanthroline; E = –1.43 V versus SCE), being an even stronger reductant in its excited state than $[Ru(bpy)_3Cl_2]$ also gave rise to **3a**, though, in lower yields (Table 1, entry 7).

8.4 synthesis of 3a and 3b: Catalyst screening and reaction optimization

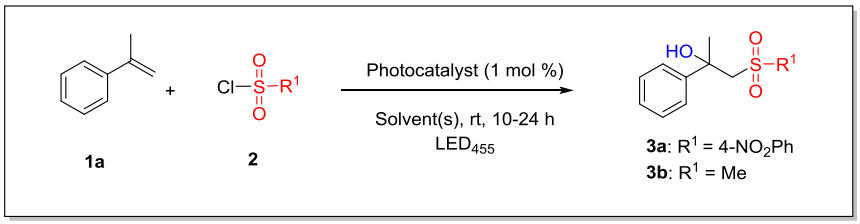

Entry	R^1 in R^1SO_2Cl	Photocatalyst (1 mol %)	Solvent(s)	Yield (%)[b]
1	4-NO_2Ph	$[Ru(bpy)_3Cl_2]$	H_2O	6
2	4-NO_2Ph	$[Ru(bpy)_3Cl_2]$	MeCN:H_2O (1:3)	40
3	4-NO_2Ph	$[Ru(bpy)_3Cl_2]$	MeCN:H_2O (1:1)	51
4	4-NO_2Ph	$[Ru(bpy)_3Cl_2]$	MeCN:H_2O (3:1)	63
5	4-NO_2Ph	$[Ru(bpy)_3Cl_2]$	MeCN:H_2O (5:1)	90
6	4-NO_2Ph	$[Ru(bpy)_3Cl_2]$	MeCN:H_2O (7:1)	69
7	4-NO_2Ph	$[Cu(dap)_2Cl]$	MeCN:H_2O (5:1)	61
8	4-NO_2Ph	*fac*$[Ir(ppy)_3]$	MeCN:H_2O (5:1)	95
9	4-NO_2Ph	no catalyst	MeCN:H_2O (5:1)	trace[c]
10	4-NO_2Ph	*fac*$[Ir(ppy)_3]$ no light	MeCN:H_2O (5:1)	trace[c]
11[d]	Me	$[Cu(dap)_2Cl]$	MeCN:H_2O (5:1)	21
12[d]	Me	$[Ru(bpy)_3Cl_2]$	MeCN:H_2O (5:1)	7

Table 8.1: Reaction conditions: [a] **1a** (1.0 mmol, 1.0 equiv), sulfonyl chloride **2** (1.5 mmol, 1.5 equiv), photocatalyst (1 mol %), solvent(s) (2 mL), LED_{455}. [b] Isolated yields. [c] Detected by TLC analysis, starting materials remain unchanged. [d] 24 h irradiation time. [e] 10 h irradiation time.

Finally, *fac*[Ir(ppy)$_3$][15] (ppy = 2-phenylpyridine; E = –1.73 V versus SCE) having the strongest reducing power after excitation of all other catalysts tested, allowed the isolation of 3a in 95% yield (Table 8.1, entry 8). Control experiments further confirmed both, light and a photoredox catalyst is required to the reaction to proceed effectively (Table 8.1, entry 9-10). Switching from the aromatic 4-nitrosulfonyl chloride (E = -0.44 V versus SCE) to the aliphatic mesyl chloride **2b**, having more negative reduction potential (E = -1.39 V versus SCE, see experimental section), only catalyst *fac*[Ir(ppy)$_3$] gave the hydroxysulfone **3b** in good yields (Table 8.1, entry 11-13). As a result, the scope and limitations for the synthesis of β-hydroxysulfones **3** was subsequently explored using the *fac*[Ir(ppy)$_3$] photocatalyst.

8.5 Scope for sulfonyl chlorides

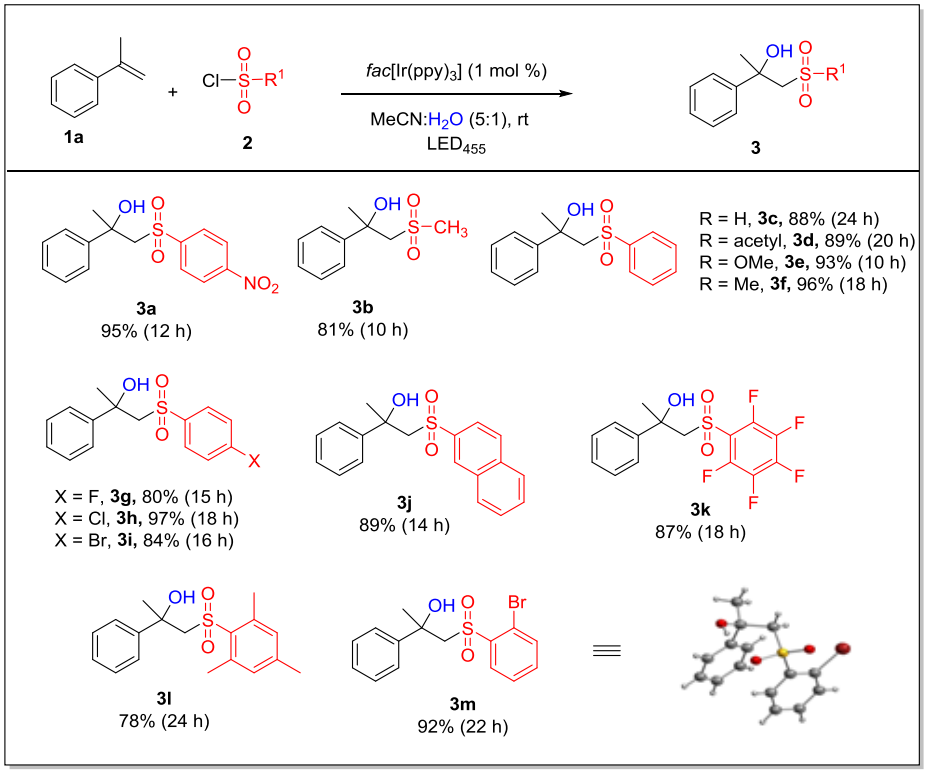

Table 8.2: Reaction conditions: α-methyl styrene **1a** (1.0 mmol, 1.0 equiv), sulfonyl chloride **2** (1.5 mmol, 1.5 equiv), *fac*[Ir(ppy)$_3$] (1 mol %), MeCN (1.67 mL), water (0.33 mL), LED$_{455}$ at room temperature.

Various sulfonyl chlorides could be efficiently coupled with α-methyl styrene **1a** (Table 8.2), demonstrating the broad functional group compatibility for the photochemical process. A series of aryl sulfonyl chlorides bearing strong or weak electron-donating groups and electron-withdrawing groups afforded the desired hydroxysulfones in excellent yields.

Notably, a nitro substituent, which is typically a limitation for photochemical[16] or radical processes,[17] was fully compatible under current conditions. Moreover, sterically bulkier groups at the sulfonyl chloride such as 2-naphthyl, pentafluorophenyl, mesityl, or ortho-bromophenyl efficiently reacted with styrenes to afford the corresponding tertiary hydroxysulfones **3j**-**3m** in 78-92% yield. Furthermore, the identity of the β-hydroxysulfones **3** was further explained by the X-ray crystal structure of *ortho*-bromo hydroxysulfone derivative **3m** (Table 8.2).

8.6 Scope for alkenes

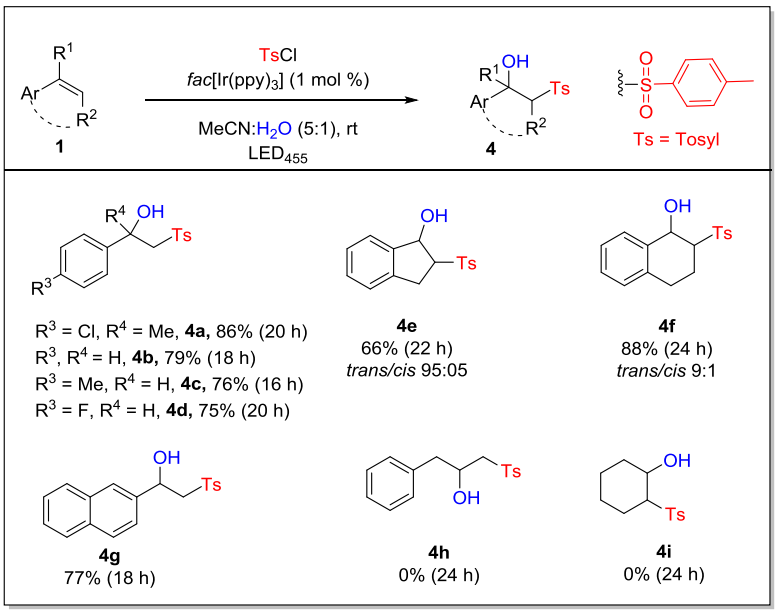

Table 8.3: Reaction conditions: Alkene **1** (1.0 mmol, 1.0 equiv), tosyl chloride **2f** (1.5 mmol, 1.5 equiv), *fac*[Ir(ppy)$_3$] (1 mol %), MeCN (1.67 mL), distilled water (0.33 mL), LED$_{455}$ at room temperature.

Furthermore, using tosyl chloride as a common sulfonyl source (Table 8.3), a range of styrene type alkenes also gave the corresponding β-hydroxysulfones in good to excellent yields, tolerating 1,1- and 1,2-disubstitution as well as a variety of functional groups in the aromatic

moiety. The limitation of the reaction was found with aliphatic alkenes that did not react at all, which is probably due to the less efficient oxidation of the alkyl radical formed after addition of RSO_2• to the alkene (*vide infra*, see mechanism).

From the last few years, our group has engaged in the development of $[Cu(dap)_2Cl]$ catalyzed, visible light mediated ATRA reactions.[18] Recently, we have shown unprecedented trifluoromethylsulfochlorination of unactivated alkenes utilizing CF_3SO_2Cl (E = -0.18 V versus SCE)[19] as a sulfonyl partner.[11] This surprising reaction contrasts the [Ru] or [Ir] catalyzed processes that resulted only in chlorinated products (Scheme 8.2).[19] In this reaction, it is assumed that $[Cu(dap)_2Cl]$ plays a dual role, i.e. acting both as an electron transfer reagent as well as coordinating the reactants in the bond forming processes.[11]

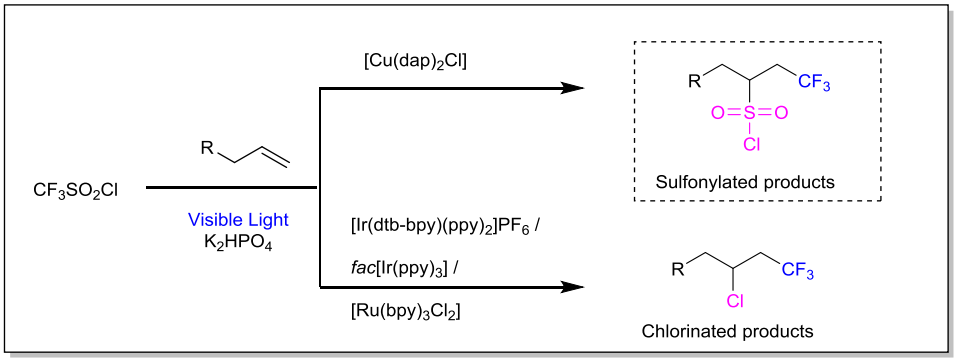

Scheme 8.2: Catalyst selective Sulfonylation vs. chlorination of unactivated alkenes

8.7 Sequential photocatalysis (One or two flask synthesis)

We thought this method could also be used as a starting point for further developments since fluorine containing compounds are valuable building blocks in pharmaceutical chemistry.[20] Therefore, along with the process towards β-hydroxysulfones developed here, we also explored the possibility to stitch two photocatalytic sequences together. Indeed, sulfonyl chlorides could be achieved by the $[Cu(dap)_2Cl]$ catalyzed ATRA process, followed by their *fac*$[Ir(ppy)_3]$ catalyzed addition to styrenes to yield **7a-7d** (Table 8.4). Noteworthy, each specific photocatalyst is necessary for the individual steps of the sequence: When *fac*$[Ir(ppy)_3]$ is used in to synthesize the sulfonyl chlorides **6a-6d**, direct addition of *trifluoromethyl* and *chloride* instead

of *sulfonylchloride* is observed, on the other hand [Cu(dap)$_2$Cl] was not redox-efficient[10] for the activation of **6a-6d** to engage in the coupling with styrenes to provide the desired hydroxysulfones **7a-7d** (Table 8.4).

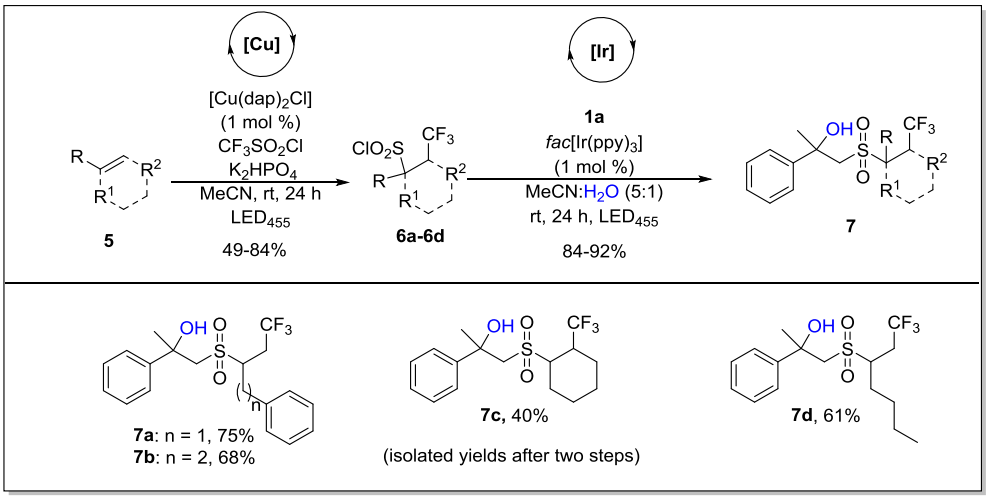

Table 8.4: Reaction conditions: (1st step) Alkene 5 (1.0 mmol, 1.0 equiv), CF_3SO_2Cl (2.0 mmol, 2.0 equiv), K_2HPO_4 (2.0 mmol, 2.0 equiv), [Cu(dap)$_2$Cl] (1 mol %), MeCN (2 mL), LED_{455} at room temperature for 24 h. (**2nd step):** α-methyl styrene 1a (1.0 mmol, 1.0 equiv), sulfonyl chloride 6 (1.5 mmol, 1.5 equiv), *fac*[Ir(ppy)$_3$] (1 mol %), MeCN (1.67 mL), distilled water (0.33 mL), LED_{455} at room temperature for 24 h.

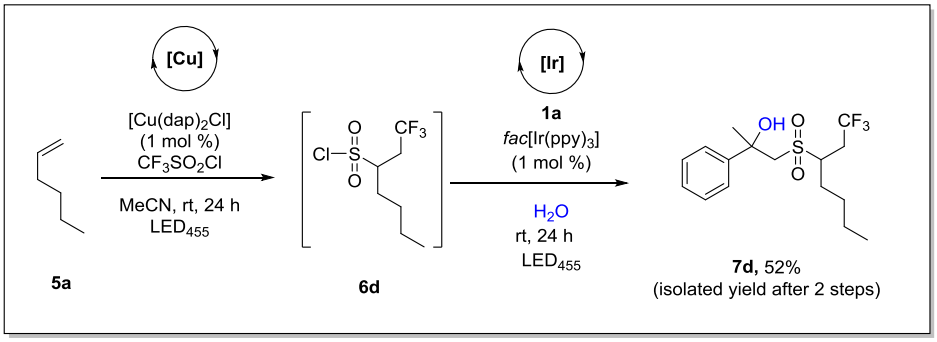

Scheme 8.3: Reaction conditions: 1-hexene **5a** (1.0 mmol, 1.0 equiv), CF_3SO_2Cl (2.0 mmol, 2.0 equiv), [Cu(dap)$_2$Cl] (1 mol %), MeCN (1.67 mL), LED_{455} at room temperature for 24 h then α-methyl styrene **1a** (1.0 mmol, 1.0 equiv, *fac*[Ir(ppy)$_3$] (1 mol %), distilled water (0.33 mL), LED_{455} at room temperature for 24 h.

This sequence can also be carried out in a single flask without the requirement to isolate the intermediate sulfonyl chlorides: e.g., **7d** could be directly obtained by first irradiating **5a** and

CF_3SO_2Cl in the presence of $[Cu(dap)_2Cl]$ (1 mol %) photocatalyst followed by the addition of distilled water, α-methylstyrene (**1a**) and *fac*$[Ir(ppy)_3]$ (1 mol %) (Scheme 8.3).

The resulting trifluoromethylated sulfones obtained from sequential photocatalysis as equimolar mixture of diastereomers, reflecting the nature of the two chronological radical addition processes. In order to arrive at diastereomerically pure compounds, the obtained hydroxysulfones can be further converted to vinylsulfones by a literature known procedure,[21] which is demonstrated with the conversion of **7b** to **8a** (Scheme 8.4).

8.8 Synthesis of vinyl Sulfones

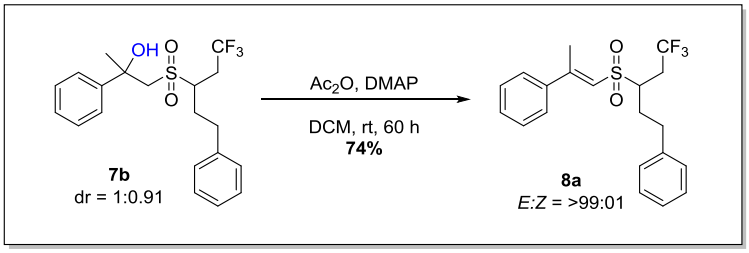

Scheme 8.4: Reaction conditions: 7b (0.5 mmol, 1.0 equiv), Ac_2O (1.0 mmol, 2.0 equiv), DMAP (1.0 mmol, 2.0 equiv), DCM (7 mL), at room temperature for 60 h.

8.9 Proposed reaction mechanism

We propose here a plausible reaction mechanism for the hydroxysulfonylation reaction. It is known that, the initial excitement of the Ir(III) photoredox catalyst should occur by irradiation with blue light to generate excited *Ir(III). Followed by single electron transfer (SET) to sulfonyl chloride **2** form the resultant sulfonyl radical **I** simultaneous with oxidation to Ir(IV). The regioselective sulfonyl radical **I** addition to styrene **1** takes place to arrive at the carbon cantered radical intermediate **II**, which subsequently undergoes oxidation to corresponding carbocation **III** by back electron transfer processes regenerating the Ir(III)-catalyst. The consequential carbocation **III** is trapped by water as a nucleophile (Figure 8.1).

In order to understand the reaction mechanism in more details, oxygen isotope labeling experiment was conducted. Indeed, it was found from the HRMS data that, the oxygen atom of the hydroxyl group in compound **3fa** was only originated from H_2O^{18} (See SI).

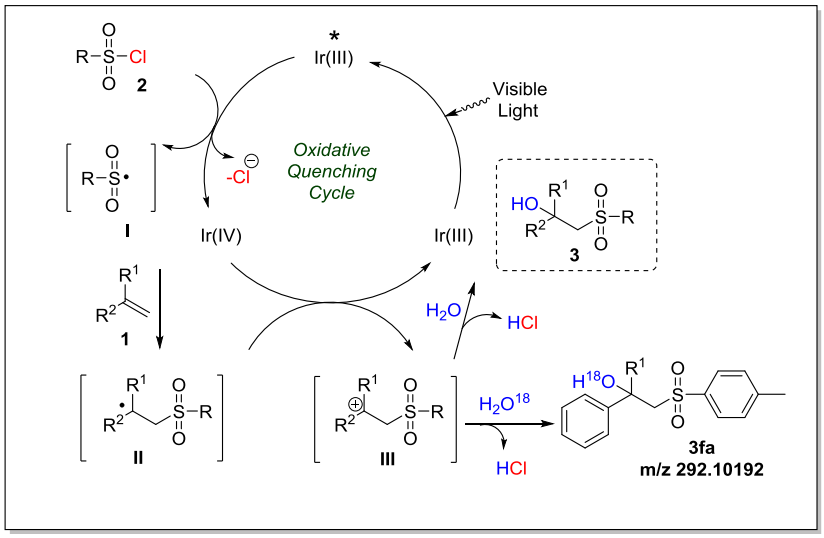

Figure 8.1: Proposed reaction mechanism for the synthesis of **3** and **3fa**.

8.10 Conclusion:

To conclude, we have developed a visible light mediated, Ir(III)-catalyzed ATRA-like reaction for the synthesis of β-hydroxysulfone derivatives from commercially available alkenes and sulfonyl chlorides. Moreover, in combination with the visible light mediated Cu(I)-catalyzed synthesis of trifluoromethyl containing sulfonyl chlorides, two different photochemical processes can be connected together in a logical way to access the β-hydroxysulfones demonstrating the possibility of sequential photochemical reactions.

8.11 Experimental section:

8.11.1 General procedure (GP-1): Scope for sulfonyl chloride

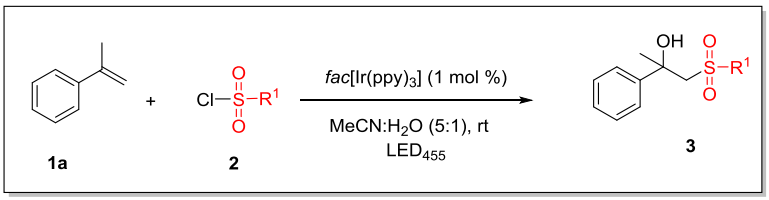

To an oven-dried Schlenk tube (10 ml size) equipped with a stir bar was added aryl sulfonyl chloride 2 (1.5 mmol, 1.5 equiv.) and *fac*[Ir(ppy)$_3$] (6.6 mg, 1.0 mol %). Then, acetonitrile (1.67 mL) and distilled water (0.33 mL) was added; the resulting suspension was deoxygenated by three freeze-pump-thaw cycles followed by the addition of the prop-1-en-2-ylbenzene (or α-methyl styrene) 1a (118 mg, 1.0 mmol, 1.0 equiv.) under positive nitrogen atmosphere. The reaction mixture was irradiated with blue light emitting diode (LED, λ_{max} = 455 nm) at room temperature. After complete conversion of starting materials (judged by TLC analysis), the reaction mixture was saturated with brine solution (15 mL) and the product was extracted with ethyl acetate (3x15 mL), the combined organic layers were dried over Na_2SO_4 and concentrated, the residue was purified by column chromatography on silica gel by using hexanes and ethyl acetate as eluents to afford the desired product 3.

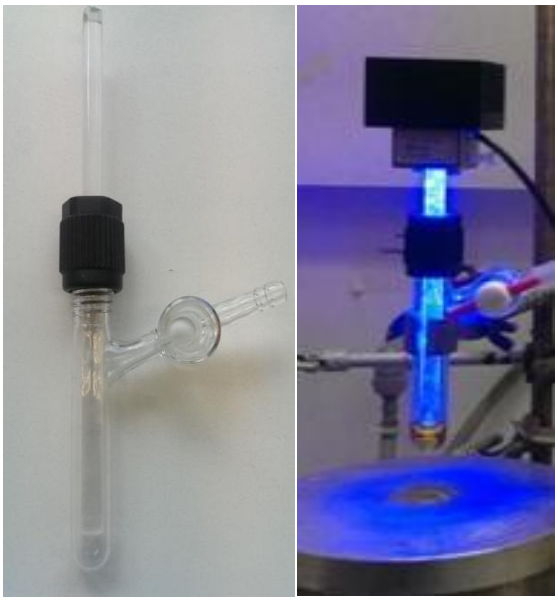

Figure 8.2: Experimental set-up for photochemical reaction

1-((4-nitrophenyl)sulfonyl)-2-phenylpropan-2-ol (3a):

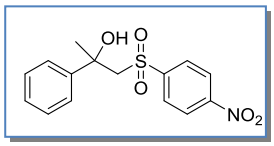

Following GP-1, **3a** was prepared from 4-nitrobenzenesulfonyl chloride **2a** (332 mg, 1.5 mmol). The crude product was purified by column chromatography (Hexanes: EtOAc, 4:1, R_f = 0.18) to afford **3a** as a colorless solid (305 mg, 95% yield).

^{1}H-NMR (300 MHz, DMSO): δ 8.29 (d, *J* = 8.6 Hz, 2H), 7.97 (d, *J* = 8.6 Hz, 2H), 7.35 (d, *J* = 7.6 Hz, 2H), 7.23 – 7.07 (m, 3H), 5.45 (s, 1H), 4.00 (ABq, *J* = 15.1 Hz, 2H), 1.60 (s, 3H).
^{3}C-NMR (75 MHz, DMSO): δ 149.70, 146.65, 146.30, 129.44, 127.52, 126.41, 124.89, 123.73, 71.55, 65.64, 29.92.
The obtained data is in accordance with the literature data.[22]

1-(methylsulfonyl)-2-phenylpropan-2-ol (3b):

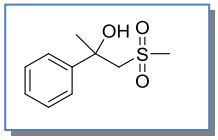

Following GP-1, **3b** was prepared from methanesulfonyl chloride **2b** (172 mg, 1.5 mmol). The crude product was purified by column chromatography (Hexanes: EtOAc, 4:1, R_f = 0.20) to afford **3b** as a colorless viscous oil (174 mg, 81% yield).

^{1}H-NMR (300 MHz, $CDCl_3$): δ 7.47 (dt, *J* = 3.2, 1.8 Hz, 2H), 7.43 – 7.37 (m, 2H), 7.34 – 7.27 (m, 1H), 3.52 (ABq, *J* = 14.9 Hz, 2H), 2.40 (s, 3H), 1.73 (s, 3H).
^{13}C-NMR (75 MHz, $CDCl_3$): δ 144.50, 128.81, 127.82, 124.81, 72.55, 65.58, 43.04, 30.61.
The obtained data is in accordance with the literature data.[23]

2-phenyl-1-(phenylsulfonyl)propan-2-ol (3c):

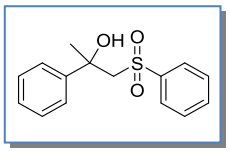

Following GP-1, **3c** was prepared from benzenesulfonyl chloride **2c** (265 mg, 1.5 mmol). The crude product was purified by column chromatography (Hexanes : EtOAc, 9:1, R_f = 0.19) to afford **3c** as a colorless solid (242 mg, 88% yield).

^{1}H-NMR (300 MHz, $CDCl_3$): δ 7.60 – 7.56 (m, 2H), 7.55 – 7.49 (m, 1H), 7.40 – 7.33 (m, 2H), 7.30 – 7.25 (m, 2H), 7.20 – 7.14 (m, 3H), 4.35 (bs, 1H), 3.68 (ABq, 14.7 Hz, 2H), 1.70 (s, 3H).
^{13}C-NMR (75 MHz, $CDCl_3$): δ 144.25, 140.20, 133.47, 129.12, 128.29, 127.51, 127.28, 124.65, 787, 66.62, 30.85.
The obtained data is in accordance with the literature data.[22]

1-(4-((2-hydroxy-2-phenylpropyl)sulfonyl)phenyl)ethan-1-one (3d):

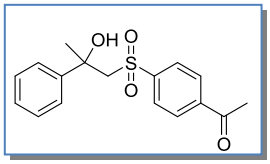

Following **GP-1**, **3d** was prepared from 4-acetylbenzenesulfonyl chloride **2d** (328 mg, 1.5 mmol). The crude product was purified by column chromatography (Hexanes : EtOAc, 4:1, R_f = 0.15) to afford **3d** as a colorless solid (285 mg, 89% yield).

^{1}H-NMR (300 MHz, $CDCl_3$): δ 7.86 (d, *J* = 8.6 Hz, 2H), 7.61 (d, *J* = 8.6 Hz, 2H), 7.22 (dd, *J* = 6.7, 3.0 Hz, 2H), 7.15 – 7.09 (m, 3H), 4.21 (bs, 1H), 3.72 (ABq *J* = 14.8 Hz, 2H), 2.61 (s, 3H), 1.67 (s, 3H).

^{13}C-NMR (75 MHz, $CDCl_3$): δ 196.69, 143.97, 143.66, 140.33, 128.71, 128.30, 127.95, 127.30, 124.72, 73.08, 66.59, 31.03, 26.97.

IR (neat, cm^{-1}): 3493, 2969, 2915, 1677, 1596, 1574, 1494, 1448, 1428, 1398, 1359, 1312, 1296, 1263, 1189, 1147, 1120, 1085, 1072, 1012, 944, 916, 863, 826, 781, 764, 749, 717, 699.

HRMS (ESI): exact m/z calculated for $C_{17}H_{22}F_5NO_4S$ $(M+NH_4)^+$: 336.1264; Found: 336.1268 $(M+ NH_4)^+$.

Mp: 137-139 ^oC (decomposed).

1-((4-methoxyphenyl)sulfonyl)-2-phenylpropan-2-ol (3e):

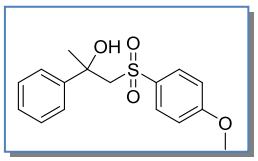

Following GP-1, **3e** was prepared from 4-methoxybenzenesulfonyl chloride **2e** (310 mg, 1.5 mmol). The crude product was purified by column chromatography (Hexanes: EtOAc, 4:1, R_f = 0.29) to afford **3e** as a colorless crystals (284 mg, 93% yield).

^{1}H-NMR (300 MHz, $CDCl_3$): δ 7.53 – 7.44 (m, 2H), 7.27 (dt, *J* = 8.5, 2.3 Hz, 2H), 7.23 – 7.14 (m, 3H), 6.84 – 6.77 (m, 2H), 4.54 (bs, 1H), 3.82 (s, 3H), 3.63 (ABq, *J* = 14.8 Hz, 2H), 1.68 (s, 3H).

^{13}C-NMR (75 MHz, $CDCl_3$): δ 163.52, 144.44, 131.75, 129.75, 128.28, 127.17, 124.67, 114.29, 784, 66.74, 55.72, 30.91.

The obtained data is in accordance with the literature data.[22]

2-phenyl-1-tosylpropan-2-ol (3f):

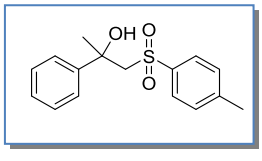

Following GP-1, **3f** was prepared from 4-methylbenzenesulfonyl chloride (tosyl chloride) **2f** (285 mg, 1.5 mmol). The crude product was purified by column chromatography (Hexanes: EtOAc, 4:1, R_f = 0.28) to afford **3f** as a colorless solid (278 mg, 96% yield).

^{1}H-NMR (300 MHz, $CDCl_3$): δ 7.50 – 7.44 (m, 2H), 7.31 – 7.25 (m, 2H), 7.22 – 7.13 (m, 5H), 4.32 (bs, 1H), 3.65 (ABq, 14.6 Hz, 2H), 2.38 (s, 3H), 1.70 (s, 3H).

^{13}C-NMR (75 MHz, $CDCl_3$): δ 144.55, 144.47, 137.31, 129.72, 128.26, 127.55, 127.15, 124.65, 787, 66.66, 30.78, 21.60.

The obtained data is in accordance with the literature data.[22]

1-((4-fluorophenyl)sulfonyl)-2-phenylpropan-2-ol (3g):

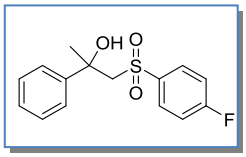

Following GP-1, **3g** was prepared from 4-fluorobenzenesulfonyl chloride **2g** (292 mg, 1.5 mmol). The crude product was purified by column chromatography (Hexanes: EtOAc, 4:1, R_f = 0.25) to afford **3g** as a colorless solid (236 mg, 80% yield).

^{1}H-NMR (300 MHz, $CDCl_3$): ^{1}H-NMR (300 MHz, $CDCl_3$) δ 7.57 – 7.48 (m, 2H), 7.27 – 7.20 (m, 2H), 7.20 – 7.14 (m, 3H), 7.05 – 6.96 (m, 2H), 4.57 (bs, 1H), 3.72 (ABq, 14.7 Hz, 2H), 1.67 (s, 3H).

^{13}C-NMR (75 MHz, $CDCl_3$): δ 167.20, 163.80, 144.01, 136.09, 130.53, 130.40, 128.33, 127.33, 124.70, 116.48, 116.18, 73.08, 66.75, 31.11.

^{19}F-NMR (282 MHz, $CDCl_3$): δ -103.97.

The obtained data is in accordance with the literature data.[7]

1-((4-chlorophenyl)sulfonyl)-2-phenylpropan-2-ol (3h):

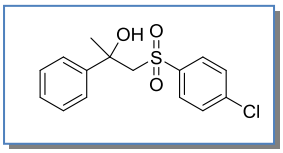

Following GP-1, **3h** was prepared from 4-chlorobenzenesulfonyl chloride **2h** (316 mg, 1.5 mmol). The crude product was purified by column chromatography (Hexanes: EtOAc, 4:1, R_f = 0.26) to afford **3h** as a colorless solid (301 mg, 97% yield).

^{1}H-NMR (300 MHz, $CDCl_3$): δ 7.47 – 7.41 (m, 2H), 7.33 – 7.27 (m, 2H), 7.25 – 7.21 (m, 2H), 7.20 – 7.15 (m, 3H), 4.53 (bs, 1H), 3.70 (ABq, *J* = 14.8 Hz, 2H), 1.67 (s, 3H).

^{13}C-NMR (75 MHz, $CDCl_3$): δ 143.96, 140.20, 138.45, 129.32, 129.03, 128.34, 127.32, 124.70, 73.07, 66.70, 31.11.

The obtained data is in accordance with the literature data.[7]

1-((4-bromophenyl)sulfonyl)-2-phenylpropan-2-ol (3i):

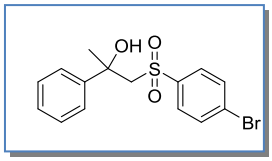

Following GP-1, **3i** was prepared from 4-bromobenzenesulfonyl chloride **2i** (383 mg, 1.5 mmol). The crude product was purified by column chromatography (Hexanes: EtOAc, 4:1, R_f = 0.28) to afford **3i** as a colorless solid (300 mg, 84% yield).

^{1}H-NMR (300 MHz, $CDCl_3$): δ 7.49 – 7.44 (m, 2H), 7.39 – 7.33 (m, 2H), 7.22 (dt, *J* = 5.4, 2.1 Hz, 2H), 7.20 – 7.15 (m, 3H), 4.53 (bs, 1H), 3.69 (ABq, *J* = 14.8 Hz, 2H), 1.67 (s, 3H).

^{13}C-NMR (75 MHz, $CDCl_3$): δ 143.93, 138.96, 132.31, 129.07, 128.81, 128.35, 127.31, 124.70, 73.06, 66.68, 31.12.

The obtained data is in accordance with the literature data.[22]

1-(naphthalen-2-ylsulfonyl)-2-phenylpropan-2-ol (3j):

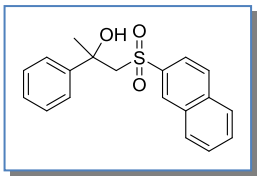

Following GP-1, **3j** was prepared from naphthalene-2-sulfonyl chloride **2j** (340 mg, 1.5 mmol). The crude product was purified by column chromatography (Hexanes: EtOAc, 4:1, R_f = 0.24) to afford **3j** as a colorless solid (290 mg, 89% yield).

^{1}H-NMR (300 MHz, $CDCl_3$): δ 8.04 (d, *J* = 1.6 Hz, 1H), 7.90 – 7.78 (m, 3H), 7.69 – 7.54 (m, 3H), 7.28 – 7.21 (m, 3H), 7.08 – 6.99 (m, 2H), 6.94 (ddd, *J* = 7.2, 3.7, 1.3 Hz, 1H), 4.70 (bs, 1H), 3.75 (ABq, *J* = 14.7 Hz, 2H), 1.70 (s, 3H).

^{13}C-NMR (75 MHz, $CDCl_3$): δ 144.04, 136.82, 135.04, 131.91, 129.79, 129.57, 129.46, 129.37, 128.11, 127.84, 127.56, 127.29, 124.59, 121.90, 73.20, 66.47, 30.97.

The obtained data is in accordance with the literature data.[7]

1-((perfluorophenyl)sulfonyl)-2-phenylpropan-2-ol (3k):

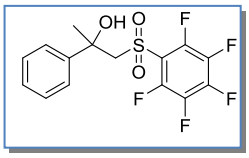

Following **GP-1**, **3k** was prepared from 2,3,4,5,6-pentafluorobenzenesulfonyl chloride **2k** (400 mg, 1.5 mmol). The crude product was purified by column chromatography (Hexanes: EtOAc, 4:1, R_f = 0.22) to afford **3k** as a colorless solid (319 mg, 87% yield).

^{1}H-NMR (600 MHz, $CDCl_3$): δ 7.31 – 7.28 (m, 2H), 7.20 (dd, *J* = 10.1, 4.8 Hz, 2H), 7.17 – 7.13 (m, 1H), 4.14 (s, 1H), 3.89 (ABq, *J* = 15.4 Hz, 2H), 1.69 (s, 3H).

^{13}C-NMR (151 MHz, $CDCl_3$): δ 145.42 (m), 143.64 (m), 142.91, 138.42 (m), 136.68 (m), 128.18, 127.65, 124.61, 72.60, 67.62, 31.20.

^{19}F-NMR (282 MHz, $CDCl_3$): δ -135.52 – -135.78 (m, 2F), -144.00 (tt, *J* = 21.1, 7.9 Hz, 1F), -158.73 – -159.11 (m, 2F).

IR (neat, cm^{-1}): 3525, 2972, 2916, 1740, 1646, 1519, 1489, 1446, 1369, 1337, 1292, 1261, 1229, 1216, 1150, 1118, 1095, 1071, 982, 943, 921, 866, 769, 753, 703.

HRMS (ESI): exact m/z calculated for $C_{15}H_{15}F_5NO_3S$ $(M+NH_4)^+$: 384.0687; Found: 384.0688 $(M+ NH_4)^+$.

Mp: 150-152 °C.

1-(mesitylsulfonyl)-2-phenylpropan-2-ol (3l):

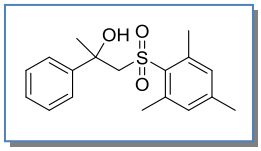

Following **GP-1**, **3l** was prepared from 2,4,6-trimethylbenzenesulfonyl chloride **2l** (328 mg, 1.5 mmol). The crude product was purified by column chromatography (Hexanes: EtOAc, 4:1, R_f = 0.66) to afford **3l** as a colorless solid (247 mg, 78% yield).

^{1}H-NMR (300 MHz, $CDCl_3$): δ 7.42 – 7.36 (m, 2H), 7.29 – 7.16 (m, 3H), 6.92 – 6.80 (m, 2H), 4.33 (bs, 1H), 3.59 (ABq, *J* = 14.4 Hz, 2H), 2.59 (s, 6H), 2.27 (s, 3H), 1.80 (s, 3H).

^{13}C-NMR (75 MHz, $CDCl_3$): δ 145.10, 143.64, 139.47, 134.39, 132.33, 128.30, 127.24, 124.46, 73.61, 66.12, 30.40, 22.82, 21.00.

IR (neat, cm^{-1}): 3498, 2978, 2941, 1738, 1600, 1561, 1492, 1443, 1401, 1379, 1299, 1268, 1242, 1151, 1111, 1075, 1034, 936, 850, 755, 721, 700.

HRMS (ESI): exact m/z calculated for $C_{18}H_{15}NO_3S$ $(M+NH_4)^+$: 336.1628; Found: 336.1633 $(M+ NH_4)^+$.

Mp: 66-68 °C (decomposed).

1-((2-bromophenyl)sulfonyl)-2-phenylpropan-2-ol (3m):

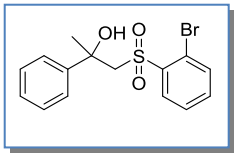

Following **GP-1**, **3m** was prepared from 2-bromobenzenesulfonyl chloride **2m** (383 mg, 1.5 mmol). The crude product was purified by column chromatography (Hexanes : EtOAc, 4:1, R_f = 0.40) to afford **3m** as a colorless needles (329 mg, 92% yield).

^{1}H-NMR (300 MHz, $CDCl_3$): δ 7.62 (dd, *J* = 7.9, 1.1 Hz, 1H), 7.51 (dd, *J* = 7.9, 1.7 Hz, 1H), 7.33 – 7.20 (m, 3H), 7.15 (td, *J* = 7.8, 1.2 Hz, 1H), 7.11 – 6.99 (m, 3H), 4.59 (bs, 1H), 4.07 (ABq, *J* = 15.1 Hz, 2H), 1.65 (s, 3H).

^{13}C-NMR (75 MHz, $CDCl_3$): δ 143.63, 138.84, 134.90, 134.33, 131.42, 128.11, 127.93, 127.33, 124.50, 120.21, 73.02, 63.80, 31.24.

IR (neat, cm^{-1}): 3493, 2973, 2944, 1740, 1568, 1494, 1444, 1426, 1378, 1363, 1305, 1241, 1154, 1109, 1090, 1042, 1020, 942, 914, 845, 757, 698.

HRMS (ESI): exact m/z calculated for $C_{15}H_{15}BrNaO_3S$ $(M+Na)^+$: 376.9817; Found: 376.9818 $(M+ Na)^+$.

Mp: 147-149 ^oC.

8.11.2 General procedure (GP-2): Scope for Alkenes

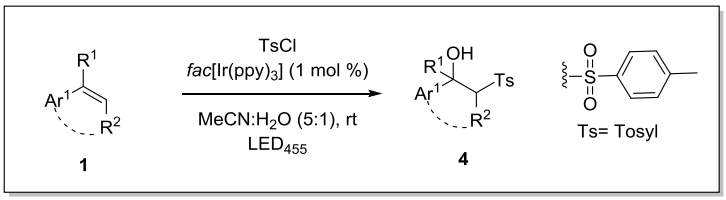

To an oven-dried Schlenk tube (10 ml size) equipped with a stir bar was added tosyl chloride **2f** (285mg, 1.5 mmol, 1.5 equiv.) and *fac*[Ir(ppy)$_3$] (6.6 mg, 1.0 mol %). Then, acetonitrile (1.67 mL) and distilled water (0.33 mL) was added; the resulting suspension was deoxygenated by three freeze-pump-thaw cycles followed by the addition of the corresponding alkene **1** (1.0 mmol, 1.0 equiv.) under positive nitrogen atmosphere. The reaction mixture was irradiated with blue light emitting diode (LED, λ_{max} = 455 nm) at room temperature. After complete conversion of starting materials (judged by TLC analysis), the reaction mixture was saturated with brine solution (15 mL) and the product was extracted with ethyl acetate (3x15 mL), the combined organic layers were dried over Na_2SO_4 and concentrated, the residue was purified by column chromatography on silica gel by using hexanes and ethyl acetate as eluents to afford the desired product **4**.

2-(4-chlorophenyl)-1-tosylpropan-2-ol (4a):

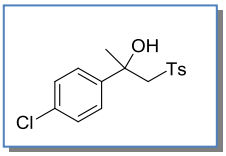

Following **GP-2**, **4a** was prepared from 1-chloro-4-(prop-1-en-2-yl)benzene (152 mg, 1.0 mmol). The crude product was purified by column chromatography (Hexanes: EtOAc, 4:1, R_f = 0.30) to afford **4a** as a colorless solid (280 mg, 86% yield).

^{1}H-NMR (300 MHz, $CDCl_3$): δ 7.42 (d, *J* = 8.3 Hz, 2H), 7.16 (dt, *J* = 4.3, 1.6 Hz, 4H), 7.12 – 7.06 (m, 2H), 4.71 (bs, 1H), 3.64 (ABq, *J* = 14.7 Hz, 2H), 2.41 (s, 3H), 1.63 (s, 3H).

^{13}C-NMR (75 MHz, $CDCl_3$): δ 144.83, 142.75, 136.88, 1387, 129.74, 128.23, 127.52, 126.25, 72.79, 66.32, 31.04, 21.62.

IR (neat, cm^{-1}): 3487, 2970, 2917, 1596, 1489, 1398, 1380, 1353, 1299, 1282, 1265, 1189, 1145, 1118, 1082, 1013, 948, 863, 824, 811, 763, 749, 702.

HRMS (ESI): exact m/z calculated for $C_{16}H_{21}ClNO_3S$ $(M+NH_4)^+$: 342.0925; Found: 342.0929 $(M+ NH_4)^+$.

Mp: 139-141 ^oC (decomposed).

1-phenyl-2-tosylethan-1-ol (4b):

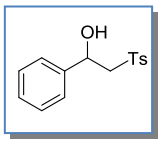

Following GP-2, **4b** was prepared from styrene (104 mg, 1.0 mmol). The crude product was purified by column chromatography (Hexanes : EtOAc, 4:1, R_f = 0.28) to afford **4b** as a colorless oil (218 mg, 79% yield).

^{1}H-NMR (300 MHz, $CDCl_3$): δ 7.82 (d, *J* = 8.0 Hz, 2H), 7.37 (d, *J* = 8.0 Hz, 2H), 7.32 – 7.24 (m, 5H), 5.24 (dd, *J* = 10.0, 1.8 Hz, 1H), 3.53 – 3.27 (m, 2H), 2.45 (s, 3H).

^{13}C-NMR (75 MHz, $CDCl_3$): δ 145.29, 140.79, 136.16, 130.13, 128.77, 128.32, 128.06, 125.71, 68.50, 63.99, 21.73.

The obtained data is in accordance with the literature data.[22]

1-(*p*-tolyl)-2-tosylethan-1-ol (4c):

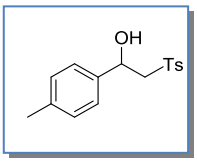

Following GP-2, **4c** was prepared from 1-methyl-4-vinylbenzene (118 mg, 1.0 mmol). The crude product was purified by column chromatography (Hexanes: EtOAc, 4:1, R_f = 0.33) to afford **4c** as a colorless solid (221 mg, 76% yield).

^{1}H-NMR (300 MHz, $CDCl_3$): δ 7.77 (dd, *J* = 18.2, 8.3 Hz, 2H), 7.34 (d, *J* = 8.1 Hz, 2H), 7.12 (dd, *J* = 18.2, 8.1 Hz, 4H), 5.18 (dd, *J* = 9.8, 1.7 Hz, 1H), 3.73 (bs, 1H), 3.54 – 3.23 (m, 2H), 2.43 (s, 3H), 2.29 (s, 3H).

^{13}C-NMR (75 MHz, $CDCl_3$): δ 145.16, 138.02, 137.99, 136.27, 130.07, 129.38, 128.07, 125.69, 68.38, 63.95, 21.71, 21.16.

The obtained data is in accordance with the literature data.[7]

1-(4-fluorophenyl)-2-tosylethan-1-ol (4d):

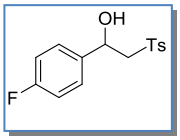

Following GP-2, **4d** was prepared from 1-fluoro-4-vinylbenzene (122 mg, 1.0 mmol). The crude product was purified by column chromatography (Hexanes : EtOAc, 4:1, R_f = 0.23) to afford **4d** as a colorless solid (221 mg, 75% yield).

^{1}H-NMR (300 MHz, $CDCl_3$): δ 7.81 (d, *J* = 8.0 Hz, 2H), 7.38 (d, *J* = 8.0 Hz, 2H), 7.32 – 7.20 (m, 2H), 7.05 – 6.92 (m, 2H), 5.23 (dd, *J* = 9.9, 1.7 Hz, 1H), 3.65 (bs, 1H), 3.36 (m, 2H), 2.46 (s, 3H).

^{13}C-NMR (75 MHz, $CDCl_3$): δ 164.13, 160.86, 145.42, 136.58, 136.53, 136.02, 130.17, 128.03, 127.55, 127.44, 115.79, 115.50, 67.88, 63.94, 21.72.

^{19}F-NMR (282 MHz, $CDCl_3$): δ -114.09.

The obtained data is in accordance with the literature data.[7]

2-tosyl-2,3-dihydro-1*H*-inden-1-ol (4e):

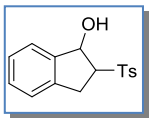

Following GP-2, **4e** was prepared from 1*H*-indene (116 mg, 1.0 mmol). The crude product was purified by column chromatography (Hexanes: EtOAc, 4:1, R_f = 0.28) to afford **4e** as a colorless viscous oil (190 mg, 66% yield, *trans/cis* 95:05).

^{1}H-NMR (300 MHz, $CDCl_3$, major isomer): δ 7.83 (d, *J* = 8.3 Hz, 2H), 7.37 (d, *J* = 8.3 Hz, 2H), 7.35 – 7.31 (m, 1H), 7.28 (dd, *J* = 6.4, 2.2 Hz, 2H), 7.22 – 7.17 (m, 1H), 5.70 (d, *J* = 4.9 Hz, 1H), 4.16 (ddd, *J* = 8.9, 6.2, 4.9 Hz, 1H), 3.65 – 3.39 (m, 2H), 2.46 (s, 3H).

^{13}C-NMR (75 MHz, $CDCl_3$, major isomer): δ 145.40, 140.28, 138.89, 134.75, 130.08, 129.66, 128.81, 128.05, 125.26, 124.59, 72.63, 60.62, 31.91, 21.75.

The obtained data is in accordance with the literature data.[24]

2-tosyl-1,2,3,4-tetrahydronaphthalen-1-ol (4f):

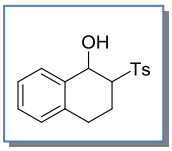

Following GP-2, 4f was prepared from 1,2-dihydronaphthalene (130 mg, 1.0 mmol). The crude product was purified by column chromatography (Hexanes: EtOAc, 4:1, R_f = 0.36) to afford 4f as a colorless solid (265 mg, 88% yield, *trans/cis* 9:1).

^{1}H-NMR (300 MHz, $CDCl_3$, major isomer): δ 7.85 (d, *J* = 7.9 Hz, 2H), 7.61 (d, *J* = 7.6 Hz, 1H), 7.40 (d, *J* = 7.9 Hz, 2H), 7.29 – 7.14 (m, 2H), 7.02 (d, *J* = 7.1 Hz, 1H), 5.21 (d, *J* = 9.2 Hz, 1H), 3.81 (bs, 1H), 3.38 (ddd, *J* = 12.5, 9.2, 3.5 Hz, 1H), 2.92 – 2.70 (m, 2H), 2.47 (s, 3H), 2.16 (ddd, *J* = 13.0, 8.1, 3.5 Hz, 1H), 1.74 (tdd, *J* = 13.0, 11.0, 6.3 Hz, 1H).

^{13}C-NMR (75 MHz, $CDCl_3$, major isomer): δ 145.55, 135.82, 134.84, 133.38, 130.06, 129.24, 128.06, 127.72, 127.68, 126.92, 67.54, 67.01, 27.97, 22.99, 21.73.

The obtained data is in accordance with the literature data.[24]

1-(naphthalen-2-yl)-2-tosylethan-1-ol (4g):[24]

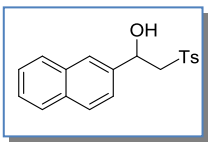

Following GP-2, **4g** was prepared from 2-vinylnaphthalene (154 mg, 1.0 mmol). The crude product was purified by column chromatography (Hexanes: EtOAc, 4:1, R_f = 0.19) to afford **4g** as a colorless solid (253 mg, 77% yield).

^{1}H-NMR (300 MHz, $CDCl_3$): δ 7.87 – 7.75 (m, 6H), 7.51 – 7.44 (m, 2H), 7.39 – 7.32 (m, 3H), 5.42 (dd, *J* = 9.8, 1.8 Hz, 1H), 3.49 (m, 2H), 2.45 (s, 3H).

^{13}C-NMR (75 MHz, $CDCl_3$): δ 145.33, 137.96, 136.11, 1389, 1385, 130.13, 128.71, 128.06, 128.03, 127.71, 126.46, 126.33, 124.81, 123.32, 68.65, 63.90, 21.72.

8.11.3 General procedure (GP-3): Trifluoromethylsulfochlorination

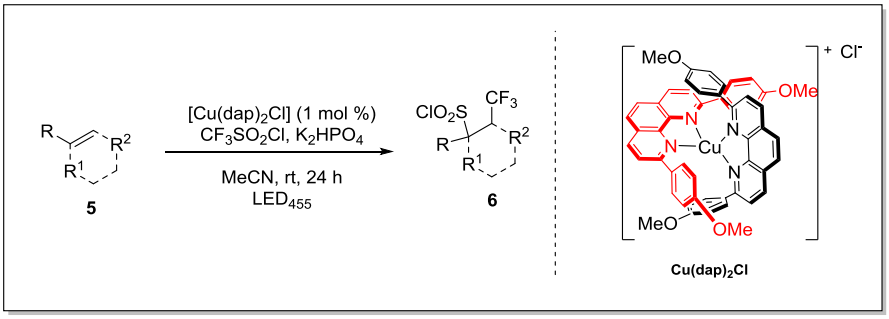

To an oven-dried Schlenk tube (10 ml size) equipped with a stir bar was charged with alkene **5** (3.0 mmol, 1 equiv), [Cu(dap)$_2$Cl] (26.4 mg, 0.03 mmol, 1.0 mol %), K_2HPO_4 (1032 mg, 6 mmol, 2 equiv) and MeCN (2.5 mL); the resulting suspension was degassed by three freeze-pump-thaw cycles followed by the addition of the triflyl chloride (1008 mg, 6 mmol, 2 equiv). The reaction mixture was irradiated for 24 hours with blue light emitting diode (LED, λ_{max} = 455 nm) at room temperature. Afterwards, the reaction mixture was quenched with water and the product was extracted with DCM (3x10 mL), the combined organic layers were dried over Na_2SO_4 and concentrated, the residue was purified by silica gel column chromatography to afford pure **6**.

4,4,4-trifluoro-1-phenylbutane-2-sulfonyl chloride (6a):

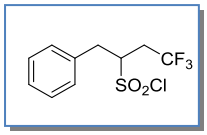

Following GP-3, **6a** was prepared using allylbenzene (354 mg, 3.0 mmol). Chromatography on silica (hexanes: EtOAc, 9:1, R_f = 0.73) afforded **6a** as a colorless oil (724 mg, 84% yield).

^{1}H-NMR (300 MHz, $CDCl_3$): δ 7.37 (m, 3H), 7.27 (m, 2H), 4.07 (m, 1H), 3.57 (dd, *J* = 14.9, 5.6 Hz, 1H), 3.26 (dd, *J* = 14.9, 6.9 Hz, 1H), 3.04 (ddd, *J* = 15.8, 10.3, 3.4 Hz, 1H), 2.66 (ddd, *J* = 15.8, 9.8, 7.3 Hz, 1H).

^{13}C-NMR (75 MHz, $CDCl_3$): 133.85, 129.49, 129.11, 128.05, 124.05, (q, *J* = 276 Hz), 70.93, 36.17, 34.16, 33.9 (q, *J* = 31.5 Hz).

^{19}F-NMR (282 MHz, $CDCl_3$): δ -63.95.

The obtained data is in accordance with the literature data.[11]

1,1,1-trifluoro-5-phenylpentane-3-sulfonyl chloride (6b):

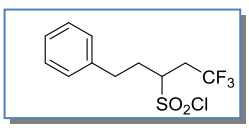

Following GP-3, **6b** was prepared using but-3-en-1-ylbenzene (397 mg, 3.0 mmol) Chromatography on silica (hexanes: EtOAc, 9:1, R_f = 0.8) afforded **6b** as a colorless oil (717 mg, 79% yield).

^{1}H-NMR (300 MHz, $CDCl_3$): δ 7.37 – 7.32 (m, 2H), 7.30 – 7.18 (m, 3H), 3.79 (ddd, *J* = 8.9, 7.8, 2.8 Hz, 1H), 81 (dqd, *J* = 15.5, 10.6, 2.7 Hz, 1H), 2.94 (t, *J* = 7.9 Hz, 2H), 2.74 – 2.47 (m, 2H), 2.41 – 2.26 (m, 1H);

^{13}C-NMR (75 MHz, $CDCl_3$): δ 138.88, 128.87, 128.65, 128.47, 126.90, 126.70, 126.37 (q, *J* = 274 Hz), 123.02, 68.86 (dd, *J* = 5.0, 2.5 Hz), 34.90 (q, *J* = 30.7 Hz), 32.13.

^{19}F-NMR (282 MHz, $CDCl_3$): δ -63.90.

IR (neat, cm^{-1}): 1603, 1696, 1455, 1372, 1317, 1260, 1245, 1148, 1119, 1072, 1024, 911, 844, 744, 698**.**

HRMS (ESI): exact m/z calculated for $C_{11}H_{12}ClF_3O_2S$ $(M)^+$: 300.01953; Found: 300.01949 $(M)^+$.

2-(trifluoromethyl)cyclohexane-1-sulfonyl chloride (6c):

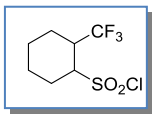

Following GP-3, **6c** was prepared using cyclohexene (243 mg, 3.0 mmol, 1 equiv.). Chromatography on silica (hexanes-EtOAc, 9:1, R_f = 0.38) afforded **6c** as a mixture of two non-separable diastereomers (60:40), colorless oil (375 mg, 49% yield).

^{1}H-NMR (300 MHz, $CDCl_3$): δ 4.01 (m, 1H), 87 (m, 1H), 2.53 (m, 1H), 2.04 (m, 3H), 1.69 (m, 4H).

^{13}C-NMR (75 MHz, $CDCl_3$,): 126.59 (q, *J* = 270 Hz), 71.03, 38.26 (q, *J* = 27.7 Hz), 23.94, 20.61, 20.43, 20.31.

^{19}F-NMR (282 MHz, $CDCl_3$): δ -67.63.

The obtained data is in accordance with the literature data.[11]

1,1,1-trifluoroheptane-3-sulfonyl chloride (6d):

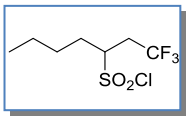

Following GP-3, **6d** was prepared using 1-hexene (252 mg, 3.0 mmol, 1 equiv.). Chromatography on silica (hexanes: EtOAc, 9:1, R_f = 0.42) afforded **6d** as a pale yellow oil (499 mg, 66% yield).

^{1}H-NMR (300 MHz, $CDCl_3$): δ 3.76 (dtd, *J* = 8.5, 5.7, 2.8 Hz, 1H), 3.07 (dqd, *J* = 15.5, 10.6, 2.8 Hz, 1H), 2.71 – 2.47 (m, 1H), 2.29 – 2.11 (m, 1H), 2.09 – 1.92 (m, 1H), 1.56 (tdd, *J* = 12.0, 6.7, 2.5 Hz, 2H), 1.39 (dq, *J* = 14.4, 7.2 Hz, 2H), 0.95 (dd, *J* = 8.9, 5.6 Hz, 3H).

^{13}C-NMR (75 MHz, $CDCl_3$): δ 124.94 (q, *J* = 277.4 Hz), 69.90 (m), 34.58 (q, *J* = 30.8 Hz), 30.11 , 27.97, 22.25, 13.53.

^{19}F-NMR (282 MHz, $CDCl_3$): δ -64.30**.**

IR (neat, cm^{-1}): 2964, 2937, 2876, 1466, 1437, 1370, 1308, 1258, 1151, 1086, 1014, 993, 917, 843, 742, 709**.**

HRMS (ESI): exact m/z calculated for $C_7H_{12}ClF_3O_2S$ $(M)^+$: 252.01948; Found: 252.01945 $(M)^+$.

2-phenyl-1-((4,4,4-trifluoro-1-phenylbutan-2-yl)sulfonyl)propan-2-ol (7a):

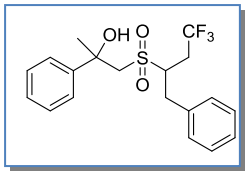

Following GP-1, **7a** was prepared from **6a** (430 mg, 1.5 mmol). The crude product was purified by column chromatography (Hexanes: EtOAc, 4:1, R_f = 0.5) to afford **7a** as a 2 non-separable diastereomers (1:1), colorless oil (343 mg, 89% yield).

^{1}H-NMR (300 MHz, $CDCl_3$): δ 7.42 – 7.28 (m, 7H), 7.23 (m, 2H), 7.19 – 7.13 (m, 1H), 4.22 (bs, 1H), 3.36 – 3.26 (m, 1H), 3.25 – 3.09 (m, 2H), 3.09 – 3.00 (m, 2H), 2.91 (qdd, *J* = 10.6, 4.4, 2.2 Hz, 1H), 2.46 – 2.14 (m, 1H), 1.67 (s, 3H), 1.62 (s, 3H – other diastereomer).

^{13}C-NMR (75 MHz, $CDCl_3$, diastereomers: 1:1): δ 144.53, 144.46, 135.79, 135.64, 129.82, 129.49, 129.10, 129.02, 128.60, 128.62, 127.79, 127.78, 127.71, 127.64, 125.66 (q, *J* = 278.09 Hz), 125.60 (q, *J* = 2888 Hz), 124.65, 124.63, 72.99, 72.86, 63.90, 63.59, 60.21 (d, *J* = 1.9 Hz), 59.91, 35.61, 34.41, 31.98 (q, *J* = 30.3 Hz), 31.02 (q, *J* = 30.4 Hz), 30.11, 30.00.

^{19}F-NMR (282 MHz, $CDCl_3$, diastereomers: 1:1): δ -63.60 and -63.77.

IR (neat, cm^{-1}): 3492, 2983, 1494, 1447, 1387, 1302, 1258, 1181, 1115, 1071, 1029, 999, 946, 917, 880, 846, 748, 697.

HRMS (ESI): exact m/z calculated for $C_{19}H_{25}F_3NO_3S$ $(M+NH_4)^+$: 404.1502; Found: 404.1504 $(M+NH_4)^+$.

2-phenyl-1-((1,1,1-trifluoro-5-phenylpentan-3-yl)sulfonyl)propan-2-ol (7b):

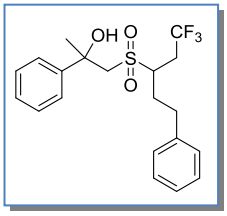

Following GP-1, **7b** was prepared from **6b** (450 mg, 1.5 mmol). The crude product was purified by column chromatography (Hexanes: EtOAc, 4:1, R_f = 0.58) to afford **7b** as a two non-separable diastereomers (0.91:1), colorless oil (344 mg, 86% yield).

^{1}H-NMR (300 MHz, $CDCl_3$): δ 7.51 – 7.39 (m, 4H), 7.38 – 7.22 (m, 4H), 7.23 – 7.16 (m, 2H), 4.28 (bs, 1H), 3.57 (dd, *J* = 25.0, 10.3 Hz, 1H), 3.32 (dd, *J* = 14.8, 4.2 Hz, 1H), 2.98 – 2.52 (m, 4H), 2.52 – 2.30 (m, 1H), 2.29 – 2.09 (m, 1H), 2.02 (qd, *J* = 10.5, 5.5 Hz, 1H), 1.78 (s, 3H).

^{13}C-NMR (75 MHz, $CDCl_3$, diastereomers: 0.91:1): δ 144.71, 144.67, 140.04, 139.90, 128.82, 128.79, 128.75, 128.60, 128.48, 128.43, 127.89, 127.87, 127.84 (q, *J* = 270.18 Hz), 126.72,

126.60, 125.63 (q, *J* = 277.11 Hz), 124.65, 124.57, 73.02, 72.93, 62.04, 61.58, 57.56, 57.51, 32.88 (q, *J* = 30.3 Hz), 32.39, 31.92, 31.26 (q, *J* = 30.4 Hz), 30.79, 30.16, 29.97, 29.67.

^{19}F-NMR (282 MHz, $CDCl_3$, diastereomers: 1:0.91): δ -63.54 and -63.96.

IR (neat, cm^{-1}): 3493, 2935, 1602, 1495, 1448, 1386, 1303, 1259, 1117, 1113, 1071, 1027, 945, 916, 880, 843, 766, 748, 698.

HRMS (ESI): exact m/z calculated for $C_{20}H_{27}F_3NO_3S$ $(M+NH_4)^+$: 418.1658; Found: 418.1661 $(M+NH_4)^+$.

2-phenyl-1-((2-(trifluoromethyl)cyclohexyl)sulfonyl)propan-2-ol (7c):

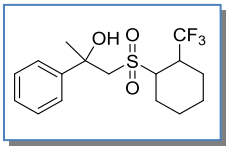

Following GP-1, **7c** was prepared from **6c** (375 mg, 1.5 mmol). The crude product was purified by column chromatography (Hexanes : EtOAc, 4:1, R_f = 0.62) to afford **7c** as a two non-separable diastereomers (1:1), colorless oil (294 mg, 84% yield).

^{1}H-NMR (300 MHz, $CDCl_3$): δ 7.46 (m, 2H), 7.38 (m, 2H), 7.33 – 7.25 (m, 1H), 4.47 (s, 1H – OH, 1st isomer), 4.43 (s, 1H – OH, 2nd isomer), 3.69 (dd, *J* = 41.1, 14.7 Hz, 1H), 3.38 (dd, *J* = 17.5, 14.7 Hz, 1H), 3.04 – 2.72 (m, 2H), 1.98 (dd, *J* = 23.6, 9.7 Hz, 2H), 1.91 – 1.80 (m, 2H), 1.76 (s, 3H 1st isomer), 1.76 (s, 3H 2nd isomer), 1.72 (d, *J* = 1.6 Hz, 1H), 1.60 – 1.43 (m, 3H).

^{13}C-NMR (75 MHz, $CDCl_3$, diastereomers: 1:1): δ 144.69, 144.57, 128.91, 128.71, 128.59, 127.77, 127.69, 127.23 (q, *J* = 278.53 Hz), 127.03 (q, *J* = 280.63 Hz), 125.19, 124.75, 124.49, 780, 72.90, 62.97, 61.60, 57.85, 56.70, 37.31 (q, *J* = 26.5 Hz), 35.10 (q, *J* = 26.8 Hz), 30.28, 30.05, 22.08, 21.63, 21.17, 21.15, 21.09, 20.78, 20.19, 19.95.

^{19}F-NMR (282 MHz, $CDCl_3$, diastereomers: 1:1): δ -67.40 and -67.53.

IR (neat, cm^{-1}): 3492, 2944, 2876, 1709, 1494, 1448, 1386, 1363, 1304, 1250, 1178, 1104, 1069, 1035, 1009, 946, 913, 873, 766, 699.

HRMS (ESI): exact m/z calculated for $C_{16}H_{25}F_3NO_3S$ $(M+NH_4)^+$: 368.1502; Found: 368.1507 $(M+NH_4)^+$.

2-phenyl-1-((1,1,1-trifluoroheptan-3-yl)sulfonyl)propan-2-ol (7d):

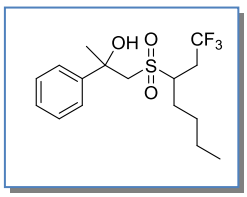

Following GP-1, **7d** was prepared from **6d** (378 mg, 1.5 mmol). The crude product was purified by column chromatography (Hexanes : EtOAc, 4:1, R_f = 0.6) to afford **7d** as a two non-separable diastereomers (1:1), pale yellow viscous oil (323 mg, 92% yield).

^{1}H-NMR (300 MHz, $CDCl_3$): δ 7.45 – 7.31 (m, 4H), 7.27 (m, 1H), 4.27 (s, 1H), 3.67 – 3.46 (m, 1H), 3.31 (dd, *J* = 14.7, 5.5 Hz, 1H), 2.89 – 2.51 (m, 1H), 2.39 – 2.05 (m, 1H), 1.73 (s, 3H), 1.64 – 1.56 (m, 1H), 1.38 – 1.08 (m, 6H), 0.90 – 0.79 (m, 3H).

^{13}C-NMR (75 MHz, $CDCl_3$, diastereomers: 1:1): δ 144.60, 144.50, 128.78, 128.75, 127.84, 127.81, 125.5 (q, *J* = 278.21 Hz), 124.62, 124.52, 123.9 (q, *J* = 277.01 Hz), 73.05, 72.88, 62.10, 61.46, 58.26, 58.06, 32.89 (q, *J* = 30.1 Hz), 31.11 (q, *J* = 30.5 Hz), 30.29, 30.23, 28.63, 28.22, 27.78, 27.29, 22.56, 22.40, 13.69, 13.66.

^{19}F-NMR (282 MHz, $CDCl_3$, diastereomers: 1:1): δ -63.96 and -64.47.

IR (neat, cm^{-1}): 3489, 2961, 2936, 1739, 1494, 1446, 1377, 1302, 1259, 1231, 1121, 946, 916, 843, 766, 699.

HRMS (ESI): exact m/z calculated for $C_{16}H_{27}F_3NO_3S$ $(M+NH_4)^+$: 370.1658; Found: 370.1662 $(M+NH_4)^+$.

8.11.4 General procedure (GP-4): One pot photocatalysis

To an oven-dried Schlenk tube (10 ml size) equipped with a stir bar was charged with 1-Hexene **5a** (84.16 mg, 1.0 mmol, 1.0 equiv), [Cu(dap)$_2$Cl] (8.8 mg, 0.01 mmol, 1.0 mol %), and MeCN (1.67 mL); the resulting suspension was degassed by three freeze-pump-thaw cycles followed by the addition of the triflyl chloride (336 mg, 2.0 equiv). The reaction mixture was irradiated for 24 hours with blue light emitting diode (LED, λ_{max} = 455 nm) at room temperature, followed by the addition of the prop-1-en-2-ylbenzene (or α-methyl styrene) **1a** (118 mg, 1.0 mmol, 1.0 equiv), distilled water (0.33 mL), and *fac*[Ir(ppy)$_3$] (6.6 mg, 0.01 mmol, 1.0 mol %) under positive nitrogen atmosphere to the reaction mixture. The resulting suspension was further irradiated with blue light emitting diode (LED, λ_{max} = 455 nm) at room temperature for 24 h. Then reaction mixture was saturated with brine solution (15 mL) and the product was extracted with ethyl acetate (3x15 mL), the combined organic layers were dried over Na_2SO_4 and concentrated, the residue was purified by column chromatography on silica gel by using hexanes and ethyl acetate as eluents to afford the desired product **7d** (183 mg, 52%).

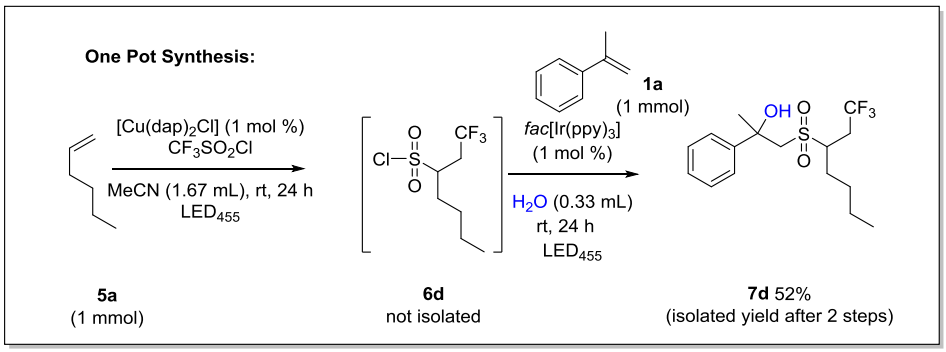

(*E*)-(5,5,5-trifluoro-3-((2-phenylprop-1-en-1-yl)sulfonyl)pentyl)benzene (8a):

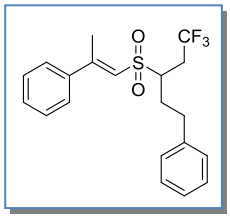

To an oven-dried round bottomed flask (25 mL size) equipped with a stir bar was charged with **7b** (200 mg, 0.5 mmol, 1.0 equiv), Ac_2O (102 mg, 1.0 mmol, 2.0 equiv), DMAP (122 mg, 1.0 mmol, 2.0 equiv), and DCM (7 mL); the resulting suspension was stirred for 60 hours at room temperature. Then reaction mixture was saturated with brine solution (15 mL) and the product was extracted with ethyl acetate (3x15 mL), the combined organic layers were dried over Na_2SO_4 and concentrated, the residue was purified by column chromatography on silica gel by using hexanes and ethyl acetate as eluents to afford the desired product 8a as a colorless oil (142 mg, 74%).

^{1}H-NMR (400 MHz, $CDCl_3$): δ 7.47 (s, 5H), 7.36 – 7.30 (m, 2H), 7.25 (t, *J* = 8.8 Hz, 3H), 6.41 (s, 1H), 3.29 (d, *J* = 5.1 Hz, 1H), 3.08 – 2.96 (m, 2H), 2.94 – 2.83 (m, 1H), 2.56 (s, 3H), 2.55 – 2.40 (m, 2H), 2.32 – 2.10 (m, 1H).

^{13}C-NMR (101 MHz, $CDCl_3$): δ 157.25, 139.86, 139.79, 134.18, 130.25, 129.94, 128.83, 128.60, 128.41, 127.18, 126.42, 126.25, 122.73, 121.67, 57.45 (d, *J* = 1.9 Hz), 32.83 (q, *J* = 30.1 Hz), 32.31, 30.33, 17.35.

^{19}F-NMR (282 MHz, $CDCl_3$): δ -63.90.

IR (neat, cm^{-1}): 2929, 1604, 1573, 1495, 1444, 1385, 1302, 1261, 1129, 1073, 1027, 826, 800, 750, 698.

HRMS (ESI): exact m/z calculated for $C_{20}H_{25}F_3NO_2S$ $(M+NH_4)^+$: 400.1554; Found: 400.1553 $(M+NH_4)^+$.

8.11.5 Reduction potentials:

Redox potentials of the sulfonyl chlorides were measured by cyclic voltammetry in acetonitrile containing tetrabutylammonium tetrafluoroborate (0.1 M) as a supporting electrolyte. All values are given versus Saturated Calomel Eletrode (SCE). Potential sweep rate was 50 mV S^{-1}.

Sulfonyl chlorides	**Reduction potential (V)**
4-nitrobenzenesulfonyl chloride (**2a**)	-0.44
methanesulfonyl chloride (**2b**)	-1.39
benzenesulfonyl chloride (**2c**)	-0.95
4-acetylbenzenesulfonyl chloride (**2d**)	-0.66
4-methoxybenzenesulfonyl chloride (**2e**)	-0.99
4-methylbenzenesulfonyl chloride (**2f**)	-0.94
4-fluorobenzenesulfonyl chloride (**2g**)	-0.90
4-chlorobenzenesulfonyl chloride (**2h**)	-0.79
4-bromobenzenesulfonyl chloride (**2i**)	-0.82
naphthalene-2-sulfonyl chloride (**2j**)	-0.74
2,3,4,5,6-pentafluorobenzenesulfonyl chloride (**2k**)	-0.56
,4,6-trimethylbenzenesulfonyl chloride (**2l**)	-0.81
2-bromobenzenesulfonyl chloride (**2m**)	-0.82

Table 8.5: Redox potential of the sulfonyl chlorides versus SCE.

8.11.6 Isotope labelling experiment with H_2O^{18}:

To an oven-dried Schlenk tube (10 ml size) equipped with a stir bar was added tosyl chloride **2f** (143mg, 0.75 mmol, 1.5 equiv) and *fac*[Ir(ppy)$_3$] (6.6 mg, 1.0 mol %). Then, acetonitrile (0.83 mL) and $H_2{}^{18}O$ (0.17 mL) was added; the resulting suspension was deoxygenated by three freeze-pump-thaw cycles followed by the addition of the prop-1-en-2-ylbenzene (or α-methyl styrene) **1a** (59 mg, 0.5 mmol, 1.0 equiv) under positive nitrogen atmosphere. The reaction mixture was irradiated with blue light emitting diode (LED, λ_{max} = 455 nm) at room temperature for 18 h. The resulting reaction mixture was saturated with brine solution (10 mL) and the product was extracted with ethyl acetate (3x10 mL), the combined organic layers were dried over Na_2SO_4 and concentrated, the residue was purified by column chromatography on silica gel by using hexanes and ethyl acetate as eluents to afford the desired product **3fa** (137 mg, 94%). The O^{18} incorporated mass of the compound **3fa** was clearly detected by HRMS analysis.

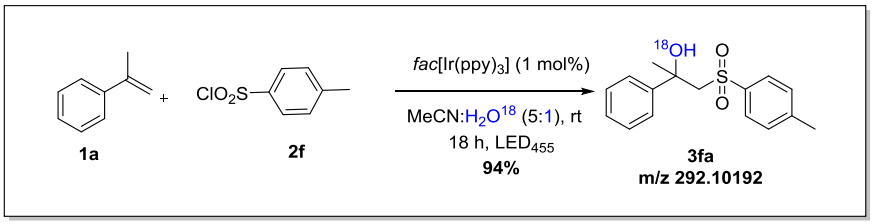

Qualitative Compound Report

Data File	pagi108638.d	**Sample Name**	SKP-O18
Sample Type	Sample	**Position**	P1-C6
Instrument Name	Instrument 1	**User Name**	jk
Acq Method	ms_160111.m	**Acquired Time**	1/11/2016 8:48:28 PM
IRM Calibration Status	Success	**DA Method**	hr_formula.m
Comment			
Sample Group		**Info.**	
Formula	C16H18[18O]O2S	**Acquisition SW Version**	6200 series TOF/6500 series Q-TOF B.05.00 (B5042.2)

Fragmentor Voltage 120 **Collision Energy** 0 **Ionization Mode** ESI

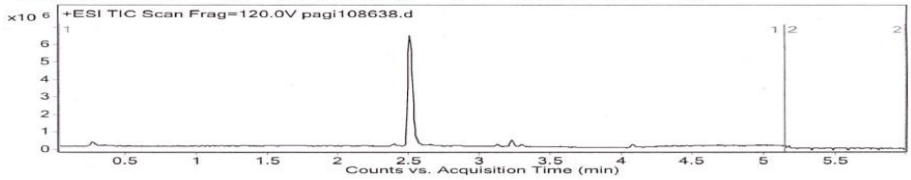

Compound Table

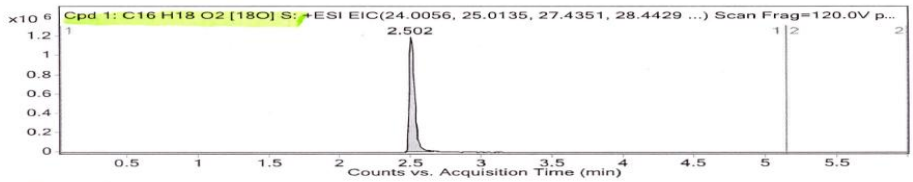

MS Spectrum

Qualitative Compound Report

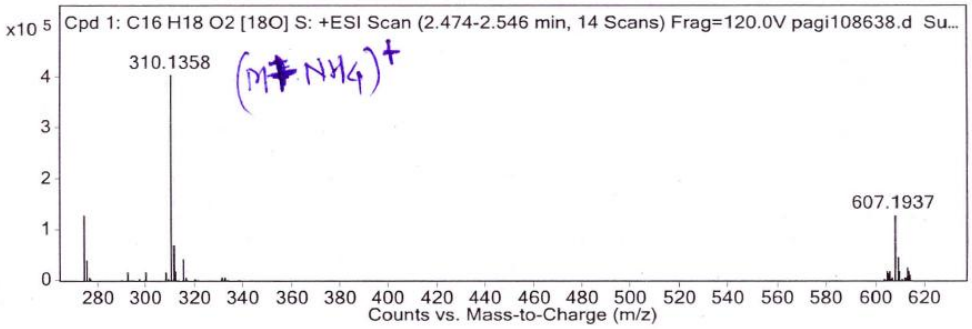

MS Spectrum Peak List

m/z	*Calc m/z*	Diff(ppm)	z	Abund	Formula	Ion
273.0945				855680.13		
278.1099	278.1095	1.23	1	57.11	C15H18NO[18O]S	(M+NH4)+[-CH4O]
292.1001	292.1014	-4.22	1	16567.57	C16H18O2[18O]S	M*+
293.1032	293.1046	-4.75	1	3071.68	C16H18O2[18O]S	M*+
294.1036	294.1003	11.34	1	3448.85	C16H18O2[18O]S	M*+
310.1358	310.1357	0.08	1	405745.19	C16H22NO2[18O]S	(M+NH4)+
311.139	311.1388	0.51	1	70491.09	C16H22NO2[18O]S	(M+NH4)+
312.1356	312.1347	2.71	1	18391.46	C16H22NO2[18O]S	(M+NH4)+
313.1363	313.1364	-0.51	1	3078.15	C16H22NO2[18O]S	(M+NH4)+
315.091	315.0911	-0.58	1	43773.08	C16H18NaO2[18O]S	(M+Na)+
316.0942	316.0944	-0.41	1	7975.66	C16H18NaO2[18O]S	(M+Na)+
317.0907	317.0901	1.99	1	2346.67	C16H18NaO2[18O]S	(M+Na)+
331.0649	331.0651	-0.6	1	7526.84	C16H18KO2[18O]S	(M+K)+
332.0682	332.0683	-0.39	1	1450.69	C16H18KO2[18O]S	(M+K)+
333.0636	333.0636	-0.08	1	887.32	C16H18KO2[18O]S	(M+K)+
607.1937	607.193	1.02	1	129123.47	C32H36NaO4[18O]2S2	(2M+Na)+
608.1963	608.1963	0.14	1	45448.06	C32H36NaO4[18O]2S2	(2M+Na)+
609.1912	609.1935	-3.91	1	20300.4	C32H36NaO4[18O]2S2	(2M+Na)+
610.1886	610.1946	-9.77	1	5972.81	C32H36NaO4[18O]2S2	(2M+Na)+
623.1675	623.167	0.78	1	293.34	C32H36KO4[18O]2S2	(2M+K)+

--- End Of Report ---

8.12 NMR spectra:

^{1}H-NMR: **3a** (DMSO-d^{6})

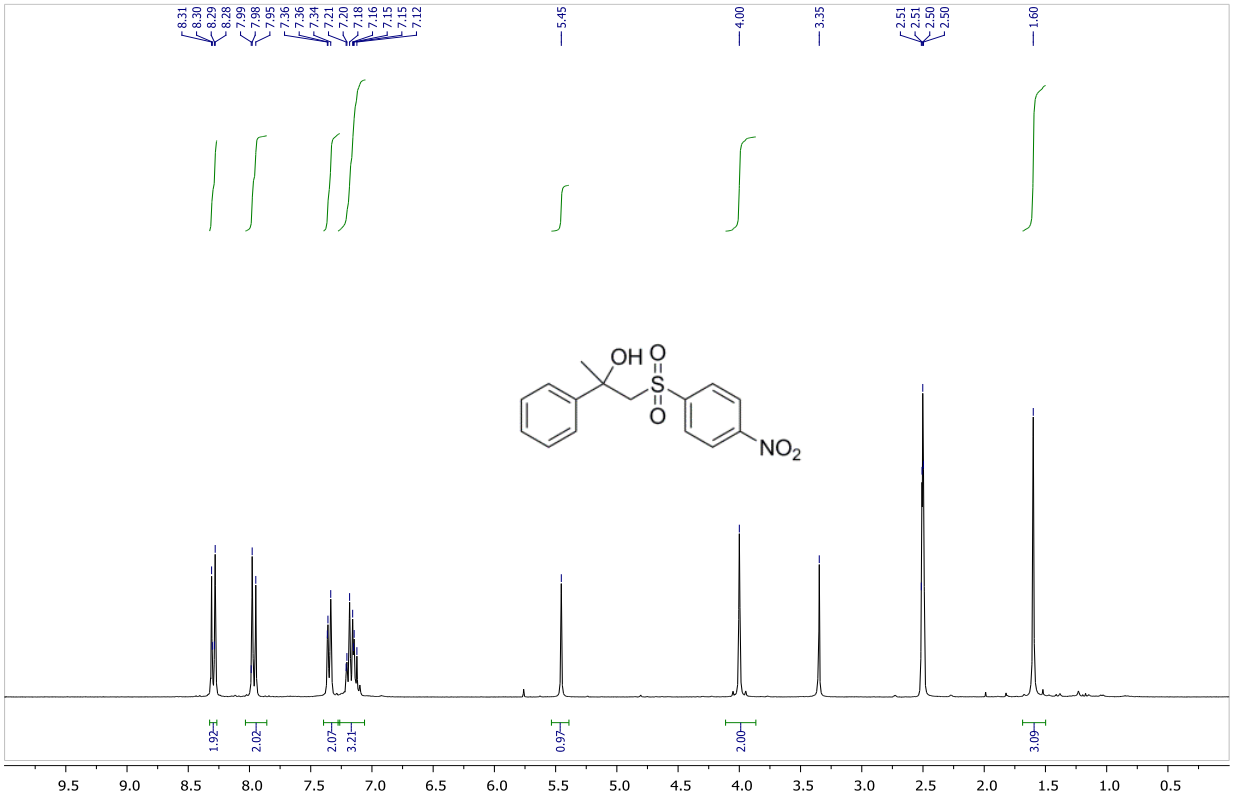

^{13}C-NMR: **3a** (DMSO-d^{6})

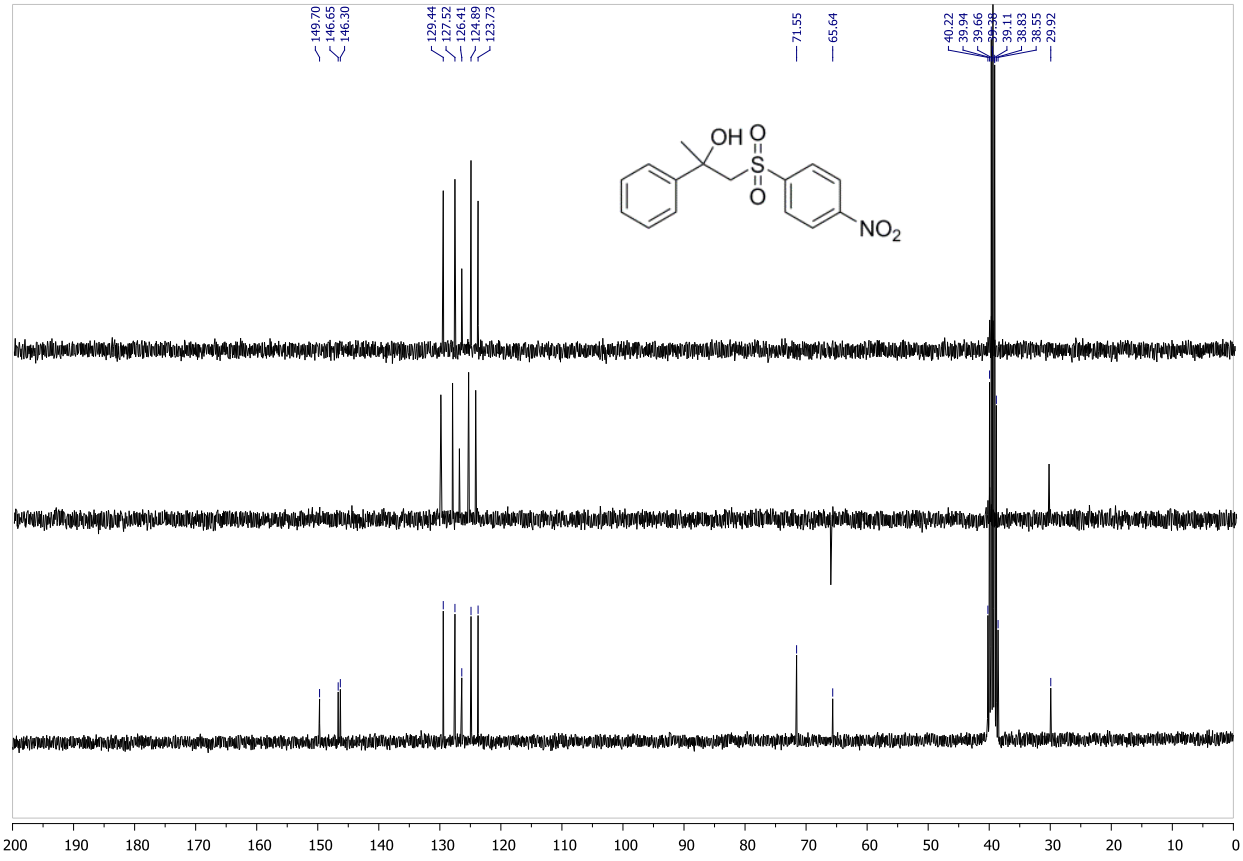

^{1}H-NMR: **3b**

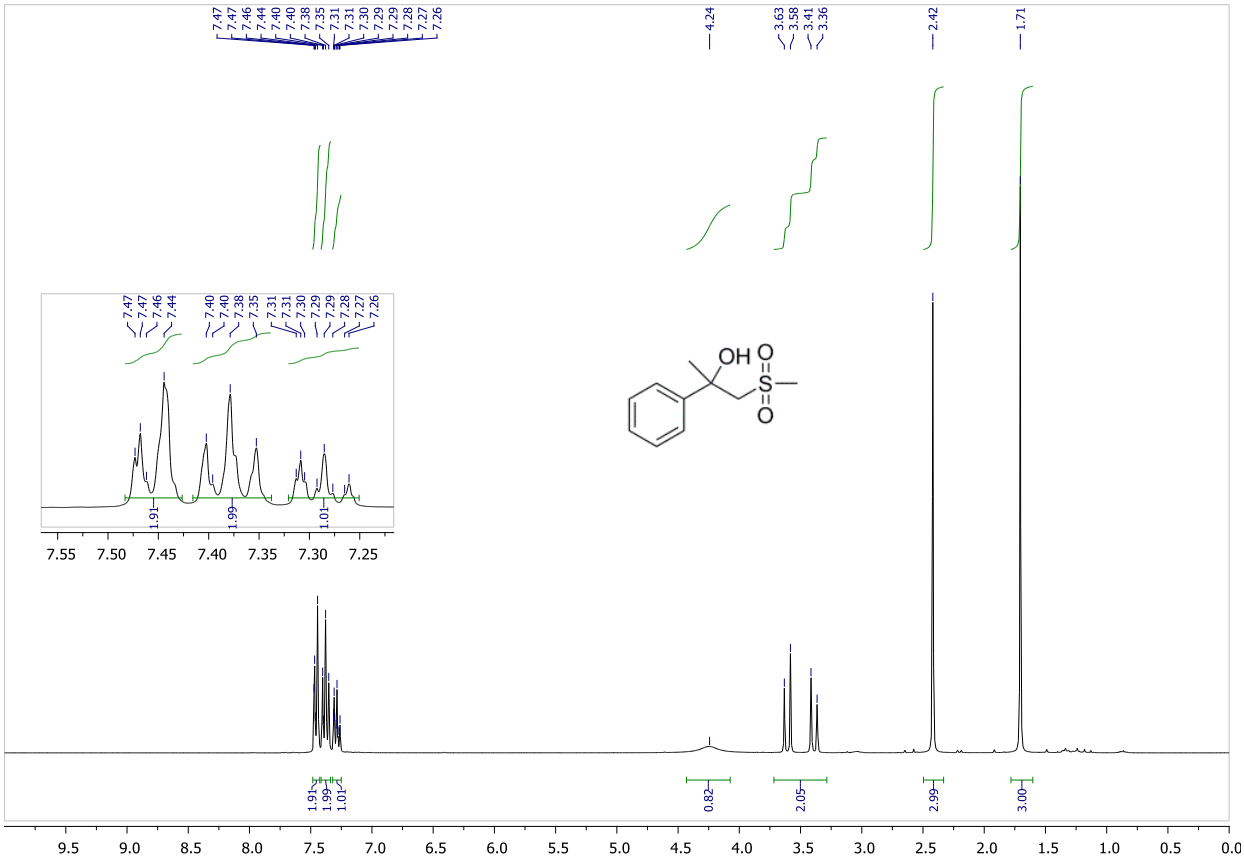

^{13}C-NMR: **3b**

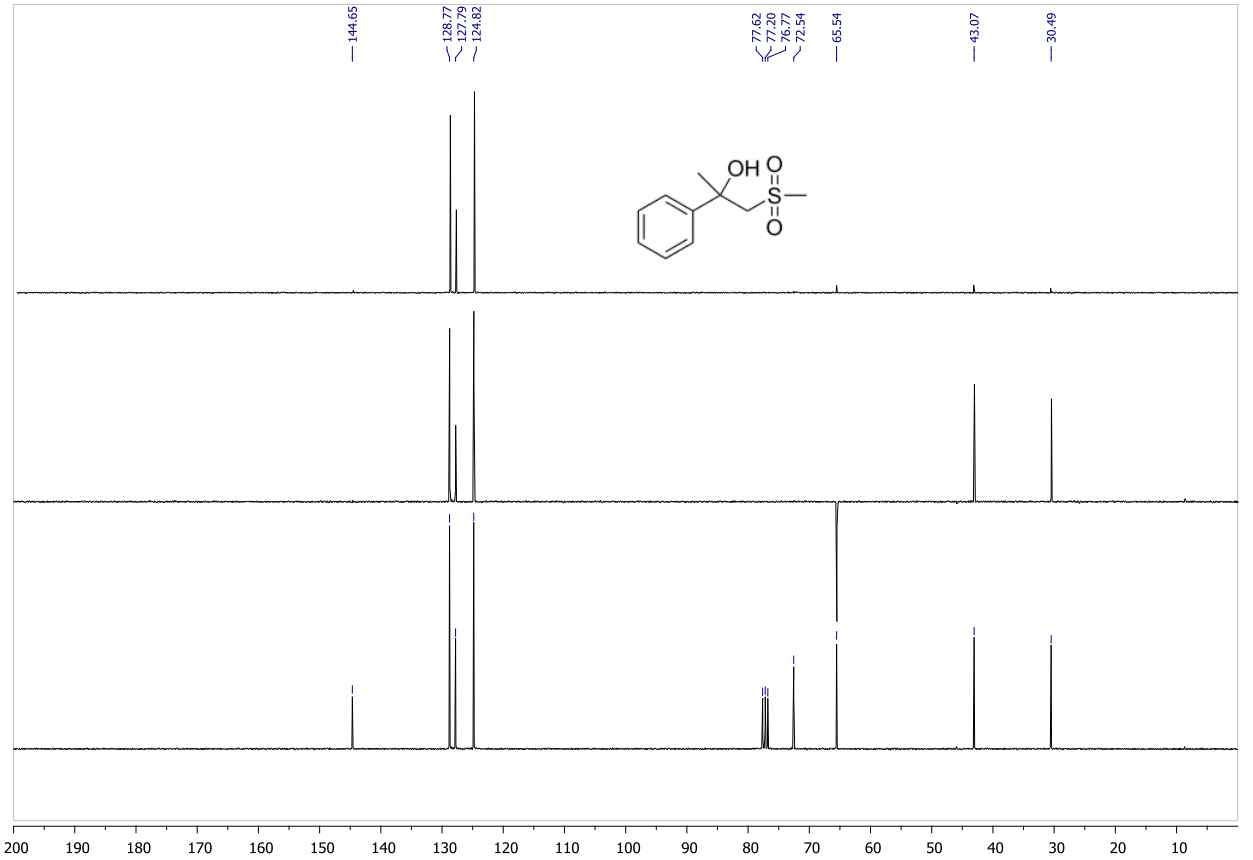

^{1}H-NMR: **3c**

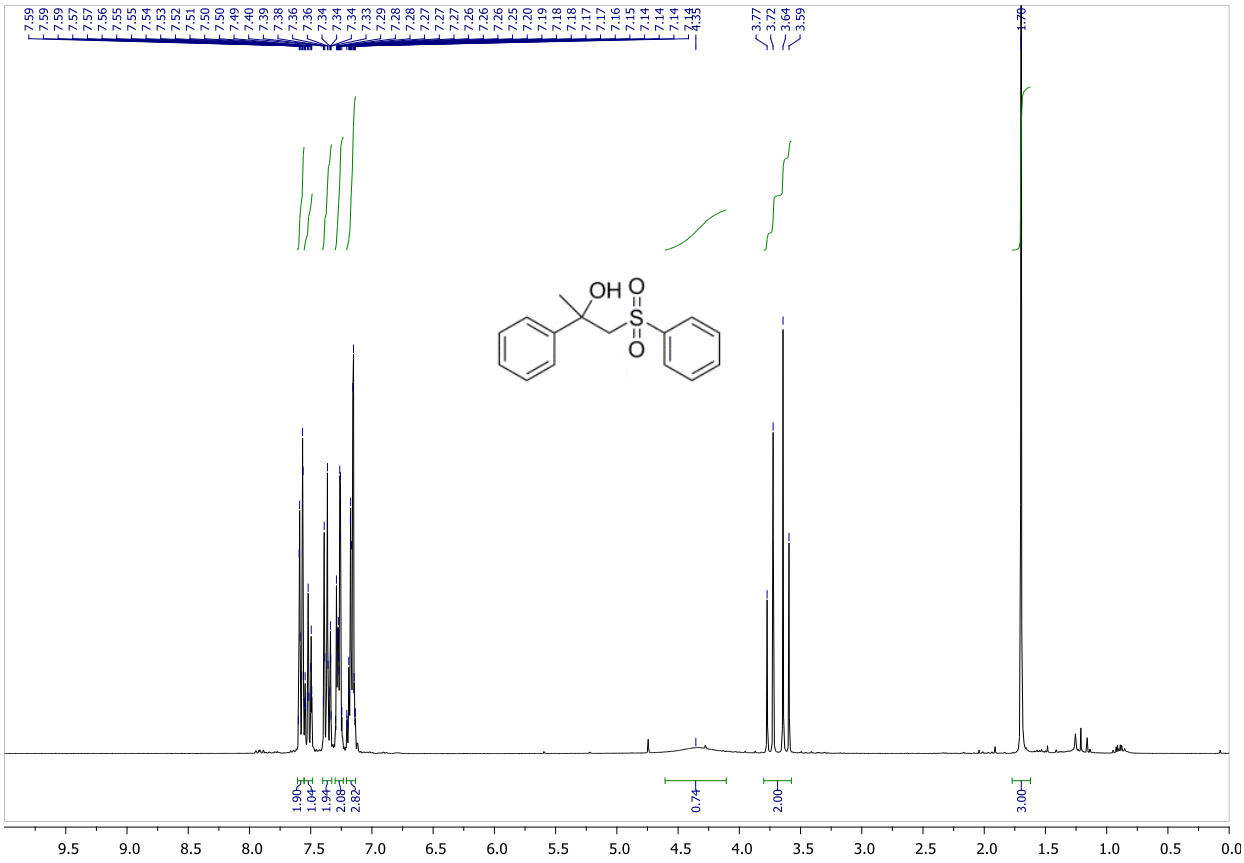

^{13}C-NMR: **3c**

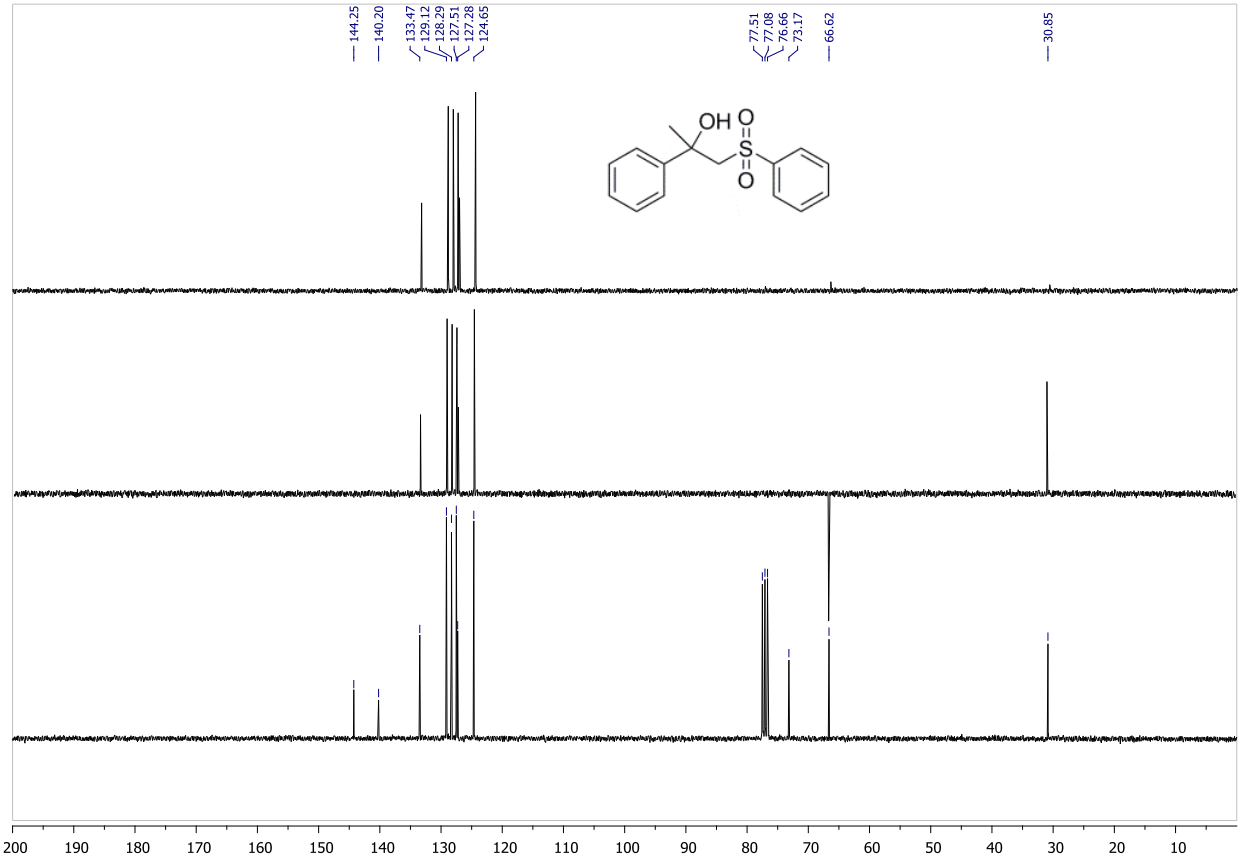

^{1}H-NMR: **3d**

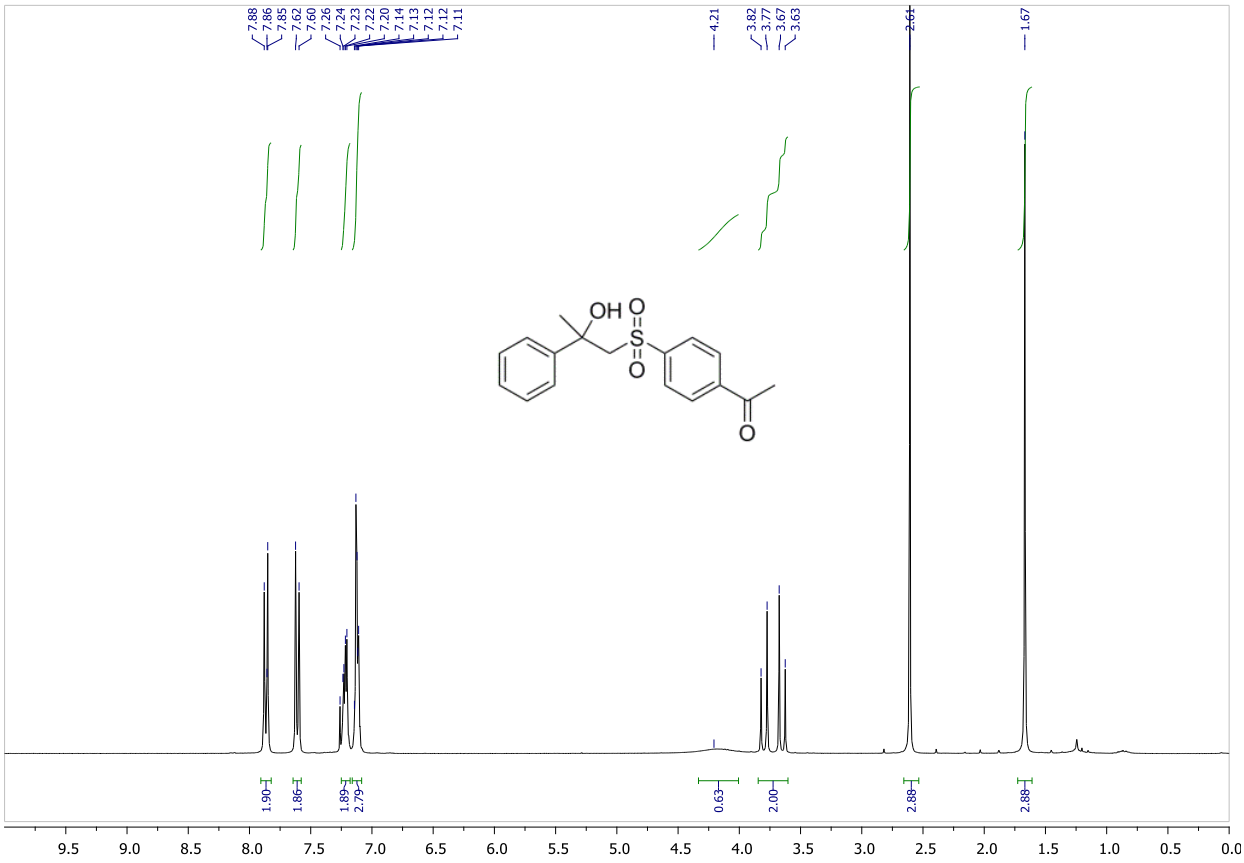

^{13}C-NMR: **3d**

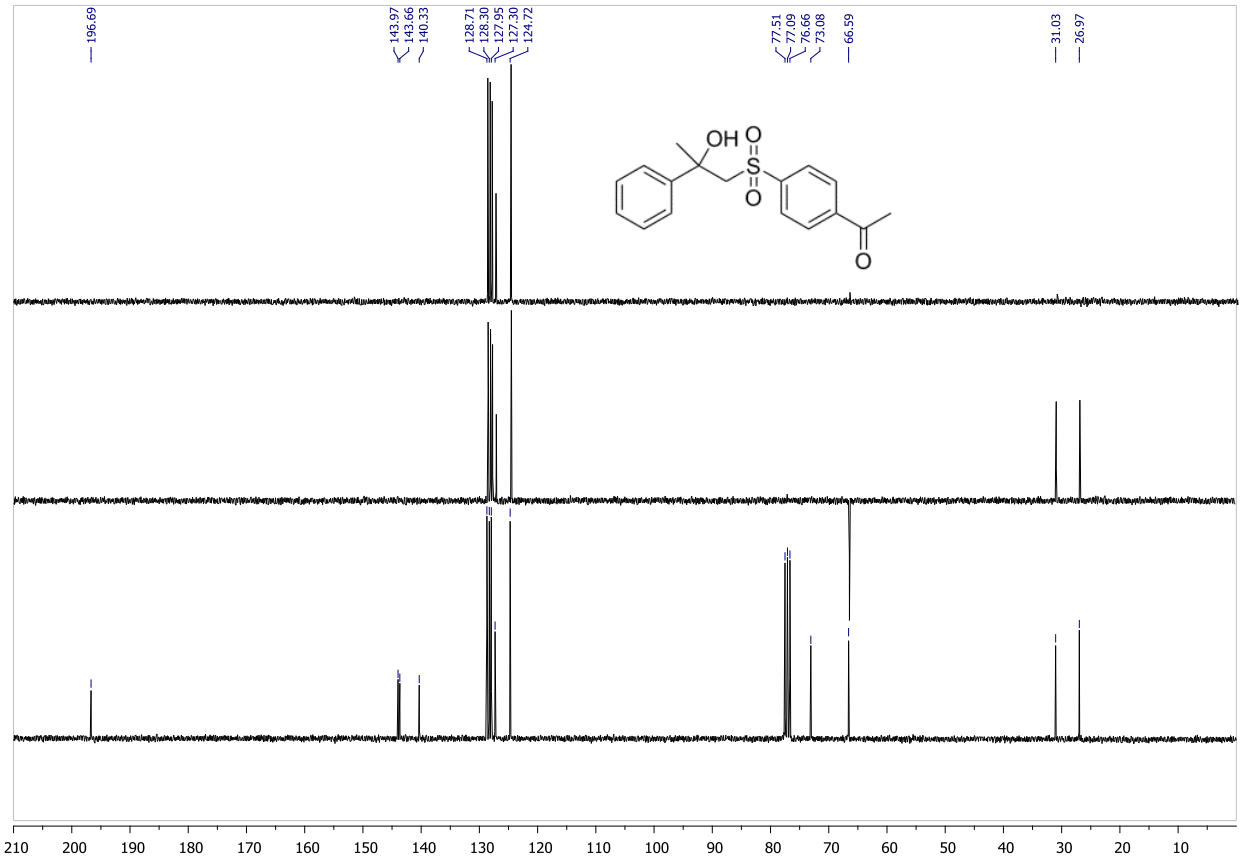

^{1}H-NMR: **3e**

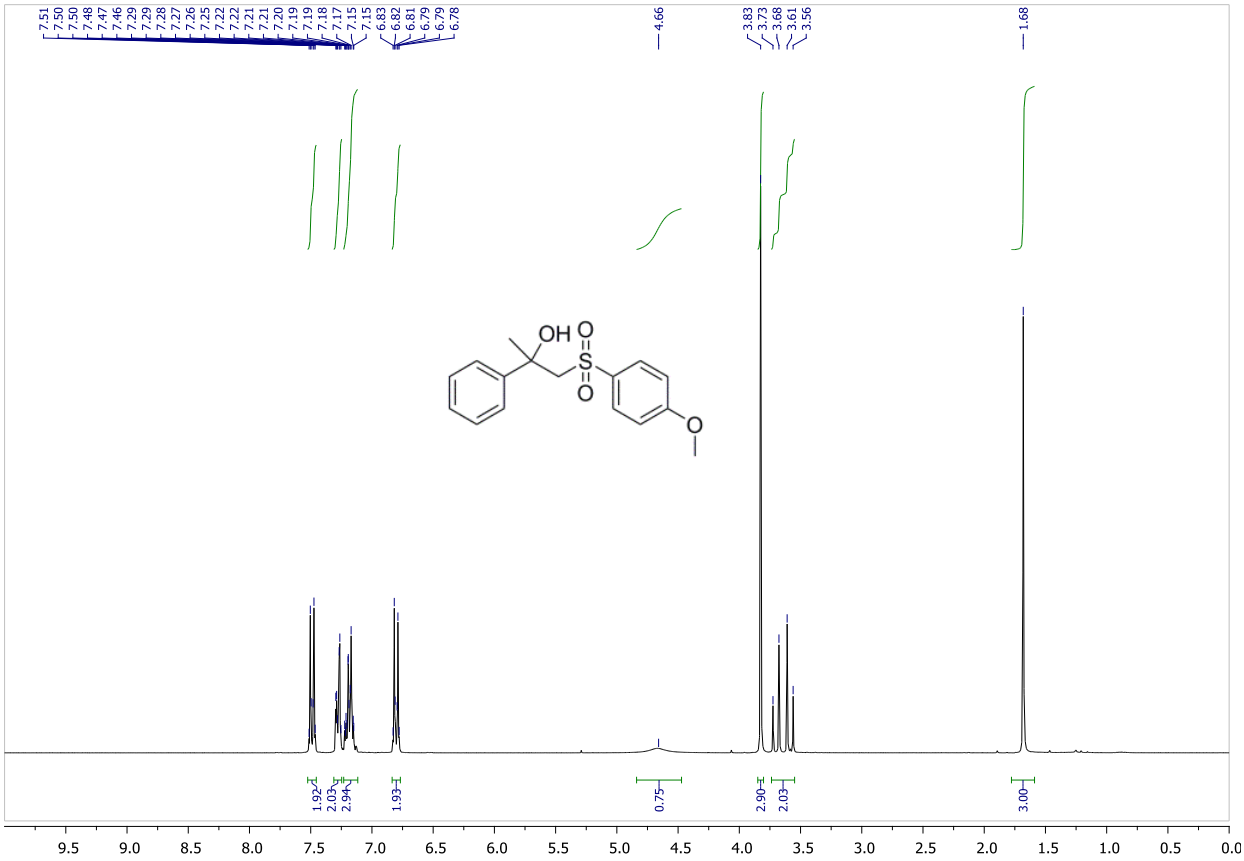

^{13}C-NMR: **3e**

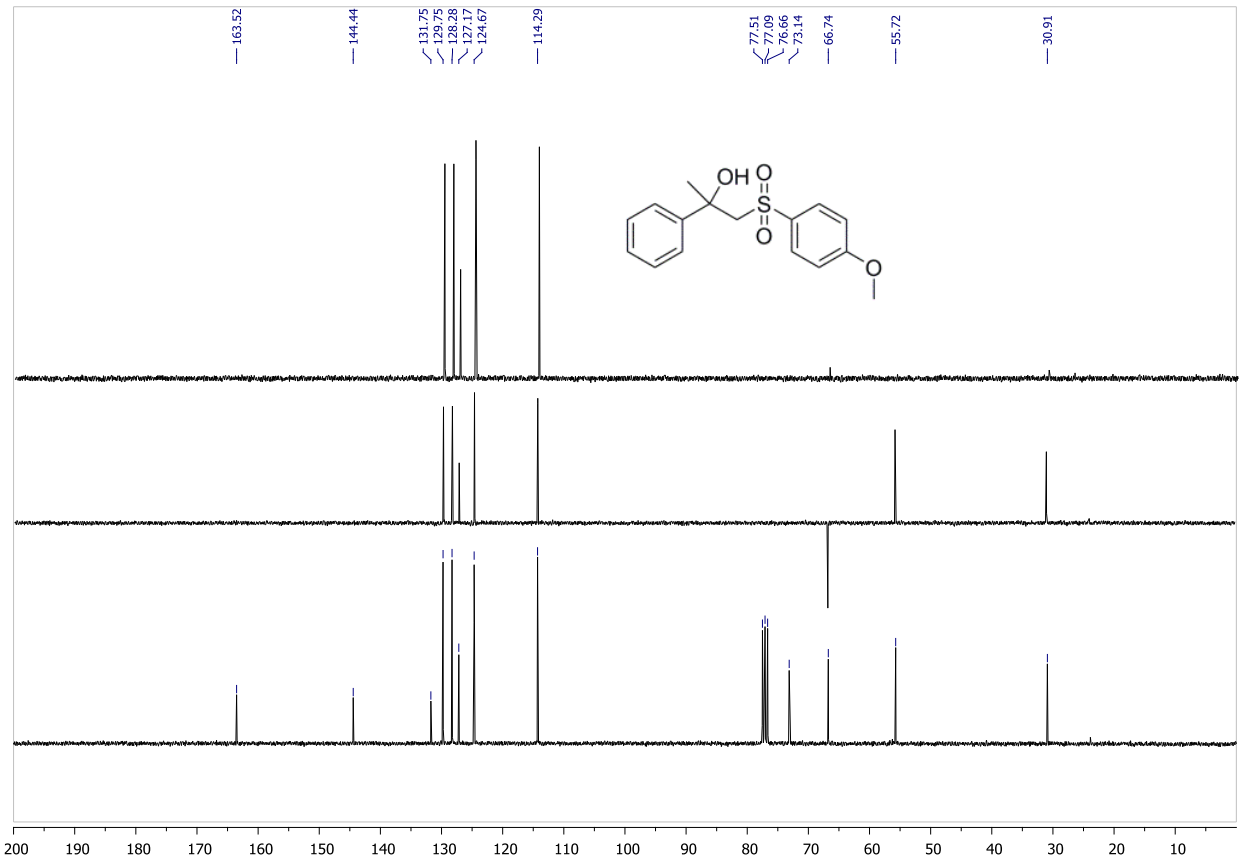

^{1}H-NMR: **3f**

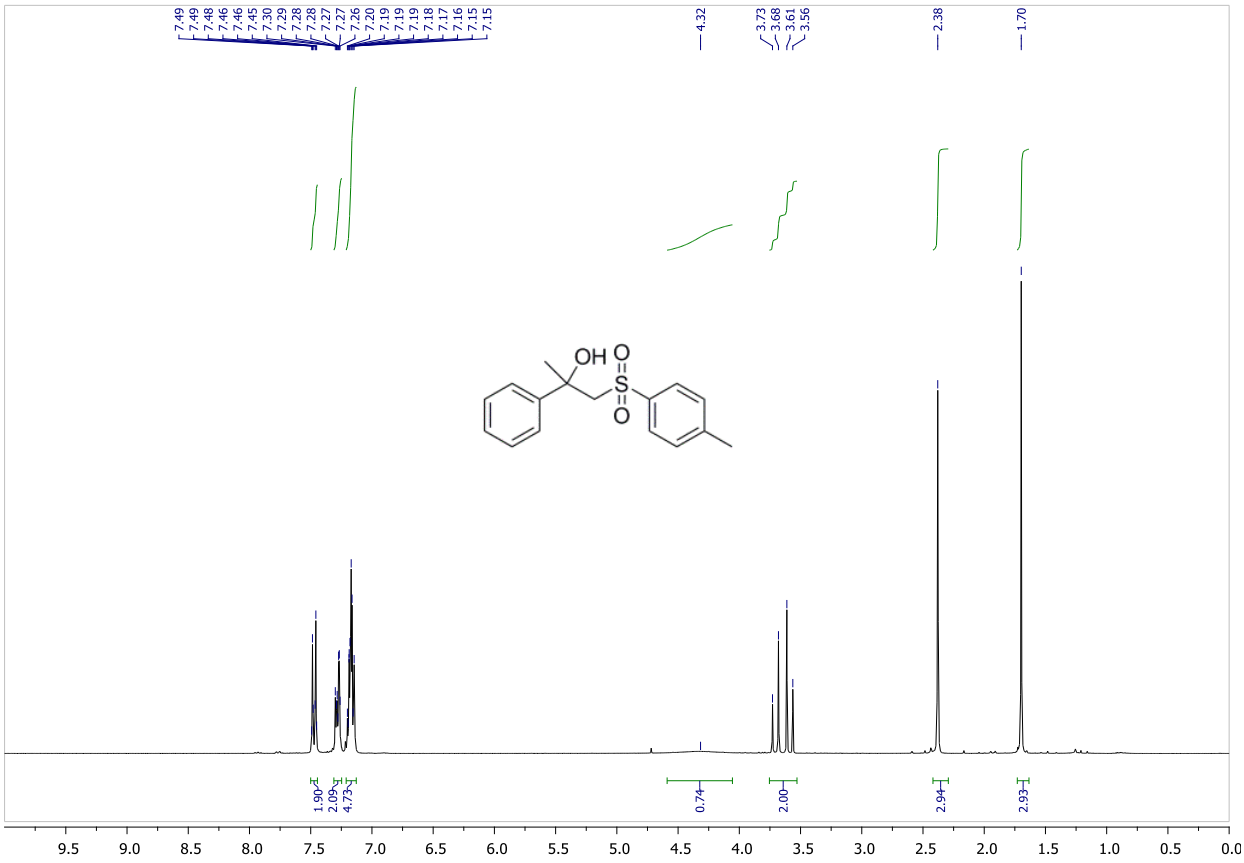

^{13}C-NMR: **3f**

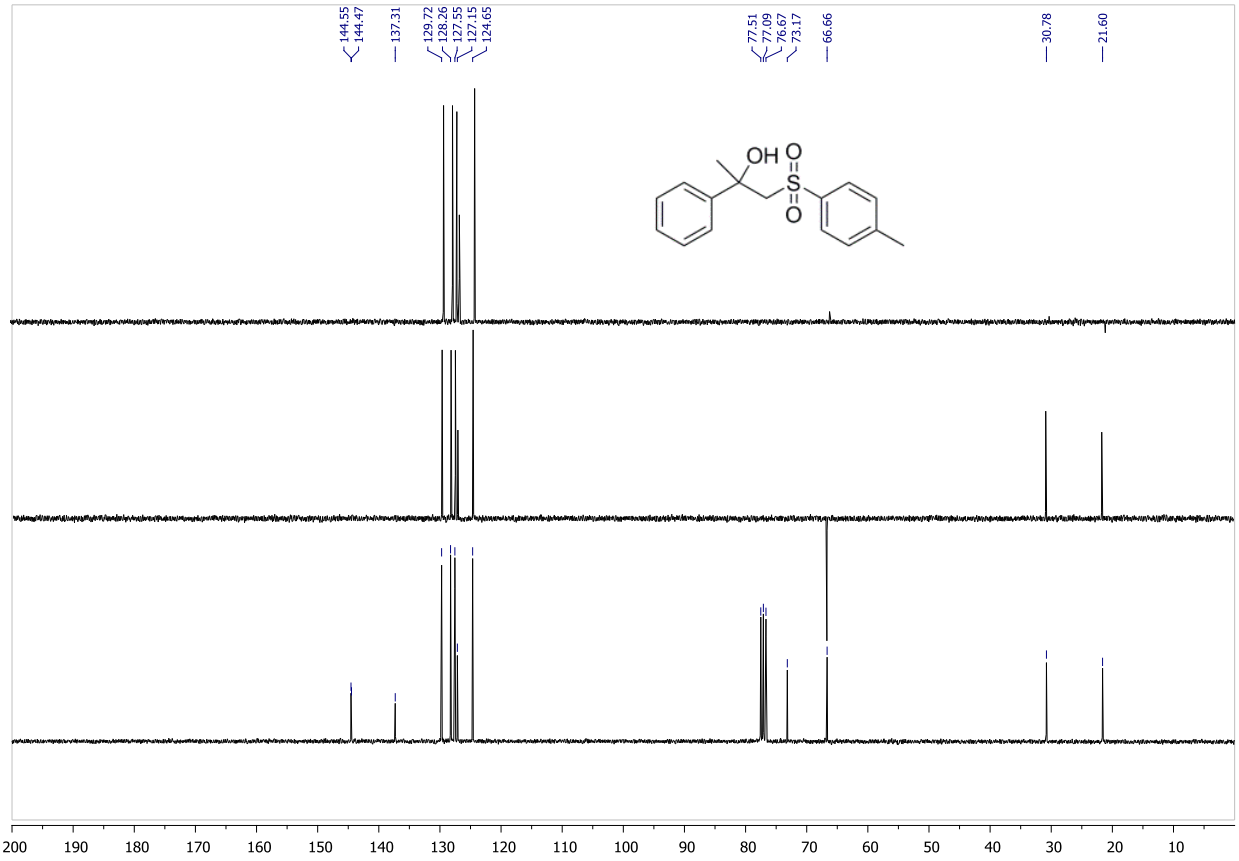

^{1}H-NMR: **3g**

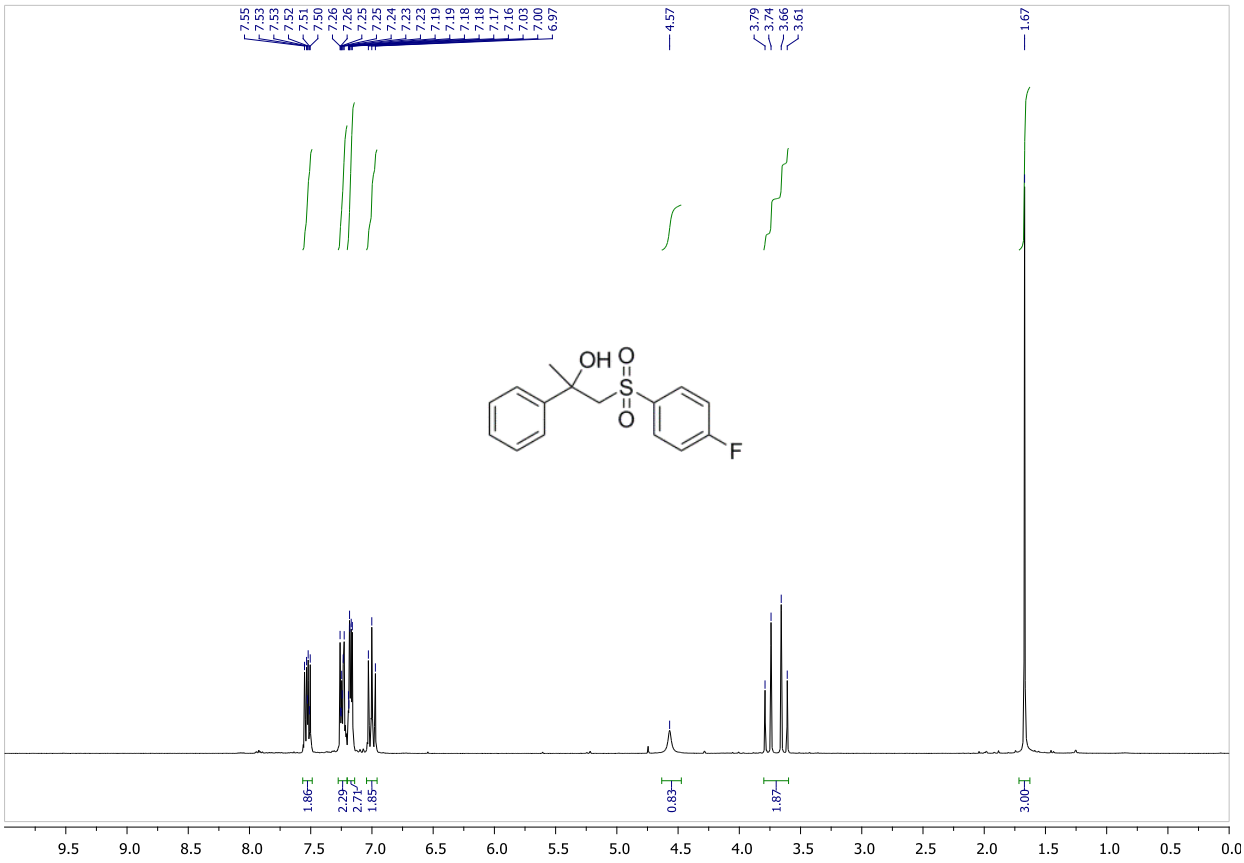

^{13}C-NMR: **3g**

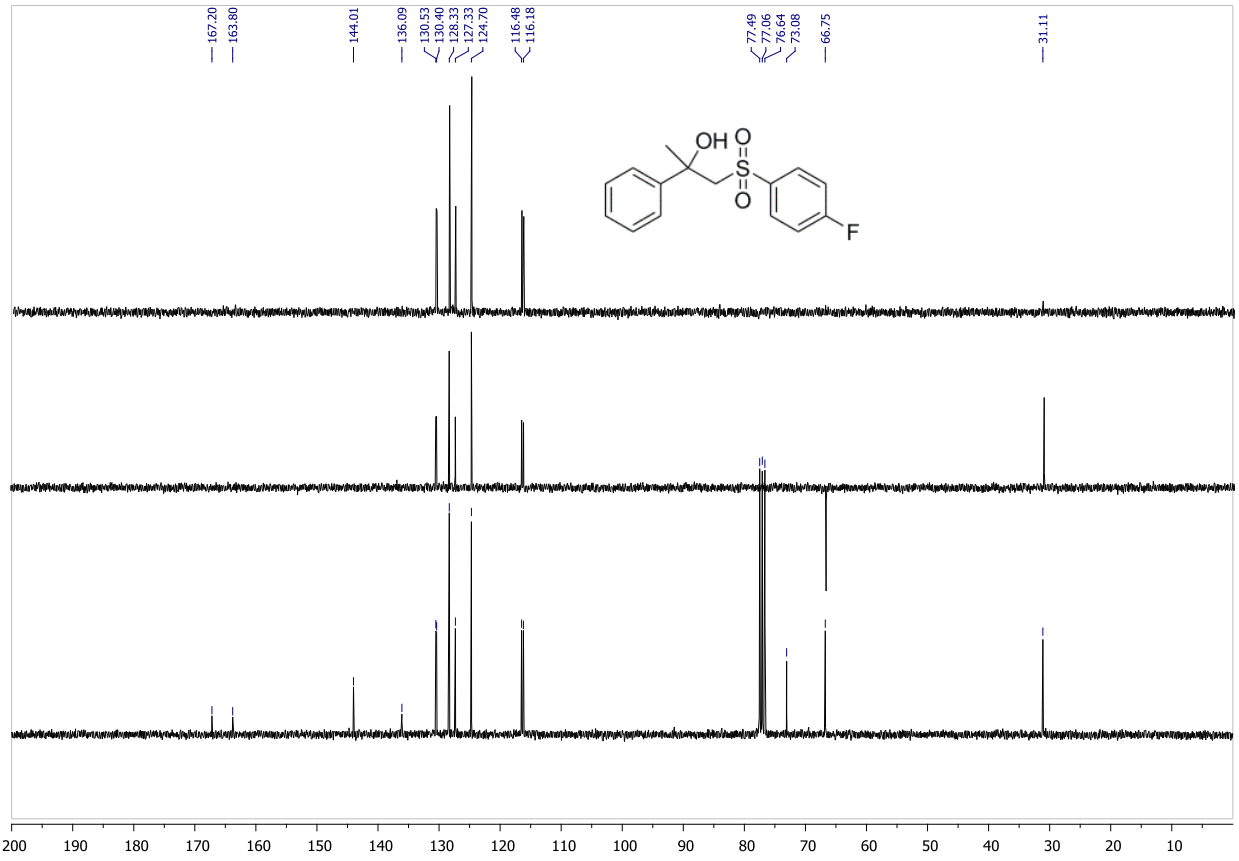

^{19}F-NMR: **3g**

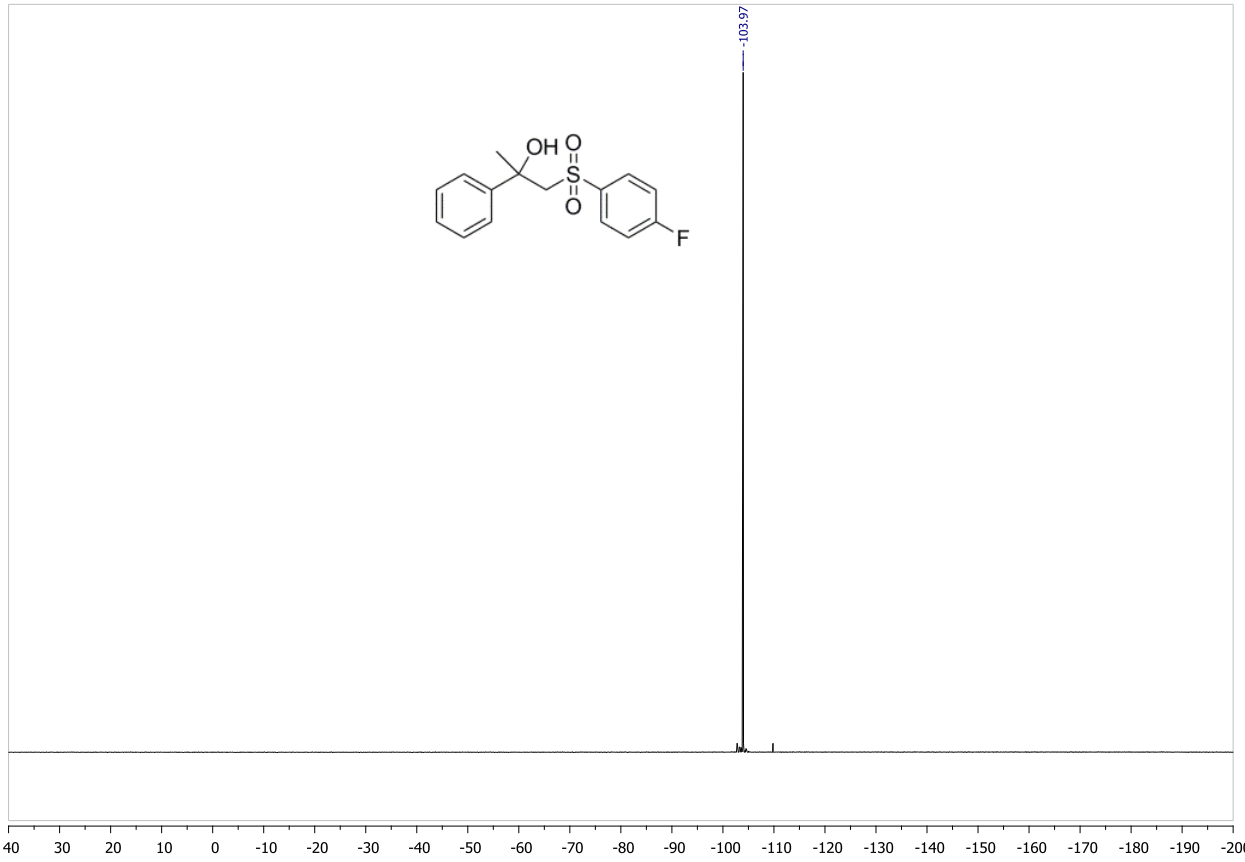
-103.97
OH
O
S
O
F
40 30 20 10 0 -10 -20 -30 -40 -50 -60 -70 -80 -90 -100 -110 -120 -130 -140 -150 -160 -170 -180 -190

^{1}H-NMR: **3h**

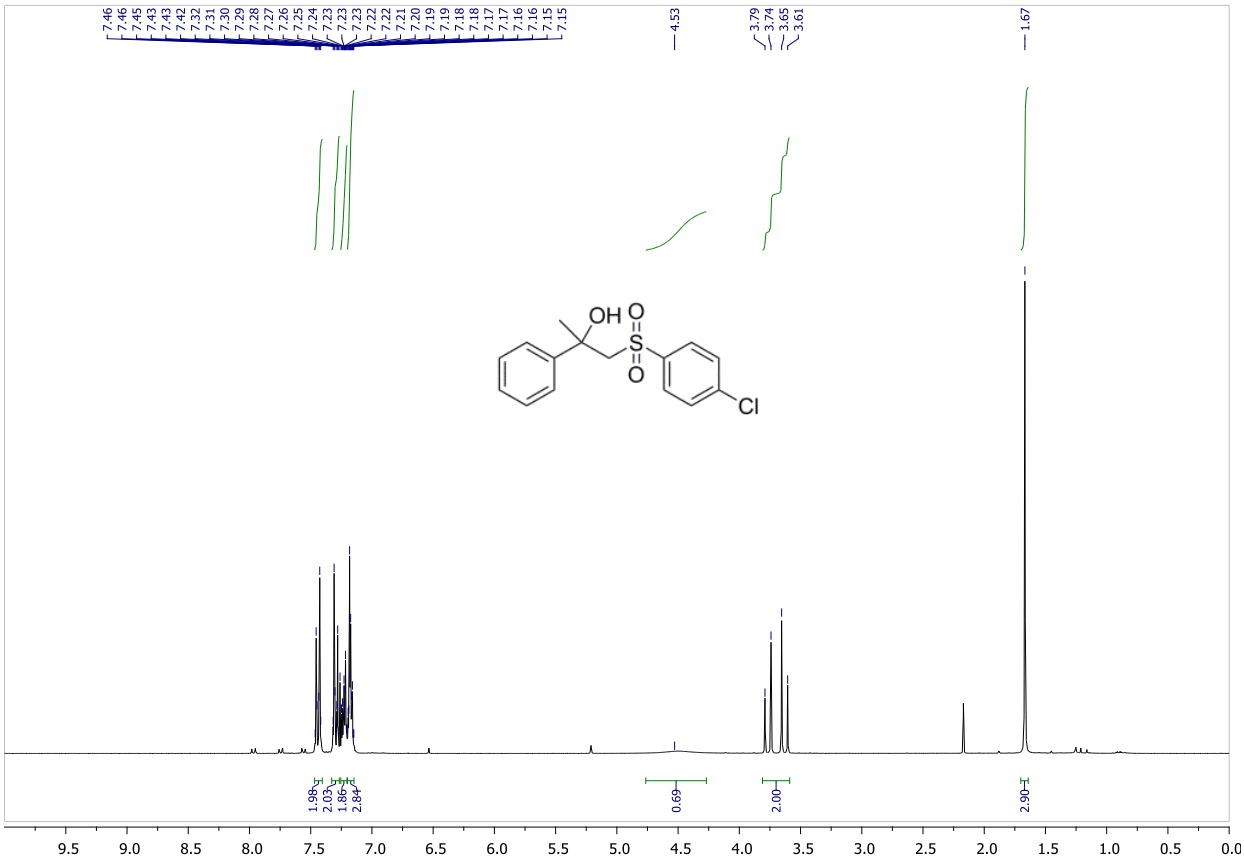

^{13}C-NMR: **3h**

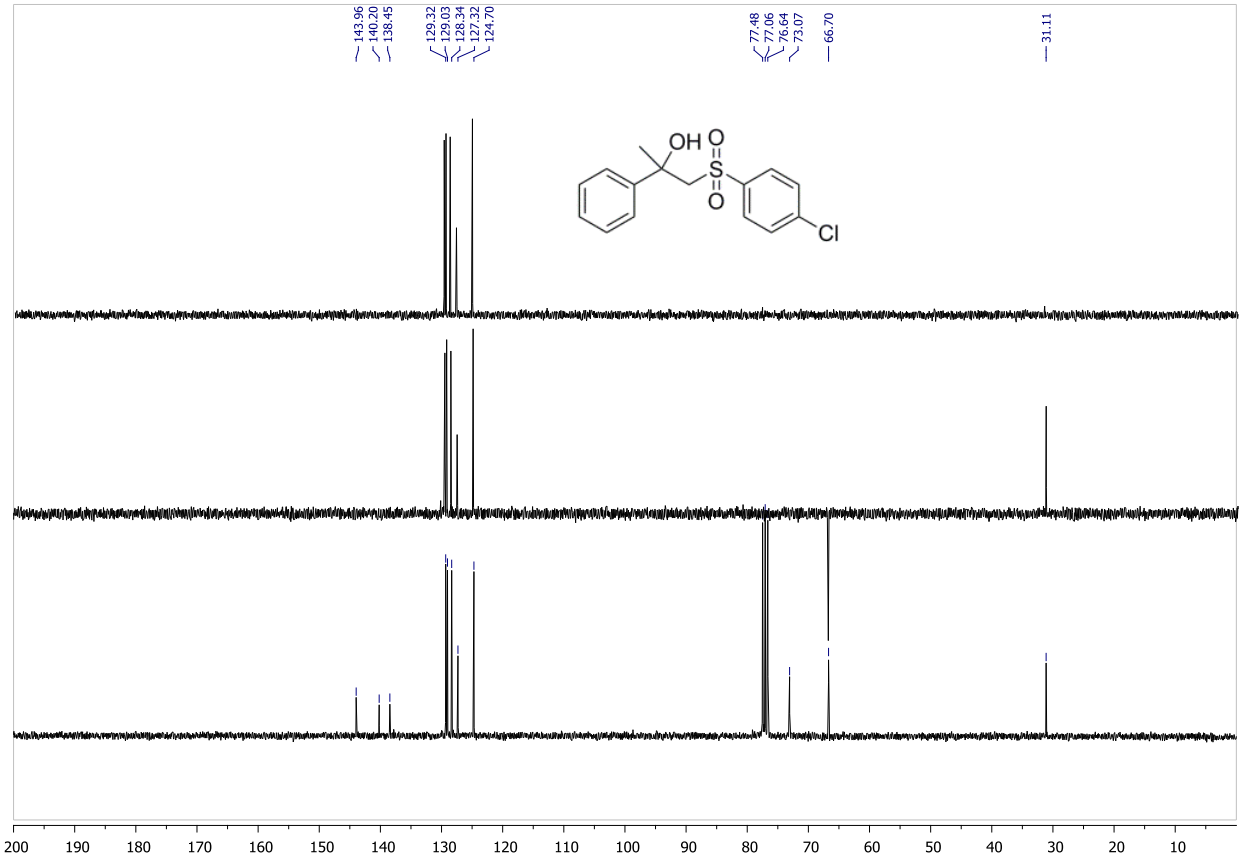

^{1}H-NMR: **3i**

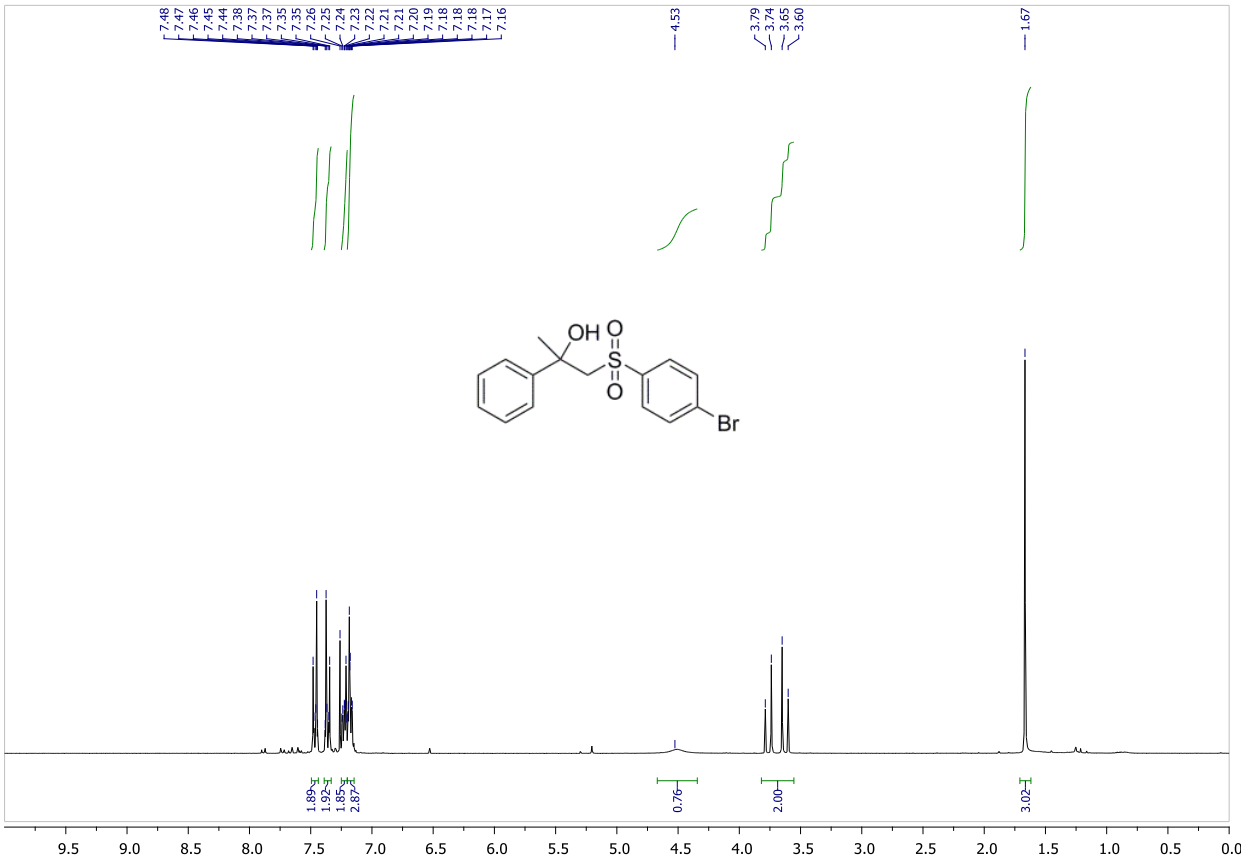

^{13}C-NMR: **3i**

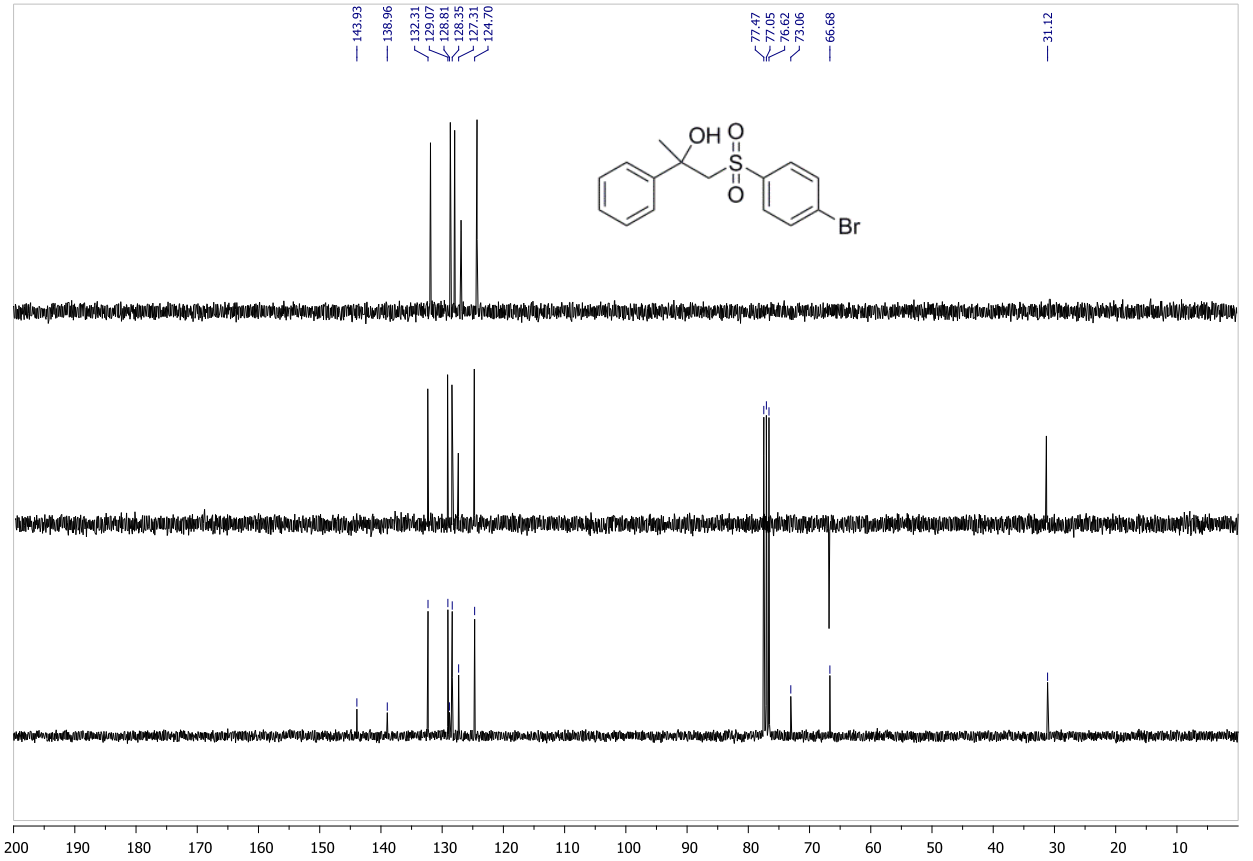

^{1}H-NMR: **3j**

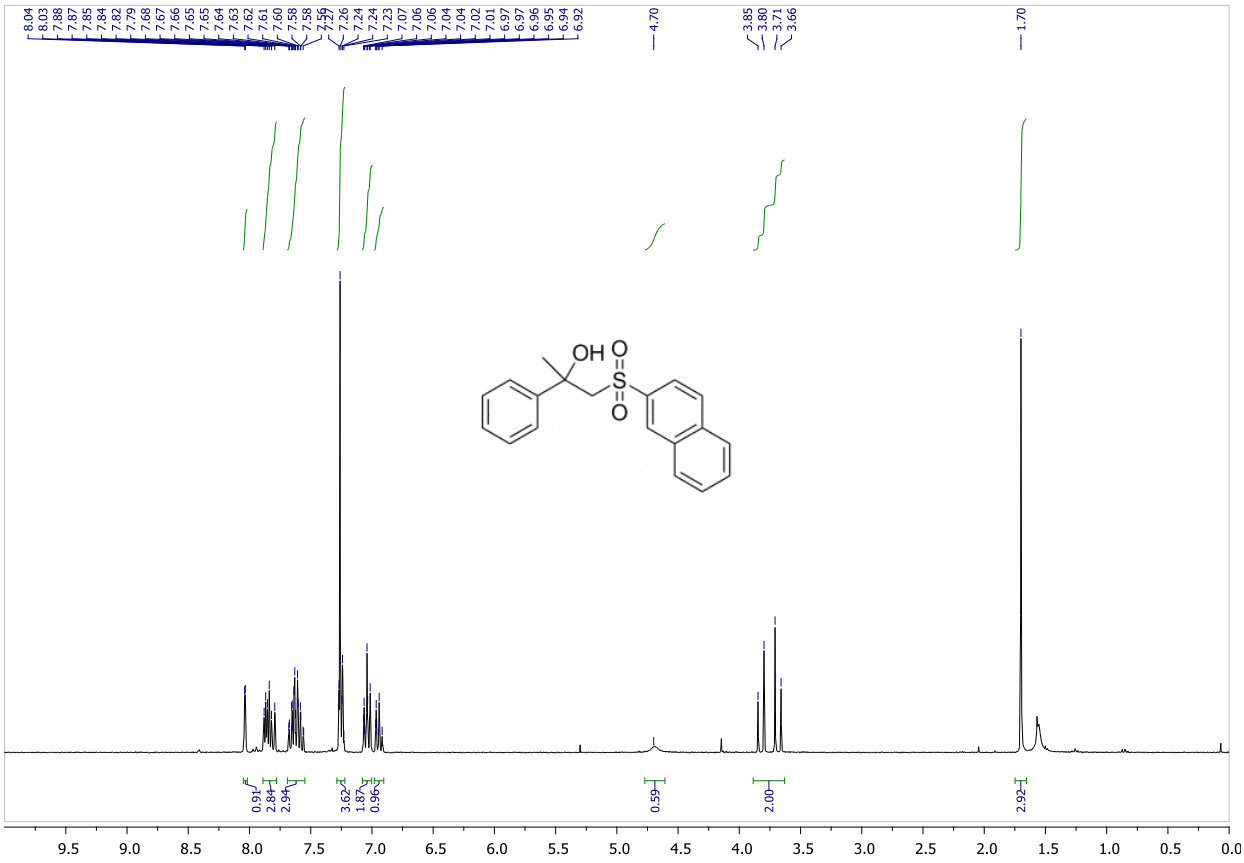

^{13}C-NMR: **3j**

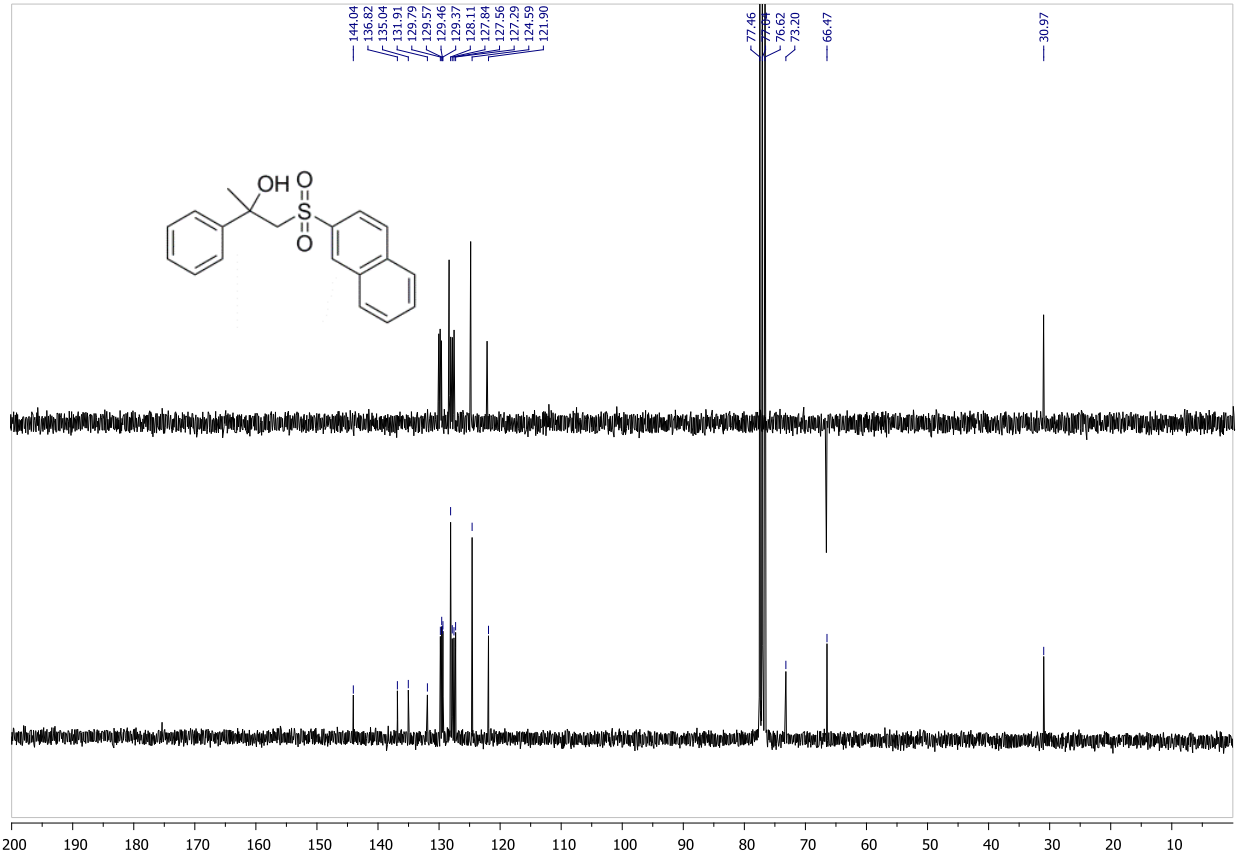

^{1}H-NMR: **3k**

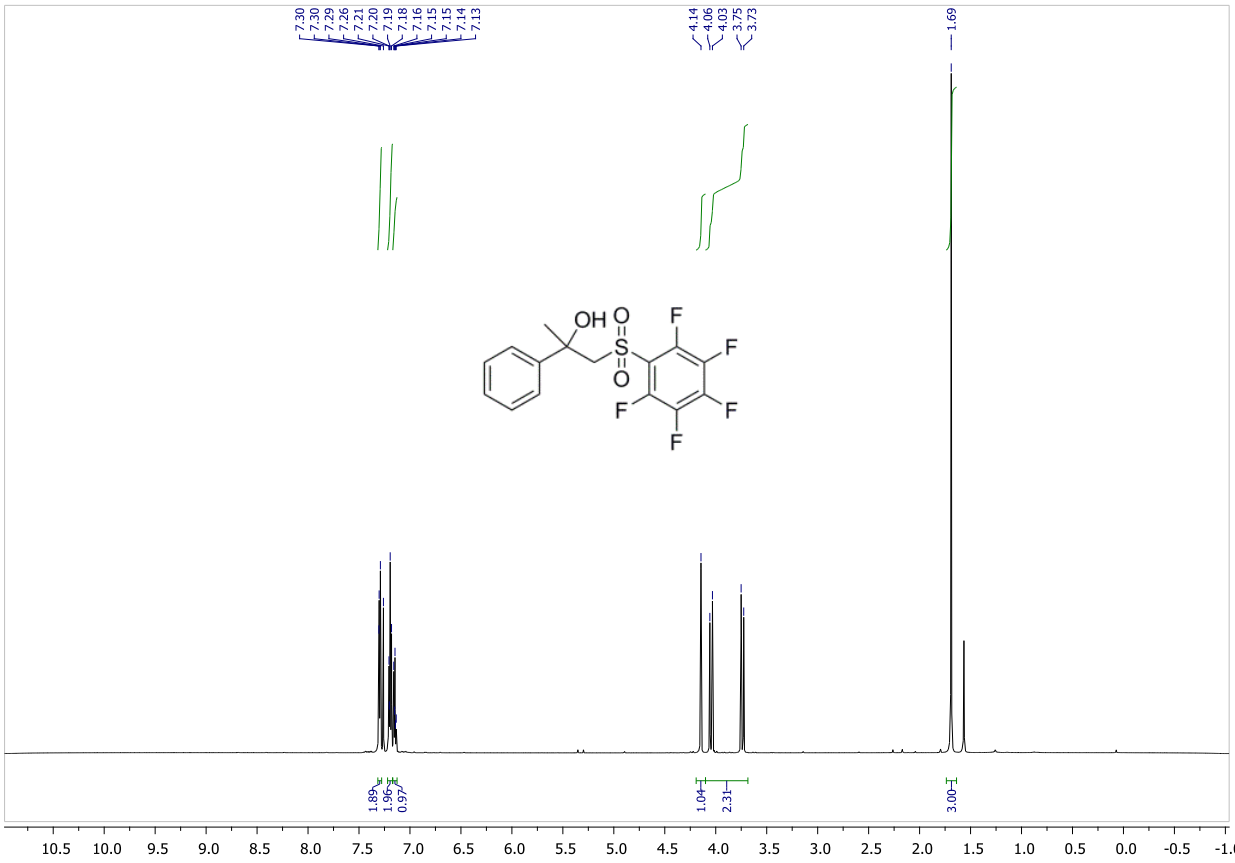

^{13}C-NMR: **3k**

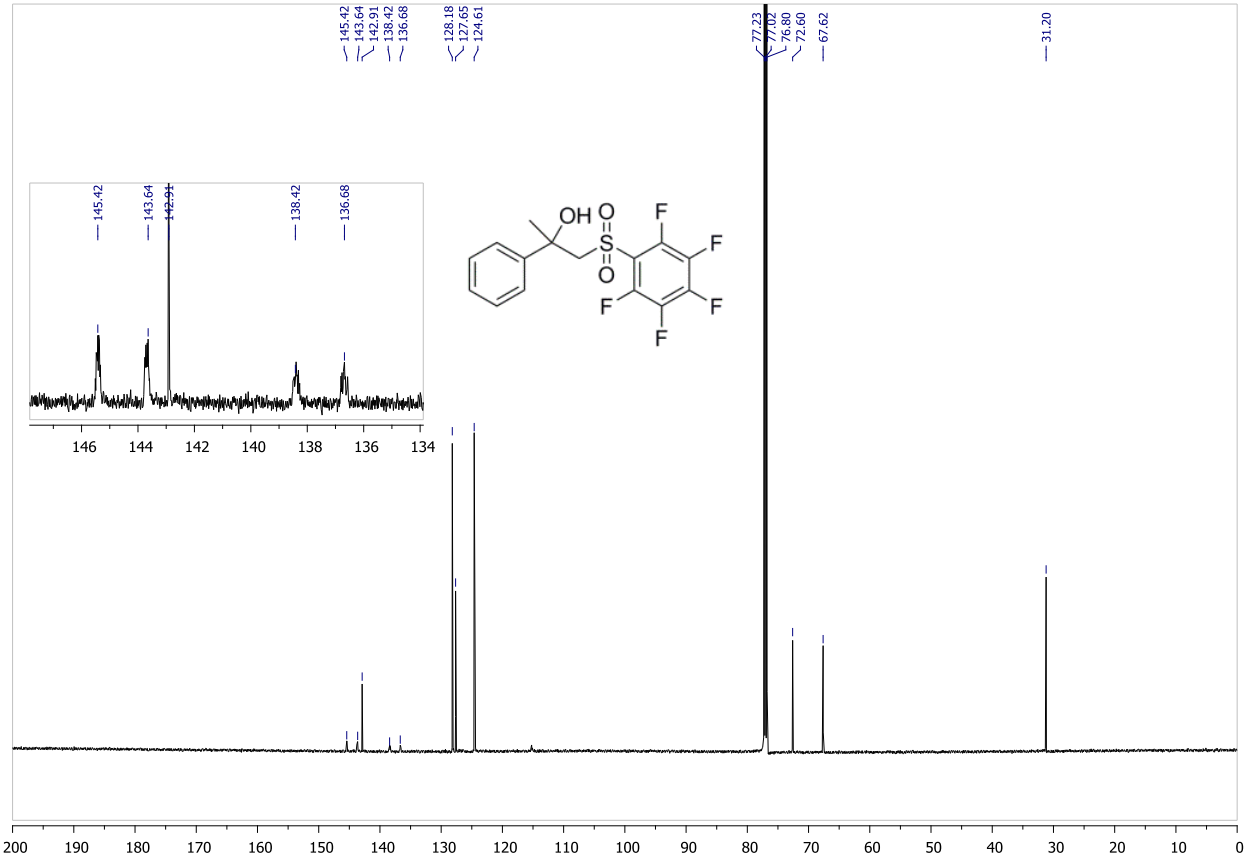

^{19}F-NMR: **3k**

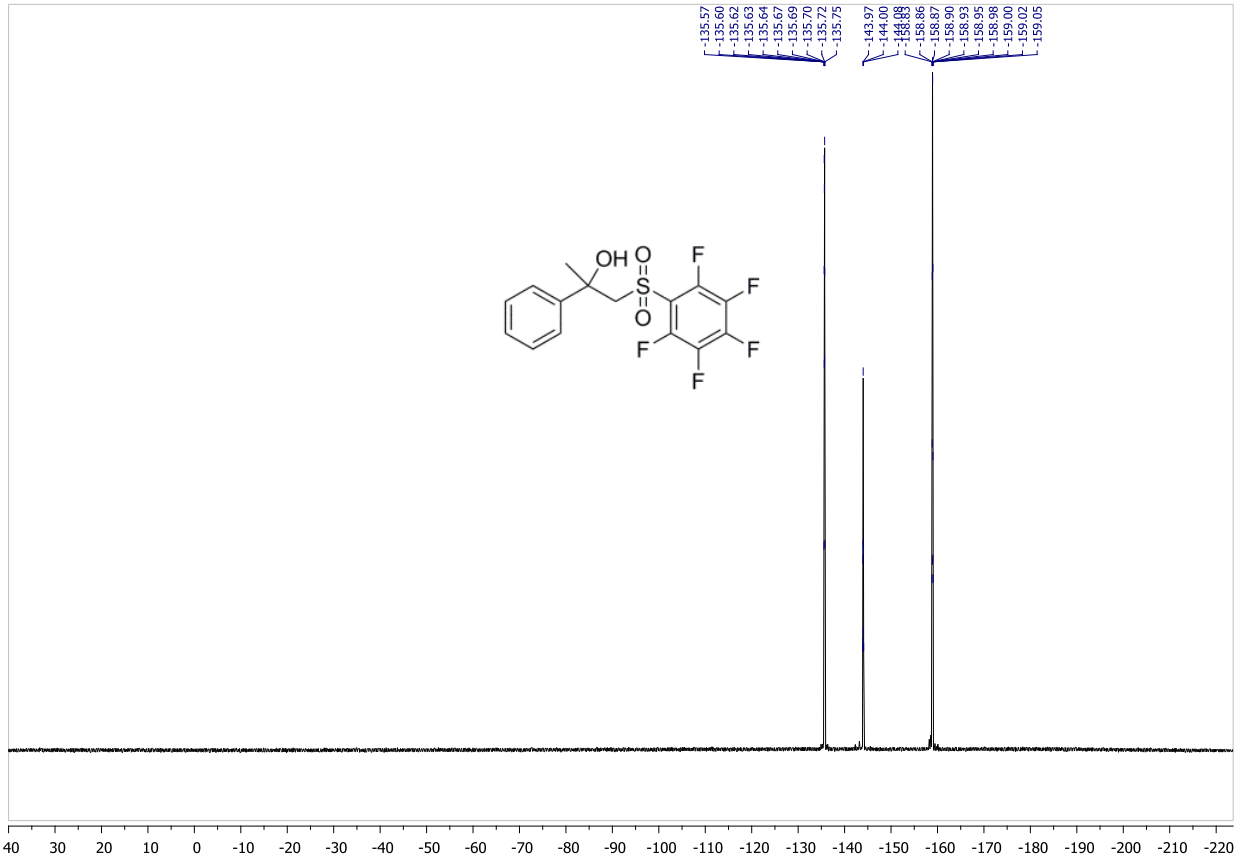
-135.57
-135.60
-135.62
-135.63
-135.64
-135.67
-135.69
-135.70
-135.72
-135.75
-143.97
-144.00
-158.83
-158.86
-158.87
-158.90
-158.93
-158.95
-158.98
-159.00
-159.02
-159.05
OH
O
S
O
F
F
F
F
F
40 30 20 10 0 -10 -20 -30 -40 -50 -60 -70 -80 -90 -100 -110 -120 -130 -140 -150 -160 -170 -180 -190 -200 -210 -220

^{1}H-NMR: **3l**

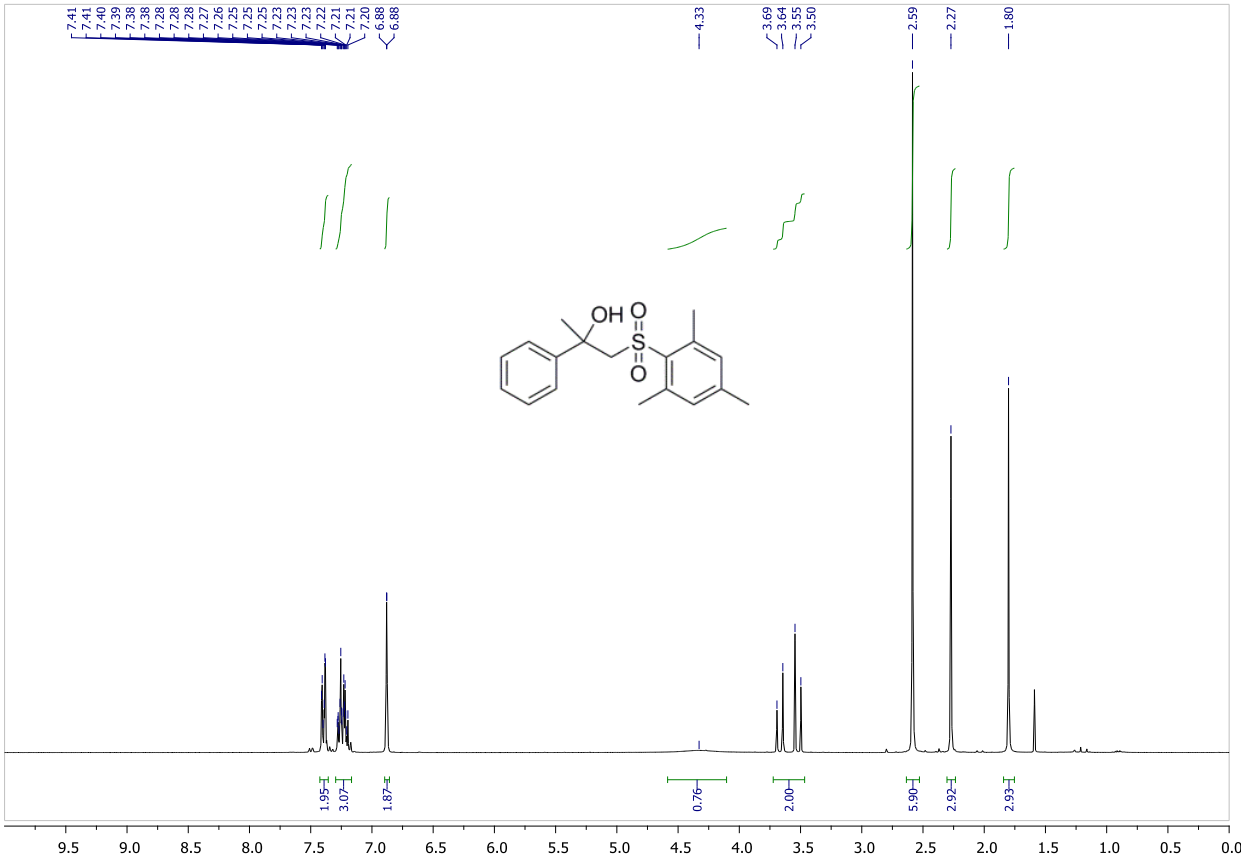

^{13}C-NMR: **3l**

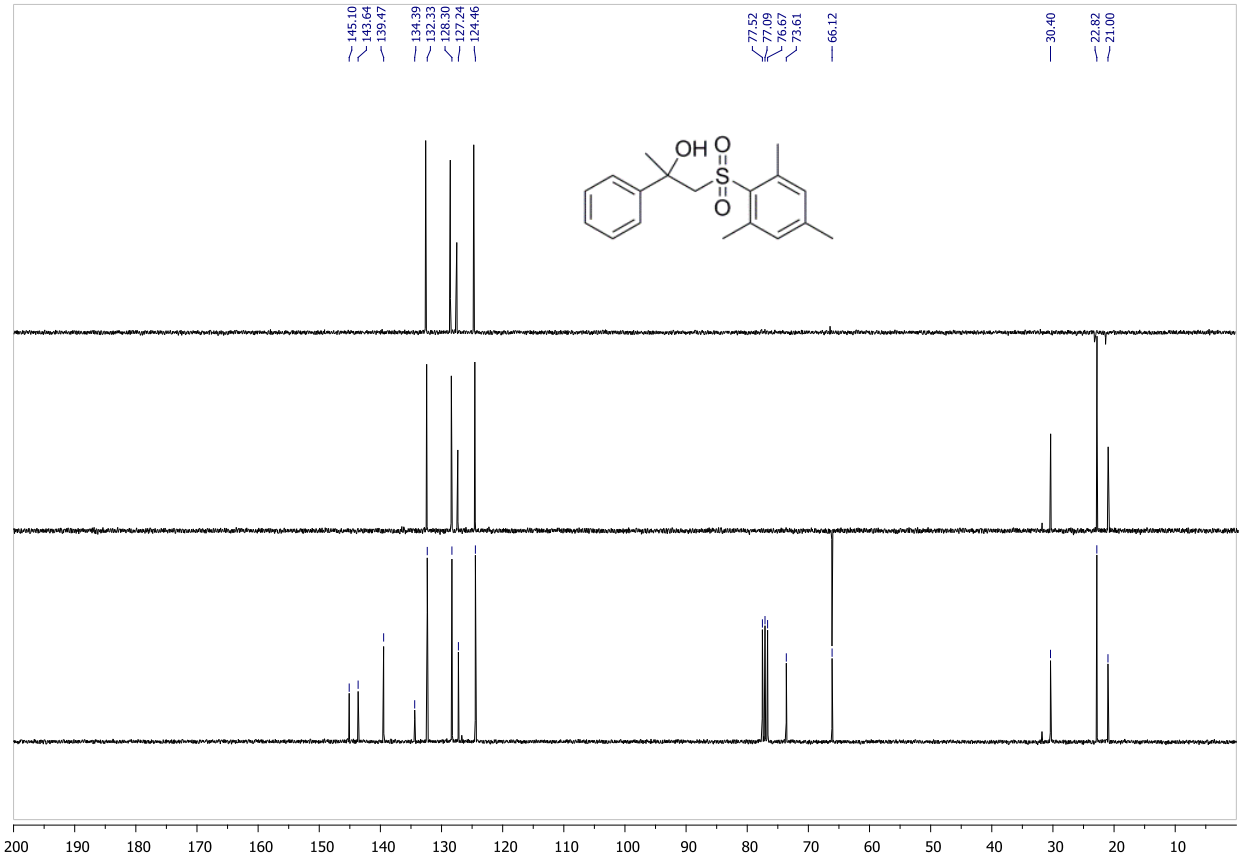

^{1}H-NMR: **3m**

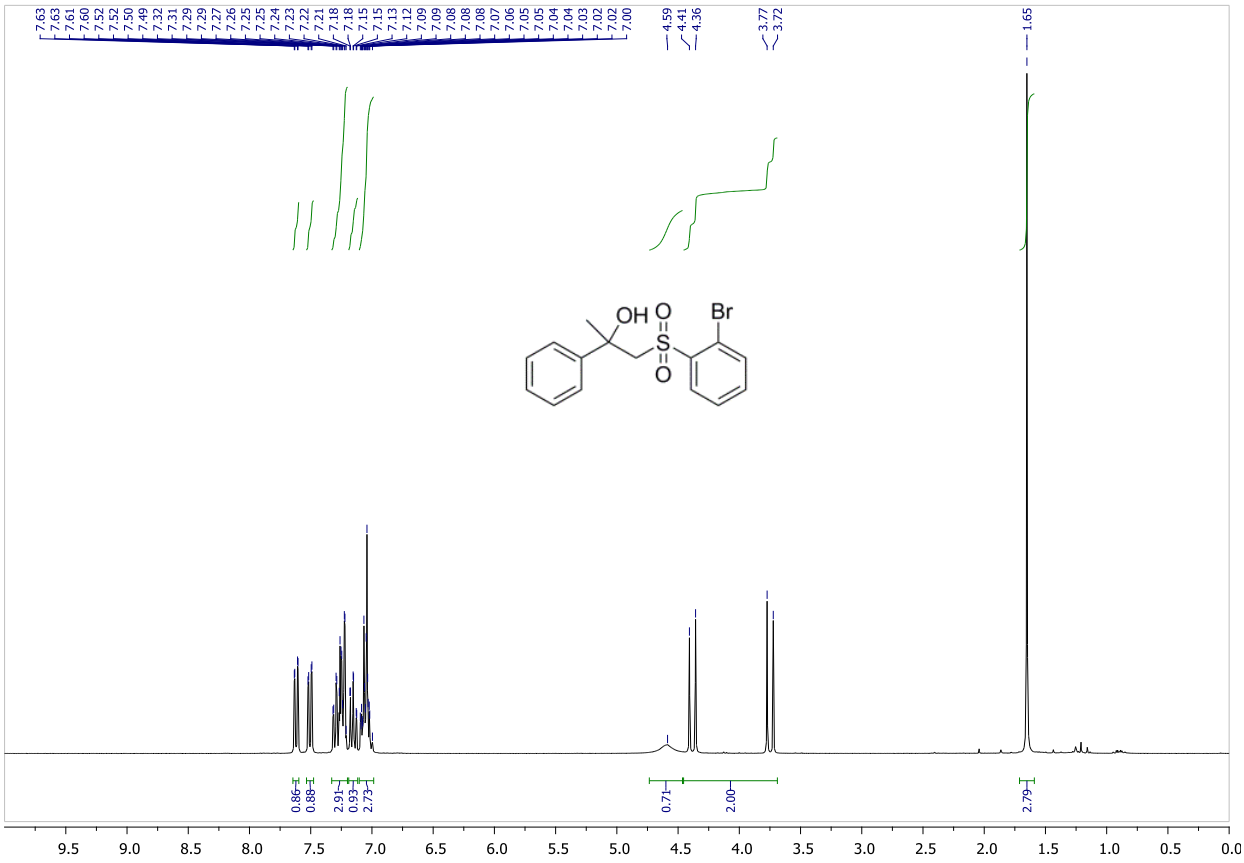

^{13}C-NMR Spectra: **3m**

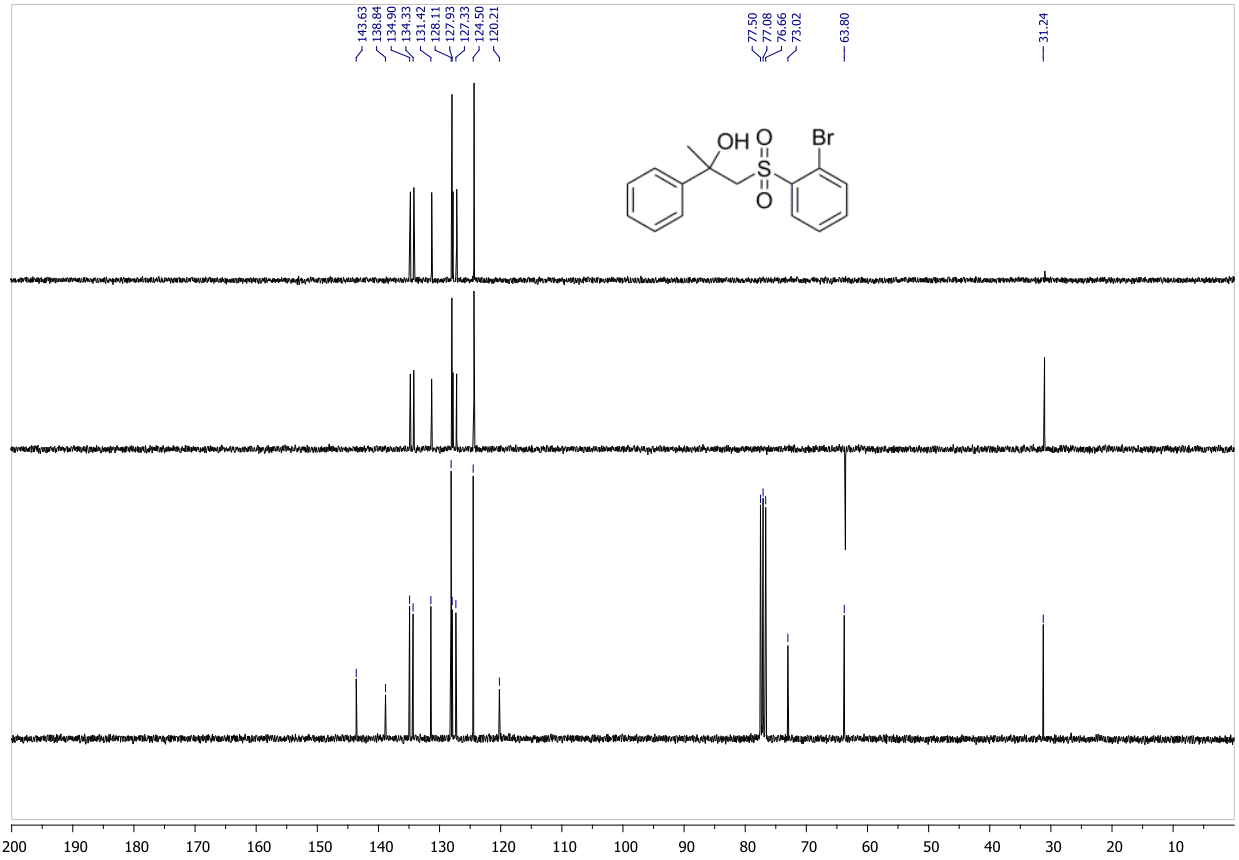

^{1}H-NMR: **4a**

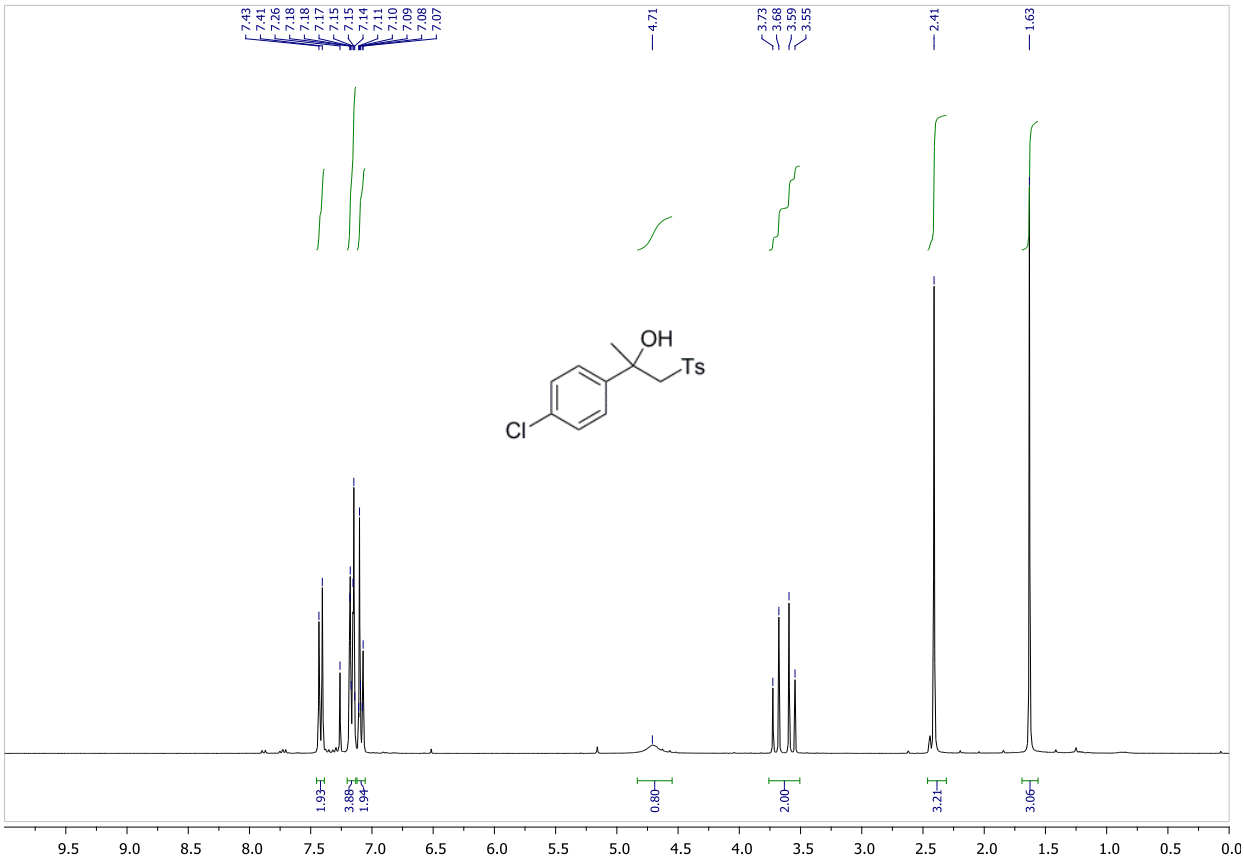

^{13}C-NMR: **4a**

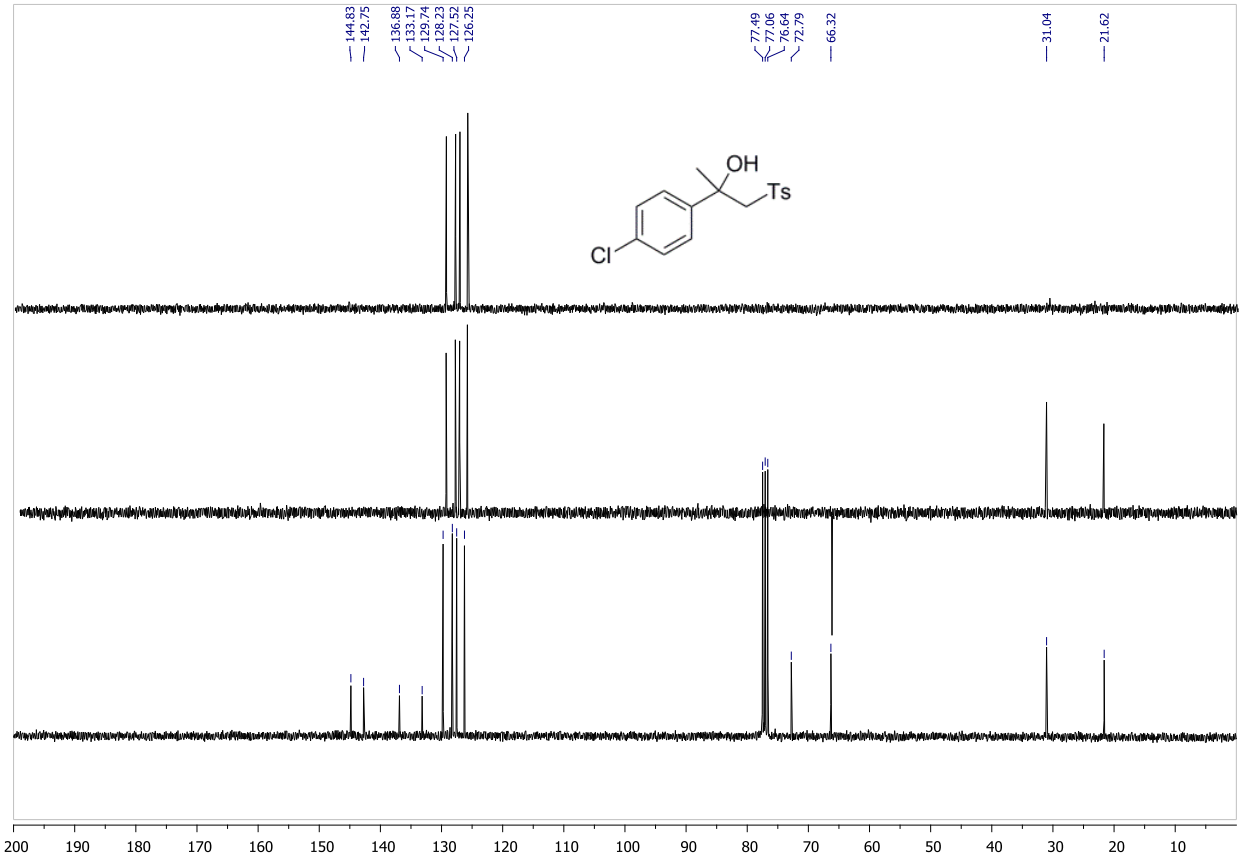

^{1}H-NMR: **4b**

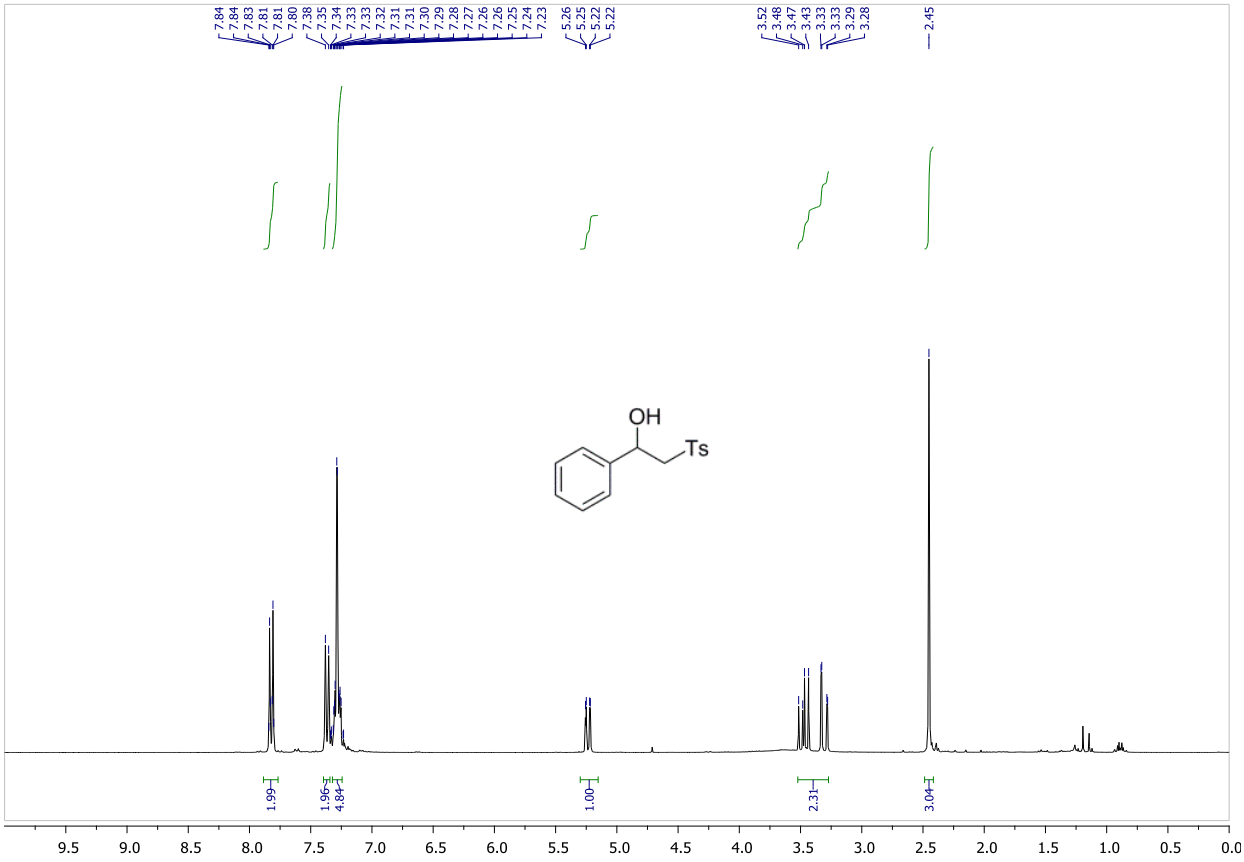

^{13}C-NMR: **4b**

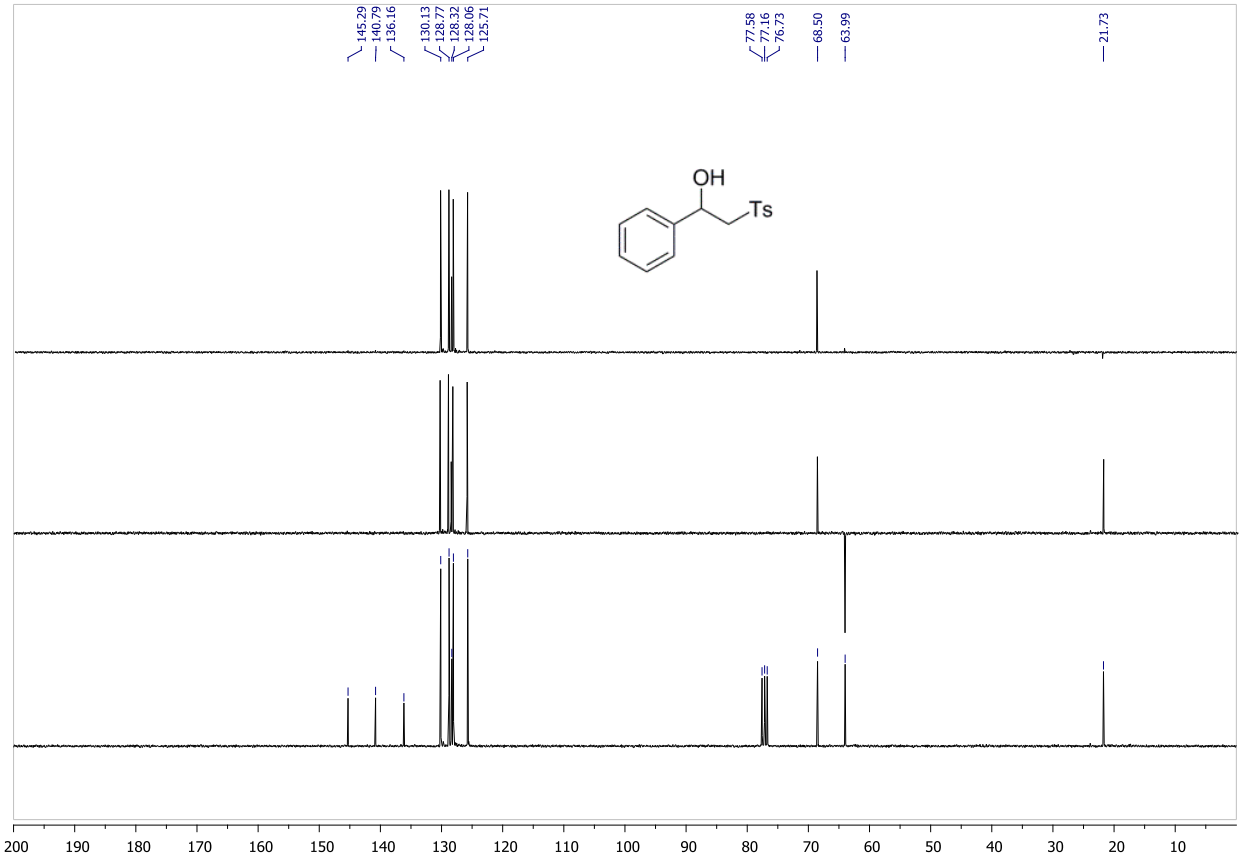

^{1}H-NMR: **4c**

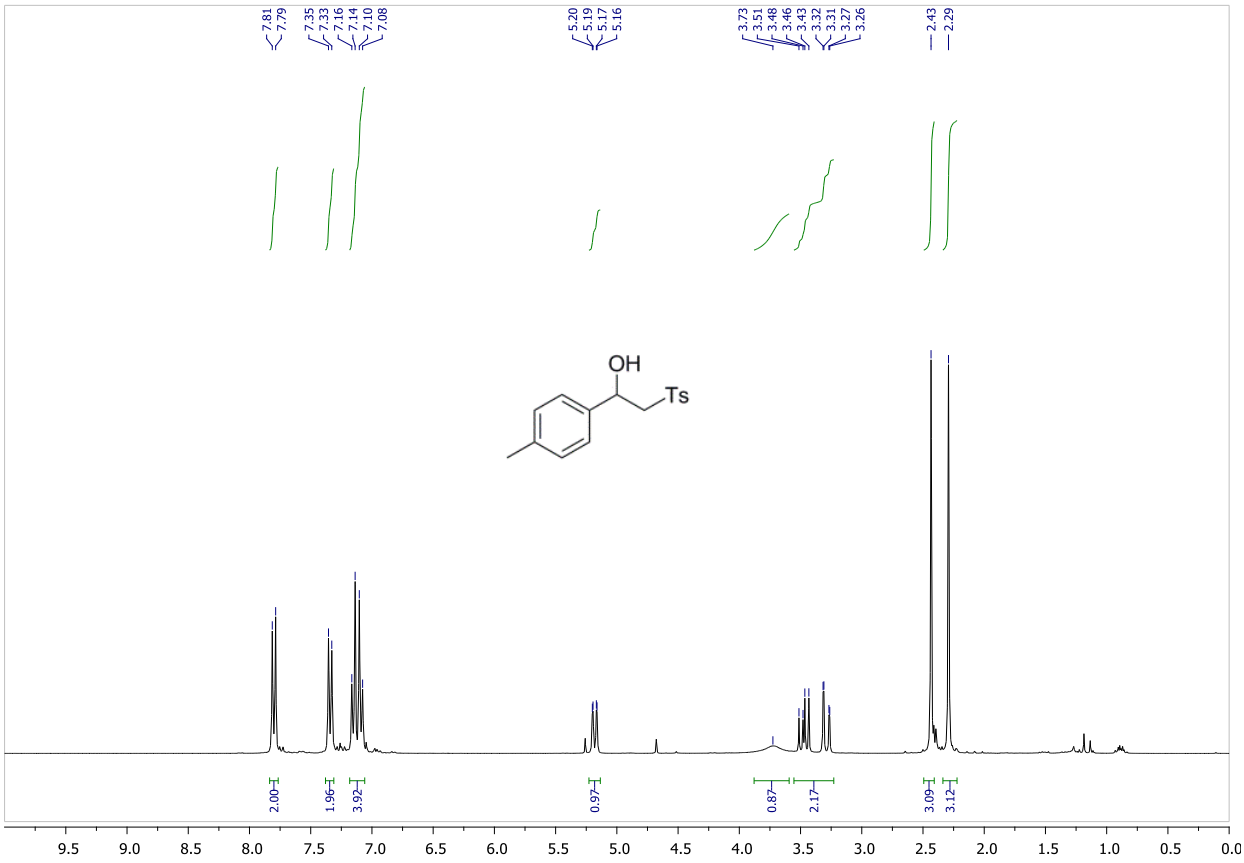

^{13}C-NMR: **4c**

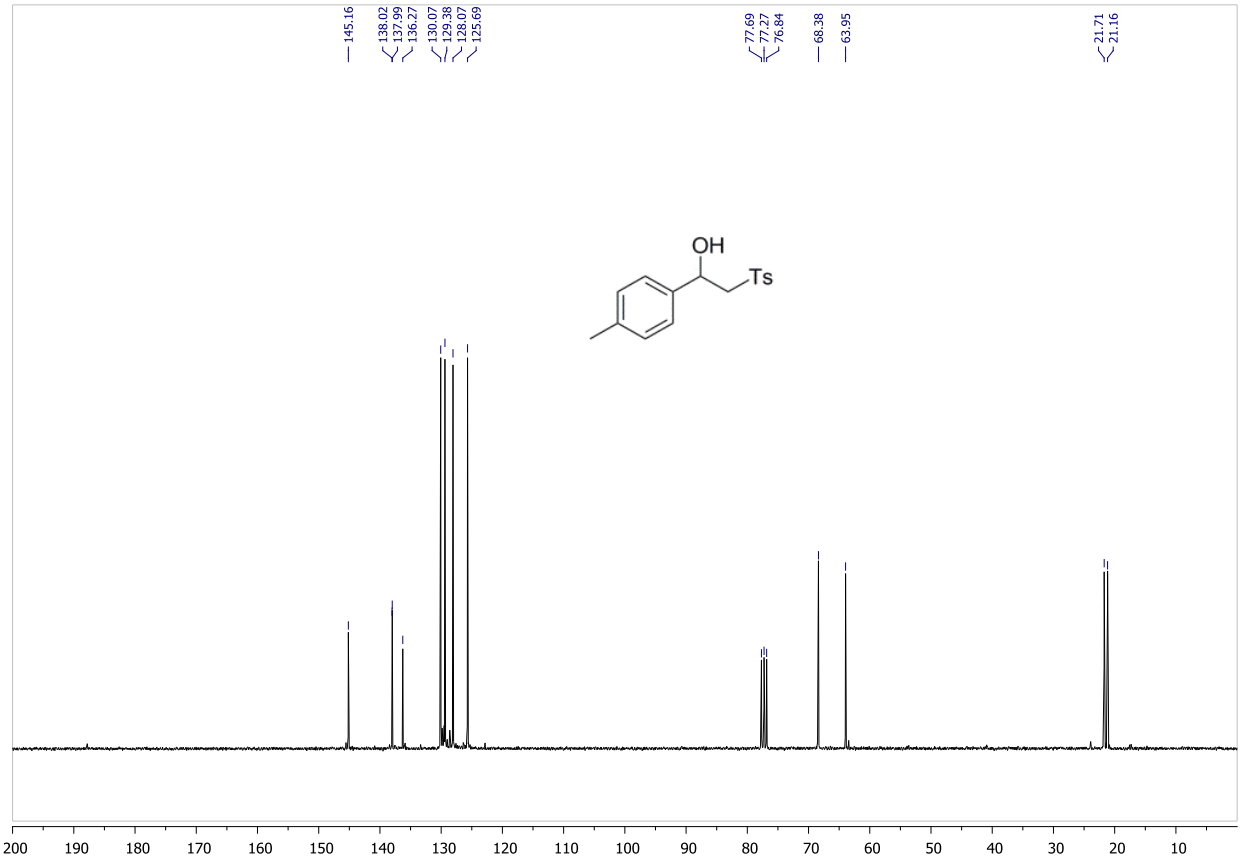

^{1}H-NMR: **4d**

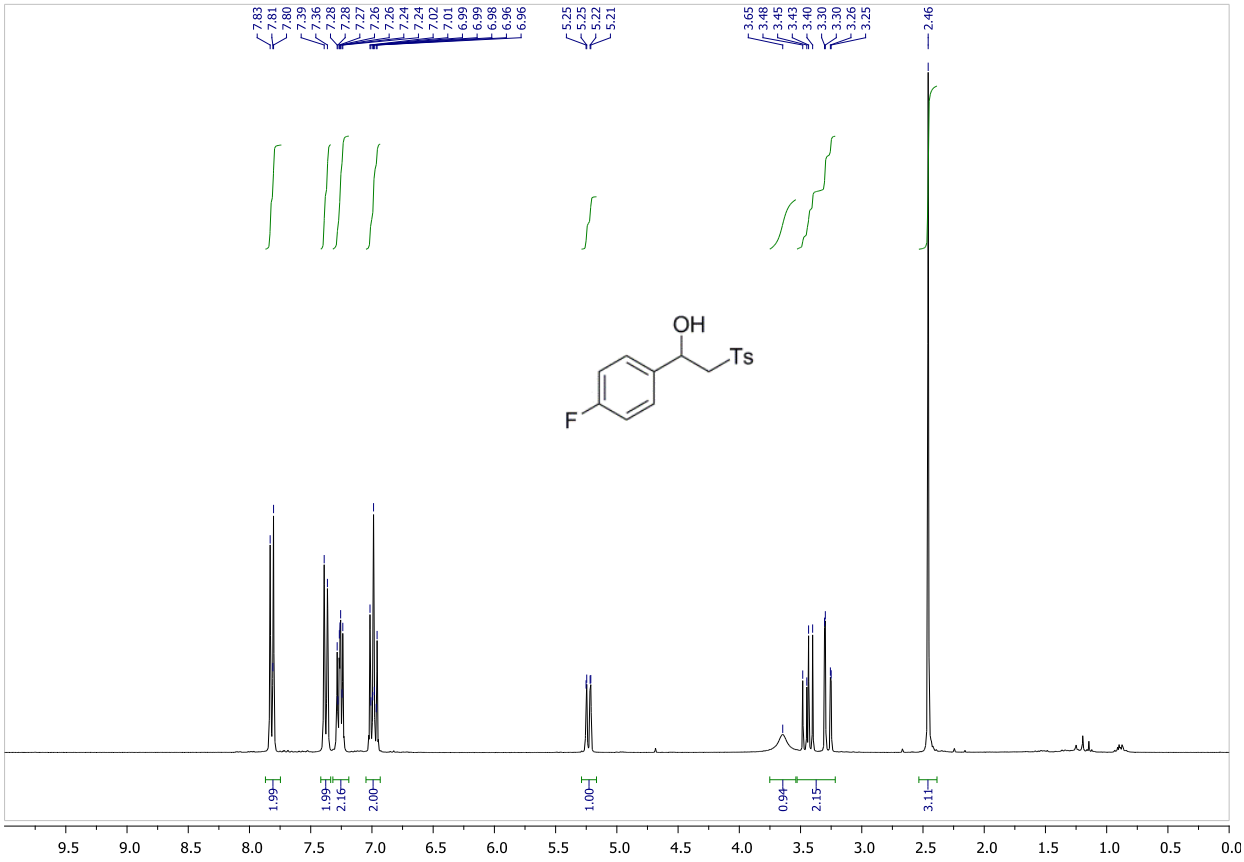

^{13}C-NMR: **4d**

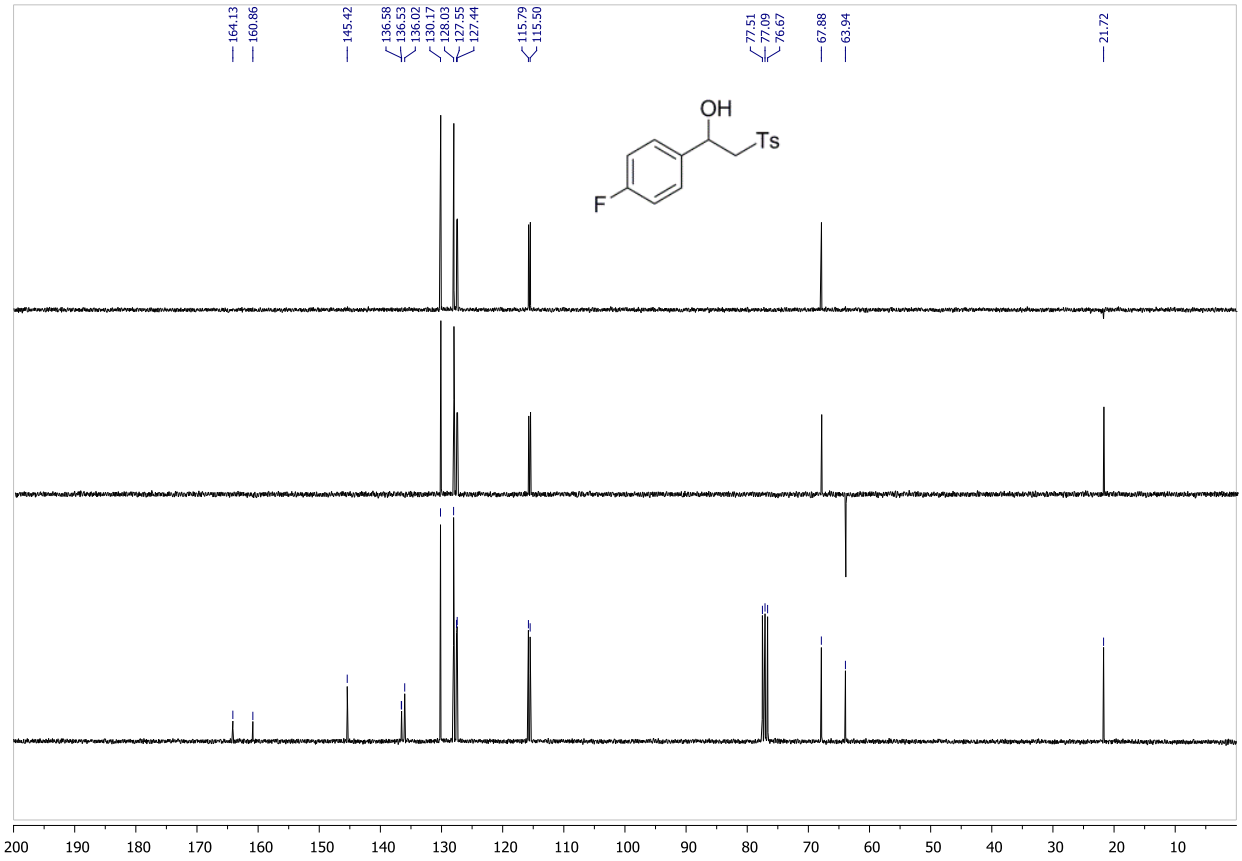

^{19}F-NMR: **4d**

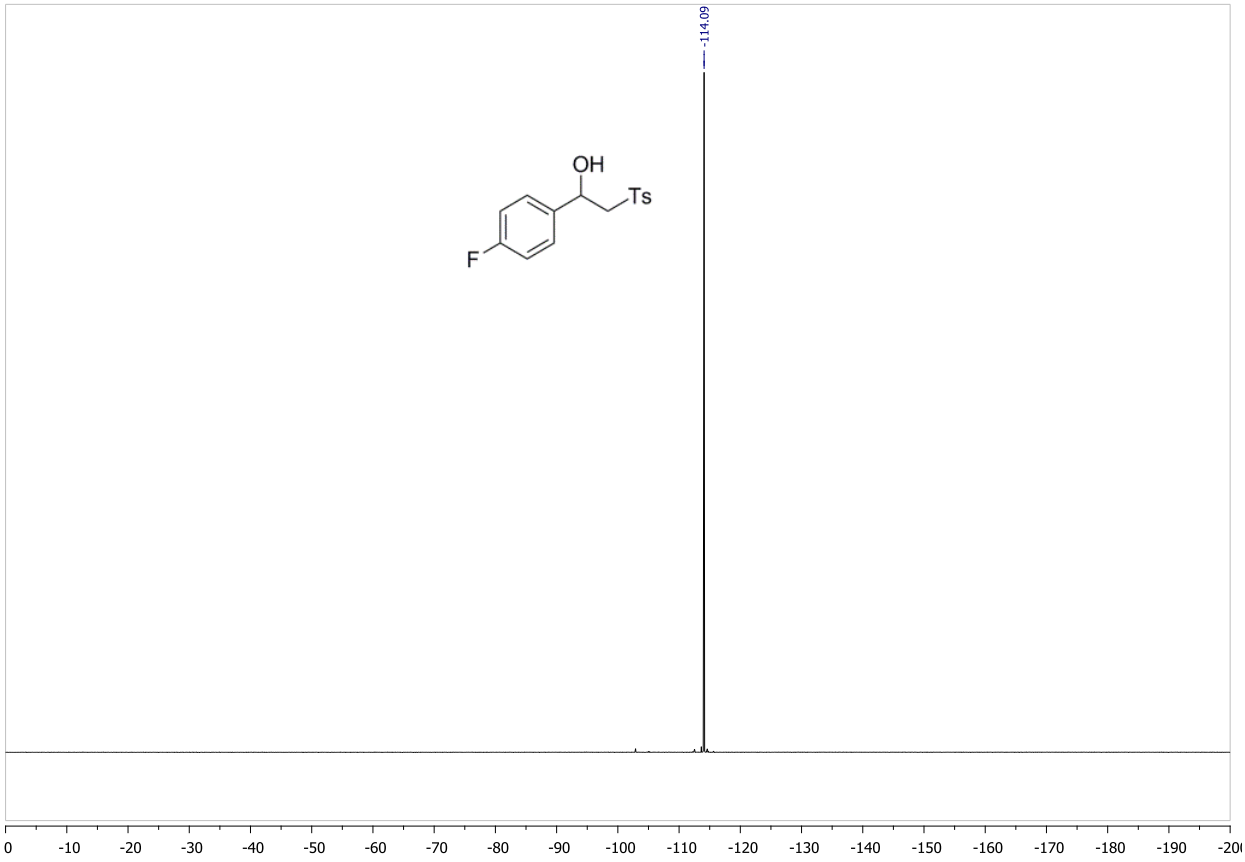
-114.09
OH
Ts
F
0
-10
-20
-30
-40
-50
-60
-70
-80
-90
-100
-110
-120
-130
-140
-150
-160
-170
-180
-190

^{1}H-NMR: **4e**

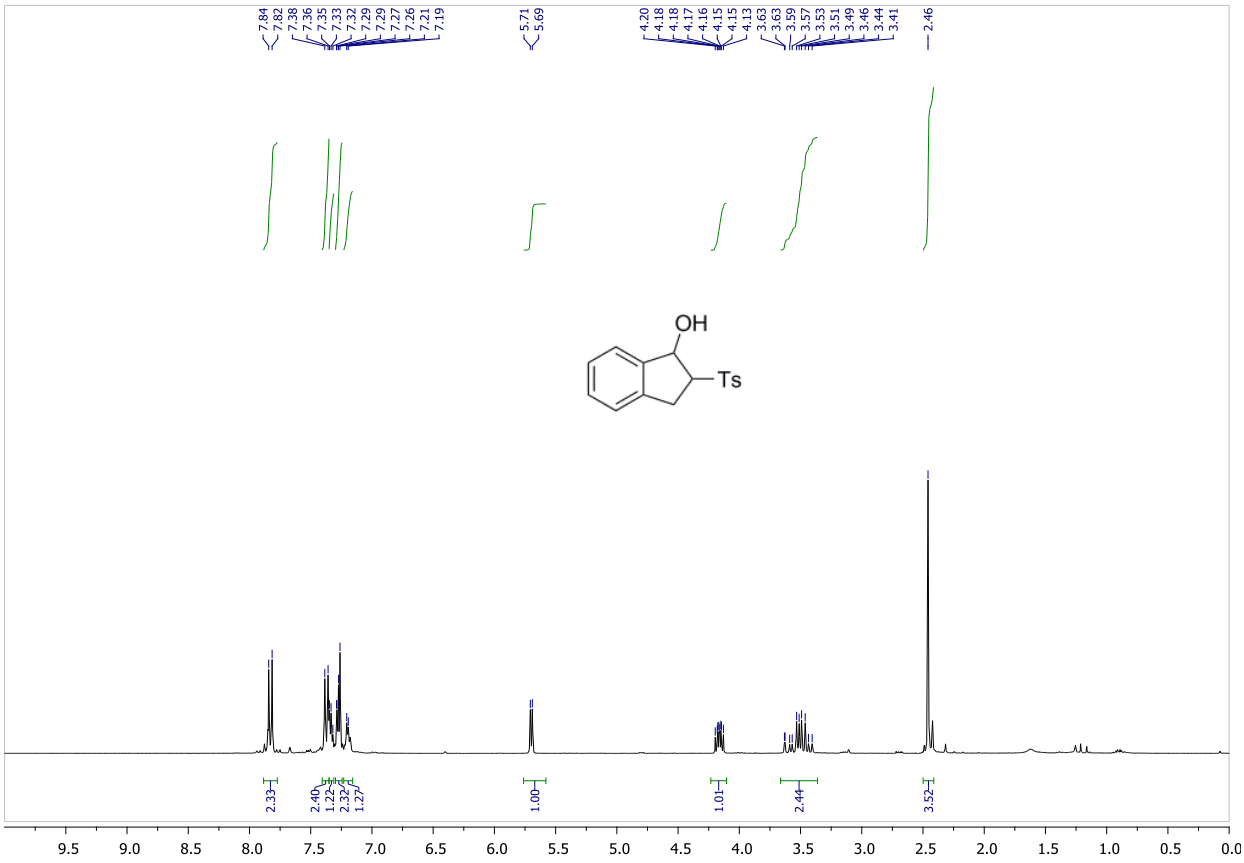

^{13}C-NMR: **4e**

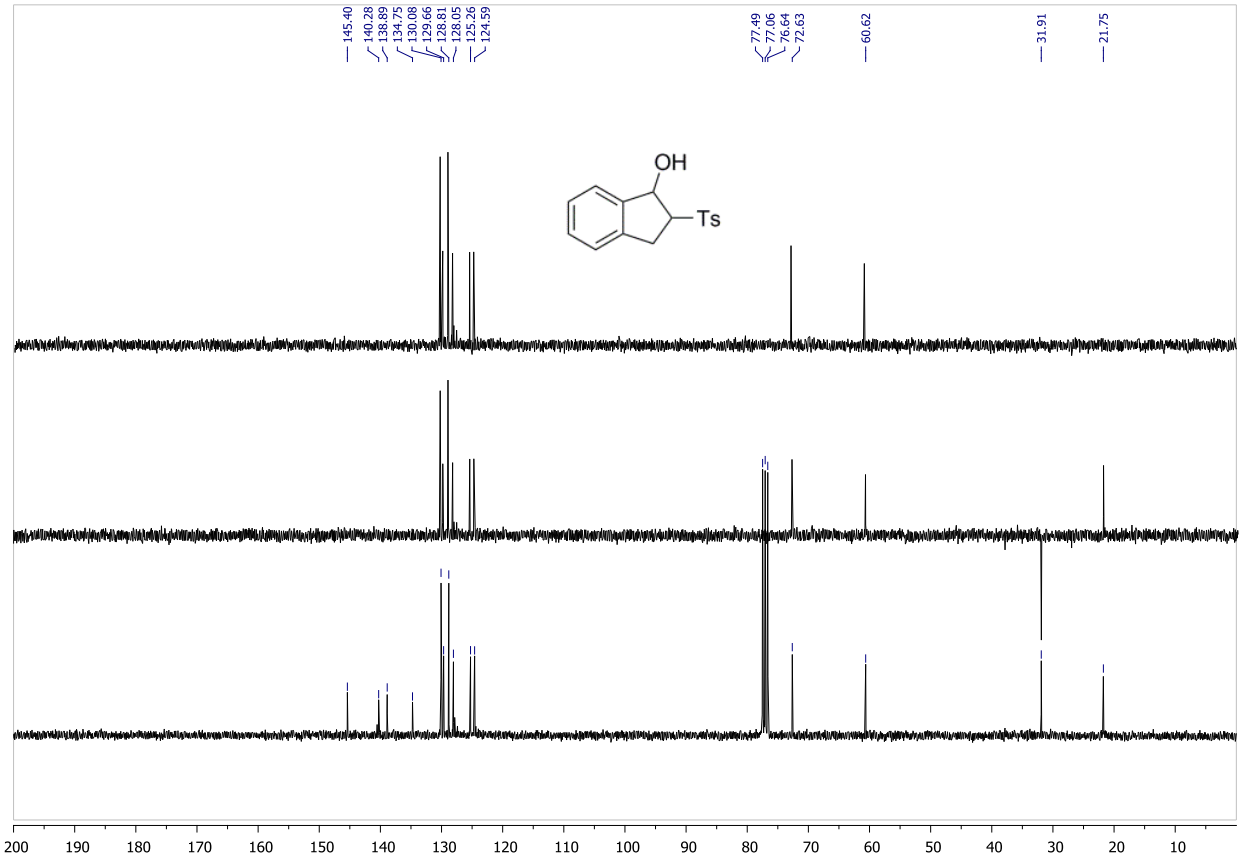

^{1}H-NMR: **4g**

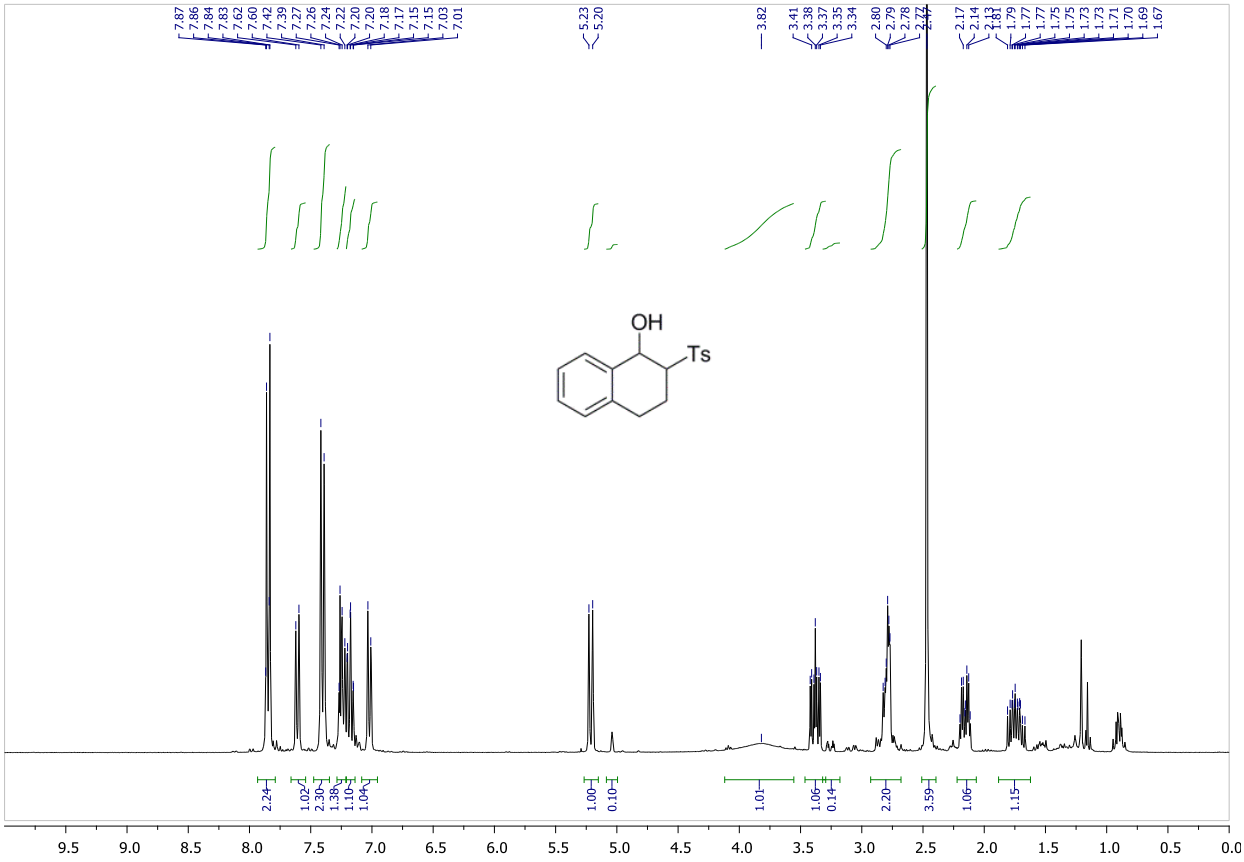

^{13}C-NMR: **4g**

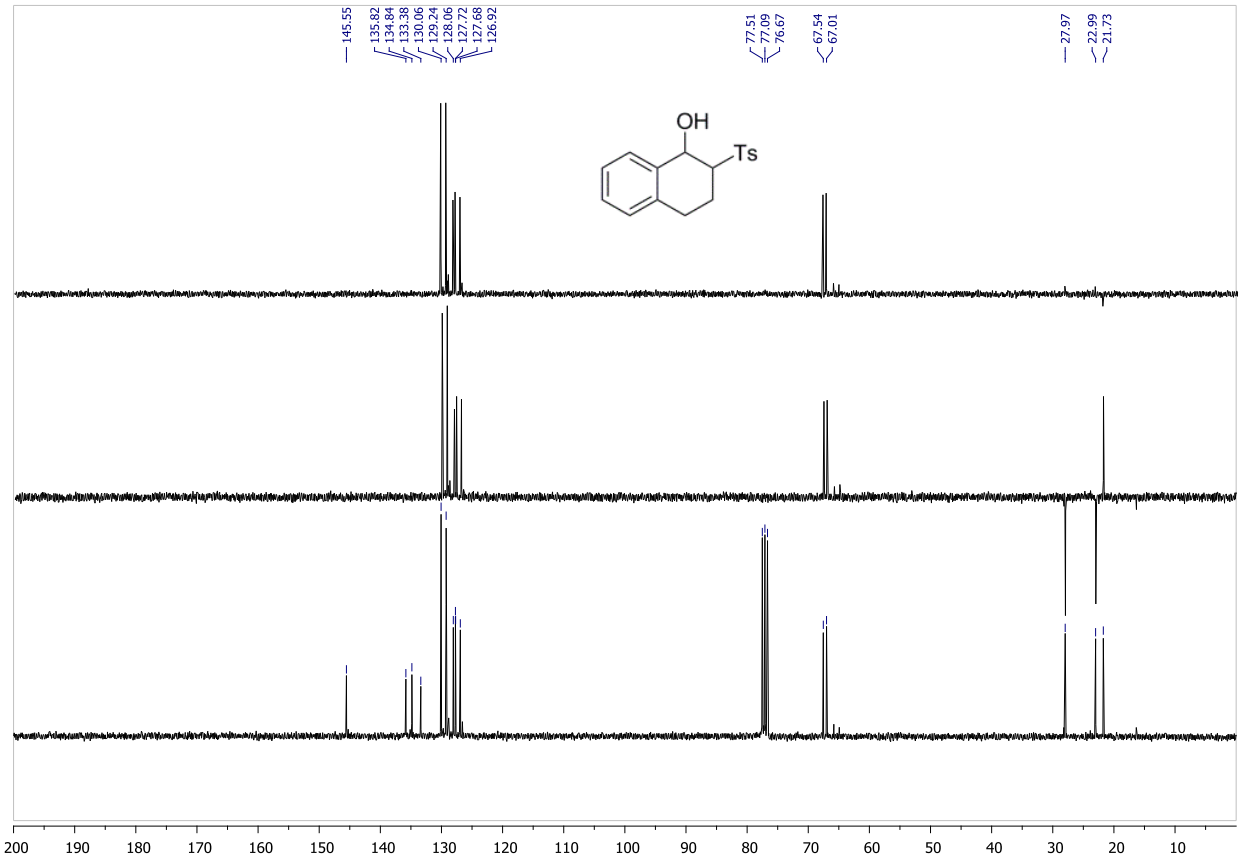

^{1}H-NMR: **4h**

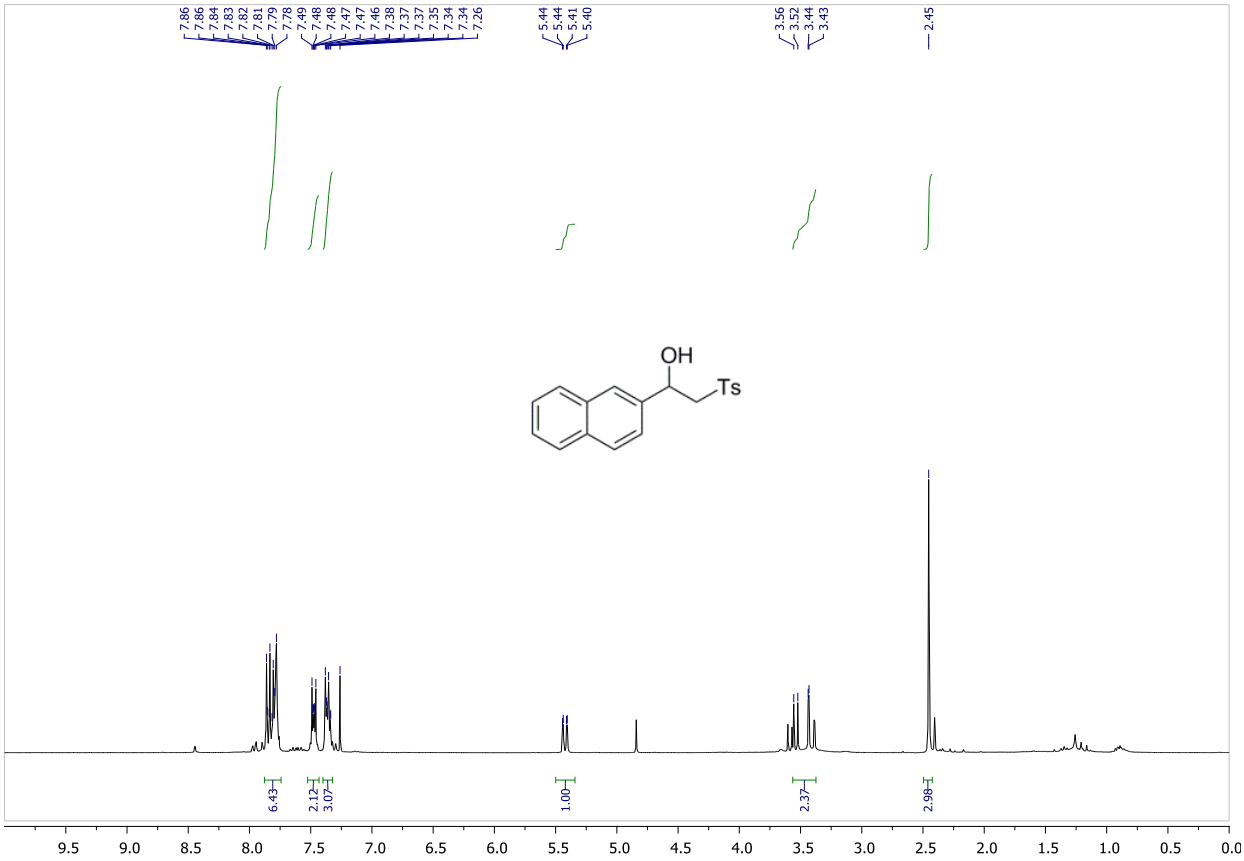

^{13}C-NMR: **4h**

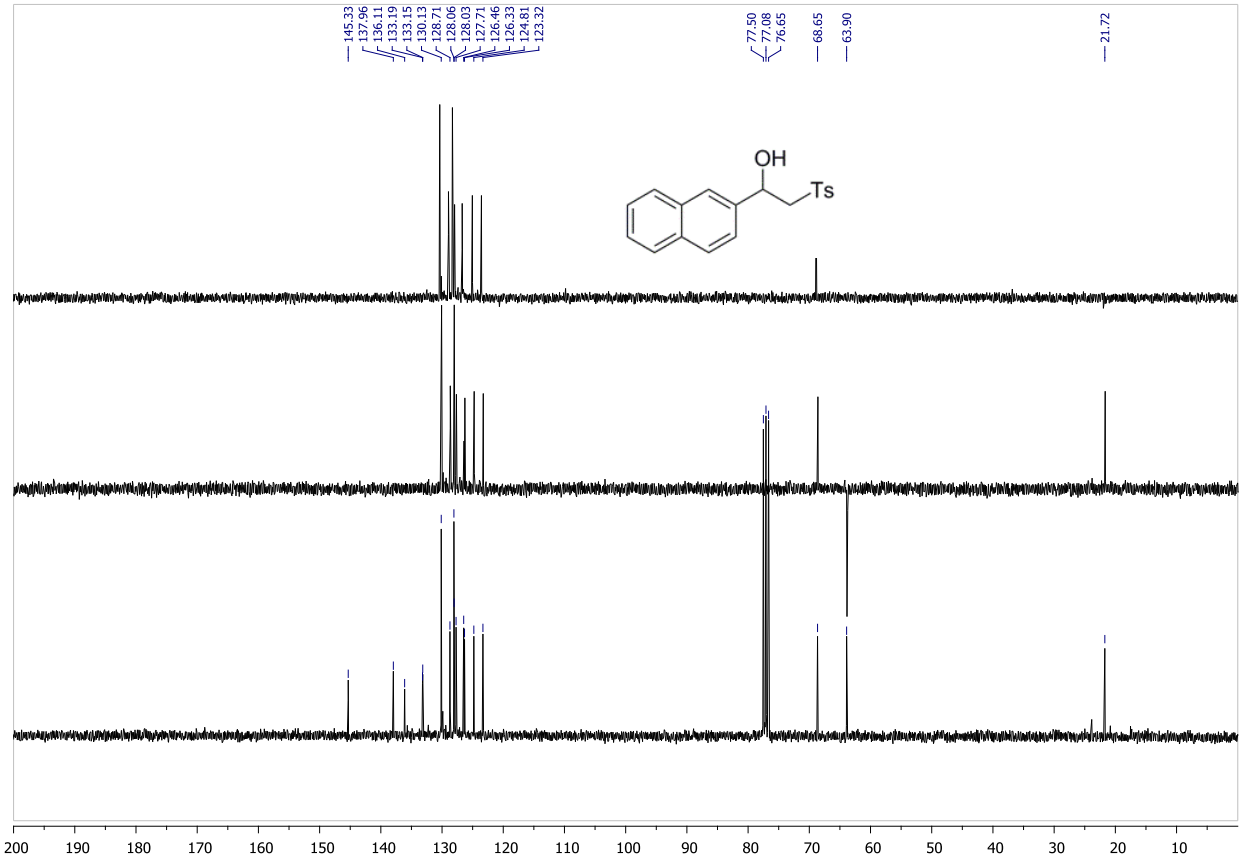

^{1}H-NMR: **6a**

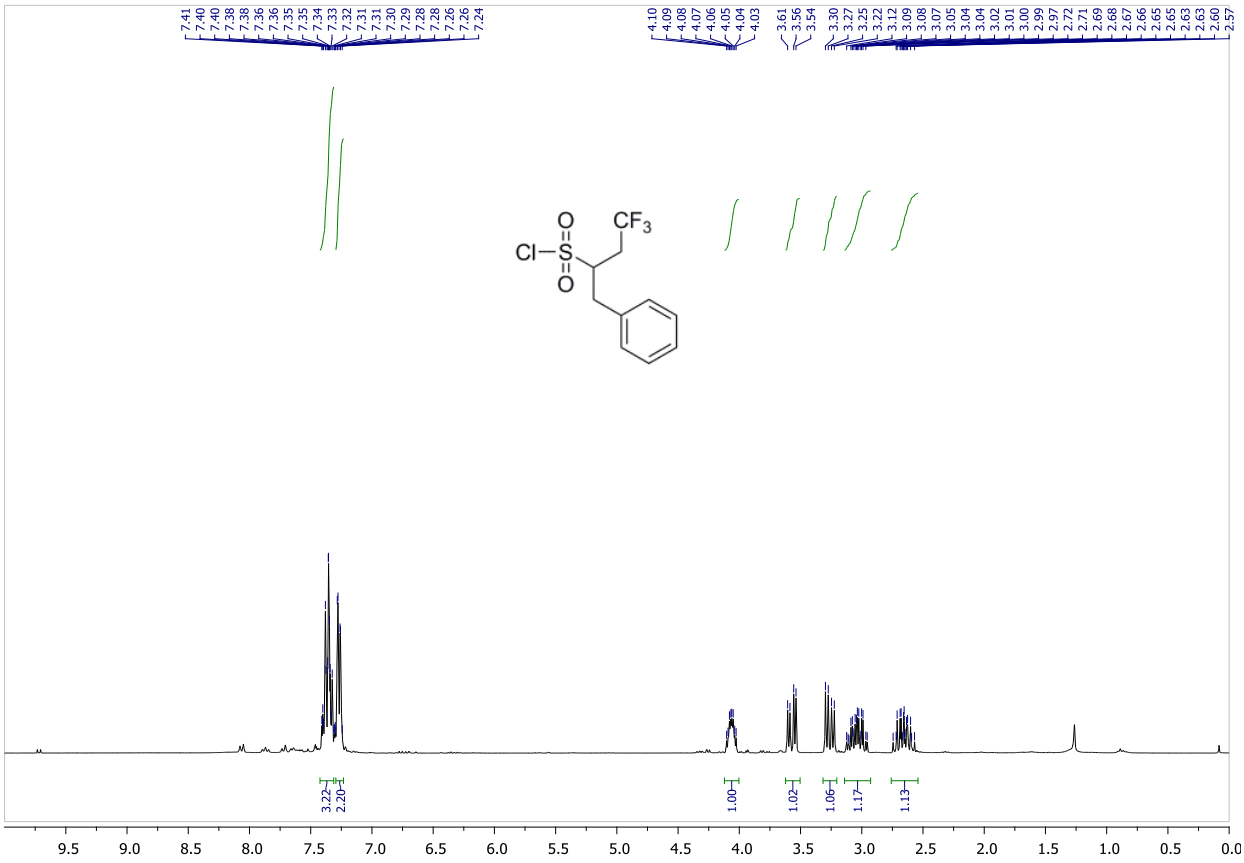

^{13}C-NMR: **6a**

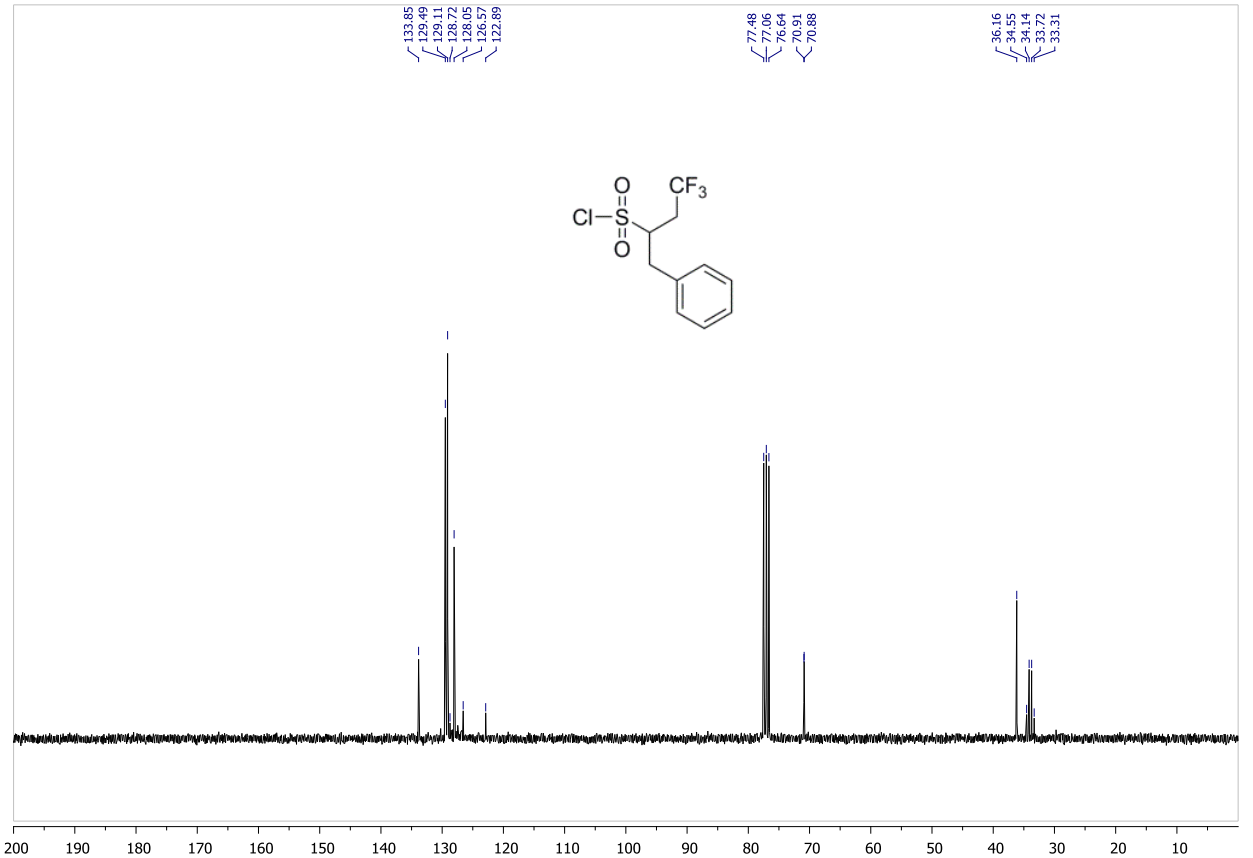

^{19}F-NMR: **6a**

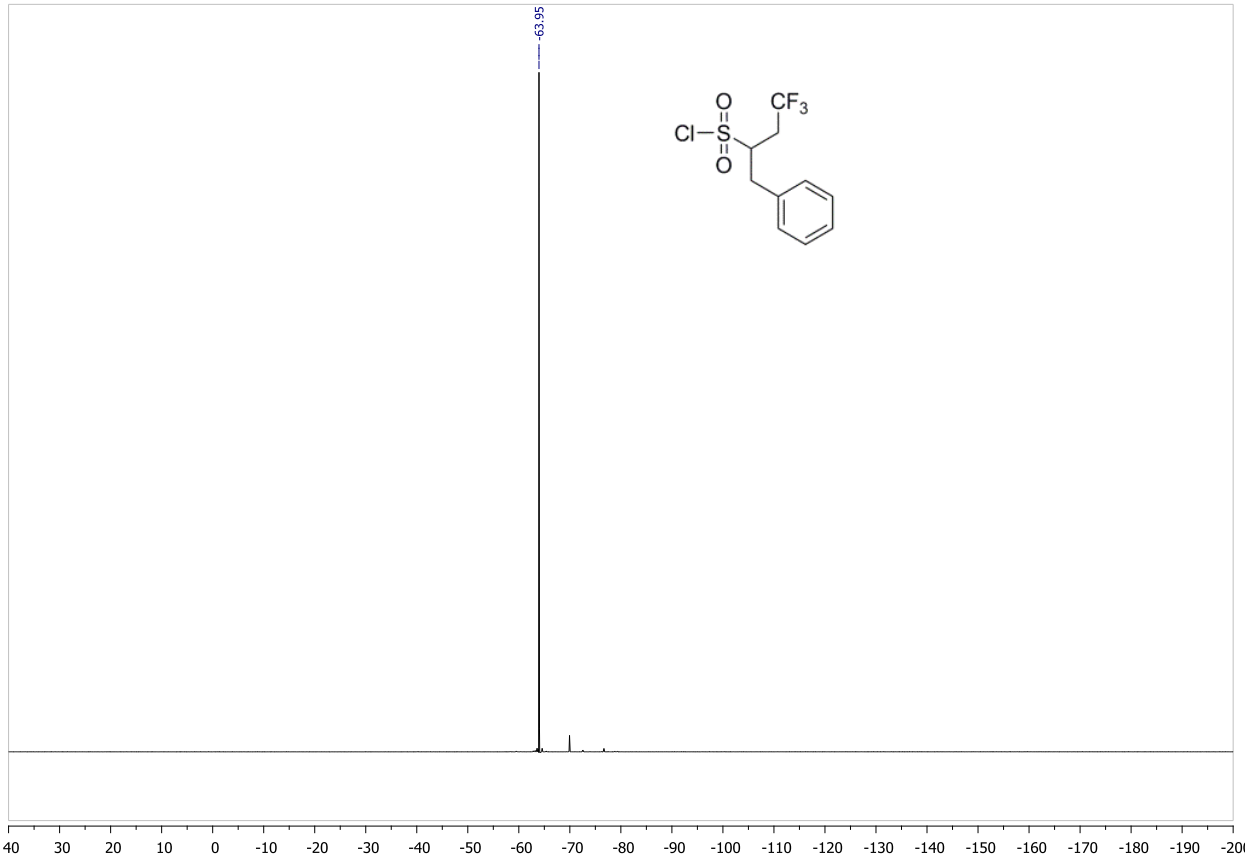
-63.95
O
CF3
Cl—S
O
40 30 20 10 0 -10 -20 -30 -40 -50 -60 -70 -80 -90 -100 -110 -120 -130 -140 -150 -160 -170 -180 -190

^{1}H-NMR: **6b**

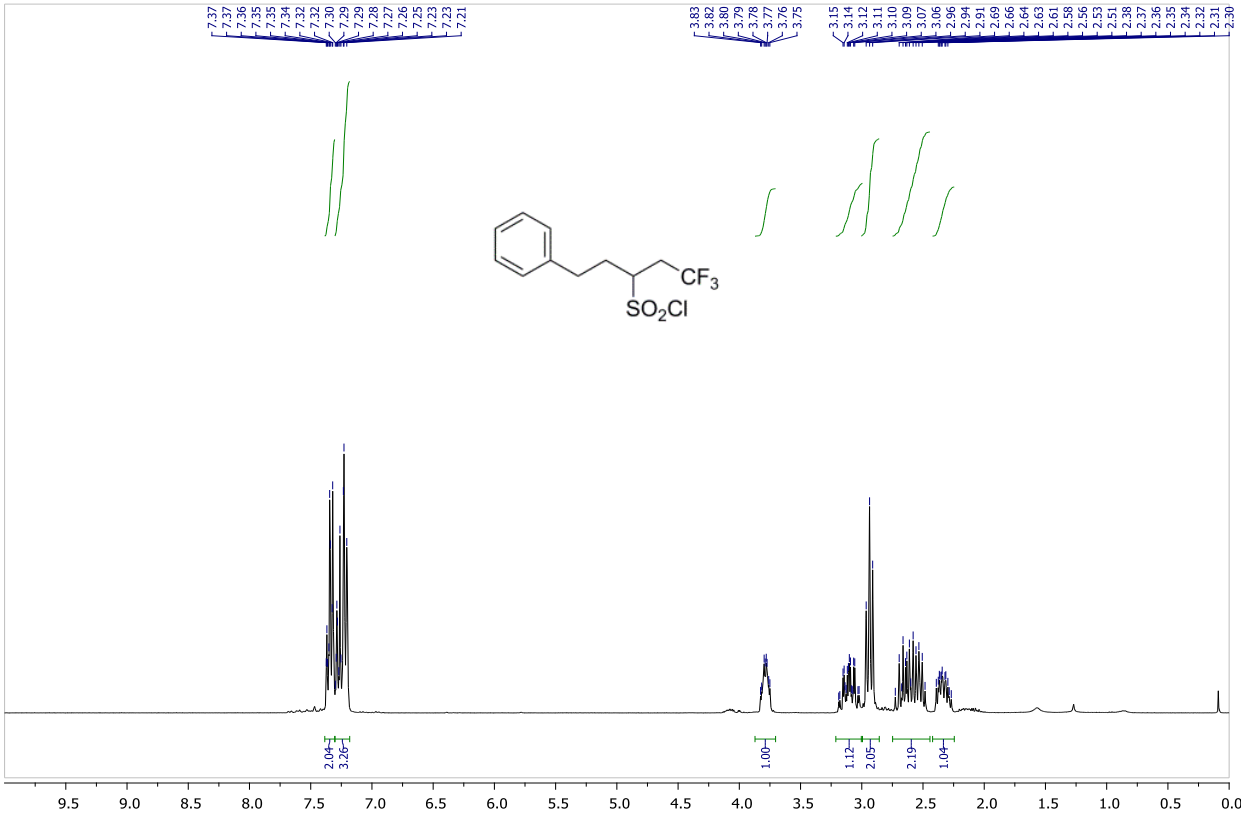

^{13}C-NMR: **6b**

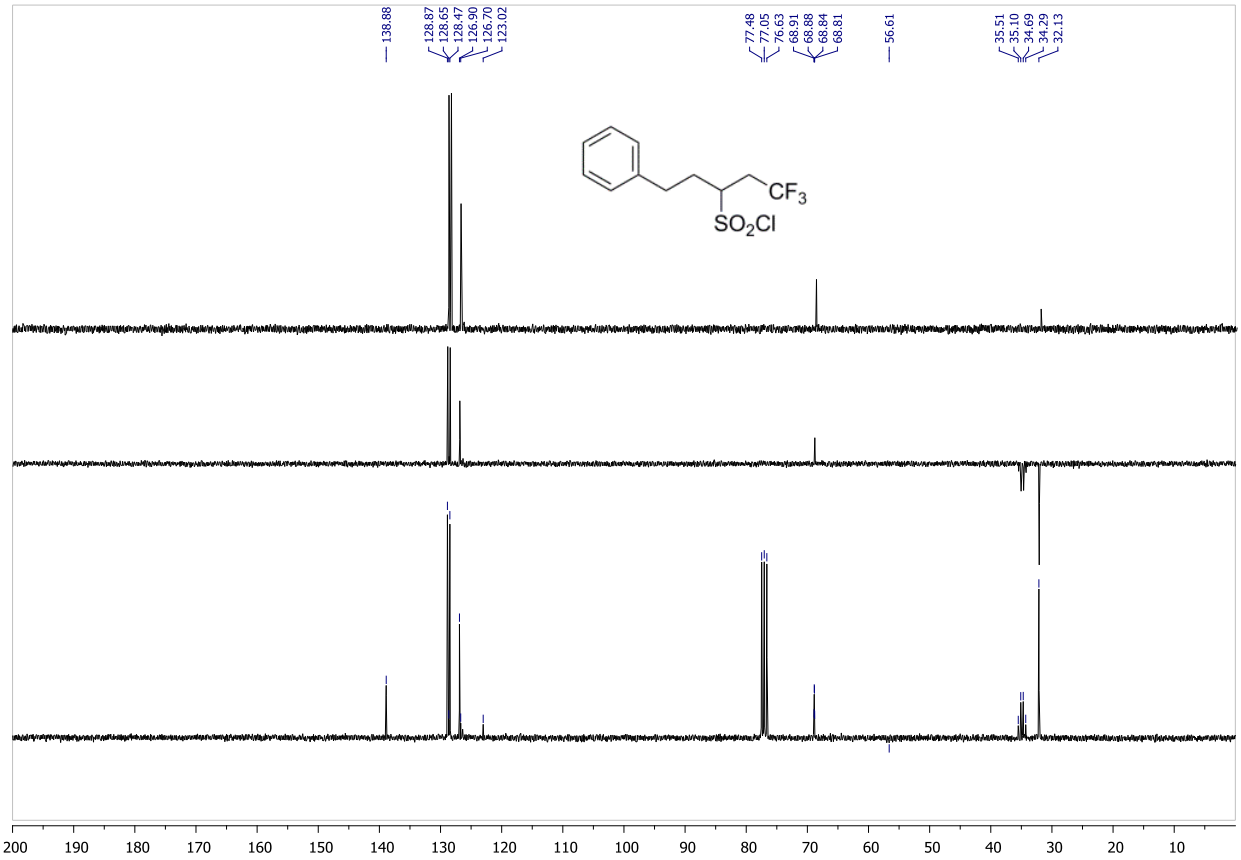

^{19}F-NMR: **6b**

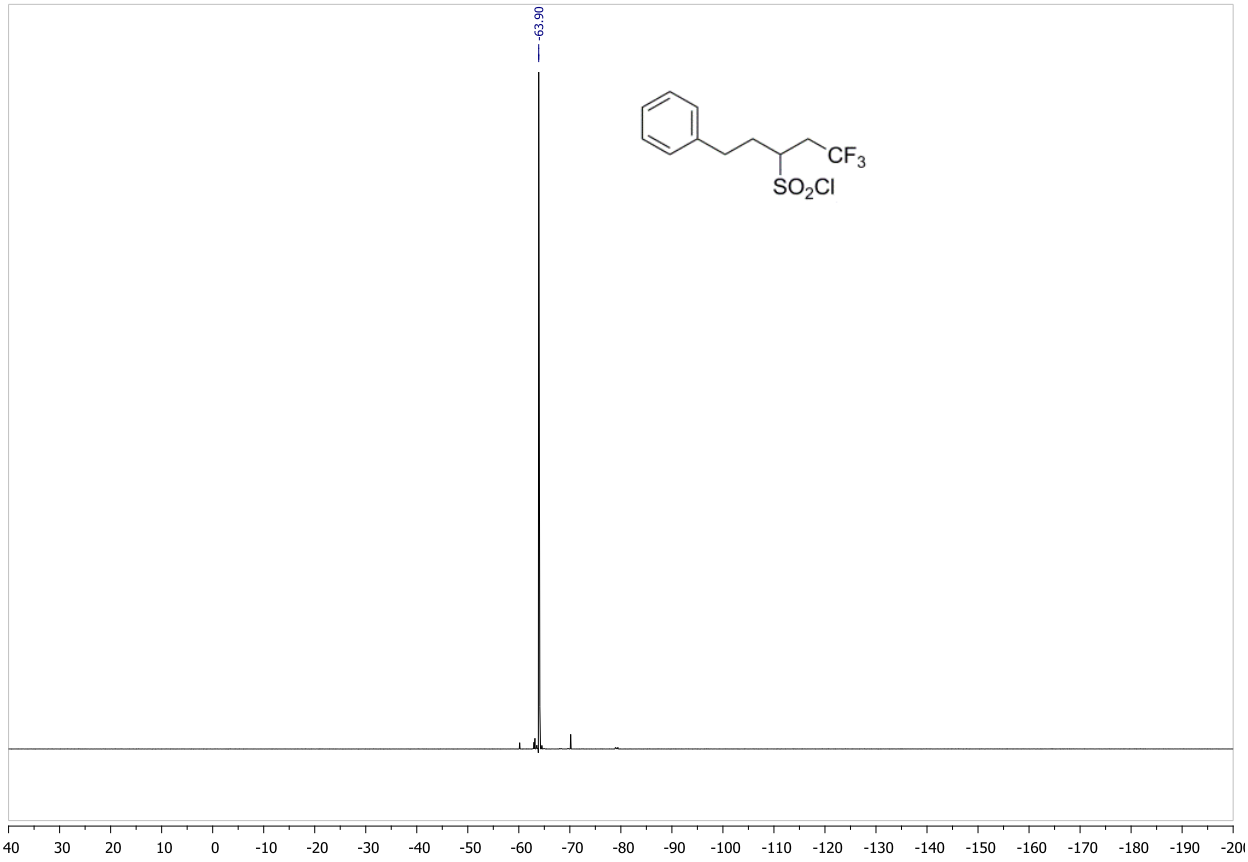
-63.90
CF3
SO2Cl
40 30 20 10 0 -10 -20 -30 -40 -50 -60 -70 -80 -90 -100 -110 -120 -130 -140 -150 -160 -170 -180 -190

^{1}H-NMR: **6c**

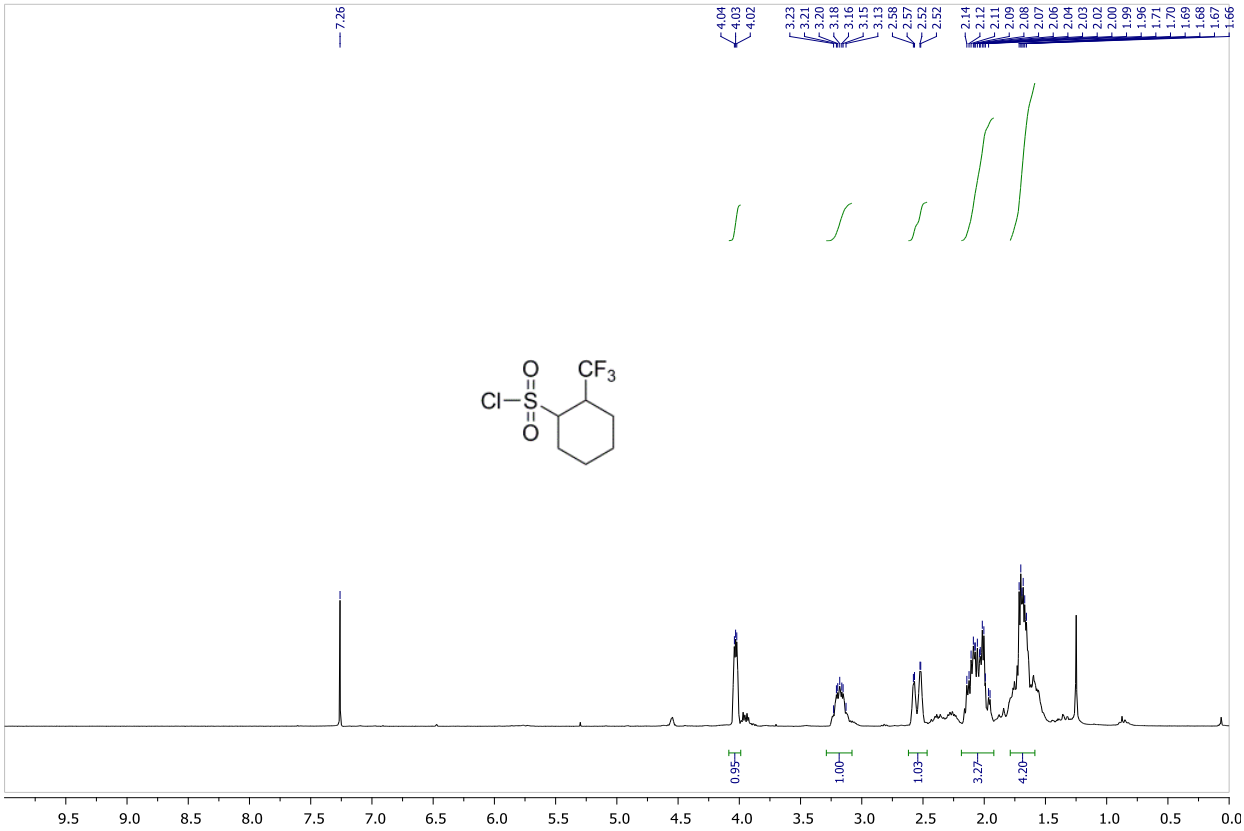

^{13}C-NMR: **6c**

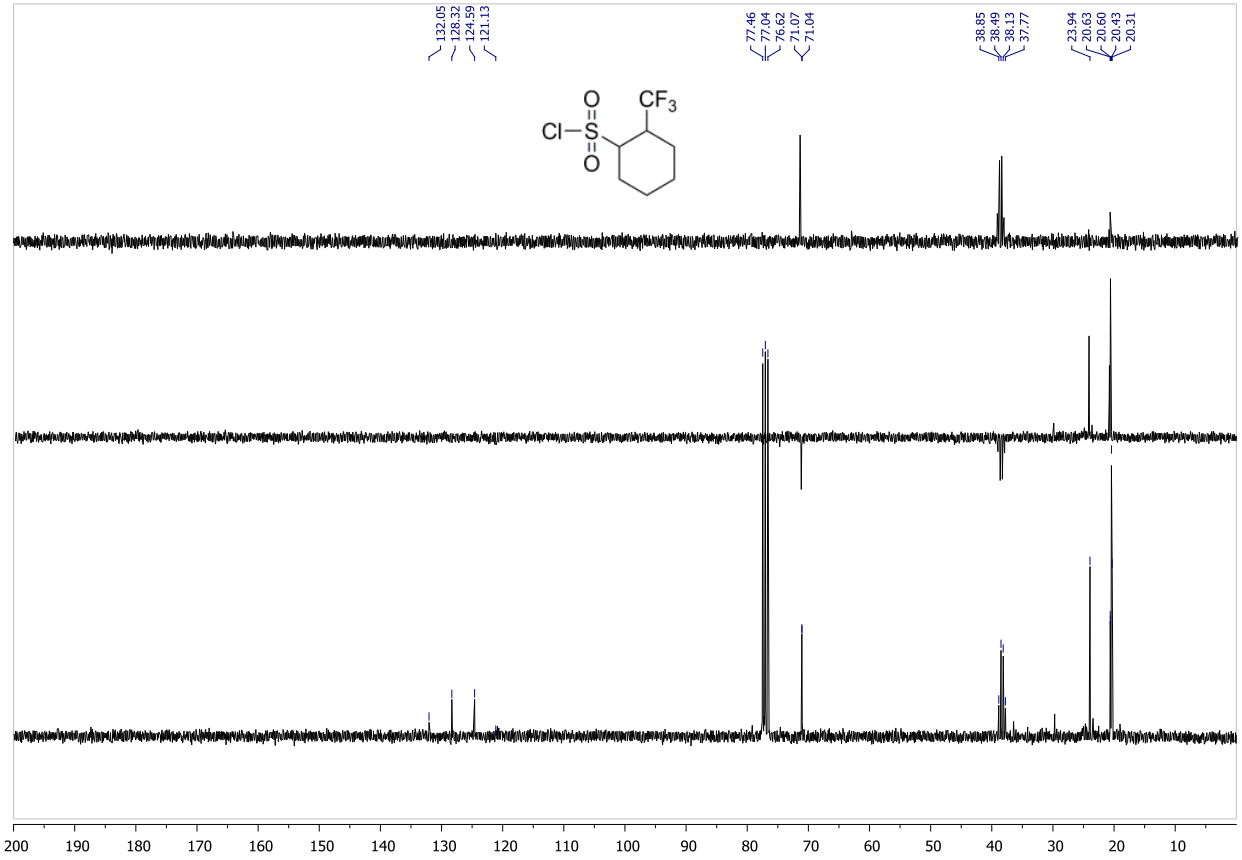

^{19}F-NMR: **6c**

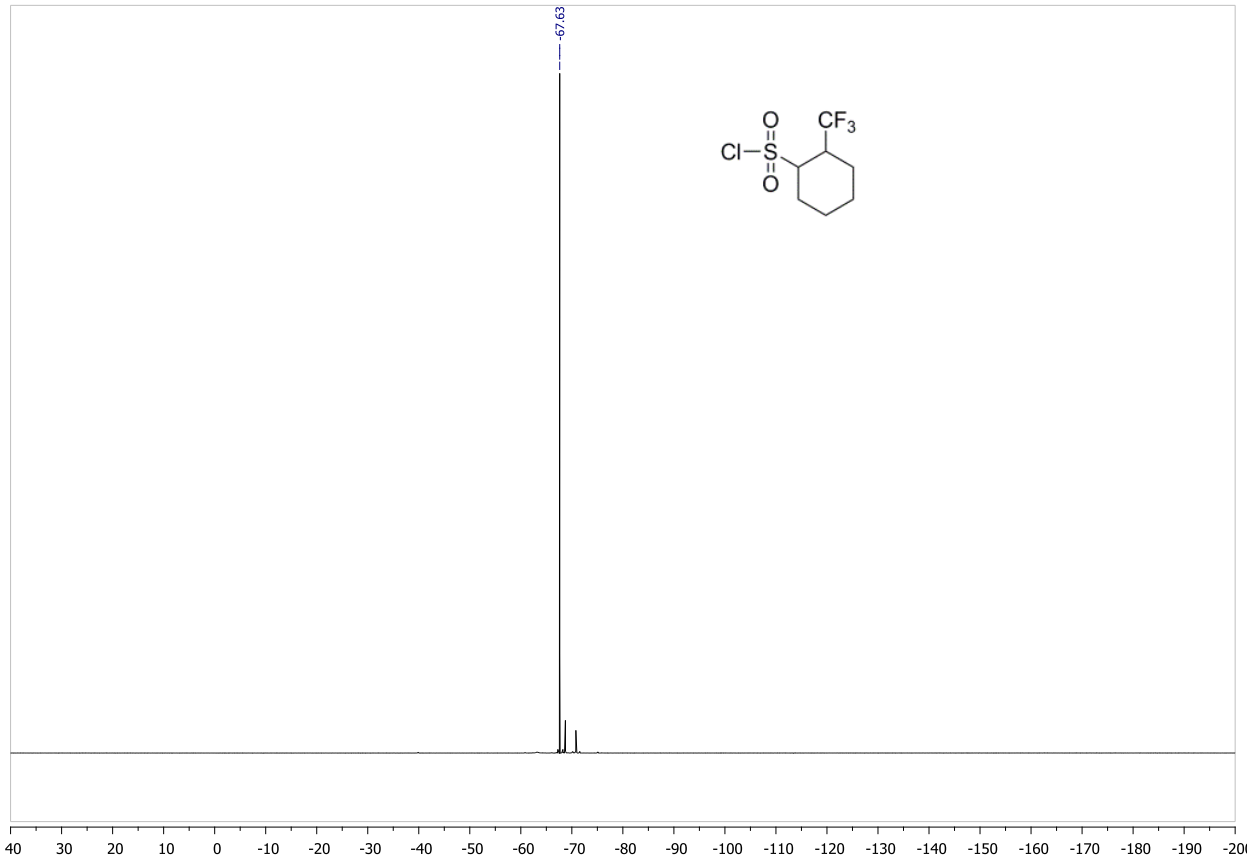
-67.63
O
CF3
Cl—S
O
40 30 20 10 0 -10 -20 -30 -40 -50 -60 -70 -80 -90 -100 -110 -120 -130 -140 -150 -160 -170 -180 -190

^{1}H-NMR: **6d**

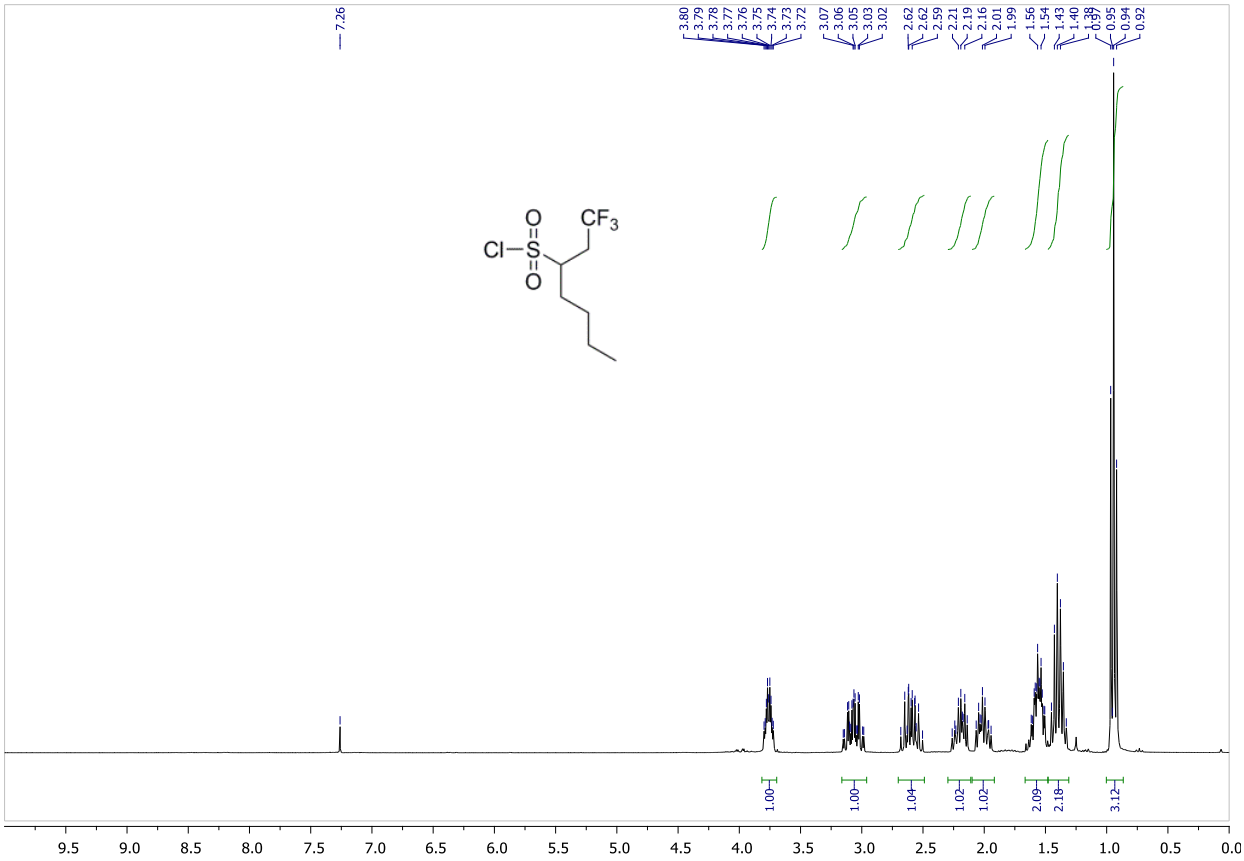

^{13}C-NMR: **6d**

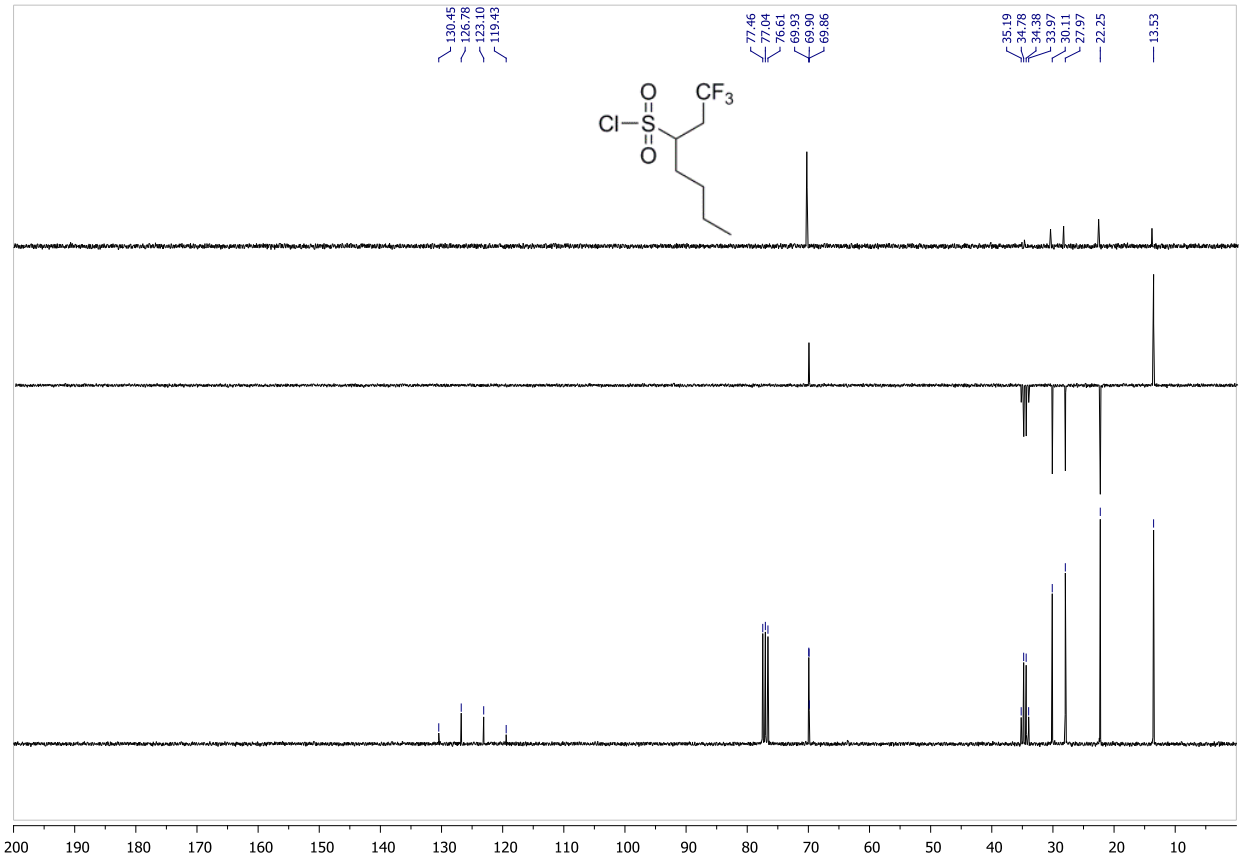

^{19}F-NMR: **6d**

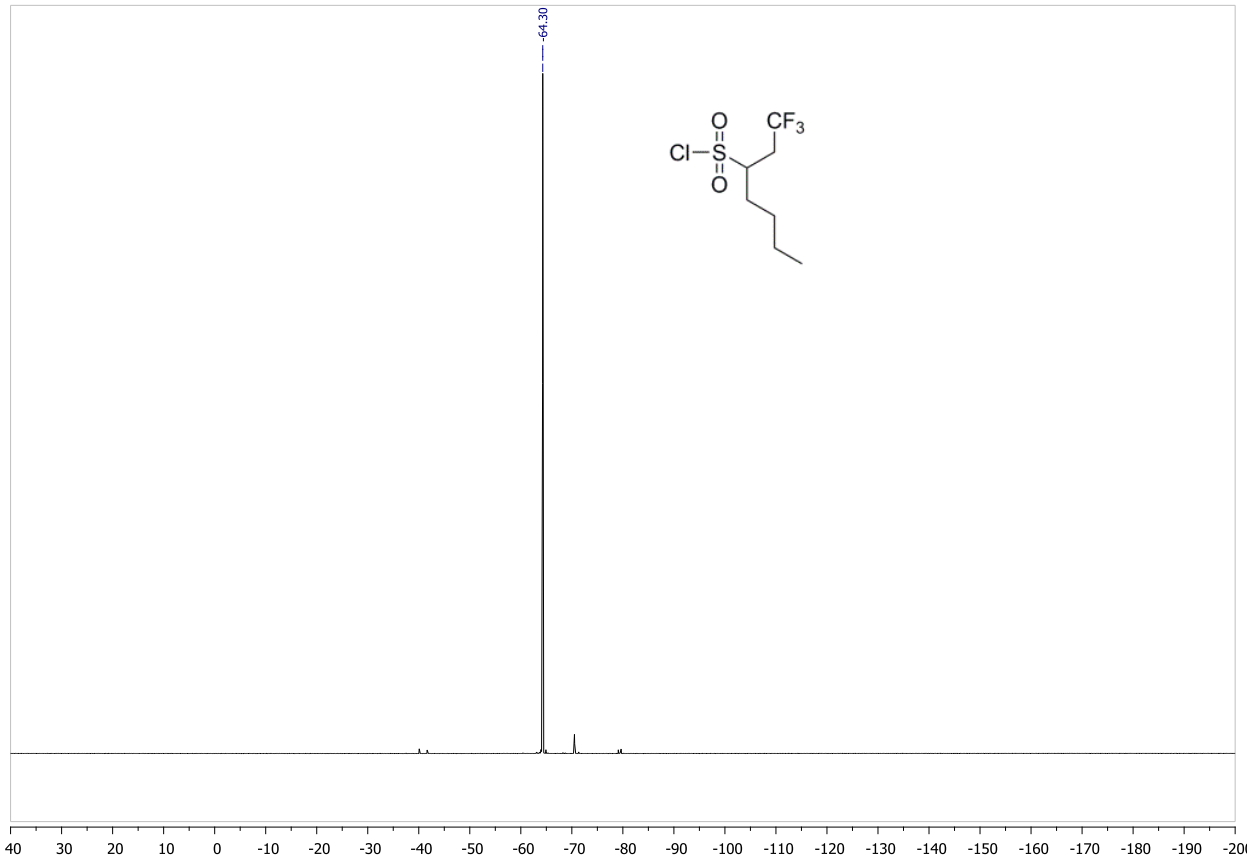
-64.30
O
CF3
Cl
S
O
40 30 20 10 0 -10 -20 -30 -40 -50 -60 -70 -80 -90 -100 -110 -120 -130 -140 -150 -160 -170 -180 -190

^{1}H-NMR: **7a**

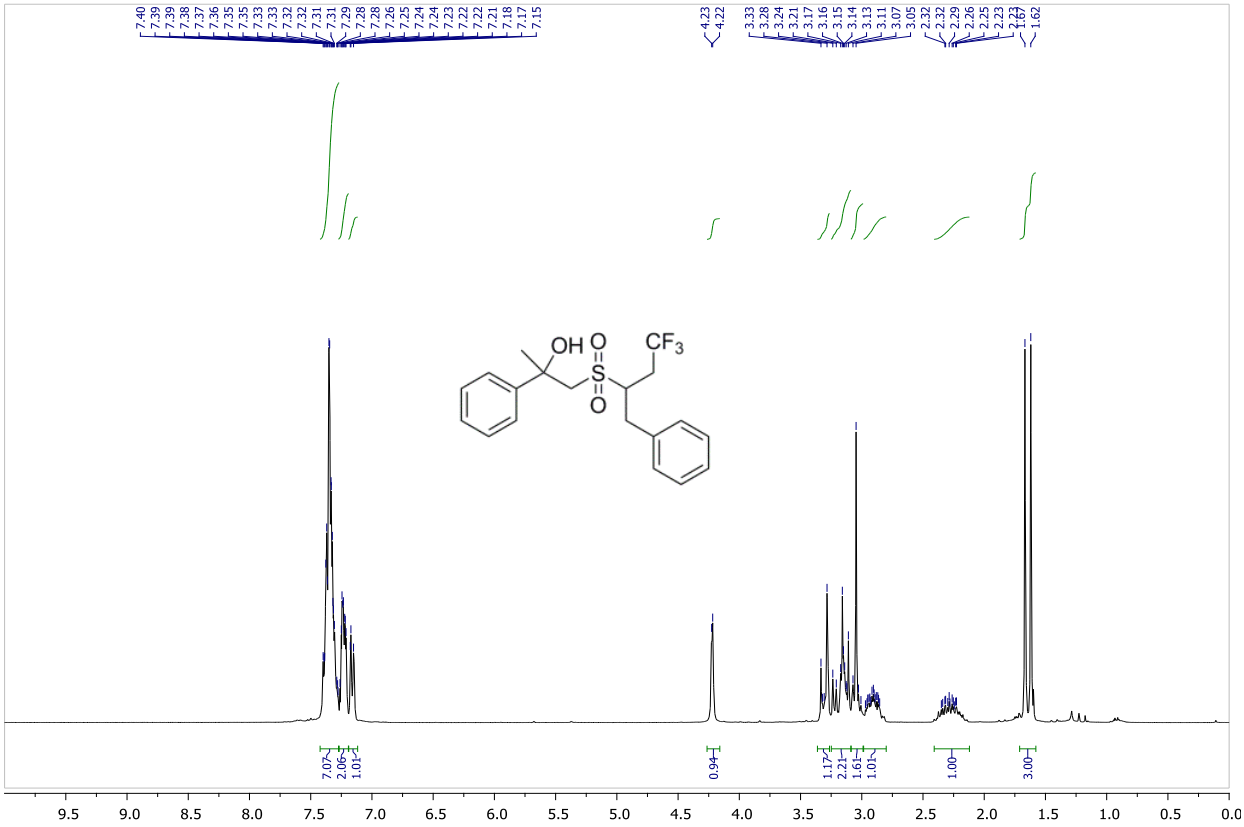

^{13}C-NMR: **7a**

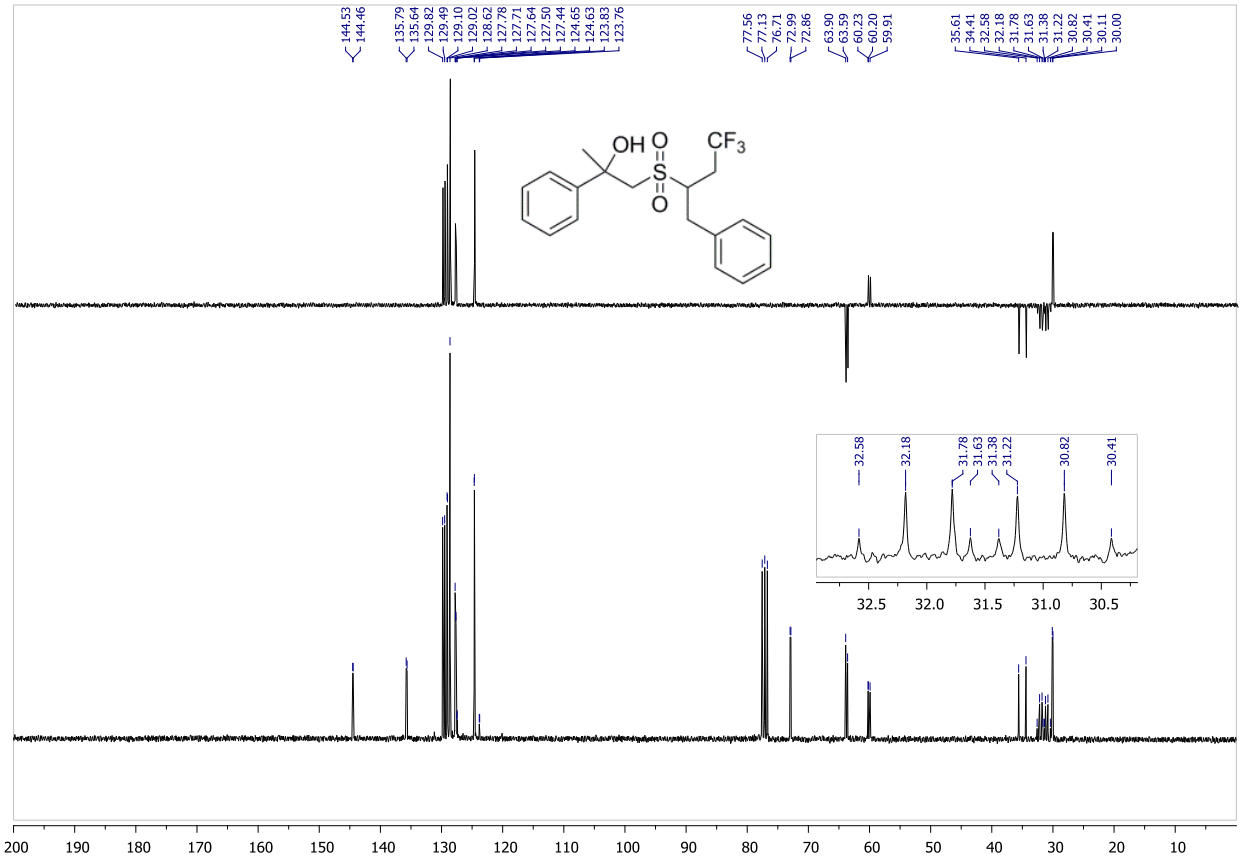

^{19}F-NMR: **7a**

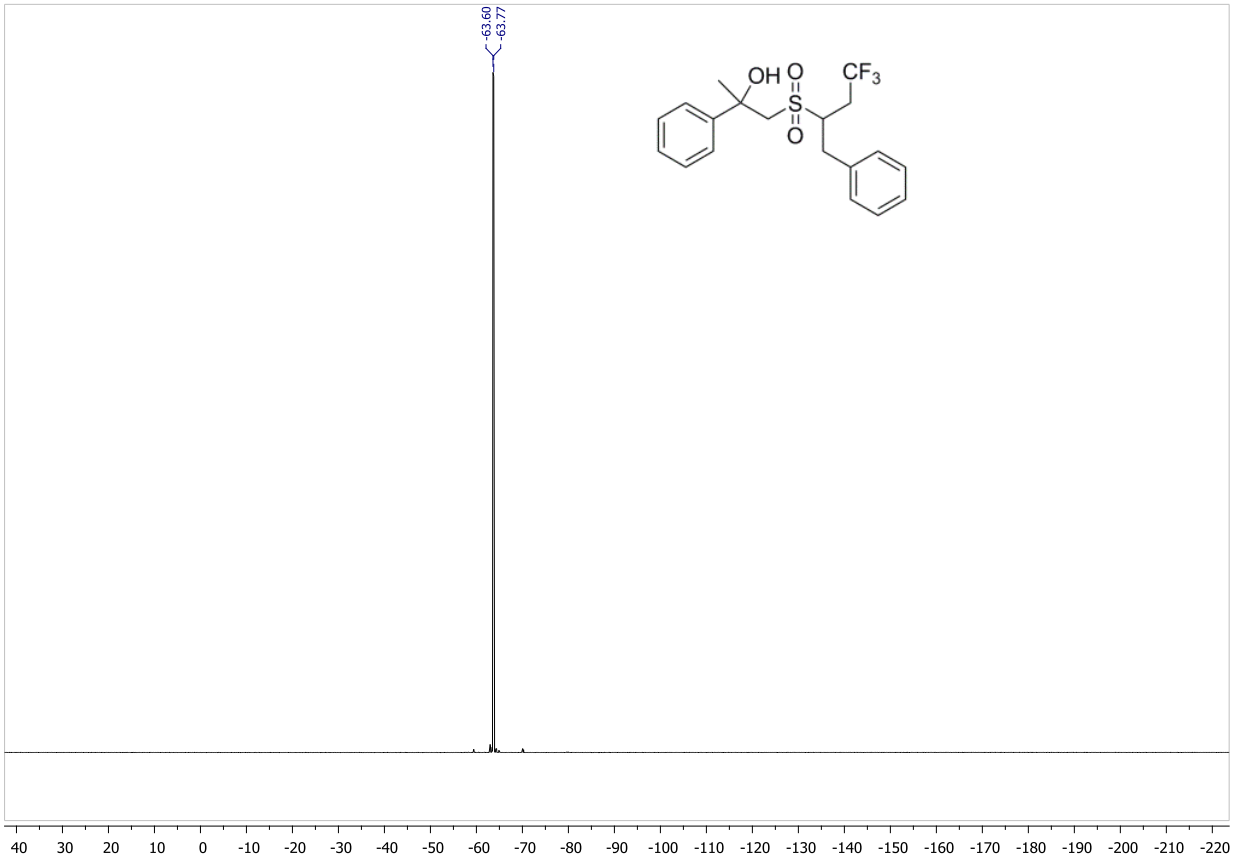
-63.60
-63.77
OH
O
S
O
CF3
40 30 20 10 0 -10 -20 -30 -40 -50 -60 -70 -80 -90 -100 -110 -120 -130 -140 -150 -160 -170 -180 -190 -200 -210 -220

^{1}H-NMR: **7b**

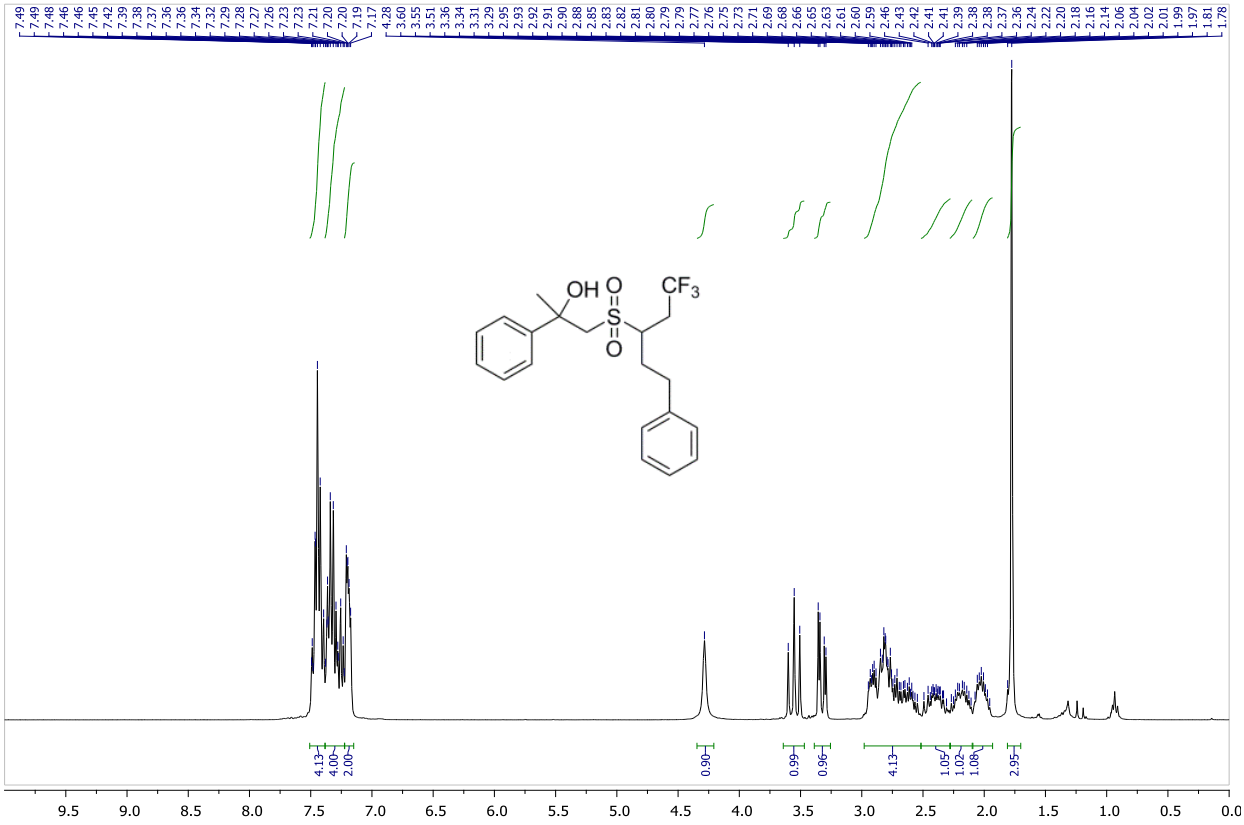

^{13}C-NMR: **7b**

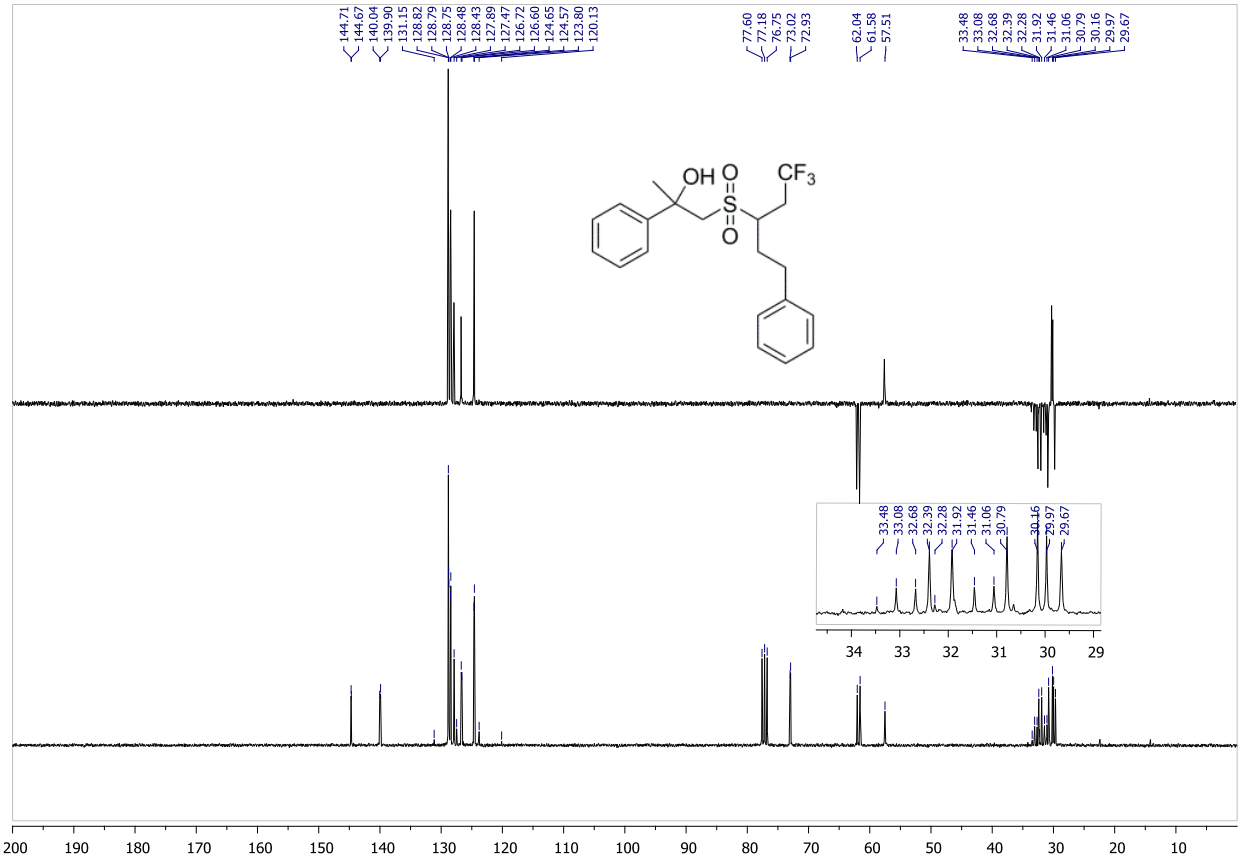

^{19}F-NMR: **7b**

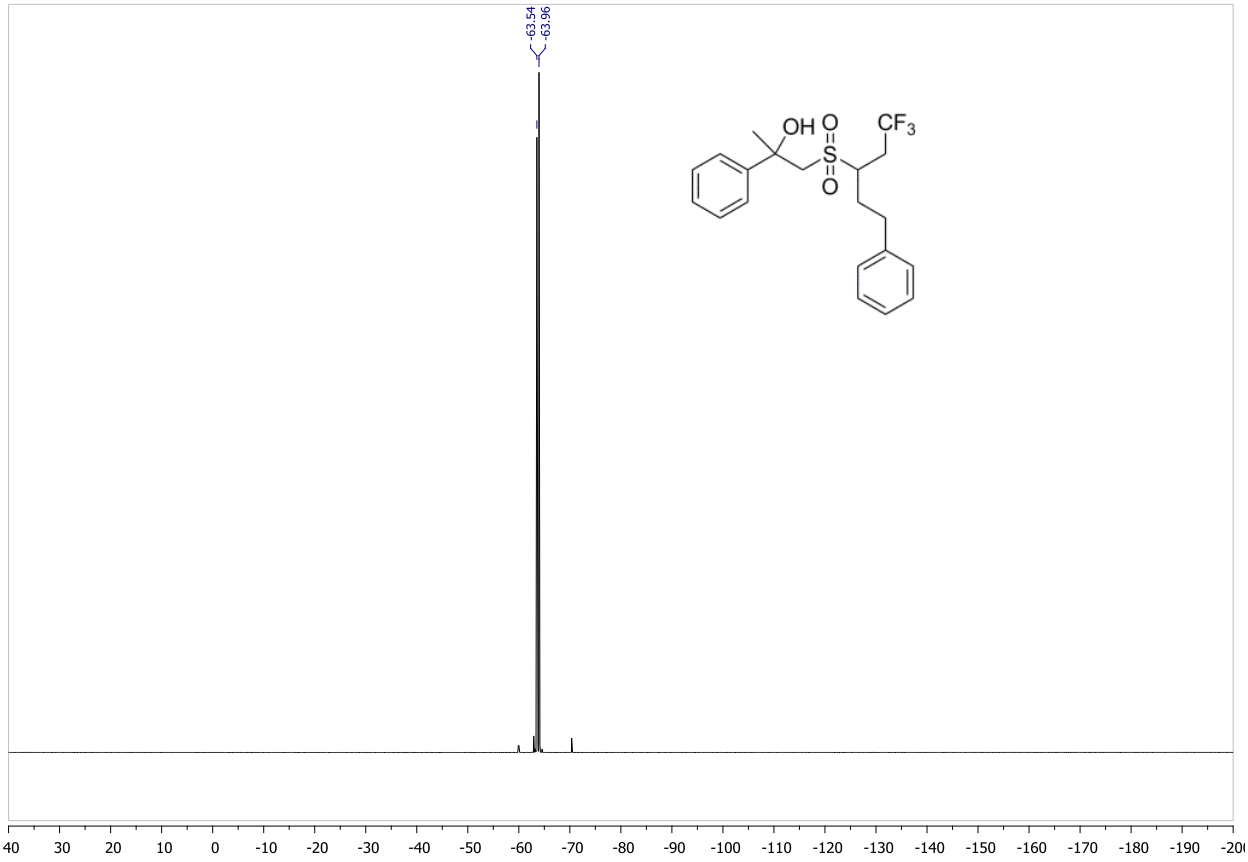
63.54
63.96
OH
O
S
O
CF3
40
30
20
10
0
-10
-20
-30
-40
-50
-60
-70
-80
-90
-100
-110
-120
-130
-140
-150
-160
-170
-180
-190

^{1}H-NMR: **7c**

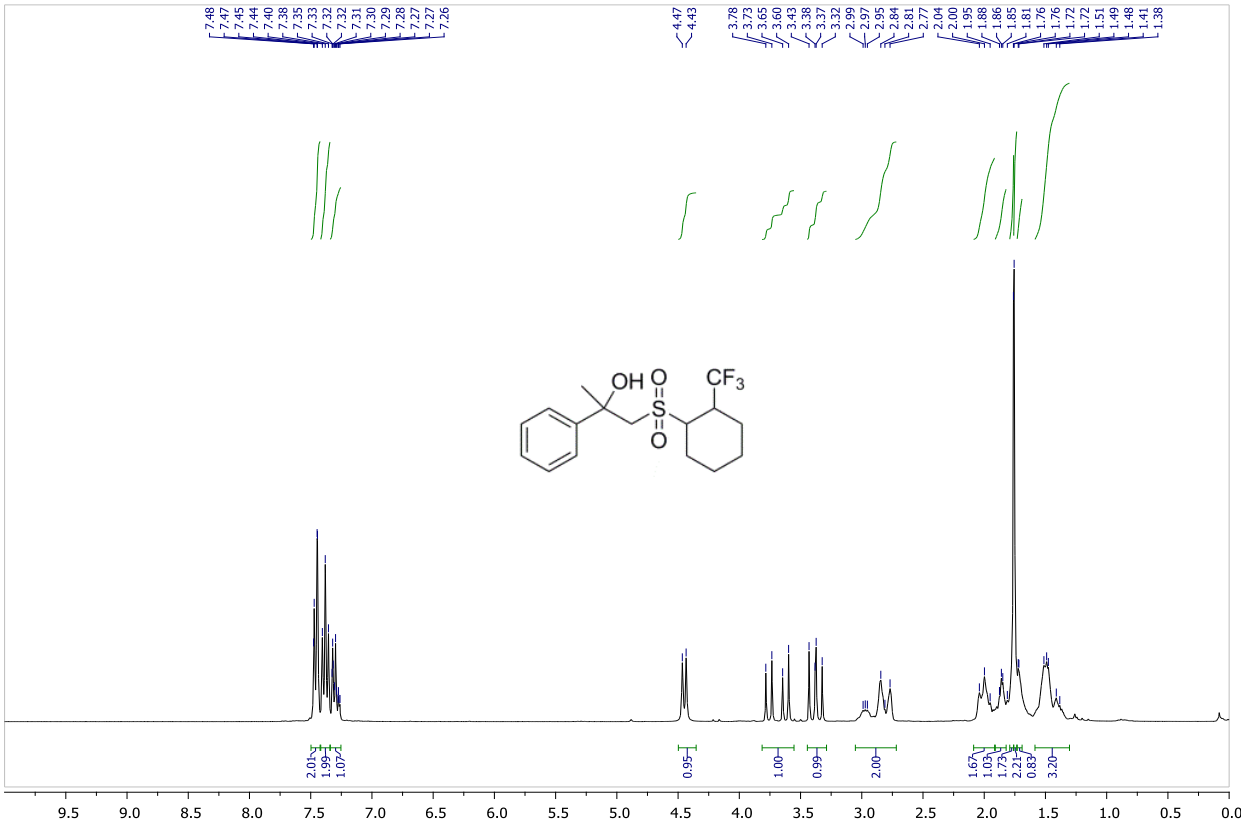

^{13}C-NMR: **7c**

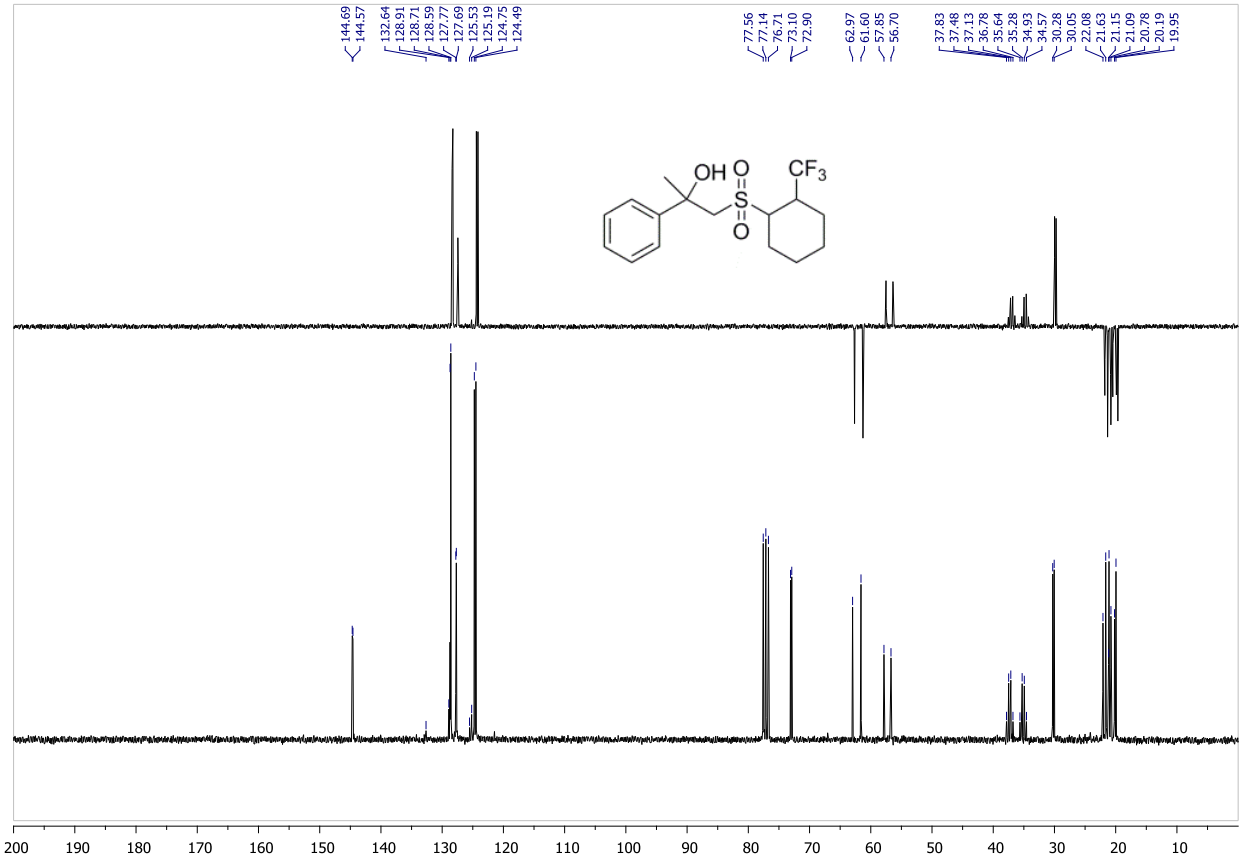

^{19}F-NMR: **7c**

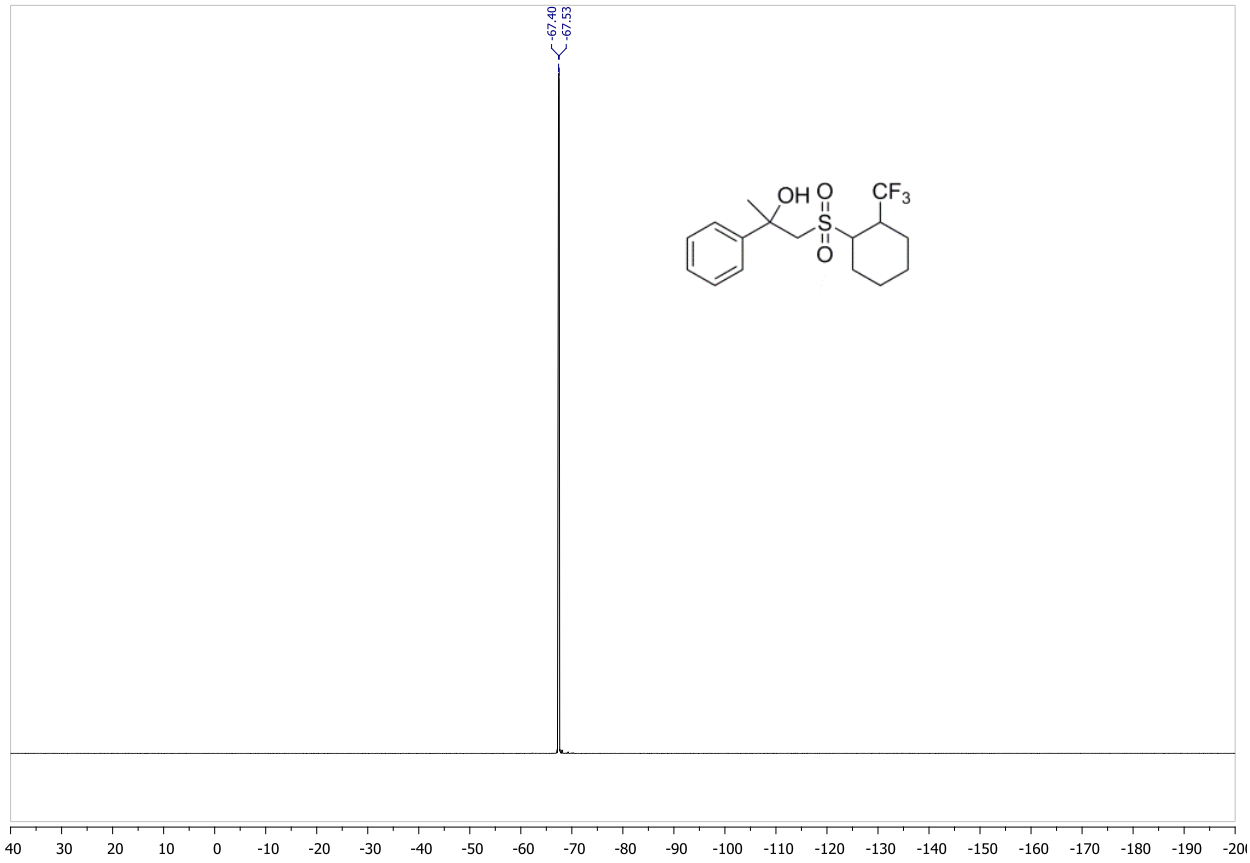
-67.40
-67.53
OH
O
S
O
CF3
40 30 20 10 0 -10 -20 -30 -40 -50 -60 -70 -80 -90 -100 -110 -120 -130 -140 -150 -160 -170 -180 -190

^{1}H-NMR: **7d**

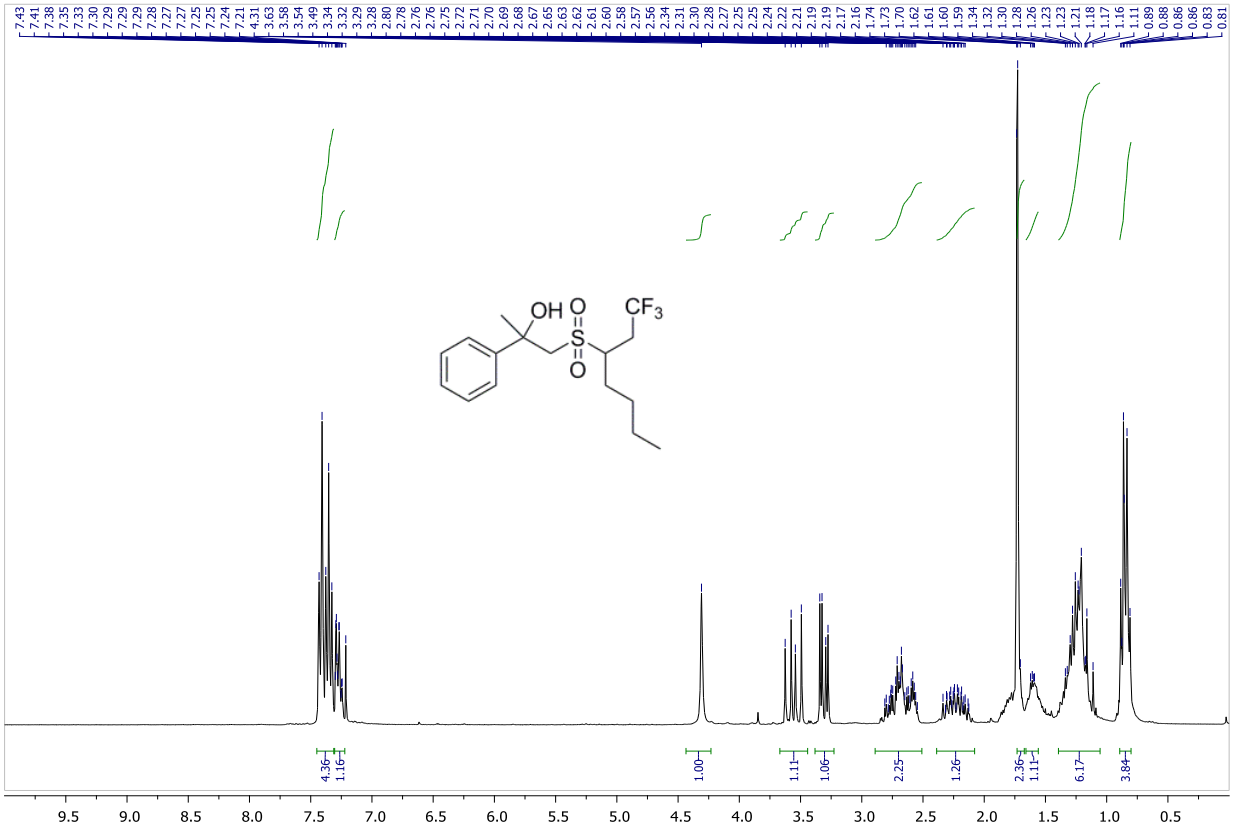

^{13}C-NMR: **7d**

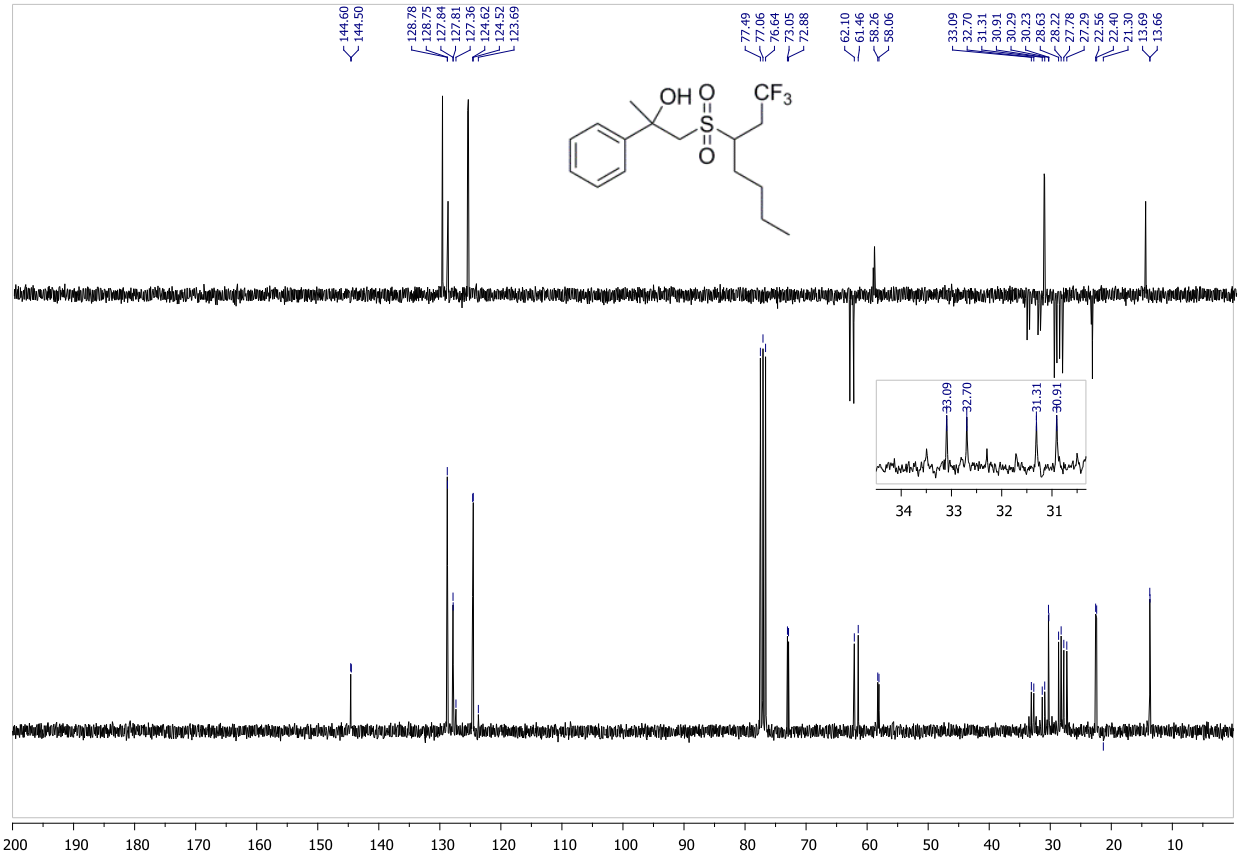

^{19}F-NMR: **7d**

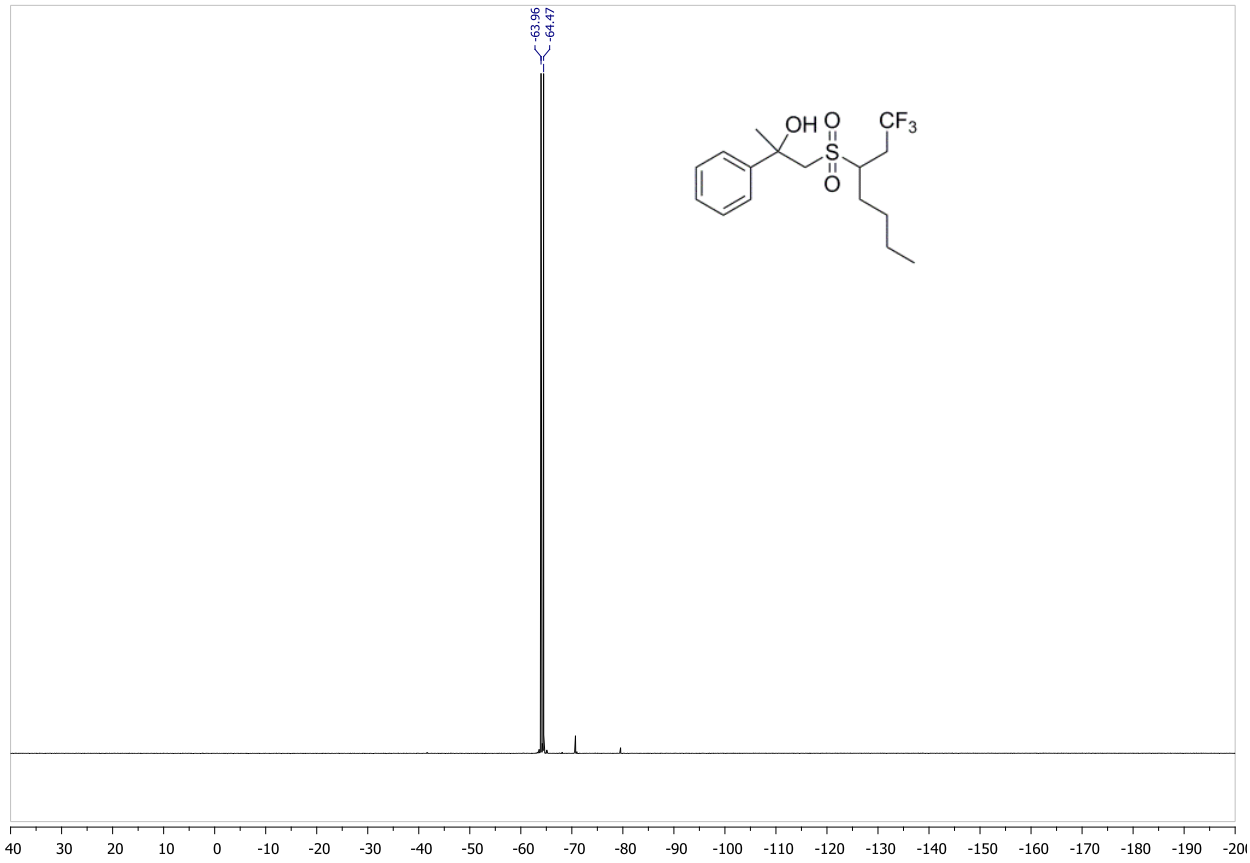
-63.96
-64.47
OH
O
S
O
CF3
40 30 20 10 0 -10 -20 -30 -40 -50 -60 -70 -80 -90 -100 -110 -120 -130 -140 -150 -160 -170 -180 -190

^{1}H-NMR: **8a**

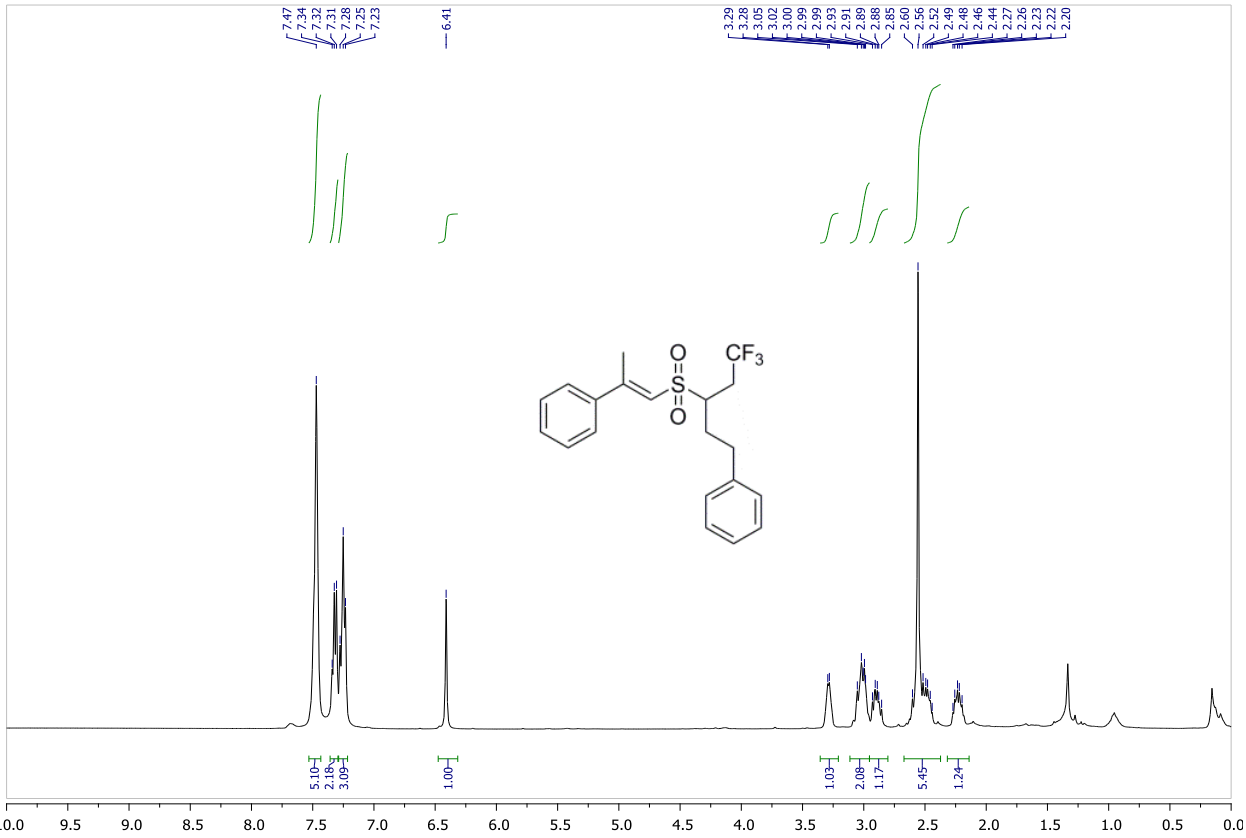

^{13}C-NMR: **8a**

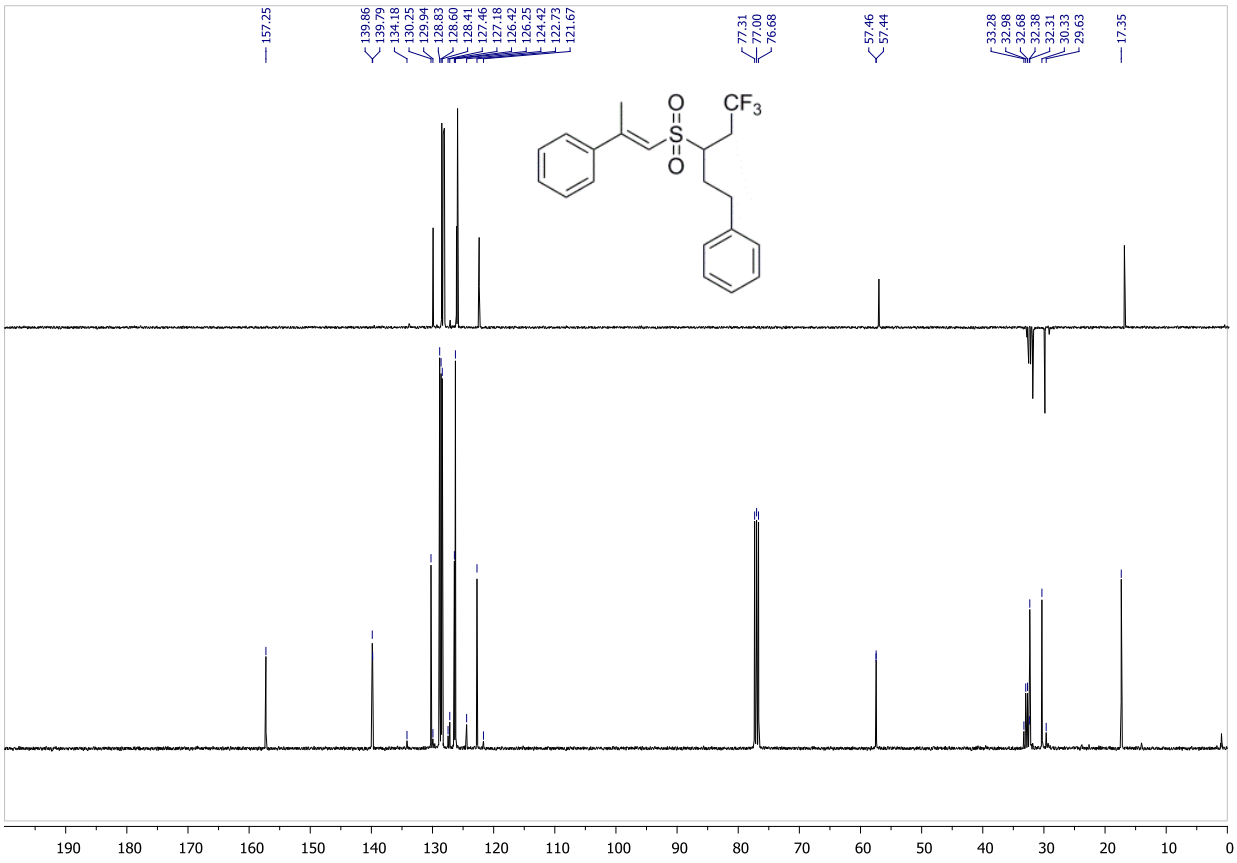

^{19}F-NMR: **8a**

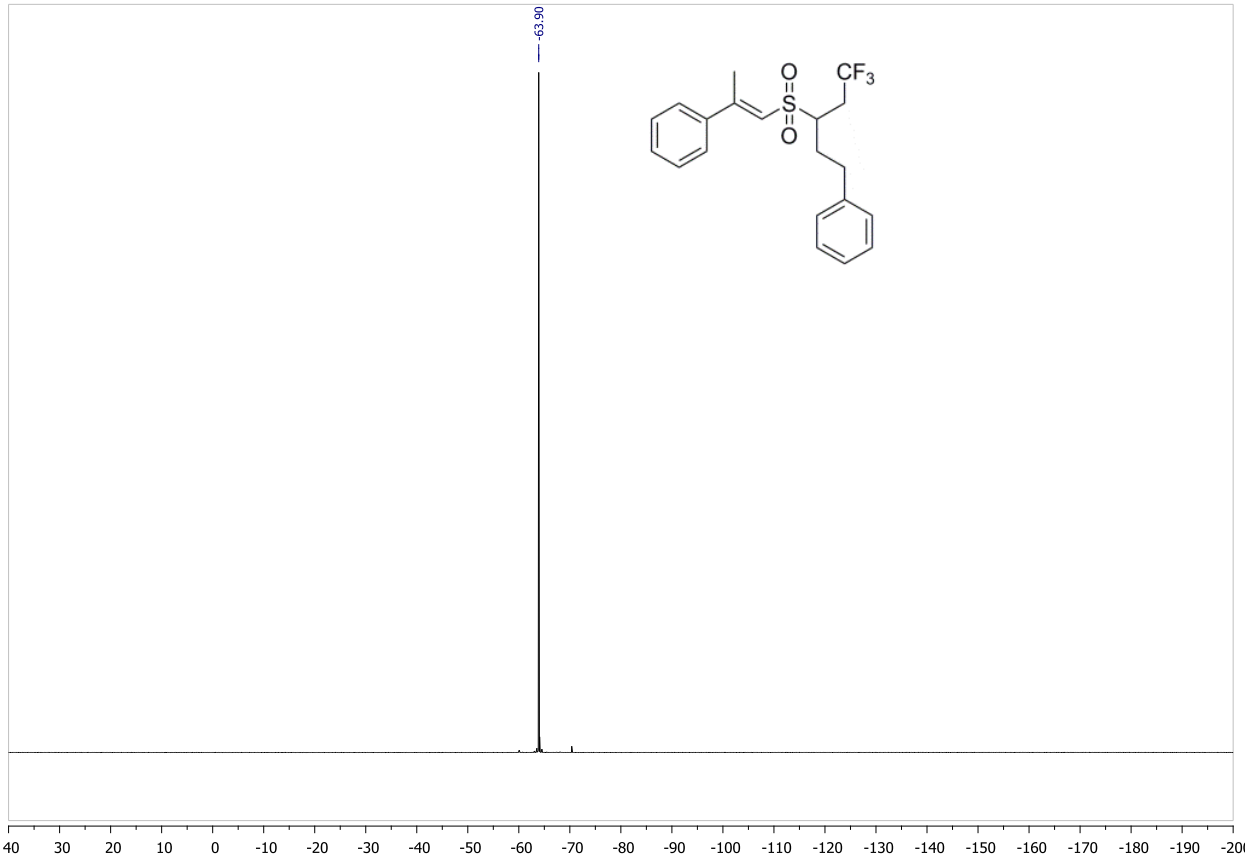

nOe: **8a**

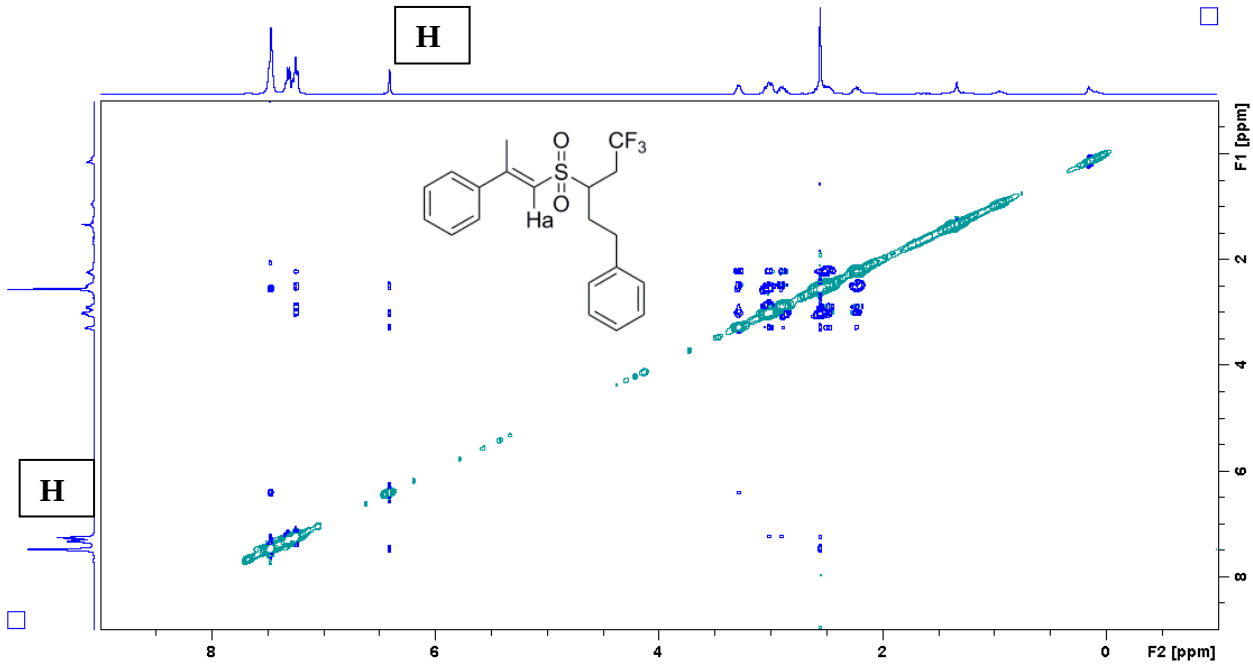

8.13 Crystal data: 3m

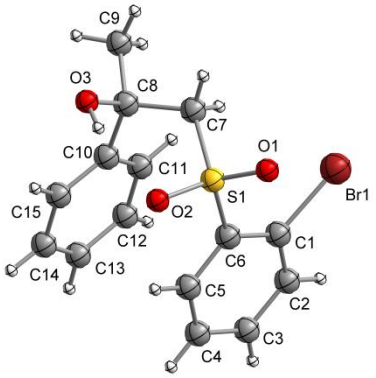

Figure 8.3: Crystal structure **of 3m**

Crystal Data: $C_{15}H_{15}BrO_3S$, M_r = 355.24, monoclinic, $P2_1$ (No. 4), a = 5.92604(15) Å, b = 12.2676(3) Å, c = 9.9444(2) Å, β = 103.755(2)°, α = γ = 90°, V = 702.21(3) Å^3, T = 123.0(2) K, Z = 2, Z' = 1, μ(CuK_α) = 5.423, 5956 reflections measured, 2628 unique (R_{int} = 0.0348) which were used in all calculations. The final wR_2 was 0.1082 (all data) and R_1 was 0.0419 (I > 2(I)).

Compound	**3m**
Formula	$C_{15}H_{15}BrO_3S$
$D_{calc.}$/ g cm^{-3}	1.680
μ/mm^{-1}	5.423
Formula Weight	355.24
Color	clear colorless
Shape	prism
Max Size/mm	0.21
Mid Size/mm	0.18
Min Size/mm	0.10
T/K	123.0(2)
Crystal System	monoclinic
Flack Parameter	0.06(4)
Hooft Parameter	0.076(12)
Space Group	$P2_1$
a/Å	5.92604(15)
b/Å	12.2676(3)
c/Å	9.9444(2)
α/°	90
β/°	103.755(2)
γ/°	90
V/Å^3	702.21(3)
Z	2
Z'	1
Θ_{min}/°	4.578
Θ_{max}/°	73.353
Measured Refl.	5956
Independent Refl.	2628
Reflections Used	2616
R_{int}	0.0348
Parameters	183
Restraints	1
Largest Peak	1.071
Deepest Hole	-0.978
GooF	1.032
wR_2 (all data)	0.1082
wR_2	0.1079
R_1 (all data)	0.0421
R_1	0.0419

Images of the Crystal on the Diffractometer

Table 8.6: Fractional Atomic Coordinates ($\times 10^4$) and Equivalent Isotropic Displacement Parameters ($Å^2 \times 10^3$) for **3m**. U_{eq} is defined as 1/3 of the trace of the orthogonalised U_{ij}.

Atom	x	y	z	U_{eq}
Br1	10142.8(9)	1539.7(6)	1408.2(6)	26.3(2)
S1	6240(3)	2321.5(13)	3254.6(16)	24.0(4)
O1	6148(10)	1165(4)	3079(6)	35.1(13)
O2	4354(9)	2844(5)	3721(5)	33.0(11)
C1	7852(10)	2631(5)	845(6)	22.5(12)
C3	6152(14)	3951(6)	-884(7)	32.2(16)
C2	7777(12)	3144(6)	-408(6)	25.8(13)
C10	8368(12)	4707(5)	4126(6)	24.1(13)
C15	6543(12)	5411(5)	4046(6)	25.3(13)
C7	8877(11)	2667(5)	4467(6)	25.2(13)
C11	9815(12)	4847(6)	3183(7)	26.2(13)
C8	8901(13)	3775(6)	5180(6)	30.8(15)
C13	7418(12)	6322(5)	2085(7)	29.3(15)
C6	6302(11)	2930(5)	1651(6)	21.7(12)
C14	6044(12)	6216(6)	3033(7)	28.1(14)
C4	4576(12)	4238(6)	-112(7)	30.1(15)
C5	4657(13)	3736(6)	1142(7)	28.2(14)
C12	9303(13)	5646(6)	2178(7)	30.5(14)
O3	7205(12)	3750(5)	6048(5)	44.0(14)
C9	11238(18)	3920(7)	6131(10)	55(3)

Table 8.7: Anisotropic Displacement Parameters ($\times 10^4$) **3m**. The anisotropic displacement factor exponent takes the form: $-2\pi^2[h^2a^{*2} \times U_{11} + ... + 2hka^* \times b^* \times U_{12}]$

Atom	U_{11}	U_{22}	U_{33}	U_{23}	U_{13}	U_{12}
Br1	25.3(3)	24.8(3)	27.9(3)	-4.4(3)	4.8(2)	4.4(3)
S1	24.9(8)	24.1(8)	23.9(7)	1.7(6)	7.7(6)	-0.7(6)
O1	44(3)	24(3)	39(3)	0(2)	13(2)	-5(2)
O2	25(2)	43(3)	35(2)	-1(2)	16(2)	1(2)
C1	19(3)	21(3)	26(3)	-1(2)	3(2)	-1(2)
C3	43(4)	29(4)	21(3)	1(3)	1(3)	-3(3)
C2	32(3)	27(3)	18(3)	-3(2)	5(2)	-3(3)
C10	30(3)	22(3)	20(3)	-6(2)	5(2)	3(3)
C15	30(3)	23(3)	22(3)	-1(2)	6(3)	1(3)
C7	31(3)	21(3)	20(3)	-1(2)	-1(2)	5(3)
C11	25(3)	30(4)	24(3)	-3(3)	7(2)	4(3)

Atom	U_{11}	U_{22}	U_{33}	U_{23}	U_{13}	U_{12}
C8	42(4)	26(3)	21(3)	-5(3)	0(3)	12(3)
C13	32(3)	26(4)	28(3)	5(3)	3(2)	0(3)
C6	21(3)	18(3)	23(3)	-3(2)	0(2)	-1(2)
C14	28(3)	24(3)	31(3)	1(2)	5(3)	6(2)
C4	32(4)	26(4)	25(3)	1(3)	-7(3)	6(3)
C5	27(3)	29(4)	25(3)	-4(3)	-2(3)	3(3)
C12	35(4)	32(4)	27(3)	2(3)	11(3)	-3(3)
O3	68(4)	40(3)	32(3)	2(2)	27(3)	6(3)
C9	63(6)	21(4)	55(5)	-4(4)	-37(5)	0(4)

Table 8.8: Bond Lengths in Å for **3m.**

Atom	Atom	Length/Å
Br1	C1	1.894(6)
S1	O1	1.429(6)
S1	O2	1.457(5)
S1	C7	1.783(6)
S1	C6	1.769(6)
C1	C2	1.387(9)
C1	C6	1.404(9)
C3	C2	1.384(11)
C3	C4	1.388(11)
C10	C15	1.372(10)
C10	C11	1.424(9)
C10	C8	1.533(10)
C15	C14	1.390(9)
C7	C8	1.531(9)
C11	C12	1.382(10)
C8	O3	1.472(9)
C8	C9	1.490(10)
C13	C14	1.391(10)
C13	C12	1.377(10)
C6	C5	1.396(10)
C4	C5	1.381(10)

Table 8.9: Bond Angles in ° for **3m.**

Atom	Atom	Atom	Angle/°
O1	S1	O2	117.8(4)
O1	S1	C7	108.7(3)
O1	S1	C6	108.5(3)
O2	S1	C7	107.2(3)
O2	S1	C6	106.5(3)
C6	S1	C7	107.8(3)
C2	C1	Br1	117.0(5)
C2	C1	C6	120.6(6)
C6	C1	Br1	122.4(5)
C2	C3	C4	119.8(6)
C3	C2	C1	120.2(6)
C15	C10	C11	118.4(6)
C15	C10	C8	122.8(6)
C11	C10	C8	118.8(6)
C10	C15	C14	121.2(6)
C8	C7	S1	115.8(5)
C12	C11	C10	119.9(6)
C7	C8	C10	111.5(5)
O3	C8	C10	111.0(6)
O3	C8	C7	108.7(7)
O3	C8	C9	107.0(7)
C9	C8	C10	110.7(7)
C9	C8	C7	107.8(6)
C12	C13	C14	119.7(6)
C1	C6	S1	124.1(5)
C5	C6	S1	117.6(5)
C5	C6	C1	118.2(6)
C15	C14	C13	119.9(6)
C5	C4	C3	120.2(6)
C4	C5	C6	120.9(7)
C13	C12	C11	120.7(6)

Table 8.10: Hydrogen Fractional Atomic Coordinates ($\times 10^4$) and Equivalent Isotropic Displacement Parameters ($Å^2 \times 10^3$) for **3m**. U_{eq} is defined as 1/3 of the trace of the orthogonalised U_{ij}.

Atom	x	y	z	U_{eq}
H3	6116	4301	-1719	39
H2	8821	2945	-929	31
H15	5624	5350	4681	30
H7A	9206	2106	5174	30
H7B	10127	2656	3990	30
H11	11104	4400	3244	31
H13	7066	6847	1392	35
H14	4792	6682	2990	34
H4	3462	4769	-440	36
H5	3601	3938	1655	34
H12	10243	5728	1557	37
H3A	6001	3461	5617	66
H9A	12384	3991	5597	82
H9B	11597	3299	6730	82
H9C	11239	4566	6677	82

8.14 References:

[1] a) G. Solladie, C. Frechou, G. Demailly, C. Greck, *J. Org. Chem.* **1986**, *51*, 1912; b) S. Robin, F. Huet, A. Fauve, H., *Tetrahedron: Asymmetry* **1993**, *4*, 239; c) A. P. Kozikowski, B. B. Mugrage, C. S. Li, L. Felder, *Tetrahedron Lett.* **1986**, *27*, 4817; d) T. Sato, Y. Okumura, J. Itai, T., *Chem. Lett.* **1988**, 1537; e) R. Tanikaga, K. Hosoya, A. Kaji, *J. Chem. Soc. Perkin Trans. 1* **1987**, 1799; f) R. A. Fromtling, *Drugs Future* **1989**, *14*, 1165; g) C. A. M. Larcheveque, *Tetrahedron* **1988**, *44*, 6407; h) R. Tanikaga, K. Hosoya, K. Hamamura, A. Kaji, *Tetrahedron Lett.* **1987**, *28*, 3705.

[2] a) R. A. Fromtling, *Drugs Future* **1989**, *14*, 1165; b) T. K. S. Oida, *Chem. Pharm. Bull.* **2000**, *48*, 694; c) H. Eto, *Chem. Pharm. Bull.* **2001**, *49*, 173.

[3] a) M. C. Bernabeu, P. Bonete, F. Caturla, R. Chinchilla, C. Najera, *Tetrahedron: Asymmetry* **1996**, *7*, 2475; b) A. K. Maiti, P. Bhattacharyya, *Tetrahedron* **1994**, *50*, 10483; c) C. C. J. Culvenor, W. Davies, N. S. Heath, *J. Chem. Soc.* **1949**, 278; d) C. C. J. Culvenor, W. Davies, N. S. Heath, *J. Chem. Soc.* **1949**, 2198; e) G. K. Biswas, P. Bhattacharyya, *Synth. Commun.* **1991**, *21*, 569; f) I. W. J. Still, F. J. Ablenas, *Synth. Commun.* **1982**, *12*, 1103; g) J. K. Crandall, C. Pradat, *J. Org. Chem.* **1985**, *50*, 1327; h) N. O. Brace, *J. Fluorine Chem.* **2000**, *102*, 21.

[4] a) B. T. Cho, D. J. Kim, *Tetrahedron: Asymmetry* **2001**, *12*, 2043; b) G. Sarakinos, E. J. Corey, *Org. Lett.* **1999**, *1*, 1741; c) G. Zhao, J.-B. Hu, Z.-S. Qian, W.-X. Yin, *Tetrahedron: Asymmetry* **2002**, *13*, 2095; d) H.-L. Zhang, X.-L. Hou, L. X. Dai, Z.-B. Luo, *Tetrahedron: Asymmetry* **2007**, *18*, 224; e) R. L. Crumbie, B. S. Deol, J. E. Nemorin, D. D. Ridley, *Aust. J. Chem.* **1978**, *31*, 1965; f) V. Gotor, F. Rebolledo, R. Liz, *Tetrahedron: Asymmetry* **2001**, *12*, 513.

[5] a) M. T. Reetz, J. Westermann, R. Steinbach, B. Wenderoth, R. Peter, R. Ostarek, S. Maus, *Chem. Ber.* **1985**, *118*, 1421; b) M. Julia, J. M. Paris, *Tetrahedron Lett.* **1973**, *49*, 4833; c) D. F. Tavares, P. F. Vogt, *Canadian Journal of Chemistry* **1967**, *45*, 1519.

[6] a) T. Taniguchi, A. Idota, H. Ishibashi, *Org. Biomol. Chem.* **2011**, *9*, 3151; b) N. Taniguchi, *J. Org. Chem.* **2015**, *80*, 7797.

[7] Q. Lu, J. Zhang, F. Wei, Y. Qi, H. Wang, Z. Liu, A. Lei, *Angew. Chem. Int. Ed.* **2013**, *52*, 7156.

[8] a) I. D. Riggi, J.-M. Surzur, M. P. Bertrand, *Tetrahedron* **1988**, *44*, 7119; b) I. De Riggi, J.-M. Surzur, M. P. Bertrand, *Tetrahedron* **1990**, *46*, 5285; c) M.-Y. C. J.-M. Fang, *Tetrahedron Lett.* **1987**, *28*, 2853; d) R. A. Gancarz, J. L. Kice, *J. Org. Chem.* **1981**, *46*, 4899; e) S.-F. Wang, C.-P. Chuang, J.-H. Lee, S.-T. Liu, *Tetrahedron* **1999**, *55*, 2273; f) W. E. Truce, C. T. Goralski, *J. Org. Chem.* **1971**, *36*, 2536; g) H. Xi, B. Deng, Z. Zong, S. Lu, Z. Li, *Org. Lett.* **2015**, *17*, 1180; h) Chanjuan Xi, Chunbo Lai, Chao Chen, Ruji Wang, *Synlett* **2004**, *9*, 1595.

[9] a) F. Teplý, *Collect. Czech. Chem. Commun.* **2011**, *76*, 859; b) J. M. R. Narayanam, C. R. J. Stephenson, *Chem. Soc. Rev.* **2011**, *40*, 102; c) K. Zeitler, *Angew. Chem. Int. Ed.* **2009**, *48*, 9785; d) T. P. Yoon, M. A. Ischay, J. Du, *Nat. Chem.* **2010**, *2*, 527.

[10] C. K. Prier, D. A. Rankic, D. W. C. MacMillan, *Chem. Rev.* **2013**, *113*, 5322.

[11] D. B. Bagal, G. Kachkovskyi, M. Knorn, T. Rawner, B. M. Bhanage, O. Reiser, *Angew. Chem. Int. Ed.* **2015**, *54*, 6999.

[12] A. U. Meyer, S. Jäger, D. Prasad Hari, B. König, *Adv. Synth. Catal.* **2015**, *357*, 2050.

[13] a) C.-J. Wallentin, J. D. Nguyen, P. Finkbeiner, C. R. J. Stephenson, *J. Am. Chem. Soc.* **2012**, *134*, 8875; b) H. Jiang, X. Chen, Y. Zhang, S. Yu, *Adv. Synth. Catal.* **2013**, *355*, 809.

[14] J.-M. Kern, J.-P. Sauvage, *J. Chem. Soc., Chem. Commun.* **1987**, 546.

[15] J. Sun, W. Wu, J. Zhao, *Chem. Eur. J.* **2012**, *18*, 8100.

[16] a) S. Paria, O. Reiser, *Adv. Synth. Catal.* **2014**, *356*, 557; b) S. Paria, V. Kais, O. Reiser, *Adv. Synth. Catal.* **2014**, *356*, 2853.

[17] a) I. Prediger, T. Weiss, O. Reiser, *Synthesis* **2008**, *2008*, 2191; b) H. Yi, Q. Liu, J. Liu, Z. Zeng, Y. Yang, A. Lei, *ChemSusChem* **2012**, *5*, 2143.

[18] a) Michael Pirtsch, Suva Paria, Taisuke Matsuno, Hiroyuki Isobe, Oliver Reiser, *Chem. Eur. J.* **2012**, *18*, 7336; b) Suva Paria, Michael Pirtsch, Viktor Kais, Oliver Reiser, *Synthesis* **2013**, *45*, 2689; c) M. Knorn, T. Rawner, R. Czerwieniec, O. Reiser, *ACS Catal.* **2015**, *5*, 5186; d) Xiao-Jun Tang, William R. Dolbier, *Angew. Chem. Int. Ed.* **2015**, *54*, 4246; e) S. Paria, O. Reiser, *ChemCatChem* **2014**, *6*, 2477.

[19] S. H. Oh, Y. R. Malpani, N. Ha, Y.-S. Jung, S. B. Han, *Org. Lett.* **2014**, *16*, 1310.

[20] a) K. Müller, C. Faeh, F. Diederich, *Science* **2007**, *317*, 1881; b) M. Shimizu, T. Hiyama, *Angew. Chem., Int. Ed.* **2004**, *44*, 214; c) S. Purser, P. R. Moore, S. Swallow, V. Gouverneur, *Chem. Soc. Rev.* **2008**, *37*, 320; d) K. L. Kirk, *Org. Process Res. Dev.* **2008**, *12*, 305; e) W. K. Hagmann, *J. Med. Chem.* **2008**, *51*, 4359.

[21] M. Patel, R. J. McHugh, B. C. Cordova, R. M. Klabe, L. T. Bacheler, S. Erickson-Viitanen, J. D. Rodgers, *Bioorg. Med. Chem. Lett.* **2001**, *11*, 1943.

[22] T. Taniguchi, A. Idota, H. Ishibashi, *Org. Biomol. Chem.* **2011**, *9*, 3151.

[23] C. Xi, C. Lai, C. Chen, R. Wang, *Synlett* **2004**, 1595.

[24] N. Taniguchi, *J. Org. Chem.* **2015**, *80*, 7797.

9 Temperature controlled selective C-S or C-C bond formations: First photocatalytic sulfonylation of unactivated heterocycles utilizing aryl sulfonyl chlorides

9.1 Abstract:

A facile method for heterocyclic sulfonylation has been developed by employing visible-light-induced photocatalysis at room temperature conditions. This strategy provides a direct access to the novel class of sulfonyl substituted heterocycles in excellent yields. The synthetic utility of this reaction attributed to the direct use of commercially available sulfonyl chlorides and unactivated heterocycles under mild reaction conditions. Furthermore, this reaction offers a simple route for the synthesis of related sulfonyl-containing biologically active molecules. On the other hand, the C-C bond formation reaction occurs with the extrusion of the SO_2 group at elevated temperature conditions, giving rise to arylated heterocycles.

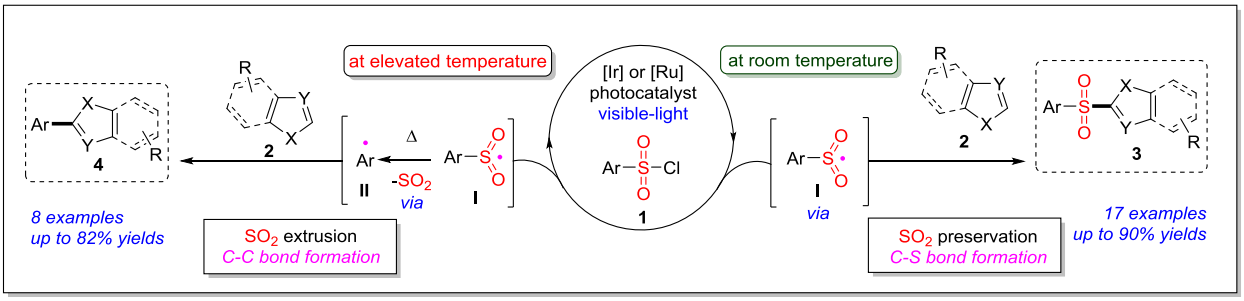

Scheme 9.1: Temperature dependent sulfonylation vs. arylation of heterocycles.

9.2 Introduction:

Sulfur-containing organic compounds have been documented as essential building blocks in synthetic as well as in medicinal chemistry.[1] The substitution of a sulfur group on the aryl or heteroaryl moiety either in the form of sulfanyl, a sulfinyl, or a sulfonyl form, which immensely

This Chapter is under final revision:

S. K. Pagire, A. Hossain, O. Reiser**.**

S.K.P. wrote the manuscript.

enhances the synthetic utility and biological activity of the resultant organic compounds.[2] In particular, sulfonyl-containing heterocycles have extensive applications in synthesis, agrochemical industries, and pharmaceuticals.[3] For example, compounds **A** and **B** are very selective and potent human immunodeficiency virus type 1 (HIV-1) reverse transcriptase inhibitors (Figure 9.1).[4] While, SR 33805 (**C**) is a potent Ca^{2+} channel antagonist, which binds allosterically to the a_1-subunit of L-type Ca^{2+} channels (K_d = 20 pM), it also inhibits PDGF-stimulated smooth muscle cell proliferation.[5] The bis-sulfone derivative **D** has been established as a cannabinoid CB_2 receptor ligands.[6] Whereas, Serotonin **E** is a 5-HT6 receptor antagonist.[3]

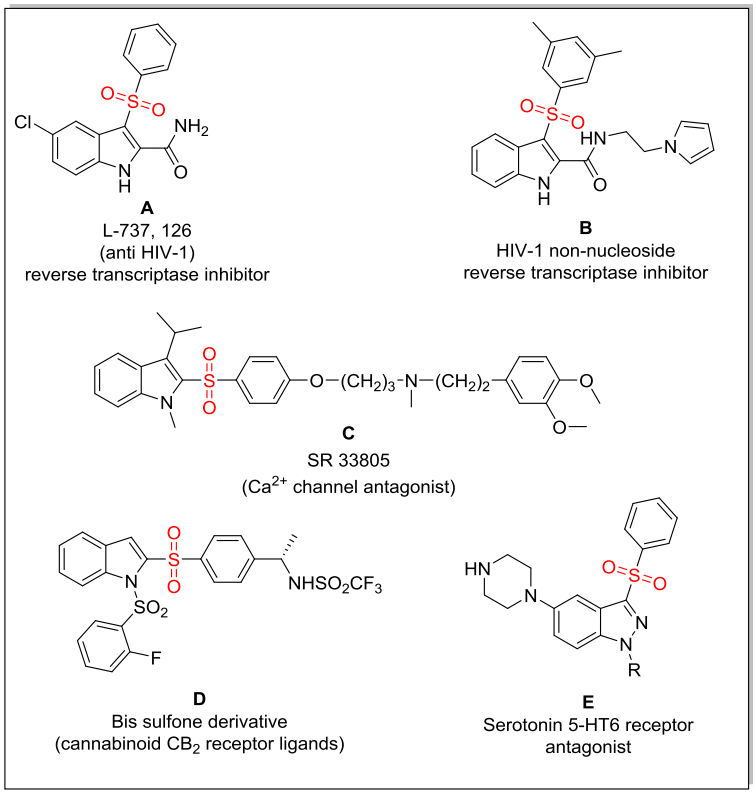

Figure 9.1: Representative biologically active molecules consisting aryl sulfonyl moiety.

As a result, the various and elegant synthetic methods have been developed in the direction of C-S bond formation by classical[7] as well as photochemical methods.[8,9] Despite the highly important several biologically active sulfonyl derivatives, the sulfonylation of desired heteroaromatics is surprisingly under-developed by straightforward routes (Figure 9.1). Therefore, direct and selective C-H sulfonylation of heterocyclic compounds has remained an

elementary challenge in organic synthesis till date. Though, there are quite a few indirect routes available for the synthesis of sulfonylated heteroarenes. Which mainly includes preactivation of heterocycles,[10,11] or need a activated (or modified) sulfonyl sources, which unfortunately limited to the specific substrates.[12,13] Furthermore, to control undesired desulfonylation[14] and over-reduction of sulfonyl groups is a challenging task.[8,15] In those cases, the re-oxidation of obtained sulfides needs to be conducted in order to recover the desired sulfonyl moiety.[16] As a consequence, these methods calls for supplementary oxidation steps,[17] which frequently require strong oxidants and suffer from harsh reaction conditions: for example, use of strong acids and organometallic reagents at elevated temperature conditions, eventually does not tolerate a variety of functional groups.[18]

In recent times, we have introduced a convenient method for the synthesis of β-hydroxysulfones from styrenes and sulfonyl chlorides utilizing visible-light-induced sequential photocatalytic strategy (Chapter 3.1).[19] As stated earlier, the aryl sulfonyl chlorides typically exist as bench-stable solids, which are commercially available, cheap, and mild sulfonylation source.[20] Despite of the sulfonylation reactions, they are also known for C-C bond formation reactions at elevated temperature conditions.[21] Therefore, obtaining temperature controlled selectivity particularly in the C-S bond formation using such reagents is another challenge.

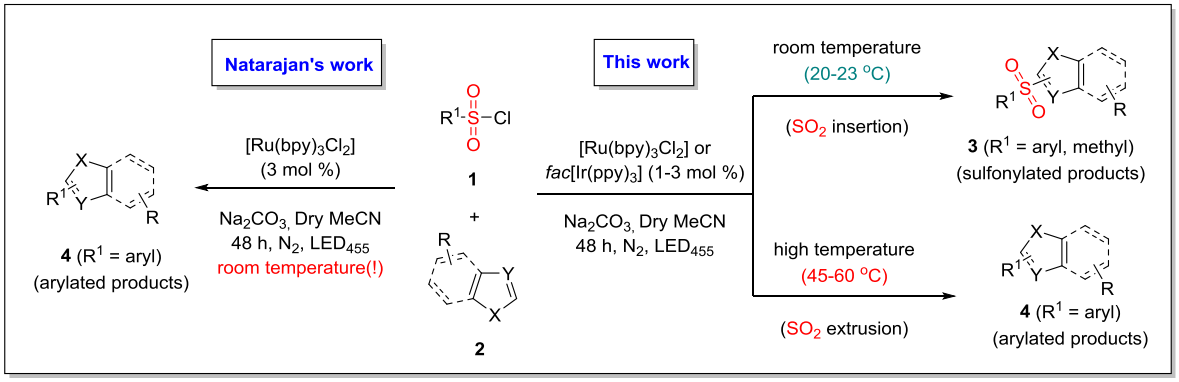

Scheme 9.2: Comparison between Natarajan's method and our method.

Within our constant interest of visible-light triggered photocatalyst controlled selective C-S bond formations with unactivated alkenes,[22] herein, we unexpectedly arrive at temperature controlled C-H functionalization of heteroaromatics utilizing sulfonyl chlorides. To our surprise, at room

temperature conditions, we observed that the sulfonyl group remained intact, though on the other hand, we were aware that, the Natarajan group[14] already showed the direct arylation under the identical conditions (Scheme 9.2). Our results therefore calls to revise the previous method and to rewrite the "exact reaction conditions" used, in particular the "reaction temperature" they employed. Rest of the parameters do not interfere with the SO_2 extrusion, which we have proved later in our group (*vide infra*).

9.3 Results and discussion:

Having all this information in mind, we began our investigations by shining blue light on benzenesulfonyl chloride **1a**, *N*-methyl pyrrole **2a** using $[Ru(bpy)_3Cl_2]$[23] ($E_{1/2\ (III/*II)}$ = -0.81 V vs SCE) catalyst with the addition of Na_2CO_3 in dry MeCN (Table 9.1, entry 1). Indeed, we predominantly found C2-sulfonylation product **3a** over C2-arylation **4a** (20 ^oC - 23 ^oC) in 67% yields at room temperature conditions.

In order to confirm our reasoning, we gradually raised the reaction temperature to 30 ^oC; indeed, the non-polar compound **4a** started to emerge (Table 9.1, entry 2). Further raising the reaction temperature to 60 ^oC, considerably provides C2-arylated product **4a** (Table 9.1, entries 3-5) in 65-66% yields without the formation of **3a**. The yield of **3a** was enhanced to 79% (Table 9.1, entry 6) by the execution of *fac*$[Ir(ppy)_3]$[24] ($E_{1/2\ (IV/*III)}$ –1.73 V vs SCE, ppy = 2-phenylpyridine) photocatalyst. To our delight, lowering the [Ir]-photocatalyst loading (from 3 mol % to 1 mol %), also provided almost the identical results (Table 9.1, entries 6-7). Further optimization exposed that, in absence Na_2CO_3, the starting materials remained unreacted, while reaction color was completely black after 48 h of irradiation (Table 9.1, entry 9). The addition of other inorganic bases such as K_2CO_3, K_2HPO_4, Na_2HPO_4 were found to be less effective (Table 9.1, entries 10-12). The controlled experiments revealed that the combination of visible-light and the photocatalyst are together necessary to accomplish the desired sulfonylation (Table 9.1, entries 13-14). In literature, there are a number of impressive methods already known for the construction of C-C bonds, which mainly includes palladium catalyzed cross-coupling reactions,[25,26] photoredox catalysis,[14,27] or dual Cu and photocatalysis.[28] Thus, we mostly focused on the synthesis of sulfonylated products. Nevertheless, we have also shown few

representative arylated examples in Table 9.2 for the direct comparison and to confirm our reasoning.

9.4 Synthesis of 3a and 4a: Catalyst screening and reaction optimization

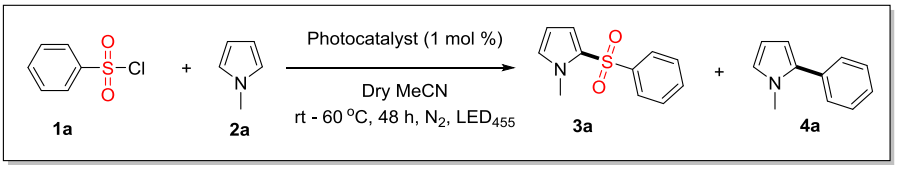

Entry	Photocatalyst (mol %)	Additive	Temperature (°C)	Yield (%)[b] 3a	4a
01	$[Ru(bpy)_3Cl_2]$ (3)	Na_2CO_3	rt[c]	67	-
02	$[Ru(bpy)_3Cl_2]$ (3)	Na_2CO_3	30	49	7
03	$[Ru(bpy)_3Cl_2]$ (3)	Na_2CO_3	35	27	31
04	$[Ru(bpy)_3Cl_2]$ (3)	Na_2CO_3	45	-	66
05	$[Ru(bpy)_3Cl_2]$ (3)	Na_2CO_3	60	-	65
06	*fac*$[Ir(ppy)_3]$ (3)	Na_2CO_3	rt	79	-
07	*fac*$[Ir(ppy)_3]$ (1)	Na_2CO_3	rt	80	-
08	*fac*$[Ir(ppy)_3]$ (1)	Na_2CO_3	45	-	75
09[e]	*fac*$[Ir(ppy)_3]$ (1)	-	rt	28	-
10	*fac*$[Ir(ppy)_3]$ (1)	K_2CO_3	rt	74	-
11	*fac*$[Ir(ppy)_3]$ (1)	K_2HPO_4	rt	71	-
12	*fac*$[Ir(ppy)_3]$ (1)	Na_2HPO_4	rt	69	-
13	No Catalyst	Na_2CO_3	rt	-	-
14	*fac*$[Ir(ppy)_3]$ (1), no light	Na_2CO_3	rt	-	-

Table 9.1: Reaction conditions: [a] Benzenesulfonylchloride **1a** (1.0 mmol, 1 equiv), *N*-methylpyrrole **2a** (1.5 mmol, 1.5 equiv), Photocatalyst (1-3 mol %), additive (1.5 mmol, 1.5 equiv), dry MeCN (3 mL), LED_{455}, 48 h. [b] Isolated yields. [c] room temperature (20 °C - 23 °C, maintained with external water bath).

9.5 Substrate scope:

By applying the optimal conditions (Table 9.1, entries 7 and 8), we turned our attention to enhance the scope of the substrates. Initially, veriety of aryl sulfonyl chlorides **1** having a range of electronic substituents were investigated with *N*-methyl pyrrole **2a** as a trapping reagent (Table 9.2). Sulfonyl chlorides **1** possessing electron donating substituents (e.g. Me, MeO) as well as electron deficient functionalities (e.g. acetyl, NO_2) were well tolerated.

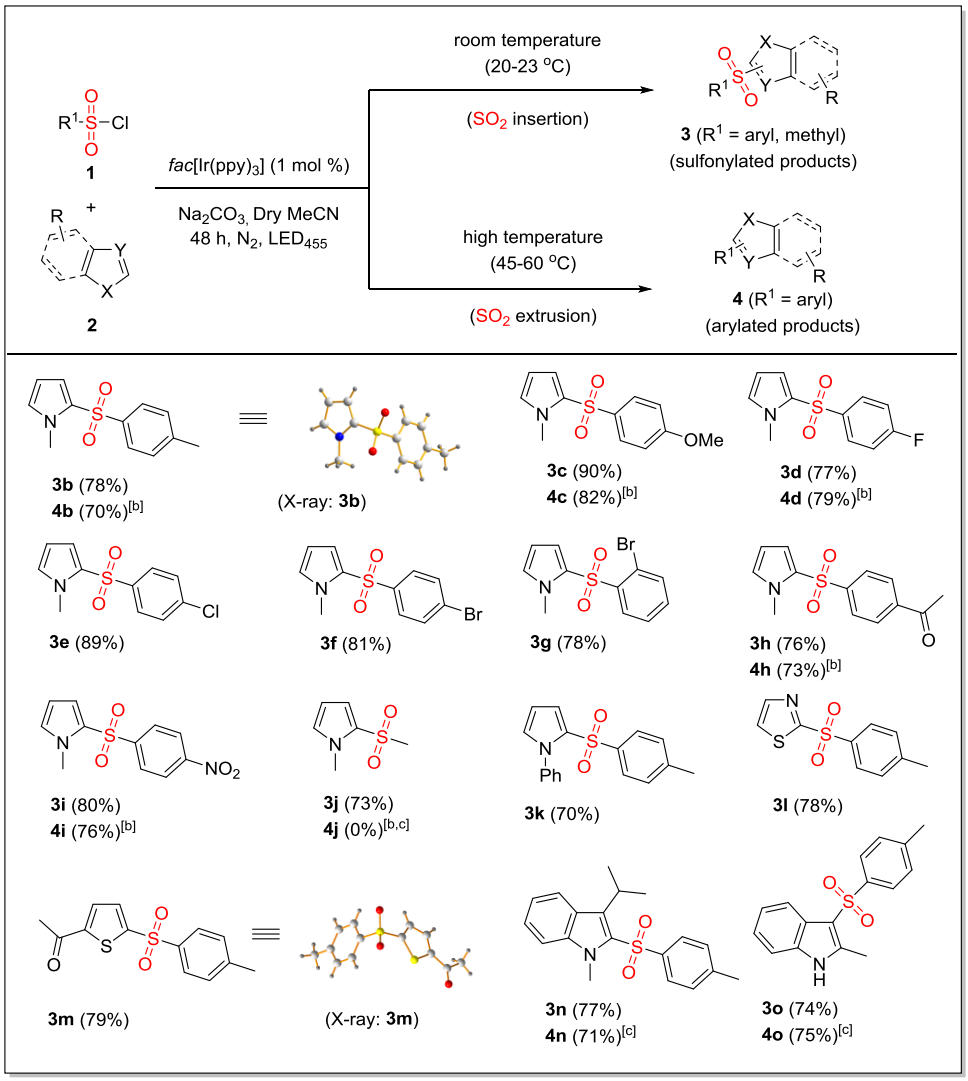

Table 9.2: Reaction conditions: [a] Aryl sulfonyl chloride **1** (1.0 mmol, 1 equiv), *N*-methylpyrrole **2a** (1.5 mmol, 1.5 equiv), *fac*[Ir(ppy)$_3$] (1 mol %), Na_2CO_3 (1.5 mmol, 1.5 equiv), dry MeCN (3 mL), LED_{455}, 48 h, rt (20 °C - 23 °C, maintained with external water bath). [b] Reaction done at 45°C. [c] Reaction done at 60 °C.

Moreover, the halogen family (F, Cl, Br) and also *ortho*-substituted bromo derivative (**3g**) were worked well under the employed conditions, providing sulfonylated products predominantly in high yields (Table 9.2). The presence of SO_2 group was already confirmed by the HRMS and NMR analysis (see experimental section). Pleasingly, structures of **3b** and **3m** were unambiguously characterized by the single X-ray crystal analysis (Table 9.2).

Furthermore, we decided to examine a scope for heterocycles **2** with Tosyl chloride **1b** as a usual coupling partner (Table 9.2). The range of heterocycles such as 2-acetyl thiophene (**3m**), thiazole (**3l**), and 2- or 3-substituted indoles (**3n**, **3o**) were regioselectively sulfonylated in good yields (Table 9.2). In particular, the selective sulfonylation of indoles was a challenging task under the similar photochemical conditions, which was earlier reported by the group of Zheng.[8] They notice a partial reduction of sulfonyl to sulfide group at >30 ^{o}C. To our great delight, under the employed controlled conditions, only desired sulfonylated products could be isolated (see experimental section). In contrast, direct arylation reactions are also achieved at 60 ^{o}C for indoles without the formation of any of partially reduced intermediates (Table 9.2). At 45 ^{o}C, the undesired products (may be partially reduced) were observed.

9.6 Applications:

Having established the sulfonylation protocol, we aimed to demonstrate the utility of this new strategy for the construction of representative valuable biologically active sulfonyl containing drug candidates which are already described in Figure 9.1. By employing the standard conditions, the direct C3-sulfonylation of indole derivative **2g** was productively achieved utilizing benzenesulfonylchloride **1a** in 72% yields (Scheme 9.3)**.**

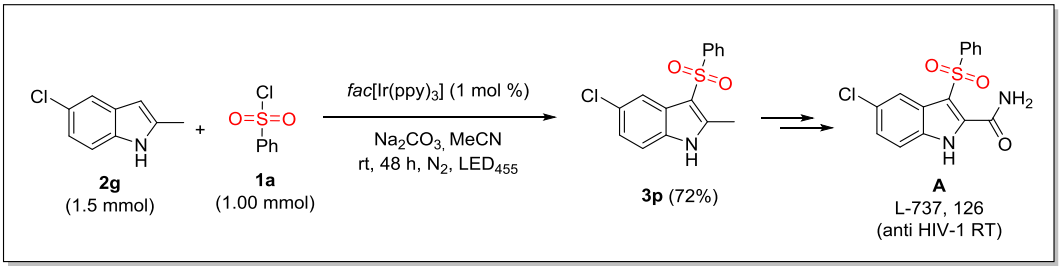

Scheme 9.3: Formal synthesis of HIV-1 RT (L-737, 126).

From the resulting 3-sulfonylated indoles **3p**, further synthesis of corresponding biologically active HIV-1 RT (L-737, 126) **A** is already established in few steps.[29] Next, we have also implement our method for the direct C2-sulfonylation of 3-substituted indole derivative **2e** which gives a key precursor **3q** in 74% yields in a single step. To our surprise, this has never done before in single step (Scheme 9.4). From intermediate **3q**, the following synthesis of a Ca^{2+} channel blocker **C** (SR 33805) was already achieved in literature.[30]

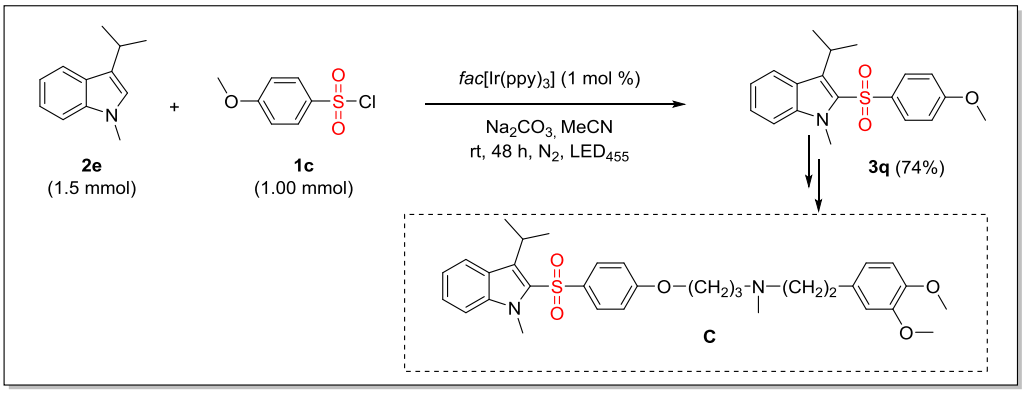

Scheme 9.4: Formal synthesis of Ca^{2+} channel blocker **C** (SR 33805).

9.7 Proposed reaction mechanism:

As reported earlier,[19] we propose the reaction mechanism utilizing the oxidative quenching cycle: Initial excitation of the Ir(III) to Ir (III)* occurs by irradiation with blue light. From this Ir(III)*, the subsequent single electron transfer (SET) to benzenesulfonylchloride **1a** occurs to generate the corresponding sulfonyl radical **I** upon chloride extrusion, concurrent with oxidation to Ir(IV). Regioselective sulfonyl radical **I** addition to *N*-methyl pyrrole **2a** takes place to form a stable carbon-centered α-amino radical intermediate **II**, which subsequently undergoes oxidation to the corresponding carbocation **III** by back electron transfer processes. The resultant carbocation **III** rapidly undergoes rearomatization triggered by sodium carbonate give rise to **3a** (Figure 3).

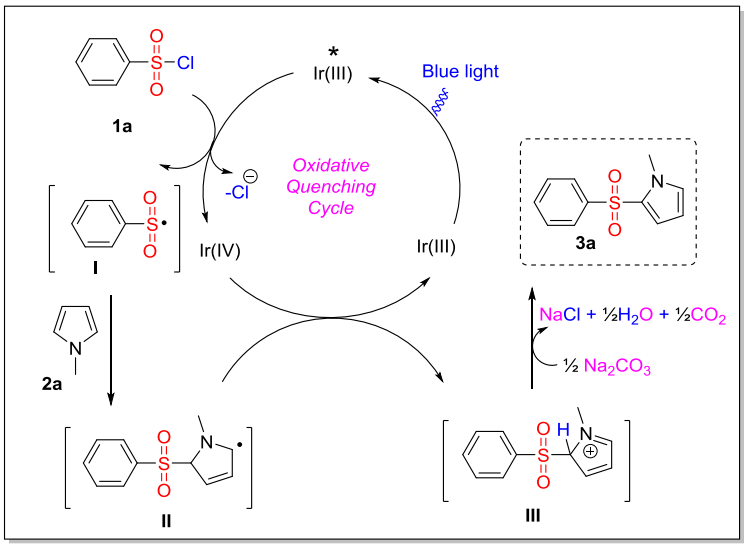

Figure 9.2: Proposed reaction mechanism.

9.8 Conclusion:

To conclude, we have developed a first visible-light photocatalyzed method for the direct sulfonylation or arylation of heterocycles at different temperature conditions without pre-activating a sulfonyl source and a heterocyclic ring. In addition, the utility of this transformation has been demonstrated via the formal synthesis of relevant biologically active molecules using readily available starting materials under sustainable reaction conditions.

9.9 Experimental section:

9.9.1 Reduction potentials:

Redox potentials of the sulfonyl chlorides were measured by cyclic voltammetry in acetonitrile containing tetrabutylammonium tetrafluoroborate (0.1 M) as a supporting electrolyte. All values are given versus Saturated Calomel Electrode (SCE). Potential sweep rate was 50 mV S^{-1}.

Sulfonyl chlorides	**Reduction potential (V)**
benzenesulfonyl chloride (**1a**)	-0.95
4-methylbenzenesulfonyl chloride (**1b**)	-0.94
4-methoxybenzenesulfonyl chloride (**1c**)	-0.99
4-fluorobenzenesulfonyl chloride (**1d**)	-0.90
4-chlorobenzenesulfonyl chloride (**1e**)	-0.79
4-bromobenzenesulfonyl chloride (**1f**)	-0.82
2-bromobenzenesulfonyl chloride (**1g**)	-0.82
4-acetylbenzenesulfonyl chloride (**1h**)	-0.66
4-nitrobenzenesulfonyl chloride (**1i**)	-0.44
methanesulfonyl chloride (**1j**)	-1.39

Table 9.3: Redox potentials of the sulfonyl chlorides versus SCE.

9.9.2 General Procedure (GP-1) for C, H-Sulfonylation:

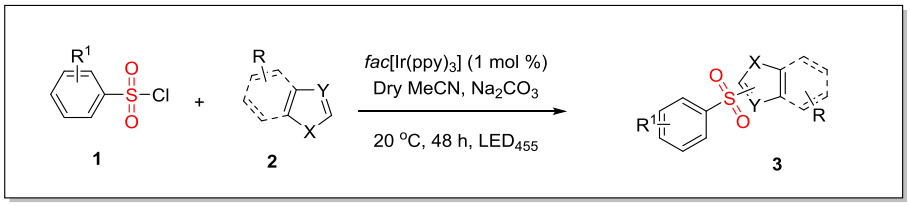

An oven dried 10 mL Schleck flask was charged with **1** (1.0 mmol, 1.00 equiv), Na_2CO_3 (159 mg, 1.50 mmol, 1.00 equiv), and *fac*[Ir(ppy)$_3$] (6.54 mg, 0.01 equiv, 1.00 mol %) in 3.0 mL dry MeCN. The resulting suspension was deoxygenated by three freeze-pump-thaw cycles. Then desired heterocyclic compound **2** (1.50 mmol, 1.5 equiv) was added under positive nitrogen atmosphere). The reaction mixture was exposed to the blue light emitting diode (LED, λ_{max} = 455 nm) at room temperature for 48 h. After complete conversion of aryl sulfonyl chloride (judged by TLC), the reaction mixture was saturated by addition of brine solution (20 mL). The aqueous phase was washed with ethyl acetate (3 x 20 mL). The combined organic fractions were dried over Na_2SO_4, concentrated *in vacuo*, and the crude residue was purified by column chromatography on silica gel by using hexanes and ethyl acetate as eluents to afford the pure product **3**.

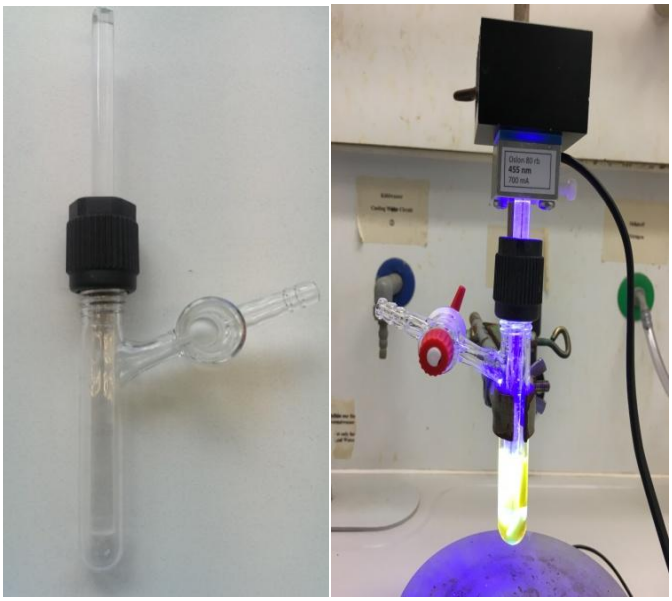

Figure 9.3: Experimental set-up for photochemical reaction.

1-methyl-2-(phenylsulfonyl)-1*H*-pyrrole (3a):

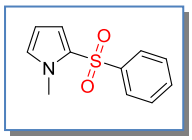

Following **GP-1**, **3a** was prepared from benzenesulfonylchloride **1a** (176 mg, 1.0 mmol, 1.00 equiv) and *N*-Methylpyrrole **2a** (122 mg, 133 µL, 1.50 mmol, 1.5 equiv). The crude product was purified by column chromatography (silica gel, hexanes–EtOAc, 7:3, R_f = 0.34) to afford **3b** as a light yellow viscous (sticky) solid (177 mg, 80% yield).

^{1}H-NMR (300 MHz, $CDCl_3$): δ 7.97 – 7.76 (m, 2H), 7.66 – 7.38 (m, 3H), 7.03 (dd, *J* = 4.0, 1.9 Hz, 1H), 6.76 (t, *J* = 2.2 Hz, 1H), 6.16 (dd, *J* = 4.0, 2.6 Hz, 1H), 3.69 (s, 3H).

^{13}C-NMR (75 MHz, $CDCl_3$): δ 142.22, 133.03, 129.87, 129.34, 127.92, 127.26, 118.97, 108.46, 35.75.

IR (neat, cm^{-1}): 2923, 1704, 1581, 1515, 1475, 1442, 1420, 1363, 1303, 1222, 1148, 1120, 1080, 1017, 994, 749, 724, 688.

EI-MS: exact m/z calculated for $C_{11}H_{11}NO_2S$ $(M)^+$: 221.05050; Found: 221.05052 $(M)^+$.

1-methyl-2-tosyl-1*H*-pyrrole (3b):

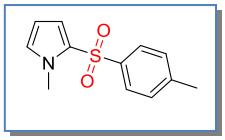

Following **GP-1**, **3b** was prepared from tosyl chloride **1b** (191 mg, 1.0 mmol, 1.00 equiv) and *N*-Methylpyrrole **2a** (122 mg, 133 µL, 1.50 mmol, 1.5 equiv). The crude product was purified by column chromatography (silica gel, hexanes–EtOAc, 4:1, R_f = 0.39) to afford **3b** as a white solid (183 mg, 78% yield).

^{1}H-NMR (300 MHz, $CDCl_3$): δ 7.78 – 7.74 (m, 2H), 7.29 (d, *J* = 8.5 Hz, 2H), 7.00 (dd, *J* = 4.1, 1.9 Hz, 1H), 6.79 – 6.61 (m, 1H), 6.15 (dd, *J* = 4.1, 2.5 Hz, 1H), 3.69 (s, 3H), 2.40 (s, 3H).

^{13}C-NMR (75 MHz, $CDCl_3$): δ 143.94, 139.32, 129.97, 129.59, 128.41, 127.40, 118.63, 108.36, 35.74, 21.71.

IR (neat, cm^{-1}): 3126, 2921, 1740, 1591, 1513, 1491, 1443, 1314, 1287, 1229, 1159, 1125, 1096, 1076, 1047, 1006, 882, 845, 818, 801, 745, 695, 658.

HRMS (ESI): exact m/z calculated for $C_{12}H_{14}NO_2S$ $(M+H)^+$: 236.074; Found: 236.0747 $(M+H)^+$.

Mp: 100-102 ^oC (decomposed).

2-((4-methoxyphenyl)sulfonyl)-1-methyl-1*H*-pyrrole (3c):

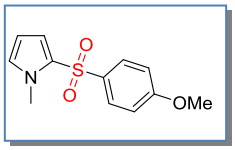

Following **GP-1**, **3c** was prepared from 4-methoxybenzenesulfonyl chloride **1c** (206 mg, 1.0 mmol, 1.00 equiv) and *N*-Methylpyrrole **2a** (122 mg, 133 µL, 1.50 mmol, 1.5 equiv). The crude product was purified by column chromatography (silica gel, hexanes–EtOAc, 4:1, R_f = 0.13) to afford **3c** as a pale yellow solid (211 mg, 84% yield).

^{1}H-NMR (300 MHz, $CDCl_3$): δ 7.89 – 7.76 (m, 2H), 7.02 – 6.90 (m, 3H), 6.76 – 6.69 (m, 1H), 6.14 (dd, *J* = 4.0, 2.6 Hz, 1H), 3.84 (s, 3H), 3.69 (s, 3H).

^{13}C-NMR (75 MHz, $CDCl_3$): δ 1691, 133.75, 129.57, 129.41, 128.77, 118.24, 114.51, 108.23, 55.80, 35.68.

IR (neat, cm^{-1}): 2924, 2854, 1704, 1592, 1573, 1458, 1397, 1364, 1315, 1290, 1259, 1154, 1128, 1079, 1022, 966, 831, 800, 749, 716, 697, 665.

EI-MS: exact m/z calculated for $C_{12}H_{13}NO_3S$ $(M)^+$: 251.06107; Found: 251.06090 $(M)^+$.

Mp: 87-89 °C (decomposed).

2-((4-fluorophenyl)sulfonyl)-1-methyl-1*H*-pyrrole (3d):

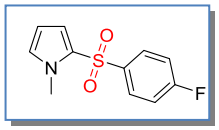

Following **GP-1**, **3d** was prepared from 4-fluorobenzenesulfonyl chloride **1d** (194 mg, 1.0 mmol, 1.00 equiv) and *N*-Methylpyrrole **2a** (122 mg, 133 µL, 1.50 mmol, 1.5 equiv). The crude product was purified by column chromatography (silica gel, hexanes–EtOAc, 9:1, R_f = 0.23) to afford **3d** as a brown solid (184 mg, 77% yield).

^{1}H-NMR (300 MHz, $CDCl_3$): δ 7.93 – 7.85 (m, 2H), 7.22 – 7.12 (m, 2H), 7.01 (dd, *J* = 4.0, 1.9 Hz, 1H), 6.77 (t, *J* = 2.1 Hz, 1H), 6.17 (dd, *J* = 4.0, 2.6 Hz, 1H), 3.70 (s, 3H).

^{13}C-NMR (75 MHz, $CDCl_3$): δ 166.98, 163.60, 138.37 (d, *J* = 9 Hz), 130.10 (d, *J* = 9.7 Hz), 127.77, 119.05, 116.63 (d, *J* = 22.6 Hz), 108.58, 35.77.

^{19}F-NMR (282 MHz, $CDCl_3$): δ -105.22.

IR (neat, cm^{-1}): 2921, 1586, 1511, 1489, 1460, 1403, 1359, 1318, 1286, 1220, 1155, 1126, 1093, 1076, 1046, 1004, 835, 813, 740, 711, 692, 663.

EI-MS: exact m/z calculated for $C_{11}H_{10}NO_2FS$ $(M)^+$: 239.4108; Found: 239.04077 $(M)^+$.

Mp: 61-63 °C (decomposed).

2-((4-chlorophenyl)sulfonyl)-1-methyl-1*H*-pyrrole (3e):

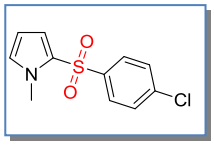

Following **GP-1**, **3e** was prepared from 4-chlorobenzenesulfonyl chloride **1e** (211 mg, 1.0 mmol, 1.00 equiv) and *N*-Methylpyrrole **2a** (122 mg, 133 µL, 1.50 mmol, 1.5 equiv). The crude product was purified by column chromatography (silica gel, hexanes–EtOAc, 7:3, R_f = 0.37) to afford **3e** as a pale yellow solid (227 mg, 89% yield).

^{1}H-NMR (300 MHz, $CDCl_3$): δ 7.84 – 7.79 (m, 2H), 7.48 – 7.45 (m, 2H), 7.04 (ddd, *J* = 5.9, 3.6, 1.8 Hz, 1H), 6.91 – 6.71 (m, 1H), 6.29 – 6.10 (m, 1H), 3.70 (s, 3H).

^{13}C-NMR (75 MHz, $CDCl_3$): δ 140.86, 139.61, 130.18, 129.70, 128.82, 127.55, 119.34, 108.73, 35.84.

IR (neat, cm^{-1}): 2923, 1702, 1579, 1512, 1474, 1392, 1313, 1290, 1228, 1159, 1130, 1086, 1048, 1006, 826, 752, 705, 690.

EI-MS: exact m/z calculated for $C_{11}H_{10}NO_2SCl$ $(M)^+$: 255.01153; Found: 255.01133 $(M)^+$.

Mp: 73-75 °C (decomposed).

2-((4-bromophenyl)sulfonyl)-1-methyl-1*H*-pyrrole (3f):

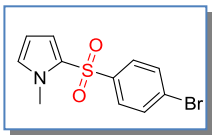

Following **GP-1**, **3f** was prepared from 4-bromobenzenesulfonyl chloride **1f** (255 mg, 1.0 mmol, 1.00 equiv) and *N*-Methylpyrrole **2a** (122 mg, 133 µL, 1.50 mmol, 1.5 equiv). The crude product was purified by column chromatography (silica gel, hexanes–EtOAc, 7:3, R_f = 0.31) to afford **3f** as a pale yellow solid (243 mg, 81% yield).

^{1}H-NMR (300 MHz, $CDCl_3$): δ 7.75 – 7.72 (m, 2H), 7.65 – 7.62 (m, 2H), 7.03 (dd, *J* = 4.1, 1.9 Hz, 1H), 6.78 (t, *J* = 2.2 Hz, 1H), 6.18 (dd, *J* = 4.0, 2.6 Hz, 1H), 3.70 (s, 3H).

^{13}C-NMR (75 MHz, $CDCl_3$): δ 141.25, 132.53, 130.07, 128.75, 127.99, 127.33, 119.22, 108.60, 35.70.

IR (neat, cm^{-1}): 2923, 1701, 1570, 1512, 1467, 1385, 1363, 1313, 1292, 1225, 1159, 1128, 1066, 1047, 1002, 818, 740, 700.

EI-MS: exact m/z calculated for $C_{11}H_{10}NO_2SBr$ $(M)^+$: 298.96101; Found: 298.96068 $(M)^+$.

Mp: 90-92 °C (decomposed).

2-((2-bromophenyl)sulfonyl)-1-methyl-1*H*-pyrrole (3g):

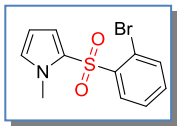

Following **GP-1**, **3g** was prepared from 2-bromobenzenesulfonyl chloride **1g** (255 mg, 1.0 mmol, 1.00 equiv) and *N*-Methylpyrrole **2a** (122 mg, 133 µL, 1.50 mmol, 1.5 equiv). The crude product was purified by column chromatography (silica gel, hexanes–EtOAc, 4:1, R_f = 0.42) to afford **3g** as a pale yellow solid (234 mg, 78% yield).

^{1}H-NMR (300 MHz, $CDCl_3$): δ 8.22 (dd, *J* = 7.8, 1.7 Hz, 1H), 7.69 (dd, *J* = 7.8, 1.3 Hz, 1H), 7.49 (td, *J* = 7.7, 1.4 Hz, 1H), 7.40 (td, *J* = 7.6, 1.8 Hz, 1H), 7.17 (dd, *J* = 4.1, 1.9 Hz, 1H), 6.79 (t, *J* = 2.1 Hz, 1H), 6.20 (dd, *J* = 4.1, 2.6 Hz, 1H), 3.66 (s, 3H).

^{13}C-NMR (75 MHz, $CDCl_3$): 140.86, 136.05, 134.29, 130.80, 130.02, 127.87, 125.86, 122.07, 121.40, 108.29, 35.96.

IR (neat, cm^{-1}): 2921, 1704, 1571, 1511, 1434, 1397, 1359, 1314, 1292, 1229, 1162, 1136, 1117, 1048, 1021, 755, 737, 700.

EI-MS: exact m/z calculated for $C_{11}H_{10}NO_2SBr$ $(M)^+$: 298.96101; Found: 298.96068 $(M)^+$.

Mp: 107-109 ^oC (decomposed).

1-(4-((1-methyl-1*H*-pyrrol-2-yl)sulfonyl)phenyl)ethan-1-one (3h):

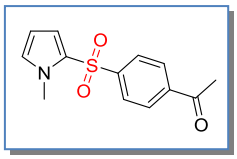

Following **GP-1**, **3h** was prepared from 4-acetylbenzenesulfonyl chloride **1h** (219 mg, 1.0 mmol, 1.00 equiv) and *N*-Methylpyrrole **2a** (122 mg, 133 µL, 1.50 mmol, 1.5 equiv). The crude product was purified by column chromatography (silica gel, hexanes–EtOAc, 1:1, R_f = 0.50) to afford **3h** as a pale yellow viscous (sticky) solid (199 mg, 76% yield).

^{1}H-NMR (300 MHz, $CDCl_3$): δ 8.07 – 8.03 (m, 2H), 7.72 – 7.56 (m, 2H), 6.77 (dd, *J* = 2.4, 1.9 Hz, 1H), 6.61 (dt, *J* = 4.2, 2.0 Hz, 1H), 6.25 – 6.06 (m, 1H), 3.53 (s, 3H), 2.64 (s, 3H).

^{13}C-NMR (75 MHz, $CDCl_3$): δ 197.35, 148.64, 138.56, 129.75, 128.99, 125.46, 125.05, 118.32, 108.65, 34.96, 26.98.

IR (neat, cm^{-1}): 2923, 1682, 1589, 1514, 1420, 1393, 1357, 1293, 1258, 1146, 1120, 1083, 1033, 1009, 957, 827, 793, 722, 676.

EI-MS: exact m/z calculated for $C_{13}H_{13}NO_3S$ $(M)^+$: 263.0699; Found: 263.0748 $(M)^+$.

1-methyl-2-((4-nitrophenyl)sulfonyl)-1*H*-pyrrole (3i):

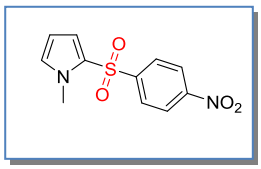

Following **GP-1**, **3i** was prepared from 4-nitrosulfonyl chloride **1i** (221 mg, 1.0 mmol, 1.00 equiv) and *N*-Methylpyrrole **2a** (122 mg, 133 µL, 1.50 mmol, 1.5 equiv). The crude product was purified by column chromatography (silica gel, hexanes–EtOAc, 4:1, R_f = 0.12) to afford **3i** as a pale yellow solid (213 mg, 80% yield).

^{1}H-NMR (300 MHz, $CDCl_3$): δ 8.36 – 8.30 (m, 2H), 8.09 – 8.03 (m, 2H), 7.11 (dd, *J* = 4.1, 1.9 Hz, 1H), 6.83 (t, *J* = 2.1 Hz, 1H), 6.23 (dd, *J* = 4.1, 2.6 Hz, 1H), 3.74 (s, 3H).

^{13}C-NMR (75 MHz, $CDCl_3$): δ 150.08, 148.03, 130.96, 128.42, 126.16, 124.55, 120.37, 109.17, 35.87.

IR (neat, cm^{-1}): 3102, 2924, 1702, 1605, 1527, 1462, 1395, 1343, 1291, 1223, 1162, 1126, 1076, 1009, 853, 763, 735, 679.

EI-MS: exact m/z calculated for $C_{11}H_{10}N_2O_4S$ $(M)^+$: 266.03558; Found: 266.03629 $(M)^+$.

Mp: 95-97°C (decomposed).

1-methyl-2-(methylsulfonyl)-1*H*-pyrrole (3j):

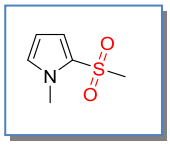

Following **GP-1**, **3j** was prepared from Methanesulfonylchloride **1j** (115 mg, 1.0 mmol, 1.00 equiv) and *N*-Methylpyrrole **2a** (122 mg, 133 µL, 1.50 mmol, 1.5 equiv). The crude product was purified by column chromatography (silica gel, hexanes–EtOAc, 4:1, R_f = 0.19) to afford **3j** as a pale yellow oil (116 mg, 73% yield).

^{1}H-NMR (400 MHz, $CDCl_3$): δ 6.90 (dd, *J* = 4.0, 1.9 Hz, 1H), 6.82 (t, *J* = 2.2 Hz, 1H), 6.18 (dd, *J* = 4.0, 2.6 Hz, 1H), 3.89 (s, 3H), 3.09 (s, 3H).

^{13}C-NMR (101 MHz, $CDCl_3$): δ 129.64, 128.28, 118.40, 108.47, 45.70, 35.89.

IR (neat, cm^{-1}): 2956, 2924, 1514, 1469, 1399, 1363, 1290, 1224, 1161, 1110, 1007, 952, 762, 738.

EI-MS: exact m/z calculated for $C_6H_9NO_2S$ $(M)^+$: 159.03485; Found: 159.03519 $(M)^+$.

1-phenyl-2-tosyl-1*H*-pyrrole (3k):

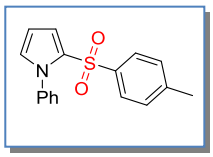

Following **GP-1**, **3k** was prepared from tosyl chloride **1b** (191 mg, 1.0 mmol, 1.00 equiv) and *N*-phenylpyrrole **2b** (214 mg, 1.50 mmol, 1.5 equiv). The crude product was purified by column chromatography (silica gel, hexanes–EtOAc, 4:1, R_f = 0.32) to afford **3k** as a white solid (208 mg, 70% yield).

^{1}H-NMR (300 MHz, $CDCl_3$): δ 7.42 – 7.32 (m, 2H), 7.32 – 7.18 (m, 4H), 7.15 (dt, *J* = 4.9, 2.5 Hz, 1H), 7.09 – 6.99 (m, 3H), 6.81 (dd, *J* = 4.7, 2.4 Hz, 1H), 6.26 (dt, *J* = 7.1, 3.6 Hz, 1H), 2.30 (s, 3H).

^{13}C-NMR (75 MHz, $CDCl_3$): δ 143.68, 138.79, 138.19, 130.83, 129.97, 129.37, 128.98, 128.63, 128.07, 127.79, 119.14, 108.84, 21.70.

IR (neat, cm^{-1}): 2921, 2852, 1738, 1719, 1495, 1441, 1391, 1304, 1287, 1209, 1168, 1138, 1088, 1076, 1034, 1018, 967, 814, 777, 757, 693, 667.

EI-MS: exact m/z calculated for $C_{17}H_{15}NO_2S$ $(M)^+$: 297.08180; Found: 297.08092 $(M)^+$.

Mp: 99-101 ^oC (decomposed).

2-tosylthiazole (3l):

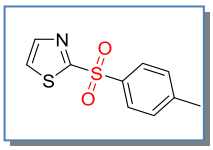

Following **GP-1**, **3l** was prepared from tosyl chloride **1b** (191 mg, 1.0 mmol, 1.00 equiv) and thiazole **2d** (128 mg, 1.50 mmol, 1.5 equiv). The crude product was purified by column chromatography (silica gel, hexanes–EtOAc, 4:1, R_f = 0.37) to afford **3l** as a white solid (186 mg, 78% yield).

^{1}H-NMR (300 MHz, $CDCl_3$): δ 7.98 (d, *J* = 8.4 Hz, 2H), 7.94 (d, *J* = 3.0 Hz, 1H), 7.65 (d, *J* = 3.0 Hz, 1H), 7.36 (d, *J* = 8.4 Hz, 2H), 2.42 (s, 2H).

^{13}C-NMR (75 MHz, $CDCl_3$): δ 166.66, 144.83, 144.39, 134.89, 129.30, 127.87, 124.86, 20.89.

The obtained data is in accordance with the literature data.[10]

1-(5-tosylthiophen-2-yl)ethan-1-one (3m):

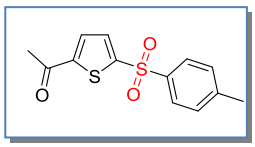

Following **GP-1**, **3m** was prepared from tosyl chloride **1b** (191 mg, 1.0 mmol, 1.00 equiv) and 1-(thiophen-2-yl)ethan-1-one **2c** (189 mg, 1.50 mmol, 1.5 equiv). The crude product was purified by column chromatography (silica gel, hexanes–EtOAc, 4:1, R_f = 0.16) to afford **3m** as a pale yellow solid (221 mg, 79% yield).

^{1}H-NMR (300 MHz, $CDCl_3$): δ 7.84 (d, *J* = 8.3 Hz, 2H), 7.60 (d, *J* = 4.0 Hz, 1H), 7.55 (d, *J* = 4.0 Hz, 1H), 7.31 (d, *J* = 8.1 Hz, 2H), 2.52 (s, 3H), 2.39 (s, 3H).

^{13}C-NMR (75 MHz, $CDCl_3$): δ 190.59, 150.25, 150.21, 145.28, 137.97, 132.79, 131.57, 130.28, 127.73, 26.94, 21.72.

The obtained data is in accordance with the literature data.[10]

3-isopropyl-1-methyl-2-tosyl-1*H*-indole (3n):

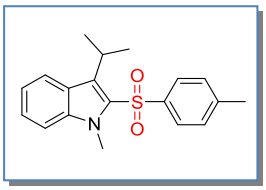

Following **GP-1**, **3n** was prepared from tosyl chloride **1b** (191 mg, 1.0 mmol, 1.00 equiv) and 3-isopropyl-1-methyl-1*H*-indole **2e** (259 mg, 1.50 mmol, 1.5 equiv). The crude product was purified by column chromatography (silica gel, hexanes–EtOAc, 9:1, R_f = 0.37) to afford **3n** as a viscous (sticky) white solid (251 mg, 77% yield).

^{1}H-NMR (300 MHz, $CDCl_3$): δ 7.92 (d, *J* = 8.2 Hz, 1H), 7.84 – 7.75 (m, 2H), 7.40 – 7.21 (m, 4H), 7.18 – 7.07 (m, 1H), 4.36 (hept, *J* = 7.1 Hz, 1H), 3.91 (s, 3H), 2.40 (s, 3H), 1.49 (d, *J* = 7.1 Hz, 6H).

^{13}C-NMR (75 MHz, $CDCl_3$): δ 144.22, 140.11, 139.10, 130.99, 130.03, 128.61, 126.78, 125.63, 124.62, 123.47, 120.03, 110.65, 31.90, 25.43, 23.11, 21.72.

IR (neat, cm^{-1}): 2960, 2929, 2872, 1732, 1596, 1509, 1460, 1367, 1327, 1299, 1180, 1155, 1089, 825, 744, 705, 687.

HRMS (ESI): exact m/z calculated for $C_{19}H_{21}NO_2S$ $(M+H)^+$: 328.1366; Found: 328.1368 $(M+H)^+$.

2-methyl-3-tosyl-1*H*-indole (3o):

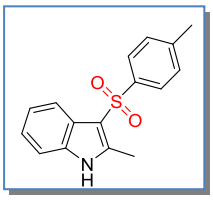

Following **GP-1**, **3o** was prepared from tosyl chloride **1b** (191 mg, 1.0 mmol, 1.00 equiv) and 2-methyl-1*H*-indole **2f** (196 mg, 1.50 mmol, 1.5 equiv). The crude product was purified by column chromatography (silica gel, hexanes–EtOAc, 4:1, R_f = 0.13) to afford **3o** as a brown solid (210 mg, 74% yield).

^{1}H-NMR (300 MHz, $CDCl_3$): δ 9.54 (s, 1H), 7.91 (d, *J* = 8.3 Hz, 2H), 7.62 (t, *J* = 8.4 Hz, 1H), 7.42 (d, *J* = 8.3 Hz, 1H), 7.33 (dd, *J* = 7.0, 1.1 Hz, 1H), 7.30 – 7.23 (m, 2H), 7.19 – 7.12 (m, 1H), 2.57 (s, 3H), 2.37 (s, 3H).

^{13}C-NMR (75 MHz, $CDCl_3$): δ 144.41, 139.06, 136.16, 130.04, 129.47, 128.28, 127.04, 126.12, 120.70, 118.51, 112.50, 21.66, 9.04.

IR (neat, cm^{-1}): 3285, 2922, 2853, 1594, 1582, 1537, 1493, 1451, 1410, 1386, 1281, 1141, 1121, 1099, 1067, 1012, 925, 809, 735, 685, 657.

Mp: 160-162 ^{o}C (decomposed).

The obtained data is in accordance with the literature data.[13]

5-chloro-2-methyl-3-(phenylsulfonyl)-1*H*-indole (3p):

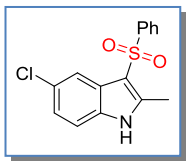

Following **GP-1**, **3p** was prepared from benzenesulfonylchloride **1a** (176 mg, 1.0 mmol, 1.00 equiv) and 5-chloro-2-methyl-1*H*-indole **2g** (247 mg, 1.50 mmol, 1.5 equiv). The crude product was purified by column chromatography (silica gel, hexanes–EtOAc, 5:1, R_f = 0.25) to afford **3p** as a white solid (219 mg, 72% yield).

^{1}H-NMR (300 MHz, $CDCl_3$): δ 9.41 (s, 1H), 8.01 – 7.90 (m, 3H), 7.55 – 7.41 (m, 3H), 7.19 (d, *J* = 8.6 Hz, 1H), 7.11 (dd, *J* = 8.6, 2.0 Hz, 1H), 2.65 (s, 3H).

^{13}C-NMR (75 MHz, $CDCl_3$): δ 143.64, 143.05, 132.96, 132.94, 129.38, 128.27, 126.51, 126.11, 123.74, 118.84, 112.62, 110.90, 13.17.

IR (neat, cm^{-1}): 3290, 1529, 1575, 1446, 1400, 1281, 1143, 1107, 1069, 1020, 999, 946, 870, 804, 735, 712, 686.

Mp: 179-181 ^{o}C (decomposed).

The obtained data is in accordance with the literature data.[29]

3-isopropyl-2-((4-methoxyphenyl)sulfonyl)-1-methyl-1H-indole (3q):

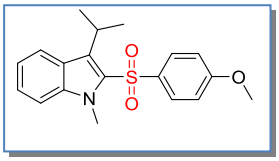

Following GP-1, **3q** was prepared from 4-methoxybenzenesulfonyl chloride **1c** (206 mg, 1.0 mmol, 1.00 equiv) and 3-isopropyl-1-methyl-1*H*-indole **2e** (259 mg, 1.50 mmol, 1.5 equiv). The crude product was purified by column chromatography (silica gel, hexanes–EtOAc, 9:1, R_f = 0.14) to afford **3q** as a viscous (sticky) white solid (253 mg, 74% yield).

^{1}H-NMR (300 MHz, $CDCl_3$): δ 7.89 – 7.84 (m, 1H), 7.82 – 7.74 (m, 2H), 7.32 – 7.21 (m, 2H), 7.12 – 7.03 (m, 1H), 6.95 – 6.88 (m, 2H), 4.30 (hept, *J* = 7.1 Hz, 1H), 3.86 (s, 3H), 3.79 (s, 3H), 1.43 (d, *J* = 7.1 Hz, 6H).

^{13}C-NMR (75 MHz, $CDCl_3$): δ 163.38, 139.12, 134.69, 130.51, 129.02, 125.56, 124.65, 123.47, 120.01, 114.61, 110.63, 55.85, 31.89, 25.44, 23.15.

IR (neat, cm^{-1}): 2958, 2922, 2869, 2850, 1733, 1592, 1577, 1495, 1459, 1365, 1323, 1295, 1258, 1178, 1148, 1129, 1088, 1021, 821, 801, 741, 686, 653; $C_{19}H_{21}NO_3S$ $(M+H)^+$: 344.1315; Found: 344.1318 $(M+H)^+$.

The obtained data is in accordance with the literature data.[30]

9.9.3 General Procedure (GP-2) for C, H-Arylation:

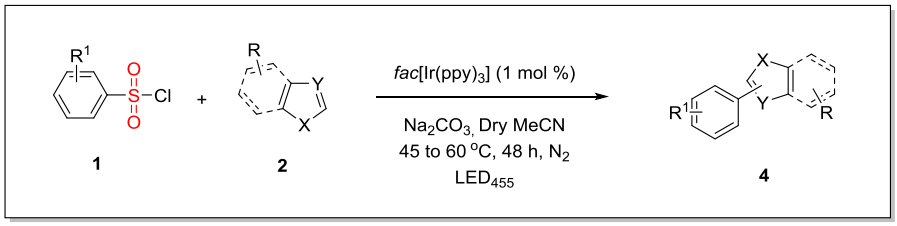

An oven dried 10 mL Schleck flask was charged with **1** (1.0 mmol, 1.00 equiv), Na_2CO_3 (159 mg, 1.50 mmol, 1.00 equiv), and *fac*[Ir(ppy)$_3$] (6.54 mg, 0.01 equiv, 1.00 mol %) in 3.0 mL dry MeCN. The resulting suspension was deoxygenated by three freeze-pump-thaw cycles. Then desired heterocyclic compound **2** (1.50 mmol, 1.5 equiv) was added under positive nitrogen atmosphere). The reaction mixture was exposed to the blue light emitting diode (LED, λ_{max} = 455 nm) at 45 (or 60 ^{o}C) for 48 h. After complete conversion of aryl sulfonyl chloride (judged by TLC), the reaction mixture was saturated by addition of brine solution (20 mL). The aqueous phase was washed with ethyl acetate (3 x 20 mL). The combined organic fractions were dried over Na_2SO_4, concentrated *in vacuo*, and the crude residue was purified by column chromatography on silica gel by using hexanes and ethyl acetate as eluents to afford the pure product **4**.

1-methyl-2-phenyl-1*H*-pyrrole (4a):

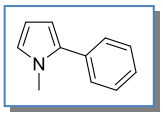

Following **GP-2**, **4a** was prepared from benzenesulfonylchloride **1a** (176 mg, 1.0 mmol, 1.00 equiv) and *N*-Methylpyrrole **2a** (122 mg, 133 µL, 1.50 mmol, 1.5 equiv). The crude product was purified by column chromatography (silica gel, hexanes–EtOAc, 3:1, R_f = 0.35) to afford **4a** as a colorless solid (117 mg, 75% yield).

^{1}H-NMR (300 MHz, $CDCl_3$): δ 7.53 – 7.41 (m, 5H), 6.83 – 6.72 (m, 1H), 6.34 – 6.30 (m, 1H), 6.30 – 6.25 (m, 1H), 3.72 (s, 3H).

^{13}C-NMR (75 MHz, $CDCl_3$): δ 134.72, 133.48, 128.77, 128.49, 126.86, 123.78, 108.78, 107.90, 35.17.

The obtained data is in accordance with the literature data.[14,26]

1-methyl-2-(*p*-tolyl)-1*H*-pyrrole (4b):

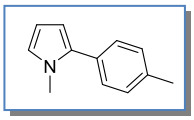

Following **GP-2**, **4b** was prepared from tosyl chloride **1b** (191 mg, 1.0 mmol, 1.00 equiv) and *N*-Methylpyrrole **2a** (122 mg, 133 µL, 1.50 mmol, 1.5 equiv). The crude product was purified by column chromatography (silica gel, hexanes–EtOAc, 3:1, R_f = 0.37) to afford **4b** as a pale yellow oil (119 mg, 70% yield).

^{1}H-NMR (300 MHz, $CDCl_3$): δ 7.76 – 7.70 (m, 2H), 7.25 (m, 2H), 6.97 – 6.88 (m, 1H), 6.72 (t, *J* = 4.7 Hz, 1H), 6.29 (dd, *J* = 4.2, 2.6 Hz, 1H), 3.97 (s, 3H), 2.42 (s, 3H).
^{13}C-NMR (75 MHz, $CDCl_3$): δ 151.82, 146.59, 139.81, 129.78, 126.59, 122.13, 110.20, 99.69, 33.54, 21.56.
The obtained data is in accordance with the literature data.[14,26]

2-(4-methoxyphenyl)-1-methyl-1*H*-pyrrole (4c):

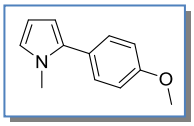

Following **GP-2**, **4c** was prepared from 4-methoxybenzenesulfonyl chloride **1c** (206 mg, 1.0 mmol, 1.00 equiv) and *N*-Methylpyrrole **2a** (122 mg, 133 µL, 1.50 mmol, 1.5 equiv). The crude product was purified by column chromatography (silica gel, hexanes–EtOAc, 3:1, R_f = 0.32) to afford **4c** as a pale yellow oil (153 mg, 82% yield).

^{1}H-NMR (300 MHz, $CDCl_3$): δ 7.87 – 7.73 (m, 2H), 7.04 – 6.93 (m, 2H), 6.93 – 6.86 (m, 1H), 6.67 (dd, *J* = 4.1, 1.5 Hz, 1H), 6.28 (dd, *J* = 4.2, 2.6 Hz, 1H), 3.95 (s, 3H), 3.87 (s, 3H).
^{13}C-NMR (75 MHz, $CDCl_3$): δ 160.97, 148.01, 146.54, 126.26, 123.80, 114.34, 110.11, 99.22, 55.74, 33.52.
The obtained data is in accordance with the literature data.[14,26]

2-(4-fluorophenyl)-1-methyl-1*H*-pyrrole (4d):

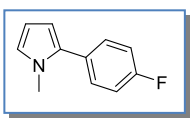

Following **GP-2**, **4d** was prepared from 4-fluorobenzenesulfonyl chloride **1d** (194 mg, 1.0 mmol, 1.00 equiv) and *N*-Methylpyrrole **2a** (122 mg, 133 µL, 1.50 mmol, 1.5 equiv). The crude product was purified by column chromatography (silica gel, hexanes–EtOAc, 3:1, R_f = 0.39) to afford **4d** as a white solid (138 mg, 79% yield).

^{1}H-NMR (300 MHz, $CDCl_3$): δ 7.39 – 7.28 (m, 2H), 7.13 – 7.02 (m, 2H), 6.69 (t, *J* = 2.2 Hz, 1H), 6.22 – 6.13 (m, 2H), 3.61 (s, 3H).

^{3}C-NMR (75 MHz, $CDCl_3$): δ 162.08 (d, *J* = 246.3 Hz), 133.70, 130.50 (d, *J* = 8.0 Hz), 129.61 (d, *J* = 3.3 Hz), 123.70, 115.46 (d, *J* = 21.4 Hz), 108.78, 107.91, 35.08.

^{19}F-NMR (282 MHz, $CDCl_3$): δ -116.05.

The obtained data is in accordance with the literature data.[14,26]

1-(4-(1-methyl-1*H*-pyrrol-2-yl)phenyl)ethan-1-one (4h):

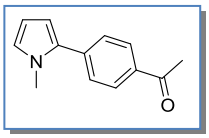

Following **GP-2**, **4h** was prepared from 4-acetylbenzenesulfonyl chloride **1h** (219 mg, 1.0 mmol, 1.00 equiv) and *N*-Methylpyrrole **2a** (122 mg, 133 µL, 1.50 mmol, 1.5 equiv). The crude product was purified by column chromatography (silica gel, hexanes–EtOAc, 3:1, R_f = 0.29) to afford **4h** as a brown solid (145 mg, 73% yield).

^{1}H-NMR (300 MHz, $CDCl_3$): δ 8.08 – 7.87 (m, 2H), 7.59 – 7.43 (m, 2H), 6.77 (dd, *J* = 7.7, 5.2 Hz, 1H), 6.35 (dt, *J* = 5.8, 2.9 Hz, 1H), 6.29 – 6.15 (m, 1H), 3.73 (s, 3H), 2.63 (s, 3H).

^{13}C-NMR (75 MHz, $CDCl_3$): δ 197.78, 138.07, 135.06, 133.56, 128.76, 128.11, 125.49, 110.38, 108.52, 35.62, 26.76.

The obtained data is in accordance with the literature data.[28]

1-methyl-2-(4-nitrophenyl)-1*H*-pyrrole (4i):

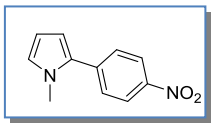

Following **GP-2**, **4i** was prepared from 4-nitrosulfonyl chloride **1i** (221 mg, 1.0 mmol, 1.00 equiv) and *N*-Methylpyrrole **2a** (122 mg, 133 µL, 1.50 mmol, 1.5 equiv). The crude product was purified by column chromatography (silica gel, hexanes–EtOAc, 3:1, R_f = 0.30) to afford **4i** as a pale yellow solid (153 mg, 76% yield).

^{1}H-NMR (300 MHz, $CDCl_3$): δ 8.32 – 8.12 (m, 2H), 7.58 – 7.43 (m, 2H), 6.85 – 6.68 (m, 1H), 6.39 (dd, *J* = 3.7, 1.8 Hz, 1H), 6.22 (dd, *J* = 3.7, 2.7 Hz, 1H), 3.72 (s, 3H).

^{13}C-NMR (75 MHz, $CDCl_3$): δ 144.92, 138.74, 131.35, 127.07, 125.60, 123.01, 110.53, 107.88, 34.73.

The obtained data is in accordance with the literature data.[14,26]

3-isopropyl-1-methyl-2-(*p*-tolyl)-1*H*-indole (4n):

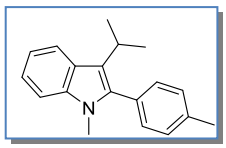

Following **GP-2**, **4n** was prepared from tosyl chloride **1b** (191 mg, 1.0 mmol, 1.00 equiv) and 3-isopropyl-1-methyl-1*H*-indole **2e** (259 mg, 1.50 mmol, 1.5

equiv). The crude product was purified by column chromatography (silica gel, hexanes–EtOAc, 95:05, R_f = 0.70) to afford **4n** as a colorless solid (186 mg, 71% yield).

^{1}H-NMR (300 MHz, $CDCl_3$): δ 7.90 – 7.83 (m, 1H), 7.41 – 7.25 (m, 6H), 7.18 (ddd, *J* = 8.0, 7.0, 1.1 Hz, 1H), 3.58 (s, 3H), 94 – 3.04 (m, 1H), 2.51 (s, 3H), 1.46 (d, *J* = 7.1 Hz, 6H).
^{13}C-NMR (75 MHz, $CDCl_3$): δ 137.98, 137.52, 136.76, 130.90, 129.71, 129.16, 126.22, 121.34, 120.59, 119.34, 118.82, 109.65, 30.76, 26.55, 23.64, 21.54.
IR (neat, cm^{-1}): 2962, 2921, 2868, 1460, 1428, 1400, 1362, 1338, 1314, 1248, 1221, 1125, 1014, 990, 827, 703.
EI-MS: exact m/z calculated for $C_{19}H_{21}N$ $(M)^+$: 263.16685; Found: 263.16657 $(M)^+$.
Mp: 89-91 ^oC (decomposed).

2-methyl-3-(*p*-tolyl)-1*H*-indole (4o):

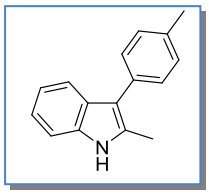

Following **GP-2**, **4o** was prepared from tosyl chloride **1b** (191 mg, 1.0 mmol, 1.00 equiv) and 2-methyl-1*H*-indole **2f** (196 mg, 1.50 mmol, 1.5 equiv). The crude product was purified by column chromatography (silica gel, hexanes–EtOAc, 9:1, R_f = 0.25) to afford **4o** as a brown solid (166 mg, 75% yield).

^{1}H-NMR (300 MHz, $CDCl_3$): δ 8.16 (bs, 1H), 7.64 – 7.53 (m, 1H), 7.38 – 7.28 (m, 1H), 7.29 – 7.10 (m, 2H), 6.99 (s, 4H), 2.51 (s, 3H), 2.27 (s, 3H).
^{13}C-NMR (75 MHz, $CDCl_3$): δ 141.12, 135.81, 135.54, 134.46, 130.45, 129.64, 125.88, 122.25, 120.78, 119.12, 110.78, 99.90, 21.00, 12.27.
The obtained data is in accordance with the literature data.[31]

9.10 NMR spectra:

^{1}H-NMR: **3a**

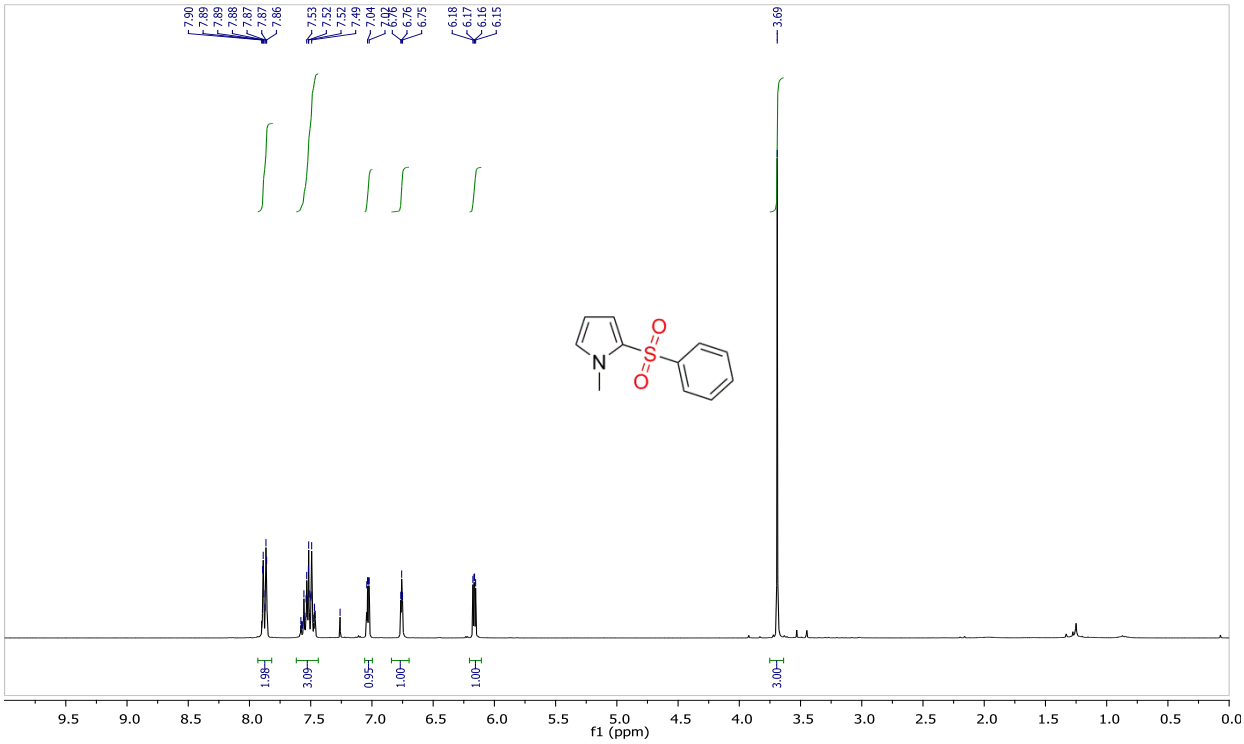

^{13}C-NMR: **3a**

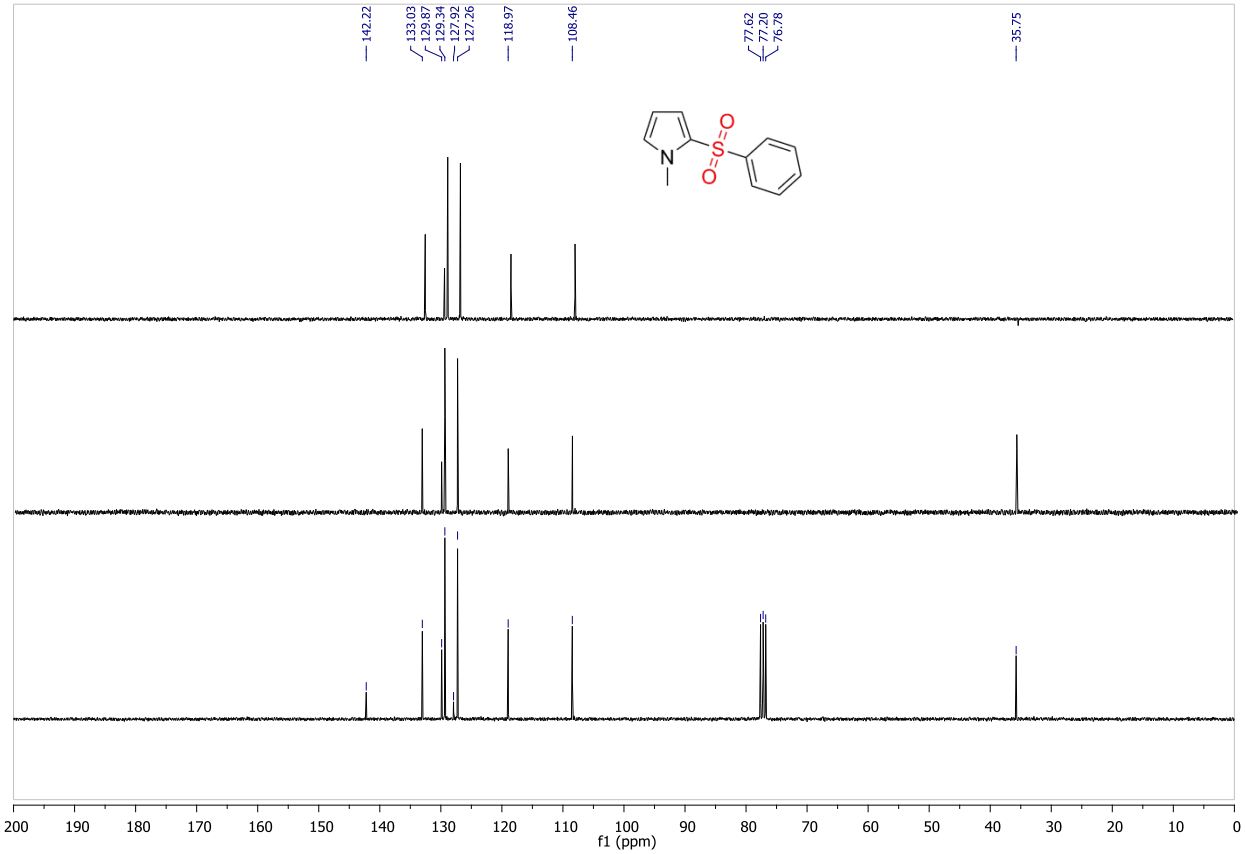

^{1}H-NMR: **3b**

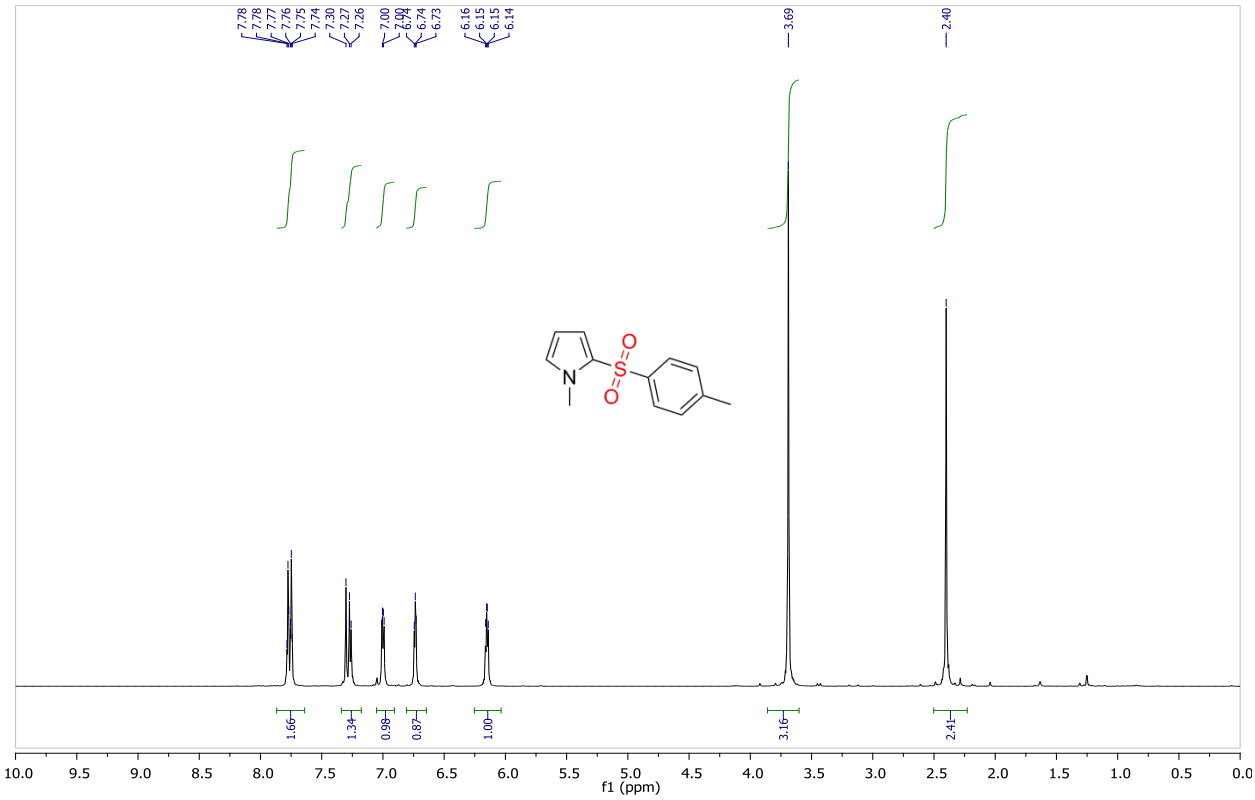

^{13}C-NMR: **3b**

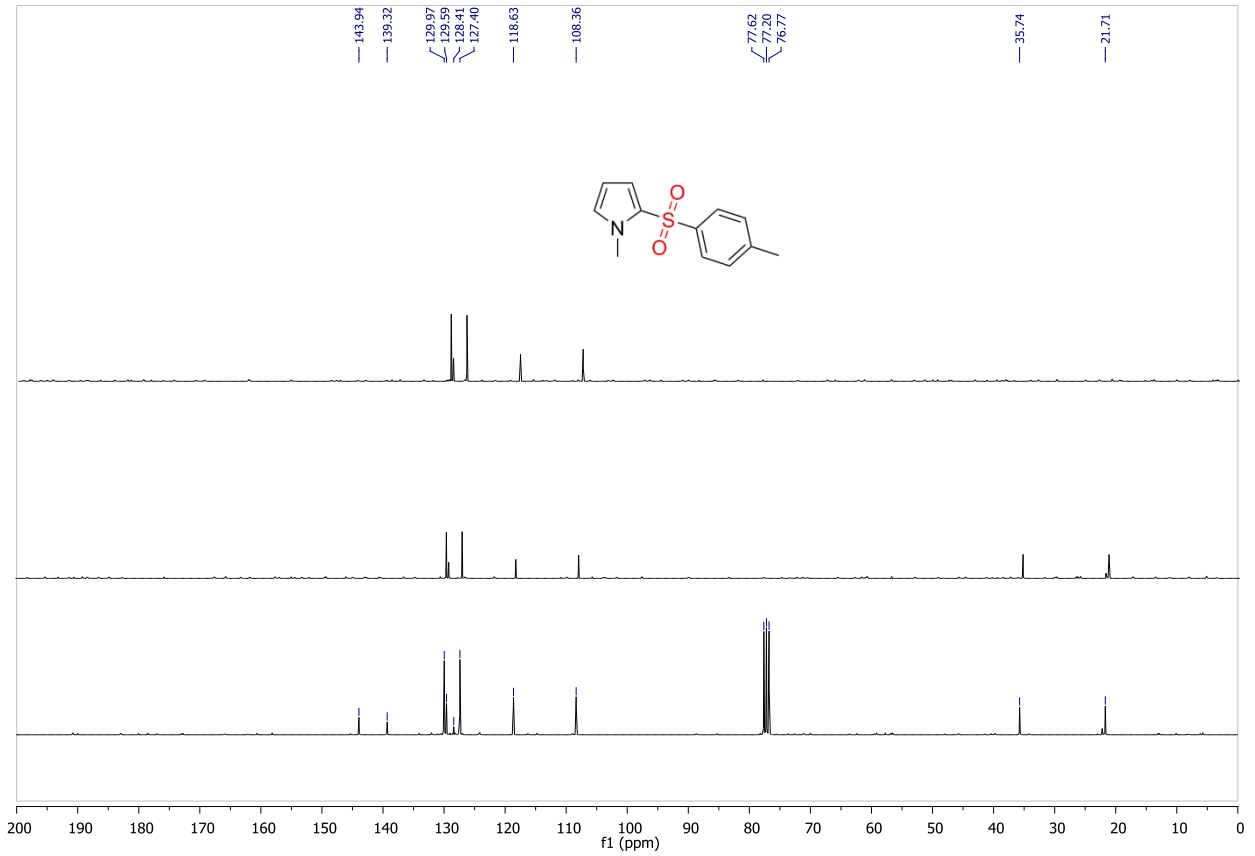

^{1}H-NMR: **3c**

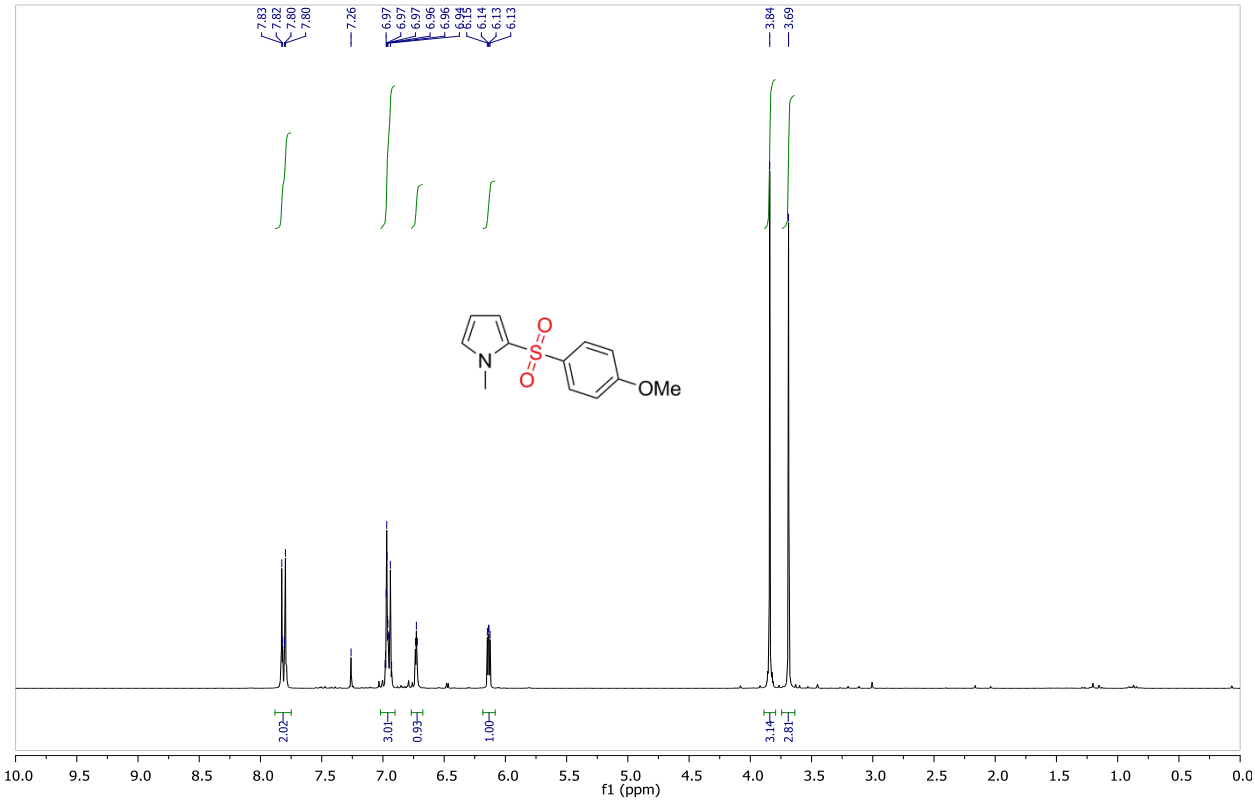

^{13}C-NMR: **3c**

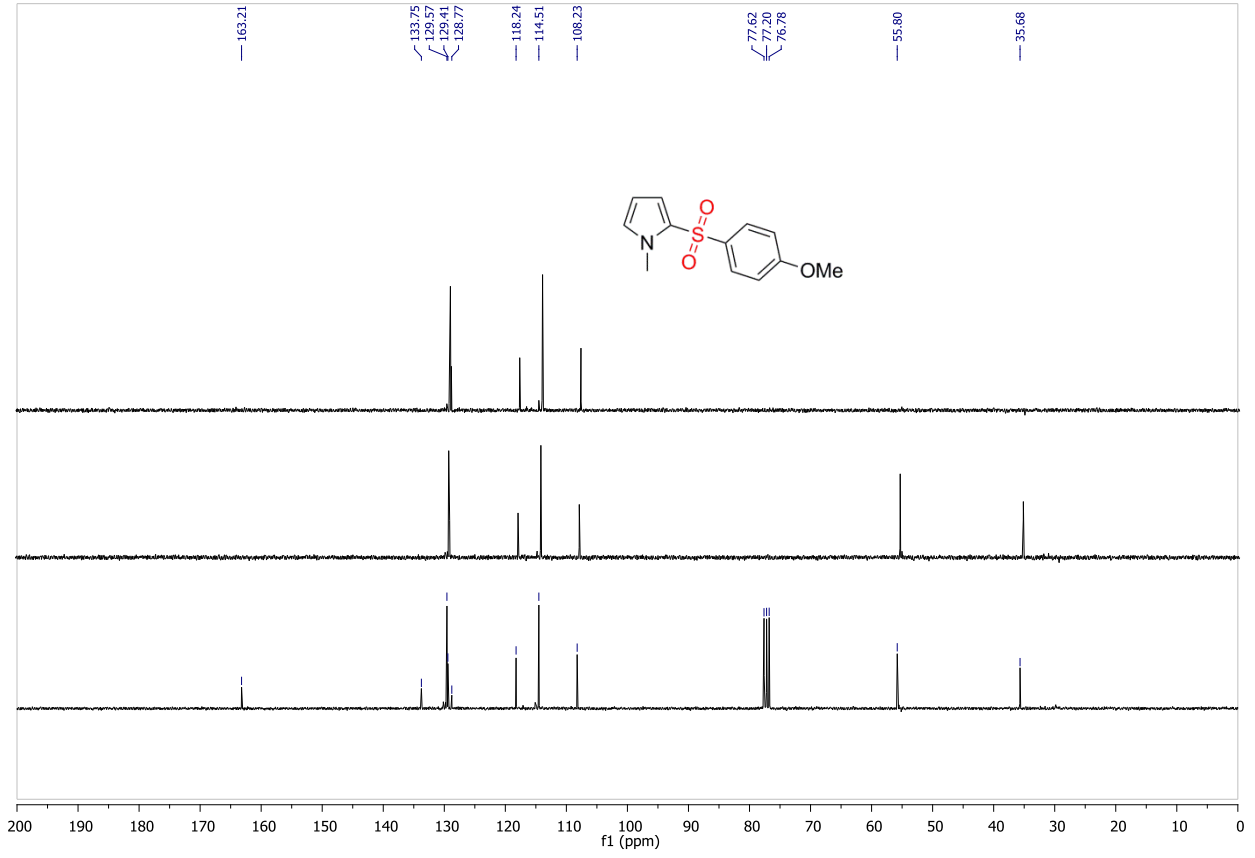

^{1}H-NMR: **3d**

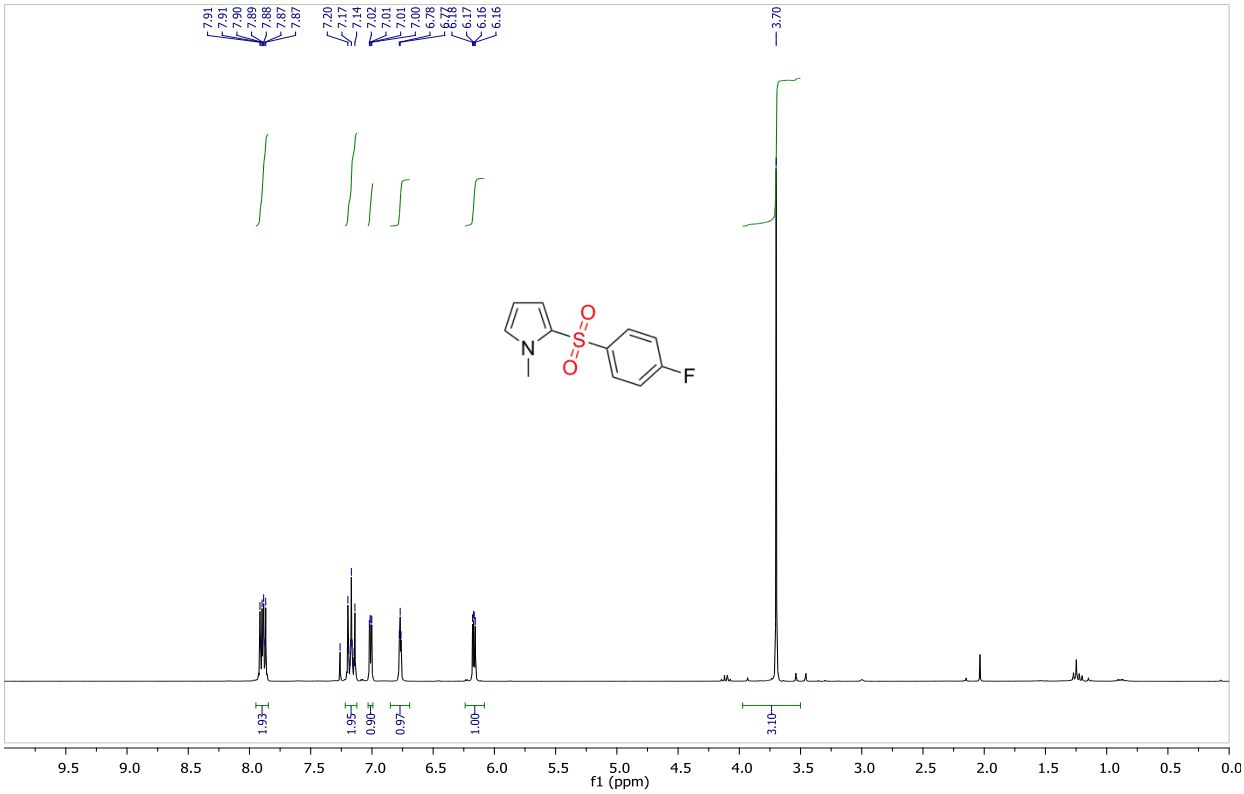

^{13}C-NMR: **3d**

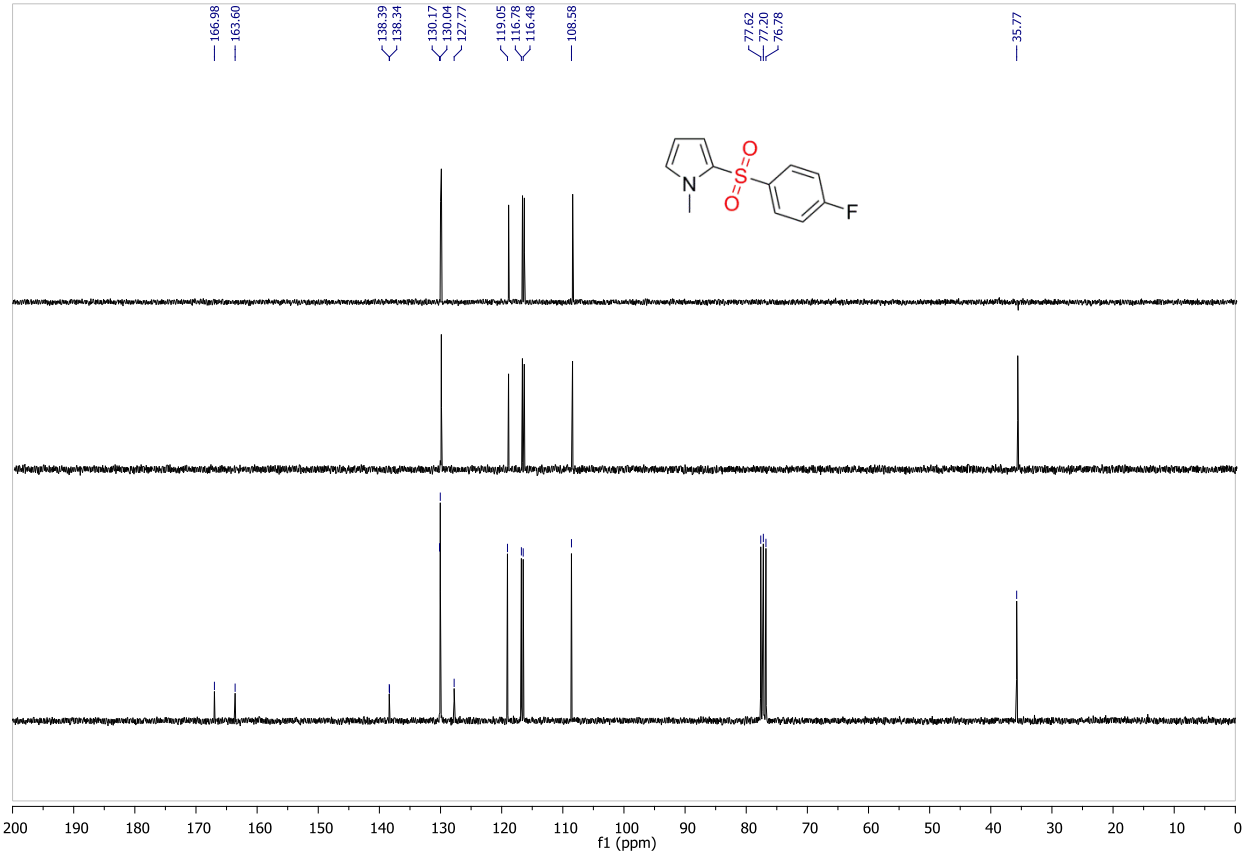

^{19}F-NMR: **3d**

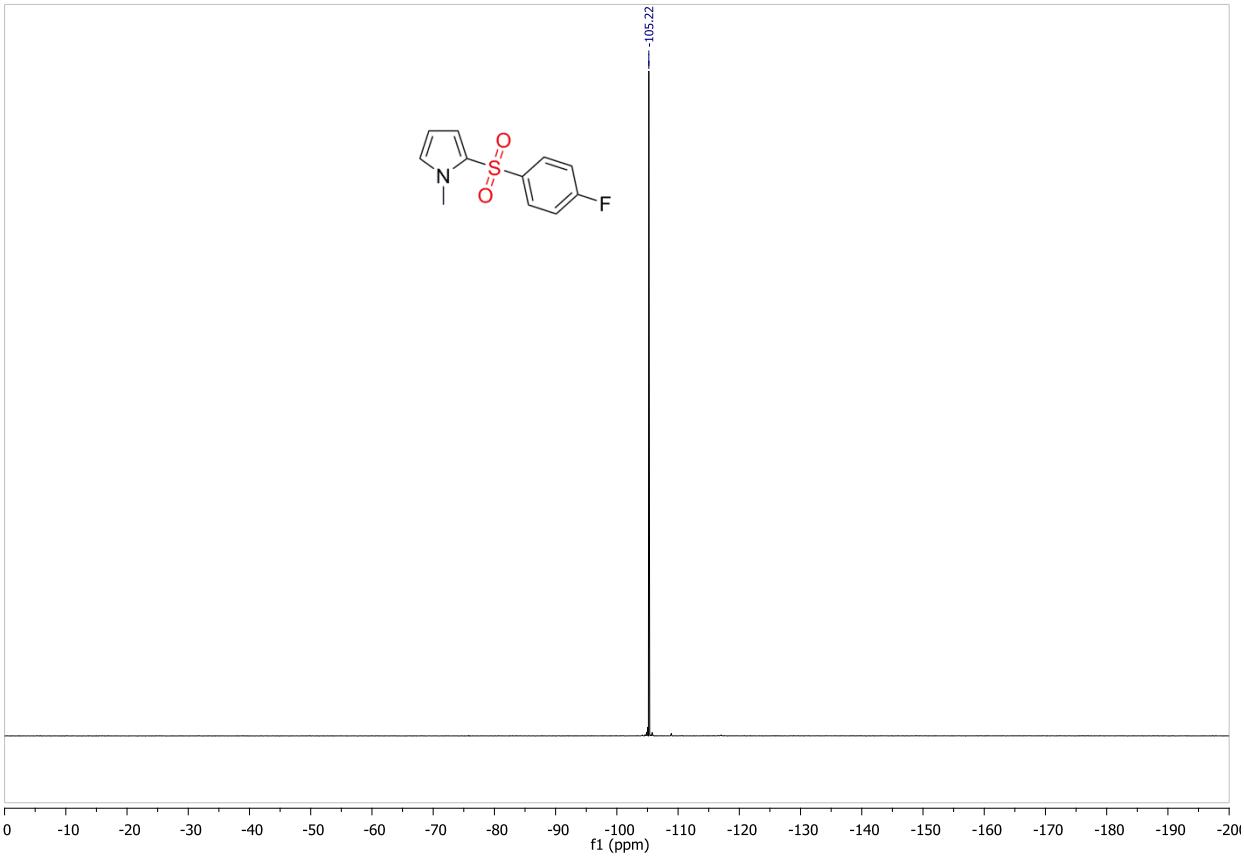
-105.22
O
S
O
N
F
0
-10
-20
-30
-40
-50
-60
-70
-80
-90
-100
-110
-120
-130
-140
-150
-160
-170
-180
-190
f1 (ppm)

^{1}H-NMR: **3e**

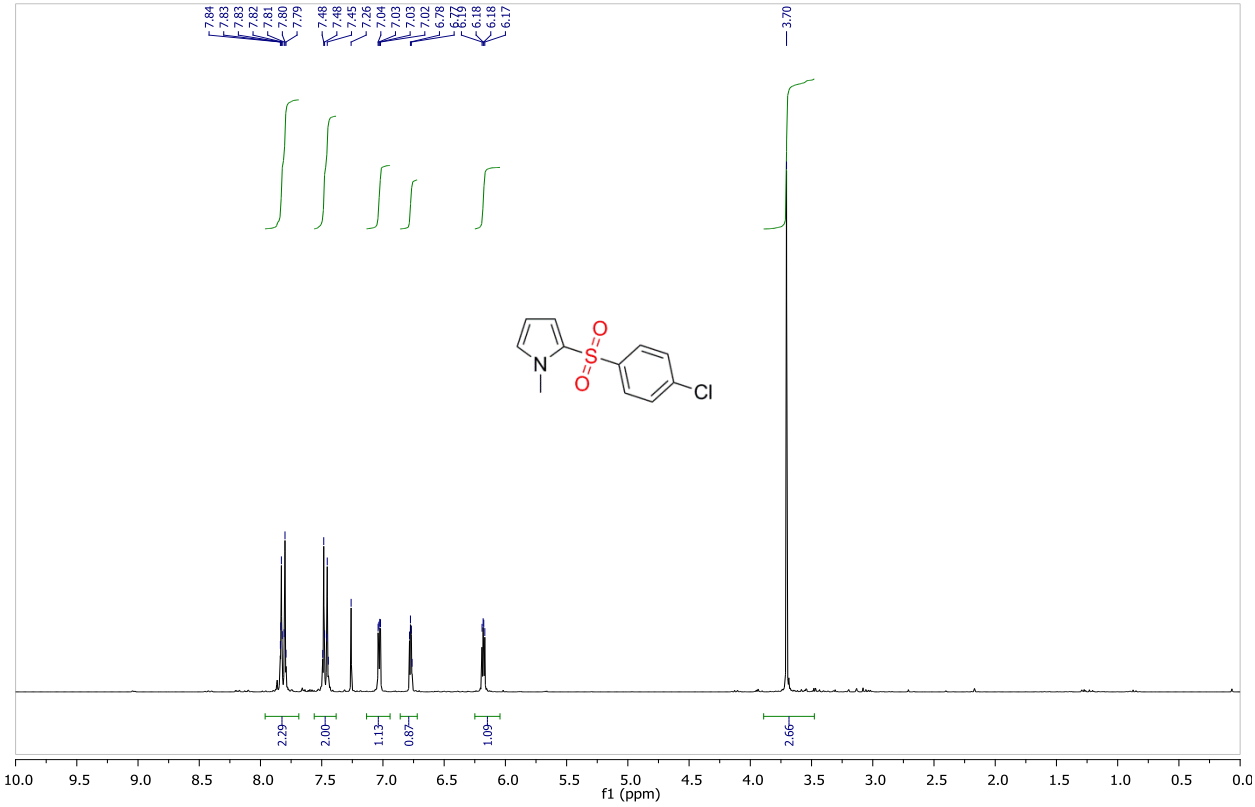

^{13}C-NMR: **3e**

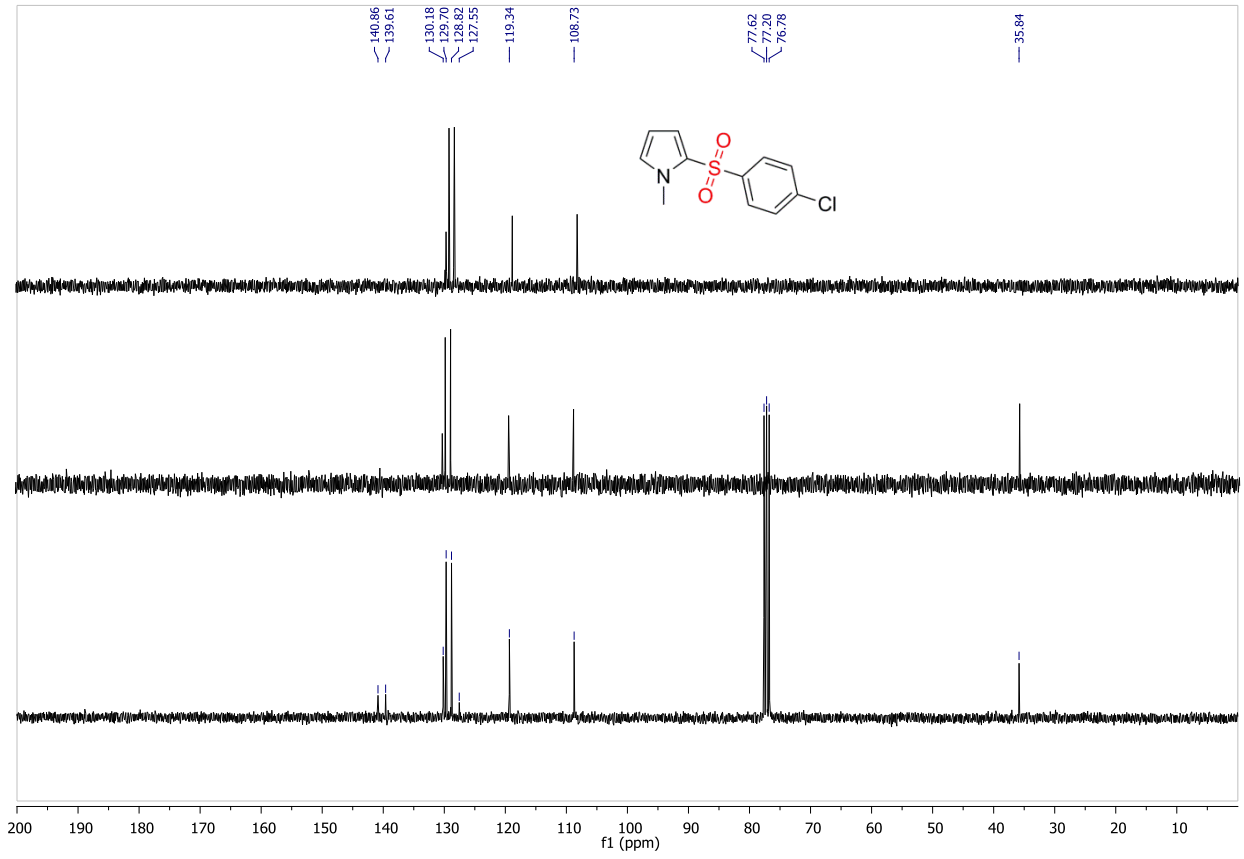

^{1}H-NMR: **3f**

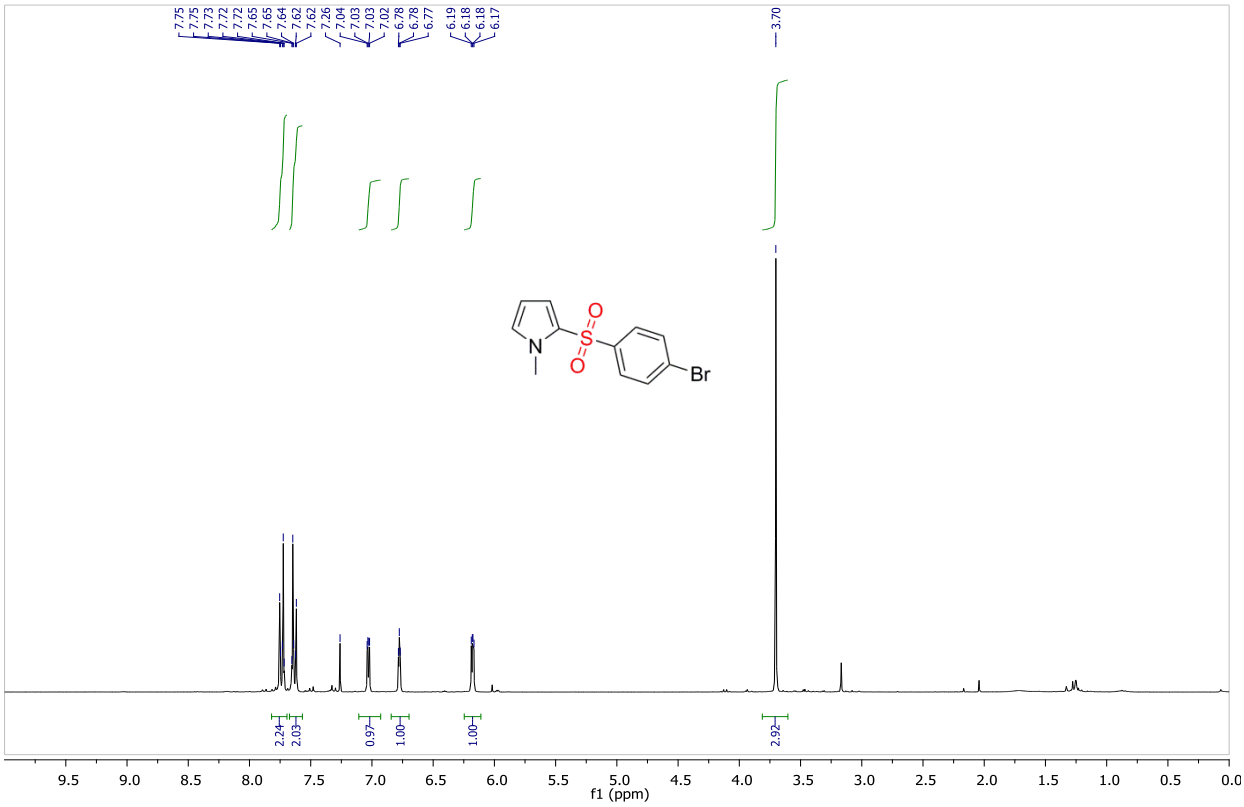

^{13}C-NMR: **3f**

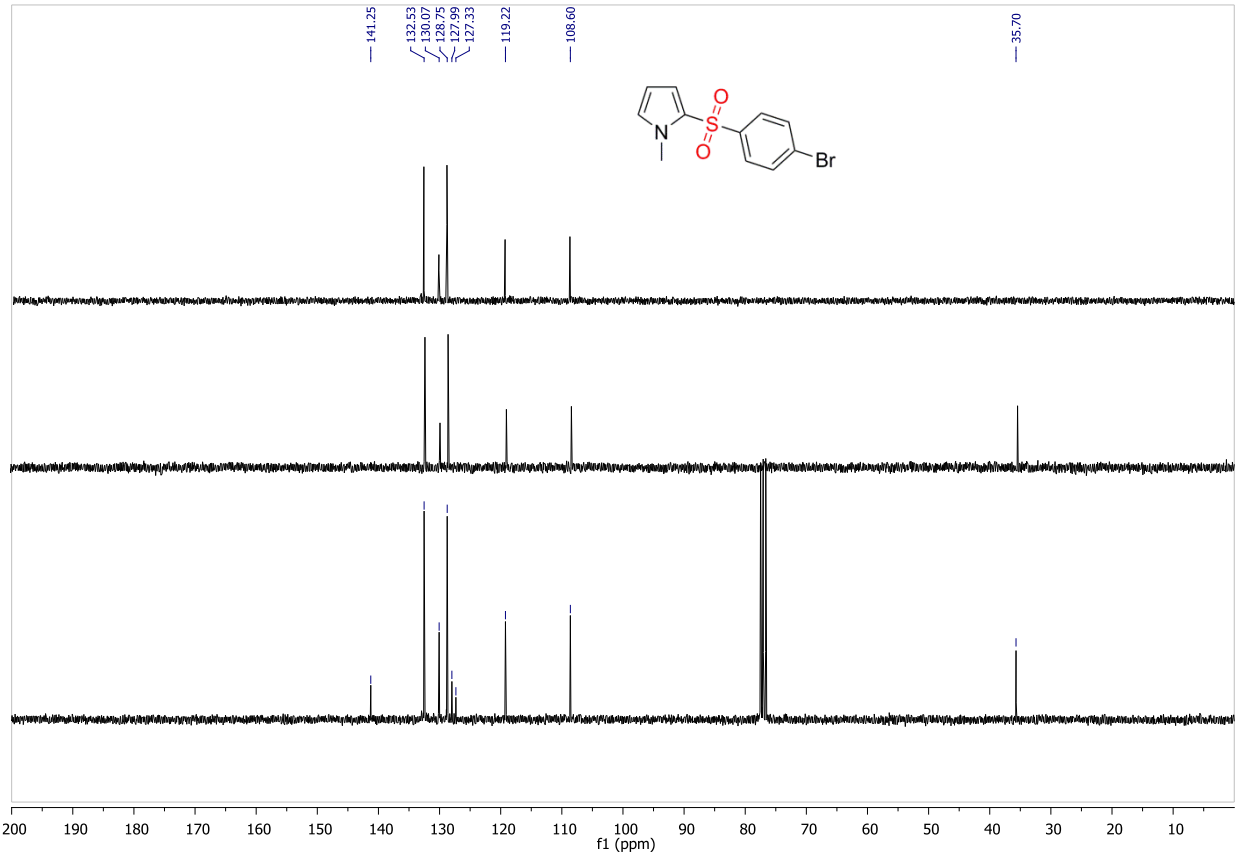

^{1}H-NMR: **3g**

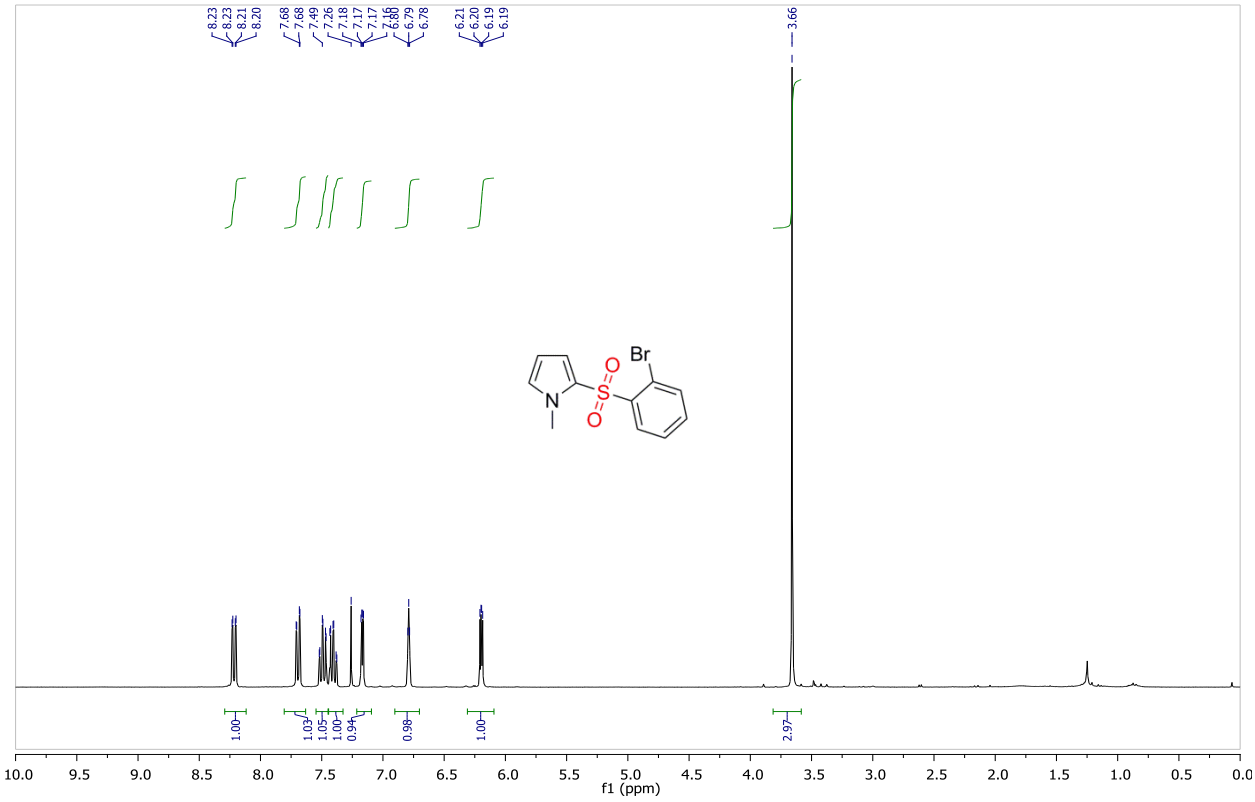

^{13}C-NMR: **3g**

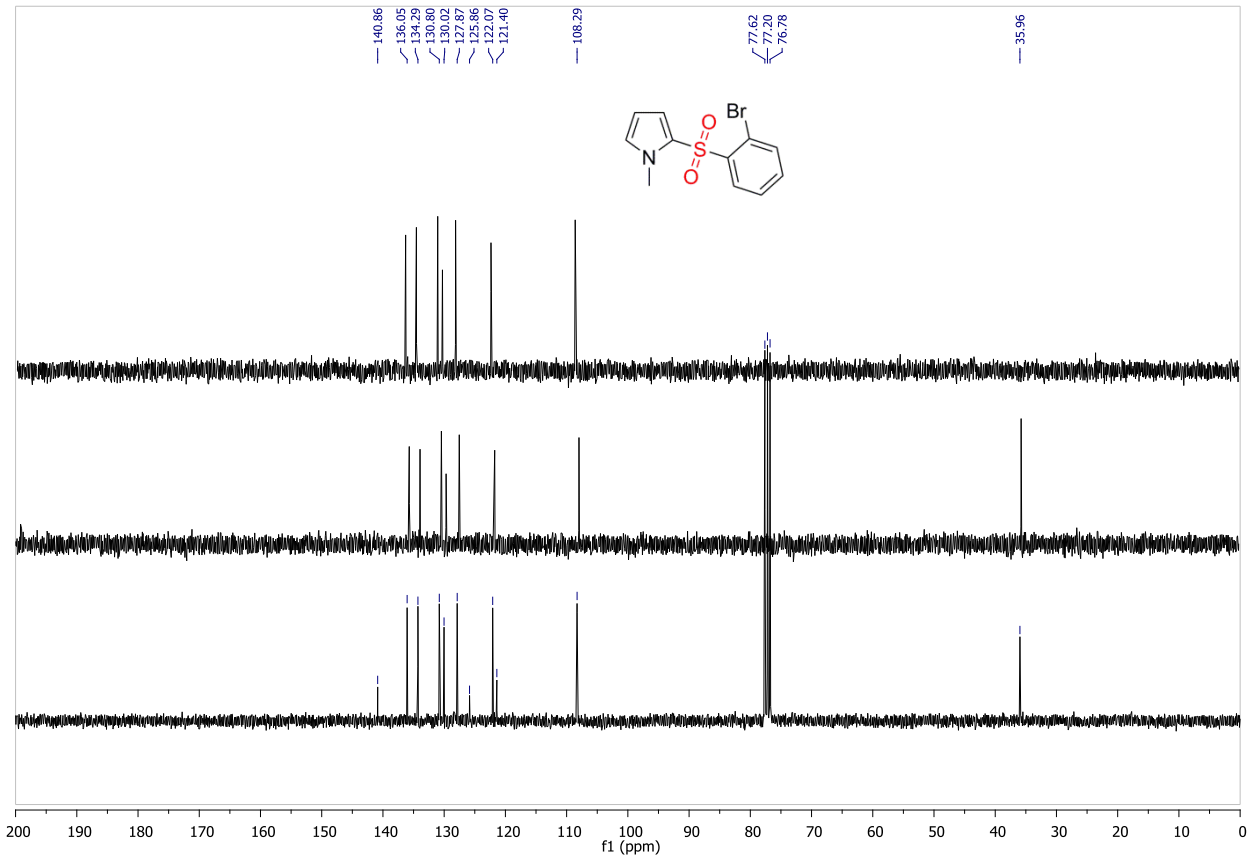

^{1}H-NMR: **3h**

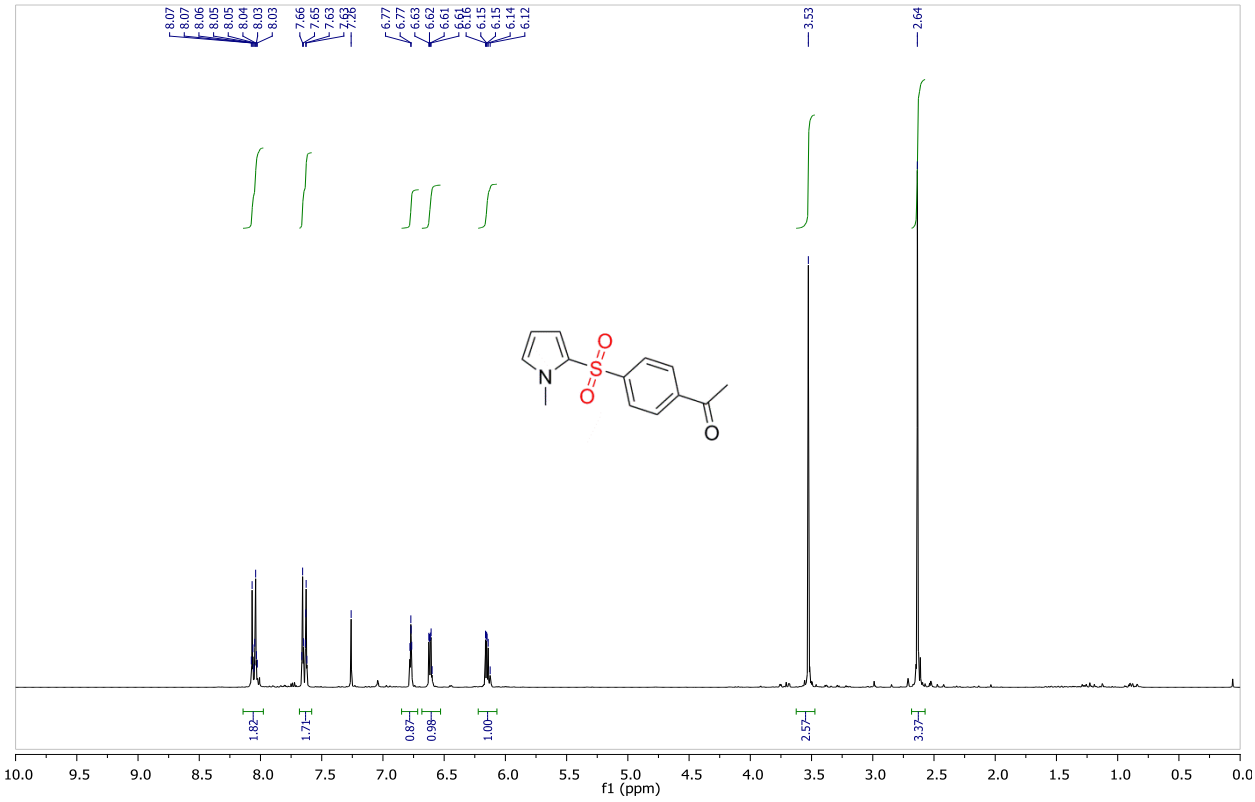

^{13}C-NMR: **3h**

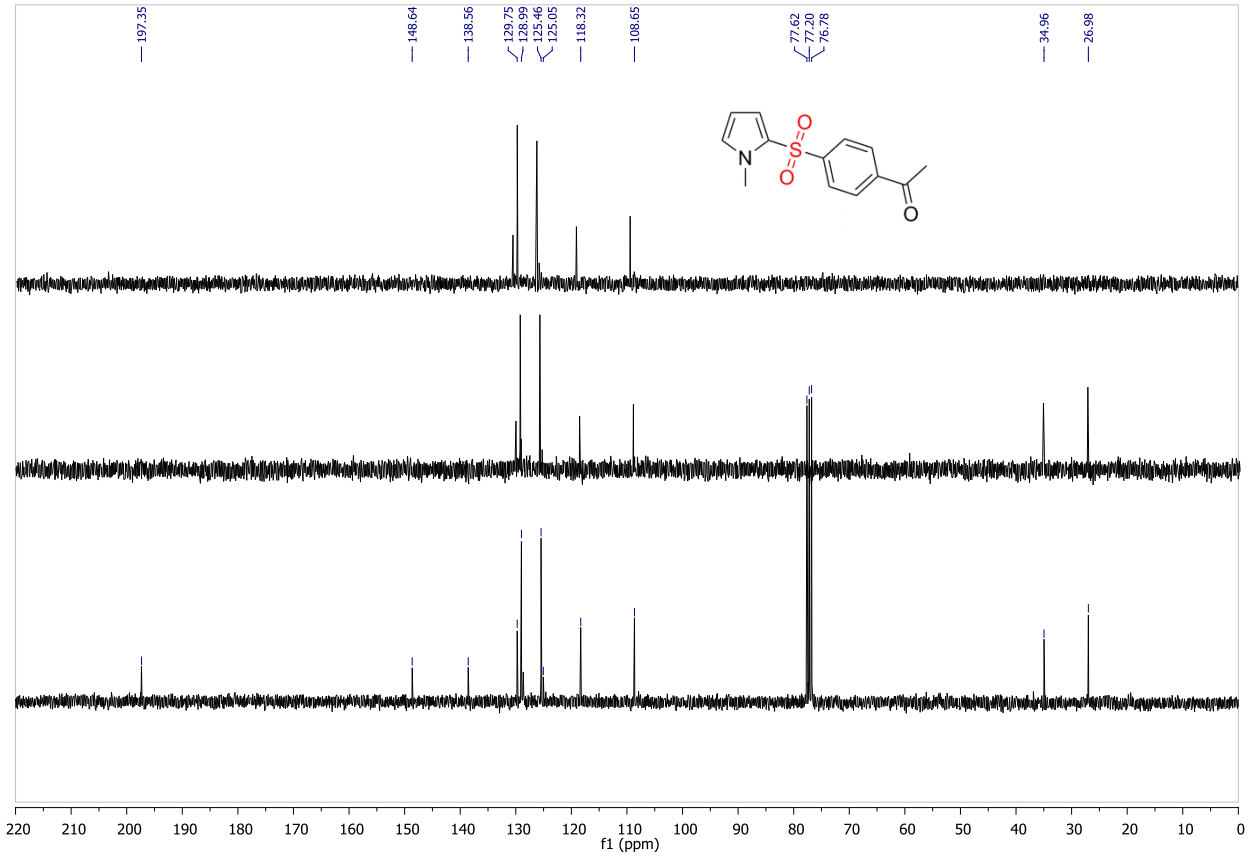

^{1}H-NMR: **3i**

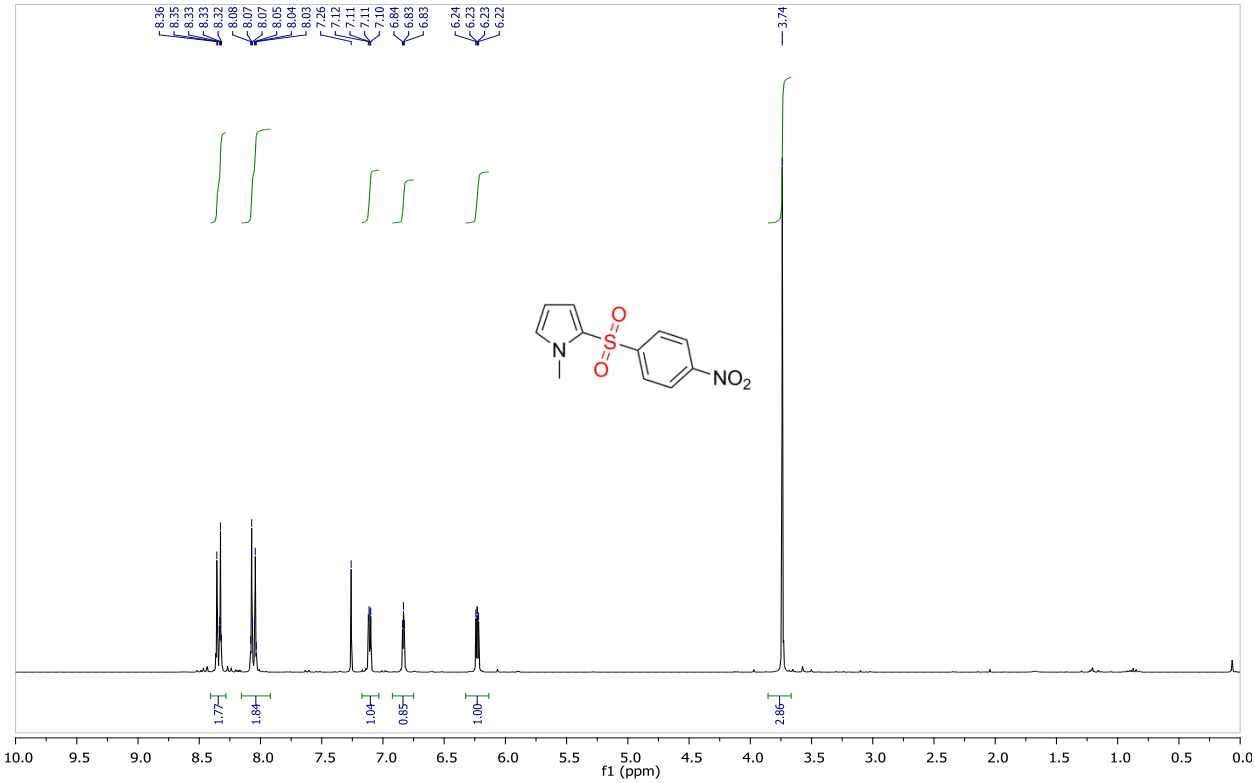

^{13}C-NMR: **3i**

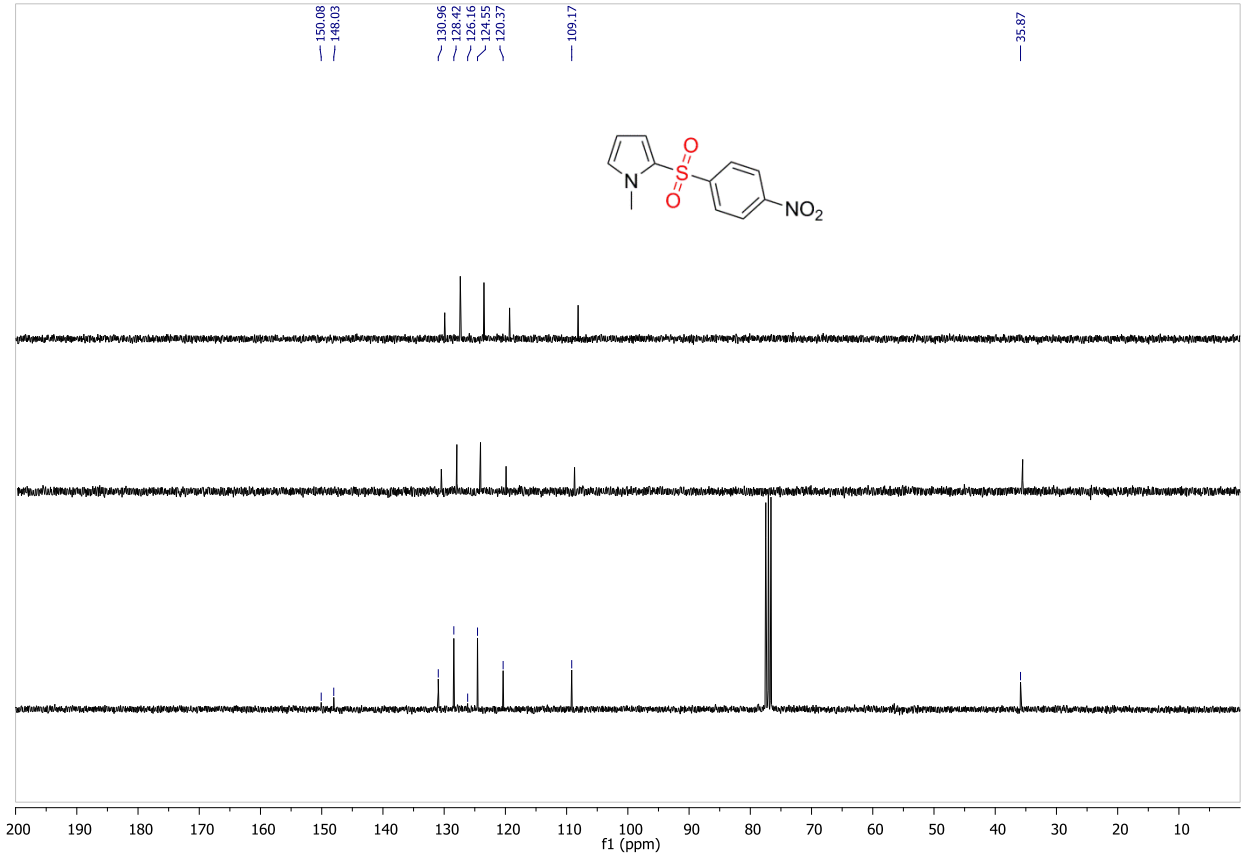

^{1}H-NMR: **3j**

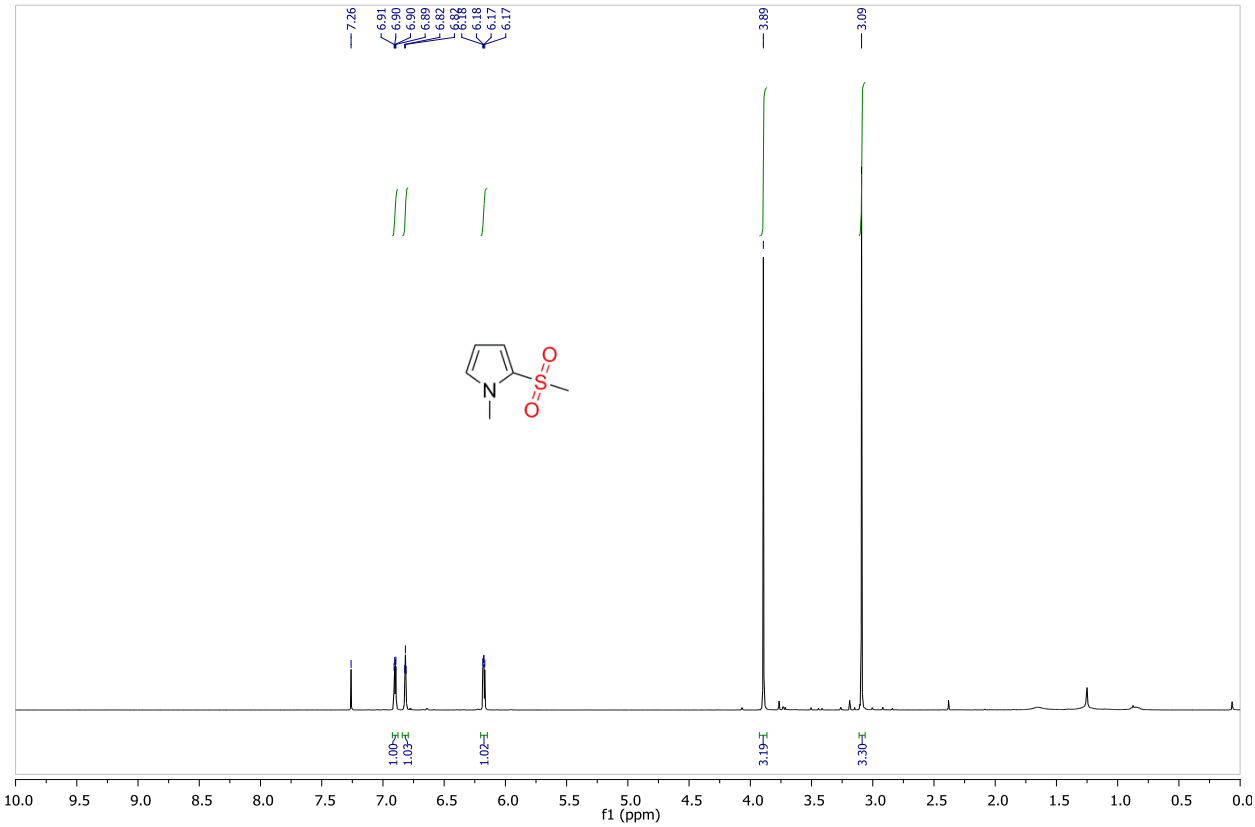

^{13}C-NMR: **3j**

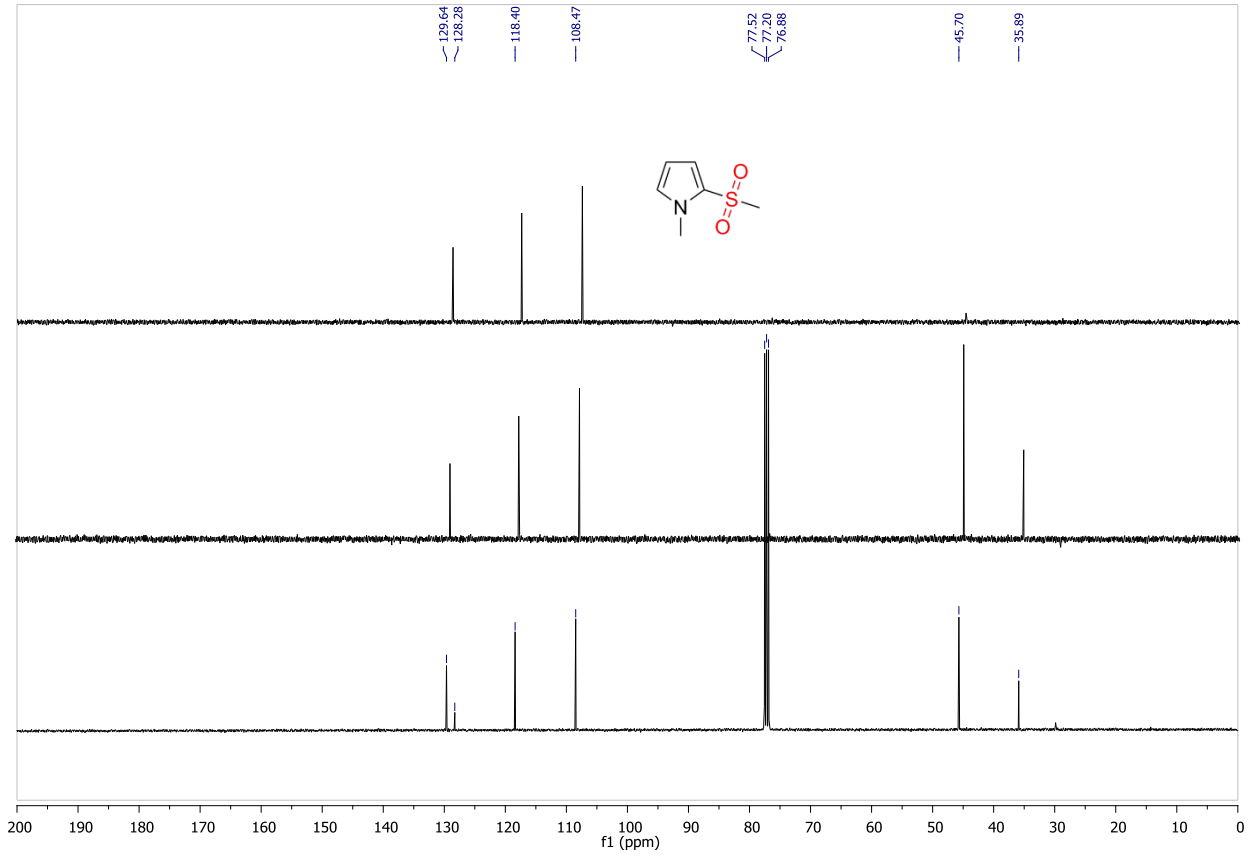

^{1}H-NMR: **3k**

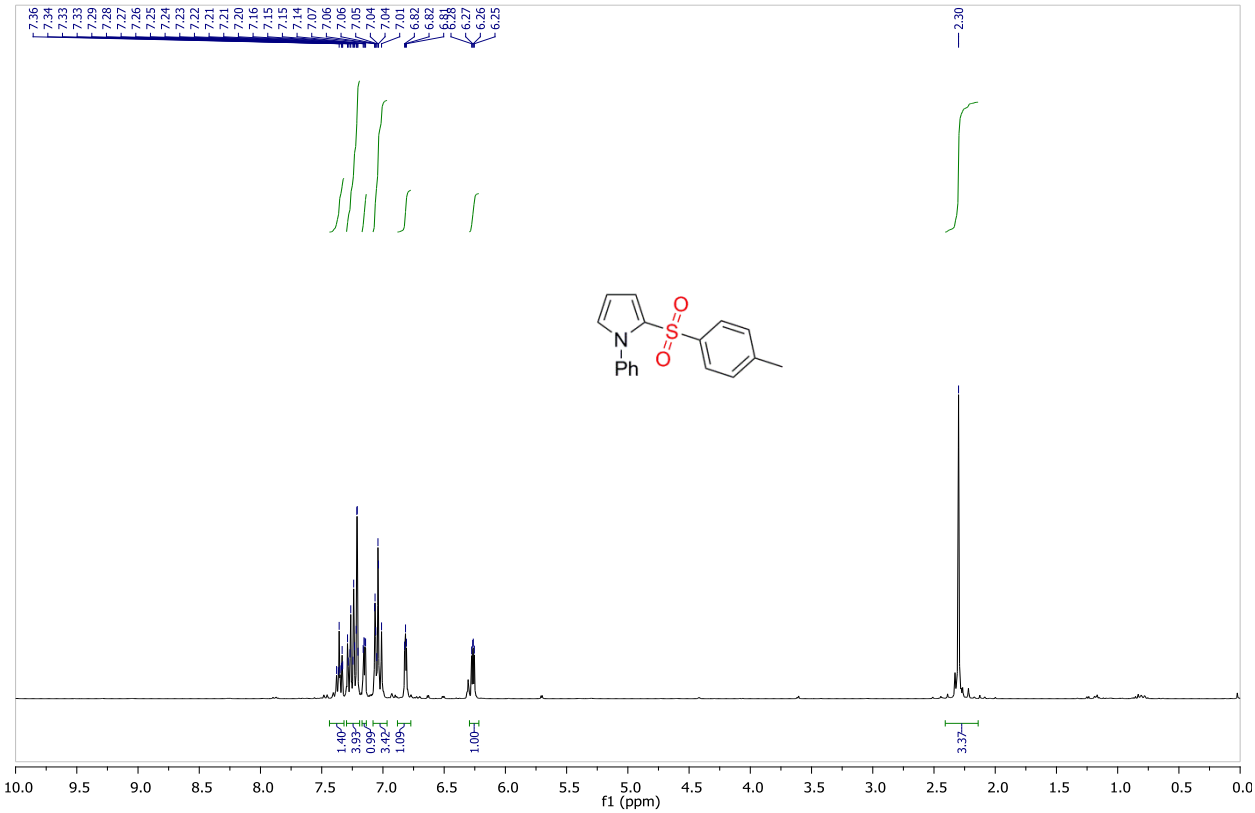

^{13}C-NMR: **3k**

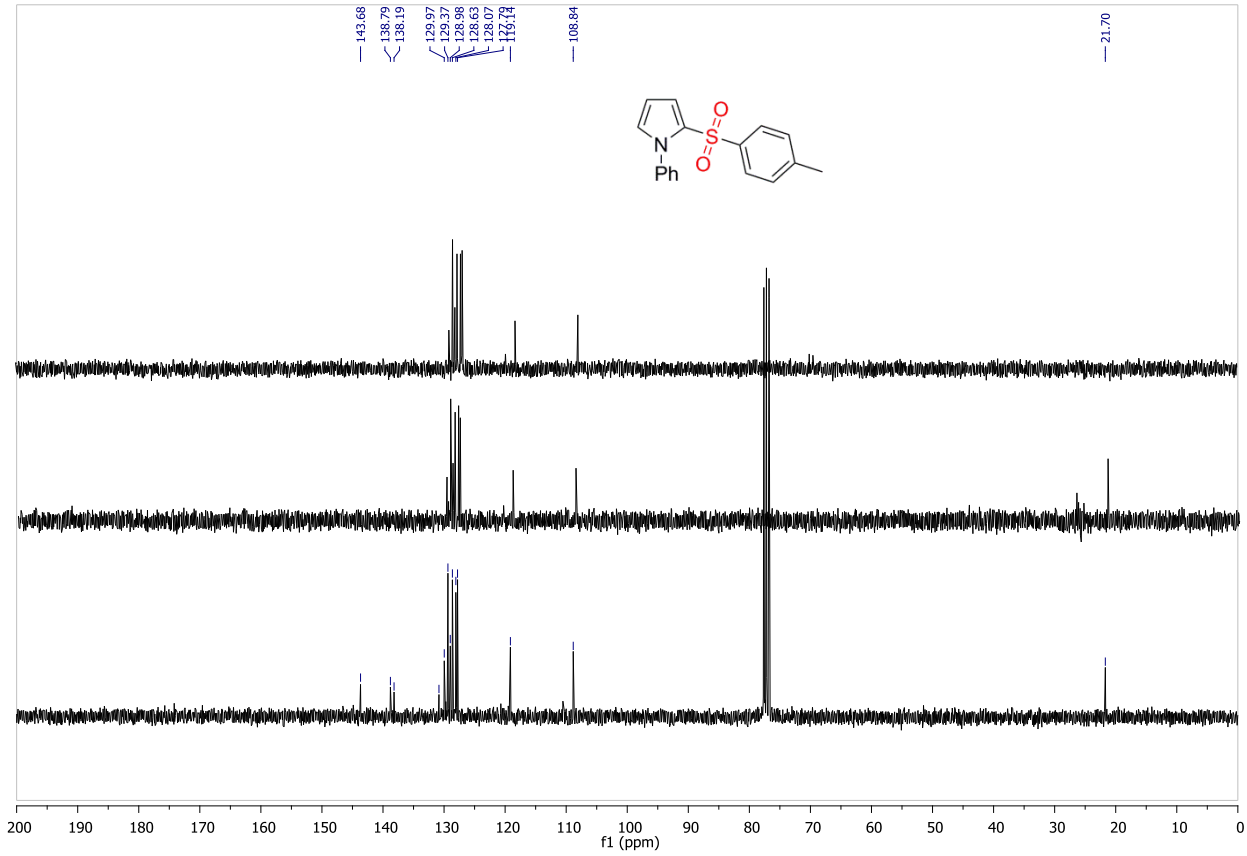

^{1}H-NMR: **3l**

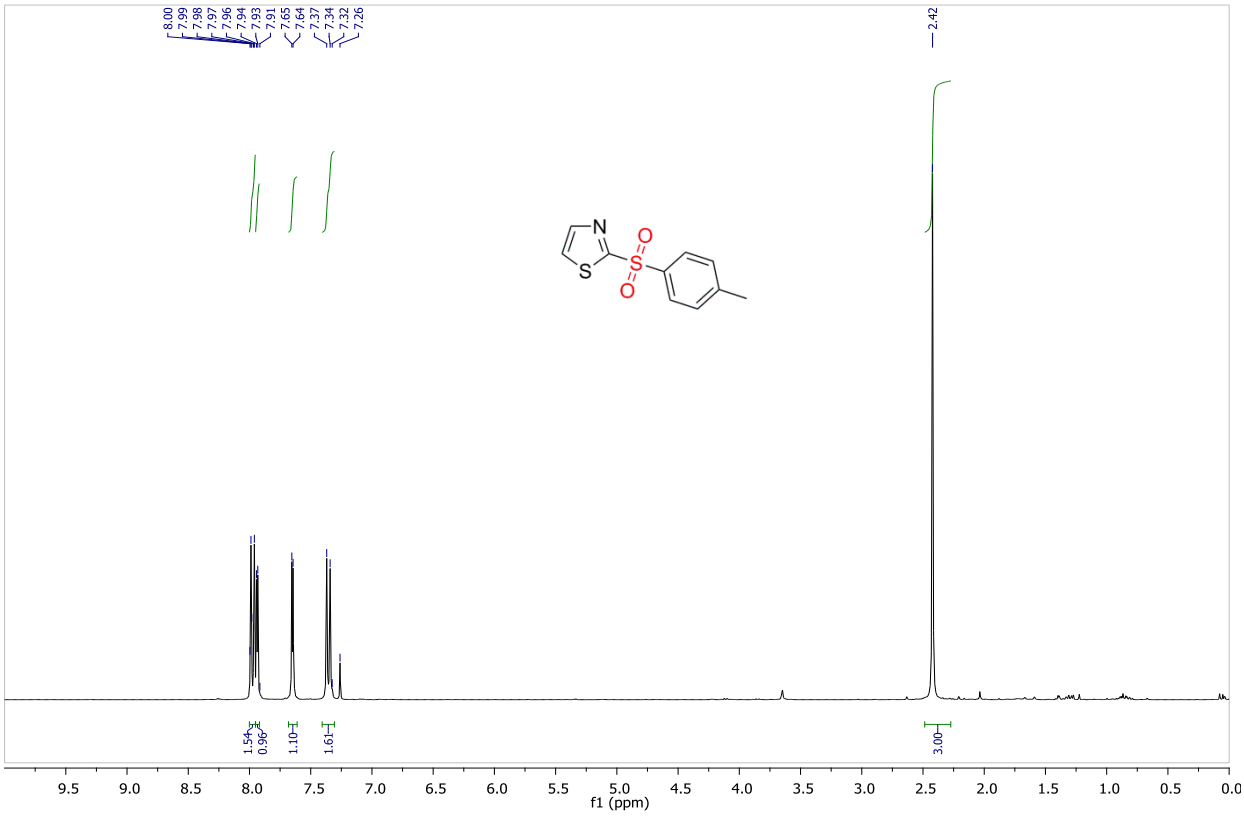

^{13}C-NMR: **3l**

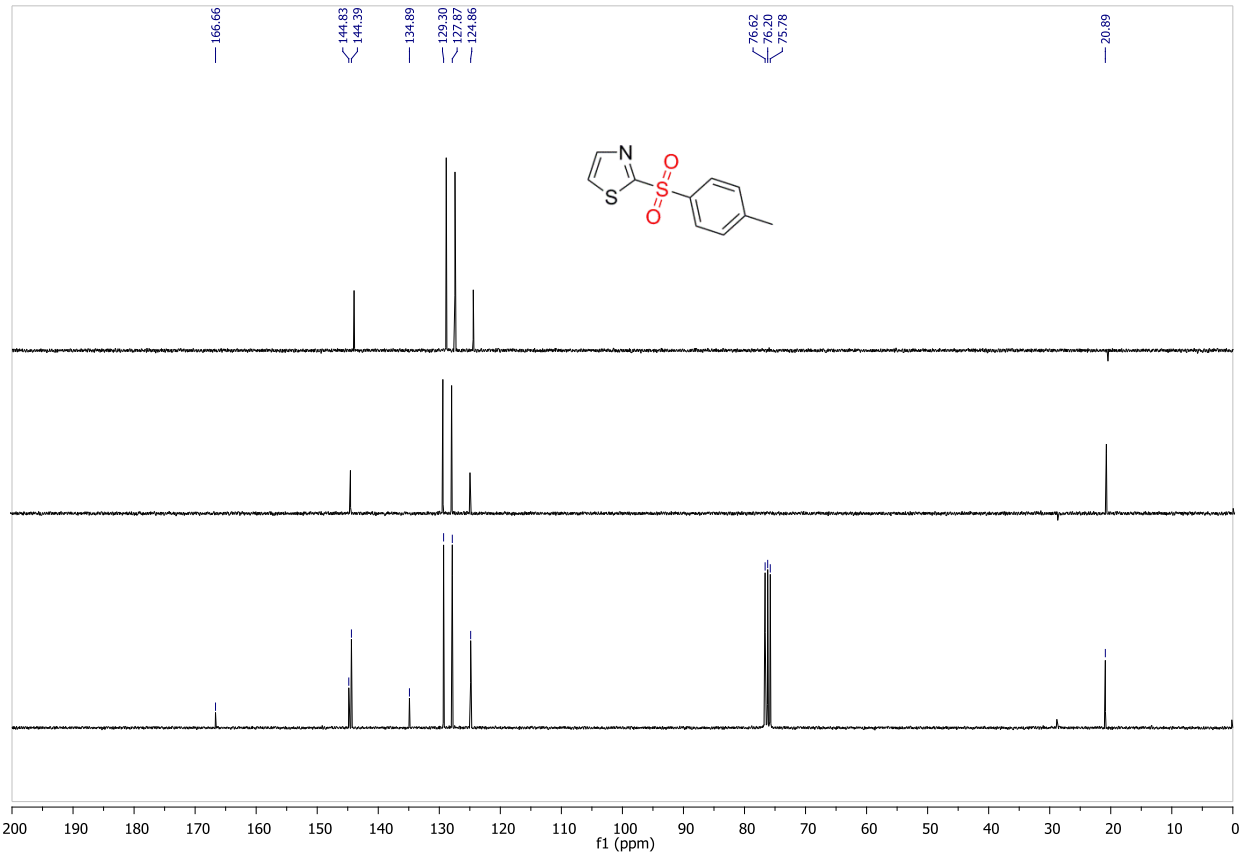

^{1}H-NMR: **3m**

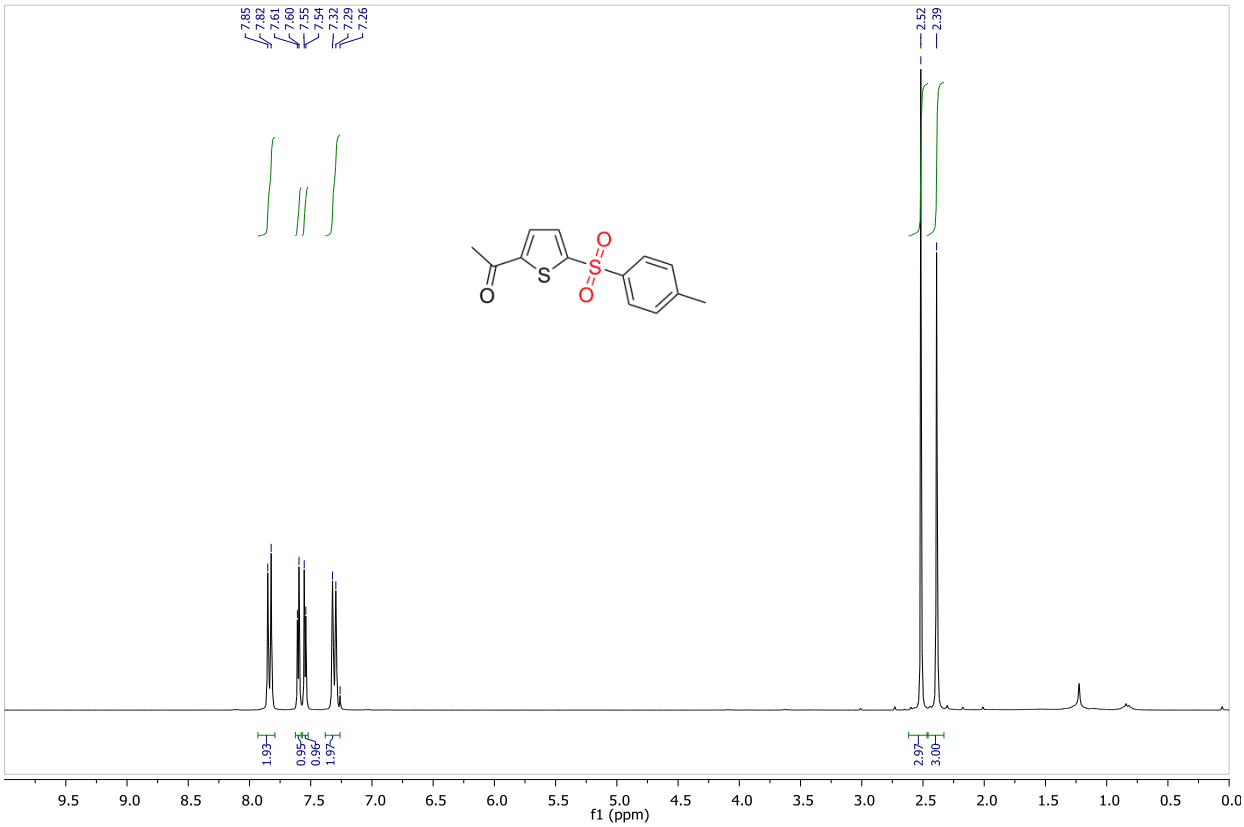

^{13}C-NMR: **3m**

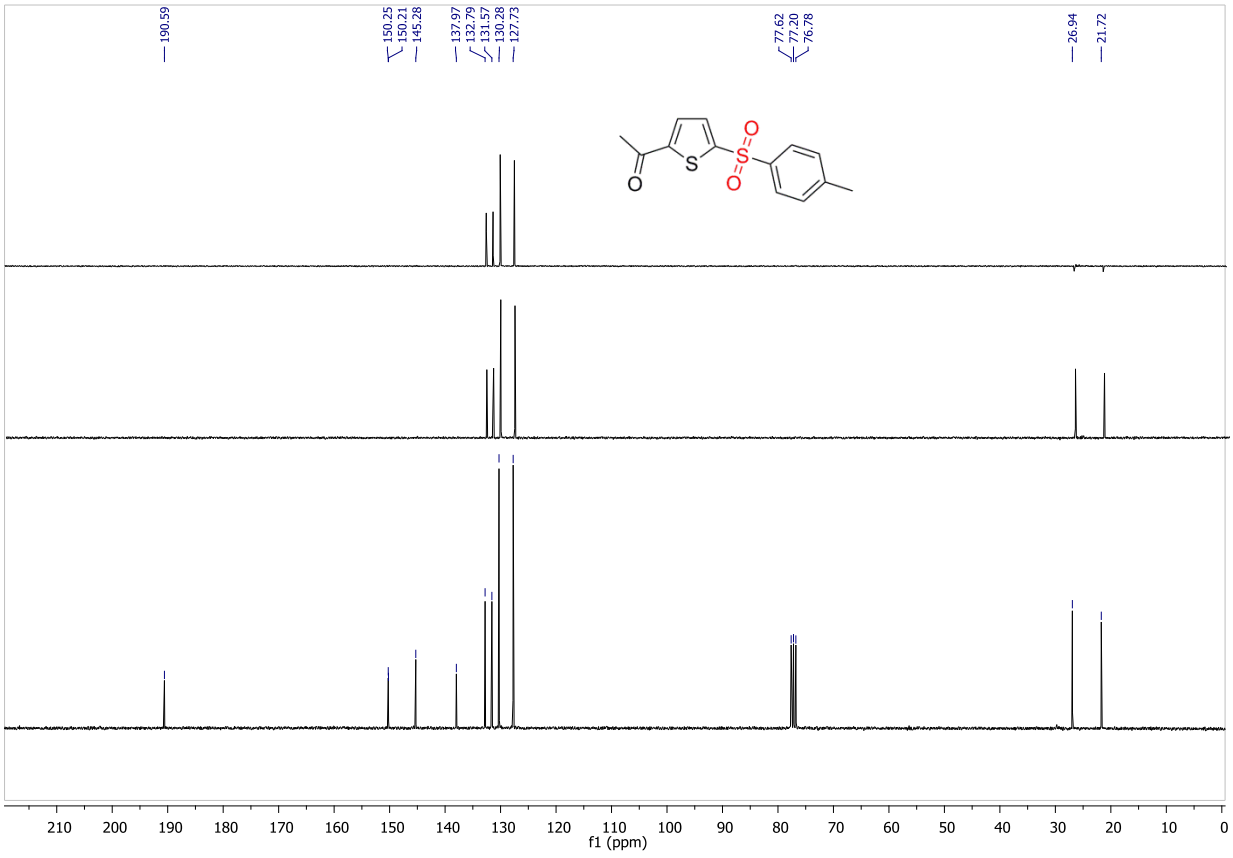

^{1}H-NMR: **3n**

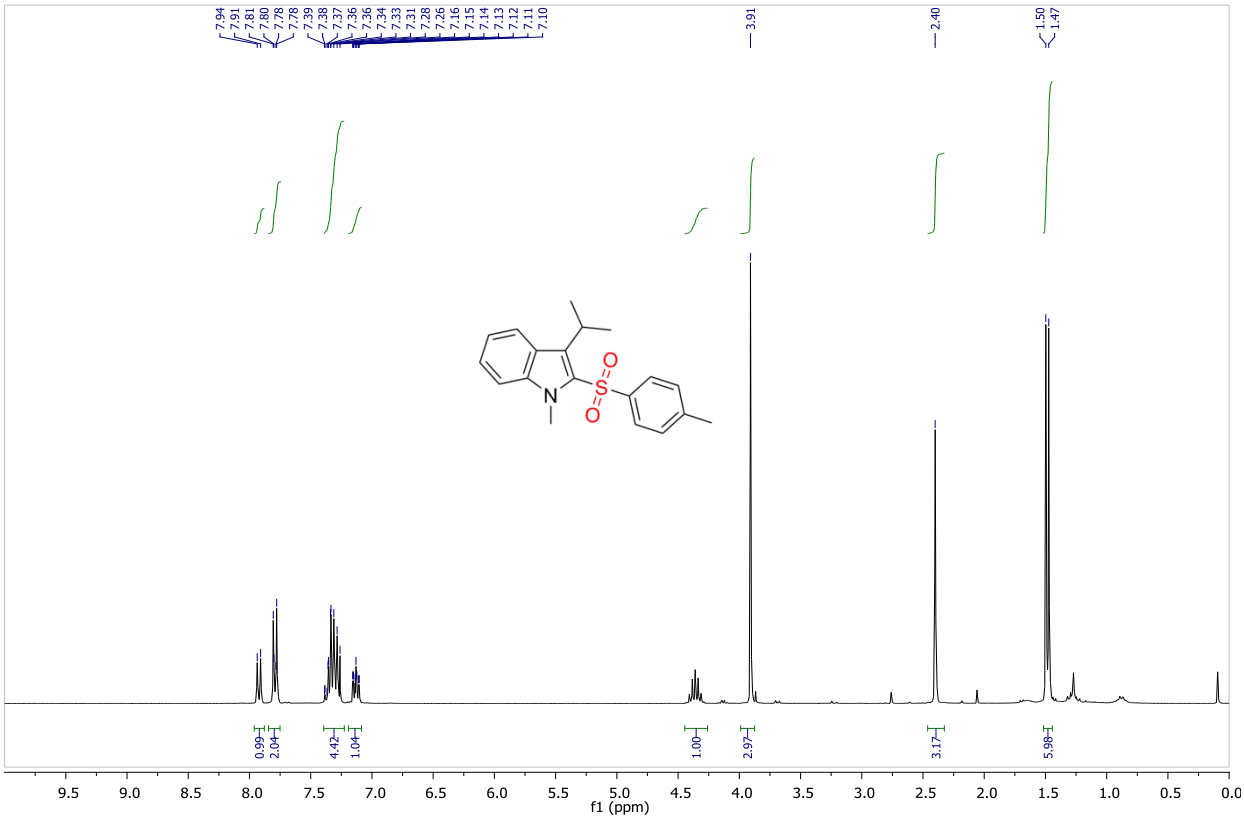

^{13}C-NMR: **3n**

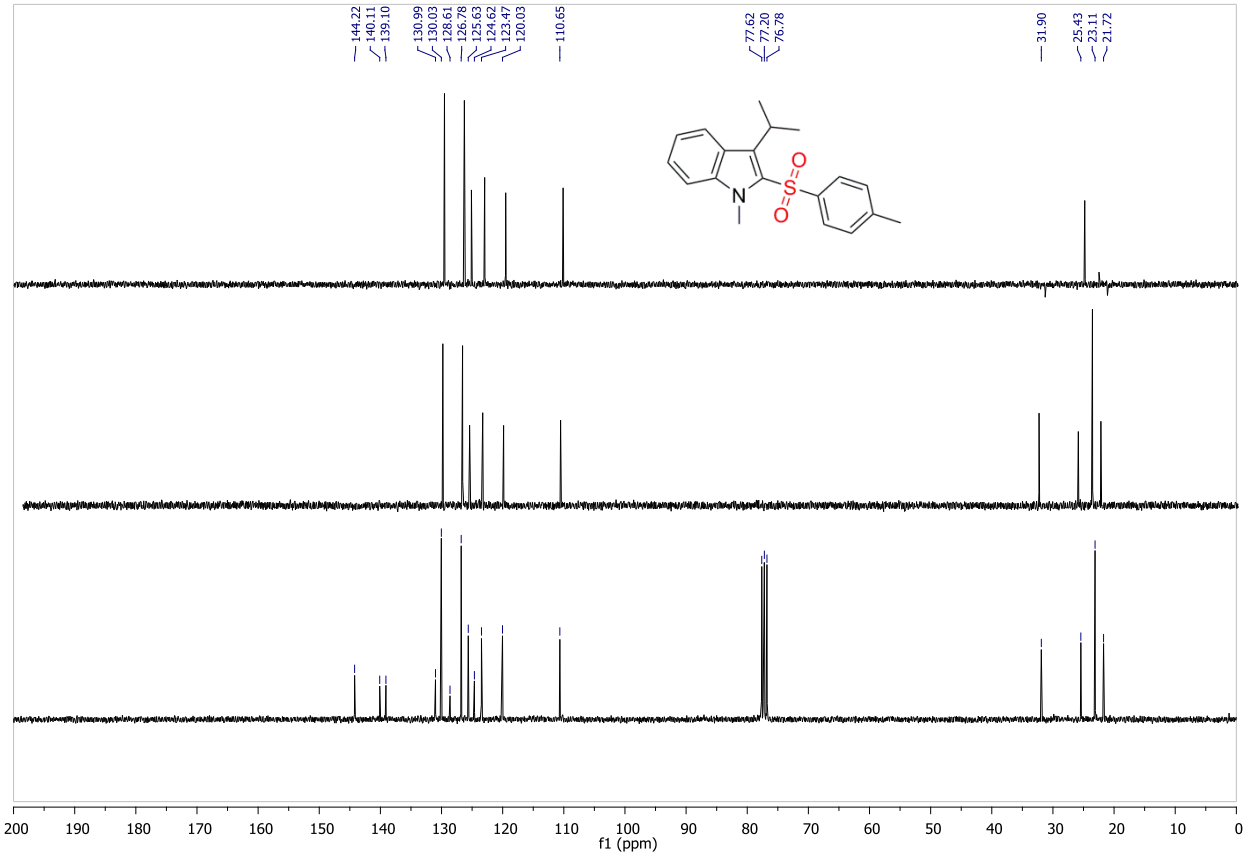

^{1}H-NMR: **3o**

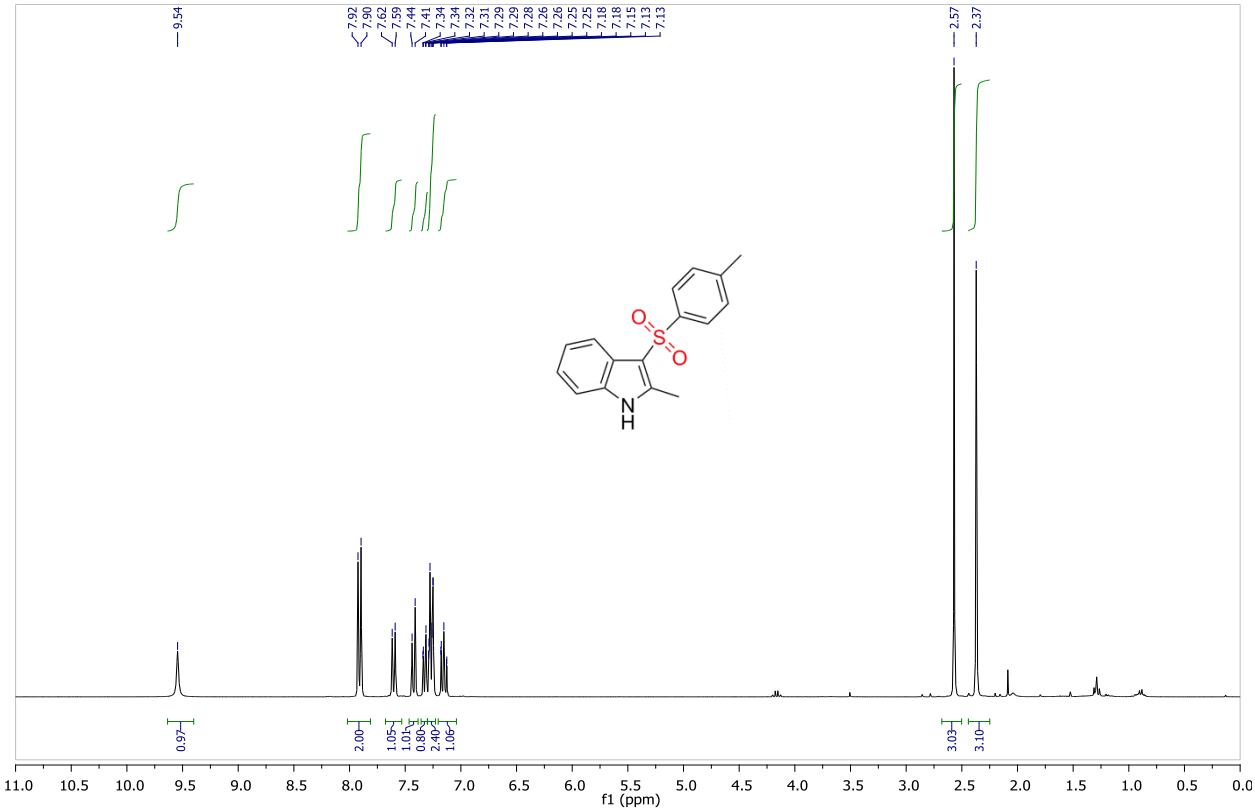

^{13}C-NMR: **3o**

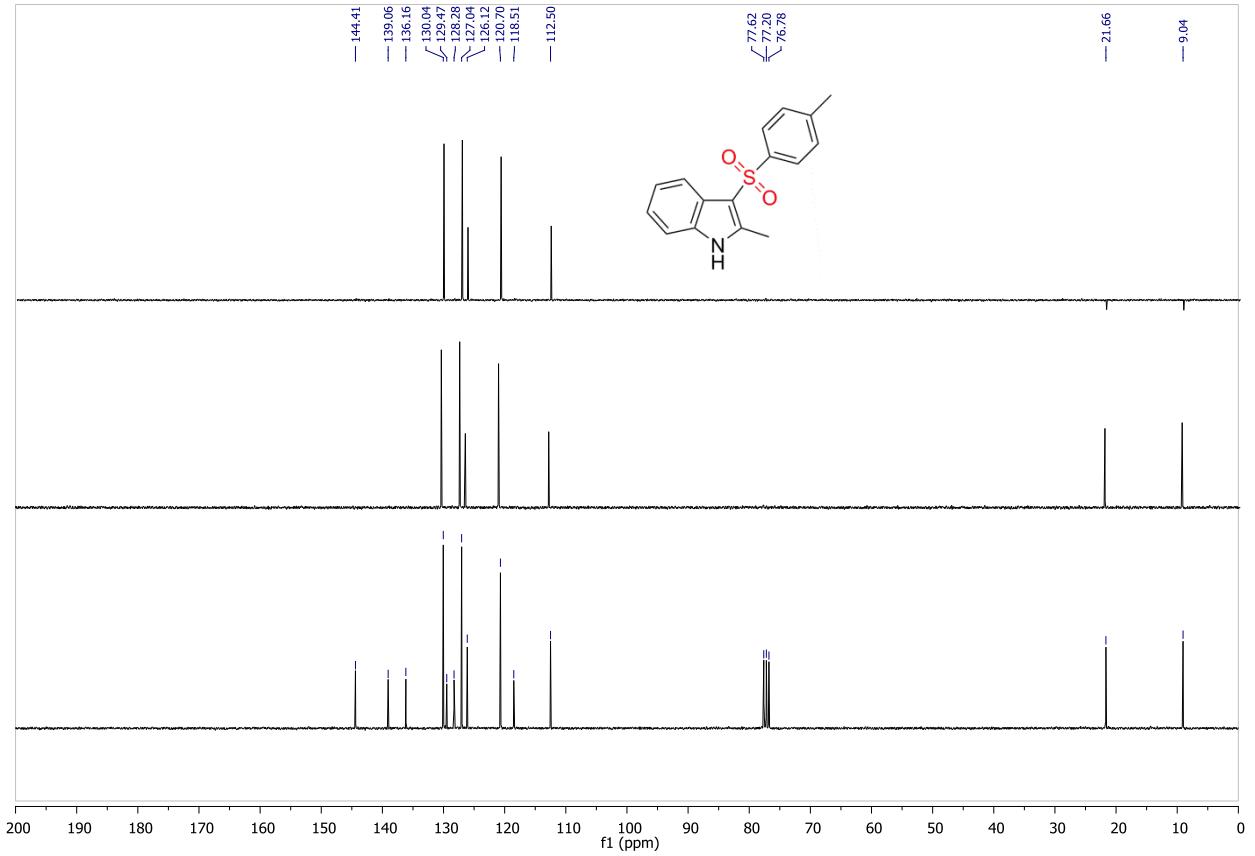

^{1}H-NMR: **3p**

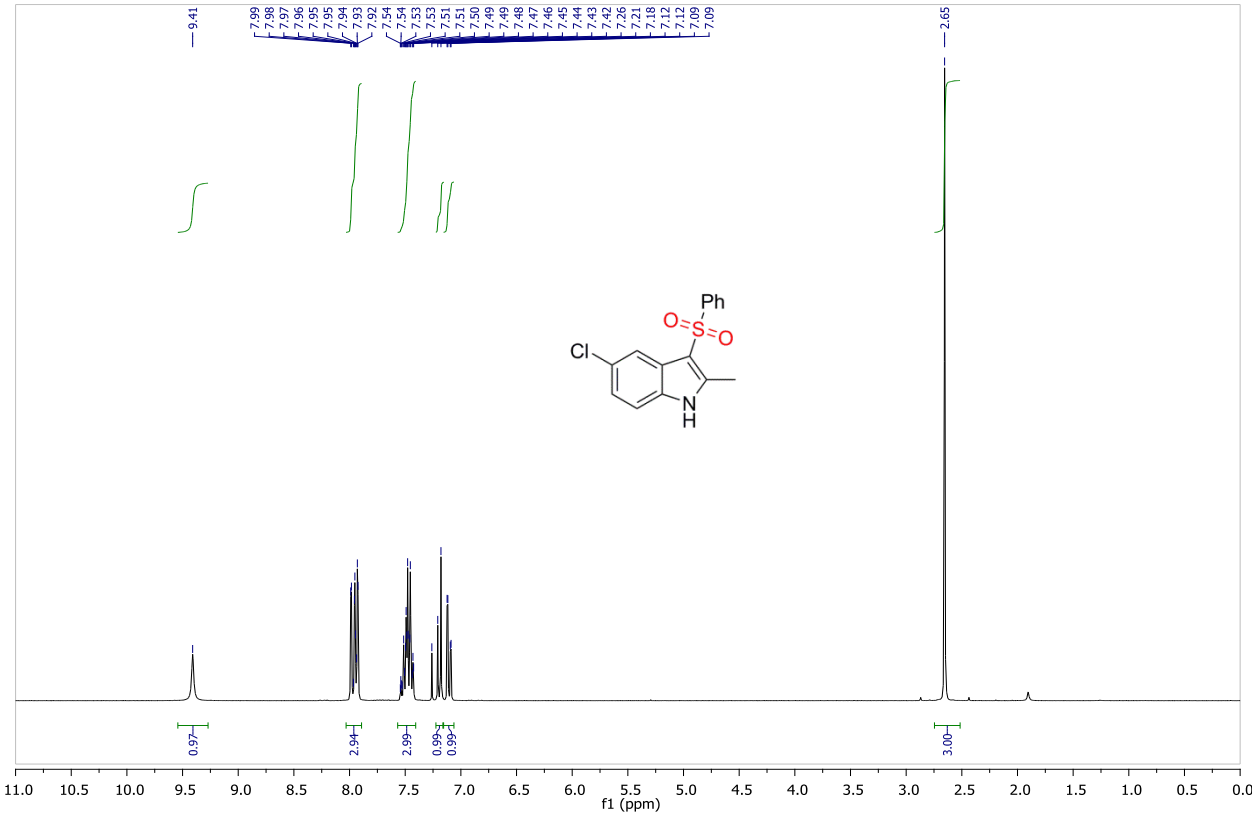

^{13}C-NMR: **3p**

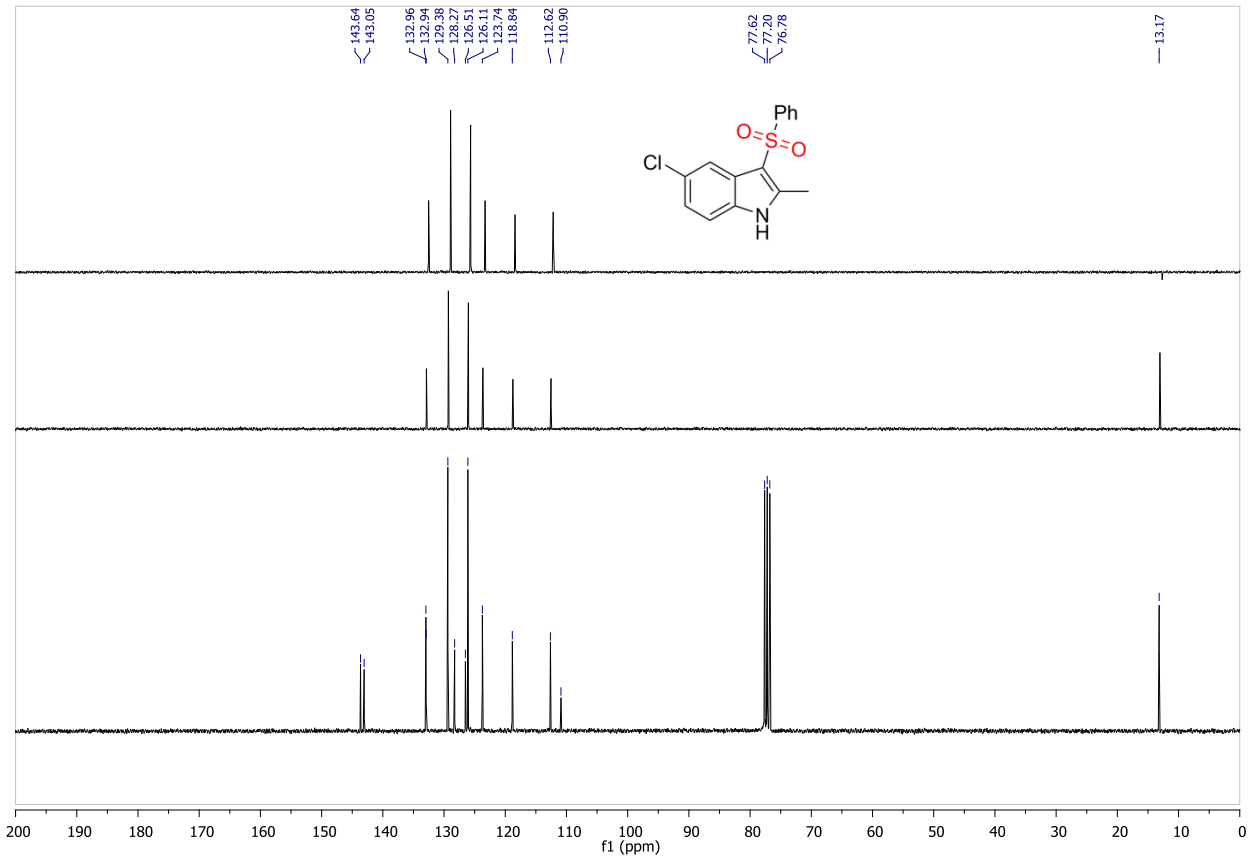

^{1}H-NMR: **3q**

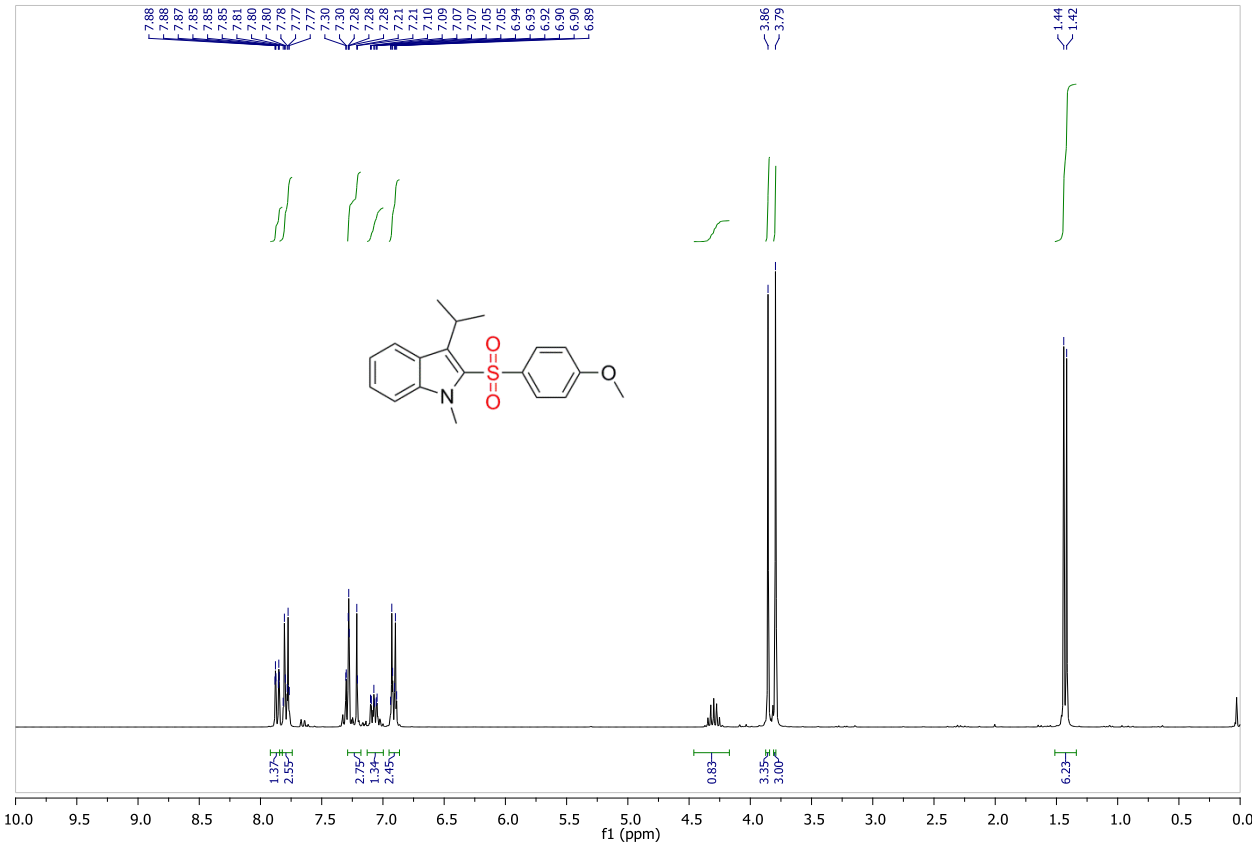

^{13}C-NMR: **3q**

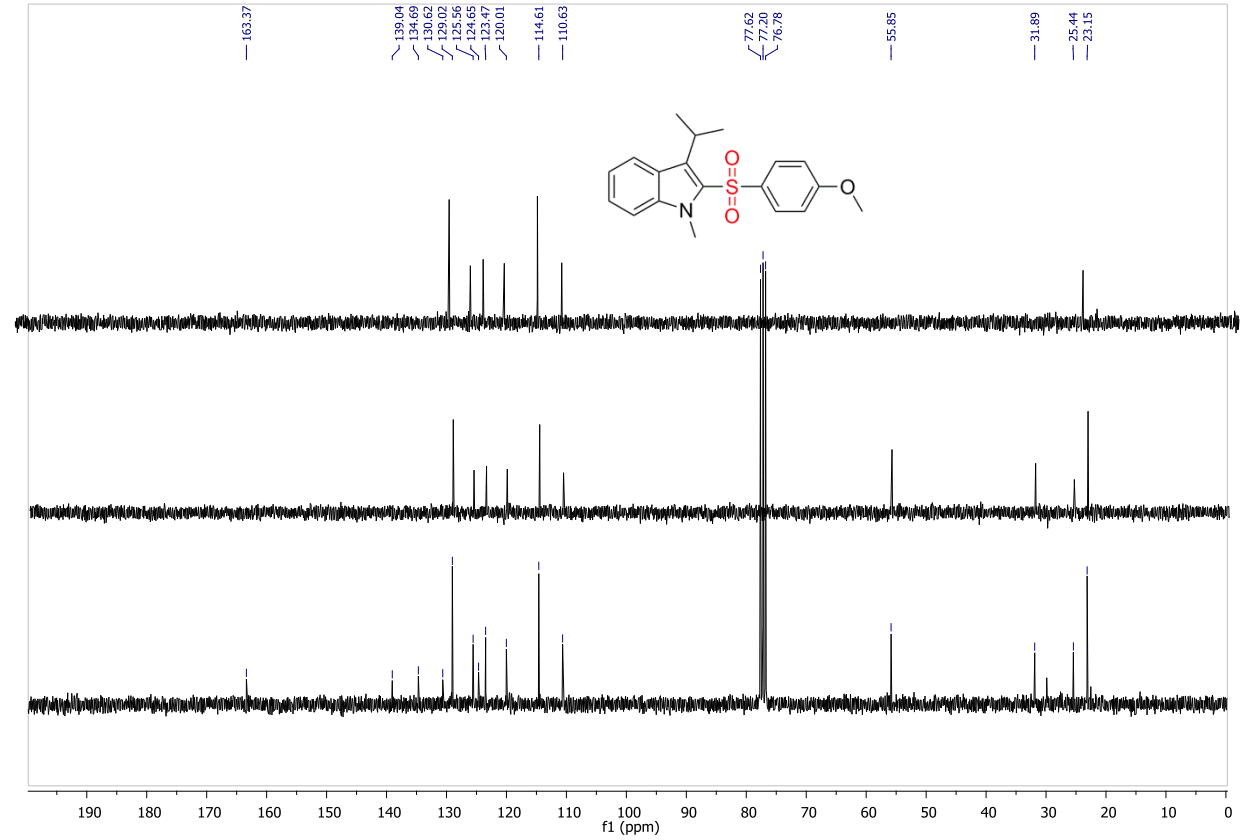

^{1}H-NMR: **4a**

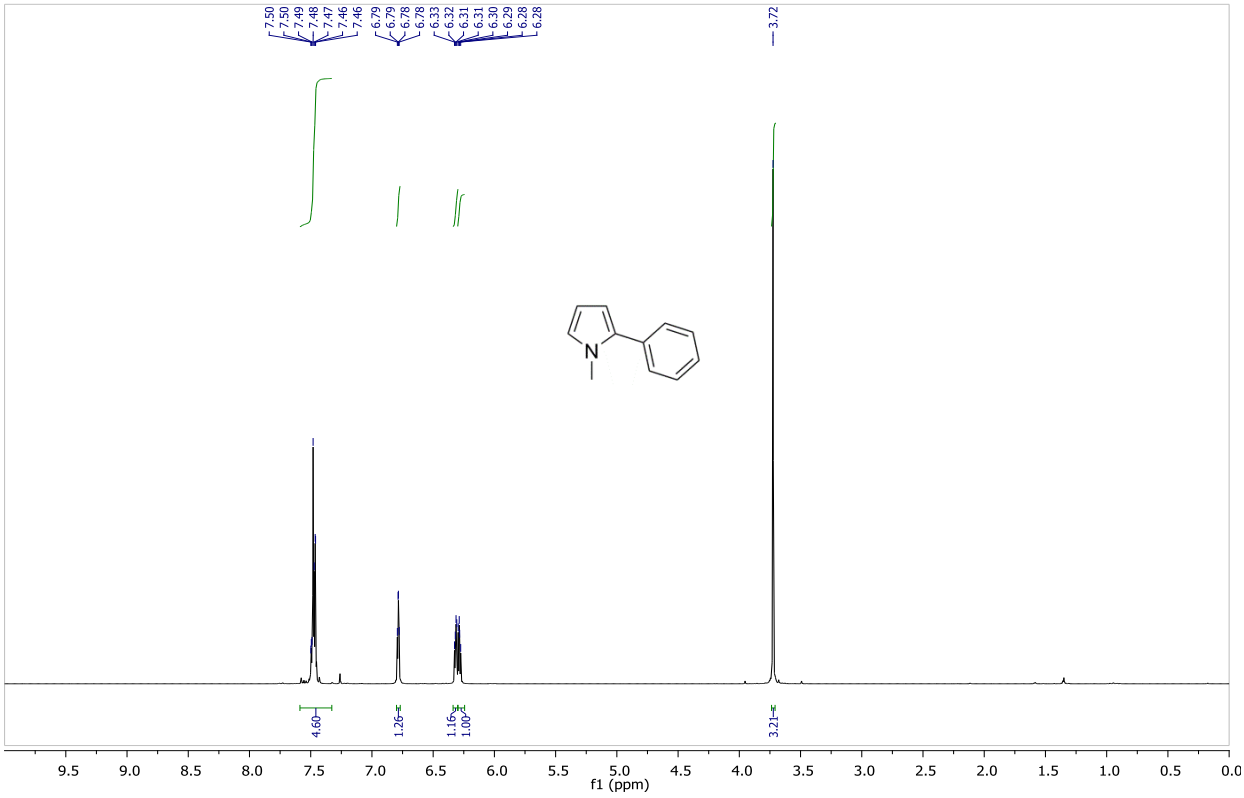

^{13}C-NMR: **4a**

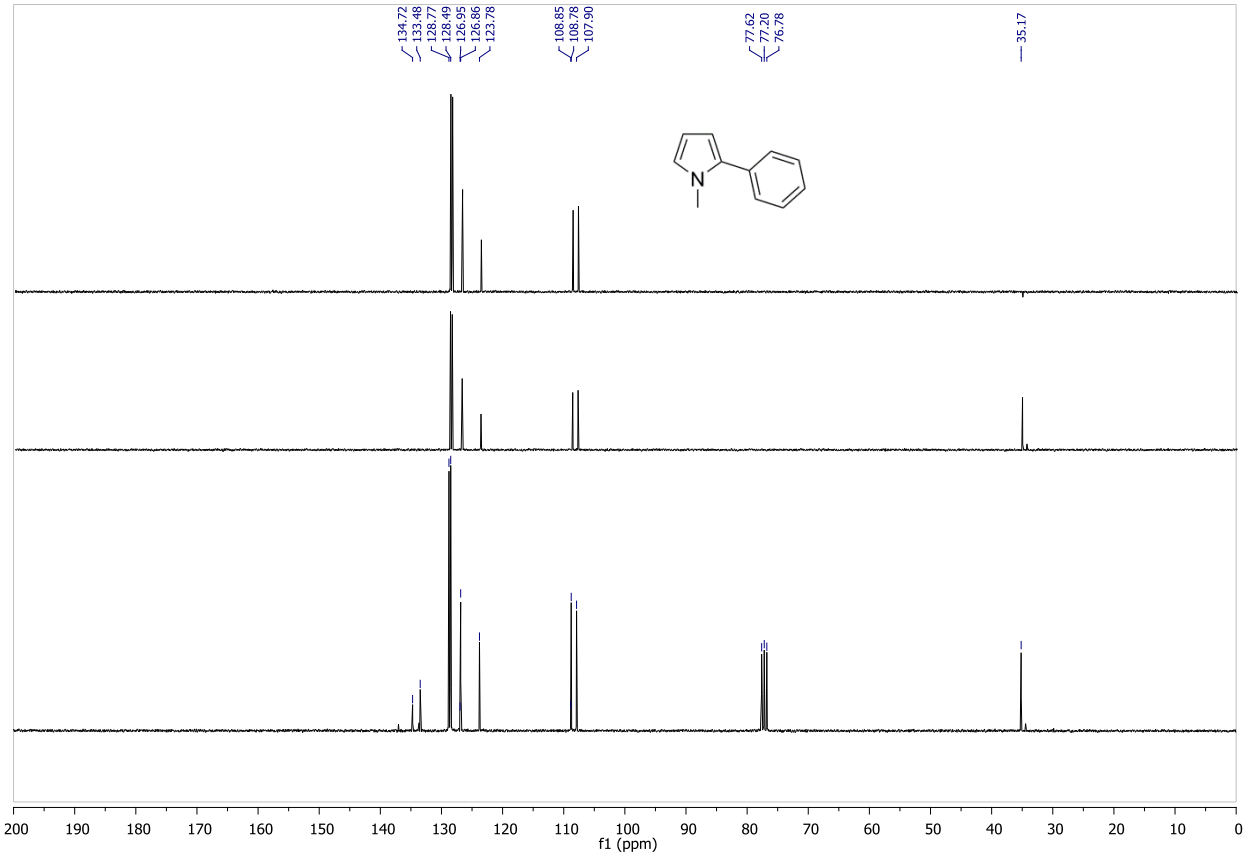

^{1}H-NMR: **4b**

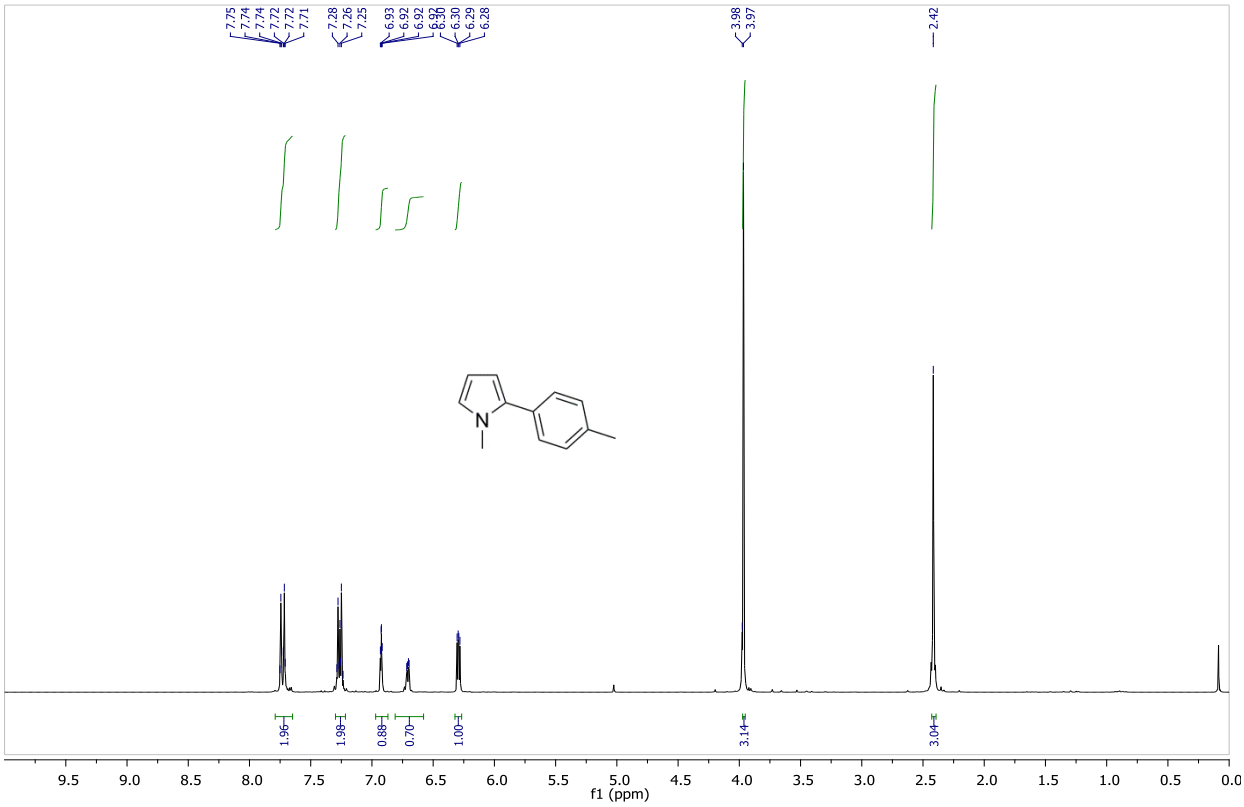

^{13}C-NMR: **4b**

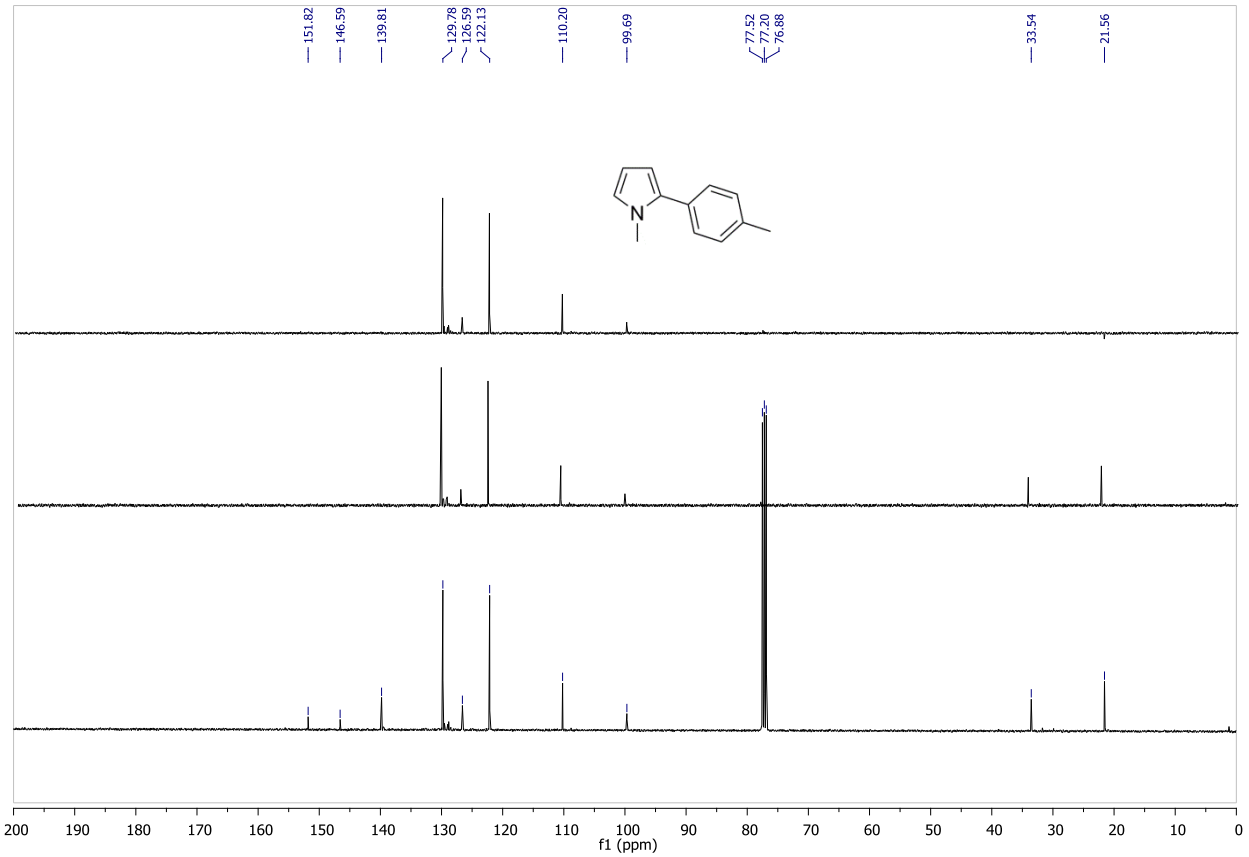

^{1}H-NMR: **4c**

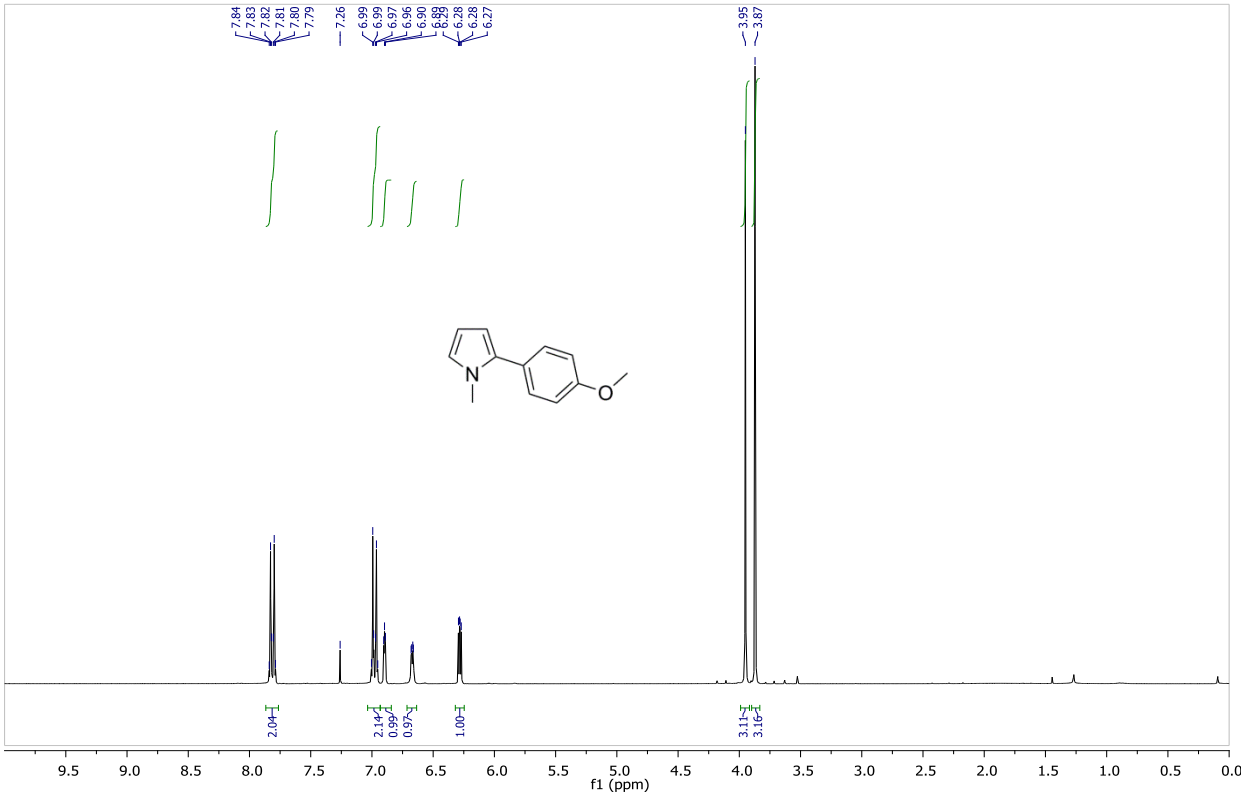

^{13}C-NMR: **4c**

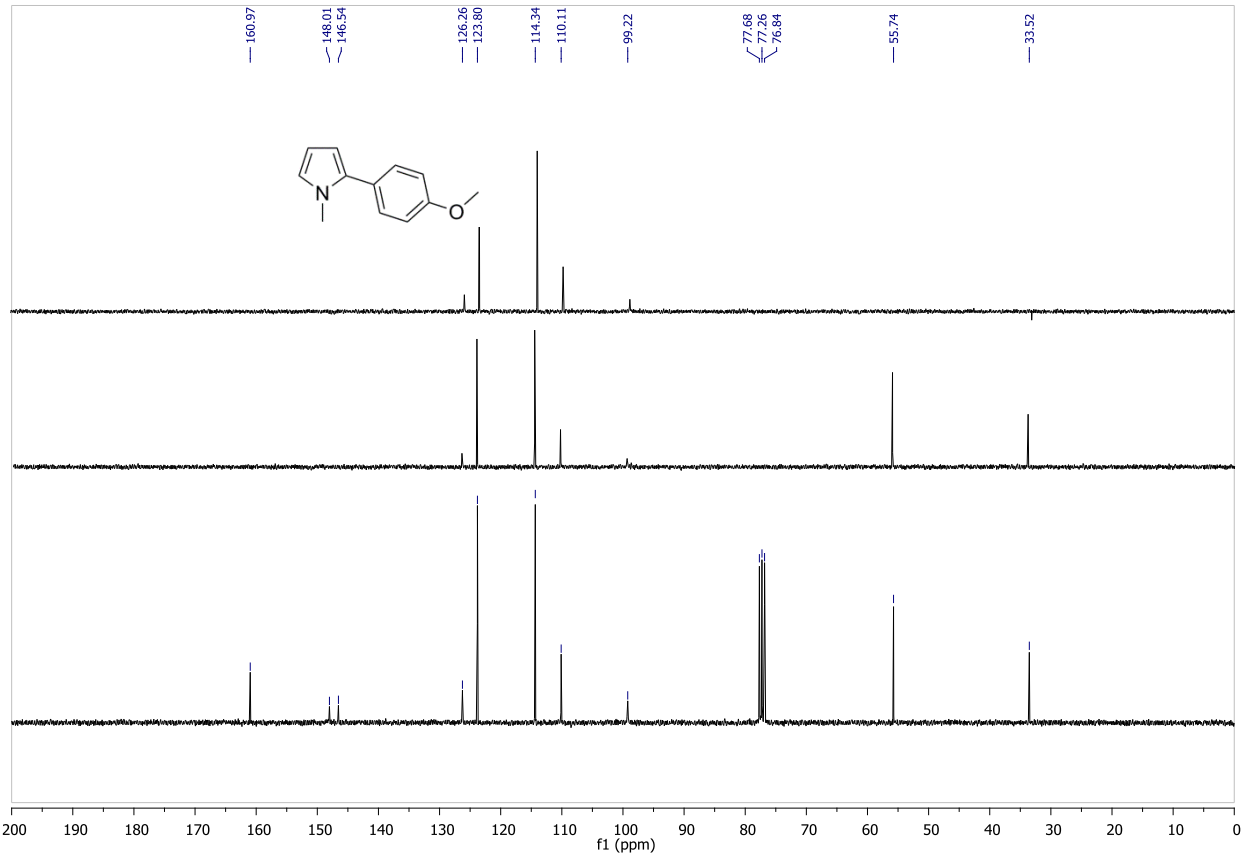

^{1}H-NMR: **4d**

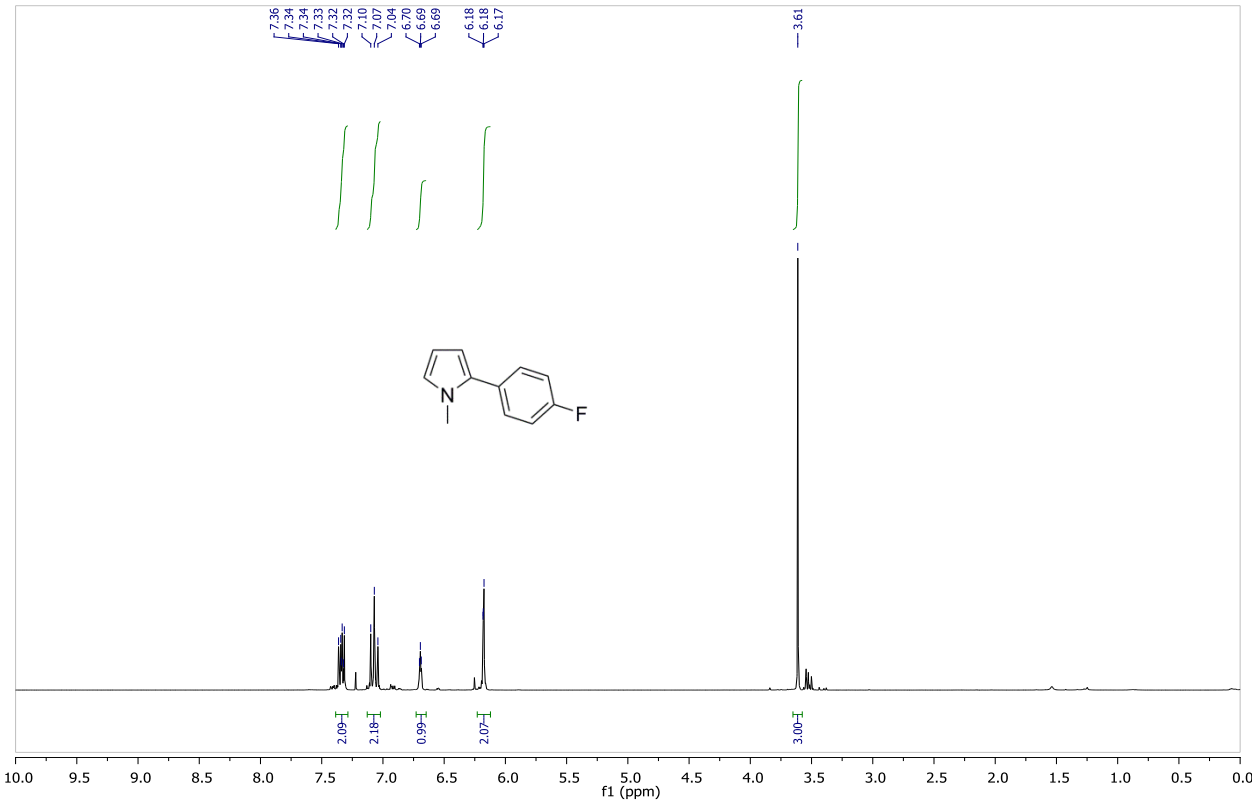

^{13}C-NMR: **4d**

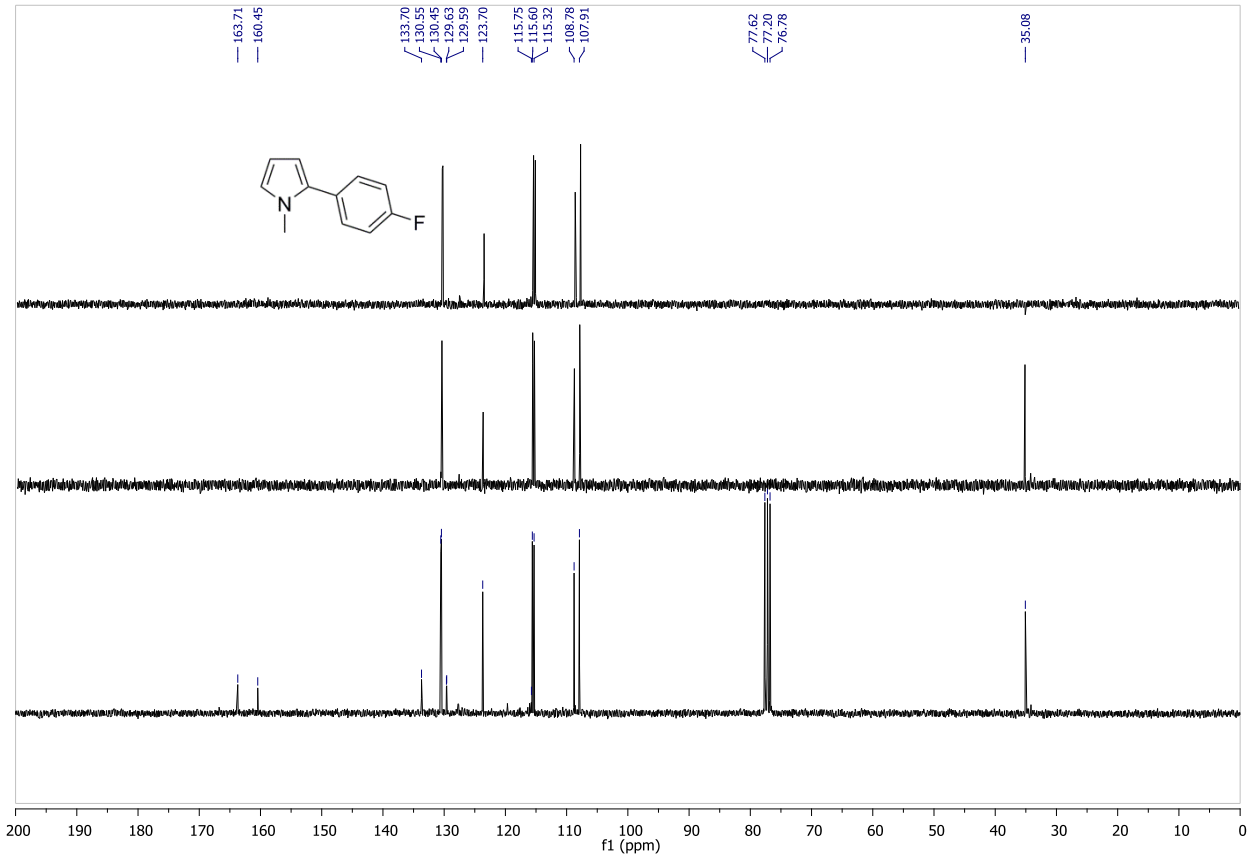

^{19}F-NMR: **4d**

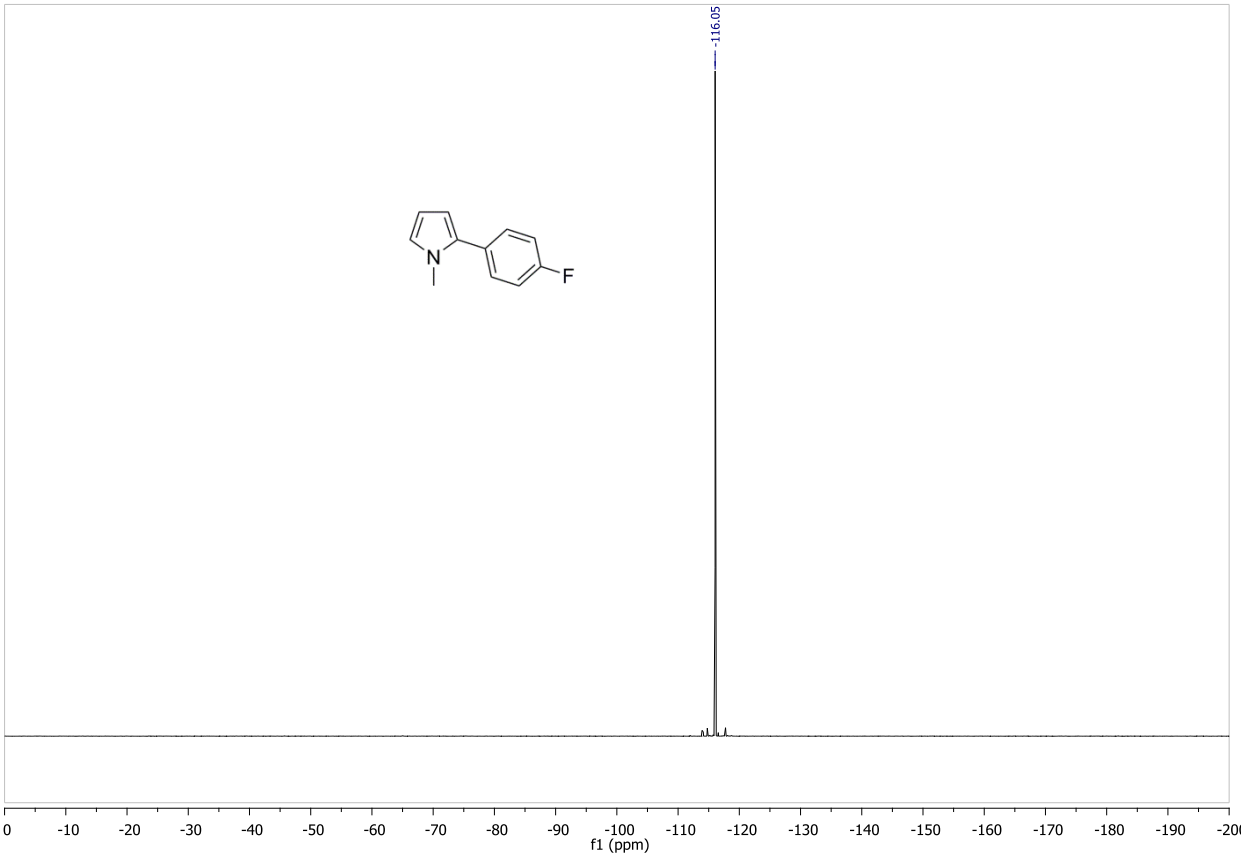
-116.05
N
F
0
-10
-20
-30
-40
-50
-60
-70
-80
-90
-100
-110
-120
-130
-140
-150
-160
-170
-180
-190
f1 (ppm)

^{1}H-NMR: **4h**

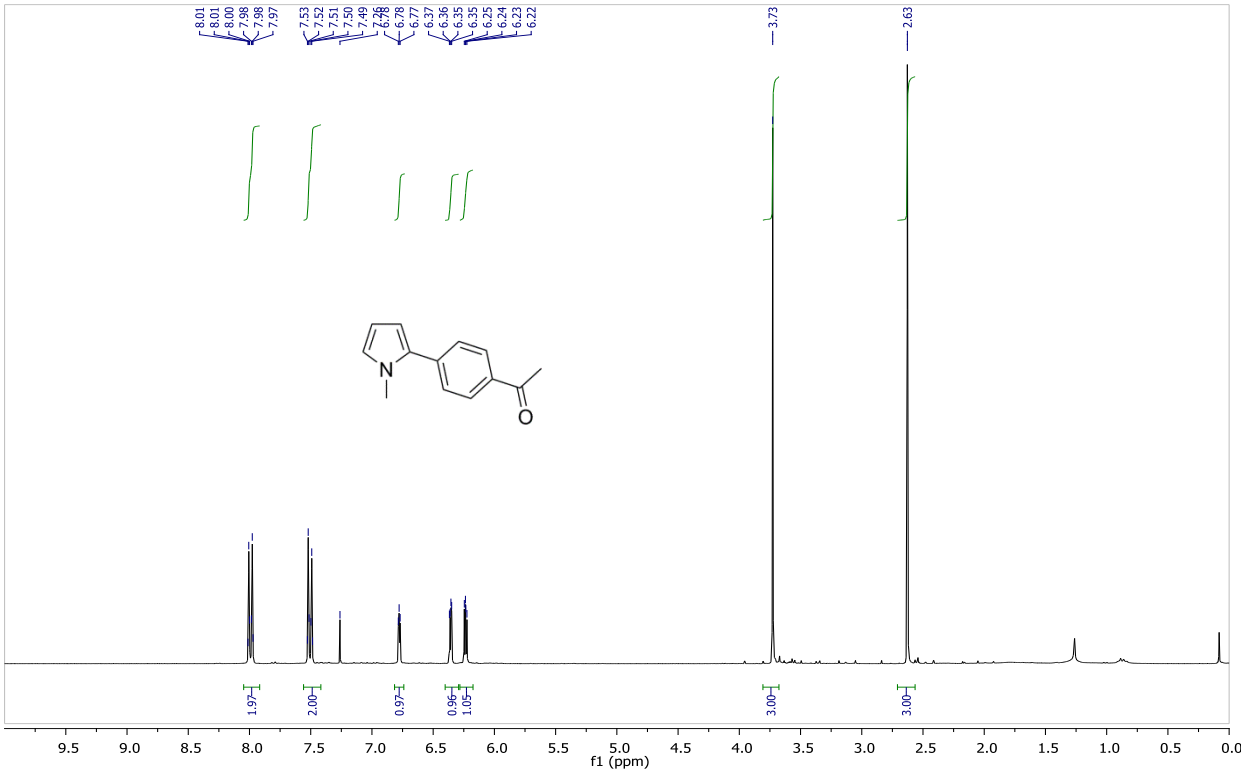

^{13}C-NMR: **4h**

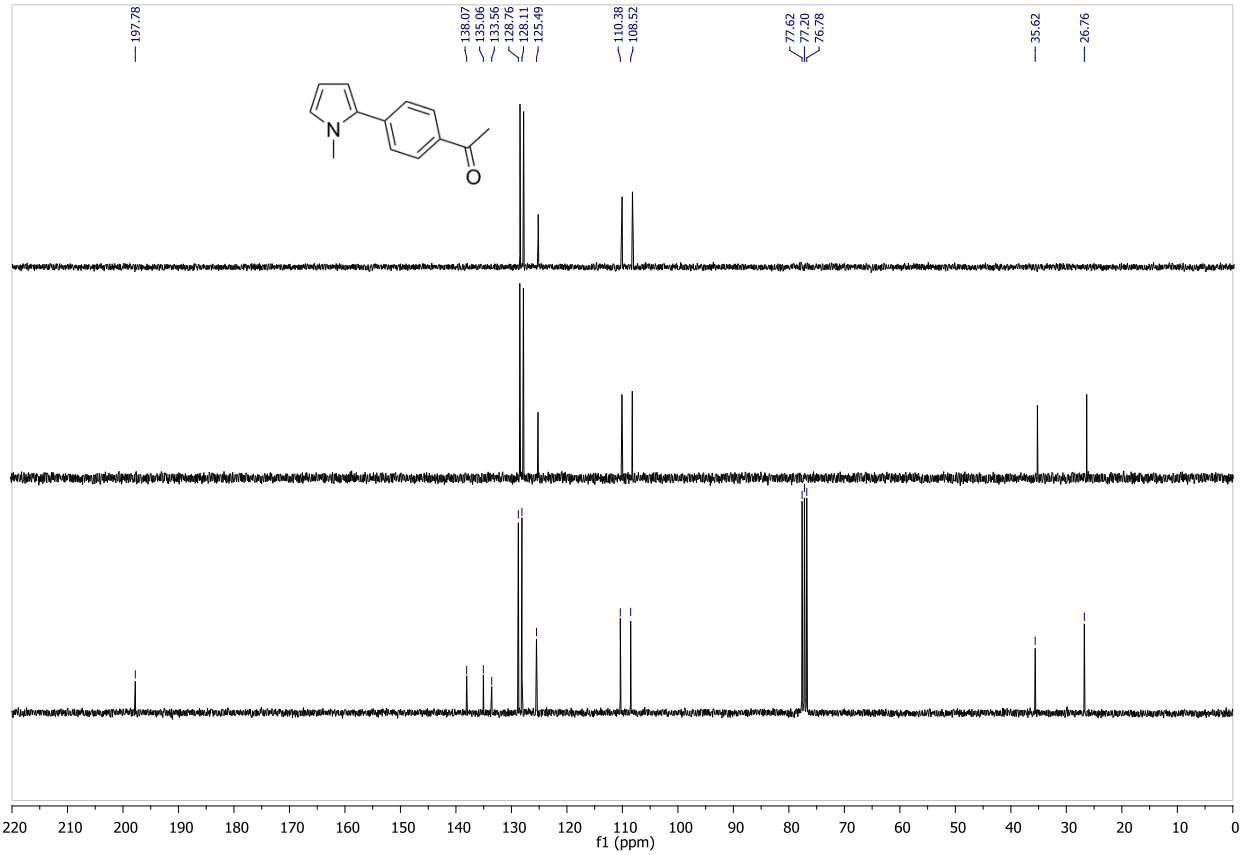

^{1}H-NMR: **4i**

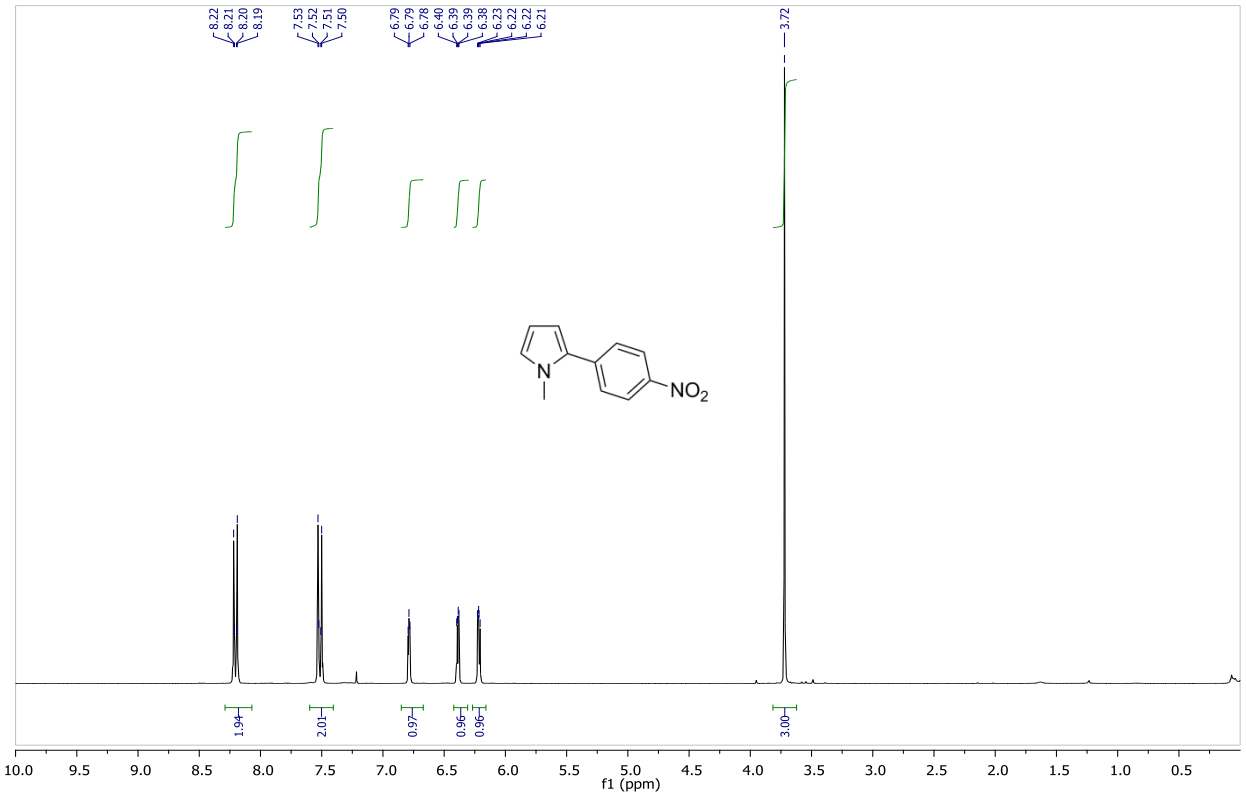

^{13}C-NMR: **4i**

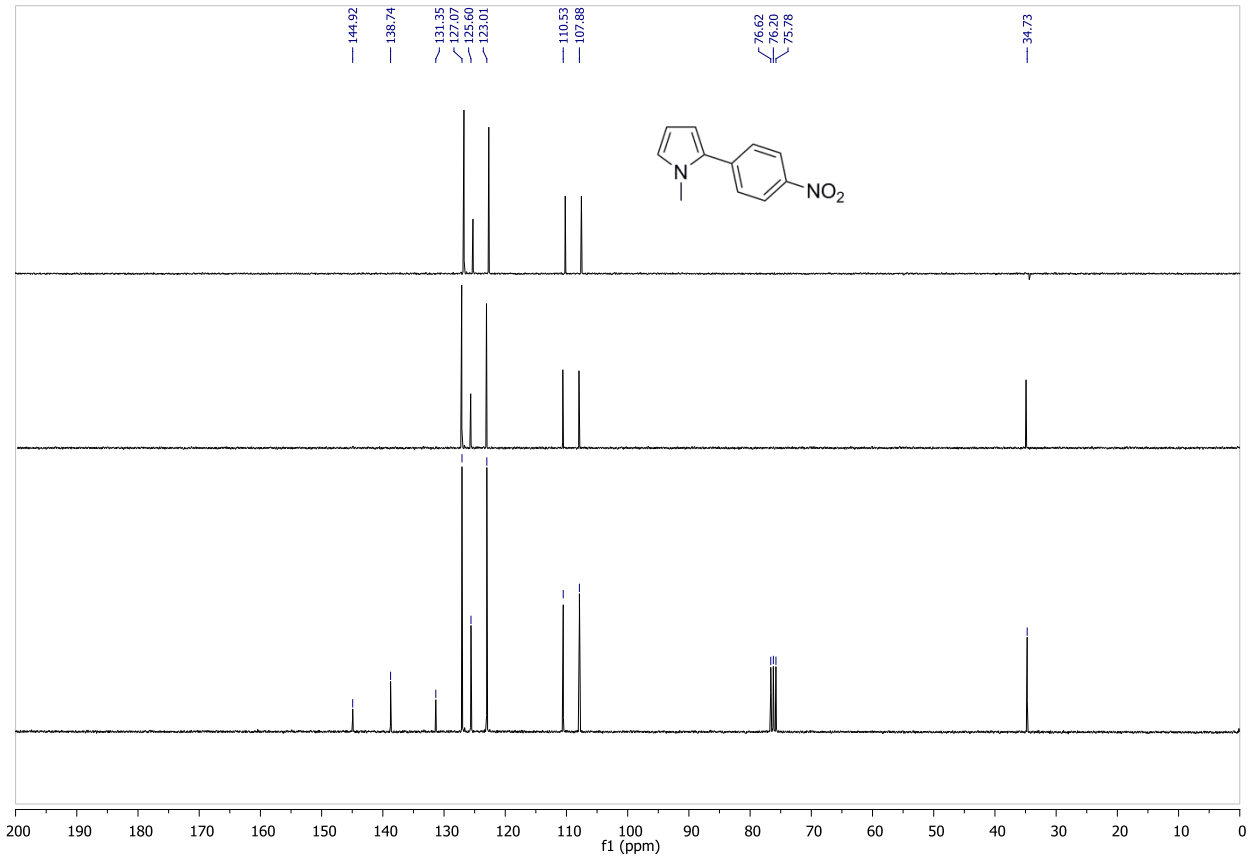

^{1}H-NMR: **4n**

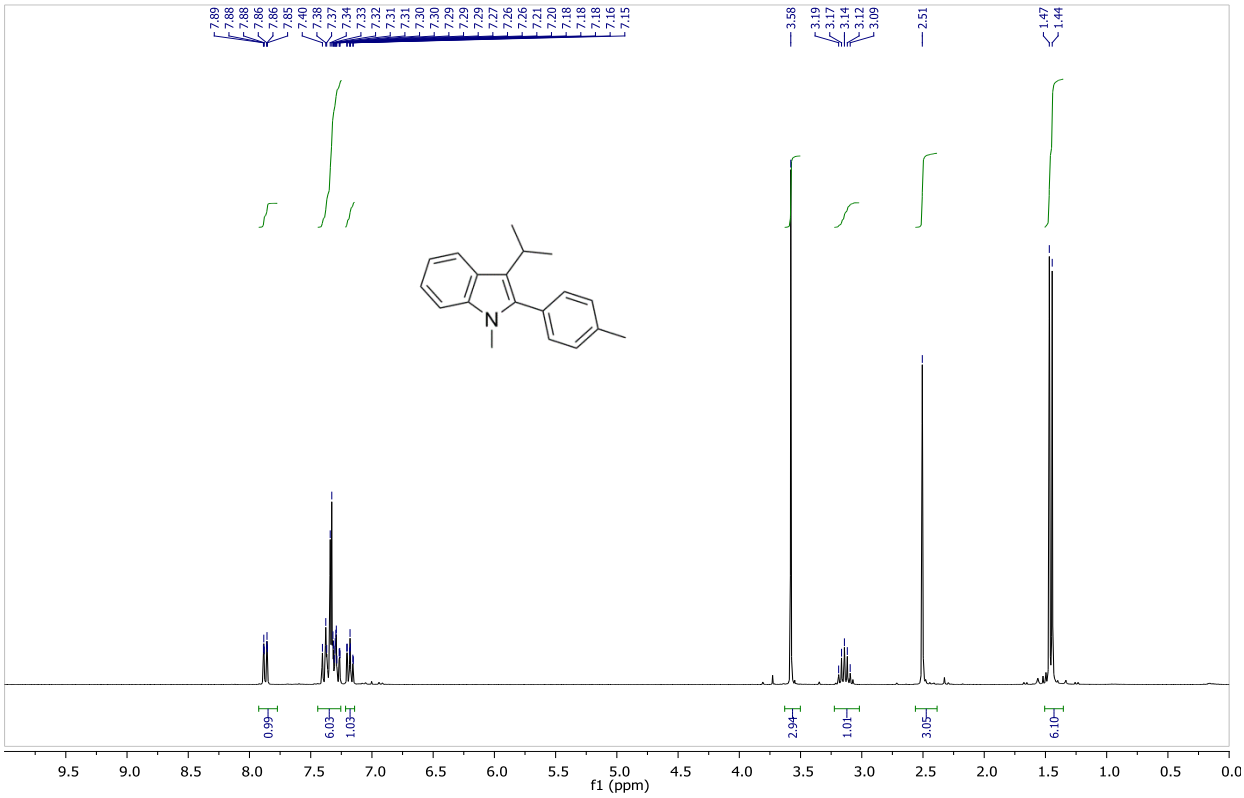

^{13}C-NMR: **4n**

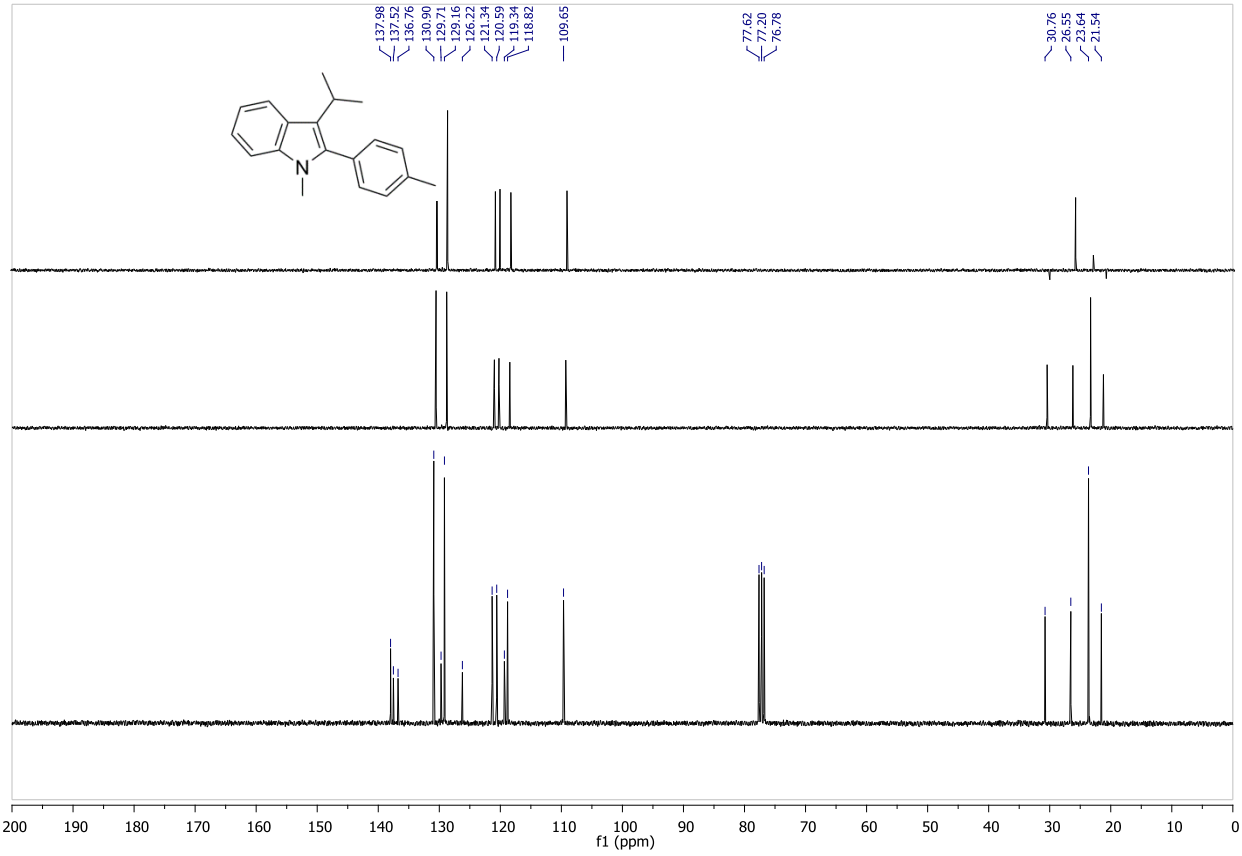

^{1}H-NMR: **4o**

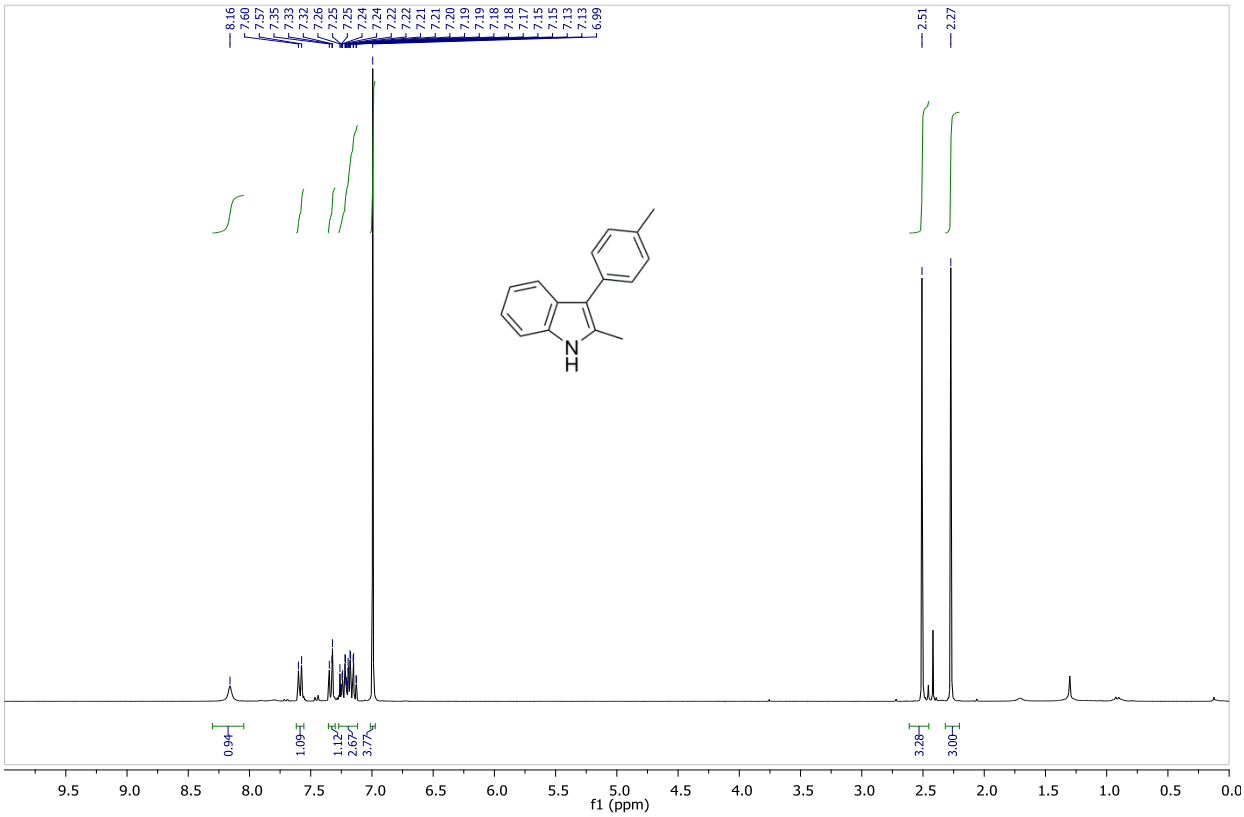

^{13}C-NMR: **4o**

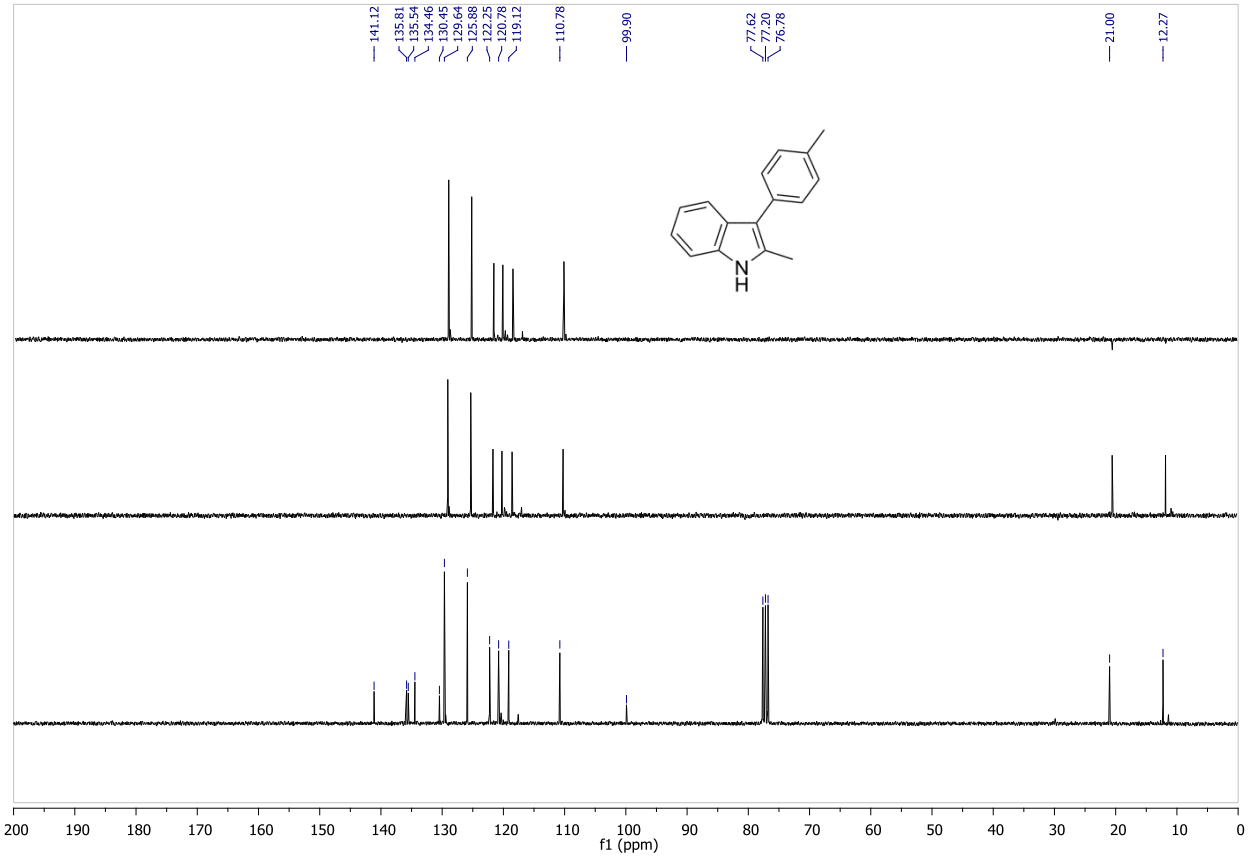

9.11 Crystal data: 3b

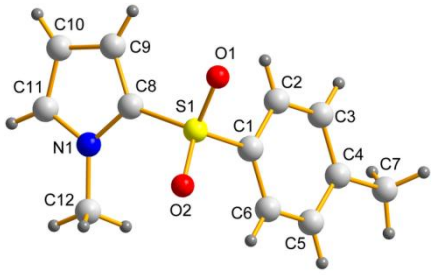

Figure 9.4: Single X-ray crystal structure of **3b**

Experimental: Single clear colorless needle-shaped crystals of (**3b**) were obtained by recrystallization from DCM/pentane (diffusion method). A suitable crystal (0.27×0.08×0.05) mm³ was selected and mounted on a MITIGEN holder with inert oil on a SuperNova, Single source at the offset, Atlas diffractometer. The crystal was kept at T = 123.00(10) K during data collection. Using **Olex2** (Dolomanov et al., 2009), the structure was solved with the **ShelXT** (Sheldrick, 2015) structure solution program, using the Intrinsic Phasing solution method. The model was refined with a version of **olex2.refine** (Bourhis et al., 2015) using Gauss-Newton minimisation.

Crystal Data. $C_{12}H_{13}NO_2S$, M_r = 235.31, orthorhombic, Fdd2 (No. 43), a = 26.8040(7) Å, b = 21.6398(5) Å, c = 7.7705(2) Å, α = β = γ = 90°, V = 4507.1(2) Å³, T = 123.00(10) K, Z = 16, Z' = 1, μ(Cu K_α) = 2.428, 6092 reflections measured, 1989 unique (R_{int} = 0.0377) which were used in all calculations. The final wR_2 was 0.0822 (all data) and R_1 was 0.0306 (I≥σ(I)).

Compound	**3b**
Formula	$C_{12}H_{13}NO_2S$
$D_{calc.}$/ g cm^{-3}	1.3870
μ/mm^{-1}	2.428
Formula Weight	235.31
Colour	clear colourless
Shape	needle
Size/mm³	0.27×0.08×0.05
T/K	123.00(10)
Crystal System	orthorhombic
Flack Parameter	-0.049(14)
Hooft Parameter	-0.033(9)
Space Group	Fdd2
a/Å	26.8040(7)
b/Å	21.6398(5)
c/Å	7.7705(2)
α/°	90
β/°	90
γ/°	90
V/Å³	4507.1(2)
Z	16
Z'	1
Wavelength/Å	1.54184
Radiation type	Cu K_α
Θ_{min}/°	5.25
Θ_{max}/°	73.42
Measured Refl.	6092
Independent Refl.	1989
Reflections Used	1950
R_{int}	0.0377
Parameters	146
Restraints	0
Largest Peak	0.2255
Deepest Hole	-0.2312
GooF	1.0527
wR_2 (all data)	0.0822
wR_2	0.0807
R_1 (all data)	0.0316
R_1	0.0306

Table 9.4: Fractional Atomic Coordinates (×10⁴) and Equivalent Isotropic Displacement Parameters (Å²×10³) for **3b**. U_{eq} is defined as 1/3 of the trace of the orthogonalised U_{ij}.

Atom	x	y	z	U_{eq}
S(1)	4168.74(16)	4658.49(19)	3472.3(6)	26.04(13)
O(1)	4346.3(6)	4999.7(7)	2004(2)	35.5(3)
O(2)	4337.1(5)	4036.0(6)	3739(2)	33.0(3)
N(1)	4282.1(6)	4914.1(7)	6940(2)	27.4(3)
C(4)	2472.4(8)	4624.5(8)	3100(2)	28.6(4)
C(2)	3256.8(8)	5174.0(9)	2865(3)	31.1(4)
C(1)	3509.7(7)	4639.2(8)	3344(3)	25.6(4)
C(9)	4448.1(8)	5721.4(8)	5234(3)	29.7(4)
C(5)	2734.4(7)	4095.2(8)	3574(3)	29.5(4)
C(8)	4311.3(7)	5106.4(8)	5245(3)	25.6(4)
C(10)	4502.6(8)	5905.6(9)	6948(3)	32.8(4)
C(6)	3251.1(7)	4097.9(8)	3680(3)	27.3(4)
C(11)	4403.6(8)	5397.8(9)	7958(3)	32.2(4)
C(7)	1912.4(9)	4623(1)	2973(3)	37.8(5)
C(3)	2742.2(8)	5158.9(9)	2732(3)	32.7(4)
C(12)	4169(8)	4299.2(9)	7577(3)	34.4(5)

Table 9.5: Anisotropic Displacement Parameters (×10⁴) **3b**. The anisotropic displacement factor exponent takes the form: $-2\pi^2[h^2a^{*2} \times U_{11} + \ldots + 2hka^* \times b^* \times U_{12}]$

Atom	U_{11}	U_{22}	U_{33}	U_{23}	U_{13}	U_{12}
S(1)	25.4(2)	27.5(2)	25.2(2)	-0.08(16)	3.70(18)	0.75(17)
O(1)	36.8(8)	42.9(8)	26.8(7)	-6.6(6)	4.9(6)	1.9(6)
O(2)	27.9(7)	32.3(7)	38.7(8)	4.1(5)	2.9(6)	-1.8(6)
N(1)	25.6(8)	30.1(8)	26.5(8)	0.7(6)	1.1(7)	3.1(7)
C(4)	29(1)	33.9(8)	22.8(10)	1.6(7)	-1.7(7)	0.3(7)
C(2)	33.1(10)	24.5(8)	35.6(11)	-1.6(7)	0.9(8)	3.5(8)
C(1)	27.1(9)	27.4(8)	22.4(9)	1.7(7)	3.0(8)	0.8(6)
C(9)	26.6(10)	29.2(9)	33.5(11)	-1.5(7)	-0.6(8)	6.2(8)
C(5)	30.5(10)	27.8(8)	30.1(10)	-2.3(7)	0.7(8)	4.5(8)
C(8)	22.0(9)	29.2(9)	25.7(9)	1.0(7)	1.1(7)	2.8(7)
C(10)	31.5(11)	31.3(9)	35.5(11)	-3.8(8)	-3.4(9)	1.1(8)
C(6)	30.5(9)	24.4(8)	27.2(10)	2.0(7)	0.5(8)	4.2(7)
C(11)	30.3(10)	37.5(10)	28.7(11)	-0.7(8)	-2.6(8)	-1.0(8)
C(7)	30.4(11)	43.7(11)	39.4(13)	4.0(8)	-4.0(9)	-0.7(9)
C(3)	34.7(11)	28.0(8)	35.4(11)	8.3(8)	-2.5(9)	2.6(8)
C(12)	40.8(12)	30.8(9)	31.7(12)	-0.7(8)	2.9(9)	7.1(8)

Table 9.6: Bond Lengths in Å for **3b**.

Atom	Atom	Length/Å
S(1)	O(1)	1.4398(17)
S(1)	O(2)	1.4356(14)
S(1)	C(1)	1.7698(19)
S(1)	C(8)	1.727(2)
N(1)	C(8)	1.383(3)
N(1)	C(11)	1.352(3)
N(1)	C(12)	1.455(2)
C(4)	C(5)	1.393(3)
C(4)	C(7)	1.504(3)
C(4)	C(3)	1.394(3)
C(2)	C(1)	1.392(3)
C(2)	C(3)	1.383(3)
C(1)	C(6)	1.386(3)
C(9)	C(8)	1.380(3)
C(9)	C(10)	1.398(3)
C(5)	C(6)	1.387(3)
C(10)	C(11)	1.376(3)

Table 9.7: Bond Angles in ° for **3b**.

Atom	Atom	Atom	Angle/°
O(2)	S(1)	O(1)	119.44(9)
C(1)	S(1)	O(1)	107.30(10)
C(1)	S(1)	O(2)	107.45(8)
C(8)	S(1)	O(1)	105.73(9)
C(8)	S(1)	O(2)	109.99(10)
C(8)	S(1)	C(1)	106.19(9)
C(11)	N(1)	C(8)	108.09(16)
C(12)	N(1)	C(8)	127.68(17)
C(12)	N(1)	C(11)	124.19(19)
C(7)	C(4)	C(5)	121.24(18)
C(3)	C(4)	C(5)	118.35(18)
C(3)	C(4)	C(7)	120.41(18)
C(3)	C(2)	C(1)	119.07(18)
C(2)	C(1)	S(1)	118.79(14)
C(6)	C(1)	S(1)	120.57(14)
C(6)	C(1)	C(2)	120.63(18)
C(10)	C(9)	C(8)	107.24(18)
C(6)	C(5)	C(4)	121.03(17)
N(1)	C(8)	S(1)	125.31(14)
C(9)	C(8)	S(1)	126.48(17)
C(9)	C(8)	N(1)	108.13(18)
C(11)	C(10)	C(9)	107.21(17)
C(5)	C(6)	C(1)	119.45(16)
C(10)	C(11)	N(1)	109.3(2)
C(2)	C(3)	C(4)	121.44(18)

Table 9.8: Hydrogen Fractional Atomic Coordinates (×10⁴) and Equivalent Isotropic Displacement Parameters (Å²×10³) for **3b**. U_{eq} is defined as 1/3 of the trace of the orthogonalized U_{ij}.

Atom	x	y	z	U_{eq}
H(2)	3431.2(8)	5536.3(9)	2637(3)	37.3(5)
H(3)	2572.7(8)	5519(9)	2390(3)	39.2(5)
H(5)	2560.2(7)	3734.4(8)	3823(3)	35.4(5)
H(6)	3422.5(7)	3739.5(8)	3974(3)	32.8(5)
H(9)	4495.2(8)	5967.4(8)	4266(3)	35.7(5)
H(10)	4589.5(8)	6298.0(9)	7333(3)	39.3(5)
H(11)	4418.0(8)	5388.9(9)	9154(3)	38.6(5)
H(7a)	1778.7(9)	4947(6)	3680(19)	56.8(7)
H(7b)	1815.0(9)	4689(9)	1798(5)	56.8(7)
H(7c)	1786(1)	4232(3)	3360(20)	56.8(7)
H(12c)	4408(4)	4010.3(17)	7170(20)	51.6(7)
H(12b)	4164(7)	4302(2)	8812(3)	51.6(7)
H(12a)	3839(3)	4179(4)	7170(20)	51.6(7)

9.12 Crystal data: 3m

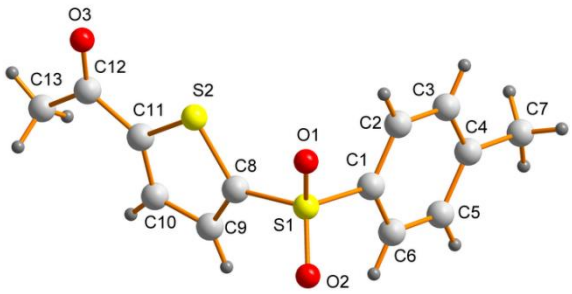

Figure 9.5: Single X-ray crystal structure of **3m**

Experimental: Single clear colorless prism-shaped crystals of (**3m**) were obtained by recrystallization from DCM/pentane diffusion method. A suitable crystal (0.26×0.20×0.17) mm³ was selected and mounted on a SuperNova, a Single source at the offset, Atlas diffractometer. The crystal was kept at T = 123.00(10) K during data collection. Using **Olex2** (Dolomanov et al., 2009), the structure was solved with the **ShelXT** (Sheldrick, 2015) structure solution program, using the Intrinsic Phasing solution method. The model was refined with version 2016/6 of **ShelXL** (Sheldrick, 2015) using Least Squares minimisation.

Crystal Data. $C_{13}H_{12}O_3S_2$, M_r = 280.35, monoclinic, $P2_1/c$ (No. 14), a = 10.1074(2) Å, b = 16.4523(3) Å, c = 7.8081(2) Å, β = 101.625(2)°, α = γ = 90°, V = 1271.77(5) Å³, T = 123.00(10) K, Z = 4, Z' = 1, μ(CuK_α) = 3.783, 13789 reflections measured, 2536 unique (R_{int} = 0.0242) which were used in all calculations. The final wR_2 was 0.0744 (all data) and R_1 was 0.0273 (I > 2(I)).

Compound	**3m**
Formula	$C_{13}H_{12}O_3S_2$
$D_{calc.}$/ g cm^{-3}	1.464
μ/mm^{-1}	3.783
Formula Weight	280.35
Colour	clear colourless
Shape	prism
Size/mm³	0.26×0.20×0.17
T/K	123.00(10)
Crystal System	monoclinic
Space Group	$P2_1/c$
a/Å	10.1074(2)
b/Å	16.4523(3)
c/Å	7.8081(2)
α/°	90
β/°	101.625(2)
γ/°	90
V/Å³	1271.77(5)
Z	4
Z'	1
Wavelength/Å	1.54184
Radiation type	CuK_α
Θ_{min}/°	5.214
Θ_{max}/°	73.712
Measured Refl.	13789
Independent Refl.	2536
Reflections Used	2443
R_{int}	0.0242
Parameters	165
Restraints	0
Largest Peak	0.396
Deepest Hole	-0.327
GooF	1.033
wR_2 (all data)	0.0744
wR_2	0.0737
R_1 (all data)	0.0282
R_1	0.0273

Table 9.9: Fractional Atomic Coordinates (×10⁴) and Equivalent Isotropic Displacement Parameters (Å²×10³) for **3m**. U_{eq} is defined as 1/3 of the trace of the orthogonalized U_{ij}.

Atom	x	y	z	U_{eq}
S2	3653.7(3)	3175.0(2)	6292.5(4)	16.66(10)
S1	6205.3(3)	3947.3(2)	8233.5(4)	15.81(11)
O1	5284.1(10)	4625.3(6)	7939.0(13)	21.4(2)
O2	6993.1(11)	3795.4(7)	9947.2(13)	22.7(2)
O3	1330.6(11)	2234.9(6)	4445.0(15)	27.6(3)
C2	6949.8(14)	4478.4(8)	5258.2(18)	17.5(3)
C10	4633.8(14)	1742.5(8)	7045.9(18)	18.7(3)
C8	5239.8(14)	3078.3(8)	7557.8(17)	16.1(3)
C11	3504.0(14)	2132.0(8)	6155.4(17)	16.8(3)
C9	5641.5(15)	2288.4(8)	7859.0(18)	18.9(3)
C12	2236.5(14)	1787.9(8)	5142.5(18)	19.0(3)
C3	7784.8(15)	4486.6(9)	4048.8(18)	20.0(3)
C4	8977.3(15)	4038.1(8)	4325.8(19)	19.1(3)
C1	7307.6(14)	4013.1(8)	6756.3(18)	15.8(3)
C6	8499.3(15)	3563.6(9)	7080.5(19)	21.0(3)
C5	9322.0(15)	3581.1(9)	5859.5(19)	22.0(3)
C13	2141.5(16)	879.6(9)	5024(2)	24.7(3)
C7	9877.2(16)	4048.8(10)	3005(2)	25.2(3)

Table 9.10: Anisotropic Displacement Parameters (×10⁴) **3m**. The anisotropic displacement factor exponent takes the form: $-2\pi^2[h^2a^{*2} \times U_{11} + \ldots + 2hka^* \times b^* \times U_{12}]$

Atom	U_{11}	U_{22}	U_{33}	U_{23}	U_{13}	U_{12}
S2	15.47(17)	14.51(17)	19.09(18)	-0.85(11)	1.30(12)	1.26(11)
S1	15.81(18)	16.22(18)	15.15(17)	-2.19(11)	2.52(13)	-0.86(11)
O1	20.8(5)	17.4(5)	26.6(5)	-3.8(4)	6.3(4)	0.8(4)
O2	23.1(5)	28.9(5)	15.1(5)	-2.0(4)	1.6(4)	-3.4(4)
O3	21.0(5)	23.7(5)	34.3(6)	-4.6(4)	-3.3(5)	2.9(4)
C2	14.6(6)	16.8(6)	20.1(7)	1.1(5)	0.9(5)	1.6(5)
C10	20.5(7)	16.0(6)	19.9(7)	1.3(5)	5.0(5)	1.1(5)
C8	16.5(6)	17.4(6)	14.4(6)	-0.4(5)	2.8(5)	-0.4(5)
C11	19.4(7)	15.7(6)	16.4(6)	-1.4(5)	6.0(5)	-1.0(5)
C9	18.4(7)	18.8(7)	18.9(7)	2.1(5)	1.9(5)	1.8(5)
C12	18.4(7)	20.9(7)	18.6(7)	-2.7(5)	5.6(5)	0.4(5)
C3	21.1(7)	20.2(7)	17.7(6)	3.4(5)	1.4(5)	-0.5(5)
C4	17.8(7)	20.0(7)	19.1(7)	-2.0(5)	3.1(5)	-2.1(5)
C1	14.4(6)	15.9(6)	16.7(6)	-1.7(5)	2.3(5)	-2.2(5)
C6	20.3(7)	22.9(7)	18.8(7)	4.5(5)	1.8(5)	3.9(6)
C5	16.9(7)	24.9(7)	23.8(7)	2.0(6)	3.0(6)	6.0(6)
C13	29(7)	20.2(7)	29.5(8)	-4.7(6)	2.9(6)	-2.2(6)
C7	29(8)	30.8(8)	22.8(7)	0.9(6)	7.9(6)	1.3(6)

Table 9.11: Bond Lengths in Å for **3m**.

Atom	Atom	Length/Å
S2	C8	1.7127(14)
S2	C11	1.7240(14)
S1	O1	1.4414(10)
S1	O2	1.4344(11)
S1	C8	1.7514(14)

Atom	Atom	Length/Å
S1	C1	1.7610(14)
O3	C12	1.2144(18)
C2	C3	1.388(2)
C2	C1	1.3837(19)
C10	C11	1.370(2)

Atom	Atom	Length/Å
C10	C9	1.409(2)
C8	C9	1.3677(19)
C11	C12	1.4761(19)
C12	C13	1.499(2)
C3	C4	1.392(2)
C4	C5	1.397(2)
C4	C7	1.507(2)
C1	C6	1.392(2)
C6	C5	1.386(2)

Table 9.12: Bond Angles in ° for **3m**.

Atom	Atom	Atom	Angle/°
C8	S2	C11	90.20(7)
O1	S1	C8	106.31(6)
O1	S1	C1	108.76(6)
O2	S1	O1	120.20(6)
O2	S1	C8	108.04(6)
O2	S1	C1	108.43(6)
C8	S1	C1	103.92(6)
C1	C2	C3	119.30(13)
C11	C10	C9	112.53(13)
S2	C8	S1	119.86(8)
C9	C8	S2	113.48(11)
C9	C8	S1	126.57(11)
C10	C11	S2	112.35(10)
C10	C11	C12	129.57(13)
C12	C11	S2	118.09(10)
C8	C9	C10	111.44(13)
O3	C12	C11	120.17(13)
O3	C12	C13	122.87(14)
C11	C12	C13	116.96(13)
C2	C3	C4	121.02(13)
C3	C4	C5	118.48(13)
C3	C4	C7	120.70(13)
C5	C4	C7	120.82(13)
C2	C1	S1	119.71(11)
C2	C1	C6	121.11(13)
C6	C1	S1	119.11(10)
C5	C6	C1	118.74(13)
C6	C5	C4	121.34(13)

Table 9.12: Hydrogen Fractional Atomic Coordinates (×10⁴) and Equivalent Isotropic Displacement Parameters (Å²×10³) for **3m**. U_{eq} is defined as 1/3 of the trace of the orthogonalized U_{ij}.

Atom	x	y	z	U_{eq}
H2	6157.95	4782.49	5063.84	21
H10	4725.46	1180.19	7106.95	22
H9	6474.25	2131.33	8517.01	23
H3	7544.28	4796.35	3037.58	24
H6	8738.48	3257.33	8096.95	25
H5	10119.81	3282.71	6065.07	26
H13A	2164.76	657.14	6166.02	37
H13B	2888.8	671.34	4569.56	37
H13C	1310.22	728.74	4259.56	37
H7A	9345.7	3946.51	1860.36	38
H7B	10556.33	3635.62	3292.29	38
H7C	10302.94	4571.05	3019.04	38

9.13 References:

[1] a) D. Granchi, A. Scarso, G. Bianchini, A. Chiminazzo, A. Minto, P. Sgarbossa, R. A. Michelin, G. Di Pompo, S. Avnet, G. Strukul, *Eur. J. Med. Chem.* **2013**, *65*, 448; b) F. Pinnen, I. Cacciatore, C. Cornacchia, P. Sozio, L. S. Cerasa, A. Iannitelli, C. Nasuti, F. Cantalamessa, D. Sekar, R. Gabbianelli, *J. Med. Chem.* **2009**, *52*, 559.

[2] a) H. J. M. Gijsen, M. A. J. de Cleyn, M. Surkyn, G. R. E. van Lommen, B. M. P. Verbist, M. J. M. A. Nijsen, T. Meert, J. van Wauwe, J. Aerssens, *Bioorg. Med. Chem. Lett.* **2012**, *22*, 547; b) S. Caddick, K. Aboutayab, R. West, *Synlett* **1993**, 231; c) T. Asai, T. Takeuchi, J. Diffenderfer, D. L. Sibley, *Antimicrob. Agents Ch.* **2002**, *46*, 2393; d) B. J. Lavey, J. A. Kozlowski, R. W. Hipkin, W. Gonsiorek, D. J. Lundell, J. J. Piwinski, S. Narula, C. A. Lunn, *Bioorg. Med. Chem. Lett.* **2005**, *15*, 783.

[3] B. Benhamu, M. Martin-Fontecha, H. Vazquez-Villa, L. Pardo, M. L. Lopez-Rodriguez, *J. Med. Chem.* **2014**, *57*, 7160.

[4] a) G. Tocco, M. Begala, F. Esposito, P. Caboni, V. Cannas, E. Tramontano, *Tet. Lett.* **2013**, *54*, 6237; b) G. La Regina, A. Coluccia, A. Brancale, F. Piscitelli, V. Gatti, G. Maga, A. Samuele, C. Pannecouque, D. Schols, J. Balzarini et al., *J. Med. Chem.* **2011**, *54*, 1587.

[5] O. Cazorla, A. Lacampagne, J. Fauconnier, G. Vassort, *Br. J. Pharmacol.* **2003**, *139*, 99.

[6] L. Tong, B. B. Shankar, L. Chen, R. Rizvi, J. Kelly, E. Gilbert, C. Huang, D.-Y. Yang, J. A. Kozlowski, N.-Y. Shih et al., *Bioorg. Med. Chem. Lett.* **2010**, *20*, 6785.

[7] a) F. Chen, Q. Meng, S.-Q. Han, B. Han, *Org. Lett.* **2016**, *18*, 3330; b) J.-K. Qiu, W.-J. Hao, D.-C. Wang, P. Wei, J. Sun, B. Jiang, S.-J. Tu, *Chem. Comm.* **2014**, *50*, 14782.

[8] M. Chen, Z.-T. Huang, Q.-Y. Zheng, *Chem. Comm.* **2012**, *48*, 11686.

[9] A. U. Meyer, A. Wimmer, B. Konig, *Angew. Chem., Int. Ed.* **2017**, *56*, 409.

[10] S. Liang, R.-Y. Zhang, L.-Y. Xi, S.-Y. Chen, X.-Q. Yu, *J. Org. Chem.* **2013**, *78*, 11874.

[11] F. Hu, X. Lei, *ChemCatChem* **2015**, *7*, 1539.

[12] P. Katrun, C. Mueangkaew, M. Pohmakotr, V. Reutrakul, T. Jaipetch, D. Soorukram, C. Kuhakarn, *J. Org. Chem.* **2014**, *79*, 1778.

[13] Y. Yang, W. Li, C. Xia, B. Ying, C. Shen, P. Zhang, *ChemCatChem* **2016**, *8*, 304.

[14] P. Natarajan, A. Bala, S. K. Mehta, K. K. Bhasin, *Tetrahedron* **2016**, *72*, 2521.

[15] F.-L. Yang, S.-K. Tian, *Angew. Chem., Int. Ed.* **2013**, *52*, 4929.

[16] a) Y. Chen, C.-H. Cho, F. Shi, R. C. Larock, *J. Org. Chem.* **2009**, *74*, 6802; b) E. Vedejs, J. D. Little, *J. Org. Chem.* **2004**, *69*, 1794.

[17] K. Kobayashi, A. Kobayashi, K. Ezaki, *Tetrahedron* **2013**, *69*, 7936.

[18] B. M. Graybill, *J. Org. Chem.* **1967**, *32*, 2931.

[19] S. K. Pagire, S. Paria, O. Reiser, *Org. Lett.* **2016**, *18*, 2106.

[20] S. J. Nara, J. R. Harjani, M. M. Salunkhe, *J. Org. Chem.* **2001**, *66*, 8616.

[21] a) G.-B. Deng, Z.-Q. Wang, J.-D. Xia, P.-C. Qian, R.-J. Song, M. Hu, L.-B. Gong, J.-H. Li, *Angew. Chem., Int. Ed.* **2013**, *52*, 1535; b) J.-D. Xia, G.-B. Deng, M.-B. Zhou, W. Liu, P. Xie, J.-H. Li, *Synlett* **2012**, *23*, 2707.

[22] a) D. B. Bagal, G. Kachkovskyi, M. Knorn, T. Rawner, B. M. Bhanage, O. Reiser, *Angew. Chem., Int. Ed.* **2015**, *54*, 6999; b) T. Rawner, M. Knorn, E. Lutsker, A. Hossain, O. Reiser, *J. Org. Chem.* **2016**, *81*, 7139.

[23] F. Teplý, *Collect. Czech. Chem. Commun.* **2011**, *76*, 859.

[24] J. Sun, W. Wu, J. Zhao, *Chem. Eur. J.* **2012**, *18*, 8100.

[25] a) F. Jafarpour, M. B. A. Olia, H. Hazrati, *Adv. Synth. Catal.* **2013**, *355*, 3407; b) M. Zhang, S. Zhang, M. Liu, J. Cheng, *Chem. Comm.* **2011**, *47*, 11522; c) A. Hfaiedh, K. Yuan, H. Ben Ammar, B. Ben Hassine, J.-F. Soule, H. Doucet, *ChemSusChem* **2015**, *8*, 1794.

[26] R. Jin, K. Yuan, E. Chatelain, J.-F. Soulé, H. Doucet, *Adv. Synth. Catal.* **2014**, *356*, 3831.

[27] L. Marzo, I. Ghosh, F. Esteban, B. König, *ACS Catal.* **2016**, *6*, 6780.

[28] B. Michelet, C. Deldaele, S. Kajouj, C. Moucheron, G. Evano, *Org. Lett.* **2017**, *19*, 3576.

[29] D. Gao, T. G. Back, *Synlett* **2013**, *24*, 389.

[30] J. Gubin, H. de Vogelaer, H. Inion, C. Houben, J. Lucchetti, J. Mahaux, G. Rosseels, M. Peiren, M. Clinet, P. Polster et al., *J. Med. Chem.* **1993**, *36*, 1425.

[31] S. Tong, Z. Xu, M. Mamboury, Q. Wang, J. Zhu, *Angew. Chem., Int. Ed.* **2015**, *54*, 11809.

10 Summary:

This thesis demonstrates the development of new and unprecedented activation methods in visible-light mediated photoredox catalysis. The established transformations not only unlocked new avenues in organic synthesis but holds enormous potential for the future advancements and sustainable developments in this field.

In chapter 1, I have outlined a short overview of visible-light-mediated processes that have been established over the years, starting with Ciamician's idea of using sunlight as a clean and unlimited energy source for organic synthesis. Therein, I have also highlighted four principal activation modes associated with visible-light photocatalysis (*i.e*, oxidative quenching, reductive quenching, energy transfer, and a photocascade process). Accordingly, I stated the diversity of various synthetic methods relies upon the ability of photoredox catalysts such as $[Ru(bpy)_3]Cl_2$, $[Ir\{dF(CF_3)ppy\}_2(dtbbpy)]PF_6$, $[Ir(ppy)_2(dtbbpy)]PF_6$, or *fac*-$Ir(ppy)_3$ to undergo a number of productive quenching pathways from the excited state. The flexibility of these catalysts has allowed for the development of a series of transformations such as diradical formation by triplet photosensitization, cycloaddition reactions, vinyl radical formation by reductive radical dehalogenations, 1,6-HAT process or α-amino functionalization, sulfonylation as well as arylation reactions, etc. Notably, these photocatalysts certainly possess a series of advantages over the classical radical chemistry in light of sustainable developments.

In chapter 2, we have summarized the visible-light mediated activation of C-X bonds, generation of vinyl radical as a key intermediate, and its applications in organic synthesis that are developed in last few years, mostly from our group.

In chapter 3, I have presented the unprecedented activation of vinyl-bromides with molecular oxygen utilizing dual energy and electron transfer modes: *Ortho*-alkynylated α-bromocinnamates can be converted by a visible-light-mediated photocascade reaction with molecular oxygen into either indenones or dihydroindeno[1,2-c]chromenes. The one-step process features key photochemical steps; thus, the initial activation of vinyl bromides through energy transfer to give α-ketoradicals in a reaction with molecular oxygen, followed by α-oxidation of an arene moiety by 6-π electrocyclization, and subsequent hydroxylation by an electron-transfer process from the

same photocatalyst leads to the dihydroindeno[1,2-c]chromenes. For this chapter, I have conducted a series of experiments in attempts of understanding the detailed reaction mechanism. While finding the mechanistic details, some of the attempts also ended up in disclosing the new reactions; for examples, visible-light mediated [2+2]-photocycloaddition of cinnamates with visible-light was unknown. As a consequence, we have subsequently developed the latter method and extended the scope of the stated transformation, which is separately described in chapter 4.

In chapter 4, an efficient method for the synthesis of substituted cyclobutanes from cinnamates, chalcones, and styrenes utilizing a visible-light triplet sensitization mode was described. This reaction provided a diverse range of substituted cyclobutanes in high yields under mild conditions without the need of external additives. Good regioselectivity was obtained due to strong π–π-stacking of arene moieties, whereas diastereoselectivity relied on the electronic effects or *ortho*-substitution of the arene substrate. Furthermore, we have also shown the utility of this transformation by formal synthesis of the lignane natural product (±)-Tanegool.

In chapter 5, a tin-free method for the synthesis of substituted indolines was described generating vinyl radicals by visible-light-promoted photocatalysis in a reductive quenching cycle. This method offered a mild, robust, and high yielding pathway to a wide range of indolines containing diverse electronic substituents. The resulting 2,3-disubstituted indolines serve as valuable precursors for the synthesis of biologically active molecules, which was demonstrated with the formal synthesis of Tryptamines and Furoindolines. Notably, we have replaced the hazardous reagents and harsh reaction conditions with the mild reaction conditions.

In chapter 6, the unprecedented discovery of Triquinacenes was outlined: We have shown for the first time, a visible-light mediated cascade of C-C bond formations with vinyl chlorides and phenyl acetylenes. Noteworthy, this process involves four highly reactive vinyl radical intermediates, which was engaged in a productive reaction cascades with two phenyl acetylene molecules, leading to the complex molecular designs in a single photochemical step under the mild reaction conditions. This reaction could also be performed in the micro-flow reactors in the short reaction time. Arguably, the single step synthesis of these types of complex architectures is certainly impossible to accomplish by employing other methods at this stage.

In chapter 7, I have highlighted the applications of sulfonyl chlorides. This has been found a cheap, biocompatible, readily available reagent for sulfonylation, trifluoromethylation or arylation reactions under visible-light conditions.

In chapter 8, the sequential [Cu] and [Ir] photocatalyzed method for the synthesis of β-hydroxysulfones from sulfonyl chlorides and styrenes in the presence of water was demonstrated. We showed here the importance of each specific catalyst that is employed in the title transformation. In turn, this paper has already received a remarkable attention from the synthetic community.

Finally, in chapter 9, I further extended the scope of sulfonyl chlorides for arylation or sulfonylation of heterocycles at different temperature conditions. We showed for the first time a comparative study on the selective C-C and C-S bond formations just by adjusting the appropriate reaction temperature.

Overall, in my PhD work, I had a chance to work in the fascinating field of visible-light photoredox catalysis. As shown, I have come across several unique reaction pathways and closely witnessed these surprising discoveries. Undoubtedly, further discovery and development of new methods utilizing visible light-mediated photoredox catalysis will continue to grow in the next years, particularly due to the redox flexibility of photocatalysts to be employed with a range of reactions. However, a detailed study of how factors such as temperature, solvent choice, catalyst choice, or additives, etc…affect the reaction outcome. Such studies will be necessary to understand how to better improve existing methods and develop new methods. More importantly, these studies may also provide answers to many of the existing anomalous results that have been observed in this field. One example of an observation that could possibly be explained by more rigorous mechanistic studies involves the specific role of oxygen for the vinyl bromide activation (Chapter 3) or the high reactivity of vinyl chlorides over vinyl bromides in Triquinacene synthesis (Chapter 6), and so on. Another observation pertains to the unexpected C-S bond formation in the trifluoromethylsulfochlorination reaction in the presence of selected [Cu]-catalyst in contrast to the [Ir]- or [Ru]-photocatalysts (Chapter 8).

Last, but not least, to understand the detailed reaction mechanism of new photoredox methods is still a challenging task. Preliminary results in our group, especially for the activation of vinyl halides indicate that particular reactions are prone to a high level of selectivity and reactivity via different reaction pathways based on the specific substituents present on the starting materials or the photocatalyst employed. The design of special substrates or identification of key intermediates involved could open new chapters along with understanding the mode of action of a photocatalyst in the overall process.

11 Zusammenfassung:

Diese Arbeit beschreibt die Entwicklung neuer Aktivierungsmethoden in der Photoredoxkatalyse mit sichtbarem Licht. Die hier beschriebenen Umwandlungen eröffnen nicht nur Wege in der organischen Synthese, sondern bergen auch enormes Potential für zukünftige Untersuchungen und nachhaltige Entwicklungen in diesem Bereich.

In Kapitel 1 wurde ein kurzer Überblick über die verschiedenen, von sichtbarem Licht getriebenen Prozesse gegeben, welche sich über die Jahre etabliert haben, angefangen mit Ciamicians Idee Sonnenlicht als saubere, unbegrenzt zur Verfügung stehende Energiequelle für die organische Synthese zu nutzen. In diesem Kapitel wurden zudem die vier grundlegen Aktivierungsmethoden der Photokatalyse mit sichtbarem Licht näher betrachtet (d.h. oxidatives Quenching, reduktives Quenching, Energietransfer und Photoredoxkaskaden). Dementsprechend wurde beschrieben, dass die Bandbreite an chemischen Transformationen von Photoredoxkatalysatoren wie $[Ru(bpy)_3]Cl_2$, $[Ir\{dF(CF_3)ppy\}_2(dtbbpy)]PF_6$, $[Ir(ppy)_2(dtbbpy)]PF_6$, oder *fac*-$Ir(ppy)_3$, von deren Fähigkeit abhängt ausgehend vom angeregten Zustand produktive Quenchingschritte durchführen zu können. Die vielseitige Einsetzbarkeit dieser Katalysatoren ermöglichte die Entwicklung diverser Umwandlungen, wie z.B. die Diradikalbildung durch Triplett-Photosensitizer, Cycloadditionsreaktionen, Vinylradikalbildung durch reduktive, radikalische Dehalogenierung, der 1,6-HAT-Prozess, α-Aminofunktionalisierung, Sulfonylierungs- sowie Arylierungsreaktionen und viele mehr. Diese Photokatalysatoren besitzen eine bemerkenswerte Reihe an Vorteilen gegenüber der klassischen Radikalchemie in Hinblick auf nachhaltige Entwicklungen.

In Kapitel 2 wurden die Aktivierung von C-X-Bindungen, die Generierung von Vinylradikalen als Schlüsselintermediate und deren Anwendung in der organischen Synthese der letzten Jahre zusammengefasst.

In Kapitel 3 wurde eine neuartige Aktivierung von Vinylbromiden mit molekularem Sauerstoff unter Verwendung von Energie- und Elektronenentransfer beschrieben. *Ortho*-alkynylierte α-Bromzimtsäuren konnten mit sichtbarem Licht in einer Photokaskadenreaktion mit molekularem Sauerstoff in Indenone sowie Dihydroindeno[1,2-c]chromene umgewandelt werden. Dieser einstufige Prozess beinhaltet photochemische Schlüsselschritte: die anfängliche Aktivierung der

Vinylbromide zu α-Ketoradikalen durch Energietransfer mit molekularem Sauerstoff, gefolgt von α-Oxidierung einer Arengruppe durch 6-π-Elektrozykliesierung und anschließender Hydroxylierung durch einen Elektronentrasferprozess desselben Katalysators, was zur Bildung von Dihydroindeno[1,2-c]chromene führt. Hierfür wurden eine Reihe an Experimenten durchgeführt um den genauen Reaktionsmechanismus zu ermitteln und zu verstehen. Diese Experimente führten auch zur Entdeckung neuer Reaktionen, z.B. die zuvor unbekannte [2+2]-Photocycloaddition von Zimtsäuren mit sichtbarem Licht. Diese wurde als Folge später genauer untersucht und das Anwendungsspektrum erweitert, was in Kapitel 4 näher beschrieben wird.

In Kapitel 4 wurde eine effiziente Methode zur Synthese von substituierten Cyclobutanen, ausgehend von Zimtsäuren, Chalconen und Styrolen und mithilfe von Triplett-Sensitizern sowie sichtbarem Licht, beschrieben. Eine Vielzahl an substituierten Cyclobutanen konnte mit dieser Methode in hohen Ausbeuten unter milden Bedingungen ohne zusätzliche Additive hergestellt werden. Die gute Regioselektivität konnte aufgrund des starken π-π-Stackings der Arengruppen erreicht werden, die Diastereoselektivität basierte auf elektronischen Effekten oder der *ortho*-Substitution des Arensubstrats. Der Nutzen dieser Transformation konnte durch die Formalsynthese des in Lignan vorkommenden Naturstoffs (±)-Tanegool aufgezeigt werden.

In Kapitel 5 wurde eine Zinn-freie Methode zur Synthese von substituierten Indolinen durch Generierung von Vinylradikalen mittels Photokatalyse unter sichtbarem Licht und reduktiven Quenching beschrieben. Diese Methode bot einen milden, robusten Weg zur Darstellung einer Vielzahl an substituierten Indolinen in hohen Ausbeuten. Die entstanden 2,3-disubstitueirten Indoline dienen als nützliche Vorstufen für die Synthese von biologisch aktiven Verbindungen. Dies wurde durch die Formalsynthese von Tryptaminen und Furoindolinen demonstriert. Hier konnten gefährliche Reagenzien und harsche Reaktionsbedingungen durch mildere ersetzt werden.

In Kapitel 6 wurde die Entdeckung einer neuartigen Methode zur Darstellung von Triquinacenen erörtert: durch eine zuvor unbekannte Kaskade von C-C-Bindungsknüpfungen von Vinylchloriden und Phenylacetlyenen unter sichtbarem Licht. Hier ist zu bemerken, dass dieser Prozess insgesamt vier reaktive Vinyradikallintermediate beinhaltete, welche in einer Reaktionskaskade mit zwei Molekülen Phenylacetylen reagierten was zur Bildung der komplexen Verbindung unter milden, photochemischen Bedingungen in einem Schritt führte.

Diese Reaktion konnte zudem auch in einem Mikroreaktor im Flow mit kurzen Reaktionszeiten durchgeführt werden. Die Einstufensynthese dieser komplexen Verbindungen ist zurzeit vermutlich durch keine andere Methode möglich.

In Kapitel 7 wurden die Anwendungen von Sulfonylchloriden näher betrachtet. Diese stellen günstige, biokompatible Reagenzien zur Sulfonylierung, Trifluoromethylierung oder Arylierung für Reaktionen unter sichtbarem Licht dar.

In Kapitel 8 wurde die sequenzielle [Cu]- und [Ir]-photokatalysierte Methode zur Synthese von β-Hydroxysulfonen ausgehend von Sulfonylchloriden und Styrolen in Anwesenheit von Wasser beschrieben. Dabei wurde die Wichtigkeit jedes verwendeten Katalysators für die Reaktion aufgezeigt. Die resultierende Publikation hat schon jetzt Aufmerksamkeit in der chemischen Gemeinschaft bekommen.

Im abschließenden 9. Kapitel wurde die Anwendungsbreite der nutzbaren Sulfonylchloride für die Arylierung oder Sulfonylierung von Heterozyklen bei verschieden Temperaturen erweitert. Eine Vergleichsstudie wurde angefertigt, welche den Einfluss der Temperatur auf die konkurrierende selektive C-C bzw. C-S-Bindungsknüpfung aufzeigt.

Während meiner Studien zu dieser Doktorarbeit hatte ich die Chance im faszinierenden Feld der Photoredoxkatalyse mit sichtbarem Licht zu arbeiten. Wie aufgezeigt war ich in der Lage über verschiedene, einzigartige Reaktionswege zu stolpern und diese überraschenden Entdeckungen näher zu untersuchen. Ohne Zweifel werden auch in den nächsten Jahren weitere Entdeckungen im Feld der Photoredoxkatalyse mit sichtbarem Licht gemacht werden und neue Methoden entwickelt werden, insbesondere aufgrund der Flexibilität der Redoxeigenschaften der Photokatalysatoren welche in vielen Reaktionen ausgenutzt werden wird. Dies erfordert jedoch die genaue Untersuchung von Reaktionsparametern, welche einen Einfluss auf den Ausgang der Reaktion haben, wie z.B. Temperatur, Lösungsmittel, Katalysator oder Additive. Diese Untersuchungen sind wichtig um bereits existierende Methoden zu verbessern und neue Methoden zu entwickeln. Zudem können diese auch Antworten auf viele ungeklärte Beobachtungen liefern welche in diesem Gebiet gemacht wurden. Ein Beispiel für eine Beobachtung welche durch genauere mechanistische Studien geklärt werden könnte ist die genaue Rolle des Sauerstoffs in der Vinylbromidaktivierung (Kapitel 3) oder die hohe Aktivität

der Vinylchloride im Vergleich zu den –bromiden in der Triquinacensynthese (Kapitel 6). Eine weitere untersuchenswerte Beobachtung ist die unerwartete C-S-Bindungsknüpfung in der Trifluoromethylsulfochlorierung, welche mit ausgewählten [Cu]-Katalysatoren, jedoch nicht mit [Ir]- oder [Ru]-Photokatalysatoren stattfindet (Kapitel 8).

Das Unterfangen den detaillierten Reaktionsmechanismus für neue Photoredoxmethoden zu verstehen ist noch immer sehr herausfordernd. Vorläufige Ergebnisse in unserer Arbeitsgruppe, speziell für die Aktivierung von Vinylhalogen, ergeben, dass hohe Selektivität und Reaktivität in bestimmten Reaktionen abhängig vom Substitutionsmuster der verwendeten Startmaterialien oder von der Wahl des Photokatalysators sind. Das Entwerfen von speziellen Substraten oder die Identifizierung der Schlüsselintermediate könnte neue Möglichkeiten eröffnen und zum Verständnis des Wirkmechanismus des Photokatalysators im gesamten Prozess beitragen.

12 Curriculum Vitae:

Santosh K. Pagire

Present Address:

Santosh K. Pagire
C/o. Prof. Dr. Oliver Reiser,
Institute of Organic Chemistry,
University of Regensburg,
D-93053 Regensburg, Germany.
E-mail: Santosh.Pagire@chemie.uni-regensburg.de / santoshpagire@gmail.com

Personal Information:

Full Name:	**Santosh Kisan Pagire**
Date of Birth:	July 21, 1988 (India)
Languages Known:	English (proficiency), Hindi, Marathi (native), and German (basic)
Nationality:	Indian
Hobbies:	reading, traveling, playing and watching cricket.
Permanent Address:	At- Pimpri Pathar, Post- Gargundi, Taluka- Parner, Dist- Ahmednagar, PIN- 414 304, Maharashtra, India.

Education and Research:

10/2013 – 12/2017 **Doctor of Philosophy (Ph.D.): Organic Chemistry** University of Regensburg, Germany.
Grade:
Research Advisor: Prof. Dr. Oliver Reiser (Dean of Research, UR)
Funding: DAAD (German Academic Exchange Service)
Ph.D. thesis title: *"Surprises and Discoveries in Visible-Light Photocatalysis"*.

05/2013 – 09/2013 **Intensive German Language Course:** Basic and advanced level course Goethe Institute, Chennai (India) and InterDaF, University of Leipzig (Germany); Organized and funded by DAAD.

06/2012 – 04/2013 **Research Assistant:** National Chemical Laboratory (CSIR-NCL), Pune, India.
Research Advisor: Dr. Subhash P. Chavan (Sci.-G).

10/2011 – 03/2012	**Research Scholar:** University of KwaZulu-Natal, Durban, South Africa [within the collaboration of Prof. Dilip D. Dhavale (India), Prof. Thavendran Govender (South Africa), and Prof. Pher G. Andersson (Sweden)].
06/2011 – 09/2011	**Lecturer:** Dhokeshwar Mahavidyalaya, Takali Dhokeshwar, Tal- Parner, Dist- Ahmednagar (Affiliated to University of Pune, India).
12/2010 – 12/2010	**National Eligibility Test (NET): Chemical Sciences**; Qualified in the first attempt with 22nd rank (all India rank from 12927 applicants and 1067 qualified students, success rate for our batch was 8.2%) conducted by CSIR-HRDG, New Delhi, India.
12/2010 – 12/2010	**State Eligibility Test (SET): Chemical Sciences**; Qualified in the first attempt (overall success rate for this examination is 3-6%); conducted by University of Pune, India.
06/2009 – 05/2011	**Master of Science (M.Sc.): Organic**, Inorganic, and Physical Chemistry University of Pune, India. Master thesis title: *"Organocatalytic Enantioselective Synthesis of Benzomorphan Analogues"* Grade: "O" (Outstanding, GPA: 5.31/6.00, 75.55%); Overall Rank**:** 04.
06/2006 – 05/2009	**Bachelor of Science (B.Sc.): Chemistry**, Physics, Botany, and Zoology University of Pune, India. Grade: *First Class with Distinction* (90.33%); Overall Rank**:** 05.

Awards and Achievements:

- Awarded a full-time **DAAD** fellowship to conduct the Ph.D. studies in Germany (2013-2017).
- Received ***iP*UR** and **GDCh** fellowships to attend the conferences in USA and Germany, respectively (2016).
- Awarded a **Junior Research Fellowship** (JRF) of the Council of Scientific and Industrial Research (**CSIR-NET**), New Delhi, India (2012-2013).
- Awarded an **Eklavya** scholarship on merit basis during M.Sc. (2009-2011).
- Awarded a **Kawathekar** scholarship on need-cum-merit basis during M.Sc. (2009-2011).

- Received **a best presentation** award in "**Prof. M. S. Wadia Lecture Competition**" (MSWLC) organized by New Arts, Commerce and Science College, Parner, Dist-Ahmednagar as a part of activities for the celebration of the international year of chemistry (2011).
- Ranked **1st** in Chemistry Entrance Test (CET, for the master program) conducted by New Arts, Commerce and Science College, Ahmednagar (2009).
- Ranked **3rd** in Chemistry Entrance Test (CET, for the master program) conducted by Abasaheb Garware College, Pune (2009).
- Ranked **5th** in Chemistry Entrance Test (CET, for the master program) jointly conducted by National Chemical Laboratory (CSIR-NCL) and Department of Chemistry, University of Pune (2009).
- **1st Prize** in cricket as a captain of the team and for the best performance throughout the series, University of Pune, India (2011).
- Ranked **2nd** for the research chemist position in the campus interview organized by Daiichi-Sankyo (also known as Ranbaxy laboratories - a pharmaceutical company), New Delhi, India (2011).

Professional References:

Prof. Dr. Oliver Reiser
Dean of Research,
Institute of Organic Chemistry,
University of Regensburg,
D-93053 Regensburg,
Germany
oliver.reiser@chemie.uni-regensburg.de

Prof. Dr. Burkhard König
Head,
Institute of Organic Chemistry,
University of Regensburg,
D-93040 Regensburg,
Germany
burkhard.koenig@chemie.uni-regensburg.de

13 Declaration:

Herewith, I declare that the current PhD thesis is an outline of my original work, which is prepared single-handed. Wherever contributions from others are involved, all of them are marked clearly, with reference to the literature, license and acknowledgement of collaborative research.

Regensburg, November 06, 2017

……...
Santosh K. Pagire

„Gedruckt bzw. veroffentlicht mit Unterstutzung des Deutschen Akademischen Austauschdienstes“